OS_1

PROGNOSIS OF THERAPY RESPONSE WITH FDG-PET IN METASTATIC COLORECTAL CARCINOMAS AFTER FOLFOX CHEMOTHERAPY

A. Dimitrakopoulou-Strauss (1), J. Rudi (2), C. Burger (3), L.G. Strauss (1). (1) German Cancer Research Center, Heidelberg, Germany; (2) Dept. of Internal Medicine IV, Univ. of Heidelberg, Germany; (3) Dept. of Nuclear Medicine, Univ. of Zurich, Switzerland.

Aim: The assessment of a new chemotherapeutic protocol (FOLFOX), including fluorouracil, folinic acid and oxaliplatin in patients with metastatic colorectal cancer using quantitative PET FDG studies.
Methods: The evaluation of the current study comprises 31 patients (pts) with liver metastases and one patient with lung metastases due to colorectal cancer. All patients were examined prior to onset of FOLFOX therapy, after completion of the first and the fourth cycle. PET with FDG was performed with dynamic data acquisition for 60 min. The evaluation of the iteratively reconstructed images was performed using a dedicated software. The following parameters were used for data evaluation: SUV, two compartment model with computation of k1-k4 and consideration of the distribution volume (VB), fractal dimension (FD, parameter for the inhomogeneity of the tumors).
Results: The evaluation includes 66 metastases. Restaging data were available in all patients, survival data were used in nine patients for reference. Discriminant analysis was used to assess the quantitative PET data, using the restaging data as reference. The analysis demonstrates, that the SUV of the first and second PET examination has an accuracy of only 60 % with respect to therapy outcome. While 77.8 % of the patients with progressive disease (PD) were correctly identified, only 55.6 % of patients with stable disease (SD) were identified, and 42.9 % of patients with partial response (PR) group were correctly classified. In contrast, the dynamic PET data (K1-k4, VB, FD) of only the first, pretherapeutic PET study provided an accuracy of 71.4 % (positive predictive value: PD: 90 %, SD: 80 %, PR: 37.5 %). When the kinetic data of the first and second PET examination were used, the accuracy increased to 91.3 % (positive predictive value: PD: 100 %, SD: 88.9 %, PR: 85.7 %). Furthermore, we were able to demonstrate a close correlation for the kinetic data and the survival. Conclusion: SUV data are of limited value for the prediction of therapy outcome, while the kinetic parameters k1-k4, VB, and FD provide superior information for the prediction of response to FOLFOX therapy.

OS_2

FDG-PET FOR EVALUATION OF RESPONSE AFTER RESECTION OF LIVER METASTASES OF COLORECTAL CANCER

W.J.G. Oyen (1), B.S. Langenhoff (2), T.J. Ruers (2), G.J. Jager (3), F.H.M. Corstens (1). (1) Dept. of Nuclear Medicine; (2) Dept. of Surgery; (3) Dept. of Radiology, University Medical Center Nijmegen, The Netherlands.

Aim. The survival of patients who develop liver metastases of colorectal cancer clearly benefit from resectability. The surgical procedure of liver metastases is frequently extended with cryosurgery (CS) or radiofrequency ablation (RFA) for additional treatment of tumor remnants. The use of CS or RFA results in persisting abnormalities on CT-scanning, which makes it very difficult to recognize residual or recurrent tumor. We evaluated the diagnostic yield of FDG-PET in the follow-up of patients after CS or RFA.

Methods. A total of 23 patients (9 female, 14 male; mean age 65 years, range 53-80 years) were studied. Contrast-enhanced CT and attenuation-corrected FDG-PET (220 MBq FDG, Siemens ECAT/ART) were performed 1, 6 and 12 weeks after metastasectomy with CS or RFA. CT and FDG-PET were interpreted independently. After final reading, correlative, retrospective reading was performed and the results were correlated to the findings at re-operation or follow-up (≥ 1 year).

Results. One week after surgery, FDG-PET showed photopenic areas in the liver. Follow-up FDG-PET became positive in 10 patients, 9 of who developed an early relapse of liver metastases. A postoperative abscess was responsible for the one false-positive study. FDG-PET was superior to CT in establishing tumor activity. Even with knowledge of the positive FDG-PET findings, CT was negative in 4 patients. FDG-PET showed the relapse 3 months before it was apparent on CT. Furthermore, 12 of the 13 patients with negative FDG-PET did not have a relapse. One patient with proven liver metastases had an unexplained false-negative study, which turned positive at follow-up PET.

	FDG (+)	FDG (-)	All
Relapse	9	1	10
No Relapse	1	12	13
All	10	13	23

Conclusions. After resection of liver metastases in combination with CS or RFA, FDG-PET is a very accurate diagnostic tool to detect relapse of tumor activity in the liver. FDG-PET provides important information when aggressive surgical treatment of liver metastases is pursued.

OS_3

SERIAL POSITRON EMISSION TOMOGRAPHY (PET) TO ASSESS THE RESPONSE OF PREOPERATIVE INDUCTION CHEMORADIOTHERAPY IN ADVANCED ESOPHAGEAL CANCER IN RELATION TO SURVIVAL

J.PH. Cambier, P. Flamen, E. Van Cutsem, A. Lerut, A. Maes, G. Bormans, K. Haustermans, N. Ectors, L. Mortelmans. Nuclear Medicine Universitaire Ziekenhuizen Leuven, Leuven, Belgium.

Aim: to evaluate with a prospective study the use of FDG-PET for prediction and assessment of response to preoperative chemoradiotherapy (CRT) in patients with locoregional advanced esophageal cancer.
Methods: thirty-seven patients with locally advanced esophageal cancer (clinical T_4) underwent a whole-body dedicated FDG-PET before and one month after CRT (concurrent 40 Gy, 5-FU and cisplatinum). Patients were classified as PET responders when the postCRT PET demonstrated a strong reduction of the FDG uptake at the primary tumor site (>80% reduction of the tumor-to-liver uptake ratio) without any abnormal FDG uptake elsewhere in the body. All other patients were classified as PET non-responders. The gold standard for response was available in 36 patients based on pathology obtain during surgery (n=30) and by guided biopsy or dedicated radiology in case of a suspicion of progressive disease (n=6).
Results: CRT response, defined as $pT_{0-3}N_0M_0$ with extensive CRT effects observed on pathology, was found in 14/36 (39%) patients. Six of these patients (17%) had a complete pathological response ($pT_0N_0M_0$). A strong correlation between lymph node involvement as shown by preCRT PET and the pathologic responsiveness was found (p=0.0005). The sensitivity of serial FDG-PET for CRT response was 10/14 (71%) and for a non-response 18/22 (82%), resulting in a overall accuracy of 78%. PET was not accurate to diagnose a complete pathological response (sensitivity: 67%, positive predictive value: 50%). The median survival time after CRT of PET responders versus PET non-responders was 16.3 vs 6.4 months (log rank test: p=0.005). Excluding the six patients with overt progressive disease who did not undergo surgery, median survival time was 16.3 and 8.0 months, respectively (log rank test: p=0.015).
Conclusions: these data indicate that PET is a strong predictor of CRT response. Response as assessed by FDG-PET is strongly correlated with pathologic response and survival.

OS_4

PROGNOSTIC VALUE OF PET AFTER THE SECOND CYCLE OF CHEMOTHERAPY AT MALIGNANT LYMPHOMA

O. Belohlavek (1), J. Slaby (2), K. Taborska (1), M. Trneny (2), P. Klener (2). (1) Dept. of Nuclear Medicine, Na Homolce Hospital, Prague, Czech Republic; (2) 1-st Dept. of Medicine, Charles University General Hospital, Prague, Czech Republic.

Aim: Positron emission tomography is often used for staging of malignant lymphomas and assessment of effect of therapy. The aim of this prospective study is to evaluate prognostic value of PET in patients with Hodgkin disease (HD) and non-Hodgkin lymphoma (NHL) after completion of the second cycle of chemotherapy.
Methods: We studied 37 patients (14 males, 23 females; 9 HD, 21 aggressive NHL, 7 indolent NHL; 26 initial diagnosis and 11 relapses). Attenuation corrected PET imaging was performed by dedicated ECAT EXACT PET scanner from the base of the skull to the upper thighs 1 hour after intravenous administration of 18F-FDG (7,6 ± 1,3 MBq/kg). PET scans were evaluated visually by one observer without knowledge of any clinical data. Patients were followed up for 1 – 13 months (mean 7 months). Kaplan-Meier statistical analysis was used. Significance of differences between groups was determined by log-rank test on the level of 5 %.
Results: During the follow up disease relapse or progression occurred at 13 patients (2 patients died) and 24 patients were disease free. After second cycle of chemotherapy PET was positive in 18 patients. In this group disease relapse or progression occurred in 11 cases. On the other hand relapse or disease progression was present in only 2 cases in the group of 19 patients with negative PET. We have found significant difference ($p<0.05$) in the duration of progression free period between groups of PET positive and negative patients.
Conclusions: Our first results suggest that PET performed after second cycle of chemotherapy can play significant role in prediction of malignant lymphoma relapse or progression.

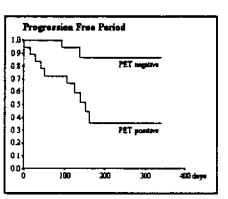

OS_5

MONITORING ISOTRETINOIN THERAPY IN METASTATIC OR RECURRENT THYROID CANCER WITH F-18-FDG PET

A.R. Boerner (1), E. Weckesser (1), M. Weckesser (2), M. Hofmann (1), T. Petrich (1), C. Boy (3), K.J. Langen (3), W.H. Knapp (1). (1) Dept. of Nuclear Medicine, Medical School Hannover; (2) Dept. of Nuclear Medicine, University Muenster; (3) Institute of Medicine, Research Center Juelich, Germany.

Introduction: In case of unsuccessful surgery, radioiodine and/or external radiation therapy, outcome is fatal in recurrent or metastatic thyroid cancer. Therapy with the vitamin A-derivative 13-cis-retinoic acid (13-cis-RA) is an additional option in advanced, otherwise untreatable differentiated thyroid cancer. The aim of this study was to clarify the clinical value of F-18-FDG-PET for monitoring the effects of 13-cis-RA therapy in these patients.
Methods: Twenty-one patients (age: 27 – 72 years) with advanced differentiated thyroid cancer underwent FDG-PET and iodine-131-whole-body scintigraphy paralelled by thyroglobulin tests before, 3, 6, and 9 months after initiation of 13-cis-RA therapy (0.3-1 mg/kg bodyweight). After 9 months 13-cis-RA therapy was terminated, and the imaging procedures were repeated 3 months later. Thyroglobulin levels, blood counts, serum lipids, and liver enzymes were monitored at identical intervals.
Results: FDG uptake (median SUV=3.2) decreased significantly during 13-cis-RA therapy (median SUV=2.2, $p<0.03$) but relapsed in six of eight patients after withdrawal of 13-cis-RA therapy (median SUV 3.8, $p<0.04$). FDG uptake 3-4 months after start of 13-cis-RA therapy was significantly lower in patients who developed increased I-131 tumour uptake than in those patients with no subsequently increased I-131 uptake (median SUV 0.6 vs. 3.4, $p<0.004$). No relationship between serum thyroglobulin level and either I-131 or FDG tumour uptake was detected. 3-4 months after start of the adjuvant therapy was a tendency toward lower FDG uptake in the tumours with a better outcome (median SUVs for CR 0.0, PR 1.6, SD 3.3, and PD 5.2) according to WHO classification.
Conclusions: FDG-PET promises to measure early redifferentiation effects of adjuvant 13-cis-RA therapy in thyroid cancer. These data indicate that reduction of FDG uptake may predict a subsequent induction of radioiodine avidity and tumour response, but the number of patients observed is still small.

OS_6

FDG-PET CORRELATES WITH THE PROGNOSIS OF PATIENTS UNDERGOING HIGH-DOSE CHEMOTHERAPY WITH STEM CELL TRANSPLANTATION FOR MALIGNANT LYMPHOMA

A. Becherer (1), M. Mitterbauer (2), U. Jaeger (3), P. Kalhs (2), H. Greinix (2), C. Poetzi (1), G. Karanikas (1), A. Kurtaran (1), G. Zettinig (1), R. Dudczak (1), K. Kletter (1)(1) Department of Nuclear Medicine; (2) Division of Bone Marrow Transplantation; (3) Department of Haematology and Haemostaseology, University of Vienna, Austria.

Aim: FDG-PET has established itself as a valuable tool in determination of viability of post-chemotherapy residual lymphoma bulks in Hodgkin's disease (HD) and non-Hodgkin's lymphoma (NHL). Therefore PET is accurate in prediction of the clinical course after conventional chemotherapy (ChT). This study aimed to determine whether this is also true after high-dose chemotherapy followed by stem cell transplantation (HDT/SCT).
Methods: In a retrospective analysis, our PET database was reviewed for patients undergoing a PET scan for lymphoma at least 3 weeks after ChT and not more than 8 weeks prior to HDT/SCT. The PET result was scored visually and quoted as negative ([-]), weakly positive ([+]), moderately positive ([++]) and strongly positive ([+++]).
Results: Out of 236 patients 16 fulfilled the inclusion criteria, 10 with NHL an 6 with HD. In the NHL group 2 had refractory disease (RD), two a responsive relapse (RR), 4 were in partial remission (PR), one in first complete remission (CR) but with high risk, and 2 in second CR. All HD patients underwent HDT/SCT because of RR. PET was [-] in 5 patients, [+] in 3 patients, [++] in 2 patients and [+++] in 6 patients. After HDT/SCT the follow-up period lasted from 4 to 28 months. One patient with a [++] PET was excluded because he died 3 weeks after HDT/SCT from transplantation associated mortality. During follow up after HDT/SCT from 4 to 28 months all 5 patients with a [-] PET and 2 with a [+] PET are in remission. All other patients relapsed within 4 to 10 months after HDT/SCT. Four of them died, three directly from lymphoma, all with a [+++] PET. Two NHL patients with age adjusted international prognostic index (Aa-IPI)=2 but [-] PET are still in remission while of those with [++] or [+++] PET, one patient with Aa-IPI=0 and three with Aa-IPI=1 relapsed.
Conclusion: FDG-PET is useful for discrimination of patients with lymphoma who have a good prognosis after HDT/SCT from those who are at high risk for a relapse. PET might therefore aid in choosing the optimal individual conditioning strategy before HDT/SCT.

OS_7

POSITRON EMISSION TOMOGRAPHY AND 18F-FLUORODEOXY-GLUCOSE FOR PREDICTION AND ASSESSMENT OF RESPONSE TO NEOADJUVANT CHEMOTHERAPY IN PATIENTS WITH ADVANCED OVARIAN CANCER

N. Avril (1), W. Kuhn (2), S. Ruthke (2), J. Nährig (3), W. Weber (1), B. Schmalfeldt (2), M. Werner (3), M. Schwaiger (1). (1) Department of Nuclear Medicine; (2) Department of Gynecology; (3) Department of Pathology, Technische Universität München, Munich, Germany.

Primary (neoadjuvant) chemotherapy is increasingly used as an alternative to standard primary surgery in patients with advanced stages of ovarian cancer. Aim of the study was to address the role of positron emission tomography (PET) using F-18 fluorodeoxyglucose (FDG) for (1.) preoperative assessment of primary (neoadjuvant) chemotherapy (CTx) in patients presenting with locally advanced ovarian cancer, and (2.) prediction of response to therapy based on changes of tumoral FDG uptake between baseline and following the 1st course of CTx.
Methods: Twenty-four patients with histologically proven advanced ovarian cancer (stage FIGO IIIC and IV) underwent neoadjuvant CTx consisting of 3 courses of carboplatin based CTx followed by cytoreductive surgery. FDG-PET scans of the abdomen and pelvis (ECAT EXACT, 320-380 MBq F-18 FDG, 10 min. emission and 10 min. transmission scanning; 3 bed positions) acquired after the 1st and 3rd (preoperatively) course of CTx were compared with the baseline scan obtained prior to treatment. Quantification of regional FDG uptake using (SUVglc) was correlated with surgical/histopathological response.
Results: Surgery and histopathology after the 3rd course of CTx revealed gross residual disease (GRD) in 14 patients and minimal residual disease (MRD) in 10 patients. The change of tumoral glucose metabolism between baseline and preoperative PET allowed assessment of response with an accuracy of 86% using a SUV decrease of 30% as threshold to differentiate between responder and non-responder. In addition, the metabolic activity of disease in preoperative PET scans correlated well with the intraoperative findings. PET correctly predicted the response in 14 out of 18 patients after the 1st course of CTx by using a cut-off defined as a decrease of SUVglc of 30% below the baseline scan.
Conclusions: This study demonstrates that in patients with advanced ovarian cancer preoperative FDG-PET imaging enables noninvasive assessment of response to neoadjuvant chemotherapy. Moreover, the decrease of tumor glucose metabolism allows prediction of the response early in the course of therapy. Monitoring response to CTx by metabolic imaging may alter the management of patients with advanced ovarian cancer by identifying a subgroup who would not benefit from surgery after neoadjuvant treatment.

OS_8

IMPACT OF WHOLE-BODY 18F-FDG PET ON THE MANAGEMENT OF PATIENTS WITH SUSPECTED RECURRENCE OF COLORECTAL CANCER

J. Setoain, F. Lomeña, M. Simo, G. Perez, J.M. Costansa, I. Carrio. CETIR, PET Center, Barcelona, Spain.

Objectives: The purpose of the study was to retrospectively investigate how ^{18}F-FDG studies influenced clinical therapeutic decision in a series of patients with colorectal cancer referred because of suspected recurrence after first curative surgery.
Methods: 41 consecutive patients underwent whole-body ^{18}F- FDG PET (370 MBq: CPET ADAC) after 6-8 hours fast. All patients had suspected recurrence of colorectal cancer based on elevated CEA levels and /or inconclusive X-ray, CT or MR examinations. PET results were confirmed by surgical resection or clinical follow-up. Major management change was considered if medical therapy was changed to surgical, and medical or surgical to no treatment. Minor management change was considered if changes were made within treatment modality.
Results: PET confirmed tumor recurrence in 25/41 (61%) patients and ruled out recurrence in 16/41 (39%) patients. Resectable liver metastasis were found in seven patients and resectable local relapse was detected in five patients. Major management changes took place in 15/41 (36%) patients: Surgery was planned in 12/41 (29%) and observed metastatic spread precluded treatment in 3/41 (7%) patients. Minor management changes occurred in 8/41 (19%) patients and no change in 18/41 (44%) patients.
Conclusion: Whole-body FDG examinations have major impact on clinical decision making in patients with colorectal cancer and suspected recurrence. Major management changes may occur in >30% of patients (EUREKA FIT0700002000693).

OS_9

TETROFOSMIN PERFUSION SCINTIGRAPHY HAS NO INCREMENTAL PROGNOSTIC VALUE IN PATIENTS WITH A LEFT BUNDLE BRANCH BLOCK

J.J.J. Borm (1), Y.G.C.J. America (1), E.E. van der Wall (2), E.K.J. Pauwels (1). (1) Nuclear Medicine; (2) Cardiology, LUMC, Leiden, The Netherlands.

Aim: To asses the prognostic and incremental prognostic value of tetrofosmin perfusion scintigraphy [TPS] in patients with a left bundle branch block [LBBB].
Methods: Long term follow-up study in consecutive patients who underwent routine TPS. Inclusion criteria: first study with left bundle branch block [LBBB] at rest. Exclusion: pacemaker induced LBBB. Recruitment from August 1995 until Februari 1999. Census date for follow-up was April 1st 1999. Analysis by means of Cox regression analysis. Endpoints: death; myocardial infarction, ECG-documented ventricular fibrillation; revascularization.
Results: 131 out of 1707 patients fulfilled the criteria. Patient characteristics were: age 65 ± 9 y; male 64%; average 2.2 riskfactors; previous infarction 31%; previous revascularization 25%. Reason for referral: de novo anginal complaints: 36%; asymptomatic patients 8%; established coronary artery disease [CAD] 43%; candidacy for implantation of a cardioverter-defibrillator 13%. Follow-up: 126 patients could be evaluated. Median follow-up of the survivors was 1.37 y [maximum 3.65 y]. Endpoints: 16 dead; 3 hard events; 14 revascularizations. The sixteen patients who died did so after median of 1.0 y [range 19 d - 3.3 y]. Normal perfusion was seen in 17 subjects; reversible defects in 34 and irreversible defects in 75. Cox regression analysis showed prognostic value for survival for perfusion results: irreversible lateral defect [chi-square 7.6, relative risk [RR] 7.6, 95% confidence interval [CI] 2.0 - 29.2]. Contributing clinical risk factors in uni-variate analysis for survival were age [RR 1.09 per year, P < 0.02]; body-mass index [RR 0.81 per unit, P < 0.05]. Stepwise analysis, with clinical data in block 1 and perfusion data added in block 2 showed for survival: (Block 1) Established CAD [RR 5.5, P 0.0017, 95% CI 1.7 - 17.7]; Age [RR 1.11/y, P 0.0035, CI 1.03/y - 1.20/y]; body-mass index [RR 0.70/unit, P 0.0003, CI 0.57 - 0.86]. Chi-square block 1: 24.1, P < 0.00005. (Block 2) No single perfusion parameter, nor any derived summary statistic contributed to the model. Similar results were obtained for hard-event-free survival. In the soft event-free survival analysis, reversible defects in th anteroseptal area were predictive for revascularization [RR 6.1, P 0.0084, CI 1.9 - 19.5], with a chi-square for change from block 1 of 6.9 [P 0.0086].
Conclusions: tetrofosmin perfusion scintigraphy has prognostic, but no incremental prognostic value in subjects with a left bundle branch block.

OS_10

TL-201 MYOCARDIAL PERFUSION SPECT EVALUATION OF SILENT CORONARY ARTERY DISEASE IN PATIENTS WITH ESSENTIAL HYPERTENSION

F. Berk (1), T. Sahin (2), H. Demir (1), E. Ural (2), S. Isgoren (1), O. Erdinçler (1), B. Komsuoğlu (2), C. Aktolun (1). (1) Department of Nuclear Medicine; (2) Department of Cardiology, Kocaeli University, Kocaeli, Turkey.

Patients with essential hypertension have a higher prevalance of silent coronary artery disease (sCAD) and significant coronary artery disease than the normal population. This study was designed to determine the prevalance of significant coronary artery disease in a group of asymptomatic essential hypertension patients and to assess the validity of non-invasive tests in a subset of these patients who undergo coronary arteriography.
METHODS: One hundred and thirty-one asymptomatic patients (75 females, 56 males, mean age 58 +/- 10 years) with essential hypertension and without any evidence of clinical coronary artery disease were studied prospectively. After a minimum of 4 days without medication, subjects underwent stress thallium-201 scintigraphy, exercise electrocardiography, and echocardiography. Coronary angiography was performed in a subset of 46 patients (34%) out of 131, with one or more positive test results.
RESULTS: Eighty-five patients (66%) were negative in both exercise ECG and stress thallium-201 scintigraphy. The prevalance of exercise-induced silent ischemia, defined by concordant ST segment depression or thallium-201 reversible perfusion defect was 34% in the study group. In coronary angiography, 23 of the ischemic patients had normal coronary arteries, 12 had one vessel disease, and 11 had two or three vessel disease. Significant coronary artery disease found to be 17%, that was higher than the prevalance in normal population. Patients with reversible perfusion defects in 2 or more segments were more likely to have significant coronary artery obstruction than patients with a perfusion defect in only 1 segment (93% vs 33%, p<0.001).
CONCLUSIONS: Significant coronary artery disease occurs more frequently in asymptomatic hypertensive patients than in normal population. Reversible Thallium-201 scintigraphic defects were both sensitive and specific for the diagnosis of epicardial coronary artery and microvascular disease.

OS_11

CORRELATION BETWEEN ANGIOGRAPHY, ECHOCARDIOGRAPHY, AND STRESS REST SCINTIGRAPHY TO EVALUATE THE FUNCTIONAL SIGNIFICANCE OF ANOMALOUS CORONARY ARTERIES

G. Rubini (1), F. Bovenzi (2), J. Bagnoli (1), C. D'Agostino (2), D. Rubini (1), A. Niccoli-Asabella (1), A. Bortone (3), N. Veneziani (3), A. D'Addabbo (1). (1) Department of Nuclear Medicine; (2) Department of Cardiology; (3) Department of Cardio-Surgery, University of Bari, Italy.

Aim: This study describes the importance of integration of data obtained from digital coronary angiography CA, Transesophageal Multiplane Echocardiography (MTE) and S/R99mTc-Sestamibi SPET in evaluating the haemodynamic significance of coronary artero-venous fistulae (CF) and of anomalous origin and decourse of coronary arteries (ACA).
Material and Methods: All pts underwent MTE to evaluate the relationship of anomalous ACA with the aorta (A) and pulmonry artery (PA), and S/R99mTc-Sestamibi SPET to detect ischaemia.
Results: CF were detected by coronary angiography in 9 pts, 5 right coronary arteries (RC) with anomalous decourse between A and PA, 1 RC with anomalous decourse posteriorly A and PA, 2 circumflex coronary (Cx) artery anomalous decourse, 2 posteriorly and 1 anteriorly aorta, single coronary artery with anterior interventricular artery (IVA) located between A and AP and Cx posteriorly. S/R99mTc-Sestamibi SPET showed ischaemia in 2 pts with CF and in all 5 pts with ACA decourse between A and PA.
In the first pt with CF CA detected a Cx fistula in the coronary sinus, S/R99mTc-Sestamibi SPET detected a reversible perfusion defect of the proximal portion of the postero-lateral wall and the lateral wall confirming the haemodynamic importance of the flow through the fistula during stress. In the second pt. with previous inferior wall myocardial infarction CA detected a CF between the IVA and the left pulmonary artery. The S/R99mTc-Sestamibi identified an irreversible perfusion defect due to previous infarction and a reversible perfusion defect of the anterior wall and apex due to ischaemia caused by the anomalous flow through the CF. The correspondence between the site of the coronary artery where the fistula originated and the reversible perfusion defects, indicates that the anomalous flow through the fistula may cause myocardial ischaemia.
Conclusions: ACA with anomalous decourse between the A and PA is associated with a myocardial perfusion defect detected by S/R99mTc-Sestamibi SPET. CF cause ischaemia only in a small number of patients. Data obtained from S/R99mTc-Sestamibi SPET in evaluating perfusion, correlated to that of coronary angiography, have shown that changes in pts with CF may be due to different coronary diseases: ischaemia due to anomalous flow through the fistula and infarction due to subocclusive RC stenosis.
S/R99mTc-Sestamibi SPET for the evaluation of myocardial perfusion is a reliable means of evaluating the functional importance of the CF detected by coronary angiography. Evaluation of the haemodynamic importance of the coronary fistulae is indispensable in programming corrective surgery.

OS_12

99M-TC-MIBI STRESS GATED SPECT CAN OBVIATE THE NEED FOR CONVENTIONAL STRESS / REST 99M-TC-MIBI SPECT IMAGING FOR THE DIAGNOSIS OF CORONARY ARTERY DISEASE

A.F. El Maghraby (1), W.M. Omar (2), Y. Baghdady (3), M. Abdelghany (3). (1) Department of Nuclear Medicine; (2) Department of Nuclear Medicine, National Cancer Institute; (3) Department of Cardiology, Cairo University, Cairo, Egypt.

Gated SPECT which is recently almost used routinely, permits simultaneous assessment of both left ventricular perfusion and function by assessing wall motions and thickening. These data have major diagnostic and prognostic importance in patients with coronary artery disease. Gated SPECT with ^{99m}Tc- MIBI has been validated extensively against a variety of techniques.
The aim of our study is to analyse wall thickening, wall motion in the post-stress perfusion imaging using ^{99m}Tc-MIBI Gated SPECT as an alternative to conventional stress-rest imaging.
METHODS AND RESULTS: We performed Gated SPECT in 47 patients. They were 30 men, 17 women with mean age 61±11 years.
Gated SPECT was acquired 45-60 min post 555 MBq ^{99m}Tc-MIBI injection at peak exercise in 20 patients or after Dipyridamole pharmacological stress in 27 patients. All patients had post-stress Gated SPECT acquisitions while only 35 patients had another set of Gated SPECT data acquired with the rest study.
The success rate of automatic Gated SPECT acquisition was 100 % and visually assessed image quality was good to excellent in 95% of the cases.
Visual analysis of the presence and reversibility of stress perfusion defects on standard imaging was correlated with the wall thickening data from the post-stress Gated SPECT images. Among the 62 segments with stress-induced perfusion defects and visually apparent wall thickening on ECG-Gated SPECT images, 57 were reversible on rest imaging (positive predictive value of 94% for wall thickening to predict stress defect reversibility). However, Of the 25 segments with stress-induced defects and no apparent wall thickening on Gated SPECT images, 10 segments (40%) demonstrated significant stress defect reversibility on rest imaging. This result represents a negative predictive value of only 60% for the lack of apparent wall thickening to predict correctly an irreversible stress defect.
CONCLUSIONS: Detection of significant wall thickening and motion by stress Gated SPECT ^{99m}Tc-MIBI imaging in a stress-induced perfusion defect highly correlates with stress defect reversibility on ^{99m}Tc-MIBI rest imaging. This may obviate the need to perform rest imaging, thereby potentially reducing the time and cost involved in myocardial perfusion imaging.
However, in absence of wall thickening, rest imaging must be performed to differentiate ischaemia from infarction in a stress induced perfusion defect.

OS_13

CAN CONTRAST-ECHO AND CONTRAST-MRI COMPETE WITH SPET IN DETECTING REGIONAL PERFUSION DEFECTS IN PATIENTS WITH MYOCARDIAL INFARCTION?

A. Giordano (1), A. Lombardo (2), L. Natale (3), M.L. Calcagni (1), L. Galiuto (2), M. Tavolozza (1), S. Maccafeo (1), F. Pasutto (1), F. Reale (1), L. Romano (1), L. Troncone (1)(1) Istituto di Medicina Nucleare; (2) Istituto di Cardiologia; (3) Istituto di Radiologia, Università Cattolica del S. Cuore, Rome, Italy.

The presence and amount of severely hypoperfused myocardium in pts with myocardial infarction has important diagnostic and prognostic value. Recent methodological advances in the field of i.v. contrast agents seem to allow both echocardiography and cardiac MRI to regionally evaluate myocardial perfusion. However, no study is presently available comparing these tests in the same pts.

Aim of this study was to verify whether i.v. contrast-echocardiography (C-ECHO) and i.v. contrast cardiac MRI (C-MRI) are capable to detect segments with severe perfusion defects, as judged by SPECT, in pts with recent myocardial infarction.

Methods: we studied 14 patients with acute myocardial infarction who underwent C-ECHO, C-MRI and SPECT within 5 days from admission and within 48 hours from each other. Pts with poor acoustic window or with contraindication to MRI were excluded. C-ECHO was performed in Harmonic-Power-Angio-mode using i.v. Levovist®; qualitative analysis of digitized images classified myocardial perfusion as present or absent using a 16 segments LV model. C-MRI was performed by i.v. Gd-DTPA and appropriate acquisition sequences; myocardial perfusion was qualitatively classified as present or absent. SPECT was performed 1-2 hours after rest i.v. injection of 740 MBq of Tc99m-Sestamibi. Segments with <50% of max. uptake were classified as severely hypoperfused segments. Comparative analysis was focused on the area perfused by the infarct-related-artery (IRA); overall, it included 96 segments.

Results: C-ECHO provided a contrast effect of diagnostic value in 75/96 segments perfused by IRA (78%). In these segments, sensitivity, specificity and accuracy values in detecting severe hypoperfusion (as judged by SPECT) were 83%, 71% and 76%, respectively. Agreement with SPECT was 76% (kappa: 0.52). In the most apical segments the agreement improved (83%, kappa: 0.66). C-MRI provided diagnostic images in all segments. Sensitivity, specificity and accuracy in detecting severe hypoperfusion were 66%, 78% and 73%, respectively. Agreement with SPECT was 73% (kappa: 0.44). In the most apical segments the agreement slightly decreased (69%, kappa: 0.38).

Conclusions: 1) C-ECHO provided good contrast images in 78% of segments, C-MRI in 100% of segments; however, pts with unfavourable acoustic window or with contraindications to MRI were excluded from the study; 2) C-ECHO and C-MRI results were often different from those of SPECT (range of agreement 69-83%); 3) to date, C-ECHO and C-MRI do not equal SPECT in feasibility and/or in accurately detecting severe perfusion defects.

OS_14

ST SEGMENT ELEVATION IN Q WAVE MYOCARDIAL INFARCTION DURING STRESS SPECT MYOCARDIAL SCINTIGRAPHY: A MARKER FOR VIABILITY

H. Salman (1), N. Hayat (1), S. Mohannadi (1), C. Patel (1), N. Ballani (2), M. Shukur (1), G. Cherian (1). (1) Nuclear Cardiology Unit, Chest Diseases Hospital and Faculty of Medicine, Kuwait; (2) Health Sciences Center, Kuwait University, Kuwait.

Recent radionuclide imaging techniques have validated the occurrence of exercise-induced ST elevation (EISTE) in Q wave leads as a marker of myocardial viability within infarcted areas.

Methods: The study comprised 30 consecutive patients (pts). All pts had uncomplicated Q wave myocardial infarction (MI): 24 anterior and 6 inferolateral MI. All pts had stable post MI angina. Twenty two pts could exercise on a treadmill (Bruce protocol) and 8 pts had dipyridamole test. SPECT scintigraphy was done using Tc-99m MIBI during stress and nitrate augmented thallium-201 (NA Tl-201) for the rest studies. Twenty pts had coronary angiography within 3 weeks of the test.

Results: Twenty four pts developed EISTE in the anterior chest leads and their scintigraphy revealed large anterior, septal and apical defect (group I) and 6 pts had EISTE in the inferior leads and large defect in the posterior segment (group II). Following rest NA Tl-201 SPECT, 20/24 pts (81%) in group I and 5/6 pts (83%) in group II showed significant uptake and viability in their respective areas. Of all these 25 pts with viability, 20 pts had coronary angiography. Sixteen pts in group I had successful revascularization: 12 pts had PTCA and 4 pts coronary bypass graft surgery (CABGS). In group II, 4 pts had successful PTCA of the culprit artery. All these pts had a very good recovery.

Conclusion: EISTE in Q wave MI during SPECT scintigraphy is an accurate marker of residual myocardial viability that could be salvaged by PTCA or CABGS.

OS_15

LOW DOSE DOBUTAMIN GATED SPECT MYOCARDIAL PERFUSION IMAGING VERSUS F-18 FLUORODEOXY-GLUCOSE PET IN THE ASSESSMENT OF MYOCARDIAL VIABILITY

O. Lindner, A. Kammeier, D. Rosanwo, P. Wielepp, W. Burchert. Institut für molekulare Biophysik, Radiopharmazie und Nuklearmedizin, Herz- und Diabeteszentrum NRW, Bad Oeynhausen, Germany.

Positron emission scanning using 18FDG is well established for the detection of myocardial viability. The aim of this study is to validate the role of low dose dobutamine infusion of 10 µg/kg/min during 99m-Tc-sestamibi ECG gated SPECT imaging (Iodo-SPECT) in the assessment of myocardial viability in comparison to FDG-PET.

Methods: 12 patients with left ventricular dysfunction underwent Iodo-SPECT and F-18 fluorodeoxy-glucose PET. Quantitative images of regional EF at rest and under low-dose-dobutamin (LDD) were generated and compared to the FDG-PET using a 20 segment model. To assess the different patterns of viability the FDG uptake was divided into 4 groups [absent < 50 % (avital), low 50 – 70 % (borderline), normal 70 – 110 % (vital) and high >110 % (hypermetabolic)] referring to the segment with maximal perfusion.

Results: The regional EF at rest and under LDD of 229 segments was examined. The segments scored as avital showed no significant increase of regional EF after LDD, whereas regional EF of the other segments increased significantly ($p < 0,05$) after LDD.

	avital	borderline	vital	hypermetabolic
No. of segments	32	40	117	40
Increase of regional EF [%]	1,7 ± 23,2	11,5 ± 16,7	6,2 ± 26,5	15,1 ± 19,4

Conclusion: Low dose dobutamin gated SPECT myocardial perfusion imaging is able to identify contractile reserve and by this means to detect viable myocardium

OS_16

POSITRON EMISSION TOMOGRAPHY EVALUATION OF METABOLISM AND PERFUSION CHANGES INDUCED BY CONVENTIONAL RIGHT- AND BIVENTRICULAR PACING IN THE PATIENTS AFFECTED BY DILATED CARDIOMYOPATHY

P. Zanco (1), G. Neri (2), F. Chierichetti (1), B. Saitta (1), S. Cargnel (1), E. Milan (1), A. Fini (1), P. Trento (1), S. Medea (1), V. Fiore (1), R. Buchberger (2)(1) Nuclear Medicine - PET Center, Az. USSL 8, Castelfranco Veneto, Italy; (2) Cardiology, Az. USSL 8, Montebelluna, Italy.

Biventricular pacing (BP) induces well-known effects on myocardial wall function, apparently providing better results in comparison to conventional right pacing (CP) in the patients affected by dilated cardiomyopathy (DC), but at the moment the secondary changes on myocardial metabolism induced by pacing devices are unclear. The aim of our study was to evaluate the possible changes on myocardial metabolism and perfusion induced by BP and CP in these patients.

Methods: To this aim 23 patients affected by DC (III NYHA functional class and ejection fraction < 35%) were submitted to cardiac Positron Emission Tomography (PET). Thirteen patients were examined during ventricular pacing (9 CP, 4 BP), while the other 10 patients were considered as controls. Metabolism was evaluated using F18-fluorodeoxyglucose (FDG), by the glucose load-insulin technique, and perfusion by N13-ammonia (NH3), injected at rest. A visual and a semi quantitative analysis were performed, calculating by ROIs the septum to lateral uptake ratio (SLR).

Results: In all the 9 patients examined during CP a selective defect in FDG uptake in the septum was present (mean SLR 0.65±0.18, $p<0.01$ with respect to controls), while both the patients submitted to BP and controls presented a homogeneous distribution of FDG in the myocardial wall (respectively mean SLR 0.85±0.23 and 0.95±0.13, p=ns). On the contrary at the NH3 PET studies no significant difference in the myocardial perfusion was found in the 3 groups of patients, both at the visual and at the semi-quantitative analysis (mean SLR CP 1.03±0.24, BP 1.00±0.35, controls 0.94±0.11, p=ns).

Conclusions: our preliminary experience could suggest that, in the patients affected by DC, conventional right pacing could induce interference in the metabolism of the septum not correlated to changes in the perfusion, while biventricular pacing improves the myocardial wall function without damages of the myocardial metabolism and perfusion.

OS_17

QUANTITATIVE GRAVITY-ASSISTED DRAINAGE IN F+20 DIURETIC RENOGRAPHY IN PEDIATRIC PATIENTS

J. Stauss, U. Porn, S. Fischer, K. Hahn. Department of Nuclear Medicine, LMU, Munich, Germany.

The **aim** of this study was to evaluate the use of quantitative gravity-assisted drainage (GAD) in pediatric patients with abnormal drainage (less than 70% of maximal activity) after standard renography.

Methods: 186 children (109 girls, 77 boys; age range 19 days to 16 years; median age, 4 years 70 days) with 273 renal units with abnormal drainage after standard renography were studied according to the following procedure: patients were asked to change from a supine to an erect position for at least 5 minutes and to void (1. GAD). Depending on the visually assessed residual activity in the pelvicaliceal system, the attending physician decided, if obstruction was excluded, then a Post Micturition Image (PM) was used to calculate the final drainage. If obstruction was considered possible, then a Furosemide study was performed. For patients studied with Furosemide, the effect of GAD was assessed by measuring drainage 1 min p.i. of Furosemide. Normal drainage (>70%) at this time was considered sufficient to exclude obstruction. If the drainage 20 min p.i. of Furosemide was abnormal (<70%), patients underwent quantitative GAD again (2. GAD) and the final drainage was determined by a PM Image.

Results: The 1. GAD caused a mean additional drainage of 22.1% ± 21.2% of the maximal activity. 91 of 273 renal units (33.3%) had a normal drainage (>70%) after GAD (in 36 units assessed by PM; in 55 units assessed 1 min p.i. of Furosemide). Referred to the number of patients 23 of 186 patients (12.4%) did not receive Furosemide and another 18 patients (9.7%) who received Furosemide did not need the diuretic study, because obstruction already had been excluded after GAD. The 2. GAD resulted in a mean additional drainage of 14.1% ± 13.5%. In 21 of 48 renal units (43.8%) the 2. GAD improved the drainage to >70%. Combined with other findings this effect caused a change in final diagnosis from obstruction to non-obstruction in 6 cases (12.5%).

Conclusions: The effect of gravity-assisted drainage made the Furosemide test unnecessary in 22.1% of patients with abnormal drainage after standard renography. Additionally GAD following the diuretic study test can change the final diagnosis to non-obstruction. Therefore GAD is a very useful procedure in F+20 diuretic renography.

OS_19

STENTS IN PAEDIATRIC UROLOGY: ASSESSMENT BY DIURETIC RENAL SCINTIGRAPHY: DO THEY WORK?

R. Howman-Giles (1), S.J. Singh, D.K. Chung, M. Patel, G.H. Smith. (1) Department of Nuclear Medicine; (2) Department of Paediatric Urology, The Children's Hospital at Westmead, Sydney, Australia.

Double J stents are being used commonly in paediatric urological practice. It has been shown that urinary drainage occurs around as well as through the lumen of this prosthesis, however several studies show the stents sometimes fail to relieve apparent renal outflow obstruction on diuretic scans.

A pilot study was performed using the diuretic renal scan on 6 paediatric cases with suspected ureteric obstruction before , during and after double J stents were placed in situ.

Methods: Six infants (ages 3 days -3.5 yrs) were examined. The double J was across the pelviureteric junction (PUJ) in 4 and vesicoureteric junction (VUJ) in 2. The diuretic renal scan (DRS) was performed after IV hydration (15mls/kg) and with Tc99m MAG3. Furosemide was given (1mg/kg) after activity was seen in the bladder. Differential function and diuretic T1/2 was performed.The T1/2 was calculated with a monoexponential curve fit.

Results: Of the 4 cases with the stent across the PUJ the T1/2 normalised in 1, no change in 2 and appeared obstructed in 1. In the 2 cases of the stent across the VUJ the T1/2 normalised in 1 (preop reimplantation of megaureter) and failed to improve in the other (postop reimplantation of megaureter). This patient required decompression with a nephrostomy tube and obstruction settled with time. Differential function improved in 3, remained stable in 2 and one patient had a single kidney.

Conclusion: This study shows a varying response on DRS in patients with double J stents. It is difficult to determine if the lack of normalisation of washout curves is due to the inability of the DRS to detect an improvement or to persistent obstruction. By qualitative assessment we feel that scans with and without a stent help to determine how significant an obstruction is. Late follow up of these patients with DRS to measure renal function is necessary to confirm relief of obstruction

OS_18

LONG-TERM FOLLOW-UP IN CHILDREN WITH UNILATERAL UPPER JUNCTION OBSTRUCTION (UJO): COMPARISON BETWEEN SURGERY AND CONSERVATIVE TREATMENT

A. Boubaker (1), J. O. Prior (1), C. Antonescu (1), B. Meyrat (2), P. Frey (2), A. Bischof Delaloye (1). (1) Department of Nuclear Medicine; (2) Department of Pediatric Surgery, University Hospital, Lausanne, Switzerland.

We evaluated the long-term outcome of renal function of the UJO (UJOK) and controlateral (NK) kidneys obtained during I-123-OIH at diagnosis and at ≥5 years follow-up in children presenting unilateral UJO.

12 children (10 M, 1 F) aged 1 month to 9 years (mean :2.4±2.9y) at diagnosis had no surgery. 32 children (21 M, 11 F) aged 10 days to 14 years (mean : 1.9±3.3y) at diagnosis had unilateral pyeloplasty. 59 children (13 M, 46 F) aged 3 to 17 years with no history of obstructive uropathy, normal differential function and ERPF were selected as controls. Separate renal function was measured by an accumulation index (AI) defined as the tracer extracted by the kidney from 30 to 90 seconds after cardiac peak activity. Normal AI in children is 11±2% of injected activity.

In non operated children, there was no difference of AI between affected and normal kidneys, neither at diagnosis nor at follow-up when it was significantly higher than controls in UJOK and NK ($p<.05$). We have separated the children who had surgery in 2 groups, one with clearly decreased function (AI<6) and one with moderately decreased or normal function (AI>6) of the UJOK. In the first group, AI significantly improved after surgery but remained inferior to normals, whereas AI of the controlateral kidneys increased above normals. In the second group, AI of the UJOK was significantly lower than that of NK. This difference disappeared after surgery, AI of both kidneys were in the range of controls.

			First RG		Follow-up	
Patients	n	Kidneys	Age	AI (mean±SD)	Age	AI (mean±SD)
No surgery	12	UJOK	1m-9y	9.06±1.75	5y-18y	12.65±1.44
		NK		9.51±1.55		12.21±1.43
Surgery AI>6	18	UJOK	2w-14y	8.68±1.57	5y-21y	11.08±2.13
		NK		11.06±1.75		11.78±1.54
Surgery AI<6	14	UJOK	10d-3y	4.36±1.57	5y-15y	7.80±3.47
		NK		10.57±3.20		13.28±2.68
Controls	59	LK	3y-17y	10.99±1.43	RK	11.06±1.50

In conclusion, children selected for conservative treatment had bilaterally normal AI that increased above normals at follow-up. Those who were operated had either moderately or severely reduced AI of the affected kidney. At follow-up AI increased in both groups, children with moderate preoperative function reduction were no longer different from normals, those with severely reduced function of the UJOK did generally not reach normal values, whereas the controlateral AI increased, probably indicating compensation.

OS_20

RELATIONSHIP BETWEEN GASTRO-OESOPHAGEAL REFLUX, LOWER RESPIRATORY INFECTIONS AND ASTHMA IN CHILDREN: PRELIMINARY REPORT OF A COORDINATED RESEARCH PROJECT (I.A.E.A.)

G. Ciofetta, P. Bernal, B. Birkenfeld, S. Boonyaprapa, S. Chen, A. Ellman, S. Fatima, P. Orcellana, J.E. Rondain, A.K. Padhy. Nuclear Medicine Section, Division of Human Health, International Atomic Energy Agency, Vienna, Austria.

Gastro-oesophageal reflux (GER), Lower Respiratory Tract Infections (LRTI) and Bronchial Asthma (BA) often coexist in children. It is not clear yet: the prevalence of GER in children with respiratory disorders, the possible cause-effect mechanism, how beneficial GER medical treatment could be in the management of LRTI and BA.

Aim: this coordinated research project (CRP) aimed to use the "milk-scan" as an objective mean for GER, Oesophageal Transit (OT) anomalies and Lung Aspiration (LA) detection and monitoring, in a wide sample of children affected by LRTI and/or BA.

Methods: all participants to the CRP adopted the same procedure. Patients with LRFT and/or BA were recruited and investigated, for diagnosing GER, suspected on clinical bases. The milk-scan was obtained by oral administration of 99mTc-sulfur-colloid labelled milk (1.8 MBq/kg, from 18 to 74 MBq); the individual formula amount was given, after 4 hours fasting; OT studies required 2 frames/sec acquisitions in the upright position, during the first ingestions. After feeding completion, a 40 min acquisition was performed at 10 to 60 sec/frame, for Gastric Emptying (GE) and GER evaluation, in the supine posture; delayed 2 to 24 hours images were added for LA detection.

Results: during the first year of the IAEA-CRP, 159 children were studied, 1/12 to 15 years aged; male to female ratio was 55,9%. OT studies were successfully obtained in 85 patients and anomalies were detected in 9 (9.4%). LA studies were completed in 87 patients and were positive in 3 (3.4%). GER was found in 100/159 children (62.9%). According to clinical diagnosis, GER prevalence was highest in BA group (69.6%), followed by Pneumonia (61,1%) and Recurrent Bronchitis (44.1%). Medical treatment for GER was given to 47 children: a significant clinical improvement was present in almost all of them. Repeated milk-scans were obtained only in 18 patients up to date: GER quantitative parameters improved in 89% of these follow-up investigations.

Conclusions: the CRP preliminary results show that GER prevalence in LRTI and/or BA is about 7 times higher than the reported normal prevalence in infancy. LA and OT anomalies did not play a major role in our sample: this is agreement with other studies in the literature, indicating that respiratory symptoms are probably due to vagally mediated mechanisms. GER diagnosis and its medical treatment are mandatory in children with LRTI/BA.

OS_21

HEPATOBILIARY SCINTIGRAPHY IN THE EVALUATION OF NEONATAL CHOLESTASIS SYNDROME

A. Mavi (1), N. Arslan (2), R. Bekis (1), H. Durak (1), B. Büyükgebiz (2), Y. Öztürk (2), B. Aslan (3). (1) Department of Nuclear Medicine; (2) Department of Pediatrics; (3) Department of ,Dokuz Eylül University, Izmir, Turkey.

AIM: The aim of this study was to assess the diagnostic role of hepatobiliary scintigraphy in the evaluation of neonatal cholestasis. METHOD: Thirtythree infants (12 girls, 21 boys; mean age 67,2±60 days) with neonatal cholestasis (8 biliary atresia, 25 neonatal hepatitis) are retrospectively evaluated. Urinary and blood amino acids, thyroid functions, antibodies against cytomegalovirus, rubella and toxoplasma, hepatitis virus serology, sweat test, serum alfa-1 antitripsin activity, reducing substance in urine, abdominal ultrasonography, hepatobiliary scintigraphy were performed all of infants and liver biopsy performed 13 of them. Dynamic images were obtained 90 minutes (1 minute/frame) after intravenous administration of 37MBq Tc-99m HIDA. If no radiopharmaceutical is noted in the bowel, planar images were obtained 2. 4. 6. and 24. hours. Images of 17 patiens (13 idiopatic neonatal hepatitis, 2 K vit. deficiency, 1 cystic fibrosis, 1 alfa-1 antitripsin deficiency) showed intestinal drenage in 32 minutes after the injection. This 17 patients having normal hepatobiliary scintigraphy were classified as group A. In 6 of 25 neonatal hepatitis (2 prematurity and sepsis, 2 idiopatic neonatal hepatitis, 1 intrahepatic biliary hypoplasia, 1 cystic fibrosis) activities were detected after 32 minutes till 24 hours in the bowel (Group B). In the scintigraphy of 8 extrahepatic biliary atresia (histologically proven) and 2 of 25 neonatal hepatitis (1 primary hemachromatosis, 1 prematurity and sepsis) intestinal dreinage was not noted until 24 hours (Group C). Each group was compared with the others according to biyochemical parameters of liver function [serum total and direct biluribin, total protein, albumin, serum aspartat aminotransferaz(AST), alanin aminotransferaz(ALT), gama glutamyl transpeptidaz(GGT), alkalen phosphataz(ALP)]. RESULTS: When we compare the results of Group A and C; T.bil. (7,3±4; 12±4,2 mg/dl), D.bil. (2,3±1,5; 6,6±2,4 mg/dl), AST (87,1±78,1; 179,2±108,4 IU/L), ALT (40,4±38,2; 105,9±63,9 IU/L) and GGT (165,5±134,8; 668,5±545,2 IU/L) were found respectively. These results were accepted statistically meaningfull ($p<0,05$). When we compare the results of Group A and B; D.bil. (2,3±1,5; 5,4±3,1 mg/dl respectively) ($p<0,03$), Group B and C; GGT (172,1±141,4; 668,5±545,2 IU/L respectively) ($p<0,02$). CONCLUSION: Delayed intestinal visualization of radiopharmaceutic is related with high levels of direct biluribin and GGT. Higher levels of GGT is also related with non-visualization of intestinal activity. There is no relationship between high levels of ALP and intestinal visualiation of activity. Absence of the intestinal excretion of the tracer is nor constantly associated with biliary atresia. Therefore, no excretion of tracer needs further investigations as liver needle biopsy.

OS_22

SOMATOSTATIN RECEPTOR SCINTIGRAPHY IN CHILDREN WITH MALIGNANT LYMPHOMAS

W. Cholewinski (1), JR. Kowalczyk (2), A. Drop (3), E. Poniatowicz-Frasunek (1), A. Nocun (1), B. Stefaniak (1), B. Chrapko (1), A. Tarkowska (1). (1) Department of Nuclear Medicine; (2) Department of Hematology and Oncology; (3) Department of Radiology, Medical University, Lublin, Poland.

AIM: The purpose of this study was to assess the diagnostic value of somatostatic receptor scintigraphy (SRS) in children with malignant lymphomas in comparison with usually applied diagnostic methods.

METHODS: The study was performed on 15 patients 4 – 17 years old (average age 13±5 years) with histopathologically confirmed diagnoses of malignant lymphoma (Hodgkin lymphoma – 7 pts, non-Hodgkin lymphoma – 8 pts). Eleven pts had completed treatment and 4 pts underwent SRS during chemotherapy.

In all patients scintigraphy was performed 24 and 48 hours after i.v. administration of an indium 111In-labelled somatostatin analog (Octreoscan 111In, Mallinckrodt Medical) using planar static technique (128x128 matrix) over selected body parts. In selected cases SPECT studies over thorax and abdomen were performed (64x64 matrix, 6° step). An Elscint Varicam double-head gamma camera with dedicated computer system was used in the tests. SRS results were compared with clinical data and imaging results. CT over thorax and abdomen was performed in all patients, MRI in 2, 67Ga scan with SPECT in 3 pts. All patients included in this study had 24 months follow up after SRS. Seven patients were referred to SRS with post-treatment residual masses in mediastinum and abdomen.

RESULTS: The presence of pathological, focal areas with increased radioisotope uptake was observed in 12 patients. There were 41 lesions in total. The above changes were observed in the cranium, neck, mediastinum, liver and abdomen. In three cases SRS and CT results were in accordance with each other (two complete remissions; change in mediastinum in one case). In 2 patients SRS results were totally discordant with CT (one true positive and one false negative result). In the remaining 9 patients' results of SRS and CT were similar in some abnormalities localisation, however SRS revealed more abnormal findings than CT. Concerning all verification methods used in this study and 24 moths clinical follow up, SRS in our study showed the sensitivity of about 85%.

CONCLUSIONS: It should be stated that: 1. Somatostatin receptor scintigraphy can be useful in the localisation of pathological changes in childhood and adolescent lymphomas, especially in the diagnosis of post-treatment pathological masses. 2. However, our data showed that somatostatin receptor scintigraphy seems to have more additional importance in the diagnostics of children malignant lymphoma and cannot replace already used methods.

OS_23

MYOCARDIAL ISCHEMIA IN CHILDREN WITH CARDIOMYOPATHY. COMPARATIVE ANALYSIS OF PET AND ECG DATA.

I. Litvinova (1), M. Litvinov (1), I. Leontieva (2), I. Sebeleva (2). (1) Independent PET-group, Moscow, Russia; (2) Department of Cardiology, Institute of Pediatrics and Pediatric Surgery, Moscow, Russia.

Recent experimental and clinical studies showed that oxidative metabolism disorders in cardiomyocyte mitochondria can be a pathogenetic base of cardiomyopathy (CMP). Besides, in children with CMP the electrocardiography (ECG) can reveal the ischemia markers, which associated with poor outcome. The aim of this study is to evaluate whether these ECG-abnormalities are indicative of myocardial ischemia.

Methods: 34 patients (pts.) aged from 2 to 13 years (8,0+3,0) with CMP (hypertrophic (HCMP) – 16, dilated (DCMP) – 18) underwent electrocardiography and PET.

Myocardial perfusion was assessed with [^{13}N]-ammonia, glucose metabolism - with [^{18}F]-fluorodeoxyglucose (FDG). For analysis we used ratio between radionuclide concentration in myocardium and blood inside cavity in steady state (Kperf, Kglu). The dynamic study with [C-11]-acetate was performed to evaluate Krebs cycle activity. Rate constant (k_{mono}) and [^{11}]-activity clearance half-time ($\_{1/2}$) were calculated using myocardial time-activity curves.

Results: ST segment depression and/or abnormal form of QRS complex were recorded in 28 (82,4%) pts. using ECG. PET images showed that perfusion was decreased only in 15 of 28 (53,6 %) children with ECG-markers of ischemia. The focal perfusion defects were diagnosised in 12 pts., in 2 of them it was located in area of the left coronary artery descending branch; perfusion was total decreased in 3 pts.). In 13 of 28 (46,4%) pts. perfusion was normal, but metabolism was decreased: glucolysis activity ($\_{glu}$ = 1,3 ± 0,3) - in 6 children, Krebs cycle activity (k_{mono} = 0.070 ± 0,007 min^{-1}, $\_{1/2}$ = 10.4 ±1,8 min) – in 4 pts. and in 3 pts oxidative metabolism data were not measured.

Conclusions: The changers of ventricular complex final part were registered on ECG in most of the patients with CMP. The PET investigations have shown, that the repolarisation disorders were caused by ischemia (focal or relative) in half of these pts. only. In the rest of them they were connected with the metabolism decrease (Krebs cycle and/or glucolysis activity) at normal blood flow. The determination of reasons cousing repolarisation desorders using PET allows to administer appropriate theraphy.

RADIOPHARMACY / RADIOCHEMISTRY

OS_24

DOTA-NOC, A HIGH AFFINITY LIGAND FOR SOMATOSTATIN RECEPTOR SUBTYPES 2, 3 AND 5

M. Ginj (1), D. Wild (1), J. Schmitt (1), B. Waser (2), J.C.L. Reubi (2), M. de Jong (3), B.F. Bernard (3), E.P. Krenning (3), H.R. Maecke (1). (1) University Hospital Basel, Department of Nuclear Medicine, Radiological Chemistry, Basel, Switzerland; (2) University of Berne, Institute of Pathology, Berne , Switzerland; (3) University Hospital Dijkzigt, Rotterdam, The Netherlands.

Tumor targeting with radiolabelled peptides has been of much recent interest. The prototypes are derivatives of somatostatin (SRIF) like DTPA-octreotide or DOTA-[Tyr^3]-octreotide (DOTA-TOC). Five SRIF-receptor subtypes (sstr) are known and shown to be expressed on different tumors. The above mentioned peptides show high affinity mainly for sstr2 and moderate affinity to sstr 5. We aimed at developing new SRIF-analogs for internal radiotherapy which recognize different subtypes to expand the present range of accessible tumors.

Methods: Using parallel solid phase synthesis we synthesised 15 new octapeptides based on octreotide replacing Phe^3 by unnnatural amino acids. DOTA was coupled to these peptides and the receptor subtype affinity profile was determined using transfected cell lines with sstr1-5. Internalisation was determined using AR4-2J cell lines and biodistribution was studied in a rat tumor model (CA 20948) and in normal rats.

Results: Parallel solid phase synthesis allowed quickly to synthesise a range of new SRIF-based radiopeptides. One of them, DOTA-[1-Nal^3]-octreotide (DOTA-NOC), showed high affinity to sstr 2,3,5 if complexed with Y(III) or In(III) (IC_{50}=3.3+/-0.2; 26+/-2 and 10+/-1.6 nM). Surprisingly the sstr2 affinity was almost 4 times higher than the one of [Y]DOTA-TOC and equal to natural SS28. Interestingly the structurally very similar regioisomer [Y]DOTA-[2-NAl^3]-octreotide has only low to moderate affinity to the 3 receptors. The rate of internalisation in this series was highest for [^{111}In]DOTA-NOC and at 4 h was more than twice that of [^{111}In]DOTA-TOC. Biodistribution data in tumor bearing and normal rats again showed very promising results. The uptake in sstr expressing tissues including the CA 20948 tumor was significantly higher for [^{111}In]DOTA-NOC compared to [^{111}In]DOTA-TOC and the tumor-to-kidney ratio was improved by a factor of 2, potentially opening the therapeutic window in a clinical setting. Blocking studies with DTPA-octreotate, a sstr2 selective ligand and cold DOTA-NOC showed high specificity of sstr receptor uptake but also differential blocking in the adrenals, pituitary and pancreas indicating that other receptor subtypes than sstr2 are being targeted.

Conclusion: Parallel solid phase synthesis along with the suitable bioassays is a powerful tool to select new radiopeptides with improved targeting properties. [^{111}In] and [^{90}Y]DOTA-NOC are very promising radiopeptides for the diagnosis and peptide receptor mediated radiotherapy of a larger range of sstr expressing tumors like thyroid, colon or pancreatic adenocarcinomas which were shown to overexpress SRIF receptor subtypes other than sstr2.

OS_25

LUTETIUM-177 MAY BE A BETTER CHOICE FOR RADIONUCLIDE THERAPY THAN IODINE-131 AND YTTRIUM-90

S. Vallabhajosula, P. Smith Jones, I. Kuji, L. Kostakoglu, S.J. Goldsmith, N.H. Bander. Departments of Radiology and Urology, New York Weill Cornell Medical Center, New York, NY, USA.

Monoclonal antibodies (MAb) and peptides labeled with β- emitting radionuclides, ^{131}I and ^{90}Y are being investigated clinically. These two nuclides have several disadvantages. ^{131}I is dehalogenated in vivo and not ideal for internalizing antibodies and peptides. Since ^{90}Y has no γ radiation, pharmacokinetics, tumor uptake and radiation dosimetry can only be estimated using a surrogate, such as ^{111}In. The high energy of ^{90}Y may be more appropriate for bulky tumors, but rad dose to bone marrow and bowel may decrease the maximum tolerated dose (MTD). ^{177}Lu has the physical characteristics similar to ^{131}I and forms stable complexes with chelating agents such as DTPA and DOTA. In addition, the γ energy (113 and 208 KeV), is optimal for imaging and pharmacokinetic studies.

Aim: To compare the biodistribution, pharmacokinetics and radiation dosimetry of ^{177}Lu-DOTA-huJ591 MAb (Lu-J591) with that of ^{90}Y-DOTA-huJ591 (Y-J591) and ^{131}I-huJ591 (I-J591).

Methods: Biodistribution and tumor uptake studies with the three agents were performed in nude mice with LNCaP prostate tumors expressing prostate specific membrane antigen (PSMA), which binds huJ591 MAb. I-J591 and In-J591 biodistribution and tumor targeting studies were performed in patients with prostate cancer.

Results: In nude mice, the tumor uptake (% I.D./g) and tumor/blood ratios with ^{177}Lu were higher compared to the values obtained with I-J591 and In-J591. In addition, Lu-J591 showed higher anti-tumor effect compared to Y-J591. With I-J591, 70% of the activity was eliminated from the body with little retention in the organs due to in vivo dehalogenation. With Lu-177, the radiation dose to organs is only 30% of Y-90 dose (shown in table).

Conclusions: ^{177}Lu biodistribution and dosimetry may eliminate the disadvantages of ^{131}I and ^{90}Y. In addition, the longer residence time of ^{177}Lu in tumor tissue may also augment the anti-tumor response.

Organ	% I.D. organ/at day 6		Radiation Dose (rads/mCi)		
	I-131-J591	In-111-J591	I-131-J591	Lu-177-J591	Y-90-J591
Liver	1.5 ± 0.6	27.0 ± 1.8	2.2 ± 0.3	7.8 ± 0.7	20.2 ± 2.1
Kidney	0.3 ± 0.2	2.7 ± 0.8	2.2 ± 0.6	6.2 ± 1.6	19.2 ± 4.1
Spleen	0.4 ± 0.2	1.8 ± 0.9	3.8 ± 1.2	6.2 ± 2.5	18.0 ± 7.0
Red Marrow	0.4 ± 0.1	0.4 ± 0.1	0.9 ± 0.1	0.5 ± 0.1	1.7 ± 0.2
Whole Body	23.8 ± 3.7	63.8 ± 3.7	0.7 ± 0.1	0.6 ± 0.1	1.8 ± 0.1

OS_26

RADIONUCLIDE THERAPY WITH [LU-177-DOTA,TYR3]OCTREOTATE: AN OVERVIEW OF TUMOUR RESPONSES AND SIDE EFFECTS IN EXPERIMENTAL MODELS

M. De Jong (1), W.A.P. Breeman (1), H.F. Bernard (1), M. Bijster (1), A. Capello (1), J. Bugaj (2), J. Erion (2), A. Srinivasan (2), E. Van Harskamp (1), W.H. Bakker (1), E.P. Krenning (1)(1) Nuclear Medicine, Erasmus University Medical Center Rotterdam, The Netherlands; (2) Mallinckrodt Medical Inc., St Louis Mo, USA.

Aim: A promising application of radiolabelled somatostatin analogues is receptor-targeted radionuclide therapy. The β-emitter Lu-177 (low energy, max 497 keV) is an interesting radionuclide for this purpose, therefore we evaluated the therapeutic potential of [Lu-177-DOTA,Tyr3]octreotate (Lu-177-DOTATATE) in experimental models.

Methods and Results: [Tyr3]octreotate, chelated with DTPA or DOTA, showed very high affinity binding to somatostatin receptor subtype 2 (sst2) in vitro. Lu-177-DOTATATE showed high tumour uptake in sst2-positive tumours in vivo in patients and rats.

The therapeutic effects of Lu-177-DOTATATE were evaluated in vitro in a single cell, colony forming assay (100 cells/well in 6-well plates, 1 h incubation with Lu-177-DOTATATE, 10 days colony growth) using the sst2-positive rat pancreatic tumour cell lines CA20948 and AR42J. These cells showed relative radioresistance in external beam radiation studies (survival after 1 and 2 Gy was 70% and 50% of control). In our in vitro system, Lu-177-DOTATATE was able to control tumour growth (0% survival), the effects were dependent on radiation dose, incubation time and specific activity used.

Radionuclide therapy in vivo in rats bearing CA20948 or AR42J tumours in their flank resulted in dose-dependent responses: 0-100% cure was reached after estimated tumour doses of 10-140 Gy. 100% cure was found beyond 60 Gy.

Dose-limiting organs were the kidneys, because of their high tubular peptide reabsorption capacity. Kidney radiation doses investigated were 20-100 Gy, with and without kidney protection by administration of positively charged amino acids. In rats with a kidney dose higher than 50 Gy, a dose-dependent transient rise in urinary protein excretion (mostly albumin, revealed by SDS-PAGE electrophoresis) was found, starting at about 80 days with complete normalisation at about 150 days post therapy. Control rats that received no radioactivity and rats with a kidney dose lower than 23 Gy had urine with normal protein content. Kidney histology showed time- and dose-dependent increase in kidney damage to severe damage found at 100 days post therapy with a dose-dependent recovery to milder stages at one year post therapy. Using D-Lysine (400 mg/kg), co-injected with the Lu-177-DOTATATE and resulting in 50% reduction of kidney radioactivity, kidney damage could be reduced.

Conclusion: this study shows the great promise of Lu-177-DOTATATE for radionuclide therapy in patients suffering from sst2-positive tumours. Furthermore, the potential of protection of the radiosensitive kidneys using positively charged amino acids, like lysine and arginine, is shown.

OS_27

IS IN-111 AN IDEAL SURROGATE FOR Y-90? IF NOT WHY?

H. Maecke (1), G. Scherer (2), A. Heppeler (1), M. Hennig (3). (1) University Hospital, Department of Nuclear Medicine, Radiological Chemistry, Basel, Switzerland; (2) University Basel, Department of Chemistry, Basel, Switzerland; (3) Hoffmann-La Roche Ltd., Basel, Switzerland.

Aim: One of the most frequently used radionuclides for internal radiotherapy is ^{90}Y because of its good availability via a $^{90}Sr/^{90}Y$ generator, its high specific activity and the high β-energy. The major draw back of ^{90}Y is the lack of γ-radiation. Usually ^{111}In serves as a surrogate for ^{90}Y to do pretherapeutic imaging and dosimetry. This is probably valid if the 2 radiometals are coupled to proteins but not if they are bound to small peptides. We and others have indeed found that labelled to DOTA-somatostatin analogues differences in the rate of internalisation and biodistribution may be found.

Methods: We undertook solid state and solution structural studies using the model peptide DOTA-D-PheNH$_2$ and the corresponding In^{III} and Y^{III} complexes by X-ray crystallography and ^1H-NMR including 2D COSY, 2D TOCSY, NOESY and ROESY to understand how the metal coordination geometry may influence structure.

Results: Potential differences between In^{III} and Y^{III} complexes may be found with respect to coordination number and complex geometry. In^{III} complexes tend to be hexa-and heptacoordinated, Y^{III} prefers coordination number 8. Both complexes crystallize with antiprismatic geometry including the amide carboxy oxygen. A difference between the two structures arises from a different conformation of the ethylenic bridges and different orientation of the side arms (clockwise or counterclockwise, ? or ?) leading to 2 pairs of isomers. Y^{III}(DOTA-D-PheNH$_2$) has the ?(????) structure (m-isomer) and In^{III}(DOTA-D-PheNH$_2$) the ?(????? configuration (M-type). More important are the structural differences in solution. The ^1H-NMR spectra of In^{III}(DOTA-D-PheNH$_2$) show broad lines in the temperature range of 280-315 K for almost all signals. A relatively sharp signal (NH) appears at 9.4 ppm. The same signal is found in the free chelator at 8.4 ppm. The low field shift strongly indicates binding of the carboxy oxygen to the metal also in solution. The broad lines are explained by an imperfect fit of In^{3+} within the DOTA-cage and consequently a more flexible macrocyclic chelate. The corresponding spectra of the Y^{III} complex also shows the low field shift of the NH proton but 2 sets of lines in the ratio of 47:53 appear. One set belongs to the cis isomer at the secondary amide bond which follows from the J_{HCNH} coupling constant of 4 Hz.This is very unusual as cis fractions in secondary amides are usually below 1%.

Conclusion: Our structural studies surprisingly showed major differences between the two metal complexes which may be responsible for pharmacological and biological differences.

OS_28

[111IN]-DOTA-LYS8-VASOTOCIN: A NEW PEPTIDE FOR OXYTOCIN RECEPTOR EXPRESSING TUMORS

M. Chinol (1), A. Nacca (1), G: Bussolati (2), P. Cassoni (2), B. Chini (3), G. Paganelli (1). (1) Nuclear Medicine Division, European Institute of Oncology, Milano-Italy; (2) Department of Biomedical Sciences and Human Oncology, University of Torino - Italy ; (3) CNR Cellular And Molecular Pharmacology Center, Milano - Italy.

The clinical use of radiolabeled peptides, mainly somatostatin analogues, opened new avenues in tumor management. In order to extend these applications, we focused on oxytocin (OT), the hypothalamic nonapeptide which binds to several tumors through specific receptors (OTR). The OT analogue lys^8-vasotocin (LVT), which retains a high affinity for OTR, was selected because the ε-amino group of lysine offered a safe binding site for the conjugation with the DOTA chelating agent.

Methods: The carboxyl group of DOTA was activated by means of a carbodiimmide reagent and then coupled to LVT. After HPLC purification, the new conjugate was radiolabeled with ^{111}In by heating at 80 °C for 25 min. Affinity constants of LVT and DOTA-LVT were determined by etherologous competition experiments using ^{3}[H]OT as radioligand. Binding studies were performed on human breast and endometrial carcinomas and glioblastoma cell lines (OTR positive) and colon carcinoma (OTR negative) determining the displacement of ^{111}In-DOTA-LVT by the two agonists OT and LVT. The entity and specificity of the receptor mediated uptake of ^{111}In-DOTA-LVT in comparison with the non-specific peptide ^{125}I-DOTA-TOC was evaluated in mice bearing OTR expressing tumors.

A mixture of 1.1 MBq of [^{111}In]-DOTA-LVT and 74 kBq of [^{125}I]-DOTA-TOC was administered intraperitoneally to each mouse. The animals were sacrificed at 3 and 24 h post-injection. Tumors and normal organs were removed and counted in a gamma ray detector.

Results: The conjugation between DOTA and LVT was complete as verified by the absence of unconjugated LVT in the reaction mixture. Radiolabeling yields were greater than 95% and a specific activity of 0.05 GBq/_M was obtained. The new conjugate showed hundred folds decreased affinity for OTR compared to unconjugated LVT whereas specific radiolabeling was observed in all the OTR positive cell lines and was negligible in OTR negative ones.

The in-vivo experiments indicated that [^{111}In] radioactivity uptake in tumor, expressed as TS/A tumor/blood ratio, was significantly higher in comparision to the brain/blood ratios either at 3h and 24h after injection. Brain tissues were harvested since is known the presence of OTR in this organ, thus confirming that the uptake in TS/A tumor was probably due to OTR overexpression.

Conclusions: These preliminary data showed that this new peptide may be promising to convey radioisotopes to OTR positive tumors although the loss of affinity for OTR needs further improvements.

OS_29

INTERNALISATION PROPERTIES OF IN-111-DTPA-DGLU-MINIGASTRIN

M. Behe (1), W. Becker (2), T. M. Behr (1). (1) Departement of Nuclear Medicine, Philipps University Marburg, Germany; (2) Departement of Nuclear Medicine, Georg-August-University Göttingen, Germany.

Aim We have developed In-111-DTPA-DGlu[1]-minigastrin for CCK-B receptor scintigraphy. 95 % of the medullary thyroid carcinomas and more than 50 % of the small cell lung cancer express the CCK-B receptor. An import property of target specific radiopharmaceuticals is the internalisation and externalisation of the compound for good diagnostic and therapeutic purpose.

Methods We used TT (human medullary cell line), H69 (humans small cell lung cancer cell line) and AR4-2J (rat exocrine pancreatic tumour cell line) for the internalisation and externalisation studies. The cells were incubated with about 1 µCi of the labelled compound for 5, 15, 30, 45, 60 and 120 minutes and for the unspecific control together with 10^{-6} M gastrin for the same time points. The cells were washed with two different procedures: 1.) 3 x 3 mL PBS and 2.) 2 x 3 mL Barbiturat buffer pH 3.5; 1 x 3 mL PBS. The cell activity were counted in a γ-counter.

For the externalisation studies the cells were incubated for 60 min with 1 µCi of the labelled compound and were washed afterwards 3 times with PBS and were the further incubated for 24 h in cell medium. After certain time points samples of the supernatant were taken, counted in the γ-counter and analysed by reversed phase HPLC.

Results The AR4-2J cell show a increasing internalisation of the specific bound peptide up to 95 % after 30 min and remains on the this plateau for the later time points. The TT cells show an plateau uptake of 87 % after 45 min whereas the H-69 cells show it after 30 min with 92 %. All three cell types show an releasing rate between 11-23 % of the specific bound peptide after 24 h. The HPLC chromatogram shows that the released radioactivity are small hydrophilic metabolites.

Conclusions The internalisation and externalisation behaviour of target specific radiopharmaceuticals is one of the most important point for diagnostic and especially for therapeutic purpose. The In-111 labelled minigastrin show a very fast and nearly quantitative internalisation. As expected for stable radiometall complexes the externalisation rate is very low. The In-111-DTPA-DGlu[1]-minigastrin is a good residualising radiopharmaceutical.

OS_31

HIGH AFFINITY CHEMOTACTIC PEPTIDES LABELED USING N-SUCCINIMIDYL 3-[131I]IODOBENZOATE

O. Pozzi, M. Edreira, E. Sajaroff. National Atomic Energy Comission, Buenos Aires, Argentine.

High affinity nca preparation is an important consideration in the utilization of chemotactic peptide agonists without toxic effects for imaging of bacterial infections.

The chemotactic peptide fNleLFNleYK, which binds with high affinity to receptor on polymorphonuclear leukocytes (PMN), was labeled with N-succinimidyl 3-[^{131}I] iodo benzoate (SIB).

The aims of this study were: radioiodination at high specific activity of chemotactic peptide inert to in vivo dehalogenation without damaging its biological activity, characterize their receptor binding affinity, biodistribution studies in normal and infected mice.

Methods: The [^{131}I]SIB was prepared from N-succinimidyl 3-(tri-n-butylstannyl) benzoate and purified by HPLC. The [^{131}I]SIB was subsequently conjugated to the peptide and purified by HPLC. The synthesis of fNleLFNleYK-SIB conjugate (cold) was made too. Biodistribution studies were performed in C57 normal mice and mice bearing an E.coli infection in the right tight. To determine the effect of labeling in vitro studies using isolated human PMN were made. The binding competition assays of the purified derivatized peptide against the tritiated chemotactic peptide [^{3}H]fMLF and fNleLFNleYK-[^{131}I]SIB conjugate , and superoxide production assay (SPA), were performed.

Results: The radiochemical yield for the synthesis of [^{131}I]SIB and fNleLFNleYK-[^{131}I]SIB conjugate were 55-85% and 59-75% respectively. In the displacing of [^{3}H]fMLF and fNleLFNleYK-[^{131}I]SIB conjugate for the derivatized peptide, binding affinity (IC_{50}): of 36 nM and 68 nM respectively were obtained. Because of both IC_{50} were higher of than those for the underivatized peptide (fNleLFNleYK), 18 nM and 11 nM respectively, the affinity of the derivatized peptide is somewhat lower than it. The SPA (IC_{50}) for the fNleLFNleYK and for fNleLFNleYK-SIB-conjugate were 2-4 nM and 2-3 nM respectively. In the HPLC separation of the labeled peptide retention time was 23 min for fNleLFNleYK and 38 min for the fNleLFNleYK-[^{131}I]SIB. The biodistribution studies showed a very low thyroid uptake (%ID): 0.11±0.05, 0.09±0.03 at 60, 120 min. The higher ratio between infected and normal leg was observed at 60 min.

Conclusions: The HPLC separation used yield essentially nca fNleLFNleYK-[^{131}I]SIB conjugate. This peptide bound specifically to human PMN and exhibited biological activity in a SPA, however its affinity is somewhat lower than the underivatized peptide fNleLFNleYK, but similar to the native chemotactic peptide fMLF. The low thyroid uptake indicate that the radiohalogenation method yield a labeled molecule very stable to in vivo dehalogenation. Rapid localization of radiolabeled peptide at the site of experimental infection was observed.

PHYSICS / INSTRUMENTATION

OS_30

SOMATOSTATIN RECEPTORS ON LYMPHOCYTES OF PATIENTS WITH GRAVES'S DISEASE STUDIED BY GA-67-LABELLED DOTA-LANREOTIDE

I. Szilvási (1), GY. Jánoki (2), E. Bartha (1), I. Virgolini (3). (1) Dept. of Nuclear Medicine, Semmelweis University, Budapest, Hungary; (2) NCPH-FJC, National Research Inst. For Radiobiol., Budapest, Hungary; (3) Dept. of Nuclear Medicine, University of Vienna, Vienna, Austria.

In-111-pentetreotide has been used for visualization of thyroid-associated ophtalmopathy. One of the pathophysiological mechanism of scintigraphy is the high number of activated lymphocytes expressing somatostatin receptors. These receptors are binding other somatostatin analogs as well. **Aim** of our study was to evaluate somatostatin receptors on lymphocytes of patients with Graves's disease using Ga-67-labelled DOTA-lanreotide. DOTA-lanreotide is a long-acting somatostatin analog. High affinity binding of this peptide to variety of tumour cells expressing somatostatin receptors was found. These receptors are expressed on lymphocytes of patients with Graves's disease.

Methods: labelling was performed by using Ga-67-GaCl3 with high specific activity. Labelling efficiency was 96.5 +/- 1.2 %. 6 patients with Graves's disease without eye symptoms (G), 6 patients with marked endocrine ophtalmopathy (O), 5 patients with Graves's disease in remission (R) and 4 normal subjects (N) were studied. Lymphocytes of peripheral blood was separated from 30 ml of blood by standard Ficoll-Uromiro gradient technique. Cells were homogenized in a buffer and incubated with standard amount of Ga-67-labelled substance for 30 minutes. Lanreotide binding sites (LBS) per 10xx5 cells were calculated measuring the specific binding of Ga-labelled DOTA-lanreotide.

Results: mean values of LBS/10xx5 cells were: G: 2.30, O: 3.55, R: 1.24, N: 0.15. All groups of patients with Graves's disease had significantly higher number of LBS on lymphocytes than normal subjects. Patients with endocrine ophtalmopathy had significantly ($p<.05$) higher LBS than patients without eye-symptoms. LBS is significantly ($p<.05$) less in patients with Graves's disease in remission.

Conclusions: number of somatostatin receptors binding Ga-67-labelled DOTA-lanreotide is increased on lymphocytes of patients with all clinical form of Graves's disease. Patients with endocrine ophtalmopathy had highly elevated number of these receptors. Ga-67-DOTA-lanreotide can be used for visualization of thyroid-associated ophtalmopathy.

OS_32

FILTERED ATTENUATION CORRECTION IN POSITRON EMISSION TOMOGRAPHY

O. Demirkaya (1), R.Y. Al Mazrou (2). (1) Department of Biostatistics, Epidemiology, and Scientific Computing; (2) Department of Biomedical Physics, King Faisal Specialist Hospital and Research Center, Riyadh, Saudi Arabia.

Aim: In this study, we propose a new attenuation correction method, filtered attenuation correction (FAC), based on the nonlinear filtration of transmission images acquired using external rod sources. Nonlinear anisotropic diffusion filters are best known for their performance in removing the noise while retaining the image sharpness. The FAC method assumes that the transmission images are not contaminated by emission photons.

Methods: The transmission image of an elliptical ECT phantom (Data Spectrum Inc., NC) with cold rods and spheres was acquired by ECAT EXACT scanner (CTI/Siemens, Inc., Knoxville, TN). The phantom (centered in the scanner) was scanned for 10 minutes in 2D mode (septa extended). Then the attenuation images were obtained by taking the log of the ratio of the blank to transmission counts. Images (µmaps) were reconstructed using a ramp filter with a cutoff frequency of 0.5 cycles/pixel. The µmap images were filtered using the anisotropic diffusion filtering technique to obtain the smooth measured µmap. The smoothed images were then forward projected to obtain the attenuation correction factor (ACF) images (sinograms). The emission image of the same phantom, filled with 4.8 mCi fluorine, positioned at the same location, and scanned using the same scanner for ten minutes, were corrected for attenuation using the smoothed ACF images. The emission images were reconstructed into a 128x128 array using Hanning-windowed ramp filter with a cutoff frequency of 0.4 cycles/pixel. The images corrected by the filtered and original ACFs were compared qualitatively.

Results: In the figure the left image shows the emission image corrected with original measured ACF while the image on the right shows the emission image corrected with the filtered ACF.

Conclusions: The preliminary results indicate that the emission images corrected by the FAC method have sharper and circular boundaries around the cold spheres and rods, and image intensity appears more uniform inside the uniform regions of the phantom. The FAC method, by reducing the amount of noise, permits the reconstruction of emission images at a higher cutoff frequency. Therefore, it may allow identical image quality to be achieved with a better resolution. The smoothed images, if used in segmented attenuation correction (SAC) method to identify the regions, may help improve the performance of the SAC method. It may also allow the use of transmission images acquired in a shorter time period. Future studies will quantitatively evaluate the impact of the FAC method on image noise and resolution as well as its application to cardiac images.

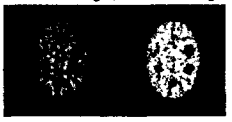

OS_33

PET EMISSION ACTIVITIES AFTER 68GE-TRANSMISSION CORRECTION OR CT-BASED ATTENUATION CORRECTION

A. Buck (1), G. Gubler (1), G. Goerres (1), S. Ross (2), A. Ronn (2), H. Altman (2), A. Tokman (2), G. vonSchulthess (1), C. Burger (1). (1) Nuclear Medicine, University Hospital, Zurich, Switzerland; (2) GE Medical Systems, Switzerland.

Objective: The contrast of the attenuation information in CT images is significantly higher than that in PET transmission images. It is therefore expected that the use of CT images for PET attenuation correction has an impact on the calculated PET emission activities. The aim of this study was to assess the quantitative difference between these two corrections.
Methods: Eight patients referred for FDG PET were scanned on a PET (GE Advance) and a CT system (GE HiSpeed CT/I Pro). Data were acquired according to a standard clinical protocol on the PET system (400 MBq 18F-FDG, Emission: 7 axial field-of-views with 2min. duration; Transmission: 4min/FOV). PET emission images were calculated using segmented transmission correction and iterative reconstruction. The same axial coverage of the patient was scanned on the CT system with 140 keV, 120mA, 5mm slice thickness, 1.7 pitch. The CT images were converted into 511keV attenuation coefficients (scaling approach) and forward projected according to the PET scanner's acquisition geometry to calculate attenuation correction factor (ACF) sinograms. These ACF sinograms were then imported into the Advance system and used for attenuation correction by a prototype reconstruction software. Volumes-of-interest (VOI) were defined manually in several organs and applied to the two sets of corrected emission images.
Results: Mean and (SD) of the ratio [CT-corrected/GE68-corrected] was 1.23 (0.10) in brain, 1.12 (0.22) in liver, 0.99 (0.22) in leg muscle and 0.94 (0.23) in lung.
Conclusions: The highest disprepancy between the two methods was found in brain, where CT correction yielded 23% higher values. This phenomenon needs further investigations if future CT corrected quantitative scans are to be compared with GE68-corrected scans. One possible reason may be that bone attenuation in the skull is not adequately assessed by one of the methods.

OS_34

ABSOLUTE RADIOACTIVITY QUANTIFICATION USING TRANSMISSION BASED SCATTER AND ATTENUATION CORRECTION

D.L. Bailey, R.E. Lewis, G.L. Clarke. Department of Nuclear Medicine, Guy's & St Thomas' Hospital, London, UK.

We have investigated the accuracy of quantitative ^{99m}Tc SPECT using the ADAC Vertex dual-head gamma camera system with scanning ^{153}Gd transmission line sources. All data are acquired in 360° mode with simultaneous emission/transmission scanning. After acquisition the transmission data are first corrected for the downscatter component from ^{99m}Tc photons in the ^{153}Gd window (<5% of ^{99m}Tc count rate). Scatter correction is applied using a transmission dependent scatter correction (TDSC) technique previously described. The data are then reconstructed using the vendor supplied ML-EM algorithm incorporating attenuation correction based on the measured transmission data. Quantitative accuracy was tested by calculating the reconstructed count rate and comparing this with aliquots counted in a calibrated gamma well counter. The calibration of the SPECT system is based entirely upon the camera's sensitivity in air with the same high resolution collimation (~55 cps.MBq^{-1}). A measured correction factor of 13.5% was employed to account for the difference in elapsed time and acquired time in the emission data, to account for the electronic transmission window. In a range of phantom experiments the error in the calculated SPECT activity concentration, over a wide range of activities, was 5.8% (range: 1.6%-13.0%). Linearity of response was also tested and accuracy confirmed. Patient cardiac blood pool SPECT studies have been performed with left ventricular (LV) activity concentration compared to that in a venous blood sample. Pilot results indicate LV activity concentrations are accurate to within 10%, but mostly underestimated. This may be due to partial volume and motion effects from the use of non-gated data. Attenuation map segmentation has been necessary in some cases due to high downscatter from ^{99m}Tc. In conclusion, the system appears to be capable of delivering accurate activity concentrations *in vivo*, with the only user-added component being the use of transmission based scatter correction and attenuation map segmentation.

OS_35

SPECT RECONSTRUCTION FROM LIST-MODE ACQUIRED DATA

L. Bouwens (1), R. van de Walle (1), M. Koole (1), Y. D'Asseler (1), S. Vandenberghe (1), R. Dierckx (2), I. Lemahieu (1). (1) ELIS-Medisip; (2) Division of Nuclear Medicine, Ghent University Hospital, Ghent, Belgium.

Aim: Recently it became possible to acquire list-mode data using a gamma camera and this not only for coincidence studies but also for SPECT. Up to now this feature was only used for dynamic imaging, to make better use of the time information. We developed a list-mode reconstruction algorithm, which uses the list-mode fine spatial and angular sampling. We can bin the detection location to a high degree a accuracy and one does not need to bin the gantry angles into predefined frames, but can record the actual angle thereby removing the impact of angular blurring with continuous rotation. Using list-mode data it becomes possible to store more information without the increase of used storage capacity.
Method: The iterative algorithm uses a new forward projector, which project the estimate of the source distribution, taking into account the attenuation of the object, to an intermediate layer between the object and the detector. This projection is called the emission radiance distribution or angular sinogram. In the backprojection the obtained radiance distribution is sampled using an accurate geometric model of the collimator. The probabilities obtained in the sampling are used in the iterative update equation, which can be derived using the probabilistic mixture approach to emission tomography. Because of the separation of the object dependent and detector dependent characteristics, it is very easy to adapt to different types of collimators, for example fan-beam or pinhole collimators.
Results: Evaluation of the performance of the list-mode reconstruction algorithm using phantom studies and list-mode data acquired with the Marconi Irix gamma camera, shows improvements in contrast and resolution recovery over methods like OSEM and RBI. These methods tend to overcorrect and deviate faster from the optimal solution at increasing number of iterations, where as the list-mode reconstruction is less influenced by the noise.
Conclusion: We have developed a first iterative reconstruction algorithm for SPECT that can use the list-mode acquired data. The better sampling of the data and the better model used in the reconstruction method lead to improved image quality. Using list-mode acquisition the energy information no longer has to be windowed, but the actual energy can be recorded. This can be used for energy and scatter correction which is part of further research.

OS_36

CORRECTION FOR DETECTION EFFICIENCY, GEOMETRY AND DEADTIME IN GAMMA CAMERA BASED PET LIST MODE RECONSTRUCTION

S. vandenberghe (1), Y. D'Asseler (1), M. Koole (1), R. Van De Walle (1), I. Lemahieu (1), R.A. Dierckx (2). (1) Medical imaging and Signal Processing; (2) Dept. of Nuclear Medicine, Ghent, Belgium.

Aim: Semi quantitative data are important for different tasks in PET imaging. We have shown the result of the detector thickness effect and the geometry on the sensitivity for different configurations before. It was shown that there is an non-uniform sensitivity due to both geometry and detector thickness. These effects need to be corrected for to obtain correct reconstructions.

Methods: Here we present a method to correct for both effects and dead time simultaneously in list mode reconstruction , which is a first important step towards quantitative data. The obtained sensitivity values, which combine the geometry and the detection efficiency, are compared with the results of Monte Carlo simulations. Dead time corrections are verified by measurements.

Results: The sensitivity values were calculated for three different configurations: a dual head configuration with heads at 0° and 180° and radii of 360 mm, a Ushape triple head configuration with heads at 0°, 90° and 270° (same radii), and a triangular triple head configuration with heads at 0°,120° and 240° and radii of 230 mm. These values were verified by performing a Monte Carlo simulations (Geant). Photons were randomly generated in a 4π degree emission cone. The same geometries were used. The ratio of detected (giving 511 keV energy) photons to the emitted photons gave the sensitivity. A good agreement was obtained The results of the dual head configuration show a perfect agreement (less than 2 %) between the simulations and the calculated values. There is also a similar behaviour for the Ushape configuration for small radii, but there is an overestimation for large radii. For the triangular configuration there is an slight overestimation for all radii. For both cases the average angle of incidence is higher as in the dual head case. The approximation that the sensitivity depends only on the thickness seems to be less correct for large angle of incidences.

Conclusions: It is shown that the absolute sensitivity for trues can be predicted by an integration over the detection efficiency. The agreement with the results of Monte Carlo simulations is almost perfect for configurations with limited angle of incidences. When large angle of incidences occur in the configuration the estimated sensitivity is higher than the real sensitivity.

OS_37

ITERATIVE RECONSTRUCTION WITH COMPENSATION OF FAN-BEAM COLLIMATOR RESPONSE IN SPECT NEURORECEPTOR IMAGING

D. Pareto (1), A. Cot (1,2), C. Falcón (1), I. Juvells (3), F. Lomeña (4), J. Pavía (4), D. Ros (1). (1) Unitat Biofísica, Facultat Medicina, UB, Barcelona, Spain; (2) Dept. Física Eng. Nuclear, UPC, Barcelona; (3) Dept. Física Aplicada i Òptica, Fac. Física, UB; (4) Servei Medicina Nuclear, Hospital Clínic - IDIBAPS, Spain

Aim: To assess accuracy enhancement in the calculation of the ratio of specific to non specific uptake in SPECT neuroreceptor ligand imaging when OSEM with compensation of attenuation and fan-beam collimator response is employed in reconstruction.
Materials and methods: A numerical phantom was simulated by using data obtained from a CT image of the Alderson phantom. The attenuation coefficients of the non-uniform attenuation map were 0.14cm^{-1} for brain and 0.29cm^{-1} for bone. Ratio of striatum uptake to background activity was established at 7/1. 2D-deterministic simulation of projections for one slice was performed by using a projector which included attenuation map and position dependent response of a fan-beam collimator (previously modelled). 60 projections each 6° of 128 bins (bin size=0.4424cm) were simulated. Poisson noise corresponding to 300 kc was included in the projections. In order to test the influence of adjacent slices and scattered photons, 3D-Monte Carlo simulation was also performed by using SimSet code. Primary and scatter photons were collected separately. 2D-reconstruction of projections was performed by using OSEM algorithm (6 subsets, 1-32 iterations) without correction of attenuation and collimator response (NANC) with only attenuation correction (ANC) and with compensation for attenuation distance-dependent collimator response (AC).
Results: The recovery of theoretical ratio in caudate (CRC) and putamen (CRP) uptake with respect to a non specific uptake in the frontal area is shown in the table as mean and standard deviations in 8 noise trials. The table shows highest values obtained from deterministic simulation, SimSet primary photons and SimSet primary and scatter photons.

	Deterministic		SimSet (primary photons)		SimSet (all photons)	
	CRC	CRP	CRC	CRP	CRC	CRP
NANC	0.55±0.04	0.65±0.01	0.44±0.03	0.57±0.03	0.37±0.03	0.46±0.02
ANC	0.71±0.06	0.82±0.02	0.57±0.04	0.73±0.04	0.48±0.04	0.59±0.03
AC	0.85±0.05	0.91±0.02	0.68±0.06	0.81±0.05	0.55±0.06	0.63±0.03

Conclusions: Our findings indicate that compensation for fan-beam collimator response results in a significant improvement in the recovery of the theoretical ratio. Comparison between 2D-deterministic and 3D-Monte Carlo simulations suggests that 3D reconstruction and scatter correction are necessary in order to achieve a more accurate quantification.
This work has been supported in part by the CICYT (SAF99/0137).

OS_38

PERFORMANCE OF ITERATIVE RECONSTRUCTION ALGORITHMS FOR SMALL ORGANS HIGH RESOLUTION SPECT IMAGING USING A PSPMT BASED DETECTOR

G. Loudos, K. Nikita, N. Uzunoglu, N. Mouravliansky, G. Matsopoulos. National Technical University of Athens, Faculty of Electrical and Computer Engineering, Athens, Greece.

Aim: Clinically used SPECT systems suffer from low resolution and sensitivity since gamma ray detectors, which are based on Anger camera, are not optimised for small organs imaging like breast, thyroid and prostate. In addition convolution algorithms that are used for slice reconstruction degrade image quality resulting to a spatial resolution of 5-8mm. The aim of this work is to show that by using a SPECT system based on a PSPMT and iterative reconstruction algorithms 3D images with 2mm spatial resolution can be obtained. In addition reconstruction of the object from slices can be performed in real time allowing 3D visualisation on the computer screen in order to acquire information from different viewing points.
Methods: The detector consists of a PSPMT coupled with a CsI crystal and the signals are digitized and transferred to the PC via a CAMAC system. Capillary phantoms with 1.1mm inner diameter at intercapillary distances of 2mm were used in order to measure resolution in 3D space. The capillaries were filled with ^{99m}Tc solution of different concentrations for evaluation of the system's response. Other phantoms have also been used and will be presented. A Maximum Likelihood Algorithm (MLA) was implemented for slice reconstruction while an Ordered Subsets Expectation Maximization algorithm (OSEM) was used for accelerating the procedure. The results were compared with those of Filtered Back Projection. A Modified Marching Cubes algorithm (MMC) allowed object reconstruction from slices and visualisation on the PC screen. A commercially available Pentium III, 800MHz, 128MB was used for reconstruction and 3D visualization.
Results: Phantom studies and use of iterative algorithms have shown a 2mm resolution in 3D space as well as detection of the differences in capillaries concentration. The MLA allowed slice reconstruction in 20secs in order to obtain quality images while the OSEM resulted to real time reconstruction. In contrast FBP showed that a 3-4mm resolution can be achieved only when the detector is placed close to the phantom and that resolution decreases significantly when the phantoms are placed in greater distances or in a water solution. Object reconstruction is performed in real time and visualization on the screen allowed rotation and zooming. Furthermore slices in several planes could be obtained instantly.
Conclusions: The developed SPECT system, which combines the excellent performance of a PSPMT and iterative image reconstruction, can be used for high resolution imaging of small organs or small animals, offering high quality 3D images in real time.

OS_39

APPLICATION OF LEVEL SETS TO REGISTRATION, CHANGE DETECTION AND VOLUME BROWSING IN SPECT

J. Carroll, K. Britton. Department of Nuclear Medicine, St Bartholomew's Hospital,UK.

Aim: To derive a region based image representation to allow the application of registration change detection and visual browsing to radiolabelled tumour detection in prostate cancer using multi-temporal SPECT data and to parathyroid detection in dual isotope tomographic data.
Methods: From a set of tomographic reconstructions, for each section we extract an object based representation of the significant regions within that section and thus by combining the objects from each section build a three dimensional indexed representation of the total tomographic volume. For each section containing G grey levels we may threshold at G different levels to give G binary images or level sets. From within these G level set images we search for the optimum threshold t which segments each section into its significant binary objects. We apply robust measures such as the Euler number , a topological invariant, over each set of G binary images to derive a histogram of changes in these measures and a subsequent threshold point t for each tomographic section. For each potential object we derive quantities such as the number of boundary points , the mean edge value derived from the original section along the object boundary , the number of pixels and shape measures such as circularity. For each set of binary objects two and three dimensional moment functions are calculated to give robust reference points for matching multi-temporal data sets as a prerequisite to change detection. By comparing homologous sections which have been previously segmented we detect significant changes by the presence of new objects or a change in shape between the respective binary segmentations. Each binary object may be rendered and displayed in a three dimensional form with areas of change mapped onto the normal blood pool reference image data in the case of change detection in radio-immune studies.
Results: We demonstrate the utility of this object based approach by considering data from patients with prostate cancer who have undergone sequential tomographic imaging with 111In labelled Prostascint (CYTOGEN Corp) and from patients undergoing 99mTc/123I tomography for parathyroid detection.
Conclusions: The use of a higher order description of tomographic data enables both image analysis such as change detection and visual image browsing to be applied to difficult tumour detection problems.

OTHER CLINICAL SCIENCE. BONE AND JOINTS

OS_40

UPTAKE OF SM-153-EDTMP IN NORMAL BONE AND IN BENIGN AND MALIGNANT BONE TUMOR TISSUE. COMPARISON WITH TC-99M-DPD

A. Riegel (1), M. Rodrigues (1), E. Schwameis (2), T. Scholze (3), S. Böhm (3), H. Sinzinger (1). (1) Department of Nuclear Medicine; (2) Department of Orthopaedics; (3) Department of Pharmacology, University Hospital, Vienna, Austria.

Sm-153-ethylenediaminetetramethylene phosphonate (EDTMP) has been used for therapy of painful skeletal metastases, mostly from breast, prostate and lung cancer. The aim of this study was to investigate and compare the uptake in-vitro of Sm-153-EDTMP (Sm) and Tc-99m-DPD (DPD) in sarcoma cells, murine and human healthy bone, and human benign and malignant bone tumor tissue. This in view of the possible clinical application of Sm in patients with soft tissue sarcoma and osteosarcoma.
Methods: After 10-120 min of incubation at 22°C and 37°C with 5µCi Sm or DPD, the uptake kinetics of these tracers in human sarcoma cells (1x10^6/ml) SW 684 (fibrosarcoma) and SW 1353 (chondrosarcoma) was assessed. Normal bone tissue from Wistar-rats, and human healthy bone (hip, tibia, tarsus, ulna) and benign and malignant (primary and metastatic) bone tumor tissue, obtained during surgical procedures, were incubated at 37°C with 10 µCi Sm or DPD during 10, 30, 60 and 120 min. The tracer uptake (as %/mg tissue) was calculated and compared.
Results: The cellular uptake of both tracers was higher at 37°C than at 22°C, indicating that it is related to cellular metabolic activity. Sm-uptake in fibrosarcoma cells (max. 10%, 20 min), chondrosarcoma cells (max. 2%, 40 min), healthy bone tissue (animal, 1-5%/mg tissue; human, 2.5-7.7%/mg tissue) and bone tumor tissue (0.2-11.2%/mg tissue) was lower (mostly non-significantly) than that of DPD. The highest Sm-uptake was found in osteoblastic or osteosclerotic lesions, in particular osteoblastoma. Osteoclastic lesions, either primary bone or metastatic, showed low Sm-uptake. No significant difference in the Sm-bone tissue uptake according to the localisation of the metastatic or primary bone tumors was found.
Conclusions: Data seem to indicate that Sm is promising for clinical application in osteoblastic subtypes of sarcoma.

OS_41

99MTC-MDP BONE SCAN TO EVALUATE MANDIBULAR RECONSTRUCTION BY AUTOLOGUS CORTICAL BONE GRAFT AFTER PARTIAL MANDIBULAR RESECTION

G. Rubini, C. Minervini, D. Rubini, A. Niccoli-Asabella, M. Mele, A. D'Addabbo. Department of Nuclear Medicine University of Bari - Policlinico, Bari, Italy.

Aim: The aim of this study was to evaluate the diagnostic accuracy of 99mTc-MDP bone scintigraphy (BS) in the follow up of bone grafts mandibular reconstruction in pts underwent maxillofacial surgery for infiltrative oral squamocellullary carcinoma.
Materials and methods: 8 pts, underwent maxillofacial surgery and partial mandibular resection followed by cortical autologus bone graft (fibula or radius) reconstruction, were enrolled. For all pts, tumor resection and microvascularized bone graft mandibular reconstruction was simultaneously performed. Head three-phase BS (128 matrix; anterior dynamic acquisition; anterior, right and left lateral static acquisition) at 8 days and 3, 6 and 12 months post surgery was performed.
Results: All our pts have an successful bone transplantation, a good post operative decourse free from surgical or vascular complications. In the 8 days BS, a high degree radiopharmaceutical uptake in vascular, blood-pool and at 3 hrs scan at the edges of the resected bone and in the cortical bone graft was showed. These results permit to demonstrate a good microvascularization of bone graft in acute phase.
The 3, 6 and 12 months post surgery BS showed a slight decrease 99m-Tc-MDP uptake at the graft edges, while in the cortical bone graft normal bone turn-over was detected. These results permit to demonstrate a high degree vascularization and bone turn-over in graft-to-mandibula connection site. Also a progressive normalization of turn-over in the autologus bone graft was found. The BS performed 12 months post surgery shows a uniform tracer uptake similar to the normal bone witch demonstrates a perfect integration of bone graft. These results are in accordance with the clinical follow up and functional recovery of all pts.
Conclusions: In pts underwent maxillofacial surgery and partial mandibular resection by autologus cortical bone graft reconstruction, BS is a useful tool monitoring the vascularization in acute and delayed phase. BS permit to demonstrate the progressive normalization of the local bone turnover. The demonstration of good vascular connection is an important predictive sign of successful bone graft implant.

OS_42

THE ROLE OF BONE SCINTIGRAPHY IN DETECTING OSTEOPOROTIC FRACTURES CORRELATED TO DIFFERENT BONE MINERAL DENSITY VALUES

D. Dodig, S. Crnkovic, M. Medvedec, M. Poropat. Clinical Department of Nuclear Medicine and Radiation Protection, University Hospital Zagreb, Zagreb, Croatia.

Aim: Reduced bone biomechanical resistance in osteoporosis is responsible for an increased risk of fractures. Since many of these events are asymptomatic or presented as nonspecific chronic pain, reliable estimation of the prevalence and proper diagnosis are of paramount importance. The aim of our study was to investigate the diagnostic usefulness of bone scintigraphy in detecting fractures in women with severe osteoporosis, comparing their frequency with bone mineral density (BMD) values.
Methods: We conducted a study of BMD at lumbar spine and femoral neck by dual-energy x-ray absorptiometry (DXA) in 110 postmenopausal female patients (median age 65 years, range 45-83) who were asymptomatic or complaining of nonspecific back pain related to degenerative joint disease, with no previous radiological or any other evidence of osteoporosis. We used the World Health Organization criteria for BMD measured to determine osteoporosis (T score <-2.5). Patients with severe osteoporosis were divided in three age matched groups according to their T scores: 45 patients in group 1, T from –3.5 to –4.0, 36 patients in group 2, T from –4.0 to –4.5, and 31 patients in group 3, T less than –4.5.Bone scintigraphy was performed in all patients 3-4 hours after injection of 740 MBq of Tc-99m-MDP. We analyzed the pattern, frequency and the location of increased uptake in different sites of the skeleton.
Results: Bone scintigraphy revealed fractures in 16/45 patients (35.6%) in group I, 14/36 patients (38.9%) in group II, and 22/31 patients (71.7%) in group III, mainly in thoracic and lumbar spine, ribs and sacrum. Statistically significant differences were found between group I and III ($p<0.05$). We also analyzed degenerative processes throughout the skeleton, and noticed statistically significant differences between the same groups in the knee joint region ($p<0.05$), suggesting more degenerative changes in patients with lower BMD values. Differences were not significant in the spinal region (46.7% in group I, 42.9% in II, 64.7 % in III) and in the hip joint region (33.3% in group I, 35.7% in II, 29.4% in III).
Conclusion: Our data show that bone scintigraphy has a significant role in assessing the location and extent of clinically and radiologically unsuspected fractures throughout the skeleton, and we recommended it as a complementary diagnostic procedure in women with severe osteoporosis whose T scores are below –3.5, particularly below –4.5.

OS_43

FLUORINE-18-FLUORO-DEOXYGLUCOSE POSITRON EMISSION TOMOGRAPHY FOLLOW-UP IN ERDHEIM CHESTER DISEASE: COMPARISON WITH X-RAY, SCINTIGRAPHY, CT AND MRI

M. Diehl, J.H. Risse, S. Sengupta, N. Hamscho, F. Grünwald. Department of Nuclear Medicine, University Hospital Frankfurt, Frankfurt, Germany.

Aim: Erdheim Chester disease is a rare form of histiocytosis, affecting the long bones and multiple inner organs. 69 cases with radiographic and bone scintigraphic studies have been reported. We present the first patient who underwent a PET-study also including a follow-up.
Methods: The PET-studies were performed with quantification using isoactivity-ROIs, determining the count rates of both humeri and femora. The results were compared to scintigraphic and radiologic findings, including MRI.
Results: FDG-PET showed an inceased metabolism in the limbs with SUV-values up to 5.01. Upon diagnosis the ratio of the count rates of lower to upper limbs showed a predominance of both femora, according to the predominant localization of pain in the legs. In the follow-up study the ratio decreased, correlating to the predominant pain in both arms.
Conclusions: The typical skeletal abnormalities in Erdheim Chester disease can be detected using FDG-PET. This seems to be due to the presence of activated histiocytic cells that are known to show an increased glucose consumption. The quantification revealed that the metabolic activity correlates well with the clinical findings of the predominant localization of pain.

OS_44

SEMIQUANTITATIVE EVALUATION OF FENESTRAL AND COCHLEAR OTOSCLEROSIS IN-VIVO: IS THE COCHLEA-CLIVUS-RATIO A USEFUL PARAMETER?

M.J. Reinhardt (1), U.H. Ross (2), R. Fischer (3), H. Palmedo (1), H.J. Biersack (1), T. Krause (1). (1) Dept. of Nuclear Medicine, Univ. Hospital Bonn, Germany; (2) Dept. of Oto-Rhino-Laryngology, Univ. Hospital Freiburg, Germany; (3) Dept. of Nuclear Medicine, Univ. Hospital Freiburg, Germany.

Aim: To find a valid parameter for differentiation of fenestral and cochlear otosclerosis in patients with progressive hearing loss.
Methods: 196 patients (118 women, 78 men; aged 45.5±12.7 years) with progressive hearing loss and 35 healthy controls (22 women, 13 men; aged 42.3±10.9 years) were included in the study. TCS was performed on a Siemens Basicam equipped with a one-pinhole collimator. Images of the middle-/ inner ear were obtained over 10 minutes in a modified Mayer position 2.5 hours after i.v. injection of 700 MBq Tc-99m DPD. Semiquantitative evaluation was done in region-of-interest technique with one region placed over the cochlea and one over the clivus. The ratio of the maximum counts per pixel in each region was assigned as cochlea-clivus-ratio (CCR). Tone- and speech audiometric and ear microscopic findings and tuning fork tests and stapedius reflex measurements confirmed clinically-suspected fenestral otosclerosis in 80 patients, cochlear otosclerosis in 28 patients and no otosclerosis in 88 patients. CCR was compared between patient groups and controls.
Results: CCR of controls was 0.55±0.11 (median 0.53, range 0.41-0.78), CCR of fenestral otosclerosis was 1.4±0.43 (median 1.33, range 1.07-2.32), CCR of cochlear otosclerosis was 2.84±1.08 (median 2.64, range 1.52-5.44), CCR of non-otosclerotic patients with hearing loss was 0.53±0.09 (median 0.51, range 0.37-0.72). There was a clear-cut CCR of 0.8, which separated otosclerotic from non-otosclerotic patients and controls. There was an overlap of CCR from 1.5 to 2.3 between fenestral and cochlear otosclerosis which affected 6.5 % of otosclerotic patients. Both groups could be significantly distinguished by CCR ($p < 0.02$, Wilcoxon-Mann-Whitney test).
Conclusion: The cochlea-clivus-ratio (CCR) is helpful in differentiating patients with progressive hearing loss in those with and without otosclerosis and further separates fenestral and cochlear otosclerosis in almost 95 % of cases, which may be difficult by visual interpretation of scintigraphic images alone.

OS_45

SKELETAL UPTAKE OF TC-99M-HDP BEFORE AND AFTER HIGH-DOSE TREATMENT WITH RE-186-HEDP AND SM-153-EDTMP

W. Brenner, C. von Forstner, C. Bruemmer, W.U. Kampen, C. Muhle, N. Czech, E. Henze. Clinic of Nuclear Medicine, Christian-Albrechts-University, Kiel, Germany.

Since the duration of pain relief after treatment with Sm-153-EDTMP or Re-186-HEDP is limited to a mean period of 2-3 months, a subsequent therapy is recommended as long as blood cell counts are in the normal range. The aim of this animal study was to calculate the bone uptake of Tc-99m-HDP as a measure of bone metabolism before and after high-dose treatment with Sm-153-EDTMP and Re-186-HEDP in order to prove or disprove posttherapeutic alterations of bone metabolism.

Methods: In a total of 12 rabbits we applied 400 MBq per kg body weight of either Sm-153-EDTMP (n = 6) or Re-186-HEDP (n = 6). One week prior to as well as 8 weeks after this treatment bone scanning was performed with 100 MBq Tc-99m-HDP. Whole-body images were acquired at 3 min, 3 h, and 24 h p.i. using a double-head gamma camera with high resolution collimators. The activities for whole body, urinary bladder and soft tissue in the flank were measured by ROI-technique in order to calculate bone uptake, urinary excretion, and remainder soft tissue activity at 24 h p.i.

Results: Prior to treatment with Re-186-HEDP the mean bone uptake of Tc-99m-HDP was 44.8 ± 6.7 % (39.2 – 54.7 %) of initial total whole-body activity. 8 weeks after treatment bone uptake was 40.4 ± 4.9 % (35.7 – 47.1 %) revealing no significant changes ($p > 0.05$) although uptake values were lower in all animals. Before and after treatment there were also no differences between the remainder soft tissue activities (17.7 ± 1.6 % versus 22.0 ± 0.4 %) and between urinary excretion rates (37.0 ± 6.1 % versus 37.7 ± 4.9 %). Similar results were obtained for Sm-153-EDTMP: bone uptake 51.1 ± 5.5 % (45.4 – 57.8 %) versus 48.0 ± 6.1 % (43.7 – 58.8 %); soft tissue retention: 16.4 ± 5.3 % versus 17.8 ± 3.5 %; urinary excretion: 31.6 ± 3.0 % versus 34.2 ± 4.7 %.

Conclusions: Thus, no significant changes of the bone uptake of Tc-99m-HDP as a measure of bone metabolism were observed in rabbits 8 weeks after high-dose treatment with Re-186-HEDP or Sm-153-EDTMP. Therefore, significant alterations of the bone metabolism which might impair bone uptake of the radiopharmaceuticals in general are not to be expected in patients undergoing a second radionuclide therapy with standard activities.

OS_46

OPTIMAL TIMING OF SCINTIGRAPHY WITH TC-99M-LABELLED ANTIGRANULOCYTE MONOCLONAL ANTIBODY FAB' FRAGMENT IN PATIENTS WITH SUSPECTED CHRONIC BONE OR SOFT-TISSUE INFECTION

I. Szilvási, ZS. Varga, Z. Nagy, E. Takács. Dept. of Nuclear Medicine, Semmelweis University, Budapest, Hungary.

Scintigraphy using Tc-99m-antigranulocyte (anti-NCA-90) monoclonal antibody Fab' fragment is a useful method in diagnosing chronic osteomyelitis and soft tissue infection. One of advantages is rapid diagnosis. However optimal timing of imaging is under discussion.

Aim of our study was to compare diagnostic accuracy of early (60 minutes), delayed (4-5 hours) and late (24 hours) images in patients with suspected chronic bone and/or soft tissue infections.

Methods: 12 orthopaedic patients (mean age: 46 yr, 7 female, 5 male) were examined. Final diagnosis was established by clinical, radiographic and microbiologic findings. 5 patients with suspected infection of endoprosthesis, 5 with suspected posttraumatic osteomyelitis were studied, 1 patient had osteosarcoma and 1 patient had neuro-osteoartropathy. 8 out of 12 patients were on antibiotic treatment. Scintigraphy was performed after injection of 750 MBq Tc-99m-anti-NCA-90 Fab' fragment. Images of the suspected area were taken after 60 minutes (E) and 4-5 hours (D). 24 hours (L) imaging was performed in 8 patients. In patients with suspected vertebral lesion SPECT was also performed at 4-5 hours. All patients underwent three-phase bone scan as well.

Results: 7 out of 12 patients had chronic infection (4 osteomyelitis, 3 infected endoprosthesis). 6 were positive on E and D imaging as well, but lesions were better visualized due to higher contrast on D images. 1 FN result was found, it was negative on the L images as well. In 5 patients without infection 3 FP results were found on the E images, but all patients were negative on D images. Patients with FP findings on E images were also positive on three-phase bone scintigraphy.

Conclusions: in patients with chronic orthopaedic infections 4-5 hours imaging has a higher diagnostic accuracy than the early imaging, because of possible nonspecific accumulation of the fragments resulting FP findings. 24 hours imaging has no advantages over 4-5 hours imaging.

OS_47

THE INFECTED JOINT REPLACEMENT: MONITORING RESPONSE TO THERAPY WITH LABELED LEUKOCYTE/MARROW IMAGING

C. Love (1), M.B. Tomas (1), S.E. Marwin (2), C.J. Palestro (1). (1) Division of Nuclear Medicine; (2) Department of Orthopaedic Surgery, Long Island Jewish Medical Center, New Hyde Park, NY, USA.

Aims: Treatment of the infected joint replacement has, as its ultimate goal, the successful replacement of the infected hardware. Successful revision depends on complete eradication of the infection. Treatment typically consists of excision of the infected prosthesis, followed by several weeks of antibiotic therapy. Antibiotic impregnated cement is often placed into the medullary cavity and joint space. Determining when and if the infection has been completely cured remains a daunting task. Laboratory tests are generally noncontributory; the C-reactive protein may remain elevated for more than a year after surgery. Joint aspiration carries the risk of reinfection. Generally, the patient is followed for several months after treatment, and a clinical decision about revision surgery is then made. Although Nuclear Medicine has an important role in the diagnosis of the infected joint replacement, there are few data about its utility in the follow-up of patients with infected joint replacements. The objective of our study was to assess the utility of leukocyte/marrow imaging for monitoring the response to treatment in patients with infected joint prostheses.

Materials and Methods: Ten patients, 5 men and 5 women 59 to 85 years old, with 5 hip and 5 knee replacements ranging from 4 weeks to 9 years of age are included in this retrospective study. All patients had histopathologically confirmed, infected prostheses and all underwent baseline and follow-up leukocyte/marrow studies after treatment. Leukocyte/marrow studies were interpreted according to generally accepted criteria: activity on the leukocyte image without corresponding activity on the marrow image was classified as positive for infection.

Results: The causative organisms were Methicillin Resistant Staphylococcus aureus (3), Staphylococcus coagulase negative (2), Trichosporon glabrata (1), Pseudomonas aeroginosa (1), bacillus species (1), and Candida albicans (1). In one patient only pus was present. Baseline leukocyte/marrow images were positive in all ten patients. Post-treatment studies reverted to normal in 9 of ten patients. Six of these patients underwent excision arthroplasty, and successful reimplantation surgery. In two patients, extensive debridement of the infected tissue was performed, but the prostheses were not removed. Both patients recovered. One patient was deemed a poor surgical risk, and underwent long-term antibiotic therapy. Clinically the infection resolved. One patient, who underwent excision arthroplasty and antibiotic therapy, had a positive post-treatment leukocyte/marrow study. Reexploration confirmed the presence of persistent infection.

Conclusions: These data suggest that leukocyte/marrow imaging may be a useful method for objectively monitoring response to therapy in patients with infected joint prostheses, and further investigation is warranted.

NEUROLOGY / PSYCHIATRY

OS_48

A PET AND SPECT COMPARISON OF THE NEW SELECTIVE SEROTONIN TRANSPORTER RADIOLIGAND ADAM IN THE CYNOMOLGUS MONKEY BRAIN

C. Halldin (1), J. Tarkiainen (1), P. Karlsson (1), P. Emond (2), Z.S. Cselényi (1), B. Gulyás (1), D. Guilloteau (2), J. Hiltunen (3), C. Jonsson (4), S. Larsson (4), L. Farde (1)(1) Karolinska Institutet, Department of Clinical Neuroscience, Psychiatry Section, Karolinska Hospital, Stockholm, Sweden; (2) Inserm U316, Université Francois Rabelais, Tours, France; (3) MAP Medical Technologies Oy, Helsinki, Finland; (4) Department of Nuclear Medicine, Karolinska Hospital, Stockholm, Sweden

Aim: The serotonin transporter (5-HTT) is the target for the majority of antidepressant drugs. For this reason *in vivo* imaging of 5-HTT could be useful but it has been restricted due to lack of suitable radioligands. Recently, a selective 5-HTT ligand (ADAM) was labeled with ^{123}I and examined in the monkey brain with SPECT. There was a high uptake in the 5-HTT rich midbrain region. Here we report a comparison in monkey of radioactive uptake after i.v. administration of ADAM radiolabeled with ^{11}C for PET and ^{123}I for SPECT.

Methods: ADAM was labeled with ^{11}C for PET and ^{123}I for SPECT respectively according to procedures previously described. Each radioligand was injected i.v. into a separate monkey and examined with PET and SPECT and respectively. The acquisition time was 90 and 200 min respectively. The experiments were repeated for each monkey with the addition of pretreatment with the SSRI citalopram (5 mg/kg) 20 min before i.v. injection of the radioligand. Regional radioactivity was obtained using a computerized monkey brain atlas for the cerebellum, midbrain, thalamus, striatum and frontal cortex. The binding potential (BP) was determined for each region using the simplified reference tissue model.

Results: After injection of each radioligand in PET or SPECT the radioactivity accumulated markedly in the midbrain, thalamus, striatum and neocortical regions. In the cerebellum the radioactivity reached a relatively low level. The BP in the PET measurements was 1.48, 0.90, 0.71 and 0.26 in each region respectively. The BP in the SPECT measurements was 0.63, 0.56, 0.50 and 0.18 in each region respectively. In the pretreatment experiments the BP was reduces by 0-60% in the PET experiments and by 30-60% in the SPECT experiments.

Conclusions: Both ^{11}C- and ^{123}I-labeled ADAM are highly potent and selective 5-HTT radioligands. The higher BP in PET could be due to less partial volume error compared to SPECT. The higher variability in pretreatment effect in the PET experiments could be due to the shorter acquisition time and subsequent lesser reliability in the BP. [^{123}I]ADAM can be considered to be a very promising SPECT radioligand. However, the relatively slow kinetics for [^{11}C]ADAM giving an equilibrium later than 2 hours makes it less suitable for PET.

OS_49

[11C]MADAM - A HIGHLY SUITABLE RADIOLIGAND FOR EXAMINATION OF THE SEROTONIN TRANSPORTER WITH PET

C. Halldin (1), D. Guilloteau (2), J. Tarkiainen (1), J. Sóvágó (1), B. Gulyás (1), J. Sandell (1), P. Emond (2), J. Vercouillie (2), S. Chalon (2), J. Hiltunen (3), L. Farde (1)(1) Karolinska Institutet, Department of Clinical Neuroscience, Psychiatry Section, Karolinska Hospital, Stockholm, Sweden; (2) Inserm U316, Université Francois Rabelais, Tours, France; (3) MAP Medical Technologies Oy, Helsinki, Finland.

Aim: The serotonergic system is involved in a variety of neurological and psychiatric disorders. Imaging serotonin transporters (5-HTT) in living human brain has been restricted due to the limited availability of radioligands with suitable *in vivo* binding characteristics. We report a preliminary PET evaluation of [^{11}C]N,N-dimethyl-2-(2-amino-4-methylphenylthio)benzylamine ([^{11}C]MADAM) a highly potent (K_d=62pM) and selective 5-HTT compound. MADAM is a methyl analogue of the recently developed SPECT tracer ADAM but is less lipophilic and suitable for a straight forward labeling using [11C]methyl iodide. For quantification aspects an equilibrium within 2 hours is preferred.

Methods: [^{11}C]MADAM was prepared using the automated [^{11}C]methyl iodide method with an incorporation yield better than 75%. MADAM and the nor-analogue precursor for labeling were obtained by the direct coupling of 4-bromo-3-nitrotoluene with N,N-dimethyl-2-thiobenzamide and N-methyl-2-thiobenzamide, followed by reduction of the amide and nitro functions. [11C]MADAM was injected i.v. into a Cynomolgus monkey and examined during baseline and pretreatment conditions with PET. Radiolabeled metabolites were measured in plasma using a gradient HPLC method.

Results: In the baseline PET experiment a high accumulation of radioactivity was obtained in the monkey brain after i.v. injection of [^{11}C]MADAM (6% after 15 min). There was a high uptake of radioactivity in the brainstem, thalamus and striatum with a lower uptake in the temporal, occipital and frontal cortex with a ratio to cerebellum of about 1.8–2.1 and 1.2-1.6, respectively, obtained at 75-85 minutes. Equilibrium was obtained in all brain regions examined within 85 minutes. In brain regions with lower density the equilibrium was obtained earlier. In a pretreatment experiment (citalopram 5 mg/kg), radioactivity in all examined brain regions was reduced to the level of the cerebellum. Mainly polar labeled metabolites were found in plasma (15-20% unchanged radioligand at 45 minutes).

Conclusions: [^{11}C]MADAM is an excellent 5-HTT radioligand with a high affinity and selectivity for 5-HTT, favorable brain kinetics and metabolism which makes it highly suitable for PET receptor occupancy studies in humans.

Time (min)	3 5 or 4.0	5.5 or 6.0	10 or 12	20	30	40	60
Healthy controls 33m/2f (KI)	42.6	11.5	6.92	5.40	6.60	6.18	
Healthy controls 18m/11f (TU)		12.8	7.31	5.65	4.60		
Depression 3m/4f (TU)		13.8	6.22	4.90	3.88		
Healthy controls 11m/0f (CU)	87.6	24.7	13.4		10.2	7.56	6.00
Depression 21m/1f (CU)	83.6	21.4	10.3		7.52	5.59	4.08
m: male; f: female							

Conclusions: This study shows that measures of unchanged [^{11}C]WAY in human plasma are similar in the three PET Centres, and that the test-retest reproducibility is high. This indicates that, despite rapid clearance of radioactivity from human plasma after [^{11}C]WAY injection, unchanged [^{11}C]WAY can be measured with fair accuracy. This permits the reliable application of bio-mathematical models requiring an arterial input function.

OS_50

RADIOACTIVE METABOLITES OF THE 5-HT1A RECEPTOR PET RADIOLIGAND, [CARBONYL-11C]WAY-100635, IN HUMAN PLASMA SAMPLES: A MULTI-CENTRE STUDY

K. Någren (1), C. Halldin (2), V.W. Pike (3), T. Allonen (1), J. Hietala (1), C.-G. Swahn (2), B. Andrée (2), L. Farde (2), S. Osman (3), P. Grasby (3). (1) Turku PET Centre, Turku University Central Hospital, Turku, Finland; (2) Karolinska Institutet, Department of Clinical Neuroscience, Psychiatry Section, Karolinska Hospital, Stockholm, Sweden; (3) MRC Cyclotron Unit, Imperial School of Medicine, Hammersmith Hospital, London, United Kingdom.

Aim: [*carbonyl*-^{11}C]WAY-100635 ([^{11}C]WAY) is currently the favoured radioligand for the study of the 5-HT_{1A} receptor in the human brain with PET. Accurate measurement of the radioactive metabolites of [^{11}C]WAY in human plasma is critical for the implementation of certain approaches to the bio-mathematical modelling of PET data acquired with this radioligand. The results obtained on [^{11}C]WAY metabolism in three European PET centres, which are summarised here, forms part of a European COST program.

Methods: Measurements of [^{11}C]WAY and its radioactive metabolites were made in Stockholm (KI) and in Turku (TU) with gradient reverse phase HPLC after plasma protein precipitation with acetonitrile and in CU:MRC & IRSL Hammersmith (CU) with isocratic reverse phase HPLC after plasma protein precipitation with methanol. The time-points after administration analyzed at the individual centres were 4–60 min (KI); 2–30 min (TU); and 1.5–60.5 min (CU).

Results: The mean values for the volunteers studied with [^{11}C]WAY in KI and TU are very similar. The mean values for the volunteers studied in CU were generally slightly higher. This small discrepancy may be due to factors such as the differences in methods and subject populations and also statistical variation. Despite the rapid metabolism of [^{11}C]WAY, the test-retest variability of the percentage of radioactivity in plasma represented by unchanged [^{11}C]WAY was low. No influence of age or gender was seen in the [^{11}C]WAY metabolism in volunteers. The mean values for the depressed patients studied with [^{11}C]WAY in TU and CU are slightly lower than the mean values for the volunteers. However, this difference is not statistically significant.

OS_51

IN VIVO HISTAMINE H-1 RECEPTOR MAPPING IN NORMAL HUMAN BRAIN USING 11C-DOXEPIN PET

A.S. Dogan (1), A.M. Catafau (1), Y. Zhou (1), A.H. Crabb (1), K. Yanai (3), S. Offord (2), J. Brasic (1), J. Hilton (1), D.F. Wong (1). (1) Dept of Radiology, Johns Hopkins Medical Institutions, Baltimore, MD, USA; (2) Aventis Pharma, Bridgewater, NJ; (3) Tohoku University, Sendai, Japan.

^{11}C-doxepin is a tricyclic antidepressant with antihistaminic potency recently developed as a PET ligand for imaging cerebral H1 receptors (H1-R) in vivo.

Objective: To assess the distribution of histamine H1-R in the normal human brain in vivo with ^{11}C-doxepin PET.

Methods: Twelve healthy volunteers (7M,5F; 25.8±9.7 yrs) underwent three ^{11}C-doxepin PET scans. Parametric images of distribution volume (DV), which represent H1-R availability, were generated by pixelwise model fitting. Parametric DV images were co-registered with MRI, on which ROIs of 13 brain regions were drawn. Average DV values were obtained for each region, and mean DVs were also calculated for all cortical regions [CX], basal ganglia (caudate, putamen, thalamus [BG]) and infra-tentorial structures (cerebellum, pons [CP]).

Results: Mean DV values obtained are reflected in Table. Friedman's test revealed significant differences among CX, BG and CP ($p<.0001$). Post-hoc Wilcoxon test showed that DV was higher in CX compared to both BG (Wilcoxon $p=0.004$) and CP ($p=0.002$). DVs were also significantly higher in BG than in CP ($p=0.002$). The highest H1-R density was found in cingulate, followed by temporal, parietal and frontal regions, and the lowest in cerebellum (Table).

Conclusion: The normal human brain shows a high density of H1-R in the cortex, a moderate H1-R density in basal ganglia, and a low H1-R density in cerebellum and pons, as demonstrated by parametric images of DV using ^{11}C-doxepin PET. The low H1-R density found in cerebellum may validate the use of this region as a reference for calculation of binding potential. This technique is useful to assess changes in histamine receptor availability in different physiologic and pharmacologic conditions.

TABLE: Mean DV ±SD of H1-R.

Cingulate	Temporal	Parietal	Sup. frontal	Prefrontal	Orbito frontal	Mesial temp.	Occipital
34.6±6.1	33.3±6.2	32.0±6.4	31.7±5.7	30.7±5.5	29.9±5.5	29.6±4.8	28.7±4.9
Thalamus	Putamen	Caudate	Pons	Cerebellum	CX	BG	CP
28.4±4.1	29.7±4.3	26.7±3.9	22.2±3.3	20.5±2.8	31.3±5.5	28.3±4.0	21.4±3.0

OS_52

IN VIVO CEREBRAL HISTAMINE RECEPTOR OCCUPANCY OF THREE ANTIHISTAMINE DRUGS: A 11C-DOXEPIN PET STUDY

A.S. Dogan (1), A.M. Catafau (1), Y. Zhou (1), K. Yanai (3), H. Ravert (1), J. Brasic (1), J. Hilton (1), S. Offord (2), R. Dannals (1), D.F. Wong (1). (1) Dept of Radiology, Johns Hopkins Medical Insts., Baltimore, MD, USA; (2) Aventis Pharma, Bridgewater, NJ, USA; (3) Tohuku University, Sendai, Japan.

Antihistamines are effective therapies for treatment of allergic disease, a condition with a prevalence of over 20%. The most troublesome adverse effect of antihistamines is sedation and cognitive impairment, thought to be a result of central H1 blockade. As many patients self medicate and take higher than recommended doses, a lack of brain H1-R occupancy is a goal in the development of new antihistamines. **Objective:** To measure the H1-R occupancy induced by the two new generation antihistamines fexofenadine (Fex), cetirizine (Cet), and the classical antihistamine diphenhydramine (Dph), using PET with the histamine H1 antagonist ligand ^{11}C-doxepin. **Methods:** Twelve healthy volunteers (7m, 25.8±9.7 yrs) underwent three ^{11}C-doxepin dynamic PET scans with arterial blood samples on two separate days. Antihistamine drugs were administered as single oral doses ninety minutes prior to PET scans. A 2-compartmental 3-parameter kinetic model was used for generating the distribution volume (DV) (=K1/k2) images. MRI and DV images were co-registered and DV values were obtained from regions drawn on MRIs (8 cortical regions, caudate, putamen, thalamus, pons, cerebellum). Percent occupancy (Occ), based on DV changes from baseline was calculated as 100*(DVdrug-DVbaseline)/DVbaseline, a negative change indicating H1-R blockade. **Results:** There was significant H1-R blockade with Dph in all regions (T-test, p=0.01) except for cerebellum, pons, and thalamus. No significant blockade was found with Fex (low and high doses). For Cet at 20 mg level, a blocking effect was found in superior frontal and orbitofrontal regions (T-test, p=0.05). The highest percent Occ in the cortex corresponded to Dph (T-test, p=0.02), and lowest to Fex (Table). **Conclusions:** Our results show that central H1-Rs are blocked by Dph significantly and not blocked by Fex even at high doses. Cet is shown to block the H1-Rs in the frontal cortex at a dose of 20 mg. ^{11}C-doxepin PET is useful to explore the central H1-R binding of antihistamine drugs in vivo.

Drug occupancy in the cortex

Dose (mg)	% Occ (mean±SD)
Fex, low (180)	-4.5±10.0
Fex, high (360)	4.9±10.9
Cet (10)	-10.4±13.5
Cet (20)	-10.5±5.5
Dph (50)	-29.8±4.2

OS_53

EVIDENCE FOR STRIATAL DOPAMINE RELEASE DURING REWARD: A PET STUDY WITH 11C-RACLOPRIDE AND A SINGLE DYNAMIC SCAN

S. Pappata (1), S. Dehaene (1), J.B. Poline (2), M.C. Grégoire (3), A. Jobert (1), J. Delforge (2), V. Frouin (2), M. Bottlaender (2), F. Dollé (2), L. Di Giamberardino (1), A. Syrota (2)(1) CEA DSV, INSERM U334, Orsay, France; (2) CEA DSV, Service Hospitalier Frédéric Joliot, Orsay, France; (3) CEA DSV, CNRS URA 2210, Orsay, France.

Aim: Release of dopamine in the ventral striatum is thought to signal reward information that may be implicated in learning. Recently PET and 11C-raclopride (11C-RAC) activation studies were proposed as a new approach to detect human striatal dopamine release in vivo during behavioural manipulation. The aim of this study was to use PET and 11C-RAC to test the hypothesis that endogenous dopamine is released in human ventral striatum during reward tasks. We used a new method that combines a single PET/dynamic study with a within-subject design, a kinetic compartmental model and the general linear model used in statistical parameter mapping (SPM).

Methods: 12 volunteers were studied, 8 while performing an intense task of speeded arithmetic with periods of monetary gain (R+) and periods of loss (R-) and 4 at rest. 90 frames of 1 min were acquired after bolus injection of 11C-RAC using the ECAT HR+ camera. Two 5 min blocks of R+ and R- in counterbalanced order were presented at 30 and 60 min after injection. We predicted dopamine release in the ventral striatum during R+ but not R- blocks. Based on simulation data and kinetic model parameters, a statistical model was defined allowing to identify and differentiate CBF effect (increased 11C-RAC binding) and DOPAMINE effect (decreased 11C-RAC binding). These effects were tested voxel by voxel using the general linear model of SPM and a group analysis (voxel $p<10^{-3}$, cluster $p<0.05$ corrected).

Results: During R+ blocks a significant DOPAMINE effect was found in the ventral striatum bilaterally (15, 15, -12; -18 9 -12, p<0.001corrected). During R- blocks, a much smaller DOPAMINE effect was observed only in the right ventral striatum (15, 18, -12, p=0.007 corrected). This resulted in a greater DOPAMINE effect in R+ than in R- . A significant CBF effect was observed in ventral striatum with no difference between R+ and R-. No significant effects were found in subjects studied at rest. After correction for movement the activation patterns were preserved at lower thresholds.

Conclusions: This study suggests that our method allows to detect and distinguish dopamine release and CBF increase during positive monetary rewards. Our results also raise the problem of possible false positive effects due to movement during single displacement cognitive studies. This application of PET and radioligands could provide new insights on the in vivo 'functional neurochemistry'.

OS_54

REGULATION OF AROMATIC L-AMINOACID DECARBOXYLASE IN VIVO FOR L-DOPA AND 5-HYDROXYTRYPTOPHAN

P. Hartvig, P. Merachtsaki, R. Torstenson, K. Forsberg, B. Långström. Uppsala University PET Centre, Uppsala University, SE-75185 Uppsala, Sweden.

Aromatic L-amino acid decarboxylase, ADDC, catalyses the decarboxylation of a wide range of aromatic amino acids including 5-hydroxy-L-tryptophan, 5-HTP and L-DOPA to the neurotransmitters serotonin and dopamine, respectively. The decarboxylation capacity in the brain is lower for 5-HTP as compared to L-DOPA. AADC enzyme was supposed not ratelimiting in the formation of serotonin and dopamine and hence not modulated by neuronal activity. Recent findings dispute this statement and the decarboxylation rate of L-DOPA is enhanced by doses of L-DOPA itself and by the co-factor for hydroxylases, 6R-L-erythro-5,6,7,8-tetrahydrobiopterin, BH_4 Brain uptake of 5HTP is favored by glucose, insulin and amino acid supplementation, thus resulting in increased brain synaptic serotonin

Aims: The goal of the present study was to elucidate mechanisms for brain uptake and modulation of the decarboxylation of 5-HTP to serotonin.

Methods: Effect of glucose and BH_4 on brain uptake of 5HTP and biosynthesis of serotonin and dopamine, respectively was investigated in Rhesus monkeys. Glucose or BH_4 were administered intravenously, with and without simultaneous tryptophan, as constant rate infusions to monkeys starting one hour prior to PET with [β-^{11}C]5-HTP as tracer quantitating the brain radioactivity uptake and the decarboxylation rate to serotonin.

Results. Glucose infusion in female Rhesus monkeys increased uptake of 5HTP whereas effect of used infusions of supplement amino acid was negative. Not any change of decarboxylation rate as compared to baseline conditions was detected following BH_4 infusion for [β-^{11}C]5-HTP, whereas in the same monkey a significantly increased synthesis rate was seen for [β-^{11}C]L-DOPA. However, a 15-to 20% lower decarboxylation rate of [β-^{11}C]5-HTP was seen with tryptophane infusion with and without simultaneous BH_4 in contrast to results in similar studies shown for L-DOPA decarboxylation rate. BH_4 treatment increased decarboxylation rate of L-DOPA but not of 5-HTP. Pyridoxine, vitamin B6 the co-factor for AADC increased serotonin synthesis rate, whereas no effect was seen on L-DOPA decarboxylation.

Conclusion. The brain uptake of the precursor for serotonin synthesis is regulated by delicate mechanisms balancing fluctuations in demand for synaptic serotonine The modulating effect of BH_4 and pyridoxine of AADC on serotonin synthesis was at variance with their modulation effect on dopamine synthesis. Still, decarboxylation of the two precursors may be controlled by a similar AADC enzyme. Other mechanisms might be operative as well, such as a different decarboxylation capacity of the substrates.

OS_55

OPTIMUM ACQUISITION PROTOCOL FOR ESTIMATING DISTRIBUTION VOLUME BY C-11 FLUMAZENIL BRAIN PET

M. Tsukamoto, C. Katoh, T. Shiga, T. Kaji, Y. Kuge, N. Tamaki. Depertment of Neuclear Medicine, Hokkaido University, Sapporo, Japan.

Aim: Although C-11 flumazenil (FMZ) has recently been used for assessing benzodiazepine receptor function, it requires long time acquisition and multiple arterial blood sampling for calculating distribution volume (DV) image. To overcome these limitations, we searched the optimal acquisition protocol to obtain a static image compatible with DV image.

Methods: In 10 normal subjects, a dynamic series of FMZ PET scans was performed for 90 minutes with multiple arterial blood sampling to measure radioactivity and labeled metabolites. For the standard, DV images were calculated with two-compartment kinetic analysis. Static images were acquired for 5 minutes during 11 to 60 minutes after tracer administration. For each subject, we investigated the correlation coefficient (r) and SEE (standard estimation error) between these ten static images and DV image using pixel by pixel methods. Correlation coefficient and SEE value were compared with each other using Wilcoxon test. The $p < 0.01$ was considered as statistically significant.

Results: The mean correlation and SEE in each static image were shown in the table. The static images acquired during 25-30 and 30-35 minutes yielded statistically strongest linear correlation (r=0.956, 0.957). While mean SEE showed the minimum value (628) in the image acquired during 35-40 minutes, there were no significant difference in SEE among the images acquired during 30-35, 35-40, 40-45 and 45-50 minutes. As a result, the optimum image was acquired during 30-35 minutes after tracer injection.

mid scan time (min.)	14	17	22.5	27.5	32.5	37.5	42.5	47.5	52.5	57.5
r (mean)	0.929	0.945	0.951	0.956	0.957	0.950	0.942	0.930	0.914	0.900
SEE (mean)	1002	867	770	686	633	628	635	654	676	688

Conclusions: In our comparative study with dynamic FMZ PET acquisition and multiple arterial blood sampling, one static scan of 30-35 minutes after tracer administration is considered to be a substitute for DV image because of its highest coefficient correlation and lower SEE. This method is simple and reliable for assessing brain benzodiazepine receptor function in clinical setting.

OS_56

CLINIC IMPACT OF SCINTIMAMMOGRAPHY WITH TECHNETIUM-99M MIBI

P. Gomez (1), M.L. Gonzalez (1), R. Garcia (1), I. Borrego (1), J. Lopez (1), R. Alvarez (1), R. Vazquez (1), L. Madrid (2), H. Maravi (2), J. Leon (2). (1) Nuclear Medicine Diagnosis Unity; (2) Surgery of Breast Unity, Seville, Spain.

AIM: The aim of this study is the evaluation of the diagnostic accuracy of scintimammography with technetium-99m MIBI in patients with suspected breast cancer.
METHODS: We have study 120 female patients from December 1998 to March 2001. All patients had a breast nodule detected by palpation or mammography. Aged 28 to 80 years, with a mean of 51.4. All the patients were performed mammography and fine-needle aspiration. Surgery and excisional biopsy were realized when the fine-needle aspiration was positive. Scintigraphy technetium-99m MIBI was realized. Imaging was performed 10 minutes after injection of 20 mCi intravenous in a outlying vein of the inferior extremities. We have obtained 3 planar proyections: one anterior in prone decubitus and two laterals. Using a special bed with two semicircular lateral holes of 15 cm of diameter that allow that breast hang freely. The time of accquisition was 10 minutes. The images were obtained and processed with a SIEMENS ORBITER camera equiped with a work station. The results of scintigraphy were comparated with anatomopatological findings.
RESULTS:
In all over 120 patients the sensitivity was 86%, specificity 89% and accuracy 88%, with a positive predictive value 75% and negative predictive value 94%.

Scintigraphy	Cancer	No Cancer	Total
+	31	10	41
-	5	74	79
Total	36	84	120

We have found 137 lesions. 126/137 (92%) lesions were palpable nodule and 11/137 (8%) were nonpalpable nodule, although they were detected by mamamography. 43/137 lesions corresponding to breast cancer (40 Infiltrating ductal carcinoma and 3 Medullary carcinoma). The tumor size ranged from 0,3 to 7 cm of diameter. All over 137 lesions the sensitivity was 84%, specificity 89% and accuracy 88%, with a positive predictive value 78% and negative predictive value 93%. The smallest detected tumor had a diameter of 1 cm. The tumor size ranged of negative falses from 0,3 to 1 cm of diameter.

Scintigraphy	Cancer	No Cancer	Total
+	36	10	46
-	7	84	91
Total	43	94	137

CONCLUSIONS: The Tc99m-MIBI scintigraphy is an non invasive and simple technique. It has a sensitivity, specificity, accuracy and predictive values adequated for diagnosis of breast carcinoma. This technique, specially in lesions of a size >1 cm, could change theinitial diagnosis of breast positive nodules and theraphy attitude reducing unnnecesary excisional biopsy. For these reasons and because the mamamography have got ratio cost-efectiveness, this diagnosis technique could be introduced in the diagnosis protocol of breast carcinoma.

OS_57

ANALYSIS OF EARLY OUTCOME FOLLOWING BREAST CANCER SURGERY OF PATIENTS INVESTIGATED BY TC-99M SESTAMIBI SCINTIMAMMOGRAPHY

D.M. Howarth (1), S. Sultana (2), D. Clark (3), R. Sillar (4), J. Booker (1), P. Tan (1), A. Smith (2). (1) Pacific Medical Imaging, Newcastle, NSW, Australia; (2) Faculty of Medicine & Health Science, Newcastle University, NSW Australia; (3) Christo Rd. Private Hospital, Newcastle, NSW, Australia; (4) Mater Hospital, Newcastle, NSW, Australia

Pre-operative Tc-99m sestamibi scintimammography (ScMam) may detect unsuspected multifocal or metastatic breast cancer lesions and better estimate the extent of disease, thus aiding breast conservation surgical planning.
Aims: To evaluate the role of ScMam in facilitating the total removal of primary breast cancer by assessing surgical outcome.
Methods: 110 Australian female patients were investigated by ScMam (ScMam group) prior to breast cancer surgery. An age and disease-matched group of 80 patients were selected from the same population that included those who were not investigated by ScMam (non-ScMam group). A comparison of the type of surgical procedure undertaken, the need for repeat operations required to remove all of the primary lesion, occurrence of early and late post-surgical complications and local recurrence/metastatic disease were the study end-points at follow-up ranging from 1 to 5 years (median follow-up: ScMam group 30 months, non-ScMam group 36 months). Prior to surgery all patients from both groups were investigated by x-ray mammography, breast ultrasound and fine needle aspiration biopsy (FNAB).
Results: The respective pre-operative diagnostic sensitivities for ScMam, x-ray mammography, breast ultrasound and FNAB were 91%, 68.5%, 74.7% and 94.3%. Significantly more lumpectomies were performed in the non-ScMam group (39% v 21%, p=0.003) and more partial mastectomies in the ScMam group (12.2% v 1.3%, p=0.006). The ScMam group had more partial mastectomies with axillary clearance (29% v 10%, p<0.003), whereas the non-ScMam group had more lumpectomies with axillary clearance (10% v 1%, p=0.003). The non-ScMam group required significantly more repeat operations to remove primary cancer remaining in the margins of the excised tumour (50% v 28%, p=0.003). This most commonly involved a wider excision procedure (28% v 4%). A greater number of ScMam group patients experienced early transient breast oedema (24% v 10%, p=0.005) but a greater number of the non-ScMam patients experienced chronic lymphoedema of the ipsilateral upper limb (16% v 7%, p=0.006). Within the limits of the early follow-up period, no difference was found in the rates of local recurrence or metastatic disease between the two groups.
Conclusion: ScMam provides valuable pre-operative information that significantly reduces the need for repeat surgery in order to completely remove the primary breast cancer. Furthermore, the reduced need for repeat surgery significantly decreases the likelihood of serious late surgical complications such as lymphoedema.

OS_58

RELATIONSHIP OF METASTATIC SPREAD WITH BLOOD FLOW IN PRIMARY NODULE IN BREAST CANCER, QUANTIFIED BY DYNAMIC 99MTC-MIBI STUDY

W.Y. Ussov (1), J.E. Riannel (1), S. Regoe (2), E.V. Barysheva (1), J. Mihailovic (2), S. Velichko (1), E.M. Slonimskaya (1), L. Stefanovic (2). (1) Tomsk Medical Research Center, Tomsk, Russia; (2) Institute of Oncology, Sremska Kamenica, Yugoslavia.

Aim of the study. It has been widely accepted that metastatic risk is definitively higher in patients with active angiogenesis and proliferative activity in primary nodule of breast cancer (BC). We have evaluated quantitative dynamic mammascintigraphy (MS) data focusing on how uptake of ^{99m}Tc-MIBI in primary nodule of breast cancer relates to presence of metastases in lymph nodes and also peripheral ones.
Material and methods. 156 ladies with breast cancer of $T_{1-3}N_{0-2}M_{0-1}$ stages were studied using routine ^{99m}Tc-MIBI (570-740 MBq) MS protocol comprising dynamic uptake (in 71) planar multiprojection study and chest SPECT with subsequent attenuation-corrected reconstruction.
BC/background and BC/Myocardium count ratios, BC node diameter, and BC blood flow were analyzed. BC blood flow (BCBF) was calculated from dynamic ^{99m}Tc-MIBI uptake data using Gjedde-Rutland-Patlak approach, as BCBF = K/E, where E is extraction fraction, K is transport constant, calculated from equation $BC/C_h = K*(\int C_h\,dt)/C_h + V_0$. BC is radioactivity in breast cancer, C_h-blood concentration of ^{99m}Tc-MIBI. Multifactor discriminant analysis of scintigraphic indices was performed in attempt to separate patients with distant metastases in sub-, supraclavicular or parasternal lymph nodes, parenchymal organs or bones revealed by methods others than MS from pts with no definitive metastatic involvement larger than N_1.
Results. We have not revealed definitive predictive role for metastatic spread for factors others than breast cancer blood flow and BC/Myocardium ratio. All patients with BC/Myocardium ratio over 0.24 did have distant metastases. Existance of distant metastases was also predicted by BCBF higher than 16 ml/min/100 cm^3. No any factor definitively predicted absence of metastases.
Conclusion. Hence, we conclude blood flow in primary nodule of breast cancer over 16 ml/min/100cm^3 coincides with presence of distant metastases of BC. Mammascintigraphy with ^{99m}Tc-MIBI, both as dynamic or static mutiplanar study can be useful for detection of patients with distant metastatic spread.

OS_59

COMPARISON OF 99MTC-MIBI PLANAR SCINTIMAMMOGRAPHY, SPECT AND GD-ENHANCED MRI IN DIAGNOSIS OF PRIMARY TUMOR AND LYMPHATIC METASTASES IN BREAST CANCER

W.Y. Ussov (1), J.E. Riannel (1), E.M. Slonimskaya (1), V.A. Dmitrichenko (2), S.G. Kutuzov (2). (1) Tomsk Medical Research Center, Tomsk, Russia; (2) Institute of Medical Engineering, Moscow, Russia.

Aim of the study. Although scintimammography (SM) with ^{99m}Tc-MIBI has been accepted as efficient technique for primary detection and follow-up of breast cancer, it hasn't been cleared out, whether SPECT provides additional value to planar SM. Thus we aimed to compare the diagnostic power of planar SM with those of SPECT in breast cancer and also with results of Gd-DTPA enhanced MRI carried out with low-field scanner.

Material and methods. 148 ladies with breast cancer of $T_{1-4}N_{0-2}M_{0-1}$ stages were referred for the study. SM and SPECT were performed with single-head camera (high-resolution collimator) immediately after injection of ^{99m}Tc-MIBI (540MBq). SPECT comprised 64 projections in 64x64 matrix over anterior haemicircle with subsequent attenuation-corrected reconstruction.

Results. Methods were as effective for tumor detection as shown below:

Planar SM, SPECTand MRI in diagnosis of primary tumor of various stages

Sensitivity	Primary tumor of breast cancer		
%	Planar SM	SPECT SM	Gd-enhanced MRI
T1	75.0	86.4	83
T2	96.4	97.1	98
T3	97.8	100	100
T4	100	100	100

Planar SM, SPECT and Gd-enhanced MRI in detection of axillary metastases, as compared to diagnosis of primary tumor.

Diagnostic indices, %	Primary tumor		Metastases			
	Plan.SM	SPECT	MRI	Plan.SM	SPECT	MRI
Sensitivity	95.0	95.9	95,4	62.1	81.6	67,8
Specificity	92.5	84.5	87,5	95.4	96.6	59,5
Diagnostic accuracy 93.6	90.1	91,3	84.7	91.1	62,9	

Conclusion. We propose the ^{99m}Tc-MIBI SPECT, although inferior to planary SM in specificity, is the most sensitive tool in diagnosis of primary tumors of T1-stage as well as of metastatic involvement of axillary lymph nodes of groups I- III. Gd-enhanced MRI does not top SPECT in any aspect.

OS_60

COMPARATIVE DATA OF MR-MAMMOGRAPHY, WHOLE-BODY PET AND SCINTIGRAPHY FOR STAGING AND PROGNOSIS OF THERAPY IN PATIENTS WITH BREAST CANCER

Y.U. Soukhov, N. Fadeev, L. Korytova, A. Arzumanov, N. Arzumanova, N. Kostenikov, T. Khazova, D. Ryjkova. Central Research Institute of Roentgenology and Radiology, St Petersburg, Russia.

PURPOSE: To compare diagnostical value of PET with 18-F-FDG, MR-mammography and mammoscintigraphy in primary breast cancer (BC) patients.

Materials: MRI, scintigraphy and PET studies were performed in 79 BC patients. Whole-body PET-scanning started 1 hr after i.v. injection of 370-500 MBq, 99mTc-MIBI in 3 projections. Planar scintigraphy was performed 10 min p.i. of 370 MBq of 99mTc-MIBI in 3 projections. The count density, measured within a region of interest, was divided by the one, measured in ipsilateral and/or contralateral area. This value represents coefficient of tracer uptake (in SUV). MR-mammography included assessment of T1 and T2 weighted images with the use of FLASH-mode and Gd-enhancement.

Results: Statistically significant correlation coefficients (tumor/background) were observed for evaluated regions of increased uptake of radiopharmaceuticals in primary lesions: MIBI > 1.61+/-0.27, FDG > 1.72+/-0.21. These data were concordant with MR findings of primary breast tumor lesions. In all cases $p<0.001$. Regional lymph nodes involvement was assumed in cases of axillary region uptake > 1.50+/-0.22 for both PET and scintigraphy. Only FDG-PET was responsible for parasternal lymph nodes detection.

Conclusion: Significant and strong correlation exists between results of MRI-mammography, mammoscintigraphy and FDG-PET in assessment of primary BC. While mammoscintigraphy and especially FDG-PET are considered as the best tools for evaluating of regional lymph nodes that enable the staging and adequate planning of radiation and chemotherapy.

OS_61

WHOLE-BODY 18F-FDG PET IN PATIENTS WITH SUSPECTED RECURRENCE OF BREAST CANCER

F. Lomeña, M. Simo, J. Setoain, G. Perez, J.M. Costansa, I. Carrio. CETIR, PET Center, Barcelona, Spain.

Objectives: The purpose of the study was to retrospectively investigate the performance of whole body ^{18}F-FDG studies in the detection of tumor relapse in patients with breast cancer and suspected recurrence after interval free of disease.

Methods: Twenty-three consecutive patients underwent whole-body ^{18}F- FDG PET (370 MBq: CPET ADAC) after 6-8 hours fast. All patients had suspected recurrence based on elevated tumor marker levels and /or inconclusive X-ray, CT or MR examinations, after interval free of disease. PET results were confirmed by surgical resection or clinical and radiological follow-up.

Results: PET detected tumor recurrence in 14/23 (61%) patients. Lesions detected: 2 local recurrences, 6 regional lymph nodes, 9 bone, 2 liver, 4 lung and 1 soft tissue recurrence. One false negative was observed in a bone lesion and one false positive was observed in the mediastinum After a follow-up period of 6-12 months, all patients with suspected recurrence and negative ^{18}F- FDG PET remained asymptomatic and without demonstrable recurrence.

Conclusion: Whole-body FDG examinations detect recurrence in ~ 60% of patients with breast cancer and suspected recurrence, indicating that ^{18}F- FDG PET may play a central role in the management of these patients (EUREKA FIT0700002000693).

OS_62

DOES IMMUNOSCINTIGRAPHY ALLOW FOR PROGNOSTIC PREDICTIONS WITH RESPECT TO THE TOXICITY AND THERAPEUTIC EFFICACY OF HERCEPTIN IMMUNOTHERAPY OF METASTATIC BREAST CANCER ?

T.M. Behr (1), M. Behe (1), C. Angerstein (2), F. Griesinger (3), C.C. Kaufmann (3), B. Wörmann (3), G. Emons (4), W. Becker (2). (1) Dept. of Nuclear Medicine, Philipps-University, Marburg, Germany; (2) Dept. of Nuclear Medicine, Georg-August-University, Göttingen, Germany; (3) Dept. of Hematology-Oncology, Georg-August-University, Göttingen, Germany; (4) Dept. of Gynecology, Georg-August-University, Göttingen, Germany

Aim: Trastuzumab (Herceptin®) is a monoclonal antibody, directed against the c-erbB-2 proto-oncogen product HER2/neu. It has been approved for immunotherapy of HER2/neu+ breast cancer. Cardiotoxicity is its major dose-limiting toxicity. The aim of this pilot study was to determine whether pretherapeutic scanning with radiolabeled trastuzumab may allow for predictions with respect to the toxicity or efficacy of Herceptin®.

Methods: Fifteen patients with metastatic HER2/neu+ breast cancer underwent immunoscintigraphy with ^{111}In-labeled trastuzumab before starting unlabeled Herceptin® therapy. All patients stained 2+-3+ for the HER2/neu receptor; all had bone and liver, some in addition lymph node, lung, and brain metastases. Scanning was performed daily for 7 days after injection of 7 mCi ^{111}In-DTPA-trastuzumab. The first two patients had been studied before with ^{131}I-trastuzumab in a protein dose escalation (1 vs. 10 mg total vs. 2-4 mg/kg body weight). All patients were treated with unlabeled Herceptin® and followed for at least 6-12 months.

Results: Optimal tumor targeting was seen at 2-4 mg/kg body weight; lower amounts led to a rapid hepatic clearance of the conjugate. ^{131}I-trastuzumab showed initially good, but over time decreasing uptake in known tumor manifestations (and concomitantly increasing thyroid uptake), whereas ^{111}In-trastuzumab displayed significantly better, constantly increasing tumor/non-tumor ratios. Eight patients with good tumor uptake responded to subsequent Herceptin® therapy, whereas 7 patients with only low uptake were non-responders. On the other hand, only 4/15 patients showed myocardial uptake; 3 of them subsequently developed cardiomyopathy, whereas in the 11 patients without myocardial uptake, no cardiac side-effects occurred.

Conclusion: These preliminary data suggest that residualizing (e.g., radiometal) labels are preferrable over radioiodine, probably due to the internalizing properties of this MAb. Pretherapeutic scanning may allow for diagnostic predictions with respect to the therapeutic efficacy and cardiotoxicity of Herceptin® treatment.

OS_63

99MTC-MIBI UPTAKE IS REDUCED IN BCL-2 OVEREXPRESSING MCF-7 BREAST CANCER CELLS

L. Aloj (1), S. Del Vecchio (1), A. Zannetti (1), C. Caracò (1), M. Salvatore (2). (1) CNR-Centro Medicina Nucleare; (2) Università Napoli. Italy.

An association between lack of 99mTc-MIBI uptake in tumors and poor treatment response has been consistently reported. It is also well documented that 99mTc-MIBI accumulates within mitochondria and that apoptosis is regulated by Bcl-2 family members at the level of mitochondrial membrane. In particular, overexpression of Bcl-2 anti-apoptotic protein prevents cells to enter apoptosis and correlates with relative resistance to chemotherapy drugs and radiation therapy. Therefore, we hypothesized that 99mTc-MIBI accumulation within mitochondria may be affected by the overexpression of Bcl-2 protein.

Aim. To test this hypothesis, 99mTc-MIBI uptake was determined in Bcl-2 overexpressing clones obtained by stable transfection of MCF-7 breast cancer cells.

Methods. The full coding sequence of human bcl-2 gene, under the control of a strong viral promoter, was introduced in MCF-7 cells using lipofectin. Stable transfectants were selected in the presence of neomycin analog, G-418 and individual clones were isolated and characterized. The expression of Bcl-2 in transfected clones was assessed by RT-PCR and Western blotting analysis. The effect of bcl-2 overexpression on Staurosporine-induced apoptosis was assessed in mock and transfected cells by DNA laddering on agarose gel electrophoresis. 99mTc-MIBI uptake was determined by incubating $1x10^6$ counts with mock and transfected cells in multiwell plates for 1 h at 37°C. After several washes in cold PBS, cells were lysed in 1M NaOH, the whole lysates were counted and the activity specifically associated to cells was expressed as the percentage of total added radioactivity per mg of protein.

Results. Nine G418 resistant clones were obtained and two of them showed increased levels of the Bcl-2 protein. Staurosporine treatment caused DNA laddering in control cells within 2 hours whereas no evidence of DNA fragmentation was observed in Bcl-2 overexpressing clones up to 4.5 hours. A dramatic decrease of 99mTc-MIBI uptake was observed in Bcl-2 tranfectants as compared to mock transfected and wild-type MCF-7 cells. Specific 99mTc-MIBI uptake normalized for protein content in Bcl-2 overexpressing clones was only 10 % that of control cells. 99mTc-MIBI uptake was promptly and partially restored by Staurosporine treatment which counteracts the effect of Bcl-2 by inducing permeabilization of mitochondrial membrane.

Conclusion. 99mTc-MIBI uptake is dramatically reduced by overexpression of Bcl-2 in MCF-7 cells. These findings indicate that lack of initial 99mTc-MIBI uptake in untreated malignant tumors may be caused by high levels of Bcl-2 thus identifying patients with an altered control of apoptosis and poor response to subsequent chemotherapy and radiation therapy.

OS_65

IMPROPER CENSORING OF FOLLOW-UP DATA IS COMMON AND RESULTS IN SIGNIFICANT BIAS IN STUDIES ON THE PROGNOSTIC VALUE OF MYOCARDIAL PERFUSION SCINTIGRAPHY

J.J.J. Borm (1), Y.G.C.J. America (1), E.E. van der Wall (2), E.K.J. Pauwels (1). (1) Nuclear Medicine; (2) Cardiology, LUMC, Leiden, The Netherlands.

Aim: To assess the extent and severity of not censoring follow-up data in studies on the prognostic value of myocardial perfusion scintigraphy [MPS].

Methods: -1- Structured review of a representative sample from published original articles. -2- Direct comparison of correctly censored follow-up data with uncensored raw follow-up data from the same clinical study. Endpoint was all-cause-death.

Results: -1- Studies on the prognostic value of MPS were selected from the MEDLINE databases. Studies were selected if they met predetermined quality criteria, including follow-up exceeding 90 days, homogenous patient group, uniform acquisition and processing. Of the 44 remaining publications, 9 failed to specify the recruitment period, 8 failed to state whether consecutive patients were studied, 7 used different acquisition techniques in a single cohort. Four were excluded for other reasons. Of the remaining 16 publications none tested for bias due to incomplete follow-up, 13 reported survival data over a time period where follow-up was grossly incomplete. None clearly stated whether censoring was used. Criteria for completeness of follow-up were not defined in any study and in most it seemed as if a minimum duration of follow-up was used as sole criterium, although such was never clearly stated. Truncation of follow-up data at a census date was never reported.

-2- Follow-up data was obtained from an ongoing study in 1268 consecutive patients. Recruitment started August 1995 and ended April 1998. A snapshot of the study-database, taken on March 15th 2000 was used for analysis. The official census data was April 1st 1999. Theoretically, 2772 patient-years of follow-up should have been obtained at the census date, versus 3785 on March 15th 2000. Actual follow-up was obtained for 2633 and 2990 patient-year respectively. So follow-up was 95% versus 79% complete. Relative risk for death abnormal versus normal MPS were 2.50 versus 2.89. Inproper censoring resulted in a bias of 16% for all-cause-death. This implies an overestimation of the risk for cardiac death by between 30% and 50%.

Conclusions: Improper censoring is a major source of bias in studies on the prognostic value of myocardial perfusion scintigraphy. It is commonly present in literature and it has a major effect on risk estimates.

CARDIOVASCULAR

OS_64

FAILURE TO PREVENT EXERCISE-SPET ISCHEMIA, IN CORONARY ARTERY DISEASE TREATED MEDICALLY BY BETA-BLOCKERS, LEADS TO A DELAYED BUT DRAMATIC WORSENING OF OUTCOME

C. Mercenier (1), N. Hassan (1), P. Olivier (1), P.Y. Marie (1), M.H. Laurens (1), A. Grentzinger (2), F. Zannad (2), N. Danchin (3), G. Karcher (1), A. Bertrand (1). (1) Department of Nuclear Medicine, CHU-Nancy, France; (2) Department of Cardiology, CHU-Nancy, France; (3) Department of Cardiology, Georges Pompidou European Hospital, Paris, France.

Aim. Beta-blockers are strong anti-ischaemic medications, able to improve the prognosis of patients with coronary artery disease. The aim of this study was to determine whether this beneficial prognostic effect might be decreased when beta-blockers fail to prevent exercise SPECT ischaemia.

Methods. We included 442 patients (59±11 years, 44 women) who had a proven history of coronary artery disease, who were treated medically by beta-blockers and referred to exercise Tl-201 SPET under their daily-life medications.

Results. Exercise ischaemia was documented in 190 patients (43%) and necrotic ("non viable") areas in 119 (27%). During a 4.0±1.7 years of follow-up, 32 patients died, 19 had non-fatal myocardial infarction and only 48 stopped their beta-blocking treatment.

Kaplan-Meyer survival curves were equivalent in patients with and in those without exercise SPET ischemia up to the end of the 2nd year of follow-up but became dramatically divergent afterwards. The respective survival rates were: at 2 years: 98±1% and 96±2%, at 4 years: 95±1% and 87±3%, and at 6 years: 92±3% and 81±5%. The best independent predictors of death were: extended necrotic area (> 30% of the left ventricle; $p < 0.001$) and exercise-SPET ischemia ($p < 0.001$). Patients free of both ischemia and extended necrosis, only had a 1.0±0.7% annual mortality rate.

Conclusion. The long-term survival of patients with coronary artery disease treated medically by beta-blockers is very high when they are free of both extended myocardial infarction and residual exercise-SPET ischemia on treatment. Surprisingly, the worsening in outcome related to residual ischemia appeared to be delayed, starting only after a 2-year "quiet" period.

OS_66

ENHANCED PROGNOSTIC STRATIFICATION OF CAD PATIENTS WITH THE USE OF STRESS AND REST TC99M-TETROFOSMIN MYOCARDIAL PERFUSION GATED-SPECT

A. Bestetti, C. Di Leo, M. Musarra, A. Triulzi, L. Tagliabue, G.L. Tarolo. Department of Nuclear Medicine, University of Milan, Milan, Italy.

Background: Sharir et al have recently shown that the addition of post-stress LFEF and end-systolic volume by Gated SPECT has incremental prognostic value compared with perfusion indexes in predicting fatal events. **The aim** of this study was to evaluate whether the change between post-stress and rest functional parameters, measured by Gated-SPECT, has incremental prognostic value compared with perfusion parameters in predicting cardiac events.

Methods: We studied 605 consecutive patients who underwent conventional diagnostic two-day stress/rest gated SPECT, thirty minutes after injection of 925 MBq of 99mTc-tetrofosmin, using a dual head SPECT camera. Of these 107 (84 M) were followed up for a mean period of 23 ± 9.6 months. Sixty-four of 107 (60%) patients had a history or ECG evidence of previous myocardial infarction and forty three (40%) had undergone surgical revascularization procedures. During the follow up, 20 events (2 cardiac deaths, 2 nonfatal myocardial infarction, 16 revascularization procedures) occurred for a 10% annual event rate. Perfusion was analyzed on ungated images using 20 segments scored on a 5-point scale (0=normal, 4=no uptake), while wall thickening was assessed visually on stress/rest end-systolic images using a 4-point score (0=normal, 3=absence of WT). LVEF and volumes were calculated using an automatic algorithm. The post-stress and rest ratio were determined for both end-diastolic (EDV) and end-systolic volume (ESV), while the post-stress LVEF change (d-LVEF) was calculated according to the following formula: (Stress LVEF-rest LVEF)/ rest LVEF*100.

Results: all the post–stress perfusion and functional parameters were more compromised in patients with cardiac events compared with patients without events, but only the post-stress/rest ESV ratio and d-LVEF reached the statistical significance (1.37 vs. 1.07; p=0.012; -8.2% vs. –4.2%; p=0.05 respectively). Cox proportional hazards analysis demonstrated that after adjusting for post-stress and rest perfusion scores and for post-stress LVEF and volumes, post-stress/rest ESV ratio added significantly prognostic information in predicting cardiac events (p=0.01). A post-stress ESV ratio > 1.12 was an optimal threshold, yielding moderate sensitivity and good specificity in the prediction of cardiac events (ROC analysis).

Conclusions: The addition of gating to routine post-stress and rest myocardial perfusion SPECT provides clinically useful risk stratification, being inexpensive, both in regard to cost and time. Post-stress ESV dilation has incremental prognostic value compared with perfusion and function indexes in predicting cardiac events.

OS_67

PARADOXICAL SEPTAL MOTION EVALUATED BY G-SPECT

P. Rossini, S. Canclini, A. Terzi, C. Pizzocaro, U. Pajoro, B. Panarotto, B. Paghera, R. Giubbini. Nuclear Medicine, Spedali Civili di Brescia, Italy.

Paradoxical septal wall motion (SWM) in pts with no previous myocardial infarct (MI) may be an artifact due to exaggerated cardiac mobility after pericardiotomy. Several techniques evaluating LV RWM (RWM) are poorly reliable for the assessment of SWM after CABG. GSPECT with perfusion tracers allows simultaneous 3-D evaluation of RWM, count-based regional wall thickening (RWT) and perfusion. After CABG a true paradoxical movement in pts with previous or perioperative anterior MI should present paradox RWM and compromised RWT in territories with perfusion defects, while pseudo-paradoxical movement should maintain normal RWT and perfusion. 56 CABG pts, 26 pts with previous anterior MI (PAMI) and 30 pts with no history of PAMI (NOPAMI) underwent rest Tc99m-Sestamibi GSPECT, according to the standard QGS protocol. Quantitative EF (%), perfusion (% of Max), RWM (mm), RWT (% increase of diastolic value) and RWT normalized to perfusion were determined using a 20 segment model. PAMI and NOPAMI pts with similar RWM impairment present significant differences both in perfusion and in normalized RWT.

	Regional EF (%)	Perfusion (%)	Wall Thick. (%)	Wall motion (mm)	Normalized Wall Thick. (%)
PAMI	2.5 ± 3	42 ± 13	29 ± 10	0.4 ± 11	12 ± 1
NOPAMI	2 ± 5	56 ± 6	30 ± 10	0.4 ± 11	16 ± 0.5
p Value	n.s.	< 0.0001	n.s.	n.s.	< 0.0001

GSPECT can identify pseudo from true paradox SWM in pts with previous CABG. It might be the method of choice for evaluating LV performance after CABG.

OS_68

THE PROGNOSTIC VALUE OF TETROFOSMIN PERFUSION SCINTIGRAPHY IN PATIENTS WITH DE NOVO CHEST PAIN

J.J.J. Borm (1), Y.G.C.J. America (1), E.E. van der Wall (2), E.K.J. Pauwels (1). (1) Nuclear Medicine; (2) Cardiology, LUMC, Leiden, The Netherlands.

Aim: To asses the prognostic value of tetrofosmin myocardial perfusion scintigraphy [MPS] in symptomatic patients with de novo chest pain.

Methods: Follow-up study in consecutive patients undergoing routine MPS. Inclusion criteria: Symptomatic patients. No history of coronary artery disease CAD [previous revascularization, myocardial infarction [MI] or 50% stenosis on previous coronary angiography]. Cardioverter-defibrillator candidates were excluded. Recruitment from August 1995 until April 1998. Census date for follow-up was April 1st 1999. Analysis by means of Cox regression analysis. Endpoints: death; myocardial infarction, ECG-documented ventricular fibrillation; revascularization.

Results: 576 out of 1269 patients were included. Patient characteristics: age 60 ± 12 y; male 50%; average 1.8 riskfactors. Follow-up: Average censored follow-up of survivors was 2.2 y [maximum 3.7 y]. Endpoints: 33 dead; 8 hard events; 39 revascularizations. The non-survivors died after mean of 1.2 y [range 25 d - 3.3 y]. Normal perfusion in 376 subjects; reversible defects in 84 and irreversible defects in 116.

Clinical risk factors in uni-variate analysis for survival:age [relative risk [RR] 1.086 per year]; gender [RR 1.9 males]; diabetes [RR 3.0]. Step-wise survival analysis, with clinical data in block 1 and perfusion data added in block 2, found: (Block 1) Age [RR 1.09/y] and gender [RR 1.5/MI] [total chi-square 23.2, P < 0.00005] (Block 2) inferolateral segment [reversible: RR 6.1, irreversible RR 6.8], antero-lateral segment [reversible RR 10.7], global perfusion [any reversibility: RR 2.1, only irreversible: RR 0.33] [change from block 1, chi-square 27.7, P 0.0001]. Total chi-square of the full model was 81.8 [P << 0.00005]. Similar results were obtained for hard-event-free survival. Using the full model 90% of the subjects was classified as at low risk [3-year survival 96%] versus 10% at high risk [3-year survival 80%], resulting in a net relative risk of 5 versus 3.5 for clinical data alone.

Conclusions: tetrofosmin perfusion scintigraphy has incremental prognostic value in subjects with de novo anginal complaints.

OS_69

LEFT VENTRICULAR EJECTION FRACTION AND INFARCT SIZE DURING ACUTE MYOCARDIAL INFARCTION AND AFTER TWO MONTHS FOLLOW-UP BY GATED-SPECT

P. Pajoro (1), P. Rossini (1), A. Terzi (1), C. Pizzocaro (1), S. Canclini (1), B. Panarotto (1), B. Paghera (1), C. Cuccia (2), M. Panteghini (3), R. Giubbini (1). (1) Nuclear Medicine; (2) Cardiology Dpt; (3) Clinical Pathology Dpt. Spedali Civili di Brescia, Italy.

Sestamibi Gated SPECT offers the possibility of simultaneous evaluation of perfusion and LV function, thus allowing the determination of rest EF and defect size (DSZ) in acute phase of MI. 21 pts (17M, 4F) were prospectively evaluated within 48 h from hospital admission for acute MI and after 2 months follow-up. EF was calculated according to the QGS protocol. DSZ was measured as a percentage of LV surface below the normal range of our normal data base. 7 pts were treated by primary angioplasty, 7 by systemic trombolysis and 7 by conventional therapy. DSZ decreased in 19/21 pts, from 14%±9% to 6%±6% (p<.001) and EF improved in 18/21 from 44%±12% to 51%±12% (p<.001). A correlation was found between EF and DSZ both in the acute phase (y = -0,4743x + 34,81; R2 = 0,3435) and at 2 months follow-up. (y = -0,3252x + 22,385 R2 = 0,4534). The correlation between early and late EF was: y = 0,8247x + 14,966; R2 = 0,6658, and between early and late DSZ was: y = 0,3396x + 0,983 R2 = 0,3167. In conclusion, a significant decrease in defect size is commonly observed at two months follow-up after acute MI in comparison to the acute phase. All pts with a DSZ < 15%, had a DSZ <8% at 2 months follow-up, whereas 7/11 pts with a DSZ > 15% in post acute phase had a DSZ >8% at follow-up. The DSZ is correlated to EF impairment both in the acute phase, and at late control. The post-acute DSZ overestimates the infarct size, but the DSZ at two months can be predicted in early imaging.

OS_70

RADIONUCLIDE MONITORING OF CARDIAC RESPONSE TO TACHYCARDIA INDUCED BY TRANS-OESOPHAGEAL AND DUAL CHAMBER PACING IN PATIENTS WITH HEART FAILURE

A. Ferro (1), M. Santomauro (2), C. Duilio (2), A. Cuocolo (1). (1) Department of Biomorphological and Functional Sciences; (2) Department of Cardiology, University Federico II, Napoli, Italy.

A comparison between pacing tachycardia induced by a normal (trans-oesophageal atrial pacing) and abnormal (DDD pacemaker) electric activation of the ventricles in patients with heart failure has not yet been reported. The present study was undertaken to assess the effects on left ventricular (LV) function with increasing in heart rate (HR) by these different pacing modes in patients with heart failure.

Methods: 15 patients (11 men and 4 women) with heart failure (LV ejection fraction 33 ± 7%) were enrolled: 7 patients had atrio-ventricular sequential pacemaker (DDD) implanted for complete heart block (group 1) and 8 patients were in sinus rhythm without any conduction defect (group 2). In this latter group an electric-catheter was placed within oesophagus to perform atrial pacing during the study. In all patients, LV function was continuously monitored by radionuclide system (Vest) under resting conditions and during two stages of pacing tachycardia: baseline HR plus 20 (intermediate level) and plus 40 (high level) beats/min. Each stage was maintained for 6 min.

Results: in group 1, LV ejection fraction decreased (p<.05) from baseline 35±3% to 26±4% at intermediate level of pacing and to 22±6% at high level, as consequence of slightly changes in end-diastolic volume and a significant (p<.05) increase in end-systolic volume in both stages of pacing tachycardia. Similarly, in group 2, LV ejection fraction reduced (p<.05) from baseline 32±9% to 24±10% at intermediate level of pacing and to 22±7% at high level, as consequence of reduction in end-diastolic volume and increase in end-systolic volume (both p<.05). In both groups of patients, cardiac output and peak filling rate showed slightly and not significant changes. No difference between the two groups of patients in all parameters considered was observed.

Conclusions: in patients with heart failure, tachycardia induced by atrio-ventricular pacing (group 1) has a negative effect on LV function. The same negative effect was also found in patients with heart failure when tachycardia was induced by a normal electric activation of the ventricles, such as trans-oesophageal atrial pacing (group 2). This suggests that HR *per se* plays a relevant role in determining our results and casts doubt on the possible advantages of biventricular pacing mode in patients with heart failure.

OS_71

PROGNOSTIC VALUE OF EXERCISE SESTAMIBI CARDIAC TOMOGRAPHY IN SYMPTOMATIC AND SYMPTOM-FREE PATIENTS AFTER PERCUTANEOUS TRANSLUMINAL CORONARY ANGIOPLASTY

W. Acampa (1), M. Petretta (2), L. Florimonte (1), A. Mattera (1), A. Cuocolo (1). (1) Department of Biomorphological and Functional Sciences; (2) Institute of Internal Medicine, Cardiology and Heart Surgery, University Federico II, Napoli, Italy.

The role of myocardial perfusion imaging in evaluating risk in patients who have had percutaneous transluminal coronary angioplasty is still unclear. This study was designed to assess the role of technetium-99m (Tc-99m) sestamibi single-photon emission computed tomography (SPECT) in calculating risk in symptomatic and symptom-free patients who have had percutaneous transluminal coronary angioplasty.

Methods: Analysis was based on 128 consecutive patients (107 men and 21 women, mean age 56 ± 9 years) undergoing symptom-limited exercise-rest sestamibi SPECT after percutaneous transluminal coronary angioplasty. Sestamibi perfusion variables were analyzed to determine their prognostic impact during 4 years of follow-up.

Results: During the follow-up there were 13 cardiac events: myocardial infarction in 7 patients, revascularization procedures in 4 patients and cardiac death in 2 patients. Reversible perfusion defects at SPECT were observed in 9 (69%) of 13 patients with events during the follow-up. Of the 115 patients without events, 92 (80%) did not have reversible defects at SPECT. A significant difference between the presence and the absence of ischemia at SPECT imaging was observed between patients with and without events (chi-square 15.0, $p < 0.0001$). The total extent of ischemia was higher in patients with events as compared to those without events (1.9 ± 1.7 and 0.47 ± 1.1, respectively, $p < 0.0001$). At Cox univariate analysis, the presence of ischemia at SPECT was associated with a major risk of cardiac events (relative risk 9.2, 95% CI 2.8 - 30.4, $p < 0.001$). At multivariate analysis, the total extent of ischemia was the strongest predictor of events (relative risk 1.65, 95% CI 1.2 - 2.2, $p < 0.001$). Finally, the incidence of events was significantly higher in the presence of ischemia at SPECT imaging in both symptomatic ($p < 0.01$) and symptom-free patients ($p < 0.05$).

Conclusion: The results of this study demonstrated that exercise sestamibi myocardial perfusion imaging provides significant prognostic information in predicting major cardiac events in both symptomatic and symptom-free patients after percutaneous transluminal coronary angioplasty.

RADIONUCLIDE THERAPY/ DOSIMETRY

OS_72

ZEVALINTM RADIOIMMUNOTHERAPY VERSUS A STANDARD REGIMEN OF RITUXIMAB IMMUNOTHERAPY FOR B-CELL NHL

D. Lamonica (1), B. Leigh (2), G. Wiseman (3), W. Erwin (4), D. Podoloff, N. Bartlett, J. Parker, S. Spies (4), T. Witzig (3), C. White (2). (1) Nuclear Medicine Section, Roswell Park Cancer Institute, Buffalo, NY, USA; (2) IDEC Pharmaceuticals Co., San Diego, CA, USA; (3) Nuclear Medicine Division, Mayo Clinic, Rochester, MN, USA; (4) Robert H. Lurie Cancer Center, Northwestern University, Chicago, IL, USA

Aims: Zevalin is an anti-CD20 murine monoclonal antibody (ibritumomab) conjugated to an MX-DTPA linker (tiuxetan) that securely chelates Yttrium-90 (^{90}Y) for therapy of B-cell non-Hodgkin's lymphoma. In a phase III randomized controlled trial Zevalin was compared with a standard course therapy of Rituxan™ (rituximab) in 143 patients with relapsed or refractory low-grade, follicular, or CD20+ transformed B-cell NHL.

Methods: The Zevalin regimen included rituximab 250 mg/m2 followed by 5mCi Indium-111 (^{111}In) labeled Zevalin for imaging/dosimetry. Therapy was performed with a second, Day 8 injection of rituximab 250/mg/m2 followed by 0.4 mCi/kg ^{90}Y Zevalin. Control arm patients received a standard course of 4 weekly doses of rituximab (375mg/m2). Patients were classified by histology to IWF A (including small lymphocytic, lymphoplasmacytic, monocytoid B, and MALT); follicular; or transformed lymphoma. Patient characteristics and baseline entry criteria in the two study arms were similar. There was no statistical difference between the Zevalin and rituximab groups in median age (60 vs. 57); disease stage (III/IV: 89% vs. 91%); tumor bulk; splenomegaly; extranodal disease; bone-marrow involvement; elevation of serum LDH (19% vs. 14%); median prior therapy regimens and resistance to last chemotherapy. IPI risk grouping and measures of baseline performance status and quality of life (FACT-G) were also similar.

Results: Overall response rate (ORR) based on International Workshop NHL Response Criteria was 80% in the Zevalin arm vs. 56% in the rituximab arm ($p=0.002$) with 30% CR (Zevalin) vs. 16% CR (rituximab) ($p =0.04$) and 4% CRu in each arm. Kaplan-Meier estimates of response duration are not statistically different at 14.2+ and 12.1+ mos. Median time to next anti-cancer therapy has not been reached for Zevalin at 32 mos. Integrated adverse events in those receiving Zevalin therapy were primarily hematologic and of brief duration. Twenty-eight percent of patients developed Gr. 4 neutropenia and 8% Gr. 4 thrombocytopenia. The median number of days below 1000 neutrophils/mm^3 was 10 for the entire population and 26 for those with grade 3 or 4 neutropenia. The median number of days below 50,000 plateletes/mm^3 was 16 for the entire population and 22 for those with grade 3 or 4 thrombocytopenia. Five patients (7%) were hospitalized for infection.

Conclusion: Zevalin radioimmunotherapy appears safe and effective. A statistically significant improvement in objective response rates is achieved with Zevalin radioimmunotherapy compared to therapy with rituximab alone.

OS_73

PRELIMINARY RESULTS OF A MULTICENTER DOSIMETRY, EFFICACY AND SAFETY STUDY WITH IODINE-131 TOSITUMOMAB IN TREATMENT OF NON-HODGKIN'S LYMPHOMA (NHL)

L. Kostakoglu (1), S.J. Goldsmith (1), F. Buchegger (2), V. Lewington (3), J.P. Leonard (1), T. Illidge (3), N. Ketterer (2), T. Kovacsovics (2), N. Valente (4), A. Bischof-Delaloye (2). (1) New York Presbyterian Weill Cornell Medical Center, New York, USA; (2) University Hospital of Lausanne And Geneva, Sz; (3) Royal South Hants Hospital, Southampton, UK; (4) Corixa Corp.,South San Francisco, USA

Iodine-131 (I-131) labeled tositumomab (Bexxar™), a IgG2a monoclonal antibody directed against the CD20 antigen, is safe and effective for low-grade and transformed low-grade NHL. The aim of this study is to evaluate its efficacy in large number of patients in a multicenter expanded access trial.

Methods: As of March 2000, 359 patients with relapsed/refractory low-grade or transformed low-grade NHL received Bexxar™ in a multicenter trial carried out at 53 centers. The study group consisted of 79% low-grade, 20% transformed low-grade, 1% intermediate-grade NHL (Median age: 58 years). Patients received dosimetric dose followed 7-14 days later by a therapeutic dose. The dosimetric dose consisted of 450mg of unlabeled tositumomab infused over an hour and then 5 mCi I-131-tositumomab. Whole body counts were obtained at 3 times over the next week to determine total body residence time to calculate mCi of I-131-tositumomab to deliver a total body dose of 65 or 75cGy.

Results: Two hundred and seventy three patients were evaluable for response. Eighty-nine percent had Stage III or IV disease, 55% had elevated LDH, 43% had bulky disease (≥5 cm), 45% had bone marrow involvement. Median number of prior chemotherapies was 2 (range: 1-10). Twenty-one percent received ≥4 chemotherapies and 79% received 1-3 chemotherapies. The radioactivity administered ranged from 44 mCi to 244 mCi (median: 80 mCi). The residence times ranged from 43 to 166 hrs (median: 98 hrs). The overall response rate was 58%; 27% had a complete response. The median duration of response and complete response have not been reached with 17-month follow-up. High tumor burden, elevated LDH and ≥4 chemotherapy were associated with lower response rates (See Table). The most common toxicity was reversible hematologic toxicity; median ANC nadir 1300 cells/mm^3, median platelet nadir 68,000 cells/mm^3. Thirty-two percent of patients developed grade 3 or 4 hematologic toxicity. Hematologic toxicity was observed in patients with bone marrow involvement or greater number of prior chemotherapies ($p<0.05$). Eight percent of patients developed HAMA and 7% had elevated TSH levels.

Conclusions: This multicenter expanded access trial demonstrates that Bexxar™ provides a safe and effective therapy modality for low-grade and transformed low-grade NHL with a high response rate.

	OVERALL RESPONSE	COMPLETE RESPONSE
PRIOR CHEMO		
1-3 chemotherapy	61%	29%
≥4 chemotherapy	44% (p: 0.044)	17% (p: 0.090)
ELEVATED LDH		
Low/Normal	70%	36%
Elevated	50% (p: 0.003)	20% (p: 0.007)
TUMOR DIAMETER		
< 5 cm	66%	35%
≥5 cm	47% (p: 0.003)	17% (p: 0.001)

OS_74

HIGH-DOSE RADIOIMMUNOTHERAPY OF MANTLE CELL LYMPHOMA WITH THE I-131-LABELED CHIMERIC ANTI-CD20 ANTIBODY C2B8 AND AUTOLOGOUS STEM CELL SUPPORT

T.M. Behr (1), F. Griesinger (2), J. Riggert (3), M. Behe (1), S. Gratz (1), G. Brittinger (2), W. Becker (4). (1) Dept. of Nuclear Medicine, Philipps-University, Marburg, Germany; (2) Dept. of Hematology-Oncology, Georg-August-University, Göttingen, Germany; (3) Dept. of Transfusion Medicine, Georg-August-University, Göttingen, Germany; (4) Dept. of Nuclear Medicine, Georg-August-University, Göttingen, Germany

Aim: CD20 has been used as target molecule for low-dose as well as high-dose, myeloablative RIT of B-cell NHL. MCL is an especially aggressive, prognostically unfavorable form of B-cell NHL. Recent evidence has failed to show convincing therapeutic efficacy of non-myeloablative RIT in MCL. The aim of this pilot study was to investigate whether high-dose, myeloablative RIT with the ^{131}I-labeled chimeric anti-CD20 antibody C2B8 (rituxan, Mabthera®, Roche) may be therapeutically effective in MCL.

Methods: A total of seven patients with chemorefractory or relapsed mantle cell lymphoma were studied so far (all of them having relapsed after high-dose chemotherapy, four of them combined with 12 Gy TBI). A diagnostic-dosimetric study was performed with 10 mCi of ^{131}I-C2B8 at a protein dose of 2.5 mg/kg. In case of splenic pooling, the protein dose was doubled in additional diagnostic scans until a more "favorable" biodistribution was obtained. Therapy was performed with myeloablative activties of 261-495 mCi of ^{131}I-C2B8 at the previously optimized protein dose, aiming at lung doses of ≤ 27 Gy. Stem cells were re-infused at whole-body activities ≤ 15-20 mCi. Clinical follow-up was obtained for up to 38 months.

Results: Overall, in 6 patients the 2.5 mg/kg protein dose was used, whereas in one patient with splenomegaly, 10 mg/kg were necessary to overcome the splenic antigenic sink. All patients re-engrafted at 7-10 days after stem cell reinfusion. Non-hematologic toxicity was restricted to mild to moderate nausea, fever, transient bilirubine or liver enzyme elevations. Despite thyroid blocking, 5/7 patients developed hypothyroidism, requiring thyroxine substitution at 6-18 months after RIT. 6 patients experienced complete and one a partial remission. 5 patients are still in CR, and 6 are still alive for up to 38 months; one patient relapsed locally at 3 months, one systemically at 26 months after RIT.

Conclusions: High-dose RIT with ^{131}I-labeled anti-CD20 antibodies seems to be associated with a high response rate at moderate toxicity in patients with MCL. Further prospective clinical studies are indicated.

OS_75

RADIOIMMUNOTHERAPY (RIT) FOR NON-HODGKIN'S LYMPHOMA. PRELIMINARY RESULTS USING I-131 LABELLED ANTI-CD-20 ANTIBODY (TOSITUMOMAB) IN 47 PATIENTS AT TWO YEARS POST-THERAPY.

H. Jan (1), K. .E. Britton (1), A. Davies (3), R. Sobnack (1), R.R. Foley (1), R. Barlow (1), S.J. Mather (2), D. Ellison (2), A.Z. Rohatiner (3), T.A. Lister (3). (1) Department of Nuclear Medicine, St. Bartholomew's Hospital; (2) ICRF; (3) Department of Medical Oncology, London, UK.

Aim: Non-Hodgkin's lymphoma becomes increasingly resistant to chemotherapy over time. Non-chemotherapeutic modalities are being investigated for their ability to induce durable remissions in patients with recurrent disease, especially in patients with resistant disease or those with short-lived responses.

Methods: 47 Patients with follicular lymphoma, majority had stage III and IV at therapy time received 131- I labelled monoclonal antibody (MoAb) anti CD-20 (Tositumomab) . The desired therapeutic dose is calculated using the total body residence time calculated from the tracer infusion (185 MBq I-131 MoAb) prior to therapy, which is designed to give a whole body dose of 75 cGy. A non-labelled MoAb was administered before tracer and therapy doses to to improve biodistribution and to saturates the Fc receptors of RES to minimise non-specific binding to normal tissues. All had HAMA test before and after therapy. The time between tracer and therapy dose was one week. The side effects were skin rash, infection, nausea, cough, constipation, headache, one GI bleeding and fever. All patients recover by week 7-9 from the side effects.

Results: At two years, 13% had complete remission, 32% partial remission, 51% progressive disease and 4% had steady disease.

Conclusion: RIT is an effective and easy therapy for Non Hodgkin's Lymphoma, it can be used as first line or in combination with chemotherapy.

OS_76

I-131 TOSITUMOMAB(BEXXAR) IN PATIENTS (PTS.) WHO FAILED THERAPY WITH RITUXAMB

A. Podoloff (1), A. Younas (1), S. Horning (2), M. Goris (2), J. Lucas (2), S. Kroll (3), J. Anderson (3), J. Vinay (4). (1) U.T. M. D. Anderson Cancer Center, Department of Nuclear Medicine, Houston, Texas, USA; (2) Stanford Univ., Palo Alto, CA ; (3) Corixa Corp., San Francisco, CA, USA; (4) Baylor College of Medicine, Dallas, TX, USA

We conducted a Phase II trial to assess the safety parameters, the overall response rate and duration of response in pts. with progressive non-Hodgkin's lymphoma after Rituxamb. Methods: 40 CD20 positive pts. with a diagnosis of follicular (grade 1 or 2,) small lymphocytic, denovo follicular grade 3 or transformed histologies who progressed after or failed to respond to Rituxamab were entered. All had bi-dimensionally measurably disease, KPS of > 60, age > 18 and written informed consent. Pts. were treated with a previously described protocol including SSKI, thyroid protection followed by 450 mg of anti-B1 antibody (unlabeled) and 5 mCi of I-131 labeled anti-B1 antibody (35 mg) for pretherapy dosimetry. Candidates were then treated with 450 mg of unlabeled anti-B1 (450mg) followed by I-131 labeled anti-B1 calculated to deliver 75 cGy or 65 cGy if the platelets were less than 150,000. Assessment of response occurred at week 7 and 13, 6 months and biannually. Median age of 57 (range 35-78.) The median time since diagnosis was 53 months (range 11-170 months.) Twenty-nine pts. had 4 or more therapies (70%.) Twelve had bone marrow involvement, 11 had disease > 7 cm, 20 had disease > 5 cm. B-2 microglobulin > 3 in 9. The response rate to Rituxamb was compared to that Tositumomab.

Results: Twenty-three/40 (58%) responded completely (CR) or partially (PR). Eight (20%) had a CR. Overall, consensus response rate was 70%. Consensus CR was 40% (N=16.) The duration of response was 15.4 months in the 23 responding pts. (95% CI 7.4 months-not reached). There is a trend in the 23 responders suggesting prolonged time to progression (not statistically significant). Overall response in the pts.who failed Rituxamab 67%, response 0-6 months 67%, response > 6 months 100%. Consensus CR in Rituxamab failed pts. 25, 50 and 100%. There was a significant difference in the response in pts. having a β-2 microglobulin of <3 from those >3.

Conclusion: We conclude that I-131 Tositumomab (Bexxar) has significant activity in indolent and transformed lymphoma that progressed after Rituxamb. The major adverse effect is reversible myelotoxicity. Tositumomab (Bexxar) appears to be effective in pts. with no or brief response to Rituxamb, (median duration of response 15.4 months).

OS_77

RADIOIMMUNOTHERAPY (RIT) OF NON-HODGKIN'S LYMPHOMA (NHL) WITH I-131 ANTI-CD20 MONOCLONAL ANTIBODY (BEXXAR™). PRELIMINARY RESULTS

C. Antonescu (1), F. Buchegger (1), M. Kosinski (1), N. Ketterer (2), T. Kovacsovics (2), C. Helg (3), A. Bischof Delaloye (1). (1) Service de Médecine Nucléaire, University Hospital Lausanne, Switzerland; (2) Centre Pluridisciplinaire d'Oncologie, University Hospital Lausanne, Switzerland; (3) Département de Médecine, University Hospital Geneva, Switzerland.

Aim: We present preliminary results of our first patients treated with labelled and non labelled anti-CD20 Mab for low grade or transformed low-grade NHL.

Methods: 11 patients (5F and 6M; aged 49.2±11.6y), with histologically proven low-grade or transformed low-grade NHL (7 stage IV and 4 stage III), were treated. All were HAMA negative, 8 had no, 3 <25 bone marrow % infiltration, . After a dosimetric phase, aimed to calculate the activity to be administered to deliver a total body dose of 75 cGy (65cGy if platelet 100-149 G/L), by the means of sequential whole body scans, a patient-specific therapeutic dose of I-131 labelled anti-CD20 (35 mg, 2921±621 MBq) was infused immediately after administration of unlabelled Bexxar™ (450 mg). Thyroid was blocked by KI (2x100mg/d) starting the day before dosimetry until 14 days after therapy. 1h before Mab infusion patients received 500mg paracetamol and 2mg clemastine to prevent major infusion reactions. Follow-up included periodical clinical examination, evaluation of blood cell counts, hepatic, renal and thyroid function, HAMA, CT-SCAN and bone marrow analysis (if infiltrated before therapy).

Results: 8 patients could be evaluated (3 were treated recently): 4 patients achieved a complete response (CR), none of them relapsed during an observation period of 3-18 months (m). 3 patients showed a good partial response (PR), 2 ongoing (3-9 m), one relapsed after 9 m. In one patient tumour progressed despite RIT. Acute side effects were generally minor (mild fever in 3, joint pain in 2, rash in 1 patient). Haematological toxicity was the most common side effect: 4 patients (3 CR) experienced grade IV thrombocytopenia, 2 with grade IV neutropenia, (nadir 5-9 weeks), that normalised after 10 weeks in 2 patients. 1 patient reached pre-treatment values of granulocytes and platelets only after 6 and 9 months, respectively. The fourth patient with progressive disease, needed cytokine support. Minor recurrent ENT and lung infections were observed in 3 patients, 1 became HAMA positive.

Conclusions: RIT using non-myeloablative doses of Bexxar™ (tositumomab and iodine I 131 tositumomab) for the treatment of CD-20 expressing low-grade and transformed low-grade NHL showed an objective response in 7/8 evaluated patients with 4 CR still ongoing (3-18 m). The only significant toxicity was haematological with uncomplicated grade IV thrombocytopenia and neutropenia in 4 and 2 patients, respectively.

OS_78

SEQUENTIAL ADMINISTRATION OF CHEMOTHERAPY FOLLOWED BY RADIOIMMUNOTHERAPY WITH IODINE-131-TOSITUMOMAB IN UNTREATED NON-HODGKIN'S LYMPHOMA (NHL)

L. Kostakoglu (1), S.J. Goldsmith (1), S. Vallabhajosula (1), M. Coleman (1), A. Morris (2), B.K. Link (3), M.S. Kaminski (4), K. Nadeau (2), N. Valente (2), J.P. Leonard (1). (1) New York Presbyterian Hospital Weill Cornell Medical Center, NY; (2) Corixa Corp, CA, USA; (3) University of Iowa Cancer Center, IA, USA; (4) University of Michigan Cancer Center, II, USA

Patients with relapsed or refractory NHL have limited therapeutic options. Iodine-131-Tositumomab (Bexxar™), a monoclonal antibody directed against the CD20 antigen, is effective in treatment of low-grade and transformed low-grade NHL. We have conducted a phase II clinical trial to assess the efficacy of sequential administration of chemotherapy followed by Bexxar™ in the initial treatment of NHL.

Methods: Forty-seven patients (median age: 48 years) with NHL were studied (44 low-grade NHL, 3 intermediate grade). All patients received combination therapy consisted of chemotherapy followed by Bexxar™ , with regimens including Fludarabine + Bexxar™:35 pts, CVP (Cyclophosphamide/Vincristine/Prednisone) + Bexxar™: 9 pts, CHOP (CVP with Doxorubicin) + Bexxar™: 3 pts. Bexxar™ therapy was administered within 6-8 weeks following the last cycle of chemotherapy. Patients received dosimetric dose followed 7-14 days later by a therapeutic dose. Whole body counts were obtained at 3 times over the next week to determine total body residence time to calculate mCi of I-131-tositumomab to deliver a total body dose of 65 or 75cGy.

Results: All patients to date have shown clinical response to combination therapy, and these are the results of the safety data on the combined modality approach. The most common toxicity was reversible hematologic toxicity; median ANC nadir 774 cells/mm^3 (range: 30-3812), median platelet nadir 57,000 cells/mm^3 (range: 4,000-126,000). Three patients (6%) developed an ANC < 100 cells/mm^3 and one patient (2%) developed a platelet count < 10,000 cells/mm^3. Ten patients required transfusional support, and 7 patients received hematopoietic growth factors. Non-hematologic toxicity was consistent with that observed with chemotherapy and radioimmunotherapy in other settings. Assessments for HAMA (Human Anti-Mouse Antibody) are currently underway in the full population of patients.

Conclusions: Bexxar™ can be safely administered in sequential combination after chemotherapy. The patient-optimized dosimetry method (based on individual whole body clearance) utilized with Bexxar™ may be particularly important in regimens combining chemotherapy and radioimmunotherapy in order to predict and minimize dose toxicity.

OS_79

BIODISTRIBUTION AND INDIVIDUAL DOSIMETRY OF I-131-LABELED RITUXIMAB IN RELAPSED NON-HODGKIN'S LYMPHOMA

K. Scheidhauer (1), I. Wolf (1), C. von Schilling (1), B. Schmidt (2), H. Baumgartl (1), G. Reidel (1), C. Peschel (2), M. Schwaiger (1). (1) Nuklearmedizin, Klinikum r. d. Isar; (2) III. Med. Klinik, TU Munich, Germany.

An individual dosimetry as basis for radioimmunotherapy of NHL is disputed, as the in-vivo distribution of radiolabeled antibodies results often in low contrast scans: delineation of organs can be difficult and pretherapeutic determination of organ and tumor activity may lead to arbitrary results. Thus aim of this study was to determine biodistribution of ^{131}I-labeled Rituximab in patients before radioimmunotherapy and to evaluate these data for reliability and plausibility.

Methods: 17 patients with relapsed NHL underwent dosimetric studies using 15-20 mg Rituximab labeled with 180-370 MBq ^{131}I. Biodistribution was determined by serial conjugated gamma camera whole body scans including ROI-technique for organ delineation, whole body probe measurements, and serial blood and urine samples up to 144 hrs p.i. Activities for therapy were calculated using the MIRDOSE 3 program for an escalating whole body dose of 50 to 65 cGy.

Results: Whole body activity showed a monoexponential decay with a half life of 40 to 110 hrs, plasma activity a biexponential decay. Tumor half lives were slightly longer than those of whole body and organs. Activity was excreted solely by kidneys, proven by urine measurements. Organ activities (mean values, 1 hr p.i.: heart 8.9%, liver 9.2%, lungs 9.5%, kidneys 3.0%) corresponded well with theoretically expected activities derived from standard organ and blood volumes and individual hematocrit values (heart 6.9%, liver 6.0%, lungs 9.8%, kidneys 4.0%). Thus, measured organ activities seem to reflect simply blood pool activity. This is further confirmed by the observation, that ratios of organ-to-whole body activity decreased over time. In contrast to this, measurable tumor masses (40 to 320 ml) showed kinetics with increasing ratios of tumor-to-whole body activity as an evidence of specific tumor binding, resulting in calculated tumor doses of 7 to 21 Gy.

Conclusions: Conjugated whole body scans together with probe measurements are suitable to provide meaningful data for dosimetry, at least in its mean value. Those dose estimates may be adequate in non-myeloablative models, as therapeutic doses are not relevant regarding organ toxicity except bone marrow. However, due to a high individual variability this may lead to an overestimation of organ doses in a myeloablative model - resulting in less applicable activity than possible - or to an underestimation with unintentional organ radiotoxicity. Therefore in myeloablative models a more exact individual dosimetry seems to be necessary as rationale for radioimmunotherapy.

ENDOCRINOLOGY

OS_80

99MTC-DTPA VERSUS MRI FOR THE ESTIMATION OF DISEASE ACTIVITY IN GRAVE'S OPHTALMOPATHY: A COMPERATIVE STUDY

L. Galuska (1), L. Galuska (1), F. Szûcs (2), E. Nagy (3), I. Garai (1), J. Szabó (3), J. Varga (1), E. Varga (3), E. Balázs (3), A. Leövey (3). (1) Department of Nuclear Medicine; (2) Department of Radiology; (3) First Department of Internal Medicine, University of Debrecen, Hungary.

Aim: In Graves' ophthalmopathy (GO), the retrobulbar inflammatory activity (RIA) needs immunosuppressive treatment, while the same therapy is useless and may cause side effects in patients with inactive disease. Of the currently used methods, clinical RIA activity scores are inaccurate, and MRI T2 relaxation time estimation and the more specific somatostatin-receptor antagonist (octreotide) scans are expensive. Our aim was to introduce a simple, cost effective method to quantitate RIA using 99mTc-DTPA.

Methods: Fifteen GO patients with asymmetric clinical eye manifestation (aged 34-56, m.v. 47 ± 8 years) were studied with both 99mTc-DTPA and MRI within two weeks. The control group consisted of five patients with no symptoms of GO. T2 relaxation time measurements were performed on the extraocular muscles, and to each involved muscle with T2 relaxation time over 70 ms, 1 score point has been assigned. The MRI severity score for a given orbit was the sum of the involved muscles, i.e. it could be 0 to 4 . Using 400-500 MBq 99m Tc DTPA intravenously, after 15 minutes a SPECT with 127 frame acquisisons was performed with a four headed Nucline X ring SPECT (MEDISO, Hungary) system. Three of the transaxial slices of the ocular region were selected and summed up in a triangle-like ROI, which contained projections of all extraocular muscles (RBROI). An identical ROI of the temporal lobe area of the brain (BROI) was selected too, and the RB/B count ratios were calculated . MR scores and RB/ B values were compared using the two sample t-test. In addition, one patient was investigated with 111In-Octreotide (Octreoscan), and Apex Helix double-headed SPECT images were also taken.

Results:

		RB/B ratio		
		Left	Right	
Controls	(n=5)	2,16+-0,42	2,26+-0,48	
MR score=0	(n=10)	2,81+-0,72	2,76+-0,45	
MR score=1-3	(n=5)	3,21+-0,68	4,04+-0,59*	*p=0,0035.

Both RB/B ratios and visual inspection helped to identify orbits with ongoing RIA activity. Disease activity was identifiably on both the 111In-Octerotide and 99mTc-DTPA images. The double headed and four headed SPECTs yielded similar images.

Conclusions: Our preliminary results suggest that RB/B values of 99mTc-DTPA retrobulbar SPECT identify disease activity in the orbits of patients with GO. Further studies are warranted to clarify if 99mTcDTPA can really become a cost effective substitute for MRI and/or octreotid imaging in the diagnosis and follow up of disease activity in GO patients.

OS_81

IMAGE FUSION AS A TOOL FOR THE IDENTIFICATION OF PERI- AND RETROORBITAL TARGETS (ANTIGENS) RELATED TO GRAVES' OPHTHALMOPATHY BASED ON CT AND 99MTC-HYNIC-TOC

R. Moncayo (1), R. Bale (2), I. Baldissera (3), R.A. Sweeny (4), C. Bacher Stier (1), C. Decristoforo (1), K. Seydl (1), M. Gabriel (1), E. Donnemiller (1). (1) Dept. of Nuclear Medicine; (2) Dept. of Radiology; (3) Dept. of Ophthalmology; (4) Dept. of Radiation Therapy, University of Innsbruck, Austria

Aim: Imaging procedures using OctreoScan have been helpful in differentiating active from inactive thyroid eye disease in Graves' hyperthyroidism (Thyroid 1997; 7:21-29). Nuclear Medicine imaging alone can suggest a peri- and retro-ocular distribution of the tracer, however a clear relation between tracer uptake and the underlying anatomy has not been achieved yet. The aim of this investigation was to evaluate a newly developed somatostatin analog tracer in the characterisation of putative antigenic targets of thyroid eye disease based on image fusion with CT.

Methods: A series of 9 patients attending the University Clinic in Innsbruck were investigated with the newly developed ^{99m}Tc-HYNIC-TOC tracer – TOC- (Eur.J.Nucl.Med. 2000; 27: 1318-1325). A conventional CT examination without contrast media was conducted 2-3 days before or after the scan. A patented reference frame (SIP Lab Innsbruck Frame) with the respective image modality-specific external markers in precisely defined positions was used for each imaging modality. This frame is securely connected to the VBH vacuum-mouthpiece, which allows identical repositioning of the frame with respect to the head (Comput.Aided Surg. 1997; 2:286-291). All studies were converted to DICOM format and transferred to the processing work station (Immerge, Sofamore-Danek, Inc). Image analysis was done using the CT images as a reference (grey color scale). Visual analysis was done by switching SPECT images on/off on a rainbow color scale.

Results: Succesful image fusion could be achieved in 7/8 patients. In one case image re-alignment failed due to a loosely fitting dental prothesis causing a shift of the head frame. Physiological proof of a "good fit" was the exact localisation of the pituitary within the sella which also permitted to set the adequate threshold. In acute exophthalmos cases TOC uptake was localised to the eye muscles and to the retrobulbar space. In both acute as well as in chronic eye disease the most common structure being recognised was the lacrimal gland. An additional strong uptake was seen in the nasopharyngeal region.

Conclusions: Our tracer has the capability to detect putative target structures located to the orbital space in active Graves' disease: eye muscles, retroorbital space, lacrimal gland and nasopharynx. TOC uptake could be explained by somatostatin receptor expression on the membrane of activated lymphocytes localized to the involved structures. We hypothesize that therapeutic measures based on somatostatin analogs will be targeting immune reactions localised in these organs.

OS_82

CORTICOSTEROIDS PREVENT AN INCREASE OF TRAB AND TPOAB IN PATIENTS WITH GRAVES DISEASE UNDERGOING RADIOIODINE THERAPY

S. Massoudi, W. Brenner, S. Brandt, E. Henze. Clinic of Nuclear Medicine, Christian-Albrechts-University, Kiel, Germany.

The aim of this study was to evaluate the course of TSH-Receptor-Antibodies (TRAb) and Thyroid-Peroxidase-Antibodies (TPOAb) after I-131 therapy in patients with Graves disease with respect to treatment with or without corticosteroids.
Methods: Out of a total of 196 patients with Graves disease undergoing radioiodine treatment with a mean activity of 950 MBq I-131 (400-2000 MBq) we evaluated 30 patients, 4 males and 26 females, aged 37–78 years who received a combination treatment of antithyroid drugs (thionamides) and thyroxine over the whole period of investigation. All patients showed up with normal fT3 and fT4 serum levels at the beginning of the therapy. 11 patients additionally received 50 mg prednisolone initially (group B) while 19 patients served as controls (group A). Serum levels of TSH, TRAb and TPOAb were measured at the beginning, and at 4 and 12 weeks post therapy (p. t.).
Results: In patients of group A prior to therapy the serum levels (median) of TSH, TRAb and TPOAb were 0.02 µU/ml, 13 U/l and 1752 U/ml, respectively. 4 weeks p. t. serum levels were 0.06 µU/ml for TSH, 22 U/l for TRAb and 1327 U/ml for TPOAb and increased significantly at 12 weeks p. t. to 3 µU/ml, 30 U/l and 3000 U/ml ($p < 0.05$ each). In patients of group B however antibody titers decreased ($p < 0.05$) while TSH serum levels showed an increase as observed in group A: TSH 0.04 µU/ml at the beginning, 0.1 µU/ml at 4 weeks, and 3.3 µU/ml at 12 weeks p. t.. The corresponding values for TRAb were 19 U/l, 15 U/l and 6 U/l, for TPOAb 1086 U/ml, 420 U/ml and 522 U/ml. No significant differences could be proven for the TSH serum levels between group A and B at all times of investigation excluding TSH-effects as a reason for the differences observed between the two groups.
Conclusions: In patients without prednisolone treatment the TRAb significantly increased as early as 4 weeks p. t. while TPOAb showed a significant increase after 12 weeks. In contrast to these data a decrease of both TRAb and TPOAb was observed in patients treated with corticosteroids. Thus, measurement of both TRAb and TPOAb clearly reflect the immunosuppressive effects of prednisolone suggesting these antibodies as follow-up parameters for the assessment of the immunological activity in patients with Graves disease.

OS_83

PROSPECTIVE EVALUATION OF PARAMETERS INFLUENCING THE OUTCOME OF 131I-THERAPY OF GRAVES DISEASE AND TOXIC NODULAR GOITER

C.K. Körber, C. Körber, P. Schneider, N. Körber-Hafner, H. Hönscheid, CHR. Reiners. Clinic and Policlinic for Nuclear Medicine University of Würzburg, Germany.

Aim: The parameters influencing the outcome of radioidine therapy are still discussed controversely for Graves«disease (GD) and toxic nodular goiter (TNG). Especially a simultaneous antithyroid medication was postulated to be a decisively negative factor for a successful ^{131}I-therapy. **Method, Activity and Patients:** All patients treated in our therapy ward in 1998 were prospectively studied to investigate the influencing parameters of sex, age, antithyroid medication, dose equivalent of medication, applied radiation dose, emptiness prior to application, achieved dose, effective half-life, target volume, TSH, fT_3 and fT_4-levels on the success rate of radioiodine therapy. For individual pretherapeutic dosimetry a calibrated uptake probe system was used. A test activity of 4-6 MBq ^{131}I (4,9±1,2 MBq, mean ± standard deviation) was administered. Iodine uptake U(t) was measured after 2 hours and at the time t_h of hospitalization (24h-9d). $U(t_h)$ was used to calculate the activity to be administered for therapy. Bockisch proposed to calculate the therapy activity from a single late uptake measurement. An extended formula (formula 2) was applied when t_h was > 3 d.

$$A(MBq) = \frac{F}{2} * \frac{V[ml] * D[Gy]}{U(th[\%] * th[d]}$$

A=activity (MBq ^{131}I), F=constant factor (=25,75), V=target volume (ml), D=target dose (GD 200 Gy, TNG 300 Gy), U=uptake at time t_h (days). Target volume was measured using ultrasound scans with a Siemens Sonoline Elegra Scanner
Results: One hundredandfiftyfour patients treated for Graves«disease and 575 patients with toxic nodular goiter were observed and classified according to their TSH-level 9-12 months after therapy. Students t-test and a multiple regression analysis model were used to quantitate the influence of the parameters on the outcome. We found, that the influene of antithyroid medication was far beyond significance. In the forward stepwise multiple regression analysis model used, only few parameters were found to have a significant influence. The models reached a significance level of p=0.05, but revealed a low overall predictive value for both groups (GD 5%, TNG 2%).

For Graves«disease only the factor target volume (ml) reached significance

	Beta	St. Error of Beta	Partial correlation	p-Level
Target volume	-0,178	0,085	-0,179	0,04

For Toxic nodular goiter applied activity (MBq ^{131}I) showed a significant influence on outcome.

	Beta	St. Error of Beta	Partial correlation	p-Level
Appl. activity	0,157	0,054	0,124	0,004

Conclusion: Thyroid volume is the only significant factor influencing the outcome of radioiodine therapy for GD as delineated by the stepwise multiple regression analysis model used. For TNG the significant factor is the applied activity. The factors investigated revealed only a marginal predicitive value on the posttherapeutic TSH-level.

OS_84

E-SELECTIN, L-SELECTIN, ICAM-1 AND IL-6 CONCENTRATIONS CHANGES IN THE SERUM OF PATIENTS WITH HYPERTHYROIDISM IN THE EARLY PERIOD OF RADIOIODINE I-131 THERAPY

D. Jurgilewicz (1), F. Rogowski (1), A. Citko (1), E. Jaroszewicz (1), U. Lebkowska (2). (1) Department of Nuclear Medicine; (2) Department of Radiology, Medical Academy, Bialystok, Poland.

Among cytokines IL-6, IL-8, E-selectin, L-selectin and ICAM-1 are the most important links in the initiation of the inflammatory process. Taking into account that inflammatory process is the basic stage of the effective radioiodine therapy we tried to compare the behaviour of the initial inflammatory factors in the early period of I-131 therapy of hyperthyroidism.
The aim of the study was to estimate the behaviour of IL-6, ICAM-1, E-selectin and L-selectin concentrations in the serum of patients with hyperthyreoidism before and during I-131 therapy.
Methods: The groups of 26 patients with Graves'-Basedow disease (GB) and 18 patients with toxic nodular goiter (SN), in the age 34-77, were studied. Control group (C) consisted of 10 healthy volunteers.
For estimation of thyroid function serum concentrations of TSH, free T4 and freeT3 were measured by IRMA or RIA kits (Polatom, Poland). IL-6, ICAM-1, E-selectin and L-selectin serum concentrations were determined using ELISA method by Bender kits (USA), respectively. Blood samples for all estimations were taken 10-12 days before and in 6th week after I-131 administration.
Treatment dose of radioiodine was calculated basing on modiefied equation for absorbed dose.
Results: Comparing to control no statisticall difference in the levels of E-selectin (C:44,4±11ng/ml) and L-selectin (C-842±168,9ng/ml) was observed before treatment (GB:E-sel.- 59,8 ±19,6ng/ml; L-sel. -1288,2±273,5ng/ml; SN: E-sel.-61,5±18,4ng/ml, L-sel.-1247,0 ±273,5ng/ml) and in the 6th week after I-131 administration (GB: E-sel.-57,3±19,5ng/ml ,L-sel.- 1142,4 ±193,4ng/ml; SN: E-sel - 62,1±20,6 ng/ml, L-sel. 1113,5±236,3ng/ml) in both groups.
In comparison to control there was no difference in initial IL-6 levels nor in GB neither in SN group, but statistically important decrease was observed in the 6th week after I-131 administration in GB patients (C- 2,07±0,2 ng/ml vs 1,79±0,16ng/ml).
ICAM-1 serum concentrations before treatment were elevated comparing to control group (C-190,2±34,7ng/ml) in both groups (GB-263,6±24,6ng/ml, $p<0,05$; SN-251,4±36,1ng/ml, $p<0,05$). In GB patients statistically significant increase of ICAM-1 was observed in the 6th week (301,1±33,2ng/ml, $p<0,05$) of I-131 therapy wheras in SN group there was no statistical difference comparing to initial values (249,7±42,6ng/ml, N.S.).
Conclusions: We conclude, that ICAM-1 and IL-6 may be important factors in the estimation of the inflammatory processes in the thyroid gland during radioiodine therapy, specially in GB disease. E- and L-selectins seems to be not helpful in the monitoring of the thyroid inflammatory changes during early period of I-131 therapy.

OS_85

A PATIENT-SPECIFIC DOSIMETRIC METHOD FOR THE RADIOIODINE THERAPY OF THE AUTONOMOUS NODULE

R. Matheoud (1), C. Canzi (1,2), E. Reschini (1), F. Zito (1,2), F. Voltini (1,2), R. Lambertini (1), P. Gerundini (1). (1) Nuclear Medicine Department; (2) Health Physics Department, Ospedale Maggiore IRCCS, Milan, Italy.

The radioiodine therapy of the autonomous thyroid nodule (ATN) has been widely used for decades, but it has been shown that the high prevalence of hypothyroidism reported in some series could be caused by the irradiation of the extranodular tissue.

Aim. This work was intended to develop a patient-specific dosimetric method based on Medical Internal Radiation Dosimetry formalism to accurately determine the ^{131}I activity to be administered to patients with ATN to deliver 150 Gy to the nodule and the correspondent dose absorbed by the extranodular tissue.

Methods. Sixteen patients with ATN were given 111 MBq of ^{123}I i.v. and their neck was imaged with a gamma camera at 2, 4, 24, 48, 72 and 120 hours after administration, to evaluate iodine kinetics for nodule and contralateral lobe. The volumes of nodule and contralateral lobe were measured on the 24 hour scintigraphic image. Two simplified methods, the first based on three uptake measurements (2, 24 and 120 hours) only (3-point method) and the second on the 24 hour uptake assuming an effective ^{131}I half-life within the nodule of 5 days ($T_{1/2}$ fixed method), were also examined and compared to the reference method.

Results. The mean ^{131}I activity to administer to the 16 patients was 449 MBq (range 81 – 903) and the mean dose to the contralateral lobe was 22.0 Gy (range 6.1 – 45.0). The precision on ^{131}I activity (depending on the precision on nodule mass, uptake and half-life) was 12% and that on the dose to the contralateral lobe (depending on the precision on activity, contralateral lobe mass, uptake and half-life) was 21%. The percentage differences in ^{131}I activity and in the dose to contralateral lobe between the reference method and the 3-point method ranged between -5.4 and 13.4%, and between -13.3 and 2.4%, respectively. The deviation in ^{131}I activity between the reference method and the $T_{1/2}$ fixed method ranged between -42.6 and 79.5%.

Conclusions. The reference method proved to be precise in the determination of ^{131}I activity to administer to ATN patients and useful in the prevision of the dose received by the contralateral lobe during the therapy. The use of the $T_{1/2}$ fixed method would lead to a considerable misestimation of the ^{131}I activity to administer, due to the great interpatient variability of functional data. The 3-point method is a reliable alternative when the clinical work load of a Nuclear Medicine department is particularly heavy.

OS_87

ABLATIVE RADIOIODINE THERAPY OF GRAVES' DISEASE - WHICH TISSUE-ABSORBED DOSE IS NECESSARY?

M.J. Reinhardt (1), H. Palmedo (1), A. Joe (2), M. Zimmerlin (2), A. Manka-Waluch (1), E. Moser (2), H.J. Biersack (1), T. Krause (1). (1) Dept. of Nuclear Medicine, Univ. Hospital Bonn, Germany; (2) Dept. of Nuclear Medicine, Univ. Hospital Freiburg, Germany.

Aim: Comparison of several tissue-absorbed doses to induce hypothyroidism within one year after radioiodine therapy.

Methods: 120 Graves' disease patients (99 women, 21 men; aged 58±14 yrs., range 29-98 yrs.; thyroid volume 30±19 ml, range 5-98 ml) at 2 centres were included in the study. Activities of 525±240 MBq (185-1110 MBq) were calculated by means of Marinelli's formula to deliver 150 Gy (N=48), 200 Gy (N=34), and 300 Gy (N=38) absorbed doses to the thyroid. The results were compared concerning thyroid metabolism one year after treatment.

Results: One year after treatment, 48 pts. were hypothyroid, 46 were euthyroid and 26 remained hyperthyroid. No significant difference in the frequency of persisting or recurrent hyperthyroidism was found between different target doses (150 Gy: 25 %; 200 Gy: 29 %; 300 Gy: 11 %). Frequency of hypothyroidism ranged from 21 % after 150 Gy to 60 % after 300 Gy absorbed doses ($p < 0.005$, Chi-square test). The therapeutically-achieved target doses did not differ significantly between patients becoming hypothyroid (259 ± 75 Gy), euthyroid (222 ± 79 Gy) or remaining hyperthyroid (213 ± 83 Gy). When analysing several factors which might further influence therapeutic outcome, only thyroid volume showed a significant relationship to the result of treatment. Patients becoming hypothyroid had a significantly smaller pretreatment thyroid volume (20±10 ml, range 5-52 ml) than those becoming euthyroid (37±18 ml, range 8-86 ml) or remaining hyperthyroid (39±21 ml, range 9-98 ml), $p < 0.01$ (Wilcoxon-Mann-Whitney test).

Conclusions: Even an absorbed dose of 300 Gy was found to be „ablative" in only 60 % of patients one year after radioiodine therapy. Especially patients with goiters of more than 50 ml might need higher doses.

OS_86

DOSE-DEPENDENT IN-VIVO OXIDATION INJURY AFTER RADIOIODINE THERAPY

H. Sinzinger (1), M. Rodrigues (1), A. Oguogho (1), U. Resch (1), B. Palumbo (2), R. Palumbo (2). (1) Department of Nuclear Medicine, University of Vienna, Vienna, Austria; (2) Department of Nuclear Medicine, University of Perugia, Perugia, Italy.

Until now, radiation hazards as a consequence of radioiodine therapy are not examined in detail.

We examined the effect of a single radioiodine therapy with 5 (n=8; 46-71a), 10 (n=6; 54-75a), 20 (n=11; 45-73a), 80 (n=6; 37-75a) ur 200 (n=6; 43-67a) mCi on in-vivo oxidation injury in blood (plasma [P], serum [Se]), urine (U) and saliva (Sa) in patients suffering from hyperthyroidism or cancer, respectively. 8-epi-prostaglandin (PG) $F_{2\alpha}$ as a marker of in-vivo oxidation injury (Sa, Se, P, U), oxidation of lipoproteins (LDL, HDL), thromboxane B_2 (Sa, Se, P, U), PGE_2, $PGF_{2\alpha}$ and circulating endothelial cells (CEC) were examined before therapy, daily for 7 days and weekly thereafter for 6 weeks.

There is a dose-dependent increase in 8-epi-$PGF_{2\alpha}$ being most pronounced saliva ($p < 0,01$), reaching a maximum between 2 and 5 days after therapy and showing a continuous decline thereafter. Also in the other compartments a significant short-term increase was seen. CEC show a significant temporary increase too. There is a long-lasting disturbance in PG-metabolism.

These data indicate a significant temporary and dose-dependent endothelial desquamation, oxidation of lipoproteins and long-lasting in-vivo oxidation injury (saliva > urine > blood) as side effect of radioiodine therapy, alltogether potentially being proatherogenic.

OTHER CLINICAL SCIENCE. NEPHRO-UROLOGY

OS_88

SMALL KIDNEY: HOW CAN WE DISTINGUISH BETWEEN NORMAL AND HYPOFUNCTIONING KIDNEY?

V. Camacho, G. Torres, M. Estorch, J.C. Martín, A. Tembl, E. Mena, Y. Aguilar, A. Flotats, A. Catafau, I. Carrió. Department of Nuclear Medicine, Hospital de Sant Pau, Barcelona, Spain.

The quantification of relative renal function based on DMSA uptake in both kidneys is an established method for the assessment of individual renal functionality. The normal range of relative function of each kidney is considered between 45% and 55%. However, when there is a small normal kidney this percentage is decreased, being sometimes difficult to distinguish a small normal kidney from an hypofunctioning kidney.

Aim: To evaluate the relative renal function by means of quantification of renal DMSA uptake corrected for kidney size.

Methods: Three hundred fifty five patients with a mean age of 13 years (range 1 month – 77 years) were explored by DMSA scintigraphy, due to several renal diseases. Relative renal function was quantified using an equation that relates DMSA uptake and renal size. However, relative renal function was quantified without correction for renal size.

Results: In 168 patients (47%) the relative renal DMSA uptake was normal either uncorrected or corrected for renal size, in 121 (34%) it was abnormal by both quantification methods, and in 66 (19%) it was abnormal only by one method. In 57 of them (86%) the relative renal DMSA uptake was abnormal only when uncorrected for renal size, and in 9 of them (14%) it was abnormal only when corrected for renal size (all of these patients presented with bilateral cortical defects). One hundred seventy seven patients (50%) presented with decreased relative DMSA uptake in one kidney, and in 56 occasions it was associated with a small normal kidney. Quantification with correction for renal size showed a normal percentage in all of these 56 patients (100%, $p<0.0005$).

Conclusion: Relative renal DMSA uptake expresses better the individual renal function when is corrected for renal size. When there is a small kidney, relative renal DMSA uptake corrected for renal size can distinguish between normal and hypofunctioning kidney.

OS_89

MONITORING ATN IN THE EARLY KIDNEY TRANSPLANT PERIOD: A PROSPECTIVE STUDY IN 42 PATIENTS, USING A FUNCTIONAL SCINTIGRAPHIC PARAMETER

A.F. El Maghraby (1), H. Boom (2), J.A.J. Camps (3), J.A.K. Blokland (3), A.H. Zwinderman (4), J.W. de Fijter (2), E.K.J. Pauwels (3).
(1) Department of Nuclear Medicine, Leiden University Medical Center, Leiden, The Netherlands and Cairo University, Department of Nuclear Medicine, Cairo, Egypt; (2) Leiden University Medical Center, Department of Nephrology, Leiden, The Netherlands; (3) Leiden University Medical Center, Department of Nuclear Medicine, Leiden, The Netherlands; (4) Leiden University Medical Center, Department of Medical Statistics, Leiden, The Netherlands

Delayed graft function (DGF) is a common complication that may affect up to 50% of cadaveric renal transplants. This clinical disorder is most frequently caused by Acute Tubular Necrosis (ATN). To assess the tubular cells function, we developed a quantitative parameter named Tubular Function Slope (TFS) derived from the upslope of the extraction phase of the ^{99m}Tc-MAG3 renogram. We investigated the TFS in a prospective study, aiming to assess its added value in the early post-transplant period.

Materials and Methods: The TFS proved to be technically applicable and reproducible in a preliminary random study of 28 scans in 10 different patients. Subsequently, a prospective study was designed which included 28 consecutive patients with immediate graft function (IGF) and 14 consecutive patients with DGF

All recipients had ^{99m} Tc-MAG3-renography on the first day after transplantation. Patients experiencing DGF were scanned every other day until function was restored. Recipients experiencing IGF were followed with ^{99m} Tc-MAG3 scan at 1 and 2 weeks after transplantation.

Results: In the IGF group the average TFS values in the initial ^{99m}Tc-MAG3 studies was (1.72±0.83) (Mean ± SD), Whereas, in the DGF group the TFS appeared to be significantly low (0.50 ± 0.29) (P value < 0.001). It showed a significant increase with improvement of the ATN condition and reached the average value of 1.5 ± 0.48 (P value < 0.01) at the time of improvement which was around 20 days after transplantation.

Six patients (40%) of the DGF group showed a complicated prolonged course of ATN. The average TFS in those patients was initially (0.35± 0.12) with stationary or minimal increase in the sequential ^{99m}Tc-MAG3 studies to reach (1.1±0.41). These values were significantly lower than the TFS values for the rest of patients with non-complicated ATN which were for the initial and follow-up ^{99m}Tc-MAG3 (0.85±0.25 and 1.9±0.36) respectively (P value < 0.01).

Conclusion: The observer-independent transplant function slope (TFS) allows the measurements of small changes in tubular cells function. TFS can differentiate between IGF and DGF grafts. More importantly, TFS is able to differentiate between cases of prolonged complicated ATN versus smoothly recovering ATN that is important for the follow up of individual DGF patients.

OS_90

RESULTS OF MYOCARDIAL PERFUSION SCINTIGRAPHY IN DIALYSIS PATIENTS AND THEIR PROGNOSTIC SIGNIFICANCE

J.R. Buscombe, E. Kingdom, S. Holt, J.G. Goghlan, A. Davenport, P. Sweney, A. Burns, A.J.W. Hilson. Royal Free Hospital, London, UK.

Patients on renal replacement therapy have a nine time risk of dying from cardiac disease and may have occult cardiac disease with minimal symptoms. The aim of this study was to review the results of performing myocardial perfusion scintigraphy (MPS) in patients on dialysis and to determine if the results predict cardiovascular outcome.

MPS was performed on 47 asymptomatic patients (25, male, mean age 55, range 21-78) 28 on haemodialysis and 19 on peritoneal dialysis. When compared to coronary angiography with a 50% stenosis as defining stenosis the sensitivity of MPS was 81% with all three false negatives being in triple vessel disease. The specificity of MPS was 45% most of the false positives were reported as having inferior ischaemia or patchy reversible defects consistent with small vessel disease. There was no correlation between a false positive MPS and left ventricular hypertrophy. In the 24 month follow up period 8 patients (17%) had a major cardiac event from which 2 died. MPS was abnormal in 6 of these patients and angiography in 5 of these, (including both of the deaths). None of the patients with triple vessel disease and a negative MPS had a cardiac event.

Assymptomatic patients on renal dialysis are at risk of ischaemic heart disease and cardiac death. Neither MPS or angiography predicts cardiac events with sufficient accuracy to rely on a single test alone

OS_91

INTRAPERITONEAL VOLUME AND LYMPHATIC ABSORPTION USING 125-I-HUMAN SERUM ALBUMIN (SARI-125) IN PERITONEAL DIALYSIS WITH A NEW GLUCOSE POLYMER SOLUTION

A. Carniato (1), G. Amici (2), F. Boccaletto (1), P. Sorce (1), F. Palermo (1). (1) Nuclear Medicine, Treviso Regional Hospital; (2) Nephrology and Dialysis, Treviso Regional Hospital, Treviso, Italy.

The assessment of intraperitoneal volume and lymphatic absorption during peritoneal dialysis is important for the prescription optimization of a new dialysis solution containing glucose polymers. Tracer dilution techniques commonly employ macromolecular substances to avoid peritoneal diffusive processes. We report the first clinical experience about the use of SARI-125 in long intraperitoneal dwells with glucose polymer solution.

Fourteen patients undergoing peritoneal dialysis for chonic kidney failure were studied with a single eight-hour intraperitoneal glucose polymer (Extraneal 7.5%, Baxter Healthcare) solution dwell. SARI-125 0.4 mg, corresponding to 370 kBq (Nycomed-Amersham-Sorin) was diluted into a 2000 ml bag of the solution after a preparation phase with 1 g of cefazolin and 0.4 mg of standard albumin for minimizing infection risk and SARI-125 adhesion to the plastic bag. After the instillation procedure plasma and dialysate samples were taken at 0, 2, 4, 6, 8 hours. The intraperitoneal fluid was completely drained and weighed after 8 hours. Dialysate samples were taken at the preceding and following exchange for residual volume calculation. The activity of the samples was determined by a gammacounter (10 minutes count). Dialysate volumes by tracer dilution were linearly corrected for tracer disappearance due to peritoneal adherence and fluid absorption rate (FAR, ml/min). Plasma tracer appearance was considered representative of the lymphatic absorption rate (LAR, ml/min) through diaphragmatic stomata and thoracic duct.

Drainage at 8 hours was 2304±280 ml, all patients had positive water extraction except two with negative balance (-277 and -288 ml). All intraperitoneal volume curves showed a regular behaviour. FAR was 0.92±0.39 ml/min and LAR was 0.16±0.14 ml/min, the same two patients with negative water balance showed high FAR (1.72 and 1.76 ml/min, respectively) and normal LAR values (0.16 and 0.14 ml/min, respectively). Residual intraperitoneal volume at the end of the test was 77±77 ml. A highly significant inverse correlation was observed between drainage volume and FAR (r=-0.831, p<0.001) and no correlation was found between drainage volume and LAR.

SARI-125 as dilution tracer showed reliable and useful results with the new peritoneal dialysis solution. The contemporary measurement of intraperitoneal volume, FAR and LAR gives important information about individual peritoneal physiology and the test results have been clinically confirmed also in the two non-responder patients.

OS_92

EARLY FUNCTION OF RENAL TRANSPLANTS: COMPARISON BETWEEN LIVING AND CADAVER DONORS

A. Boubaker (1), J. O. Prior (1), V. Bettschardt (2), F. Mosimann (2), G. Halabi (3), J.-P. Wauters (3), A. Bischof Delaloye (1). (1) Department of Nuclear Medicine; (2) Department of Surgery; (3) Department of Nephrology, University Hospital, Lausanne, Switzerland.

In this study we compared renal function in the 5 first days after transplantation for transplants obtained from living (group A) or cadaver (group B) donors.

A total of 125 renographies (47 Tc-99m-MAG, 78 I-123-OIH) performed 1 to 5 days after transplantation were reviewed. Group A consisted of 27 patients (13M, 14F) aged 20 to 69 years (mean : 41±13y) : 17 patients(8M, 9F, aged 20 to 58y) were studied with I-123-OIH, 10 patients (5M, 5F, aged 23 to 69y) with Tc-99m-MAG3. Group B consisted of 98 patients (63M, 35F) aged 16 to 69 years (mean : 47±12y) : 61 patients (40M, 21F, aged 16 to 69y) were studied with I-123-OIH, 37 patients (23M, 14F, aged 24 to 65y) with Tc-99m-MAG3. Renal graft function was measured by an accumulation index (AI) defined as the percentage of tracer extracted by the kidney 30 to 90 seconds after vascular peak activity after background and depth correction.

Renographies were performed 1 to 5 days (mean : 3±1d) after transplantation for both groups. AI obtained with Tc-99m-MAG3 were lower than AI obtained with I-123-OIH in both groups of patients (p<.05). No difference of AI was observed between group A and group B with Tc-99m-MAG3 and I-123-OIH.

	Living donors				Cadaveric donors			
	n	Age (y)	Mean±SD	Range	n	Age (y)	Mean±SD	Range
Tc-99m-MAG3	10	23-69	5.52±2.03	2.57-8.33	35	24-65	5.11±2.17	1.50-10.56
I-123-OIH	17	20-58	7.02±1.90	4.50-12.03	61	16-69	6.46±2.50	1.82-12.37

7 living donors had renographies performed before surgery, 3 were studied with Tc-99m-MAG3, 4 with I-123-OIH. First examination in the receivers were performed with the same tracer. We compared AI of the graft obtained in the donor before nephrectomy with AI measured in the receivers. AI obtained with Tc-99m-MAG3 were lower than AI obtained with I-123-OIH in donors and receivers. AI was lower in the receiver when compared with AI obtained in the donors before nephrectomy.

		Donor		Receiver	
	n	Age (y)	Range	Age (y)	Range
Tc-99m-MAG3	3	44-57	4.28-8.02	15-69	2.57-6.51
I-123-OIH	4	36-67	6.44-11.12	35-50	4.22-6.70

In conclusion, AI obtained with Tc-99m-MAG3 were lower than AI obtained with I-123-OIH in both groups of patients. No difference in AI was observed between the living and cadaver donors. For both tracers, AI measured in donors before nephrectomy was higher than AI obtained in the receivers.

OS_93

TUBULAR FUNCTION SLOPE IN INITIAL 99M-TC-MAG3 RENOGRAPHY AFTER RENAL TRANSPLANTATION PREDICTS LONG TERM GRAFT OUTCOME

A.F. El Maghraby (1), H. Boom (2), J.A.J. Camps (3), J.A.K. Blokland (3), A.H. Zwinderman (4), J.W. de Fijter (2), E.K.J. Pauwels (3).
(1) Department of Nuclear Medicine, Leiden University Medical Center and Department of Nuclear Medicine, Cairo University, Cairo, Egypt ; (2) Department of Nephrology, Leiden University Medical Center, Leiden, The Netherlands; (3) Department of Nuclear Medicine, Leiden University Medical Center, Leiden, The Netherlands; (4) Department of Medical Statistics, Leiden University Medical Center, Leiden, The Netherlands

Many studies found that the impact of Delayed Graft Function (DGF) lies in its effect on graft survival and outcome in the first year. In order to monitor renal tubular function we developed a quantitative parameter named Tubular Function Slope (TFS). In the present study we assessed the relevance of the TFS on the outcome and graft function at 6 months.
Materials and Methods All recipients who received a cadaveric graft from 1998 until 1999 underwent ^{99m}Tc-MAG3 renography on the first day after transplantation. Recipients experiencing DGF were scanned every other day until function was restored and after 1 week, 2 weeks, 3 and 6 months. Recipients experiencing Immediate Graft Function (IGF) were scanned at 1 week, 2 weeks, 3 and 6 months. Initial TFS's were compared with consecutive TFS's and related with renal function.
Results Forty-two patients entered the study. Fourteen grafts experienced DGF and 28 grafts experienced (IGF). The statistical change-point model curves for both IGF and DGF show striking differences both at the initial period and during follow-up (P=0.004) figure 1.
In the IGF group the average TFS values (Mean ± SD) in the initial 99mTc-MAG3 studies were (1.72 ± 0.83), while it was 0.50 ± 0.29 For the DGF group.
The TFS values after 3 and 6 months were (2.8±1.06) and (3.03±1.17) for the IGF group and (1.82±0.61) and (1.86±0.75) for the DGF and were significantly different from each other. The correlation coefficients of basal TFS with TFS values at 6 months were 0.80 in the IGF group, whilst in the DGF group the r-value was 0.90.

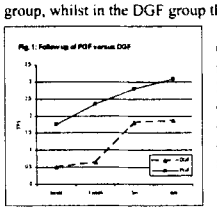

Conclusion In this study we show that with a new sensible marker for tubular function in the ^{99m}Tc-MAG3-renography, DGF influences renal function compared with grafts experiencing immediate graft function and that this difference still exists after 6 months of follow-up. This is consistent with our epidemiological findings that DGF influences graft function and not graft survival

OS_94

COMPARISON OF GLOMERULAR FILTRATION RATE MEASURED BY CAMERA-BASED TC-99M DTPA CLEARANCE WITH PLASMA CLEARANCE OF I-125 IOTHALAMATE

H.R. Balon (1), CYO. Wong (1), O. Lang (2), E. Roff (1), R.A. Ponto (1).
(1) Department of Nuclear Medicine, Wm. Beaumont Hospital, Royal Oak, MI, USA; (2) Department of Nuclear Medicine, Charles University, 3rd School of Medicine, Prague, Czech Republic.

Aim: 1. To compare GFR results obtained by the Gates camera-based method (GCBM) with GFR measured by plasma clearance of I-125 iothalamate (Cl-iothal) as the gold standard, in order to determine if the simpler GCBM is adequate in routine clinical practice. 2. To evaluate the reproducibility of GCBM. 3. To correlate calculated GFR estimate (EstGFR) with Cl-iothal.
Methods: 56 pts (24 M, 32 F), mean age = 70.3 y, (range 42-85), serum creatinine range 71-690 _mol/l, had GFR determined on the same day by Cl-iothal (1.3 MBq iv , 6 plasma samples over 4-6 hrs) and by GCBM (110 MBq Tc-99m DTPA, renal uptake @ 2-3 min). GCBM data were processed independently by 3 technologists using an automated commercially available algorithm. Each pt's EstGFR was calculated from age, weight, creatinine by Cockroft & Gault formula (CGF). Results were analyzed using Pearson correlation and paired t-test.
Results: Multiple-sample Cl-iothal ranged from 5.3 to 130.8 ml/min (mean=57.3), means of GCBM triplicates from 12.2 to 198.2 ml/min (mean=76.9), EstGFR from 7.8 to 100.2 ml/min (mean=50.4). The Gates method yielded significantly higher GFR values than Cl-iothal: mean difference = 19.6 ± 33.6 ml/min ($p<0.0001$ by paired t-test); and significantly higher values than EstGFR (mean difference = 26.5 ± 35.9 ml/min ($p<0.0001$by paired t-test). The mean difference between EstGFR and Cl-iothal was –6.9 ± 11.9 ml/min ($p<0.0001$). There was a positive correlation between Cl-iothal and GCBM (correlation coefficient r = 0.649 [$p<0.0001$]). There was a very strong positive correlation between EstGFR and Cl-iothal (r = 0.924, [$p<0.0001$]), as well as among the 3 technologists for GCBM (r values for technologist 1vs2, 2vs3, 1vs3 were 0.99, 0.993, 0.989, respectively [$p<0.0001$]).
Conclusions: Although the Gates method is highly reproducible based on repeat analysis of the same data acquisition, Gates GFR values are significantly different from the plasma disappearance method. This finding is supported in the literature. As an alternative to multiple-sample Cl-iothal, we propose combining EstGFR and GCBM. When clinically significantly different results are obtained, Cl-iothal should be performed. The day-to-day reproducibility of Gates GFR has to be investigated to determine if this method can be used for serial measurements, when interval change, rather than absolute values may be of clinical interest.

OS_95

TOWARDS OBJECTIVE TIME-ACTIVITY CURVES OF RENAL CORTEX

H. Bergmann (1), C.C. Nimmon (2), K.E. Britton (2), M. Samal (3,4).
(1) Department of Biomed. Eng. and Physics, University of Vienna, Austria; (2) Department of Nuclear Medicine, St. Bartholomew's Hospital, London, UK; (3) Charles University Prague, Czech Republic; (4) L. Boltzmann Institute of Nuclear Medicine, Vienna, Austria

Aim: Time-activity curves of renal cortex can reflect abnormal parenchymal function better than curves from the entire parenchyma or the whole kidney. The problem is to accurately and precisely measure cortical dynamics using a narrow peripheral ROI. The aim of our study was to assess several techniques to obtain more objective cortical time-activity curves.
Methods: Five methods for objective cortical ROI definition were evaluated: (1) thresholding parenchymal factor image, (2) masking parenchymal factor image, (3) subtraction of medullary from parenchymal factor curves, (4) using a peripheral strip of pixels inside the whole-kidney ROI, and (5) using the outer rim of the whole-kidney ROI. In all methods, only the lateral part of the resulting ROI was used to obtain the cortical time-acitivity curve. Curves (1) - (3) were obtained using fuzzy ROIs, (4) - (5) using standard binary ROIs. For each curve, cortical transit time was then calculated using the matrix method and compared with the values obtained by an experienced expert using manually drawn ROIs and optimized deconvolution.
Results: With the exception of (5), all curves (n = 55) produced cortical transit times reflecting loose but statistically significant correlation with the expert's values (0.53, 0.59, 0.63, 0.41, and 0.15). The differences between methods (1) - (4) were not significant. The smallest value of the averaged paired differences between test and expert transit times was obtained with method (3): 3 ± 29 s. All other methods produced transit times 20-40 s shorter than the expert (on average in the range of 170-190 s vs 200-220 s). Cortical fuzzy ROIs appear to perform better than binary ROIs. The problem encountered was very small peripheral pixel values in the cortical fuzzy ROIs. The lack to detect clearer differences between the methods for selection of the ROIs may reflect suboptimal performance of the simple matrix method used for deconvolution.
Conclusions: Objective assessment of cortical dynamics is feasible but will require not only a standardized and reproducible definition of cortical ROIs but also a more robust deconvolution procedure.

OTHER CLINICAL SCIENCE. INFECTION AND INFLAMMATION

OS_96

ACCURACY OF 99MTC-LEUKOCYTE SCINTIGRAPHY IN THE DIAGNOSIS OF POST-STERNOTOMY MEDIASTINITIS RELAPSE

R. Lebtahi (1), C. de Labriolle-Vaylet (2), J.L. Trouillet (3), A. Hitzel (1), F. Harel (1), D. Daou (1), L. Sarda (1), M. Faraggi (1), N. Delahaye (1), C. Gibert (3), D. Le Guludec (1)(1) Department of Nuclear Medicine, Bichat Hospital, Paris, France; (2) Department of Nuclear Medicine, St-Antoine Hospital, Paris, France; (3) Department of Intensive Care Unit, Bichat Hospital, Paris, France.

Aim: A prospective study was performed to evaluate the accuracy of leukocyte scintigraphy for the diagnosis of recurrence of mediastinitis. 33 patients (23 males, mean age 68 ± 7), surgically treated for a first episode complicating cardiac surgery using closed drainage and Redon catheter, were suspected to relapse despite sustained antibiotic therapy.
Methods: The delay between the last sternotomy and scintigraphy was 2-3 weeks. Thoracic planar images were acquired 1 hr, 4 hrs and 24 hrs post injection of 150 MBq of 99mTc-HMPAO-labeled autologous granulocytes. A scan was considered as positive if abnormal uptake was found on 4 and 24 hrs images (or only at 24 hrs images). Final diagnosis was assessed by an additional surgery and/or by histology and bacterial growth on cultures and by a 6 to 9 month clinical and biological follow-up for all but 4 patients who died.
Results: A high vascular background was present on 1-hr images, and the 4 and 24 hrs images were more useful for the detection of infection. One patient was positive only on 24 hrs images. Scintigraphic findings were considered as positive for infection in 20/33 patients. One scan was falsely negative, due to a misinterpretation at the beginning of the study, and a second scan was clearly positive 3 weeks later. One scan was falsely positive in presence of a mild abnormal uptake persistent on 24 hrs images. Finally, results were 19 true positive, 12 true negative patients, 1 false positive and 1 false negative results. Leukocyte scintigraphic results obtained in mediastinitis relapse yielded a sensitivity of 95%, a specificity of 92%.
Conclusion: Leukocyte scintigraphy accurately identifies patients who are relapsing after post-operative mediastinitis. 24hour images are required for accurate interpretation.

■ OTHER CLINICAL SCIENCE. INFECTION AND INFLAMMATION

OS_97

A PILOT STUDY ON INFECTION IMAGING WITH 99MTC-BIOTIN IN PATIENTS WITH PROSTHETIC HIP REPLACEMENT

G. Mariani (1), C. Augeri (1), L. Molfetta (2), M. Chinol (2), B. Nock (4), G. Villa (1), F. Buffoni (1), P. Erba (1), M. Carletto (1), G. Paganelli (3), H.R. Maecke (4)(1) Nuclear Medicine Service, DiMI - University of Genoa, Genoa, Italy; (2) Division of Orthopedics - University of Genoa, Genoa, Italy; (3) Division of Nuclear Medicine, European Institute of Oncology. Milan, Italy; (4) Nuclear Medicine service, University Hospital, Basel, Switzerland

Scintigraphy with radiolabeled autologous leucocytes (WBC) represents the „gold standard" nuclear medicine procedure for imaging infection. However, this procedure is time-consuming, expensive, and involves some biological hazard to both patients (pts) and personnel. Preliminary data obtained during validation of the avidin/111In-biotin approach for imaging infection have suggested some potential of 111In-biotin *per se* to accumulate at sites of infection. In this pilot study we explored the potential of 99mTc-biotin as an infection imaging agent in pts with orthopedic infections.

Methods: N_4-lys-biotin (50 µg in sodium citrate) was labeled with 1110 MBq (30 mCi) of freshly eluted $99mTcO_4^-$ by incubation with 30 µg stannous chloride at pH 10-12 for 1 hr; labeling efficiency was > 95% by TLC analysis. Sixteen pts bearing a total of 20 prosthetic hip replacements were enrolled in the study (9 women and 7 men, mean age 73.2 yr, 64-89 yr). Eight pts had previously undergone removal of their hip prosthesis because of infection, while infection was suspected in the remaining 8 pts. Scintigraphy was recorded 20 min, then 1, 4 and 24 hr after the i.v. injection of 99mTc-biotin. Within 48 hr of the 99mTc-biotin study, all pts also underwent scintigraphy with 99mTc-HMPAO-WBC.

Results: Out of the 20 hips evaluated, 15 turned out to be infected while in the remaining 5 cases pain was only caused by bone-prosthetic loosening and/or conditions other than infection. In 12/15 infected sites scintigraphy was concordantly positive with both 99mTc-biotin and 99mTc-HMPAO-WBC, 99mTc-biotin yielding higher target-to-nontarget ratios than 99mTc-HMPAO-WBC in 4 cases and similar values in the other cases. Discordant patterns were observed in the remaining 3 infected sites, 99mTc-biotin being positive with a negative 99mTc-HMPAO-WBC scan in 2 cases, and the opposite in 1 case. The 99mTc-biotin and 99mTc-HMPAO-WBC scans were concordantly negative in the 5 non-infected sites. Positivity of 99mTc-biotin was obvious already at 4 hr, without any additional information provided by the 24-hr scintigraphy.

Conclusion: The results obtained in this study indicate the high feasibility and the excellent infection imaging properties of 99mTc-biotin scintigraphy in pts with prosthetic joint replacements, thus warranting further clinical validation studies in various conditions of infection/inflammation.

OS_98

99MTC-INTERLEUKIN-8 FOR IMAGING ACUTE OSTEOMYELITIS

S. Gratz, H. Rennen, O. Boerman, W. Oyen, F. Corstens. University Medical Center Nijmegen, Nuclear Medicine, Nijmegen, The Netherlands.

Introduction: Accurate diagnosis of osteomyelitis remains a clinical problem. Various nuclear medicine imaging techniques (e.g. bone scan with ^{99m}Tc-MDP) are sensitive in detecting acute osteomyelitis, but lack in specificity. We evaluated the performance of ^{99m}Tc-IL-8 in an experimental model of acute osteomyelitis. Methods: Acute pyogenic osteomyelitis was induced in 10 rabbits by applicating 0.5 ml of 5% sodium morrhuate and $5x10^6$ cfu (0.5 ml) of Staphylococcus aureus into the medullary cavity of the right femur. A sham operation was performed on the left femur. Ten days after surgery, rabbits were subdivided in two groups of 5 animals and were injected either with 18.5 MBq ^{111}In-granulocytes or 18.5 MBq ^{67}Ga-citrate and imaged both 24 hr p.i. and 48 hr p.i.. On day 12, rabbits received either 18.5 MBq ^{99m}Tc-MDP or 18.5 MBq ^{99m}Tc-IL-8 and for serial images were aquired at 0, 1, 2, 4, 8, 12, 24 hr p.i.. Uptake in the infected femur was determined by drawing regions of interest. Ratios of infected (target)-to-sham (background) (T/B)-operated femur were calculated. After the last images, the rabbits were killed and the right femur was scored for microbiological and histopathological evidence of osteomyelitis. Results: Eight out of ten rabbits developed acute osteomyelitis. The extent of infection was best seen with ^{67}Gallium-citrate and delayed bone scan, whereas diaphyseal photopenia was noted with both ^{99m}Tc-IL-8 and ^{111}In-granulocytes. The uptake in the infected region did significantly differ between ^{67}Ga-citrate (4.9 ± 0.8 %ID (at 48 hr p.i.)) and ^{99m}Tc-MDP (4.7 ± 0.7 %ID) compared with ^{99m}Tc-IL-8 (2.2 ± 0.2 %ID (at 4 hr p.i.)) and ^{111}In-WBC (0.8 ± 0.2 %ID (at 48 hr p.i.)) ($p<0.0042$). In contrast, the ratios of infected-to-sham operated femur (T/B) were significantly higher for ^{99m}Tc-IL-8 (T/B 6.2 ± 0.3 (at 4 hr p.i.)) compared with ^{67}Ga-citrate, ^{99m}Tc-MDP and ^{111}In-WBC with 1.5 ± 0.4, 1.9 ± 0.2 and 1.4 ± 0.1 respectively ($p<0.0001$). Radiography correctly visualized acute osteomyelitis in only two out of eight cases. Conclusions: In the present study, in terms of uptake ^{99m}Tc-IL8 showed comparable imaging results to ^{99m}Tc-MDP and ^{67}Ga-citrate, which were superior to ^{111}In-granulocytes. In terms of T/B (Target to Background) ratios, ^{99m}Tc-IL-8 performed much better than the other imaging agents due to fast background clearence. The ease of preparation, the good image quality and the lower radiation burden suggest that ^{99m}Tc-IL-8 might be a suitable imaging agent for the scintigraphic evaluation of acute osteomyelitis.

OS_99

THE ASSESSMENT OF DIAGNOSTIC VALUE OF 99MTC INFECTON BY MEANS OF WHOLE-BODY SCANS IN PATIENTS WITH BONE AND JOINT DISEASES

W.A. Mielcarek (1), E. Dziuk (1), I. Drabek (1), M. Baranski (2), M. Marciniak (3), J. Pietrzykowski (1). (1) Centre of Nuclear Medicine ; (2) Septic Department of the Institute of Traumatic Surgery, Orthopaedy and Neurosurgery; (3) Department of Radiobiology and Radiation Protection, Military Institute of Hygiene and Epidemiology, Warshaw, Poland.

The radiolabelled with 99mTc ciprofloxacin (Infecton) offers simply method to image the sites of infection.

Aim of the study. The evaluation of diagnostic utility of the new radiopharmaceutical Infecton.

Material. The study includes 21 consecutive patients (females – 9, males 12, aged 18 –76 yrs, mean age 50 yrs) investigated for presence of the sites of infection.

Method. 23 whole-body scans (WBS) were performed at 1 hr and 4 hrs and sometimes 24 hrs p.i. using double headed gamma camera Varicam equipped with LFOV low-energy collimators. The spot view of chosen regions of the body were also performed.

Results. Rapid paper chromatography showed labelling efficacy over 92 % (mean 98.1 %). 40 sites of the abnormal accumulation of the Infecton were detected. 27 of them were bacterial infection sites confirmed by clinical data. 5 suspected sites/patients were not infected and were negative on performed scans. WBS showed in 6 patients (mean age 63.5 yrs) changes (n=13) which were not clinically or microbiologically assessed as infective or were asymptomatic. One result was false negative. On the patients basis the sensitivity, specificity and accuracy were respectively 94.4%, 60%, 87%, on the findings basis were 96.4%, 27.8% and 69.6%, when assessed only in cases (n=19) with microbiological data 93.3%, 50% and 84.2%.

Conclusion. Investigation with Infecton seems to us useful for determining the extent of the infection and probably for infection monitoring with good sensitivity. In our opinion specificity is decreased because WBS revealed also non-bacterial, inflammatory changes, especially in elderly patients.

OS_100

COULD BONE SCINTIGRAPHY BE AVOIDED IN THE DIAGNOSIS OF INFECTED JOINT PROSTHESIS?

A. Benítez (1), A. Muñoz (1), J.A. Hernández-Hermoso (2), Y. Ricart (1), M. Castell (1), C. Díaz (1), J. Martín-Comín (1). (1) Department of Nuclear Medicine; (2) Department of Traumatology, Hospital de Bellvitge, L'Hospitalet de Llobregat, Spain.

Aim: The aim of this work was to analyse the possibility of suppress bone scintigraphy in the diagnosis protocol of infected joint prostheses in order to short the time for diagnosis.

Material and method: A retrospective analysis has been realised in 80 p (25 men) with suspicion of joint prosthesis infection: hip in 47 p, knee en 28 p, shoulder in 1 p The request for the study was to evaluate infection in the remaining 4 p with osteosynthesis post bone fracture. Bone scintigraphy (BS) with 99mTc-MDP, leukocyte scintigraphy (LS) with 99mTc-HMPAO and bone marrow scan with 99mTc-microcolloid (BMS) was performed in all patients. The interval between studies was 48h. The final diagnosis was established by surgical samples cultures. The interval time between prosthesis graft and bone scan was evaluated.

Results: Infection was confirmed in 29 out of the 80 patients. BS was positive in all patients. The interval time between surgery and scintigraphy was 1- 5 years in 57 p, 6 -10 years in 10 p and more than 10 years in 13 p. Sensibility (S) was 100% and positive predictive value (PPV) 36,2% (29 TP, 51 FP). The LS was positive in 64 p. The S was 96,5%, the specificity (Sp) 29,4% and the PPV 43,7% (28 TP, 15 TN, 1 FN, 36 FP). The BMS was no congruent with the LS in 28 p (1FP) and congruent in 52 p (2 FN). The combination LS + BMS showed a S of 93,1% , a Sp of 98% and a PPV of 96,4% (27 TP, 50 TN, 2 FN, 1 FP).

Conclusions:

1). The combination LS-BMS is the most accurate technique in the diagnosis of infected joint prosthesis.

2). The BS does not significantly help to the final diagnosis.

3). The suppression of BS in the diagnosis protocol provides an earlier diagnosis, reduces radiation burden to the patient and the number of visits to the nuclear medicine department.

OS_101

PROSPECTIVE COMPARISON OF 99M TC CIPROFLOXACIN (INFECTON) SPECT AND FDG PET FOR THE DIAGNOSIS OF CHRONIC OSTEOMYELITIS IN THE CENTRAL SKELETON: PRELIMINARY RESULTS

F. De Winter (1), F. Gemmel (1), C. Van De Wiele (1), D. Vogelaers (2), D. Uyttendaele (3), B. Poffijn (3), O. De Winter (1), R.A. Dierckx (1). (1) Division of Nuclear Medicine; (2) Department of Internal Medicine-Section Infectiology; (3) Division of Orthopedics, Ghent University Hospital, Belgium.

With conventional noninvasive techniques, the accurate diagnosis of chronic osteomyelitis in the central skeleton remains a diagnostic challenge due to the presence of bone marrow and/or metallic implants. Both infecton scintigraphy and FDG PET are promising techniques for this indication due to low bone marrow uptake when compared to gallium and white blood cell scanning. We prospectively evaluated their relative effectiveness in this particularly difficult patient population.

Methods: Forty-four patients with suspected chronic osteomyelitis of the central skeleton were evaluated with infecton SPECT. Of these, 38 patients in whom a complete microbiological/histopathological (n=18) or clinical (n=20) diagnosis was obtained, were included in this analysis. Patients with recent surgery were not excluded, since this would not reflect the clinical situation. Infecton SPECT was performed on a Marconi IRIX triple headed gamma camera 3 hours after 60 minutes after injection of 370 MBq 99m Tc ciprofloxacin (20 angular steps over 6° of 60 seconds each). PET was performed on a Siemens ECAT 951/31 scanner 60 minutes after injection of 370 MBq FDG (minimum 8 minutes per bed position, no AC). PET and SPECT images were scored visually by two independent blinded readers on a five point score scale, according to the readers' confidence of osteomyelitis. Disagreements were solved by consensus.

Results: Fourteen patients had chronic osteomyelitis and 25 proved to be free of infection. FDG PET was true positive in 14 patients, true negative in 19 patients and false positive in 5 patients. Infecton SPECT was true positive in 11 patients, true negative in 20 patients, false positive in 3 patients and false negative in 4 patients. This results in a respectively sensitivity, specificity and accuracy of 100%, 79% and 87% for FDG PET and 79%, 83% and 82% for infecton SPECT.

Conclusions: According to these preliminary results infecton SPECT has an accuracy that is in the same range of FDG PET. The added value of FDG PET is its very high negative predictive value. Due to lower cost however, infecton SPECT seems to be preferable as a first line strategy.

OS_102

POSITRON EMISSION TOMOGRAPHY WITH FLUORINE-18 DEOXYGLUCOSE IN THE DIAGNOSIS OF SPONDYLODISCITIS

H. Palmedo (1), A. Schmitz (2), J. Risse (3), MJ. Reinhardt (1), T. Krause (1), A. Matthies (1), O. Schmitt (2), HJ. Biersack (1). (1) Department of Nuclear Medicine, University of Bonn, Bonn , Germany; (2) Department of Orthopaedics, University of Bonn, Bonn , Germany; (3) Department of Nuclear Medicine, University of Frankfurt, Frankfurt, Germany.

The aim of the study was to evaluate the diagnostic accuracy of positron emission tomography with Fluorine-18 Deoxyglucose (FDG-PET) in patients with spondylodiscitis.

Material and Methods: Twenty patients who presented with a clinically suspected spondylodiscitis were included in the study. After injection of 280-370 MBq F-18 FDG, a PET scan was performed in the suspected area (PET scanner Ecat Exact Siemens/CTI, iterative reconstruction, at least three bed positions and in a fasting state). Transmission-corrected and non-corrected images were scored independently during a blind read by two experienced nuclear medicine physicians. These results were compared to the histopathological findings which served as the gold standard.

Results: A histopathological specimen was gained in 15 patients. FDG-PET showed a true positive result in 12 out of 12 histopathologically proven spondylodiscitides. Standard uptake values ranged from 4.4 to 13.2. In 2 patients who demonstrated unsuspicious histological findings, FDG-PET was true negative. PET showed a positive scan in a patient in who histology revealed an osteosarcoma. These data resulted in a sensitivity of 100% and in a diagnostic accuracy of 93%.

Conclusions: These first results demonstrate that positron emission tomography with Fluorine-18 Deoxyglucose is very sensitive in the detection of spondylodiscitides.

OS_103

THE VALUE OF FDG-PET FOR THE DETECTION OF INFECTED HIP PROSTHESIS

B. Vanquickenborne, A. Maes, F. Van Acker, J. Stuyck, M. Mulier, J. Nuyts, L. Mortelmans. Gasthuisberg university hospital, Leuven, Belgium.

INTRODUCTION: Accurate differentiation between infected and uninfected prosthesis remains a challenge because of the limitiations of the current tests. Recently, FDG-PET has proved to be useful for the detection of inflammation.

AIM OF THE STUDY: To evaluate the accuracy of PET combined with bone scintigraphy (BS) in the detection of infected hip prosthesis and to compare it with the results obtained through BS combined with leucocyte scintigraphy (LS).

MATERIALS AND METHODS: Seventeen patients with a hip prosthesis suspected for infection were included prospectively and underwent a BS, LS and PET scan within a two week period. Seven volunteers with an asymptomatic hip prosthesis were used as a control group and underwent a BS and PET scan. Three volunteers had bilateral prosthesis. Bacteriology of specimens obtained by surgery or needle aspiration or clinical follow-up up to 6 months were used as gold standard. Planar images of the BS and LS (4 and 24 hours p.i.) were performed. Additionally, SPECT images of LS were also obtained. Pelvic and hip region PET scans were performed with a dedicated PET scanner (HR+ Siemens) after a 10 mCi FDG injection. Two experienced observers analysed the LS images by comparing the uptake in the hip region to the controlateral bone marrow. These images were scored in combination with the BS as positive, negative or equivocal. PET scans were analysed alone using the tracer pattern shown in the control group. These PET findings were then compared to BS. To calculate sensitivity and specificity, equivocals were considered as positive.

RESULTS: Analysis of planar BS and LS resulted in a 75 % sensitivity and a 78 % specificity. LS SPECT images showed a better lesion contrast, resulting in a 88 % sensitivity and a 100 % specificity. 24 hour images provided no additional value. Analysis of PET images alone resulted in a 88 % sensitivity and a 78 % specificity. PET and BS comparison did not improve our results. We found a sensitivity of 88 % and a specificity of 68 %.

CONCLUSION: In our preliminary study, FDG-PET scan alone shows the same sensitivity as the conventional bone and leucocyte scintigraphy, although possibly with a somewhat lower specificity. If a PET camera is available, FDG PET seems to be a time and cost effective technique. Further confirmation in a larger patient group will be necessary.

NEUROLOGY / PSYCHIATRY

OS_104

MEASURING PROGRESSION OF DOPAMINE TRANSPORTER LOSS IN HEMI-PARKINSON'S DISEASE WITH I-123 BETA-CIT SPECT

A. Varrone (1), K.L. Marek (2), D. Jennings (2), R.B. Innis (3.4), J.P. Seibyl (1.3). (1) Department of Diagnostic Radiology, Yale University School of Medicine, New Haven, CT, USA; (2) Department of Neurology, Yale University School of Medicine, New Haven, USA; (3) Department of Psychiatry, Yale University School of Medicine, New Haven, CT, USA; (4) VA Connecticut, West Haven, CT, USA

Previous studies have demonstrated a bilateral loss of dopamine transporter (DAT) in hemi-Parkinson's disease (hemi-PD) patients. The loss of DAT in the striatum ipsilateral to the affected side is less pronounced than the one in the contralateral striatum; this finding clearly demonstrates an impairment of nigrostriatal projections in an asymptomatic stage of PD. Therefore, hemi-PD may be an adequate model to study the presymptomatic stage of the disease. The aim of this study was to evaluate the disease progression in hemi-PD patients using [^{123}I]β-CIT SPECT, to assess whether ipsilateral and contralateral striata showed a different rate of DAT loss.

Methods: Thirty-one hemi-PD patients (17 male, 14 female, mean age 58 ± 9 years) underwent two [^{123}I]β-CIT SPECT studies with an interval of 22.4 ± 0.9 months. The outcome measure was V_3'' (specific:nondisplaceable ratio). The DAT loss in the ispilateral and contralateral striata was measured as: 1) Absolute loss of DAT (V_3'' points) per year; 2) Percent change of V_3'' per year.

Results: The reduction of V_3'' points/yr in the ispilateral striatum was significantly higher than the one in the contralateral striatum (-0.42 ± 0.41/yr vs. -0.34 ± 0.34/yr, p=0.039 by paired t-test), whereas there was no difference in the percent change of V_3''/yr between ispilateral and contralateral sides (-9.34 ± 8.48 %/yr vs. -8.98 ± 8.55 %/yr).

Conclusions: In hemi-PD there is a higher loss in the number of transporter sites in the ipsilateral compared to the contralateral striatum; however, the DAT loss is likely to be an exponential process, with no difference in the rate of progression between the two striatal sides. This result is also supported by the clinical and imaging findings of preserved asymmetry of the dopaminergic impairment throughout the whole disease course.

OS_105

INFLUENCE OF SUBTHALAMIC NUCLEUS STIMULATION ON THE RATE OF DISEASE PROGRESSION IN PATIENTS WITH PARKINSON'S DISEASE

P.D. Mozley, H.I. Baltuch, M.B. Stern, A.D. Siderowf, J. Jaggi, J. Kulinski, K. Plossl, L. Harper Mozley, A. Cotter, H. Saghari, T. Jacobson University of Pennsylvania, Phildadelphia, PA USA.

Aim: To determine whether chronic electrical stimulation of the subthalamic nuclei (STN) through neurosurgically implanted electrodes slows the rate of disease progression in patients with Parkinson's disease.
Background: Excitatory glutaminergic stimulation of the substantia nigra by the STN may contribute to oxidative stress and accelerate neurodegeneration in patients with Parkinson's disease. Electrical stimulation reduces dyskinesias, decreases the length of off periods, and allows drug dosages to be lowered. It follows that electrical stimulation may slow the rate at which dopaminergic neurons degenerate, and may even rescue them.
Methods: The sample included 21 patients who were studied 1 to 3 weeks prior to surgery and agreed to be followed with serial images of their dopamine transporters every 6 months. They were compared to 173 other patients with parkinsonian movement disorders and 102 controls. All scans were acquired with 740 MBq of [Tc-99m]TRODAT-1 on a triple-headed camera. Data sets consisting of 12 sequential 5 minute frames obtained from 3 to 4 hours post injection were backprojected and filtered. Specific uptake values (SUVs) were calculated for subregions of the basal ganglia and related to performance scores on neuropsychological tests administered during the uptake period.
Results: All 21 neurosurgical patients had advanced disease with severe dyskinesias. Of these, 7 had virtually no visualizable uptake in the basal ganglia. Only 8 of the other 173 patients seemed as severely affected, and 2 of these also had dyskinesias. No patient with relatively preserved activity in the caudate had dyskinesias. Quantification showed that 58% of the surgical candidates had caudate uptake values that were less than 20% of the values in controls. Follow up showed that 57% of the surgical patients had less uptake after 6 months despite subjective improvement in all but one; however, 43% had quantitatively, as well visually, increased uptake after 6 months. One of these patients was able to stop taking medicines altogether. Statistically significant changes could not be detected in the 58 other patients who were studied twice or more, nor in the 70 controls who were studied twice or more.
Conclusions: The findings suggest that dyskinesias are associated with severely decreased dopamine transporter levels. While most all patients experience dramatic symptomatic relief from surgical implantation of electrodes, serial measures of physiology suggest that some patients continue to deteriorate anyway, while transporter levels clearly increase in others.
Supported by NIH RO1 AG17524.

OS_106

[123I]IBZM-SPECT IN ADVANCED PARKINSON'S DISEASE AS DIAGNOSTIC TOOL IN PREOPERATIVE ASSESSMENT

S. Asenbaum (1), W. Pirker (1), T. Traub (2), T. Brücke (3), F. Alesch (4), R. Dudczak (2). (1) Department of Neurology; (2) Department of Nuclear Medicine; (3) Department of Neurology, Wilheminenspital, Vienna; (4) Department of Neurosurgery, University of Vienna, Austria

With the development of invasive therapies as deep brain stimulation (DBS) in idiopathic Parkinson«s disease (PD) an exact diagnosis and a distinct exclusion of atypical parkinsonian syndromes as multiple system atrophy (MSA) is important. As [^{123}I] iodobenzamide (IBZM), binding on dopamine(DA) D2-receptors, can differentiate between these disorders, this method was performed in daily clinical routine to increase the diagnostic accuracy of PD before DBS.
Methods: 11 patients (pts; 46-66 years old, 9 male) with PD (duration 5-20y, mean 11y) were investigated with IBZM and SPECT. All pts fulfilled the criteria of the CAPSIT-PD protocol (Defer et.al.1999) inclusively a test of dopaminergic responsiveness. In 5 pts a previously existing dopaminomimetic therapy was stopped at least 5 days before the SPECT study, the remaining therapy including L-dopa was continued till the examination day. For semiquantification a binding ratio striatum/frontal cortex (SFR) was calculated and compared with the data of a control group (n=7; 36-87y) and of MSA pts (n=10; 44-88y). Diagnosis of MSA based on the clinical criteria of Quinn 1994.
Results: Age did not differ between the controls and pts (F=2.4, p<.11). One-way ANOVA revealed significantly higher SFR in controls (r=1.62, SD.08) than in pts (F=23.9, p<.0001), as well in controls vs. PD (r=1.50, SD.08; F=9.6, p<.007) and PD vs. MSA (r=1.38, SD.08; F=11.0, p<.004). No influence of recently taken dopaminomimetic therapy was obvious. No clear correlation existed between SFR and duration of PD.
Conclusion: In [^{11}C] raclopride-PET studies alterations of striatal DA D2 receptors have already been indicated in pts with advanced PD. An influence of chronic dopaminergic therapy, leading to postsynaptic receptor downregulation, or structural adaptations of the postsynaptic side, as a reaction to neuronal loss presynaptically, are discussed. In this IBZM-SPECT study a discrete, but significant reduction of striatal IBZM binding could now be delineated in our small group with advanced PD as well. For clinical application as preoperative management, these slight decreases of striatal IBZM binding have to be considered carefully not to overinterpret the results with regard to real degeneration of striatal neurons. Although investigated MSA pts revealed significantly lower SFR than PD, on the other hand an overlap between PD and MSA existed. Therefore careful interpretations of IBZM SPECT studies in advanced PD are necessary.

OS_107

PREDICTIVE VALUE OF CLINICAL EVALUATION AND I-123 BETA-CIT SPECT IMAGING FOR THE DIAGNOSIS OF PARKINSON'S DISEASE AND MULTIPLE SYSTEM ATROPHY

A. Varrone (1), K.L. Marek (2), D. Jennings (2), R.B. Innis (3.4), J.P. Seibyl (1.3). (1) Department of Diagnostic Radiology, Yale University School of Medicine, New Haven, CT, USA; (2) Department of Neurology, Yale University School of Medicine, New Haven, CT, USA; (3) Department of Psychiatry, Yale University School of Medicine, New Haven, CT, USA; (4) VA Connecticut, West Haven, CT, USA

Multiple system atrophy (MSA) is an akinetic-rigid syndrome that can be difficult to distinguish from Parkinson's disease (PD) in some patients. The aim of this study was to assess the predictive values of clinical ratings - Hoehn & Yahr stage and Unified Parkinson's Disease Rating Scale (UPDRS) – and dopamine transporter (DAT) imaging with [^{123}I]β-CIT SPECT, for the diagnosis of PD and MSA.
Methods: One hundred and fifty-seven PD (102 male, 55 female, mean age 61 ± 12 years) and 26 MSA (19 male, 2 female, mean age 66 ± 12 years) patients were studied. Outcome measure of striatal DAT density was V_3'' (specific:nondisplaceable ratio), expressed as percent of control value.
Results: MSA patients were more severely impaired than PD, as shown by higher Hoehn & Yahr stage (2.8 ± 1.0 vs. 1.7 ± 0.6, $p < 0.0001$) and UPDRS scores (motor UPDRS: 31.9 ± 15.1 vs. 18.4 ± 8.4, $p = 0.0002$), and showed a more symmetric DAT loss, as demonstrated by lower V_3'' in the striatum ipsilateral to the more affected side (44.0 ± 20.2 % vs. 53.1 ± 13.8 %, $p = 0.004$) and by lower striatal asymmetry index (7.0 ± 17.5 % vs. 17.2 ± 12.6 %, $p = 0.0004$). Logistic regression analysis showed that Hoehn & Yahr stage was the strongest predictor of disease diagnosis among the clinical variables. Among SPECT imaging outcome measures, only the striatal asymmetry index provided a small, but significant, predictive value when combined to the Hoehn & Yahr stage.
Conclusions: Imaging of the DAT demonstrates a similar pattern of nigrostriatal impairment in PD and MSA and does not provide a relevant contribution to the differentiation of the two disorders in addition to clinical ratings.

OS_108

WILL ENDOCRINOLOGICAL CHALLENGE TESTS REPLACE SPECT IMAGING IN THE DIFFERENTIAL DIAGNOSIS OF PARKINSONISM?

M. Choukèr (1), E. Friess (2), G. Pöpperl (1), J. Winkelmann (2), C. Trenkwalder (2), K. Hahn (1), K. Tatsch (1). (1) Dept. of Nuclear Medicine, University of Munich, Munich, Germany; (2) Max Planck Institute of Psychiatry, Neurology Section, Munich, Germany.

Aim: In the early stage of disease it is often difficult to distinguish between Parkinson's disease (PD) and other parkinsonian syndromes (PS) such as MSA or PSP. However, with respect to prognosis and treatment strategy it is important to establish the diagnosis reliably. In the past SPECT imaging of the pre- and postsynaptic dopaminergic system has proven to be helpful in the differential diagnosis of parkinsonism. In a recent study dopaminergic sensitivity in parkinsonian patients was investigated by an endocrinological challenge test measuring the growth-hormone (GH) response to a subthreshold dose of apomorphine (APO). There was an enhanced GH response to the dopaminergic stimulus, which was significantly higher in PD patients than in those with PS or controls. Aim of this study was to compare the results of the endocrinological challenge test with SPECT findings for the differential diagnosis of parkinsonism.
Methods: 35 patients with the clinical diagnosis of parkinsonism (PD: n=23; PS: n=12) were investigated with [I-123]IPT- and [I-123]IBZM-SPECT for assessment of the pre- and postsynaptic dopaminergic system, respectively. For semiquantitative evaluation specific binding of the ligands to the striatum was calculated (SB_{IPT}, SB_{IBZM}). In addition GH response to low dose APO was tested.
Results: In 31/35 the clinical diagnosis of parkinsonism was confirmed by SPECT investigations (PD: 20/23; PS: 11/12) showing the typical characteristics of specific tracer binding (PD: normal SB_{IBZM} and reduced SB_{IPT}; PS: reduced SB_{IBZM} and reduced SB_{IPT}). In 20/35 the clinical diagnosis was confirmed by the endocrinological challenge test. After low dose APO 14/23 PD patients showed a dramatical increase in GH plasma concentration but 9/23 only a minor GH response. 6/12 PS patients showed the expected low, but 6/12 also an unexpected high response to low dose APO.
Conclusions: Our study confirms that combined evaluation of the pre- and postsynaptic dopaminergic system with SPECT may reliably distinguish between PD and PS of other etiology. The GH response to a subthreshold dose of APO seems to be helpful to identify the specific deficit of the central dopaminergic system in patients with parkinsonism, currently, however, this method is not ready to replace SPECT yet. Further studies are warranted to improve and refine (e.g. optimizing cut-off thresholds for GH response) the new endocrinological challenge test before it may be used as a diagnostic tool for the differential diagnosis of parkinsonism in the clinical setting.

OS_109

[TC-99M]TRODAT-1: DIAGNOSING PARKINSONIAN MOVEMENT DISORDERS WITH A SINGLE TRACER

P.D. Mozley (1), A. Cotter (1), A.D. Siderowf (1), J. Kulinski (1), J.S. Schneider (2), N. Leopold (3), G.H. Baltuch (1), K. Plossl (1), L.M. Harper Mozley (1), H.I. Hurtig (1), M.B. Stern (1)(1) University of Pennsylvania, Philadelphia USA; (2) Thomas Jefferson University, Philadelphia USA; (3) Crozer Medical Center, Pennsylvania USA.

AIM: [Tc-99m]TRODAT-1 selectively binds dopamine transporters. This study quantified its effectiveness for differentiating patients with idiopathic Parkinson's disease (PD) from patients with other causes of parkinsonism. Methods: The sample consisted of 150 patients meeting research criteria for PD, 23 of whom had clinical hemi-PD, 36 patients with either multiple systems atrophy (MSA) or progressive supranuclear palsy (PSP), and 102 healthy human controls. SPECT scans of the brain were acquired on a triple headed camera 3 to 4 hours after the i.v. injection of 740 MBq (20 mCi) of [Tc-99m]TRODAT-1. Neuropsychological tests were administered during the uptake period. Mean counts per pixel were measured manually in regions of interest (ROIs). Results: Image analysis showed that the mean putamen to caudate ratio was higher in controls than in any patient group (p< 10EE-9) and higher in patients with MSA than PD (p<10EE-4). However, there was overlap: 7 patients with clinically advanced MSA had no detectable uptake in any subregion of the striatum, and as a result were indistinguishable from 21 patients with longstanding PD who had similar findings. When patients who were diagnosed less than 2 years before presentation were compared, it was clear that the two diseases could usually be distinguished from each other by observing areas of retained TRODAT activity in the putamens of patients with MSA, while patients with early PD or hemi-PD had no visible posterior putamen activity on either side. Patients with very early PSP seemed to have uniformly decreased uptake in both the caudate and putamen, but the uptake in PSP patients with advanced disease was about as chaotic as patients with early MSA. No neuropsychological test could distinguish between the patient groups. There were significant relationships between performance scores and uptake values in controls, but not in patients. Conclusions: The findings indicate that early, but not late, MSA can frequently be distinguished from PD with [Tc-99m]TRODAT-1 by detecting areas of retained uptake in the putamens of patients with MSA, but not PD. Patients with early, but not late, PSP seem to be distinguished from patients with MSA by noting uniformly decreased uptake in all regions of the striatum. The findings seem to be in contradistinction to studies with other tracers that have not been able to differentiate between these groups. Enough resolution to make the proper diagnosis may reflect the favorable imaging characteristics of technetium and several advantageous biological properties of TRODAT.

Conclusion: The uptake of presynaptic dopaminergic PET tracers is not markedly reduced in the substantia nigra of early PD patients. This may be related to some limitations of this study. It may however suggest that, at an early stage of the disease, the degenerative process affects more the striatal synaptic terminals than the dopaminergic neuronal bodies in the substantia nigra.

OS_110

THE UPTAKE OF PRESYNAPTIC DOPAMINERGIC LIGANDS IS NOT MARKEDLY REDUCED IN THE SUBSTANTIA NIGRA OF EARLY PARKINSON'S DISEASE PATIENTS: A PET STUDY

M.J. Ribeiro (1), M. Vidailhet (2), C. Loch (1), P. Hantraye (3), Y. Samson (1,4), P. Remy (1,3). (1) Service Hospitalier Frédéric Joliot, DSV-CEA, Orsay, France; (2) Service de Neurologie, Hôpital de Saint-Antoine, Paris, France; (3) URA Cea-cnrs 2210, Orsay, France; (4) Urgences Cérébro-Vasculaires, CHU Pitié-Salpétrière, Paris, France

Aim: Neuroprotective strategies in early Parkinson's disease (PD) aim at reducing the degeneration of dopaminergic neurons in the substantia nigra (SN) of these patients. To evaluate neuroprotective drugs, it might be useful to directly assess the loss of dopaminergic neurons in the SN using positron emission tomography (PET) and presynaptic dopaminergic tracers. We compared with PET the uptake of ^{18}F-L-DOPA and of ^{76}Br-FE-CBT, a ligand of the membrane dopamine transporter, in the SN of early PD and age-matched controls.
Methods: Nine untreated early PD patients (51.3 ± 4.5 year-old, UPDRS motor score = 13.3 ± 6.4) and 5 controls (51.0 ± 4.8 year-old) were studied with ^{18}F-L-DOPA and ^{76}Br-FE-CBT using a 3D acquisition and a high-resolution tomograph. The subject's movements were restrained using a molded headholder. Attenuation coefficients were measured and for both ligands, emission scan lasted 90 min after injection. Circular regions-of-interest were positioned on the PET images, based on coregistered individual MRI. The ^{18}F-L-DOPA uptake (Ki) in the SN was calculated using a multiple-time graphical analysis using occipital as non-specific input function. The nigral ^{76}Br-FE-CBT binding potential (BP) was calculated using a Logan analysis with an occipital reference region. The Ki and BP values of the patients were normalised to the respective mean of control values. The SN Ki and BP values were compared to control values according to the side opposite to the less and more clinically affected hemibody of the patients
Results: ^{18}F-L-DOPA uptake was in the range of control values (Table). The reduction of ^{76}Br-FE-CBT BP was not statistically significant, even in the SN contralateral to the more clinically affected hemibody (Table). These results contrast with the marked reduction of both tracers uptake found in the putamen of the same patients (^{18}F-L-DOPA and ^{76}Br-FE-CBT normalised uptake reduced to 0.63 and 0.43, respectively).

Table - Mean normalised Ki and BP values in the substantia nigra contralateral to the more and less clinically affected sides of the patients.

	Ki	BP
More affected	0.87 ± 0.33	0.76 ± 0.50
Less affected	1.00 ± 0.21	0.87 ± 0.46

OS_111

DOPAMINE TRANSPORTERS IN EARLY AND LATE ONSET PARKINSON'S DISEASE:A PET STUDY WITH [11C] FE-CIT

C. Gobbo (1), A. Antonini (4), R.M. Moresco (2), G. Lucignani (3), R. De Notaris (4), P. Barone (4), A. Carpinelli (2), A. Panzacchi (3), G. Pezzoli (4), F. Fazio (1-2). (1) Scientific Institute H San Raffale Milan Italy; (2) University of Milan Bicocca , INB-CNR; (3) University of Milan; (4) University of Naples, ICP Milan , Italy

Aim: Parkinson's disease is characterized by a progressive loss of nigrostriatal dopamine neurons. The dopamine transporter (DAT) is a sensitive marker of this loss. Little data exist on the assessment of DAT levels on early onset PD patients, particularly in subjects with autosomal recessive PD. The Aim of this study was to compare striatal DAT binding in early and late onset PD patients.Methods: Twenty patients with PD and ten controls were studied by PET and [^{11}C]FE-CIT. Disease duration was < 5 years, H&Y stage was I - II. Nine patients had early onset (age 38±6 years) 3 of them had a mutation of the parkin gene (autosomal recessive PD) and 11 had late onset PD (age 60±7 years). Control subjects were divided in young (N=5 ; 35±9 years) and old (N=5; 60±10 years). Subjects underwent a 90 min. dynamic PET study. ROIs were drawn on the head of the caudate nucleus and on the putamen of both hemispheres and on the cerebellum (reference region). Specific uptake (striatum - cerebellum)/cerebellum, was measured between 60-90 minutes from injection.Results: Mean values of FE-CIT specific uptake are reported below:

	Caudate	Putamen
PD (early)	2.9±0.8	1.2±0.5
Control (young)	4.0±0.3	3.9±0.3
PD (late)	3.1±0.7	1.7±0.5
Control (old)	4.1±0.5	4.1±0.6

A reduction of DAT was observed in both groups of PD patients, relatively to age matched normal controls, particularly in the putamen (early PD: -68%; late PD -58%, respectively; p<0.001). In this region a higher loss of dopaminergic nerve endings was observed in early onset as compared to late onset PD (p<0.001). The 3 patients carrying the parkin mutation showed the lowest mean specific uptake of [^{11}C]FE-CIT in the putamen: 0.94±0.4. Conclusion: These results suggest a different degree of striatal degeneration in patients with early vs. late onset PD. The rate of neuronal degeneration is under investigation in longitudinal studies.

OS_112

THE OPTIMUM PATIENT PREPARATION FOR MYOCARDIAL PERFUSION SCINTIGRAPHY

P. Dibbets-Schneider, M.P.M. Stokkel, E.K.J. Pauwels. Department of Nuclear Medicine, Leiden University Medical Center, Leiden, The Netherlands.

Myocardial perfusion scintigraphy (MPS) is a powerful diagnostic tool to assess ischemia of the heart. Several factors, such as low statistical count rate and movement artifacts, may influence image quality. With the use of Tc-99m labeled compounds artifacts commonly occur due to the high activity in the bowel nearby the heart, as these agents are excreted both via the liver and kidney. The aim of the present study was to find the optimum patient preparation to minimise the radioactivity in the surrounding area of the heart.

Methods: Ten groups consisting of 15 patients each underwent a different preparation scheme. Between the administration of 500 MBq Tc-99m Tetrofosmin and acquisition milk, water, chocolate or a combination of stimuli was given at different time intervals. Before SPECT acquisition, an anterior static image was performed on which standard ROI's were drawn in the liver, colon, background and lung. The average counts in each region was expressed as a percentage of the average counts measured in the region of the heart.

Results:

Grp	Stimulus	Interval injection-stimul. (min)	Interval injection-acquis. (min)	Liver (%)	Back-ground (%)	Colon (%)	Lung (%)
1	200 ml milk	10	69	85	80	102	52
2	200 ml milk	20	66	93	79	91	50
3	200 ml milk	30	64	102	79	109	48
4	200 ml milk*	40	-	-	-	-	-
5	200 ml milk/ 400 ml water	10	58	105	76	85	50
6	200 ml milk/ 400 ml water	20	68	102	76	84	53
7	200 ml milk/ 400 ml water	30	65	95	73	79	50
8	45g chocolate	10	76	73	61	66	42
9	45g chocolate	20	72	80	68	73	45
10	45g chocolate	30	71	93	75	90	46
11	No preparation	-	63	112	81	95	52

*Due to the bad image quality, i.e. the artifacts, this group was stopped after 4 patients.

The difference in time-interval between injection and acquisition between the groups was nog significant. In group 8, count-rates were significant lower than in the other groups, especially in the liver and colon.

Conclusion: The optimum patient preparation for MPS is 45 g chocolate 10 minutes p.i. In case the patient is not allowed to eat chocolate, 200 ml milk 20 minutes p.i. and 400 ml water is a reasonable alternative.

OS_113

THE COEXSISTENCE OF HIATAL HERNIA AND DUODENAL GASTRIC REFLUX OF TC99M MIBI

A. Arroyo (1), H. Semaan (2), Y. Patel (1). (1) Department of Nuclear Medicine, St. Vincent Mercy Medical Center, Toledo Ohio, USA; (2) Department of Radiology, The Medical College of Ohio (MCO), Toledo Ohio, USA.

Background: Duodenal gastric reflux of Tc99m-MIBI is common and can result in interference with the evaluation of myocardial uptake. It is unknown wether a relation between the presence of hiatal hernia and duodenal gastric reflux of Tc99m-MIBI exist.

Objective: The purpose of the present study was to determine if a relationship exists betweenhiatal hernia and duodenal gastric reflux.

Materials and methods: The medical records and the Tc99m-MIBI studies of 1153 patients, 392 females and761 males referred for evaluation of possible ischemic heart disease performed over a period of 6 months in our institution were reviewed. The cases of hiatal hernia and duodenal gastric reflux were reported.

Results: 52 patients had hiatal hernia proven by Computed Tomography, barium upper gastrointestinal studies or plain X-ray films. 233 patients had duodenal gastric reflux of Tc99m-MIBI. 3 patients had co-existence of duodenal gastric reflux and hiatal hernia.

Discussion: Duodenal gastric reflux of Tc99m-MIBI excreted from the liver and gallbladder is frequently noted during cardiac imaging, and it is reported to be approximately 24% of all patients, in previous studies. The presence of hiatal hernia brings the activity closer to the heart and would result in a more significant interference with the evaluation of myocardial uptake. Hiatal hernia is a common condition in elderly people. If a relation between hiatal hernia and duodenal gastric reflux existed, maneuvers such as lying down on their right side for 20 minutes prior to the cardiac acquisition may be helpful. Unfortunately this relationship was not proven in our protocol.

Conclusion: There was no correlation between the presence of a hiatal hernia and duodenal gastric reflux in our study.

OS_114

THE FREQUENCY OF EXTRA-CARDIAC UPTAKE DURING TC99M SESTAMIBI MYOCARDIAL PERFUSION IMAGING

A. Arroyo (1), H. Semaan (2), Y. Patel (1). (1) Department of Nuclear Medicine, St. Vincent Mercy Medical Center, Toledo Ohio, USA; (2) Department of Radiology, The Medical College of Ohio (MCO), Toledo Ohio, USA.

Background:
Technetium-99m sestamibi has been reported to localize in a variety of benign and malignant tumors. Its most common use is in cardiac imaging. Three-dimensional reconstruction that might be helpful in the detection of non-cardiac conditions is not often performed.
Objective:
The aim of our study was to determine the frequency and the diagnostic value of extra cardiac activity during Tc99m-sestamibi cardiac imaging.
Materials and methods:
The medical records and the 3-D reconstruction of Tc99m sestamibi studies of 1153 patients, 392 females and 761 males referred for evaluation of possible ischemic heart disease performed over a period of 6 months in our institution were reviewed, and the cases of unsuspected extra-cardiac activity were reported.
Results:
Three patients showed activity within previously unknown lung tumor. Two patients had activity within a hiatal hernia associated with duodeno-gastric reflux. One patient demonstrated activity within an undiagnosed breast cancer, and one patient displayed activity within a thyroid tumor.
Discussion:
Cases of extra-cardiac uptake during Technetium-99m sestamibi cardiac stress imaging are reported in the literature. We found that is not uncommon to make the diagnosis of non-cardiac condition during routine cardiac imaging. The frequency of incidental detection of undiagnosed condition is 0.6% in our institution.
Conclusion:
Careful attention should be made during the evaluation of the 3-D reconstructed images from myocardial perfusion studies. Non cardiac abnormal activity could be detected, and might be relevant for patient care.

OS_115

EFFECT OF DIFFERENT ATTENUATION CORRECTION METHODS ON SUV MEASUREMENTS FOR 18F-FDG PET BRAIN STUDIES

M. Schiavini, F. Zito, A. Bruno, R. Leo, M. Castellani, F. Voltini, G. Tafuni, P. Gerundini. Nuclear Medicine Department, Ospedale Maggiore IRCCS, Milano, Italy.

Introduction: An accurate quantitative estimation of cerebral metabolic rate with ^{18}F-FDG positron emission tomography (PET), requires emission image corrections for brain photon attenuation. Aim of this work was to compare the accuracy of the standardized uptake value (SUV) measured with different attenuation correction procedures, now available on modern PET scans to improve the patient throughput. Methods: Three different attenuation correction procedures were analysed based on m-map obtained with: -pre-injection transmission scan (preT) considered as reference, -post-injection transmission scan (piT) and –segmentation of the post-injection transmission scan (spT). The different methods were evaluated on the 3D-Hoffman brain phantom filled with a ^{18}F aqueous solution (about 5000Bq/cc) and on 13 patients with cerebral diseases. Patients were given 111-185MBq of ^{18}F-FDG i.v.. Emission and transmission scans were performed with an ECAT Exact HR plus system. Emission studies were acquired for 20 min in 3D mode while pre-post injection transmission scans for 10 min in 2D windowed mode. Transaxial sections were reconstructed with filtered back projection algorithm smoothed with Hann filter (cut-off 0.5). For the different images, SUV (Bq/cc) was assessed by drawing regions of interest on central and peripheral cerebral regions. The SUV values obtained with the piT and spT procedures were compared with the preT ones in terms of percent differences.

Results: For all studies, the SUV values obtained with piT and spT procedures were lower than preT ones. On average the percent differences of piT and spT SUV values were respectively -10% and -9%, for both central and peripheral brain areas.

Conclusion: In the present study it is demonstrated that the SUV of piT and spT attenuation corrected images is about 10% lower than the preT one. When an higher level of accuracy is required and the patient throughput is not a constraint, the preT procedure should be preferred.

OS_116

THE MYOCARDIAL GATED SPECT ACQUISITION PARAMETERS FOR THREE HEADED GAMMA CAMERA AND TECNETIATE AGENTS

M. Servadei, C. Zampagna, A. Dalmonte, M. Fossati, B. Frontali, F. Medri. Nuclear Medicine Dpt, Faenza, Italy.

INTRODUCTIONS: the recent implementation of software programs with sophisticated tools in gated spet myocardial scintigraphy (GSM) makes critical the optimisation of the acquisition data. In this study we decided to evaluate the best GSM parameters to acquire a rapid but always diagnostic exam with the three headed gamma camera in use in our centre (PICKER PRISM 3000 equipped with parallel hole collimators and automatic elaboration QGS program by Germano). We also did a control to verify the exam reproducibility after the parameters set.

MATERIALS: assuming that 40 seconds for each step was a good compromise to obtain a sufficient counts number, time bins and number of steps were chosen according to the results of a double GS acquisition in 2 groups of 10 pt each. In the I group we acquired with time bins 16 and 8 (120 steps), in the II group we used 72 and 120 steps (time bin 8).

RESULTS: in any case the application of the automatic QGS was effective and in particular the mean Ejection Fraction (EF) changed of 0,8% (I group) and 1,2% (II group). The End Diastolic Volume (EDV) and End Systolic Volume (ESV) had a mean variation that was slightly greater in group II but no bigger than 2,2 ml. Using the parameters 72 steps of 40 seconds each with time bins 8 (exam length of 18 minutes) we tested the reproducibility of the exam in 10 pt. with two subsequent GS performed in clinical identical situations. In these cases EF, EDV and ESV showed similar results with a mean variation of 0,4%, 0,2ml and 0,6ml.

CONCLUSIONS: the selected parameters are effective in performing an adequate and fast GS acquisition. In our opinion this group of parameters is also the best indicated for the GS stress test using a three headed camera.

OS_117

COMPARISON OF FDG-UPTAKE IN MYOCARDIUM, SKELETAL MUSCLES AND LIVER IN DIABETIC AND NON-DIABETIC PATIENTS

U. Dopichaj-Menge, V. Ivancevic, D. L. Munz. Clinic for Nuclear Medicine and PET Center Berlin, University Hospital Charite, Berlin, Germany.

Aim: F-18-labeled FDG is the radiopharmaceutical applied most frequently for PET in oncological patients. The rationale for this procedure is the enhanced utilisation of glucose in tumor cells. To further enhance FDG uptake in tumor cells the patients should be in a fasting state for 6 to 12 hours. Obviously, this fasting period cannot be maintained in diabetic patients. The aim of this study was to comparatively investigate FDG uptake in diabetic and non-diabetic patients and to derive conclusions regarding the preparations of diabetic patients for FDG-PET.

Methods: 37 FDG-PET investigations in 32 patients (16 women ,16 men; age range, 36 - 54 years) were enrolled. 10 of the patients suffered from type I diabetes mellitus and 8 from type II. There were 19 non-diabetic patients. The duration of the fasting periods und blood glucose levels were documented before FDG injection. FDG-uptake was analyzed visually and semiquantitatively using ROIs drawn in representative regions of the myocardium, sceletal muscles and liver. Myocardial uptake was judged visually as faint or pronounced. For semiquantitative analysis different ratios were used: myocardium/ upper arm (myo/ua), myocardium/liver (myo/li), and upper arm/liver (ua/li).

Results: Fasting period for the type I patients was 0 – 6.5 hours (median 0.5 h), blood glucose levels ranged from 65 – 173 mg% (median 118 mg%). Type II diabetics fasted for 5 – 15 h (median 13.5 h) and had blood glucose levels ranging from 75 – 124 mg% (median 99 mg%). Non-diabetic patients fasted for 4 – 24 h (median 15 h) and had blood glucose levels ranging from 65 – 109 mg% (median 83 mg%). Pronounced myocardial FDG uptake was encountered in 8 patients (80%) with type I, in 4 patients (50%) with type II, and in 10 (53%) of the non-diabetic patients. The results of the semiquantitative analysis are summerized as follows:

	type I	type II	non-diabetics
myo/ua	4.9	3.9	3.6
myo/li	4.0	1.5	1.6
ua/li	0.8	0.3	0.3

Conclusion: FDG uptake patterns of type II diabetic and non-diabetic patients are almost identical. Type I diabetics show pronounced myocardial FDG uptake more frequently and seem to have a comparatively higher FDG uptake in sceletal muscles as documented by ratio analysis. A longer fasting period in type I diabetics might possibly result in an FDG uptake pattern more similar to that of type II diabetics and non-diabetic patients. However, a prospective investigation with special medical guidance of these patients will be necessary in order to investigate this hypothesis.

OS_118

THE USE OF [18F]-FDG IN THE SEARCH FOR INFECTIOUS LESIONS:FALSE POSTIVE BECOMES DIAGNOSTIC TOOL. WHAT DOES IT MEAN FOR THE PATIENT AND THE TECHNOLOGIST?

L. Currie, J.N. Talbot, C. Audri, V. Dayre, E. Fontana, C. Lafon, L. Leroux, C. Machacek, E. Nival. Service of Nuclear Medicine, Hospital Tenon, Paris, France.

The search for primary lesions and metastatic disease in oncology has been metamorphosised in the last few years by the improvements in nuclear medicine imaging technology, the arrival of [18F]- fluo-deoxy-glucose (FDG), dedicated PET and hybrid triple head cameras capable of coincidence imaging when fitted with thick crystals.

However, it was discovered that in certain cases a false positive result for the detection of cancerous tissue could be recorded in patients with infection. The fixation, occurring due to the activation of the macrophages to combat the infection, could be used positively to localise infectious lesions using [18F] –FDG.

At hospital Tenon, Paris, the medical team has opted to replace [67Ga]-Gallium citrate scintigraphy with [18F] –FDG detected with the same hybrid triple head camera. As the average examination time for [18F] –FDG is around 2 hours, replacing 5 days for [67Ga]Gallium citrate this releases more appointment possibilities for such cases, involving the Nuclear Medicine technologist more frequently than before with extremely sick patients, largely immobile, often in acute pain with fever.

This increased contact with potentially contagious illnesses involves changes in the organisation of work to protect the patient, staff and other patients susceptible to infection i.e. immuno-supressed patients, involving more specialised patient care and more specific hygiene procedures.

In comparison with [67Ga]- gallium citrate examinations taking on average 5 days [18F]-FDG allows a much faster localisation of lesions in cases where time is very important for clinical management of very sick patients.

The resolution of the images is better than with [67Ga]Gallium citrate due to the suppression of the middle energy collimators.

As the uptake of [18F]-FDG by the digestive tract is less than [67Ga]- gallium citrate there is no need for a laxative or an enema to clear bowel activity.

Finally the dose delivered to the patient is reduced by a factor of 5.

OS_119

CORRELATION BETWEEN NONSPECIFIC FDG UPTAKE AND GLUCOSE LEVEL, AGE, FASTING PERIOD

A.P. Meeuwis, P.J. Kok, M. Groot de, F.H. Corstens, W.J. Oyen.
Department of Nuclear Medicine, University Medical Nijmegen, The Netherlands.

Aim: FDG uptake in the myocardium, stomach and bowel is frequently increased on PET scans, interfering with scan reading. The aims of this study were to investigate if blood glucose level, age, fasting period could provide an explanation for this unwanted FDG-uptake, or if there is a patient-specific pattern.
Methods: 175 oncology patients (113 men, 62 woman, mean age 57 yr) referred for whole-body FDG-PET were included. The fasting period ranged from 6 to 22 hours (median 13 hours). Blood glucose levels were measured before FDG injection. One hour after intravenous injection of 220 MBq FDG, emission and transmission images (Siemens ECAT/ART) were recorded. The emission data were corrected for attenuation, followed by iterative reconstruction. Uptake in myocardium, bowel and stomach was scored visually by three independent investigators. The correlation co'fficient was calculated between FDG uptake and these parameters. Another group of 25 patients (16 men, 9 woman) who were referred for whole-body FDG-PET at least three times, underwent a total of 92 scans which were evaluated similarly to identify possible patient-specific patterns.
Results: No significant correlation between glucose, age, fasting period and FDG uptake was found. However, high glucose levels (> 7.5 mmol/l) always resulted in absent or minor FDG uptake in the myocardium. In the patients who underwent multiple PET-scans, there seemed to be a patient-specific pattern. In 13 (52%) patients there was no or only minor change of nonspecific uptake on the PET-scans. If there was a change in uptake in one organ, uptake in a second organ changed in only 9 % of scans without a discernible pattern. In 3 (12%) patients, the uptake in the myocardium varied widely from none to high, not correlated with glucose level or change of tumor load.
Conclusions: Increased FDG-uptake in myocardium, bowel and stomach was not correlated to glucose level, age or fasting period. However, when glucose levels were high, no myocardial uptake was seen. Patients seem to show patient-specific uptake patterns for myocardium, stomach and bowel. If there was a change in nonspecific uptake it was not correlated to a change of tumor load.

DIAGNOSTIC ONCOLOGY

OS_120

ACCURACY OF PEROPERATIVE GAMMA PROBES IN LOCALIZING SENTINEL LYMPH NODE FOR BREAST CANCER : COMPARISON OF THREE PROBES IN 40 PATIENTS

C. Curtet (1), J. .M. Classe (1), F. Dravet (1), M. Fiche (3), C. Sagan (3), C. Rousseau (1), J.F. Chatal (1,2), I. Resche (1). (1) Service de medecine nucléaire Centre régional de Lutte contre le cancer 44805 nantes saint herblain ; (2) INSERM U 463, 9 quai moncousu 44035, Nantes, France; (3) Service Anatomo-pathologie hopital nord 44805, Nantes, France.

Gamma probes are used in radioguided surgery to identify sentinel lymph nodes (SLN). Three commercial gamma probes; Modelo 2 (Novellec), Navigator (Auto Suture) and Neoprobe 2000 (Breast Care) were evaluated in this study for localisation of SLN in breast cancer patients , using BgO, CdTe, CZT detectors respectively .
Methods : Forty patients with infiltrative breast carcinoma were enrolled (10 T0, 21 T1, 9 T2).Two 0,1 ml injections of 15 - 18 MBq Tc99m (100nm) sulfur colloid were administred in peritumoral space. Twenty one patients had planar lymphoscintigraphy (LS) when injected 20 h before surgery. Two groups of patients were defined relative to the intreval between injection and peroperative radiodetection : group A 20 hours before surgery, group B 2 hours before surgery. Patent blue was injected in surgery room. Peroperative radiodetection was performed with the three probes on background, axilla, SLN, and lymphadenectomy. SLN were radiodetected when S / B ratio was > 2. All nodes underwent standard pathological analysis wih serial sections at 150 _m intervals, and HES / Immnohistochemistry (Cytokeratin)).
Results : 17 of the 21 LS were positive, 9 of them had one spot, and 13 SLN were radiodetected in the surgery room, and 8 had 2 or more spots, and 18 SLN were radiodetected. Probes counts (cps) were as fellows : group A (n= 23 patients and group B (n=17 patients),

	Group A			Group B		
	Modelo 2	Navigator	Neoprobe	Modelo 2	Navigator	Neoprobe
Back-ground	9,5 ±,2	0,8 ± 2	1,3 ± 08	73,2 ± 32,7	3,9 ± 3,1	7 ± 2,5
SLN	244,8 ± 511	45 ± 101	46,5 ± 38	889,2 ± 106,7	138,3 ± 199,6	223 ± 368

A total of 77 SLN were radiodetected, (40 SLN in group A. 37 SLN in group B).In group A 37 /40 were detected with Modelo2, 21 /40 wih Navigator, and 24 / 40 with Neoprobe 2000 , and 7 metastasis (3 micometastasis) were found; In group B 37 SLN were detected , 36 / 37 with modelo2, 33 / 37 with navigator, and 34 / 37 with neoprobe 2000, and 11 metastasis (4 micrometastasis) were found. Only 15 of the 40 patients with metastasis required axillary lymph nodes removal, 15 / 15 patients were detected by Modelo 2, 13 / 15 with Navigator and 14 / 15 by Neoprobe 2000.
Conclusion : Radiodetection was better when patients were injected 2 hours before surgery. Count differences. with the gamma probes were detector related. Therefore, probes that are less optimal in their localizing properties may influence the success of SLN radiodetection . It is important for the surgeon to understand the major factors that can affect the performance of each probe. These results need to be confirmed with a larger series.

OS_121

A SIMPLE METHOD FOR CONTEMPORARY LOCALIZATION OF NON PALPABLE BREAST CANCER AND SENTINEL NODE (SN)

L. Feggi (1), E. Basaglia, S. Corcione, P. Querzoli, L. Bergossi, G. Soliani, N. Prandini, P. Carcoforo. (1) Nuclear Medicine and Radiology, St. Anna Hospital, Ferrara, Italy; (2) Clinical General Surgery and Pathology, University of Ferrara, Italy.

One of the most important aspects in the management of non palpable breast cancer is the need of an accurate and exact localization either of the tumor and also of the sentinel node to perform a correct surgical biopsy and to avoid unnecessary axillary nodes dissections. We propose a simple method for the contemporary radioguided localization of non palpable breast cancer and SN, by injecting only a 99mTc nanocolloid (Nanocoll®, Amersham).
Material and methods: We used our method in 65 patients (median age 60 years; range 46-80) with mammographic or ultrasonographic evidence but without clinical evidence of tumor. All patients had previous cytology of malignancy or, at least, high suspicious of malignancy and need of surgical removal of breast lesion. In all patients we injected, by ecographic or radiostereotactic guide, the nanocolloid in a total volume of 0.3-0.4 cc, giving half of the radiopharmaceutical intratumorally and half immediately superficially to the tumor. When the lesion had no mass but is represented only by calcifications the injection is completely made between these calcifications. We supplied the colloid in the afternoon 15-23 hours before lymphoscintigraphy (LS) and surgery, with a dose calculated in order to have about 10 MBq of 99mTc at the moment of surgery. During scintigraphy we tattoo the cutaneous projections of SN: a gamma ray detection probe is then used to locate breast cancer and SN and guide its surgical removal.
Results: The procedure got success in permitting us localizing occult breast lesion in every patient and permitted SN localization with selective biopsy in all patients but two (96.9%). Lesions were always localized at first attempt and were always contained into excision edges with shortest distance between tumor and specimen edges > 1 cm. The histological examination showed nodes which were free of disease in 52 cases, and metastatic in 11 cases (9 with micrometastases, one of which in intenal mammary chain): false negative SNs were not encountered .
Discussion: If you have an high probability of malignancy in non palpable breast lesion and a good coordination between surgeon, radiologist and nuclear medicine physician, the single radiotracer method to localize contemporary non palpable breast cancer and SN gives great benefits under the economic point of view, with reduction of the costs. Then, it is appreciated also under the psychological point of view, with patients who observe the fast surgical solution of their problem.

OS_122

LYMPHOSCINTIGRAPHY FOR INTERNAL MAMMARY CHAIN DETECTION IN BREAST CANCER

G. Paganelli (1), L. Travaini (1), G. Trifirò (1), C. De Cicco (1), G. Viale (3), M. Cremonesi (1), G. Prisco (1), V. Galimberti (2), A. Luini (2), U. Veronesi (2). (1) Nuclear Medicine and Medical Physics Divisions; (2) Senology Division; (3) Pathology Division, European Institute of Oncology - Milano, Italy.

In breast cancer patients the detection of SNs outside the axilla generally occurs in 1-2% of the cases after superficial injection of the tracer. Aim of this study was to verify if a deep injection can allow the visualization of internal mammary chain nodes (IMC) in a higher percentage of cases.

Methods: 200 eligible patients with T_1-T_2 N0 lesions of the inner quadrants were enrolled into the study. A superficial injection was performed in 100 pts (group I), and a deep injection in the others (group II). In this first phase of the study, patients with outer quadrant lesions were excluded from IMC biopsy because an additional surgical excision should have been required. However, a control group of 200 pts with outer quadrant lesions was studied by lymphoscintigraphy as well.

Results: In group I (superficial injection) SNs were visualized in 99 pts, in group II (deep injection) SNs were visualized in 96 pts. SN at IMC was visualized in 65.6 % of cases (63/96 pts) in group II, *vs* 2.1 % (2/99 pts) in group I. In the control group (outer quadrants) deep injection allows the visualization of IMC in 10% of cases. IMC localization was prevalently in the 2nd, 3rd and 4th intercostal spaces. Radioguided biopsy of the IMC was performed in 62/63 pts with a stage migration in 7% of cases.

Conclusions: Deep injection allows to localize SN at IMC in more than 60% of inner quadrant breast lesions, probably due to the deeper location of IMC lymphatic vessels. Axillary plus IMC biopsy provided stage migration in 7% of pts with cancer located in the inner quadrants.

OS_123

SENTINEL NODE IMAGING AND 18F-FDG PET FOR STAGING THE CLINICALLY NO NECK IN ORAL SQUAMOUS CELL CARCINOMA

N.C. Hyde (1), E.M. Prvulovich (2), W.A. Waddington (2), M. Keshtgar (2), D. Visvikis (2), L. Newman (1), P.J. Ell (2). (1) Department of Maxillofacial Surgery, University College London Hospitals NHS Trust, London, UK; (2) Institute of Nuclear Medicine, Royal Free and University College London Medical School, UK.

Aims: Accurate staging of the clinically N0 neck in patients with oral squamous cell carcinoma is sub-optimal as conventional imaging techniques are associated with high false negative/positive rates. The aim of this study is to evaluate the accuracy of ^{18}F-FDG 3D positron emission tomography (PET) and sentinel lymph node (SLN) imaging and biopsy in determining the true disease status of the loco-regional lymphatics.

Methods: 15 patients with biopsy proven oral carcinoma and clinically N0 necks underwent pre-operative ^{18}F-FDG PET and SLN imaging. A 3D PET acquisition (emission/transmission imaging) of the whole body and the head and neck followed an intravenous injection of 370MBq of ^{18}F-FDG. SLN technique was performed using 4 peri-tumoural injections of ^{99m}Tc labelled albumin colloid each of 10MBq. Dynamic and static imaging followed in the antero-posterior and lateral projections. At operation 1ml of 2.5% Patent Blue Dye and a hand held gamma probe (1500 Neoprobe) were used in combination to identify and remove the SLN. Surgery then continued along conventional lines including a selective or modified radical neck dissection. Histology of the resultant specimen was correlated with that of the SLN and pre-operative imaging.

Results: In all patients SLN harvesting was feasible. In 12/15 patients the SLN(s) and the residual neck dissection were -ve for tumour. In 2/15 patients the SLN(s) were +ve for tumour as were other neck nodes. In 1/15 patients the SLN was -ve but another tumour +ve node was identified in the neck. This patient occurring early in our series with a SLN close to the primary tumour. ^{18}F-FDG PET failed to identify nodal disease in all three patients with histologically proven lymph node metastases. The size or these nodes ranging from 12mm x 10mm x 3mm to 25mm x 15mm x 10mm.

Conclusion: SLN imaging and biopsy with probe and Patent Blue Dye guided harvest is feasible in patients with oral squamous cell carcinoma and can predict cervical nodal status. ^{18}F-FDG PET may be less useful.

OS_124

SENTINEL LYMPH NODE BIOPSY IN PAPILLARY THYROID CANCER

M. Catarci (1), G. Longo (1), M.G. De Filippo (2), S. Drago (1), R. Massa (3), A. Romanzi (4), L. Montemurro (3), M. Carboni (3), G. Pasquini (4), G.B. Grassi (1). (1) Surgical Oncology, San Filippo Neri Hospital, Rome, Italy; (2) Nuclear Medicine, San Giuseppe Hospital, Marino, Italy; (3) 2nd Surgical Clinic, University of Rome ; (4) General Surgery, Velletri Hospital, Italy

Aims: The role and the extension of lymphadenectomy for papillary thyroid cancer (PTC) with occult lymph node metastases is controversial. The concept of sentinel lymph node biopsy (SLNB) was recently applied also to differentiated thyroid cancer using intraoperative injection of a vital dye. The feasibility and the technical details of using preoperative lymphoscintigraphy coupled with intraoperative vital dye and gamma probe scanning were investigated in this pilot study.

Methods: Over a seven months period, eight consecutive patients with preoperative suspicion of PTC at FNAB were enrolled in the study. They were all submitted to preoperative lymphoscintigraphy with ^{99m}Tc-labelled colloidal albumin (Nanocoll, Sorin Biomedica, Saluggia, Italy) at different dosages (Fig. 1). Two to three hours later, they were all submitted to total thyroidectomy with SLNB guided by intraoperative injection of a vital dye (Blu Patent V 2,5%) and scanning with a hand-held gamma probe (Navigator, U.S.S.C., Norwalk, U.S.A.). Lymph node dissection was completed in the area in which the sentinel node was located. Two cases were excluded from final analysis: in one the final pathology revealed a follicular adenoma and in the other there was inadvertent injection of the tracer outside the tumor into a blood vessel followed by early migration of the tracer to the liver.

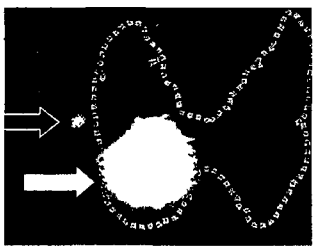

Figure 1: Preoperative lymphoscintigraphy, 25 minutes after intratumoral injection of 0.1 mL of ^{99m}Tc-labelled colloidal albumin (22 MBq). It shows a 39 mm nodule in the lower half of the right lobe corresponding to a papillary carcinoma (full white arrow) and its sentinel lymph node (empty arrow) located along the right jugular chain.

Results: The sentinel node was identified using all the three methods in all cases (100%). Considering one of the methods alone, identification rates were 66%, 50% and 83% for preoperative lymphoscintigraphy, vital dye, and probe scanning, respectively. One sentinel node was identified in 4 cases and two in the other two cases. The optimal dosage of the tracer appeared to be at 22 MBq.

Conclusions: These results underline the necessity to use the combination of nuclear medicine imaging and lymphatic vital dye in order to enhance the identification rate of sentinel node also in thyroid cancer. It is now necessary to check the diagnostic accuracy of this procedure through a controlled trial involving a more extended lymph node dissection in the neck.

OS_125

DEGREE AND TIMING OF RECOVERY IN HIBERNATING MYOCARDIUM, AFTER EFFICIENT REVASCULARIZATION, IN PATIENTS WITH ANTERIOR MYOCARDIAL INFARCTION

R. Petrovici, R. Capalneanu, C. Medrea, A. Iancu, A. Molnar, M. Barsan. Department of Cardiology, Heart Institute Cluj-Napoca, Romania.

Purpose: The assessment of improvement in systolic function and 99m Tc-MIBI uptake, after efficient revascularization in hibernating myocardium, consecutive to anterior myocardial infarction

Methods: 78 patients (age 52±15 years, 56 men and 22 women) were followed between May 1996 and January 2001, all with anterior myocardial infarction older than 2 months and presence of hibernation. LV ejection fraction was 34±11%. 43 patients had an interventional revascularization and 35 a surgical one. At follow-up, exclusion criteria were: restenosis, graft occlusion and cardiac events. Before revascularization, all patients were explored with delayed (4 hours) 99m-Tc MIBI nitroglycerine Quantitative Gated SPECT. The myoacardium was divided in 19 segments and uptake was graded from 0 to 3. Hibernation was identified as a decreased uptake with wall-motion abnormalities and end systolic thickening on QGS. After revascularization, the patients underwent rest 99m-Tc-MIBI QGS, at 3,6,12 and 18 months.

Results: From 107 segments identified as hibernating before revascularization, at 3 months post revascularization, 20% had improved uptake, at 6 months 43%, at 12 months 62%, at 18 months 81%.

LV ejection fraction improved ≥ 5% whenever uptake normalised. No correlation was found between the extent of hibernation and the time or the degree of recovery, similar uptake having different outcomes, from slight improvement to complete recovery and normalization of a supposed antero-septal Q-wave MI with antero-apical aneurysm.

Conclusions: Recovery of hibernation post-revascularization is a slow process. The scintigraphic identification of hibernation with delayed 99m-Tc MIBI nitroglycerine QG-SPECT can predict improvement, but not the time and the degree of recovery. The scintigraphic extent of hibernation is not predictable for the post-revascularization outcome.

OS_126

STATE OF MYOCARDIAL PERFUSION EARLY AFTER SOLE TMLR AND AFTER TMLR COMBINED WITH CABG

A. Teresińska (1), M. Œliwiński (2), B. Szumilak (1), S. Konieczna (1), M. Szymańska (2), P. Hendzel (2), Z. Juraszyński (2), A. Wojnowski (2), A. Dębski (3). (1) Department of Nuclear Medicine; (2) Cardiosurgery Clinic; (3) General Cardiology Clinic, National Institute of Cardiology, Warsaw, Poland.

Background: Transmyocardial laser revascularisation (TMLR), performed as a sole procedure or in combination with CABG, causes symptoms alleviation in high percentage of patients with advanced CAD, not amenable to complete revascularisation by CABG. Laser-stimulated angiogenesis is considered as one of the mechanisms responsible for clinical improvement but because angiogenesis is a time-prolonged process, lack of perfusion improvement early after TMLR was suggested in the literature.

Aim: The aim of this work was to assess changes in perfusion very early and 3 months after sole TMLR or after TMLR+CABG.

Methods: TMLR was performed by high-power CO_2 laser. If possible, 1-5 bypasses were implemented (av.1,7±0,9 per patient). Tc-99m-MIBI SPECT (rest and stress) was performed in 102 patients before operation (SPECT-0), very early after (av. 3 weeks, SPECT-early) and 3 months (SPECT-3m) after TMLR (44 pts) or TMLR+CABG (58 pts). In TMLR group, perfusion was studied also 6 and 12 months after operation (SPECT-6m and SPECT-12m). Perfusion was assessed in 17 segments (seg) of the LV. Only changes in transient perfusion defects detected in SPECT-0 are presented (and related to SPECT-0).

Results: In TMLR group, after exclusion of 4 septal segments never treated by laser: in SPECT-early, perfusion did not change in 58% ($CI_{0,95}$=50-66%) and improved in 28% of seg ($CI_{0,95}$=22-36%). In SPECT-3m, perfusion did not change in 53% ($CI_{0,95}$=49-59%) and improved in 26% of seg ($CI_{0,95}$=21-31%). The results were similar in next studies (SPECT-6m: 51% and 30%, SPECT-12m: 50% and 29%). In TMLR+CABG group: in SPECT-early, perfusion did not change in 30% ($CI_{0,95}$=22-39%) and improved in 58% of seg ($CI_{0,95}$=48-66%). In SPECT-3m, perfusion did not change in 25% ($CI_{0,95}$=21-29%) and improved in 56% of seg ($CI_{0,95}$=51-61%). Analysing only the revascularised segments (by bypasses), similar results were obtained: perfusion improved in 60% of seg in SPECT-early and in 63% of seg in SPECT-3m. Interestingly, analysing only the lasered segments (after exclusion of bypassed and septal segments), also similar results were achieved: perfusion improved in 54% of seg in SPECT-early and in 48% of seg in SPECT-3m (percentage significantly higher than in TMLR group).

Conclusions: During first 3 months after sole TMLR, in segments with preoperatively transient defects, perfusion increases in approximately 30% of lasered segments (similarly to the state observed 6 and 12 months after operation). If TMLR is combined with CABG, perfusion increases in approximately twice higher number of segments and it concerns to bypassed segments as well as lasered segments. So the level of perfusion improvement in lasered areas can be dependent on the level of the perfusion in the neighbouring areas.

OS_127

PREVENTION OF IN-STENT RESTENOSIS WITH LIQUID-FILLED 188-RE BALLOON: THE DRESDEN IN-STENT RESTENOSIS RADIATION TRIAL (DIRRT)

J. Kropp (1), K. Reynen (2), U. Koeckeritz (2), G. Wunderlich (1), A. Schmeisser (2), F.F. Knapp (3), R.H. Strasser (2), W.G. Franke (1). (1) Department of Nuclear Medicine, Technical University, Dresden, Germany; (2) Department of Cardiology, Technical University, Dresden, Germany; (3) Nuclear Medicine Group, Oak Ridge National Laboratory, Oak Ridge, USA.

Aim: In some studies intracoronary radiation therapy (IRT) to minimize the restenosis rate after PTCA proved to be effective. We evaluated the performance, safety and effectiveness of IRT with ^{188}Re-perrhenate filled into a standard PTCA balloon. This kind of IRT allows a self-centering homogenous dose distribution to the vessel wall.

Methods: 41 patients (pts) with a mean age of 60 years (33 m, 8 fm) with in-stent restenosis (type B in 39 %, type C in 61 %) and proven ischemia were included. After routine re-PTCA with or without additional stent implantation a second standard balloon was placed into the PTCA area and filled with β-emitting liquid ^{188}Re at 3 atm. Irradiation time was 540 +/- 155 sec to achieve a dose of 30 Gy at 0.5 mm depth of the vessel wall.

Results: In only one procedure there was a disconnection of the ^{188}Re containing system and the catheter but no contamination of the cath table or lab was measured. In 16 coronaries 21 stents were additionally implanted. In the follow-up 4 stent thromboses (1 day, 37 days, 2 x 6 months) with subsequent myocardial infarction were noticed, all in pts with additionally implanted stents. 36 pts (88 %) had control angiography after 4 to 6 months after therapy. Restenosis (stenosis > 50 %) was shown in 9 of 14 pts (64 %) with additionally implanted stents but only in 4 of 22 pts (18 %) with PTCA alone. Reocclusion was noticed in 3 (21 %) pts with additional stent but only in 1 pt (5 %) without.

Conclusions: Intracoronary radiation therapy (IRT) with β-emitting liquid-filled ^{188}Re balloon is a safe and effective therapy method which might be used routinely. Long-term results seem satisfactory in a patient group with in-stent restenosis and high risk of re-restenosis. But the positive effect of irradiation is abolished if an additional stent after PTCA is needed. These data justify a prospective double-blind randomized study which has already started.

OS_128

COMPARISON BETWEEN SONO VUE TM, A NEW SECOND GENERATION ECHO-CONTRAST AGENT, AND SPECT FOR THE EVALUATION OF MYOCARDIAL PERFUSION IN PATIENTS WITH FIXED ISCHEMIC DEFECTS: INITIAL RESULTS

L. Agati (1), D. Bokor (3), G. Veneroso (1), C. Di Russo (1), M.P. Madonna (1), T. Montesano (2), M. Ciancamerla (2), G. Ronga (2). (1) Department of Cardiology, University ; (2) Department of Clinical Sciences, University ; (3) Bracco SpA, Milan, Italy.

SonoVueTM (Bracco SpA) is a new echo-contrast agent made of microbubbles stabilized by phospholipids and containing sulphur hexafluoride. The objectives of this study were to optimize imaging/dosing parameters and evaluate SonoVue™ potential role in the assessment of myocardial perfusion defects in patients previously evaluated by SPECT.

Methods: This study was conducted in 11 CAD patients with a prior myocardial infarction and a fixed defect on recent Tc-99m sestamibi SPECT. Sono Vue™ was administered during rest as an IV bolus of 0.5 to 2 ml + 3 ml saline solution flush (4 sec injection rate) or as an infusion of 120 to 240 ml/hrs (2-4 ml/min) using Agilent Sonos 5500 or ATL HDI 5000 and real time color and grayscale imaging (rt-MCE). Two blinded reviewers evaluated all SPECT and rt-MCE images. Safety was assessed for 72 h post Sono Vue™. Myocardial perfusion was assessed using a 12-segment model (4-2-chambers apical views for rt-MCE, and horizontal and vertical long axis views for SPECT). For each segment a contrast score was calculated by both methods according to the following scale: 1. Artifact, 2. Segment not visible, 3. Normal myocardial perfusion, 4. Patchy perfusion, 5. Myocardial perfusion defect

Results: Optimized imaging conditions for rt-MCE were obtained with both platforms at 1-1.5 ml bolus and at 3-4 ml/min infusion rate. The best setting for Agilent was : Mechanical Index (MI) 0.10 (-21.5 db), color gain 60%, Pulse Repetition Frequency(PRF) max, Frame Rate (FR) 14Hz, Flash at MI 1.4 for 3-4 frames; for ATL was: MI 0.09, color gain 60%, PRF 3000 Hz, FR 24Hz, Flash at MI 1.1 for 3 frames, Dynamic Range low, Line Density C, Wall Filter high. Using these imaging/dosing parameters an excellent myocardial opacification was obtained in all patients. Good overall concordance between SPECT defect detection (79%), localization (70%) and scoring (71%) and Sono Vue™ rt-MCE imaging was achieved.

Conclusions: Preliminary data from this pilot study suggest that when appropriate imaging/dosing was used, Sono Vue™ is an excellent contrast agent for rt-MCE using different imaging platforms.

OS_129

THE TL-201 SPET ABNORMALITIES, DOCUMENTED AT REST IN DILATED CARDIOMYOPATHY, ARE RELATED TO A LOWER THAN NORMAL MYOCARDIAL THICKNESS BUT NOT TO AN EXCESS IN MYOCARDIAL WALL STRESS

N. Hassan (1), J.M. Escanyé (1), O. Claudon (2), N. David (1), P. Olivier (1), P.Y. Marie (1), J.C. Mayer (1), A. Naoun (1), Y. Juillière (2), G. Karcher (1), A. Bertrand (1)(1) Department of Nuclear Medicine; (2) Department of Cardiology, CHU-Nancy, France.

Aim It has been hypothesised that the ^{201}Tl-SPET abnormalities, which are documented in patients with dilated cardiomyopathy, might be related to local excesses in the left ventricular wall stress, leading to slow down the diastolic perfusion of myocardium. This study was aimed to analyse this hypothesis.

Methods. We included 6 normal subjects and 7 patients with idiopathic dilated cardiomyopathy who had ^{201}Tl-SPET at rest. An index of wall stress was calculated at end-diastole on a 13-segment division of the left ventricle and by applying the Laplace Law equation, thickness and curvature radii being calculated for each segment using 2 orthogonal MRI slices.

Results. Among all patients, 21 analysed segments had ^{201}Tl-SPET defects (D+) and 67 had none (D-). Myocardial thickness was lower in D+ (0.88±0.30 cm) than in D- (1.23±0.33 cm, p = 0.0002) and in segments from normal subjects (0.99±0.15 cm, p = 0.04). The index of end-diastolic wall tension was also lower in D+ (2.5±1.0 10^3N.m^{-2}.mmHg^{-1}) than in D- (3.3±1.1 10^3N.m^{-2}.mmHg^{-1}, p = 0.02) and in segments from normal subjects (3.2±1.2 10^3N.m^{-2}.mmHg^{-1}, p = 0.04). Lastly, the index of end-diastolic wall stress, determined by the ratio: wall tension index / myocardial thickness, was equivalent in D+, in D- and in segments from normal subjects (respectively: 3.0±1.4, 2.8±1.2 and 3.2±1.6 10^5N.m^{-3}.mmHg^{-1}).

Conclusion. In patients with dilated cardiomyopathy, the abnormalities documented by ^{201}Tl-SPET at rest are related to a lower than normal wall thickness, suggesting a mechanism of partial volume effects. These thinner areas are also submitted to a lower diastolic wall tension and this might protect the diastolic myocardial perfusion from any deleterious excess in wall stress.

OS_131

SKELETAL UPTAKE OF 99M-TC-HDP REMAINS UNALTERED AFTER TREATMENT OF ANKYLOSING SPONDYLITIS WITH THE ALPHA-EMITTER 224-RA

U. Kampen, W. Brenner, J. Prause, N. Czech, C. Muhle, E. Henze. Clinic of Nuclear Medicine, Kiel University, Germany.

Aim: Treatment of ankylosing spondylitis by ten cumulative injections of 1MBq 224-RaCl each is an effective analgetic therapy and got its re-approval in Europe in 02/2000. The α-emitting radionuclide is incorporated as a Calcium-analogue into sites of newly formed tissue mineralization and leads to a local irradiation with its high energy and a very short tissue penetration. Aside from the reduction of pain, a significant protraction of increasing osteogenesis is discussed due to a direct antiosteoblastic effect. Aim of this study was to quantify bone metabolism by ROI-measurement of skeletal tracer uptake in two-phase bone scanning both prior to and after treament with 224-RaCl.

Methods: Until now, eight male patients, aged from 36 to 83 years were treated with 10 MBq 224-RaCl for ankylosing spondylitis. Whole-body bone scintigraphy was performed prior to and eight weeks after therapy by i.v. injection of 600 MBq 99m-Tc-HDP. Images in both ventral and dorsal projections were acquired 3 minutes and 3 hours after tracer injection. Skeletal tracer uptake reflecting osteoblastic activity was calculated by ROI-analysis, subtracting both the bladder and a soft tissue reference-ROI from whole body activity at both imaging times (Brenner et al. 1997).

Results: Mean skeletal tracer uptake prior to 224-RaCl treatment was calculated as 21,0 ± 3,9% of the injected activity (range: 16,0 to 26,0%). Eight weeks after therapy the same mean value of 21,0 ± 3,4% was found (range: 16,5 to 25,4%). In the individual patient, the mean alteration of skeletal uptake was only 1% (range: -0,6 to +5,6%). No harmful side effects were seen after treatment with 224-RaCl.

Conclusions: No reduction of osteoblastic activity reflecting bone metabolism could be found by means of ROI-analysis in bone scanning with 99m-Tc-HDP up to eight weeks after treatment of ankylosing spondylitis with 10 MBq of the α-emitter 224-RaCl. Thus, the proven delay of ankylosis during clinical follow-up seems to be a result of eased physical therapy due to the alleviated pain. There is still no evidence for a direct antiosteoblastic effect of 224-RaCl on a cellular level.

RADIONUCLIDE THERAPY / DOSIMETRY

OS_130

TREATMENT OF ANKYLOSING SPONDYLITIS WITH 'THE NEW' RADIUM-224 CHLORIDE

J. Prause, W.U. Kampen, W. Brenner, C. Muhle, N. Czech, E. Henze. Clinic of Nuclear Medicine, Christian-Albrechts-University, Kiel, Germany.

Radium-224, a calcium-analogue and alpha-emitting radionuclide, is incorporated into sites of newly formed tissue mineralization. It is approved in Europe since January 2000 for the treatment of patients with ankylosing spondylitis. Lokal radiation leads to reduction of pain and an improved mobility. The aim of this study was to evaluate the analgetic effect and the influence of Ra-224Cl on spine mobility.

Methods: We treated a total of 11 male patients with ankylosing spondylitis grade II - III and pain under antiphlogistic drug therapy (mostly NSAID's). The treatment consisted of 10 injections of 1 MBq Ra-224Cl each, given at weekly intervals. Blood cell-counts, serum C-reactive Proteine, electrolytes, ESR and liver enzymes were measured weekly. For clinical evaluation we used fingertips-to-floor distance, Schober- and Ott-Test for lumbal and thoracal spine mobility, occiput-to-wall Test, chest expansion and evaluation of pain symptoms 1 week prior to therapy and 4 weeks after the last radionuclide injection.

Results: The fingertips-to-floor distance decreased by 5 cm (range: 0 - 14 cm), the Ott-Test decreased by 0.7 cm (range: 0 - 1 cm) and the Schober-Test increased by 0.5 cm (range 0 - 1.5 cm). The occiput-to-wall distance decreased by 1.2 cm (range 0 - 6 cm), the chest expansion showed no significant changes. The analgetic / antiphlogistic drugs were completely stopped in 3 and reduced in 6 of 11 patients. No change in drug therapy occured in one case and one patient had no drugs prior to treatment. C-reactive Proteine decreased, all the other blood parameters investigated showed no significant changes.

Conclusion: In our preliminary study we observed a good analgetic effect of Ra-224Cl. However the stiffness of the spine showed no significant changes. This might be due to our comparatively short follow-up period since metabolic effects such as reduced tissue mineralization are considered long-term effects. Ongoing studies will prove this hypothesis. Substantial benefit from radionuclide therapy with Ra-224Cl will have patients without advanced spinal ankylosis but severe pain despite antiphlogistic drug therapy.

OS_132

THERAPY WITH RHENIUM-186 HEDP IN MEDICATION-REFRACTORY PATIENTS WITH PAINFUL MULTIFOCAL ARTHRITIS: PRELIMINARY RESULTS OF A PROSPECTIVE STUDY

H. Palmedo (1), JK. Rockstroh (2), M.J. Reinhardt (1), K. Schliefer (2), J. Risse (3), C. Menzel (3), HJ. Biersack (1). (1) Department of Nuclear Medicine, Bonn, Germany; (2) Department of Internal Medicine, Bonn, Germany; (3) Department of Nuclear Medicine, Frankfurt, Germany.

Polyarthritis associated to a variety of systemic diseases can be difficult to treat if patients do not respond to anti-inflammatory therapy or if severe side effects appear. The aim of this ongoing study was to evaluate the effect of systemic therapy with rhenium-186 HEDP on disease activity in patients with polyarthritis. Method: 8 patients (4 rheumatoid arthritis, 3 psoriatic arthritis, 1 systemic lupus erythematosus) with 77 affected joints received a total of 10 injections of rhenium-186 HEDP with a standardized average dosage of 570 MBq (range 496-688 MBq). Assessment of pain and disease activity was performed according to the core set of the American College of Rheumatology including the parameters tender joint count, swollen joint count, patient's global assessment of disease activity, physician's global assessment of disease activity, acute phase reactant value. Follow-up was performed monthly after treatment for at least 9 months. Results: In 6 out of 8 patients (75%), a single rhenium-186 HEDP injection led to an improvement of disease activity. The duration of response was 3 months at an average (range 2 to 13 months). A decrease of painful and swollen joint count was observed in 5 (average decrease of 6.2 joints) and 4 (average decrease of 2.25 joints) patients, respectively. Patient's and physician's global assessment of disease activity correlated well with improvement of painful or swollen joints. In four patients, erythrocyte sedimentation rate showed a mean decrease from a pretherapeutic value of 57 mm/h to 30 mm/h. Repetitive therapy performed in two patients prolonged the duration of response. Conclusions: Our preliminary data show that systemic low dose treatment with Rhenium-186 HEDP can reduce disease activity in patients with polyarthritis due to rheumatoid arthritis, psoriatic arthritis and systemic lupus erythematosus. It seems that repetitive therapy can prolong the duration of response. Further investigations are justified to confirm these encouraging results.

OS_133

A CLINICAL FOLLOW-UP STUDY OF RADIATION SYNOVECTOMY

W. Brenner, W.U. Kampen, E. Henze. Clinic of Nuclear Medicine, Christian-Albrechts-University, Kiel, Germany.

The aim of this prospective study was to evaluate the clinical outcome after radiation synovectomy in patients suffering from synovialitis as proven by three-phase bone scanning.
Methods: After treatment with intraarticular application of either Y-90-colloid, Re-186-colloid or Er-169-citrate, all 178 patients with a total of 551 treated joints were divided into three subgroups according to the underlying ethiology of their disease: rheumatoid arthritis (I), inflammatory joint disease other than rheumatoid arthritis (e.g psoriatic arthritis, postinfectious arthritis etc.) (II), osteoarthritis (III). All patients were examined 12-18 months after therapy with a standardized questionnaire concerning pain improvement, improvement of the grade of handicap during daily activities as well as questions according to the ARA criteria for rheumatoid arthritis judging each question by the categories excellent improvement, moderate improvement, unchanged or worsened.
Results: In 67 % of all joints a moderate to excellent improvement was found. The best results were obtained in patients with rheumatoid arthritis: in 74 % of these subjects a clinical improvement could be proven compared to a success rate of 51 % in patients of group II and of only 35 % in patients with osteoarthritis. An aggravation of the clinical symptomes up to 18 months after therapy occured in only 2 % of the treated joints in group I and II while in patients with osteoarthritis a clinical worsening was found in 8 %. Major side effects such as infection or necrosis were observed in none of the patients. In patients with rheumatoid arthritis radiation synovectomy yielded the best results in the proximal interphalangeal joints (85 %) while in wrist joints improvement was achieved in only 62 %. In patients of group II best results were obtained for the knee joints (75 %) while treatment of finger joints was successful in only 8 %. In case of osteoarthritis an improvement was found in only 24 % of the joints of the upper limb while radiation synovectomy was successful in 44 % of the ankle and knee joints.
Conclusions: Radiation synovectomy is an effective and safe therapeutic modality for patients suffering from inflammatory joint disease with the best clinical results obtained in rheumatoid arthritis. In case of osteoarthritis with proven synovitis the success rate however was rather low in joints of the upper limb suggesting radiation synovectomy in these patients only as a last attempt prior to surgical treatment.

OS_134

EXPERIMENT STUDY OF 188RE-SULFIDE RADIOSYNOVECTOMY IN RHEUMATOID ARTHRITIS MODEL OF RABBIT

L.Y. Zhang, G. Chen, X.F. Jiang, P.Y. Li. Department of Nuclear Medicine, Ruijin Hospital, Shanghai Second Medical University, Shanghai, China.

Objective: 188Rhenium is a new therapeutic isotope interested by many researchers. The purpose of this study is to evaluate the effect of 188Re-sulfide to synovium and cartilage in animal model.
Materials and methods: 14 rabbits of antigen-induced rheumatoid arthritis model were studied. In 10 models, 4 knee joints of each rabbit were divided into two groups. For the therapeutic group, 18.5MBq/0.2ml 188Re-sulfide suspension was injected intra-articularly, and 0.2ml saline was used for control group. Histopathology study on paraffin sections of synovial tissues was performed in two groups 21 days after the administration of 188Re-sulfide. To evaluate the injury caused by the radiation to the cartilage covering articular surface, the other 4 rabbit models were injected intra-articularly with 188Re-sulfide suspension in four different dosages ranging from 7.4MBq/0.2ml to 37MBq/0.2ml. 6-8 months after administration, the effects of the 188Re-sulfide to cartilage were assessed by means of undecalcification sections with H-E stain.
Results: The knees of rheumatoid arthritis rabbit model in control group were swollen and hyperemia with inflammatory cells infiltration and proliferated synoviocytes filled in synovial tufts. After treatment with intra-articular injection of 188Re-sulfide suspension, the inflammatory cells reduced markedly, adipose cells in fat pad atrophied and the synovium became thinner in all specimens inspected. The examination of cartilage indicated that cartilaginous tissues remain normal in structure when 7.4MBq/0.2ml, 14.8MBq/0.2ml or 22.2MBq/0.2ml 188Re-sulfide suspension was injected respectively. But when the dosage of 188Re-sulfide suspension was increased to 37MBq/0.2ml, the cartilaginous tissues became thinner, the structure disturbed and the tidal-line disappeared.
Conclusion: 188Re-sulfide radiosynovectomy did play a part in the improvement of synovitis in rheumatoid arthritis. For clinical application, dosage calculation is important to avoid side effect such as cartilage damage.

OS_135

BIOLOGICAL EVALUATION AND PET EXAMINATION IN MONKEY OF [3H]- AND [11C]-5-METHYL-6-NITROQUIPAZINE - A POTENTIAL SEROTONIN TRANSPORTER RADIOLIGAND FOR USE BOTH IN VITRO AND IN VIVO

C. Halldin (1), J. Sandell (1), J. Sóvágó (1), Y.H. Chou (1), B. Gulyás (1), S. Chalon (2), M. Yu (3), P. Emond (2), D. Guilloteau (2), K. Någren (3), L. Farde (1)(1) Karolinska Institutet, Department of Clinical Neuroscience, Psychiatry Section, Karolinska Hospital, Stockholm, Sweden; (2) Inserm U316, Université Francois Rabelais, Tours, France; (3) Turku PET Centre, Radiopharmaceutical Chemistry Laboratory, Turku, Finland.

Aim: Neuronal uptake of serotonin (5-HT) occurs via a serotonin transporter (5-HTT) protein which plays a major role in the regulation of synaptic 5-HT levels. PET examination of the 5-HTT would be of great value in order to better understand the pathophysiological mechanisms of several neurodegenerative and mental illnesses such as Parkinson's disease and depression, as well as to quantify 5-HTT-occupancy in relation to antidepressant drug treatment. 6-nitroquipazine is one of the most selective and potent 5-HTT inhibitors known. The 5-position has been shown to be suitable for halogen substitution yielding halogenated analogues equipotent such as [^{123}I]5-iodo-6-nitroquipazine and [^{76}Br]5-bromo-6-nitroquipazine. The present work deals with the synthesis, radiolabeling and biological examination of a 5-methyl-6-nitroquipazine analogue, [^{3}H or ^{11}C]MNQP.
Methods: The stannyl precursor was synthesized according to a procedure reported previously. [^{3}H or ^{11}C]MNQP was prepared from the stannyl precursor in a two-step procedure. The first step was a palladium-promoted cross-coupling reaction with [^{3}H or ^{11}C]methyl iodide and finally, the BOC-group was removed with TFA. The dissociation constant of [^{3}H]MNQP was determined using rat frontal cortex cell homogenates. [^{11}C]MNQP was injected i.v. into a Cynomolgus monkey and examined during baseline and pretreatment conditions with PET. Radiolabeled metabolites were measured in plasma using a gradient HPLC method.
Results: The isolated yield of [^{3}H or ^{11}C]MNQP after purification by reversed-phase HPLC was 60% within 40 minutes, with a specific radioactivity of 3 and 25 GBq/μmol, respectively, and a radiochemical purity >99%. The dissociation constant (K_d) of [^{3}H]MNQP was found to be 51±7pM. After i.v. injection of [^{11}C]MNQP in a Cynomolgus monkey the radioactivity in brain was high (4.5%). The radioactivity was high in regions known to contain 5-HTT sites such as the thalamus and brainstem. The ratio of the thalamus to cerebellum and brainstem to cerebellum were about 1.5 at 90 minutes. Pretreatment with the selective 5-HTT inhibitor citalopram (5 mg/kg, 30 min b.i.) reduced the specific uptake in these regions by 60-70%. [^{11}C]MNQP was mainly metabolised to more polar metabolites as measured by HPLC (60% unchanged at 30 minutes).
Conclusions: In conclusion, 5-methyl-6-nitroquipazine can be efficiently radiolabeled using [^{3}H or ^{11}C]methyl iodide. [^{3}H]MNQP has a high *in vitro* affinity for 5HTT. Pretreatment with citalopram indicates that [^{11}C]MNQP binds specifically to the 5-HTT in the primate brain *in vivo*.

OS_136

RADIOSYNTHESIS, METABOLISM, AND BIODISTRIBUTION OF [BR-76]BROMOPACLITAXEL ([BR-76]BPAC), A POTENTIAL PET TRACER FOR PACLITAXEL

C. Kao, D. Kiesewetter, E. Jagoda, Y. Ma, L. Ravasi, L. Szajek, W. Eckelman. Positron Emission Tomography Department, National Institutes of Health, Bethesda, Maryland, USA.

Aim: Multidrug resistance often causes failure in chemotherapy by removing drugs such as paclitaxel from tumor cells through p-glycoprotein (Pgp). Thus, paclitaxel labeled with positron emitting bromine-76 (T1/2: 16.2 h) coupled with PET has the potential to assess the efficacy of cancer treatment using paclitaxel. This abstract reports on radiosynthesis, biodistribution in rats, and *in vivo* and *in vitro* metabolism of [Br-76]BPAC.
Methods: Radiosynthesis. Natural arsenic metal (0.2 g) was bombarded by He-3 particle (17.7 MeV) and the resulted irradiated target was mixed with sodium dichromate (1.5 g) and aqueous H_2SO_4 (10 ml, 50% v/v). The mixture was heated at 125°C for 30 min and Br-76 was distilled into a NH_4OH solution. Trimethylstannylpaclitaxel (0.04 mg, 0.04 ml CH_3CN), [Br-76]NH_4Br (0.01 ml H_2O, 90 MBq), and peracetic acid (0.03 ml, 0.3% in HOAc) were mixed and heated at 70°C for 10 min. The product was purified by reversed phase HPLC. Biology. Supernatant from [Br-76]BPAC/human hepatocyte incubation (37°C) were analyzed by LC/MS for *in vitro* metabolism. Adult male rats injected with [Br-76]BPAC were sacrificed at 1 and 4 h post injection (p.i.), and organs were counted for the activity. Blood and liver samples were taken and their CH_3CN extracts were analyzed by TLC for metabolites.
Results: Distillation of Br-76 from the irradiated target yielded [Br-76]NH_4Br in 59±14% (n=17) with minimal chemical contaminants. One step electrophilic bromodestannylation yielded [Br-76]BPAC in 57.4±6.3% (n=5). Radiochemical purity remained >95% for at least 30 h in EtOH. *In vitro* metabolism study showed the Br-76 compound was 65% intact after 4 h incubation with human hepatocytes. The rest of activity was represented by only one metabolite. Biodistribution data (as Differential Uptake Ratio: %ID/g x body wt(g)/100, n=5) revealed that liver (2.70±0.27) and kidney (2.22±0.26) had the most activity at 1 h p.i. Plasma clearance was rapid (0.10±0.01, 1 h p.i.) but metabolism was slow. The compound was approximately 50% parent in blood for both 1 and 4 h. *In vivo* liver metabolism showed 50% as intact [Br-76]BPAC at 1 h and 46% at 4 h.
Conclusions: We have prepared [Br-76]BPAC with high radiochemical purity under facile condition. Metabolism and biodistribution studies suggested this compound suitable for *in vivo* imaging. The results warrant further studies to investigate [Br-76]BPAC usefulness as a paclitaxel marker.

OS_137

I123 AND F18 LABELLING AND IN VIVO EVALUATION OF ORG 13063, SPECT AND PET RADIOLIGANDS FOR THE 5-HT1A RECEPTOR

M. Vandecapelle (1), F. De Vos (6), H. Vermeirsch (2), K. Strijckmans (3), K. Audenaert (6), D. Leysen (4), G. De Ley (5), R. Dierckx (6), G. Slegers (1). (1) Department of Radiopharmacy; (2) Department of Morphology; (3) Department of Analytical Chemistry, Institute for Nuclear Sciences, Ghent University, Ghent, Belgium.

Aim: Org 13063 or 4-fluoro-N-{2-[4-(6-trifluoromethyl-2-pyridinyl)-1-piperazinyl]ethyl}benzamide (⊥.F) is a full 5-HT_{1A} agonist with high affinity (pK_i=9.3) and selectivity (1000 fold (towards 5-HT_{2A}) and higher) for this receptor subtype and has a calculated lipophilicity value (clog P) of 3.44. The iodine derivative (⊥.I) of Org 13063 was found to have lower *in vitro* affinity (pK_i=8.2) without loss of selectivity and was considerably more lipophilic (clogP=4.28). Our aim was to label and evaluate these ligands for PET and SPECT.

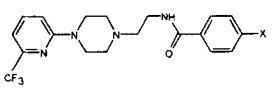

X = F ⊥.F
X = ^{18}F ⊥.^{18}F
X = I ⊥.I
X = ^{123}I ⊥.^{123}I
X = NO2 ⊥.NO2

Methods and Results: 4-[^{123}I]Iodo-N-{2-[4-(6-trifluoromethyl-2-pyridinyl)-1-piperazinyl] ethyl}benzamide (⊥.^{123}I) was synthesized by electrophilic iododestannylation of the tributyltin derivative using n.c.a. [^{123}I]NaI and chloramine-T (20 min, ambient temperature). Radiochemical yield averaged around 60 % with radiochemical purity higher than 99 %. Specific activity was at least 222 GBq/µmol (6 Ci/µmol). Biodistribution studies with ⊥.^{123}I were performed in rats leading to 0.22 % ID in the brain at 5 min *p.i.* At none of the selected time points, radioactivity concentration of brain was significantly higher than that of blood and no specific binding of this tracer could be demonstrated. The combination of agonist action with relatively high lipophilicity and relatively low affinity probably explains the predominance of non specific binding in the brain.

We tried to enhance the ratio specific to non specific binding by labelling of ⊥.F with ^{18}F. This should give better results because of the higher affinity of this ligand for the 5-HT_{1A} receptor and its lower clogP value.

4-[^{18}F]Fluoro-N-{2-[4-(6-trifluoromethyl-2-pyridinyl)-1-piperazinyl]ethyl}benzamide (⊥.^{18}F) was synthesized by nucleophilic aromatic substitution on the nitro precursor in a microwave oven (5 min, 700 W). Overall radiochemical yield was 20 % (EOB), chemical and radiochemical purity were respectively higher than 95 and 99 %. Specific activity was always higher than 18.5 GBq/µmol (500 mCi/µmol). Biodistribution studies in rabbits were performed leading to 0.77 % ID in the brain at 5 min *p.i.* Radioactivity concentration of brain was significantly higher than that of blood but no specific binding of this tracer could be demonstrated.

Conclusions: As we expected, brain to blood ratios turned out to be much better for ⊥.^{18}F than for ⊥.^{123}I, probably because of its lower lipophilicity. Allthough, the affinity of ⊥.^{18}F is 10 times higher than that of ⊥.^{123}I, no specific binding could be demonstrated in the different 5-HT_{1A} rich brain regions. Affinity probably still isn't high enough because of the agonistic activity of the tracer.

OS_138

SYNTHESIS, BIODISTRIBUTION AND BLOCKING STUDIES IN MICE OF A NEW 123I-LABELED DOPAMINE D3 ANTAGONIST

L. Staelens (1), F. Dumont (1), F. Devos (1), R. Oltenfreiter (1), M. Vandecapelle (1), I. Goethals (2), R.A. Dierckx (2), G. Slegers (1). (1) Laboratory of Radiopharmacie, Ghent University, Ghent, Belgium; (2) Department of Nuclear Medicine, University Hospital, Ghent, Belgium.

Although many neurotransmitter systems are implicated in the pathophysiology of schizophrenia, treatment is usually based on blockade of dopamine transmission. Recent developments in molecular biology lead to the classification of dopamine receptors in five subtypes. For one of these, the D_3 receptor, it has been postulated that receptor levels are elevated in schizophrenia. The development of a labeled selective ligand for the D_3 receptor could be useful to better understand the biological basis of schizophrenia. the aim of this work was to synthesize 4-[^{123}I]iodo-N-(4-(4-(2-methoxyphenyl)-1-piperazinyl)butyl)-benzamide, and to investigate its biodistribution and specificity for the D_3 receptor.

Methods: The ^{123}I labeled compound was synthesized by electrophilic iododestannylation of the tributyltin derivative (1µmol) using CAT (1µmol), HOAc (5µl) and n.c.a. [^{123}I] NaI (10 min, ambient temperature). 37 kBq of the ^{123}I labeled compound dissolved in a mixture water/ethanol (99/1) was injected i.v. into the tail vein of NMRI mice. At various time points p.i. the mice were sacrificed and dissected. Biodistribution studies were performed until 48 hours p.i.. For blocking studies the mice were injected with cold product (1mg/kg) 10 minutes before tracer injection.

Results: Radiochemical yield was approximately 70 %. Chemical and radiochemical purity were respectively >99 % and >95 %. Biodistribution studies showed penetration through the blood brain barrier and accumulation in the brain (brain blood ratio is 10 after 10 min). Pretreatment with cold product resulted in a decrease of accumulation of the tracer in the brain (brain blood ratio is 1.6 after 10 min).

Conclusion: Both biodistribution and blocking studies show that 4-[^{123}I]iodo-N-(4-(4-(2-methoxyphenyl)-1-piperazinyl)butyl)-benzamide is a potential SPECT tracer for in vivo visualization of the dopamine D_3 receptor.

OS_139

PHARMACOLOGICAL CHARACTERIZATION OF N,N-DIMETHYL-2(2-AMINO-4-METHYLPHENYLTHIO)BENZYLAMINE OR MADAM AS A RADIOLIGAND OF THE SEROTONIN TRANSPORTER WITH HIGH AFFINITY AND SELECTIVITY

D. Guilloteau (1), J. Tarkiainen (2), L. Garreau (1), J. Vercouillie (1), P. Emond (1), J.C. Besnard (1), C. Halldin (2), S. Chalon (1). (1) INSERM U316, Lab Biophysique, Tours, France; (2) Karolinska Institutet, Dept Clin Neurosci, Stockholm, Sweden.

Aim: The serotonin transporter (SERT) has a major role in serotoninergic neurotransmission and can be involved in several pathological situations such as depressive disorders. Several radiolabeled compounds have been proposed to study this transporter *in vitro* and *in vivo* by PET or SPECT. Among them, the iodinated diphenyl sulfide derivative ADAM appears to be the best tracer in terms of affinity and selectivity properties for SPECT exploration. However, this tracer labelled with ^{11}C is not suitable for PET exploration due to its long specific binding kinetics. In order to obtain a tracer with high affinity and selectivity for the SERT and *in vivo* binding kinetics suitable for PET, we developed a derivative of ADAM: the N,N-dimethyl-2(2-amino-4-methylphenylthio)benzylamine or MADAM. We describe here the pharmacological characterization of this compound.

Methods: [^{3}H]MADAM was prepared from its desmethylated precursor and was obtained with a specific radioactivity of 85 Ci/mmol. *In vitro* binding experiments were performed on rat cortical membranes to determine the affinity and selectivity of MADAM using different competitors of the serotonin, dopamine and noradrenaline transporters. Autoradiographic experiments were performed on cerebral slices from rats which serotoninergic pathway was normal or lesioned with 5,7-dihydroxytryptamine (40 µg infused in the dorsal and medial raphe 3 weeks before brain removal for binding studies).

Results: [^{3}H]MADAM bound to the SERT with a Kd of 59.62 ± 8.93 pM and Bmax of 543 ± 181 fmol/mg protein (n = 5 independent experiments each performed in triplicate). The rank order of potency of competing drugs was MADAM = ADAM > paroxetine > citalopram > PE21 > nisoxetine > desipramine = GBR 12935. Autoradiographic studies showed a high and specific binding of [^{3}H]MADAM in areas rich in SERT such as the frontal cortex, dorso-lateral thalamus, superior colliculus, dorsal and medial raphe. This binding was almost totally abolished on cerebral slices from animals lesioned with 5,7-dihydroxytryptamine.

Conclusions: MADAM is a SERT ligand with very high affinity and selectivity. These findings associated with preliminary *in vivo* experiments are in agreement with the use of this tracer for *in vitro* and PET study of the SERT.

NEUROLOGY / PSYCHIATRY

OS_140

INSULAR CORTEX INVOLVEMENT IN MESIOTEMPORAL LOBE EPILEPSY USING POSITRON EMISSION TOMOGRAPHY

V. Bouilleret (1), S. Dupont (1), L. Spelle (1), M. Baulac (2), Y. Samson (1), F. Semah (1). (1) SHFJ, CEA, DRM, Orsay, france; (2) Pitie Salpetriere, Paris, France.

Aim: Somesthetic and emotional symptoms which are common in patients with mesial temporal lobe epilepsy (MTLE) are usually related to hippocampo-amygdalar complex involvement. Recent stereo-electroencephalographic studies have shown a relationship between such symptoms and epileptic insular discharges. To further investigate this problem, we carried out a PET study using fluorodeoxyglucose (^{18}F-FDG) and flumazenil (^{11}C-FMZ) in patients with MTLE. The aim of our study was to assess the existence of a cortical insular involvement, to examine its clinical correlates and the relationship between the postoperative outcome and the insular involvement.

Methods: FDG and FMZ PET studies were carried out in 18 patients with MTLE. A statistical parametric mapping (SPM96) was performed to analyze the data in comparison to 18 healthy volunteers. For each set of FDG and FMZ images a group and an individual analysis were performed. Focusing on the metabolic abnormalities, we also investigated the role of insular cortex in the symptoms experienced by the patients and we also studied the prognostic value of insular metabolic abnormalities.

Results: Highly significant (p<.001) hypometabolism and BZR binding decreases were detected in the insular cortex. Insular involvement (mainly ipsilateral to the seizure focus) was present in 70% of the patients. Emotional symptoms correlated with hypometabolism in the anterior part of the ipsilateral insular cortex, while somesthetic symptoms correlated with hypometabolism in the posterior part (p=.001). No relationship between postoperative outcome and ipsilateral insular hypometabolism was found.

Conclusions: Unilateral MTLE is associated with insular hypometabolism and BZR loss. Our results also suggest that the anterior part of the insular cortex is involved in the emotional symptoms while the posterior insular cortex is involved in the somesthetic symptoms. Hypometabolism localized to the insula did not influence the postoperative outcome after anterior lobectomy.

OS_141

A PET STUDY OF THE STRIATAL DOPAMINE UPTAKE IN PATIENTS WITH EPILEPTIC SEIZURES ASSOCIATED WITH RING CHROMOSOME 20 MOSAICISM

M.J. Ribeiro (1), F. Semah (1), P. Remy (1), F. Dollé (1), V. Bouilleret (1), A. Depaulis (2), A. Biraben (3). (1) Service Hospitalier Frédéric Joliot, DSV-CEA, Orsay, France; (2) Inserm U398, Strasbourg, France; (3) Unité d'Epileptologie, CHU, Rennes, France.

Aim: Several recent studies reported the electroclinical features in patients with epileptic seizures associated with ring chromosome 20 mosaicism. In these patients, ictal EEG do not always demonstrate a correlation between EEG abnormalities and clinical symptoms, like „absences" seizures with pseudo-focal onset or hypertonic seizures while EEG demonstrated generalized patterns. One of the most striking feature is the long duration of the seizures, lasting for more than 10 to 15 minutes. Recent animal studies suggested that the epileptogenic network might be controlled by inhibitory network involving the basal ganglia. To test this hypothesis we performed positron emission tomography (PET) with ^{18}F-L-DOPA.
Methods: Ten patients (7 males, 3 females; 22.9±7.0 years old) with a drug-resistant form of epilepsy and a mosaicism with one of the cell clones carrying a ring chromosome 20 were studied in PET with ^{18}F-L-DOPA using an ECAT EXACT HR+. The uptake constant (Ki, min^{-1}) of this radiotracer was calculated in the caudate nucleus and the putamen of each patient, using the occipital activity as a non-specific input function. The results obtained were averaged over both hemispheres and compared to the corresponding mean values calculated in controls studied with ^{18}F-L-DOPA in our center (6 males, 2 females; 40.4±14.9 years old).
Results: The Ki values (table 1) measured in epileptic patients were decrease in both striatal structures when compared with those obtained to the control subjects ($p<0.01$ and $p<0.05$, for caudate nucleus and putamen respectively):

Table 1- Ki (min^{-1}) values (mean±standard deviation) obtained for caudate and putamen nuclei respectively in epileptic patients and in normal subjects.

	Ki (min^{-1}) Caudate nucleus	Ki (min^{-1}) putamen
Epileptic patients	0.0107±0.0010	0.0105±0.0011
Normal subjects	0.0126±0.0013	0.0117±0.0010

Conclusion: These preliminary results showed that the dopaminergic function is altered in epileptic patients with a drug-resistant form of epilepsy associated to a ring chromosome 20 mosaicism. They suggested that the dopaminergic system could explain the absence of specificity of the seizures of this kind of epilepsy and that it might be involved in the long duration of the seizures in these patients.

OS_142

VALIDATION OF INTRACAROTID AMOBARBITAL TEST WITH HMPAO BRAIN SPECT

F.J. Setoain (1), F. Lomeña (1), S. Arroyo (2), D. Pareto (1), J. Pavá (1), A.M. Catafau (3), J. Rumiá (4), F. Martin (1), M. Ortega (1), F. Pons (1). (1) Nuclear Medicine Department, Hospital Clinic. Barcelona; (2) Neurology Department, Hospital Clinic. Barcelona; (3) Nuclear Medicine Department, Hospital de Santa Creu i Sant Pau. Barcelona; (4) Neurosurgery Department, Hospital Clinic. Barcelona, Spain

Aim: The intracarotideal amobarbital (ICA)test or Wada test is performed in patients with temporal lobe seizures (TLS), before temporal lobectomy (TL), in order to predict postoperative speech and memory dysfunction. Because of the variability in vascular supply of the hippocampal formation, amobarbital may not anesthetize the hippocampus, producing a erroneous interpretation of the Wada test in predicting memory dysfunction. Our aim was to evaluate with HMPAO brain SPECT if the hippocampus has been anesthetized with the ICA injection, in order to determine the validity of the memory test results during the Wada test.
Methods: ICA test was performed on 39 patients with intractable TLS prior to surgery. There were 18 males and 21 females with a mean age of 30 ± 9 years. Memory was evaluated with the Wechsler Memory Scale to quantify memory function before and during one year follow-up after TL.
Following the catheterization of the internal carotid artery, 125 mg of amobarbital was injected on the side of the seizure focus. A dose of 740 MBq of HMPAO-Tc99m was injected intravenously immediately after the patients developed a contralateral hemiparesis. An interictal SPECT with the same procedure was used as a baseline SPECT, in order to compare the perfusion changes after amobarbital. Both SPECTs were reoriented and normalized according to total pixel counts in the brain and then subtracted from each other to obtain a difference image. A 5% discontinuing parametric color scale was used to quantify the perfusion reduction percentage (PRP) produced with the ICA injection. We consider the hippocampus inactive if PRP in the hippocampus was 25% or greater than the PRP in the lateral temporal lobe.
Results: Mean blood flow reduction percentage (PRP) of amobarbital in brain (%):

Frontal	Parietal	Lateral Temporal	Contralatera Cerebellum	Occipital	Mesial Temporal
11	11.1	9.8	11.4	2.6	2.3

Brain SPECT demonstrated that the hippocampus was only anesthetized in 33% (13/39) of cases. Memory evaluation during Wada test was actually only reliable in 13 of these patients. Any of this 13 patients developed postoperative amnesia. SPECT showed that the hippocampus was not anesthetized in 26 patients (66%) and 9 of these 26 patients (34.5%) developed memory impairment after the TL.
Conclusions: SPECT could be useful for evaluating hippocampal function during the Wada test. There is a high risk of amnesia after TL where hippocampus has not been anesthetized during ICA test.

OS_143

I-123-IOMAZENIL BRAIN SPECT IN DRUG RESISTANT EPILEPSY

M. Piga (1), R. Fele (1), G.L. Loi (1), A. Serra (1), M. Puligheddu (2), F. Marrosu (2). (1) Nuclear Medicine; (2) Neurology, University Hospital, Cagliari, Italy .

The amino acid gamma-aminobutyric-acid (GABA) prevails in the CNS as an inhibitory neurotransmitter that mediates its effects through GABA-gated Cl(-)-channels ($GABA_A$). $GABA_A$ receptors ($GABA_AR$) are selectively modulated by benzodiazepines (BDZ). The blockade of the $GABA_AR$ make epileptiform bursts appear in response to focal stimuli indicating that $GABA_AR$ inhibition exert an important role in controlling neuronal excitability. The aim of this study was to evaluate the BDZ receptors brain distribution in drug resistant epileptic patients.
Methods: a total of six patients affected by severe drug resistant epilepsy, 3 with primary generalized epilepsy and 3 with complex partial seizures, were studied. All patients underwent a complete neurological examination including standard, video and 24-hours Holter EEG. Magnetic resonance imaging (MRI) with contrast-enhancement was performed in order to role out secondary epilepsy . Two hours delayed brain SPECT was made after injection of 111 MBq I-123-iomazenil (^{123}I-IMZ) using dual head γ-camera equipped with high resolution fan-beam collimators. Results are blindly evaluated by visual analisys by two expertised phisicians.
Results: Although the patients studied belong to both generalized and partial epilepsy, they present the common trait of complete resistence to traditional and new antiepileptic drugs (AEDs). EEG results were congruent with severe interictal epileptiform activity, lateralized and/or generalized during the wakefulness and non-rem sleep. MRI yielded normal findings ruling out, among other, temporal-mesial sclerosis and vascular abnormalities. ^{123}I-IMZ Spect showed focal (1 subject) or patched (4 patients) low concentration of cortical $GABA_AR$, while, the only patient showing normal pattern was affected by a less severe form of generalized epilepsy. Interestingly, the patient showing a focal decrease in ^{123}I-IMZ uptake presented interical regional spiking EEG activity congruent with SPECT localization of $GABA_AR$ reduction. Normal $GABA_AR$ concentration was observed in extraneocortical areas including cerebellum.

Patient	Epilepsy	EEG	MRI	^{123}I-IMZ SPECT
C.L.	Complex partial	Focal spiking activity	Normal	Patched decrease
L.M.	Complex partial	Focal spiking activity	Normal	Patched decrease
P.AL.	Primary generalized	Generalized s.a.	Normal	Patched decrease
M.E.	Primary generalized	Generalized s.a.	Normal	Normal
M.F.	Primary generalized	Generalized s.a.	Normal	Patched decrease
S.M.	Simple partial	Focal spiking activity	Normal	Focal decrease

Conclusions: Our results show that $GABA_AR$ are altered in both generalized and partial AEDs resistant epilepsy. This finding, is, for some extent, at variance with the results obtained in other studies which highlighted the significant $GABA_AR$ decrease in focal epilepsy. However the condition of drug resistence emphasize the capital role played by $GABA_AR$. It is well know from stereo-EEG studies the crucial role played by the cortex in synchronizing the epileptic discharge in both genearalized and partial epilepsy. Since most of the AEDs act enhancing the GABA cortical competence in all forms of epilepsy we suggest that the decrease of BDZ receptors may be a common mechanism in drug resistant epileptic activity.

OS_144

ICTAL/POSTICTAL BRAIN SPECT PERFUSION PATTERN MODEL IN THE LOCALIZATION OF EPILEPTOGENIC FOCI: A PROSPECTIVE STUDY

K. Borbély (1), A. Balogh (2), V. Juhos (2), A. Sólyom (1). (1) National Institute of Neurosurgery, Budapest, Hungary; (2) Szent-István Hospital, Budapest, Hungary.

Objectives: SPECT has been proved to be a sensitive and specific method in the presurgical evaluation of patients with complex partial seizures. Ictal minus interictal rCBF analysis is a routine part in the assessment of epileptogenic foci. During ictal studies patients might have secondary generalizations or rCBF changes might appear not only in the epileptogenic area, but also in remote areas of the brain. The precise note of the time of the tracer injection for SPECT is the key in interpreting the brain perfusion changes. We studied ictal/postictal rCBF patterns in the brain tissue within, adjacent to, and remote from the epileptogenic foci in 56 patients with complex partial seizures.
Methods: The assessment included neurological examination, ictal semiology, interictal and ictal electrophysiological recording, MRI, and neuropsychological evaluation. Baseline, ictal and/or postictal SPECT studies were carried out with a standard technique for each patient. SPECT data were analysed visually and by a special region of interests (ROIs) program. Circular ROIs were placed over the basal ganglia, frontal, temporal, parietal, occipital cortex, and cerebellum. ROIs were normalized to the whole brain average. The statistical analysis was considered significant at $P \leq 0.05$. MRI was positive in 39 patients, while in 17 cases there were no abnormalities. SPECT results were compared to electrophysiological and surgical findings.
Results: The baseline SPECT demonstrated a significant hypoperfusion (P>0.05) in the epileptogenic area in 34/56 (60,7%) cases. 48/56 (85.7%) of the ictal studies showed a marked hyperperfusion (P>0.005) in the epileptogenic area with low cerebellar tracer uptake (P>0.05). In 23/56 (41.1%) patients the early postictal studies demonstrated moderate or high tracer uptake in the epileptogenic region (P>0.05) with diffuse perfusion abnormalities in the surrounding tissue. Late postictal studies (12/56, 21.4%) showed hypoperfusion (P>0.05) in the epileptogenic area with moderate or high tracer uptake in the surrounding tissue. The results of the ictal/postictal studies correlated well with the electrophysiological, and surgical data.
Conclusions: Ictal SPECT presents precise localization of the epileptogenic areas. The method is particularly useful in patients with normal MRI findings. Surgical resection of ictal onset zone identified by ictal SPECT and concordant electrophysiological recording appears to have good postsurgical outcome. The sensitivity and reliability of postictal SPECT might be improved by applying the perfusion pattern model (progression from ictal hyper- to excessive hypo-, then finally to persistant interictal hypoperfusion with a combination of cerebellar perfusion pattern), and by noting the precise time of injection for SPECT studies.

DIAGNOSTIC ONCOLOGY

OS_145

TRANSPORT MECHANISM AND UPTAKE OF DIFFERENT AMINO ACIDS IN TUMOR CELLS, LYMPHOCYTES AND XENOTRANSPLANTED TUMORS

H. Philippi, B. Stoeber, M. Herz, F. Rau, H.-J. Wester, M. Schwaiger, R. Senekowitsch-Schmidtke. Nuklearmedizinische Klinik der Technischen Universität Muenchen, München, Germany.

Aim: The amino acid tracer ^{11}C-methionine used for tumor diagnosis with PET also shows an uptake by inflammatory tissue, thus leading to false positive results. The potential of ^{18}F labeled amino acid derivatives to differentiate between tumor and inflammation was investigated by uptake studies in tumor cells and stimulated lymphocytes.
Methods: The uptake of the amino acids [methyl-^{3}H]-methionine (Met), L-[^{18}F]-fluoroethyl-tyrosine (FET) and L-[^{18}F]-fluoroethylcysteine (FEC) was analyzed in SW707 human colon carcinoma cells, C6 rat glioma cells, human lymphocytes, as well as in SW707 cells xenotransplanted into nude mice. About 5 x10^5 cells of each cell line were incubated at 37¡C for 3 hours in a buffered medium containing either different concentrations of unlabeled amino acids (5-200mg/L), concanavalin A (10mg/400µL; Con A, mitogenic to lymphocytes) or the transport inhibitors (90 mM) 2-amino-norbornane-carboxylic acid (BCH, L-system), α-(methylamino)-isobutyric acid (MeAIB, A-system) or L-Serin (ASC-system). 0.37 MBq of each amino acid tracer were added and incubated at 37°C for 10 minutes. Uptake was stopped by ice-cold PBS, cells were washed three times and tracer uptake was analyzed. Biodistribution and tumor uptake of FET, FEC and Met in nude mice were determined 30 minutes after i.v. injection of 370 kBq in 100µL.
Results: The amount of tumor uptake was different in the various cell types investigated. C6 cells showed the highest uptake for all three tracers. A slightly lower uptake was found in SW707 cells. In Con A stimulated lymphocytes the uptake of the ^{18}F labeled amino acids was negligible, while methionine uptake was significantly higher than in both tumor cells lines. Because BCH reduced the uptake of FET, FEC and Met to approximately 10 %, these amino acids are transported predominantly by the L-system. In xenotransplanted nude mice FET and Met were accumulated predominantly in tumor (FET: 5.7 % ± 0.8% ID/g, Met: 1.8 ± 0.2% ID/g) and in pancreas (FET: 22.5% ± 13.7% ID/g, Met: 13.2 ± 2% ID/g), FEC in tumor (5.4% ± 0.8%ID/g) and kidney (9.3% ± 1.8% ID/g). The tumor-to-blood ratios for FET, FEC, and Met were 2.1, 2.5, and 2.6, respectively.
Conclusion: The results show that the ^{18}F labeled amino acid derivatives may differentiate between tumor and inflammatory tissue, as deduced from their low uptake by stimulated lymphocytes.

This work was supported by Deutsche Krebshilfe Nr. 10-1421-Se 2

OS_146

MEASUREMENT OF THE REGIONAL EXTRACELLULAR SPACE IN BRAIN TUMORS BY [76BR]BROMIDE PET

M. Bruehlmeier (1), U. Roelcke (2), S. Ametamey (1), P. Bläuenstein (1), J. Missimer (1), R. Pellikka (1), J.T. Locher (3), P.A. Schubiger (1). (1) Paul Scherrer Institut, Center for Radiopharmaceutical Science, Villigen, Switzerland; (2) Cantonal Hospital Aarau, Department of Neurology, Aarau, Switzerland; (3) Cantonal Hospital Aarau, Department of Nuclear Medicine, Aarau, Switzerland.

Background and aim: Bromide dilution in plasma is a useful measure of extracellular space (ECS) in whole body. We aimed to quantitatively assess the *regional* ECS (rECS) in brain tumors using [^{76}Br]bromide and PET.
Methods: [^{76}Br]bromide was produced via ^{76}Kr by 60 MeV proton irradiation of a NaBr target. We performed dynamic PET scans of brain tumors in 9 human patients during 0 – 90 minutes p.i. 39 – 59 MBq [^{76}Br]bromide, while [^{76}Br]bromide concentrations were measured in 19 arterial blood samples. A 2-tissue-compartment model and Patlak plots were applied for kinetic analysis. Late PET scans and venous plasma radioactivity were used to calculate the apparent distribution volumes ($DV_{apparent}$= tissue/plasma) after 24 hours p.i. in 6 patients.
Results: In all tissues, bromide distributed rapidly in a reversible tissue compartment (C1), with a subsequent slow influx into a second compartment (C2). Measures of C1 (V_d, K_1/k_2) were higher than normal in most tumors, while C2 (K_1, k_3/k_4) was also increased in some instances, e.g. in patient 1 and 5. Patlak plots provided more robust parameter estimation than the 2-tissue model.

Table: Pharmacokinetics of [^{76}Br]bromide in brain tumors, compared with normal tissue. Diagnosis: ANAC=anaplastic astrocytoma WHO III, GBM=Glioblastoma multiforme WHO IV, TNC = tumor not confirmed, OLAS=oligoastrocytoma WHO II, MEN=meningioma. Therapy: PR=partial resection, GT=gross total resection, RT=radiotherapy. Missing values (–): no tumor or tumor not visible on PET.

patient	age	sex	diagnosis	therapy	Patlak plot		2-tissue-model		PET
					V_d	K_i [min^{-1}]	K_1/k_2	k_3/k_4	24h $DV_{apparent}$
1	35	m	ANAC	PR, RT	0.218	0.00365	0.1000	7.95	0.817
2	41	f	GBM	GT	0.609	0.00031	0.277	1.24	0.718
3	66	f	TNC	no therapy	–	–	–	–	–
4	62	m	OLAS	Biopsy	–	–	–	–	–
5	46	f	ANAC	GT, RT	0.396	0.00211	0.119	4.060	0.868
6	71	f	MEN	GT	0.667	0.00039	0.406	0.683	not avail.
7	31	m	ANAC	GT, RT	0.534	0.00118	0.202	2.27	0.731
8	40	m	ANAC	PR, RT	0.374	0.00200	0.311	1.12	not avail.
9	63	f	ANAC	PR, RT	0.300	0.00049	0.141	1.22	0.349
normal brain (mean, n=9)				cerebrum	0.272	0.00049	0.137	1.23	0.440
				cerebellum	0.179	0.00040	0.097	1.29	0.339

Conclusions: We propose that [^{76}Br]bromide distribution in C1 reflects the rECS, revealing extracellular tumor edema of various degrees. C2 indicates [^{76}Br]bromide uptake into a second tissue compartment, e.g. intracellular influx. The assessment of the rECS may provide insights into tumor pathophysiology with implications for therapy (e.g. drug dilution and delivery).

OS_147

COMPARISON OF THE DISTRIBUTION OF THE HYPOXIC CELLS IN MURINE TUMORS WITH THAT OF BLOOD FLOW OR GLUCOSE METABOLISM. -AN AUTORADIOGRAPHIC STUDY USING A NEW 18F-LABELED 2-NITROIMIDAZOLE ANALOG, [18F]FRP-170 AND [14C]IODOANTIPYRINE OR [14C]DEOXYGLUCOSE

Y. Takai (1), N. Tujitani (2), T. Kaneta (1,3), T. Hakamazuka (1), S. Yamada (1), H. Wada (4), M. Yuki (4), R. Iwata (4), T. Ido (4). (1) Department of Radiation Oncology, Tohoku University, Sendai, Japan; (2) Pola Chemcal Industries, Yokohama, Japan; (3) Department of Radiology, Hiraka General Hospital, Yokote, Japan; (4) Cyclotoron and Radioisotope Center, Tohoku University, Sendai, Japan

Purpose: Recently, it has been reported that hypoxia induces hypoxia inducible factor that induces a variety of genes which are known to have an important role in the growth of tumors. In such a situation, imaging and quantification of hypoxic cells in tumor is thought to be very important to predict prognosis and to select the patients for bioreductive drugs, in addition to the prediction of radiosensitvity. We have recently succeeded in synthesizing fluorine-18 labeled fluoroRP-170 ([^{18}F]FRP-170) as a new hypoxic cell marker. RP-170 (1-[2-hydroxy-1-(hydroxymethyl)-ethoxy] methyl-2-nitroimidazole) was a potential radiosensitizer with low lipophylicity developed by POLA chemical industries.

A purpose of this study is to evaluate the usefulness of the new hypoxia maker and to investigate the distribution of hypoxic cells in comparison with the distribution of blood blow or glucose metabolism using double-tracer autoradiograpy.

Materials and Methods: WHT/Ht albino mice bearing the squamous cell carcinoma (sqcc) or fibrosarcoma in the both axillas were used. Biodistribution and the tumor-to-blood ratios of [^{18}F]FRP-170 were investigated 120 hours after iv injection. Double-tracer autoradiography for tumors was performed with 4-[N-methyl-^{14}C] iodoantipyrine ([^{14}C]IAP) and [^{18}F]FRP-170. [^{14}C]IAP was used as a tracer of blood flow. Another double-tracer autoradiograpy was done with 2-[1-^{14}C]-deoxy- D-glucose ([^{14}C]DG) and [^{18}F]FRP-170. The first autoradiographic exposure for 10 hrs detected the distribution of [^{18}F]FRP-170, then [^{14}C] images were obtained by second exposure for 7 days.

Results: The uptake rates (%injected dose/g tissue) of various tissues except for liver and kidney were less than that of tumors. The tumor-to-blood ratios were 1.97(1.36_2.9) for sqcc and 2.50 (1.72_3.60) for fibrosarcoma. Double-tracer autoradiograms with [^{18}F]FRP-170 and [^{14}C]IAP revealed that the distribution of [^{18}F]FRP-170 was just reversed to the distribution of [^{14}C]IAP. This means that the uptake of [^{18}F]FRP-170 occurs in the region of low blood flow. On the other hand, double-tracer autoradiograms with [^{18}F]FRP-170 and [^{14}C]DG revealed that the uptake of [^{18}F]FRP-170 was found as a part of [^{14}C]DG uptake region. These two kinds of double-tracer autoradiographies revealed that hypoxic tumor cells labeled with [^{18}F]FRP-17 were produced in the viable (glucose metabolizing) cell layers with low blood flow.

Conclusions: We conclude from these data that [^{18}F]FRP-17 is a promising new hypoxia tracer in patients. Most hypoxic cells will be produced completely in the viable cell layers with low blood flow, not in the peripheral region of viable cell layers.

OS_148

EVALUATION OF A FLUORINATED CYCLIC RGD GLYCOPEPTIDE FOR PET-IMAGING

W.A. Weber (1), R. Haubner (1), H.J. Wester (1), M. Herz (1), C. Bodenstein (1), W. Linke (1), S.I. Ziegler (1), H. Kessler (2), M. Schwaiger (1). (1) Department of Nuclear Medicine; (2) Institute of Organic Chemistry and Biochemistry, Technische Universität München, Germany.

Aim: The αvβ3 integrin is an important cell adhesion molecule involved in tumor induced angiogenesis and metastasis. This integrin binds to several matrix proteins with an exposed Arg-Gly-Asp (RGD) sequence. Inhibition of αvβ3 is currently being evaluated as a new strategy for tumor specific anti-cancer therapy. For this purpose cyclic RGD containing peptides with high affinity and selectivity for the αvβ3 integrin have been developed. In this study we evaluated whether PET and the fluorinated glycopeptide cyclo(-Arg-Gly-Asp-D-Phe-Lys(N-(2-[^{18}F]fluoropropyonyl)-7-amino-L-glycero-L-galacto-2,6-anhydro-7-deoxyheptanoic acid)) (Galacto-RGD) may be used to assess αvβ3 expression in-vivo and to monitor the blockade of the receptor by specific antagonists.

Methods: Nude mice bearing xenografts of the human melanoma cell lines M21 (αvβ3 positive) and M21-L (αvβ3 negative) were studied 2-3 weeks after tumor inoculation using a small animal PET system (Munich Avalanche Diode PET). Furthermore, „mixed" tumors containing between 25 and 75% αvβ3 positive M21 cells were imaged. PET imaging was started 60 min after injection of 4-8 MBq ^{18}F-Galacto-RGD (1-3 slices, acquisition time 4 min/slice). Mice bearing M21 tumors were also studied after pretreatment with various amounts of an unlabeled αvβ3 receptor ligand (cyclo(-Arg-Gly-Asp-D-Phe-Val). The unlabeled ligand was i.v. injected 10 min prior to tracer injection at a dose of 6 mg/kg - 18 mg/kg.

Results: αvβ3 positive M21 tumors demonstrated a marked tracer uptake and image contrast (tumor/background ratio (t/b): 5.8 ± 1.3) whereas αvβ3 negative tumors showed similar tracer uptake as surrounding normal tissues. In the tumors containing M21 and M21 negative cells, the intensity of tracer uptake correlated with the percentage of αvβ3 positive cells. Pretreatment with increasing doses of the unlabeled αvβ3 receptor ligand, lead to a steady decrease of the tumor background ratio of αvβ3 positive tumors. At a dose of 18 mg/kg, tumor uptake was reduced to background level (t/b: 1.3 ± 0.11).

Conclusion: ^{18}F-Galacto-RGD is a promising tracer for imaging αvβ3 expression and to monitor receptor blockade during therapy with αvβ3 ligands.

OS_149

IN VIVO IMAGING FOR THE EARLY DETECTION AND MONITORING OF HUMAN BREAST CANCER IN ANIMAL MODEL DURING THERAPY

T.R. Chaudhuri (1), B.E. Rogers (2), A.F. LoBuglio (3), K.R. Zinn (1). (1) Department of Radiology, Division of Nuclear Medicine; (2) Department of Radiation Oncology; (3) Department of Medicine, Comprehensive Cancer Center, University of Alabama at Birmingham, Birmingham, AL 35294, USA.

Aim. The purpose of the present study was to develop a sensitive non-invasive imaging method for the early detection and monitoring of breast tumors during therapy.

Methods. Human breast tumor cells (MCF-7, and T47D), and mouse breast tumor cells (CRL2116) were transfected with a replication deficient adenoviral (Ad) vector encoding GFP (Ad-GFP). The GFP-positive tumor cells were first implanted subcutaneously at variable cell numbers (10 cells-1000 cells) to examine the resolution. Therapeutic intervention study was carried out as follows: The GFP-positive tumor cells, MCF-7 and T47D (1million/ mouse) were implanted separately in two groups of six nude mice subcutaneously. In one group of six mice, adriamycin (50 micrograms/mouse) was injected directly into the implanted tumor cells 24 hours after implantation. Mice were imaged in vivo with a fluorescence stereomicroscope at 1 hour after the tumor implantation and after 3 and 5 days. Images were collected with an optronic digital camera. Following in vivo imaging of intact mice on 3rd and 5th days, GFP-positive tumors and tissue biopsy were collected for culture and further examination by inverted fluorescence microscope.

Results. GFP-positive breast cancer cells as low as 10 were visualized in vivo by light-based imaging. For therapy study, at 1 hr, 3 day and 5 day imaging, the GFP-positive cancer cells in all control mice showed brilliant green light emitting regions on the tumor implantation sites. However, the 3rd and 5th day images of adriamycin-treated mice showed gradual decrease of green fluorescence and change of brilliant green color of the tumor to light orange (due to adriamycin uptake). Control images showed blood vessels infiltrating the tumor regions. No green fluorescence was detected on 5th day in the mice treated with adriamycin. However, the tumor sites became more brilliant orange. Both MCF-7 and T47D cells grew from all GFP-positive tissue biopsies. Orange cells were confirmed to be dead by trypan blue stain. Subcutaneous images showed angiogenesis around the tumors. Reduction of tumor size, gradual change of original tumor color (GFP) to orange (due to adriamycin incorporation) and finally disappearance of GFP were captured in images over time.

Conclusions. The present study provides the evidence for the application of fluorescent stereomicroscopy as an in vivo tool for the detection and monitoring of human breast tumors in mice models without contrast agent or surgery, with potential applications in humans. The light-based imaging will be useful for new drug development research.

OS_150

99MTC LABELED N4-FUNCTIONALIZED STABLE NEUROTENSIN ANALOGS EFFICIENTLY LOCALIZE IN AN EXPERIMENTAL TUMOR MODEL

B. Nock (1), A. Nikolopoulou (1), T. Maina (1), E. Stathopoulou (1), P. Conrath (2), D. Tourwe (2), E. Chiotellis (1). (1) Institute of Radioisotopes - Radiodiagnostic Products, NCSR ; (2) Vrije Universiteit Brussel, Brussels, Belgium.

Recent evidence has shown that neurotensin (NT) receptors are overexpressed by human neoplastic cells, as in the case of exocrine pancreatic carcinoma. As a part of our ongoing work aiming toward the development of radiolabeled NT analogs for diagnostic or therapeutic application we report on two modified NT(8-13) sequences, functionalized with tetramines and labeled with ^{99m}Tc. Preclinical evaluation of these compounds performed in HT-29 cell lines and in tumor bearing mice is described herein.

Methods: The N4-Gly-Lys-(R)-Arg-Pro-Tyr-Tle-Leu-OH, NT1, and N4-Gly-Arg-(R)-Arg-Pro-Tyr-Tle-Leu-OH, NT2, derivatized NT(8-13) sequences were obtained by SPPS and labeled with ^{99m}Tc using $SnCl_2$ as reductant in the presence of citrate. The binding capabilities of new peptides for the NT receptor was tested by proper assays in HT-29 cell preparations. Stability of ^{99m}Tc NT 1 and 2 was studied in mouse plasma employing HPLC techniques. Internalization of ^{99m}Tc NT 1 and 2 in the same cell line was tested over time after incubation at 37°C. Biodistribution was performed in athymic mice bearing an experimental tumor grown in their flanks after inoculation of a HT-29 cell suspension 10-15 days prior to the experiment.

Results: The N4 functionalized NT(8-13) analogs, NT1 and 2, bind with a high affinity to the NT1 receptor subtype overexpressed in the colorectal adenocarcinoma HT-29 cells with respective IC_{50}s 1.5 and 0.9 nM (IC_{50}= 0.6 nM for native NT). Both analogs could be quantitatively labeled with ^{99m}Tc leading each to a single hydrophilic and high specific activity product. Both ^{99m}Tc NT 1 and 2 were found stable in murine plasma up to 2 h incubation, while they internalize very rapidly in HT-29 cells at 37°C. After intraveneous injection in athymic mice bearing the experimental HT-29 tumor they both showed a rapid accumulation of radioactivity in the tumor as well as in the NT receptor-rich intestinal wall, which could be blocked by a bolus injection of 300 μg NT together with the radioligand. Radioactivity washed out rapidly from all other tissues into the urine via the kidneys and the urinary system leading to high target to non-target ratios for both ^{99m}Tc NT 1 and 2.

Conclusions: Owing to their plasma stability, rapid wash out and fast localization in target cells the two novel ^{99m}Tc labeled NT analogs combine excellent characteristics for application in the diagnosis of NT positive neoplasms in patients employing SPECT.

OS_151

SUBCELLULAR LOCATION OF N-(2-DIETHYLAMINOETHYL)-4IODOBENZAMIDE : TOPOGRAPHIC AND QUANTITATION ANALYSIS BY SECONDARY ION MASS SPECTROMETRY

F. Chehade (1), C. De Labriolle-Vaylet (2), E. Hindie (2), N. Moins (3), M.F. Moreau (3), G. Slodzian (4), A. Veyre (3). (1) Hammoud Hospital, Sidon, Lebanon; (2) Hopital Saint Antoine, Paris, France; (3) Inserm U484, Clermont Ferrand, France; (4) Laboratoire de physique des solides, Orsay, France

Introduction : Uptake mechanism, intracellular concentration and stability of radiopharmaceuticals are becoming prerequisite data needed before their clinical introduction in nuclear medicine for either scintigraphic diagnosis or systemic radiotherapy.
Materials and Methods : Iodine-123-labeled N-(2-diethylaminoethyl)-4iodobenzamide (^{123}I-BZA) has been proposed for the imaging of ocular and skin malignant melanomas. We used the secondary ion mass spectrometry (SIMS) to study the subcellular locations and concentrations of BZA. Analysis was carried out on mice C57BL/6 J1 co, inoculated with pulmonary colonies of B16 murine melanoma. We also studied the normal pigmented structure of the eyeball. SIMS allows imaging of BZA through detection of native iodine-127 atom (^{127}I) of this molecule. BZA stability was further assessed after labeling it with carbon 14 (^{14}C) and after comparing the obtained ^{127}I and ^{14}C atoms images. Moreover, the intra-cellular concentration of ^{14}C-BZA was estimated by measuring the local ratio of ^{14}C and carbon 13 (^{13}C), a natural isotope existing in tissues with a known abundance. ^{14}C/^{13}C ratios measured at 2, 14, and 72 hours after injection allowed us to asses the intracellular kinetic of BZA.
Results : Our results demonstrate selective localization of BZA in the pigmented cells of melanoma tissue, choroidal melanocytes and retinal pigmented epithelium of teh eyeball. Molecule localization is intracytoplasmic, reproducing the distribution of melanin in normal and tumor cells. ^{127}I and ^{14}C showed similar distribution patterns indicating stability of BZA bound to melanin. Intra-cellular measurements of ^{14}C/^{13}C isotopic ratios at different times, showed slow cellular clearance of the molecule with a biological half-life of 38 h. in tumor tissue, 47 h. in choroidal melanocytes, and 58 hours in the retinal pigmented epithelium.
Discussion : Selective and specific localization of BZA in the pigmented cells explains both high sensitivity and specificity of ^{123}I-BZA scintigraphy for melanotic tumors. Results of this work can serve as a model for the radiation dose calculation at cell level. The microanalytical technique adopted here (SIMS) is of special relevance to select other iodobenzamide that has the highest concentration and longest biological half-life in tumor cells for internal radiotherapy.

CARDIOVASCULAR

OS_153

INFLUENCE OF LEFT BUNDLE BRANCH BLOCK ON MYOCARDIAL FLUORODEOXYGLUCOSE UPTAKE AND PERFUSION: EVALUATION USING QUANTITATIVE POSITRON EMISSION TOMOGRAPHY

P. Zanco, F. Chierichetti, S. Cargnel, E. Milan, B. Saitta, P. Trento, S. Medea, V. Fiore, M. Marcolin, A. Fini. Nuclear Medicine - PET Center, Az. USSL 8, Castelfranco Veneto, Italy.

Septum reverse mismatch (SRM) in cardiac Positron Emission Tomography (PET), defined as a reduced uptake of F18-fluorodeoxyglucose (FDG) in comparison with N13-ammonia (NH3) was referred in the patients affected by left bundle branch block (LBBB). The exact understanding of the underlying cause is lacking. In particular it is unclear if the FDG defect could be secondary to perfusion damages induced by the altered motion of the septum, presented in LBBB patients.
To this aim 10 patients (9M, 1F, aged 60-72 yr., mean 66) affected by permanent, complete LBBB were enrolled and submitted using a dedicated scanner to glucose load-insulin FDG PET and rest NH3-PET. A visual analysis and a semi quantitative analysis were performed, calculating by ROIs the septum to lateral uptake ratio (SLR). The myocardial blood flow (MBF) was also quantitatively calculated in *ml/min/g* using a dynamic acquisition and a modified Patlak method. The coronary angiography and echocardiography were also performed. The mean ejection fraction was 36±6 (range 25-40). Five patients presented a significant stenosis of LAD and LCx at the coronary angiography, while 3 patients presented only stenoses in RCA and LCx and no significant coronary stenosis was found in the other 2 patients.
All the LBBB patients presented an FDG uptake defect in the septum, with a reverse mismatch with respect to NH3-PET. At the semi quantitative analysis the mean septum/lateral ratio was 0.60±0.19 for FDG (range 0.27-0.85) and 1.04±0.16 for NH3 (range 0.78-1.36), $p<0.001$. No correlation between the dysfunctional area at the echocardiography and the site of the FDG uptake defect was found.
At the quantitative analysis the mean MBF in the septum was 0.73±0.21 (range 0.39-0.97), without significant differences in comparison with the lateral wall assumed as reference (mean MBF 0.69±0.21, range 0.45-1.05, p=ns).
In conclusion our study could suggest that the change in FDG uptake referred in the LBBB patients should be considered as a primary phenomenon, independent from damages in perfusion and wall motion.

OS_152

A PHASE II CLINICAL TRIAL OF N-(2-DIETHYLAMINOETHYL)-2-IODOBENZAMIDE, A NEW SPECIFIC MELANOMA IMAGING AGENT

J. Bonafous (1), N. Moins (2), M.F. Moreau (2), P. Labarre (2), D. Mestas (1), M. D'Incan (3), F. Bacin (3), F. Chossat (4), J. Papon (2), M. Bayle (2), A. Veyre (1,2)(1) Médecine Nucléaire, Centre J.Perrin, Clermont-Ferrand, France; (2) Unité 484 INSERM, Clermont-Ferrand, France; (3) Services de Dermatologie et Ophtalmologie, CHU, Clermont-Ferrand, France; (4) CIS Bio International, Gif-sur-Yvette, France

We have been the first to propose a series of iodobenzamide derivatives showing an affinity for melanoma tissue, as potential imaging agents for melanoma scintigraphy. Due to its in vivo behaviour in preclinical studies, *N*-(2-diethylaminoethyl)-2-iodobenzamide (BZA2) has been selected for a phase II clinical trial.
The aim of this study was to assess the diagnostic value of BZA2 scintigraphy in melanoma.
Methods: Forty patients were divided into three groups: group I, primary ocular melanoma, 12; group II, metastasic cutaneous melanoma, 14; group III, clinical remission,14. A dose of 130 MBq of [^{123}I] BZA2 was injected IV after blocking thyroid by potassium iodide (1h before, 500 mg per os). Whole-body images were performed 2, 4 and 6 hours post-injection and complementary images of suspicious areas were taken. The pharmacokinetic parameters were determined in blood and dosimetry was evaluated from whole-body scintigraphy.
Results: No side effects or adverse reactions were noticed after the injection of [^{123}I]BZA2. The performances of the method in melanic tumour detection were good with a specificity of 100% (no false positive results), and a sensitivity of 78%: 4 small primary ocular lesions (< 3mm) were not imaged, but all the metastasic lesions were visualized, except one amelanotic. Moreover, negative BZA2-scintigraphy in cases of suspicious lesions allowed the correction of three diagnoses: the prostatic origin of bone metastases for two patients and the endocrine tumour origin (APUD system) of an ocular lesion. Finally, the negative BZA2-scintigraphy in a patient suspected of relapse in CT could have avoided a "white" laparotomy. These different examples underline the benefit of such a specific tracer for this pathology.
Conclusions: The whole-body BZA2-scintigraphy allowed the detection of primary ocular melanoma and metastases and moreover a differential diagnosis between melanoma and simulating lesions, leading to a better staging of the disease and a good management for the patient treatments.

OS_154

RANDOMISED TRIAL EVALUATING CHANGES OF MYOCARDIAL PERFUSION DUE TO EXERCISE TRAINING VERSUS PERCUTANEOUS TRANSLUMINAL CORONARY ANGIOPLASTY (PTCA) IN PATIENTS WITH CORONARY ARTERY DISEASE (CAD)

K. Kendziorra (1), R. Hambrecht (2), C. Walther (2), S. Möbius-Winkler (2), M. Förster (1), R. Kluge (1). (1) Department of Nuclear Medicine; (2) Heart Center Leipzig, University of Leipzig, Germany.

Physical exercise is known to improve not only exercise capacity but probably also the frequency of cardiac events in patients with CAD. The aim of our study was to evaluate changes in stress perfusion after one-year exercise training in comparison to the effects of PTCA in patients with CAD.
Method: In 33 male patients with angiographically confirmed significant coronary stenosis in one target vessel; myocardial perfusion scintigraphy was performed at baseline and 12 months after randomisation into either a physical exercise group (19 patients) or a PTCA-group (14 patients). SPECT was performed after treadmill stress and at rest with 400 MBq Tc-99m-tetrofosmine and a dual-head camera (Vertex ADAC Lab.). Images were quantified using circumferential count rate profiles in 16 wall segments and compared to baseline. According to the relative count rates ischemic segments were classified as areas with ≥85% of maximum perfusion in rest and <85% under stress.
Changes of regional perfusion were calculated for four groups of segments: A) ischemic segments in the target region of the coronary stenosis at baseline; B) ischemic segments outside the target region at baseline; C) ischemic segments at baseline or follow-up in the target region; D) ischemic segments outside the target region at baseline or follow-up. The individual stress limit was quantified by using the rate pressure product to gain a reproducible parameter for maximum exercise capacity.
Results:

	Exercise training-group			PTCA-group		
	Count rate in stress studies		Significance	Count rate in stress studies		Significance
Group	Baseline	12 months		Baseline	12 months	
A	73,8 %	81,1 %	P<0,01	79,2 %	90,4 %	P<0,01
B	76,7 %	90,0 %	P<0,01	77,2 %	84,7 %	P=0,27
C	75,8 %	80,3 %	P=0,01	82,8 %	86,6 %	P=0,21
D	81,7 %	86,5 %	P=0,19	82,8 %	81,9 %	P=0,87

There was no significant change in rest perfusion.
Conclusions: Our data indicate a significant improvement in stress myocardial perfusion in the physical exercise group after 12 months. The ischemia is reduced not only in the target region of the leading stenosis but also in other ischemic myocardial areas. In contrast, after PTCA stress perfusion improved only in the initially ischemic parts of the target area. Further follow-up studies will investigate the impact of exercise training on prognosis of the CAD.

OS_155

ATTENUATION CORRECTION IN DUAL-ISOTOPE TL-201 (REST) AND TC-99M SESTAMIBI (STRESS) MYOCARDIAL SPECT

G. Storto, J. O. Prior, N. Besseghir, A. Bischof Delaloye. Department of Nuclear Medicine, CHUV University Hospital, Lausanne, Switzerland.

Background: Attenuation correction (AC) in diagnosis of coronary artery disease (CAD) using a dual-isotope Tl-201 rest/Tc-99m Sestamibi stress protocol has not yet been completely evaluated. We studied the influence of AC in detecting CAD using myocardial gated single-photon emission computed tomography (GS).
Methods: Seventy-nine patients, 48 (32 Women,16 Men, aged 65±9y) with low pre-test likelihood of CAD (group N), and 31 (6W, 25M, aged 67±12y) with previous myocardial infarction or angiographically documented coronary stenoses (group P), underwent Tl-201 rest (111MBq) and Tc-99m Sestamibi stress (900MBq) myocardial GS. Transmission and emission images were acquired simultaneously on a dual-head camera (Siemens E.-Cam) equipped with Gd-153 sources and processed by iterative reconstruction. Short-axis images were qualitatively evaluated and quantitative analysis was performed in non-corrected (NC) and AC studies by dividing the left ventricular wall into 21 segments. Segments were judged moderate-severely ischemic when improvement at rest was greater than 25%. Statistical analysis used a χ^2 and a Student's t-test with a significance level of ($p<0.05$).
Results: In group N all patients presented ejection fraction (EF) >55%, and of 1008 segments considered, 975 (96%) in NC and 983 (97%) in AC studies were normal, without significant difference ($p=0.79$), this result was confirmed when regional analysis was performed. In group P, EF ranged from 16% to 55%, in a total of 651 segments, 38 (6%) and 35 (5%) were judged ischemic in NC and AC studies, respectively ($p=0.62$). Interestingly when regional perfusion was analyzed, significant differences were found in the number of ischemic segments in the anterior wall which was 7/155 (4%) for NC and 15/155 (10%) for AC studies ($p<0.05$) and in the inferior region 21/155 (13%) for NC and 6/155 (3%) for AC studies ($p<0.01$). When relative activity between NC and AC Tc-99m Sestamibi studies was compared, a significant difference ($p<0.0001$) was found in anterior wall with NC>AC and inferior wall with NC<AC. Activity in Tl-201 studies increased after AC only in the inferior segments but less than Tc-99m studies.
Conclusion: AC did not change the diagnosis in normal patients. In patients with decreased Tc-99m Sestamibi stress uptake in anterior or in inferior wall, AC might lead to overstimation of ischemia in the anterior and understimation in the inferior wall. The increase of Tl-201 activity at rest, in the inferior wall, did not change overall interpretation of the dual-isotope study.

OS_156

COMPARISON BETWEEN VISUAL AND SEMIQUANTITATIVE ANALYSIS OF THE EFFECT OF ATTENUATION CORRECTION WITH SCATTER COMPENSATION ON THE MYOCARDIAL DISTRIBUTION OF 99MTC MIBI IN PATIENTS WITHOUT CORONARY ARTERY DISEASE

F.J. Pena, J. Jimenez-Bonilla, I. Banzo, C. Guede, R.H. Allende, R. Quirce, J.M. Carril. Servicio de Medicina Nuclear, HU Marqués de Valdecilla, Santander, Spain.

Aim: Before any new instrumental technique is applied in the clinical situation, the knowledge of its effects on the normal population is recommended. The aim of this work was to study the effect of attenuation correction and scatter compensation (AC+SC) in the distribution of MIBI in a normal population without coronary artery disease (CAD) and to compare the visual interpretation with the semiquantitative analysis of the data obtained.
Methods: A rest myocardial MIBI SPECT was performed in 27 patients without CAD referred for a non-myocardial MIBI scan. A double headed camera with linear sources of ^{153}Gd was used. Simultaneous transmission/emission acquisition was performed. Both in non-corrected (NC) and AC+SC studies, either males and females, a 4-points (4=normal, 0=defect) visual score was used by three experienced physicians. Left myocardium (LM) was divided into 9 segments: apex (AP), anterior wall (AW), inferior wall (IW), lateral wall (LW), and septum (S), either basal and apical. For semiquantitation LM was divided into 33 segments: 5 in AP and 7 in each wall. The volume-weighted average counts were calculated for each segment in NC and AC+SC, in female and male. For each segment the increase of tracer uptake (↑), the decrease (↓) or the absence of changes (=) after AC+SC was considered.
Results:

Females	AP	AAW	BAW	AIW	BIW	ALW	BLW	AS	BS
Visual	↑	↓	=	↓	↑	↑	↑	↑	=
Semiquant	↓	↓	↓	↑	↑	↓	=	↓	=

Males	AP	AAW	BAW	AIW	BIW	ALW	BLW	AS	BS
Visual	↓	=	↓	↑	↑	=	=	=	=
Semiquant	↓	↓	↓	↑	↑	↓	=	↓	↑

Visual analysis showed no significant differences (SD) between AC+SC and NC, but semiquantitation detected SD in all territories. NC studies showed SD between males and females in 12/33 segments, specially in AP and IW. After AC+SC the SD were found only in 6/33 segments. Average uptake on NC were 76.4 ± 13.96% in females and 71.36 ±13.7% in males. On AC+SC values were 72.92 ± 10.83 and 79.49 ± 7.83, respectively
Conclusions: AC+SC studies showed more uniform uptake than NC studies,either in males and females. The AC+SC produced changes in all myocardial walls more relevant in AW and IW. Visual analysis of LW, SW and AP was discrepant in males and females. In all these territories, except in basal septum in males, the semiquantitative analysis showed a decrease of uptake.

OS_157

COMPARISON OF 180-DEGREE AND 360-DEGREE DATA ACQUISITION IN GATED BLOOD POOL TOMOGRAPHY

C. Vanhove, N. Walgraeve, L.O. Dierickx, P.R. Franken. Department of Nuclear Medicine, Free University Brussels (AZ-VUB), Brussels, Belgium.

Aim. The optimal clinically relevant demonstration of the superiority of 180- versus 360-degree image acquisition in gated blood pool tomography (GBPT) has not been performed.
Methods. GBPT were acquired in 25 consecutive patients after injection of 740 MBq of Tc99m labelled Human Serum Albumin. Projection images were acquired on a triple-head gamma camera: 360-degree clockwise step-and shoot rotation; 32 stops (96 projections); 30 sec. per stop; 64x64 matrix; 8 time-bins. Projection images were reconstructed using the 360-degree data and again using only data acquired from LPO to RAO. Redistributing the counts in the 360-degree image set using binominal deviates equalized the global count densities. Finally, images were reoriented according to the left ventricular long axis and LVEF and volumes were measured using a new algorithm (QUBE) based on a three-dimensional segmentation technique, combining threshold and local gradient methods. The LVEF were validated against planar radionuclide angiocardiography (PRNA).
Results. For the measurement of the LVEF, no significant differences could be found between the 360- and the 180-degree image sets. Compared to PRNA however, a better correlation was found when a 360-degree acquisition ($r=0.89$; GBPT=0.97PRNA+5.12) was used compared to a 180-degree acquisition ($r=0.83$; GBPT=0.85PRNA+12.94). In addition, the systematic error (3.56% vs 5.24%) and the random errors (7.88% vs 9.40%) determined by Bland-Altman analysis were less when the 360-degree image collections were used. For left ventricular volumes, linear regression analysis showed a good correlation between both acquisition methods as well for end-diastolic volumes ($r=0.93$) as for end-systolic volumes ($r=0.92$). On average, however, left ventricular volumes were 22% smaller when 180-degree image acquisition was used.
Conclusions. Although there was no significant difference in the determination of LVEF using 180- or 360-degree acquisition in GBPT, 360-degree acquisition showed superior agreement with PRNA.

OS_158

DOES ATTENUATION-CORRECTION USING MULTIPLE LINE-SOURCES IMPROVE MYOCARDIAL SESTAMIBI SPECT?

H. Hoeffken (1), B. Maisch (2), T.M. Behr (1). (1) Dept. clinical nuclear medicine; (2) Dept. Cardiology, Hospital of the Philipps-university Marburg, Marburg, Germany.

In order to evaluate the impact of attenuation correction on the quality of myocardial scintigraphy, we investi-gated 61 patients suffering from CAD. The impact of attenuation correction on sensitivity and specificity in the diagnosis of coronary artery stenoses >50% was studied as well as its influence on regional myocardial uptake dependent on the patients' extent of overweight.
Methods: 35 of the 61 patients had stenoses ≥50% (14 with single-,13 two- and 8 three-vessel disease), 26 patients <50%. A Tc-99m-sestamibi one day stress rest protocoll was used. SPECT-images were acquired using a dual head gamma camera with detectors in 90¡ position. Transmission data were obtained from an array of 14 Gd-153 line sources opposite each detector. The scintigrams were evaluated quantitatively, sensitivity and specificity were determined by ROC-analysis. Additionally, the regional uptake values in the anterior, lateral, inferior, septal and apical myocardial regions obtained with attenuation correction were compared with those obtained without attenuation correction in patients without and with 10% and 20% overweight, respectively.
Results: As expected from physical aspects, there was no significant difference in changes of regional myocardial uptake related to attenuation correction in the 3 patient groups without and with 10% or 20% overweight: In all three groups the highest impact of attenuation correction was found in the inferoseptal and posterior myocardial regions. Independent of the patient«s weight, there was an increase in regional uptake of 11.7 - 12.8% in the inferoseptal and 16.1 - 17.4 in posterior region related to attenution correction. Due to attenuation correction, the sensitivity for the detection of CAD increased from 63% to 71% without loss of specificity (69%). Best improvement was found in the detection of RCA stenoses: Sensitivity and specificity increased from 67% and 83% to 81% and 93%.
Conclusions: Thus, attenuation correction with line source arrays may be able to avoid false positive results in the RCA region mainly caused by attenuation artifacts. According to our results there is a significant impact in regional uptake not only in patients with overweight, but also in normalweighted patients, leading to the assumption that attenuation correction is useful in all patients, regardless of the patients weight.

OS_159

BACK-PROJECTION VS ITERATIVE 99MTC-SESTAMIBI GATED-SPECT RECONSTRUCTION IN THE EVALUATION OF LEFT VENTRICULAR EJECTION FRACTION AND VOLUMES: A COMPARISON WITH CONTRAST LEFT VENTRICULOGRAPHY

C. Cittanti (1), E. Succi Leonelli (2), P. Colamussi (1), M. Giganti (1), G. Percoco (2), F. Ferrari (2), A. Filice (1), R. Ferrari (2), A. Piffanelli (1). (1) Nuclear Medicine Section; (2) Cardiology Section, University of Ferrara, Ferrara, Italy.

Aim: ECG synchronization during myocardial tomoscintigraphy (G-SPECT) adds to standard perfusion images both left ventricular volumes (LVV) and ejection fraction (EF) data that constitute important parameters in the diagnosis and prognostic stratification of coronary artery disease. Nevertheless only a few data concerning the impact of synchronized images reconstruction modalities on EF and LVV quantification are available in a clinical setting. The purpose of this study was to evaluate left ventricular volumes and function by 99mTc-sestambi G-SPECT using two different tomographic reconstruction methods (filtered back-projection or iterative algorithms) in comparison with contrast left ventriculography (LVG).
Methods: We retrospectively evaluated 34 subjects affected by ischemic heart disease who underwented standard two-day 99mTc-sestamibi G-SPECT protocol (8 frames/cardiac cycle) using a 90° double-detector camera (Vertex - ADAC). Rest synchronized projection data were reconstructed with both filtered back-projection (FBP) and iterative (IT) algorithms; end diastolic volume (EDV), end systolic volume (ESV) and EF were obtained for each subject using an extensively validated software (AutoSPECT Plus – Cedars Sinai). All patients underwented angiographic evaluation of LVV and EF using the Dodge biplane method. Linear regression and paired t-tests were used to compare G-SPECT data with angiographic parameters for all subjects.
Results: Linear regression analysis demonstrated Pearson correlation coefficients respectively of 0.80 for EDV, 0.92 for ESV and 0.87 for EF [FBP vs LVG], and of 0.83 for EDV, 0.93 for ESV and 0.91 for EF [IT vs LVG]; paired t-test analysis did not show any significant difference between ESV evaluated with both FBP and IT methods in comparison to angiographic values. However, paired t-test revealed G-SPECT EDV and EF significantly lower data than LVG for both tomographic reconstruction modalities. Finally, despite very strong correlations between FBP and IT parameters (r=0.99 for EDV, ESV and EF), paired t-test analysis showed significantly lower values of EDV and ESV with higher LVEF data ($p<0.001$) in IT than in FBP reconstructed images.
Conclusions: According to international literature G-SPECT gives significantly lower estimates of EDV and EF than LVG measurements, probably because of inclusion of greater outflow tract amounts in standard angiographic models. However, G-SPECT provides LVV and EF values that correlate well with angiographic data. In particular IT method showed a better correlation with LVG for both LVV and EF estimates than FBP. Larger clinical studies are needed to confirm these findings.

OS_160

ATTENUATION CORRECTION IMPROVES DIAGNOSTIC VALUE OF MYOCARDIAL SPECT IN PATIENTS WITH SUSPECTED CORONARY HEART DISEASE USING CORONARY ANGIOGRAPHY AS REFERENCE

A. Kjaer, A. Cortsen, H. Hasseldam, B. Rahbek, J. K. Madsen, B. Hesse. Department of Clinical Physiology and Nuclear Medicine, Rigshospitalet, University of Copenhagen, Denmark.

Aim: To investigate the diagnostic value of attenuation correction in myocardial scintigraphy (SPECT) in coronary disease, using angiography (CAG) as reference.
Methods: SPECT was performed in 53 patients (mean age: 53 years, 38 men) with a Millennium MG (GEMS) dual head camera, ^{99m}Tc-sestamibi, ^{153}Gd transmission line sources for attenuation correction, and scattered photons acquired in a window below the ^{99m}Tc peak. Images processed by filtered back projection (FBP) and iterative algorithm with scatter subtraction and attenuation correction (SCAC) were evaluated and compared with regard to reversible/irreversible defects in 5 regions of the left ventricle (anterior, lateral, inferior, septal and apical) by consensus reading without knowledge of clinical or angiographic data. If there was a difference in the interpretation of SPECT, CAG was used as reference.
Results: In 31 patients conclusions were identical. In 22 patients interpretation differed: (suspicion of) 15 irreversible (11 inferior, 2 anterior and 2 septal) and 6 reversible (5 inferior and 1 apical) defects disappeared with SCAC. Four irreversible (1 anterior and 3 inferior) were changed to reversible defects after SCAC. CAG, performed in 12 of the patients with changed interpretation, supported interpretation of SCAC images in 10 cases and FBP images in 1 case. In one case CAG supported neither.
Conclusions: The interpretation was changed - definitely or from "suspicion of" – by attenuation/scatter correction in almost half of the studies. Using CAG as reference the diagnostic accuracy was improved in 83% of discrepant cases.

RADIONUCLIDE THERAPY / DOSIMETRY

OS_161

RADIOTHERAPY DOES NOT IMPROVE PROGNOSIS OF PATIENTS WITH DIFFERENTIATED THYROID CARCINOMA

D. Sandrock, D. Noack, K. Baba, D.L. Munz. Clinic for Nuclear Medicine, University Hospital Charité, Berlin, Germany.

Aim: The impact of (percutaneous) radiotherapy on prognosis in patients with differentiated thyroid carcinoma is controversially discussed. The randomisation for currently beginning multicenter studies (e.g., Puskas and Schober, Nuklearmedizin 1999; 38:328-332), however, is slowly ongoing due to the traditional therapy algorithms of different institutions and problems to obtain informed consent of suitable patients. It was, therefore, the aim of this study to analyse data from a *very special "retrospective"* group of patients.
Methods: In the years 1970 to 1991 the decision for percutaneous radiotherapy (neck, supraclavicular groin; telecobalt, fast electrons 40/50 Gy) was – according to the (complete) records – not systematically made and not only given to pT4-tumors (late correct diagnosis from reference pathologist, availability of therapy facilities, different oppinions by different chiefs at different times...). Therefore, there is a group of 178 patients having follicular and 132 papillary carcinoma *with* radiotherapy (RT) and a comparable group (162 follicular, 143 papillary) *without* radiotherapy (No RT). All patients received otherwise a standard treatment (surgery, lymphadenectomy [if appropriate], radioiodine, suppressive thyroxine medication). The mean follow-up time was 9.8 years.
Results: Both groups did not differ significantly in the parameters age, sex, TNM-stage, and survival (COX-regression). Survival rates are given in the table below (carcinoma related mortality). There is also no difference in survival for T4-patients (41 patients *with* vs. 34 *without* radiotherapy).
Conclusion: Radiotherapy has – according to our analysis of comparable groups – no benefit for survival in patients with differentiated thyroid carcinoma – including the subgroup of T4-patients.

Survival	RT T1-4	No RT T1-4	RT T4 No	RT T4
5 years	94 %	92 %	81 %	85 %
10 years	89 %	87 %	67 %	70 %

OS_162

THYROID REMNANTS ABLATION BY MEANS OF 131I – IS IT POSSIBLE TO PREDICT EFFICACY OF THE THERAPY ?

Z. Adamczewski (1), A. Lewinski (2), S. Mikosinski (1), J. Makarewicz (1), A. Karwowska (1). (1) Department of Nuclear Medicine, District Hospital, Zgierz, Poland; (2) Department of Thyroidology, Medical University, Lodz, Poland .

Aim: Assessment of effect of dosimetric parameters and TSH levels on ablation effectiveness in patients with differentiated thyroid carcinoma.
Material and methods: One hundred patients were included in the study, 88 women (age 13-75 years, mean 44,9±12,3) and 12 men (age 9-79 years, mean 48,5±21,9). In 54 cases (54%) papillary and in 46 cases (46%) follicular thyroid carcinoma was diagnosed. In every patient neck ^{131}I uptake, effective ^{131}I half-live time [EHL] and thyroid mass [M] was determined. TSH level was determined after > 4 weeks of L-T4 withdrawal. Standard ablative activities modified based on prognostic factors were administered. Activities of administered ^{131}I ranged from 1643 MBq (44,4 mCi) to 4048 MBq (109,0 mCi). Therapy effectiveness was controlled 3-6 months after ablation under endogenous TSH stimulation (TSH ≥ 25µIU/ml). Neck ^{131}I uptake <1% and lack of focal radioiodine uptake in scintigrams were regarded as successful ablation.
Results: No focal uptake of radioiodine in the neck was found in 80 patients (80%), in 20 patients (20%) ablation was regarded as unsuccessful. Doses absorbed by the thyroid remnants were calculated retrospectively. Correlation was found between the absorbed dose and the ablation effectiveness ($rs=0,23$; $p<0,05$). It was found that in a group of patients who received 2400Gy or more for thyroid remnants the ablation effectiveness was 90,7% (n = 43, successful ablation 39 patients). No relationship was found between ablation effectiveness and administered activity of radioiodine. It was demonstrated that in a group of patients with unsuccessful ablation the thyroid remnants mass was significantly greater then in a group with successful ablation ($p<0,05$). Therapy effectiveness in a group of patients with thyroid remnants mass < 1,5g was 91%, whereas in patients with greater mass it was only 68%. Comparison of the uptake and EHL in both groups yielded no significant differences. Negative correlation was found between thyroid remnants mass and TSH level in patients before ablation ($rs= - 0,34$; $p<0,001$).
Conclusions: 1. Ablation effectiveness correlates with radiation dose absorbed by the thyroid remnants. 2 No relationship has been observed between the applied ^{131}I activities and the effectiveness of ablation. 3. The mass of remaining thyroid remnants is an important parameter, affecting ablation effectiveness. 4. The negative effect of the mass of thyroid remnants on ablation effectiveness can result from lower dose absorbed by the thyroid remnants and/or weaker stimulation of thyrocytes by endogenous TSH.

OS_163

TREATMENT WITH ISOTRETINOIN AND RECOMBINANT HUMAN TSH IN DEDIFFERENTIANTIATED THYROID CARCINOMA

E. Seregni, G. Savelli, L. Maffioli, F. Pallotti, E. Bombardieri. Istituto Nazionale Tumori, Milano, Italy.

Aim Dedifferentiation associated with the loss of radioiodine (RI) uptake is a common event in patients affected by progressive thyroid carcinoma. Retinoids are known to induce tumor differentiation and evidences have shown that isotretinoin (13-cis-retinoid acid) is effective in redifferentiate thyroid cancer and to reinduce RI uptake. In patients with dedifferentiated thyroid carcinoma the hormonal withdrawal can induce tumor progression. High TSH levels for few days can be obtained by recombinant human TSH (rh-TSH). Aim of the present investigation is to evaluate the efficacy of isotretinoin associated to rh-TSH in patients with dedifferentiated thyroid carcinoma.

Methods Five metastatic patients with negative ^{131}I whole body scan entered the study. The main characteristics of patients are reported in the table. All patients had undergone total thyroidectomy and several courses of RI therapy. Isotretinoin (Roaccutan, Hoffmann-La Roche) treatment at dosage of 1.5 mg/kg body weight was started at 4 months before RI therapy. 0.9 mg of rhTSH (Thyrogen, Genzyme) was i.m. administered in two consecutive days. RI therapy, with a standard dose of 7.4 GBq of ^{131}I, was performed 24 hours following the final rh-TSH injection.

ID	Gender	Age	Primary tumour	Disease extension	Tireoglobulin;(mIU/L)		
					Pre-isotretinoin	Pre-rh-TSH	Peak value
1	F	66	Follicular, oxyphilic variant	Lung, skeleton	40	160	826
2	F	78	Papillar, oxyphilic variant	Lung, nodes	60	68	69
3	M	60	Follicular, oxyphilic variant	Lung, nodes	407	797	1129
4	F	69	Papillar, oxyphilic variant	Lung	173	228	584
5	M	69	Papillar, tall-cell variant	Lung	2	2	5

Results All patients experienced isotretinoin-related side effects including muco-cutaneous reactions (such as erythema of the skin, cheilitis, and xerosis), myalgia, alteration of the lipidic profile that required appropriate treatment. No adverse reactions secondary to rh-TSH administration were observed. After rh-TSH treatment all patients exhibited adequate circulating levels of TSH ranging from 150 to 410 mUI/L. Tireoglobulin before starting therapy and after isotretinoin and rhTSH treatments are reported in the table. In 1 patient (ID1) we found a markedly increase of RI uptake in neoplastic lesions. In the other 4 patients no significative RI uptake was achieved.

Conclusions In our experience the combined therapy of isotretinoin plus rh-TSH induced RI uptake in only 1 patient with RI negative thyroid carcinoma. Further investigations are needed in order to verify if the failure of redifferentiation can be due to an alteration of retinoic acid metabolic pathway or to a non adequate TSH stimulation.

OS_164

FACTORS INFLUENCING THE DOSIMETRY AND THE THERAPEUTIC OUTCOME OF RADIOIODINE (I-131) THERAPY QF DIFFERENTIATED THYROID CANCER

T.M. Behr (1), M. Behe (1), S. Gratz (1), M. Hüfner (2), W. Becker (3). (1) Dept. of Nuclear Medicine, Philipps-University, Marburg, Germany; (2) Dept. of Endocrinology, Georg-August-University, Göttingen, Germany; (3) Dept. of Nuclear Medicine, Georg-August-University, Göttingen, Germany.

Aim: Almost twenty years ago, Maxon *et al.* published (N. Engl. J. Med. 1983; 309: 937) and updated (J. Nucl. Med. 1992; 33: 1132) a detailed analysis of factors that influence the dosimetry and efficacy of the $Na^{131}I$ therapy of DTC. The aim of this study was to re-investigate whether these factors hold true for a different patient population (Europe vs. the United States) with a lower alimentary iodine supply, and to identify additional variables affecting the outcome of DTC therapy.

Methods: Sixty-seven patients (39 papillary, 23 follicular, 3 Hürthle cell, 2 partially anaplastic cancers) were given 30-350 mCi $Na^{131}I$ for remnant ablation (n=37) or treatment of metastatic disease (n=30). Fourteen additional patients underwent a prior "diagnostic" dose (2-100 mCi) within one week before the actual therapy. All had stopped thyroid hormone intake for ≥ 4 weeks. For dosimetry, quantitative conjugate view whole-body scans were performed daily for ≥ 96 h.

Results: The mean ^{131}I uptake values were ~ 3-fold higher in remnants (18.2 μCi/mCi×g) than in metastases (5.6 μCi/mCi×g), whereas effective $t_{1/2}$s were not significantly different. The biological $t_{1/2}$s in remnants and metastases were strongly dependent upon TSH values (the higher the TSH, the shorter the biological $t_{1/2}$), whereas surprisingly, no correlation was found between TSH values and uptakes: e.g., at TSH ≥ 50 μU/ml, mean radiation doses to remnants or metastases were lower by one order of magnitude than at physiological TSH. Mean doses to remnants were 8.6 Gy/mCi (range 0.4-62.5 Gy/mCi), mean doses to metastases 2.8 Gy/mCi (range 0.2-17.5 Gy/mCi). In patients having received a prior "diagnostic" dose, stunning began at activities > 2 mCi (corresponding to radiation doses > 6 Gy). Actual doses, and not administered activities were best predictors of therapeutic success (reliable remnant ablation at ≥ 300 Gy, metastasis ablation at ≥ 80-200 Gy).

Conclusions: Threshold doses for successful tissue ablation were similar in this study as compared to those published earlier. The finding that increasing TSH levels do not seem to enhance the uptake, but dramatically decrease the biological $t_{1/2}$s, thus radiation doses, stands in clear contrast to the traditional paradigm and warrants further investigation.

OS_165

THE EFFICIENCY OF PLANNING OF THERAPEUTIC 131I ACTIVITIES IN THE RADIOIODINE THERAPY OF DIFFERENTIATED THYROID CANCER

B. Sinyuta, D. Dzhuzha. Department of Nuclear Medicine, Institute of Oncology, Kiev, Ukraine.

The efficiency of radioiodine therapy (RIT) in combined treatment of the differentiated thyroid cancer (DTC) could be increased by calculation of the values of individual therapeutic 131I activities using parameters of the pharmacokinetics of the diagnostic radioiodine activities. With the aim to evaluate the efficiency of planning the therapeutic radioiodine activities for ablation of thyroid residual tissue and lymph node metastases treatment results were analysed.

Methods: The study included 66 patients with DTC aged 25-68. The diagnostic scintigraphy was made using 70-80 MBq of 131I 4-6 weeks following thyroidectomy. The thyroid residual tissue was diagnosed in 52 patients, thyroid residue with lymph node metastases – in 14. RIT was performed with empirical therapeutic activities according to the spread of the process. The suppressive hormonal therapy with L-thyroxin was carried out after RIT. Control scintigraphy was made 4-6 months following RIT. Retrospective calculation of the therapeutic radioiodine activities for creation of ablative radiation adsorbed dose was performed using the parameters of 131I pharmacokinetics registered during diagnostic scintigraphy. Radiation adsorbed doses in thyroid remnants and lymph node metastases were estimated according to MIRD recommendations.

Results: The patients were divided into two groups. The first group consisted of 41 patients in whom therapeutic activities were equal or higher than calculated activities. In the second group 25 patients had therapeutic activities less than the planned ones. In the first group the positive effect after the first course of RIT was reached in 34 patients (82.9%). In the second group the positive effect was observed in 10 patients (40%). Difference between efficiencies in group 1 and 2 was significant ($p<0.002$). 2 patients of the first group had negative results of RIT despite the high radiation adsorbed doses. In these cases lung metastases were diagnosed on therapeutic scans. In another 5 patients from this group thyroid stunning caused negative results. Radiation adsorbed doses after administration of the diagnostic activity varied from 28.2 to 47.7 Gy and were comparable to radiation adsorbed doses after administration of therapeutic activity.

Conclusions: Administration of the calculated therapeutic activities of 131I can improve the results of the first course of RIT. Negative results of the planning of RIT may be due to the aggressive course of DTC, high tissue radioresistance and the effect of thyroid stunning.

OS_166

THE INFLUENCE OF DIAGNOSTIC RADIATION ADSORBED DOSES AND TIME INTERVAL ON THE DEGREE OF THYROID STUNNING

B. Sinyuta, D. Dzhuzha. Department of Nuclear Medicine, Institute of Oncology, Kiev, Ukraine.

The effect of the thyroid stunning (TS) is one of the factors, which can significantly change the efficacy of the radioiodine therapy (RIT) in differentiated thyroid cancer (DTC). The aim of this investigation was to evaluate the influence of diagnostic radiation adsorbed doses (RAD) and time interval between diagnostic scintigraphy and RIT on the degree of the TS.

Methods: The study included 69 patients aged 25-74 receiving combined treatment for DCT. The diagnostic scintigraphy was made using 70-80 MBq of 131I 4-6 weeks following thyroidectomy. All patients had only thyroid residual tissue. RIT was performed with empirical or calculated therapeutic activities ranging from 1.9 to 4.7 GBq. The time interval between diagnostic scintigraphy and RIT varied from 1 to 227 days. Control scintigraphy was done 4-6 months after RIT. The RAD in thyroid remnants were estimated according to MIRD recommendations.

Results: All patients were divided into four groups: with diagnostic RAD lesser 10 Gy, 10-19.9 Gy, 20-29.9 Gy and more than 30 Gy. The mean diagnostic RAD were in groups 4.6±0.5 Gy, 14.5±0.7 Gy, 24.8±0.5 Gy and 47.1±4.3 Gy, respectively. The mean reduction of the D/A therapeutic index relative to that of the diagnostic one equaled 36.9±8.2%, 72.1±4.5%, 73.5±5.9% and 85.8±3.1%, respectively. The difference was significant between groups 1 and 2 ($p<0.001$), while it was not between groups 2 and 3, 3 and 4. The diagnostic RAD was 9.0±0.6% of total RAD on the first day, 25.4±1.8% on the second day and 33.9±2.8% on the third day. The influence of the time interval on the TS was studied in two groups of patients receiving more than 10 Gy of the diagnostic RAD. In the first group (n=8) the time interval was 1-3 days (1.75±0.27 days), in the second one (n=46) it was more than 3 days (64.5±7.4 days). The reduction of D/A therapeutic indices was 58.0±7.3% and 81.4±2.5%, respectively ($p<0.01$).

Conclusions: The TS may appear after diagnostic scintigraphy with 70-80 MBq when RAD of several Gy was reached in thyroid residuum. The TS increased significantly at value of diagnostic RAD more than 10 Gy. The administration of RIT during 1-3 days after administration of the diagnostic activity can decrease the effect of the TS.

OS_167

SELF-STUNNING IN THYROID ABLATION - EVIDENCE FROM A COMPARATIVE STUDY OF 131I AND 123I AS DIAGNOSTIC AGENTS

A.A. Bolster (1), M.F. Dempsey (1), T.E. Hilditch (1), R.M. McMenemin (2), N.S. Reed (2). (1) Department of Nuclear Medicine; (2) Beatson Oncology Centre, Western Infirmary, North Glasgow University Hospitals NHS Trust, Scotland, G11 6NT.

Aim
This study aims to determine whether the use of ^{123}I iodide to assess thyroid cancer patients before radioiodine ablation can obviate the 'stunning' problem associated with diagnostic ^{131}I. A quantitative approach is used, employing a dual head gamma camera in the measurement of thyroid uptake.
Methods
Twenty-eight patients who had recent surgery for thyroid cancer, and had not commenced thyroid hormone replacement therapy, were investigated using ^{131}I iodide [120MBq]. Uptake in the thyroid bed was measured at 3 days. An ablation dose of ^{131}I iodide [4000MBq] was administered 3-38 [17.1±11.0 S.D.] days later and uptake in the thyroid bed measured once or twice, 1-3 days post therapy. For measurements post therapy, the gamma camera was operated in the high-count rate mode with appropriate correction factors to compensate for any count loss.
A further 15 patients were given ^{123}I iodide [200MBq] as the diagnostic agent and uptake measured at 24 hours. The ablation dose was administered 5-61 [25.6±14.9] days later and uptake measured also at 24 hours. Two patients required thyroid hormone replacement therapy [T3] in the interim but this was discontinued 2 weeks before thyroid ablation.
Results
Reduced uptake post therapy [$p<0.001$] was observed in 27 of the 28 patients given diagnostic ^{131}I, being, overall, 37.8±23.0% [range 5.9-100%] of the uptake after the diagnostic dose. There was no correlation between the degree of stunning and time delay before the ablation dose, nor evidence of rapid loss of radionuclide from the thyroid bed 1-3 days post therapy. In the patients given diagnostic ^{123}I, reduced uptake post therapy was observed in 13 of the 15 patients [$p<0.01$] and overall the mean value was 67.0±33.8% [range 15.6-151.6%] of the diagnostic uptake. In two cases the uptake post therapy was increased. The stunning observed in the group given ^{123}I was significantly less [$p<0.002$] than in the group given ^{131}I.
Conclusions
Stunning was observed using ^{123}I and this effect cannot be explained by errors in the estimation of relative uptake due to different tissue absorption of the ^{131}I and ^{123}I photons, nor by the radiation dose delivered by the ^{123}I. However the ablation dose itself may cause stunning because the cumulated activity, over the first few hours of uptake, may not be insignificant when compared to all the cumulated activity from a diagnostic dose of ^{131}I.

OS_168

IS RADIOIODINE THERAPY ALWAYS USEFUL IN PATIENTS WITHOUT RESIDUAL THYROID TISSUE AFTER TOTAL THYROIDECTOMY FOR DIFFERENTIATED THYROID CANCER (DTC)?

M. Salvatori, V. Rufini, G. Perotti, L. Marchetti, M.L. Maussier, L. Troncone. Department of Nuclear Medicine, Università Cattolica del Sacro Cuore, Rome, Italy.

The recent tendency to perform ^{131}I ablative therapy after total thyroidectomy for DTC without pre-ablative diagnostic ^{131}I scintigraphy has the object to avoid thyroid stunning, to reduce the costs and to decrease the hypothyroidism burden for the patient (Nucl Med Commun 21:529,2000).On the other hand the risk of this approach is to perform some inappropriate therapy in pts. without residual thyroid tissue. The aim of this retrospective study was to evaluate the incidence of inappropriate ^{131}I therapy in 102 consecutive patients without residual thyroid tissue at pre-therapy diagnostic evaluation out of the 760 treated after surgery with radioiodine during the 1995-1999 period.
There were 85 females and 17 males with a median age of 46.7 years (range 17 – 76). The histological types included 50 conventional papillary,31 follicular variant of papillary carcinoma, 3 tall cell variant of papillary carcinoma,14 follicular well- differentiated carcinoma and 4 follicular carcinoma oncocytic type. Before ^{131}I therapy, these pts. showed an absence of residual thyroid tissue by strict criteria of evaluation (Tg off L-T4 <2 ng/ml and absence of Ab-Tg with TSH > 30 µUI/ml; RAIU in the neck <0.2% at 24 hr.; no or faint visualization of thyroid tissue with a diagnostic dose of radioiodine).All pts. were treated with a fixed 1850 MBq dose of radioiodine except 32 pts. treated with 3700 MBq (all pT4 pts. and 10 pts. with aggressive histological patterns). In spite of the absence of residual thyroid tissue, the ^{131}I therapy was performed in order to detect previously unknown locoregional or distant metastases by post-therapy ^{131}I scan (PTWBS) performed 3-4 days after therapy.
At PTWBS faint radioiodine uptake in the thyroid bed in 19 pts.(18.6%) and negative results in the remaining 83 pts. (81.3%) was noted . During the successive follow-up (range 12-60 mos., median 18.9 mos.) only two pts. showed locoregional metastases (2 females with pT4 tall cell variant of papillary carcinoma and pT2 follicular well-differentiated thyroid cancer 12 mos. after radioiodine therapy).
In conclusion, our results confirm the high negative predictive value of Tg off L-T4 for residual or metastatic thyroid tissue and show that in 11% of pts. (83/760) with DTC a ^{131}I treatment without pre-ablative diagnostic evaluation may be cause of inappropriate therapy because they are lacking in residual thyroid tissue and locoregional or distant metastases.

OTHER CLINICAL SCIENCE. ENDOCRINOLOGY

OS_169

EVIDENCE FOR SPATIAL HETEROGENEITY IN INSULIN- AND EXERCISE INDUCED INCREASES IN GLUCOSE UPTAKE. STUDIES IN NORMAL SUBJECTS AND PATIENTS WITH TYPE 1 DIABETES

J. Knuuti (1), P. Peltoniemi (1), H. Yki-Järvinen (2), H. Laine (1,3), V. Oikonen (1), T. Rönnemaa (3), K. Kalliokoski (1), O. Raitakari (1), P. Nuutila (1,3). (1) Turku PET Centre; (2) Department of Medicine; (3) Department of Medicine, University of Turku, Turku, Finland.

Aim: It is unknown whether resistance to insulin- or exercise-stimulated glucose uptake reflects a spatially uniform or nonuniform decrease in glucose uptake within skeletal muscle.
Methods: We compared the distributions of muscle glucose uptake and blood flow in eight patients with type 1 diabetes (age 24±1 years, BMI 22.0±0.8 kg/m^2) and seven age- and weight-matched normal subjects using positron emission tomography, [^{18}F]-fluoro-deoxy-glucose and [^{15}O]-water. Both groups were studied during euglycemic hyperinsulinemia and one-legged exercise. Heterogeneity was evaluated by calculating relative dispersion (standard deviation divided by mean*100 %) of glucose uptake (RD_g) and flow (RD_f) in all pixels within a region of interest in femoral muscle.
Results: The exercise-induced increment in glucose uptake but not in blood flow was significantly lower in the type 1 diabetic patients than in the normal subjects (94±21 vs 186±29 µmol/kg·min). RD_g, but not RD_f was increased in the insulin resistant type 1 diabetic patients both at rest (RD_g 31±1 vs 25±2 %, patients with type 1 diabetes vs normal subjects, $p<0.05$) and during exercise compared to normal subjects (27±1 vs 21±2 %, respectively, $p<0.05$). Exercise increased both glucose uptake and blood flow several-fold and significantly decreased both RD_g and RD_f. RD_g was inversely associated with total glucose uptake ($r=-0.54$, $p<0.001$, pooled data) and was highest in the most insulin-resistant patients.
Conclusions: We conclude that both glucose uptake and blood flow are characterized by heterogeneity in human skeletal muscle, which magnitude is inversely proportional to respective mean values. This implies that an increase in glucose uptake in human skeletal muscle is not a phenomenon, where each unit increases its glucose uptake by a fixed amount but rather a spatially heterogeneous process.

OS_170

3-PLANE WHOLE BODY SCINTIGRAPHY AND I-131-SPECT IN THYROID CANCER

P. Mariß (1), J. Herrmann (2), S. Herbrik (1), D. Emrich (1). (1) Gemeinschaftspraxis Radiology/Nuclear Medicine Dr. Stuckenholz & Partner, Germany; (2) Medizinische Klinik I, Städtische Kliniken Bielefeld, Germany.

Aims: Total thyroidectomy (TT) and high dose radioiodine therapy (RIT) represent the essential therapeutic options in differentiated (papillary and follicular) thyroid carcinoma (DTC). Thyreoglobulin (TG) determination and whole body I-131-scintigraphy (WBS) are the most important follow up procedures. Planar WBS shows some methodological impairments. Therefore we performed a prospective comparative study between the usual 2-plane WBS (2PWBS) and a new 3-plane WBS (3PWBS) combined with a cervical-thoracic I-131-spect investigation (CTIS) in patients with DTC under post-therapeutic conditions.
Methods: In 56 pts (38 female and 18 male) with DTC (papillary n=39, pT2-4 N0-1 M0-1 and follicular n=17, pT1-4 N0-1 M0-1) 4-5 w after TT and 6-8 d after RIT (3,7 GBq) a 2PWBS (180 degree v/d) (Elscint SP6) and a 3PWBS (120 degr. v/rdo60/ldo60) (IRIX, Marconi Picker) followed by CTIS were performed within 6 h. The spect image reconstruction was achieved by filtered back projection and by iterative reconstruction as well.
Results: In 43 from 56 pts identical results between 2PWBS and 3PWBS with CTIS respectively were obtained. In 6 pts additional metastases were detected by CTIS. One thoracic enrichment was identified as a physiological iodine accumulation in thymus. In 5 pts additional information was won in thyroid remnant or in a cervical lymph nodes. One pt showed a "false positive" liver accumulation in a histologically proven dysontogenetic liver cyst.
Conclusion: This preliminary study seems to demonstrate a qualititative improvement in scintigraphic images of the thyroid remnant, cervical lymph nodes and I-131-accumulating metastases in DTC using a modified whole body scintigraphy in combination with cervical-thoracic-spect tomograms in comparison to the conventional planar scintigrams. By application of recombinant TSH and by implementation of a Monte-Carlo-simulation in image reconstruction a further amelioration can probably be realized.

OS_171

BONE MINERAL METABOLISM DURING ANTI-THYROID THERAPY FOR ENDOGENOUS SUBCLINICAL HYPERTHYROIDISM

F. Berk (1), M. Akkoyun (2), H. Demir (1), O. Erdincler (1), S. Isgoren (1), B. Cetinarslan (2), C. Aktolun (1). (1) Department of Nuclear Medicine; (2) Department of Endocrinology, Kocaeli University, Kocaeli, Turkey.

Patients with subclinical hyperthyroidism (reduced serum TSH and normal free T4-T3 concentrations) usually have a slightly increased bone turnover that may reduce the bone mineral mass. In this study, we evaluated the effects of antithyroid drug treatment on bone metabolism in endogenous subclinical hyperthyroidism; when euthyroidsm is restored.

METHODS: Eighteen pre-menapousal women with endogenous subclinical hyperthyroidism (TSH <0.1 Mu/L), associated with multinodular or diffuse goitre were included the study. Patients were followed prospectively for a year during and after propycil treatment. Serum concentrations of free T4, free T3, TSH, ALP, and bone mineral density (BMD) were measured at regular intervals. BMD was measured at lumbar L2-4 vertebrae and femoral neck by dual energy x-ray absorbtiometry (DEXA, Norland XR-26). All pre and post-treatment results were compared with controls.

RESULTS: Significant ($p<0.01$) decline in FT4, FT3 was observed; beginning in 6 weeks, after the commencement of propycil therapy and stabilized thereafter. The mean TSH values increased to the target level. Significant changes in serum ALP (89.33± 33.87) levels were not observed. (BMD results are summarized in table below) Significant BMD changes were not observed.

BMD results (gr/cm2)	Baseline	On anti-thyroid therapy
L2-L4 BMD	1.06 ± 0.15	1.05 ± 0.15
Femoral neck BMD	0.89 ± 0.13	0.88 ± 0.12

CONCLUSION: Our findings suggest that; treatment with anti-thyroid therapy in perimenouposal women with endogenous subclinical hyperthyroidism do not affect the short term bone mineral metobolism in the axial skeleton. The precise effects of drug treatment on long term bone mineral metabolism is yet to be investigated with further studies.

OS_172

ENHANCEMENT OF RADIOIODINE UPTAKE IN HYPERTHYROID PATIENTS WITH HYDROCHLOROTHIAZIDE: PRELIMINARY RESULT OF A PROSPECTIVE RANDOMIZED CONTROL STUDY

S. Tepmongkol. Division of Nuclear Medicine, Department of Radiology, Chulalongkorn University, Bangkok, Thailand.

Aim : To determine whether hydrochlorothiazide (HCTZ) could improve radioiodine uptake in low-uptake hyperthyroid patients.

Methods : Eighteen hyperthyroid patients with low 3 hr and 24 hr I-131 uptake were studied. Patients were divided into 11 patients in HCTZ group and 7 in control group. The second uptake was done two weeks later. Patients in both groups had low-iodine diet after the first uptake. In HCTZ group, 50 mg. of HCTZ was administered twice a day for 5 days prior to the second uptake. Impovement of uptake at 3 and 24 hr. were compared between the first and the second uptake within group and between groups.

Results : In control group, there was significant improvement of uptake at 3 hr compared to baseline (P=0.03) but no significant change at 24 hr (p=0.937). In HCTZ group, significant improvement at both 3 hr.(p=0.004) and 24 hr. (p=2.2E-05) were observed. Patients in HCTZ group had statistically more improvement of uptake at 24 hr. compared to the control group (p=0.002), however, no significant difference was found at 3 hr. (p=0.326). There was 7.18 fold average improvement of uptake in HCTZ group, whereas only 1.33 fold in control group at 24 hr.

Conclusions : Administration of HCTZ significantly improves 24 hr radioiodine uptake in high-iodide pool, low-uptake hyperthyroid patients compared with patients who had low-iodine diet alone.

OS_173

STEPWISE-ADAPTATED ABSORBED DOSE CONCEPT IN MULTIFOCAL AND DISSEMINATED THYROID AUTONOMY - RESULTS IN 145 CASES

M.J. Reinhardt (1), D. von Mallek (1), M. Zimmerlin (2), A. Joe (2), T. Krause (1), E. Moser (2), H.J. Biersack (1), H. Palmedo (1). (1) Dept. of Nuclear Medicine, Univ. Hospital Bonn, Germany; (2) Dept. of Nuclear Medicine, Univ. Hospital Freiburg, Germany.

Aim: Some years ago a modified dose concept for radioiodine treatment of multifocal and disseminated thyroid autonomy has been developed (1). This concept stepwise adapts the tissue absorbed dose to the pertechnetate thyroid uptake between 150 Gy and 300 Gy. The present study prospectively investigates the results obtained following this concept.

Methods: 145 patients with multifocal or disseminated thyroid autonomy (103 women, 43 men; aged 71±10 years; thyroid volume 65±40 ml) were treated with radioiodine. Activity applied was calculated by means of Marinelli's formula. The entire thyroid was determined as target volume. Target dose was choosed according to the pertechnetate thyroid uptake under TSH-suppression (TcTUs): 150 Gy for TcTUs 1.5-2.5 %, 200 Gy for TcTUs 2.51-3.5 %, 250 Gy for TcTUs 3.51-4.5 % and 300 Gy for TcTUs > 4.5 %. Therapeutic success was defined as normalisation of TcTUs (< 1.5 %) one year after therapy.

Results: Success rate and frequency of hypothyroidism with the present dose concept are summarised in table 1.

TcTUs (%)	Target dose (Gy)	Patients (N)	Thyroid vol. (ml)	Success rate	Hypothyroidism
1.5-2.5	150	62	67 ± 46	58/62 (93.5 %)	2/62 (3.2 %)
2.51-3.5	200	30	66 ± 41	27/30 (90 %)	0
3.51-4.5	250	25	51 ± 28	24/25 (96 %)	0
>4.5	300	28	73 ± 33	26/28 (92.9 %)	0
Total	-	145	65 ± 40	135/145 (93.1 %)	2/145 (1.4 %)

Table 1. Results of radioiodine therapy for Plummer's disease using a TcTUs-adapted dose concept

Conclusion: Elimination of functional autonomous thyroid tissue can be obtained with a single radioiodine therapy even in patients with large goiters and severe autonomy in 93 %. The overall rate of hypothyroidism using the presented dose concept remains below 1.5 %.

Reference: Reinhardt M, Emrich D, Krause T, et al. Improved dose concept for radioiodine therapy of multifocal and disseminated thyroid autonomy. Eur J Endocrinol 1995; 132: 550-556

OS_174

ECTOPIC THYROID TISSUE ON THYROID SCAN WITH TC-99M PERTECHNETATE AND I-131 IN PATIENTS WITH ATHYROTIC HYPOTHYROIDISM

B.C. Ahn, S.W. Lee, J. Lee, K.B. Lee. Department of Nuclear Medicine, Kyungpook National University Hospital, Taegu, Korea.

We previously reported clinical characteristics of 41 cases with surgically proven thyroglossal duct cyst, which was never seen on thyroid scan with ^{99m}Tc-pertechnetate. Thyroglossal duct cysts seldom contain sufficient follicular tissue to be imaged in euthyroid state, but they could be easily visualized on thyroid scan in patients with athyrotic hypothyroidism. We performed this study to find the incidence of ectopic thyroid tissue on thyroid scan in thyroidectomized patients with hypothyroidism.

Methods: We reviewed ^{99m}Tc-pertechnetate (Tc-scan) and ^{131}I scan (I-scan) of 110 patients (male:female=15:95, mean 44 yrs) with differentiated thyroid carcinoma who had underwent total thyroidectomy without thyroid hormone replacement for more than 4 weeks. Planar and pinhole images of neck with ^{99m}Tc-pertechnetate were acquired and followed by ^{131}I imagings after high dose radioiodine therapy (ranging from 100 mCi to 200 mCi) within 7 days. Two nuclear medicine physicians performed visual interpretation.

Results: Serum TSH levels of all patients were more than 30 mIU/L. Fifty-three out of 110 patients (48%) showed focal or linear abnormal tracer uptake at midline of upper anterior neck. Tc-scan and I-scan of each patient showed corresponding result in all cases.

Conclusion: The incidence of ectopic thyroid tissue is strikingly high than previously reported. Especially in patients with athyrotic hypothyroidism, ectopic thyroid tissues are frequently visualized on both Tc-scan and I-scan, although clinically unsuspected.

OS_175

AN INVESTIGATION OF THE USE OF AN ARTIFICIAL NEURAL NETWORK TO PREDICT THE OUTCOME OF I-131 THERAPY FOR HYPERTHYROIDISM

J.M. Warwick, B.B. Van Heerden. Department of Nuclear Medicine, University of Stellenbosch, Tygerberg Hospital, Tygerberg, 7505, South Africa.

Aim: A large number of factors have a variable and complex influence on the effectiveness of I-131 treatment for hyperthyroidism. Despite extensive work in this field, it is currently not possible for the physician to accurately predict the I-131 dose required for the patient to become euthyroid post-therapy, without the need for long term thyroxine therapy. The aim of this study was to investigate the ability of an Artificial Neural Network (ANN) to predict the result of I-131 therapy in patients with hyperthyroidism.
Methods: This study used data from 242 doses of I-131, administered to 226 patients by the Nuclear Medicine hyperthyroidism clinic of our institution during 1998. Eight pre-treatment factors from clinical, biochemical and scintigraphic assessment, and a follow up free thyroxine value at least 3 months after therapy were obtained for each of the doses. These data were then divided into 3 sets. The training and validation sets were used to train an ANN by means of the backpropagation algorithm, to predict the outcome of therapy using the pre-treatment factors. Data from the testing set was then used to evaluate the performance of the trained ANN. Receiver operating characteristic analysis was used to determine optimal thresholds to predict which patients would be hypothyroid or hyperthyroid following therapy.
Results: An ANN output value less than 16 was predictive of hypothyroidism following therapy, with a sensitivity of 74%, specificity of 80% and an accuracy of 77%. An ANN output value greater than 21 was predictive of hyperthyroidism following therapy, with a sensitivity of 44%, specificity of 82% and an accuracy of 74%.
Conclusions: Using appropriately chosen thresholds, the ANN output was a highly specific and moderately sensitive predictor of the outcome of I-131 therapy in these patients. This study suggests that ANN's may provide a novel and potentially widely applicable approach to predicting the results of I-131 therapy for hyperthyroidism. This may provide clinicians with a tool to assist in improving their dosing regime.

OS_176

INFLUENCE OF ABNORMAL LONG CONTINUAL ANTITHYROID DRUGS TREATMENT ON OUTCOME OF 131I THERAPY IN GRAVES' DISEASE

M. Bogicevic, M. Rajic, S. Antic, M. Vlajkovic, G. Lilic, M. Lazarevic, D. Mitic, V. Stefanovic. Department of Nuclear medicine, Clinical Center, Nis, Yugoslavia.

Introduction: Radioiodine therapy is commonly proposed for treatment of diffuse toxic goiter if it is not possible to eliminate hyperthyroidism with antithyroid drugs up to 18 months. Continual medical therapy was preformed for much longer time period in some patients in our country due to inability to import enough amounts of 131I because of very poor finance resources in several last years. The **aim** of this study was to evaluate influence of abnormal long continual antithyroid drug treatment on effectiveness of radioiodine therapy in patients with Graves' disease. **Methods:** 15 females and 7 males aged from 34 to 67 years, were received empirical dose of 131I (111-259 MBq), 5-7 days after antithyroid medications were discontinued. One dose of 131I was applied to 15 patients, 2 doses in 6, and 3 doses in one patient. Thyroid function was assessed by radioimmunoassays of TT4 (nmol/l), TT3 (nmol/l) and TSH (mU/l). **Results**:

Drugs (years)	**No**		Before 131I	After 18 months	r	p
< 1.5		TT3	4.42 ± 1.28	2.35 ± 1.34	-0.028	
(1.15±0.24)	11	TT4	228 ± 35	170 ± 63	-0.012	N.S.
		TSH	0.136 ± 0.021	2.71 ± 2.20	-0.256	
> 1.5		TT3	4.62 ± 2.74	2.08 ± 1.13	0.046	
(4.75±1.50)	11	TT4	238 ± 46	164 ± 46	-0.305	N.S.
		TSH	0.175 ± 0.097	2.29 ± 1.87	0.139	

The results displayed showed that previous medicament treatment duration did not correlated with hormone levels at 18 months after radioiodine administration in both groups. At that time hyperthyroidism was eliminated in 40.9% patients (in 55.6% pts. on drug treatment < 1.5 yr. and 59.1% pts. on drug treatment < 1.5 yr.). **Conclusion:** The findings presented showed no differences in outcome of radioiodine treatment in patients with enorm long continual thyrostatic therapy related to those with customary lasting of drug therapy.

PHYSICS / INSTRUMENTATION

OS_177

A METHOD FOR THE CALCULATION OF THE GEOMETRIC SENSITIVITY FOR STATIONARY 3D PET USING A TRIPLE-HEADED GAMMA CAMERA

Y. D'Asseler (1), S. Vandenberghe (1), M. Koole (1), L. Bouwens (1), R. Van De Walle (1), I. Lemahieu (1), R.A. Dierckx (2). (1) ELIS-Medisip; (2) Department of Nuclear Medicine, Ghent University Hospital, Ghent, Belgium.

Aim : Recently, the use of triple-headed gamma cameras for PET imaging has been suggested. With the heads in a triangular configuration, and moved as close together as possible, allmosty all LOR's are detected using only one camera position, so stationary PET becomes feasible. Various techniques have been devised to compensate for missing data. In order to reconstruct data acquired with this technique, it is important to know how the 3D geometric sensitivity varies throughout the FOV . We devised a method to calculate this sensitivity.
Methods : The calculation of the geometric sensitivity for 3D PET using a stationary triple-headed gamma camera is based on the calculation of the solid angle subtended by two detector heads from a given voxel. Solid angles for each detector pair are then added to obtain the total sensitivity. To calculate the solid angle, first, the central projection through the voxel under consideration of the first detector plane onto the second detector is calculated, this will give a rectangular area. The cross section of this area with the second detector is then determined. This will again give a rectangular area, and this area will define the solid angle. We divide the rectangle into two triangles, which we project onto a unit sphere. The area of the spherical triangles, giving the solid angle, are calculated from the angles of the triangle.
Results : Sensitivity profiles for an existing triple-headed configuration (IRIX, Marconi Med.) were calculated, for different radii of the detector heads. As expected, these profiles show a decrease in sensitivity at the location of the gaps between the different camera heads. However, sensitivity is greater than zero at all places within the FOV. Sensitivity reaches a local minimum at the center of the FOV.
Discussion : Our method for the calculation of 3D geometric sensitivity will be used as a first step in the reconstruction of images acquired with a stationary gamma camera. Whereas sensitivity for a given pixel is always greater than zero, this is not the case for the LOR's : some LOR's will not be detected at all due to the gaps between the detector heads. In future work, we will implement a method to compensate for these missing data, and will evaluate the artifacts due to these missing data.

OS_178

STUDY OF HOLE ARRAY PATTERN ARTIFACTS IN MULTIHOLE COLLIMATORS

A.R. Formiconi, F. Di Martino, D. Volterrani, A. Passeri. Dept. Clinical Pathophysiology, University of Florence, Italy.

Recently, a theoretical description of any kind of collimator has been proposed by one of the authors. In this work, the theory was used to study the response to extended uniform sources, so that hole array effects can be easily studied.
The dependence of such effects on the detector-collimator distance was assessed and the existence of optimal detector-collimator distances for which they are minimized was found.
Our theoretical predictions were compared with experimental data obtained with a specific camera-collimator system. A large field of view camera equipped with an high-energy general purpose collimator for I-131 with round holes placed in an hexagonal lattice was used. A series of images of a flood source placed on the collimator external face, each with a different detector-collimator distance was acquired.
The qualitative analysis of the images clearly showed the existence of optimal distances to reduce the hole array artifacts. The quantitative analysis data showed that the theoretical predictions were in agreement with the experience.
These results may be useful for the design of new collimators, for the optimal arrangement of camera-collimator system and they may also foster the study of some artifacts compensation methods.

OS_179

COUNT RATE CHARACTERISTICS OF PET WITH BROMINE-76

M. Lubberink (1), H. Schneider (2), M. Bergström (2), H. Lundqvist (1).
(1) Section of Biomedical Radiation Sciences, Uppsala University, Uppsala, Sweden; (2) Uppsala University PET Centre, Uppsala, Sweden.

A number of nuclides used in PET, such as ^{76}Br, ^{110m}In or ^{86}Y, emit gamma radiation in cascade with positrons. Essentially true coincidences involving this gamma radiation lead to an increased image background, which can be corrected for using a projection tail fit subtraction prior to image reconstruction. The aim of this study was to investigate the effect of gamma radiation on ^{76}Br count rate linearity and noise equivalent count rates.
Methods: Measurements were done using a Scanditronix/GEMS 4096+ scanner with fixed septa, and a Siemens/CTI ECAT Exact HR+ with retractable septa. Dynamic scans of uniformly filled phantoms with high initial radioactivity concentrations of ^{76}Br or ^{11}C were made during several half-lives of the respective nuclide. Noise equivalent count (NEC) rates were calculated using the following equation:

where T is the net trues rate, S is the scatter rate, G is the gamma coincidence rate, R is the randoms rate and f is the fraction of the sinogram taken up by the object. A count rate model, involving both singles and coincidence dead time, was developed.
Results: The HR+ peak 3D NEC rate is approximately 35 kcps at 12 kBq/ml for ^{76}Br, compared to >150 kcps at >18 kBq/ml for ^{11}C. In 3D mode, the total randoms rate is higher than the net trues rate at any activity concentration. In 2D mode, the total randoms rate exceeds the net trues rate at 23 kcps and 10.5 kBq/ml. The standard dead time correction of the HR+, based only on measured singles rates, is not valid for gamma-emitting PET nuclides. The prompts rate relative to singles rate is much higher than for ^{11}C at any radioactivity concentration, both in 2D and in 3D mode, which causes an underestimation of the dead time. The suggested count rate model predicts accurately both ^{11}C and ^{76}Br system dead time. The 4096 dead time correction, based both on singles and on prompts rates, has a linear result, but radioactivity concentrations are overestimated.
Conclusions: Noise equivalent count rates at clinically relevant radioactivity concentrations are approximately ten times higher for ^{11}C than for ^{76}Br. A dead time correction based not only on singles rates, or a dedicated singles-based dead time correction for each gamma-emitting nuclide, is necessary for quantitative imaging of ^{76}Br and other gamma-emitting PET nuclides with the ECAT Exact HR+.

OS_180

PERFORMANCE EVALUATION OF A NEW THICK SLOTTED NAI CRYSTAL SINGLE PHOTON AND COINCIDENCE IMAGING GAMMA CAMERA

W. D. Erwin (1), M. W. Groch (1), S. M. Spies (1), J. F. Caruba (2), J.T. Chapman (2), R. E. Malmin (2), T. D. Rempel (2), J. M. Soldner (2).
(1) Department of Nuclear Medicine, Northwestern University Medical School, Chicago, USA; (2) Siemens Medical Systems, Hoffman Estates, USA.

The purpose of this investigation was to evaluate the single photon and coincidence imaging performance of a new generation, slotted crystal gamma camera (e.cam$^{duet™}$, Siemens Medical Systems), consisting of dual scintillation detectors with StarBrite® (Bicron) NaI crystals (25 mm (1") thick, 12.5 mm (1/2") slotted exit window, 90x66 array of 6x6 mm pixels, 0.5 mm slots), and automated corrections for the energy-dependent response of the crystal.
Methods: Single photon measurements consisted of: 1) NEMA intrinsic spatial resolution, linearity, uniformity and energy resolution, 2) NEMA SPECT reconstructed spatial resolution, 3) intrinsic bar and orthogonal hole patterns, 4) system sensitivity versus radionuclide (^{67}Ga, ^{111}In, ^{131}I) and 5) SPECT performance phantom (4.8-12.7 mm "cold" rods, 9.5-31.8 mm "cold" spheres). ^{18}F coincidence measurements (with septa, 30 % energy window at 511 keV, timing window = 12 nsec) consisted of 1) NEMA NU2 2000 peak noise equivalent count rate (NEC) and scatter fraction, 2) NEMA NU2 1994 spatial resolution and system sensitivity, and 3) PET performance phantom (10-32 mm "hot" spheres, 8:1 target-to-background ratio).
Results: Measured single photon spatial resolution, linearity and uniformity were as follows:

	NEMA	Resolution	NEMA	Linearity	NEMA	Uniformity
	FWHM	FWTM	Differential	Absolute	Integral	Differential
CFOV	5.2 mm	9.9 mm	0.2 mm	0.3 mm	2.4 %	1.5 %
UFOV	5.3 mm	10.1 mm	0.2 mm	0.7 mm	3.2 %	1.6 %

Energy resolution was 9.4 % FWHM. SPECT reconstructed resolution was: 12.0 mm (central), 12.3 (radial) and 9.2 (tangential). Bar and orthogonal hole patterns demonstrated acceptable resolution and excellent linearity. Sensitivities measured were (e.cam^{duet}:9.5 mm ($^3/_8$") crystal system): 1.33 (^{67}Ga), 1.52 (^{111}In) and 1.91 (^{131}I). Coincidence results were: spatial resolution (mm FWHM): ≤ 4.7 (central axial), ≤ 5.3 (central transaxial); peak NEC ≥ 2.0 kcps; scatter fraction: ≤ 19%; and sensitivity: ≥ 804 cps/MBq/ml. All 6 spheres of the performance phantom were visualized. E.cam^{duet} performance measurements and clinical images compared favorably to, and will be shown in comparison to, those from conventional 9.5 mm and 15.9 mm ($^5/_8$") crystal gamma cameras.
Conclusions: These initial results demonstrate that the e.cam^{duet} system is capable of generating diagnostic quality images at all photon energies, providing significantly increased medium-to-high energy and coincidence system sensitivity while maintaining good low energy imaging performance. To date, 22 single photon (all energies) and 14 coincidence patient scans of excellent image quality have been obtained.

OS_181

INITIAL CLINICAL EVALUATION OF A THICK, SLOTTED NAI CRYSTAL DESIGN FOR SINGLE PHOTON AND COINCIDENCE IMAGING

S. M. Spies (1), W.G. Spies (1), M. W. Groch (1), J. M. Soldner (2), W. D. Erwin (1). (1) Department of Nuclear Medicine, Northwestern University Medical School, Chicago, USA; (2) Siemens Medical Systems, Hoffman Estates, USA.

The purpose of this study was to evaluate the clinical performance of a prototype dual detector gamma camera/coincidence imaging system employing a new sodium iodide slotted crystal design (e.cam$^{duet™}$, Siemens Medical Systems), compared to conventional single photon gamma cameras and a dedicated BGO PET tomograph. The slotted 25 mm (1") thick crystal is designed to provide increased sensitivity for 511 keV coincidences, while minimizing the loss of spatial resolution at low-to-medium energies associated with a 25 mm thick crystal.
Methods: A variety of clinically requested and indicated radionuclide imaging procedures were performed on 36 patients. After completion of the routine study and informed consent, duplicate imaging was performed using Duet. The 22 single photon studies included whole body (^{99m}Tc bone, ^{67}Ga citrate, ^{111}In leukocyte, Na^{131}I), non-circular orbit SPECT (^{99m}Tc bone, and ^{99m}Tc/^{201}Tl dual isotope stress/rest myocardial perfusion in the 90 degree detector configuration) and ^{99m}Tc planar lung perfusion. ^{18}FDG dedicated PET followed by coincidence imaging with Duet was performed on 14 patients. The results of all imaging studies were reviewed by two experienced Nuclear Medicine physicians, and a qualitative assessment of image quality and clinical interpretation was performed for each pair of data sets.
Results: The new detector system produced images of diagnostic quality at all energies evaluated. The minimal degradation in spatial resolution at low energies (^{201}Tl, ^{99m}Tc) was deemed not clinically significant. The ^{67}Ga citrate and ^{111}In leukocyte images demonstrated excellent image quality, with 33% and 50% increases in sensitivity, respectively, compared to a 9 mm ($^3/_8$") thick crystal system. The Na^{131}I images were also excellent, and demonstrated a nearly 100% increase in sensitivity. Coincidence images identified abnormalities visualized with dedicated PET in all but one patient. The lesion missed by Duet was a small pulmonary nodule faintly visible on the dedicated PET images.
Conclusions: The results of this preliminary study demonstrate the feasibility of using the crystal technology employed in the Duet system for routine clinical radionuclide imaging at all photon energies.

OS_182

PRELIMINARY RESULTS OF CT-SPECT TOMOGRAPHY FOR BREAST CANCER STUDY

A. Del Guerra (1), M. Gambaccini (2), G. Di Domenico (2), A. Taibi (2), A. Tuffanelli (2), G. Zavattini (2), R. Pani (3). (1) Dipartimento di Fisica, Universita' di Pisa, Pisa, Italia; (2) Dipartimento di Fisica, Universita' di Ferrara, Ferrara, Italia; (3) Dipartimento di Medicina Clinica e Sperimentale, Universita' La Sapienza, Roma, Italia.

AIM: Conventional mammography is still the most sensitive imaging technique for early detection of breast cancer. The low capability to differentiate malignant from benign lesions, lead to the use of invasive technique for obtaining a complete diagnosis. To improve the specificity of non-invasive technique, we are developing a new tomographic system combining 99m-Tc scinti-mammography and X-ray CT.
METHODS: The SPECT system is made of two detector heads. Each head consists of a CsI(Tl) scintillator matrix (2x2x0.5 cm^3) composed of 8x8 small crystals (2.5x2.5x5 mm^3). The matrix is directly coupled to a small position sensitive photomultiplier (Hamamatsu - R5900-C8) and each head is equipped with high sensitive collimator.
CT scanner has a quasi-monochromatic X-ray source which produce a 28 keV fan-beam and a linear digital detection system. The CT-detector is made up of an array of photodiodes coated with a ceramic ultra fast scintillator.
The X-ray source, the CT-detector and the SPECT modules are on a rotating gantry, the CT field of view is 13 cm trans-axially and 2 mm axially, the SPECT field of view is 2cm trans-axially and 2 cm axially.
The SPECT modules are standing in front so as the X-ray source and CT-detector. The system can be rotate over 180 degrees with 2 degrees step. Fast iterative algorithms have been implemented to reconstruct SPECT and CT data. An accurate alignment procedure of two systems has been implemented to make simpler the fusion of CT and SPECT images.
RESULTS: The imaging capabilities of CT-SPECT system have been tested by using a phantom, specifically designed, consisting of outer plexiglas cylinder (diameter 8 cm, height 10 cm) containing a hydro-alcoholic solution whose x-ray attenuation properties are similar to the breast tissue. An inner cylinder (diameter 0.8 cm, height 1 cm) filled with water has been used to simulate the tumour. A CT image has been acquired before filling the phantom with 99m-Tc: the activity concentration ratio is of 1:10 (outer-inner).
The reconstructed SPECT images have been corrected for attenuation by extrapolating CT data to 140 keV and the two modalities images have been combined together with image fusion technique. The hot region corresponding to the tumour is clearly visible in the combined images.
CONCLUSIONS: The CT-SPECT tomograph seem to be a promising tool for breast cancer diagnosis.

OS_183

MEASUREMENT OF KR81M GENERATOR OUTPUT WITH AN INSERT FOR AN IONISATION CHAMBER: DERIVED CALIBRATION FACTORS FOR A DISTRIBUTED KR81M GAS VOLUME

W.H. Thomson, S. Buckley, P. Childs, N. Franklin. Physics and Nuclear Medicine, City Hospital , Birmingham , UK.

Kr81m generators are commonly used for lung ventilation studies. However few departments perform any quality control of the activity of Kr81m gas from the generator. The output of the generator can be measured with a simple insert placed inside an ionisation chamber. With a continuous gas flow, the activity in the chamber is constant and equal to the available Kr81m gas output activity of the generator. A calibration factor is required for the ionisation chamber and we have derived this empirically.

Method: The insert consists of four discs which create three sections in series within the chamber. The output from a Kr81m gas generator is fed continuously to the lower section and the remaining two sections act as baffles. With a continuous gas flow the activity inside the chamber is constant and equal to the available Kr81m gas activity. The generator must be in equilibrium (ie at least 2 minutes since any gas flow).

Results: The activity reading is independent of flow rate. However at low flow rate, transit decay may occur. Also the steady reading starts to fall when gas leakage occurs. With 400ml.min-1 the reading falls by 5% after 25sec and with 1200ml.min-1 the reading falls by 5% after 15ec.

We have calculated the appropriate calibration factor for the Capintec chamber for Kr81m gas measured with this technique. Imaging the chamber insert with a gamma camera shows that the Kr81m gas fills each of the insert sections in the chamber in the proportions 65:25:10. The geometrical characteristics of the chamber response were measured with a small point source of Tc99m. With 100% as the centre base value, the maximum variation in reading radially was 107% radially and 51% vertically.

Integrating the Kr81m gas volume distribution with the variation in geometrical response showed that the insert response was theoretically less than 1% higher than the value at the centre of the chamber base. This demonstrates the consistency of the calibration factor noted by Capintec, but for a 'P6 vial' type geometry and the derived value using our insert.

Conclusion: A simple insert for an ionisation chamber allows the output strength of the Kr81m generator to be measured. The gas distribution gives a calibration factor equivalent to that of a standard vial geometry.

OS_184

THE IMPORTANCE OF A COPPER FILTER FOR IONISATION CHAMBER MEASUREMENTS OF I123 AND IN111 ACTIVITY

W.H. Thomson, J. Cullis, A. Mills, D. Kershaw, S. Hesslewood. Physics and Nuclear Medicine, City Hospital, Birmingham, UK.

Large variations in measured activity can be obtained with radionuclides which emit a high percentage of low energy X-rays. Changes in activity measurements from vial to syringe of over 80% can be obtained for I123 and of over 40% for In111.

Method: Copper filters have been shown to eliminate this variation for I123 (1). The calibration technique in this previous work was based on Tc99m. However this technique is not sufficiently accurate for the higher energies of In111.

We have derived empirically the reduction in ionisation chamber reading with gamma ray energy. These data allow the chamber calibration factor to be calculated for a radionuclide when measured with the copper filter. In addition we have modelled (in MATHCAD) the reduction factor of the copper filter with energy. This model shows a very good relationship with the empirical data.

Results: A copper wall thickness of 0.5mm is sufficient to effectively eliminate the X-ray emissions of I123 and In111 from measurement in an ionisation chamber. The reduction in reading with energy is shown in the table.

Energy (kev)	75	122	140	190	250	320	662
Measured	56%	84%	86%	91%	93%	97%	97.5%
Modelled	55%	84%	87%	91%	93%	94%	95%

The 159kev gamma ray of I123 is reduced by 12% and the 185 and 245 Kev gamma rays of In111 are reduced by 11% and 7%.

The model also showed that a variation in copper wall thickness of 10% only changed the reading for I123 by 2%.

With a copper filter, the variations in measured activity are reduced to only 4% for I123 and 2% for In111 for a range of glass vial types and syringe sizes. This allows departments to be confident about the levels of activity they are administering to patients. Such filters are now becoming commercially available. The data presented here was carried out on Capintec calibrators, but will allow calculation of the factor for the use of copper filter for other systems.

Conclusion: A copper filter should always be used for ionisation chamber measurements of I123 and In111. The filter could also be used with other radionuclides where low energy emissions are significant eg Xe133 and Sm153.

1. Ionisation Chamber measurements of I123 using a copper filter. Thomson WH et al; Rad. Isotopes in Clin.Med. and Res. Birkhauser-Verlag 1997.

NEUROLOGY / PSYCHIATRY

OS_185

SIMULTANEOUS ASSESSMENT OF THE PRE- AND POSTSYNAPTIC DOPAMINERGIC SYSTEM IN PATIENTS WITH PARKINSONISM

G. Pöpperl (1), C. Hamann (1), J.P. Sieb (2), S. Dresel (1), K. Hahn (1), K. Tatsch (1). (1) Department of Nuclear Medicine, University of Munich, Munich, Germany; (2) Max Planck Institute of Psychiatry, Neurology Section, Munich, Germany.

Aim: Simultaneous assessment of the dopamine transporter (DAT) using [Tc-99m]TRODAT-1 and dopamine D2 receptors using [I-123]IBZM would allow perfect coregistration of the pre- and postsynaptic dopaminergic system with a single investigation. Aim of this study was to evaluate the potential benefit of this approach in pts with idiopathic (IPS) and non-idiopathic (PS) parkinsonian syndromes.

Methods: 11 pts with known parkinsonism (7 x IPS; 4 x non-IPS; age: 53±13 yrs) and 2 healthy volunteers (age: 32±6 yrs) were injected with 800 MBq [Tc-99m]TRODAT-1 followed 1 h later by 185 MBq [I-123]IBZM. A single SPECT scan was performed 3 h after the first injection using a triple headed gamma camera (Picker Prism 3000; asymmetric energy windows). Specific binding for the striatum (S), the caudate (C) and putamen (P) was calculated using the ROI technique based on a fixed template.

Results: Findings of the simultaneous investigations are summarized in the table below. Corresponding to the known results of separately performed DAT and receptor studies in the simultaneous investigation IPS pts showed a reduced DAT (P more affected than C, marked asymmetry with lower striatal binding contralateral to the more affected body side) and normal receptor binding (slight asymmetry with upregulation contralateral to the more affected body side) whereas in non-IPS pts both, DAT and receptor binding was markedly reduced. IBZM binding was slightly lower in IPS pts than in controls most reasonable due to the marked age difference between these groups. There was some cross contamination of I-123 in the Tc-99m window, which can be corrected for, however, even prior to correction image quality and specific binding of the dual-isotope studies was similar to that known from single-isotope studies.

Conclusions: Simultaneous assessment of the pre- and postsynaptic dopaminergic system in parkinsonian patients is feasible and presents the characteristic findings well known from studies addressing the DAT and receptor site separately. Furthermore, this approach is time- and cost-effective, convenient for the patient and may even provide superior diagnostic results due to the perfect coregistration.

	Controls			IPS			non-IPS		
	S	C	P	S	C	P	S	C	P
TRODAT-1	0.95±0.01	1.06±0.09	0.90±0.06	0.55±0.14	0.73±0.22	0.42±0.08	0.53±0.09	0.60±0.12	0.51±0.08
IBZM	0.94±0.13	1.00±0.13	0.94±0.13	0.83±0.13	0.89±0.14	0.86±0.14	0.65±0.09	0.74±0.06	0.64±0.17

OS_186

PARAMETRIC MAPPING OF 123I- FPCIT (DATSCAN) BINDING IN NORMAL VOLUNTEERS AND PARKINSON'S DISEASE

D. Visvikis (1), S. Gacinovic (1), K. Erlandsson (1), J.D. O'Sullivan (2), A.J. Lees (2), R. Katzenschlager (2), D.C. Costa (1). (1) Institute of Nuclear Medicine, Middlesex Hospital, London, UK; (2) Department of Neurology, University College London, London, UK.

Introduction: ^{123}I labelled FPCIT (DaTSCAN™) has high affinity to the dopamine transporter system (DaT) in the pre-synaptic neurone. It is now routinely used to demonstrate nigrostriatal dopaminergic degeneration in Parkinsonian patients. This study was designed to compare two different methods of analysis for the calculation of DaTSCAN™ binding to the striatum: (i). the reference tissue model (RTM), and (ii). the specific to non specific ratio analysis at equilibrium.

Objectives: We have investigated in a group of patients and normal volunteers the use of the reference tissue model in order to (i). obtain parametric images of binding potential on a pixel by pixel basis, and (ii) to subsequently validate the use of the equilibrium analysis.

Methods: Five normal volunteers and ten Parkinsonian patients were scanned on a Marconi 3000XP up to 3.5 hours following bolus injection of 185MBq of DaTSCAN™. Principal component analysis of the dynamic datasets was used to obtain time activity curves (TACs) for various areas of the brain (striatum, occipital cortex, cerebellum). The occipital cortex and the cerebellum were used to describe the kinetics of the non-displaceable tissue compartment. Parametric images of the binding potential in the striatum were obtained using both the Logan reference tissue method (Logan et al, JCBFM 16, 1996) and the basis function method (Gunn et al, Neuroimage 6, 1997).

Results: The mean striatal binding potential using the RTM was 1.49±0.39 and 2.98±0.24 for the patients and the normal volunteers respectively. There was no statistically significant difference between the results from the two reference tissue models. There was good correlation between the calculated BP from the equilibrium analysis and the reference tissue model (r^2=0.95). The equilibrium analysis tended to overestimate the BP, with a larger effect observed in the case of the normal volunteers.

Conclusions: Parametric images of dopamine transporter activity using DaTSCAN™ have been derived. Equilibrium analysis compares favorably to RTM and it is easier to implement. However, parametric maps of binding potential can be combined with statistical analysis in order to provide higher sensitivity in studying different stages of disease evolution, and this is already under evaluation.

OS_187

SAFETY OF [TC-99M]TRODAT-1

P.D. Mozley, L.I. Araujo, J. Kulinski, A. Cotter, K. Plossl, C.F. Keeney, H. Saghari, E.D. Barraclough. Division of Nuclear Medicine, University of Pennsylvania, Philadelphia, PA, USA.

Aim: To determine whether the intravenous injection of a formulation containing [Tc-99m]TRODAT-1 produces an observable effect on humans.
Background: TRODAT is a SPECT imaging agent that, like cocaine, binds dopamine transporters. Its Technetium-99m label and many favorable biological properties have contributed to its rapid adoption by several laboratories around the world, even though few studies of its safety have been published.
Methods: The sample consisted of 194 patients with parkinsonian movement disorders who participated in 265 studies and 112 healthy human volunteers. They were placed in a supine position on an imaging table for at least 20 minutes before and after injection. Vital signs and electrocardiograms (EKGs) were acquired at 5 minute intervals. Each 740 MBq (20 mCi) dose contained between 0.067 to 0.13 mg of radiolabeled plus unlabeled TRODAT. Blood was serially aspirated before and after injection.
Results: A single patient had a shift in the site of her atrial pacer and went into a sinus rhythm of 120 beats per minute starting 20 minutes after administration which lasted for less than 1 minute. One control expressed feelings of unusual relaxation which lasted for about 15 seconds. About 10% of patients and controls reported perceiving a smell of alcohol starting about 10 seconds after injection which lasted 3-5 seconds. Otherwise, there were no apparent effects on any subject. During the first 5 minutes after injection, blood pressure increased slightly in 59% of the patients and 66% of the controls. In patients, the systolic blood pressure increased from a group mean of 133.5 to 137.9 ± 22 mm Hg ($p < 10EE-9$) while the diastolic blood pressure rose from 73.6 to 75.1 ± 9 mm Hg ($p < 0.00002$). Heart rate dropped continuously throughout the study, including a change from 68.8 to 68.2 ± 12 beats per minute during the first 5 minutes after injection ($p = 0.024$). The QTc interval increased ($p<0.001$). Otherwise, there were no detectable drug effects on the EKG tracings. White blood cell counts increased from 6.2 ± 2.0 to 6.5 ± 1.8 1000/uL ($p=0.042$).
Conclusion: Injecting a formulation containing TRODAT is associated with statistically significant effects on hemodynamics and white blood cell physiology which resemble the peripheral, but not the central, profile of cocaine. However, the effect does not appear to be clinically meaningful. It follows that TRODAT is probably a safe radiopharmaceutical for imaging dopamine transporters when administered in this dose range.

OS_188

IMAGING DOPAMINE TRANSPORTERS IN RATS USING PINHOLE SPECT

J. Booij (1), K. de Bruin (1), J.B.A. Habraken (1), P. Voorn (2). (1) Department of Nuclear Medicine, Academic Medical Center, Amsterdam, The Netherlands; (2) Department of Anatomy, Vrije Universiteit, Amsterdam, The Netherlands.

Aim: Imaging of striatal dopamine transporters (DAT) is adequate to detect loss of nigrostriatal dopaminergic neurons in parkinsonian syndromes. It would be of value to image DAT also in small animals since this offers the opportunity to perform repeated studies within the same animal. The pinhole collimator has been used extensively to obtain greater detail in planar imaging. Utilising pinhole SPECT is difficult, however, since it requires a heavy detector to rotate around a small object with a constant radius of rotation. Small misalignments may generate a displaced center of rotation causing artefacts. To circumvent this problem, we developed an animal pinhole SPECT system in which the collimated detector is fixated and the object rotates, and tested its feasibility to image DAT in rat brain.
Methods: A perspex cylinder was mounted on a step-motor driven system and positioned exactly above the pinhole collimator of an ADAC ARC3000° camera with a 1 mm pinhole insert. Into the cylinder an anaesthetised animal can be fixated. The step-motor makes 50 steps per 360° rotation. Filtered back projection, adapted to pinhole SPECT, was used for reconstruction. Phantom experiments were performed to assess the spatial resolution and uniformity of the system and to test the system for distortion artefacts. In a second series of experiments, striatal DAT was imaged in seven male control rats and four unilateral-lesioned rats (n = 4, dopaminergic lesioning by stereotactic injection of 6-hydroxydopamine) 2 h after injection of approximately 75 MBq ^{123}I-FP-CIT (DaTSCAN; acquisition 45 s per step). ROI's were placed over the striatum (bilaterally) and cerebellum (non-specific binding).
Results: The line source experiment showed a spatial resolution in air of 1.3 mm full width at half maximum with a 33 mm radius of rotation. The system showed good uniformity and no distortion artefacts. In control rats, striatal binding was visible at both sides (Figure 1). Striatal/cerebellum ratios (mean left and right) ranged from 1.5 to 2.9. In unilateral treated rats, striatal binding was only visible at the non-lesioned side (Figure 1; ratios ranging from 1.6 to 2.1). Binding ratios were significantly lower at the lesioned side (paired t-test; 1.2 to 1.5).
Conclusion: A rotating pinhole SPECT system may be feasible to image DAT in rats.

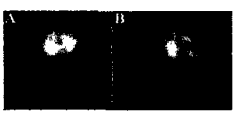

Figure 1: Coronal SPECT images showing striatal DAT binding bilaterally in control rats (A), and only binding at the non-lesioned side in unilateral-treated rats (B).

OS_189

STRIATAL REDUCTION OF ACETYLCHOLINESTERASE IN PROGRESSIVE SUPRANUCLEAR PALSY REVEALED BY PET AND QUANTITATIVE 11C-PHYSOSTIGMINE ANALYSIS

S. Pappata (1), G. Blomqvist (1), P. Damier (2), B. Tavitian (1), L. Traykov (3), A. Jobert (1), B. Dubois (4), C. Crouzel (1), L. Di Giamberardino (1). (1) INSERM U334,CEA-SHFJ, Orsay, France; (2) Clinique Neurologique, CHU Nantes, France; (3) Inserm U324, Paris, France; (4) Inserm Epi 007, Hôpital De La Salpêtrière, Paris, France

Aim: Reduction of cholinergic neurochemical markers has been reported post-mortem in the striatum, the thalamus and brainstem nuclei of patients with Progressive Supranuclear Palsy (PSP). Surprisingly, the in vivo activity index (k3) of AChE was found to be decreased only in the thalamus using PET and 11C-MP4A. In this study we used PET and 11C-Physostigmine (11C-PHY), a more suitable AChE tracer than MP4A for calculation of AChE in regions with high enzyme activity, to assess quantitatively whether a reduction in striatal AChE concentration may be detected in PSP in vivo and correlated with the clinical deficit found in these patients.
Methods: 10 patients (72 ± 8 yr) were studied. Motor and intellectual functions were evaluated with UPDRS (part III), MMSE and Mattis Scale. Sequential PET frames were acquired during 60 min after 11C-PHY injection using the ECAT 953B camera. A simplified reference tissue model with one reversible tissue compartment and three parameters (DVR, R and k2) was applied to data obtained from the caudate, the putamen the thalamus, the pons and the whole cerebral cortex. The white matter was used as reference. Regional DVR values obtained in patients were compared to those of 5 healthy volunteers (57±15 yr) using Student's t-test. Spearman correlation analysis was used to test DVR-clinical relationships.
Results: In PSP there was a mild but significant reduction of DVR in the caudate, putamen and thalamus (table). Striatal and thalamic DVR values were significantly and negatively correlated to UPDRS scores (caudate and thalamus $p<0.05$, putamen $p<0.02$). No significant correlation was found with MMSE and Mattis scores.

	caudate	putamen	thalamus
PSP (DVR)	1.869± 0.054 **	1.912 ± 0.106 **	1.329 ± 0.086*
Controls (DVR)	2.031 ± 0.034	2.146 ± 0.158	1.449 ± 0.038

* = $p<0.05$; **=$p<0.01$

Conclusions: These results show that PET and quantified 11C-PHY-AChE binding allow to detect significant losses of AChE in the striatum and thalamus of PSP patients. The decline of AChE in these structures seems to be related to extrapyramidal rather than cognitive disturbances.

OS_190

BINDING POTENTIAL EVALUATION OF 123I-PE2I, A NEW SPECIFIC DOPAMINE TRANSPORTER LIGAND, BY KINETIC APPROACH IN HEALTHY AND MPTP-TREATED MONKEYS

C. Caroline (1), S. Chalon (2), B. Aesch (3), E. Bezard (2), S. Benderbous (2), J.C. Besnard (1), D. Guilloteau (2), J.L. Baulieu (1). (1) Department of Nuclear Medicine CHU Tours France; (2) Inserm U316 Tours France; (3) Department of Neurosurgery CHU Tours France.

Aim : Because of difficulties in the diagnosis of Parkinson's disease and the development of neuroprotective drugs, it seems more and more useful to look at nigro-striatal neurons degeneration. ^{123}I-PE2I is a reversible high specific dopamine transporter (DAT) ligand with rapid kinetic. Because of its properties and based upon the 3-compartments model, we apply Logan's graphical method to quantify the binding potential (BP) of this new ligand.
Methods : ^{123}I-PE2I (84.0 +/- 8.4 MBq) was injected in 3 healthy cynomolgus monkeys (Macaca *fascicularis*, mean age = 3.1 +/- 0.3 years, mean weight = 2.9 +/- 0.2 kg) and in one chronically MPTP-treated. SPECT images (Ceraspect® DSI) was obtained by thirty 3.3 minutes sequential acquisitions over 120 minutes after bolus injection. We performed femoral arterial blood sampling only in healthy monkeys every 30 seconds for the 5 first minutes after injection, then every 1 minute during 15 next minutes, every 5 minutes for 1 hour then every 15 minutes until the end of 125 minutes post-injection. We have defined specific and non specific activity ($kBq.mL^{-1}$) in striatal (S) and occipital (Occ) regions of interest (ROI) and plasma activity (Cp, $kBq.mL^{-1}$). Logan's graphical method was applied by plotting [integral(0,T)S(t)dt] / S(T) versus [integral(0,T)Cp(t)dt] / S(T) (plot 1) and [integral(0,T)S(t)dt] / S(T) versus [integral(0,T)Occ(t)dt] / S(T) (plot 2). BP was defined by slopes of plotting. In MPTP-treated monkey, acquisitions were done at days 6, 12 and 15 according to the same protocol.
Results : A linearization of the plots was observed with correlation coefficient of 0.999 for plot 1 and 0.992 +/- 0.006 for plot 2 in the 3 healthy monkeys. BP was equal to 2.56, 1.74 and 1.64 in each monkey. In the MPTP-treated monkey, BP decreased from 2.6 at day 0, to 1.96 (-24.6%) at day 6, 1.36 (-47.7%) at day 12 and 1.25 (-52%) at day 15.
Conclusions : These preliminary data indicate that ^{123}I-PE2I BP could be evaluated by using Logan's graphical method because of its rapid kinetic and reversible binding and that this quantitative analysis of ^{123}I-PE2I uptake allowed quantitative assessment of presynaptic dopaminergic lesions specifically induced by MPTP in a monkey toxic model.

OS_191

DEMENTIA WITH LEWY BODIES DIFFERENTIATED FROM ALZHEIMER'S DISEASE ON TC-99M-HMPAO SPECT USING STATISTICAL PARAMETRIC MAPPING

E.D. Williams (1), S.J. Colloby (1), S.M. Paling (1), K. Lobotesis (1), J.D. Fenwick (2), C. Ballard (1), I. McKeith (1), J.T. O'Brien (1).
(1) Institute for the Health of the Elderly; (2) Regional Medical Physics Department, Newcastle General Hospital, Newcastle upon Tyne, UK.

The purpose of this study was to investigate differences in regional cerebral blood flow (rCBF) between subjects with dementia with Lewy bodies (DLB), Alzheimer's disease (AD) and healthy volunteers using the statistical parametric mapping (SPM99) technique.
Methods: Seventy-one patients with dementia according to DSM-IV (forty-eight AD, 23 DLB according to NINCDS-ARDRA and DLB concensus criteria, respectively) and 20 age - matched control subjects participated. Tc-99m hexamethyl propylene amine oxime (HMPAO) SPECT brain scans were acquired for each subject using a rotating gamma camera (IGE CamStar XR/T). The SPECT images were spatially normalised , group comparisons performed by SPM99, and areas showing significant differences were located. In addition, covariate analysis was undertaken on the standardised images taking the age of patients at assessment and mini mental state examination (MMSE) scores as variables.
Results: Significant (p=0.0005 uncorrected) perfusion deficits in the parietal, temporoparietal and frontal regions of the brain were observed in the AD group compared with the control subjects. Significant reductions (p=0.0005 uncorrected) in perfusion in the parietal, occipital and frontal regions were found in the DLB group with respect to normal control subjects. Comparing the two dementia groups, there were perfusion deficits (p=0.01 uncorrected) in both the parietal and occipital regions of the brain in DLB compared with AD, in a region which included part of the primary visual cortex (V1/V2). Covariate analysis indicated that age and MMSE also affect rCBF in patients with dementia. These findings amplify results from a region-of-interest analysis of the image data, which was inevitably not as comprehensive in its coverage of the whole brain.
Conclusions: Voxel-based analysis demonstrated differences in cerebral blood flow patterns, not only between controls and dementia patients, but also between AD and DLB, consistent with but more extensive than those found by region-of interest analysis.

OS_192

BRAIN SPECT IN PATHOLOGICAL AGING BRAIN: LEWY BODY DISEASE AND AGE-ASSOCIATED MEMORY IMPAIRMENT

A. Bianchi (1), B. Palumbo (1), L. Parnetti (2), D. Siepi (1), S. Amici (2), A. Lanari (2), S. Carluccio (1), V. Gallai (2), R. Palumbo (1). (1) Dept. of Nuclear Medicine, University of Perugia; (2) Dept. of Neuroscience, University of Perugia, Italy.

Aim: The purpose of the study was to investigate the capability of brain SPECT to individuate specific hypoperfusion patterns able to characterize different pictures of cognitive impairment which can offer some difficulty in differential diagnosis in clinical practice.
Methods: Brain SPECT with ^{99m}Tc-ECD (740 MBq iv) was performed in 20 patients withAge-Associated Memory Impairment (AAMI) according to Crook's criteria, in 15 with Lewy Body Dementia (LBD) according to Mc Keith's criteria, in 59 with probable Alzheimer Disease (AD) according to NINCDS-ADRDA criteria, in 16 with Fronto-temporal dementia (FTD) according to Lund and Manchester criteria and in 20 with Vascular Dementia (VaD) according to DSM-IV R criteria. SPECT images were acquired by a four head brain dedicated system (SELO-CERTO96). Each hemisphere was divided in 12 bilateral symmetrical (Right=R, Left=L) regions of interest (ROIs) (1=Ant-temp., 2=Pons, 3=Cerebellar, 4=Ant-front., 5=Mid-front., 6=Sylvian, 7=Temporo-Parietal-Occipital, 8=Occipital, 9=Thalamic, 10=Sup-front., 11=Central-Pariet, 12=Post-pariet) and each was compared to the mean of the cerebellar ROIs as reference region.
Results: A globally impaired perfusion was observed in AD patients, being significantly decreased in temporo-parieto-occipital and deep structure ROIs as compared to AAMI (6L, 6R, 7L, 7R, 8R, 9R, p varying from <0.05 to <0.001), and in the left thalamic ROI (9L, p<0.05) when compared to VaD. A reduced perfusion was also found in LBD, particularly in the occipital and thalamic regions, being significantly decreased in the right regions as compared to AAMI (7R, 8R, 9R, p<0.05). Furthermore a significantly impaired perfusion was evidenced in FTD vs AAMI (7R), in VaD vs LBD (6R, 8R) and vs AAMI (8L) (p<0.05).
Conclusions: a relevant hypoperfusion is generally present in dementia patients. LBD shows an occipital hypoperfusion which, if confirmed in a larger series, may represent a potential diagnostic marker.

TECHNOLOGY PROGRAM

OS_193

PREPARATION OF 99MTC-TETROFOSMINE WITH HIGH RADIOACTIVE CONCENTRATION

S. Steien, K. Nordling. Hedmark Central Hospital, Elverum, Norway.

The aim of the study was to measure the radiochemical purity and stability of ^{99m} Tc-Tetrofosmine when using a higher radioactive concentration and volume than recommended by the manufacturer.
Method:
Tetrofosmin was prepared with 15,0 GBq ^{99m}Tc diluted with 0,9% sodium chloride until a total volume of 10 ml. Except the radioactive concentration and total volume the preparation followed the procedure as recommended by the manufacturer
The radiochemical purity was measured by thin-layer chromatography with Gelman ITLC/SG-strips with 35:65 acetone:dichlormethane mixture as the solvent phase. After chromatography the strip was cut in three pieces. Free pertechnetate runs to the top piece of the strip (C). Reduced hydrolysed pertechnetate and any hydrophilic complex impurities remain at the bottom of the strip (A) . ^{99m} Tc-tetrofosmin runs to the middle part of the strip (B). The tree parts of the strips was measured in a Capintec dose calibrator, and radiochemical purity was calculated (equation 1): B x 100%/A+B+C.
The radiochemical purity of each preparation was measured twice; in the morning immediately after preparation and incubation in room temperature for 15 minutes and just before the last injection 7,5 – 8 hours later.
Results:
We have prepared Tetrofosmin with 15,0GBq ^{99m}Tc to a total volume of 10 ml 15 times. The average radiochemical purity in these preparations was calculated to be 96% (range 94-97%). The general stability of the radiopharmaceutical was good. The mean measured radiochemical purity after 7,5-8 hours was 94% (range 91-96%).
Conclusion:
The results show that Tetrofosmin can be prepared with a higher specific radioactive concentration and a larger total volume than that recommended by the manufacturer.
We believe our procedure is acceptable as long as the quality of the prepared tetrofosmin is measured before using the radiopharmaceutical and after 7,5-8 hours.

OS_194

IMPROVED QUALITY CONTROL METHOD FOR 99M-TECHNETIUM-TETROFOSMIN

E.B. Koenders (1), O.C. Boerman (1), J. Bakker (2), F.H.M. Corstens (1). (1) Dept. of Nuclear Medicine; (2) Dept. of Clinical Pharmacy, UMC St Radboud, Nijmegen, The Netherlands.

Aim: The noninvasive assessment of myocardial viability in patients with coronary artery disease has proven clinically useful. New ^{99m}Tc-labeled perfusion agents such as ^{99m}Tc-tetrofosmin and ^{99m}Tc-sestamibi have emerged as alternatives to ^{201}Tl for imaging of regional myocardial perfusion. Tetrofosmin (Myoview) Nycomed-Amersham is manufactured as an instant kit, and can be readily and efficiently labeled with ^{99m}Tc (10 min, room temperature). The ^{99m}Tc-tetrofosmin solution may contain impurities like: $^{99m}TcO_2$, $^{99m}TcO_4^-$ and ^{99m}Tc-gluconate. Therefore, the radiochemical purity of the labeled product has to be determined before administration of the radiopharmaceutical to the patient. In our laboratory, occasionally, the standard ITLC quality control method suggested that the preparation contained an excess of $^{99m}TcO_4^-$. We developed an extra ITLC procedure to accurately assess the radiochemical purity of ^{99m}Tc-tetrofosmin.
Methods: The ITLC method recommended by the manufacterer was used: silicagel strips (Gelman Sciences, Ann Arbor, MI) were developed with aceton/dichloormethane (35/65). As a gold standard the preparation was analysed by reversed phase HPLC. In addition, a TLC method, using Whatman#1 paper strips and saline as the mobile phase, was developed.
Results: Generally, the ITLC method recommended by the manufacterer, allowed the discrimination of ^{99m}Tc-tetrofosmin (Rf = 0.7) from $^{99m}TcO_2$ (Rf = 0.0) and $^{99m}TcO_4^-$ (Rf = 1.0). However, occasionally no activity at Rf = 0.7 was observed. Instead, a broad peak at Rf= 0.6-1.0 was observed, suggesting the presence of a large amount of $^{99m}TcO_4^-$. However, HPLC-analysis indicated that the ^{99m}Tc-tetrofosmin content of these preparations exceeded 95%. The abnormal ITLC profile was due to an artifact, mainly caused by the use of moistened ITLC strips. However, our attempts to prevent the artefact by storing the ITLC strips in an dessicator did not prevent the artefact in all cases. HPLC-analysis is too time-consuming to serve as a quality control method in routine clinical practice. The additional TLC method (Whatman#1 strips developed with saline) accurately discriminated between $^{99m}TcO_4^-$ (Rf=1.0) and ^{99m}Tc-tetrofosmin (Rf=0.1-0.4). –
Conclusions: In summary, ITLC chromatography as recommended by the manufacturer in combination with chromatography on Whatman#1 in saline allows the reliable and rapid determination of the radiochemical purity of ^{99m}Tc-tetrofosmin in routine clinical practice.

OS_195

COMPARISON OF THE BIOLOGICAL EFFECT IN ESCHERICHIA COLI OF THE COMPOUNDS PRESENT IN TWO KITS (PHYTIC AND GLUCOHEPTONIC ACIDS) USED IN NUCLEAR MEDICINE TO PREPARE RADIOPHARMACEUTICALS LABELED WITH TECHNETIUM-99M

G.L. Lima-Filho (1), M.L. Assis (1), M.T. Catanho (2), R.S. Freitas (1), A. Caldeira-de-Araújo (1), M. Bernardo-Filho (1,3). (1) Departamento de Biofísica e Biometria, Instituto de Biologia Roberto Alcantara Gomes, Universidade do Estado do Rio de Janeiro, Rio de Janeiro, RJ, Brasil; (2) Departamento de Biofísica e Radiobiologia, Centro de Ciências Biológicas, Universidade Federal de Pernambuco, Recife, PE, Brasil; (3) Pesquisa Básica, Instituto Nacional do Câncer, Rio de Janeiro, RJ, Brasil.

Radionuclides are incorporated in a variety of chemical or cellular structures that may be interest because of their favorable biochemical, physiologic, or metabolic properties, as radiopharmaceuticals. In the preparation of the kits to prepare radiopharmaceuticals labeled with technetium-99m (99mTc), it is necessary a reducing agent and stannous chloride is widely utilized. However, authors have reported that this reducing agent has undesired effects, as genotoxic and mutagenic actions in bacteria and a carcinogenic inducer in rats. The study with strains of Escherichia coli (E.coli) indicates that stannous chloride induce lesions in the deoxyribonucleic acid (DNA) evaluated by the cellular inactivation and with isolated DNA, this reducing agent is capable to induce breaks in the DNA. AIM: We decided to compare the biological effect in E. coli of the compounds present in two kits (phytic – PHY and glucoheptonic – GHA acids) used in nuclear medicine to prepare 99mTc-radiopharmaceuticals. PHY-99mTc is normally used for hepatic and splenic scintigraphy, while GHA-99mTc is mainly utilized for renal and cerebral scintigrahies. We have investigated the biological effect of the reducing agent isolated and in the association form with phytic acid or glucoheptonic acid. METHODS: We determined the survival fraction (SF) in a culture of a DNA repair proficient mechanism Escherichia coli AB 1157 strain that was treated with the solutions in the concentrations used in the kits: (i) stannous chloride, (ii) phytic acid, (iii) glucoheptonic acid, (iv) phytic acid and stannous chloride and (glucoheptonic acid and stannous chloride). RESULTS: The SF of this strain was not altered when phytic acid and glucoheptonic acid solutions were used. The SF of the culture decreased with the treatment with stannous chloride. When the culture was treated with the compounds of the kits put together (phytic acid and stannous chloride or glucophetonic acid and stannous chloride), the lethal effect ot the reducing agent is abolished. CONCLUSION: The phytic and glucoheptonic acids present a protection action against the stannous chloride effect. As this effect is due to the generation of reactive species (ROS), we can speculate that the phytic acid and the glucoheptonic acid have similar effects and would act as a chelating of the stannous ion and/or a scaveneger of ROS. This information is highly significant to the nuclear medicine practitioners and these results increase our knowledge about the biological effects concerning to the kits normally utilized in nuclear medicine procedures, evaluating the benefit/risks arising from their use.

OS_196

AN AUDIT OF THE ACQUISITION AND PATIENT PARAMETERS IN GAMMA CAMERA PET IMAGING WITH MCD-AC IN CANCER PATIENTS UNDERGOING SERIAL SCANS

A. Dynes, A. Dynes, R. Hampson, G. Mufti, M. Buxton-thomas. Department of Nuclear Medicine, King's College Hospital, Haematology Department, KCH, London, UK.

The purpose of this study is to audit whether the minimum data set established for our database for acquisition parameters and patient preparation (glucose levels, administered activity, scanning time post-injection.) were adhered to using the above ADAC Vertex Plus Gamma Camera PET/SPECT system with Molecular Coincidence Detection and Attenuation Correction (MCD-AC). I also hope to demonstrate the value of serial G.C.PET in the management of oncology patients, particularly those with Hodgkin's Disease (HD) or Non-Hodgkins Lymphoma (NHL).
Method:
217 scans on 197 patients have been performed in the past 20 months on 1 or 2 days/week. 48% of these patients were referred for Lymphoma and 30% for Lung Cancer, either suspected or confirmed.19 patients have had multiple scans to a total of 48. 15 patients (79%) for lymphoma, 2 with Breast cancer (11%), 1 with Ca Colon (5%) and 1 with Malignant Melanoma (5%). 1 patient has had 5 scans, 2 have had 4 scans, 3 have had 3 scans and the remaining 13 patients have had 2 scans each. The referral reasons include staging, response to treatment, recurrence or metastases, change in tumour grade, whether a lesion seen on MRI/CT is necrotic/fibrotic change or recurrence and routine follow-up.I used the database established when we started G.C.PET to examine patients' blood glucose level, injected activity, scanning time post-injection and any adverse occurences and whether there were any significant differences in any particular patient undergoing serial scans. I also examined the acquisition parameters for each scan, e.g. time/azimuth, number of bed positions, etc.
Results:
Acquisition parameters were reproduced on each occasion. All but 2 patient had glucose levels within the acceptable range of 4 - 8 µmols/litre. 2 diabetic patients, 1 with Ca Colon and 1 NHL had levels of 10.2 and 11.0 and 10.8 and 10.4 respectively for the 2 scans, although acceptable images were acquired in each case. Administered activities ranged from 70-180 MBq 18F-FDG (Mean 129MBq) and imaging commenced 60-90 minutes post-injection (Mean 66 minutes)
Conclusion:
Minor differences in the patient preparation factors did not appear to affect the quality of scans and images for any particular patient were comparable. Gamma Camera PET(MCD-AC) offers a relatively cheap and effective method of monitoring this group of patients, gives high-quality reproducible images and is acceptable to patients.

OS_197

INTRODUCTION AND IMPACT OF AN ATTENUATION CORRECTION SYSTEM FOR MYOCARDIAL PERFUSION SCINTIGRAPHY

S. Jonkman, G. Akkerman, L. Poot, P.L. Jager. Department of Nuclear Medicine, University Hospital, Groningen, The Netherlands.

Introduction: Attenuation correction (AC) is a new feature in myocardial perfusion imaging, just like gating of SPECT images. The true clinical value of AC is currently unknown.
Aim: To study the consequences of the introduction of AC in routine daily practice, the feasibility of combined gated SPECT and AC, and to study first clinical results.
Methods: This study was performed on a Siemens E.cam dual-head gammacamera, equiped with the Profile attenuation correction system. This camera is equiped with two wings which are filled with an array of 14 Gd-153 (100 keV, T1/2 242 days) line sources each. Acquisition of 64 projections of 20 seconds each was performed 60 min after injection of 600 MBq Tc-99m-SestaMIBI in stress and at rest (on a separate day). Simultaneously emission, transmission and scatter images were obtained using four energy windows. Matrix size was 128 x 128 word. Gated acquisition was performed during the rest acquisition. Images were reconstructed using filtered back projection (uncorrected) and iterative methods (AC images). The uncorrected and AC results were compared by a nuclear medicine physician.
Results: Simultaneous acquisition of AC has no influence on the total acquisition time of 15 min. Reconstruction took significantly longer, up to 15 min, even using state-of-the art ICON computer systems. Also simultaneous acquisition of gated SPECT is feasible and does not require more technologist time. Furthermore, very large data files are generated (up to 45 MB), which requires special archiving and storage logistics. 4 of the expensive Gd-153 line sources have to be replaced twice a year. As a first impression, in circa 35% of the first 47 patients, AC images of the inferior myocardial wall gave better results. However, interfering extracardiac activity in liver or stomach frequently troubled the interpretation.
Conclusion: AC can easily be implemented in a nuclear medicine department with a few adaptations. Routine combination of AC acquisition with gated SPECT is feasible and is currently our standard procedure. Clinical benefit appears to be positive.

OS_198

SPECT ARTIFACTS RELATED WITH HEART POSITION IN A CIRCULAR ORBIT: A CARDIAC PHANTOM STUDY IN A 90 DEGREE DUAL-HEAD SYSTEM

M. Deger, S. Inanir, M. Balikci, H.T. Turoglu. Department of Nuclear Medicine, Marmara University Medical Faculty, Istanbul, Turkey.

In single-headed gamma cameras, the organs that are not centrally located in the body can be centered in the axis of rotation during SPECT acquisition, which is achieved with the movement of table in the axis direction. However, dual-head gamma cameras do not allow the table movement in this direction. In this study, we investigated the effect of the heart position in the center of rotation or in an eccentric position during Thallium-201 SPECT studies in this type of dual-head gamma camera.
Methods: A cardiac insert of a Data Spectrum cylindrical phantom was used. The myocardium component of the cardiac phantom was filled with thallium-201. A 90° (L-shaped) dual-head gamma camera system was used. Two sets of SPECT data were collected with the heart in the center of rotation as well as in an eccentric position. For the latter, the cardiac phantom was positioned in an anatomically realistic fashion in the cylinder, which is simulating the position of the heart in the human body. SPECT data were collected from the 45 degrees right anterior oblique to the 45 degrees left posterior oblique projection in a total of 180 degrees' circular orbit (each detector was rotated over 90°). The heads were equipped with low energy general purpose collimator and double photopeak of thallium-201 was used (72 keV with 20% window and 167 keV with 15% window). Thirty two frames were recorded and the counts/frame were similar to that of cardiac patients. The planar images were processed using Cequal processing program. Then, the short and long axis slices as well as the polar maps were generated.
Results: The reconstructed images with the heart in the eccentic position showed significant image distortion and created artifactual defects.
Conclusions: Inspite of the use of circular orbit, these artifactual defects seem to be related with varying distance of the heart from the detectors.

OS_199

WHAT'S DAT? A TECHNOLOGIST'S EXPERIENCE WITH A NEW BRAIN AGENT

C. .I. Hamilton, P. Ryan, D. Marshall. Department of Nuclear Medicine, Medway NHS Trust, Gillingham, Kent, UK.

Aim. The aim of this study was to evaluate and develop a workable protocol for a new brain agent our department had decided to try out. The agent in question is called DaTSCAN, which is used to detect the loss of functional dopaminergic neuron terminals, in the striatum of patients with clinically uncertain Parkinsonian Syndromes, in order to help differentiate between those and Essential Tremor.

Methods. The patients first arrive for iodine blocking, using Potassium Iodate 180mgms orally. One hour later, the DaTSCAN labelled to ^{123}Iodine, was given very carefully given through a butterfly. Then a three hour minimum time lapse between injection and scan was required. The scan was performed using an ADAC Vertex double headed gamma camera, 360^0 Circular motion, 30 sec. asimuths, 128x128 matrix. It was imperative the camera was within 2 cms of the patient's face in the anterior position. the head was positioned so that the OMBL was perpendicular to the camera head, and carefully secured in an appropriate head pad. The resultant Spect images were processed using a filter. The appropriate axial images, showing the were dully summed, ROIs were drawn round the to give an accurate statistical result. These results were compared to statistics and images obtained from an appropriate phantom.

Results. We have up to date performed 8 successful scans using this agent:

Patient	Age	Male/Female	Results	Comments
	65	M	-ve	Normal scan no evidence of Parkinsons.
	88	M	+ve	Very strong evidence of Parkinsons.
	84	F	+ve	Positive scan
	85	M	+ve	Strong evidence of a Parkinsons.
	75	M	+ve	Positive scan.
	81	M	+ve	Good evidence of a Parkinsons.
	80	F	-ve	Negative scan, Essential Tremors
	83	F	+ve	Strong positive scan.

Conclusions. The DaTSCAN is a very expensive agent, costing nearly £600/patient. It is an extremely time consuming procedure, taking up to 5 hours to complete. Considerable staff involvement and expertise is required to obtain successful results. Careful administration of the agent is essential. But the hardest part is obtaining good quality images, keeping the patient's head perfectly still with the camera face only 2 cms. from their face, not an easy task if the patient is suffering tremors. The results so far have been very encouraging and we look forward to completing many more.

OS_200

DOES THE TECHNETIUM-99M PERTECHNETATE THYROID UPTAKE DEPEND ON IODINE SUPPLY AND CAN THIS RECOGNIZED BY SPOT MEASUREMENTS OF IODINE URINARY EXCRETION ?

S. Dunkelmann, F. Rudolph, A. Koch, J. Schefthaler, P. Groth, C. Schuemichen. Clinic of Nuclear Medicine, Rostock, Germany.

Global technetium-99m pertechnetate thyroid uptake under TSH suppression (TcTUs) obtained by quantitative thyroid scintigraphy is believed to depend mainly on the number of autonomous cells and on a molecular level on the number of Na^+/I^- symporters expressed. It is used for estimation of functional relevance or of the target volume prior to radioiodine therapy (RIT) in patients with multifocal (MFA) or disseminated (DISA) thyroid autonomy. However the TcTUs may be inversely influenced by the individual iodine supply, routinely measured by urinary excretion of iodine. This was analysed in a larger number of patients.
Methods: The retrospective analysis included 1323 patients treated for thyroidal autonomy by RIT and 165 patients successfully treated. Prior to RIT all patients were exo- or endogenously suppressed (TSH<0.1 µU/mL). No patient had a history of iodine excess. Urine was collected immediately before injection of 75 MBq $^{99m}TcO_4^-$, iodine in the urine was determined by a modified method after Wawschinek, iodine in serum by an HPLC method. In one of us the TcTU was measured three times: 1st day baseline, 2nd day simultanous injection of 1 mg iodide and $^{99m}TcO_4^-$ and 5th day control.
Results: Serum concentration of iodine was closely related to urinary excretion of iodine at corresponding time (r = 0.68), but urinary excretion of iodine did not influence the TcTUs up to values of 800 µg iodine/g creatinine:

Iodine in Urine (µg/g creatinine)	0 - 49	50 - 99	100 - 149	150 - 199	200 - 299	300 - 499	< 500
TcTUs (%)	3.78	2.73	2.67	2.71	3.04	2.41	3.10

Similar results but on a much lower level were obtained after successful RIT.
After intravenous injection of 1 mg iodide the serum concentration was raised shortly from 4.22 µg/L to 75.8 µg/L but this had no negative influence on the TcTU (1.50 % versus 1.57 %, corrected for residual activity from day before), 4 days later TcTU dropped to 1.23 %.
Conclusion: The transport capacity of the Na^+/I^- symporter is extremely high and the expression of the symporter is regulated by the iodine supply only with some delay. As a consequence, any influence of the mean iodine supply (within a normal range) on the TcTU/TcTUs cannot be recognized by a spot measurement of iodine excretion in the urine.

DIAGNOSTIC ONCOLOGY

OS_201

COMPARISON OF SENTINEL-NODE BIOPSY AND POSITRON EMISSION TOMOGRAPHY WITH FDG IN THE STAGING OF MALIGNANT MELANOMA

H. Palmedo (1), S. Ezziddin (1), G. Reinhard (2), D. Von Mallek (1), P.J.M. Mulkens (2), R. Reich (3), T. Bieber (2), H.J. Biersack (1), M.J. Reinhardt (1). (1) Department of Nuclear Medicine; (2) Department of Dermatology; (3) Department of Oral and Maxillofacial Surgery, University of Bonn, Bonn, Germany.

The aim of this ongoing study is to compare diagnostic accuracy of sentinel-node scintigraphy/biopsy and FDG-PET for the primary staging of malignant melanoma.
Methods: In 52 patients (mean tumor diameter mTD=1.93 mm; stage Ia-IIIb), dynamic and static images of the lymphatic areas were acquired after peritumoral, subdermal injection (6 sites of 7-11 MBq ‡ 0.3 ml) of Tc-99m Nanocoll. The sentinel node(s) was scintigraphically documented and its site was marked on the skin. Using a hand held probe (C-Trak), the node(s) was intraoperatively identified and removed and histopathologically and immunhistochemically evaluated. In 23 patients (mTD=2.05 mm), whole-body PET was performed previous to sentinel-node scintigraphy)Ecat Exact Siemens/CTI, iterative reconstruction, 370 MBq FDG i.v., imaging 1h p.i., fasted state).
Results: Scintigraphic detectability of one or more sentinel nodes was 100% (52/52 patients). A total of 98 sentinel nodes could be scintigraphically detected (average 1.87 SLN/patient, range 1-6). All of these nodes were intraoperatively identified and removed. In 9 patients (17%), histopathology revealed lymph node metastases (11 lymph nodes). Regional lymph node dissection did not demonstrate further lymph node metastases in these patients. Fifteen of the 23 patients who had a PET scan showed a negative SLN-biopsy and PET result. In the remaining 5 patients (primary melanoma mTD=2.31mm), sentinel node biopsy proved one lymph node metastasis (mTD=3mm). PET scans demonstrated a true positive result of the affected lymphatic bassin in 2 of these patients.
Conclusions: Using scintigraphic imaging and a gamma probe, sentinel node biopsy allows rapid localization and subsequent removal of sentinel nodes. The results of our study show that FDG-PET is inferior to sentinel node biopsy in the detection of smallest and microscopic metastases of the lymph nodes.

OS_202

SERIOUS INFLUENCE OF SURGICAL INTERVENTION ON IDENTIFICATION AND LOCALIZATION OF SENTINEL NODES (SNS) IN CUTANEOUS MELANOMA OF TRUNK

S. Maza (1), H. Winter (2), V. Ivancevic (1), L. Geworski (1), E. Dröger (2), W. Sterry (2), D.L. Munz (1). (1) Clinic for Nuclear Medicine; (2) Clinic for Dermatology, Charite, Berlin, Germany.

Aim: In SN diagnostics using lymphoscintigraphy and/or gamma probe and/or blue dye detection only "SNs of the injection site" can be identified and localized. It is very important to apply the lymphotropic tracer as close as possible to the primary tumor (PT), biopsy area or biopsy scar. Due to considerable manipulation of lymph drainage pattern by biopsy/operative intervention (e.g. wound-healing, hematoma, lymphocele, large safety distance to the primary tumor, plastic rotation flap...) Munz et al. claimed already at the beginning of the 80s (e.g. Lymphology 1982; 15: 143-7) to perform lymphoscintigraphy in MM preoperatively. With support of a classification of the lymphatic drainage status (D-status) of a PT developed by our group (Nuklearmedizin 2000; 39: 88-91) the effects of biopsy/surgery in truncal melanoma on SN diagnostics should be clarified in this study.

Methods: From 1/1995 to 12/2000 516 patients were enrolled (176 female, 340 male; age 11-91). After intracutaneous injection of Tc-99m nanocolloid (40-150 MBq; 0.05 ml/deposit) surrounding the tumor (214x) or biopsy scar (302x) static and dynamic lymphoscintigraphy was performed in various views with a gamma camera (LEAP collimator, 256x256 Matrix) until 2 h p.i. Based on the number of draining node locations (NL) and number of sentinel nodes (SN) the D-status encompasses four classes (I-IV) and various subclasses (A-E).

Results: The following table shows an increase in number of both draining lymph node groups and SNs when lymphoscintigraphy was performed postoperatively, irrespective of tumor location inside or outside lymphatic watersheds. This shift was most pronounced after plastic rotation flap insertion.

		Pre-Op		Post-Op	
		inside watershed	outside watershed	inside watershed	outside watershed
D-class I	A	22	78	20	91
	B	4	24	9	47
D- class II	A	37	14	53	26
	B	10	4	11	4
	C	1	2	4	
D- class III	A	7		6	3
	B	1			2
	C			2	
	D				
D- class IV	A	2			3
	B		2		1
	C-E				

Conclusion: SN-diagnostics in truncal melanoma should be performed preoperatively if possible. Due to surgical intervention and its effects on lymphatic drainage patients can loose the chance of detecting the "true" SNs of their melanoma.

OS_204

CUTANEOUS MELANOMA'S SENTINEL NODE (SN) DETECTED WITH LYMPHOSCINTIGRAPHY AND GAMMA PROBE: POLYMERASE CHAIN REACTION (PCR) VERSUS HISTOPATOLOGY IN MICROMETASTATIC INVOLVEMENT EVALUATION

D. Donner (1), P. Cristofolini (2), S. Boi (3), A. Palermo (1), E. Lorenzi (1), R. Togni (3), S. Girlando (3), R. Visentin (1), M. Camerani (1).
(1) Department of Nuclear Medicine; (2) Department of Dermatology; (3) Department of Patology, S. Chiara Hospital, Trento, Italy.

The aim of our study was to evaluate the accuracy of PCR techniques versus immunohistochemical stains (IH) in detecting micrometastasis in SNs.
Methods: we performed a day surgery approach of SN study in **112** patients (pts) affected by cutaneous melanoma (CM) of the limbs or of the trunk. **10** pts had a melanoma thickness ranging from 0 to 0,74 mm; **44** pts from 0,76 mm to 1,5 mm, **41** pts from 1,6 to 4 mm and **17** pts had thickness from 4,1 to 12 mm. Each patient underwent lymphoscintigraphy (LS) with a dynamic acquisition, a static view to mark the SN projection in the skin and a postoperative static imaging to confirm the SN excision. We injected in 3-4 subcutaneous sites all around the melanoma or the surgical scar of the previous excision, 74 MBq of 99mTc-Lymphoscint in 0,2 ml of saline solution. A gamma probe mapping of the operating field was done before, during and after surgery. After removal, the SN was immediately sent to pathology lab where IH and PCR were performed.
Results: **176** SNs were located and removed (in **54** pts double SN were detected in **2** pts triple), 1 SN was detected but not removed. All **176** SNs have been analysed with IH and PCR. The metastatic spread in SN was demonstrated by the two techniques as follow: **IH: 32/176(18%) SNs positive, 144/176(84%) SNs negative; PCR: 84/176(48%) SNs positive, 92/176(52%) SNs negative.** All SNs IH positive (**32**) were PCR positive too. **34/112(30%)** pts were only PCR positive. We attempt to compare also the results of PCR with melanoma's thickness. Wilcoxon's statistical test was used to comparing differences between different categories that were formed according to PCR (negative and positive PCR) and melanoma's thickness (p=0.227, 2-tailed, 95% of confidence).

PCR	**Melanoma's thickness [mm]**				
	Patient's N.	Mean	Std. Déviation	Minimum	Maximum
Positives	**54**	**3.06**	**2.49**	**0.5**	**12.0**
Negatives	**58**	**1.86**	**1.52**	**0.5**	**10.0**
Wilcoxon's test: **p= 0.012**; 2-tailed; alfa=0.05					

Conclusions: LS is an accurate diagnostic tool for SN localization in melanoma. In our opinion, PCR techniques may have an important prognostic role in management of patient with CM especially considering that we find a significative difference, in Breslow thickness, between PCR positive and PCR negative patients groups.

OS_203

LYMPHOSCINTIGRAPHY IN CUTANEOUS MELANOMA. THE IMPORTANCE OF EARLY IMAGES

L. Rettenbacher (1), J. Koller (2), H. Kaessmann (1), G. Galvan (1).
(1) Institut für Nuklearmedizin; (2) Dept. of Dermatology, Landeskliniken Salzburg, Austria.

In more than 50% of the patients lymphoscintigraphy shows several radioactive lymph nodes in one basin. The exact identification of the sentinel lymph node is only possible by the visualization of the lymph channel. The aim of our study was to evaluate the importance of early images.
Methods: A total of 115 consecutive patients with cutaneous melanoma were studied. Lymphoscintigraphy was performed with Tc-99m-labeled nanocolloid. The tracer (30 MBq) was injected intradermally around the biopsy site in a mean volume of 0,3 ml. We performed dymamic and early static images up to 15 minutes and delayed images 30 and 60 min p.i. The early and delayed images were compared in order to determine the SLN.
Results: The SLN identification rate in this study was 99% (114/115). In 90% of the patients lymph channels were visible but only on the early images in 75%. In 55% of the patients multiple radioactive lymph nodes were visualized in the drainage basin. In 25% of the patients the exact identification of the SLN was only possible viewing the dynamic and early images.
Conclusions: In patients with cutaneous melanoma lymphoscintigraphy reveals multiple radioactive lymph nodes in the drainage basin in 55%. The dynamic and early images were necessary for the exact identification of the SLN in 25% of the patients.

OS_205

PRELIMINARY RESULTS OF SENTINEL LYMPH NODE RADIOGUIDED SURGERY IN PROSTATE CANCER

M. Rudoni (1), G.M. Sacchetti (1), L. Leva (1), E. Inglese (1), G. Monesi (2), D. Minocci (2), B. Frea (2). (1) U.O.A. Medicina Nucleare, Ospedale Maggiore, Novara, Italy; (2) Clinica Urologica, Università A.Avogadro, Novara, Italy.

Following the widespread use of radioguided surgery (RGS) in melanoma and brest cancer, we applied this new surgical strategy in prostate cancer (PC) considering the well-known variability of its lymphatic drainage.
Aims - The aims of this study were: 1) to evaluate the accuracy of RGS in detection of prostatic sentinel lymph node (SLN); and 2) to verify if the pelvic lymphadenectomy (LAD) is an accurate mean for detecting solitary micrometastases.
Methods – Thirtythree pts (age range 59 – 74; PSA range 2.7 – 51 ng/mL; staging range pT2a-pT3b) with PC confirmed by transerctal biopsy, were submitted to radical prostatectomy and to bilateral LAD. No neoadiuvant theraphy was started in these pts. Three hours or the day before surgery a dose of 99m-Tc labelled nanocolloid particled ranging from 15 to 111MBq in a volume < 1 ml was injected into two sites of PC after needle positioning by echography. Serial imaging at 20 and 90 min from tracer administration was obtained with a gamma camera.
A "blood pool" imaging of the same view, obtained 48 hrs before, was used for a more correct anatomical mapping.
A skin landmark was a useful tool for intraoperatory searching of SLN. The sites of intratumor injection were not masked during the intraoperatory probe scanning. We separately considered: 1) the first radioactive lymphnode (SLN); 2) other radioactive lymphnodes; and 3) non-active lymph nodes.
Results –Thirtytwo SLN in 33 pts were identified. Sixteen SLN were located in unusual sites, considering the conventional LAD. Four SLN were positive for micrometastases and two of these was positioned outside the ususal LAD territory. No micrometastases were found in all the remaining lymphnodes (active and non-active).
Conclusions – These preliminary results are in agreement with the few previous scientific contributions on this topic and prospect the following advantages: 1) to reduce the extent and duration of surgery; and 2) to reevaluate the conventional sites of lymphatic drainage.

OS_206

THE CAPILLARY TRANSIT OF FATTY ACIDS IS IMPAIRED IN REPERFUSED MYOCARDIUM

W.-S. Richter, N. Ernst, S. Fischer, D.L. Munz. Clinic for Nuclear Medicine, University Hospital Charité, Berlin, Germany.

Aim: A reduced uptake of long-chain fatty acids has been described in stunned myocardium. Since the capillary wall has been identified as the major barrier for uptake of fatty acids, we hypothesized that a disturbance at the capillary wall may be responsible for the reduced extraction during reperfusion.The aim of this study was, therefore, to examine the first-pass extraction and the capillary permeability surface (PS) product for I-123-iodophenyl pentadecanoic acid (IPPA) in isolated hearts at control conditions and during reperfusion.
Methods: 16 isolated hearts of male Wistar rats (300g) were subjected to retrograde perfusion with constant flow (Krebs Henseleit buffer with 10 mmol/l glucose + 5 IE insuline). IPPA extraction was measured using the indicator dilution technique with Tc-99m albumine as the reference. The PS product was calculated from Renkin-Crone equation ..PS...= -F..ln (1-E....).... Flow was reduced to 25% of control for 20 min in 10 hearts, remaining 6 hearts served as control. Measurements were performed 5 min before low flow, and at min 5, 15, 30, 34, 60, 75, and 90 during reperfusion.
Results: Before low flow, the first pass extraction of IPPA was 53.5 +/- (mean +/- 1 SE) and the PS product was 6.01 +/- 1.05 ml/g...min. During reperfusion, IPPA extraction was slightly and the PS product severely reduced (compared with the control group). Individual values are shown in the table.
Conclusion: During reperfusion the capillary transit of long chain fatty acids is impaired. Simultaneously, the relatively discrete reduction of net fatty acid extraction (compared with the reduction of the PS product) is compatible with an increased intracellular fatty acid retention.

Min Reperf.	5'	15'	30'	45'	60'	75'	90'
Net extraction	91.5+/-1.5	93.3+/-1.7	93.0+/-1.5	94.3+/-1.5	92.4+/-3.3	93.6+/-3.6	96.0+/-4.9
PS product	20.3+/-1.4	21.8+/-1.6	21.9+/-1.7	22.2+/-1.9	22.9+/-2.6	22.7+/-2.7	25.3+/-1.7

all values in % of control group

OS_207

ALTERATIONS OF MYOCARDIAL PRESYNAPTIC SYMPATHETIC INNERVATION EVALUATED WITH C-11-HED PET IN PATIENTS WITH MULTI-VESSEL CORONARY ARTERY DISEASE BUT WITHOUT HISTORY OF MYOCARDIAL INFARCTION

H. Bülow (1), F. Bengel (1), F. Stahl (2), B. Lauer (2), S.G. Nekolla (1), G. Schuler (2), M. Schwaiger (1). (1) Department of Nuclear Medicine, Technische Universität München, München, Germany; (2) Department of Cardiology, Herzzentrum der Universität Leipzig, Leipzig, Germany.

Objective: In patients with myocardial infarction, it has been shown that the extent of left-ventricular sympathetic denervation exceeds the size of scar tissue. Little, however, is known about regional innervation in patients with coronary artery disease but without previous myocardial infarction.
Methods: Using PET with N-13 ammonia and C-11 HED, resting perfusion and presynaptic sympathetic innervation were studied in 8 patients (7m,1w; 58±9 years) with angiographically proven multi-vessel coronary disease. Pts had no history of myocardial infarction, preserved global left ventricular function and no diabetes mellitus. 7 of 8 pts had a history of bypass surgery (>8 months prior to the study). From the PET data, polar maps of static myocardial perfusion and of HED retention were calculated, and regionally compared to normal databases.
Results: Mean HED retention in the 8 patients was 8.3±2.1 %/min, and was abnormally low (<2.5 SD) in 50±40% of the left ventricular myocardium. Resting myocardial perfusion was normal in 23 of the studied 24 vascular territories. One territory with decreased flow was excluded from further analysis. Despite normal resting perfusion, significantly reduced HED retention, indicating dysinnervation, was found in 12/23 (52%) vascular territories (6/8 patients). 7 of the 12 dysinnervated vascular territories (58%) showed high degree stenosis at angiography (>= 99% or occlusion with collateralisation). The other 5 vascular territories showed an subtotal stenosis or and occluded coronary artery with an open bypass graft in 4 segments and a stenosis of 50% in 1 segment. Of the vascular segments with normal innervation 9/11 (82%) had no higher degree stenosis. Stress testing (perfusion scintigraphy and/or exercise ECG) was performed on 7 of 8 pts and revealed evidence of exercise-induced ischemia for 5 of 5 pts with dysinnervated vascular territories and no signs of ischemia in 2 of 2 pts without dysinnervation.
Conclusion: In patients with advanced coronary artery disease and normal LV function, autonomic nerve damage can occur despite normal perfusion at rest and no history of myocardial infarction. Although the precise mechanism cannot be elucidated, dysinnervation may be a result of ischemic episodes which did not cause myocyte necrosis. This would be consistent with the hypothesis previously derived from infarct patients that sympathetic neurons are more susceptible for ischemic damage than myocytes.

OS_208

ADIPOSE TISSUE GLUCOSE UPTAKE DETERMINED IN HUMANS WITH 18-F-FDG AND PET

P. Nuutila (1), K. Virtanen (1), P. Peltoniemi (1), P. Marjamäki (1), P. Lönnroth (2), J. Knuuti (1). (1) Turku PET Centre, Turku, Finland; (2) University of Gothenburg, Gothenburg, Sweden.

Positron emission tomography (PET) has been widely used in the assessment of skeletal muscle glucose uptake and perfusion in humans, but not in the assessment of adipose tissue. Quantitative [^{18}F]-2-fluoro-2-deoxy-D-glucose ([^{18}F]-FDG) results depend partly on the lumped constant (LC), which accounts for the difference in the transport and phosphorylation between [^{18}F]-FDG and glucose. To determine LC for adipose tissue, we estimated LC for [^{18}F]-FDG directly by combining [^{18}F]-FDG, PET with subcutaneous microdialysis. Abdominal subcutaneous adipose tissue perfusion was measured using [^{15}O]-labelled water and PET. Fourteen healthy males (age 31.5 ± 1.4 yr) with a wide range of body mass index (mean 27 ± 1 kg/m2) were studied during euglycemic hyperinsulinemia (1 mU/kgámin for 110 min). The glucose concentration was measured in arterial plasma and in subcutaneous interstitial fluid simultaneously with the abdominal [^{18}F]FDG PET scanning. Adipose tissue glucose uptake was calculated by means of microdialysis (rGUMD) and data were compared with those from PET scanning in the same adipose tissue region (rGUFDG) as well as in femoral muscle.
A significant correlation was found between rGUMD and rGUFDG ($r = 0.82$, $P < 0.01$). Regional glucose uptake in adipose tissue measured with microdialysis was 11.8 ± 1.7 µmol·kg tissueámin-1 in the nonobese and 7.6 ± 0.8 µmol·kg tissueámin-1 in the obese subjects ($P < 0.05$) respectively. When measured with [^{18}F]FDG and PET, the uptake was 14.9 ± 2.9 and 7.3 ± 0.8 µmol·kg tissueámin-1 , respectively ($P < 0.05$). The LC value averaged 1.14 ± 0.11 and was similar in the obese and nonobese subjects (1.01 ± 0.15 vs 1.26 ± 0.15, respectively, NS). Muscle glucose uptake was 4-5 times more efficient than in adipose tissue. In conclusion, [18F]FDG PET is a feasible and non-invasive tool to investigate adipose tissue glucose metabolism noninvasively in humans. Direct measurements with these two independent techniques suggest an LC value of 1.14 for [18F]FDG in human subcutaneous adipose tissue during insulin stimulation. The LC appears not to be altered in insulin resistant subjects. Moreover, glucose uptake seems to be decreased in subcutaneous adipose tissue in obese subjects.

OS_209

DECREASED LEFT VENTRICULAR GLUCOSE UTILISATION IN RIGHT HEART FAILURE DUE TO PULMONARY HYPERTENSION

R. Kluge (1), A. Seese (1), T. Lincke (1), H. Wirtz (2), J. Winkler (2). (1) Department of Nuclear Medicine; (2) Medical Department I, University of Leipzig.

Aim: Recent studies suggest that changes of energy substrate metabolism may be crucial for the development of heart failure in patients with pressure overload. Aim of the present study was the regional myocardial glucose uptake in patients with right ventricular (rv) pressure load due to pulmonary hypertension with or without rv failure.
Methods: In 40 patients (group A: without rv failure, n = 18; group B: with rv failure, n = 22) myocardial glucose utilization and perfusion were investigated under resting conditions with F-18-FDG (PET, Siemens ECAT exact HR+) and Tc-99m-tetrofosmine (SPECT, Vertex, ADAC Lab.), respectively. Region-of-interest technique was used to calculate ratios of mean count densities of the free right (r) and left (l) ventricular walls (tetrofosmine r/l and FDG r/l). Glucose utilisation rate (GUR) was calculated by use of the graphical method of Patlak.
Results: Mean pulmonary artery pressure (mPAP) and tetrofosmine r/l were similar in groups A and B. FDG r/l, however, was significantly higher in group B.

	Group A	Group B	Significance
mPAP (mmHg)	50.5 ± 22.2	56.1 ± 14.6	no
Tetrofosmine r/l	0.66 ± 0.11	0.63 ± 0.10	no
FDG r/l	0.69 ± 0.20	1.00 ± 0.35	$p < 0.05$
GUR_{right} (µmol/100g*min)	14.3 ± 6.9	16.1 ± 5.7	no
GUR_{left} (µmol/100g*min)	28.6 ± 12.3	18.7 ± 7.4	no, $p = 0.07$

There was a close inverse correlation between the degree of pressure load (mPAP) and the GUR in left ventricular myocardium in group B ($r = -0.77$, $p<0.001$) but no significant correlations in group A ($r = -0.3$) or in right ventricular myocardium (Group A: $r = 0.46$, group B: $r = -0.2$).
Conclusion: Rv failure due to pulmonary hypertension was accompanied by a pressure load-dependent decrease of glucose utilisation in lv myocardium, while no significant changes occurred in the overloaded rv myocardium. These changes could be due to decreased enddiastolic volumes of the left ventricle and thereby decreased wall stress and work load.

OS_210

TREATMENT OF DIABETIC DB/DB MICE WITH THE NEW INSULIN-SENSITIZING DRUG GW1929 RESULTS IN ALTERATIONS IN GLUCOSE HANDLING AND LIPID METABOLISM - STUDIES WITH [I-125]-BMIPP AND [F-18]-2-FDG

F. F. Knapp (1), A. L. Beets (1), E. J. Michaud (1), B. H. Jones (1), H. J. Verberne (1,2), G. Sloof (2), K. K. Brown (3), B. R. Henke (3). (1) Nuclear Medicine Group, Oak Ridge National Laboratory (ORNL), Oak Ridge, Tennessee, USA; (2) Nuclear Medicine Department, Free University of Amsterdam, Amsterdam, The Netherlands; (3) GlaxoSmithKline, Inc., Research Triangle Park, North Carolina, USA.

Aims: New thiazolidinedione (TZD)-type insulin-sensitizing drugs are now widely used in Type 2 diabetic patients. The molecular target is the peroxisome proliferator-activated receptor gamma (PPARγ), associated with transcriptional regulation of genes involved in transport, utilization and storage of glucose (G) and fatty acids (FFA). The goals of this study were to evaluate the effects of GW1929, a novel non TZD compound, on G and FFA uptake in diabetic mice.

Methods: 60 d old mice (n=6/group) were studied: Group I - db/db (T) mice, 15 mgm/gm body weight/day of GW1929 by food-admixture; Group II -aged-matched lean db/+ (NT) and Group III - db/db (NT) mice – received standard chow. After 12 days, a [I-125]-BMIPP/[F-18]-2-FDG mixture was administered i.v. to 3 mice/group. Mice were sacrificed 120 min p.i., major organs (15) removed, counted for F-18/I-125, lipids extracted (Folch) and analyzed by TLC. Blood was drawn from the remaining non-injected mice (n=3/ group) for serum analysis.

Results: Group I T mice (Table; mean values) showed a dramatic decrease in serum G, TG (triglycerides) and FFA levels compared to db/db NT. 2-FDG tracer uptake was significantly increased in heart (H) and other insulin-sensitive tissues of Group I T mice but not in non-target tissues such as liver (L). CD36 (FFA transporter) is upregulated by PPARγ agonists, but BMIPP uptake in H was decreased compared to Group II and III mice. There was an unexpected alteration in the tissue lipid profile in Group I T mice (DG = diglycerides), suggesting similarity of H lipid stores to NT lean controls and TG storage was promoted in adipose (A) but not other tissues.

Conclusions: GW1929 treatment of db/db mice results in a dramatic increase in target tissue G uptake and alteration in FFA metabolism compared to NT db/db controls . TG/DG ratios in H and A are more like lean controls. These data demonstrate the benefits of using radiotracers to detect changes in therapeutic-targeted gene expression.

				% Injected Dose/gram Tissue				BMIPP –	
	Glucose	TG	FFA	2-FDG		BMIPP		TG/DG Ratio	
Mouse Group	(mg/dL)	(mg/dL)	(mEq/L)	H	L	H	A	H	A
I - db/db T	260	43	0.61	24.89	0.84	9.53	0.82	1.80	2.14
II - db/+, NT	229	105	0.44	25.68	0.65	14.31	2.03	1.15	1.85
III - db/db, NT	538	236	1.96	9.06	0.97	13.37	0.76	3.45	0.54

DIAGNOSTIC ONCOLOGY

OS_211

POSITRON EMISSION TOMOGRAPHY IN THE STAGING OF PATIENTS WITH ESOPHAGEAL CARCINOMA

A. Bruno (1), M. Castellani (1), L. Antoniazzi (2), L. Bonavina (2), M. Schiavini (1), A. Peracchia (2), P. Gerundini (1). (1) Department of Nuclear Medicine; (2) Department of Surgery, University of Milan, Ospedale Maggore-IRCCS, Milano, Italy.

Accuracy of staging is critical to select the most appropriate treatment for esophageal cancer. Aim of the study was to determine whether PET may change the staging. We investigated 37 consecutive patients (28 M; mean age 57 yrs.; range 32-83) with total body FDG-PET as part of routine staging (n = 11) or restaging after neoadjuvant therapy (n = 26). Twenty-Three patients underwent surgery, 21 of whom through a transthoracic approach. In 9 patients only palliative endoscopic treatment was performed. The remaining 5 patients were submitted to further chemotherapy and/or radiotherapy. Histological diagnosis was squamous cell carcinoma in 18 patients, adenocarcinoma in 17, and undifferentiated carcinoma in 2. PET scan was performed 45 min. after e.v. injection of 370 MBq of 18F-FDG, acquiring emission and transmission data. PET tomograms were evaluated analyzing both emissive and attenuation corrected slices. The results of PET were compared to traditional spiral CT.

Overall, PET scan allowed to confirm the presence of metastatic disease in 14 patients (37.8 %). Moreover, it was able to reveal 25 new metastatic localizations in 23 patients (62.1%), 15 of whom after chemoradiation therapy. The sites of metastasis were bone (24 %), mediastinal nodes (16%), celiac nodes (12%), cervical nodes (12%), liver (8%) and other (16%). In two patients, the persistent primary tumor after neoadjuvant therapy was not evident at CT scan.

Compared with conventional imaging studies, FDG PET modifies staging of esophageal cancer and has a great impact on the therapeutic strategy, particularly after neoadjuvant therapy.

OS_212

THE UTILITY OF WHOLE-BODY POSITRON EMISSION TOMOGRAPHY (PET) WITH 18-F-FLUORO-DEOXY-D-GLUCOSE (FDG) FOR DIAGNOSIS OF RECURRENT GASTRIC CANCER

T. De Potter, P. Flamen, A. Maes, E. Van Cutsem, G. Bormans, L. Mortelmans. Gasthuisberg University Hospital, Leuven, Belgium.

PURPOSE: Available biochemical and radiological parameters offer little diagnostical advantage over clinical surveillance alone and do not excel at confirming suspected relapse. This retrospective study was designed to assess the accuracy of FDG-PET in diagnosing recurrence of gastric cancer.

PATIENTS AND METHODS: Thirty-three patients who had surgical treatment for gastric cancer with curative intent and underwent an FDG-PET for suspected recurrence were retrieved from the PET database. All patients were reviewed with full knowledge of prior conventional diagnostic workup (CDW). Results were compared to a gold standard, consisting of histological confirmation or radiological and clinical follow-up.

RESULTS: The gold standard established disease recurrence in 20/33 patients (prevalence: 61%). Sensitivity and specificity of FDG-PET for diagnosis of recurrence was 14/20 (70%) and 9/13 (69%), respectively. Positive and negative predictive value was 14/18 (78%) and 9/15 (60%), respectively. Of the 6 false negative cases, 4 had intra-abdominal lesions (2 peritoneal and one liver metastasis, one local recurrence). In the subgroup with previous signet cell differentiation in the primary tumor (n=13, disease prevalence: 62 %), specificity was 3/5 (60%) and sensitivity 5/8 (62.5%). Survival analysis for the entire patient group using Kaplan-Meier statistics yielded a prolonged survival in the PET negative group (median: 11.9 months) versus the PET positive group (median: 5.6 months) ($P = 0.01$). In the group with proven recurrence (n = 20), median survival for the PET negative group was 15.9 months versus 4.5 months for the PET positive group ($P = 0.03$).

CONCLUSION: Because of its poor sensitivity and low negative predictive value, FDG-PET is not suited for screening purposes in the follow-up of treated GC. However, FDG-PET appears to provide important additional information concerning the prognosis of recurrent gastric cancer.

OS_213

IMAGE FUSION OF FDG-PET AND SPIRAL-CT IN THE DIAGNOSIS OF FOCAL PANCREATIC LESIONS

H. Amthauer (1), M. Böhmig (2), E. Lopez-Hänninen (1), S.M. Niehues (1), S. Rosewicz (2), A.J. Lemke (1), J. Langrehr (3), N. Hosten (1), R. Felix (1). (1) Klinik für Strahlenheilkunde; (2) Medizinische Klinik m.S. Hepatologie und Gastroenterologie; (3) Klinik für Allgemein- und Transplantationschirurgie, Charité, Campus Virchow-Klinikum, Berlin, Deutschland.

Evaluation of the diagnostic value of FGD-PET / CT image fusion in patients with focal pancreatic lesions.

Methods: As part of a prospective multimodal diagnostic program, 45 patients with focal lesions of the pancreas were included in this study. The data gained by 18-F-FDG-PET- and Spiral-CT-scans was fused on an AVS platform (Advanced Visualization System, Neuss, Germany) by a custom-made software developed at our department. The actual registration was performed by a voxel-based method. Evaluation of the findings concerned dignity, topographic assignment, infiltration of surrounding tissue, lymph-node metastases as well as distant metastases and was carried out by two independent observers. A histological verification of the diagnosis was done after surgical resection (n=24), laparatomy (n=14) and biopsy (n=7).

Results: Out of the total of 45 patients, 31 turned out to suffer from malignoma whereas benign processes of the pancreas were diagnosed in 14 patients. The detection of a pancreatic malignoma by FDG-PET-scans showed a sensitivity of 85,4 %, a specifity of 60,9 %, a PPV of 82 %, a NPV of 66,7% and a correctness of 77,5 %. In 15 out of 38 operated patients (39 % of all cases), an improved topographic assignment of PET-scan-findings was possible due to image fusion (Differentiation of organ metastases vs nodal metastases: n=4, verification of multifocal pancreatic lesions: n=2, delimitation from the duodenum: n=3, delimitation from the gut: n=6). In the evaluation of regional lymph-node involvement, PET-scans alone showed a sensitivity of 18 % (4/22) whereas fused images had a sensitivity of 29 % (6/22). Infiltration of surrounding tissue was shown correctly in 12 of 18 cases (67 %). Distant metastases occurred in 11 of 31 patients and were detected by PET-scans with a sensitivity of 91 % (10/11).

Conclusions: The use of FDG-PET is of high value for the evaluation of the dignity of a focal pancreatic lesion. Furthermore, it allows a sensitive detection resp. exclusion of distant metastases of pancreatic neoplasms. Additional diagnostic information can be obtained by consecutive image fusion with abdominal CT-scans. Thus, the greatly enhanced accuracy of topographic assignment is especially valuable for the preoperative phase and regional staging procedures.

OS_214

FDG-PET IMAGING IN DETECTING RECURRENT OR METASTATIC COLORECTAL CANCER IN PATIENTS WITH ELEVATED CEA LEVELS

F. Ponzo, H.M. Zhuang, L.B. Lacorte, A. Alavi. Hospital of the University of Pennsylvania, USA.

Patients with recurrent or metastatic colorectal cancer often have elevated plasma CEA levels. The CEA levels are therefore used as a marker of tumor recurrence in these patients. Traditionally, CT was used as the first imaging modality to evaluate such patients. The **aim** of this study was to determine the efficacy of FDG-PET in detecting recurrent or metastatic lesions in patients with history of colorectal cancer and a newly elevated CEA.

Methods: We retrospectively reviewed seventy-one FDG-PET scans in patients with history of colorectal cancer and possible recurrence. All patients had elevated CEA levels with either a negative CT results (n = 41) or without prior CT examination (n = 30). The PET images were acquired using a C-PET camera (ADAC). All patients were followed by a minimum of 8 months with either surgical pathology (n = 52) or conventional imaging technique (CT or MRI, n = 19).

Results: Forty-nine patients had true-positive FDG-PET scans, including 25 of those with negative CT findings. Four patients had false-positive results, all of which were detected by surgery. Sixteen patients had true-negative results. The CEA levels of some of these patients fell without known reasons. Two patients had false-negative results. The sensitivity, specificity, accuracy, positive predictive value, negative predictive value of FDG-PET in this group of patients are 96.1%, 80.0%, 91.5%, 92.5% and 88.9%, respectively.

Conclusion: FDG-PET is highly accurate in evaluating recurrence and metastasis in patients with history of colorectal cancer and elevated level of CEA. Considering that CT is not accurate enough to detect recurrent or metastatic lesions, using FDG-PET to replace CT as the first imaging modality in these patients may be both life- and cost-saving.

OS_215

THE ROLE OF 18F-DG IN THE PRESURGICAL RECTAL CANCER

F. Chierichetti (1), C. Capirci (2), G. Crepaldi (3), P.L. Zanco (1), A. Fini (1), C. Polico (2). (1) U.O. Medicina Nucleare - Centro PET, Castelfranco Veneto; (2) U.O. Radioterapia Rovigo; (3) Div. Oncologia , Rovigo, Veneto, Italy.

AIM OF THE STUDY: F18-DG (fluorine18-deoxyglucose) PET (positron emission tomography) is well established in the follow up of colorectal cancer to select patients who will benefit of surgery if the disease is not spread. The recent introduction of radio and chemotherapy before surgery in rectal cancer has changed the approach to these tumors and is giving a better prognosis to these patients. The aim of our study was to investigate a possible role of F18-DG PET in the evaluation of neoplastic response to chemo-radiation neoadjuvant therapy.

PATIENTS AND METHODS: 26 patients (range 46-80 years) with bioptically proved rectal cancer (T3 in 23 and T4 in 3) where studied with F18-DG PET by a dedicated tomograph (ECAT EXACT 47, Siemens) 30 days after the end of radiotherapy. In 2 out of 26 patients there was a radiological evidence of metastatic disease (M+) and in 18 patients local nodal involvement was documented.

RESULTS: all patients were submitted to surgery. Neoadjuvant radio-chemotherapy changed previous T evaluation in 19 (in 5 cases to T0!) and previous N staging in 11 pts (from N1 to N0). At surgery, 5 patients had no cancer cells in the primary site of disease and 5 presented micro foci of tumor. F18-DG PET was correctly negative in the 5 cases with no cancer cells found at surgery after treatment (T0) and was faintly positive in the 5 cases with micro persistence of local disease at surgical approach. In the group of 16 patients with locally proved disease after treatment with masses from 1 to 5.5 cm diameter, F18-DG PET was false negative in 9 cases with residual masses at surgery. Among this last group, PET, even if negative on primitive site, was the only diagnostical tool to evidentiate lung metastases, furtherly proved, in a patient and in another one (PET positive also in rectum) it identified further sites of metastases thus changing previous staging.

CONCLUSIONS: in this our preliminary experience, on pre-surgical subjects, F18-DG PET was sensitive to detect spread disease (2 patients M+ at previous evaluation resulted in 3 cases at final diagnosis affected of M+) thus changing the final staging as already shown in patients with previous colorectal cancer. PET was less sensitive to detect local tumor viability: in 57% of cases (12 out of 21) it was negative for local persistence of disease. Nevertheless, these patients are candidates for surgery. We believe that a follow up is required to show that negative PET on local site of tumor may be of prognostic value, as demonstrated in other kind of tumors. PET negative is probably a marker of a long term disease free.

RADIOPHARMACY / RADIOCHEMISTRY

OS_216

OPTIMIZATION OF BISPECIFIC ANTIBODY PRETARGETING OF RENAL CELL CARCINOMA USING A 99MTC-LABELED BIVALENT PEPTIDE

F.G. van Schaijk (1), A.C. Soede (1), J. van Eerd (1), W.J. McBride (2), G.L. Griffith (2), E. Oosterwijk (1), F.H.M. Corstens (1), O.C. Boerman (1). (1) Department of Nuclear Medicine, University Medical Center Nijmegen, Nijmegen, The Netherlands; (2) Immunomedics, Morris Plains, NJ, USA.

Objective: Pretargeting could optimize radioimmunotherapy (RIT). We aim to optimize RIT for renal cell carcinoma (RCC) using the biologically produced anti-RCC x anti-DTPA bispecific antibody (bsMAb: G250 x DTIn-1). In order to develop this method for therapeutic application a bivalent chelate [K(DTPA-In)-Y-K(DTPA-In)-K(N_2S_2)] was synthesized that can be labeled with ^{99m}Tc as well as with ^{188}Re. Here we report the optimization of the pretargeted tumor targeting with the ^{99m}Tc-labeled bivalent peptide as compared to the ^{111}In-labeled P-K(DTPA)-Y-K(DTPA) peptide. Methods: In nude mice with human RCC (SK-RC-52) xenograft tumors were pretargeted with G250 x DTIn1 bsMAb. 24 hours later mice received ^{99m}Tc- or ^{111}In-labeled bivalent peptide (max. specific activity ^{99m}Tc-peptide: 10.5 Ci/μmol, RCP = 94 %, max. specific activity ^{111}In-peptide: 10.3 Ci/μmol, RCP = 82 %). At various timepoints after injection of the radiolabeled peptide mice were killed and the distribution of the radiolabel was determined. Results: In the first experiments the optimal peptide dose was determined: mice were pretargeted with a fixed bsMAb dose of 0.1 nmol and after 24 hrs mice received 0.3 - 12.6 pmol ^{99m}Tc-labeled peptide. At a peptide dose of 3.8 pmol optimal tumor uptake (32.6 ± 6.1 %ID/g, 6 h pi) and tumor-to-blood ratio (6.4 ± 1.2, 6 h pi) were obtained. Subsequently, the optimal bsMAb dose was determined at a fixed ^{99m}Tc-labeled peptide dose of 3.8 pmol. Tumors were pretargeted with 0.1 - 1.0 nmol G250 x DTIn1 bsMAb. Optimal tumor uptake was obtained at 0.2 nmol G250 x DTIn1 bsMAb (tumor uptake 37.0 ± 19.3 %ID/g, tumor-to-blood ratio 3.50 ± 2.22). Pretargeted tumors can also be targeted very effectively with the ^{111}In-labeled peptide. At optimized conditions (0.1 nmol bsMAb, 0.8 pmol peptide) tumor uptake of the ^{111}In-labeled peptide was very high (45.5 ± 10.6 %ID/g, 4 h pi) and the tumor-to-blood ratio was 12.0 ± 3.5 at 4 h pi. Conclusion: In this model pretargeted RCC tumors can be targeted rapidly and effectively with a radiolabeled bivalent peptide which can be labeled with ^{99m}Tc as well as with ^{188}Re. This approach will be further developed for pretargeted RIT using ^{188}Re-labeled peptide.

OS_217

IMMUNORADIOMETRIC ASSAY OF SERUM CHROMOGRANIN-A AND NEURON-SPECIFIC ENOLASE IN DIAGNOSIS OF SMALL-CELL LUNG CANCER

L. Giovanella (1), L. Ceriani (1), M. Bandera (2), S. Garancini (1). (1) Department of Nuclear Medicine, University Hospital ; (2) Department of Pneumology, University Hospital, Varese, Italy.

Aims

Aim of our work was (1) the evaluation of the diagnostic performance of serum chromogranin-A (CgA) in small cell lung cancer (SCLC) and (2) the comparison between CgA and neuron-specific enolase (NSE).

Methods

We enrolled 74 consecutive patients with cytological or histological diagnosis of SCLC. The staging of the disease was performed according the UICC criteria. Patients were classified as limited disease (LD) or extensive disease (ED). Before any therapy a blood sample was taken: serum CgA and NSE were assayed by immunoradiometric methods (NSE Prolifigen®, Byk Sangtec, Sweden and CgA RIA CT, Cis BioInternationale, France). A group of 100 patients affected by benign pulmonary diseases was used as control.

Results

A cut off level of 100 ng/mL and 12.5 μg/L was employed for CgA and NSE, respectively. The sensitivity of NSE and CgA was 45% and 51% respectively. A simultaneous positivity of both markers was observed in 26% of cases while a positivity of "one or both" markers was observed in 70% of patients. The specificity of NSE, CGA, NSE+CgA, NSE and/or CgA was 94%, 92%, 96% and 90% respectively. The distribution of both markers in SCLC patients differs significantly respect the control subjects (U-test, $p<0.001$). The sensitivity of NSE and CgA was 25% and 43% in LD and 66% and 62% in ED (X^2-test, $p<0.001$ for NSE, $p<0.01$ for CgA) . The distribution of both markers differs significantly in LD respect ED (U-test, $p<0.001$ for NSE, $p<0.01$ for CgA).

We also evaluated the influence of haemolysis on serum levels of both markers by adding increasing concentrations of haemolysed serum to normal serum samples: CgA levels were not affected by haemolysis while NSE greatly increased when haemolysis occurs.

Conclusions

In conclusion, NSE and CgA showed a comparable sensitivity in SCLC diagnosis. On the other hand, CgA is more sensitive than NSE in LD and, consequently, the association of NSE and CgA should be employed to enhance the overall diagnostic sensitivity and accuracy. Additionally, CgA was not affected by haemolysis while NSE levels greatly increased in haemolysed serum.

OS_218

PRECLINICAL EVALUATION OF A NEW SINGLE CHAIN AGAINST CA 19-9 ANTIGEN AND COMPARISON OF THE BIODISTRIBUTION CHARACTERISTICS WITH IT'S PARENTAL ANTIBODY

S. Guhlke (1), B. Stommel (1), H. Bender (1), P. Karwath (1), A. Hombach (2), C. Heuser (2), H. Abken (2), H.J. Biersack (1). (1) University of Bonn, Clinic for Nuclear Medicine, Bonn, Germany; (2) University of Cologne, Innere Medizin, Cologne, Germany.

The aim of the study was to test whether the radioiodinated new single chain (scFv) against CA 19-9 could be a useful agent for the diagnosis (or treatment) of pancreas, stomach and/or colorectal carcinoma. Therefore a) the radioiodination, b) specific antigen binding after iodination and c) the biodistribition in mice were studied.
Methods: We have optimized the iodination of both, the scFv and it's parental Mab against CA 19-9.
The radiolabeled proteins were purified by gel-chromatography and radiochemical purity was checked by thin layer chromatography. To test the binding specifity of the I-131-ScFv, supernatants of the human colon carcinoma cell lines H498 (CA 19-9 positive) and H716 (negative control) were applied to CA 19-9 Mab coated wells. Dilutions of the iodinated ScFv were incubated to the antigen coated wells and finally the ratio of bound to non-bound I-131-ScFv was determined. Biodistribution studies were performed using nude mice.
Results: Optimal radiochemical yields of I-131-ScFv were 40-60% with >95% radiochemical purity after gel-chromatography. I-131-ScFv binding to antigen negative control wells was within background while binding to antigen positive wells reached a concentration dependant maximum of 40-50%, thus demonstrating highly significant binding of the iodinated ScFv to the CA-19-9 antigen. The biodistribution data for the I-131-ScFv revealed an initial fast blood clearance with values of 18% ID/g at 20 min p.i and 8 % at 4,5 h. Excretion was predominantly renal (55 % ID/g at 20 min; 6 % at 4,5 h). Hepatic uptake was low with maximum liver values of 10 % ID/g at 20 min. As expected blood clearance of the parental I-131-Mab was considerably slower with 28% ID/g at 30 min and still 24 % at 4.5 h. Excretion followed mainly hepatic pathways (20 % ID/g at 4,5 h) accompanied by low renal excretion (7% ID/g at 4,5 h p.i. in kidneys).
Conclusions: The preliminary data show highly promising binding and biodistribution characteristics of this first radiolabeled single chain against CA 19-9 antigen.

OS_219

CLINICAL EVALUATION OF THE 2ND GENERATION RADIO-RECEPTORIAL ASSAY FOR ANTI-TSH RECEPTOR ANTIBODIES (TRAB)

L. Giovanella, L. Ceriani, S. Garancini. Department of Nuclear Medicine, University Hospital, Varese, Italy.

Detection of autoantibodies to the TSH receptor by radioreceptorial assays (RRA) is largely requested in clinical practice for the diagnosis of Graves' disease and its differentiation from diffuse thyroid autonomy. Additionally, TRAb measurement during antithyroid drug treatment can be useful to evaluate the risk of disease's relapse after therapy discontinuation. Nevertheless, some patients affected by Graves' disease are TRAb negative when 1st generation assay is used. Recently a new RRA method for TRAb assay was developed by using human recombinant TSH-receptor and solid-phase technique.
Aim
Aim of our work was the comparison between 1st and 2nd generation TRAb assays in Graves' disease diagnosis.
Methods
We evaluated the diagnostic performance of a newly developed 2nd generation TRAb assay (DYNOtest™ TRAK human, BRAHMS Diagnostica GmbH, Germany) in 46 patients affected by Graves' disease with negative 1st generation TRAb assay (TRAK Assay™, BRAHMS Diagnostica GmbH, Germany) . A control groups of 50 Graves' disease patients with positive 1st generation TRAb assay, 50 patients affected by Hashimoto's thyroiditis and 50 patients affected by nodular goiter were also examined.
Results
41out of 46 patients affected by Graves' disease with negative 1st generation TRAb assay showed a positive 2nd generation test. The overall sensitivity of the 2nd generation test was significantly improved respect the 1st generation assay in Graves' disease patients (_^{2}=22.5, p<0.0001). 1 and 3 out of 50 patients affected by Hashimoto's thyroiditis were positive by 1st and 2nd generation TRAb assay, respectively. All these patients showed primary hypothyroidism. No differences resulted in euthyroid Hashimoto's thyroiditis sub-group and in nodular goiter control group.
Conclusions
The 2nd generation TRAb assay is clearly more sensitive than the 1st generation test and should be used in clinical practice to minimize the incidence of TRAb negative Graves' disease. Long-term prospective studies are needed to evaluate the prognostic role of 2nd generation TRAb assay in Graves' disease treated by antithyroid drugs.

OS_220

COMPARISON OF SELECTIVE INHIBITION OF P-GLYCOPROTEIN-MEDIATED TRANSPORT OF 99MTECHNETIUM-MIBI BY PSC833, R101933 AND GG918

J. Vergote, PX. Charlopin, D. Saintier, JL. Moretti, JC. Kouyoumdjian. Laboratory of radiopharmacology, University Paris 13, France.

BACKGROUND : Drug resistance is a major impediment to the successful treatment of human cancers. The earlier-identified resistance mechanisms has been the overexpression of the mdr1 gene product : P-glycoprotein (Pgp). The multidrug resistance associated protein (MRP1) is also described as a protein associated with multidrug resistance in vitro. It is known that ^{99m}Tc-MIBI uptake is drastically reduced in cancer cells that express the Pgp or the MRP1.
AIM : The Pgp reversing effect of R101933 and GG918 was evaluated with ^{99m}Tc-MIBI on cultured cancer cell lines and compared to the PSC833 effect.
METHODS : ^{99m}Tc-MIBI radioactivity incorporation was determined into two cell lines : K562/R and GLC4/R which overexpress Pgp and MRP1, respectively. The cells were incubated at 37¡C in the absence or presence of different concentrations of one reversal agent (R101933 or GG918 or PSC833).
RESULTS : ^{99m}Tc-MIBI accumulation in GLC4/R was similar with or without these reversal agents. The uptake of ^{99m}Tc-MIBI observed in K562/R increased with the increasing PSC833 or R101933 or GG918 concentrations. At 2µM PSC833, 5µM R101933 and 10µM GG918, the accumulation of radioligand in K562/R was comparable to parental sensitive cell line (K562/S).
CONCLUSION : In the presence of PSC833 or R101933 or GG918, ^{99m}Tc-MIBI accumulation in cells expressing Pgp was increased and was not changed in cells with MRP1. PSC833 have got a higher potency to inhibit Pgp-mediated transport *in vitro* but R101933 and GG918 are both valuable Pgp new generation reversal agents if their relative toxicity is not considered.

CORRELATIVE IMAGING

OS_221

A NEW CONCEPT OF A UNIFIED APPROACH IN THE TREATMENT OF BRAIN TUMORS

R. Bale (1), R.A. Sweeny (2), R. Moncayo (3), W. Eisner (4), J. Burtscher (4), M. Vogele (1), E. Donnemiller (3), K. Seydl (3), P. Lukas (2), K. Twerdy (4), W. Jaschke (1)(1) Dept. of Radiology I; (2) Dept. of Radiotherapy; (3) Dept. of Nuclear Medicine; (4) Dept. of Neurosurgery, University of Innsbruck

Aim: The fundamental idea is the application of the VBH mouthpiece as an individualized reference base for a unified, multidisciplinary diagnosis and therapy by allowing image fusion of CT/MR/SPECT/PET, and fixation for radiotherapy and neurosurgery. We report our first clinical experiences with this new device in various disciplines.
Methods: The VBH mouthpiece is an individualized vacuum dental-cast, which is attached to the upper palate by under-pressure. For immobilization of the patient's head the VBH mouthpiece is secured to a base plate by hydraulic arms. The frame provides external reference points for image fusion, computer aided surgery and radiotherapy. The diagnostic studies are performed with the VBH mouthpiece. Image-fusion is based on reference points on the frame. Biopsy is performed with frameless stereotactic navigation. If a surgical intervention is necessary, the image guided surgery relies on the fiducials on the frame, thus necessitating another additional scan. For radiotherapy the patient is repositioned with the original VBH mouthpiece, thus necessitating the fabrication of a mask. For follow-up subsequent image acquisitions are performed with the frame.
Results: The VBH head holder has been used successfully for fractionated radiotherapy, brachytherapy, and computer assisted surgery. Funtional imaging by SPECT can be easily fused to any other diagnostic modality (CT or MRI). The VBH head holder offered a rigid, accurate, and reproducible fixation and accurate external reference points for registration and image fusion.
Conclusions: Application of the mouthpiece is an important step towards unified, multidisciplinary diagnosis and therapy by allowing image fusion of CT/MR/SPECT/PET, use of imaging data, fixation for radiotherapy (external beam, brachytherapy, radiosurgery) and neurosurgical applications.

OS_222

SPECT / CT FUSION IMAGING IN HYPERPARATHYROIDISM: A HELPFUL DECISION MAKING FOR ENDOSCOPIC SURGERY.

P. Martin (1), M. Krzemien (2), S. Güler (2), N. Hermanus (2), J. Paternot (1), R. Gheldof (1), C. Ponnen (2), F. Guerrerolimeros (3), A. Jortay (4), P. Bergmann (1), M. Verhas (1)(1) Nuclear Medicine; (2) Radiology; (3) Internal Medicine; (4) Surgery, Brussels University, CHU Brugmann, Brussels, Belgium

With increasing development of endoscopic surgery for hyperparathyroid disease, most precise localization of abnormal gland became a major preoperative tool. Present study was undertaken to evaluate the feasibility of imaging fusion of highly sensitive and specific 99mTc MIBI SPECT imaging of parathyroid lesion with less sensitive but much more precise anatomically location given by CT.

27 consecutive patients (20 women -7 men) underwent a 99mTc MIBI SPECT (IV 740 MBq) and a CT with contrast of neck and mediastinum to detect abnormal gland. 4 external anatomical marks consisted in a tiny drop of 67 Ga for SPECT, jointed with a metallic cutting for CT. Scintigraphic acquisition (double isotope) was performed, 30 minutes after injection, using a SOPHA DSX rectangular tomocamera (-90°, +90°; 128x128 matrix, 32 projections; zoom 1,33; pixel size 3,4 mm). General Electric CT images were reconstructed using a 512x512 matrix, 2 mm thick slices. Both studies were aligned with external marks, fusion imaging being thereafter performed. Before the fusion of images, SPECT and CT were analyzed by independent observers. Thereafter, fusion of images was done. At the present time, 14 out of 27 patients underwent parathyroidectomy.

Taken separately, agreement between SPECT and CT was found in 22/27 patients (82%). After analysis of fusion images, the agreement percentage was 96%, according to the fact that non specific CT images could have a clear hypermetabolic SPECT signal, indicating lower sensitivity of CT. In the 14 patients who underwent surgery, taken separately, SPECT detected correctly the lesion in 13/14 patients (Sensitivity of 92%). Since there was no false positive lesion, specificity was 100%. CT detected a lesion in 12/14 cases (Sensitivity 85%, specificity 100%). When both procedures were combined, lesion was precisely located in 13/14 cases, the advantage of fusion in this particular disease being its highly anatomical precision, allowing most precise surgical procedure.

We conclude that the highly sensitive and specific signal of 99mTc MIBI SPECT in the detection of parathyroid adenoma makes it a powerful test to detect the presence of a lesion. However, its lack of precise anatomical location can be a handicap in case of endoscopic surgery. Combination of SPECT and CT in this particular situation is of major interest to maximally reduce risk and surgery time in the management of parathyroid disease.

OS_223

VALUE OF CEREBRAL BLOOD FLOW SPET IN DEMENTIA COMPARED WITH MAGNETIC RESONANCE IMAGING

K. Machida (1), N. Honda (1), M. Hosono (1), Y. Shimizu (1), S. Kosuda (1), H. Matsuda (2), M. Ohshima (3), T. Momose (4), K. Koizumi (5), T. Matsumoto (6), J. Hashimoto (7)(1) Department of Radiology,SMC,Saitama Medical School,Kawagoe,Japan; (2) Department of Radiology, National Psychiatric Center,Tokyo; (3) Department of Radiology,Teikyo University,Tokyo, Japan; (4) Department of Radiology,University of Tokyo, Tokyo, Japan

Magnetic resonance imaging (MRI) is the imaging technique of choice for most central nervous system disorders. Cerebral blood flow SPET has been shown to exhibit characteristic patterns in dementia enabling differential diagnosis. The purpose of the study was to determine which of SPET or MRI was superior for the differentiation of dementia when each was interpreted by dedicated subspecialties.

Methods: Fifty-seven cases of dementia, who underwent both MRI of the brain and SPECT by either Tc-99m ECD (n = 44) or I-123 IMP (n = 13) were collected from 4 institutions. Gold standard was set to diagnoses made by experts in the source institutions. There were 19 cases of Alzheimer's disease (AD), 8 of multi-infarction dementia (MID), 2 of Pick disease, 6 of other dementias, and 22 of normal. Image interpretation experiment was done with clinical information provided in two separate occasions: first, SPET images were inspected by 10 nuclear medicine physicians (NMP) of variable experience (1 to 30 years); second, MRI of the brain was interpreted by 4 board-certified neuroradiologists and 3 experienced NMP. Listed diagnoses were rated according to a 5-point scale in the both occasions. Receiver-operating characteristics (ROC) curves were generated using the ratings as operating points. Area under the ROC curve (Az) was calculated and unpaired *t*-test was done between the two sessions.

Results: There was no statistical difference ($p > 0.05$) between the Az's of the individual sets of imaging modalities and doctor subspecialties (Table). Skill of MRI interpretation of the three nuclear medicine physicians indicated by Az was not inferior to the skill of the neuroradiologists when diagnostic consideration was limited to dementia. However, the ROC curves showed considerable variation in the Az, and the variation was greatest in the differentiation of AD and MID.

Area under the ROC curve

Modality/Itpr	N–Dementia	N–(AD/MID)	N–AD	AD-MID
SPET/NMP (n = 10)	0.715	0.671	0.610	0.672
MRI/NR (n = 4)	0.815	0.785	0.759	0.766
MRI/NMP (n = 3)	0.771	0.714	0.686	0.555

*Itpr: interpreters, N: Normal, AD: Alzheimer's disease, MID: multi-infarction dementia NR: Neroradiologist, NMP: Nuclear medicine physician

Conclusions: CBF SPET has comparable power of differentiation as MRI when the both are interpreted by corresponding subspecialties in dementia. Training of SPET interpretation is mandatory because inter-observer variation is great.

OS_224

THORACIC DUCT SCINTIGRAPHY BY ORALLY ADMINISTERED 123I-BMIPP - NORMAL FINDINGS AND A CASE REPORT

A. Qureshy, K. Kubota, S. Ono, T. Sato, H. Fukuda. Tohoku University, Department of Nuclear Medicine & Radiology, Institute of Development, Aging & Cancer, Sendai Shi, Japan.

AIM: The aim of the study was to investigate the use of orally administered I-123 BMIPP for thoracic duct imaging in normal and pathological states and to study the tracer distribution and dynamics in the normal subjects.

Material & Methods: The radiotracer was administered with solid (in 3 normal subjects and one patient) or liquid meals (in other 3 normal subjects). Solid meals contained relatively more fat content than the liquid meal. Images were acquired to trace the passage of radiotracer from the intestine to systemic venous circulation via lymphatic route. Multiple static planar images were acquired in anterior and posterior views. Blood samples were analyzed for radioactivity and serum triglyceride levels.

Results: In normal subjects I-123 BMIPP was absorbed from the intestine and reached the venous circulation via the thoracic duct. The thoracic part of the duct was successfully visualized in all normal subjects within 80 minutes. The radiotracer dynamics varied according to the type of administered meal. The patient had chylomediastinum and right chylothorax and underwent thoracic duct ligation. In the patient, marked stasis in the collateral lymphatic channels was seen, together with chylous leakage into the mediastinal space and right pleural cavity. There was a delay in the passage of tracer to the general venous circulation. Normal thoracic duct was not seen in this patient.

Conclusion: Scintigraphy by orally administered I-123 BMIPP is a simple method to image thoracic duct and to monitor its lesions. The meals with higher fat content results in better BMIPP absorption and may be used as a standard method.

OS_225

COMPARISON OF SPIRAL CT ANGIOGRAPHY (CT) VS. V/Q SCANNING FOR DIAGNOSING PULMONARY EMBOLI (PE) IN HIGH CLINICAL RISK PATIENTS

A. Dhupa (1), M. Dakhel (2), M. Kumar (3), S. Heiba (2), S. Bhaskaran (2), J. Cicenia (3), P. Tietjen (3), M. Abdel-Dayem (2). (1) Pulmonary Service, Department of Medicine, St. Vincent's Catholic Medical Centers of New York; (2) Nuclear Medicine Service, Department of Radiology, St. Vincent's Catholic Medical Centers of New York; (3) Department of Medicine, St. Vincent's Catholic Medical Centers of New York, USA.

AIM: Compare results of Ventilation Perfusion (V/Q) scanning and spiral CT angiographs (CT) in the diagnostic work-up of pulmonary emboli (PE).
METHODS: A retrospective review of 46 pts. who had high clinical suspicion for thromboembolic disease was performed. All 46 pts. had V/Q scans using Tc99m-MAA and Tc99m-PYP for aerosol ventilation, CT angiogram (High Speed Advantax, GE) of the chest .Only 33 pts. had lower extremity Doppler Ultrasound (DU) studies. Results were compared to those of Pulmonary Angiography (PA) where available (9 pts.).
RESULTS: For V/Q 35 pts. (76%) had low probability (LP) (6/35 + ve CT) 6 pts (13%) had intermediate probability (IP) (3/6 positive CT) and 5 (10.8%) high probability (HP) (1/5 + ve CT). Total concordance 39/46 (84.6%) and discordance 13/46 (32.6%). Of the 9 pts. who had PA 3/9 were negative by PA, CT negative and all were LP V/Q. Additional 3/9 positive PA had negative CT in 2/3 and V/Q was IP in 2 and LP in 1. The remaining 3 pts. were positive by PA and CT but V/Q were 1 HP, 1 IP and 1 LP. DU was positive in 4/33 (12.1%) and negative 29/33 (87.9%).
CONCLUSIONS: Our data suggests that V/Q and CT angiogram are complementary to each other. Pulmonary angiography still remains the gold standard and should be used in presence of high clinical suspicion of PE and negative V/Q and CT angiograms.

OS_227

GABAERGIC DYSFUNCTION IN PRADER-WILLI SYNDROME: PRELIMINARY FINDINGS WITH 11C-FLUMAZENIL AND POSITRON EMISSION TOMOGRAPHY

G. Lucignani (1), L. Bosio, A. Panzacchi, R.M. Moresco, I. Coppa, L. Ravasi, F. Fazio, G. Chiumello. (1) Medicina Nucleare Ospedale L. Sacco, Università di Milano, Italia; (2) Clinica Pediatrica III, Università di Milano, Istituto Scientifico, H San Raffaele, Milano, Italia; (3) INB-CNR, Università Di Milano-bicocca, Istituto Scientifico H San Raffaele, Milano, Italia.

Introduction. Prader-Willi Syndrome (PWS) is a multi-system defect characterized by delayed mental and physical development, hyperfagia and gross obesity, bizarre, antisocial and maladaptive behaviors, self-injury and reduced sensitivity to pain. PWS patients have a typical deletion of chromosome 15 (15q11-q13) or maternal disomy, entailing a deletion of the gene encoding the $GABA_A$ receptor b_3-subunit. Mean plasma GABA levels in PWS patients are 2 to 3 folds higher than in non-retarded moderately obese control subjects.
Aim of this study was to assess the GABAergic function in PWS patients by studying the benzodiazepine (BZD) receptor subunit of the GABA receptor. To this end we used positron emission tomography and [C-11] Flumazenil, a marker of the density and affinity of the BZD receptors in brain.
Methods. Six subjects with genetic diagnosis of PWS (mean age 22.8, range 18.8-28.8 yrs) and seven age matched normal control subjects were enrolled for the study. PET studies were performed with a GE Advance scanner. Each subject underwent a 60 min dynamic emission scan after the i.v. injection of 1.85-3.7 MBq/kg of [C-11]Flumazenil. Attenuation correction was achieved by a 15 min pre-injection transmission scan. Transaxial PET images were reconstructed with a Hanning filter. Circular ROIs (1.25 cm diameter) were drawn on the images over different cortical and subcortical regions. ROIs tracer concentrations data were analyzed to calculate the binding potential (BP) of [C-11] Flumazenil by a simplified reference tissue model developed by Gun et al., by use of the pons as the reference region.
Results Discrete significant reduction of the [C-11] Flumazenil BP was found in brain of PWS patients compared to normal subjects. Statistically significant differences ($p<0.05$) were found in three regions: the anterior cingulate gyrus (-17%), the insula (-17%), and the thalamus (-12%).
Conclusions: These preliminary findings, demonstrate a selective GABAergic dysfunction in the brain of patients with PWS, in some of the areas involved in the processing of somatosensory stimuli.

NEUROLOGY / PSYCHIATRY

OS_226

NEUROCHEMISTRY OF PERSONALITY TRAITS: A [18F]FESP PET STUDY

R.M. Moresco (1), A. Vita (3), C. Messa (1), M. Dieci (3), C. Gobbo (2), A. Panzacchi (4), F. Tenconi (3), G. Invernizzi (4), F. Fazio (1-2). (1) INB-CNR,University of Milan Bicocca; (2) Scientific Institute H San Raffaele Milan; (3) DSM Melegnano; (4) University of Milan, Italy

Aim The in vivo evaluation of the neurochemistry of personality traits is of particular interest. Using Positron Emission Tomography (PET) and [^{11}C]raclopride, an association between striatal D_2 dopamine receptors and emotional detachment has been reported using two different personality questionnaire (L. Farde et al., 1997; A Breier et al., 1998). In this study we investigated the relationship between the three personality dimensions evaluated by means of the Tridimensional Personality Questionnaire (CR Cloninger et al., 1987), i.e. „novelty seeking", „reward dependence" and „harm avoidance", and the in vivo binding of [^{18}F]FESP in the cortex and basal ganglia of a group of healthy volunteers.
Methods Eleven healthy volunteers (8M, mean age 27±4, range 22-32 yrs.) were enrolled for the study and underwent a PET scan. Specific binding of [F-18]FESP, to either striatal D_2 or cortical $5HT_{2A}$ receptors was measured between 90 and 120 minutes after injection using the cerebellum as a reference region. PET images were analyzed using both a manual (ROIs) and an authomatic operator independent (SPM96) technique. Spearman correlation coefficients were calculated among each of the three personality dimensions total score, age and the mean, right and left BI values and a multiple linear regression analysis, considering: each cortical region and age as independent variables and the personality dimension as the dependent variable. For these analyses, all data were transformed into rank values.
Results The personality dimension „harm avoidance" showed a significant inverse correlation to [^{18}F]FESP binding in the cerebral cortex, particularly in the frontal cortex (R square= -0.709, p=0.0145) and left parietal cortex (R=-0.629), p=0.038) but not in the basal ganglia (r=-0.176 , p=0.651). Similar results were obtained using SPM setting a p thresholds of 0.05. On the contrary no significant correlation of [^{18}F]FESP binding were observed with „novelty seeking" or „reward dependence" in any of cerebral area examined.
Conclusion In the cerebral cortex, high values of [^{18}F]FESP binding values are associated to an high tendency to avoid danger in otherwise normal subjects, indicating an involvement of serotoninergic system and in particular of $5HT_{2A}$ receptors, in this trait of personality. The results of our as well as previous studies on personality dimensions indicate not only the existence of a relationship between specific behavioral and neurobiological factors but more in general, represent important findings to sustained the concept that variability of PET data may be strongly explain by neurochemical aspects.

OS_228

VISUALISATION OF ACTIVATED MICROGLIA IN MULTIPLE SCLEROSIS PATIENTS

J.A. Versijpt (1), J. Debruyne (2), K. Van Laere (1), F. De Vos (1), J. Keppens (1), K. Strijckmans (1), E. Achten (3), G. Slegers (1), J. De Reuck (2), J. Korf (4), R.A. Dierckx (1)(1) Division of Nuclear Medicine and Radiopharmacy, Ghent University, Belgium; (2) Department of Neurology, Ghent University Hospital, Belgium; (3) Department of Radiology, Ghent University Hospital, Belgium; (4) Department of Biological Psychiatry, Groningen, the Netherlands

Aim: Activated glial cells are implicated in regulating and effecting the immune response that occurs within the CNS as part of multiple sclerosis (MS). The peripheral benzodiazepine receptor (PBR) is expressed on microglial cells and upregulated after neuronal injury. [^{11}C]PK11195 is a specific and selective PET ligand for the peripheral benzodiazepine receptor. The aim of the present study was to investigate the utility of [^{11}C]PK11195 imaging in MS patients and compare relative uptake values for different kinds of lesions with findings of coregistered MR scans.
Methods: Seven controls (average age 33 yrs; SD 7.5, range 23-41 yrs) and 22 MS patients (average age 43.5 yrs; SD 7.0, range 37-51 yrs) were included. All subjects underwent MR scanning (proton-density, T2-weighted, T1-weighted, and T1-weighted after gadolinium injection), perfusion PET scanning (Siemens ECAT 951/31) with [^{15}O]CO_2 and [^{11}C]PK11195 scanning after the injection of 370 MBq [^{11}C]PK11195 (perfusion and receptor PET in the same session). Receptor, perfusion, and MR images were realigned into Talairach coordinates by means of perfusion PET and T1-weighted MR templates. A semiquantitative approach was used providing relative binding indices with normalisation on cortical grey matter. Relative binding indices were assessed for normal and normal-appearing white matter, grey matter (cortical and central grey matter), T2-weighted lesions and Gadolinium-positive T1-weighted lesions.
Results: Relative uptake in controls for yielded 100.26 ± 9.8 and 100.46 ± 9.3 respectively, indicating the minimal aspecific binding in normal control CNS. Relative uptake values for normal-appearing white and grey matter in patients was slightly higher compared to white and grey matter in controls (respectively 101.44 ± 10.8 and 101.05 ± 9.1), however, not reaching significance. Ten patients had Gadolinium-positive T1-weighted MR scans. Relative focal uptake in these Gadolinium-positive T1-weighted MR lesions was highly significant increased (110.37 ± 14.6; p=0.002). Relative uptake in T2-weighted lesions varied from decreased to increased depending on clinical relapse and the presence of Gadolinium-positive T1-weighted MR lesions at the time of [^{11}C]PK11195 scanning.
Conclusions: Semiquantitative [^{11}C]PK11195 PET, as a cellular measure of disease activity, is able to demonstrate activated microglia *in vivo* in MS patients in areas of focal pathology identified by T1- and T2-weighted MRI and to a lesser extent in normal-appearing and grey matter.

OS_229

REGIONAL DIFFERENCES OF BRAIN SEROTONIN SYNTHESIS IN PATIENTS WITH IRRITABLE BOWEL SYNDROME REVEALED BY USING A-[11C]METHYL-L-TRYPTOPHAN, PET AND STATISTICAL PARAMETRIC MAPPING

M. Diksic (1), A. Nakai (1,4), Y. Kumakura (1), M. Boivin (2), P.R. Neto (1), D. D'Souza (3), K. Kersey (3). (1) Montreal Neurological Institute, McGill University, Montreal, QC, Canada; (2) Centre Hospitalier de l'Universite de Montreal, Montreal, QC, Canada; (3) Glaxo Wellcome Inc, Mississauga, ON, Canada; (4) Department of Pediatrics, Fukui Medical University School of Medicine, Fukui, Japan

Objective: To compare brain serotonin (5-HT) synthesis rates, using PET and α-[11C]methyl-L-tryptophan as the tracer, during rectal distension in patients with IBS (Irritable Bowel Syndrome), on alosetron versus placebo treatment.
Subjects and Methods: All IBS patients were non-constipation-predominant. The diagnoses of IBS were made based on the Rome I criteria. Six male and six female IBS patients were scanned. In a randomized, double-blinded, crossover manner, each subject received alosetron (a 5-HT3 antagonist) or placebo for 14 days, separated by a two-week washout. On Day 14, rectal distensions (a model for IBS pain) commenced just before the PET scan and continued for 20 minutes. Eighty-min dynamic PET studies were performed using ECAT-HR+ scanner. Functional 5-HT synthesis images were linearly standardized to Talairach space, normalized to the global mean, smoothed to 14 mm, and analyzed with SPM 99. A separate comparison was done in males and females.
Results: There were significant gender-treatment interactions in 5-HT synthesis in the caudate nucleus, globus pallidus, cerebellum, and cingulate gyrus. In addition there were several regions in which 5-HT synthesis rates were greater in males than those in females during alosetron treatment, whereas there was no region in which females had a greater synthesis rate than males.
Discussion and Conclusion: It is possible that the gender differences observed in regional brain 5-HT synthesis are related to a larger predominance of IBS symptoms in females. Treatment with a 5-HT3 antagonist may result in differential affects in brain 5-HT synthesis in males and females. Study S3B10901 was supported by GlaxoWellcome Inc.

OS_230

BRAIN PERFUSION RATIOS BY 99MTC HMPAO UTILISING A MEAN VALUE OF THE VISUAL CORTEX TO THE CEREBELLUM RATIO DERIVED FROM A NORMAL DATABASE

C.A. Sanchez (1), R. Rodriguez (1), M. Cisnero (2), O. Rizo (3), R. Palmero (1), N. Rodriguez (4), A. Aguila (1). (1) Ciren-Hospital; (2) ISSM; (3) ISTN; (4) CIMEQ-hospital, La Habana, Cuba

Previous results shows that the cerebellum (CER) is the best reference to calculate relative indexes of perfusion (IP) by brain SPECT, but it can not be used on patients with bilateral cerebellar affection (BCA). In these cases visual cortex (VC) or an average of the whole brain activity is recommended. Besides the fact that VC and WB are less reliable than CER, it is impossible to compare SPECT scans when they have been normalized with different values. Method: To overcome that, we developed a method to calculate IP utilizing a reference value defined as (VC / <f>), where <f> is the mean value of the VC/CER ratio derived from a normal database, which was assumed to be constant. We called this value „ the Pseudocerebellum" (PCER). For clinical validation, we first tested statistically the VC/CER ratio on a group of 60 [^{99m}Tc]-HMPAO SPECT scans of 20 normal subjects and 40 neurological patients with positive SPECT but without involvement of VC and CER. Afterwards, to prove that $IP_{PCER} \approx IP_{CER}$, we calculated the mean value of the absolute differences $\langle |IP_{CER} - IP_{PCER}| \rangle$ on two groups of scans from subjects without involvement of VC and CER: 10 normal subjects (GI); and 40 patients (GII). Finally, the method was tested in a third group of SPECT scans on 30 patients with BCA (G III). It was tested using an indirect procedure. Results: The VC/CER ratio was approximately constant with gender and age (age range = 16 - 87 years) with a confident level of 95 %; $\langle |IP_{CER} - IP_{PCER}| \rangle$ was 1.22 % ± 0.35 and 1.20 % ± 0.42 for GI and GII, respectively, which is less than the within-subject replicability of the HMPAO SPECT studies; and it was proved indirectly that IP_{PCER} is a valid procedure to evaluate relative perfusion on patients with BCA (GIII) and quantitatively comparable to using CER as reference region. Conclusion: The VC/CER ratio has very little inter-subject variations in individuals where these structures are not affected. Using this fact we developed a valid procedure to calculate IP equivalent to using CER as a reference value but with the advantage that it is independent of the perfusion status of CER.

DIAGNOSTIC ONCOLOGY

OS_231

EPITHELIAL MEMBRANE ANTIGENE (EMA) AND NM23 SUPPRESSOR GENE IN PAPILLARY AND FOLLICULAR THYROID CARCINOMAS

V. Pesutic-Pisac (1), A. Punda (2), V. Capkun (2), S. Tomic (1), S. Petric (3), M. Marinkovic (4), A. Stanicic (2), A. Pranic-Kragic (2), V. Markovic (2), D. Radovic (2), L.J. Juretic-Kuscic (2)(1) Department of Patology, Clinical Hospital Split, Split, Croatia; (2) Department of Nuclear Medicine, Clinical Hospital Split, Split, Croatia; (3) Department of Otorinolaryngology, Clinical Hospital Split, Split, Croatia; (4) Department of Cytology, Clinical Hospital Split, Split, Croatia

Aim. Wishing to improve the efficiency of the „Team for thyroid diseases", that exists in our clinical hospital last ten years, we made a clinicopathologic study of papillary (PC) and follicular carcinomas (FC) treated in ten years period from 1988 to1998. We noticed their incidence increment, so we wanted to make a reliable data base for better diagnostic procedure, therapy and follow up.
Methods. We analysed 106 papillary and 26 follicular carcinomas according to sex, age, size, location, histological type, metastasis and survival rate. We determined immunoreactivity for EMA and candidate metastasis-suppressor gen nm23 and their relationship to presenting clinical and pathologic features. All the patients, before surgery, had performed cytology diagnosis, scintigraphy, ultra sound and hormone status analysis. All of them with definitive pathology diagnosis of PC and FC were treated with total thyroidectomy.
Results. Among interesting results we stress the raise of female:male ratio (6,5:1), high percentage of multicentric PC (41%) but with no statistically significant association with propensity to metastasize and existence of metastases only in minimally invasive FC that showed vascular invasion in tumor capsula. The high expression of EMA and, at the same time, low grade expression of nm23 gene have been shown to correlate with high metastatic potential in papillary ($p<0,001$) and follicular ($p<0,001$) carcinomas. Furthermore, there were no statistically significant association between their expression and sex, age or tumor size.
Conclusions. Although the survival rate was excellent (97%), all patients that passed away had carcinomas associated with unfavorable factors – men, older age, follicular carcinoma, tumor size >2,5 cm, lymphonode metastases, distant metastases, high grade EMA and low grade nm23. According to these results we decieded to performe routinely immunostaining for EMA and nm23 on all papillary and follicular carcinomas.

OS_232

PAPILLARY MICROCARCINOMA OF THE THYROID GLAND: RETROSPECTIVE ANALYSES OF CLINICAL PRESENTATION AND OUTCOME

Z. Ozcan (1), H. Ozkilic (1), O. Omur (1), S. Erhamamci (1), O. Ozyurt (1), A. Dirlik (1), M. Kayalioglu (1), M. Tuncyurek (2). (1) Department of Nuclear Medicine; (2) Pathology Department, Ege University Medical Faculty, Izmir, Turkey.

Aim: Papillary microcarcinoma (MC) of thyroid is a specific subgroup of papillary thyroid carcinoma defined as a tumor measuring 10 mm or less in maximum diameter. It has known to have excellent prognosis, however, some controversy exists since its diagnosis, treatment, and natural history are not well defined. The aim of this study was to elucidate the clinical presentation and outcome in papillary MC in comparison with those of papillary thyroid carcinoma (PC).
Methods: We retrospectively reviewed clinical variables of 89 MC patients diagnosed from a total series of 341 PC patients. MC group included 76 female and 13 male with a mean age of 43.5 yrs. Histologic diagnoses were obtained from surgical material in 75 pts who underwent thyroid surgery for various thyroid diseases and from biopsy in 14 pts. All pts underwent TSH suppressive therapy after sub-total thyroidectomy. Radioiodine therapy following near-total thyroidectomy was applied in 64 pts. Clinical follow-up including serum thyroglobuline measurements were available in 80 pts while 9 pts were lost to follow up. Mean duration of follow-up was 38.5 months (4-120 mo).
Results: In MC group, mean tumor size was 0.65 cm, and tumor diameter was less than 0.5 cm in 17 cases. The primary tumor was unifocal-unilateral in 58 (65 %), multifocal-unilateral in 18 (20 %) and multifocal-bilateral in 13 (15 %) pts. Vascular invasion of the tumor was noted in 5 cases. Lymph node metastases were detected at initial presentation in 14 (15.7 %) pts in which 8 had admitted to the hospital with cervical enlargement. Distant metastases (lung and bone) were noted in 2 pts (2.2 %) who also had co-existing lymph involvement. The frequency of lymph and distant metastases were 23.4 % and 5.2 % respectively in PC pts and statistically significant difference (chi-square, $p>0.05$) could not be demonstrated in these variables. Clinical course of all MC pts, except 2 cases with cervical lymph node involvement at initial presentation, were favorable. Ten of PC pts showed progression of the disease so far.
Conclusion: Our results imply that, papillary MC pts may have metastases at initial presentation in a similar ratio with those of papillary thyroid carcinoma. Therefore, close clinical follow-up with systemic metastatic scanning is suggested. Although MC has a relatively benign course, more aggressive strategy including near-total thyroidectomy followed by radioablation may be required in a sub-group of pts with multifocal tumors, lymph node involvement and distant metastases.

OS_233

I-123 SCAN COMPARED TO POST-THERAPY I-131 SCAN FOR THE DETECTION OF REMNANT OR METASTASIS OF DIFFERENTIATED THYROID CANCER (DTC)

N. Alnafisi (1), W. Delfyett (1), M. Yun (1), A. Alavi (1), S. Mandel (2). (1) Division of Nuclear Medicine; (2) Division of Endocrinology, Hospital of the University of Pennsylvania, Philadelphia, USA.

AIM: I-123 has a great potential role for the detection of remnant or recurrence of DTC by providing superior image quality and avoiding thyroid stunning associated with I-131 scan. The aim of this study is to assess the usefulness of I-123 compared to post-therapy I-131 scan.
METHODS: One hundred and forty nine patients with previous thyroidectomy for DTC (129 papillary, 13 follicular and 8 Hurthle cell cancer) were included in this study. 133 patients were scanned for detecting post-surgical remnants and 16 patients were surveyed for recurrence or metastasis as they had previous ablation therapies. Each patient had a diagnostic whole body scan acquired at 24 hr after the oral administration of 1.5 to 2 mCi of I-123 sodium iodide and a post-therapy scan acquired 7 days following the oral administration of 60 to 200 mCi of I-131 sodium iodide. The therapy dose was given on the same day of the diagnostic scan. Serum TSH was elevated (> 30 micro IU/ml) in all patients. I-123 and post-therapy I-131 scans were compared for the detection of remnant or recurrence of DTC.
RESULTS: I-123 and I-131 scans were concordant positive in 129 patients showing foci in the neck, lungs and in the bone. In 12 patients (4 surveillance and 8 post-surgical remnant), I-131 scan showed more lesions than I-123: in the neck in 12 patients and in the ovary in one. I-123 was totally negative in 3 of these 12 patients. In the remaining 8 patients (all post-surgical remnants), I-123 scan was superior to I-131 showing additional foci in the neck. I-131 was totally negative in 3 of these 8 patients. I-123 diagnostic scan predicted 98% of the patients with positive post-therapy I-131 scan.
CONCLUSION: Diagnostic I-123 scan is comparable to post-therapy I-131 scan for the detection of remnant or recurrence of DTC. The decision on which patients to treat and on the therapeutic dose of I-131 can be justified based on the diagnostic I-123 scan.

OS_234

CHARACTERIZATION OF 111IN LABELED CCK8 PEPTIDE COUPLED TO A NOVEL DTPA-LIKE DERIVATIVE IN CCK-B RECEPTOR OVEREXPRESSING CELLS

L. Aloj (1), A. Zannetti (1), C. Caracò (1), S. Del Vecchio (1), D. Tesauro (2), S. De Luca (2), A. Brunetti (3), S. Aime (4), G. Morelli (2), C. Pedone (2). (1) CNR-Centro Medicina Nucleare; (2) CNR -centro Biocristallografia; (3) Ist. di Radiologia, Università ; (4) Dip. di Chimica IFM, Università di Torino, Italy

Regulatory peptides and their analogs are being extensively investigated as radiopharmaceuticals for cancer imaging. Receptors of the cholecystokinin (CCK) family have been shown to be overexpressed in different types of neuroendocrine tumors.
Aim. To evaluate the binding properties of the CCK8 peptide tagged with a DTPA-like derivative (DLD) and test whether the 111In-labeled conjugate (111In-DLD-CCK8) is suitable for receptor imaging.
Methods. CCK8 was synthesized by solid-phase technique and covalently coupled to DLD through its amino terminus. The compound was subsequently released from the support by acid treatment and labeled with 111In-Citrate. Thin layer chromatography was performed to assess radiochemical purity. Saturation and competitive binding assays were performed on NIH-3T3 cells stably transfected with a cDNA encoding for the human CCK-B type receptor (NIH-3T3/CCK-BR) and wild type NIH-3T3 cells. The binding parameters, Bmax and Kd, were determined using the GraphPAD Inplot program. To test receptor internalization upon binding of the ligand, parallel binding experiments were performed at 4°C and 37°C. After 90 min incubation, surface bound peptide was removed by a 5 min. acid treatment. Stability was assessed by incubation of 111In-DLD-CCK8 with human serum for 24 h at 37°C followed by FPLC analysis.
Results. 111In-labeling efficiency of DLD-CCK8 conjugate and radiochemical purity of the labeled compound exceeded 97%. The binding of 111In-DLD-CCK8 to receptor negative wild-type NIH-3T3 cells was unsaturable and the amount of bound radioactivity was negligible even at the highest concentration of labeled compound. The specific binding of the radiolabeled peptide to NIH-3T3/CCK-BR was saturable and 25-fold higher compared to receptor negative cells. Scatchard analysis of experimental data obtained by NIH-3T3/CCK-BR cells at 4°C showed a Bmax of 4.1±0.33E5 sites/cell and an apparent Kd in the nanomolar range. The specific binding determined at 37°C was two-fold higher as compared to that obtained at 4°C. Acid treatment reduced specific surface bound radioactivity by 80% in cells assayed at 4°C whereas less than 30% decrease was observed in cells incubated at 37°C, suggesting internalization of the receptor/ligand complex. After 24 h incubation of 111In-DLD-CCK8 with serum, less than 5% of total activity added was found to be associated with high molecular weight proteins.
Conclusion. 111In-labeled DLD-CCK-8 peptide showed high specific binding to CCK-B receptor, high target-to-non target ratios and optimal stability in serum indicating that it can be suitable for receptor imaging.

OS_235

99MTC LABELED [TYR3]OCTREOTATE TETRAMINE-MODIFIED ANALOGS CONTAINING ASP LINKERS: EFFECTS ON AFFINITY, TISSUE DISTRIBUTION AND TUMOR UPTAKE IN ANIMAL MODELS

T. Maina (1), A. Nikolopoulou (1), B. Nock (1), C. Tsipra (1), P. Sotiriou (2), V. Magafa (2), D. Maidas (3), P. Cordopatis (2), E. Chiotellis (1).
(1) Institute of Radioisotopes - Radiodiagnostic Products, NCSR ;
(2) Department of Pharmacy, University of Patras, Patras, Greece;
(3) Institute for Isotopic Studies, Athens, Greece.

The search for somatostatin (SMS) receptor-specific agents has identified so far several radiolabeled octreotide analogs useful for the effective detection or treatment of SMS-positive neoplasms. In a previous study, we have reported on some ^{99m}Tc labeled N4-functionalized [Tyr^3]octreotate analogs showing promising biological characteristics for clinical application. With the purpose of further increasing radioligand hydrophilicity, and thereby clearance, we report herein on two additional [Tyr^3]octreotate analogs carrying Asp spacer(s) between the N4 ligand and the peptide chain. The effects of these modifications on the affinity and in vivo properties of novel compounds are discussed.
Methods: The N4-Asp-[Tyr^3]octreotate, **1**, and N4-Asp-Asp-[Tyr^3]octreotate, **2**, were synthesized by SPPS techniques. Labeling with ^{99m}Tc proceeded in alkaline medium using $SnCl_2$ in the presence of citrate. The affinity of new peptides for the SMS receptors was tested by competition binding experiments in rat cortex and AR42J cell membrane homogenates. Biodistribution of ^{99m}Tc **1** and **2** was initially performed in healthy mice and later on in tumor bearing athymic mice. The experimental tumor was grown in their flanks after subcutaneous injection of a AR42J cell suspension 10-15 days prior to the biodistribution experiment. Receptor blocking experiments were conducted by injection of 100 μg [Tyr^3]octreotate together with the radioligand.
Results: The binding capabilities of **1** and **2** for the SMS receptor were found increasingly affected by progressive introduction of Asp linkers both in AR42J (respective IC_{50}s: 0.45 and 2.3 nM; for [Tyr^3]octreotate 0.32 nM) and in rat cortex membranes (respective IC_{50}s: 0.56 and 6.2 nM; for [Tyr^3]octreotate 0.30 nM). As shown by HPLC, labeling with ^{99m}Tc was quantitative with ^{99m}Tc **2** showing a more hydrophilic profile than ^{99m}Tc **1**. Both ^{99m}Tc **1** and **2** washed out rapidly from all non-target tissues into the urine via the kidneys. While specific uptake in the pancreas and adrenals decreased from ^{99m}Tc **1** to **2** in healthy mice, an equally high tumor specific uptake of 23-25 %ID/g at 1 h pi for ^{99m}Tc **1** and **2** was observed. This discrepancy may be related to a different SMS receptor subtype(s) occurrence in normal and neoplastic tissue.
Conclusions: The rapid body wash out and the specific fast localization of ^{99m}Tc **1** and **2** in AR42J tumor cells validate these two agents as candidates for the scintigraphic localization of SMS-positive tumors in patients.

OS_236

IMAGE FUSION OF COMPUTED TOMOGRAPHY AND SOMATOSTATIN-RECEPTOR-SCINTIGRAPHY AND ITS DIAGNOSTIC VALUE FOR THE LOCALIZATION OF NEUROENDOCRINE TUMORS

H. Amthauer (1), N. Hosten (1), A.J. Lemke (1), M. Gutberlet (1), J. Ruf (1), B. Wiedenmann (2), R. Felix (1). (1) Klinik für Strahlenheilkunde; (2) Medizinische Klinik m.S. Hepatologie und Gastroenterologie, Charité Campus Virchow-Klinikum, Berlin, Deutschland.

This study assessed the informational value of fused images gained from computed tomography (CT) and somatostatin-receptor-scintigraphy (SRS) for the preoperative diagnosis and localization of metastasized neuroendocrine tumors of the gastrointestinal tract and the pancreas.
Methods: 21 patients with metastasized neuroendocrine tumors were included in this study. In 12 cases, the primary tumor was located in the gastrointestinal tract, the other 9 patients had a primary lesion of the pancreas. All patients received CT -and SRS-scans, whose data was used in the consecutive image fusion. Image fusion was performed on an AVS platform (Advanced Visualization System, Neuss, Germany) by a custom-made software developed at our department. The actual voxel-based data registration was carried out by the method of "normalized mutual information". The next step was a comparison of the topographic accuracy between SRS- and CT-scans interpreted separately and their consecutively fused image. Therefore, all findings were grouped into 59 anatomical regions. Areas with increased activity (segments of the liver/lymph-node metastases/organ metastases) were consecutively ranked on a scale from 1 to 5 by two independent observers (from "1: no topographic assignment possible" to "5: unambiguous topographic assignment"). Histological verification of image-diagnosed findings followed in 12 patients after resection of the tumor, in 9 patients after needle-biopsy.
Results: Compared to SRS alone, CT/SRS Image showed an improved topographic assignment in 29,5% of the lesions in all 21 patients. In 7/12 operated patients (12/26 lesions), this enhanced accuracy relevantly influenced the therapeutic approach (localization of an involved liver segment: n=6, differentiation between nodal and organ metastases: n=3, verification of multifocal pancreatic metastases: n=2, verification of splenic infiltration: n=1). The median value for accurate topographic assignment of all lesions was significantly higher in fused CT/SRS images compared to the sole use of CT- and SRS-scans without image fusion (Observer A: 4,5 vs. 3,3, observer B: 4,4 vs. 3,8. Chi square: $p > 0,05$).
Conclusion: CT/SRS Image fusion improves the topographic assignment of pathologic SRS findings in patients with neuroendocrine tumors. As a consequence, the use of the above presented method had a relevant impact on further therapeutic procedures in one third of all patients examined.

OS_237

CHOLECYSTOKININ(CCK)–B/GASTRIN-RECEPTOR BINDING PEPTIDES FOR DIAGNOSIS AND THERAPY OF METASTATIC MEDULLARY THYROID CANCER

T.M. Behr (1), M. Behe (1), M. Gotthardt (1), C. Angerstein (2), A. Heufelder (3), W. Becker (2). (1) Dept. of Nuclear Medicine, Philipps-University, Marburg, Germany; (2) Dept. of Nuclear Medicine, Georg-August-University, Göttingen, Germany; (3) Dept. of Endocrinology, Philipps-University, Marburg, Germany.

Aim: In medullary thyroid cancer (MTC), elevated calcitonin levels may indicate metastatic disease although all diagnostic modalities fail in its localization (occult disease). On the other hand, patients with advanced metastatic disease are left with few therapeutic options. We have developed radiopeptides with high affinity to the CCK-B receptor expressed on more than 95% of MTCs. The aim of this study was to investigate their role in the staging and therapy of MTC.

Methods: Forty-five patients with metastatic MTC were investigated. All had undergone ultrasonography, whole-body CT and MRI, bone scanning and somatostatin receptor scintigraphy. As a result, 23 suffered of known, 22 of occult disease. CCK-B receptor scintigraphy was performed with 5-7 mCi of ^{111}In-labeled DTPA-*D*-Glu^1-minigastrin. Eight of these patients with advanced metastatic disease were injected with potentially therapeutic doses of a ^{90}Y-labeled derivative at 4-6-weekly intervals (30-50 mCi/m^2 per injection for a maximum of 6 injections).

Results: The normal organ uptake was confined to the stomach as a result of CCK-B specific binding, and to the kidneys as excretory organs. All tumor manifestations known from conventional imaging were visualized as early as 1 h p.i., with increasing tumor-to-background ratios over time; at least one lesion was detected in 20/22 patients with occult disease (patient-based sensitivity 91%; 9 of them surgically confirmed, 11 remaining unconfirmed positive). Among them were local recurrences, lymph node, pulmonary, hepatic, splenic and bone metastases. Three patients treated with the ^{90}Y derivative at 30 mCi/m^2 per injection did not show any signs of toxicity, whereas all 3 patients treated at 40 mCi/m^2 developed transient hematologic toxicity. One of 2 patients treated at the 50 mCi/m^2 level developed transient grade-4 thrombocytopenia and grade-1 nephrotoxicity. This patient experienced a partial remission, a second patient a minor response, 4 stabilization of their previously rapidly progressing disease.

Conclusions: These data suggest that CCK-B receptor ligands are a promising new class of receptor binding peptides for the staging and therapy of MTC.

OS_238

ABSENCE OF THERAPEUTIC EFFICACY OF THE SOMATOSTATIN ANALOGUE LANREOTIDE IN ADVANCED BILIARY TRACT CANCER IN SPITE OF SOMATOSTATIN RECEPTOR EXPRESSION IN VIVO

T. Traub (1), W.C.C. Fiebiger (2), W. Scheithauer (2), A. Kurtaran (1), C. Gedlicka (2), G.V. Kornek (2), R. Dudczak (1), M. Raderer (2), I. Virgolini (1). (1) Deptartment of Nuclear Medicine; (2) Deptartment of Oncology, University of Vienna, Austria.

Carcinoma of the biliary system is a rare tumour entity, and patients with advanced disease face a dismal prognosis. Because of the absence of standard chemotherapy for advanced biliary caracinoma and reports of expression of receptors for somatostatin (SST), we have performed a phase II study to evaluate the clinical potential of the long acting SST-analogue lanreotide (LAN) for treatment of this disease.

Methods: Twenty consecutive patients with histologically verified cholangiocellular or gallbladder cancer were enrolled in the study. Before initiation of therapy, SST-receptor scintigraphy using ^{111}In-DOTA-LAN was carried out in 8 patients to check for in vivo expression of SST-receptors. Thirty mg of a slow release formulation of LAN were administered by deep intramuscular injection every two weeks until progression or patients wish to withdraw. Restaging by means of computed tomography was performed every eight weeks, and response was assessed according to WHO standard criteria. In addition, weight, performance status, analgesic intake and subjective pain perception were recorded every four weeks along with evaluation of tumor markers CEA and Ca 19-9.

Results: Tumor sites were visualized by means of ^{111}In-DOTA-LAN in all 8 patients. A total of 161 injections were administered, the median number per patient being 5 (range; 2 – 36). Side effects were generally mild, only two patients complained of mild nausea and one patient had meteorism attributed to therapy. Therapeutic results, however, were disappointing, with only one patient demonstrating complete remission (CR), which lasted for 18 months before diagnosis of recurrence. Four patients had stable disease (SD) lasting between 3.5 – 9 + months accompanied by weight gain and improvement in performance status in two cases, while the remaining 15 patients progressed during therapy. The median time to progression was 2.5 months (range; 1 – 18), and the median survival was 4.5 months (range; 1.5 – 18+ months). No clear cut correlation between scan result and therapeutic outcome could be demonstrated, as not only the patient with CR and two with SD, but also 5 patients with progressive disease had a positive scan result.

Conclusion: Our data show that gallbladder and cholangiocellular carcinoma express SST-receptors in vivo as judged by ^{111}In-DOTA-LAN scintigraphy. In spite of this fact, LAN did not display therapeutic activity in this study.

CARDIOVASCULAR

OS_239

TRANSIENT LEFT VENTRICULAR DILATION DURING MYOCARDIAL PERFUSION GATED-SPECT IN HYPERTENSIVE PATIENTS

A. Bestetti, C. Di Leo, A. Alessi, L. Tagliabue, G.L. Tarolo. Department of Nuclear Medicine, University of Milan- HSPaolo, Milan, Italy.

Background. The apparent dilation of the left ventricular cavity on myocardial perfusion imaging in the presence of extensive epicardial vessel stenosis has been referred to as transient ischemic dilation. Transient ischemic LV cavity dilation during stress myocardial perfusion imaging has become a generally accepted marker of severe extensive myocardial ischemia. The aim of the study was to assess whether there may be other causes of ischemic dilation of the left ventricle in the absence of a significant post-stress perfusion defects. Methods: 672 patients (mean age: 62.3; range 29-86 yrs.) underwent conventional diagnostic two-day stress/rest gated SPECT with 99mTc-tetrofosmin: 607 patients (mean age: 62.5 yrs., range: 34-86 yrs.) had known or suspected CAD, while 65 (mean age: 60 yrs, range: 29-80 yrs.) had low pre-test likelihood of CAD (<10%), a normal post-stress perfusion scan and no hypertension. Fifty three percent of CAD patients had a history of MI. Perfusion was analyzed on ungated images using 20 segments scored on a 5-point scale. LVEF and volumes were calculated using an automatic algorithm (QGS). The post-stress and rest ratio was determined for end-systolic volume (ESV-ratio). Results: In the control group, the mean value of ESV ratio was 1.01 ± 0.12. The best threshold for transient dilation ratio abnormality was the mean value plus two standard deviations obtained in the control group, or a ESV-ratio > 1.25. LVEF as well as volumes, were not significantly different in the post-stress and rest status or using physical or pharmacological stress. Seventy seven of 607 CAD patients (12%) showed a ESV-ratio > 1.25. This last group was further divided according to the value of summed stress score (SSS) into two subgroups: a) patients with normal perfusion (SSS ≤4) (15 patients); b) patients with perfusion defects (SSS >4) (62 patients). Seven of 15 patients with normal perfusion (46%) were hypertensive and four had non ischemic dilated cardiomyopaty (no coronary artery stenosis). Conclusions: transient ischemic dilation is not a specific marker for severe coronary artery disease in a population with a high prevalence of hypertensive or dilated heart disease.

OS_240

EJECTION FRACTION EVALUATION BY GATED MYOCARDIAL PERFUSION SPECT : COMPARISON BETWEEN GATED SPECT QUANTIFICATION (GSQ) AND EMORY CARDIAC TOOL BOX (ECTB)

M.R. Boussaha, G. Storto, C. Antonescu, A. Bischof Delaloye. Department of nuclear medicine, CHUV University Hospital, Lausanne, Switzerland.

AIM : To retrospectively compare the results of two semi-automated methods for the evaluation of left ventricular ejection fraction (LVEF) in patients with suspected coronary artery disease (CAD) by gated myocardial perfusion SPECT (MPS).

METHODS: 164 consecutive patients (women 61, men 104, age 61,1 ±11y) with suspected CAD underwent gated myocardial perfusion SPECT. 81 studies were performed with Tl-201 (111 MBq), 29 with one day protocol Tc-99m Sestamibi (740 MBq) and 55 using a dual-isotope protocol. Images were acquired with a 180° angle on a dual-head camera (Siemens E.-Cam ; LEHR collimator) and processed by filtered back projection (Butterworth; cut-off 0,55; order 5; 8 images/cycle). Rest LVEF, end-diastolic volume (EDV) and end-systolic volume (ESV) were computed using GSQ (Germano et al, 1995) and ECTB (Garcia et al, 1990). Statistical analysis was performed using a Student's t-test with a significance level of ($p<0.01$). Patients were stratified according to myocardial perfusion patterns assessed on short axis, vertical and horizontal long axis MPS by 3 operators and corroborated with clinical, echocardiographic and angiographic data. In 15 patients LVEF was measured by angiography.

RESULTS : 56 patients had normal perfusion, 54 were judged mild-moderately and 27 severely ischemic, while 28 presented myocardial infarction without associated ischemia.

	LVEF		EDV		ESV	
	GSQ	ECTB	GSQ	ECTB	GSQ	ECTB
Normal	63,7±7	74,8±8	67,2±23	96,3±36	25,3±12	25,0±14
Mild-moderate ischemia	55,1±5	65,8±7	82,2±22	107,5±30	37,5±12	37,2±13
Severe ischemia	45,6±6	55,5±6	122±41	159,1±55	70,3±35	69,8±28
Myocardial infarct	41,9±19	52,7±13	106,7±46	145,4±53	66,3±37	72,2±43

Significant differences were systematically found for the LVEF and EDV values ($p<0.0001$) in all sub-groups with GSQ< ECTB, whereas ESV were not different ($p=0.63$). When the LVEF values of the two methods (GSQ = 42,7±11 and ECTB =52,3±14) were compared with angiography (51,4±14 ; range 27-72%) the results matched with those obtained by ECTB ($p=0.77$) while GSQ values were significantly lower ($p<0.01$).

CONCLUSION : In comparison with ECTB, functional data obtained by GSQ showed significantly lower values for LVEF and EDV, whereas ESV were the same. The differences were observed in normal and all degrees of abnormal MPS. LVEF obtained by ECTB matched with angiography whereas those measured by GSQ were systematically lower.

OS_241

EVALUATION OF THE ROBUSTNESS OF THE 'GERMANO' SOFTWARE FOR GATED SPECT ANALYSIS

J.J.J. Borm (1), Y.G.C.J. America (1), N. Groen (1), E.E. van der Wall (2), E.K.J. Pauwels (1). (1) Nuclear Medicine; (2) Cardiology, LUMC, Leiden, The Netherlands.

Aim: To evaluate claims regarding excellent reproducebility for left ventricle ejection fraction [EF], end-disastolic left ventricular volume [EDV] and regional wall motion score [RWM] for the 'Germano' software for gated SPECT analysis.
Background: The operator dependency regarding the selection of the volume containing the left ventricle and its re-orientation was not documented in literature.
Methods: -1- Gated SPECT using 500 MBq 99m-technetium tetrofosmin. Acquisition with a triple-headed camera; acquisition time 35" per frame, 90 frames, 64x64 matrix, 16 bins. -2- The Germano algorithm was reviewed in detail and potential weaknesses were identified. -3- A series of specific patterns of defects and artifacts were defined; for example: large apical defect, or extensive inferior wall defect combined with extensive amounts of activity just below the diaphragm. For each pattern typical cases were selected and used as so-called prototypes for further analysis. -4- The effects of variation of choices made by the operator, to define and re-orient the volume containing the left ventricucle were systematically evaluated. Evaluations included systematically changing the number and position of selected slices [vertical direction, septum - lateral direction], orientation [in the sagital and transversal plane]. Once the sub-space containing the left ventricle was defined, the software was used without further operator interventions. Results were expressed as a coefficient of variation [COV]. It was visually verified that the entire left ventricle remained within the operator-defined subspace.
Results: To date, two prototypes are fully evaluated: -type A: large apical defect with extensive activity below the diaphragm; -type B: large defect of septum extending into the apical area. For changes in size and position in the vertical direction, the COV for all parameters was below 5%; for changes in septum-to-lateral direction, the COV for regional wall motion scores exceeded 20% in some segments in prototype A. Changes in the re-orientation [rotation, 5-degree steps] also resulted in COV's exceeding 5% in some segments in both prototypes. COV for global parameters remained below 8%. Repeated reconstructions, but with constant width and angles for slice selection and re-orientation, showed COV's below 5% for EF and EDV, versus COV's up to 20% for RWM scores.
Conclusions: Estimates for ejection fraction and end diastolic volume are robust, but estimates for regional wall motion show considerable operator dependency.

OS_242

DETECTION OF STRESS-TEST INDUCED LEFT VENTRICULAR WALL MOTION ABNORMALITIES USING LOW-DOSE THALLIUM GATED SPECT AND ITERATIVE RECONSTRUCTION

Z. Jurasinovic, S. Tezak, R. Petrovic. Clinical Department of Nuclear Medicine and Radiation Protection, University Hospital Zagreb, Zagreb, Croatia.

The aim of our study was to investigate the feasebiliy and usefulness of low-dose thallium gated SPECT in patients who come to our
Methods: We studied 41 consecutive patients (28 male, 13 female, age 38-76, median age 57) with suspected or known coronary artery disease. Stress thallium gated SPECT was performed with a tripple-head gamma camera 10 minutes after stress-test (either bicycle exertion or dipyridamol) and injection of 74 MBq Tl-201, followed by redistribution study after 4 hours in 39 patients. Two patients underwent rest-redistribution viability study with the same imaging protocol. Images were reconstructed using iterative algorithm
(OS ML-EM, offset 0 cm, 2 iterations) and post-reconstruction filtering with Butterworth filter (order 5, Nyquist cutoff frequencies from 0.19 to 0.26). Ungated images were reconstructed with standard filtered backprojection using commercially available software.
Results: It was possible to distinguish attenuation from perfusion defects in 22 patients (23 attenuation defects overall, 18 situated in inferior and 5 in anterior left ventricular wall) by evidencing wall thickening in gated SPECT images.
In order to analyse stress induced regional wall motion abnormalities we divided left ventricular myocardium in nine segments: anterior, lateral, inferior and septal wall were divided in proximal and distal part, while apex formed the ninth segment. Nine patients had normal both perfusion and wall motion study. In 56 out of 369 segments reversible (ischaemic) defects were found, while 33 perfusion defects showed no sign of redistribution (scarring). In 46 out of 56 ischaemic defect (82%) we found evidence of wall motion abnormalities (hypo-, dys- or akinezia). The same motion abnormalities were found in 31 (94%) out of 33 irreversible perfusion defects.
Conclusion: unlike gated SPECT with technetium-labelled agents, thallium gated SPECT is performed immediately after stress-testing thus enabling the detection of regional left ventricular wall motion abnormalities in addition to myocardial perfusion imaging alone, which could improve patient management in cases of coronary artery disease.

OS_243

LVEF MEASURED WITH GATED MYOCARDIAL SPECT 3 HRS AFTER 99MTC-TETROFOSMIN ADMINISTRATION AT PEAK EXERCISE

A. Tarkowska, W. Cholewinski, B. Stefaniak, A. Olesiuk, E. Poniatowicz-Frasunek, B. Chrapko, P. Maj. Department of Nuclear Medicine, Medical University, Lublin, Poland.

Our earlier observations revealed that in about 60% of pts with coronary artery disease (CAD), LVEF measured with gated myocardial SPECT (gSPECT) 1 hr after tetrofosmin injection at peak exercise was significantly lower than at rest.The aim of this study was to check whether the above decrease of LVEF persists as long as 3 hrs post radiotracer injection during stress.
Methods: The study population comprised 20 pts with CAD, confirmed by coronary angiography. All subjects underwent gSPECT 1 hr after 99mTc-tetrofosmin administration at rest (R-gSPECT) and, on the next day, 1 hr and 3hrs after tetrofosmin injection at peak exercise (respectively, S1-gSPECT and S3-gSPECT). In each of the above examinations data acquisition was performed using a double-head camera, over a 180° circular orbit, with 8 sequences/cardiac cycle. The method of Germano et al was applied to calculate LVEF.
Results: LVEF measured with S3-gSPECT (S3-EF) amounted to 47.0±8.6% and was significantly lower than EF calculated from R-gSPECT (R-EF)(52.0±8.8%; $p<0.001$) and from S1-gSPECT (S1-EF)(50.9±8.3%; $p<0.001$). In relation to R-EF, decreased values of S3-EF LVEF were observed in 16/20 pts. In 14 out of these subjects LVEF measured with S3-gSPECT was lower than that with S1-gSPECT; in one case both values were similar and in one subject S3-EF was a little higher than S1-EF. In 4/20 pts no differences were observed between EF values obtained with R-gSPECT, S1-gSPECT and S3-gSPECT. No relationship was found between changes of LVEF occuring after administration of tetrofosmin at peak exercise on one hand and heart rates during data acquisitions, heart rate at peak exercise, as well as degree of applied load and work performed during physical stress on the other.
Conclusion: In majority of pts with CAD decrease of LVEF measured by gated myocardial SPECT under stress conditions persists during 3 hrs after termination of physical exercise. Further studies are necessary to identify mechanisms responsible for this phenomenon. However, the more pronounced reduction of LVEF observed 3 hrs after stress than after 1 hr suggests that in pts with ischaemic heart disease the physical exercise may result in impairement of LV function which may tend to intensify during several hours.

OS_244

INFLUENCE OF VENTRICLE SIZE ON THE RESULTS OF LEFT VENTRICULAR EJECTION FRACTION FOUND BY QUANTITATIVE GATED SPECT

A. Kelles (1), P. Martin (1), E. Tran-ngoc (2), B. Peperstraete (2), J. Paternot (1), R. Gheldof (1), P. Decoodt (2), M. Verhas (1). (1) Department of Nuclear Medicine, CHU Brugmann, Brussels, Belgium; (2) Department of Cardiology, CHU Brugmann, BRUSSELS, Belgium.

In 108 patients (67± 12 y), the ejection fraction (LVEF) calculated by automated Quantitative Gated SPECT (QGS), according to Germano et al., was compared to that determined by Equilibrium Radionuclide Angiography (ERA).
Methods. ERA was performed after IV injection of 5 mg cold Ppi followed by 740 MBq ^{99m}Tc, using a single head Siemens camera equipped to detect cardiac cycle. Within the same week, after injection of 99mTcMIBI, a QGS-EF was performed with a Multispect Siemens tomocamera (8 frames/cycle, 3 x 32 projections, 40 sec each). Largest diameter (d) of non gated coronal slices was measured as an index of LV size.
Results. The interobserver reproducibility calculated by QGS and ERA was high (QGS: $r= 0.96$, $p<0.0001$, ERA: $r=0.89$, $p< 0.0001$). A linear relationship could describe the relation between LVEF determined by QGS and ERA (QGS-EF= 1.71 + 0.98 ERA-EF, $r=0.66$, $p<0.0001$). For the whole group, the Bland-Altmann trend graph demonstrated a positive regression slope of 0.42 and an intercept at −18.47 {QGS-ERA= -18.47 + 0.42 (QGS + ERA)/2 }. An underestimation of QGS for the lower EF was indicated by the negative intercept. The positive regression slope demonstrates an overestimation of the QGS for the higher EF. We therefore analyzed possible influence of LV size on both methods and found different relationships: QGS EF = 186 − 101 x d (cm) + 13.5 d^2 (cm^2) ($r=0.82$) and ERA EF = 29 + 48 x d (cm) - 21 d^2 (cm^2) ($r=0.72$). When a theoretical EF for 17 LV size values was calculated by each method, an exponential relation was found between QGS and ERA-EF: QGS-EF = 7 x $e^{(0.04 * ERA\text{-}EF)}$, ($r= 0.9$). These results confirm previous observations that as a mean, QGS-EF found in women are higher than in men (in the present study 7%).
Conclusion: QGS provides a highly reproducible estimate of LVEF. However, QGS seems to be affected by the diameter of the left ventricle. In very small and very large ventricles the edge detection might not be ideal, thereby overestimating dilated ventricles and underestimating small ventricles.

OS_245

USEFULNESS OF A SKELETON TO ASSESS REGIONAL MYOCARDIAL WALL MOTION BY TC-99M MIBI ECG-GATED SPECT

C. Thouly (1), D. Mestas (1), J. Lipiecki (2), J.Y. Boire (3), F. Cachin (1), K. Massaloux (1), T. Nguyen (4), J. Maublant (1). (1) Department of Nuclear Medecine, Centre Jean Perrin, Clermont Ferrand, France. ; (2) Department of Cardiology, Centre Hospitalier Regional Universitaire, Clermont-Ferrand, France; (3) Erim, Faculty of Medecine, Clermont Ferrand, France; (4) General Electric Sopha Medical Vision International

Objectives : Gated single photon emission computed tomography (GSPECT) has been extensively used to assess global left ventricular (LV) function, but there are very few reports regarding its value for assessment of regional wall motion (WM). Endocardial wall determination remains subject to a part approximation. Since the homotopic skeleton of the LV can be more easily defined in GSPECT, we evaluated its usefulness in assessing the LV WM.
Methods : 23 patients with a myocardial infarction underwent within a week biplane contrast angiography (CA) (reference method) and ^{99m}Tc -MIBI GSPECT with 16 frames per cycle. The LV skeleton, i.e., a one-pixel thick central surface, was generated for each frame. In order to compare WM on similar sections in CA and in GSPECT, only the middle vertical and short axis views were analyzed. WM was read independently with the three modalities (CA, skeleton and myocardium) as well as in another set of views on which the skeleton was superimposed to the myocardium. The WM score ranged from 0 (normal) to 3 (dyskinetic) and a 7-segment model was used. WM was read blindly by two observers and a consensus was reached when necessary.
Results : 15 of the 161 segments were not interpretable by GSPECT because of a lack of myocardial activity. In the remaining segments, the precise agreement between GSPECT and CA endocardial WM was only fair 60 % (K=0.35) but the agreement for +/-1 WM score unit was excellent 96% (K=0.90). Most of the discrepancies were due to segments scored as hypokinetic in GSPECT and normal or akinetic in CA. The overall and +/- 1 WM score unit agreement between GSPECT endocardial WM and skeleton motion was good (85%, K=0.75) and excellent (95%, K=0.90), respectively. A high correlation was observed (r=0.95, y=0.83x+1.72). The chi-square test showed no difference between GSPECT endocardial WM and skeleton motion.
Conclusion : Skeleton motion analysis is of similar value than endocardial WM analysis in GSPECT. This non equivocal geometric landmark of the myocardium could be used to evaluate WM in GSPECT.

OS_246

LEFT VENTRICULAR EJECTION FRACTION MEASURED WITH 201-TL MYOCARDIAL GATED SPECT : FACTORS AFFECTING ITS VARIABILITY

D. Daou (1), C. Coaguila (1), B.O. Helal (1), T. Fourme (2), I. Carel (2), R. Lebtahi (3), M. Faraggi (3), M. Slama (2), D. Le Guludec (3). (1) Department of Nuclear Medicine, Antoine Beclere Hospital, AP-HP, Clamart, France; (2) Cardiology Department, Antoine Beclere Hospital, AP-HP, Clamart, France; (3) Department of Nuclear Medicine, Bichat Hospital, AP-HP, Clamart, France.

Aim: Coupling myocardial perfusion to function in a single acquisition is interesting. Previous studies reported the use of myocardial perfusion ^{201}Tl ECG-gated SPECT (GSPECT) for this objective and reported good correlation between left ventricular ejection fraction (LVEF) measured with ^{201}Tl GSPECT versus other modalities. We aimed to define the factors that may influence the variability of LVEF measured with GSPECT.
Methods: Sixty-nine patients with CAD had rest ^{201}Tl GSPECT (8 frames/RR). Planar left anterior oblique (LAO) rest radionuclide angiography was acquired on the same day and processed at 8 frames/RR (gold-standard). The LVEF was also calculated on ^{201}Tl GSPECT with the Cedars-Sinai (QGS) and the MultiDim software (MD). The random error (RE) for QGS and MD-LVEF were calculated after correction for systematic error (as defined by the linear correlation between QGS-LVEF and MD-LVEF versus LAO-LVEF). The correlation between LVEF-RE for QGS and MD versus other reported variables were studied with univariate analysis and forced into multivariate analysis: LAO-LVEF, abdominal uptake superimposed on myocardial activity (visually estimated), myocardial ^{201}Tl counts, distance scan, rest myocardial visual score (from 0=normal to 4=absent uptake), previous myocardial infarction.
Results: On univariate analysis, LVEF-RE with QGS and MD were correlated to LAO-LVEF (r=0.6, p=0.0001 for both). The LVEF-RE with QGS (but not with MD) was also correlated to myocardial count statistics (r= -0.3; p=0.017). All the other above reported factors were not correlated to the LVEF-RE with QGS and MD. On multivariate analysis, the QGS-LVEF-RE (r=0.74; p=0.0001) was correlated positively to LAO-LVEF (p=0.0001) and abdominal ^{201}Tl uptake (p=0.016) and negatively to myocardial counts (p=0.005); and MD-LVEF-RE (r=7;p=0.0001) was correlated positively to LAO-LVEF (p=0.0001) and abdominal ^{201}Tl uptake (p=0.013).
Conclusion: With ^{201}Tl GBPS, QGS and MD LVEF are influenced by LAO-LVEF and abdominal ^{201}Tl uptake. QGS as opposed to MD is influenced by myocardial count statistics.

RADIONUCLIDE THERAPY / DOSIMETRY

OS_247

INTRAPATIENT COMPARISON BETWEEN OCTREOSCAN111 AND OCTREOTHER DOSIMETRY: POTENTIAL EFFECTIVENESS AND SAFETY

R. Barone (1), S. Walrand (1), F. Jamar (1), J. De Camps (1), L.K. Kvols (2), E.P. Krenning (3), C. Smith (4), S. Pauwels (1). (1) Department of Nuclear Medicine, Université Catholique de Louvain, Brussels, Belgium; (2) Lee Moffitt Cancer Center, University of South Florida, Tampa, FL, USA; (3) Department of Nuclear Medicine, University Hospital Dijkzigt, Rotterdam, The Netherlands; (4) Novartis Pharmaceutical Corporation, East Hanover, NJ, USA

Aim: Octreother (^{90}Y-DOTA-Tyr$_3$-octreotide) and OctreoScan111 (^{111}In-DTPA-octreotide) are used for peptide targeted radiotherapy of somatostatin receptors positive tumors. We estimated in the same patient OctreoScan111 and Octreother dosimetry in order to compare their potential effectiveness (tumor dose) and safety (kidney and red marrow). Octreother dosimetry was measured using PET and ^{86}Y-Octreother.
Methods Six patients with neuroendocrine tumors underwent quantitative OctreoScan111 SPECT and ^{86}Y-Octreother PET scan at 24 h and 48 h at 1 week interval. All studies were performed with coinfusion of amino acids for renal protection. PET and SPECT were reconstructed using iterative algorithms, incorporating attenuation and scatter corrections. Tissue uptakes (ID%) were calculated and used to compute mean residence times (MRT). Doses to tissues were further estimated using MIRDOSE 3.0 software.
Results Mean Octreother kidney, red marrow and tumor exposure were significantly higher compared to OctreoScan111 (1.9±0.5 *vs* 0.15±0.04 mGy/MBq; 0.28±0.13 *vs* 0.04±0.01 mGy/MBq and 3.5±2.4 *vs* 0.12±0.1 mGy/MBq respectively; p<0.01). Tumor to kidney and tumor to red marrow dosimetry ratios were higher for Octreother compared to OctreoScan111 (1.6 *vs* 0.8 p= 0.07; 12 *vs* 3 p<0.0001 respectively). We estimated in each patient the maximal allowed dose (MAD) as the dose delivering 23 Gy to the kidneys and for this dose tumor and red marrow dosimetry were computed. Mean tumor irradiation estimated for the MAD was higher with Octreother compared to OctreoScan111 (45.1±34.9 *vs* 21.4±15.5 Gy; p< 0.001), conversely, mean red marrow exposure was lower for Octreother (3.6±2 Gy *vs*; 7.1±2.2 Gy p<0.001).
Conclusions: Octreother has a better dosimetry profile with more favourable tumor to target organs than with OctreoScan111.

OS_248

SAFETY AND EFFICACY OF [Y-90-DOTA,TYR(3)]-OCTREOTIDE (Y-90-SMT487; OCTREOTHER) PEPTIDE RECEPTOR RADIONUCLIDE THERAPY (PRRT). PRELIMINARY RESULTS OF A PHASE-1 STUDY

R. Valkema (1), F. Jamar (2), W.H. Bakker (1), J. Norenberg (3), C. Smith (4), B. Stolz (4), L. Kvols (3), S. Pauwels (2), E.P. Krenning (1). (1) Department of Nuclear Medicine, Erasmus University Medical Centre, Rotterdam, The Netherlands; (2) Department of Nuclear Medicine, Universite Catholique Louvain, Brussels, Belgium; (3) Moffitt Cancer Center, Tampa, FL, USA and University of New Mexico, Albuquerque, NM, USA; (4) Novartis Pharma, East Hanover, NJ, USA

Aim. To define maximum tolerated single and 4-cycle doses of OctreoTher for PRRT in patients (pts) with advanced somatostatin receptor-positive tumours.
Methods. Presently, 42 pts (23 women, 19 men) are enrolled. 21 pts had carcinoid tumors, 10 islet cell carcinoma and 21 other neuroendocrine tumors. At baseline 34 pts were progressive, 8 had stable tumors. Before treatment, all pts underwent quantitative PET with ^{86}Y-SMT487, to predict renal exposure expected with ^{90}Y-SMT487. The cumulative radiation dose to kidneys was limited to 27Gy. Since i.v. amino acids (AA) were shown by ^{86}Y-SMT487 to reduce renal exposure, all pts received AA concomitant with OctreoTher. In 31 pts the intention was to give 4 cycles of escalating doses of 25, 50, 75 and 100 mCi/m^2 , repeated every 6 to 9 weeks. Pts received lower dose/cycle if the cohort dose would induce renal radiation exposure beyond this limit. In 11 pts escalating single doses of 100, 125, and 150 mCi/m^2 were given, but the number of additional cycles was limited by the renal exposure. The median follow-up is 15 months.
Results. Toxicity (tox): With cycle doses from 36 to 291 mCi and cumulative doses from 47 to 733 mCi, the maximum tolerable dose has not been reached. Three pts had dose-limiting tox: 1 liver tox grade-3, 1 thrombocytopenia grade-4, and 1 myelodysplastic syndrome (2 yr after start and previous chemotherapy). Renal tox was mild, 2 pts with grade-1 protenuria and 1 with grade 2 serum-creatinine. In 10 pts after 2 yr a 37% increase in serum-creatinine and a 16% to 18% decrease in creatinine clearance occurred. Hematology: 5 pts thrombocytopenia grade-3 and 1 grade-4 (5/6 pts had prior chemotherapy); 9 pts grade-2 and 6 grade-3 leukopenia, usually reversible; 9 pts grade-2 and 4 pts grade-3 anemia. Endocrine: no dysfunction of pituitary axes (thyroid, adrenal, gonadal), no diabetes mellitus; in men a >80% decrease in serum-inhibin-B with concurrent rise in serum-FSH suggested a negative effect on spermatogenesis.
Tumor responses: In 32 pts (planned dose given) 3 partial remission, 3 minor remission, 1 mixed response, 17 stable and 8 progressive. In 2/2 insulinoma and 1/1 gastrinoma pts, hormone values normalized. Sixteen pts had symptomatic improvement.
Conclusion. Renal toxicity is mild in OctreoTher therapy, with individualized (renal) dosimetry and coinfusion of protective AA. Prior chemotherapy predisposes to hematological toxicity. The antitumour effects and symptomatic improvement are most encouraging. Further studies with this promising agent are in progress.

OS_249

RECEPTOR-TARGETED RADIONUCLIDE THERAPY USING RADIO-LABELLED SOMATOSTATIN ANALOGUES: TUMOUR SIZE VERSUS CURABILITY

M. De Jong (1), W.A.P. Breeman (1), H.F. Bernard (1), W.H. Bakker (1), A. Van Gameren (1), J. Bugaj (2), J. Erion (2), A. Srinivasan (2), H.R. Maecke (3), E.P. Krenning (1). (1) Nuclear Medicine, Erasmus University Medical Center Rotterdam, The Netherlands; (2) Mallinckrodt Medical Inc., St Louis Mo, Usa; (3) Nuclear Medicine, Kantonspital Basel, Switzerland.

Aim: radionuclide therapy using somatostatin analogues labelled with the β-emitters Y-90 (high energy) or Lu-177 (low energy) is most promising. In rat models, we evaluated the therapeutic effects of different somatostatin analogues, [Y-90-DOTA,Tyr3]octreotide (DOTATOC) and [Lu-177-DOTA,Tyr3]octreotate (DOTATATE), currently used in clinical radionuclide therapy studies. Furthermore, we investigated the influence of tumour size on tumour response.

Methods: rats were bearing somatostatin receptor-positive CA20948 or AR42J tumours of different size (0.1 – 15 cm2) at therapy start. Rats received one or two (one week apart) iv injection(s) (277.5 - 555 MBq for Lu-177-DOTATATE; 370 MBq for Y-90-DOTATOC). Controls did not receive radioactivity. Rats were followed at least 150 days post therapy, the rat equivalent of the human 5-year survival.

Results: tumour responses appeared to be dependent on tumour size at therapy start in rats bearing CA20948 tumours. For Lu-177-DOTATATE a dose-response was found, leading in rats bearing small tumours (about 1 cm2) to 100% cure (555 MBq, estimated tumour dose 60 Gy). In rats bearing bigger tumours (mean 5 cm2) only 50% cure was reached after 555 MBq. This in accordance with a computer model (J Nucl Med 1995;36:1902) that calculated high tumour cure probability for Lu-177 in small tumours. Rats bearing AR42J tumours (higher uptake) also showed 100% cure after 555 MBq Lu-177-DOTATATE (tumour dose: 140 Gy). However, here the effects were independent of tumour size (100% cure in small-big tumours), so when the radiation dose to the tumour was high, Lu-177-DOTATATE could cure both small and larger tumours.

In contrast, injection with DOTATOC labelled with 370 MBq Y-90 (tumour dose: 60 Gy) resulted in 100% cure in medium-sized CA20948 tumours (mean 8 cm2), but not in tumours smaller than 1 cm2 (50% cure) or tumours bigger than 14 cm2 (0% cure). So, for Y-90-DOTATOC an optimal tumour cure size was found, also in accordance with the mentioned computer model. In smaller tumours part of the Y-90-radiation energy will not be absorbed in the tumour, whereas in very large tumours the increased number of clonogenic and probably hypoxic tumour cells explains the failure to reach cure.

Conclusion: this study shows the great promise of radionuclide therapy with Lu-177- and Y-90-labelled somatostatin analogues. It emphasises the concept that especially the combination of Y-90- and Lu-177-somatostatin analogues is most promising, to reach a wider tumour size region of high curability.

OS_250

90Y-DOTATOC RECEPTOR MEDIATED RADIOTHERAPY: A PHASE I STUDY

G. Paganelli (1), L. Bodei (1), M. Cremonesi (1), C. Grana (1), M. Bartolomei (1), L. Travaini (1), M. Fiorenza (1), H.R. Maecke (2), M. Chinol (1). (1) Nuclear Medicine and Medical Physics Divisions, European Institute of Oncology - Milano, Italy; (2) Institute of Radiochemistry, University Hospital - Basel, Switzerland .

High activities of ^{90}Y-DOTA-D-Phe^{1}-Tyr^{3}-Octreotide (DOTATOC) can be injected in patients (pts), affected by somatostatin receptor positive tumors, with low myelotoxicity. However, the predicted absorbed dose for kidneys (3.3 ± 2.2 mGy/MBq) raises concern on nephrotoxicity. As results from external radiotherapy, delayed kidney toxicity is limited to a ~25 Gy cumulative dose. Amino acids infusion partially reduces (20-30%) the radiation exposure of the kidneys after radiolabeled peptides injection. Accordingly, a dose of around 10-12 GBq of ^{90}Y-DOTATOC could be injected as maximum total activity. Based on this defined cumulative dose, the aim of this study was to determine the maximum dosage per cycle of ^{90}Y-DOTATOC after amino acid infusion. Methods: Forty pts, divided in 8 groups, received 2 cycles of ^{90}Y-DOTATOC, with activities increasing by 0.37 GBq per group, starting from 2.96 to 5.55 GBq. All pts received amino acid infusion (lysine + arginine) immediately before therapy.

Results: Sixty percent of pts presented grade I-II gastrointestinal toxicity (nausea and vomit) after amino acid infusion whereas none showed adverse reactions after ^{90}Y-DOTATOC injection up to the dose of 5.55 GBq/cycle. Reversible grade III haematological toxicity was found in 3/7 (43%) of pts injected with 5.18 GBq which was defined as the MTD per cycle. Objective therapeutic responses were documented.

Conclusions: Five GBq per cycle is the recommended dosage of ^{90}Y-DOTATOC. Although none of our pts has shown acute kidney toxicity, delayed kidney toxicity remains the major concern limited to a ~25 Gy cumulative dose. Further studies towards more efficacious renal protecting agents are needed, to increase the cumulative injectable activity.

(Work supported by grants of the Italian Association for Cancer Research (AIRC) and Swiss National Science Foundation (31-52969.97))

OS_251

RADIATION DOSIMETRY AND RADIOTHERAPY PLANNING FOR PEPTIDE RECEPTOR RADIONUCLIDE THERAPY WITH 177LU-DOTA-TYR3-OCTREOTATE (LU-O) IN HUMANS

P.P.M. Kooij (1), M.W. Konijnenberg (2), D.J. Kwekkeboom (1), W.H. Bakker (1), E.P. Krenning (1). (1) Department of Nuclear Medicine, University Hospital Rotterdam, The Netherlands; (2) Research and Development,Mallinckrodt, Petten, The Netherlands.

Aim: A new radiopharmaceutical (Lu-O), the somatostatin analogue with the highest tumor uptake found in rats and humans, has been developed for peptide receptor radionuclide therapy (PRRT). ^{177}Lu (T1/2=6.71d) emits both beta- (47, 111 and 149 keV) and gamma-radiation (113 and 208 keV). We determined the radiation dose in humans for Lu-O, with emphasis on radiation dose estimates for the kidneys (limit 23 Gy) and bone marrow (limit 2 Gy) as these organs will determine the maximum tolerated radioactivity (MTR) in radiation therapy.

Methods: 5 Patients with tumors, showing low uptake and being localised outside the organs with physiological uptake (kidneys, spleen and liver), were investigated. Urine excretion and plasma radioactivity were measured during at least 24h. Patients were scanned at regular intervals up to 408h pi. The bone marrow dose was based on both the total body activity and the plasma curve. Also in 4 of these patients the effect of an amino acid co-infusion (AA) to reduce renal uptake was studied.

Additionally in a group of 18 patients the radiation dose to the kidneys was determined to estimate variability in renal MTR.

Results: The radiation dose (average±sd, n=5) to the kidneys, liver and spleen was resp. 1.36±0.32, 0.19±0.05 and 1.89±0.37 mGy/MBq. The radiation dose to red marrow according to ICRP30 and total body radioactivity was 0.066±0.010 mGy/MBq. A more recent method and using plasma-based cumulated activity in red marrow gives a value as low as 0.021±0.009 mGy/MBq.

Co-infusion with AA (n=4) showed a 40% reduction of the radiation dose to the kidneys and about 30% reduction in radiation dose to liver and spleen. No substantial effect on radiation doses to other organs and tumors was observed.

In a group of patients (n=18, with AA) with varying tumor uptake (up to more than 30% of the injected dose) the radiation dose to the kidneys varied from 0.44 to 0.92 mGy/MBq.

Conclusions: Based on these data all further patients were treated with co-infusion of AA. Because of the large variation in radiation dose to the kidneys individual dosimetry is necessary to calculate the renal MTR for the maximum dose of 23 Gy, without exceeding a bone marrow radiation dose of 2 Gy.

OS_252

DOSIMETRY WITH 86Y-DOTATOC AND 111IN-OCTREOTIDE: ARE THE DIFFERENCES RELEVANT FOR THERAPY PLANNING?

J. Förster (1), M. Engelbach (2), J. Brockmann (3), H. Reber (1), H.-G. Buchholz (1), F. Rösch (3), H. Herzog (4), P. Bartenstein (1). (1) Department of Nuclear Medicine, University Mainz,Germany; (2) Department of Internal Medicine, University Mainz,Germany; (3) Institute of Nuclear Chemistry, University Mainz,Germany; (4) Institute of Medicine, Research Center Jülich, Germany

Aim: The somatostatin analogue ^{90}Y-DOTATOC is used for treatment of patients with neuroendocrine tumors. An accurate pretherapeutic dosimetry would allow for an individual planning of the optimal therapeutic strategy.

In this study, the biodistribution and resulting dosimetric calculations for therapeutical exposure with ^{90}Y-DOTATOC of critical organs and tumor masses based on the chemically identical PET-tracer ^{86}Y-DOTATOC are compared to a conventional dosimetric approach based on ^{111}In-Octreotide.

Methods: So far, 3 patients with metastases of carcinoid (>4 weeks no therapy with unlabeled somatostatin) were investigated. Dynamic and static PET investigations up to 30 hr p.i. were performed (77-185 MBq ^{86}Y-DOTATOC). Serum and urine activity was measured simultaneously. Within 1 week, conjugated planar whole body (for quantification) and SPECT investigations with ^{111}In-Octreotide (110-180 MBq, using a protocol equivalent to ^{86}Y-DOTATOC) and CT-scans (for ROI definition) were performed. The regional tissue uptake with either tracer was alternatively regarded as valid for ^{90}Y-DOTATOC compound. Based on the biodistribution data of ^{111}In-Octreotide as well as ^{86}Y-DOTATOC, the dose estimates were calculated using the IMEDOSE software and the MIRDOSE3 technique.

Results: Serum kinetics and urinary excretion of both tracers showed no relevant differences. Estimated doses for ^{90}Y-DOTATOC therapy of critical organs were similar for both tracers (^{111}In-Octreotide vs. ^{86}Y-DOTATOC in mean mGy/MBq, respectively): liver 0.6 vs. 0.8, kidneys 2.8 vs. 2.4, and spleen 2.9 vs. 2.6. In contrast, large differences in dose estimation were found in tumor masses. The dose estimations for tumor masses based on ^{86}Y-DOTATOC were more than 50% higher than those based on ^{111}In-Octreotide. Furthermore, there was a large variability across the patients in the kinetics of ^{86}Y-DOTATOC in spleen (residence time ranging from 0.1-2 hr) and kidneys (0.7-1.7 hr).

Conclusions: Our data suggest that dosimetry for ^{90}Y-DOTATOC therapy based either on ^{86}Y-DOTATOC or ^{111}In-Octreotide results in similar organ doses whereas estimation of tumor doses shows relevant discrepancies. Therefore it is questionable if the planar scintigraphy based dosimetry with ^{111}In-Octreotide is accurate enough to assess reliably the achievable tumordose for therapy with ^{90}Y-DOTATOC. However an individual pretherapeutic dosimetry appears necessary considering the large differences in organ doses between single patients. If possible, this should be performed with the chemically identical PET-tracer ^{86}Y-DOTATOC.

OS_253

TREATING SOMATOSTATIN RECEPTOR POSITIVE TUMOURS WITH RADIOLANREOTIDE

R. Buscombe (1), M.E. Caplin (1), J. Hepplewhite (1), G. Johnson (1), P.L. Bouloux (1), T. Meyer (1), D. Hochhauser (1), C. Bouvier (1), I. Virgolini (2), T. Ah Yong (3), A.J.W. Hilson (1)(1) NET Clinic, Royal Free Hospital, London, UK; (2) University Hospital Lienz, Austria; (3) Queen Elizabath Hospital, Hong Kong, China.

Targeted therapy with Y-90 Lanroetide may be appropriate in patients who have tumours which express somatostatin receptors. Many of these patients, for example those with carcinoid, do not respond to chemotherapy or external radiotherapy. The aim of this study is to review our experience in using Y-90 Lanreotide on such tumours

A total of 53 cycles of Y-90 lanreotide have been given to 23 patients over an 18 month period. All patients had failed or found to be unsuitable for other cancer treatments. There were 15 patients with carcinoid, 5 with gliomas, 1 fibrolamellar cancer, 1 ACTH secreting cancer and one malignant histiocytoma. Patients were infused with 0.8-1.2 GBq on a 3-4 week basis for 3 treatments and if there was response this was repeated afer a 3 month gap. Those with intra-cerebral tumours were treated with 200-400 MBq Y-90 Lanreotide intra-arterially into the tumour bed.

Most patients had fatigue for 7-10 days post treatment. There has been mild bone marrow toxicity in 4 patients and no renal toxicity. Response as measured by >50 reduction in tumour size on CT has occurred in 6 patients, stability of previously growing disease in 8 patients. All the remaining 9 patients with progressive disease have died of their disease. Poor prognostic indicators are massive tumour bulk and bone or lung metastases.

Y-90 Lanreotide can induce stability or regression in 56% of patients but may not be appropriate for those with very advanced disease

OS_254

TREATMENT WITH LU-177-DOTA-TYR3-OCTREOTATE IN PATIENTS WITH SOMATOSTATIN RECEPTOR POSITIVE TUMORS: PRELIMINARY RESULTS

D.J. Kwekkeboom (1), B.L. Kam (1), W.H. Bakker (1), P.P. Kooij (1), A. Srinivasan (2), J.L. Erion (2), J.L. Bugaj (2), M.A. Schmidt (2), M. de Jong (1), E.P. Krenning (1). (1) Department of Nuclear Medicine, University Hospital Rotterdam, Rotterdam, the Netherlands; (2) Mallinckrodt Medical, St Louis, Missouri, USA.

In patients with somatostatin receptor positive tumors, scintigraphy with In-111-DTPA-octreotide (OctreoScan) can be used diagnostically and DOTA-Tyr3-octreotide, labelled with Y-90, is effective for peptide receptor radionuclide therapy (PRRT). Because of favourable characteristics in vitro and in animal experiments, as well as in the initial comparison with OctreoScan in patients, showing a 3-4 fold higher binding to most tumors, the newly synthesized somatostatin analogue DOTA-Tyr3-octreotate, labelled with the beta and gamma emitting radionuclide Lu-177 was used for PRRT in 36 patients (125 administrations).

Methods: Interim analysis in patients who had received at least 300 mCi (11 GBq) was performed in 26 patients with mostly neuroendocrine tumors. All patients had progressive disease before enrollment. None had yet received their maximum cumulative dose (approximately 600-800 mCi (22-30 GBq)). All had aminoacid co-infusion to reduce kidney dose.

Results: Nausea, vomiting, and mild abdominal discomfort were present in 31%, 9%, and 11%, respectively. Mild (WHO tox grade 1) leucocytopenia, thrombocytopenia, and anemia occurred in 5, 3, and 10 patients, respectively. Lymphocytopenia occurred in 21 patients. Serum creatinine did not change significantly in any patient.

Minor CT-assessed tumor shrinkage was noticed in 8 patients and partial remission in 1. Three patients had tumor progression, and in 14 no changes were seen. Tumor markers were elevated in 22 patients. In 2/8 patients with shrinkage on CT >50% decrease of tumor markers was found; in 2/11 patients with unaltered CT and in 2/3 with progression >50% increase was found.

Conclusion: The interim results of PRRT with Lu-177-DOTA-Tyr3-octreotate are very promising and may indicate that this radiopharmaceutical is at least as effective as the Y-90 labelled somatostatin analogues currently used for PRRT.

RADIOPHARMACY / RADIOCHEMISTRY

OS_255

IMAGING EVALUATION OF TC-99M-LABELED RECOMBINANT ADENOVIRUS

K.R. Zinn (1), T.R. Chaudhuri (1), N. Belousova (2), A.J. Davis (1), D.T. Curiel (2), V.N. Krasnykh (2). (1) Department of Radiology; (2) Department of Medicine, Gene Therapy, University of Alabama at Birmingham, Birmingham, AL, USA.

Aim. A new capability to ^{99m}Tc label and image recombinant Ad was developed, using direct labeling of a 6-His tag genetically fused to the Ad fiber protein.

Methods. In 3 separate experiments, a 6His-tagged Ad vector encoding luciferase was incubated for 2 h at 37°C with a preformed ^{99m}Tc(I) carbonyl chelate, prepared as described by Waibel et al (Nat Biotech 17, 897-901,1999). Following dialysis for 4 h, the binding of ^{99m}Tc-Ad to confluent 293 cells in a 24-well plate was tested. Adherent cells were washed, recombinant Ad5 knob added to half the wells (300 ug/ml, 0.2 ml/well), and plates were incubated with a series of 1:5 Dilutions („D" 1,2,3,4; 3 reps each) of ^{99m}Tc-Ad (0.2 mL/well; D1=$1x10^{10}$ Ad particles) for 2 h. Gamma camera images were collected during the incubation, and again at the end, after extensive washing. After an additional 18 h at 37°C, the cells were lysed for luciferase measurement. In parallel, ^{99m}Tc-Ad was i.v. injected into mice (3/Exp.); either nude mice (Exp. 1) or BABL/C mice (Exp. 2-3). The mice were imaged at 10 min with a gamma camera equipped with a pinhole collimator, then terminated for the vector biodistribution studies.

Results. Quality control analyses showed 95% of ^{99m}Tc to be Ad bound. Imaging detected specific uptake of ^{99m}Tc in the 293 monolayer of cells for D1-D3, consistent with binding and internalization of ^{99m}Tc-Ad. The % ^{99m}Tc-Ad bound was a constant 22% of added ^{99m}Tc-Ad for D1-D3, and reduced to ~3% in the presence of recombinant knob. Luciferase assays indicated effective gene transfer. Relative light units were consistent with the ^{99m}Tc-Ad5 dilutions, and a similar inhibition pattern was found with excess knob. Mice images at 10 min after i.v. injection showed a distinct pattern of the vector uptake by the liver, with 77±4, 68±2, and 67±6% of the dose in that organ, for Exp. 1,2,3, respectively. On a weight basis, spleen and lung were 2nd and 3rd for organ uptake.

Conclusion. Recombinant 6His-tagged Ad vector was successfully radiolabeled with ^{99m}Tc. The integrity of the Ad was preserved, as demonstrated by in vitro and in vivo studies. The short half-life (6 h) for ^{99m}Tc is an advantage to determine in vivo Ad localization. After 2 days (8 half-lives for ^{99m}Tc) an expressed reporter receptor, for example hSSTr2, can be imaged with a ^{99m}Tc-labeled hSSTr2-avid peptide as previously reported (J Nucl Med 41:887, 2000).

OS_256

IN VITRO AND IN VIVO PROPERTIES OF MORPHOLINOS AS RADIOPHARMACEUTICALS

D.J. Hnatowich, G. Liu, K. Mangera, N. Liu, S. Gupta, M. Rusckowski. Department of Radiology, University of Massachusetts Medical School, Worcester, MA, USA.

Morpholinos (MORFs), a new class of synthetic oligomers with a nuclease resistant, nonionic and water soluble phosphorodiamidate backbone, may represent an alternative to DNAs and PNAs in radiopharmaceutical design.

Aim: We investigated the in vitro and in vivo properties of MORFs labeled with Tc-99m.

Methods: Three MORFs (15, 18 and 25 mer), along with their complements, were obtained with a primary amine attached via a six-member alkyl linker. The amine was conjugated with NHS-MAG3 to permit radiolabeling with Tc-99m.

Results: By surface plasmon resonance at room temperature, the association rate constant for hybridization of each MORF to its complement (cMORF) was essentially equal to that of DNAs and PNAs. Hybridization of Tc-99m-MORF in vitro to free cMORF and to a cMORF polymer was rapid (2-3 min) and nearly quantitative (90%) under a variety of conditions. By SE HPLC, the stability of the Tc-99m-MORF was found to be greater than 85% over 24 hrs in 37°C serum with minimal protein binding. In normal mice, the Tc-99m-MORF showed rapid pharmacokinetics with only 8% remaining in the whole body at 24 hrs. In vivo targeting with Tc-99m-MORF of cMORF beads in one thigh of normal mice compared to MORF beads in the contralateral (control) thigh showed study/control thigh ratios of 4-7 between 3 -24 hrs. Preliminary to a test of pretargeting, the anti-CEA IgG antibody MN-14 (Immunomedics) was conjugated with 18 mer MORF. Nude mice bearing LS174T tumors each received 50 µg of conjugated antibody 48 hrs prior to the administration of 0.5 µg (200 µCi) of Tc-99m labeled 18 mer cMORF. Control animals received the labeled cMORF without the prior administration of the antibody. Imaging was performed at 3 and 24 hrs post administration of Tc-99m. At 24 hrs, an average of only 11% of the radioactivity remained in the whole body in the study animals and, of this, 3% was in tumor. The next highest organ was kidney with 2% and all other organs were less than 1%. Corresponding values for the control animals were 5% (whole body), 0.06% (tumor) and 1.8% (kidneys). All images reflected the high tumor uptake and low uptake in normal tissues in the study mice.

Conclusions: These results demonstrate that MORF oligomers hybridize in vitro and in vivo with affinity/kinetics and in vivo stability/pharmacokinetics suitable for radiopharmaceutical design. In particular, effective pretargeting in a mouse tumor model was accomplished through their use.

OS_257

THE POTENTIAL OF SPIEGELMERS FOR IN VIVO IMAGING

B. Tavitian (1), B. Kühnast (1), S. Klussmann (2), I. Doignon (1), B. Wlotzka (2), B. Rousseau (3), J.M. Verbavatz (3), F. Dollé (4), A. Syrota (4). (1) CEA DSV, Inserm Eritm 0103, Orsay, France; (2) Noxxon Pharma AG, Berlin, Germany; (3) CEA DSV, DBCM, Saclay, France; (4) CEA DSV, Service Hospitalier Frédéric Joliot, Orsay, France

Aptamer oligonucleotides evolved *in vitro* as ligands for a variety of targets including small molecules, peptides and protein domains, are an interesting potential source of radiopharmaceuticals. We have explored with PET an original class of aptamers, the Spiegelmers, in which D-ribose and D-deoxyribose found in natural RNA and DNA, respectively, are replaced by their corresponding enantiomeric L-forms.

Methods Two Spiegelmers, one L-RNA and one L-DNA, having a model sequence without target binding properties, were explored. Labelling was performed by conjugation between the Spiegelmers bearing a 3'phosphorothioate monoester group and a radio[halogeno]benzyl-bromoacetamide : *N*-(4-[^{18}F]fluorobenzyl)-2-bromoacetamide or *N*-(4-[^{125}I]iodobenzyl)-2-bromoacetamide. Dynamic whole body PET acquisition was performed in baboons with the Siemens EXACT-HR+ camera in order to establish the whole body pharmacokinetics of [^{18}F]-labelled Spiegelmers, and their plasmatic and urinary metabolism were studied with radioHPLC.

Results After purification by RP-semipreparative-HPLC, the labelling method allowed to prepare 20 to 30 mCi (EOB) of fluorinated Spiegelmers and 150 to 200 µCi of iodinated Spiegelmers, respectively, with high specific radioactivity in both cases. PET images and time-activity curves showed that initial radioactivity concentrations in organs were dependant on blood flow for both L-DNA and L-RNA. In plasma, heart, lungs and liver, the distribution phase was followed by a decrease of the radioactivity more rapid for L-DNA than for L-RNA. In kidneys, the L-DNA followed a pattern of distribution/elimination of the radioactivity, whereas the L-RNA accumulated significantly until 140 minutes (0.25% of ID at 140 min.) followed by a slow decrease. In brain and muscles the radioactivity concentrations never exceeded 0.008% of ID.

Analysis of metabolism showed that [^{18}F]-labelled Spiegelmers remained undegraded in the plasma up to 3 hours after injection, although limited degradation was found in urines collected 6 hours after injection.

To improve the resolution of the radioactivity distribution in the kidneys, the iodine-125 labelled L-RNA Spiegelmer was injected to rats and the kidneys were removed 30 minutes after injection, frozen and cut. Microautoradiography revealed radioactivity only in the tubules of the renal cortex and no radioactivity was detected in the glomerules and in the medulla. Metabolic studies showed that the Spiegelmers remained undegraded in the kidneys.

Conclusion Favourable whole body pharmacokinetics and metabolic stability characterize the Spiegelmers as potent and promising aptamer-type radiopharmaceuticals.

OS_258

MONITORING OF GENE THERAPY IN LDL-RECEPTOR DEFECT WITH IN-111-LDL. DURATION OF GENE EXPRESSION AND DOSAGE OF GENETIC VECTORS

W. Burchert (1), H. Schmidt (2), P. Gielow (3), G. Cichon (4), T. Petrich (3), C. Büttner (2), M. Dogar (2), M. Manns (2), W.H. Knapp (3). (1) Inst. f. Molekulare Biophysik, Radiopharmazie und Nuklearmedizin, Herz- und Diabeteszentrum NRW, Ruhr-Universität Bochum, Germany; (2) Abt. f. Gastroenterologie, Medizinische Hochschule Hannover, Germany; (3) Klinik für Nuklearmedizin, Medizinische Hochschule Hannover, Germany; (4) Max-Delbrück-Zentrum f. Molekulare Medizin, Berlin, Gemany

Aim: A gene therapy for familial hypercholesterinemia is under development. This disease is caused by a deficiency of the hepatic low density lipoprotein (LDL)-receptor (LDLr). In an animal model (WHHL-rabbits). the efficacy of the gene therapy was monitored with a ^{111}In-LDL scintigraphy The aim of this study was to evaluate the duration of therapy induced phenotypic changes, and to characterize the effect of different vectors dosage in vivo.

Methods: LDL was isolated from human plasma and labelled with ^{111}In . After injection of 3.5-5 MBq planar images were acquired 4 and 24 h p.i. (ME collimator, Siemens DIACAM). Gene therapy was performed using 10%, 50%, 100% and 200% of the usual vectors dosage (approx. 1 x 10^{13} pfu, adenovirus V, CMV promotor, hLDL insert) in two WHHL-rabbits, respectively. To asses the time course of the induced phenotypic changes scintigraphic investigations were performed 14 days before and 5, 30, 60, and 110 days after completion of gene therapy in each rabbit. The tracer uptake was quantified by the ratio of liver to heart (blood pool) activity.

Results: In all rabbits a significant increase of the liver / heart ratio (L/H) was found 5 days after gene therapy (L /H = 11.3 ± 1.7; 4 h p.i.) as compared to pretherapeutic values (L/H = 1.5 ± 0.2; 4 h p.i.). Similar uptake ratios were found at 4 h and 24 h p.i.. Following the time course a slight decrease of the specific liver uptake was found at 30 days after therapy (L/H = 7.0 ± 1.5; 4 h p.i.). Up to 110 days an elevated liver uptake as compared to the values before therapy was observed (60 days: L/H = 6.0 ± 1.1; 110 days: L/H = 7.3 ± 0.9). No significant differences were found between the rabbits with different vectors dosage neither early nor late after therapy.

Conclusions: The maximal therapeutic effect was found 5 days after gene therapy. An increased hepatic accumulation of ^{111}In-LDL even after 110 days after gene therapy suggested a long standing therapeutic effect. The in vivo imaging of the phenotypic expression could be performed as early as 4 hours after tracer application.

OS_259

LIPOSOME-ENCAPSULATED 99MTECHNETIUM MIBI ACCUMULATION IN SENSITIVE AND MULTIDRUG RESISTANT LUNG ADENOCARCINOMA GLC4 CELLS.

J. Vergote (1), H. Belhaj-Tayeb (1), D. Briane (2), G. Leger (1), JL. Moretti (1). (1) Laboratory of Radiopharmacologie, University Paris 13, France; (2) Laboratory of Cellular and Molecular Oncology, University Paris 13, France.

Background : Polyethyleneglycol (PEG) liposomes have been shown to be excellent vehicles for lipophilic anthracycline antibiotics or ^{99m}Tc-radiopharmaceuticals.

Aim : Encapsulating ^{99m}Tc-MIBI into labelled pegylated liposomes would be a good candidate to explore the accumulation in GLC4 small-lung cancer cells which overexpress or not the multidrug resistance related protein MRP1.

Methods : Using rhodamine B labelled liposomes, we explored by fluorescence microscopy the influx and the localisation of these liposomes into GLC4 cells. En capsulated ^{99m}Tc-MIBI was obtained in response to K^+ diffusion potential. Untrapped ^{99m}Tc-MIBI in liposomes preparations (SUVs) was removed by passing the SUVs through a Sephadex G-25 Column. ^{99m}Tc-MIBI uptake was quantified by measuring radioactivity retained in GLC4 cells incubated at 37°C for 60 min with encapsulated or free ^{99m}Tc-MIBI.

Results : The efficiency with which ^{99m}Tc-MIBI was encapsulated in liposomes was 45 % - 50 %. ^{99m}Tc-MIBI labelled pegylated liposomes accumulation in sensitive and resistant GLC4 cells was higher compared to free radiotracer. The uptake of liposome-encapsulated ^{99m}Tc-MIBI in resistant cells was lower than the uptake in sensitve cells. Encapsulation did not modify the capacity of ^{99m}Tc-MIBI to distinguish between the two types of cells.

Conclusion : ^{99m}Tc-MIBI labelled pegylated liposomes do not affect its accumulation in tumour cells and is a promising radiopharmaceutical for imaging multidrug resistance related protein in tumour cells.

OS_260

SYNTHESIS OF [99MTC]-EDTMP USING PERRHENIC ACID AS CARRIER - RADIOPHARMACEUTICAL AND CLINICAL RESULTS

M. Mitterhauser (1), A. Krcal (2), R. Dudczak (2), T. Traub (2), S. Oflouglu (2), H. Viernstein (3), C. Pirich (2). (1) Hospital Pharmacy, General Hospital of Vienna; (2) Univ. Clinic of Nuclear Medicine, General Hospital of Vienna ; (3) Inst. of Pharmaceutic Technology and Biopharmaceutics, University of Vienna.

Aim: An increased uptake of bone-seeking radiopharmaceuticals into malignant bone lesions is a prerequisite for adequate bone scanning. Visual image analysis is impaired due to high soft-tissue activity with currently available [^{99m}Tc]-EDTMP-kits. This study aimed to compare carrier-added [^{99m}Tc]-EDTMP with carrier-free [^{99m}Tc]-EDTMP and [^{99m}Tc]-DPD as a tracer used in clinical routine.

Methods: 15µg - 150µg perrhenic acid were added to [^{99m} Tc]-pertechnetate (>6GBq in 2ml phys. saline). The solution was transferred into a vial containing 1mg of EDTMP, 4mg stannous(II)chloride and 10mg ascorbic acid under inert conditions. Under vigorous stirring the reaction mixture was heated to 45°C for 10min. After cooling down to room temperature the labelling mixture was sterile filtrated (0.22µm). Quality control was performed using radio-ITLC (acetone or ethanol as solvent: R_f perrhenate/pertechnetate 0,87, colloid/product 0.05; phys. saline as solvent: R_f colloid 0.00, perrhenate/pertechnetate and product 0.9) allowing rapid and efficient assessment of the labelling results. Carrier free [^{99m}Tc]-EDTMP and [^{99m}Tc]-DPD were prepared according to instructions. Clinical studies were performed in 29 patients according to a routine bone scanning protocol by injecting 740 MBq of the respective tracer and whole body imaging 3h thereafter.

Results: Radiochemical purity and yield relied on various parameters such as concentration of carrier and reducing agent and reaction conditions (pH and temperature). Labelling yields varied with means of 22% (n=4; 150µg carrier), 80% (n=10; 15µg carrier) and 91% (n=5; carrier free). In all experiments radiochemical purity was >96%.

In clinical studies quantitative analysis demonstrated a significant ($p < 0.05$) increase in bone/soft tissue ratio and bone lesion/normal bone ratio as compared to both carrier-free [99mTc]-EDTMP and [99mTc]-DPD. These results were supported by visual image analysis.

Conclusion: Our new method of „co-labelling" allows fast and efficient preparation of Re/[^{99m}Tc]-EDTMP offering promising properties for its evaluation in controlled clinical trials.

Fig. 1 shows a typical image of prostate cancer metastasis (3 hrs after injection of carrier added [^{99m}Tc]-EDTMP)

OS_261

UPTAKE CHARACTERISTICS AND MECHANISMS OF TC-99M-MIBI, TC-99M-TETROFOSMIN AND TC-99M-FURIFOSMIN IN SARCOMA CELLS.

M. Rodrigues (1), A. Arakil Aghajanian (1), W. Kalinowska (2), C. Zielinski (2), H. Sinzinger (1). (1) Department of Nuclear Medicine; (2) Clinical Division of Oncology, Department of Internal Medicine I, University Hospital, Vienna, Austria .

Tc-99m-methoxyisobutylisonitril (MIBI), Tc-99m-tetrofosmin and Tc-99m-furifosmin have been widely used in the imaging of several tumor types, but the mechanisms of their tumor cellular uptake are not yet precisely known. The aim of this study was to assess and compare the in-vitro uptake characteristics and mechanisms of Tc-99m-MIBI, Tc-99m-tetrofosmin and Tc-99m-furifosmin in well-characterized human malignant soft tissue sarcoma cell lines; this in view of the possible clinical application of these tracers in soft tissue sarcoma.
Methods: The kinetics of cellular uptake [at 22¡C, 32¡C and 37¡C, 10-120 minutes after incubation with the tracer (7.4x10E5 Bq)] and washout (30 and 60 minutes after incubation with the tracer) of Tc-99m-MIBI, Tc-99m-tetrofosmin and Tc-99m-furifosmin, and the possible involvement of cell membrane ion transport systems and mitochondrial membrane potential on the accumulation of these tracers in soft tissue sarcoma cells (1x10E6 cells/ml) was investigated. The chemical agents ouabain (cation channel inhibitor), verapamil (calcium channel inhibitor), nigericin (increases mitochondrial potential and disrupts the cell membrane potential) and carbonyl cyanide m-chlorophenylhydrazone (CCCP) (depolarizes the mitochondrial membrane) were used for this purpose.
Results: Tumor cellular uptake of Tc-99m-MIBI, Tc-99m-tetrofosmin and Tc-99m-furifosmin depends not only on the chemical structures and physical properties of these tracers, but also on the degree of cellular metabolic activity. Passive transport through the plasma membrane and the negative intracellular charge of both mitochondria and cell membranes play a role in the cellular uptake of these tracers. The tumor cellular uptake of Tc-99m-MIBI and Tc-99m-tetrofosmin is mainly dependent on both the mitochondrial membrane potential and the plasma membrane, whereas the uptake of Tc-99m-furifosmin shows much more dependence on the passive transport through the plasma membrane. The uptake of Tc-99m-MIBI, Tc-99m-tetrofosmin and Tc-99m-furifosmin could not be increased by verapamil.
Conclusions: Tc-99m-MIBI, Tc-99m-tetrofosmin and Tc-99m-furifosmin seem to be equally promising for the in-vivo imaging and characterization of soft tissue sarcoma. Verapamil is not a promising agent for increasing sensitivity of scintigraphy with these tracers in patients with soft tissue sarcoma.

OS_262

HIGH PLASMA CONCENTRATIONS DURING THE DISTRIBUTION PHASE IS A LIKELY REASON FOR RAPID RADIOLIGAND METABOLISM IN PET-STUDIES

S. Sestini (1), C. Halldin (2), L. Farde (2). (1) Department of Clinical Physiopathology - Nuclear Medicine Unit, University of Florence, Florence, Italy; (2) Department of Clinical Neuroscience-Psychiatry Section, Stockholm, Sweden.

High plasma concentrations during the distribution phase is a likely reason for rapid radioligand metabolism in PET-studies
Objectives: to determine the pharmacokinetic phase-distribution or elimination- during which a brain PET experiment works by using PET input function data in a classical pharmacological acceptance. Results were used to discuss reasons for the somewhat unexpected observation of rapid radioligand metabolism in PET-studies. Methods: Comparisons were made between: (A) distribution and elimination half-lives of 9 PET input function curves of [11C]raclopride (bolus i.v.) (PETc) and distribution and elimination half-lives of 13 plasma curves of unlabelled raclopride (10 min infusion i.v.) used as reference curves (REFc) due to the long time sampling (30h); (B) volumes of distribution during terminal phase for PETc (Vd^{PET}) and REFc (Vd^{REF}) and at steady state for REFc (Vss^{REF}). The % of raclopride in plasma during time and at steady-state, dilution of drug in body V(t), and % of metabolite fraction in plasma were calculated and plotted. Results: differences were found between elimination half-lives of PETc (0.5±0.2h) and REFc (9.8±4.5h) as well as distribution half-lives of PETc (0.018±0.02h) and both distribution (0.6±0.1h) and elimination half-lives of REFc (p=0.0001). Importantly, no differences were present between *elimination* half-lives of PETc and the *distribution* half-lives of REFc (p=0.1). Moreover, the Vd^{PET} (13.6±10.8L) was lower than Vd^{REF} (82.2±30.5L) and Vss^{REF} (59.4± 20L) (p=0.0001). Accordingly, the % of [11C]raclopride in plasma at 50 min was 10% of the dose whereas the value for % of unlabelled raclopride at 30h was close to that of steady-state (4%). The V(t) plots showed a wide time-lag between the final value of PETc (38L) and REFc (1015L). The plots of metabolites fraction showed that radioligand metabolites were rapidly formed. Conclusions: the present results show that behaviour of radioligands during a PET scan can be described as „distribution phase". This is a likely reason for rapid radioligand metabolism in PET-studies: during distribution phase, ratio of the tracer concentration in plasma to the extra-plasmatic body spaces has not been reached steady state and high plasma concentration affords for a considerable fraction of radioligand subjected to metabolic enzymes.

OTHER CLINICAL SCIENCE. LUNG

OS_263

Abstract withdrawn

OS_264

DIFFERENTIATION BETWEEN NON-CARDIOGENIC AND CARDIOGENIC PULMONARY OEDEMA: DIFFERENCE IN PLASMA DISAPPEARANCE RATE CONSTANTS OF 67GA-TRANSFERRIN ?

J. Verheij (1), P.G.H.M Raijmakers (2), A.B.J Groeneveld (1), A. van Lingen (2), L.G. Thijs (1), G.J.J. Teule (2). (1) Department of Acute Internal Medicine; (2) Department of Nuclear Medicine, Free University Hospital, Amsterdam, The Netherlands.

Pulmonary oedema resulting from increased permeability, associated with the Adult Respiratory Distress Syndrome (ARDS) is often hard to differentiate clinically from cardiogenic pulmonary oedema (CPE). Methods have been developed to measure the increase in permeability in the presence of ARDS and to discriminate between the two types of oedema. These techniques are using a probe system to measure the increase of a labelled protein, for example ^{67}Ga-transferrin, in the lungs concomitantly with the plasma disappearance of the tracer in the blood. A pulmonary leak index (PLI) is obtained and the PLI is proven to be a useful tool to differentiate between pulmonary oedema associated with ARDS or CPE. With the data obtained to calculate the PLI, we studied the kinetics of the tracer in the blood to see if the plasma disappearance of ^{67}Ga-transferrin alone could make a distinction between the oedema types.
Methods: We studied three groups of patients: one group of patients with clinically defined ARDS (n=13), one group of patients with CPE (n=8) and a Control group (n=10) with patients scheduled for aortic surgery. Ten blood samples were obtained in 60 minutes after i.v. administration of 3,7 MBq ^{67}Ga-citrate. The disappearance of ^{67}Ga-transferrin is very well described (r^2>0,95) by a bi-exponential model with two disappearance rate constants (min^{-1}, SPSS 9.0.1).
Results: Description of the plasma disappearance of ^{67}Ga-transferrin in the blood by a bi-exponential model associated with two plasma disappearance rate constants (k_1 and k_2), shows a significant increase of both the k_1 and k_2 in the case of ARDS and no overlap with CPE (Fig). The parameters in CPE are in the normal range.
Conclusions: Description of the plasma disappearance of ^{67}Ga-transferrin in the blood using a model with a bi-exponential fit and two plasma disappearance rate constants can help to differentiate between pulmonary oedema resulting from ARDS or CPE.

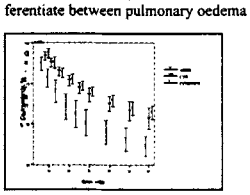

OS_265

QUANTITATIVE ANALYSIS OF INHOMOGENEITY IN VENTILATION SPECT

J. H. Xu (1), M. Moonen (1), A. Johansson (1), A. Gustafsson (2), B. Bake (1). (1) Institute of Heart and Lung Diseases; (2) Department of Radiation Physics, Sahlgrenska University Hospital, Gothenburg, Sweden.

Aim: The aim of this study was to evaluate a method for quantification of inhomogeneity in ventilation SPECT.
Methods: Nine emphysematous patients, nine life-long non-smokers and nine smokers were included in the study. The SPECT investigation was performed after 50 MBq ^{99m}Tc-Technegas had been inhaled by each subject in supine position, with a single head gamma camera, equipped with a general purpose parallel collimator using 64 projections (20 seconds each) over 360°. Data were acquired in 128×128 matrices. Attenuation correction was applied based upon CT density map. Lung ROIs were delineated manually on CT images and then positioned on SPECT images. Several attenuation corrected transaxial SPECT slices (thickness 1 cm, spacing 3.5 cm) were acquired. Each SPECT slice was divided into several 2×2 cm^2 square regions. Inhomogeneity was assessed by the coefficient of variation (CoV) of the pixel-counts within 2×2×1 cm^3 volumes (micro-level) and by the CoV of the total counts of these 2×2×1 cm^3 volumes (macro-level).
Results: The frequency distribution of micro-level CoVs concentrated at low values (usually lower than 30%) in non-smokers, whereas it dispersed largely (up to >150%) in emphysematous patients. In 7 smokers, CoVs distributed within non-smokers' range, whereas the other two distributed between non-smokers' and emphysematous patients'. The pooled mean values of micro-level CoVs and the macro-level CoVs in each subject clearly separated the patients from the others. Parametric images of micro-level CoV showed the localisation and severity of the diseased lung.
Conclusion: The present method enables the quantification and localisation of inhomogeneity in ventilation SPECT images.

OS_266

THE PERFORMANCE OF DIAGNOSTIC TESTS FOR ACUTE PULMONARY EMBOLISM IN PATIENTS WITH COPD

I.J.C. Hartmann (1), P.J. Hagen (2), M.P.M. Stokkel (3), O.S. Hoekstra (2), C.F. Melissant (1), P.E. Postmus (2), M.H. Prins (4). (1) University Medical Center, Utrecht, The Netherlands; (2) Free University Hospital, Amsterdam, The Netherlands; (3) Leiden University Medical Center, Leiden, The Netherlands; (4) Academic Medical Center, Amsterdam,The Netherlands

In patients with chronic obstructive pulmonary disease (COPD), differentiating a pulmonary embolus (PE) from an exacerbation of COPD is difficult since clinical signs and symptoms of both diseases overlap. In this study, the effect of the presence of COPD on the accuracy of clinical probability estimate (CPE), spiral CT angiography (SCTA), D-dimer testing, ventilation/perfusion (V/Q) scintigraphy and pulmonary angiography for the diagnosis of PE was assessed.
Methods: From May 1997 through March 1998, 627 consecutive in- and outpatients with suspected PE were investigated in six teaching hospitals. In these patients D-dimer testing, CPE, V/Q scintigraphy, SCTA and/or pulmonary angiography were performed according to a strict diagnostic protocol. Patients were categorized independently as having COPD or not.
Results: COPD diagnosis could be confirmed in 91 patients (15%). PE prevalence was similar in patients with and without COPD (29% and 31%, respectively), notwithstanding the larger proportion of non-diagnostic V/Q-scan results in patients with COPD (59% versus 33%, $p < 0.001$). The distribution of CPE and the diagnostic value of the D-dimer essay, SCTA, and pulmonary angiography were comparable among patients with and without COPD.
Conclusion: The presence of COPD does not influence the diagnostic value of D-dimer testing, SCTA and pulmonary angiography. Furthermore, V/Q scintigraphy remains a valuable screening test in patients with COPD. Normal and high-probability V/Q scan results are observed in a substantial proportion of patients with COPD.

OS_267

URGENT REQUESTS FOR LUNG SCANS: COMPARISON OF UTILIZATION RATES

F. Ponzo, L.B. Lacorte, H.M. Zhuang, B. Moussavian, P.D. Mozley, A. Alavi. Hospital of the University of Pennsylvania, Philadelphia, USA.

Aims of this study was to compare the effectiveness of performing non-elective V/Q scans after the close of regular business hours.
Methods: The results of 1,667 consecutive V/Q scans were retrospectively reviewed, of which 418 were ordered by the Emergency Department (ER) and 1249 by other physicians. The results were divided into 2 groups. The low-risk group included those read as normal, very low and low probability. The high-risk group included those read as intermediate and high probability.
Results: The average age of the patients from the ER averaged 50.9 ± 18.6 years old, which was significantly younger than patients from other physicians (62.3 ± 19.2) ($p<0.01$). Image analysis showed that 89.7% (375) of the V/Q scans ordered by the ER were in the low-risk group, while 10.3% (24 intermediate and 19 high probability) were in the high-risk group. By comparison, 80.8% (1009) of the V/Q scans ordered by other specialties were in the low-risk group while 19.5% (153 intermediate and 87 high probability) were in the high-risk group. The ratio of the high risk group to low risk group between the study ordered by ER physicians and by other physicians were statistically significant ($p<0.01$). Conclusion: The results suggest that ER physicians have a lower threshold for ordering V/Q scans than other physicians. Only approximately 10% of the patients have a post-test probability of PE that is intermediate or greater. This suggests that the test may not be having a significant impact on patient care when the study is ordered urgently by ER physicians. It also indicates that issues of utilization and cost effectiveness deserve systematic study.

OS_268

COMPARISON OF THE LUNG CLEARANCE RATES OF TC99M-DTPA, GA-67 SCINTIGRAPHY AND OTHER PULMONARY TESTS, IN PATIENTS WITH PULMONARY SARCOIDOSIS

M. Argon (1), Z. Aytemur (2), N. Moğulkoc (2), H. Özkılıc (1). (1) Department of Nuclear Medicine; (2) Deparment of Chest Disease, Ege University Medical School, Izmir, Turkey.

The aim of this study was to determine the value of the lung clearance rates of Tc99m-DTPA (CR-DTPA) (as a measure of the alveolo-capillary permeability) and the value of Ga-67 scintigraphy in pulmonary sarcoidosis (PS). The CR-DTPA and scintigraphic results were compared with radiological findings, pulmonary function tests (PFT), diffusion capacity of CO (Dlco) and the percentage of the lymphocyte in bronchoalveolar lavage fluid (BAL) in patients pts with PS-Pts.
Methods: 32 PS-pts and 16 healthy non-smoking volunteers as controls were studied. Ga-67 scintigraphy and CR-DTPA was studied in 32 patients, FEV1-FVC was assessed in 29 patients, Dlco in 17 patients and 19 BAL in 19 patients. Radiological appearances were assessed as stages I, II, III and scintigraphic appearances as stages 0,1,2,3 (S0: normal, S1: hilar and mediastinal uptake, S2: as S1, plus lung uptake, S3: only lung uptake) were used. To assess intensity of Ga-67 uptake, the uptake was graded from 0 to +4, using the uptake by the liver as a control.
Results: There was no significant correlation between the intensity of Ga-67 uptake and PFT, Dlco, BAL, radiological or scintigraphic stages. But in Stage III-3 pts (i.e. those who had lung fibrosis) the lung uptake was low. Stage I, II-1, and 2 patients had high torakal uptake that were active PS-pts and had granuloma formation/lymphocytic alveolitis. There was no significant correlation between the localisation of Ga-67 uptake and Dlco or BAL, but in stage 2-3, patients had low PFT. Between radiological stages and scintigraphic stages a significant correlation was seen. CR-DTPA were 1.075±0.3, 1.11±0.3, 1.5±0.1, 1.55±0.4 % min^{-1} in controls, stages I, II, III respectively. CR-DTPA was increased in those who had low PFT. There was poor correlation between CR-DTPA and Dlco, but none with BAL. In stage 2-3 pts who had increased lung Ga-67 uptake, CR-DTPA was increased. Conclusion: CR-DTPA is a non-invasive test and can show lung damage in early period of illness that can't be shown by radiology. By Ga-67 uptake in lung parenchyma, to distinguish fibrosis (which is an irreversible defect) from granuloma and alveolitis which can be treated was possible. Scintigraphic staging can be used to facilitate the understanding and description of the activity of disease and the results of scintigraphy.

OS_269

EVALUATION OF F-18-FDG DUAL-HEAD TOMOGRAPHY WITH COINCIDENCE IN THE DETECTION OF LUNG LESIONS

R.F. Wang, X.X. Wang, H.Y. Chen, T.L. Liu, J. Li, J.H. Lin. Department of Nuclear Medicine,Peking University First Hospital, Beijing, China.

Aim: To evaluate the ability of FDG-18F dual-head tomography with coincidence (DHTC) to differentiate benign from malignant lung lesions.
Methods: Twenty-seven patients with lung lesions showing abnormal on chest roentgenograms and confirmed histopathologically from thoracotomy (n =17), thoracoscopy (n = 2), bronchoscopy (n = 3), tumor needle aspiration (n = 4) and thoracic fluid smear (n = 1) were enrolled in this study. The acquisitions were taken using ADAC Epic Vertex plus dual head molecular coincidence detection (MCD/AC) system. The images with attenuation correction (AC) and without AC (NAC) were reconstructed iteratively, and interpreted by more than two experienced physicians. The ratios of tumor-to-background (T/B) were calculated in both AC and NAC images, with the ratio of T/B >2.0 being considered as the malignant lesions.
Results: Twenty of 21 patients with lung malignant lesions showed significantly increasing glucose uptake with T/B > 2.0. The sensitivity was 95.2%. One false negative case was adenocarcinoma. Six patients with benign lesions didn't demonstrate abnormal glucose accumulation with T/B < 2.0. No false positive was noted. The specificity was 100%. The positive predictive value, the negative predictive value and the accuracy was 100%, 85.7% and 96.2%, respectively.
Conclusion: FDG-18F DHTC imaging which is an attractive alternative to PET imaging because of its wide accessibility, relatively lower costs and versatility of tracer administration in the clinical setting accurately differentiates malignant from benign lung lesions. It could be a useful noninvasive approach to evaluate indeterminated lung lesions, which will provide us with more accurate and valuable diagnostic information.

OS_270

LUNG PERMEABILITY AND HIGH RESOLUTION COMPUTERIZED TOMOGRAPHY (HRCT) IN SYSTEMIC SCLEROSIS (SS)

N. Prandini (1), R. La Corte (2), R. Galeotti (3), L. Feggi (1), A. Ciprian (1), S. Panareo (1), D. Santilli (2), F. Trotta (2). (1) Department of Nuclear Medicine, S.Anna Hospital, Ferrara; (2) Department of Rheumatology, S.Anna Hospital, Ferrara, Italy; (3) Institute of Radiology, University of Ferrara, Italy.

To evaluate alveolar epithelial damage in PSS, we studied pulmonary epithelial permeability by measuring the clearance of inhaled 99mTc-DTPA aerosol and performing thin slice CT scan, chest x-ray and pulmonary function tests in 79 patients (3 males and 76 females) with a mean age of 53 years (aging 20-74). All the patients suffered of SS (22 diffuse and 57 limited variants) from 5-600 months (mean 115): 34 pts hadn't lung symptoms and had a normal chest x-rays. Forty-one patients had normal function respiratory tests.
HRCT demonstrated lung fibrosis in 87% of the patients instead of lung permeability which resulted severely increased in 25 patients (half time < 40 minutes), mild increased in 13 (half time 40-60 min) and normal in 41 patients. The mean half time resulted of 42.4 minutes in SSD and of 64.1 minutes in SSL patients, while no significant correlations were found between lung permeability and the clinical and instrumental parameters (age, disease age, HRCT scores, chest x-rays, respiratory function tests). Twenty of 41 patients with normal Tc99m-DTPA lung clearance resulted with important HRCT alterations (score > 5): this can suggest that epithelial permeability can be reduced in patient with fibrosis and important reduction of lung perfusion.
These findings indicate that pulmonary interstitial lesions in PSS are accompanied by alveolar epithelial damage, and that the clearance of 99mTc-DTPA may be an early predictor of interstitial change but we can found a pseudo-normalization of lung clearance in advanced stage of disease.

OS_271

SCINTIGRAPHIC PROCTOGRAPHY HIGHLIGHTS DIFFERENCES IN RECTAL EVACUATION IN TWO GROUPS OF CONSTIPATED PATIENTS

A. .A. Darakhshan (1), M.K. Khela (2), F.D. Castillo (2), S.M. Scott (1), P.J. Lunniss (1), M. Newell (3), N.W. Garvie (2), N.S. Williams (1). (1) Academic Department of Surgery; (2) The Wingate Institute; (3) Department of Nuclear Medicine; (4) Clinical Physics Group, St Bartholomew's and The Royal London Hospital School of Medicine and Dentistry, London, UK

Aim: The electrically stimulated gracilis neosphincter (ESGN) procedure is a treatment for end stage faecal incontinence. Paradoxically, a proportion of these patients suffer from rectal evacuatory dysfunction (RED) following surgery. Scintigraphic proctography has some advantages over barium proctography, allowing quantifiable assessment of the rate, duration and efficiency of rectal evacuation and also localisation of rectocoele stool retention. We aimed to determine whether differences existed between patients diagnosed with RED as a cause of their constipation, and those with RED following ESGN surgery.
Methods: Twenty patients were studied, 10 (7 F) with RED following ESGN surgery and 10 (9 F) with RED confirmed on barium proctography. Radioactive Cobalt-57 markers were taped over the pubis, coccyx and the lumbosacral junction. Artificial stool (porridge oats, water, 100MBq of Technetium-99m DTPA) was instilled into the patient's rectum up to the maximum tolerated volume. With the patient seated on a commode, dynamic images at 1 frame/second were obtained for a period of 60 seconds at rest, and thence during evacuation. For analysis, lines drawn between the markers allowed delineation of the theoretical pelvic floor, and the upper limit of the pelvic cavity. Measurements of anorectal angles (ARA), pelvic floor position and movement, rectal and rectocoele emptying rates, and stool retention post evacuation were made.
Results: Differences in pelvic floor position at rest were found between the ESGN and constipated groups (median distance: 73 and 44 mm, respectively, $P<0.008$, paired t-test), as well as pelvic floor descent on straining (4.5 and 32 mm, $P<0.003$) and the upper ARA during maximum straining (median 169 and 178°, $P<0.04$). There were also differences in rectocoele activity at rest (211 and 85 counts/sec, $P<0.05$) and total rectocoele evacuation (42 and 80 %, $P<0.03$), but not rectocoele evacuation rate (0.46 and –0.9 %/s, $P=0.056$). Linear regression analysis demonstrated a correlation between the rectal evacuation rate and the rectocoele evacuation rate in ESGN patients ($r^2=0.59$, $P<0.01$), but not in constipated patients ($r^2=0.08$, $P=0.42$).
Conclusions: Scintigraphic proctography provides a practical and accurate method for assessment of rectal evacuation in patients following ESGN surgery. A comparison with constipated patients demonstrated a lowering of the pelvic floor with minimal movement during evacuation. Reduced rectocoele evacuation was also seen in the ESGN group, a problem that may be confounded by a theoretically non-compliant gracilis sling around the anal canal.

OS_272

SCINTIGRAPHIC MEASUREMENT OF SEGMENTAL COLORECTAL TRANSPORT DURING DEFECATION

N. Olsen (1), K. Krogh (2), P. Christensen (2), J.L. Madsen (3), S. Laurberg (2). (1) Department of Nuclear Medicine, Aarhus University Hospital, Aarhus, Denmark; (2) Department of Surgery L, Section AAS, Aarhus University Hospital, Aarhus, Denmark; (3) Department of Nuclear Medicine, Hvidovre Hospital, Copenhagen, Denmark.

Aim: The aim of the present study was to measure the segmental colorectal transport during defecation by use of a new scintigraphic method.
Methods: 18 healthy young men were studied. They were grouped according to the size of their defecation on the day of scintigraphic investigation. It was characterized by themselves as normal (8 men, group 1); smaller or much smaller than normal (8 men, group 2), no defecation (one man), and larger than normal (one man). The age was in median 31 years (24-36) in group 1 and 32 years (24-46) in group 2 (p>0.10). In-111 labeled polystyrene pellets (PP, 2 MBq p.o./day) were given in the morning on the two days just before the investigation. The first scintigraphy was performed with the subject fasting. It was followed by the intake of a standard meal and a visit to the toilet room. A second scintigraphy was performed immediately after the defecation. Each scintigraphy was performed by a dual-headed Picker gamma camera. The acquisition time was 10 min. Regions of interest were delineated manually around the ascending colon, the transverse colon, the descending colon, and the rectosigmoid. Geometric mean of anterior and posterior counts of a given segment was used as attenuation correction. The antegrade and retrograde transport of PP from each segment were computed and expressed in per cent of the counts found in the segment before defecation (ST). Assuming ordered evacuation of the colorectum, a defecation score (DS) was calculated as the extent of colorectal emptying expressed in per cent of counts found in each segment before defecation. Values are given as median (range).
Results: The retrograde ST did not differ from zero in any segment and did not differ between the two groups of men (p > 0.10). The antegrade ST had the following values in group 1 and group 2, respectively: 10 (0-60) and 0 (0-15) in ascending colon (p>0.10); 46 (0-130) and 1 (0-26) in transverse colon (p<0.05); 82 (9-179) and 1 (0-34) in descending colon (p<0.01); and 98 (82-333) and 31 (3-66) in rectosigmoid (p<0.01). DS was 99 (83-169) in group 1 and 31 (3-66) in group 2 (p<0.01).
Conclusions: The results indicated that normal defecation i young healthy men was associated with an antegrade transport mainly from the rectosigmoid but also from the descending colon and to a minor degree the transverse colon. No significant retrograde transports were detected. Defecations smaller than normal were associated with significantly smaller antegrade transports from rectosigmoid, descending colon and transverse colon.

OS_273

ASSESSMENT OF THE GALLBLADDER MOTILITY AFTER GASTRIC SURGERY BY INFUSION CHOLESCINTIGRAPHY

V. Artiko. Institute for Nuclear Medicine Clinical Center of Serbia, Beograd, Yugoslavia.

The aim of the study is the estimation of the gallbladder (GB) motility in the controls (C, n=8), patients after partial gastrectomy (Billroth I -B I, n=7 and Billroth II- B II, n=7), gastroplasty (G, n=7) and in those after total gastrectomy (PG, n=10) in order to assess the influence of the truncal vagotomy (GP, PG) and exclusion of the duodenal transit (B II, PG) of food on the GB motility.
The study was performed during (3 h,10 ml/h) infusion of 150 MBq, 0.25 mg/ml 99m-Tc-EHIDA, preceded by a loading dose. Test meal was given in 120. min.
In the patients with preserved n. vagus and duodenal transit (BI), ejection fraction (EF=66.4+/-9.2%), emptying time (ET=35.1+/-6.2 min) and ejection rate (ER=2.1+/-0.5%/min) were almost physiological ($p > 0.05$) (C;EF=76.7+/-17.9%; ET=37.8+/-11.4 min and ER=2.1+/-0.45%/min). In the patients with exclusion of duodenal transit (RV BII), EF values were (58.3+/-11.4%) slightly, but not significantly decreased ($p > 0.05$) in comparison to C and RV BI while ET and ER were completely undisturbed (39.0 min and 1.61+/-0.46 %/min). In those with truncal vagotomy (GP), EF was slightly decreased (54.4+/-14.4%), ER unchanged (1.8+/-0.84%/min) while ET (23.3+/-7.5 min) was significantly ($p < 0.05$) decreased in comparison to C, RV BI and RV BII. In the PG, with both truncal vagotomy and exclusion of the duodenal transit, EF, ET and ER (23.3+/-8.5%; 23.5+/-7.6 min; 0.92+/-0.40 %/min) were significantly ($p < 0.05$) decreased in comparison to C, RV BI, RV BII and GP.
We can conclude that truncal vagotomy, especially if accompanied by the exclusion of duodenal transit cause GB motility disorders. So, in the choice of gastric surgery, advantage must be given to the methods that preserve n. vagus and duodenal transit as often as it can, in order to avoid formation of GB calculosis.

OS_274

GALLBLADDER MOTILITY AFTER GASTRIC SURGERY ESTIMATED BY INFUSION CHOLESCINTIGRAPHY

V. Artiko (1), V. Obradovic (1), M. Petrovic (2), N. Petrovic (1), M. Milicevic (2), V. Bosnjakovic (1), K. Kostic (1). (1) Institute for Nuclear Medicine; (2) Institute for Digestive Diseases, Clinical Center of Serbia, Belgrade, Serbia.

Aims and material: The aim of the study is the estimation of the gallbladder (GB) motility in the controls (C, n=8), patients after partial gastrectomy (Billroth I -B I, n=7 and Billroth II- B II, n=7), gastroplasty (G, n=7) and in those after total gastrectomy (PG, n=10) in order to assess the influence of the truncal vagotomy (GP, PG) and exclusion of the duodenal transit (B II, PG) of food on the GB motility.
Method: The study was performed during (3 h,10 ml/h) infusion of 150 MBq, 0.25 mg/ml 99m-Tc-EHIDA, preceded by a loading dose. Test meal was given in 120. min.
Results: In the patients with preserved n. vagus and duodenal transit (BI), ejection fraction (EF=66.4+/-9.2%), emptying time (ET=35.1+/-6.2 min) and ejection rate (ER=2.1+/-0.5%/min) were almost physiological ($p > 0.05$) (C;EF=76.7+/-17.9%; ET=37.8+/-11.4 min and ER=2.1+/-0.45%/min). In the patients with exclusion of duodenal transit (RV BII), EF values were (58.3+/-11.4%) slightly, but not significantly decreased ($p > 0.05$) in comparison to C and RV BI while ET and ER were completely undisturbed (39.0 min and 1.61+/-0.46 %/min). In those with truncal vagotomy (GP), EF was slightly decreased (54.4+/-14.4%), ER unchanged (1.8+/-0.84%/min) while ET (23.3+/-7.5 min) was significantly ($p < 0.05$) decreased in comparison to C, RV BI and RV BII. In the PG, with both truncal vagotomy and exclusion of the duodenal transit, EF, ET and ER (23.3+/-8.5%; 23.5+/-7.6 min; 0.92+/-0.40 %/min) were significantly ($p < 0.05$) decreased in comparison to C, RV BI, RV BII and GP.
Conclusion:We can conclude that truncal vagotomy, especially if accompanied by the exclusion of duodenal transit cause GB motility disorders. So, in the choice of gastric surgery, advantage must be given to the methods that preserve n. vagus and duodenal transit as often as it can, in order to avoid formation of GB calculosis.

OS_275

SCINTIGRAPHIC EVALUATION OF RETROGRADE COLONIC WASH-OUT TREATMENT

P. Christensen (1), N. Olsen (2), K. Krogh (1), T. Bacher (2), S. Laurberg (1). (1) Surgical Research Unit, Department of Surgery L, Section AAS; (2) Department of Nuclear Medicine, Aarhus University Hospital, Aarhus, Denmark.

Aim: Retrograde colonic wash-out with the Enema Continence Catheter (ECC) is a well established treatment for faecal incontinence and constipation in selected patients. The aim of the study was to evaluate the internal effect of the ECC in three groups of patients by a new scintigraphic method using dual isotope technique.
Methods: Eighteen patients treated with ECC on a regular basis were investigated. Five patients had a neurogenic colorectal dysfunction (NCD), 6 had idiopathic faecal incontinence (FI) and 7 had idiopathic constipation (IC). ^{111}In-labelled polystyrene pellets (2 MBq p.o./day) were given on 2 days before the investigation to label the solid bowel content. ^{99m}Tc-DTPA was mixed with about 730 ml irrigation fluid to assess its front within the colorectum. Scintigraphy was performed before and after a standardised wash-out procedure. A two-headed Picker gamma camera was used to image the whole abdomen. The acquisition time was 10 min. Regions of interest were delineated manually around the caecum and ascending colon, the transverse colon, the descending colon, and the rectosigmoid. Geometric mean was used for attenuation correction. Assuming ordered evacuation of the colorectum, the contribution of each colonic segment to the total emptying was expressed in percent of the original segmental counts. The segmental contributions were added into a defecation score (0-400). Values are given as median (range).
Results: The defecation score was 59 (21-130) in IC which was significantly different from 204 (108-323) in NCD and 188 (155-234) in IC ($p<0.05$). Thus emptying of the rectosigmoid and most of the descending colon was found in NCD and FI whereas only 59 % of the rectosigmoid was emptied in IC. The front of irrigation fluid reached in median just beyond the hepatic flexure and correlated with the defecation score ($r^2 = 0.58$, $p<0.001$).
Conclusions: The scintigraphic results indicated that the effect of retrograde colonic wash-out was significantly higher in NCD and FI than in IC. The effect was correlated to the front of the irrigation fluid within the colorectum.

OS_276

SEGMENTAL COLONIC TRANSIT IDIOPATHIC CONSIPATION BY MEANS OF GALLIUM-67 AND IN-111 DTPA

L. Samanides, G. Limouris, V. Voliotopoulos, A. Frantzis, A. Stavraka-Kakavaki, L. Vlachos. Areteion University Hospital,Nuclear Medicine Dept., Athens, Greece.

Introduction:Aim of the present study was the measurement of segmental colonic transit for the assessment of severe constipation by means of Ga-67 citrate.Ga-67 citrate data were compared with those of In-111 DTPA, performed to the same population(11 non-constipated control subjects,9 patients with idiopathic constipation)with a time interval of 10 days between the two examinations.
Methods:After oral administration of 3 Mbq of Ga-67 citrate and 4 Mbq of In-111 DTPA in solution,serial abdominal images were performed up to 96 hr. p.i.Data were generated from(i)the geometric means of segmental retention of both tracers,(ii)the mean activity profiles and(iii)the colonic tracer half clearance times.
Results:Between control subjects and constipated patients no differences in segmental retention of either tracer or in mean activity profiles were observed.Results in constipated subjects were significantly different compared to those in controls.The mean half-clearance times of tracers for control were 26.2hr for Ga-67 citrate and In-111 DTPA respectively and 72.6 hr for Ga-67 citrate and 68.8 hr for In-111 DTPA in constipated patients.
Conclusion:Oral Ga-67 citrate seems to be a safe alternative to In-111 DTPA for segmental colonic transit measurment.Compared to In-111 DTPA the method has the same accuracy and is considerable cheaper.

OS_277

Abstract withdrawn

OS_278

RELATIONSHIP BETWEEN GASTROESOPHAGEAL REFLUX, LOWER RESPIRATORY TRACT INFECTION AND ASTHMA IN CHILDREN: A PRELIMINARY REPORT

P. Bernal (1), P. Panqueva (1), A. Cerquera (1), J. Morales (1), P. Pacheco (1), M. Sierra (1), J. Lozano (1), A. Soricelli (2), A. Padhy (2).
(1) Department of nuclear medicine, Hospital San Ignacio, Bogota, Colombia ; (2) Nuclear Medicine Section, International Atomic Energy Agency, Vienna, Austria.

Gastroesophageal Reflux (GER) is frequent in children, it is associated with heterogeneous symptoms and it has been demonstrated to perpetuate the pulmonary symptoms. GER is a potentially curable pathology, hence it is important to identify „significant" (more than 6% of time monitored , ph < 4 and for a period of 5 minutes) GER at an early stage in order to initiate appropriate treatment and prevent lung infection and chronic lung disease. GER Scintigraphy is a highly sensitive technique, easy to perform with minimum radiation dose and at very low cost. It allows the quantification of Esophageal Transit and Gastric Emptying simultaneously.
Objective: To identify the correlation between GER and Pulmonary Symptoms.
Methods: 36 children (16 male, 20 female; 4-84 months of age) with symptoms of GER, lung infection or respiratory symptoms (wheezing syndrome, Asthma) were studied for evidence of GER. 15 (41.6%) patients had symptoms of GER, 16 (44.4%) Bronchitis or Broncho-obstructive symptoms and 5 (13.8%) had history of Broncho-pneumonia confirmed by X-ray. GER Scintigraphy was carried out using a gamma camera with low energy and high resolution collimator, linked to a computer following a fasting period of at least 4 hours. The studies began with the esophageal Transit, after the oral administration of Non- absorbable radioactive material (18.5 MBq - 37MBq) in 3 cc of the patient's usual formula (orange juice or milk). Later on the gastric capacity was completed with non-radioactive liquid and dynamic imaging of the upper abdomen and thorax was done with the patient in decubitus position for 30 minutes. Static images were obtained at 1,4 and 24 hrs. to evaluate GER and lung aspiration.
Results: All 36 children studies had evidence of GER. Seven out of 15 children with gastrointestinal symptoms had abnormally prolonged gastric emptying. Eight out of 21 children with predominantly respiratory symptoms also had prolonged gastric emptying. There was no scintigraphic evidence of lung aspiration in the late images in any of the children studied. Esophageal transit was observed to be normal in all children.
Conclusions:Preliminary results suggest a strong correlation between GER and Pulmonary symptoms. All patients are being followed up. In several patients medical treatment for GER had shown significant improvement in respiratory symptoms. Results will be discussed.

NEUROLOGY / PSYCHIATRY

OS_279

REGIONAL CHANGES IN DOPAMINE FUNCTION OF DEPRESSED PATIENTS WITH RETARDED OR IMPULSIVE DEPRESSION

V. Bragulat (1), M.L. Paillère-Martinot (3), E. Artiges (1,2), V. Frouin (2), J.L. Martinot (1,2,4). (1) INSERM U334, Orsay, France; (2) Service Hospitalier Frédéric Joliot, DSV-CEA, Orsay, France; (3) Service de Psychiatrie, Hôpital de la Salpêtrière, Paris, France; (4) Service de Psychiatrie, Hôpital Albert Chenevier, Créteil, France

Aim : In depressed patients with blunted affect and psychomotor retardation, we previously reported a decreased left caudate presynaptic dopamine function, using positron emission tomography with [^{18}F] Fluorodopa and striatal regions-of-interest defined on MRI images (1). However, the regional dopaminergic dysfunction during the depressed state might be more widespread in cortical, cingulate, limbic and thalamic regions, which receive afferences from the meso-cortico-limbic dopaminergic pathways.
Methods : Depressed patients selected for psychomotor retardation and blunted affect (RD; n=6) were compared with depressed patients selected for high impulsivity (ID; n=6), and healthy subjects (n=6). We determined the regional presynaptic dopaminergic function by re-analysing raw [^{18}F]-Fluorodopa images (1) with the SPM99 voxel-based method (2). For each subject, parametric images of the influx constant Ki were obtained from the [^{18}F]-Fluorodopa images, and afterwards coregistrated on the anatomical MRI. The parametric Ki [^{18}F]-Fluorodopa images normalized onto the Talairach stereotactic space were subsequently obtained by applying the normalization matrix of the MRI images to the coregistrated Ki parametric images.
Results :The Ki decrease in left caudate was replicated in RD, validating the method. In RD, Ki value decreases were detected in thalami, and increases in both amygdalae and subcallosal gyrus. In the patient group, significant covariations were found between affective flattening or retardation scores, and Ki values in thalamus, amygdalae, subcallosal gyrus, and anterior cingulate. The covariation between affective flattening or psychomotor retardation scores were negative in the thalamus and positive in the limbic or paralimbic regions. Impulsivity scores covaried conversely in subcortical and limbic regions. Results in patients with retarded depression were consistent with those reported in Parkinson's disease patients studied with an analogous methodology (2).
Conclusion : Altered presynaptic dopamine function can be detected *in vivo* in subcortical, limbic and paralimbic regions in depressed patients with blunted affect and psychomotor retardation.

References
American.Journal of Psychiatry, Feb. 2001
Rashki et al., Brain 1999 122 : 1637 - 50

OS_280

CEREBRAL BLOOD FLOW CHANGES AS ASSESSED BY 99M-TC-HMPAO SPECT IN TWO SUBGROUPS OF MAJOR DEPRESSIVE DISORDER PATIENTS

M.M.E. Pagani (1), A. Gardner (2), D. Salmaso (3), G. Lindberg (2), C. Jonsson (4), H. Jacobsson (4), A.M. Danielsson (4), A. Sanchez-Crespo (4), P.O. Schnell (4), T. Hälström (2), S.A. Larsson (4)(1) Institute of Neurobiology and Molecular Medicine, CNR, Rome, Italy; (2) Neurotec, Section of Psychiatry And Department of Medicine, Karolinska Institute, Huddinge University Hospital, Stockholm, Sweden; (3) Institute of Psychology, CNR, Rome, Italy; (4) Section of Nuclear Medicine, Department of Hospital Physics, Karolinska Hospital, Stockholm, Sweden

Aim: The Karolinska Scale of Personality (KSP) rates 135 items with a four-point response format summed up to 15 scales focused on personality traits that are thought to have biological correlates. It includes scales associated with vulnerability to depressive disorder. Altered scores have been reported in Major Depressive Disorders (MDD), including patients suffering of Psychic Anxiety (ANX) and Socialisation (SOC) disorders. The aim of this study was to identify the cortical and subcortical brain regions showing regional cerebral blood flow (rCBF) changes in patients with altered Anxiety and Socialisation KSP scores.
Methods: The rCBF distribution at rest in two sub-groups of 19 MDD patients each with high ANX score and low SOC score was compared to that of 28 normal controls (CTR). 99mTc-HMPAO SPECT, using a three-headed gamma camera, was performed and intersubject group analysis was carried out by a Computerised Brain Atlas able to standardize brain anatomy in 3D space. The uptake in 27 functional subvolumes of the brain bilaterally, including the most of Brodmann (B) areas, basal ganglia and thalamus, was analyzed by analysis of variance. The significance level was set at $p = 0.05$.
Results: No age difference was found between the groups. Both patients to control comparisons showed a significant global interaction ($p<0.02$). No effect of hemispheres was found in neither comparison. In the CTR/ANX comparison, group x VOI interaction was significant in the prefrontal cortex for B9, B10, B46, basal ganglia and the thalamus. Significant interactions where also found in CTR/SOC comparison in B9, B10, in auditory cortex, in the Broca area, thalamus and putamen. In all these regions there was a significant rCBF increase. The KSP scores did not correlate to rCBF in any of the functional subvolumes.
Conclusions: Two sub-groups of major depressed patients selected according to their altered Anxiety and Socialisation KSP scores showed significant rCBF increases. These changes were evident in the prefrontal cortex and central structures in both pathological groups. Patients with Socialisation disorders showed an increased flow also in auditory and language production cortex. These findings confirm rCBF changes in psychiatric disorders and encourage the use of standardisation software for comparison to normal controls and for making group and individual diagnosis.

OS_281

ACUTE REGIONAL CEREBRAL BLOOD FLOW CHANGES IN DEPRESSED PATIENTS RECEIVING REPETITIVE TRANSCRANIAL MAGNETIC STIMULATION

W. Haindl (1), C. Loo (2), P. Mitchell (2), P. Sachdev (2), X. Zheng (1), S. Som (1), B. Walker (1). (1) Department of Nuclear Medicine; (2) Department of Psychiatry, Prince of Wales Hospital, Sydney, Australia.

Electroconvulsant therapy (ECT) is very effective in treatment resistant severe depression with response rates of 70-90%. However, ECT has major limitations including the need for anaesthesia and memory difficulties. Repetitive transcranial magnetic stimulation (rTMS) has been used as a diagnostic technique in neurology and recent reports suggest a potential therapeutic benefit in depressed patients. rTMS is now under assessment as a possible alternative therapy for resistant depression but its mechanism of action is unclear.

Aim: Frontal lobe perfusion reduction is a common finding in depression. The aim of this study was to determine if the use of rTMS results in acute regional cerebral blood flow (rCBF) changes in the frontal lobes.

Methods: In this study, 5 patients (3 females, 2 males aged 36 to 66 years mean 48.6 years) with major depression underwent SPECT brain scanning using a Picker 3000 triple headed camera. Each patient had a baseline rCBF scan following the IVI injection of 500MBq of Tc-99m-HMPAO during sham rTMS. On the following day, each patient received another 500MBq injection of Tc-99m-HMPAO during rTMS to the left dorsolateral prefrontal cortex. A Magstim Super Rapid magnetic stimulator with a 70mm figure eight coil was used. The stimulator parameters were: 15Hz, 90% of resting motor threshold, 1s on 3s off for 30 trains prior to injection and 15 to 30 trains following injection. Each patient continued to receive their usual medication during this period. The reconstructed SPECT data sets were normalised to the global mean and registered to the Talairach template. Statistical Parametric Mapping (SPM) and ROI analyses were performed.

Results: Compared with the baseline group, the rTMS group showed a significant perfusion increase in the pre-frontal cortices, especially on the left ($p<0.05$).

Conclusions: This study demonstrates the ability of rTMS to acutely increase frontal lobe perfusion. This increase in frontal lobe perfusion is a possible mechanism for the therapeutic action of rTMS when it is used as an adjunct to pharmacological therapy or as an alternative to ECT in resistant depression.

OS_282

STRIATAL DOPAMINERGIC D2 RECEPTOR DENSITY: A PROGNOSTIC MARKER IN SCHIZOPHRENIA?

A.M. Catafau, I. Corripio, V. Perez, A. Tembl, J.C. Martin, V. Camacho, A. Flotats, M. Estorch, E. Alvarez, I. Carrio. Department of Nuclear Medicine, Hospital Sant Pau, Barcelona, Spain.

Imaging studies of striatal dopaminergic D2 receptor (D2R) density in neuroleptic-naive schizophrenic patients have been reported controversial results. Some studies have found increased D2R in these patients, whereas other studies fail to show differences from normal controls. Furthermore, a consistent relationship between D2R and clinical parameters at diagnosis has not been demonstrated. However, the association between D2R and prognostic factors has not been studied so far. Although DSM-IV prognostic factors and previous psychosocial adaptation are widely used to predict clinical outcome in schizophrenic patients, subjectivity is a major drawback. Therefore, a prognostic marker would be useful. Aim: To investigate the relationship between striatal D2R density and prognostic factors in neuroleptic-naive schizophrenic patients.

Methods: ^{123}I-IBZM SPECT was performed on 13 neuroleptic-naive schizophrenic patients (DSM-IV criteria; 8 m, 22.7±3.5 yrs), using a double-headed camera fitted with fanbeam collimators. D2R density was assessed by means of striatum/occipital uptake ratios (S/O). Psychopathological evaluation was performed using the PANSS and BPRS scales. Previous psychosocial functioning was evaluated by means of the Premorbid Adjustment Scale (PAS). Based on the 4 DSM-IV criteria for good prognosis, patients were divided in two groups: good prognosis if two or more criteria were fitted (n=7), and bad prognosis if < 2 criteria were fitted (n=6). S/O ratios previously obtained from a control group of 10 healthy volunteers (5m, 33.8±8 yrs) were used for comparison.

Results: Patients with bad prognosis showed higher S/O ratios (1.86±0.13) than patients with good prognosis (1.63±0.09) and the control group (1.70±0.12) (ANOVA p=0.007, post-hoc Scheffé p<0.05). PAS scores were significantly different between patients with good and bad prognosis (36±10 vs. 74±27, Mann-Withney U-test p=0.006). A direct correlation of S/O ratios and PAS scores was found (Spearman r=0.64, p=0.02).

Conclusions: Striatal D2R density in naive schizophrenic patients relates to DSM-IV prognostic factors and premorbid adjustment criteria (PAS). Therefore, striatal D2R density may predict clinical outcome and offer prognostic information in neuroleptic-naive patients. (FIS 00/0335)

OS_283

STRIATAL AND EXTRA-STRIATAL D2/D3 RECEPTOR BLOCKADE OF LOW-DOSE RISPERIDONE TREATMENT: AN [123I]-EPIDEPRIDE STUDY

R.A. Bressan (1), K. Erlandsson (2), H.M. Jones (1), R.S. Mulligan (2), P.J. Ell (2), L.S. Pilowsky (1). (1) Institute of Psychiatry, London, UK. ; (2) Institute of Nuclear Medicine, University College Medical School, London, UK.

Aim: The limbic cortical selectivity over striatal D_2/D_3 receptor blockade by atypical antipsychotics is a putative mechanism for their therapeutic efficacy without extrapyramidal side effects. We report preliminary SPET scans of schizophrenic patients using the high affinity radioligand [^{123}I]-epidepride to evaluate the limbic selectivity of blockade of low dose risperidone.

Methods: Dynamic SPET data were obtained during 6 hours postinjection (151MBq), using a high-resolution triple-headed brain scanner (Marconi Prism 3000XP). Reference region model analysis was performed to obtain binding potential values relative to a cerebellar reference area. Estimates of receptor occupancy were made relative to a normal volunteer control group (n=5).

Results: Six patients treated with low-dose risperidone (mean=2.6 mg) showed moderate levels of occupancy in striatum (43%) and thalamus (58%), but high levels of occupancy in temporal cortex (73%) and frontal cortex (76%) (see figure 1).

Conclusion: Although risperidone has high affinity for D_2/D_3 receptors, these results suggest that treatment with low doses unlike typical antipsychotics induce high temporal cortex/striatum ratios. It seems that risperidone, like atypical antipsychotics with low D_2/D_3 affinity such as clozapine, olanzapine and quetiapine, has limbic selectivity

Figure 1: BP values for normal volunteers and schizophrenic patients in striatum, temporal cortex, thalamus, and frontal cortex.

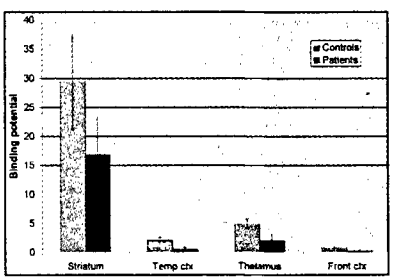

OS_284

DOPAMINE D2 RECEPTOR SPECT IN SCHIZOPHRENIC PATIENTS TREATED BY QUETIAPINE

L. Pavics (1), G. Szekeres (2), E. Ambrus (1), A. Juhasz (2), SZ. Keri (2), Z. Kovacs (2), L. Galuska (3), Z. Janka (2). (1) Department of Nuclear Medicine, University of Szeged, Szeged, Hungary; (2) Department of Psychiatry, University of Szeged, Szeged, Hungary; (3) Department of Nuclear Medicine, University of Debrecen, Debrecen, Hungary.

Quetiapine is a novel antipsychotic substance with a relatively short half-life and a low affinity for dopamine D2 receptors. PET and SPECT studies demonstrated individually different D2 receptor occupancies during quetiapine monotherapy.

In the present study, the D2 receptor occupancy was investigated in quetiapine-treated schizophrenic patients for detection of the relationship between the scintigraphic pattern and clinical sign and symptoms.

Method: In 10 schizophrenic patients (7 women, 3 men, age ±SD: 34±7 PANSS score: 72 ±20), IBZM SPECT (185 MBq, acquisition was started 90 min p.i.) was performed during the introduction of quetiapine therapy (600-800 mg/day) and during a lower maintenance dose (200-400 mg/day). All the patients were receiving quetiapine monotherapy. Simultaneously with the SPECT investigations, visual contrast standardised rating scales were used to determine the sensitivity, clinical symptoms and exrapyramidal signs. For evaluation of the SPECT images, visual interpretation and striatum/occipital lobe (S/O) activity ratio calculation were applied.

Results: The striatum/occipital lobe ratio was 1.7±0.23 (SD) in the first investigation and in the second one 1.68±0.12 (SD). The receptor occupancy was individually different, but no significant difference was observed in relation to the quetiapine dose used. There was no difference in visual contrast sensitivity and no patients displayed extrapyramidal signs. In 6 subjects in a clinically steady state, the S/O ratio increased by 1-35% on decrease of the dose of quetiapine, without a long-term relapse, but in 4 the decreased S/O ratio (9-29%) was accompanied by clinical relapse of the disease. The endogenous dopamine release, transporter changes and the roles of other receptors might be responsible for this finding.

Conclusion: There is no direct relationship between the quetiapine dose and D2 receptor occupancy. Other receptors should also be investigated for clarification of the effect of quetiapine in schizophrenics.

OS_285

TEMPORAL LOBE DYSFUNCTION IN AUTISM: A PET AUDITORY ACTIVATION STUDY

N. Boddaert (1), P. Belin (1), N. Chabanne (2), M.C. Mouren-Simeoni (2), C. Barthelemy (3), M.J. Ribeiro (1), Y. Samson (1,4), M. Zilbovicius (1,3). (1) Service Hospitalier Frédéric Joliot, DSV-CEA, Orsay, France; (2) Hôpital Robert Debré, Paris, France; (3) Unité INSERM U316, CHU Bretonneau, Tours, France; (4) Hôpital la Salpétrière, Paris, France

Aim: We have recently described a bitemporal hypoperfusion at rest in children with primary autism (Zilbovicius et al., 2000). This dysfunction is centered in the associative auditory and adjacent multimodal cortex located in the superior temporal gyrus (STG) and in the superior temporal sulcus (STS). In healthy volunteers, these regions are highly activated by complex synthetic sounds containing speech-like spectral modulation (SM) (Thivard et al., 2000). A dysfunction of the auditory cortex may explain sensory abnormalities and language impairments in autism. Therefore, we performed an auditory activation study in autistic children in order to investigate the cortical response to speech like auditory stimuli.
Methods: A PET $H_2{}^{15}O$ activation study was performed in eleven autistic children (mean age ± sd: 9.2 ± 4.5 years) and 6 non autistic children (mean age ± sd: 7.2 ± 2.4 years) after slight premedication. rCBF was measured in two conditions : a) rest and b) passive listening to synthetic sounds containing speech-like SM. We used auditory stimuli that contained spectral maxima (like the formants of speech) that were changing in time. They were synthesized using Klatt cascade/parallel speech synthesizer, and consisted of complex sounds with a central 200 ms steady-state period surrounded by initial and final changes in frequency of the spectral maxima. Data analysis was conducted using SPM96 (multi-study design).
Results: Compared to rest, passive listening to sounds containing speech-like spectral modulations induced a significant bilateral activation of the primary auditory cortex and the superior temporal gyrus in both groups. However, a direct comparison of the two groups revealed a significantly (Z score = 3.28; $p < 0.001$) higher activation of the left posterior STG in the non-autistic group. This posterior auditory associative region was deactivated in the autistic group.
Conclusions: These findings suggest that autism is associated with an abnormal pattern of activation of the left speech related cortical areas. This could be implicated in the communication impairments and in the inadequate behavioral response to sounds characteristics of autism.

OS_286

BINDING POTENTIAL FOR I-123 ALTROPANE IS INCREASED IN STRIATUM OF YOUNG ADHD PATIENTS: RESULTS OF A MULTI-CENTER TRIAL

A.J. Fischman, A.A. Bonab, D. Feifel, C. Hoh, R.A. Barkley, R. Lichio, J.J. McGough, F. Mishkin, P. Tuite, B.K. Madras, M.E. LanserDepartment of Nuclear Medicine, Massachusetts General Hospital, Boston MA, USA.

Aim: Attention deficit hyperactivity disorder (ADHD) is one of the most common psychiatric conditions in children. Currently, the most effective treatments for ADHD are drugs that block dopamine transporter (DAT) sites, i.e. methylphenidate and amphetamine. Also, several studies have implicated variations in DAT alleles in the pathophysiology of ADHD. Recently, we demonstrated that DAT binding potential (B'max/Kd) measured by SPECT with the highly selective DAT ligand, I-123 Altropane, was elevated in 7 adults (age 24-54) with ADHD (The Lancet 1999; 354: 2132-2133). Unfortunately, since BP normally decreases with age and only one patient <30 years of age was studied, it remains uncertain if SPECT with I-123 Altropane is useful for detecting ADHD in young adults and children.
Methods: To address this issue, a multicenter trial was performed at 4 major academic centers in the United States. Twenty ADHD patients (age 18-40) and 20 age matched healthy volunteers were recruited for this study. All subjects were injected with approximately 5 mCi of I-123 Altropane and serial SPECT images were acquired over 60 min. Time-activity curves (TAC's) derived from striatal regions of interest (STR) and occipital cortex (OCC, a reference region devoid of DAT sites) were used to calculate the function, STR - OCC, which defines the time dependence of bound tracer. By fitting these data to a gamma variate function and division of the maximum by the value of the OCC TAC at the same time, an equilibrium estimate of BP was derived.
Results: Of the 40 subjects that were studied, evaluable SPECT data was obtained in 24 cases (16 controls and 8 ADHD patients). The primary reason for the large number of unevaluable cases was head motion during acquisition of the SPECT data. Nonetheless, for the evaluable subjects, BP extrapolated to age 25 was consistently elevated (mean ± sem) in ADHD patients compared with controls; 3.08 ± 0.16 vs. 2.37 ± 0.057, $p<0.001$.
Conclusions: These results indicate that striatal DAT density is elevated by approximately 30 % in young adult ADHD patients and suggest that Altropane SPECT could be of value in diagnosing this condition.

DIAGNOSTIC ONCOLOGY

OS_287

UTILITY OF FDG PET IN UNKNOWN PRIMARY TUMORS (UPT)

R.C. Delgado Bolton (1), A. Ortega (2), R. de Juan Rubio (1), A. González-Maté (1), M.J. Pérez-Castejón (2), M. Domper (2), A. Jiménez Vicioso (2), R. Montz (2), J.L. Carreras Delgado (1). (1) Nuclear Medicine, Hospital Clínico San Carlos, Madrid, Spain; (2) Instituto PET Dr Carreras, Madrid, Spain.

Aim: To evaluate the utility of PET with FDG in patients with unknown primary tumors (UPT). UPT is defined as the presence of microscopically confirmed metastatic malignancy in the absence of an identifiable primary tumor site. Detection of the primary tumor site and careful staging of the UPT are of utmost importance as the therapeutic approach depends on both aspects.
Methods: FDG PET scans were performed in thirty-six patients following extensive but inconclusive diagnostic work-up. Patients were divided into two groups: (1) Twenty-one patients with *strict* UPT presenting metastatic cervical adenopathy (n=7) or extracervical metastasis (n=14). (2) Fifteen patients with *non-strict* UPT in which, despite negative clinical and diagnostic procedures, malignant disease was suspected but not confirmed microscopically (n=15). FDG PET results were verified either histologically or by clinical follow-up.
Results: The thirty-six patients were divided into the two groups mentioned previously: (1) In 21 patients with *strict* UPT, FDG PET suggested the site for the primary tumor in 13 patients located in the lung (n=8), cholangiocarcinoma (n=1), breast (n=1), ovarian (n=1), lymphoepithelioma (n=1), lung or pancreas (n=1). In 12 (57%) FDG PET was true-positive, the only false-positive identifying metastatic lesions but no primary tumor. FDG PET did not identify a primary tumor in the remaining 8 patients, being false-negative in two of them, as a primary tumor was later identified in pancreas (n=1) and tongue (n=1). In the other 6 patients (28.6%) no primary site has been found after a follow-up of 2-24 months. (2) In 15 patients with *non-strict* UPT, FDG PET showed potential primary tumor sites in 9 patients located in the lungs (n=3), colorectal (n=2), pancreas (n=1), biliary tract (n=1), parotid gland (n=1). In 8 (53%) FDG PET was true-positive. FDG PET did not reveal lesions suspected to be primary in 6 patients, being false-negative in one of them in which a pancreatic tumor was identified in a later phase. In the other 5 patients (33%) no primary tumor was found at clinical follow-up (2-24 months). Sensitivity (S), Specificity (E), Positive Predictive Value (PPV), Negative Predictive Value (NPV) and Accuracy (Ac) were: Group (1): S=0.86, E=0.86, PPV=0.92, NPV=0.75, Ac=0.86. Group (2): S=0.89, E=0.83, PPV=0.89, NPV=0.83, Ac=0.87.
Conclusions: FDG PET is a useful diagnostic tool in patients with UPT because it is able to detect the unknown primary tumor in 57% of *strict* UPT and 53% of *non-strict* UPT. Furthermore, FDG PET could be of help in accurately staging the malignant disease.

OS_288

18-FDG-PET IN MEDULLARY THYROID CANCER: RESULTS OF A MULTICENTRE STUDY

M. Diehl (1), J.H. Risse (1), K. Brandt-Mainz (2), M. Dietlein (3), K.M. Bohuslavizki (4), P. Matheja (5), H. Lange (6), J. Bredow (7), C. Körber (8), F. Grünwald (1). (1) Departments of Nuclear Medicine, Frankfurt/Main ; (2) Essen; (3) Cologne; (4) Hamburg, Germany

Aim: The aim of this study was to evaluate the clinical value of fluorine-18 fluorodeoxyglucose positron emission tomography (FDG-PET) in medullary thyroid cancer (MTC) in comparison to ^{111}In-Pentetreotide (SMS), ^{99m}Tc-V-DMSA (DMSA), ^{99m}Tc-Sestamibi (MIBI), computed tomography (CT) and magnetic resonance imaging (MRI).
Methods: One hundred PET examinations in 85 patients (40 m, 45 f) with elevated tumor marker levels and/or pathologic findings in other imaging methods were evaluated retrospectively. Histological confirmation of fifty-five lesions was obtained.
Results: The results are shown in the table.

	Number of studies	Positive lesions*	Total positive°	Lesion detection proba-bility	Number of histo-logic exa-minations	True positive	False positive	True negative	False negative
CT	64	56	119	47%	21	8	4	1	8
MRT	37	36	73	49%	26	14	3	6	3
Octreo	46	22	89	25%	24	3	1	11	9
MIBI	8	1	17	6%	9	1	0	5	3
DMSA	33	19	65	29%	18	3	2	7	6
PET	100	123	181	68%	55	32	3	11	9

Number of lesions classified as positive with each imaging technique* and total number of positive lesions detected with all imaging methods in these patients°

FDG-PET showed a sensitivity of 78 % and a specificity of 79 %. The sensitivity and specificity of SMS were 25 % and 92 %, of DMSA 33 % and 78 %, of MIBI 25 % and 100 %, of CT 50 % and 20 % and of MRI 88 % and 67 %, respectively.
Conclusions: The highest lesion detection probability for tumor tissue of MTC was found in FDG-PET. PET also showed a high sensitivity and specificity. PET was superior to the other morphologic and functional imaging methods. Only MRI showed results comparable to PET. Therefore, it is concluded that FDG-PET is a useful method in the diagnosis and follow-up of MTC.

OS_289

METASTATIC LYMPH-NODES IN CERVICAL CANCER: DETECTION WITH MRI OR FDG-PET?

M.J. Reinhardt (1), T. Bauknecht (2), C. Ehritt-Braun (3), C. Ihling (4), D. Vogelgesang, A. Joe, H. Palmedo (1), E. Moser, H.J. Biersack (1), T. Krause (1). (1) Dept. of Nuclear Medicine, Univ. Hospital Bonn, Germany; (2) Dept. of Gynecology, Univ. Hospital Bonn, Germany; (3) Dept. of Diagnostic Radiology, Univ. Hospital Freiburg, Germany; (4) Institute of Pathology, Univ. Hospital Freiburg, Germany

Aim: To compare sensitivity and specificity of magnetic resonance imaging (MRI) with that of positron emission tomography (PET) using fluoro-deoxy-glucose (FDG) for detection of metastatic lymph nodes in patients with cervical cancer.
Methods: Abdominal FDG-PET and MRI were performed prior to radical hysterectomy and radical pelvic lymphadenectomy including the paraaortic lymph nodes in 35 patients (aged 49±13 years) with FIGO stage IB or IIA cervical cancer. Nine lymph node sites were evaluated in each patient. Malignancy criteria were a lymph node diameter of 1 cm or more at MRI and a focally increased FDG-uptake at PET. The findings of FDG-PET and of MRI were compared with histology of the removed tissue.
Results: Histological examination revealed pN0-stage cancer in 24 patients and pN1-stage cancer in 11 patients. On a patient basis, N-staging resulted in sensitivities of 0.91 with FDG-PET and 0.73 with MRI and specificities of 1.0 with FDG-PET and 0.83 with MRI. The positive predictive value (PPV) of FDG-PET was 1.0 and of MRI, 0.67 (not significant). Metastatic involvement of lymph node sites was identified by FDG-PET with a PPV of 0.9 and by MRI of 0.64 ($p<0.05$, Fisher's exact test).
Conclusion: Metabolic imaging with FDG-PET is an alternative to morphological MR imaging for detection of metastatic lymph nodes in patients with cervical cancer. FDG-PET may be more accurate than MRI for adapting the extent of the field of radiation because a single metastatic lymph node site can be identified with a significantly higher positive predictive value.

OS_290

THE ROLE OF 18FDG-PET IN INITIAL STAGING AND THERAPY CONTROL OF TESTICULAR GERM CELL TUMOURS

W.J.G. Oyen (1), J.R. Spermon (2), L.F. de Geus-Oei (1), L.A.L.M. Kiemeney (3), J.A. Witjes (2), F.H.M. Corstens (1). (1) Department of Nuclear Medicine; (2) Urology; (3) Epidemiology, University Medical Center Nijmegen, The Netherlands.

Aim. This study investigated the role of ^{18}Fluoro-2-deoxyglucose (^{18}FDG) in initial staging of clinical stage (CS) I and II nonseminomas (NSGCT) and in restaging of (non)seminomas after chemotherapy.
Methods. 57 FDG-PET studies were performed in 40 patients. FDG uptake was interpreted visually and when possible the standardized uptake value (SUV) was determined. A FDG-PET scan was performed in 5 patients with CS I and in 7 with CS II NSGCT. The scans were validated by histology. CS I patients underwent a retroperitoneal lymph node dissection because of vascular invasion in the primary tumour.
Twenty-eight scans were performed after completion of chemotherapy (21 NSGCT, 7 seminomas (SGCT)), and validated by histology or clinical follow-up. In 8 patients also a serial FDG-PET scan was performed to monitor the treatment response.
Results. In CS I NSGCT, FDG-PET staging was equivalent to CT staging. One small lesion, consisting of mature teratoma (MT), was missed by both FDG-PET and CT scan. In CS II NSGCT, the FDG-PET missed two lesions (MT and small component of embryonal cell carcinoma) whereas CT classified all correctly.
In restaging NSGCT after chemotherapy, increased accumulation of FDG-PET was detected in 10 of the 21 scans. Two lesions represented persistent malignant residual mass. In two patients only increased pulmonary uptake was found, while necrosis was found retroperitoneally. Both showed no evidence of disease at follow-up. In six scans inflammatory components were seen, supplemented with MT in four of them. Eleven FDG-PET studies were negative. In seven of them MT was found both in the primary tumour and residual mass. The remaining four were negative staged on histology (n=2) or showed no evidence of disease at follow-up (n=2). Of interest, none of them had a MT in the primary tumour.
Six of seven patients with SGCT were correctly staged. One false-positive result was obtained due to inflammation of the residual mass. In the other patients FDG-PET scan correctly predicted absence of tumourviability.
Serial FDG-PET showed a decrease of metabolic activity in two patients whereas the size of the retroperitoneal mass did not change.
Conclusions. In primary staging, FDG-PET has no benefit over CT. However, it might be useful in CS II to prevent false-positive lesions on CT. In restaging, FDG-PET predicts fibrotic residual mass in SGCT and possibly also in NSGCT without a teratoma component in the primary tumour. Serial FDG-PET might be useful in predicting the therapy response.

OS_291

DETECTION OF RECURRENCE OF OVARIAN CANCER : PERFORMANCE OF [18-F]-FDG SCAN USING A DUAL-HEAD COINCIDENCE GAMMA CAMERA (CDET)

K. Kerrou, F. Montravers, D. Grahek, N. Younsi, V. De beco, C. Colombet-lamau, Y. Petegnief, JN. Talbot. Service de Médecine Nucléaire, Hôpital Tenon, Paris, France.

Aim : The aim of this study was to evaluate the role of [F-18]-FDG-CDET in the detection of recurrence of ovarian cancer.
Methods and patients: After a fast of 6 hours, the patient (pt) was injected I. V. with 150-250 MBq of [F-18]-FDG and imaging (whole-body scan and at least a tomoscintigram) was started 60 min. later, using a PICKER Prism XP 2000 CDET gamma camera.
Between July 1997 and December 2000, 79 patients were studied for suspected recurrence of ovarian carcinoma.
To date, the results of 49 patients are evaluable with reference to histology after surgery or long-term follow-up. From these, 22 pts were referred for occult recurrence (OR) defined by an increase in serum CA-125 levels with negative conventional imaging and the remaining 27 pts for equivocal aspect at conventional imaging (ECI).
Results: [18-F]-FDG was true positive (TP) in 36 cases all confirmed by histology after surgery (17 OC and 19 ECI). [18-F]-FDG was true negative (TN) in 10 cases (4 OC and 6 ECI) as confirmed by spontaneous normalization of CA-125 levels and no events during a 20-month follow-up for 7 pts and histology after surgery for 3 pts.
[18-F]-FDG was false negative (FN) in 3 pts (2 OC and 1 ECI) with one brain metastasis, one lymph node of less than 10 mm size and one patient with continuing increase of CA-125 and still negative conventional imaging in the follow-up
In summary, the overall sensitivity, specificity and accuracy on a per patient basis were respectively 36/39 (92%), 10/10 (100%) and 46/49 (94%) for FDG-CDET while sensitivity, specificity and accuracy of conventional imaging was respectively 19/39 (49%), 4/10 (40%) and 23/39 (59%).
Conclusion: These results showed a very good performances of [18-F]-FDG scan on CDET gamma cameras, for the detection of recurrence of ovarian cancer.

OS_292

CARBON-11 ACETATE PET IMAGING IN PROSTATE CANCER PATIENTS WITH RISING PSA AFTER RADICAL THERAPY: PRELIMINARY RESULTS

A. Kurtaran (1), S. Wachter (2), A. Becherer (1), S. Ofluoglu (1), J. Schmaljohann (1), B. Djavan (3), R. Dudczak (1), K. Kletter (1). (1) Department of Nuclear Medicine; (2) Department of Radiotherapy; (3) Department of Urology, University of Vienna, Austria.

Despite recent advances in imaging techniques localization of local as well as metastatic disease of prostate cancer after radical therapy (radical prostatectomy, radiation therapy) continues to be a diagnostic challenge. Recent reports suggested a promising clinical value of C-11 acetate PET imaging in prostate cancer.
Aim: This study aims to evaluate the potential role of C-11 acetate PET imaging in patients with rising PSA after radical therapy in choosing the appropriate treatment option (local vs. palliative therapy).
Methods: Nine clinically asymptomatic patients with rising PSA and evidence of recurrent/metastatic disease by bone scan and/or CT/MRI have been evaluated. C-11 acetate dynamic imaging of the prostate region was performed after i.v administration of 700 MBq of C-11 acetate followed by whole body scan. C-11 acetate PET images were analyzed by visual interpretation. In case of abnormal C-11 acetate uptake in previously unknown localizations, additional radiological work up was performed.
Results: In one patient with suspected solitary tumor site by bone scan, no correlation could be found by either C-11 acetate nor CT/MRI study. Increased C-11 acetate uptake was found in 8 out of 9 patients corresponding to the pre-known lesions (bone Mts, lymph-node involvement, local recurrence). In addition, increased C-11 acetate uptake were documented in previously unknown localizations.

Conclusion: Our preliminary data demonstrate the clinical feasibility of C-11 acetate PET whole body imaging in patients with prostate cancer and rising PSA after radical therapy. C-11 acetate PET imaging may therefore be helpful to select patients with local disease from those having distant metastases to choose the most approriate therapy option.

OS_293

DISTRIBUTION AND RELEVANCE OF SATELLITE LESIONS DIAGNOSED WITH METABOLIC IMAGING OF THE LUNGS

C. Schiepers (1), C.S. Yap (1), M. Fishbein (2), J.E. Filmont (1), M.E. Phelps (1), J. Czernin (1). (1) Ahmanson Biological Imaging Center; (2) Pathology, UCLA School of Medicine, Los Angeles, California, USA .

Aim: Lung lesion characterization, staging and re-staging of lung cancer are well known indications for FDG PET imaging. A high sensitivity has been reported for solitary nodules (SPN) as well as a false positive rate of 10-20% dependent on geography. The performance for multiple lobar lesions, i.e. T4 staging, is not clear. We retrospectively evaluated studies with ≥2 parenchymal lung lesions on PET that had a final pathological diagnosis.
Methods: Referrals for characterization or staging of lung lesions between January 98 and August 00 were selected. There were 314 patients, 29 of whom (9.2%) had 2 or more hypermetabolic lung lesions. Lesions in the mediastinum were specifically excluded. In total 12 males and 17 females, with median age 65, range 43-82 yr. were analyzed.
Results: Referral indication was lesion characterization in 21% and staging in 79% of patients. By pathology, there were 73% adeno-carcinomas, 14% squamous and 1 small cell lung cancer. Half of the adenos were BAC. The PET lesions involved lung cancer in 26 primaries (Sensitivity 90%), in 52% of first satellite and 40% of second satellite lesions. Lesion size in cm (mean±sd) was 3.8±2.5 for primaries and 1.7±0.9 for first satellites. Stratification into mild, moderate and intense uptake patterns yielded: moderate or intense uptake for all primaries, compared to mild to moderate uptake for most satellites. The lesions were most often located in the upper lobes: primary tumors 72% (24% right 48% left), first satellite 69%, and second satellite 62%. Satellites diagnosed as false positive by PET were caused by inflammation in 44%, pneumonia in 21%, and granuloma in 14% of patients. The remaining 21% represented metastatic lobar lymph nodes and are, therefore, true positive lesions.
Conclusions: In patients with multiple parenchymal lung lesions, the diagnostic performance of whole body PET for the primary tumor is no different than for SPNs, whereas satellite lesions represented cancer in 62%. Most of the lesions were in the upper lobes (about 70%). About three-quarters of the lesions were adeno-carcinomas, half of which BAC, known to have multi-focal involvement. The primary tumor had generally significantly higher uptake than the satellites. These findings do not support opinions of poor performance of metabolic imaging for T-staging.

OS_294

QUANTITATIVE FDG-PET STUDIES FOR THE DIFFERENTIATION OF MALIGNANT AND BENIGN BONE LESIONS

A. Dimitrakopoulou-Strauss (1), T. Heichel (2), L. Bernd (2), B. Lehner (2), C. Burger (3), V. Ewerbeck (2), L.G. Strauss (1). (1) Dept. of Oncological Diagnosis and Therapy, German Cancer Research Center, Heidelberg, Germany; (2) Dept. of Orthopedic Clinics, Univ. of Heidelberg, Germany; (3) Dept. of Nuclear Medicine, Univ. of Zurich, Switzerland.

Aim: Assessment of the value of quantitative FDG-PET studies for the differentiation of benign and malignant bone lesions.
Methodology: The evaluation comprises a total of 108 patients. Malignancies were confirmed in 40 cases, while benign lesions were found in 50 patients. Thirty six of the 50 benign lesions were histologically confirmed. The FDG studies were accomplished as dynamic series for 60 minutes. The evaluation of the FDG kinetics was performed using the following parameters: SUV, global influx, computation of the transport constants K1-k4 with consideration of the distribution volume (VB) according to a two-tissue compartment model, fractal dimension based on the box counting procedure (parameter for the inhomogeneity of the tumors).
Results: The mean SUV, the vascular fraction VB, K1 and k3 were significantly higher in malignant tumors as compared to benign lesions (t-test, $p<0.05$). However, FDG SUV alone was found to be of limited value due to an overlap in the uptake values, which limits the diagnostic accuracy. Based on the discriminant analysis, SUV alone revealed a sensitivity of 81.5 %, a specificity of 71.7 % and a diagnostic accuracy of 70.7 %. The fractal dimension demonstrated a sensitivity of 78.1 %, a specificity of 78.6 % and an accuracy of 73.4 %. The combination of SUV, fractal dimension, VB, K1 to k4 and global influx revealed the best results with a sensitivity of 92 %, a specificity of 81.8 % and an accuracy of 85.7 %. Bayesian analysis demonstrated true positive results (with a diagnostic accuracy of $p=0.8$) even for a low prevalence of disease (prevalence of disease $p=0.235$) if the full kinetic data are used in the evaluation.
Conclusion: The evaluation of the full FDG kinetics and the application of discriminant analysis are required and superior to one static measurement for the differential diagnosis of intraosseous bone lesions.

CARDIOVASCULAR

OS_295

CONTINUOUS LEFT VENTRICULAR FUNCTION MONITORING DURING EXHAUSTING EXERCISE IN ATHLETES WITH ELECTROCARDIOGRAPHIC VENTRICULAR REPOLARIZATION ABNORMALITIES

A. Flotats (1), R. Serra-Grima (2), V. Camacho (1), M. Estorch (1), E. Mena (1), A. Tembl (1), JC. Martín (1), AM. Catafau (1), X. Borràs (2), J. Cinca (2), I. Carrió (1)(1) Nuclear Medicine Department; (2) Cardiology Department, Hospital Sant Pau, Barcelona, Spain.

Aim: The clinical significance of ventricular repolarization abnormalities (VRA) in trained athletes remains uncertain. The aim of the study was to analyze the dynamic response of left ventricle (LV) during exhausting exercise in male trained athletes with VRA in the ECG.
Methods: Eighteen athletes with VRA (negative T waves ≥ 2mm in up to 3 ECG leads at rest) and 17 with no VRA underwent monitoring of LV function with a miniaturized radionuclide detector (C11 Vest) during bicycle upright exhausting exercise test. All athletes were symptom free. Age and physical performance between both groups were comparable.
Results: One athlete with VRA was excluded due to hypertrophic cardiomyopathy. The rest of athletes showed normal ventricular dimensions for highly conditioned sportsmen. During the exercise test, athletes with VRA showed a tendency to normalize the ECG abnormalities, with no significant ST segment changes in athletes with no VRA. Both groups of athletes showed similar heart rate (HR), LV volumes, LVEF, cardiac output, stroke volumes (SV) and peak ejection and filling rates at baseline, 50% and 75% of maximal HR, and at peak HR. Both groups attained a similar workload corrected by body weight at physical exhaustion. However, athletes with VRA showed a significant decrease of end-systolic volume (ESV) at 50% of maximal HR leading to an increase of LVEF and SV at 50% of maximal HR. In athletes with no VRA the peak filling rate significantly increased from 75% of maximal HR to peak HR.
Conclusions: The presence of ventricular repolarization abnormalities in highly trained athletes appear to have no functional implications and therefore should not preclude physical training. Ventricular repolarization abnormalities may be associated with an early hyperdynamic cardiac response during intense physical exercise. Vest can be used to evaluate cardiac responses during bicycle exhausting exercise.

OS_296

PULMONARY THROMBO-ENDARTERECTOMY AND HOSPITAL MORTALITY IN CHRONIC POST-EMBOLIC PULMONARY HYPERTENSION: VALUE OF PRE-OPERATIVE RIGHT VENTRICULAR FUNCTION EVALUATED WITH ECG-GATED BLOOD-POOL SPECT

D. Daou (1), C. Coaguila (1), O. Sitbon (2), T. Fourme (3), B.O. Helal (1), F. Parent (2), M. Humbert (2), M. Slama (3), D. Le Guludec (4), G. Simonneau (2). (1) Department of Nuclear Medicine, Antoine Beclere Hospital, AP-HP, Clamart, France; (2) Pulmonary Department, Antoine Beclere Hospital, AP-HP, Clamart, France; (3) Cardiology Department, Antoine Beclere Hospital, AP-HP, Clamart, France; (4) Department of Nuclear Medicine, Bichat Hospital, AP-HP, Clamart, France

Objective: In patients with advanced chronic post-embolic pulmonary hypertension (CPE-PH), pulmonary thrombo-endarterectomy (PTE) is proposed as an effective treatment. Despite much improvement in patient's management and careful selection of patients, the operative mortality of PTE is still high with reported values varying between 10 and 20%. We aimed to study the pre-operative predictors of PTE mortality.
Methods: Thirty-nine consecutive patients with CPE-PH referred for the preoperative work-up of their right ventricular (RV) function with ECG-gated blood-pool SPECT and having PTE have been studied.
Results: During the post-operative hospital period, 87 % of patients survived the PTE operation (Group A) while 13% (n=5 patients) died (Group B). The mean age was significantly different between the 2 groups: 48±16 vs 65±6 ($p=0.025$). The sex (15/34 vs 3/5 males), the NYHA classification for dyspnea (3±0.7 vs 3.2±0.5), the rest heart rate (79±17 vs 72±8 beats/min), the left ventricular ejection fraction (78±17 vs 62±28 %; $p=0.07$) and RV ejection fraction calculated with GBPS (39±11 vs 30±9; $p=0.10$) were not significant predictors of mortality. Similarly, the different hemodynamic parameters (thermodilution) as reflected by mean right atrial pressure (9±7 vs 11±4 mmHg), mean pulmonary artery pressure (55±13 vs 55±9 mmHg), cardiac index (2.1±0.6 vs 1.8±0.2 l/min/m2) and total pulmonary resistance (28±11 vs 30±6 UIxm2) were not predictive of post-operative mortality in respectively GroupA vs Group B. But, the indexed RV end-diastolic and end-systolic volumes (respectively 135±36 vs 171±41 ml/m2, $p=0.04$ and 77±28 vs 112±39 ml/m2, $p=0.017$) as well as pulmonary venous saturation (Svo2) were significantly different between the 2 groups: 61±9 vs 45±9 % ($p=0.002$).
Conclusion: Age, RV volumes and Svo2 may be useful preoperative predictors of hospital mortality in patients with CPE-PH undergoing PTE.

OS_297

AMBULATORY MONITORING OF LEFT VENTRICULAR FUNCTION AT REST AND DURING WALK TEST IN PATIENTS WITH HEART FAILURE UNDERGOING TWO DIFFERENT PACING MODES

A. Ferro (1), M. Santomauro (2), C. Duilio (2), A. Cuocolo (1).
(1) Department of Biomorphological and Functional Sciences;
(2) Department of Cardiology, University Federico II, Napoli, Italy.

The clinical benefit of atrio-ventricular pacemaker rate responsive (DDDR) when compared to traditional ventricular pacemaker at fixed heart rate (VVI) in patients with heart failure is somewhat conflicting. The aim of this study was to assess the effects on left ventricular (LV) function at rest and during moderate physical activity of these two different pacing modes in patients with heart failure. Methods: 8 patients with nonischemic heart failure were studied. All patients had DDDR pacemaker implanted for complete heart block and baseline LV ejection fraction <50%. LV function was continuously monitored by a radionuclide system (Vest). After 10 min at rest, all patients performed 6 min walk-test followed by 10 min of recovery. Thereafter, DDDR was changed in VVI no rate responsive and 6 min later patients repeated walk-test. Results: at rest, during VVI activation, LV ejection fraction, end-diastolic volume, end-systolic volume and peak filling rate showed a slightly but not significant decrease when compared to DDDR, while cardiac output significantly ($p<.05$) reduced after VVI stimulation. Heart rate (HR) increased from baseline to peak of walk test from 95±14 to 109±15 bpm ($p<.01$) only during DDDR activation. Moreover, at peak of both walk tests, all parameters of LV systolic and diastolic function increased ($p<.01$), without any difference between DDDR and VVI. Nevertheless, when value of rest-peak variations were analyzed, LV ejection fraction and peak filling rate showed a higher increase ($p<.05$) during VVI as compared with DDDR. Conclusions: in patients with heart failure, there is a significant reduction of cardiac output and a slight but not significant decrease of LV ejection fraction and peak filling rate after VVI activation as compared to DDDR at rest. These findings may be explained by the lack of atrial contribution during VVI. On the contrary, an opposite effect is found during moderate physical activity as demonstrate by the greater improvement of LV ejection fraction and peak filling rate after VVI. This could account for a negative effect of heart rate *per se* and/or for an excessive load secondary to both atrial contribution and increase in HR.

OS_298

LEFT VENTRICULAR EJECTION FRACTION AND VOLUMES FROM GATED BLOOD POOL TOMOGRAPHIES: A COMPARISON BETWEEN TWO AUTOMATIC ALGORITHMS

C. Vanhove, N. Walgraeve, H. Everaert, P.R. Franken. Department of Nuclear Medicine, Free University Brussels (AZ-VUB), Brussels, Belgium.

Aim. Two different algorithms, which are fast, automatic and operating in the three-dimensional space were compared in the same group of patients to compute left ventricular ejection fraction (LVEF) and volumes from gated blood pool tomography. One method, dependent on surface detection, was developed at the Cedars-Sinai Medical Center (QBS), while the other method, developed at the Free University of Brussels (QUBE) used image segmentation.
Methods. Gated blood pool tomograms (GBPT) were acquired in 92 consecutive patients after injection of 740 MBq of Tc99m labelled Human Serum Albumin. After reconstruction and reorientation according to the left ventricular long axis, LVEF and volumes were measured using the QBS and QUBE algorithms. The LVEF were validated against planar radionuclide angiocardiography (PRNA).
Results. The software success rates were 87% for QBS and 97% for QUBE. Agreement between LVEF measured with QBS and QUBE ($LVEF_{QBS}=0.91LVEF_{QUBE}-0.85; r=0.87$) and agreement between both methods and PRNA was good ($LVEF_{QBS}=1.04LVEF_{PRNA}-4.75; r=0.80$ and $LVEF_{QUBE}=0.98LVEF_{PRNA}+4.42; r=0.82$). For left ventricular volumes, linear regression analysis showed a good correlation between both methods concerning end-diastolic volumes ($r=0.81$) and end-systolic volumes ($r=0.91$). On average, end-diastolic volumes were similar and end-systolic volumes were slightly higher with QBS compared to QUBE. Consequently, significantly lower LVEF were observed using QBS compared to QUBE.
Conclusions. A good correlation was observed between QBS and QUBE for both left ventricular volumes and ejection fraction. In addition, measurements of LVEF obtained with both algorithms correlated fairly with those obtained from conventional PRNA over a wide range of values.

OS_299

SEVERE AORTIC VALVE REGURGITATION ASSESSING: STRESS DOBUTAMINE ECHOCARDIOGRAPHY (SDE) OR STRESS EQUILIBRIUM RADIONUCLIDE ANGIOCARDIOGRAPHY (S-ERNA)?

E. Perrone (1), M. Stanislao (2), S. Modoni (1), G. Valle (1), G. Petracca Ciavarella (1), V. De Rito (2), G. Martino (1), L. Trotta (1), R. Fanelli (2), V. Frusciante (1). (1) Department of Nuclear Medicine; (2) Department of Cardiology, Casa Sollievo della Sofferenza, san Giovanni Rotondo, Italy.

INTRODUCTION: Severe aortic valve regurgitation patients require a careful monitoring in order to properly addresss medical or surgical therapy. At this regard both scintigraphic and echocardiographic techniques have been proposed. Aim of our research has been a comparison of these techniques.
PATIENTS AND METHODS: Twenty-six consecutive patients (20 M, 6 F, mean age 46 year, SD± 13 yea) with severe (18 cases) or moderate (8 cases) aortic valve regurgitation were studied both with SDE and S-ERNA, in order to detect left ventricular (LV) disfunction as evaluated by an insufficient left ventricular ejection fraction increase. All patients underwent a basal study.
In SDE studies dobutamine infusion was performed at 5 gamma/Kg/min for 5 minutes followed by 10 gamma/Kg/min for 3 minutes up to 40 gamma/Kg/min
S-ERNA was performed by intravenous injections of stannous pyrophosphate followed at 15-20 minutes by a second injection of 740 Mbq of 99mTc-pertechnetate.
Heart rate, ECG, blood pressure, LV diastolic volume, LV systolic volume were also recorded. Comparison between SDE and S-ERNA in LV ejection fraction (LVEF) changes both in basal conditions and under stress was performed by Linear Regression Analysis (LRA)
RESULTS: A good correlation was observed between DSE ans S-ERNA at rest ($r=0,73$) and improving of correlation was observed under stress ($r=0,86$). A bias of DSE versus S-ERNA was observed at rest (-1,7%) and at peak stress (-1,3). Both diastolic and systolic volumes were significantly smaller at peak stress at DSE than S-ERNA. Despite the high correlation observed, only half of patients positive for LV dysfunction at S-ERNA were also positive at DSE when a rest to peak dose increase criterion in LVEF of ≤ 5% was used. To increse sensitivity a more strict criterion (increase in LVEF ≤ 10%) was necessary.
CONCLUSIONS: DSE gained a large popularity in aortic valve regurgitation patient assessment. The present study confirms its role kept in mind both that dobutamine administration is not entirely comparable to physical effort (expecially in LV dimensional changes) and that a different sensitivity threshold of DSE (LVEF changes from basal to peak ≤ 10%) must be used in comparison to S-ERNA (LVEF changes from basal to peak ≤ 5%).

OS_300

BIVENTRICULAR PACING TO CORRECT INTERVENTRICULAR DYSSYNCHRONY IN PTS WITH ISCHEMIC CARDIOMYOPATHY: ASSESSMENT BY RNV AND PHASE ANALYSIS

L. Ceriani (1), E. Verna (2), L. Giovanella (1), S. Caico (2), S. Ghiringhelli (2), S. Garancini (1). (1) Department of Nuclear Medicine; (2) Department of Cardiology ,Ospedale di Circolo e Fondazione Macchi - University Hospital of Varese, Varese, Italy.

BACKGROUND: Preliminary data demonstrated acute improvement in hemodynamic parameters and reduction of interventricular dyssynchrony with increase in the left ventricular ejection fraction (LVEF) during atrial sensed biventricular pacing (BiVP) in pts with idiopathic dilated cardiomyopathy (DCM) presenting with left bundle branch block (LBBB).
AIM: To evaluate the effects of BiVP on contractile synchrony and left ventricular function in patients with ischemic cardiomyopathy (ICM) and intraventricular conduction delay (LBBB) by using phase analysis of radionuclide ventriculography (RNV).
METHODS: Fourteen patients with ICM and LBBB underwent RNV studies either in sinus rhythm or during BiVP. Phase image analysis was applied to the scintigraphic data and mean phase angles were computed for the right (RV) and left ventricle (LV). LV mean phase angle of the normokinetic LV segments (NKLV) was also calculated separately. Mean interventricular phase delay (Df) was computed as an index of contraction synchrony by using either mean total LV phase angles (TotDf) or mean NKLV phase angles (NKDf). LVEF was calculated at baseline and during BiVP.
RESULTS: During BiVP mean LVEF increased from 24 ± 10% to 26.6 ±10.9% (p =ns). A significant increase in LVEF (> 5%) during BiVP was observed in only 5/14 patients (36%). There were no significant changes in global interventricular synchrony as measured by TotDf (17.6±12.4 vs 19.1±12.3 degrees; p =ns). By considering only the normokinetic LV segments (NKLV) BiVP improved interventricular synchrony and NKDf decreased from 23.1± 13.6 to 15.4±7.8 degrees; $p = 0.02$. The degree of dyssynchrony present in sinus rhythm correlated with the magnitude of improvement in synchrony during BiVP ($r = 0.82$, $p < 0.005$). There were no correlation between LVEF changes and improvement in both TotDf and NKDf during BiVP.
CONCLUSIONS: Contrary to previous findings in patients with DCM in this series of patients with ICM we did not observe significant improvements in global LVEF and interventricular synchrony after BiVP, althought BiVP may effectively reduce interventricular Df of the normokinetic LV segments (NKDf). The extent of regional LV akinesia and non-viable myocardium in patients with ICM and BiVP may actually limit the contribution of improved interventricular synchrony to the global LVEF.

OS_301

REPEATABILITY OF LEFT AND RIGHT VENTRICULAR FUNCTION MEASURED WITH ECG-GATED BLOOD-POOL SPECT VERSUS PLANAR RADIONUCLIDE CARDIAC ANGIOGRAPHY

D. Daou (1), C. Coaguila (1), I. Pointurier (1), B.O. Helal (1), T. Fourme (2), I. Carel (2), R. Lebtahi (3), M. Faraggi (3), M. Slama (2), D. Le Guludec (3). (1) Department of Nuclear Medicine, Antoine Beclere Hospital, AP-HP, Clamart, France; (2) Cardiology Department, Antoine Beclere Hospital, AP-HP, Clamart, France; (3) Department of Nuclear Medicine, Bichat Hospital, AP-HP, Clamart, France.

Aims: The use of ECG-gated blood-pool SPECT (GBPS) for the evaluation of systolic left (LV) and right ventricular (RV) function may present some advantages over planar radionuclide angiography (RNA). But, the reliability of GBPS for the measurement of LV and RV EF and volumes (V) as reflected by interstudy variability has not been studied. Moreover, this reliability has not been compared to the robust reliability of LVEF with planar RNA. We aimed to define and compare the intraobserver, interobserver and interstudy reliability of GBPS and planar left anterior oblique (LAO) RNA for the measurement of LV ejection fraction (EF). Were also studied the reliability of GBPS for the measurement of RVEF, LVV and RVV.

Methods: Ten patients with CAD had RNA studies acquired as follows. First, LAO (best septal) then GBPS RNA acquisitions (LAO-1; GBPS-1) were realized by one technician. Then, the patients were allowed to rest in the waiting room for at least 15 min and a second set of acquisitions (LAO-2 and GBPS-2) were realized by another technician. The LAO acquisitions were processed with a widely validated software while the GBPS were processed using a semi-automatic software based on the maximal activity threshold method (35%) after manual segmentation of the LV. The LV and RV volumes were calculated and LV and RV EF were derived. All 4 acquired studies were processed by 2 different observers with one-week interval between the first and second set of images. The % variation between 2 measurements was calculated as the % of their difference normalized to their average.

Results: The intra-observer, inter-observer and inter-study % variation calculated with LAO versus GBPS RNA were respectively (-1±4% versus -2±4%; NS), (-2±3% versus -1±5%; NS) and (-3±15% versus 0±10%; NS) for LVEF. With GBPS, these were respectively 4±4%, 2±9% and -1±17% for RVEF; 0±5%, -1±10% and 2±10% for LVV; and -3±11%, 2±12% and 1±18% for RVV.

Conclusion: GBPS presents very reliable estimate of LV and RV EF and V. This was comparable for LVEF between GBPS and planar LAO RNA.

RADIONUCLIDE THERAPY / DOSIMETRY

OS_303

3-STEP LOCOREGIONAL RADIOIMMUNOTHERAPY WITH 90Y-BIOTIN IN 42 GLIOMA PATIENTS: A PHASE I-II STUDY

M. Bartolomei, M. Ferrari, L. Travaini, M. Cremonesi, C. Grana, C. De Cicco, L. Bodei, D. Militano, M. Gatti, M. Chinol, G. PaganelliNuclear Medicine and Medical Physics Divisions, European Institute of Oncology - Milano, Italy.

Aim: The aim of this study was to investigate the safety profile and antitumor efficacy of a pre-targeting 3-step method employing ^{90}Y-biotin in the locoregional radioimmunotherapy (RIT) of recurrent high grade glioma.

Methods: Fourty-two patients underwent second surgical debulking and implantation of a catheter into the surgical resection cavity (SRC), in order to administer the radioimmunotherapeutic agents. Thirteen patients with anaplastic astrocytoma (AA) and 29 patients with glioblastoma (GBM) were injected first with biotinylated anti-tenascin MoAbs (2 mg), then with avidin (10 mg; 24 h later) and finally ^{90}Y-biotin (18 h later). Each patient received two of these treatments, 8-10 weeks apart. The injected activity ranged from 0.555 to 1.110 GBq. Dosage was escalated by 0.185 GBq in four consecutive groups: group A (0.555 GBq): 6 pts; group B (0.740 GBq): 10 pts; group C (0.925 GBq): 20 pts; group D (1.110 GBq): in 6 pts. Toxicity and adverse effects were evaluated according to the established criteria. The objective response was evaluated by CT or MR images before and 60 days after the second locoregional RIT.

Results: The treatment was well tolerated without acute side effects up to 0.925 GBq. The maximum tolerated activity was 1.110 GBq limited by neurologic toxicity (in 3 out 6 pts of group D). None of the patients developed haematologic toxicity. In 3 patients infection occurred around the catheter. The average absorbed dose to the normal brain was minimal compared with that received at the SRC interface. At first follow-up, partial (PR) and minor (MR) responses were achieved in 8 GBM (3 CR; 1 PR; 4 MR) and 5 AA patients (2 CR; 1 PR; 2 MR) with an overall objective response rate of 31%. Stable disease (SD) was observed in 12 GBM and 7 AA patients (45%). There was disease progression in 9 GBM patients and in one AA patients (24%). Presently, 17/42 pts are still in follow-up. The median overall survival time, derived from survival curves, resulted in 16.5 months (21.5 for AA and 14.6 for GBM).

Conclusions: At the dosage of 0.7-0.9 GBq per cycle, 3-step locoregional RIT was safe and produced an objective response in 13/42 patients (31%). Based on these encouraging results, further studies employing this treatment soon after first debulking are justified.

OS_302

THE ASSESSMENT OF TRANSIENT ISCHEMIC STUNNING DURING STRESS GATED SPECT THALLIUM-201 MYOCARDIAL PERFUSION IMAGING (MPI): EFFECT ON SYSTOLIC LEFT VENTRICULAR FUNCTION

S. Heiba (1), J. Santiago (1), M. Mirzaitehrane (2), S. Jana (1), F. Dede (3), H. Abdel-Dayem (1). (1) Nuclear Medicine Service, Department of Radiology, St. Vincent's Catholic Medical Centers of New York; (2) Department of Cardiology, St. Vincent's Catholic Medical Centers of New York; (3) International Research Fellow, Turkish Science Foundation, Marmara University, New York, USA.

AIM: Transient ischemic stunning was assessed during routine stress gated SPECT Thallium-201 MPI by wall motion (WM) and wall thickening (WT) changes using both semiquantitative and quantitative methods. Transient ischemic stunning was also correlated to calculated left ventricular ejection fraction (LVEF) from both early and delayed images.

Methods: 82 patients (52 men), mean age 60, had treadmill exercise (57) or dobutamine stress (25) early/delayed gated SPECT Thallium-201 MPI. Myocardial images were divided into 20 segments and scored using a scale of 5 points for perfusion, 4 points for WM and 3 points for WT by two observers. Summation reversibility score (SRS) was used for perfusion as well as for WM and WT changes to assess the extent and severity of myocardial ischemia and stunning respectively. Early/delayed LVEF using commercial software was examined with respect to all variables.

Results: Patients were classified according to perfusion, WM and WT into normal (NL), patient with fixed abnormalities (FA) and patients with improved abnormalities with/without fixed abnormalities (IMP). There was good correlation between patients' perfusion and WM, perfusion and WT as well as WM and WT (Spearman correlation = .77, .80 and .90 respectively). The mean LVEF from early and delayed images were analyzed according to perfusion, WM and WT different groups as shown in the following table. There was more significant decrease in early LVEF when compared to delayed ones as patient's WM or WT SRS increased while no significant difference was seen in patients with ischemia but no transient stunning regardless of the perfusion SRS.

Conclusion: In stress Thallium-201 MPI, transient ischemic stunning is frequently associated with myocardial ischemia and equally detected by WM and WT assessments from gated SPECT images. Significant decline in early stress image's LVEF from delayed one is, however, related to the transient stunning, particularly when the extent and severity of stunned myocardium is considered, and not to ischemic changes alone.

			Perfusion			WM			WT
LVEF	NL	FA	IMP	NL	FA	IMP	NL	FA	IMP
	(n: 31)	(n: 7)	(n: 44)	(n: 32)	(n: 21)	(n: 29)	(n: 35)	(n: 16)	(n: 31)
Early	61.7	46.3	46.9	63.9	44.5	44.4	62.8	38.4	46.9
Delayed	63.8	46.9	50.5	66.3	43.9	50.1	65.7	36.5	51.9
P value	.08	.79	.006	.1	.66	<.0001	.02	.22	<.0001

OS_304

90Y-DOTATOC LOCOREGIONAL APPROACH: DOSIMETRY IN GLIOMA PATIENTS

M. Ferrari (1), M. Cremonesi (1), M. Bartolomei (1), M. Stabin (2), S. Agosteo (3), M. Chinol (1), L. Leonardi (1), E. Sacco (1), H. Maecke (4), G. Paganelli (1). (1) Divisions of Nuclear Medicine and Medical Physics, European Institute of Oncology, Milan, Italy; (2) Department of Radiology and Radiological Sciences Vanderbilt University, Nashville, TN, USA; (3) Dipartimento di Ingegneria Nucleare, Politecnico di Milano, Italy; (4) Nuclear Medicine Department, University of Basel, Switzerland

Locoregional (LR) administration of ^{90}Y-conjugates after surgical debulking is a promising treatment for gliomas. LR protocol with the somatostatin analogue DOTATOC labeled with ^{90}Y was developed. Its potentiality was investigated in 10 patients (pts) by evaluating the absorbed dose delivered to brain adjacent tissue (BAT). Escalating activities of 370-740 MBq were injected into the surgical resection cavity (SRC) via an appropriate catheter. Scintigraphic images were acquired at 1 and 16 h, along with blood and urine sampling up to 48 h post injection. A dosimetric model based on Monte Carlo simulations combined to the MIRD formalism was developed to evaluate the residence time in SRC (t_{SRC}) and absorbed doses in BAT. The activity (A) in the SRC was considered equal to the total A injected less A in the blood and less the cumulative A eliminated in the urine. BAT was divided in adjacent shells 1 mm thick to evaluate the dose distribution around the SCR. The cavity radius (r) and the depth of diffusion of the radioconjugate through the BAT (d) were varied in order to adapt the model to different patients' situations. Based on the most likely diffusion of the DOTATOC through the tissue the parameter d ranged from 0 to 3 mm. Patients were divided in two groups - group I (4 pts): SCR connected to ventricula, group II (6 pts): SRC not connected to ventricula.

Higher cumulative %IA in the urine (30% to 50% at 50h) and irregular biodistribution were found in group I, with liquor and kidney uptake. In group II, clearance from SRC was slow as confirmed by pharmacokinetics: the blood curve reached low %IA and a slight slope and cumulative %IA in the urine ranged between 10% and 30% at 50%. In group II, mean t_{SRC} was 60 ± 10 h: in case of no diffusion, absorbed doses to shell II resulted 560 and 60 Gy/GBq for r=12 and 25 mm; in case of r=12 mm and slight diffusion (d=1 mm), absorbed dose to shells I, III and VI were 1300, 2500, and 270 Gy/GBq. Mean dose to normal brain resulted 15 mGy/GBq.

These results indicates that LR ^{90}Y-DOTATOC therapy allows to deliver very high doses to target tissue sparing normal brain. Further developments of the model will allow to improve the dosimetric evaluations in normal organs when SRC is connected to ventricula.

OS_305

DIFFUSIBLE BRACHYTHERAPY (DBT) WITH RADIOLABELLED SUBSTANCE P IN HIGH GRADE GLIOMAS:FIRST OBSERVATIONS

T. Schumacher (1), K. Eichhorn (1), S. Hofer (2), S. Good (1), K. Eisenwiener (1), H. Maecke (1), E. Nitzsche (1), J. Mueller-Brand (1), A. Merlo (2). (1) Department of Nuclear Medicine and Radiochemistry; (2) Department of Neurosurgery, University Hospital of Basel, Switzerland.

Aim: Improvement of local tumor control and prolongation of survival in high grade glioma patients after extensive debulking surgery.
Method: Since January 2000 17 glioblastoma patients were included into this pilot study. After extensive debulking,1 to 3 port-a-caths were implanted into the resection cavity or into solid tumor remnants. In 1 to 9 sessions, we injected a total dose of up to 14.800 MBq (400 mCi) of ^{90}Y-DOTA-Substance P. Scintigraphic images were obtained 5 minutes, 24 and 48 h post injection. The observation period after primary diagnosis ranges from 3 to 21 months, or up to 15 months after the first brachytherapy.
Results: Eventhough the observation interval is too short for most patients, several encouraging responses were obtained. In the first patient treated with dBT as monotherapy, recurrence-free survival lasted 8 months, and the patient is still alive 14 months after initial surgery. Another patient is still recurrence free 16 months after initial diagnosis. However, in four patients, rapid tumor recurrence and/or tumor progression was observed.
Conclusions: The intracavitary brachytherapy with ^{90}Y-DOTA-Substance P seems to be a promising approach in high grade gliomas bearing NK1-receptors. After extensive surgery of the primary tumor this therapy may represent a supplementary option.

OS_306

COMPARISON OF TRACER-BASED, WEIGHT-BASED AND STANDARD THERAPY ADMINISTRATION FOR I-131 MIBG THERAPY OF NEUROBLASTOMA

G. .D. Flux (1), S. .C. Chittenden (1), K.M. Pomeroy (1), M.J. Guy (1), M.A. Flower (1), S.T. Meller (2). (1) Department of Physics; (2) Department of Paediatric Oncology, Royal Marsden NHS Trust, Sutton, UK.

The aim of this study was to assess the potential advantages from using a tracer dose of either I-123 or I-131 mIBG prior to administration of I-131 mIBG radionuclide therapy.
Methods: 24 therapy administrations were given to 15 paediatric patients (age range 2-21 years, weight range10-95 kg) with neuroblastoma, 9 of whom were treated twice. For each treatment a tracer dose of either I-123 or I-131 mIBG was given prior to therapy to establish the administered activity necessary to deliver a whole-body (WB) dose of 2 Gy. WB counts were acquired with a ceiling-mounted NaI detector and doses calculated according to standard MIRD methodology. Therapy WB doses were compared with those predicted by the tracer administration, those that would have been predicted using weight-based formulae and those that would have been delivered using a standard administration of 7400 MBq.
Results: Administered therapy activities required to deliver a 2 Gy whole-body dose ranged from 4.4 GBq to 57.9 GBq. The optimum activity administration was determined by prior administration of a tracer, whereas a standard administration of 7400 MBq would have resulted in underdosing by up to 87% or overdosing by up to 68%. 6 of the 15 patients had two therapies given within 8 weeks, 2 within 5 months and 1 after 3 years. In these cases the therapy for the second was predicted by the kinetics of the first to within 28% in all but the one case with a 3 year separation between therapies. For this patient, the kinetics of the first therapy, if used, would have resulted in underdosing by 72%. The use of weight-based formulae would have predicted the WB doses with greater accuracy than the standard administration, but less accurately than using the tracer.

Conclusions: The optimum activity required for a first I-131 mIBG therapy for neuroblastoma is best predicted by a prior tracer administration of either I-123 or I-131 mIBG. In the absence of this, careful use of a weight-based formula is substantially more accurate than administering a standard dose. In the case of repeat therapies with a relatively short interval between administrations, the results of the first therapy may be used to predict the administered activity for the second.

OS_307

IN VIVO QUANTIFICATION OF RADIOACTIVITY USING ITERATIVE RECONSTRUCTED SPECT. A NEW APPROACH FOR PEPTIDE RECEPTOR RADIONUCLIDE THERAPY DOSIMETRY

B.L.R. Kam, R. Valkema, P.P.M. Kooij, A.E.M. Reijs, E.P. Krenning. Department of Nuclear Medicine, University Hospital Rotterdam, The Netherlands.

Aim: Peptide receptor radionuclide therapy (PRRT) with octreotide analogs labelled with radionuclides such as ^{111}In, ^{90}Y and ^{177}Lu, is an important new treatment for neuro-endocrine and other receptor-positive tumors. For the optimal strategy to achieve maximal treatment dose, accurate radioactivity quantification in organs and tumors is essential, since the radiation to the kidney and bone marrow is dose limiting. Quantification with conventional planar scintigraphy or SPECT with filtered back projection has limitations such as tumor-organ overlap and streak artifacts. This study evaluates in patients SPECT quantification using iterative reconstruction with the maximum likelihood expectation maximization (MLEM), with attenuation correction using the Chang algorithm, compared to planar quantification (PLAN).
Methods: Eighteen patients without abdominal pathology underwent ^{111}In-pentetreotide (Octreoscan®) planar and SPECT imaging. SPECT was reconstructed with MLEM (20 iterations) and 0.09 cm^{-1} attenuation correction. Measurements of counts (SPECT) were calculated to MBq using a conversion factor of 250 cts sec^{-1} MBq^{-1} calibrated in phantom ^{111}In experiments. In vivo measurements for kidneys and spleen were performed using manually drawn regions of interest (ROI) on transverse slices. Two independent observers performed this in twelve patients to evaluate interobserver variability. To evaluate the effect of attenuation correction, the body contour was independently applied by two investigators. Only the maximum counts per slice in the right kidney were evaluated, to avoid ROI-effects. Planar quantification was performed with geometric mean calculation and standard dose calibration.
Results: The percentages of injected dose for spleen, right and left kidney for planar imaging are 2.3±1.2%, 2.9±0.9% and 2.7±0.9% respectively and for SPECT 2.6±1.3%, 3.0±0.8% and 2.9±0.8% respectively. Between both observers, the SPECT radioactivity's were highly correlated (r=0.98), however one systematically measured 7.8±8.3 % more. Both observers had a good correlation with PLAN for all organs (SPECT=0.75*PLAN+1.35; r=0.85; p<0.01 and SPECT=0.73*PLAN+1.78; r=0.82; p<0.01) and for organs separately (right kidney r=0.77 and 0.73, left kidney r=0.79 and 0.75, spleen r=0.93 and 0.91). The two attenuation corrected sets had a significant difference in maximum counts (11.1±8.5 %; p<0.01).
Conclusion: Quantification with SPECT using MLEM and Chang attenuation correction is a suitable method to measure organ radioactivity. More accurate results may be obtained using patient based attenuation correction maps and standardized ROI measurements. The next step is to validate this method in patients with abdominal pathology and with other radiopharmaceuticals such as ^{177}Lu-Octreotate.

OS_308

EFFECT OF OMEPRAZOLE ON RENAL UPTAKE OF 111-IN-DTPA-OCTREOTIDE

R. Barone (1), M. de Jong (2), B.F. Bernard (2), A. Van Gameren (2), E.P. Krenning (2), S. Pauwels (1), F. Jamar (1). (1) Department of Nuclear Medicine, Université Catholique de Louvain, Brussels, Belgium; (2) Department of Nuclear Medicine, University Hospital Dijkzigt, Rotterdam, The Netherlands.

Aim: Coinfusion of basic amino acids (aa) can reduce the non-specific renal uptake of radiolabeled somatostatin analogues and protect kidneys during peptide radiotherapy. Preliminary results obtained in patients, suggest that the renal protection obtained with mixed aa infusion is more pronounced in patients chronically treated with proton-pump inhibitors. The aim of this study was to investigate in an animal model whether acute or chronic treatment with omeprazole, alone or in combination with aa infusion, can reduce renal uptake of ^{111}In-DTPA-octreotide.
Methods: Kidney uptake of ^{111}In-DTPA-octreotide (0.5 μg, 3 MBq) was studied in 8 groups of male Wistar rats (200-250 g):1) controls, 2) acute i.v.omeprazole (40-20 or 10 mg/kg), 3) chronic omeprazole pretreatment (40 mg/kg/day i.v. over 21 days), 4) Lys-Arg (200-240 mg/kg) i.v.coinjection, 5) Proteinsteril Hepa 8% (380 mg/kg) i.v. coinjection, 6) Lys-Arg (200-240 mg/kg) i.v. coinjection + chronic omeprazole pretreatment, 7) Proteinsteril Hepa 8% (380 mg/kg) i.v. coinjection + chronic omeprazole pretreatment, 8) Proteinsteril Hepa 8% (380 mg/kg) i.v. coinjection + acute i.v.omeprazole (40 mg/kg). Rats were placed in metabolic cages and sacrificed at 24h. Organs were isolated and counted for radioactivity. Results are reported as relative to controls.
Results: The Lys-Arg solution was the most effective regimen with a 53% of reduction of ^{111}In-DTPA-octreotide renal uptake; the commercially available mixed aa solution decreased kidney uptake by 25%. Acute bolus injection of high doses of omeprazole caused a 20% inhibition of kidney uptake. No effect was observed with the others regimens of omeprazole administration. Further, no additive effect of omeprazole to the effect of aa was noted.
Conclusions: Acute administration of high dose of omeprazole could contribute to reduce the renal uptake of radiolabeled somatostatin analogues. In spite of the clinical observation, no effect on renal peptide re-uptake was exerted by the chronic administration of the proton-pump inhibitor. Due to species specificity, it is possible that the rat model is not appropriate for the study of omeprazole.

OS_309

153SM-EDTMP THERAPY DECREASES ADHESION MOLECULES IN PATIENTS SUFFERING FROM BREAST CANCER

H. Sinzinger (1), B. Palumbo (2), R. Palumbo (2), K. Weiss (3).
(1) Department of Nuclear Medicine, University of Vienna, Vienna, Austria; (2) Department of Nuclear Medicine, University of Perugia, Perugia, Italy; (3) Department of Radiology and Nuclear Medicine, Hospital of Wiener Neustadt, Austria.

A great numer of prognostic markers for disease activity and progression have been identified. Among them are adhesion molecules (AM) involved in the metastasation process by increasing the adhesiveness of malignant cells to the vascular wall thus indicating disease activity. We therefore determined the AM (ICAM-1, VCAM-1 and E-selectin) using an ELISA in 16 female and 1 male patient (aged 42 – 76 years) with breast cancer and multiple painful bone recurrences undergoing single therapy with 30 mCi (1,1 GBq) ^{153}Sm-EDTMP before, 3, 6, 9 and 12 weeks after therapy and in 7 of them undergoing a second treatment. ^{153}Sm-EDTMP causes a variable but significant ($p < 0,01$) decrease in the AM in most of the patients reaching a maximum effect at 9 and 12 weeks after therapy. No correlation to bone pain palliation, number of lesions or haematologic response was recorded. Repeated treatment induced a further significant drop in AM. This effect may be due to prostaglandin liberation after radiation-induced cell damage reflecting antimetastatic potential. These findings suggest a decreased expression of AM which is an important determinant of disease activity and tumor metastasation indicating that repeated systemic ^{153}Sm-EDTMP-treatment decreases or retards metastatic spread.

OS_310

CHARACTERIZATION OF THE NEOPLASTIC TISSUE RESPONSE AFTER IODINE-131-LIPIODOL TREATMENT IN PATIENTS WITH HEPATOCELLULAR CARCINOMA

L. Ruffini (1), R. Bottelli (2), A. Rampoldi (3), D. Zanni (4), C. Zavaglia (2).
(1) Oncology and Haematology Department - Nuclear Medicine Unit; (2) Internal Medicine Department; (3) Radiology Department; (4) Physics Institute, Niguarda Hospital, Milan, Italy

Arterial injection of Iodine-131-Lipiodol showed good results in patients with unresectable hepatocellular carcinoma (HCC).
Aim of the study was to characterize the biological response of the tumor mass to the treatment evaluating induced tumor necrosis and Lipiodol retention in the neoplastic lesions.
Forty patients receveid I131-Lipiodol (2.2 GBq, 60 mCi) into the hepatic artery after tranfemoral cannulation. Before and one month after the treatment spiral CT was performed in all patients to evaluate tumor size changing due to necrosis and Lipiodol uptake. Tumor extent was estimated by a score system ranging from 0 (progression of the disease) to 4 (complete response with no evidence of neoplastic tissue); 1 unchanged, 2 tumor size reduction >25% <50%, 3 reduction >50%. Lipiodol uptake in the neoplastic lesions was measured for each patient according to Maki grading score ranging from 1 to 4 (1 Lipiodol uptake <10%, 2 <50%, 3 >50%, 4 complete filling of the tumor mass 100%).
The mean value of Lipiodol uptake in the lesions was 2.25 ± 1.06. Shrinkage of the neoplastic tissue was shown in 82% of the treated patients (33/40). Complete response (grade 4) was determined in 7 patients (5 pts with a grade 4 Lipidol uptake, 2 pts with a grade 3 uptake). Grade 3 tumor response was shown in 14 pts (8 pts with a grade 3 uptake, 6 with a grade 2 uptake); grade 2 tumor response in 12 pts (5 pts with a grade 3 uptake, 7 with a grade 2 uptake); grade 1 tumor response in 7 pts (4 pts with a grade 1 uptake, 3 pts with a grade 2 uptake). No progression of the disease was shown.
In conclusion, reduction of the tumor mass or, at least, stabilization of the disease was obtained in most of the patients. Treatment efficacy seems to be correlated with Lipiodol uptake: no patients with low uptake value (Maki score 1) showed tumor mass reduction. It may possible that stabilization of the disease in these patients may be dependent only by radiation effect.

OTHER CLINICAL SCIENCE. ENDOCRINOLOGY

OS_311

RETINOIC ACID RE-DIFFERENTIATION THERAPY FOR THYROID CANCER

L. Ruffini. Oncology and Hematology Department - Nuclear Medicine Unit, Niguarda Hospital, Milan, Italy.

Prognosis of differentiated thyroid carcinoma is strictly related to the capability of tumor cells to concentrate radioiodine. A significant minority of patients show de-differentiation of the neoplastic tissue with loss of iodine uptake capability giving rise to tumors that are refractory to conventional therapy (surgery, radiodine therapy, levothyroxine) with a worse prognosis.
Retinoic acid (RA) is a regulator of cell proliferation and differentiation well characterized by several in vitro and in vivo studies.
Aim of the study was to evaluate efficacy and feasibility of re-differentiation therapy with RA in patients with differentiated thyroid cancer.
Ten consecutive patients (3 men, 7 women, aging from 36 to 72 yrs) with thyroid cancer (follicular carcinoma 6, papillary carcinoma 4) were enrolled. All patients showed advanced tumor stage with local recurrence and distant metastases (2 patients had liver metastases).
Iodine uptake was efficient at the presentation and it was possible to perform ablation of the thyroid remnant with Iodine-131 in all the patients. Tumoral iodine uptake progressively decreased after repeated I-131 treatment in 6 patients and six months after remnant ablation in 4 patients. All the patients were administered with 13-cis-retinoic acid (Roaccutan) for 2 months. The initial dose was 1.5 mg/kg/die. At the end of the treatment patients were submitted to I-131 therapy.
Recovery of iodine uptake was shown in 4 of 10 patients allowing the performance of further radioiodine therapy. Dramatic evidence of significant uptake in all the lesions was shown in one patient. Whole body scan revealed renewed mild I-131 uptake in 3 patients. No I-131 uptake was shown in 6 patients. Thyroglobulin as index for redifferentiation of tumor cells increased in 7 pts, decreased in 2 and did not change in 1. Retinoic acid dosage was progressively reduced until 1 mg/kg/die in 3 patients because of the occurrence of nasal bleeding and dry skin. Biochemical values (controlled before treatment and then, every 2 weeks) did not show significant changes in any patient.
In conclusion, RA re-differentiation therapy may represent an alternative therapeutic approach to otherwise untreatable thyroid tumors, expecially considering the mild side effects related to the treatment.

OS_312

INSULAR THYROID CARCINOMA: PROGNOSTIC SIGNIFICANCE OF DIFFERENT MORPHOLOGIC PATTERNS

V. Rufini (1), G. Fadda (2), A. M. Samanes Gajate (1), M. C. Garganese (1), E. D. Rossi (2), M. Salvatori (1), M. L. Maussier (1), L. Troncone (1).
(1) Department of Nuclear Medicine; (2) Department of Human Pathology and Histology, Università Cattolica del Sacro Cuore, Rome, Italy.

Insular thyroid carcinoma is relatively uncommon malignancy with a morphologic picture and clinical behaviour in an intermediate position between differentiated and anaplastic carcinomas. It is considered to be an aggressive tumour mostly when the insular component (IC) is predominant in the overall neoplastic tissue. Aim of the study is to investigate whether a high or a low percentage of IC may influence the biological behaviour of this cancer -including I-131 uptake and thyroglobulin (TG) secretion- as well as the prognosis. Out of 674 patients submitted to total thyroidectomy for thyroid cancer during the period 1992-1999, 26 cases (3.8%) had histopathological findings showing the presence of IC. IC was predominant (≥ 50%) in 11 patients, focal (≤ 50%) in 15. They were 12 males and 14 females, aged 14-78 yr. Surgical staging of the primary tumour was: T1b in 1, T2 in 7, T3 in 12, and T4 in 6. Cervical lymph node metastases were detected at surgery in 4 cases. Six patients (all with predominant IC), had distant metastases detected by imaging at post-surgical evaluation; two patients (1 with focal, 1 with predominant IC) developed distant metastases 6 and 7 years after initial surgery, respectively. All patients were studied with I-131 WBS and TG assay and were treated with I-131 therapy. Among metastatic patients, TG values were elevated (ranging from 487 and 10,900 ng/ml) in all cases; I-131 WBS was negative in 3 out of 8 (all with predominant IC), even after a therapeutic dose of I-131, so they were treated with radiation therapy and/or chemotherapy; 3 patients with distant metastases died 5, 11 and 28 months from diagnosis, respectively. Two patients developed local recurrence and 3 lymph node involvement after 3-6 years from diagnosis. After a mean follow-up of 40.8 months (range 5-107) 14 patients (12 with focal IC) are alive without evidence of disease.
In conclusion: the prevalence of IC influences the clinical behaviour of thyroid cancer. A predominant pattern is associated with a more advanced stage of disease at diagnosis and a more aggressive clinical course and mortality; in this group there is a higher incidence of local recurrences and metastases which in some cases do not concentrate I-131 and are not responsive to other current available therapies. A focal pattern is associated to a less aggressive clinical course and mortality; the presence of differentiated areas suggests that I-131 may have an important diagnostic and therapeutic role.

OS_313

STUDY ON THE ISOLATION PERIOD OF PATIENTS WITH METASTATIC THYROID CANCER TREATED BY I-131 ACCORDING TO A NEW GUIDELINE IN JAPAN

S. Tsuchimochi, M. Nakajo, H. Tanabe, M. Nakajo Jr, T. Umanodan. Department of Radiology, Kagoshima University Hospital, Kagoshima, Japan.

In Japan, a new guideline for the release of patients administered I-131 was issued by the Ministry of Welfare on June, 1998: The dose rate; < 30 uSv/h at 1 m or the activity in the body; < 500 MBq. This study was designed to set the appropriate isolation period enough to satisfy these limits. A total of 29 patients with the history of total thyroidectomy and metastasis were selected for this study. In these patients, 28 patients were treated with 3.7 GBq of NaI-131 (72 times), and one patient was once treated with 5.55 GBq of NaI-131. This study also included 2 patients (4 courses) who treated with split dose of NaI-131 (740 MBq/week x 5 weeks). Measurements of the external exposure dose (uSv/h) at 1 m and the urinary excretory radioactivity (MBq) were performed at various times. There was a good correlation of the external exposure dose between standing and sitting postures. The difference in the external exposure dose before and after urination (x uSv/h) had a significant correlation with the urinary excretory radioactivity (y MBq); $y = 16.6x + 24.8$, $r = 0.96$, $p < 0.001$. Also, there was a significant correlation between the predicted value of residual radioactivity in the body (y' MBq) and the external exposure dose (x' uSv/h); $y' = 20.8x' + 31.5$, $r = 0.98$, $p < 0.001$. In the patients treated with 3.7 GBq of NaI-131, the mean and S.D. value of the external exposure dose (uSv/h) changed as follow: after 6 hr; 168±40, 24 hr; 52±23, 48 hr; 20±15, 72 hr; 10±9 and 96 hr; 8±9. The percentages of the patients satisfied the new guideline were as follow; 21.7% at 24hr, 81.2% at 48hr and 100% after 72hr. Therefore 3-day isolation is sufficient for the patients administered 3.7 GBq of NaI-131.

OS_314

TO WAIT OR NOT TO WAIT?

M. Medvedec, D. Grosev, S. Loncaric, Z. Pavlinovic, D. Dodig. University Hospital Rebro, Department of Nuclear Medicine and Radiation Protection, Zagreb, Croatia.

Aim: Thyroid stunning has been speculated to be avoidable in thyroid cancer patients if a) therapeutic I–131 is administered immediately following positive diagnostic scintigraphy with I–131 (thus diminishing the fraction of diagnostic radiation dose absorbed in remnant thyroid until therapeutic administration of I–131), or if b) I–131 therapy is postponed for a week or more following administration of the imaging I–131 activity (thus assuring time for thyroid remnant recovery). The aim of our work was to test those hypothesis.
Methods: Forty one patients totally thyroidectomized for thyroid cancer were sub-grouped in 20 (p6) and 21 (p7) patient, in regard to the time interval (1/4 6 and 3/4 7 days) between the diagnostic and the therapeutic administration of I–131, respectively. p6- and p7-patients received 2.6±0.9 and 2.6±1.0 GBq I–131 (p=n.s.) 4.8±1.1 and 9.0±2.6 days ($p<0.01$) after 92±42 and 86±32 MBq I–131 (p=n.s.), respectively. Individual absorbed doses and dose-rates were calculated from serial measurements of remnant thyroid uptake using conventional probe system and beta-gamma exposure rate meter, in conjunction with thyroid remnant mass, which was assessed from two orthogonal pinhole gamma camera images.
Results: In both groups of patients initial diagnostic absorbed dose-rates were 0.3±0.2 Gy/h (p=n.s.). Pre-therapeutically absorbed fractions of the diagnostic doses were Dp6=16±14 Gy and Dp7=26±21 Gy (p=n.s.). Due to the different timing of I–131 administration, the reduction of the total diagnostic absorbed dose was 30±18% and 18±14% ($p<0.05$) in p6 and p7, respectively. Observed therapeutic absorbed doses were respectively 55±24% and 56±30% (p=n.s.) of diagnostically predicted values in p6 and p7. Analogous relative initial dose-rates were 72±27% and 76±36 % in p6 and p7, respectively.
Conclusions: Shorter interval between diagnostic and therapeutic administration of I–131 in thyroid cancer patients may significantly decrease diagnostic absorbed dose, but has no influence on the maximal absorbed dose rate. The usual values of those two dosimetric parameters are probably still above clinically acceptable thresholds. Longer inter-administration interval may help remnant thyroid to recover, but it seems that it should be much longer than seven days. We recommend more radical changes of the standard post-surgical treatment with I–131 in thyroid cancer patients, in order to avoid the effect of thyroid stunning.

OS_315

DOES RADIOIODINE INFLUENCE FUNCTIONING PULMONARY METASTASES FROM THYROID CANCER?

E. Hindié (1), D. Mellière (2), I. Hallaj (3), C. Jeanguillaume (2), H. Boulahdour (4), L. Perlemuter (2), C. Vaylet (1), C. N'Guyen (1), T. Kiffel (1), S. Askienazy (1). (1) Department of Nuclear Medicine, Hôpital St-Antoine, Paris, France; (2) Hôpital Henri Mondor, Créteil, France; (3) Hôpital Necker, Paris, France; (4) CHU Jean Minjoz, Besançon, France.

Pulmonary metastases that capture iodine are the most frequently observed metastases in patients with differentiated thyroid cancer. They are usually diagnosed on chest X-ray and, in many reports, they more often occur late after thyroid surgery. Ten-year survival averages 40%. Because some authors doubt any beneficial role of ^{131}I in preventing or treating these metastases, we reviewed our findings.
Methods: Data from 509 patients with differentiated thyroid cancer were reviewed. Total thyroidectomy + ^{131}I ablation had been performed in 76% of cases. Functioning pulmonary metastases occurred in 20 patients. Seven of them also had bone metastases. Patients with negative chest X-ray constitute Group I, and those with positive chest X-ray Group II. All 20 patients received repeated treatments with ^{131}I. In addition, three patients had pulmonary metastectomy, and four had bone surgery or bone irradiation therapy.
Results: Functioning metastases were present at initial work-up in 19 patients (95%) and occurred late in only one. *Group I (11 patients):* Pulmonary invasion was diagnosed on the whole-body scan during routine ^{131}I ablation. In 56% of these patients, serum thyroglobuline measurement alone would not have contributed to diagnosis (average level of only 12 ng/mL, off-thyroid hormone therapy). Lasting remission was obtained in 8 patients (average cumulated ^{131}I activity = 289 mCi). Two patients showed persistent uptake. One died from local recurrence. *Group II (9 patients):* The average cumulated ^{131}I activity was 922 mCi. Lasting remission was obtained in three patients. Four others had substantial improvement in radiological findings and are continuing treatment. Two patients died. Ten-year survival overall was 82%. Average follow-up for the 17 survivors was 11 years.
Conclusions: Comparison with other published reports suggests that ^{131}I has a major influence on the natural history and course of functioning metastases, in that it provides: 1) prevention, 2) early diagnosis, and 3) improved survival.

OS_316

THE USE OF RECOMBINANT HUMAN TSH IN THE EVALUATION OF PATIENTS WITH DIFFERENTIATED THYROID CARCINOMA

PH. Rondogianni (1), V. Vlassopoulou (2), I. Tzavara (3), PH. Giannakopoulos (2), CH. Giannopoulou (1), H. Nikolou (2), N. Thalassinos (2), I. Houssianakou (1). (1) Department of Nuclear Medicine ; (2) Department of Endocrinology, Diabetes & Metabolism; (3) Department of Endocrinology, Athens, Greece.

The evaluation of patients with differentiated thyroid carcinoma with I-131 whole body scan(WBS) and thyroglobulin measurement(Tg) must be performed in the presence of high TSH levels to stimulate iodine uptake and production of Tg by thyroid remnants or metastatic tissue.Recombinant human TSH(rhTSH) has been developed to facilitate monitoring of patients with differentiated thyroid carcinoma on thyroxine (T4) suppression therapy.In this study we tried to evaluate Tg values and WBS results after rhTSH in patients who face other serious medical problems that may deteriorate off T4 therapy or patients unable to generate endogenous TSH and to compare rhTSH results with those off T4.
Methods. We studied 19 patients with differentiated thyroid carcinoma after total thyroidectomy and I-131 ablation of the thyroid remnants.All were on T4 suppression therapy. rhTSH was administered every 24h in two doses 0,9 mg each.WBS was obtained 24 h after the second dose while in all patients serum Tg and TSH were measured at baseline,24 h, 48h, 72h,and 96h after the final dose of rhTSH .Nine patients have also had a WBS after T4 withdrawal at least 2 months after the second dose of rhTSH while in 8 patients among them a therapeutic dose of I-131 was administered followed by a WBS 5 days later.
Results. On T4 therapy, suppressed TSH values at baseline rose significantly after the first rhTSH injection and remained at high levels the day of I-131 administration.Twelve patients had undetectable Tg values at baseline and in 8 among them Tg remained undetectable after rhTSH administration while in the rest 4 patients it ranged from 13-77 ng/ml.In 7 patients the detectable baseline Tg values rose significantly the 3^{rd}-5^{th} day after the 1^{st} rhTSH injection.WBS images were concordant after rhTSH and off T4 in 7 patients, while 2 patients WBS was superior after T4 withdrawal.As expected ,the sensitivity of WBS was superior after a therapeutic dose of I-131.
Conclusions.rhTSH administration is an alternative and effective mean of follow-up in thyroid carcinoma patients when T4 withdrawal is not easy.

OS_317

FOLLOW-UP OF PATIENTS WITH INITIALLY BENIGN THYROID NODULES

D. Huiæ, I. Braèiæ, S. Lonèariæ, M. Halbauer, A. Kneževiæ-Obad, D. Dodig. Department of Nuclear Medicine and Radiation Protection, University Hospital, Zagreb, Croatia.

AIM: Fine-needle aspiration (FNA) biopsy represents the most important method for evaluation of patients with thyroid nodules. This technique can identify cells that appers suspicious, malignant or benign. The aim of this study was to evaluate the realibality of initially benign FNA diagnosis over a 5-year follow-up period.
METHOD: The study included 163 patients (154 female, 9 male, median age 46 yr) with 202 thyroid nodules initially diagnosed as a benign lesions by FNA biopsy. Median nodule size was 1.9 cm. By ultrasound, 63 patients had a solitary nodule and 100 had multinodular goiters. Repeated FNA biopsies (one or more, total 454 FNA) controlled by ultrasound were performed in all patients most often because of an increase in size of nodule and because of scintigraphic („cold" lesions) or echographic (hypoechogenic lesions) findings.
RESULTS: After repeated biopsies 186 (92%) nodules remained benign, 15 (7.5%) were suspicious for follicular tumour, and one was malignant (0.5%). Six of 15 patients with suspicious citology had surgery with resected lesion being benign in all. The one malignant citology was confirmed on surgery (papillary carcinoma).
CONCLUSION: For patients with an initially benign diagnosis on FNA biopsy, clinical findings and suspicious scintigraphic or echographic presentation of the nodules are not associated with a high yield of malignancy on repeated aspiration. However, at the present time, it still seems reasonable to performe at least one repeat aspiration to confirm the original benign diagnosis.

OS_318

CALCITONINE SCREENING IN PATIENTS WITH NODULAR GOITER FOR DETECTION OF MEDULLARY THYROID CANCER

P. Mariß (1), A. Kammeier (1), M. Thermann (2), D. Emrich (1), U. Raute-Kreinsen (3). (1) Gemeinschaftspraxis Radiology/Nuclear Medicine Dr. Stuckenholz & Partner, Bielefeld, Germany; (2) Klinik für Allgemein- und Visceralchirurgie, Städtische Kliniken Bielefeld, Germany; (3) Institut für Pathologie, Städtische Kliniken Bielefeld, Germany.

Aims: Medullary thyroid carcinoma (MTC) is an uncommon malignant neoplasm developed from C-cells and secreting calcitonin with a poor prognosis. Serum calcitonin is regarded as a tumor marker of MTC and is especially used in post-surgical follow-up. Because of radical surgery is the only curative therapeutic method it is necessary to detect the tumor in an early stage. Methods: Therefore we performed a prospective study concerning routine screening of basal calcitonin levels measured with monoclonal antibodies (Calcitonin-U.S. IRMA, BioSource, normal values $\leq$ 10 pg/ml) in patients with nodular goitre and without previously known family history of MTC. In all patients anamnestic data were obtained; clinical examination, ultrasonography, scintigraphy with Tc-99m-pertechnetate and thyroid function test were performed. Within 27 months 2750 pts (78,8 % female, 21,2 % male) were screened. The measurement was repeated when calcitonin levels were elevated. Thyreoidectomy was only recommended if the calcitonin levels remained higher than 30 pg/ml. Results: 15 pts showed elevated serum calcitonin ($\geq$ 30 pg/ml), among these pts 12 had an histological MTC (calcitonin 39 – 404 pg/ml). All these pts did not show specific symptoms. 2 pts (calcitonin levels between 30 and 36 pg/ml) represented a benign histology, whereas in one of them slightly elevated calcitonin persisted after thyroidectomy. One patient (calcitonin of 35 pg/ml) was not operated until now. In 6 cases the tumor was of T1 state, 4 had T2, 1 T3, all lymph node negative. Regional lymph node metastasis (N1) were detected in one patient (T4, calcitonin 39 pg/ml). In 10 cases with MTC RET protooncogene screening was negative, in one patient screening was not performed until now, one patient died after thyroidectomy because of complications caused by a second neoplasm (esophageal carcinoma). Conclusion: We conclude that preoperative determination of basal calcitonin is helpful in differential diagnosis of nodular goitre, especially to detect MTC in an early state without nodular metastasis and with a relatively good prognosis.

INFECTION AND INFLAMMATION

OS_319

INFECTION IMAGING WITH TC-99M-LABELED C5A AND C5A-ANTAGONISTS

H.J. Rennen (1), O.C. Boerman (1), W.J. Oyen (1), S.A. Cain (2), P.N. Monk (2), J. Kohl (3), F.H. Corstens (1). (1) Department of Nuclear Medicine, University Medical Center Nijmegen, Nijmegen, The Netherlands; (2) Department of Molecular Biology and Biotechnology, University of Sheffield, Sheffield, UK; (3) Institute of Medical Microbiology, Medical School Hannover, Hannover, Germany.

Aim: The complement anaphylatoxin C5a and its natural metabolite C5a des Arg^{74} (C5adR) are involved in several stages of the inflammatory process. Both act on a common receptor on different cell types, including neutrophils and monocytes. The receptor binding affinity of C5a exceeds that of C5adR by 1-2 orders of magnitude. The biologic potency of C5adR is considerably reduced as compared to that of C5a. Here we tested in extenso both proteins for their potential to image infections. In addition, in search for a C5a receptor antagonist with less biological potency, two C5adR mutants with C-terminus mutations were investigated: the C5adR mutant with Lys^{68} substituted by Glu^{68} (C5adR E68) and a mutant with a C-terminus heptapeptide substitution.
Methods: The proteins were labeled with ^{99m}Tc via the hydrazinonicotinamide (HYNIC) chelator. In vitro receptor binding assays were performed using purified human leukocytes. The preparations were tested for imaging of infection in a rabbit model of soft-tissue infection. Biodistribution of the radiolabel was determined both by γ-camera imaging and by counting dissected tissues at 5 h p.i..
Results: Receptor binding fractions were 40% and 50% for ^{99m}Tc-labeled C5a and C5adR resp. In the rabbit model, ^{99m}Tc-labeled C5a delineated the abscess much more clearly than the labeled C5a antagonists. C5a and C5adR showed in vivo an abscess uptake of 0.115 and 0.025 %ID/g resp. Abscess/muscle ratios were 76 and 14, abscess/blood ratios 9.1 and 2.6 resp. Quantitative analysis of the images revealed abscess-background ratios improving with time up to 5.9 and 2.1 for C5a and C5adR. The radiolabel was excreted mainly renally for both preparations. Gamma camera imaging rapidly visualized the abscess from 1 h p.i. onwards for C5a. In addition, radiolabeled C5adR E68 showed an in vitro and in vivo behaviour similar to C5adR. The C5adR heptapeptide mutant showed in vivo a relatively high liver uptake and a strongly reduced abscess uptake.
Conclusion: For infection imaging ^{99m}Tc-labeled C5a showed the most optimal in vivo characteristics. However, C5a is an extremely bioactive protein, impeding its clinical use as an infection imaging agent. The naturally occurring antagonist C5adR and the mutant C5adR E68 are less biologically potent but showed suboptimal imaging characteristics, presumably due to their lower binding affinity for the C5a-receptor. The C5adR heptapeptide mutant showed to be unsuitable for infection imaging in the rabbit model of infection.

OS_320

MONITORING THE EFFICACY OF ANTIBACTERIAL TREATMENTS OF INFECTIONS WITH 99MTC-LABELLED ANTIMICROBIAL PEPTIDES

M. Welling (1), A. Paulusma-Annema (2), E.K.J. Pauwels (1), P.H. Nibbering (2). (1) Department of Nuclear Medicine; (2) Department of Infectious Diseases, Leiden University Medical Center, Leiden, The Netherlands.

^{99m}Tc-labelled synthetic fragments derived from the microbicidal domain of the human cationic antimicrobial peptide ubiquicidin (UBI), i.e. UBI 18-35 and UBI 29-41, that have been shown to discriminate between bacterial infections and sterile inflammation are now studied to monitor the efficacy of antibacterial treatment of experimental infections.
In this study we injected radiolabelled (non-microbicidal doses) of these UBI peptides into mice with an experimental thigh muscle infection with S. aureus, K. pneumoniae, or multidrug resistant S. aureus (MRSA). Next, we monitored the efficacy of treatment of these infections with classical antibiotics or an antibiotic peptide, i.e. the first eleven N-terminal amino acids of human lactoferrin (hLF 1-11), respectively. Accumulation of the radiolabelled UBI peptides at the site of infection is expressed as the ratio of the amount of radioactivity in the infected thigh (T) and the non-infected thigh (NT), further referred to as T/NT.
In our studies we found a good correlation (0.954, $p<0.05$) between the number of viable bacteria in the infected thigh muscle and the T/NT ratio's at 60 min after injection of the radiolabelled UBI peptides. In the present study we observed a significant reduction ($p<0.01$) in the T/NT ratio's (1.34 ± 0.04) for UBI peptides in S. aureus infected mice treated with an effective dose of cloxacillin, but not in animals treated with suboptimal doses of this bactericidal antibiotic (T/NT 2.48 ± 0.35). Similar results were seen in mice with a S. aureus infection that were treated with an optimal dose of erythromycin, a bacteriostatic antibiotic. The efficacy of the various antibiotic treatments in the animals was confirmed with microbiological assays. In addition, we found a significant reduction ($p<0.005$) in the T/NT ratio's in mice with an intramuscular infection with multi-drug resistant S. aureus (MRSA) after treatment with an optimal dose of hLF 1-11 (T/NT 2.01 ± 0.14), but not in animals injected with a suboptimal dose of this antibiotic peptide (T/NT 2.91 ± 0.27).
In conclusion, radiolabelled UBI 18-35 and UBI 29-41 can be used to monitor the efficacy of antibacterial treatment of infections with both (drug-resistant) Gram-positive and negative bacteria Gram-negative in laboratory animals.

OS_321

A NEW ANIMAL-MODEL TO INVESTIGATE TC-99M-HYNIC-PEG-LIPOSOMES INDUCED SIDE-EFFECTS

P. Laverman (1), J. Szebeni (2), L. Baranyi (2), W.J.G. Oyen (1), G. Storm (3), F.H.M. Corstens (1), O.C. Boerman (1). (1) Department of Nuclear Medicine, University Medical Center Nijmegen, Nijmegen, The Netherlands; (2) Department of Membrane Biochemistry, Walter Reed Army Institute of Research, Silver Spring, MD, USA; (3) Department of Pharmaceutics, Utrecht University, Utrecht, The Netherlands.

Aim: For many years we have investigated the potential of Tc-99m-labeled PEG-liposomes for imaging infection and inflammation. The preclinical results were promising and resulted in two clinical studies. In these clinical studies we showed that Tc-99m-labeled HYNIC-poly-ethyleneglycol (PEG)-liposomes can visualize infectious and inflammatory foci with high specificity and sensitivity. However, due to the occurrence of adverse reactions in 5 out of 44 patients we terminated these studies prematurely. The present study aimed to develop a pig-model to further investigate these side-effects and methods to circumvent these reactions.
Methods: Male Yorkshire swine (25-40 kg) were anesthetized by inhalation anesthesia with 1% halothane. The animals were instrumented to allow continuous monitoring of systemic blood pressure (SAP), pulmonary blood pressure (PAP) and ECG, along with many other physiological and biochemical parameters. Liposomes were prepared according to routine procedures. Liposomal formulations were administered in the jugular vein as bolus.
Results: Injection of 0.2 µmol of unlabeled HYNIC-PEG-liposomes lead to significant changes in blood pressure in all 5 pigs studied. These changes were caused by complement activation resulting in a massive release of thromboxane A_2 and other vasoconstrictive mediators. Subsequent liposome injections in the same animal after 1 hour did not lead to hemodynamic changes. A single injection of 0.9 µmol HYNIC-PEG-liposomes caused the death of one pig. Similar reactions were observed after injection of long-circulating liposomes without PEG-coating (n=5 pigs). Hypotension with dyspnea and chest or back pain (i.e., possible symptoms of pulmonary hypertension) are characteristics of hypersensitivity reactions. These symptoms observed in pigs are remarkably similar to the adverse reactions observed in the patient studies. Injection of the complement inhibitor recombinant soluble receptor type 1 (sCR1) or the cyclooxygenase inhibitor indomethacin prior to the liposome administration prevented the occurrence of the hypersensitivity reactions. These findings were confirmed by in vitro complement activation assays. All liposomal formulations tested caused complement activation in human serum which could be inhibited by coincubation with the inhibitors described above.
Conclusion: Our data indicate that pigs provide a highly sensitive animal model to study hypersensitivity reaction to liposomes. The complement activation-triggered cardiopulmonary reaction of pigs may also provide unprecedented sensitivity for biocompatibility screening of other i.v. (radio)pharmaceuticals.

OS_322

IN VITRO ASSESSMENT OF TC-99M MIBI UPTAKE IN MYCOBACTERIUM TUBERCULOSIS CULTURES

C. Stefanescu (1), D. Boisteanu (2), D. Diculencu (2), V. Rusu (1), A. Iacobovici (3), O. Dorneanu (4), I. Raileanu (1). (1) Biophysics and Nuclear Medicine Department,UMF; (2) Pneumophtysiology Department, UMF; (3) Biochemistry Department,UMF; (4) Microbiology Department,UMF, Iasi, Italy

Aims: To understand the in vivo scintigraphic Tc-99m MIBI findings in pulmonary tuberculosis we have proposed to investigate, in vitro, if Mycobacterium Tuberculosis cultures have a significant radiotracer uptake, in comparison with normal cell types known to have high (myocytes) or low (fibroblasts) uptake.
Methods: Mycobacterium Tuberculosis cultures were realised on Löwenstein Jensen medium by standard methodology, 21 days cultures being used in our experiment. The normal cells were neonatal rat heart myocytes and fibroblasts. Final plating was done to have an almost complete cell monolayer the day of the experiment, in culture dishes. The cells were incubated with a 1.85 kBq/ml concentration Tc-99m MIBI, at 37°C, using three dishes for each cell type. A kynetic three point (15, 60 and 90 minutes) was realised for Mycobacterium Tuberculosis. The incubation was stopped by rapidly washing the dish cells, three times, with a 4°C physiological saline solution. Cells were than supperficialy scrapped and withdrawn in saline physiological solution for counting the uptaked radioactivity. Protein concentration was determined using Lowry method. Freely culture medium was also incubated with the radiotracer to exclude the possible influence on the cell data. Results were expressed in percent of the total added radioactivity amount, per mg proteines and like percentage in comparison with myocites uptake, considered 100%. Statistical comparisons were done using student t test for paired data (comparison v.s. fibroblasts uptake).
Results: Cellular uptake of the radiotracer in different cell lines is summarized in the following table:

Cells	Incubation time interval (cpm/mg proteines, % of total added radioactivity) Mean ± standard deviation	Relative uptake (%, in comparaison with myocytes, considered 100%)	Relative uptake
Mycobacterium Tuberculosis	15 minutes	0.0395 ± 0.0057, p<0.001	106.47
	60 minutes	0.0181 ± 0.0026, p<0.002	48,79
	90 minutes	0.0206 ± 0.0042, p<0.005	55,52
Myocites	60 minutes	0.0371 ± 0.0051, p<0.001	**100**
Fibroblasts	60 minutes	0.0151 ± 0.0019	40.70

The results were corrected for the precise amount of activity added and for the radioactivity decay of Tc-99m.
Conclusions: Mycobacterium Tuberculosis proved to have high Tc-99m MIBI uptake at 15 minutes in comparison with other kinetics points. This uptake is almost as high as myocytes 60 minutes uptake (known as a higher normal cell uptake). These in vitro uptake results could explain the more positives scintigraphic images in BK positive patients obtain at 15 minutes, in comparison with the delayed images.

OS_323

RAPID IMAGING OF EXPERIMENTAL COLITIS WITH 99MTC-INTERLEUKIN-8 IN RABBITS

S. Gratz, H. Rennen, O. Boerman, W. Oyen, F. Corstens. University Medical Center Nijmegen, Nuclear Medicine, Nijmegen, The Netherlands.

Introduction: Radiolabeled autologous leukocytes (WBC) are the gold standard for imaging inflammatory bowel disease (IBD). For the rapid and adequate management of patients with IBD, there is need for a new agent, which is at least as good as radiolabeled WBC, but easier to prepare and without its inherent risks. In the present study, the potential of Interleukin-8 labeled with ^{99m}Tc via hydrazinonicotinamide (HYNIC) to image IBD was investigated in a rabbit model of acute colitis and compared to that of ^{99m}Tc-HMPAO-labeled granulocytes.
Methods: In rabbits with chemically-induced acute colitis, inflammatory lesions were scintigraphically visualized following injection of either IL-8 or purified granulocytes both labeled with ^{99m}Tc. Gamma camera images were acquired at 0, 1, 2 and 4 hrs p.i.. At 4 hr p.i. the rabbits were killed, and the uptake of the radiolabel in the dissected tissues was determined. Furthermore, the dissected colon was imaged and the inflammatory lesions were scored macroscopically. For each affected colon segment, the colitis index (CI, affected colon-to-normal colon uptake ratio) was calculated and correlated to the macroscopically scored severity of inflammation.
Results: Both agents visualized the colitis within 1 hr p.i.. ^{99m}Tc-HYNIC-IL-8 images of the colonic abnormalities were more accurate, the intensity of uptake in the affected colon continously increased until 4 hr p.i., whereas no further increase after 1 hr p.i. was noticed scintigraphically for ^{99m}Tc-HMPAO-granulocytes. The absolute uptake in the affected colon was much higher for IL-8 than for the radiolabeled granulocytes with %ID/g 0.41 ± 0.04 and 0.09 ± 0.05 at 4 hr p.i. respectively. With increasing severity, the CI at 4 hr. p.i. for ^{99m}Tc-HYNIC-IL-8 was 4.4 ± 0.6, 13.5 ± 0.5 and 25.8 ± 1.0; for granulocytes 1.5 ± 0.1, 3.4 ± 0.2 and 6.4 ± 0.5 respectively. The CI correlated with the severity of the inflammation (r=0.95, p<0.0001 for IL-8 and r=0.95, p<0.0001 for granulocytes).
Conclusions: Within 1 hr p.i. visualization of the extent of colonic inflammation in vivo was possible with ^{99m}Tc-HYNIC-IL-8 and ^{99m}Tc-HMPAO-granulocytes. Within 2 hr p.i. ^{99m}Tc-IL-8 allowed a good and at 4 hr p.i. a meticulous evaluation of the severity of IBD. ^{99m}Tc-HMPAO-granulocytes were able to delineate the extent of IBD within 2 hr p.i., whereas an accurate estimation of severity of inflammation was not possible. ^{99m}Tc-HYNIC-IL-8 is an inflammation imaging agent that showed promising results in this study.

OS_324

ANTI-GRANULOCYTE ANTIBODY SCINTIGRAPHY IN DIAGNOSING LEFT VENTRICULAR ASSIST DEVICE INFECTION

V. Ivancevic (1), C. de Jonge (2), D. Sandrock (1), W. Konertz (2), D.L. Munz (1). (1) Clinic for Nuclear Medicine; (2) Clinic for Cardiothoracic Surgery, University Hospital Charité, Humboldt University, Berlin, Germany.

Aim: The left ventricular assist device (LVAD) has had tremendous impact on the management of patients with end-stage heart failure. However, incidence of post-implantation infection ranges from 40% to 55% with a mortality rate of 50%. Delineation of an infectious focus within the LVAD very often fails using conventional imaging methods. We thus investigated the diagnostic performance of anti-NCA 95 anti-granulocyte antibody (BW 250/183) scintigraphy in this serious complication of LVAD implantation.
Methods: Sixteen BW 250/183 scans were performed in 8 patients (1 female, 7 males; age range, 7-60 years) with suspected LVAD infection. Two patients had one follow-up scan each, while there were 3 patients with 2 follow-up scans. Having acquired a blood pool image of the abdominal/thoracic area, planar spot, whole-body, and SPECT studies were performed up to 24 hours after injection. Scintigraphic results were verified by blood or specimen culture, surgery, and/or follow-up with antibiotic therapy. The scans were interpreted visually without knowledge of other test results. Based on the blood pool images, LVADs were divided into driveline, pump, and inflow or outflow tracts for better topographic alignment of scintigraphic hot spots or areas.
Results: Twelve/15 scans were true positive, 3 true negative, and one false negative. Sixteen scintigraphic foci were identified, 7 in the driveline, 5 in the pump, and 4 in the inflow or outflow tracts. In 9/16 investigations a single infectious focus was detected. Five of these single foci were located in the driveline, and 2 in the pump and inflow or outflow tracts, respectively. One of 2 patients with one BW 250/183 follow-up scan each, was false negative, but turned to true positive on follow-up and died after removal of his LVAD. The other patient being true positive became true negative under antibiotic therapy and is doing well. Two/3 patients with 2 follow-up scans each remained true positive throughout the follow-up. One of them died, while heart transplantation was performed in the other. The third patient was true positive in the first 2 investigations, turned to true negative under antibiotic therapy and finally recovered.
Conclusion: This preliminary data indicates that BW 250/183 scintigraphy represents a reliable method for identifying infectious foci located in LVAD systems and seems to be useful in monitoring antibiotic therapy in these patients. The single most frequent location of infection within the LVAD is the driveline.

OS_325

VALUE OF IMMUNOSCINTIGRAPHY IN PATIENTS AFTER IMPLANTATION OF AN ENDOVASCULAR ABDOMINAL AORTIC STENT

B.I. Kettner (1), V. Ivancevic (1), D. Sandrock (1), R.I. Rueckert (2), D.L. Munz (1). (1) Clinic for Nuclear Medicine; (2) Clinic for Surgery, University Hospital Charité, Berlin, Germany.

Aim: Endovascular stent implantation in patients with aortic aneurysm is a new minimal invasive method. It is unclear, however, wether the fever reaction after stenting, known as âpost implantation syndrome„ is an unspecific inflammatory reaction or a certain type of infection. Aim of this study was therefore to clarify this question using a murine monoclonal antigranulocyt antibody. Method: Up to now 15 consecutive patients (13 male, 2 female, 65 years, 45-82 years) were investigated on day 1 and 8 after surgery. After i.v. injection of 400 MBq Tc-99m antigranulocyte antibody (BW 250/183), whole body acquisitions (4, 24 h p.i and SPECT of the abdomen (24 h p.i.) were performed using a double head gamma camera (Multi-SPECT2*, Siemens, Erlangen, Germany). Analysis was done visually and in ROI-technique (background corrected ratio of bone marrow BMU, aortic stent ASU and spleen SU on 4, 24 h whole body scans). Results: Except for one clinically apparent post implantation syndrom, tracer accumulation of the aortic stent was only faint (table). The highest uptake overall was observed in the spleen. In one patient an infection of the aortic stent (leucocytes and c-reactive protein elevated) with positiv scintigraphic scan (uptake: 1,5 and 1,8 after 4 and 24 h postoperatively.) occured, required an operative revision. An acute inflammation with dominating granulocytes could be confirmed histologically.

Conclusion: The antibody can be used for the diagnosis of a stent infection characterized by an accumulation of granulocytes. Perioperative fever in patients after stent implantation due to aortic aneurysm is *not* associated with a significant accumulation of granulocytes.

OS_326

DETECTION OF INFECTIONS OF PROSTHETIC VASCULAR GRAFT BY THE 99MTC-HEXAMETHYLPROPYLEAMINEOXIME-WBC IMAGING

G. D'Errico, V. Valenza, M.L. Maussier. Nuclear Medicine Institute, Catholic University of Rome, Italy.

Introduction: fortunately the frequency of the infection, the most serious and severe complication of prosthetic vascular graft after reconstructive vascular surgery, is low. An early and accurate detection of this catastrophic complication is important to prevent the high incidence of morbidity and mortality. The clinical diagnosis of graft infection can be difficult because presenting often non-specific symptoms as well as the diagnosis by conventional radiographic methods such as arteriography and ultrasonography. The aim of this report is to evaluate, retrospectively, the diagnostic accuracy of this isotopic method in ruling out vascular graft infection.
Material and methods: for this purpose the Authors analysed 59 scans (3 patients were restudied two times and 1 patient four times) performed at our institution in 49 patients (aged from 52 to 81 years, mean 67±8.5 years; 38 males and 11 females) suspected to be affected by aortoiliofemoral (1), aortoaortic (12), iliofemoral (2) , aortobifemoral (25) and 9 by peripheral graft infections. All the patients were evaluated with CT (by Authors considered as a golden standard method) and/or US and ^{99m}Tc-HMPAO-WBC scintigraphy and underwent red cell sedimentation rate (RCSR) and C Reactive Protein assay (CRPassay).
Results: ^{99m}Tc-HMPAO-WBC scan was in agreement with CT/US in 56/59 cases [94.9%] {33/56 positive results (58.9%) and 23/56 negative (41.1%)}; in one positive case the isotopic method showed two anatomic locations of graft infection while correlative CT study detected only one site; in two cases the positive result of ^{99m}Tc-HMPAO-WBC-scan, in agreement with non specific symptoms and high RCSR, even if disagreeing with other imaging diagnostic methods, induced the surgeons to reoperate (with confirmation of the scintigraphy features). All the 9 patients suspected to be affected by peripheral graft infections showed negative feature at ^{99m}Tc-HMPAO-WBC-scan and not-isotopic diagnostic techniques.
Conclusions: The retrospective results lead to consider, according to other works, the ^{99m}Tc-HMPAO-WBC scan an accurate diagnostic method for evaluation of suspected prosthetic vascular graft infection.

NEUROLOGY / PSYCHIATRY

OS_327

PREDICTIVE ROLE OF ADENOSINE / 99MTC-HMPAO BRAIN SPECT STRESS-TEST IN PATIENTS WITH CAROTID ARTERY DISEASE

W.YU. Ussov (1), V.E. Sinitsyn (2), V. Obradovic (3), N.YU. Efimova (1), G. Dragutinovic (3), I.Y.U. Efimova (1), V.M. Trivozhenko (1), M.P. Plotnikov (1). (1) Tomsk Institute of Cardiology; (2) Mjasnikov Institute of Clinical Cardiology, Moscow; (3) Serbian Clinical Center, Beograd, Russia.

Patterns of ^{99m}Tc-HMPAO SPECT in adenosine stress-test were analysed versus long-term clinical follow-up in patients with internal carotid artery stenosis.
26 patients(pts) with atherosclerotic carotid disease detected by echo-Doppler study of carotids and verified also using digital subtractive angiography were referred. Degree of stenosis was quantified as {1 - (Lumen at site of minimal stenosis)/(Lumen at proximal non-stenotic site)}. In everybody the ^{99m}Tc-HMPAO SPECT study was performed twice: at rest and during stress-test with intravenous injection of adenosine (100 µg/kg body weight) infused via an intravenous cannula for one minute, with the patient in the supine position. Asymmetry of cortical blood flow was quantified from rest and adenosine stress test studies as ratio (asymmetry index AI) of mean counts over regiones of middle cerebral artery blood supply. Cerebral damage was evaluated quantitatively by means of brain MRI-study performed in T1, T2, T2* and proton density weighted modes.
Patients were classified according to three patterns (ptn.) of vascular reactivity. Ptn.I comprised eight pts with one-sided internal carotid artery's stenosis over 0.5, without neurologic deficit or MRI signs of cortical damage. Ptn.I demonstrated symmetric distribution of ^{99m}Tc-HMPAO at rest (AI=0.99 s.d.0.01) and decreased uptake over stenosis-dependent haemisphere vs. normal one at adenosine test (AI = 0.91 s.d.0.04). Seven pts of Ptn. II with patent carotid lumen (stenosis for < 0.3) due to carotid endarterectomy (in five) or stenting (in two) did have cortical damage from previous stroke(s), evident on MRI, mild neurologic symptoms and decreased perfusion on stenosis-dependent side of previous stroke (AI = 0.91 s.d.0.03). Adenosin test augumented blood supply to this side with more even interhaemispheric distribution of ^{99m}Tc-HMPAO (AI = 0.96 s.d. 0.03). Ptn.III comprised eleven pts with predominantly monolateral internal carotid artery stenosis over 0.5 in whom the mono- or multilocational cortical damage was also present. In these the mild rest interhaemispheric asymmetry (0.96 s.d.0.03) was deteriorated at adenosine test (0.93 s.d. 0.03).
The subsequent two-year follow-up revealed clinical neurologic ischaemis events (as frequent TIAs (in three) minor strokes (in two) and strokes (in two) only in patients (four with Ptn.I and three with Ptn.III) in whom the adenosine test enhanced interhaemispheric asymmetry of ^{99m}Tc-HMPAO uptake for > 0.05.
Hencefore we conclude that, first, the ^{99m}Tc-HMPAO SPECT adenosin stress is a reliable functional test in patients with extensive atherosclerosis and can be used for detection of patients with decreased cerebral perfusion reserve in whom the risk of future cerebral vascular ischaemic events is elevated.

OS_328

HEMODYNAMIC CHANGE AFTER PERCUTANEOUS TRANSLUMINAL ANGIOPLASTY AND STENTING

T. Mochizuki (1), Y. Sugawara (1), T. Kikuchi (1), S. Nakata (1), K. Kikuchi (1), H. Miki (1), J. Ikezoe (1), T. Ueda (2). (1) Department of Radiology, Ehime University School of Medicine; (2) Department of Neurosurgery, Ehime University School of Medicine, Japan.

Purpose: Percutaneous transluminal angioplasty (PTA) and stenting have been increasingly applied to major cerebral artery stenosis. However, cerebral hemodynamic change after PTA and stenting has not been disclosed well. The aim of this study was to evaluate hemodynamic change in both the ipsilateral and contralateral sides to PTA by measuring cerebral blood flow (CBF) and vascular reserve (CVR).

Methods: We investigated 39 PTAs (including 10 stents) in 29 patients with internal carotid artery (ICA) or middle cerebral artery (MCA) stenosis. Quantitative measurement of CBF (ml/100g/min) was performed at rest and after acetazolamide (ACZ) challenging by Xe-133 dynamic SPECT methods. The CVR was defined as the percent increase of CBF after ACZ. The mean values of CBF and CVR were obtained in the bilateral MCA territories, and they were compared before and after PTA (day 4-35, mean 15 days after PTA).

Results: In the MCA territories ipsilateral to PTA, the CVR increased significantly after PTA (15.1 ± 18.1 vs. 29.9 ± 15.4 %, $p < 0.0001$), whereas the CBF at rest increased little (38.2 ± 8.7 vs. 40.5 ± 9.8 ml/100g/min, $p=0.06$). In 12 cases of subnormal CBF and CVR before PTA, although the CBF did not change after PTA (31.2 ± 5.0 vs. 31.8 ± 6.1 ml/100g/min), the CVR remarkably increased (1.5 ± 12.9 vs. 18.1 ± 12.6 %, $p<0.0001$). In the contralateral MCA territories, both the CBF and CVR increased after PTA (CBF: 40.6 ± 8.9 vs. 42.2 ± 10.1 ml/100g/min, $p=0.08$, CVR: 26.5 ± 14.7 vs. 31.6 ± 17.8 %, $p = 0.037$). In 7 patients with bilateral steno-occlusive lesions, substantial increase of CVR were observed in the contralateral MCA territories (12.0 ± 13.3 vs. 29.1 ± 14.2 %, $p = 0.018$). However, in one patient with bilateral severe ICA stenoses, the steal phenomenon (CVR = - 26%) occurred in the contralateral MCA territory after the initial PTA and stenting. After the second stenting on the contralateral ICA stenosis, remarkable improvement of CVR were obtained in both the MCA territories (-26 % to 34%, 6% to 39%).

Conclusion: Measurement of CBF and CVR is useful to evaluate therapeutic effect after PTA and stenting. Hemodynamic change could occur in the contralateral hemisphere.

OS_329

A STATISTICAL ANALYSIS OF CEREBRAL CORTICAL PERFUSION CHANGES FOLLOWING CAROTID ENDARTERECTOMY

W. Haindl (1), R. Lundqvist (3), S. Som (1), G. Mitchell (1), J. Frawley (2). (1) Department of Nuclear Medicine, Prince of Wales Hospital, Sydney, Australia; (2) Department of Vascular and Transplantation Surgery, Prince of Wales Hospital, Sydney, Australia; (3) Centre for Image Analysis, Uppsala University, Uppsala, Sweden.

Carotid endarterectomy (CEA) is widely used and effective in the prevention of stroke and transient ischaemic attack (TIA) in patients with significant internal carotid artery (ICA) stenosis. Improvement in ICA blood flow can be demonstrated postoperatively by duplex ultrasonography but little is known about the effect of CEA in changing or reversing abnormal cortical perfusion patterns.

Aim: The aim of this study was to demonstrate an improvement in cortical perfusion following CEA and to determine which cortical regions most benefit from this procedure.

Methods: 15 patients, 10 males and 5 females (57 to 81 years, mean 69.7years) with high grade (at least 70%) unilateral ICA stenosis were scanned using a Picker 3000 gamma camera. Prior to surgery, each patient was injected with 500MBq of Tc-99m HMPAO and a baseline (BL) study was obtained. During the BL acquisition the patient received an IVI infusion of 1gm of acetazolamide (ACZ). On completion of the BL acquisition a second 500MBq scanning dose was given and a combined scan (BL plus post ACZ scanning doses) was acquired. The two scans were co-registered using Computerised Brain Atlas (CBA) software and the decay corrected BL scan was subtracted from the combined scan to produce true post ACZ images. 5 patients had right ICA stenosis and their images were mirrored to produce 15 patient studies with left ICA. Each patient was rescanned by the 1 to 6 months following CEA. The preoperative and postoperative scans were co-registered and volume of interest (VOI) analysis was performed. CBA software was used to warp the images to a standard brain template for statistical parametric mapping (SPM) analysis. Regions of significant postoperative perfusion increase were displayed on a surface rendered brain.

Results: Both the VOI and SPM analysis demonstrated improved perfusion in the BL images in the lateral frontal, superior temporal and posterior parietal regions. The ACZ images showed the most marked perfusion improvement in the tip of the frontal lobe medially, with slightly less marked improvement in the inferior aspect of the temporal lobe and in the posterolateral parietal lobe.

Conclusions: Following unilateral CEA, resting cortical perfusion is improved in the ipsilateral middle cerebral artery distribution. The most significant postoperative perfusion improvement following ACZ is in the watershed regions at the borders of the middle cerebral arterial distribution suggesting normalisation of previously precarious perfusion.

OS_330

FUNCTIONAL ACTIVITY IN THE DAMAGED HEMISPHERE AND RECOVERY FROM ACUTE STROKE : A BRAIN PERFUSION SPECT STUDY

A. Kissarova (1), K. Nedelchev (2), G. Tranulov (1), D. Minchev (2), E. Georgieva (1). (1) Department of Radiology and Nuclear Medicine; (2) Department of Neurology, Varna University of Medicine, Varna, Bulgaria.

Aims: Brain SPECT is often useful in the clinical practice since it provides information that cannot be obtained by structural neuroimaging techniques. The present study aims at assessing the correlations of perfusion patterns in the damaged hemisphere and the recovery of the motor deficits after stroke.

Methods: Perfusion changes induced by finger-to-thumb opposition task performed with the paretic arm were evaluated in 17 patients with unilateral ischemic stroke using 99m-Tc-HMPAO SPECT. The study took place within 4 weeks from stroke onset and was performed in two stages. The first included perfusion SPECT study at rest - baseline. The second one included stress perfusion SPECT study (finger-thumb opposition task). Ten symmetric regions of interest (ROI) were specifically designed and the right-to left ratios from each ROI were analysed.

Results: The increased perfusion in the damaged hemisphere under stress was established in 10 petients. The motor task induced a perfusion increase in the damaged hemisphere with respect to the baseline ($p=0.024$). In the remaining 7 patients the increased perfusion was observed in the unaffected hemisphere. The patients with increased perfusion in the damaged hemisphere recovered their motor activity after about two months. Conversely, in patients with no recovery, an additional increase of the perfusion asymmetry was observed during task performance indicating a functional activation of the undamaged hemisphere.

Conclusions: These results suggest that satisfactory recovery of the neurological deficits after stroke requires the presence of functional activity in the damaged hemisphere early after stroke onset. Brain perfusion SPECT study may be used for the early prognosis of the motor activity recovery after stroke.

OS_331

SPINAL CORD STIMULATION AND BRAIN PERFUSION SPET IN CHRONIC STROKE PATIENTS

M.L. Calcagni (1), M. Visocchi (2), A. Giordano (1), L. Romano (1), I. Bruno (1), A.M. Samanes Gajate (1), G. Galli (1). (1) Institute of Nuclear Medicine, Università Cattolica del S. Cuore, Rome, Italy; (2) Institute of Neurosurgery, Università Cattolica del S. Cuore, Rome, Italy.

Spinal Cord Stimulation (SCS) is a well known therapeutic tool for the treatment of functional neurological deficits: spasticity, benign chronic pain, bowel and bladder dysfunction, pheriperal vascular disease, angina. Towards the end of the 80ties there was a big deal of interest in studying SCS related cerebral blood flow changes. It was demonstrated that SCS induces significant cerebral blood flow changes as studied with Transcranial Doppler Sonography, Near Infrared Spectroscopy, Electromagnetic Flowmetry, ^{133}Xe-SPET but the brain perfusional improvement was an inconstant finding. Unfortunately, few pts with cerebrovascular diseases treated with SCS have been studied with brain perfusion techniques, in no case using high resolution regional methods.

The aim of this study was to evaluate the CBF in 8 chronic stroke pts wearing cervical epidural quadripolar electrode both in basal conditions and during SCS. All pts complaint some of the main neurological symptoms dealing with SCS indications. The pts (7 males, 1 female; mean age 58±12yrs), underwent to neuroradiological imaging (CT or MRI) and to brain perfusion SPET with 740 MBq of ^{99m}Tc-ECD using a dedicated tomograph in basal condition (SPET-OFF) and, 3 days later, during SCS (SPET-ON), with the same parameters. Both studies (SPET-OFF and SPET-ON) were analysed semiquantitatively in 23 ROIs according to a previously published method (JNM 1990), using as reference the cerebellar ROI with highest activity. For the statistical analysis we used Wilcoxon signed rank test.

Results: we found a significant hypoperfusion in SPET-ON, when comparing with SPET-OFF, in the regions affected by stroke, namely: right and left frontal regions, right and left central regions, right and left thalamus and pons (one tail $p<.025$; two tail $p<.05$). In region unaffected by stroke, no significant improvement of cerebral perfusion was observed. All pts improved the pre-operative neurological symptoms.

Conclusions: our preliminary results demonstrate that in chronic stroke pts during SCS, there is a further hypoperfusion in cerebral regions affected by stroke, with a trend toward a redistribution of CBF in unaffected regions. These findings support the hypothesis that stroke may impair local autoregulation by reducing vasodilatation induced by SCS (neuromodulation), as already described in pts with a diffuse atherosclerosis. Despite the apparent discrepancy between the worsening of hypoperfusion in affected areas along with a clinical improvement, it seems that SCS effects might be not related with focal lesional vascular pattern (ischemic penumbra) but with a different function and/or anatomic targets.

OS_332

CEREBRAL FDG PET FINDINGS IN PATIENTS WITH CADASIL

K. Tatsch (1), S. Fieber (1), K. Hahn (1), T. Gasser (2), M. Dichgans (2). (1) Department of Nuclear Medicine; (2) Department of Neurology, University of Munich, Munich, Germany.

Aim: Cerebral autosomal dominant arteriopathy with subcortical infarcts and leucoencephalopathy (CADASIL) is an inherited microangiopathy caused by mutations in the Notch3 gene on chromosome 19. Clinically the disease is characterized by recurrent ischemic episodes and progressive cognitive deficits. In MRI studies diffuse white matter signal intensity abnormalities and circumscribed subcortical lesions suggestive for small infarcts have been observed. In a recent MRI study bilateral temporopolar and superior frontal involvement of the white matter combined with further lesions in the basal ganglia, thalamus, brain stem and cerebellum have been reported whereas the cortex was relatively spared. Aim of our study was to evaluate the rCMRGl in CADASIL patients to characterize the metabolic situation in this disorder.
Methods: In a total of 9 patients with CADASIL (5 women, 4 men; age range: 47-64 yrs) quantitative brain PET was performed after i.v. injection of 120 MBq [F-18]FDG (Siemens HR$^+$; 3D; cold transmission; rCMRGl according to Sokoloff). For further processing modified BRASS software running on a Hermes work station (Nuclear Diagnostics) was used to automatically fit the individual patient studies to a normal template established from 12 healthy controls. Pixelwise comparison with the normal template was performed for each individual pt study as well as a grouped data set including all pt studies. PET results were related with clinical findings (e.g. disability ranking, cognitive deficits, psychiatric symptoms).
Results: 8/9 patients presenting with marked abnormalities in rCMRGl had pathologic disability scores and cognitive deficits. In the only pt without disability and normal cognitive function PET findings were almost normal. Group comparison has shown that rCMRGl was predominantely reduced in the bilateral temporal cortex, the superior frontal cortex, basal ganglia and thalamus. Furthermore there was evidence for crossed cerebellar diaschisis with lower cerebellar glucose metabolism contralateral to the more affected cortex.
Conclusions: Functional FDG PET studies in pts with CADASIL have revealed severe changes in cerebral glucose metabolism. Findings seem to correspond with the disability stage and the presence and severity of cognitive deficits/psychiatric symptoms. Interestingly, group comparisons have shown that glucose metabolism was predominantely reduced in the cortical regions adjacent to the zones of the most severely affected white matter (temporopolar and superior frontal). Whether reduced glucose metabolism in CADASIL is subsequently caused by subcortical vascular involvement, affection of subcortical structures and cortical projections, or by (limited) neuronal loss in the cortex has to be further established.

OS_333

COMPARISON OF HEMISPHERICAL CEREBRAL BLOOD FLOW IN VARIOUS CEREBRAL DISEASES WITH QUANTITATIVE HMPAO IMAGING

I. Garai (1), E. Szomják (2), J. Varga (1), C.S. Tóth (4), S. Olvasztó (4), A. Ficzere (3), L. Galuska (1). (1) Department of Nuclear Medicine; (2) 3rd Department of Internal Medicinery; (3) Department of Neurology; (4) 1st Department of Surgery, University of Debrecen, Hungary

Aim: The dynamic imaging of the inflow of HMPAO to the brain has proved to allow the estimation of hemispherical cerebral blood flow (CBF) using the Patlak plot. In our work we compared the hemispherical CBF (in ml/min/100g) of different patient groups.
Methods: 52 patients (migraine: 12, serious carotid stenosis right before endarterectomy: 12, hypertension without any antihypertension therapy: 15, healthy controls: 12) underwent baseline and acetazolamide 99mTc-HMPAO brain perfusion studies. (Only acetazolamide HMPAO studies were performed in case of the 12 healthy patients because of ethical reasons.) Dynamic studies were acquired by a double detector gamma camera with a large field of view (HELIX, Elscint). Special difference images were created to make the definition of the aortic arch and hemispherical brain regions easier and more reproducible. A semiautomatic method was developed to determine the transit time from the aorta to the brain, making the generation of the Patlak plot even more robust.
Results: The baseline CBF values did not ($p>0.1$), while those after acetazolamide provocation did significantly depend on the disease (ANOVA, $P<0.001$). Patients suffering from migraine showed significant increase in the global CBF values after acetazolamide provocation (paired t-test, $P<0.05$), but we could not find any effect of the provocation in patients before carotid endarterectomy, indicating the lack of brain perfusion reserve capacity. When comparing the results of the acetazolamide study in patients to those of the control group, the CBF values were significantly lower in carotid stenosis (two-sample t-test, $p<0.001$), but did not differ in migraine ($p>0.1$), and only slightly in hypertension ($p=0.05$).

	Baseline study		*Acetazolamide study*	
Group	*N*	*CBF (mean±SD)*	*N*	*CBF (mean±SD)*
Healthy control			12	68.5 ± 9.7
Migraine	13	55.8 ± 12.9	11	67.5 ± 12.1
Carotid	10	49.9 ± 9.4	12	49.6 ± 8.4
Hypertension	9	54.4 ± 10.1	15	60.7 ± 9.7

Conclusion: Using quantitative analysis of HMPAO brain studies we could compare objectively the CBF of patients suffering from different diseases. Especially the CBF values after acetazolamide provocation could separate disease states effectively. The quantitative results may help us in planning the therapy (e.g. selecting the right operation technique).

OS_334

99MTC-ECD BRAIN PERFUSION IN OBSTRUCTIVE SLEEP APNOEA SYNDROME: A NEW SPET FINDING

M.L. Calcagni (1), A. Giordano (1), F. Mormile (2), L. Romano (1), D. Selvaggio (2), A. Petrone (2), I. Bruno (1), A.M. Samanes Gajate (1), L. Troncone (1). (1) Institute of Nuclear Medicine, Università Cattolica del S. Cuore, Rome, Italy; (2) Institute of Respiratory Physiology, Università Cattolica del S. Cuore, Rome, Italy.

Recently, haemodynamic changes in CBF have been described in pts with Obstructive Sleep Apnoea Syndrome (OSAS). Few studies have investigated CBF in OSAS pts with nuclear techniques.
The **aim** of this study was to evaluate the brain SPET pattern of pts with OSAS and to correlate the SPET abnormalities with respiratory function and neuropsychological tests (NP). We studied 35 OSAS pts: 24 males, 11 females, mean age 62±10yrs and Body Mass Index (BMI) 32±7. All pts underwent to polysomnography, lung function tests, NP tests, and brain SPET with 740 MBq of ^{99m}Tc-HMPAO using a dedicated tomograph. Brain SPET was analysed semi-quantitatively in 29 ROI, as compared to 12 control subjects matched for age and sex.
Results: in 19 OSAS pts we found a significant hypoperfusion in temporal, parietal and frontal lobes (Group A), while in 16 OSAS pts the brain perfusion was normal (Group B). When comparing respiratory function and NP tests in the two groups, we found that the 19 OSAS pts of Group A tended to be older (64±6yrs *vs.* 59±14yrs, p= .07), had a greater BMI (35±7 *vs.* 29±5, p= .014), had a lower PaO_2 (69±10mmHg *vs.* 82±12mmHg, p= .002), had a higher $PaCO_2$ (42±5mmHg *vs.* 39±3mmHg, p= .028), had a lower %FEV1 (74±23 *vs.* 91±16, p= .012), and a higher number of altered cognitive tests (4.8±4 *vs.* 1.6±1, p= .020) than the 16 OSAS pts of Group B. Unexpectedly, the Apnoea Hypopnea Index (AHI), an index of the night-time spent in hypoxia, tended to be lower in Group A than in Group B (40±23 vs. 53±22, p=.06).
Conclusions: in OSAS pts the CBF abnormalities often involve frontal-temporal-parietal lobes; the brain perfusion deficits correlate with the degree of obesity and with the severity of the respiratory function alterations (FEV1, PaO_2, $PaCo_2$) rather than the duration of apnoea episodes. Our results provide deeper insights in the physiopathological mechanisms of this not uncommon disease.

TECHNOLOGY PROGRAM

OS_335

COMPUTER ASSISSTED LEARNING AND ASSESSMENT IN NUCLEAR MEDICINE EDUCATION

K.G. Holmes (1), B. Nixon (2). (1) University of the West of England ; (2) PaxSys, Bristol, UK.

Background
Nuclear medicine education aims to provide the tools and environment for the introduction and further education of nuclear medicine specialists. This education needs to be based on modern technologies, computer literacy and evidence based practice. Education needs to be continuously updated and suited to the requirements of the learners.
The potential for learning with computers has several applications for students in the field of Nuclear Medicine. Computers allow the possibility of a distance learning course to become a reality. Students can learn at their own pace in the comfort of their workplace or home. The Internet allows worldwide access to modules written by „experts" in their field and these modules can be updated regularly to keep apace with changes in practice. Conferencing facilitates live time communication with tutors and Nuclear Medicine experts.
Method
The design and construction of a case study file is well under way and once the „database" of clinical cases has been established it can provide a powerful tool for reference and learning. Collaboration between Nuclear Medicine Specialists, academic centres and the industry has begun the process of data collection and refinement. This paper will explore the potential uses and pitfalls of computer assisted learning for students in Nuclear Medicine. A database of verified clinical cases is being collated as a teaching and assessment tool. This can be used in learning, self-evaluation and as for OSCE assessment in an interactive environment. The current applications and future developments of this and other computer learning resources will be explored. The possible role in continuous professional development (CPD) in nuclear medicine will also be discussed.
Conclusions
Computer assisted education has applications for newcomers to the profession, to update and develop specialists and widen access. It means education is feasible for small cohorts at a time and place of their choice.

OS_336

FOLLOW-UP OF THE CONTAMINATION RISK IN TECHNEGAS-VENTILATION

I. Spaepen (1), L. Verhaegen (1), H. Vanbilloen (2), E. Vandegaer (1), P. Dupont (1), A. Maes (1), A. Verbruggen (2), L. Mortelmans (1).
(1) Department of Nuclear Medicine, U.Z. Gasthuisberg, Leuven, Belgium; (2) Laboratory of Radiopharmaceutical Chemistry, KU Leuven, Belgium.

Accurate contamination measurements are mandatory when applying Technegas ventilation. Although the particle size of Technegas is more uniform than most other aerosols, small particles are present which attach to objects in the surrounding area of the Technegas generator. The following adaptations can be made to the generator: 1. a box attached to the front valve of the gas preparation chamber; 2. a dome on a flexible arm which can be positioned above the patient's face during the inhalation; 3. a nipple on which the mouthpiece can be placed after the procedure. Items 1 to 3 are all connected with a powerful air exhaust pump with efficient filter.

Regular contamination measurements (n=60 patients) on a number of body parts of the technologist show that the adaptations have led to lower levels of contamination. No contamination was found on hair, chest, right upper arm and left arm. In a minority of cases contamination was observed on mask (2/60), right lower arm (2/60) and left hand (9/60). The most frequent contaminations were found on the right hand (16/60). This was mainly due to holding the mouthpiece by the technologist in case of uncooperative patient.

The syringe with the daily dose is shielded with 3 mm lead. When the syringe is not transported horizontally, there is a risk of leakage of radioactive solution into the needle cap. This highly radioactive drops are a source of contamination whenever the needle cap is removed. This problem can be solved by replacing the needle. Alternatively, fixing the syringe in a holder during transport can prevent leakage.

Furthermore, filling the crucible for every new patient causes a high radiation exposure. Using a longer needle can reduce the radiation dose rate. In addition to this, the radiation exposure during the frequent filling procedure is divided by two by using 2 syringes a day.

When the procedure is finished, the patients is asked to inhale a few times without supply of radioactive gas. However, the tubing and especially the outlet filter remain radioactive and have to be removed immediately in a lead container.

It can be concluded that lower levels of contamination are obtained, both due to technical adaptations to the Technegas ventilation system and supplementary radiation protection measures. It is our believe that once the technical and radiation protection measures are realised, the training and the motivation of the individual technologist becomes more important.

OS_337

RADIATION SAFETY DURING TREATMENT OF NEUROENDOCRINE TUMOURS WITH HIGH DOSE INDIUM-111 OCTREOTIDE

C.N. Boot, M.P.M. Stokkel, J.A.K. Blokland, E.K.J. Pauwels. Department of Nuclear Medicine, Leiden University Medical Center, Leiden, The Netherlands.

DTPA-D-Phe(1)-Octreotide labeled with Indium-111 (In-111) proved to be a very useful imaging tool for Somatostatin receptor positive tumours. Recent reports on high dose In-111 Octreotide have also shown promising results with respect to the treatment of these tumours. In the present study, we have measured the doses of radiation to the personell at different time intervals after treatment with In-111 Octreotide.

Methods: In 5 consecutive in-patients (18 treatments; mean dose 8000 MBq) treated with In-111 Octreotide, dose rates were obtained up to 3 hrs after the injection and on day 1, 2 and 3. The following sites were measured with a dose rate monitor at 50 cm to obtain an average value: upper chest, upper abdomen and bladder. Furthermore, the cumulative whole body dose was registered using a small dosimeter during all procedures.

Results: Mean values of 18 treatments in 5 consecutive patients.

Time p.i. (hrs)	Procedure	Mean Dose Rate (mSv/hr)	WB uptake in patient (% o.i.d.)	Mean Exposure time (min)	Mean Dose (mSv)
T=0,0	Injection / DRM	0,80	100	2	0,0142
T=0,5	Removal infusion / DRM	0,72		2	0,0080
T=1,0	DRM	0,64		1	0,0036
T=2,0	DRM	0,56		1	0,0034
T=3,0	DRM	0,48	62	2	0,0036
T=24	DRM	0,24		1	0,0022
T=24	Whole body scintigraphy*		16	12	0,0036
T=48	DRM	0,16		1	0,0016
T=48	Whole body scintigraphy*		14	12	0,0020
T=72	DRM	0,08		1	0,0012
T=72	Whole body scintigraphy*		13	12	0,0011
Total				47	0,0450

DRM=dose rate measurement *WBS performed by technologists

Currently, dose rate measurements and whole body scintigaphy are only performed at 72hrs p.i.., which will lower the cumulative whole body dose to 0,025 mSv.

Conclusion: The radiation risk to staff members and technologists seems very low during an in-patient treatment with a high dose In-111 Octreotide. According to the safety regulations no special radiation protection measures or personal dosimetry is required under the given conditions.

OS_338

RADIOIODTHERAPY IN GRAVES'DISEASE - FIRST RESULTS OF AN INDIVIDUAL DOSE CALCULATION STRATEGY

S. Dunkelmann, E.A. Iber, F. Rudolph, A. Koch, J. Schefthaler, P. Groth, C. Schuemichen. Clinic of Nuclear Medicine, University of Rostock, Germany .

Aim: To achieve a success rate ≥ 90 % in radioiodine therapy in Graves'disease, the radiation dose delivered to thyroid has to be increased to ≥ 200 Gy. On the other hand, a radiation dose of 80 Gy is sufficient for a success rate of 50 %. Hence a majority of patients will receive an unnecessar high activity of radioiodine. To avoid this, an individual radiation dose strategy was used and evaluated for its clinical usefulness. Methods: We prospectively investigated 171 unselected patients with Graves'disease receiving a first radioiodine therapy. Thyreostasis was discontinued at least 2 days before application of radioiodine. Individually-calculated radiation doses, based on the pretherapeutic data of thyroid volume, the functional and antibody (only TRAb) status, and iodine turnover equivalents such as early and late uptake values, ranged from 125 to 250 Gy. Corresponding activities of I-131 were calculated using the formula of Marinelli. Additionally most patients received cortisone (initial 25 mg/d) for 6 weeks in decreasing dosage. Patients not treated with cortisone for medical reasons received an additional 25 Gy. Patients were examined ≥ 6 months after radioiodine therapy. TSH was used as a measure of success. Results: A mean dose of 170 Gy was delivered to the thyroid. Overall success rate was 73.5 %, about 25 % of patients remained manifest or subclinically hyperthyoid. The highest success rate of 90 % was achieved with the basis dose of 125 Gy, the success rate decreased linearily and significantly ($r = 0.90$) from low to high doses. Only one patient received 250 Gy, this patient became euthyroid. No differerences were seen in patients with or without cortisone treatment. Of all variables used in this strategy only the thyroidal uptake of $^{99m}TcO_4^-$ was able to discriminate between success and failure of therapy as examined by multivariate analysis. Results were related to individual radiation doses as follows:

G	HD (Gy)	n	euthyroid (%)	hypothyroid	hyperthyroid	Success (%)
I	125	20	70	20	5	90
II	150	59	45.8	25.4	28.8	71.2
III	175	43	50.1	38.5	19	81
IV	200	32	40.6	25	34.4	65.5
V	225	16	37.5	12.5	50	50
Mean	170		48.2	25.3	26.5	73.5

Conclusion: Individual dose calculation in radioiodine therapy of Graves'disease is possible without negatively affecting the overall success rate, but the strategy needs further refinement.

OS_339

LEGISLATION: AN IMPETUS FOR A DATABASE TO DOCUMENT RADIATION PROTECTION DATA AND OPTIMISE PATIENT PLANNING FOR RADIONUCLIDE THERAPY

L.K. Janssen-Pinkse, A. van der Ree, F. Smit, I.J. Stroomnat, B.L. Wemmenhove, E. Busemann Sokole, B.L.F. van Eck-Smit. Department of Nuclear Medicine, Academic Medical Centre, Amsterdam, The Netherlands.

Background: The Euratom directives are implemented through radiation protection regulations within each European Union country. One requirement is that every radionuclide therapy be fully documented. This includes information about the treatment and medication given, patient information provided, and all radiation measurements obtained. In order to fulfil this requirement and to simplify the documentation, an electronic database was built to incorporate all these aspects for each therapy protocol applied within the department.

Methods: The database was constructed in FileMaker Pro. Each record created represents an individual therapy. The program is fed data at each step of the therapy, starting with the referral to the hospital discharge.

We handle up to 7 different protocols, each with its own logistics, such as for in and outpatients. Every step of the therapy is crucial. The program guides the user at each step, plans the logistical matters, prints the appropriate patient information, and prints radiation protection forms for documenting measurements. In addition it is programmed to calculate the therapy dose to be administered.

Users of the database are divided into groups with different data input privileges. For example, the administrative group input general patient data and plan initial diagnostic procedures for the therapy, whereas nuclear medicine physicians and radiation protection personnel input data at later stages. All groups are able to trace the progress of a therapy. Moreover, schematic therapy overviews can be made for sub-department use.

Results: The database was originally designed for radiation protection purposes, but is now a complete planning system for radionuclide therapy. The database is accessible at different locations via the hospital intranet. Since January 2001 the database has been implemented and tested alongside the old planning system. Users were instructed, and debugging took place to optimise the database. It has resulted in streamlining the whole process. Patients have responded favourably to tailor-made information.

Conclusion: The database fulfils expectations both for legal aspects of radiation protection and for therapy planning. The next step is to connect the database to the nuclear medicine management system and the module for ordering radionuclides.

OS_340

DEVELOPMENTS IN TECHNICAL REPORTING.

K.G. Holmes (1), G. Vivian (2). (1) University of the West of England; (2) Derriford Hospital NHS Trust, Bristol, UK.

Methods
In 1999 the University of the West of England in Bristol began the first postgraduate Technical Reporting module for technologists employed in Nuclear Medicine. The module's aims include the development of the clinical skills of the practitioner enabling them to describe, discuss and evaluate radionuclide imaging procedures, within a framework of ethical, legal and management issues fostering effective, rational decision-making.
It also aims to recognise the professional barriers that may cause inhibition of this process. Assessment was by logbook, Objective Structured Clinical Examination (OSCE) and an assignment 'The extended role of the technologist in the light of clinical governance' This paper explores the results and developments from two cohorts of students.
Results
All 18 students successfully completed the OSCE with a range of marks from 80-95%. This compared favourably with a logbook that compared the students' reports with a supervising Radiologist mentor. In all the cohorts of students undertook over 4,000 examinations on which they produced a Technical Report. Overall disagreement with their mentor was less than 4% for lung, renal and bone scans. A joint publication was undertaken by students from the award in Synergy and this coincided with a presentation of the results from the first cohort at the Spring BNMS in April 2000.
Conclusions
The results from this module demonstrate that appropriately trained Technologists can undertake Technical Reporting to a high level of agreement with their medical colleagues. While most students will not report studies alone all identified that the module enhanced their professional practice and procedures. Two protocols for double reporting scans has been developed at separate sites and are in the process of being implemented. This should result in more timely and accurate reports and improve patient management.

OS_341

MULTI-GATED BLOOD POOL REPORTING: THE ROLE OF THE CLINICAL TECHNOLOGIST

I. Jones, N. Storry, A. McCance, A. Tukan. Nuclear Medicine Service, Southern Derbyshire Acute Hospitals NHS Trust, Derby, UK.

Multi-Gated Blood Pool Acquisition (MUGA) is increasingly requested by Cardiothoracic Physicians and Oncologists to evaluate heart function prior to and during treatment. Cardiologists or radiologists normally report them. However, in the UK, there is little or no formal basic Multi-Gated Blood Pool report training. In our institution, a District General Centre, we have adopted a different strategy, by extensive tuition and developing a training package clinical technologist now report.
Aim
In the UK clinical technologists routinely perform blood pool imaging. We therefore considered a natural extension of their role would be to perform and interpret these studies.
Methods
Two experienced technologist were trained in reporting by:
Developing an in-house training course
Individual teaching and supervision in clinical cases by an experienced cardiac clinician.
Audit and review of studies and reports.
Results / Conclusions
Both technologists now routinely perform and interpret MUGA studies following written authorisation by the Cardiac Clinicians. A third technologist is in training. This protocol has worked very successfully. Since the technologist service started, there has been a dramatic increase in turn round times for reports from 5-7 days to 1-2 days. Feedback from the clinicians has been very positive. At all times, clinical responsibility remains with the consultant cardiologists in charge of the cardiac imaging

OS_342

CONVENIENT ARCHIVING AND PRESENTING SCINTIGRAPHY IN COMBINATION WITH OTHER DIAGNOSTIC RESULTS.

J. van den Hurck (1), S. Versmissen (2), T. Mechelen van (1), J.P.H. Cambier (1), R. Starmans (3), M. Plaizier (1). (1) Department of Nuclear Medicine, Dr. B. Verbeeten Instituut, Tilburg, The Netherlands; (2) Department of Information Technology, Dr. B. Verbeeten Instituut, Tilburg, The Netherlands; (3) Department of Mathamatics and Computer Science, University of Utrecht, Utrecht, The Netherlands.

Aim:
For educational and presentational purposes, our institute needed an information system to store and easily retrieve interesting nuclear data together with other relevant images and medical documents. The idea was to develop a system based on conventional database technology, which can easily be maintained and which is suitable for multi-users. The retrieved data should be applicable in current presentation programs.

Methods:
Database:
We used a relational database implemented in Access 97. The patients identification data were taken from the „Hospital Information System". The actualised medical histories of the patients were summarised by keywords such as mammacarcinoma, thyroid cancer, thyroid cyst, bone metastases, hypertension, pyelonefritis, hyperthyreoidie and carcinoid. The images (nuclear, CT, MRI, etc) and other relevant medical documents were described by up to 80 keywords including bone metastases, renal artery stenosis, toxic adenoma, cold nodule etc. Selections of cases and documents can be made with conventional querying techniques.
Images and other medical documents:
The scintigraphic results were added to the database via DICOM files (ADAC Dicom software according ACR-NEMA Dicom 3.0 standard). The report of the nuclear physician could be found in the database as a Word 97 file. Radiological results and other relevant medical documents were scanned with a UMAX Super Vista s-12 scanner (UMAX DATA SYSTEMS INC) and viewed by Osiris Imaging Software (version 3.6 PC/Windows 32 bits, Informatics Center University Hopital of Geneva 1211 Geneva 14). Special attention was paid to the quality of the radiological images after the scanning.
Results:
Approximately 40 patients are stored into the database, gradually more cases will be added. The database is easily assessable by a user-friendly interface. Images from the database can be simply presented in PowerPoint 97. The quality of the scanned images is good.
Conclusion:
We developed a database system combining nuclear results with relevant radiological images and other medical data. Case and document selection are based on relevant keywords on the patient history, image characteristics and data of other documents.

DIAGNOSTIC ONCOLOGY

OS_343

INFLUENCE OF THE P-GLYCOPROTEIN INHIBITOR VERAPAMIL ON THE ACCUMULATION OF CATIONIC TRACERS IN BREAST CELLS AND TISSUES

S. Haq (1), M. Rodrigues (1), S. Granegger (1), W. Kalinowska (2), L. Auerbach (3), G. Oberhuber (3), C. Zielinski (2), H. Sinzinger (1). (1) Department of Nuclear Medicine,University Hospital of Vienna; (2) Clinical Division of Oncology, Department of Internal Medicine I, University Hospital of Vienna; (3) Department of Special Gynaecology, University Hospital, Vienna, Austria.

Production of transmembrane efflux pump P-glycoprotein (Pgp) by tumor cells may cause increased efflux of tracers, and therefore account for lower tumor to background ratios. Inhibition of Pgp-mediated efflux of Tc-99m-MIBI and Tc-99m-tetrofosmin by the addition of a competitive inhibitor of Pgp such as verapamil might be an approach to increase accumulation of tracers in tumor cells and to improve sensitivity of scintigraphy with these tracers. The aim of this study was to evaluate the effects of verapamil on the Tc-99m-MIBI and Tc-99m-tetrofosmin accumulation in in-vitro well-characterized human breast cancer and non-tumor breast cell lines, as well as in breast adenocarcinoma and normal breast tissue.
Methods: The human adenocarcinoma breast cells MCF-7 (differentiated epithelial-like) and SK-BR-3 (poorly differentiated epithelial-like), and the non-tumor breast cells HBL-100, preincubated 15 or 30 minutes with 10 or 100µM verapamil, or not, were incubated with 7.4x10E5 Bq Tc-99m-MIBI and Tc-99m-tetrofosmin for 10, 30 and 60 minutes. In each experiment (n=6 each), a control cell accumulation of the tracer was obtained for that batch of cells (1x10E6 cells/ml). Normal breast and differentiated adenocarcinoma breast tissue, n=6 each, obtained during surgery in patients without previous treatment for breast disease, was incubated at 37°C with 7.4x10E5 Bq or 7.4x10E6 Bq Tc-99m-MIBI and Tc-99m-tetrofosmin for 15 or 30 minutes, with or without preincubation with 10 or 100µM verapamil. Accumulation of the tracer in cells or breast tissue was expressed as a % of the respective control values of tracer accumulation, or as %/mg tumor tissue, respectively.
Results: A decline in Tc-99m-MIBI and Tc-99m-tetrofosmin accumulation was found with verapamil in breast cancer cells and tissue, whereas in non-tumor breast cells and normal breast tissue verapamil increased the accumulation of both tracers. These effects of verapamil were neither dose- nor incubation time-dependent.
Conclusions: Differences in metabolic capacity between cell types may account for this heterogeneity of tracer accumulation found with verapamil. Might be that breast cancer cells may overexpress other types of transporters, which might also modulate intracellular tracer accumulation and not likely be inhibited by verapamil, or that sublethal injury to the cells could not be distinguished from a successive reverse of Pgp in the breast cancer cells and tisues investigated. Verapamil does not seem useful in addition of Tc-99m-MIBI and Tc-99m-tetrofosmin for in-vivo study of breast cancer.

OS_344

VERAPAMIL DECREASES ACCUMULATION OF TC-99M MIBI AND TC-99M TETROFOSMIN IN HUMAN BREAST CANCER AND SOFT TISSUE SARCOMA CELLS

M. Rodrigues (1), W. Kalinowska (2), A. Arakil Aghajanian (1), C. Zielinski (2), H. Sinzinger (1). (1) Department of Nuclear Medicine; (2) Clinical Division of Oncology, Department of Internal Medicine I, University Hospital, Vienna, Austria.

One major mechanism leading to the development of multidrug resistance (MDR) is the increased expression of the transmembrane efflux pump P-glycoprotein (Pgp). Tc-99m MIBI (MIBI) and Tc-99m tetrofosmin (TF) are recognized by the Pgp. Verapamil has been shown to be a competitive inhibitor of Pgp, and was one of the first MDR reversing agents identified. The aim of this pre-clinical in-vitro study was to evaluate the effects of verapamil on the accumulation of MIBI and TF in well-characterized human breast cancer and soft tissue sarcoma cell lines. This to address the possible increase in sensitivity of tumor detection with MIBI or TF with verapamil, and the value of these tracers for the functional detection of MDR in patients with breast cancer and soft tissue sarcoma.

Methods: Human adenocarcinoma breast cells MCF-7 (differentiated epithelial-like) and SK-BR-3 (poorly differentiated epithelial-like) and human soft tissue sarcoma cells SW 982 (synovial sarcoma) and SW 1353 (chondrosarcoma) were incubated with either (final concentration) 10 or 100 μM of verapamil, for 15 or 30 min. Thereafter, cells ($1x10^6$ cells/1 ml culture medium) were incubated with $7.4x10^5$Bq MIBI or TF for an additional 10, 30 or 60 min. The MIBI and TF accumulation in these cells at 10, 30 and 60 min after incubation with these tracers was compared with respective control cells, i.e. without preincubation with verapamil. At least six probes of each combination of the experimental conditions (i.e. concentration and incubation time with verapamil, and incubation time with tracer) were studied.

Results: Addition of verapamil caused a decline in accumulation of MIBI (2.29-55.22%) and TF (1.09-51.98%). This decrease was found at all incubation times with the tracers. The effects of verapamil on the cellular accumulation of MIBI were neither dependent on the dose (except in SW 982 cells), nor dependent on the time of preincubation with verapamil. Accumulation of TF was dose- as well as preincubation time-dependent in SK-BR-3 and SW 982 cells only.

Conclusions: Verapamil is not a promising agent for increasing sensitivity of scintigraphy with MIBI or TF, or for evaluating Pgp tumor status in these types of tumors.

OS_345

COMPARISON OF THE KINETICS OF TC-99M-SESTAMIBI, TC-99M-TETROFOSMIN, AND DOXORUBICIN IN A MULTIDRUG RESISTANCE TUMOR CELL LINE

K. Utsunomiya (1), J.R. Ballinger (2), M. Piquette-Miller (3), A.M. Rauth (3), M. Ichise (4), I. Narabayashi (1). (1) Department of Radiology, Osaka Medical College, Osaka, Japan; (2) Department of Nuclear Medicine, Cambridge University, Cambridge, UK; (3) Department of Faculty of Pharmacy, University of Toronto, Toronto, Canada; (4) Nuclear Medicine, University of Toronto, Toronto, Canada

Aim: To determine whether Tc-99m-Sestamibi (MIBI), Tc-99m-Tetrofosmin (Tfos), and Doxorubicin are substrates for P-glycoprotein (Pgp) and Multidrug resistance protein (MRP) transporters and compare their kinetics.

Methods: The accumulation and efflux of MIBI, Tfos, and Doxorubicin in breast cancer MDR1 transfected cell line (MCF7/BC-19) were studied both in the presence and absence of the various inhibitors of Pgp and/or MRP activity {GG918, PSC833, verapamil (Vrp), cyclosporin A (CsA), and buthionine sulfoximine (BSO)}. The radioactivity in the cell was measured in a gamma well counter for MIBI and Tfos study. Flow cytometry with fluorescence detection was used for Doxorubicin study. Reverse-transcriptase polymerase chain reaction (RT-PCR) analysis was used for the detection of Pgp, MRP1 and MRP2 mRNA expression of the cells.

Results: RT-PCR analysis of the MCF7/BC-19 cells detected expression of a high level of Pgp and low levels of both MRP1 and MRP2. MIBI, Tfos, and Doxorubicin accumulation was increased ($p<0.001$) in the presence of GG918, PSC833, Vrp and CsA, but not BSO, and efflux is decreased ($p<0.05$) in the presence of GG918 and PSC833, but not Vrp, CsA, and BSO, which is a specific inhibitor of MRP. Dose dependency in GG918 (0 to 0.1 mM) and PSC833 (0 to 5 mM) inhibition was observed. Synergistic effects of inhibitor combinations of GG918+BSO and PSC833+BSO were seen with accumulation and efflux of MIBI, Tfos, and Doxorubicin. The absolute accumulation of MIBI was ~2-fold higher than that seen with Tfos. However, no qualitative differences in inhibitors were seen between MIBI and Tfos.

Conclusion: All of MIBI, Tfos, and Doxorubicin are substrates for the MRP transporter as well as the Pgp transporter; and PSC833, Vrp, CsA, and BSO - but not GG918 - can inhibit MRP activity. The kinetics of MIBI and Tfos are similar to those of Doxorubicin and these may be suitable radiotracers for detecting Pgp and MRP –mediated drug resistance in human cancers.

OS_346

THE USE OF 99MTC-SESTAMIBI SCINTIGRAPHY IN THE CHARACTERIZATION AND FOLLOW-UP OF MYELOMA BONE DISEASE

G. Villa (1), G. Agnese (1), E. Balleari (2), P. Bianchi (1), F. Buffoni (1), M. Carletto (1), S. Garrè (2), M. De Lucchi (2), R. Ghio (2), M. Mariani (1). (1) Nuclear Medicine Service; (2) Hematology/Oncology Unit, DiMI - University of Genoa, Genoa, Italy.

The aim of this study was to evaluate the role of whole-body scintigraphy with ^{99m}Tc-Sestamibi (^{99m}Tc-MIBI) in the detection of bone marrow involvement in patients (pts) with multiple myeloma (MM) and in the follow-up of pts in relation to therapy.

Sixty-two pts with MM (31 men and 31 women) and 28 pts with monoclonal gammopathy of undetermined significance (MGUS) (17 men and 11 women) were enrolled in this study. At the time of first ^{99m}Tc-MIBI scintigraphy, 47/62 MM pts had active disease (AD), while 10/62 were in complete remission (CR) and 5/62 in partial remission (PR) after chemotherapy. Anterior and posterior whole-body scans were obtained 10 min after the i.v. injection of 740 MBq of ^{99m}Tc-MIBI. The scans were scored semiquantitatively according to extension and intensity of tracer uptake.

All 28 MGUS pts had a negative ^{99m}Tc-MIBI scan. As to the MM pts, 49/62 pts (44 with AD, 4 with PR and 1 with CR) had a positive ^{99m}Tc-MIBI scan, while the ^{99m}Tc-MIBI scan was negative in 13/62 pts (9 with CR, 1 with PR and 3 with AD). Thus, the overall resulting sensitivity of the scintigraphic procedure was 92.3% while specificity was 97.4%.

A total of 27 follow-up scans with ^{99m}Tc-MIBI were performed in 20 MM pts after high-dose chemotherapy, with an average follow-up duration of 12.8 ± 7.8 months (median 12 months, range 3 to 33 months). The follow-up ^{99m}Tc-MIBI scintigraphy was positive in 9/10 of the AD pts, while 6/8 negative scans were observed in the CR pts patients (one of the two positive scans showed extra-medullary localizations only), and the two PR pts exhibited, respectively, a negative scan and a mild scintigrafic positivity. The overall resulting sensitivity and specificity of the follow-up scan were, respectively, 90% and 87%.

The results obtained in this study provide additional evidence indicating that ^{99m}Tc-MIBI scintigraphy closely reflects myeloma disease activity in the bone marrow, and that a negative ^{99m}Tc-MIBI scan in pts with MM clearly, though not absolutely, indicates clinical remission of the disease. ^{99m}Tc-MIBI scintigraphy is also useful for monitoring the effects of therapy.

OS_347

QUANTITATIVE STUDY OF BLOOD FLOW IN SARCOMAS FROM DYNAMIC 99MTC–MIBI SCINTIGRAPHY: VALIDATION AND CLINICAL FOLLOW-UP STUDIES

W.Y. Ussov (1), A.M. Peters (2), E.V. Barysheva (1), M. Myers (2), O.YU. Borodin (1), Y.U.I. Tyukalov (1). (1) Tomsk Medical Research Center, Tomsk, Russia; (2) Hammersmith Hospital, London, England.

Aim. Although ^{99m}Tc-MIBI has been shown as providing imaging of bone sarcomas, quantitative analysis of ^{99m}Tc - MIBI uptake remains unemployed in diagnosis and follow-up of musculoskeletal tumors. We analysed uptake kinetics of ^{99m}Tc-MIBI in bone sarcomas in attempt to develop a technique for quantification of blood flow in vital tumor tissue.

Material and Methods Assuming ^{99m}Tc-MIBI uptake to sarcoma unidirectional for early few minutes after injection, the Gjedde-Rutland-Patlak (GRP) approach was applied, delivering classic equation: where $C_{tum}(t)$ is radioactivity in sarcoma, $\_{h}$ -blood concentration of ^{99m}Tc-MIBI, $\_$ - transport constant. Plotting as X, and as Y, the $\_$ can be obtained as slope . $\_$ is clearance equal to product *(retention fraction) * (tumor blood flow)*: $K = E * TBF$. TBF can be then calculated as ratio K/E. E was calculated from $A(t)$ and $C_h(t)$ time series as asymptote of ^{99m}Tc-MIBI retention function $h(t)=F^{-1}\{F[A(t)]/F[C_h(t)]\}$, where F is Fourier transforms, and corrected for intravascular component. In 32 patients with various musculoskeletal tumors the dynamic scintigraphy was performed with bolus injection of 540 MBq of ^{99m}Tc - MIBI and acquisition of tumor uptake of radioactivity with simultaneous blood sampling. From the blood input and tumor curves the TBF were calculated as descibed above. Correction for intravascular component was performed using pre-injected ^{99m}Tc-human serum albumin. Validation study with intraaortal catheter injection of ^{99m}Tc-labelled macroaggregates of albumin (MAA) was carried out in 12 patients.

Results. Validation with ^{99m}Tc-MAA revealed significant correlation ($r=0,89$; $p<0,002$) between TBF values calculated from dynamic ^{99m}Tc-MIBI uptake data and from ^{99m}Tc-MAA reference method. TBF values observed in patients varied from 49,5 (sd 2,6) ml/min/100 g in malignant osteoblastoclastomas and 31.7 (sd 10,1) ml/min/100 g in osteogenic sarcomas down to 23,1 (sd 1,6) ml/min/100 g in reticulosarcomas, 17,4 (sd 7,2) ml/min/100 g in Ewing sarcomas, 14,3 (sd 2,1) ml/min/100 g in fibrosarcomas, 12,6 (sd 0,6) ml/min/100 g in chondrosarcomas. In 3 patients (Ewing's sarcoma, reticulosarcoma and haemangiopericytoma), in whom the chemotherapy was proven effective later on from analysis of bioptate we observed early (within three days) postchemotherapy drop of TBF for > 1/3 of initial value. In patients with no effect of chemotherapy there was no early decrease in TBF.

Conclusion. Dynamic analysis of ^{99m}Tc-MIBI kinetics in sarcomas provides correct information on blood flow in the neoplasm. Early postchemotherapy decrease in tumour blood flow probably predicts the effect of chemotherapy in musculosceletal sarcomas.

OS_348

99MTC-MIBI AS PREDICTOR OF CHEMOTHERAPY RESPONSE IN BONE SARCOMA

H. Moustafa (1), R. Riaad (2), W. Omar (2), A. Zaher (2), E. Ebeed (3). (1) Nuclear Medicine, Cairo University, Egypt; (2) Nuclear Medicine, National Cancer Institute, Egypt; (3) Pediatric Oncology, National Cancer Institute, Egypt.

Chemotherapy is the initial treatment in bone sarcoma, which may be followed by surgery, or radiotherapy in patients with good response.

Aim of the work is to assess the response to therapy using Tc-99MIBI in relation to histopathological evaluation.

Methods: 28 patients with bone sarcoma (18 osteosarcoma and 10 Ewing sarcoma), aged from 8 to 19 years were included. The group compromised 24 males and 4 females. Pre-chemotherapy assessment was done using 20 mCi of ^{99m}Tc-MDP WBS with imaging at 10 min., 3 hours to assess the primary lesion and exclude metastatic spread. Whereas 20 mCi ^{99m}Tc-MIBI were injected and imaged at 20 min., and 2 hours were obtained before and after 3-4 courses of chemotherapy. Correlation of Tc-MIBI scan with the percentage of necrosis histopathologicaly was possible in 19 patients following surgical removal of involved limb. The remaining 9 patients were assessed clinically and radiologically versus Tc-MIBI scan for a period ranging from 6 to 12 months.

Results: Good response was evident in 12 patients with marked changes in qualitative images from high to no or mild uptake with significant decrease in mean ^{99m}Tc-MIBI ratio 2.57, 2.07 in early, and late images to 0.95 & 0.89 respectively ($P < 0.01$). 9 patients of osteosarcoma in this group showed > 90% necrosis in the surgically removed limb, while the other 3 Ewing sarcoma had no viable tumor in ^{99m}Tc-MIBI scan with no evidence of clinical or radiologic recurrence for 6-12 months.

The second group with **partial response** showed some change in qualitative images from high to moderate degree in post chemotherapy scans. Also, mean quantitive Tc-MIBI in early & late images were 5.03, 5.02 before chemotherapy and changed to 2.77, 2.43 following chemotherapy with significant difference ($P< 0.05$). The percentage of necrosis in this group ranged between 50 and 90%.

The third group with **no response** had no change in qualitative images before and after chemotherapy. Also, the mean early & late quantitive Tc-MIBI ratio before chemotherapy were 2.93, 2.69 with no change following chemotherapy with mean values of 3.8, 2.8 respectively. This group had necrosis < 50% histopathologicaly.

Conclusion: Tc-MIBI scan is a good method for assessment of chemotherapy response with significant correlation to histopathologic change.

OS_349

INTEREST OF 99MTC-MIBI SPECT IN THE RECURRENT BRAIN TUMOR DIAGNOSIS: A RETROSPECTIVE STUDY IN 201 SCANS

F. Prigent (1), F. Dubois (2), S. Blond (2), M. Steinling (1). (1) Dept Nuclear Medicine; (2) Dept Neurosurgery, Hopital R Salengro, Lille. France.

Aim : Standard treatment of glioma consists in surgery followed by radiation therapy. After this treatment, deterioration clinical status can be due to either radiation damages or recurrent initial tumor. CT and MRI are not always able to distinguish between tumor viability and radiation necrosis. The aim of this study was to assess the usefulness of brain SPECT with ^{99m}Tc-MIBI to establish this differential diagnosis, in a large series of 201 examinations.

Method : 81 patients, treated for low (II) or high (III/IV) glioma, were studied retrospectively. The tomoscintigraphy was performed one hour after intraveinous injection of 555 MBq of ^{99m}Tc-MIBI. Twelve transversal slices parallel to the orbitomeatal plane were obtained, coronal and sagittal views were reconstructed. A MIBI uptake index was computed as the ratio of counts in the lesion to counts in the controlateral region. When this index was superior to 2, it was considered as pathological. SPECT was compared to stereotactic biopsy, imaging evolution or clinical course at 6 months.

Result : 201 tomoscintigraphies were peformed. Most patients had several exams. 102 scans were true positive in patients affected by clinical and/or radiological and/or histological tumor recurrence. 82 scans were true negative in patients who did not show any signs of tumor recurrence 6 month after the last tomoscintigraphy. 6 scans were false positive (corresponding to 3 patients) : 2 patients with an inflammatory reaction after a stereotactic radiosurgery, 1 with no explanation up to now. 11 scans were false negative (corresponding to 5 patients) : 1 patient with a deep peri-ventricular lesion, which detectability is limited by choro•d plexus uptake, 2 patients with no contrast enhancement on MRI (no abnormal permeability of blood-brain-barrier), 2 patients with a temporal tumor. The sensitivity for tumor recurrence was 90%, the specificity 91,5% and the accuracy 90,5%. When we study separately low and high grade glioma, sensitivity for tumor recurrence was respectively 91% and 89%, specificity 100% and 83% and global accuracy 95% and 87%. We had no false positive in the low grade group, and the MIBI SPECT permits the diagnose of anaplasic degenerence sometimes earlier than clinical or MRI signs of recurrence.

Conclusion : Our results confirm, on the largest series to this day, the utility of MIBI SPECT in the follow-up of treated gliomas. This imaging appears accurate to diagnose early tumor recurrence. This study suggests the usefulness of repeated ^{99m}Tc-MIBI SPECT in low grade gliomas to detect the relapse and to adapt the clinical managmentearly.

OS_350

SESTAMIBI SPET FOR THE EVALUATION OF MEDIASTINAL INVOLVEMENT IN PATIENTS WITH LUNG CANCER

G. Savelli (1), A. Chiti (2), H. Dool (3), E. Bombardieri (1). (1) Istituto Nazionale Tumori,Milano, Italy; (2) Istituto Clinico Humanitas, Milano, Italy ; (3) Leiden University Medical Centre,Leiden,The Netherlands.

Aim: To assess if ^{99m}Tc-Sestamibi SPET is able to modify the management of patients with lung neoplasms.

Methods: Fifty-seven patients with clinically and radiology suspicion of lung cancer were enrolled in this study. For all patients a histological diagnosis was made, 47 patients had non-small-cell lung cancer: 3 had small-cell lung cancer: and 4 patients had non-neoplastic lung disease. Two patients had a lung carcinoid: and one had a metastasis from gastric cancer. In order to evaluate the mediastinum, the staging procedures included computed tomography (CT) and ^{99m}Tc-Sestamibi Single Photon Emission Tomography (SPET). The final diagnosis of the lymph nodes was obtained in 11 patients by mediastinoscopy and in 46 by surgery. Radionuclide imaging was performed 15 minutes after the intravenous administration of 740-925 MBq of ^{99m}Tc-Sestamibi. Data were acquired with a Picker Prism 3000 triple headed gamma-camera, matrix 128x128. The attenuation correction was performed by means of a ^{153}Gd source and reconstruction with iterative algorithm.

Results: Mediastinal lymph node involvement was demonstrated in 22 of 57 patients by pathology. ^{99m}Tc-Sestamibi SPECT correctly staged 20 of 22 patients with mediastinal lymph nodes metastases. Twenty-seven out of 35 patients without mediastinal lymph nodes metastases, were correctly staged by ^{99m}Tc-Sestamibi. The overall sensitivity was 90.1%, specificity 77.1%, positive predictive value (PPV) 71.4%, negative predictive value (NPV) 93.1%, accuracy 82.5%. CT reported resulted in a sensitivity of 77.3%, specificity of 57.1%, PPV 53.1%, NPV 80% and accuracy 64.9%. The relative figure of merit are reported in the table. In 18 cases both the CT and the ^{99m}Tc-Sestamibi SPET were negative. In this group, ^{99m}Tc-Sestamibi SPET and CT correctly identified 17 patients (94.4%). In 20 cases both the CT and the ^{99m}Tc-Sestamibi SPET were positive. Again, ^{99m}Tc-Sestamibi SPET and CT correctly identified 17 patients (85%).

	^{99m}Tc-Sestamibi SPET	CT
Sensitivity	(20/22) 90.1%	(17/22) 77.3%
Specificity	(27/35) 77.1%	(20/35) 57.1%
Positive predictive value	(20/28) 71.4%	(17/32) 53.1%
Negative predictive value	(27/29) 93.1%	(20/25) 80.0%
Accuracy	(47/57) 82.5%	(37/57) 64.9%

Conclusions: The evaluation of mediastinum is pivotal in the clinical management of lung cancer, addressing patients towards surgery or chemoradiotherapy. In this setting, ^{99m}Tc-Sestamibi SPET has showed to be a very useful tool, providing valid information in the clinical decision making.

CARDIOVASCULAR

OS_351

ATHEROSCLEROTIC PLAQUE DETECTION IN DIET INDUCED BALB/C MICE

C. Mari, M. Blankenberg, H.W. Strauss. Nuclear Medicine division, Stanford Hospital. Stanford, California, USA.

The evolution of the atherosclerotic plaque from fatty streak to ruptured plaque is accompanied by specific pathophysiologic changes as: cell activation (smooth muscle cells, lymphocytes, macrophages), cellular apoptosis and neovascularization in the plaque. The detection of these molecular changes using specific tracers could permit the identification of active atherosclerotic plaques (by using an appropriate device).

Aim: To evaluate four different specific tracers in the identification of active atherosclerotic plaques by means the detection of their molecular changes.

Methods: We studied 18 male BALB/C mice (known to develop atherosclerosis induced high fat diet). Mice were placed on a high fat high cholesterol diet for 6-12 weeks. They were classified in four different groups and injected with four different tracers that specifically detect a molecular change in the atherosclerotic plaque: 1) Tc99m-Annexin V (apoptosis); 2) 201-thallium (plaque neovascularization); 3) F18-FDG (macrophage metabolism); 4) In111-pentatreotide (increased somatostatin receptors in activated lymphocytes and proliferative smooth cells). Mice aortas were removed, open longitudinally and autorradiographed. Autorradiographs were studied semiquantitatively and compared to histology.

Results: (table).

Conclusion: All four agents showed some uptake in the atherosclerotic lesions of BALB/C mice, suggesting the all four could be useful in the detection of active atherosclerotic plaques by means their molecular changes. However, Annexin V detecting apoptosis showed the best results for atherosclerotic plaque detection in diet induced BALB/C mice.

OS_352

MYOCARDIAL PERFUSION SCINTIGRAPHY FOR THE SCREENING OF CANDIDATES FOR IMPLANTATION OF A CARDIOVERTER-DEFIBRILLATOR IS COST-EFFECTIVE

J.J.J. Borm (1), M.J. Schaly (2), Y.G.C.J. America (1), E.E. van der Wall (2), E.K.J. Pauwels (1). (1) Nuclear Medicine; (2) Cardiology, LUMC, Leiden, The Netherlands.

Aim: To assess the cost-effectiveness of the routine use of myocardial perfusion scintigraphy [MPS] in candidates for placement of a cardioverter-defibrillator [ICD].
Methods: Retrospective evaluation of consecutive patients at our institution that underwent MPS and were considered potential ICD-candidates, based on Class I indications according to the 1998 ACC/AHA recommendations [J Am Coll Cardiol 1998; 31: 1175-1209]. During the study, it was policy to refer all potential candidates for MPS. Electrophysiological testing was routinely performed to assess the response on therapeutic measures, such as anti-arrhythmic medication, RF-ablation and revascularization. Myocardial perfusion scintigraphy with tetrofosmin was performed as previously described. Survival curves and event-free survival curves according to Kaplan and Meier were obtained.
Results: 88 consecutive patients were included. Patient characteristics: age 61 ± 11 y; male 83%, on average 1.6 risk factors for coronary artery disease; previous myocardial infarction 56%, CABG 15%, PTCA 7%. Normal perfusion was seen in 10 subjects. Three of them received an ICD. Irreversible defects were encountered in 48 subjects, resulting in 24 ICD implantations. A total of 29 subjects showed reversible defects. These were considered primary target for MPS-guided therapy. In 6 of them only reversible defects were seen and none received an ICD, and only 2 underwent revascularization. Four out of 23 subjects with combined reversible and irreversible subjects could be treated with medication alone. A further 7 initially received an ICD, but in one case secundary revascularization was required. In the other 6 subjects, the area of ischemia and the arrhythmogenic focus did not match. Twelve subjects underwent revascularization as primary therapy. In 5 subsequent ICD implantation was necessary. On survival analysis a 3-fold reduction in mortality was seen among ICD-recipients, when compared to event-free survival with ICD-recorded ventricular fibrillation as surrogate endpoint. Overpacing ventricular tachycardia was not used as a surrogate endpoint. The survival among non-recipients was also good. MPS resulted in 17 subjects with reversible defects successfully treated by medication or revascularization. Those receiving medication had smaller reversible defects than those undergoing revascularization.
Conclusions: Routine use of perfusion scintigraphy in ICD-candidates is cost-effective, saving 17 ICD implants at a cost of 88 MPS procedures and a further 9 PTCA and 7 bypass procedures.

OS_353

USE OF HEART-LUNG MACHINE HAS IMPACT ON RENAL FUNCTION DURING HEART SURGERY

D. Sandrock (1), W. Heldwein (2), S. Morgera (2), H. Müller (1), K. de Jonge (3), D.L. Munz (1). (1) Clinic for Nuclear Medicine, University Hospital Charité, Berlin, Germany; (2) Clinic for Nephrology; (3) Clinic for Cardiovascular Surgery, Berlin, Germany.

Aim: During use of a heart-lung machine (HLM) in cardiac surgery there is an altered circulation (changes of volume and pressure, flow instead of pulse wave circulation) resulting in a decrease of urine excretion during the intervention. Aim of this study was to quantify intraoperatively the renal function, in particular the renal blood flow.
Methods: At start of a cardiosurgical intervention (bypass, valve replacement) in 45 patients (13 women, 32 men, aged 68 +/- 10 years, 9 patients > 75 years, 10 with diabetes, 3 with heart insufficiency, 3 with renal impairment) 10 MBq I-123-orthoiodohippurate (OIH) were injected i.v. Venous blood samples were drawn at standardised and documented time points (start HLM, 12 min after start, end HLM; 15 min after end HLM again 10 MBq I-123-OIH for better count statistics) and measured in a gamma well counter. From these data renal plasma flow was (corrected for intraoperative volume changes) calculated and compared with creatinine clearance (as an equivalent of glomerular filtration rate).
Results: In *all* patients there was a decrease of renal plasma flow during the use of HLM. The mean clearance decreased from 238 +/- 84 ml/min before HLM to 75 +/- 37 ml/min after start HLM, and further to 42 +/- 19 ml/min at end HLM. 15 min after end HLM clearance increased back to 179 +/- 70 ml/min. This represents a decrease to 32 % (early HLM) and 18 % (end HLM) of the original value (with a re-increase to 75 % after HLM). In the subgroups age > 75 years, diabetes, heart/renal impairment there was the same clearance „behavior„ as in the „normal„ patients. The changes of the renal plasma flow were more prominent than those of the glomerular filtration (with a modest correlation).
Conclusion: During the heart-lung machine in cardiac surgery there is a (partially) reversible decrease of renal plasma flow independent of age or other diseases.

OS_354

LOW HEPATIC ACTIVITY OF TECHNETIUM-99M SESTAMIBI IN PATIENTS USING DRUGS INDUCING THE CYTOCHROME P450 OXIDASE SYSTEM

S.S. Nielsen (1), S. Tigaran (2), M. Rehling (1). (1) Department of Clinical Physiology and Nuclear Medicine; (2) Department of Neurology, Aarhus University Hospital, Denmark.

Aim: We have noticed strikingly low hepatic activity after injection of Tc99m-Sestamibi (MIBI) in patients receiving drugs known to cause induction of hepatic enzymes. The aim of the study was to examine if hepatic induction gives less hepatic activity of MIBI than normally found.
Materials and methods: Fourteen patients receiving enzyme inducing drugs (induction group) were examined along with a control group of 25 patients (controls) not receiving enzyme inducing drugs. Coronal slices from reconstructed myocardial SPECT images were summed and regions of interest were drawn over the upper right quadrant of the liver. Dose of MIBI, time from injection to scanning, weight and age was noted.
Results: (mean ± SEM). Hepatic activity was significantly lower in the induction group than the control group (3236±865 vs 7263±1453 counts/pixel, p<0.0001). There was no difference between groups regarding dose (690±6.2 vs 701±6.3 MBq), time to scanning (59±7.4 vs 60±3.2 min) or weight (77±5.7 vs 78±3.9 kg). Age in the controls were higher than in the induction group (53±1.9 vs 41±2.6 years).
Conclusion: Hepatic activity of MIBI is lower in patients receiving enzyme inducing drugs than in controls indicating that hepatic clearance of MIBI is accelerated by drugs causing hepatic induction.

OS_355

ASSESSMENT OF SILDENAFIL (VIAGRA) EFFECTS ON DIPYRIDAMOLE STRESS MYOCARDIAL PERFUSION IN PATIENTS WITH ERECTILE DYSFUNCTION AND ATYPICAL CHEST PAIN USING QUANTITATIVE MYOCARDIAL PERFUSION SPECT

G.J. Cheon (1), D.S. Lee (1), Y.K. Kim (1), K.W. Kang (3), E.C. Park (2), J.S. Paick (2), J.-K. Chung (1), C.W. Choi (4), S.M. Lim (4), S.W. Hong (4), M.C. Lee (1)(1) Department of Nuclear Medicine, Seoul National University, Seoul, Korea; (2) Department of Urology, Seoul National University, Seoul, Korea; (3) Department of Nuclear Medicine, National Cancer Center, Seoul, Korea; (4) Department of Nuclear Medicine, Korea Cancer Center Hospital, Seoul, Korea

The ACC/AHA Expert Consensus Document recommended the use of sildenafil in cardiac patients after cardiac risk stratification through tests such as treadmill ECG test. The exercise ECG test, however, has a lower sensitivity and non-diagnostic cases for the detection of coronary artery disease. The purpose of this study was to evaluate the ability of the stress myocardial perfusion SPECT to assess the stratification of cardiac risk in patients with erectile dysfunction.
Methods: Seven patients with erectile dysfunction and atypical chest pain underwent dipyridamole (n=6) or exercise (n=1) stress ^{99m}Tc-MIBI myocardial SPECT before (pre-Viagra stress SPECT) and at one hour after sildenafil 100 mg oral administration (Viagra-challenged stress SPECT). During the dipyridamole stress (0.56 mg/kg/4min), blood pressure was monitored in every two minutes. Regional myocardial perfusion was quantitated using automatic quantitative software. We evaluate the correlation of regional stress myocardial perfusion between at pre-Viagra and at Viagra-challenge.
Results: Dipyridamole stress-induced decrease of systolic blood pressure (dSBP, 22±12 mmHg) did not differ significantly from sildenafil challenged dipyridamole stress-induced dSBP (24±12 mmHg, p=n.s.). Sildenafil and dipyridamole did not have the synergistic effects to provoke severe hypotension, which was reported to be provoked by nitrate compounds. Five patients in the intermediate graded risk group and 2 in the low graded risk group, as determined by clinical assessment, were re-stratified as belonging to the low cardiac risk group by the preserved perfusion reserve on stress myocardial SPECT. Quantitative regional myocardial perfusion on sildenafil challenged stress myocardial SPECT was correlated well with the regional perfusion on baseline stress myocardial SPECT (r=0.967). Sildenafil challenged stress regional perfusion (70±14%) did not differ significantly from basal stress regional perfusion (69±14%, p=n.s.).
Conclusions: As pre-Viagra stress myocardial SPECT can predict sildenafil challenged stress myocardial perfusion, stress myocardial SPECT can be used to stratify the cardiac risk during Viagra administration in patients with erectile dysfunction and atypical chest pain. Sildenafil challenged dipyridamole stress myocardial SPECT was determined to be safe, in contrast to the combination of sildenafil and nitrate.

OS_356

TC99M ANTIGRANULOCYTE SCINTIGRAPHY IN DETECTION OF MYOCARDIAL INFLAMMATION - PRELIMINARY RAPORT

A. Hubalewska (1), D. Dudek (2), A. Staszczak (1), J. Dubiel (2), Z. Szybinski (1). (1) Nuclear Medicine Unit, Chair and Department of Endocrinology, CMUJ; (2) Chair And Department of Cardiology, CMUJ, Krakow, Poland.

The histopathological evidence of myocardial inflammation can be confirmed only in about 10% of patients with signs of unexplained cardiomyopathy. It is difficult to identify myocardial inflammation patients using clinical criteria, laboratory tests, ECG and ultrasonography. Currently, a myocardial biopsy is required to establish the diagnosis of myocarditis. The invasive nature, risk, fact that the focal inflammation of the heart is more frequent than disperse, and expense of myocardial biopsy indicate the value of a non-invasive method of diagnose. Confirmation of the myocardial inflammation is also important before the transplantation of the heart. There are several radiopharmaceuticals that have been used over the years for inflammation imaging, such as 67Ga, Tc99m-nanocolloids, 111In-leucocytes, and as the gold standard radiolabeled autologous blood cells (WBCs). The last mentioned method is difficult and time-consuming.

The aim: The aim of the study was to evaluate the sensitivity of Tc99m-AntiGranulocyte BW 250/183 scintigraphy in detection of present cardiac inflammation.

Materials and Methods

Two dimensional scintigraphy and SPECT mode with the use of Tc99m-AntiGranulocyte (Tc99m labelled antigranulocyte monoclonal specific antibody) was performed in 5 patients after biopsy confirmed myocardial inflammation. 750MBq Tc99m-AntiGranulocyte was injected iv. before acquisition. The data acquisition was repeated 24 h later. Patients after examination were treated with the use of anti-inflammatory drugs.

In all patients the same examination was performed 3-5 month after the first study when the control myocardial biopsy was negative.

Results: In all patients the first scintigraphic scans revealed accumulation of the tracer in cardiac area confirming the process of inflammation.

In the examination performed after anti-inflammatory treatment accumulation of the tracer was present in one patient. In this case the accumulation of the tracer was detected on the inferior myocardium wall but the biopsy was taken from the anterior myocardium wall, and repeated scintigraphic scan (performed 3 month later) was negative.

Conclusions: In our study the accordance of Tc99m-AntiGranulocyte two dimensional and SPECT mode scintigraphy and myocardial biopsy in recognition of present myocardial inflammation was observed.

It seems that Tc99m-AntiGranulocyte scintigraphy might be recommended in patient with suspected myocarditis.

OS_357

DAS CORONARY ARTERY ANEURYSM IN KAWASAKI DISEASE CAUSE EXERTIONAL MYOCARDIAL ISCHEMIA? AN EXERCISE TL-201 SCINTIGRAPHIC EVALUATION

T. Mochizuki (1), M. Miyagawa (1), Y. Sugawara (1), T. Kikuchi (1), T. Tsuda (1), S. Nakata (1), J. Ikezoe (1), Y. Murakami (2), E. Yamamoto (2), T. Higaki (2), K. Kida (2)(1) Department of Radiology; (2) Department of Pediatrics, Ehime University School of Medicine, Ehime, Japan.

Purpose: Although Kawasaki disease is well known to complicate coronary artery aneurysm, it is uncertain whether the aneurysm causes myocardial ischemia on exercise. The purpose of this study was to investigate whether the aneurysm in Kawasaki disease causes exertional myocardial ischemia, using exercise/redistribution (EX/RD) myocardial perfusion scintigraphy (MPS).

Methods: Materials consisted of 29 patients with Kawasaki disease, having or having had coronary artery complication. Ages ranged from 2 to 24 years old with a mean of 10. All patients underwent both coronary angiography and EX/RD Tl-MPS. In case of patients under 7 years, we applied standard dose of intravenous dipyridamole (Dp) loading instead of exercise. Three major coronary arteries were classified into four categories: (1) having stenosis _75% (ST), (2) normal, (3) having aneurysm < 8mm (AN-1), and (4) having aneurysm_ 8mm or long segment _2cm (AN-2). The Tl-MPS was performed after intravenous administration of 74 to 111 MBq of ^{201}Tl, using 3-headed SPET system (step and shoot, 20 steps _ 3 = 60steps, 30 sec/step). The delayed scan (RD imaging) was acquired 3 hours after the early scan (EX or Dp imaging). Tomographic images in cardiac axes were reconstructed from the transaxial images obtained by the filtered back projection method without attenuation correction. Bull's Eye maps of the EX/RD scans and of washout rate were generated. We evaluated the Tl-MPS visually using both tomographic images and Bull's Eye maps. Each territory of the three major coronary arteries (RCA, LAD and LCX) was judged as negative or positive. Therefore, 87 territories (29 patients _ 3 coronary arteries) were investigated in total.

Results: There were 2 territories of ST, 67 of normal, 10 of AN-1, and 8 of AN-2. The Tl-MPS was positive in 2/2 ST, 2/67 normal, 1/10 AN-1, and 5/8 AN-2. Most of the coronary arteries, which were normalized in the follow up, showed normal Tl-MPS.

Conclusions: Although smaller aneurysm (AN-1) does not cause exertional myocardial ischemia, large (giant) aneurysm (AN-2) often causes exertional myocardial ischemia in Kawasaki disease.

OS_358

EXERCISE TL-201 SCINTIGRAPHY OR MULTI-DETECTOR-ROW CARDIAC CT, WHICH TO CHOOSE FOR THE EVALUATION OF THE COMPLICATED CORONARY ARTERY IN KAWASAKI DISEASE

T. Mochizuki (1), M. Miyagawa (1), Y. Murakami (2), E. Yamamoto (2), T. Higaki (2), K. Kida (2), Y. Sugawara (1), R. Kikuchi (1), T. Tsuda (1), J. Ikezoe (1). (1) Department of Radiology; (2) Department of Pediatrics, Ehime University School of Medicine, Ehime, Japan.

Purpose: Recently released multi-detector-row CT (MDCT) can potentially evaluate coronary arteries. The purpose of this study was to compare exercise/redistribution (EX/RD) ^{201}Tl myocardial perfusion scintigraphy (MPS) and MDCT in the evaluation of coronary artery aneurysm and stenosis in Kawasaki disease.

Methods: Materials consisted of 15 patients with Kawasaki disease, having coronary artery complication. Ages ranged from 3 to 24 years with a mean of 14. All patients underwent both coronary angiography (CAG) and EX/RD Tl-MPS. Of these, 8 patients underwent MDCT. In each major coronary artery territory, we visually evaluated the Tl-MPS as normal or abnormal, using both tomographic images and Bull's Eye maps. We investigated the sensitivity of the Tl-MPS in the diagnoses of stenosis (75%) and aneurysm (5mm). The MDCT data were acquired using a contrast material (300mg-I/ml, 1.5 ml/sec i.v., 50-100ml) during a single breath hold (about 30 sec). Diameters of the major coronary arteries (Segment#: 1, 5, 6, 11) and the aneurysms measured by CAG and MDCT were compared.

Results: Among the 45 coronary territories (15 pts x 3 coronary territories), there were 2 territories of stenosis, 19 of aneurysms, and 24 of normal. Tl-MPS was positive in 2/2 stenoses and in 8/19 aneurysms. All 24 territories of normal coronary artery were negative. The MDCT depicted all coronary aneurysms. Diameters measured by CAG and MDCT were correlated well ($r=0.98$, $p<0.0001$, $n=42$ measured points in total).

Conclusions: EX/RD Tl-MPS is useful to evaluate myocardial perfusion abnormality due to stenosis or large aneurysm, while the MDCT is useful to detect and measure coronary aneurysm. Tl-MPS and MDCT should be cooperative rather than competitive as non-invasive tests for coronary artery evaluation in Kawasaki disease.

RADIONUCLIDE THERAPY / DOSIMETRY

OS_359

A COST-UTILITY ANALYSIS (CUA) IN THE TREATMENT OF PAINFUL BONE METASTASES IN PROSTATE CANCER PATIENTS: 89-SR VERSUS ASSOCIATION OF CISPLATIN AND 89-SR

R. Sciuto (1), A. Festa (1), R. Pasqualoni (1), A. Semprebene (1), G. Petrilli (1), P. De Carli (2), H. Fattahi (2), C.L. Maini (1). (1) Dpt. of Nuclear Medicine, ; (2) Dpt. of Urology, Rome, Italy.

The aim of the study was to compare the cost/utility of the standard treatment with 89-Sr alone versus an alternative intervention with a combined treatment (89-Sr plus low-dose of cisplatin) in prostate cancer patients with painful bone metastases.

Methods: the cost-utility analysis was performed with the following steps. *First,* the health state pertinent to the standard intervention and its alternative was defined using the results of a controlled randomized trial on 70 patients with metastatic prostate cancer (measure of quality of life score by an „ad hoc method"). *Then,* the amount of time spent in each health state is estimated for the two alternatives as all the patients were followed until death. Quality adjusted life years (QALYs) were so obtained multiplying the quality of life score for the respective time spent, representing the utility measures or „benefits". *Finally,* the costs were computed considering all the specific costs (direct and indirect) related to the intervention of the two arms. For the CUA, the cost/benefit ratio in each Arm of treatment was considered.

Results:

	COSTS *(Euro)*	BENEFITS (Qalys)	C/B ratio *cost/qaly*
Arm A			
Cisplatin + 89Sr	93.037	8,98	10.360
Arm B			
Cisplatin + placebo	84.933	4,34	19.569

Sensitivity analysis demonstrated that these results maintain their value even if costs or the benefits vary up to 50% of the observed values.

Conclusions: the combined treatment of cisplatin and 89-Sr resulted not only more effective in improving quality of life in prostate cancer patients but also economically sound as cost-utility analysis showed a lower cost-benefit ratio.

OS_360

THE RELATIONSHIP BETWEEN SKELETAL METASTATIC LOAD AND THERAPEUTIC ACTIVITY REQUIREMENT IN PROSTATE CANCER

V. McCready (1), J. O'Sullivan, F. Buffa, G. Cook, G. Flux, D. Dearnaley, R. Grant. (1) Department of Nuclear Medicine; (2) Department of Medical Physics; (3) Department of Radiotherapy, Royal Marsden Hospital, Sutton Surrey, UK.

Aim
To analyse labelled phosphate bone scans quantitatively in patients with prostatic metastases to investigate if patients with more metastases should be given higher activities of therapeutic agents.
Methods
Some studies suggested that patients with widespread metastases treated with fixed activities of Sr 89 chloride respond less well than those with fewer metastases. In this study whole body MDP scans of 11 patients performed under standard conditions prior to high activity Re186 HEDP therapy were analysed. Anterior and posterior views were analysed by placing regions of interest (ROI) around the whole scan to measure the total activity in the body, the outline of the skeleton, excluding the renal and bladder activity to measure the total activity in the skeleton, and around each metastasis. The total number of the cells (pixels) within the ROIs encircling the metastases was measured and this was expressed as a percentage of the total number of the cells within the skeleton. Likewise the total activity (counts) in the metastases was calculated and expressed as a percentage of the activity in the skeleton. A measure of the total metastatic involvement (metastatic load) was calculated by multiplying the percentage of the cells (area) involved by the activity in the metastases expressed as a percentage of the activity in the skeleton. The average uptake per cell of the metastases was calculated. The correlation between the metastatic load and the uptake per cell of the metastases and the number of metastases was investigated.
Results
The total bone activity ranged from 70-86% of the whole body activity. The metastatic load ranged from 4 -396 units while the uptake per cell ranged from17 counts (17 metastases, load = 32 units) to 92 counts (9 metastases, load = 24 units). There was no correlation between the metastatic load and the number of individual metastases and the average counts per cell in the metastases (r=0.244 and 0.11 respectively).
Conclusions
Widespread metastatic disease does not necessarily result in lower average activities in the metastases. Our study with MDP has shown that there is no significant difference in uptake in metastases in those patients with widespread or localised disease. If these results were confirmed in Sr 89 studies then the differential response must be due to factors other than the difference in uptake.

OS_361

ANTITUMOR EFFECTIVENESS OF MULTPLE COURSES OF SM-153-EDTMP IN BONE METASTASES FROM DIFFERENT CANCERS

P. Riva, G. Franceschi, N. Riva, M. Casi, M. Santimaria. Istituto Oncologico Romagnolo, Forli', Italy.

Aim: To evaluate the feasibility, the tolerance and the antitumor activity of multiple (up to 4) cycles of Sm-153-EDTMP in patients with bone metastases.
Material an Methods: 60 evaluable tumour patients (35 prostate, 35 breast, 3 lung, 4 others) with istologically proven tumour and documented bone metastases, were treated with Sm-153-DTMP (CIS-SCHERING), whose mean dose was 37 Mbq/kg per cycle. 29 cases presented more than 10 skeletal lesions (group 3), 11 had 5-10 lesions (group 2) and 20 pat. were bearing less than 5 neoplastic involvements (group 1). 33 patients received a single adminstration (SA). In 27 cases, in order to improve the results, we gave multiple treatments (MT), every 3 months . 19 cases had 2 cycles, 7 were treated 3 times and 1 received 4 administrations.
Results: In the SA group the toxicity was mild. We recorded 1 case of anaemia (grade II) 12 cases of grade I and 10 of grade II trombocitopenia. In MT patients, we registered in 4 cases grade I and in 7 grade II transient trombocitopenia.
The clinical effects in SA group were : complete pain disappearance in 11 (33.3%) cases (mean duration 3 months): 12 group 1, 3 group 2 and 7 group 3; significant pain reduction in 13 (39.3%) cases (mean duration 4.8 months): 4 group 1, 8 group 2, and 14 group 3, while in 9 (27.2%) cases: 4 group 1 and 8 group 3, no change occurred. In one (3.03%) breast tumour pat. we observed a complete regression of the lesions (scintigraphy and CT scan). In 3 cases (9.09) a decrease in number and size of lesions was documented. In the MT group, we observed a complete pain disappearance in 11 (40.7%) cases: 5 group 1, 1 group 2 and 5 group 3; a pain reduction in 13 (48.1%) cases: 2 group 1, 3 group 2 and 8 group 3, while in 3 (11.1%) cases no subjective response was obtained. Moreover In 7 (25.9%) cases (6 prostate and 1 breast) a reduction in number and volume of lesions was radiologically recorded.
Conclusions: Repeated treatments with Sm-153-EDTMP, can be safely given, up to 4. This approach can control the pain but, in some cases, can exert a cytolitic effect, with radiological evidence of decrease of tumour size or of its complete disappearance. The therapy is effective both in pat. with reduced tumour burden, and in cases with diffuse lesions.

OS_362

DETERMINATION OF OPTIMUM RADIONUCLIDE COCKTAIL REQUIRED TO ABLATE SKELETAL METASTASES OF VARYING SIZE

F.M. Buffa, G. Flux, R. McCready. Joint Department of Physics, Institute of Cancer Research, London, UK.

AIM: To develop a method for optimising radionuclide cocktail composition for the ablation of metastases situated within heterogeneous media, such as skeletal metastases.
METHODS: Changes in energy deposition distribution and biological effectiveness of different radionuclides, depending on range and dose rate, have already been shown in homogenous media, with uniformly distributed activity. Here, a theoretical model is developed based on Monte-Carlo (MC) energy deposition calculations (EGS system) for media with heterogeneous density. Metastatic lesion geometry is simulated as bone specula of varying shapes and size surrounded by tissue. Geometrical parameters are varied to produce different bone-to-tissue volume proportions, and various histological pathlength distributions are considered. Calculations are performed using both uniform and heterogeneous distribution of radionuclide activity across the specula surface. The surviving fraction (SF) of clonogenic metastatic cells is estimated using a linear quadratic model accounting for dose-rate effects. Values for the biological parameters of the SF model are chosen from published data, and it is assumed that metastatic cells have radiobiological properties similar to cells at the primary site. SF distribution in the tissue is computed with varying radionuclides and geometry. From this distribution, the probability of metastatic lesion control (MLC) is calculated, using both a Poisson model and a model based on birth-and-death statistics to account for cellular re-growth during irradiation.
RESULTS: Choice of particle transport parameter values is important when working with condensed histories MC, as it can influence the simulation. Results obtained using different parameter values were assessed against published data for point-source emitters in water. Good agreement was seen when parameter values similar to published data were chosen. Calculations for the cocktail study are performed at the convergence point for the parameter values. A comparison of absorbed fraction calculations when homogeneous density is assumed and when tissue-bone heterogeneity is accounted for, shows differences of up to 20%. This confirms the inadequacy of homogenous density simulations for cocktail optimisation studies in skeletal metastases. The MC energy deposition calculations are being incorporated into the SF model, and the MLC estimated for various radionuclide cocktail compositions and geometry parameter choices. The MLC probability will then be maximised for the optimum radionuclide cocktail for various geometry choices.
CONCLUSIONS: This method enables optimisation of radionuclide cocktail composition when targeting radiation to sites of heterogeneous density, such as skeletal metastases.

OS_363

IS HAEMATOLOGICAL TOXICITY OF 153 SM-EDTMP THERAPY IN SKELETAL METASTASES DOSE DEPENDENT?

D. Kendler, H. Erler, E. Donnemiller, M. Gabriel, R. Moncayo, G. Riccabona. Department of Nuclear Medicine, University of Innsbruck, Austria.

153Sm EDTMP has been accepted as a highly effective radiopharmaceutical for pain palliation in patients with disseminated bone metastases. In a previous analysis of our results we found a good therapeutical response particularly in patients with a radiation dose to the lesions of at least 10 Gy. In this study we decided to estimate prospectively the activity necessary to achieve this dose in the bone lesions considering haematological toxicity and tumor spread.
Methods: A total of 56 patients with disseminated skeletal metastases underwent 62 therapies (6 patients were treated repeatedly). According to recommended standardised therapeutic activities and also based on our dosimetric trials we administered 37 MBq/ kg BW in 15 cases, 55 MBq/ kg BW in 31, and 74 MBq/ kg BW in 15. Patients were followed according to a defined protocol with pain diary, haematological samples and clinical examination at 3, 6 and 12 weeks after treatment. Statistical evaluation was performed by paired-samples t-test.
Results: In all patients where a target dose of 10 Gy or more was achieved, we could observe a very good therapy response. Haematological side effects were analysed according to the 3 dose groups (Table).

Blood values 3 weeks after therapy	37 MBq/kg BW		55 MBq/kg BW		74 MBq/kg BW	
	mean %	drop	mean %	drop	mean %	drop
Erythrocytes (Mill.)	3,5	3	3,5	11	3,7	2
Haemoglobin (g %)	11,0	3	10,6	7	11,2	3
Leukocytes	4.900	37	3.800	31	4.300	37
Platelets	105.000	44	121.000	49	109.000	62

Conclusions: Our results show that: 1) maximal decrease of all haematological parameters was observed 3 weeks following treatment and was mostly transient and not severe, 2) the largest change involved the platelet count, 3) individual dosimetry adapted to tumor spread can improve therapy results, an adequate pain palliation therapy in patients with very large tumor volume and pathological blood counts due to previous treatment can, however, be limited by myelotoxicity of Sm-153, but 4) there is no significantly increased myelotoxicity in the group which received 74 MBq/kg BW in comparison with the other groups when the pretherapeutic values are normal, 5) haematological treatment was necessary only in patients presenting anaemia already before samarium therapy.

OS_364

REDUCED BONE UPTAKE OF SM-153-EDTMP AND RE-186-HEDP IN RABBITS CAUSED BY THE CYTOPROTECTANT AMIFOSTINE

W. Brenner, C. Bruemmer, C. von Forstner, W.U. Kampen, N. Czech, C. Muhle, E. Henze. Clinic of Nuclear Medicine, Christian-Albrechts-University, Kiel, Germany.

In rabbits undergoing high-dose treatment with Sm-153-EDTMP or Re-186-HEDP a highly significant cytoprotective effect to platelets could be proven for amifostine. However, since amifostine is known to potentially affect bone metabolism, the aim of this study was to exclude any drug effects impairing the skeletal uptake of these radiopharmaceuticals.
Methods: In 24 rabbits we applied 1000 MBq of either Sm-153-EDTMP (n =12) or Re-186-HEDP (n = 12). 6 animals of each group received 500 mg amifostine i.v. (SmA, ReA) 15 min prior to the injection of the radiopharmaceutical while the other 6 animals of each group served as controls (SmC, ReC). Whole-body images were acquired at 3 min, 3 h, and 24 h after injection of the radiopharmaceutical using a double-head gamma camera in order to quantify skeletal uptake, soft tissue activity, and urinary excretion by ROI-technique.
Results: Bone uptake in percent of initial total whole-body activity of both Re-186-HEDP and Sm-153-EDTMP was significantly decreased in animals treated with amifostine: ReA: 15.8 ± 3.1 %, ReC: 30.9 ± 1.9 % ($p < 0.001$); SmA: 31.7 ± 8.9 %, SmC: 44.0 ± 6.5 % ($p < 0.05$). For Re-186-HEDP both in rabbits treated with and without amifostine the remainder soft tissue activities were identical (ReA: 14.8 ± 3.2 %, ReC: 14.0 ± 2.7 %) while the urinary excretion was higher for the amifostine group: ReA: 69.4 ± 2.5 %, ReC: 55.1 ± 3.8 %, $p < 0.001$. For Sm-153-EDTMP the soft tissue activity was higher in the amifostine group (SmA: 18.4 ± 7.0 %, SmC: 9.8 ± 4.4 %, $p < 0.05$) while urinary excretion was similar in both groups: SmA: 49.9 ± 11.8 %; SmC: 46.3 ± 7.5 %.
Conclusions: Amifostine significantly reduced the bone uptake of Re-186-HEDP and Sm-153-EDTMP. In animals treated with Re-186-HEDP the non-skeletal bound activity was excreted while for Sm-153-EDTMP a shift towards the soft tissue was observed. Due to its chemical structure, amifostine, a potentially complex-forming compound, might be able to rearrange the rhenium- and samarium-bisphosphonate complexes and form new rhenium-amifostine or samarium-amifostine complexes resulting in a decreased bone uptake and different biodistribution pattern.

OS_365

RADIATION ABSORBED DOSE OF RHENIUM-188-HEDP IN BONE METASTASES, BONE MARROW AND BONE SURFACE

K. Liepe (1), R. Hliscs (1), J. Kropp (1), R. Runge (1), FF. Knapp (2), WG. Franke (1). (1) Dept. Nuclear Medicine, Technical University, Dresden, Germany; (2) Nuclear Medicine Group, Oak Ridge Lab., Oak Ridge, TN, USA.

Aims: Labeling of HEDP with generator-produced rhenium-188 was has been reported in preliminary studies for the palliative treatment of metastatic bone pain, but kinetic and radiation-absorbed doses have not been well-documented. The aim of this study was to establish dosimetric data of rhenium-188-HEDP applied to painful bone metastases.
Methods: Thirteen male patients with prostate cancer were treated with 2700 to 3459 MBq (mean dose: 2989 MBq) of rhenium-188-HEDP. Patients typically underwent whole body scans 3, 20, and 28 hours after therapy. From these data the effective half-life and radiation absorbed dose in bone surface and in 29 bone metastases were calculated. The bone marrow dose was calculated with the activity in the bone (distribution of 50% at the trabecular and cortical bone) and in the blood, with measuring of the activity in the blood about 24 hours. Blood counts were sampling within 6 weeks (weekly).
Results: Following mean radiation absorbed doses were found: in bone metastases of 9.5 Gy (range: 1.2 to 17.6), in bone marrow of 1.8 Gy (range 1.3 to 2.6) and in bone surface of 2.4 Gy (range: 1.8 to 3.5). We observed a comparable mean effective half-life of 15.8 hours (h) (range: 10.1 to 23.3) in bone metastases and of 15,6 h (range: 11.2 to 21.5) in bone, these correspond with a long biological half-life of 242.7 h and 202.8 h, respectively. The platelet counts shown a mean decrease of 30 ± 14% from the value before therapy at 2.8 ± 0.7 weeks, the leukocyte counts of 25 ±17% after 3.8 ± 0.7 weeks. The relationship between radiation absorbed doses in bone marrow and percent changes in platelet counts shown a weak correlation ($r = 0.5449$).
Conclusion: The high uptake of rhenium-188-HEDP results in a high mean radiation absorbed dose of 9.5 Gy in comparison to a lower dose in bone surface of 2.4 Gy. A mean radiation absorbed dose in bone marrow of 1.8 Gy not lead to any clinical significantly thrombocytopenia or leukopenia.

OS_366

IS 153SM-EDTMP BONE UPTAKE INFLUENCED BY BIPHOSPHONATES?

H. Sinzinger (1), F. Chehne (1), B. Palumbo (2), C. Pirich (1), C. Kratzik (3), K. Weiss (4), R. Palumbo (2). (1) Department of Nuclear Medicine, University of Vienna, Vienna, Austria; (2) Department of Nuclear Medicine, University of Perugia, Perugia, Italy; (3) Department of Urology, University of Vienna, Vienna, Austria; (4) Department of Radiology and Nuclear Medicine, Hospital of Wiener Neustadt, Austria

More than 80% of prostate cancer patients develop bone recurrences and severe secondary pain. ^{153}Sm-therapy has been performed so far mainly as a single shot therapy in late disease stages. Repeated application of biphosphonates may result in a stunning effect. Therefore, patients repeatedly treated with 30 mCi (1,1 GBq) ^{153}Sm-EDTMP or being already on biphosphonates might show a decrease in bone uptake. In order to study this question , we assessed the bone uptake in 10 patients (aged 59 –76 years) with prostate cancer and multiple painful secondary bone lesions who at the time of the first therapy were not on biphosphonate. ^{153}Sm-EDTMP-treatment was repeated after 3 months in presence of biphosphonates which were started about one week after the first ^{153}Sm-EDTMP-therapy. All other treatment was unchanged throughout the observation period. The retained activity in bone was calculated using whole body scintigraphy (acquisition 15cm/min) performed immediately after tracer application and after 6 hours. Bone uptake of ^{153}Sm-EDTMP ranged from 53 – 85 % and revealed no significant intraindividual difference with and without biphosphonate treatment; no stunning was observed. Pain relief onset and duration of effect as well as flare phenomenon and its duration were comparable in presence and absence of biphosphonates. As biphosphonates are an essential part of the therapeutic strategy, these findings indicate that treatment can be continued without affecting ^{153}Sm-EDTMP bone uptake and eventual therapeutic benefits.

OTHER CLINICAL SCIENCE. ENDOCRINOLOGY

OS_367

DIAGNOSTIC IMAGING OF ADENOMAS OF THE PARATHYROID GLAND: USE OF MRI, SCINTIGRAPHY AND IMAGE FUSION IN THE PRE-OPERATIVE PHASE

J. Ruf (1), E. Lopez-Hänninen (1), F. Ulrich (2), T. Steinmüller (2), M. Gutberlet (1), A. Müller-York (1), H. Amthauer (1), R. Felix (1). (1) Klinik für Strahlenheilkunde; (2) Klinik für Allgemein- und Transplantationschirurgie, Charité Campus Virchow-Klinikum, Berlin, Deutschland.

Endoscopic minimal-invasive resection of adenomas of the parathyroid gland is an alternative to open surgery. The aim of this study was to evaluate the informational value of pre-operative MRI and in combination with parathyroid scintigraphy as fused images.
Methods: 28 patients suspected of suffering from primary hyperparathyroidism were recruited for this study (11 female, 17 male, age ranging from 28 to77 years). MRI imaging was conducted with a 1,5 T scanner (Magnetom SP 63, Siemens, Erlangen, Germany). Transversal and coronary scans were performed both T1- and T2-weighted, slice thickness was 4 mm. T1-weighted scans were repeated after the administration of intravenous contrast medium. Non-conclusive MRI-findings were followed by Tc-99m-MIBI scintigraphy using both planar and SPECT imaging-techniques. In case of scintigraphic evidence for an adenoma, the data acquired by both examinations was fused for a better localization of the adenoma. These image fusions were performed by a self-created software on an AVS-platform (Advanced Visualization systems, Neuss, Germany). All imaging findings were correlated to the result of post-operative histology.
Results: Adenomas of the parathyroid gland were intra-operatively verified in 22/28 patients. Pre-operative MRI-scans were able to detect 18/22 adenomas (82% sensitivity). These were subdivided into 2 qualitative groups: a) hyperintense in T2 / isointense in T1 (66%) and b) isointense in both modalities (25%). All cases showed an intensive contrast enhancement. 10 out of 28 Patients received scintigraphic examinations. In 6 of these cases image fusion was subsequently performed. This lead to unambiguous detection of adenomas in 5 cases, 1 patient was diagnosed false-positive.
Conclusions: MRI-imaging proves to be a sensitive method for the diagnosis of adenomas of the parathyroid gland. An improved localization can be achieved by the use of scintigraphy and subsequent image fusion, especially in the case of negative MRI-scan results. Thus, this diagnostic approach promises great benefit for the pre-operative planning phase of endoscopic adenoma resection. Image fusion might be especially useful for the detection of recurrent disease and mediastinal localization, where conventional diagnostic methods are of limited value.

OS_368

PROSPECTIVE PET STUDY WITH 11C-METHIONINE IN PATIENTS WITH HYPERPARATHYROIDISM

D. Otto (1), M. Behrend (2), A.R. Börner (1), G. Oetting (1), E. Weckesser (1), M. Hofmann (1), T. Petrich (1), W.H. Knapp (1). (1) Department of Nuclear Medicine; (2) Department of Surgery, Medical School Hannover, Hannover, Germany.

Prospective PET study with ^{11}C-methionine in patients with hyperparathyroidism
Aim: The aim of our study was to evaluate the role of PET with ^{11}C-methionine in the preoperative localisation of parathyroid adenoma and hyperplasia. The optimum time interval for imaging post injection of ^{11}C-methionine was to be determined.
Methods: 15 patients (4 of them with secondary, 10 with primary hyperparathyroidism (HPT) and one patient with recurrent carcinoma of the parathyroid gland) who had no or only faint focal MIBI accumulation underwent PET with ^{11}C-methionine (900-1100 MBq ^{11}C-Methionine, Siemens ECAT 922, iterative reconstruction (OSEM), matrix 128x128). Emission scans were started 25 and 40 min. p.i.. Standard uptake values (SUV«s) were calculated for the thyroid and parathyroid glands and the cervical spine (control). In all patients dual phase MIBI scintigraphy as well as cervical ultrasound preceeded PET immediately. After surgery PET findings were histologically verified.
Results: In 13/15 patients PET showed areas of pathological activity accumulation. In 1 out of these 13 patients the focal accumulation was only weakely delineated. In a subgroup of ten patients with adenomas/carcinoma 10 out of 11 hyperactive lesions were detected with PET. In 4 patients with secondary HPT 11 out of 16 hyperplastic parathyroid glands were detected. The highest tumor-to-cervical spine ratio was observed 25 min. p.i. in all patients, the highest tumor-to-thyroid ratio 40 min. p.i.. In two cases the parathyroid adenomas were contrasted only in the scan 40 min. p.i..
Conclusions: ^{11}C-methionine PET is a promising method in the preoperative identification of hyperactive parathyroid glands especially if MIBI scintigraphy is non-diagnostic. In order to obtain optimum separation of parathyroids and adjacent structures, early and late PET scans are mandatory.

OS_369

PARATHYROID IMAGING WITH TC-99M-MIBI: HOW MUCH DEPEND THE RESULTS OF PARATHYROID SCINTIGRAPHY QN THE GOLD-STANDARD?

M. Gotthardt (1), B. Lohmann (1), D. Brandt (1), U. Welcke (1), H. Hoeffken (1), C. Nies (2), A. Bauhofer (3), H. Sitter (3), M. Rothmund (2), K. Joseph (1), T.M. Behr (1)(1) Department of Nuclear Medicine; (2) Department of Surgeryy; (3) Department of Theoretic Surgery, Philipps-University, Marburg, Germany.

Aim: We investigated the specificity and sensitivity of presurgical Tc-99m-MIBI parathyroid imaging and ultrasonography (US) in a setting with specialized endocrine surgeons.
Methods: All patients who underwent Tc-99m-MIBI parathyroid imaging and subsequent surgery because of primary (PHPT) or secondary hyperparathyroidism (SHPT) between 1991 and 1999 were included into our study. The intraoperative findings served as gold standard. From 178 patients examined in this period of time, 140 were eligible for our study The others had to be excluded because they had not been operated on at all or the operation had not been performed by a specialized endocrine surgeon. In 40 of these patients, the results of US were equivocal or missing, data of the remaining 100 patients are shown in parentheses. 109 patients had PHPT, 39 patients had SHPT. The total number of patients diagnosed correctly was calculated for each method itself and for the combination of both methods. Sensitivity and specificity were calculated from the total number of adenomas found as well as positive (PPV) and negative predictive values (NPV).
Results: A totally correct diagnosis was made in 44% (49.4%) of patients with PHPT and in 29% (31.6%) of patients with SHPT scintigraphically. The results for US were 38.3% in PHPT and 26.3% in SHPT, respectively. Using the combination of both imaging modalities resulted in 48.1% of correctly diagnosed patients with PHPT and 31.5% in the case of SHPT. The sensitivity of MIBI-scanning, as calculated from the total number of adenomas was 43.5% (51.6%) and the specificity was 90.1% (89.3%). US showed values of 47.2% for sensitivity, and 84% for specificity. For scintigraphy, PPV was 75% (73.2%) and NPV was 79% (76.4%). US reached values of 63% for PPV and 73.4% for NPV.
Conclusion: Both, US and scintigraphy, performed by experienced physicians, show lower sensitivities and specificities than stated in the literature. We believe that the quality of surgery as gold standard may be the reason for these findings as the results of parathyroid surgery are very much dependent on the expertise of the surgeon. In contrast to other studies, in our study only specialized endocrine surgeons operated on all patients. We thus conclude that the clinical value of parathyroid scintigraphy may have been overestimated. A careful surgical exploration is essential, even if parathyroid imaging has been performed prior to operation.

OS_370

COMPARISON OF PINHOLE/HIGH RESOLUTION PARALLEL HOLE AND EARLY/LATE TC99M-MIBI IMAGES IN PARATHYROID IMAGING

U. Yararbas, R. Erinc, I. Karapolat, K. Kumanlioglu. Department of Nuclear Medicine, Ege University, Izmir, Turkiye.

Tc99m-MIBI is widely used for parathyroid imaging currently. Although several imaging protocols have been proposed, there is no consensus on ideal protocol. The aim of this study is to compare the sensitivity of pinhole and high resolution parallel hole images and also early and late images using Tc99m-MIBI in the detection of hyperfunctioning parathyroid tissue.

Methods: Twenty patients (age range: 21-67, 17 female, 3 male) which were referred for parathyroid imaging with the suspicion of hyperparathyroidism according to clinical and laboratory data were included in the study. Including criteria for study group was having positive pinhole double phase MIBI scan that was later proved to be true positive. Parathyroid pathology was adenoma in 12 patients and secondary hyperplasia in 8 patients. Twentieth min and 3rd hr pinhole and parallel hole images obtained after the injection of 20 mCi Tc99m-MIBI were used.

Results:

	Pinhole		Parallel hole	
	20 min	3 hr	20 min	3 hr
Adenoma (12 pts)	12 positive	11 positive 1 negative	11 positive 1 negative	7 positive 2 equivocal 3 negative
Hyperplasia (8 pts)	7 positive 1 negative	7 positive 1 negative	4 positive 3 equivocal 1 negative	2 positive 3 equivocal 3 negative

Based on pinhole images; 1 patient with adenoma and 1 with hyperplasia showed rapid washout and were not visible on late images. On the other hand, in 1 patient with hyperplasia only late image showed hyperplastic glands after the washout of physiological MIBI uptake of thyroid gland. In parallel hole imaging, 11 out of 12 patient with adenoma and 4 out of 8 patient with secondary hyperplasia could have been imaged at 20th min. Late imaging with parallel hole collimator failed to demonstrate 3 adenomas and 3 hyperplasias. Additionally 3 adenomas in late images and 3 hyperplasias in both early and late images had low lesion/background ratios that caused equivocal results.

Conclusion: Pinhole images are found to be clearly superior to parallel hole images especially in patients with secondary hyperplasia. Early images are more sensitive than late images but late images are also necessary since in 1 hyperplasia only late view showed parathyroid pathology.

OS_371

MINIMALLY INVASIVE PARATHIROIDECTOMY: SCINTIGRAPHY WITH TC-99M SESTAMIBI AND PROBE-GUIDED SURGERY

A.M. García Vicente (1), A. Soriano (1), J. Martín (2), S. Rodado (1), J. Hernández (2), V. Poblete (1). (1) Department of Nuclear Medicine; (2) Department of Surgery, Alarcos Hospital, Ciudad Real, Spain.

Aim : The most common pathologic finding in sporadic primary hyperparathyroidism is a single adenoma. The success of parathyroid surgery is determined by the identification and removal of the adenoma responsible. The aim of our study was to minimise interventional techniques, hospital stays and overall costs of patients with parathyroid adenoma who do not require a complete neck exploration.
Methods: 15 patients (13 females and 2 males) with biochemical and clinical evidence of primary hyperparathyroidism were included in our study. The medium age was 64,6 (28-82). All the patients underwent ^{99m}Tc sestamibi and ^{99m}Tc Pertecnetate neck scans in previous days. On the day of the operation we administrated a dose of 740-925 MBq ^{99m}Tc sestamibi. The scintigraphy and radio-guided surgery were performed two to three hours afterwards using an 10 mm hand-held gamma probe. Count rates (cts / 10 sec) were measured in four neck quadrants defined by the upper and lower poles of the thyroid gland on each side.
Results: a 2-3 cm incision was made according to the expected location of the adenoma as determined by both sestamibi scanning and measurement of gamma emissions with the probe. We identified 13 adenomas by scintigraphy which were removed with a 2 cm incision. 2 cases showed inconclusive scintigraphic results and required the incision to be expanded since two enlarged glands were found. These patients were finally diagnosed as having double adenoma.
The quadrant with the radioactive gland has a count rate at least 25 % higher than the other quadrants. Removal of the adenoma resulted in a decline in radioactivity in that quadrant with equalisation of all neck quadrants. Ex vivo counts identified parathyroid tissue versus fat and lymph node. The histopathologic examination and a decrease of the PTH levels at 30 and 60 minutes after removal of the adenoma confirmed the correct surgery.
Conclusions: A preoperative sestamibi scan is specific enough in identifying solitary adenoma to allow unilateral exploration. The use of a gamma probe as a surgical tool converts the sestamibi to a functional and anatomical scan eliminating the need for any other preoperative localising study.
This technique allows: minimally invasive unilateral neck exploration with a small scar and better cosmetic results, reduces operative and anaesthetic times, requires minimal time spent in the hospital and achieves a reduction in overall cost.

OS_372

THE ROLE OF GAMMA PROBE LOCALIZATION IN PATIENTS WITH PRIMARY HYPERPARATHYROIDISM

C. Demirkurek (1), I. Adalet (1), T. Terzioglu (2), S. Ozarmagan (2), A. Bozbora (2), N. Ozbey (3), Y. Kapran (4), S. Cantez (1). (1) Department of Nuclear Medicine; (2) Department of Surgery; (3) Department of Endocrinology; (4) Department of Pathology, Istanbul Faculty of Medicine, Istanbul, Turkey

Aim:The purpose of this study was to evaluate the potential value of preoperative and intraoperative gamma probe localization of parathyroid lesions with Tc-99m sestamibi (MIBI) in patients with primary hyperparathyroidism.
Methods:We studied 18 consecutive patients (16 female and 2 male, age range, 12-75 years; mean 54 years) with biochemically proven primary hyperparathyroidism (PHP). Five patients had nodular goiter. All patients were imaged 2-20 days prior surgery with tetrofosmin-teknesyum subtraction (TTS) scintigraphy. On the day of surgery, all patients underwent dual phase MIBI scintigraphy (740 Mbq). Anterior neck and thoracic images were acquired in a gamma camera using LEHR collimator at 10 minutes and 1.5 hr post injection. . Focal areas of increased uptake were marked on the skin. In the operating room, using the Navigator (USSC,USA) gamma probe, presurgical counts were determined in the four cervical quadrants. Counts were similarly measured in the same position following opening of the deep fascia. If focal uptake was clearly seen, the gamma probe was then used to guide the location of the hot spot and thus tissue dissection until the adenoma was found. Four quadrant counting was repeated at the end of the operation to make sure that no hot spots were left. Scintigraphic findings and gamma probe counts were compared with surgical and histopathological results.
Results: Eighteen patients were studied. Seventeen parathyroid lesions were excised in 17 PHP patients. Fourteen patients had parathyroid adenoma, 3 had parathyroid hyperplasia and one had multinodular goiter. Mean operation time was 53 minutes (range 19-100min). The sensitivity of TTS, dual phase MIBI scintigraphy and gamma probe localization were 92%, 94% and 100% respectively. Mean count rate for parathyroid lesions and background were 7952.59± 4491.37 and 3874.76±2413.34 respectively. There was significant difference between parathyroid lesions and background counts (p=0). Three parathyroid adenomas (retro-tracheal, anterior mediastinal and within carotid sheath) that was initially could not be found with a classical exploration at the beginning of the operation were localized with the help of gamma prob. All patients had normal calcium postoperatively.
Conclusion:.We concluded that gamma probe localization of parathyroid lesions with Tc-99m sestamibi has a potential value. It faciliates surgery and reduces operation time.

OS_373

RADIO-GUIDED SURGERY (RS) IN PRIMARY HYPERPARATHYROIDISM (PHPT): A NEW TECHNIQUE BASED ON INTRAOPERATIVE ADMINISTRATION OF A LOW TC-99M MIBI DOSE

D. Rubello (1), A. Piotto (2), M.R. Pelizzo (2), D. Casara (1). (1) Servizio di Medicina Nucleare 2, Azienda Ospedaliera di Padova, Padova, Italy; (2) Clinica Chirurgica 3, Università di Padova, Padova, Italy.

The role of RS was evaluated in 84 pHPT pts preoperatively studied with 99mTcO4/MIBI scan and neck US and then operated by the same surgeon. Quick PTH (QPTH) was intraoperatively measured. 70 pts with evidence of a single PA and a normal thyroid were selected for minimally invasive RS (MIRS). In pts with concomitant thyroid nodules (TNs) (n. 11) or multi-glandular disease (MGD) (n. 3), IGP was used during bilateral neck exploration (BNE). IGP protocol: 1) in the operative room a low MIBI dose (37 MBq) was injected, 2) after 20 min, patient's neck was scanned with the probe to individualize the PA; 3) in the case of MIRS, the PA was removed through a 2-2.5 cm skin incision; 4) radioactivity was measured on PA in vivo and ex vivo, thyroid, background, parathyroid bed after PA removal, and TNs. Surgical findings were: single PA in 78 pts, parathyroid carcinoma (PC) in 2, MGD in 4. MIRS was successfully performed in 67 of the 70 selected pts (95.7%). Conversion to BNE was needed in 3/70 pts (4.3%): in 2 cases because a PC was diagnosed at frozen section, in 1 case because QPTH remained elevated after removal of the preoperatively visualized PA and another occult PA was found. Interestingly, it was possible to perform MIRS also in 5 pts with persistent/recurrent HPT, thus limiting the surgical trauma. Among pts with MGD, IGP was helpful in 1 case to localize a thymic parathyroid gland. Among pts with TNs, IGP was helpful in 1 case to localize a PA ectopic to carotid bifurcation; however, it has to be pointed out that in 5 cases, the MIBI uptake was higher in TNs than in PA thus making it difficult to intraoperatively individualize the PA. We can conclude that: a) in primary HPT pts with a high probability of a single PA and a normal thyroid, IGP appears to be a very useful technique to perform MIRS; b) MIBI dose as low as 37 MBq appears to be adequate for MIRS; c) QPTH measurement is strongly recommended in pts selected for MIRS; d) MIRS can be useful also in pts with persistent/recurrent HPT with the aim of minimizing surgical trauma of re-operation and possible related risk of complications; e) with the exception of PA located in ectopic sites, IGP does not appear to be a recommendable technique in HPT pts with concomitant MIBI avid TNs.

OS_374

PARATHYROID SCINTIGRAPHY WITH DOUBLE SUBTRACTIONS IMAGES

F. Chehade, N. Droubi, A. Ghazawi, G. Ramadan, W. Dayeh, M. Saab. Hammoud Hospital,Sidon,Lebanon.

Background : According to literature data, to perform parathyroid subtraction scintigraphy with tecnetium-99m-labeled sestamibi or tetrofosmin (TM), the thyroid gland delineation is made either simultaneously using iodine-123-sodium iodide, or 24 hours later using technetium-99m-labeled pertechnetat (TP). We describe a one-day protocol of parathyroid scintigraphy using technetium-99m-labeled tracers based on double subtractions images.
Method : During the first 10 minutes following 7.4 MBq/Kg of TM injection, an anterior view of the neck and mediastinum is obtained using a parallel-hole collimator. Next, the pin-hole collimator is installed, and a first 10 minutes „TM" image of the thyroid area is recorded. Then 2.8 MBq/Kg of TP are injected. Ten minutes later and avoiding patient movement, a second 10 minutes „TM+TP" image is recorded. „TM" image subtraction from „TM+TP" image aims to generate the „TP" image of thyroid. In order to identify enlarged parathyroids, the generated thyroid „TP" image is subtracted from „TM" image, which contains activity of both thyroid tissue and enlarged parathyroids.
Subjects : We have used this protocol on 12 patients with primary hyperparathyroidism referred between the years 1998 and 2001 for a preoperative localization of hyperfunctionning parathyroids. The tetrofosmin was used in 6 patients and the sestamibi in 6 others.
Results : In 1 case, anterior view of the mediastinum revealed a mediastinal focal uptake of tetrofosmin in parathyroid adenoma. The double subtractions images correctly localized 2 hyperplastic parathyroids in 1 case (sestamibi), and 10 solitary parathyroid adenomas in 10 cases (5 tetrofosmin and 5 sestamibi). Tow out of these last 10 cases, and in addition to the specific tetrofosmin focal uptake showed 1 and 2 non-specific focal uptake, respectively, corresponding to thyroid adenomas.
Discussion : Successful results of scintigraphic protocol with double subtractions images are observed using either tetrofosmin or sestamibi, showing high sensitivity in 12 cases with primary hyperparathyroidism, and high specificity in cases without thyroid nodules. In this one-day protocol the gamma camera occupation time as well as the time spent by the patient are short (40 minutes). This protocol requires only one isotope, the technetium-99m, which is always available in almost nuclear medicine laboratories. The short time break of 10 minutes separating acquisitions of „TM" and „TM+TP" images makes negligible effect of TM tissue clearance on the images subtraction.

PHYSICS / INSTRUMENTATION

OS_375

NONLINEAR 3D REGISTRATION OF F-18 FDG THORACIC PET WITH CT UTILIZING PET TRANSMISSION MAPS

P.J. Slomka (1), D. Dey (1,2), C.H. Przetak (3), R.P. Baum (3). (1) Diagnostic Radiology and Nuclear Medicine, University of Western Ontario, London, Canada ; (2) JP Robarts Research Institute, London, Canada; (3) PET Center, Zentral Klinic, Bad Berka, Germany.

Aim: Image fusion of anatomical CT and functional PET can potentially improve the diagnostic value of PET and increase the role of PET in image guided therapy. However PET emission and transmission images are typically acquired during normal patient breathing and often in a different body position than CT. Therefore non-linear image registration is required to obtain correct 3D alignment.
Methods: We have implemented a practical, fully automated algorithm for non-linear 3D image registration of wholebody PET and thoracic CT images, which compensates for the non-linear deformation of lungs and surrounding tissues. We utilize PET transmission images to derive the non-linear transformation between PET and CT anatomical configurations. The algorithm automatically compensates for the differences in the axial scan coverage. Initially, linear 9-parameter registration, using normalized multi-variate mutual information is performed to approximately align the CT with the ensemble of emission and transmission PET volumes. Multi-resolution approach is used to avoid local minima and accelerate the computation of this step. Subsequently we automatically detect lung surfaces on PET transmission maps and CT volumes via outward sampling and define a large number of corresponding 3D point pairs (500). These landmark pairs allow us to perform a thin-plate-spline elastic deformation of PET emission and transmission volumes to match breath-hold CT volumes. Thirteen PET (CTI) and CT (Siemens, Somatom 2+) scans have been evaluated by this method. In 3 patients the CT was acquired during 2 breathing patterns (normal and breath-hold), to directly compare the non-linear alignment of PET with CT and alignment of breath-hold with non-breath-hold CT.
Results: In all 13 patients the automatic alignment was successful as visually assessed by two observers. The non-linear adjustment after the initial linear registration was up to 30 mm, especially in the areas of the diaphragm. The non-linear step has significantly improved the registration between the breath-hold CT and PET. The total time for the registration is approximately 80 seconds for the linear component and 7 minutes for the non-linear component.
Conclusions: We developed a practical technique for the automatic nonlinear registration of thoracic CT with wholebody PET. This technique may be applied for multimodality fusion of PET and CT acquired on separate scanners at different times and with different breathing patterns.

OS_376

TESTING OF NON-RIGID REGISTRATION PROCEDURES FOR NUCLEAR MEDICINE IMAGE FUSION: ESTIMATING DEFORMATION

A. Todd-Pokropek. Dept of Medical Physics and Bioengineering, UCL, London, UK.

Aim.
While rigid body image registration has been validated using, in particular, markers, non-rigid registration is much more difficult to validate since some kind of matching function must be defined throughout the volume being registered. Non-rigid registration is particularly important when building atlas data against which statistical tests of significance of uptake in nuclear medicine data need to be made. Here the aim has been to assess non-rigid methods of registration and deformation based on optic flow and thin plate spline interpolation.
Method.
Phantom and patient test images have been acquired which have been distorted using various known deformations, and then their characteristics, in particular noise properties, modified. The model of deformation used is based on assumptions about tissue characteristics and should be representative of real deformations that could occur. However it is not essential that this underlying model be perfect. The registration algorithm is then run backwards to re-register the modified deformed data with the original images. This process produces a deformation map being a vector field for the whole volume. This can then be directly compared to the original distortion vector field, and various error estimates for the mismatch over the whole volume computed. This mismatch can be in amplitude and direction. By analogy a method based on the comparison of electromagnetic fields has been adopted.
Results.
The main purpose of this paper is to describe a methodology for optimising algorithms. The specific results will depend on the particular features of the algorithm being tested , in particular the underlying model for interpolation. Two different algorithms have been intercompared and in particular the constraints (local divergence of the vector field, size of the local region in particular) have been tested. The particular aim was to establish that when the imposed deformation was considerably different for different regions, for example in the centre and on the edge of the brain, this deformation could be accurately captured.
Conclusions.
The conventional quadratic distance between known points is a bad estimate to use to assess non-rigid registration. A robust statistic has been developed which can be used to optimise non-rigid algorithms. While the task being tested is simpler than the real clinical task, it is believed that this method provides an adequate framework for the first essential step in the validation of such algorithms.

OS_377

INTER-INDIVIDUAL SPECT BRAIN SCAN REGISTRATION BASED ON A COMBINED INTENSITY AND GRADIENT SIMILARITY CRITERION

R. Lundqvist (1), S. Som (2), E. Bengtsson (1), L. Thurfjell (3). (1) Centre for Image Analysis, Uppsala University, Uppsala, Sweden; (2) Department of Nuclear Medicine, The Prince of Wales Hospital, Sydney, Australia; (3) ReachIn Technologies, Stockholm, Sweden.

Inter-individual image registration involves the use of an optimisation algorithm, image transformations and an appropriate cost function for measuring similarity between images. Earlier work regarding voxel-based inter-individual registration of SPECT images mostly have used cost functions based on voxel intensity distributions in the images. We have noticed that this information is not always sufficient to produce satisfying registration results. For that reason, we have developed a new cost function, which combines intensity and gradient information from the images.
Methods: Normalised mutual information (NMI) based on image intensities has been used for image registration during some time. The mutual information concept can be extended to include multivariate observations of the data. In our new cost function, the intensity and gradient magnitude value of each voxel in the two images are used when evaluating the mutual information criteria, which leads to the creation of a 4D histogram. The goal of the optimisation algorithm in this case can be summarised as minimising the dispersion of the 4D-histogram.
Registration results produced by the intensity-gradient cost function have been compared to cross-correlation and NMI measures applied on intensity or gradient information alone, for a number of previously known hard SPECT images to register. The images have been registered to a computerised brain atlas, which makes it possible to evaluate the registration quality by analysing the fit to the brain atlas.
Results: The comparisons of different cost functions show that the combined intensity-gradient NMI measure produces more robust results than the univariate cost functions using either intensity or gradient information. These findings are apparent for both the cross-correlation and the NMI cost function. The atlas brain surface generally is more tightly fit to the image brain and the plane between the hemispheres is also better located.
Conclusions: The combined intensity-gradient NMI cost function has been shown to produce an improvement of the registration accuracy in many cases, compared to cost functions using intensity or gradient information alone. It is slightly slower to compute than univariate cost functions, but the increase in accuracy motivates its use. Future work involves studying the effects of pre-filtering and subsampling of images prior to registration. The registration dependence on the number of bins used in the joint histograms also needs to be further investigated.

OS_378

A NEW MAXIMIZATION OF MUTUAL INFORMATION BASED METHOD FOR MULTIMODALITY IMAGE REGISTRATION

L. Freire (1), F. Godinho (2). (1) Instituto de Biofísica e Engenharia Biomédica, FCUL, Lisboa, Portugal; (2) Instituto de Medicina Nuclear, Hospital Santa Maria, Lisboa, Portugal.

In this work we propose a new method for MRI-PET registration based on the maximization of Mutual Information (MI) criterion. The main difference, relatively to the widespread MI method, relies in the elaboration of the joint-histogram of the two images one wants to realign; for each pair of corresponding voxels, the joint-histogram update is not unitary, but dependent on the spatial frequency associated to the MRI voxel. The validation of the method is done using two simulated data-series and a comparison between the widespread MI method and the one proposed here is presented.
Methods: We used a self-developed algorithm, which allows the user to specify the type of joint-histogram update. For spatial frequency dependent (SFD) joint-histogram update, we compute a high-frequency (HF) MR image by subtracting the original image from its 3D-gaussian-smoothed version (7mm FWHM). We used a linear transfer function to calculate the contribution of each voxel pair; it ranges from 0.25 (for voxels in 'flat' regions) to 1 - for voxels whose value in HF MR-image is above a user-supplied threshold (default: approximately 10% of brain's average value. Optimization is performed using Powell's multidimensional search method. Interpolation is cubic-spline.

Multimodality registration was performed using an emulated PET image, obtained from a MR-T1 weighted image. Two data-series of 36 PET images were generated applying random, normally distributed $\sim N(0,5)$(mm, deg), translations and rotations, respectively, in order to simulate initial misregistrations between the PET images and the MR image. Accuracy and robustness of each method is inferred through the mean error in translation, E_t (mm) and rotation, E_r (deg), and corresponding standard deviation (SD) values, for the two simulated data-series.
Results: Results refer to the two methods (MI and MI with SFD joint-histogram update - *sfd*MI). Mean errors are small, which indicate that both methods are accurate. The small SD values suggest that routines are robust. Moreover, it is possible to see that *sfd*MI errors are systematically smaller, particularly when correcting for rotation.

	Simulated Translation (n=36)		Simulated Rotation (n=36)	
	*sfd*MI	MI	*Sfd*MI	MI
Mean $E_t \pm$ SD	0.404±0.151	0.439±0.187	0.379±0.145	0.468±0.138
Mean $E_r \pm$ SD	0.456±0.221	0.482±0.299	0.656±0.246	0.843±0.487

Conclusion: We presented the basics of a new MI based registration method. Further work must be done in order to validate the method with real data and to evaluate the influence of other transfer functions.

OS_379

CONSTRAINED, LOCALIZED WARPING REDUCED REGISTRATION ERRORS CAUSED BY HYPOPERFUSION IN BRAIN SPECT

P.E. Radau, P.J. Slomka. Department of Nuclear Medicine, London Health Sciences Centre; Department of Medical Biophysics, University of Western Ontario, London, Canada.

The constrained, localized warping (CLW) algorithm was developed to minimize the registration errors caused by hypoperfusion lesions. ^{99m}Tc-HMPAO SPECT brain perfusion images from 21 Alzheimer patients and 35 controls were analyzed. CLW automatically determines homologous landmarks on patient and template images. CLW was constrained by anatomy and where lesions were probable. CLW was compared with 3rd-degree, polynomial warping (AIR 3.0). Accuracy was assessed by correlation, overlap, and variance. 16 lesion types were simulated, repeated with 5 images. The errors in defect volume and intensity after registration were estimated by comparing the images resulting from warping transforms calculated when the defects were or were not present. For normal studies, registration accuracy was very similar between CLW and polynomial warping methods, and showed marked improvement over linear registration. However, with studies that have simulated lesions the polynomial warping caused large errors in defect volume (< -10%) and intensity (> +2.5%) for most defects. The lesions had minimal effect on the CLW algorithm accuracy, with small errors in volume (> -4%) and intensity (< +2%). The accuracy improvement compared with not warping was nearly constant regardless of defect: +1.5% overlap and +0.001 correlation. CLW is recommended because it caused small errors in defect estimation and improved the registration accuracy in all cases.

Fig. 1. Warping of a study with a simulated lesion. Images are transverse SPECT images. From left to right, the study has been registered with a linear transform only (left), with the CLW method (middle), or with the polynomial AIR method (right). Arrows illustrate regions where AIR warping has erroneously changed the defect, compressing the defect's volume and increasing its intensity.

OS_380

BRAIN BENZODIAZEPINE RECEPTOR CHANGES IN PATIENTS WITH MILD HEAD TRAUMA USING AUTOMATED TEMPLATE-BASED QUANTIFICATION

T. Kauppinen (1), A. Ahonen (1), V. Tuomivaara (2), J. Hiltunen (3), K. Bergström (4), J. Kuikka (4), P. Tornianen (2), M. Hillbom (2). (1) Division of Nuclear Medicine, Helsinki University Central Hospital, Helsinki, Finland; (2) Dept. of Neurology and Div. of Nucl. Med., Oulu University Hospital, Oulu, Finland; (3) MAP Medical Technologies Oy, Tikkakoski, Finland; (4) Dept. of Clin. Phys. and Nucl. Med., Kuopio University Hospital, Kuopio, Finland

Aim: Visual interpretation is generally used to interpret images in patients even though it is a highly subjective method. ^{123}I-labeled NNC 13-8241 is a novel partial benzodiazepine agonist with high affinity to the benzodiazepine receptors (BZR) in the brain. It is well documented that in mild head traumas CT or even MRI is not reliable to show small cortical defects. To evaluate possible neuronal damage nineteen patients with mild head trauma and 18 healthy volunteers were studied. The aim of this study was to create a normal reference template (based on normal volunteers) and 3D brain model for analysing BZR distribution and then evaluate 19 patients compared to the template.
Methods: The image acquisition was carried out with a dual-head gamma camera with high resolution fan-beam collimators (with 541 mm focus) and with the radius of rotation between 140-160 mm. The studies were acquired into 128x128 matrix size using 60 s per projection angle, resulting on average 50 kcts per projection. Iterative reconstruction program OS-EM was used. The number of subsets was chosen to be 8 with 5 iterations. Attenuation correction was performed during reconstruction using Chang's first order approximation (μ= 0.110 cm^{-1}). Nineteen patients with mild head trauma and 18 healthy age-matched volunteers were studied. Fifty three brain regions were determined by using MR images. ROIs were drawn into MR image and copied onto the SPECT image. Using defined ROIs a 3D brain model was created. Volunteers data were registered and combined together as a reference template. Correspondingly, the patient studies were registered and compared then to the template.
Results: Statistically significant regional BZR differences were found when the group of patients with mild head trauma was compared to the reference template. These were found in middle frontal gyrus and post- and precentral gyrus. The regional defects of the trauma patients varied up to −11.0 % compared to the normal template. Surprisingly, increased and abnormally high benzodiazepine receptor uptake was found in pons.
Conclusions: The results suggest that the 3D template-based brain model helps in regional analysis and reveals the patophysiological findings in mild head trauma better than pure visual image interpretation. Automated template-based quantification of the BZRs was proved to be a useful revealing several regional abnormalities in brain BZR distribution in patients with mild head trauma.

OS_381

EVALUATION OF AN AUTOMATIC CLASSIFIER FOR SPECT ALZHEIMER'S DISEASE DIAGNOSIS.

O. Migneco (1), J. Stoeckel (2), G. Malandain (2), P. Koulibaly (1), PH. Robert (3), N. Ayache (2). (1) Department of Nuclear Medicine, University of Nice-Sophia-Antipolis, Nice, France; (2) Epidaure Project, Inria, Sophia-antipolis, France; (3) Department of Psychiatry, CHU Pasteur, Nice, France.

HMPAO brain SPECT provides useful information for the diagnostic of Alzheimer's disease (AD). Nevertheless, the reading of the scans can be misleading in the early stages. The aim of our work was to develop a tool to help to differentiate AD from normal subjects (NS). For this purpose, we used a classifier, the Fischer Linear Discriminant (FLD) to assign one of the two class labels (AD or NS) to a given SPECT. The classifier has to be first „trained" with n subjects with their class labels to define the parameters of the two classes. Afterward, the classifier is able to calculate the „distance" between one particular SPECT and each class. The SPECT is supposed to belong to the closest class. In essence, the FLD compares the voxels values of the tested SPECT to the mean voxels values of the SPECTs used to build the classes. This comparison is weighted by the voxels covariance matrix of the two classes which gives more importance to the more differential voxels. 29 patients with probable AD (mean Mini Mental Test score: 23.5) and 50 NS were studied. The NS were extracted from the normal database of the SNM Brain Imaging Council. All brain SPECTs (AD and NS) were acquired using a triple-head gamma camera (Prism 3000, Picker, OH) and 128x128 pixels matrices. Reconstruction was performed by filtered back projection using only a ramp filter and an additional low-pass post-filtering (Butterworth, order: 6, cut-off: 0.3). Chang attenuation correction was applied to the transverse slices (coefficient: 0.07). The SPECTs were co-registered with an affine transformation. A brain mask was applied in order to exclude non-cerebral voxels. Intensity normalisation was performed by mean of the total counts in the brain. Then, each volume was sub-sampled by a factor of 4. The classifier was trained 79 times with a training set of 78 SPECTs leaving out one different SPECT each time. This SPECT was used to test the classifier. In this way, the tested SPECT was independent of the training SPECTs. The SPECTs were successfully classified in 89.9 %, 82.8 % and 94.0 % cases respectively for the total, the NS and the AD population. The AD patients were also assessed by 4 independent blinded experts. They were successfully classified in 58.6 %, 75.9 %, 58.6 %, 72.4 % cases respectively for each expert. We conclude that the classifier approach is a promising tool to diagnose AD.

OS_382

QUANTITATIVE SPECT AND VOLUMETRIC MRI FOR DISCRIMINATION BETWEEN NORMAL CONTROLS AND PRECLINICAL ALZHEIMER'S DISEASE

G. El Fakhri (1), M.F. Kijewski (1), J.B. Hilson (1), K.A. Johnson (1), R.E. Zimmerman (1), J.A. Becker (1), R. Killiany (2), K. Jones (3), M.S. Albert (4). (1) Harvard Medical School and Brigham & Women's Hospital; (2) Boston University School of Medicine; (3) Harvard Medical School and Brandeis University; (4) Harvard Medical School and Massachusetts General Hospital, Boston, USA

Quantitative brain SPECT and volumetric MRI have been assessed on the basis of performance in discriminating preclinical Alzheimer's disease (AD)from normal controls.
Methods: 14 normal controls (mean age = 71 years, Clinical Dementia Rating CDR = 0.0), who remained normal for at least 3 years after scans were acquired, and 12 subjects (75 years) with questionable AD at baseline (CDR = 0.5) who later developed AD were examined. A T1-weighted SPGR MRI and a Tc-99m HMPAO SPECT study were performed in each case. All SPECT studies (120 projections, 128x128) were acquired in 13 energy windows (80-156 keV) and corrected for scatter using a multispectral fitting method. MRI scans were registered to the SPECT data and segmented to yield the exact attenuation map for each study. SPECT data were reconstructed using OSEM (6 subsets, 15 iterations) while modelling attenuation, intrinsic detector resolution, and geometric collimator response in the projector/backprojector. Mean perfusion (adjusted to the total number of counts using analysis of covariance) and volume were considered in 5 structures (left/right pairs): the rostral anterior (rcing), caudal anterior (ccing) and posterior (pcing) cingulate, the entorhinal cortex (ento) and the superior temporal sulcus (sts). Perfusion differences between the two populations observed in SPECT, as well as differences in volume observed in MRI, were assessed by discriminant analysis, which yielded for each subject a likelihood ratio of being preclinical AD rather than normal. From these, areas under the ROC curve (Az) for discrimination were obtained using a fitting program (ROCKIT).
Results: The areas under the ROC curve associated with a 5-feature analysis were 0.952±0.042 with SPECT data alone and 0.980±0.041 with MRI alone. The structures ranked by decreasing discriminant power were ccing, rcing, ento, sts and pcing for SPECT and ccing, ento, pcing, rcing and sts for MRI. Using joint SPECT+MRI information yielded the best results even with a small number of features (Az =0.981±0.030 for rcing+ccing SPECT + ento+ccing MRI).
Conclusion: Normal controls and preclinical AD can be discriminated with very high accuracy with either SPECT or MRI and may be best achieved by using combined perfusion (SPECT) and volume (MRI) information.

OTHER CLINICAL SCIENCE. INFECTION AND INFLAMMATION

OS_383

INFECTION IMAGING WITH TC-99M-LABELED INTERLEUKIN-8 USING FIVE DIFFERENT COLIGAND FORMULATIONS

H.J. Rennen (1), J.E. van Eerd (1), W.J. Oyen (1), F.H. Corstens (1), O.C. Boerman (1). (1) Department of Nuclear Medicine, University Medical Center Nijmegen, Nijmegen, The Netherlands.

In previous studies interleukin-8 (IL-8) was labeled with ^{99m}Tc via the hydrazinonicotinamide (HYNIC) chelator using tricine as coligand. This preparation showed excellent characteristics for imaging of infection in a rabbit model of soft-tissue infection. In the present study the propylaldehyde hydrazone formulation of HYNIC was introduced to stabilize HYNIC-IL-8. Subsequently, the effect of the coligand on the in vivo behavior of Tc-99m-labeled IL-8 was investigated using 5 different coligand formulations and 5 rabbits per coligand.
Methods: HYNIC-conjugated IL-8 was labeled with ^{99m}Tc in the presence of either (A) tricine, (B) ethylenediaminediacetic acid (EDDA), (C) tricine together with trisodium triphenylphosphinetriphosphate (TPPTS), (D) tricine with nicotinic acid (Nicotinic) or (E) tricine with isonicotinic acid (Isonicotinic). Biodistribution of the radiolabel was determined both by γ-camera imaging as well as by counting dissected tissues at 6 h p.i.
Results: The use of HYNIC with the protected hydrazine group resulted in a product with significantly increased stability. Consequently, the labeling efficiency of the preparation remained high, also after long term storage at minus 20^{0}C. Specific activities (MBq/µg protein) were highest for (Iso)Nicotinic 40-80 > TPPTS 40 > Tricine 15 > EDDA 7. Abscess/muscle ratios were highest for Nicotinic 248 > Isonicotinic 204 > EDDA 116 > Tricine 94 > TPPTS 36. Abscess/blood ratios were highest for EDDA 22 > Nicotinic 19 > Isonicotinic 17 > Tricine 10 > TPPTS 8. Abscess uptake exceeded 5.5%ID for all formulations except TPPTS: 1%ID. Kidney uptake (%ID/g) was lowest for Isonicotinic 1.75 < Nicotinic 1.91 < Tricine 2.59 < TPPTS 2.69 < EDDA 2.86. Gamma camera imaging rapidly visualized the abscess from 2 h p.i. onwards for all formulations with highest abscess/background ratios at 6 h p.i. for Isonicotinic 29 > EDDA 23 > Nicotinic 22 > Tricine 15 > TPPTS 4.
Conclusion: IL-8 can be rapidly and easily labeled with ^{99m}Tc using HYNIC as a chelator and using various coligands. The choice of the coligand had a profound effect on the in vivo behavior of the ^{99m}Tc-labeled IL-8. In the rabbit model, the most optimal infection imaging characteristics were found for formulations using tricine/(iso)nicotinic acid as coligands combining a high specific activity (40-80 MBq/µg) with high abscess/muscle ratios (>200) and high abscess/background ratios (>20).

OS_384

INFECTION IMAGING WITH TC-99M-LABELED CXC-CYTOKINES: IL-8, GCP-2 AND PF-4

H.J. Rennen (1), O.C. Boerman (1), C. Frielink (1), W.J. Oyen (1), A. Watz (2), F.H. Corstens (1). (1) Department of Nuclear Medicine, University Medical Center Nijmegen, Nijmegen, The Netherlands; (2) Theodor Kocher Institute, University of Bern, Bern, Swiss.

The CXC-cytokines interleukin-8 (IL-8) and granulocyte-chemotactic-protein-2 (GCP-2) act on human neutrophils via two neutrophil receptors (CXCR1 and CXCR2), the CXC-cytokine platelet-factor-4 (PF-4) only interacts with the CXCR2 receptor. In a recent study ^{99m}Tc-labeled IL-8 showed excellent characteristics for imaging of infection in a rabbit model of soft-tissue infection. In the present study the in vitro and in vivo characteristics of radiolabeled IL-8 were compared to that of radiolabeled GCP-2 and PF-4.
Methods: The three CXC-cytokines were labeled with ^{99m}Tc via the hydrazinonicotinamide (HYNIC) chelator, using tricine as a coligand. In vitro receptor binding assays were performed using Jurkat transfectants bearing either CXCR1 or CXCR2. The preparations were tested for imaging of infection in rabbits with E.coli infections in the left thigh muscle. Biodistribution of the radiolabel was determined both by γ-camera imaging and by counting dissected tissues at 6 h p.i.
Results: The receptor binding capacity for ^{99m}Tc-labeled IL-8 exceeded 50% for both receptortypes CXCR1 and CXCR2. Receptor binding capacities were considerably lower for ^{99m}Tc-labeled GCP-2 and PF-4. In the rabbit model IL-8, GCP-2 and PF-4 showed an abscess uptake of 0.22, 0.065 and 0.014 %ID/g at 6 h p.i. resp. Abscess/muscle ratios were 67, 18 and 5.5 resp. for these proteins. Abscess/blood ratios were 5.3, 1.8 and 0.75 resp. Quantitative analysis of the images revealed abscess-background ratios improving with time up to 11, 3.5 and 1.5 for IL-8, GCP-2 and PF-4 resp. The radiolabel was excreted almost exclusively renally for IL-8, while GCP-2 and PF-4 also cleared via the hepatobiliary route. Gamma camera imaging rapidly visualized the abscess from 2 h p.i. onwards for IL-8 and GCP-2, with best results for IL-8.
Conclusion: This study shows that for infection imaging ^{99m}Tc-labeled IL-8 is the superior agent. High affinity for both CXC-receptors seems to be a prerequisite for adequate infection imaging.

OS_385

TC-99MWBC SCAN FINDINGS IN FEMALE PATIENTS WITH ACUTE LOW ABDOMINAL PAIN

T. Lantto (1), E. Lantto (2), R. Mokka (3), T. Ranta (3), P. Ylikangas (4). (1) Centre for Laboratory Medicine, Tampere University Hospital, Tampere, Finland; (2) Department of Radiology, Tampere University Hospital, Tampere, Finland; (3) Departments of Surgery and Gynecology, Päijät-Häme Central Hospital, Lahti, Finland; (4) Department of Nuclear Medicine, Päijät-Häme Central Hospital, Lahti, Finland

Acute low abdominal pain (LAP) is a common disorder in female patients (pts) in emergency departments of the hospitals. The pain may be either gynaecological or gastrointestinal origin. The diagnosis should be reached quickly to eliminate serious late complications. Tc-99mWBC scan has offered a method to rapidly diagnose and localize inflammatory processes.
The aim of this study was to evaluate the usefulness of Tc-99mWBC scan in female pts with LAP.
We retrospectively evaluated the findings of WBC scans of 63 consecutive female patients imaged because of unexplained LAP with fever and/or palpable mass. The results were compared with the final diagnoses, which based on physical examination, radiological imaging, clinical course, scopies and operations.
Thirty-two pts were sent for imaging by the gynaecologist and 31 pts came from the other departments. Fifty-four of the 63 pts were examined by gynaecologist and 35/63 by a surgeon.
The final diagnosis was in 25 pts gynaecological (GYN) and in 25 pts gastrointestinal (GI), in 5 pts other low abdominal disorder was found (OTHER) and in 8 pts the final diagnosis was not reached.
In the 25 GYN pts WBC was positive in 6/7 of tubo-ovarial abscesses, in 7/7 of salpingo-oophoritis and it was negative in 5/5 endometritis and 6/6 benign ovarial tumours. In the GI pts WBC was positive in 15/16 pts with acute diverticulitis and in 3/3 appendicitis, 2/2 terminal ileitis, 2/2 acute cholecystitis, in 1 omental strangulation and 1abscess. In the OTHER group 2 pts had deep femoral trombosis, 1 pt post partum sacroilitis and 1 pt enlarged inguinal lymph nodes. All these were correctly diagnosed in WBC scan. A patient with post sectional pain and fever had placental chorionamnionitis , which was negative in WBC scan. In the 8 pts whose final diagnosis was not reached, WBC scan was positive in 3 pts and negative in 5 pts.
There were no significant differences in CRP and white blood cell values between the various groups. The only significance was the older mean age of the pts with acute diverticulitis compared with the pts with GYN infectious disease ($p< 0.001$).
As a conclusion can be said that Tc-99m WBC scan shows reliably the infectious processes in patients with low abdominal pain and can be used in complicated cases. The age of the patient helps in the differential diagnosis of the diseases.

OS_386

111-IN-LABELLED LEUKOCYTE SCAN IN ACUTE PROSTATITIS

F. Lomeña (1), J.J. Mateos (1), M. Velasco (2), J.P. Horcajada (2), C. Piera (1), M. Ortega (1), F. Martín (1), F. Pons (1), J. Mensa (2). (1) Department of Nuclear Medicine; (2) Department of Infectious Diseases, Hospital Clínic, University of Barcelona, Spain.

AIM: i) To evaluate the usefulness of 111-Indium-labelled leukocyte scan (LS) for diagnosing acute prostatitis. ii) to determine if the LS is an accurate method to assess the response to antibiotic treatment
METHOD: We prospectively studied 15 males (age 65±10 year) with clinical suspicion of acute prostatitis (fever + cystitic syndrome + painful digital rectal examination). We used as a control group 7 women (age 32±18 year) with clinical suspicion of acute pyelonephritis and the same male patients of the study group after finishing antibiotic therapy.
We performed in all patients and controls, urine fluid culture (UFC) and LS, 24 and 48 hours after endovenous injection of 300 μCi of 111-Indium-oxine-labelled leukocytes. After 2-4 weeks of antibiotic treatment, a second LS was performed.
RESULTS: The UFC was positive for E. Coli on 11/15 males and 6/7females. In 4/15 males, the UFC was negative. In 1/7 males the UFC was positive for Klebsiella. All patients showed LS with intense uptake in the prostatic region. Additionally, 1 male had abnormal uptake in testicular regions, due to acute epididymo-orchitis and another in left kidney. All female didn't show uptake in the perineal region, although all of them showed kidney uptake (right 4/7; left 2/7; bilateral 1/7).
After therapy the LS was normal in 14/15 male patients. The only one positive LS after therapy was due to a re-infection. All females showed a normal second LS.
CONCLUSIONS: i) LS is a useful method in diagnosing acute prostatitis, and additionally pyelonephritis. ii) LS LS is an accurate method to assess the response to antibiotic treatment.

OS_387

FEVER OF UNKNOWN ORIGIN- PROSPECTIVE COMPARISON OF 18 FDG- IMAGING WITH A DOUBLE HEAD COINCIDENCE CAMERA (DHCC) AND GA-67 CITRATE SPECT

J. Meller, G. Altenvoerde, K. Lehmann, C. Sahlmann, I. Meyer, M. Behe, H. Luig, W. Becker. Department of Nuklear Medicine, University of Göttingen, Germany.

Aim: ^{67}Ga-citrate is currently considered as the tracer of choice in the diagnostic workup of fever of unknown origin (FUO). [18F] 2ω-deoxy-2-fluoro-D-glucose (FDG) has been shown to accumulate in malignant tumors but also in inflammatory processes. The aim of our study was the prospective evaluation of FDG- imaging with a double head coincidence camera (DHCC) in patients with FUO in comparison to planar and SPECT ^{67}Ga-citrate scanning.
Patients and Methods: This study is a prospective analysis of 28 FUO-patients who underwent ^{18}F-FDG-DHCC imaging which included transaxial (TT)and longitudinal whole body tomography (LT) one hour after intravenous injection of 300 MBq FDG. In 18 of these subjects ^{67}Ga-citrate whole body- and SPECT imaging was performed 48-72 following the intravenous injection of 200 MBq ^{67}Ga-citrate. The ^{67}Ga-citrate and FDG images were interpreted by two investigators both blinded to the results of other diagnostic modalities.
Results: 36% (10/28) of the patients had infection, 21% (6/28) had autoimmune diseases, 14% (4/28) had neoplasms and 22% (6/28) other diseases. Fever remained unexplained in 7% (2/28) of the patients.
Of the 20 patients studied, FDG-imaging was positive and essentially contributed to the final diagnosis in 14 (50%). Sensitivity of FDG-TT in detecting the focus of fever was 85% and specifity 85%. Positive and negative predictive values were 92% and 75% respectively.
If the analysis was restricted to the 18 patients who were investigated both with ^{67}Ga-citrate- and F-18-FDG sensitivity was 81% and specifity 86%. Positive and negative predictive values were 90% and 75% respectively. The diagnostic accuracy of LT-FDG-tomography was lower (sensitivity: 36%, specifity: 86%, positive and negative predictive values: 80% and 46% respectively).
^{67}Ga- citrate SPECT yielded a sensitivity of 67% in detecting the focus of fever and a specifity of 78%. Positive and negative predictive values were 75% and 70% respectively. A low sensitivity (45%), but combined with a high specifity (100%) was found in planar ^{67}Ga- citrate imaging. Positive and negative predictive values were 100% and 54% respectively.
Conclusion: In the context of FUO FDG transaxial tomography performed with a DHCC is superior to ^{67}Ga- citrate SPECT. This seems to be the consequence of superior tracer kinetics of FDG compared with those of ^{67}Ga- citrate and of a better spatial resolution of a DHCC-system compared with SPECT imaging. In patients with FUO FDG-imaging either with dedicated PET or DHCC should considered as the procedure of choice.

OS_388

IMAGING INFLAMMATION IN CAROTID ATHEROSCLEROTIC PLAQUE USING FDG-PET

T.D. Fryer (1), J.H.F. Rudd (2), E.A. Warburton (3), H. Jones (2), J.C. Clark (1), P. Johnstrom (4), A.P. Davenport (4), N. Antoun (1), P. Kirkpatrick (1), J.D. Pickard (1), P.L. Weissberg (2)(1) Wolfson Brain Imaging Centre; (2) Cardiovascular Medicine; (3) Stroke Medicine, Addenbrookes Hospital, Cambridge, UK; (4) Clinical Pharmacology, University of Cambridge, UK

Aim: Atherosclerotic plaque rupture, with its life-threatening sequelae, is usually a consequence of inflammatory cell activity within the plaque. Current vascular imaging techniques provide anatomical data but give no indication of the degree of plaque inflammatory activity. *In-vitro* imaging of excised carotid plaques revealed FDG uptake in areas dominated by inflammatory cells. Consequently, we applied FDG-PET to image *in vivo* inflammation within carotid artery atherosclerotic plaque, with the aim of differentiating unstable from stable plaques.
Methods: Six patients with symptomatic carotid artery disease underwent PET scanning after administration of 370 MBq FDG. Three of the patients had bilateral carotid disease, with only one side symptomatic. Late imaging (4 x 5minute frames at approximately 100 and 195 minutes post-injection) in 3D mode was employed as earlier preliminary studies using 2D imaging for 60 minutes post-injection provided poor plaque signal-to-noise ratio. Blood sampling was performed over the entire post-injection time period but scanning was not due to patient comfort reasons. Fiducial markers and a rigid cervical collar were employed to facilitate co-registration of the PET images to a contrast CT scan performed at the end of the study.
Results: Symptomatic plaques had a statistically significant ($p<0.006$) higher plaque-to-blood FDG concentration ratio than asymptomatic ones at 195 minutes post-injection: (1.9 ± 0.2) compared to (1.1 ± 0.2), respectively. The concentration ratios for the two plaque types were less well separated at 100 minutes post-injection: (1.1 ± 0.2) compared to (0.8 ± 0.1). Co-registration with CT was a significant aid in determining the plaque region in the PET images, particularly for the asymptomatic plaques.
Conclusions: These preliminary results indicate that FDG-PET imaging approximately three hours post-injection may be able to differentiate symptomatic (unstable) from asymptomatic (stable) carotid plaques. Further work is underway to examine the plaque FDG kinetics and to correct the plaque FDG concentration for partial volume error.

OS_389

SPLENIC FDG PET UPTAKE IS INCREASED IN EARLY HIV INFECTION

S. Iyengar, M. Osman, D. Schwartz, B.B. Chin. Department of Radiology, Johns Hopkins Medical Institutions, Baltimore, USA.

Whole body FDG PET may be able to detect increased glycolytic activity of lymphocytes in regions of residence after viral infections. The aim of this study is to determine if early HIV infection is associated with increased FDG uptake in the spleen.
Methods: 11 control subjects referred for evaluation of malignancy had negative PET studies. Controls had no prior malignancy, active infection, spleen or liver disease. Seven patients with early HIV infection were diagnosed within several months of initial infection and did not receive prior HIV drug therapy. Whole body FDG PET studies with post-injection transmission scanning were reconstructed with iterative reconstruction and segmented attenuation correction. Standardized uptake values corrected for ideal body mass, spleen to liver uptake ratios, and visual interpretations of spleen to liver ratios were used to evaluate splenic FDG uptake.
Results: The mean spleen SUV in the HIV group was significantly higher than in the control group (2.44 ± 0.20 versus 1.44 ± 0.09; $p<0.0001$). The mean liver SUV was not significantly different in the HIV group compared to controls (1.6 ± 0.07 versus 1.84 ± 0.11; $p=0.3$). Spleen to liver ratios in the HIV group were significantly higher compared to the control group (1.44 ± 0.10 versus 0.78 ± 0.02; $p<0.000001$). Visually, the spleen uptake was greater than or equal to liver uptake for all HIV patients; spleen uptake was lower compared to liver uptake in all controls. All HIV patients also had abnormal lymph node uptake in multiple lymph node basins.
Conclusion: Early HIV infection is associated with abnormally high splenic FDG uptake that likely represents lymphocyte activation of the immune system. HIV infections may result in a widespread pattern of increased FDG uptake in spleen and lymph nodes that should not be confused with malignancy.

OS_390

18F-FDG-PET IN INFLAMMATORY DISEASE

D. Otto, A.R. Börner, E. Weckesser, M. Hofmann, T. Petrich, W.H. Knapp. Department of Nuclear Medicine, Medical School of Hannover, Hannover, Germany.

Aim: Cell culture and human studies show accumulation of FDG not only in malignant tumours but also in inflammatory lesions. The aim of our study was to establish the clinical value of FDG-PET in patients with fever of unknown origin (FUO) and in patients with mycosis during treatment.
Methods: 27 patients (15 patients with FUO, 3 patients with suspected arteriitis and 9 patients with known mycotic foci for therapy monitoring) underwent FDG-PET (200-900 MBq ^{18}F-FDG, Siemens ECAT 922, iterative reconstruction (OSEM), matrix 128x128, emission scan 90 min. p.i.). Standard uptake values (SUV's) were used for quantitation of focal uptake.
Results: Foci were localised with FDG-PET in 7/15 patients (47%) with FUO (SUV«s 2.4-6.4). All of them were verified by follow up. FDG accumulation in lymph nodes was observed in 3/15 patients (20%) with viral or hematological diseases. In 5/15 patients (33%) no pathological focal FDG uptake was noted. Based on the reference clinical diagnosis, sensitivity of FDG-PET for localisation of inflammatory foci was 100%. In one patient with aortitis high FDG accumulation in the aortic wall was found, two other patients with suspected aortitis (not confirmed during follow-up) had normal FDG scans. 6/9 patients with invasive mycosis on antimycotic treatment showed increased FDG uptake (SUV's 1,8-3,8) by known inflammatory foci on antimycotic therapy. Therapy management was influenced by PET results in three negative cases (change to oral therapy) and in all positive cases (continued or intensified i.v. medication).
Conclusions: These results support the role of FDG-PET as a highly sensitive method to identify focal inflammations. Accumulation of FDG in affected lymph nodes in patients with viral or hematological disease should be considered. For monitoring of antimycotic therapy the identification of residual active disease appears feasible.

NEUROLOGY / PSYCHIATRY

OS_391

SPECT IMAGING OF SEROTONIN TYPE 2A RECEPTORS IN ALZHEIMER'S DISEASE

J.A. Versijpt (1), K. Van Laere (1), F. Dumont (2), D. Decoo (3), P. Santens (3), K. Audenaert (1), G. Slegers (2), J. Korf (4), R. Dierckx (1). (1) Division of Nuclear Medicine, Ghent University, Belgium; (2) Department of Radiopharmacy, Ghent University, Belgium; (3) Department of Neurology, Ghent University, Belgium; (4) Department of Biological Psychiatry, Groningen, Netherlands

Aim: The serotonin receptor is generally involved in behaviour, learning, and memory. More specifically, the serotonin type 2A ($5HT_{2a}$) receptor has been suggested to stimulate the amyloid precursor protein secretion which could eventually lead to the formation of the amyloid neuritic plaques, typically seen in Alzheimer's disease (AD) patients. ^{123}I-5-I-R91150 is a radio-iodinated $5HT_{2a}$ receptor antagonist with high affinity and selectivity (K_d=0.11 nM). The aim of the present study was to determine whether there are abnormalities in the *in vivo* status of the $5HT_{2a}$ receptor binding potential in AD patients compared to age-matched healthy subjects.
Methods: Nine AD patients (mean age 80 yrs, range 73-88) and 10 age-matched healthy subjects were included. AD patients underwent a screening for depressive symptoms by means of the geriatric depression scale and and extensive neuropsychological testing battery (Amsterdam dementia screening test, ADS6) to assess the cognitive status (mean MMSE 17/30). All subjects were scanned on a triple-headed gamma camera after the injection of 185 MBq ^{123}I-5-I-R91150 (specific activity 10 Ci/μmol). After reconstruction (FBP, TEW scatter and uniform attenation correction), emission images were realigned into Talairach coordinates by means of the sequentially-scanned transmission images. A semiquantitive analysis was performed, providing ratios of binding potential compared to the cerebellum (void of $5\text{-}HT_{2a}$ receptors) for 26 cortical, 6 subcortical, 2 cerebellar, and one pons 3D-volumes of interest.
Results: A statistically significant decreased binding potential in AD patients compared to controls was found in the anterior and posterior cingulate, the left temporal anterior and the right temporal region, the right lateral frontal and the right sensorimotor region.
Conclusions: These SPECT imaging results are in agreement with previous postmortem and PET studies, and confirm the fact that the $5HT_{2a}$ receptor is differentially affected in AD patients compared to normal aging. This has implications for both the etiological basis and the therapeutic management of AD.

OS_392

ASSESSMENT OF PERFUSION EFFECTS OF CHOLINESTERASE INHIBITORS IN ALZHEIMER'S DISEASE BY 99MTC-ECD BRAIN SPECT

D. Volterrani (1), R. Ceravolo (2), G. Manca (1), S. Suriano (1), G. Tognoni (2), G. Boni (1), G. Dell'Agnello (2), M. Grosso (1), L. Murri (2), R. Bianchi (1). (1) Division of Nuclear Medicine; (2) Division of Neurology, University of Pisa, Pisa, Italy.

Alzheimer's Disease (AD) is associated with a loss in presynaptic cholinergic function, and cholinesterase (ChoE) inhibitors improve and/or stabilize the cognitive impairment in AD patients. However, the regional metabolic/perfusional correlates of treatment with ChoE inhibitors are unknown. Aim of this study was to identify the relationship between the cognitive benefit observed with the ChoE inhibitors and the changes in regional cerebral perfusion.
Methods: Fiveteen patients with mild to moderate AD were evaluated with ^{99m}Tc-ECD SPECT, before and after 6 months treatment with ChoE inhibitors (donepezil, and rivastigmine). Patients were gradually increased to donepezil 10 mg and rivastigmine 12 mg. Clinical evaluations included the Mini Mental State Examination (MMSE) as well as the Neuropsychiatric Inventory (NPI). Clinically significant cognitive and behavioral improvement was found with ChoE inhibitors treatment (MMSE improvement of 2 points; total NPI improvement of 4.8 points). SPECT acquisitions were carried out by using a dual head gamma camera equipped with LEHR collimators about 30 min. after i.v. tracer injection (740 MBq). FBP and a Butterworth prefiltering (cut-off 0.50 cycles/cm, order 10) were used for images recontruction. Uniform attenuation correction was also applied. Reconstructed data, after smoothing with a 12 mm Gauussian Kernel and spatial normalisation onto a SPECT template, were analysed by Statistical Parametric Mapping (SPM99).
Results: SPM analysis showed a significant increase ($p < 0.01$) of regional cortical perfusion after ChoE inhibitor therapy with respect to baseline in dorso-lateral pre-frontal areas and anterior cingulate bilaterally. No regional decrease of perfusion was observed after ChoE inhibitors treatment.
Conclusions: Our preliminary data suggest the presence of relationship between the cognitive benefit observed with the ChoE inhibitors and ^{99m}Tc-ECD SPECT findings. The clinical benefits reported with ChoE inhibitors can be correlated with specific increase of regional cortical perfusion of attentional and limbic networks.

OS_393

CONTRIBUTION OF TC99M-ECD BRAIN PERFUSION SPECT TO ALZHEIMER'S DISEASE WITH DELIRIUM

F. Chierichetti (1), G.L. Bianchin (2), M. Calabrò (3), G. Salce (2), P.L. Zanco (1), B. Saitta (1), S. Medea (1). (1) U.O. Medicina Nucleare - Centro PET, Castelfranco Veneto, Italy; (2) U.O. Psichiatria, Montebelluna, Italy; (3) U.O. Geriatria, Montebelluna, Italy.

AIM OF THE STUDY: the problem of delirium in elderly patients, without a previous history a psychiatric disease, is of relevance both to assess the diagnosis of dementia and to establish an appropriate treatment. The aim of our study was to investigate a possible role of brain perfusion SPECT.
PATIENTS AND METHODS: 26 old patients (mean age 72 years old) with delirium were considered respect a control group of 28 patients with final diagnosis of probable Alzheimer's disease. Both of them were studied by EMMS (Expanded Mini-Mental-State), Hachinski Score, Moda (Milan Overall Dementia Assessment), DSM-IV and ICD-10 for dementia, thyroid function, folates and B12 assessment in blood, echoDoppler of intracranial vessels, EEG and MRI. All patients were submitted to Tc99m-ECD SPECT using a double head camera (ECAM, Siemens) equipped with fan bean collimator. The scintigraphic data were evaluated both by a visual and a semi-quantitative analysis. All subject were drug-free and we selected only patients affected of mild to moderate dementia. Clinically relevant depression (as assessed by appropriate tests) was not present in both group. Previous head trauma, psychiatric and/or cererebrovascular diseases were excluded. 12 subjects with delirium were studied also to re-test after six months.
RESULTS: the final diagnosis for patients affected of dementia and delirium was probable Alzheimer's disease. While the control group's SPECT data showed hypoperfusion of the posterior cortex, mono and or bilateral, with relative sparing of frontal cortex, sensori-motor cortex, basal ganglia and thalamus, the patients with delirium presented a clear involvement (hypo but also hyperperfusion) of frontal cortex, thalamus and basal ganglia. In this last group we found also posterior cortex hypoperfusion, but monolateral. After a six months follow up, the group of 12 patients reaximined by SPECT, even if demented, had a better clinical assessment after therapy for delirium, but they still presented a severe impairment of frontal cortex.
CONCLUSIONS: as known from previous reports, delirium in brain degenerative diseases, such as Lewy's body dementia is characterized, in perfusion SPECT imaging, by hypoperfusion of posterior, occipital cortex. On the contrary, in pure psychiatric pathology, delirium affects anterior, frontal cortex. The results of our preliminary experience seem to show that delirium in dementia is associated with frontal derangement and this is not reversed by therapy. A possible explanation is that this is another kind of Alzheimer's dementia, probably with a different prognosis respect to typical Alzheimer's disease.

OS_394

LACTATE-INDUCED CEREBRAL BLOOD FLOW CHANGES IN ALZHEIMER'S DISEASE

L. Pavics (1), J. Kalman (2), T. Sera (1), G. Kis (2), M. Szecsi (2), P. Turi (2), L. Csernay (1,3), Z. Janka (2). (1) Department of Nuclear Medicine, University of Szeged, Szeged, Hungary; (2) Department of Psychiatry, University of Szeged, Szeged, Hungary; (3) International Medical Center, Szeged, Hungary.

Lactate, as a metabolite of glycolysis, is the primary source of energy of the nervous system. In vitro and in vivo experiments have shown the neuroprotective effect of lactate and improvement of the brain function after ischaemic injury. Intravenous infusion of lactate increases the global cerebral blood flow (CBF). In Alzheimer's disease (AD), there are characteristic regional blood flow abnormalities, and in the cerebrospinal fluid, abnormal lactate levels are detected. Since disturbed CBF and vasoregulation are detected in AD, the effects of intravenous Na-lactate on the CBF and related metabolic parameters were examined in order to assess the CBF response in the AD brain.
Methods: In 20 (14 women, 6 men, age ± SD: 74±7 years) AD patients (DSM-IV, MMS: 13±6), a self-control study was performed. rCBF SPECT (99mTc-HMPAO) investigations were carried out during the infusion of 5 mg/kg body weight 0.5 M Na-lactate and in the control state (0.9% saline infusion) one week apart. The rCBF changes were analysed by Statistical Parametric Mapping. ECG, blood pressure, heart rate, venous blood pH, pCO2, bicarbonate, serum lactate and cortisol levels were measured before and after the SPECT investigation. Acute Panic Inventory and anxiety rating scales were used to assess the psychiatric effect of lactate.
Results: The serum lactate level increased on average from 0.8 mM/L to 4.6 mM/L or to 6.1 mM/L 10 and 20 minutes, respectively, after lactate infusion. Compensatory changes were found in the venous blood pH, pCO2 and bicarbonate levels. Significant psychiatric symptoms and blood pressure and heart rate increases were not observed. The serum cortisol level increased slightly. At the baseline investigation, in 8 patients bilateral temporoparietal, in 4 cases temporal and in 8 patients other localisation hypoperfusions were detected. The lactate infusion produced statistically significant ($p<0.05$) rCBF decreases in the temporooccipital and occipital regions independently of the rCBF abnormality detected in the control investigation. The diminished cortisol level elevation indicates a blunted stress response to lactate, and the cholinergic deficit in AD might be responsible for the rCBF changes.
Conclusions: In AD, lactate infusion produces a relative hypoperfusion in the occipital areas and there is no significant beneficial effect on the diseased regions in an acute experiment. The exact mechanism of these changes warrants further elucidation.

OS_395

NORMAL OR ALZHEIMER«S DISEASE? – AUTOMATED INTERPRETATION OF CEREBRAL BLOOD FLOW IMAGES USING ARTIFICIAL NEURAL NETWORKS

L. Edenbrandt (1), S. Warkentin (2), M. Ohlsson (3), L. Minthon (4), P. Wollmer (2). (1) Dept. of Clinical Physiology, Lund University, Lund, Sweden; (2) Dept. of Clinical Physiology, Malmoe University Hospital, Malmoe, Sweden; (3) Dept. of Theoretical Physics, Lund University, Lund, Sweden; (4) Dept. of Psychiatry, Malmoe University Hospital, Malmoe, Sweden

Aim: Artificial neural networks have previously been applied to automated interpretation of myocardial perfusion images, lung scintigrams and captopril renograms. It has also been shown that physicians benefit from the advice of such neural networks. The purpose of this study was to develop neural networks for the classification of cerabral blood flow images into either normal or consistent with Alzheimer«s disease.
Methods: The study population consisted of one group of 92 normal healthy subjects and one group of 132 patients with Alzheimer«s disease. The normal subjects underwent physical examination, psychiatric screening and routine laboratory investigations in order to exclude somatic and psychiatric illness. Alzheimer«s disease was diagnosed according to established criteria (DSM-IV and NINCDS-ARDA).
The regional cerebral blood flow was measured by the non-invasive 133-Xe inhalation method. A 64-detector system (Cortexplorer 64, Ceretronix) with scintillation detectors arranged in a helmet around the head was used. The subjects inhaled a mixture of 133-Xe and air for 1 minute. During the following 10 minutes the subjects breathed normal air and the clearance of the isotop was measured. Blood flow values were calculated from these clearance values and the results were presented in blood flow images. The images reflected the blood flow in the superficial cortical areas.
Artificial neural networks with a multilayer perceptron architecture were trained using the back propagation updating algorithm. The blood flow images were used as inputs to the networks. No other data were available for the networks. A 3-fold cross validation procedure was used in order to obtain as reliable performance as possible.
Results: The performance of the neural network, measured as the area under the receiver operating characteristic curve, was 0.94. The sensitivity for Alzheimer«s disease was 84 % at a specificity of 90 %.
Conclusions: Artificial neural networks can be trained to interpret cerebral blood flow images for the diagnosis of Alzheimer«s disease. These results indicate that this type of networks may be useful as decision support tools for the nuclear medicine physicians. The network«s high performance indicates that the cerbral blood flow images contain most of the information needed for the diagnosis of Alzheimer«s disease.

OS_396

NEURODEGENERATIVE DEMENTIA ANS BRAIN FUNCTIONNAL IMAGING/ A RE-EVALUATION

M. Steinling (1), M. Steinling (1), P. Charpentier (2), L. Defebvre (2), P. Lecouffe (1), A. Duhamel (4), C. Delmaire (1), F. Pasquier (2). (1) Nuclear medicine; (2) Department of Neurology; (3) Department of Statistics, Universitary Hospital, Lille Cedex, France.

Background: Ideas concerning Alzheimer's functional imaging patterns have changed within time from the initial typical „finger-print" to the current predominating conception of heterogeneity of Alzheimer' Disease. Furthermore, the identification of new nosological forms of neurodegenerative Dementia such as Lewy Body Disease (LBD) requires a re-evaluation of the patterns observed in brain functional imaging in such diseases.
Methods: We studied 60 demented patients, divided into three groups, fulfilling respectively the clinical criteria for Alzheimer's disease (AD), Lewy body disease (LBD) and Fronto-temporal Dementia (FTD). All the patients were examined by following administration of 555 MBq of freshly prepared ^{99m}Tc-HmPAO using a dedicated cerebral SPECT system (Tomomatic 564) .Ten pairs of regions of interest were plotted on a transverse section passing through CM + 5 cm plane, and the standardised values with respect to mean cerebellum activity were analysed by non-parametric univariate statistical test, pairwise comparisons, then by applying a previously established cut-off (at 80 % and 82.5 %) and finally by discriminant analysis.
Results: The different methods used reaffirmed already established data concerning fronto-temporal dementia: anterior and inferior frontal, fronto-lateral and posterior frontal decreases (Fig; **A**); for LBD a severe diffuse decrease in the frontal regions and also in the posterior association cortex (bilaterally in the temporo-parieto-occipital and parieto-occipital regions). (Fig; **C**):

Fig: Significantly decreased Rois for FTD, AD and DLB

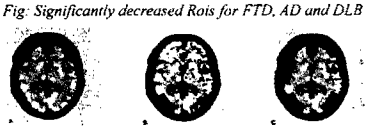

In contrast, for patients with Alzheimer's disease (**B**), the decrease was strictly limited to the posterior association cortex and this was slightly more severe on the left side than the right. The original description of bi-temporal-parieto-occipital damage, sparing the frontal cortex was thus once more found, irrespective of the severity of the cognitive decline.
Discussion: The major simplification concerning the pattern observed in Alzheimer's disease (the finger print sign) can be explained by the fact that patients suffering from LBD were previously included in the groups of patients affected by Alzheimer's disease, contributing to the pseudo heterogeneity of AD on SPECT or TEP. These results have major implications for the clinical use (differential diagnosis) of SPECT in neurodegenerative Dementia.

OS_397

RELATIONSHIP BETWEEN ELECTROENCEPHALOGRAPHIC AND CEREBRAL BLOOD FLOW CHANGES IN FRONTOTEMPORAL DEMENTIA

F. Nobili (1), G. Agnese (1), P. Erba (1), P. Vitali (2), T. Prastaro (2), S. Carozzo (2), N. Girtler (2), C. Bordoni (2), M.,. Bagnasco (1), G. Mariani (1), G. Rodriguez (2)(1) Nuclear Medicine Service, DiMI; (2) Clinical Neurophysiology Service, University of Genoa, Genoa.

Reduced blood flow in the frontotemporal regions is usually reported to occur earlier than electroencephalograhic (EEG) changes during frontotemporal dementia. The aim of this study was to characterize further such discrepancy and, moreover, to explore the relationship between EEG and regional cerebral blood flow (rCBF) findings, which is at present poorly known.
Methods: Ten patients with frontotemporal dementia (7 women and 3 men, mean age 64.1 ± 11.3 yr) underwent quantitative EEG (qEEG) as well as brain SPECT with 99mTc-HMPAO and a brain-dedicated high-resolution camera (CERASPECT, Digital Scintigraphics, Waltham, MA). Their mean score at the Mini-Mental Status Examination (MMSE) was 16.4 ± 11.3. Among the neuropsychological tests, Verbal Fluency was chosen for correlative purposes (mean score 13.1 ± 10.6). qEEG Mean Frequency was computed between 2 Hz and 13 Hz in the F1, F2, F3, F4, and O1 channels (faster activities were excluded because 8 patients received neuroactive drugs). SPECT regions of interest were drawn on the frontal, fronto-basal and left occipital cortex in a normal elderly subject and then automatically transferred to patients. rCBF values were expressed as ratios to the cerebellum. Correlation was searched for between cortical rCBF and the nearest EEG values: F2-4 for frontal rCBF, F1-F2 for fronto-basal rCBF, and O1 for occipital rCBF.
Results: A significant positive correlation was found between rCBF and qEEG Mean Frequency in the right frontal region ($r = 0.57$; $p<0.05$), whereas a correlative trend, though statistically non significant, was observed in the left ($r = 0.45$) and in the right ($r = 0.33$) fronto-basal regions. The Verbal Fluency score was related to left frontal rCBF ($r = 0.59$; $p<0.05$) but not to left frontal qEEG Mean Frequency.
Conclusion: These results confirm the role of rCBF assessment in frontotemporal dementia, and also show that there is indeed some relationship between qEEG and rCBF changes in the frontal lobes of patients with frontotemporal dementia of varying severity. However, such changes do not appear to occur simultaneously during the course of the disease; the overall findings justify the design of a follow-up study aimed at elucidating the mechanism(s) underlying this chronological discrepancy.

OS_398

IMPACT OF COMBINED BRAIN PERFUSION AND CEREBROSPINAL FLUID SPECT ON MANAGEMENT OF PATIENTS WITH DEMENTIA DUE TO NORMAL-PRESSURE HYDROCEPHALUS

K. Borbély, M. Kordás, S. Czirják, I. Nyáry. National Institute of Neurosurgery, Budapest, Hungary.

Once a diagnosis of dementia is established, the irreversible and degenerative types of dementia should be differentiated from those which are potentially treatable causes. Normal-pressure hydrocephalus (NPH) is a reversible and poorly understood cause of mental impairment that is characterized by a triad of gait disturbance, urinary incontinence, and cognitive decline. CT and MRI can display the exact size and shape of the ventricules, however are unable to predict response to shunting as well as MRI cerebrospinal fluid (CSF) flow studies.
Purpose: To determine the impact of combined Tc-99m-HMPAO/ECD brain perfusion SPECT and Tc-99m-DTPA CSF SPECT in the preoperative evaluation of patients with hydrocephalus.
Methods: 137 consecutive studies were carried out where patient management was of concern with a standard technique for each patient (555 MBq 99mTc-HMPAO/ECD; 250 MBq Tc-99m-DTPA, 1/3/6/24 h planar, 6/24h SPECT; double head ADAC SPECT camera). Brain perfusion SPECT studies were analysed visually and by a special region of interests (ROIs) program. Circular ROIs were placed over the striatum, thalamus, white matter, frontal, temporal, parietal, occipital cortex, and cerebellum. Regional brain perfusion was normalized to the whole brain average. The statistical analysis was considered significant at $P \leq 0.05$. The results of combined rCBF and CSF SPECT were correlated with CT, MRI, and clinical findings.
Results: In 106 cases the hydrocephalus appeared to be communicating by CSF SPECT, whereas in 31 cases it was noncommunicating. In 24 cases there was a contradiction between the findings (communicating versus non-communicating) of the CT/MRI and CSF SPECT. The results of brain perfusion SPECT correlated well with clinical data. 79 ventriculoperitoneal shunt implantations were carried out on the basis of combined rCBF and CSF SPECT studies. Brain perfusion SPECT studies in 79 patients (57.7%) except for hydrocephalus, demonstrated periventricular hypoperfusion ($P>0.00005$) with additional bilateral hypoperfusion in the thalamus ($P>0.01$), frontal lobe ($P>0.03$), (in 28 cases in the frontal & temporal regions ($P>0.02$). 58 patients (42.3%) were not operated upon due to the compensated CSF hydrodynamics and/or no sign of perfusion deficits except for hydrocephalus or had perfusion patterns demonstrating other types of dementia, including vascular dementia). Subsequent two year patient follow-up demonstrated a positive correlation between perfusion patterns and clinical findings.
Conclusions: RCBF SPECT functional data are highly useful for selection of candidates with dementia due to NPH for shunt implantation and timing of surgery. Combined brain perfusion SPECT and CSF SPECT studies are helpful in the management of patients with hydrocephalus.

DIAGNOSTIC ONCOLOGY

OS_399

CAN THE DIFFERENCE OF THE LEVELS OF GLUCOSE-6-PHOSPHATASE EXPLAIN THE MECHANISM OF FDG-PET DUAL TIME POINT IMAGING?

F. Ponzo, H.M. Zhuang, F.M. Liu, M. Pourdehnad, N.V. Ghesani, A. Alavi. Hospital of the University of Pennsylvania, USA.

Based on recent data, dual time point imaging increases the accuracy of FDG-PET in patients with suspected malignancy due to the fact that FDG uptake by most benign lesions peaks much earlier than most malignant lesions. However, there is no clear-cut theory to explain why dual time FDG-PET can distinguish malignant from benign lesions. The **aim** of our study is to determine whether the levels of glucose-6-phosphotase (G6Pase) in different tissues can contribute to distinct time-curve of FDG uptake by those tissues. **Methods:** 43 patients with confirmed malignancy who underwent FDG-PET dual time point imaging and also showed cardiac uptake on the images were retrospectively analyzed. The maximum SUV values at 2 time points from the following anatomic sites was measured: tumor; septum of heart; skeletal muscle and bone marrow. These tissues were chosen because it is known that both cancerous and cardiac tissues have very low levels of G6Pase in contrast to skeletal muscle and bone marrow, which have high level G6Pase. **Results**: The average change of the SUV in different tissues at the second time point compared to the first time point are as follow: skeletal muscle: -2.7%; bone marrow: +1.4%; cancer: +18.9%; heart: +13.8%. There is no statistical difference of the changes of SUV between the first and second time point for muscle and bone marrow ($p>0.05$). In contrast, there is significant difference of the SUV change for both tumor and heart ($p<0.01$). **Discussion**: FDG is trapped inside cells via 6-phosphorylation. High levels of G6Pase would reduce the intracellular levels of FDG-6-phosphate time by dephosphorylation and enabling transport out of cells over time. In contrast, low levels of G6Pase would allow continuous intracellular FDG accumulation over time since there is little dephosphorylation. G6Pase is present in high levels in most normal organs (except heart) but is low in most cancer cells. Our data demonstrate that organs having lower levels of G6Pase (tumor and heart) reveal increasing SUV over time in dual time imaging while organs with normal level of G6Pase (skeletal muscle and bone marrow) did not. **Conclusion**: The differences in the levels of G6Pase between malignant and normal tissues can, at least partially, explain why dual-time point imaging is useful in differentiating malignant from benign lesions.

OS_400

18F-FDG PET INFLUENCE ON DECISION MAKING IN PATIENTS WITH LUNG NODULES

G. Pepe (1), C. Rossetti (2), E.G. Vanoli (2), C. Landoni (4), L. Gianolli (2), L. Galli (2), U. Pastorino (3), P. Zannini (2), L. Mezzetti (1), F. Fazio (4). (1) University Of Milan, Milan, Italy; (2) Scientific Institute H.San Raffaele, Milan, Italy; (3) European Institute of Oncology, Milan, Italy; (4) INB-CNR; University of Milan-bicocca, Milan, Italy

AIM OF THE STUDY: evaluation of PET influence in managing patients with lung nodules.
MATERIALS AND METHODS: Three recruitment centres representing the major referring local thoracic surgery institutions were involved in the study. The clinical data (including laboratory and conventional instrumental findings) of 45 consecutive patients (35 males, 10 females, mean age 63.5 years) referred for PET evaluation of lung nodules before surgery were analysed. Patients with history of previous malignancy were not enrolled. Patient population was subdivided into three groups according to their clinical history: GROUP 1) Patients under evaluation for possible primary carcinoma (n=9). GROUP 2) Patients with diagnosis of cancer to be evaluated for staging purposes (n=24). GROUP 3) Patients during follow-up after adjuvant therapy (n=12). For each patient a detailed case report was prepared in an anonymous format. The clinical reports were divided on the recruitment centre basis. In particular, three experienced thoracic surgeons, one for each recruitment centre, evaluated their own patient group. Every case report was blindly submitted to the evaluation in two different steps: firstly, without knowing the results of the PET study, the surgeons filled up a questionnaire indicating their management of choice. Subsequently, the same clinical histories were analysed together with the relative PET report using the same questionnaire. Patient management choices with and without knowledge of the PET study were then compared.
RESULTS: Out of 45 patient studies, management choice changed in 21 cases (47%) when the results of the 18F-FDG PET study were added to the clinical data. In particular, management changed in 6 patients (67%) in Group 1, 11 (46%) in Group 2 and 4 (33%) in Group 3.
CONCLUSIONS: In our population, 18F-FDG PET modified the clinical management in 47% of patients with lung nodules. In particular, PET appears to change the therapeutic approach both in the early diagnostic (67%), as well as in staging process (46%).

OS_401

STAGING AND THERAPY FOLLOW-UP WITH FDG-PET IN SMALL-CELL LUNG CANCER (SCLC)

T. Schumacher, A. Joe, I. Brink, M. Mix, E. Moser, E. Nitzsche. Department of Nuclear Medicine, Albert Ludwigs-Universität, Freiburg, Germany.

Aim: The staging procedures for small cell lung cancer do not differ appreciably from those for other forms of lung cancer. For practical purposes the TNM stages are usually collapsed into a simple binary classification - limited disease and extensive disease. This study was performed to answer the question, whether FDG-PET imaging permits proper work-up of patients presenting with small cell lung cancer for both, primary and follow-up staging compared to currently recommended staging procedure.
Methods: 36 FDG-PET examinations were performed in 30 patients with histologically proven small-cell lung cancer. 24 patients were examined for primary staging while four were imaged for therapy follow-up only. Two patients received both, primary staging, and up to four examinations for therapy follow up. Static PET imaging was performed according to a standard protocol. Image reconstruction was based on a ordered subset expectation maximization algorithm including post-injection segmented attenuation correction. Results of FDG-PET imaging were compared to those of the sum of other staging procedures.
Results: Identical results from FDG-PET and the sum of other staging procedures were obtained in 23 of 36 examinations (6 x limited disease, 12 x extensive disease, 5 x no evidence of disease). In contrast to the results of conventional staging, FDG-PET imaging indicated extensive disease resulting in an up-staging in seven patients. One patient without evidence for tumour in conventional investigations following treatment was suggestive for residual viability of the primary tumour in FDG-PET. Furthermore, discordant results, however not affecting staging into limited or extensive disease, were observed in five patients with respect to lung, bone, liver and adrenal gland findings. Moreover, FDG-PET imaging appeared to be more sensitive for detection of metastatic mediastinal and hilar lymph nodes and bone metastases. Finally, all findings considered suspicious for tumour involvement by the other staging procedures were without exception also detected by FDG-PET.
Conclusion: It is concluded, that FDG-PET offers the potential of a simplified staging tool for small cell lung cancer.

OS_402

COMPARISON OF LUNG LESION VOLUME BY PET AND CT

C. Schiepers (1), D. Yue (1), M. Dahlbom (1), M. Brown (2), M. McNitt-Gray (2), M.E. Phelps (1), J. Czernin (1). (1) Ahmanson Biological Imaging Center; (2) Radiological Sciences, UCLA School of Medicine, Los Angeles, California, USA.

Aim: The role of metabolic imaging in oncology is well established. Lesion size and volume are important parameters for clinicians, and help determine therapeutic options for the patient. Helical CT is very accurate for measuring lesion size in 3D. We compared size and volume of lung lesions determined with FDG-PET to those derived from CT.
Methods: Twelve patients were studied, 8 with primary and 4 with metastatic lung cancers. There were 8 females and 4 males with an age range 47-69 yr. Seventeen isolated lung lesions were available for analysis. PET and CT were performed within 1 month. PET studies were standard attenuation corrected whole body scans, and CT scans had a collimation and reconstruction interval of 5 - 10 mm and a pitch of 1 - 2. CT volume was determined with a 50% threshold between tumor and lung parenchyma density, and counting all voxels included. Intensity weighting of voxels was used as a refinement for partial-voluming artifacts. For PET, two methods were used. *Clinical*: by counting the number of transverse, coronal and sagittal planes in which the lesion was visible, and converting this to the diameter of the lesion in 3 dimensions. *Threshold*: by using the isocontour at 50% of the SUVmax of the tumor, and determining maximum lesion diameter in all 3 dimensions. An ellipsoid model was used to calculate tumor volume from the 3D diameters.
Results: Measured volumes ranged from 1-90 ml on CT, and 2-125 ml on PET. Generally, PET overestimated lesion size and volume, especially the clinical method of counting planes. The PET thresholding method furnished a slope closer to unity with a higher correlation coefficient r (see Table).

CT voxels	PET method	Intercept	Slope	r
All	Clinical	10.9	1.32	0.79
Weighted	Clinical	11.1	1.80	0.80
All	Threshold	2.5	0.99	0.92
Weighted	Threshold	2.9	1.34	0.91

Conclusions: Lesion size can be determined with attenuation corrected, whole body PET scans. Volumes are generally over-estimated by PET, but correlate linearly to CT. These findings are important for clinical applications such as therapy monitoring during chemo and/or radiation therapy.

OS_403

FDG PET WITH DUAL-HEAD GAMMA-CAMERA (GPET) VERSUS DEDICATED PET (DPET) IN PATIENTS WITH SUSPECTED LUNG CANCER

P. Oturai (1), J. Mortensen (2), H. Enevoldsen (3), A. Eigtved (2), H. Hansen (4), K. Olesen (4), P. Clementsen (3), B. Jensen (3), V. Backer (3), L. Friberg (1). (1) Department of Clinical Physiology and Nuclear Medicine, Bispebjerg Hospital, Copenhagen, Denmark; (2) Department of Clinical Physiology and Nuclear Medicine, Rigshospitalet, Copenhagen, Denmark; (3) Department of Internal Medicine, Bispebjerg Hospital, Copenhagen, Denmark; (4) Department of Radiology, Bispebjerg Hospital, Copenhagen, Denmark

Aim: To evaluate the clinical usefulness of gPET with F18-FDG compared with dPET in diagnosis and staging of patients with suspected malignant lung tumours.
Methods: 46 patients, mean age 61±11 years and 70% males, having chest X-rays showing suspected malignant lung tumours, were included in the study. Only patients with FEV_1>2 were included. Whole body scans were performed twice on the same day, 60 and 180 min after administration of 400 MBq F18-FDG, with dPET (GE, Advance) and gPET (Marconi, Axis, _inch thick crystals). Non-corrected and attenuation-corrected images were visually analysed without knowledge of other imaging and clinical data with the exception of the chest X-ray. The patients were scored according to the TNM lung cancer classification system (Tumour/lymph Nodes/Metastases; stage 0-IV).
Results: No malignancy (T0N0M0, stage 0) was found in 11 patients by gPET. However, dPET showed signs of malignancy in 3 of these patients. Using gPET, a median TNM-stage of IIa was observed among all patients, whereas dPET found a generally slightly more advanced disease stage, IIb. Full agreement between the two PET techniques was seen in 28 patients (61%). The Cohen's kappa coefficient (κ) was 0.51, suggesting moderate agreement between the two methods regarding precise staging. Clinical significance was assessed by grouping the patients into 3 groups: no signs of malignancy (stage 0), malignancy and operation possible (stage Ia-IIIa) and malignancy and operation not possible (stage IIIb-IV). Full agreement was present in 39 patients (85%); κ=0.76, substantial agreement. Consequently, discordant staging was observed in 7 patients. In 3 patients no signs of malignant tumours were seen by gPET, whereas dPET found small (T1) solitary pulmonary tumours suggesting malignancy. Two patients had signs of metastases with dPET, while no metastases were seen by gPET. One patient demonstrated substantially more advanced local tumour invasion and lymph node involvement by dPET compared with gPET. In contrast, gPET suggested lymph node involvement and metastases in one patient who only showed a solitary lung tumour by dPET. As no histological or surgical data were available at the time of the present evaluation no calculations of true/false positive/negative findings were made.
Conclusions: A substantial level of agreement (κ=0.76) between dPET and gPET regarding clinical significance of diagnosis and staging of patients with suspected malignant lung tumours was observed. This suggests gPET to be a useful tool in the diagnosis and treatment of patients with suspected lung cancer.

OS_404

CLINICAL IMPACT OF FDG PET IMAGING IN ONCOLOGY PATIENTS BY GAMMA CAMERA COINCIDENCE (GPET) IN COMPARISON WITH A DEDICATED (DPET) SYSTEM

R. Nuñez, C.O. Wong, S. Raman, S. Dees, D. Kondas, D. Fink-Bennett, H.R. Balon, H.J. Dworkin. Department of Nuclear Medicine. William Beaumont Hospital. Royal Oak. Michigan. USA.

Objectives. To asses the differences in patient management in oncology patients, that results from the clinical information obtained by FDG PET imaging with DPET in comparison with GPET.
Methods: FDG PET images obtained by GPET in 27 patients (pts) with histologically proven cancer (18 pts) and in 9 pts with a single pulmonary nodule of equal or more than 1 cm. in diameter, were read blindly by two nuclear medicine physicians before the DPET images. After fasting for at least 4 hours, all pts. underwent initially DPET, 60 minutes after the intravenous injection of 370-555 MBq of FDG follow by GPET. The GPET images were acquired on the average 3 hours after DPET imaging, with a residual dose calculated to be around 111-185 MBq. Differences in pt. management were assessed on the basis of the change in clinical staging or number of lesions detected by DPET in comparison with GPET.
Results: GPET detected 38(59%) of a total of 65 lesions picked up by DPET. There was congruent (detection of the same number of lesions) interpretation of GPET in comparison with DPET in 15/27(56%) pts. In 5 of the 12 non-congruent cases there was a change in clinical management ($p<0.001$). In 4 of them from a change in the tumor stage, and in 1 pt. from detection of additional unknown tumor sites that prompted a change in the surgical approach. In addition, DPET had in overall a considerable better image quality than GPET, which allowed for better anatomical localization.
Conclusion: 1) Differences in the information obtained by DPET in comparison with GPET, changed the clinical management in 5/27 (19%) pts
2) The superior quality of the DPET images increases the confidence in the accurate anatomic localization of the lesions and the assessment of tumor burden.

OS_405

OPTIMIZING 3D WHOLE BODY ACQUISITION FOR ONCOLOGIC IMAGING ON THE ECAT ACCEL LSO PET SYSTEM

T. Bruckbauer (1), M. Casey (1), P.E. Valk (2), J. Rao (2), B.R. Finley (2), B. Farboud (2). (1) CTI PET Systems, Inc., Knoxville, Tn, USA;
(2) Northern California PET Imaging Center, Sacramento, CA, USA.

Aim. The first commercially available LSO whole body tomograph with a 6 ns coincidence-timing window offers unprecedented count rate performance for 3D whole body acquisitions, while maintaining sensitivity compared to BGO based systems. The goal of this study was to analyze this capability and establish a 3D scanning protocol with decreased patient scanning time and increased patient throughput.
Methods. NEC count rate studies were performed according to the NEMA NU 2 - 2000 draft to analyze the imaging behavior at count rates obtained with the current clinical protocol (injecting 15-18 mCi FDG, waiting for 45 min, and acquiring 2D data for 8 min per bed position). Patient data obtained on the previously installed ECAT EXACT and the LSO scanner were analyzed for true and random events. Thirty patients were scanned with an additional 2D scan following the 3D whole body acquisition to analyze differences in the images. Additional dynamic emission scans were taken at selected bed position to analyze the effect of random smoothing on the reconstructed images. The current whole body protocol was optimized to handle multiple motions simultaneously to reduce overhead using interleaved scanning. Several patient scanning situations were simulated and the patient scanning time requirements were analyzed.
Results. The NEMA count rate tests indicated an 85 % improvement of the NEC counts in 3D mode over the 2D mode previously used on the ECAT EXACT. The scanning protocol was therefore changed from 8 min per bed position to 5 min per bed position. The resulting patient images were of high quality and the 3D/2D comparisons revealed no systematic differences. The effects of smoothed random events on the image quality were assessed. The dynamic data from these scans indicate that 2 min emission scans will be sufficient to produce whole body scans of diagnostic quality.
Conclusion. A 3D whole body protocol using 3 min emission and 2 min transmission data acquisition resulted in high quality patient images. Initial results indicate that 4 min acquisition time per bed position, resulting in 30 min total interleaved acquisition time for 75 cm axial length scanned, will provide high-quality oncologic whole-body images.

OS_406

FRACTAL DIMENSION: A NEW PARAMETER FOR QUANTIFICATION OF DYNAMIC PET STUDIES

A. Dimitrakopoulou-Strauss (1), L.G. Strauss (1), C. Burger (2).
(1) German Cancer Research Center, Heidelberg, Germany;
(2) Dept. of Nuclear Medicine, Univ. of Zurich, Switzerland.

Quantification of dynamic FDG-PET studies is generally a problem. The introduction of the SUV at the end of the 80ιs was a good compromise, since SUV is relatively robust and reproducible at least for the same system and comparable time p.i. Compartimental approaches may be time consuming and require an input function, which is in some cases a problem. Limited data exist about the use of non-compartimental approaches for the quantification of dynamic PET data. We examined the value of the fractal dimension (FD), a parameter based on the chaos theory. FD is a parameter which is associated with tumor heterogeneity.
Methodology: The evaluation includes 108 patients with primary bone lesions (40 histologically proven malignancies and 50 benign lesions), 90 patients with soft tissue lesions (49 histologically proven tumors and 15 benign soft tissue lesions) as well as 31 patients with liver metastases from colorectal cancer. The FDG studies were accomplished as dynamic series for 60 minutes. The evaluation of the FDG kinetics was performed using the the 55-60 min SUV and the fractal dimension, based on the quantitative evaluation of the time-activity data using the box counting method for the pixelwise calculation of FD.
Results: Generally, the mean SUV were higher in malignant bone and soft tissue tumors as compared to benign lesions. While FDG SUV was helpful to differentiate benign and malignant tumors, there was some overlap, which limited the diagnostic accuracy. Based on the discriminant analysis of the bone lesions data, SUV alone revealed a sensitivity of 81.5 %, a specificity of 71.7 % and a diagnostic accuracy of 70.7 %. The fractal dimension was superior and demonstrated a sensitivity of 78.1 %, a specificity of 78.6 % and an accuracy of 73.4 %. A more detailed analysis based on six diagnostic categories (GI-GIII, scar, inflammation,lipoma) in patients with soft tissue lesions demonstrated that FD was superior to SUV for the diagnosis of G II and G III tumors, while no significant difference was found for G I tumors and lipomas. Treated liver metastases demonstrated a lower FD in comparison to normal liver parenchyma.The combination of SUV and FD was superior for the differentiation of treated liver metastases.
Conclusion: The combination of SUV and the evaluation of the FD based on the time activity data is a promising approach for the evaluation of oncological PET studies with FDG.

CARDIOVASCULAR

OS_407

PHARMACOKINETICS AND BIODISTRIBUTION OF 99MTC-PHENTHIOATE-ANNEXIN V IN PATIENTS WITH MYOCARDIAL DISEASE

H.H. Boersma (1), G.J. Kemerink (1), P.W. Thimister (1), L. Hofstra (3), I.H. Liem (1), L.M.L. Stolk (2), M.T. Pakbiers (1), D.M.M. Janssen (1), C.P.M. Reutelingsperger (4), A.J. Beysens (2), G.A.K. Heidendal (1)
(1) Department of Nuclear Medicine; (2) Department of Clinical Pharmacy and Toxicology; (3) Department of Cardiology;
(4) Department of Biochemistry, Maastricht University, The Netherlands

Aim: 99mTc-Annexin V(99mTc-AnxV) has been used successfully to detect early stages of apoptosis in animals, as well as in humans with acute myocardial infarction. To validate our imaging protocols, we conducted a study on pharmacokinetics and biodistribution of 99mTc-phenthioate-AnxV (99mTc-p-AnxV, Apomate) in patients with myocardial disease.
Methods: 99mTc-p-AnxV (800 μg, 562 ± 118 MBq) was administered i.v. to 12 patients with myocardial disease. Both 99mTc-radioactivity (n=10 patients) and the plasma concentration of Tc-p-AnxV antigen were measured (n=12) until 4 h after administration. Urine samples were collected (n=5). Stability of the 99mTc-ligand to Annexin V was assessed *in vivo*. Pharmacokinetic parameters were calculated by non-linear regression analysis using a weighted least-square simplex algorithm (MW/ Pharm 3.30). A dual head gammacamera was used to obtain biodistribution data (n=5). At about 1 h, 4 h and 20 h p.i. whole body scans were performed. Organ uptake was estimated after correction for background, attenuation and scatter.
Results: Pharmacokinetics of Tc-p-AnxV could be described using a two compartment model. 81.1 ± 14.2 % of the Tc-p-AnxV-radioactivity disappeared from plasma during the α-phase of the curve. Further pharmacokinetic parameters are shown in Table 1. In urine, 56.9 ± 11.4 % (n=5) of the radioactivity was excreted 0-20 h after administration. Binding of 99mTc to Annexin V was stable in plasma of patients up to 20 h after i.v. injection. Radioactivity strongly accumulated in kidneys and liver (at 70 min p.i. 28±10 % and 18±4%, respectively). Uptake in the target tissue was negligible from a dosimetric point of view. The biological half-life of the activity in the total body was 17±8 h (n=5).
Conclusions: Pharmacokinetics of the AnxV-protein in the second compartment is complicated to determine.99mTc-p-AnxV has a high uptake in the kidneys and liver, in fact a factor of 1.3-1.6 higher than found for the previously studied ^{99m}Tc-(n-1-imino-4-mercaptobutyl)-AnxV. The biological half-life is shorter, however, but still long compared to the physical half-life of 99mTc. The observed biodistribution and the radioactivity pharmacokinetics indicate that 99mTc-p-AnxV is suitable to perform imaging in the thorax region, but not in the abdomen.

Table 1: Pharmacokinetic parameters of 99mTc radioactivity and Tc-p-Ann V concentrations. Data are presented as mean ± standard deviation.

Parameter type of measurement	*t_.α (min)*	*t_§ (h)*	*V.α (L)*	*CL (L/h)*
99mTc-radioactivity, plasma	19 ± 12	3.6 ± 2.4	3.6 ± 1.8	2.8 ± 1.2
99mTc- radioactivity, blood	21 ± 9	Incalculable	5.6 ± 2.1	3.6 ± 2.7
Annexin V-antigen, plasma	20 ± 14	Incalculable	5.6 ± 4.4	4.4 ± 4.0

OS_408

ALTERED SYMPATHETIC INNERVATION IN HYPERTROPHIC CARDIOMYOPATHY

P. Sipola (1), E. Vanninen (2), H.J. Aronen (3), J. Kuusisto (4), K. Lauerma (3), P. Jääskeläinen (4), K. Peuhkurinen (4), M. Laakso (4), J.T. Kuikka (2). (1) Department of Radiology, Kuopio University Hospital, Kuopio, Finland; (2) Department of Clinical Physiology and Nuclear Medicine, Kuopio University Hospital, Kuopio, Finland; (3) Department of Radiology, Helsinki University Central Hospital, Helsinki, Finland; (4) Department of Medicine, Kuopio University Hospital, Kuopio, Finland

AIM: Risk of malignant arrhythmias is correlated to extent of left ventricular (LV) hypertrophy in patients with hypertrophic cardiomyopathy (HCM). On the other hand, abnormalities in myocardial sympathetic innervation are also associated to many arrhythmogenic heart diseases. To evaluate the association between myocardial hypertrophy and global and regional myocardial sympathetic function in patients with genetically determined HCM.
Methods: Planar and SPET I-123 metaiodobenzylguanide (MIBG) imaging were performed 15 min and 4 h after tracer injection in 21 patients with HCM caused by the substitution Asp175Asn of the alphatropomyosin gene (10 men/14 women, 44±11 years (mean±SD)) and in nine controls (4/5, 46±6 years). Heart-to-mediastinum (H/M) ratio, and myocardial washout of tracer were calculated. Both global and segmental analyses were performed. In patients with HCM wall thickness was assessed at 3 free wall and at 2 septal segments at short axis orientation at the mid ventricular level, and body surface adjusted LV mass were evaluated with 3D cine magnetic resonance imaging.
Results: At 4h, global H/M ratio was lower (1.57±0.16 vs 1.77±0.20;P=.008) and washout faster (47±1% vs 40±1%;P=.012) in HCM patients compared to controls. Washout correlated with body surface adjusted LV mass (r=.42;P=.056). At 4h, segmental H/M ratio was lower (0.45±0.12 vs 0.56±0.11;P=.001) and washout faster (51±12% vs 42±12%;P=.002) in segments ≥ 15 mm thick than in segments < 15 mm. Segmental H/M ratio at 4h (r=-.27;P=.005) and washout (r=.21;P=.028) correlated with segmental wall thickness.
Conclusion: Increased I-123 MIBG washout was observed in hypertrophied myocardium in patients with HCM caused by the substitution Asp175Asn of the alphatropomyosin gene. This may be due to increased sympathetic activity or reflect reduced number of sympathetic nerve terminals in these segments.

OS_409

CARDIAC BETA-ADRENORECEPTORS EVALUATED IN VIVO USING C-11 CGP12388 IN THE ISOLATED RAT HEART.

M. Momose (1), D. Raffel (2), S. Reder (1), P. Watzlowik (1), K. Eich (1), N. Nguyen (1), P. Elsinga (3), W. Vaalburg (3), F. Bengel (1), M. Schwaiger (1). (1) Nuklearmedizinische Klinik der TU Muenchen, Germany; (2) Department of Radiology, University of Michigan, Ann Arbor, USA; (3) PET Center, Groningen University Hospital, The Netherlands.

C-11CGP12388(CGP-12388), a post-synaptic adrenergic receptors ligand, was recently developed as an in-vivo tracer for the evaluation of beta-receptors in the heart. Biodistribution studies of CGP-12388 have shown similar tracer distribution and retention in the heart compared to CGP-12177. While the production of CGP-12177 is laborious and often troublesome, CGP-12388 is easily labeled via a reductive alkylation using C-11 acetone by a reliable remote controlled synthesis. The purpose of the study is to evaluate the kinetics of CGP-12388 using the perfused rat heart model.
Methods: Normal male Sprague-Dawley rats were anesthetized, and hearts were cannulated for retrograde perfusion with Krebs-Henseleit bicarbonate buffer according to Langendorff. Studies were performed at constant coronary flow of 12 ml/min with (n=4) and without(n=6) propranolol, and 6 ml/min without propranolol (10_M) (n=4). After allowing 15 minutes for stabilization, 20-30_Ci of CGP-12388 was injected directly into the heart from the side tubing of the cannula under the constant perfusion. Time-activity curves were monitored for 60 minutes from the injection using BGO-detectors. The total distribution volume (Dvtot) and Koff values were calculated by 3-compartmental model analysis.
Results: The Dvtot and Koff values in each group are listed below. The Dvtot and Koff for the control studies (12 ml/min vs. 6 ml/min) were not significantly different from each other. On the other hand, the propranolol Dvtot was significantly smaller than the corresponding 12 ml/min control studies (*p=0.0007), indicating low nonspecific binding.

	12ml/min	Beta-block	6ml/min
Dvtot(ml/g)	8.6+/-2.5	1.85+/-0.34*	10.3+/-5.7
Koff (/min)	0.19+/-0.04	-	0.18+/-0.05

Conclusions: These results suggest non-flow dependent receptor binding of CGP-12388 in the heart with little nonspecific retention, which indicate that CGP-12388 is a promising PET tracer for the evaluation of cardiac beta-receptors.

OS_410

IMPAIRMENT OF CARDIAC ADRENERGIC KINETIC OF 123-I-MIBG IN RAT MODEL OF HEART FAILURE

D. Agostini (1), P. Mulder (2), F. Dronne (1), Y. Darlas (1), C. Thuillez (2), G. Bouvard (1). (1) Department of Nuclear Medicine, CHU Cote de Nacre, Caen, France; (2) Department of Pharmacology,CHU Charles Nicolle, Rouen, France.

Aim of the study. We examined cardiac adrenergic function using 123-meta-iodobenzylguanidine (MIBG) scintigraphy in rat with heart failure after myocardial infarction (MI).
Methods. MI was produced in 10-week-old male Wistar rats by left coronary artery ligation. After 10 weeks, 27 rats were included (13 MI :441±57 g and 14 SHAM :459±54 g, P=NS). Transthoracic echocardiography studies were performed using an echocardiographic system equipped with a 7-MHz transducer to determine LVEF. Then, they were anesthesized with pentobarbital and received an I-123-MIBG injection by right external jugular vein. A two-sequential acquisition started as follows : 60-min (15s/frame) and 180-min (5-min/frame) using a double-head gamma-camera (Picker Axis), LEHR collimator, peak of 159 keV of 123-I, matrix frame 128x128, zoom 2. ROIs (8 pixels) were drawn over the heart and the tail to plot cardiac activity kinetics over the 4-hours of imaging. The raw curves of MIBG were fitted to a mono-compartment model. The activity within the ROIs were decay corrected and expressed as a (% uptake x [(body weight (g)/ heart weight(g)] and called standardized uptake value (%SUV).
Results. In rats with MI, LVEF by echocardiography was decreased 10 weeks after ligation of LAD (23±1% vs 47± 3%, P=0.001).The rats were sacrified and heart weighted (MI :1.78 ± 0.37 g vs SHAM :1.14 ± 0.11 g, P=0.0006). Compared with SHAM animals, MI with heart failure induced significant increases in heart weight, heart weight/body weight ratio (0.88 ± 0.07 vs 0.18 ± 0.14, P=0.001). The infarcted zone of LV measured by cardiac histomorphometry was moderate 28±6%. The %SUV was significantly decreased in MI from 10 min to 4 hrs. (*p<0.05).

Conclusion. Moderate myocardial infarction induces severe impairment of cardiac sympathetic innervation assessed by neuronal uptake kinetic of MIBG in rats model of heart failure with myocardial infarction.

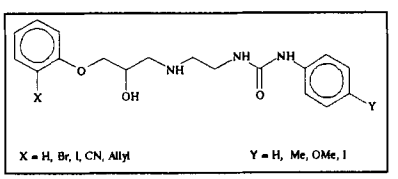

OS_411

REVISITING BETA-1-ADRENOCEPTOR ANTAGONISTS

B. Riemann (1), C. Puke (1), U. Kirchhefer (2), K. Schäfers (1), V. Pike (3), M. Schäfers (1), W. Schmitz (2), O. Schober (1). (1) Department of Nuclear Medicine, Münster University, Münster, Germany; (2) Institute of Pharmacology and Toxicology, Münster University, Münster, Germany; (3) MRC Cyclotron Unit, Hammersmith Hospital, London, United Kingdom.

Aim: Chronic human heart failure is characterized by a selective reduction in β_1-adrenoceptors (β_1-ARs) without change in β_2-AR density. To date, neither a single-photon emission tomography (SPECT) nor a PET radioligand is available for the selective imaging of cardiac β_1-ARs. It was the aim to synthetize a [^{123}I]iodine labelled derivative of the highly β_1-selective AR antagonist ICI 89.406 which may be suitable for SPECT imaging of cardiac β_1-ARs. Methods: Using in vitro competition studies with mouse ventricular membrane preparations (n = 4-6), the affinities and selectivities of ICI 89.406 and 12 of its newly synthesized derivatives (Fig.) were determined indirectly. To this end, their high- and low-affinity inhibition constants K_{I1} (for β_1-AR) and K_{I2} (for β_2-AR) were calculated.

Results: Three of the newly synthesized derivatives of ICI 89.406 were 2-7 fold more β_1-selective than the parent compound (Table). We are currently radiolabelling I-ICI-H.

	K_{I1} [M]	K_{I2}[M]	β_1-Selectivity
I-ICI-I	4.3e-11	3.4e-8	802.9
Br-ICI-Br	1.9e-10	7.4e-8	385.1
I-ICI-H	4.5e-11	1.2e-8	265.1
ICI 89.406	1.3e-9	1.6e-7	122.9

Conclusion: We conclude that the radioactive forms ([^{123}I] or [^{125}I]) of the modified compound may be a promising new tool for pharmacokinetic studies and the selective labelling of β_1-AR subtypes in patients using SPECT, respectively.
(Supported by the IZKF Münster) www.ega.it/eanm2001

OS_412

COMPARISON OF GD-DTPA

M. Gutberlet (1), H. Amthauer (1), H. Hausmann (2), H. Siniawski (2), M. Fröhlich (1), S. Mehl (1), J. Ruf (1), R. Hetzer (2), R. Felix (1). (1) Department of Radiology,Charité Campus Virchow-Klinikum, Berlin, Germany; (2) Department of Cardiac Surgery, German Heart Institute, Berlin, Germany.

Aim: A close correlation seems to exist between the ălate enhancement„ (LE) of myocardium after the administration of Gd-DTPA in MRI and non-viable scar tissue (1, 2). It was the aim of this pilot study to evaluate, whether this LE correlates with the assessment of viability in myocardial scintigraphy.
Methods: We examined 12 patients (69 +/- 10 years, ejection fraction 33 +/- 10%) before CABG surgery and 8 of them additionally after the operation using a 1.5 T MRI scanner (ACS-NT Gyroscan, Best, Netherlands) and a fast inversion recovery sequence in breath hold (TR=7.7 ms, TE=4.5 ms, flip-angle 25¡, section-thickness=8 mm, matrix=256x256). The sequence was used before and 20-30 minutes after the intravenous administration of 0.05 mmol/kg/ body weight Gd-DTPA. The images were obtained in three short-axis slices (distal [apical], middle and basal), a four-chamber and a two-chamber view to represent the entire left ventricle. Wall motion abnormalities and stress-perfusion were assessed by CINE-MRI and gated ^{99m}Tc-MIBI-SPECT in the same orientations using dobutamine for stress testing. Viability of the myocardium was finally assessed by gated rest ^{201}Tl-SPECT. For the qualitative assessment of viability a 12-segment model of the left ventricle was used. The myocardium was differentiated in scar tissue (trans- or intramural) and viable myocardium. A segment with a nonreversible perfusion defect in gated SPECT and a late enhancement in MRI was defined as non-viable myocardium. In all patients with pre- and postoperative examinations complete revascularization had been performed.
Results: Image quality was sufficent in all patients for qualitative assessment. The mean value of ejection fraction in the patients examined after CABG surgery (n=8, 3-6 months) was 39% (+/- 9). 30/ 144 segments were defined as non-viable (6/30 intramural) by gated SPECT. 24/ 144 segments (21/24 intramural) were assessed as non-viable by MRI-LE. All patients, who were examined before and after CABG surgery, showed their late enhancement at the same segments at both examinations.
Conclusions: MRI-LE seems to be an easy method to visualize non-viable myocardium. The location of subendocardial defects and therefore the differentiation of intramural or transmural defects as well as a quantification of the size and extend of scar tissue might be possible. This is important in chronic coronary artery disease to detect myocardial areas which might have a benefit from revascularization and could recover contractile function and which not.
Sandstede et al. AJR 2000; 174(6): 1741-1743
Kim et al. Circulation 1996; 94: 3318-3326

OS_413

99MTC-APROTININ SCINTIGRAPHIC DETECTION OF MYOCARDIAL AMYLOIDOSIS: LONG-TERM FOLLOW-UP OF 78 PATIENTS

C. Aprile (1), G. Merlini (2), R. Saponaro (1), G. Palladini (2), G. Cannizzaro (1). (1) Nuclear Med. Fond.S.Maugeri, Cl.Lav&Riab, IRCCS-Pavia; (2) Biotech. Res.Lab.-University Hosp. S.Matteo, IRCCS-Pavia, Italy.

Aim of this work was to evaluate the figure of merit of cardiac scintigraphy with 99m Tc-Aprotinin (TcA) to detect myocardial amyloid involvement in comparison with common diagnostic modalities, the gold standard being the clinical evolution in a long-term follow-up (f.u.)
Methods: The results of 103 TcA studies performed in 78 patients affected by AL amyloidosis, were re-evaluated after a long-term follow-up. On the basis of ECG and US findings, these pts. have been classified into four categories according to pre-test probability to have myocardial involvement: A-no suspicion, B-suspected, C- high probability or clear evidence without signs of congestive heart failure (CHF), D-as in B but accompanied by CHF.
Results: At the end of the observational period 29 pts were still alive, 35 had died, 6 were lost; the total f.u. time was 1563 months (median: 31.3 mo. for alive, 11.9 for deceased pts).
Scan results are reported in the following table (C+/-: signs of cardiac involvement present/absent).

Pre-test score	Scan	Alive	Non card. death, C-	Non card. death C +	C +	Cardiac death,	*lost*
A	-	26	3				*2*
	+	1			[1]	1	
B	-	2	2			2	*1*
	+			1	3	4	*1*
C	-	1	1				
	+			5	4	1	
D	-						
	+			4	3	8	*2*

Congo-Red-staining of myocardial tissue confirmed scan results in 6 pts (5 positive and 1 negative).
In group A, TcA scan correctly identified 1 pt who had developed signs of cardiac involvement in the course of f.u.; only one false positive was observed in group A and two false negative cases in group B, while all other pts were correctly classified allowing risk stratification. Therefore, if we include the two lost pts with evidence of cardiac deposits of group D+, an overall accuracy of .96 was observable (sensitivity and specificity .95 and .97 respectively) with a positive and negative predictive value of .97 and .95 respectively. These values are definitely superior to those obtainable with echo and electrocardiographic findings: overall accuracy of .72 for CSA (cross-sectional-area), .69 for ECG low voltage, .65 for voltage/mass ratio and .62 for granular sparkling.
Conclusions:TcA scan appears to be a useful tool to image myocardial amyloidosis, with an overall accuracy superior to common diagnostic modalities, allowing earlier diagnosis and risk stratification.

This work was supported in part by „Progetto di "Ateneo"-University of Pavia

OS_414

DETECTION OF CORONARY ARTERY STENOSIS INDUCED ISCHEMIA WITH CU-ATSM-PET

M.J. Welch, J.S. Lewis, P. Herrero, T.L. Sharp, J.A. Engelbach, R.J. Gropler. Radiological Sciences, Washington University School of Medicine, Saint Louis, USA.

Cu-ATSM is a hypoxia-avid tracer for the selective identification of hypoxia. We have previously reported our findings into the utility of Cu-ATSM-PET for the rapid non-invasive delineation of myocardial hypoxia using two canine models, namely (1) the induction of myocardial hypoxia by the generation of global hypoxia and (2) induction of acute myocardial ischemia using thrombogenic coils. This current study investigated the detection of coronary artery stenosis induced ischemia with Cu-ATSM-PET. Coronary artery stenosis was induced in mongrel dogs by the insertion of a Teflon stenosis into the LAD coronary artery under fluoroscopic guidance. The first ^{64}Cu-ATSM scan was performed within 1-h of stenosis placement. Immediately after the first scan the animals were titrated with dobutamine over a 30-min period to a final dose of 40 μg/kg/min. At this point ^{64}Cu-ATSM was given again and the second scan commenced. Tracer kinetics were assessed by a simple two-compartmental model. In this model the flow is represented by K1 (mL/min/g). ^{64}Cu-ATSM enters the myocyte at a rate of k_3 (min^{-1}) which under normoxic conditions, washes out of the cell at a rate of k_4 (min^{-1}). The ratio of k_3/k_4 represents the retention of Cu-ATSM. Under resting conditions, tracer activity in the anterior region was diminished consistent with hypoperfused but normoxic myocardium. In contrast, during dobutamine, the anterior myocardium shows increased tracer activity, in spite of diminish perfusion to this region, suggesting the presence of hypoxia. For example in one dog, myocardial blood flow (K1) in the normal regions was higher than that in the apex both at rest (0.54 ± 0.07 vs. 0.26 ± 0.08 mL/g/min) and stress (2.65 ± 0.84 vs. 0.88 ± 0.11 mL/g/min). When the clearance of the tracer (k_3/k_4) was examined, lower retention was noted in the normal region compared to the apex under resting conditions (2.59 ± 1.81 vs. 33.8 ± 13.1 min^{-1}), which becomes markedly different under stress (0.29 ± 0.27 vs. 6.20 ± 4.08 min^{-1}) in spite of diminished perfusion. Cu-ATSM-PET offers a viable alternative to the reported SPECT agents and its economic and rapid production makes this tracer an attractive agent for PET imaging. Consequently we are undertaking a pilot clinical study in our institution, to test the feasibility of Cu-ATSM-PET to detect myocardial hypoxia in patients with newly diagnosed or known coronary artery disease. Supported by DOE grant DE-FG02-87ER60512 and NIH Grant 2-PO1-HL-13851-32.

OS_415

PHASE I DOSE ESCALATION TRIALS WITH HUMANIZED J591 MONOCLONAL ANTIBODY SPECIFIC TO PSMA: PHARMACOKINETICS AND BIODISTRIBUTION STUDIES WITH 111IN-DOTA-HUJ591

J. Goldsmith, S. Vallabhajosula, I. Kuji, L. Kostakoglu, P. Smith-Jones, N.H. Bander. New York Weill Cornell Medical Center, New York, USA.

We have previously shown in pre-clinical studies that radiolabeled monoclonal antibodies (MAb) specific to the extracellular domain of prostate-specific membrane antigen (PSMA) are potentially useful for radioimmunodiagnosis and radioimmunotherapy of prostate cancer (PC). **Aim:** To study the pharmacokinetics, biodistribution and tumor targeting of ^{90}Y-DOTA-huJ591 (Y-J591) using ^{111}In-DOTA-huJ591 (In-J591) as a chemical and biological surrogate. **Methods:** In patients with PC, two different Phase I dose-escalation protocols are being studied. In the first study designed to determine the maximum tolerated dose (MTD) of huJ591 (cold MAb), 4 groups of patients (n=13) received a single injection of huJ591 MAb (25-200 mg/m^2) mixed with 185 MBq of In-J591. In a second study, designed to determine the MTD of Y-J591 (0.185-1.1 GBq/m^2), 2 groups of patients (n=10) received In-J591 (185MBq/20 mg J591). Serial blood samples and total urine was collected for 7 days. Imaging studies were performed at 1 hr and on days 1,2,3 and 6-7. Plasma time-activity was analyzed using mono and bi-exponential curve fitting. **Results:** The rate of clearance of In-J591 was dependent on MAb mass administered. The half-life of beta component was 48±16 hrs at 12 mg/m^2 and 118±32 hrs at 100-200 mg/m^2. The liver uptake was highest (27±1.7% at day 6) at low antibody mass and gradually decreased (10-12%), saturating at 50-100 mg. Total urinary excretion of In-111 activity was 4 -16% over 7 days. 19/23 patients have well documented metastatic lesions (soft tissue and bone) based on CT/MRI or bone scans. In all 19 patients, imaging studies showed tumor targeting of In-J591 regardless of huJ591 MAb mass administered. The radiation dosimetry with In-J591 and Y-J591 is shown below. Rad dose to marrow was estimated based only on blood activity. The estimated radiation dose to the tumor (n=10) with Y-J591 is 20±13 rads/mCi. **Conclusions:** Imaging studies clearly demonstrate specific tumor localization of radiolabeled huJ591 MAb. Radiation dosimetry of Y-J591 is favorable to administer up to 50 mCi/m^2 as a single dose. The hematological toxicity, however, may also depend on the specific uptake of tumor cells in bone marrow.

	In-111-DOTA-huJ591	Y-90-DOTA-huJ591
Organ	Rads/mCi	Rads/mCi
liver	2.85 ± 0.25	20.16 ± 2.10
Kidney	2.05 ± 0.33	19.21 ± 4.14
LLI wall	1.36 ± 0.21	16.01 ± 3.30
Spleen	1.89 ± 0.56	18.04 ± 6.53
Bone Marrow	0.44 ± 0.03	1.71 ± 0.21

OS_416

INDUCTION OF RADIOACTIVE ASTATINE AND IODINE UPTAKE IN CANCER CELL LINES EXPRESSING THE HUMAN SODIUM IODIDE SYMPORTER

T. Petrich, E. Pötter, H.J. Helmecke, G.J. Meyer, W.H. Knapp. Department of Nuklear Medicine, Hanover University Medical School, Hanover, Germany.

Several recent studies have investigated the sodium iodide symporter (NIS) in order to establish a radioiodine (^{131}I) concentrator gene therapy for non-thyroid cancer.
Aim: Here we examined the role of human NIS (hsNIS) for concentrating the α-particle emitting halogen astatine (^{211}At) as potential new radioagent in cancer gene therapy in comparison to radioiodine.
Methods: A mammalian expression vector containing the hsNIS cDNA under control of the CMV-promoter was constructed and used for transfection of human cancer cell lines. Five stable hsNIS-expressing cell lines (3 derived from thyroid carcinomas, 1 colon carcinoma, 1 glioblastoma) were established by antibiotic selection and their properties with respect to radioactive iodine, astatine and technetium uptake were characterized *in vitro*. Tumor imaging and biodistribution studies were carried out in a xenograft nude mice model by scintigraphy. +
Results: In contrast to the respective control cell lines, the hsNIS-expressing cell lines accumulated radioiodide. Steady state radionuclide uptake attained approximately 300-fold (^{123}I), 350-fold (^{99m}Tc-pertechnetate) and 40-fold (^{211}At) basal values. Accumulation of ^{211}At was inhibited by sodium perchlorate like iodide and pertechnetate uptake and displayed dependency on extracellular Na^+-ions as well. Radionuclide efflux was fast with a slightly slower efflux of iodide compared to ^{211}At ($T_{1/2eff}$ = 5 min vs 3 min). *In vivo* uptake in hsNIS-expressing tumors was up to 70 times (^{123}I), 25 times (^{99m}Tc-pertechnetate) and 10 times (^{211}At) higher than in control tumors or normal tissues except stomach (3-5 times) and thyroid gland (5-10 times). 33.9% and 13.6% of administered activity of ^{123}I and ^{211}At, respectively, was found in hsNIS-tumors by ROI analysis. The effective half life *in vivo* was significantly longer than in cell culture (6.4 h for ^{123}I, 5.0 h for ^{211}At), and preliminary dose calculations indicated adequate tumor dosage factors.
Conclusion: The transfection of a hsNIS-expression vector enables tumor cells of different origins to specificly and significantly take-up different iodide analogues *in vitro* and *in vivo*. The data provide first direct evidence that the high-energy α-emitter ^{211}At is efficiently transported by hsNIS with characteristics comparable to radioiodine and that ^{211}At may direct significantly higher doses to tumors than ^{131}I.

OS_417

REDUCTION OF COLLAGEN TYPE II SYNTHESIS IN CHONDROCYTES AFTER INCUBATION WITH THE BETA-EMITTER 90-YTTRIUM IN THREE-DIMENSIONAL CELL CULTURE - IMPLICATIONS FOR RADIATION SYNOVECTOMY

U. Kampen (1), J. Ailland (2), B. Kurz (2), W. Brenner (1), M. Schuenke (2), E. Henze (1). (1) Clinic of Nuclear Medicine, Kiel University, Germany; (2) Institute of Anatomy, Kiel University, Germany.

Aim: Intraarticular injection of _-emitting radionuclides, known as radiation synovectomy, is a frequently applied treatment in patients suffering from inflammatory-rheumatoid arthritis or even osteoarthritis. The colloidal particles are taken up by the synovial lining cells, depositing their high energy electrons and thus leading to cell death in the inflamed synovial layer. Radiation synovectomy results in alleviation of pain, decreasing joint effusion and finally to improved joint mobility. Possible cytopathologic effects on other diarthrodial tissues, e.g. articular cartilage or subchondral bone are yet not studied intensely. Thus, the aim of this study was to search for possible cell damage and impaired metabolism of chondrocytes, grown in a three-dimensional cell culture system, after incubation with the _-emitter 90-Yttrium used for radiation synovectomy in knee joints.
Methods: Primary monolayer and three-dimensional alginate cultures of bovine articular chondrocytes as well as monolayer cultures of bovine synoviocytes were incubated with 0, 0,375, 1 and 3 MBq 90-Y/ml culture medium from day 3 to day 7. Trypan blue / FDA-staining as well as morphology was used for characterization of cell viability, membrane integrity was tested by LDH quantification. Analysis of thiobarbituric acid reactive substances in culture supernatants showed the extent of possible membrane lipid peroxidation. Chondrocyte metabolism was studied by immunohistochemical staining of type II collagen as well as by the degree of incorporation of 3-H Proline. Photometrical detection of nitrite in the supernatants showed the extent of NO production.
Results: Both synoviocyte and chondrocyte monolayer cultures displayed pronounced cell death after incubation with 90-Y, confirmed by a dose dependent increase of LDH activity. In 3d alginate chondrocyte cultures, cell viability was near 100%, there was no rise in LDH and no lipid peroxidation was found even under highest radiation exposure. However, immunohistochemistry and 3-H Proline incorporation displayed a dose-related decrease of collagen type II synthesis. Increasing NO production was seen in both culture supernatants and cell-free medium.
Conclusions: Beta-radiation of 90-Yttrium leads to dose dependent cell death in proliferating cells. In 3d alginate cultures, the degree of chondrocyte proliferation is very low, resembling the situation in vivo and leading to near total cell viability even under highest radiation doses. However, biosynthesis of collagen type II, being the most prominent structural proteine in articular cartilage is decreased in an dose-related manner. A possible role of the radiogenic increase in NO, known to induce apoptosis, needs to be investigated in further studies.

OS_418

SM-153 LABELED MONOCLONAL ANTIBODIES FOR RADIOIMMUNOTHERAPY

D. Fani (1), S.C. Archimandritis (1), S. Xanthopoulos (1), P. Bouziotis (1), S. Potamianos (1), G. Loudos (2), A.D. Varvarigou (1). (1) N.C.S.R. ; (2) Department of Physics, University of Athens, Breece.

The aim of this study is the development of labelled Monoclonal Antibodies with Sm-153 for application in Radioimmunotherapy. The study was initiated on the polyclonal antibody IgG and was applied thereafter on the monoclonal antibody anti-CEA, which selectively localizes in colon cancer.

Methods: For the labeling of the antibodies with Sm-153 we used diethylenetriaminepentaacetic acid (DTPA) as the intermediate chelating agent, which is linked to the antibody via a dicyclic anhydride, in a molar ratio of 1:10 Ab:DTPA. The labeling is performed with the addition of $^{153}SmCl_3$ solution to a solution containing the Ab-DTPA immunoconjugate. The purification and the quality control of the final product are performed with gel filtration (Bio Gel P30). The radiochemical purity is confirmed with a combination of radiochemical techniques (HPLC, ITLC-SG, SDS-PAGE).

Results: A variety of factors which possibly affect the labeling have been studied, so as to find those which lead to a labeled product with high yield and radiochemical purity. The factors which were proven to affect labeling were mainly pH and the concentration of the antibody, both during labeling and during the formation of the immunoconjugate. The labeling is performed at a range of pH 5-7, for 60 min at room temperature. Using different concentrations of antibody (3, 9 and 15 mg/ml) for the formation of Ab-DTPA and different concentrations of immunoconjugate for labeling, it was shown that higher labeling yields were achieved by increasing the concentration of both. The labeling yield reached a maximum of 90%. The labeled antibody ^{153}Sm-antiCEA was biologically evaluated in normal Swiss mice, after intravenous injection in the tail vein. Slow blood clearance was observed, while the liver and muscles showed high uptake. Intravenous injection in nude mice transplanted with colon cancer cells afforded imaging of the experimental tumor on a _-camera.

Conclusions: With the above methodology a high labeling yield is achieved, so the intermediate purification step of the final product can be avoided. This final step has been necessary until now in antibody labeling studies with Sm-153, in order to obtain a high purity product. Visualization of the experimental induced tumors was succesful with intravenous administration of ^{153}Sm-antiCEA in nude mice.

OS_419

RADIOPEPTIDE THERAPY WITH CHOLECYSTOKININ(CCK)–B/GASTRIN RECEPTOR LIGANDS: TOXICITY AND THERAPEUTIC EFFICACY OF AUGER ELECTRON- VERSUS ALPHA- OR BETA-EMITTERS

T.M. Behr (1), M. Behe (1), C. Angerstein (2), W. Becker (2). (1) Dept. of Nuclear Medicine, Philipps-University, Marburg, Germany; (2) Dept. of Nuclear Medicine, Georg-August-University, Göttingen, Germany.

Aim: In our previous work, we have developed CCK-B receptor ligands for therapy of CCK-B receptor expressing tumors (e.g., medullary thyroid cancer [MTC] or small cell lung cancer [SCLC]). The aim of this study was to assess their toxicity and anti-tumor efficacy, labeled with high-LET emitters (e.g., Auger e— or α-) emitters as compared to low-LET β—emitters.

Methods: A minigastrin derivative, which rapidly internalizes after receptor binding, was derivatized with a novel DTPA-based chelator with improved stability for various radiometals, such as β— (^{90}Y, ^{153}Sm), Auger e— (^{111}In, ^{67}Ga, ^{140}Nd) or α-emitters (^{213}Bi/^{213}Po, ^{225}Ac). Biodistribution studies were performed in nude mice bearing MTC xenografts. The maximum tolerated doses (MTDs) of each agent were determined. Groups of mice were injected with the various radiopeptides, whereas controls were left untreated. Myelo-, 2nd organ toxicity and tumor growth were monitored.

Results: In accordance with uptake values of ≥ 30 %ID/g, the kidney was the first dose-limiting organ with all radiolabels. With all β- and α-emitters, renal doses of ≥ 90 Gy led to acute, ≥ 60 Gy to chronic radiation nephropathy. With the Auger e⁻ emitters, renal doses approximately twice these thresholds were tolerated. Whereas no gastrointestinal (GI) toxicity was observed with β-emitters despite their pronounced CCK-B receptor mediated uptake in the gastric mucosa, at their respective MTDs all high-LET (Auger e⁻ and α) emitters led to hemorrhagic gastritis. At equitoxic dosing, all high-LET (i.e., Auger e⁻ and α) emitters were significantly (~2-3-fold; $p<0.01$) more therapeutically effective than the β-labeled conjugates. Permanent cures were exclusively observed with Auger e⁻ and α, not with β—emitters.

Conclusions: These data suggest that high-LET emitters may be therapeutically more effective than β—emitters. Surprisingly, MTDs were very similar between α- and β—, but higher with the Auger-e—emitters, which may be due to their short path length, selectively irradiating the tubulus cells. The more local energy deposition of high-LET radiation in the gastric mucosa may explain why GI toxicity exclusively occurs with high-, but not with low-LET emitters.

OS_420

PRODUCTION OF BISMUTH-212 FOR THERAPEUTIC APPLICATIONS

J.L. Whitlock (1), E.P. Horwitz (2), J.J. Hines (2), M.L. Dietz (3), J. Rotmensch (1), R.C. Reba (2). (1) Department of Obstetrics and Gynecology-Oncology, University of Chicago, Chicago IL, USA; (2) Department of Radiology, University of Chicago, Chicago IL, USA; (3) Department of Chemistry, Argonne National Laboratory, Argonne IL, USA.

Aim: To develop a novel extraction chromatographic system for the production of highly pure bismuth-212 for use as a therapeutic agent in the treatment of microscopic carcinoma.

Methods: The separation of Bi-212 is achieved by periodically eluting Pb-212 sorbed on a lead-selective resin. The Pb-212 is obtained from Ra-224, which is separated from a U-232/Th-228 (t1/2=1.9y.) stock solution using extraction chromatographic resins. This approach provides a simple and effective means of separating and purifying Bi-212. The bismuth-212 is eluted from the lead-selective resin with HCl and the resultant solution is neutralized with NaOH, resulting in BiOCl as the final product.

Results: Clinical applications of Bi-212 require that it be free of chemical and radionuclide impurities that would diminish its therapeutic effectiveness and increase the toxicity to the patient. It is therefore essential that the Bi-212 be separated completely from its parent, Pb-212, and any traces of Ra-224, Th-228, and U-232. Using the above method, one obtains a highly pure, water-soluble Bi-212 product containing less than a few ppm of the parent isotopes. Also, given the relatively short half-life of Bi-212 (t1/2 = 60 min), it is important that any separation scheme employed be simple and rapid. With the above method, the separation of Bi-212 from Ra-224 requires only ~5 minutes when an automated generator system is employed.

Conclusions: A new generator system has been developed that provides a rapid and effective means of obtaining clinically useful quantities of Bi-212 for intraperitoneal therapy of micrometastases (University of Chicago) or for chelation to antibodies for radioimmunotherapy (National Cancer Institute, NeoRx, and University of Missouri).

This work was supported by the Office of Isotopes for Medicine and Science, United States Department of Energy under grant number DE-AC05-00OR22725.

OS_421

A BI-213 COUPLED MONOCLONAL ANTIBODY WITH HIGH SPECIFIC BINDING TO INTRAPERITONEAL CARCINOMATOSIS LOOKS PROMISING FOR LOCOREGIONAL ALPHA-RADIOIMMUNOTHERAPY

R. Huber (1), C. Seidl (1), K.-F. Becker (2), C. Schuhmacher (3), R. Molinet (4), Ch. Apostolidis (4), T. Nikula (4), M. Schwaiger (1), R. Senekowitsch-Schmidtke (1). (1) Nuklearmedizinische Klinik der Technischen Universitaet Muenchen, Muenchen, Germany; (2) Institut fuer Pathologie der Technischen Universitaet Muenchen, Muenchen, Germany; (3) Chirurgische Klinik der Technischen Universitaet Muenchen, Muenchen, Germany; (4) Institut fuer Transurane, Europaeische Kommission, Karlsruhe, Germany

Aim: Radioimmunotherapy (RIT) with tumor-specific α-emitter conjugated antibodies is a promising concept in the treatment of disseminated tumor growth following locoregional application. In diffuse-type gastric cancer characterised by intraperitoneal tumor spread, the cell adhesion molecule E-cadherin is mutated in 50% of all cases investigated so far. Bi-213 antibodies recognising mutated E-cadherin, without any crossreactivity to wild-type E-cadherin therefore look promising for RIT of this type of cancer.

Methods: A peritoneal carcinomatosis model was established by i.p. inoculation of 10^7 tumor cells transfected with the mutated E-cadherin gene in athymic nude mice. The development of carcinomatosis and ascites were observed by weekly MRI. For therapeutic studies and investigation of the overall toxicity, the animals were injected i.p. with 22 MBq Bi-213 immunoconjugate.

Results: 3-4 weeks after tumor cell inoculation, MRI demonstrated the development of disseminated peritoneal tumor spread with ascites in 40% of all cases; this is similar to the clinical situation in human diffuse-type gastric cancer. Biodistribution studies with Bi-213 MAb resulted in an uptake of 62% ID/g in small i.p. tumor nodules, one and three hours after i.p. injection. The selective binding of the radioimmunoconjugate to the i.p. tumor nodules up to 48 h compared to controls could be visualised by scintigraphic imaging after i.p. injection of In-111 MAb. After injection of therapeutic activities, survival rates significantly increased by up to 108 days compared to 30 days for untreated controls. Leucocyte and platelet counts showed a decrease 3 days after Bi-213 MAb injection with a recovery to pretreatment values at day 25 p.i..

Conclusions: The results indicate the promising potential of a tumor specific Bi-213 coupled MAb, for treatment of peritoneal carcinomatosis after locoregional application.

OS_422

HEALTH PHYSICS ASPECTS OF ROUTINE PREPARATION OF 177LU-DOTA-TYR3-OCTREOTATE FOR PEPTIDE RECEPTOR RADIONUCLIDE THERAPY

W.H. Bakker (1), C.J. Eggels-Hofman (2), L.C. de Jong (1), M.E. van der Pluijm (1), G.A. van der Wagt (1), P.J. Kicken (2), E.P. Krenning (1).
(1) Department of Nuclear Medicine; (2) Department of Health Physics, University Hospital, Rotterdam, The Netherlands.

Aim: Application of radioactive somatostatin analogs in patients to demonstrate somatostatin receptor positive tumors, has gained a wide-spread use in Nuclear Medicine. Nowadays, therapeutic applications are developing rapidly. This study presents dosimetric implications for workers preparing a new somatostatin analog for radionuclide therapy, ^{177}Lu-DOTA-Tyr^3-octreotate.

Methods: The preparation is done in a closed laminar air flow isolator according to GMP-guidelines. ^{177}Lu is shipped in a small conical vial, containing 1 mL 0.05 M HCl with up to 37 GBq ^{177}Lu-chloride. Labeling is started 3-4 days after production of ^{177}Lu when the shortlived contaminant ^{176m}Lu is decayed. For each labeling 125 % of the needed therapeutic activity (i.e. maximum 28 GBq) is drawn into a syringe and injected into the labeling vial with peptide solution. The vial is heated 30 min at 80 C. After cooling to room temperature the solution is diluted with saline to 8 mL and filtered through a 0.22 µm Millex-GV-filter into a sterile vacuum vial. After further dilution to 18 mL, quality control (ITLC & HPLC) is performed. Thereafter individual patient doses are transferred into infusion bottles (final infusion volume 80 mL). TLD's were placed on the top and at the place of a ring, on both thumbs, index and middle fingers of the workers. To estimate the effective doses of workers, electronic jobdose meters were worn on the chest.

Results: On eight occasions 10-50 GBq ^{177}Lu was used by four workers. The top of the right middle finger of all (right-handed) workers showed the highest equivalent dose: 53±12 (mean±sd) µSv/administered GBq. Consequently, 400 patient treatments of 7.4 GBq each in one year, prepared by four workers will result in a maximum equivalent finger dose of 39±9 mSv (about 10 % of the annual Dutch dose limit of 500 mSv). Mean equivalent finger top and ring doses are then 23±11 mSv and 14±6 mSv, respectively. Those 400 patient treatments will result in an effective dose for each worker of 0.5-1.5 mSv/year (less than 10 % of the Dutch annual dose limit of 20 mSv).

Conclusions: Extra occupational dose due to labeling procedures on this scale will remain below 10 % of the Dutch dose limits, and will therefore, as such, not be an obstacle for routine preparation of ^{177}Lu-DOTA-Tyr^3-octreotate for application in tumor patients.

Conclusions: The use of the residualizing radiolabels ^{88}Y and ^{177}Lu in combination with a mAb directed against an internalizing antigen results in higher uptake and better retention of the radiolabel in the tumor. However, the uptake in bone of these two radionuclides was also higher, which could lead to higher radiation doses to the bone marrow.

OTHER CLINICAL SCIENCE. PRECLINICAL STUDIES

OS_423

BIODISTRIBUTION OF RADIOLABELED HLL2 IN MICE WITH LYMPHOMA: QUEST FOR THE MOST SUITABLE RADIONUCLIDE

E.J. Postema (1), C. Frielink (1), W.J.G. Oyen (1), J.M.M. Raemaekers (2), F.H.M. Corstens (1), O.C. Boerman (1). (1) Dept. of Nuclear Medicine; (2) Dept. of Hematology, UMC St Radboud, Nijmegen, The Netherlands.

Radioimmunotherapy (RIT) is a promising new treatment modality in patients with non-Hodgkin's lymphoma. One of the monoclonal antibodies (mAbs) used is hLL2, a humanized mAb directed against the CD22 antigen on the malignant B-cells. This mAb can be labeled with various radionuclides. To determine the most suitable radionuclide for RIT with mAb hLL2 the biodistribution of hLL2 labeled with ^{131}I-, ^{186}Re-, ^{177}Lu-, and ^{88}Y was studied in nude mice with subcutaneous human lymphoma xenografts.

Methods: hLL2 was labeled with ^{131}I according to the iodogen method, with ^{186}Re using MAG3 as a chelator, and with ^{88}Y and ^{177}Lu using isothiocyanatobenzyl derivatized DTPA. Human Ramos lymphoma xenografts were induced in cyclophosphamide pretreated athymic BALB/c mice. Mice were injected intravenously with radiolabeled hLL2. To determine the non-specific tumor uptake, one group of mice received ^{88}Y-labeled cG250, a mAb that is non-reactive with Ramos cells. The biodistribution of the radiolabel was determined 1, 3, and 7 days p.i. The radioactivity of samples of blood, muscle, tumor, lung, liver, spleen, kidney, duodenum, and bone was measured. The amount of radioactivity in each sample was expressed as % injected dose per gram (%ID/g).

Results: Radiolabeled hLL2 had a higher tumor uptake than the nonspecific mAb at all time-points, irrespective of the radiolabel used. Tumor uptake of ^{88}Y- and ^{177}Lu-hLL2 increased with time, whereas uptake of ^{131}I- and ^{186}Re-hLL2 decreased with time. Activity in the femur (without bone marrow) on day 7 p.i. was higher for ^{177}Lu- and ^{88}Y-hLL2 than for ^{131}I- and ^{186}Re-hLL2.

	blood level, 7 days p.i. (%ID/g ± SD)	tumor uptake, 1 day p.i. (%ID/g ± SD)	tumor uptake, 3 days p.i. (%ID/g ± SD)	tumor uptake, 7 days p.i. (%ID/g ± SD)	femur uptake, 7 days p.i. (%ID/g ± SD)
^{131}I-hLL2	5.3±0.9	5.3±1.3	4.6±0.8	3.4±1.5	0.18±0.05
^{186}Re-hLL2	6.9±1.3	9.8±4.4	7.5±1.4	4.8±0.1	0.10±0.04
^{177}Lu-hLL2	9.5±0.6	8.3±1.8	10.4±0.6	11.1±0.6	1.29±0.50
^{88}Y-hLL2	5.7±2.3	6.6±1.6	14.1±3.2	8.3±3.2	1.55±0.53
^{88}Y-cG250	11.4±0.8	3.4±0.5	3.3±0.3	2.9±0.2	1.38±0.49

OS_424

POSITION SENSITIVE PHOTOMULTIPLIER TUBE BASED DETECTOR FOR SMALL ANIMAL RADIOPHARMACOLOGICAL STUDIES

G. Loudos (1), D. Maintas (4), K. Nikita (1), N. Uzunoglu (1), N. Giokaris (2), C. Papanikolas (2), A. Varvarigou (3), S. Archimandritis (3), K. Stefanis, S. Majewski, R. Pani(1) National Technical University of Athens, Athens, Greece; (2) Institute of Accelerating Systems and Applications, Athens, Greece; (3) National Center for Scientific Research ; (4) Athens Medical Center, Institute of Isotopic Studies, Athens, Greece

Aim: The aim of this work was to develop a PSPMT based detector for small animal radiopharmacological studies with high resolution and sensitivity. We have previously described the characteristics of the system and the possibilities of both planar and tomographic acquisition.

Methods: The detector is based on a PSPMT and a 4.6cm in diameter CsI pixelized crystal. The intrinsic resolution was measured with a linear source and the collimator removed and the spatial resolution with capillary phantoms. In addition phantoms of 2mm sources with different concentrations were used. All the experiments were performed in both planar and tomographic mode. We have tested the system in tumor bearing nude mice with ^{153}Sm anti CEA MAB and ^{99m}Tc labelled somatostatine analogue. We have also tested the system in rats after the administration of 1 to 2 mCi of ^{99m}Tc MIBI in order to visualize the myocardine of the left ventricle in planar and tomographic mode, by using a Maximum Likelihood Algorithm. The images were compared with those from a conventional clinically used gamma camera.

Results: Phantom studies have shown that 2mm resolution and linearity are maintained in the entire field of view and activity differences can be detected accurately. The image obtained after the injection of ^{153}Sm labelled MAB antibodies was very sensitive to detect small tumors with target to background ratio of the order 4:1, similar to the data acquired by post mortem measurements. In addition after the injection of somatostatic analogue the primary tumor was detected as well as small metastatic tumors, whose existence was confirmed by post mortem measurements. Finally the myocardine scintigraphy after the injection of ^{99m}Tc MIBI showed excellent visualization of the myocardine in planar and tomographic mode. The comparative images with the hospital system showed significantly better depiction with the developed system.

Conclusions: Phantom and small animal experiments showed that the developed system offers a 2mm resolution in both 2D and 3D and high sensitivity. The comparative studies with a commercially available system verified that it can be used for the evaluation of new radiopharmaceuticals in small animals.

OS_425

EVALUATING THE EFFECT OF HALOTHAN AND THE PROTECTIVE EFFECT OF CATECHINE ON LIVER PARENCHYM WITH HEPATOBILIARY SCINTIGRAPHY

M. Yuksel (1), B. Karamanloglu (2), E. Temiz (3), Y.S. Salihoglu (1).
(1) Department of Nuclear Medicine; (2) Department of Anaesthesia and Reanimation; (3) Department of General Surgery, Trakya University, Edirne, Turkey.

Halothan and its metabolites cause liver damage after repeated anesthesia via decreasing liver blood flow and generating free radical species. Catechine suppresses lipid peroxidation and increases enzymatic activity, therefore it seems to be capable of preventing liver parenchym against the direct toxic effect of halothan. We aimed to investigate the role of hepatobiliary scintigraphy(HBSc) in detectiong liver parenchymal damage after halothan anesthesia and the protective effect of catechine.
Methods: Total of 30 rabbits(A:control; B:Halothan C:Catechine+Halothan n=10 each group) were investigated. Rabbits in group B only with halothan and in group C with catechine pretreatment+halothan were anaesthetised 2 hours/day for seven days. Dynamic scintigrams were taken for 60 minutes(1frame/min) after injecting Tc-99m-mebrofenin, and the time of peak uptake(TPU) and the time for half of the activity to clear from the liver($T_{1/2}$) were calculated. Rabbits were sacrificed. Then for electron microscopic examination tissue specimens were taken from liver, and malonilaldehyde(MDA), superoxide dismutase(SOD), glutathione peroxidase(GSH-Px) and catalase levels(CAT) were measured in hepatic tissue.
Results: TPU and $T_{1/2}$ of the controls were significantly lower than groups B and C, $p<0.0002$ and $p<0.0002$ for TPU respectively, and $p<0.0002$ and $p<0.0003$ for $T_{1/2}$ respectively. TPU and $T_{1/2}$ of group B were significantly higher than group C, $p<0.0003$ and $p<0.0003$, respectively. Hepatic MDA level of the controls were significantly lower than group B and C, $p<0.0002$ and $p<0.0002$, respectively. SOD, GSH-Px and CAT levels of the controls were significantly higher than groups B and C, $p<0.0002$, $p<0.0001$ and $p<0.003$ for control vs. B respectively, and $p<0.0005$, $p<0.0002$ and $p<0.03$ for control vs. C, respectively. MDA level of group B was significantly higher than group C, $p<0.0002$. SOD, GSH-Px and CAT levels of group B were significantly lower than group C, $p<0.0002$, $p<0.0002$ and $p<0.003$, respectively. Electronmicroscopic examination showed that rabbits pre-treated with catechine had less tissue damage compared with those rabbits without catechine pre-treatment.

	TPU (min)	$T_{1/2}$ (min)	MDA (nmol/ mgprotein)	SOD (U/mgprotein)	GSH-Px (nmol/mgprotein)	CAT (U/mgprotein)
A	3.7±0.8	13±1.8	0.36±0.05	2.83±0.14	221.6±5.10	284.25±44.10
B	15.1±2.2	38.4±5.2	1.16±0.20	1.93±0.08	145.8±2.25	184.95±51.70
C	9.3±2.1	25.01±6.2	0.69±0.04	2.49±0.13	200.8±2.15	256.23±12.86

Conclusion: According to our results, we suggested that catechine protects liver parenchyma against the toxic effect of halothan and its metabolites and that hepatobiliary scintigraphy is a useful noninvasive method for detecting the protective effect of catechine on liver parenchyma after halothan anesthesia.

OS_426

UPTAKE OF RADIOLABELED MORPHICEPTIN AND ITS ANALOG BY EXPERIMENTAL MOUSE MAMMARY CARCINOMAS

M. Mirowski (1), R. Wiercioch (1), D. Pawlak (3), J. Switalska (3), G. Birnbaum (3), E. Byszewska (3), A. Janecka (2). (1) Department of Biochemistry, Faculty of Pharmacy, Medical University, Lodz, Poland; (2) Department of Chemistry, Medical University, Lodz, Poland; (3) Radioisotope Center POLATOM, Otwock-Swierk, Poland.

Morphiceptin is three-aminoacid peptide with high affinity to the _ opioid receptor. Recently we have synthesized morphiceptin with additional tyrosine (Tyr-Pro-Phe-Pro-NH_2) and its analog with DCl_2Phe modification (Tyr-Pro-DCl_2Phe-Pro-NH_2).
Aim of the present study was to determine biodistribution and binding of labeled morphiceptin and its analog with experimental mouse mammary tumors.
Methods: Iodination of morphiceptin and its analog (^{125}I, ^{131}I) was based on the chloramine T method. Tumors were growth in C3H/Bi mice by injection of cell suspension prepared from spontaneously growing mammary tumors. The binding of labeled compounds with cytosolic proteins and with cell membranes from the tumors was established by the ligand binding experiments and by electrophoresis. Biodisribution study was done in healthy and in tumor-bearing mice.
Results: The histological analysis by eosin and hematoxylin method (E&H) showed that above 90% of investigated tumors could be classified as adenocarcinomas. Electrophoresis of labeled morphiceptin and its analog on cellulose acetate membranes (non-denaturing conditions), after incubation with extract from mammary tumors, showed additional radioactive band. Polyacrylamide gel electrophoresis with sodium dodecyl sulfate (denaturing conditions) of labeled morphiceptin, after incubation with mammary tumor extract with the use of cross-linking reagent, showed also additional radioactive band with molecular weight about 65 kDa. The level of binding of ^{131}I-morphiceptin and its analog with tumor proteins in *in vitro* experiments was similar. However, membranes have about 10 times more binding capacity in comparison to cytosolic proteins. Both labeled compounds in biodistribution studies showed increased accumulation in the tumor with maximum at 30 min since injection. However, morphiceptin analog containing DCl_2Phe in comparison to unmodified compound, showed higher accumulation at this time. The accumulation of ^{131}I- Tyr-Pro-DCl_2Phe-Pro-NH_2 and ^{131}I- Tyr-Pro-Phe-Pro-NH_2 in the tumors (%ID/g) was 5.2 and 3.4 after 0.5hr, 2.7 and 3.3 after 2hr and 1.4 and 1.7 after 4 hr, respectively.
Conclusion: Morphiceptin and its analog have relatively high affinity to the mouse mammary adenocarcinomas.

OS_427

CEREBROSPINAL FLUID CLEARANCE STUDIES IN RABBITS

L. Aloj (1), G. Fatone (2), C. Mainolfi (1), B. Lamagna (2), L. Meomartino (2), A. Potena (2), B. Alfano (1), A. Brunetti (1,2). (1) CNR-Nuclear Medicine, University Federico II, Naples, Italy; (2) Veterinary Radiology and Clinical Vet. Sc. Dept, University Federico II, Naples, Italy.

AIM: Quantitative measurement of CSF dynamics could be helpful in the evaluation of a series of Central Nervous System (CNS) disorders both in animal and in humans. The purpose ofthe present study was to set up a method for quantitative measurement of Cerebro-spinal fluid (CSF) dynamics using a conventional gamma camera based procedure and ^{99m}Tc-DTPA.
METHODS: Studies were performed in 14 normal rabbits (weight range 2-3Kg) after i.m. premedication with acetylpromazine (0.5 mg/Kg) atropine (0.025 mg/Kg) and diazepam (1mg/Kg) followed by administration of ketamine (20 mg/Kg) repeated at 40 min intervals during the study. Dynamic studies with a LFOV camera equipped with a low energy collimator,were performed over a 3 hour period of time (36 frames ;300 sec/frame) following administration of 4-5 MBq (150 microliters) ^{99m}Tc-DTPA in the cisterna magna, in right lateral recumbency. Cross calibration of scintigraphic counts was performed with measurement of activity on a urine specimen collected at the end of the experiment. Data analysis was performed by drawing irregular ROIs over brain, spine, kidneys and bladder. Time activity cuves were generated for all regions . A simplified model based on the assumption of unidirectional transfer of ^{99m}Tc-DTPA from CSF to the urinary system was used for data analysis . A mono-exponential fitting of the spinal clearance curve starting after the first 30 minutes was obtained to estimate a series of parameters including CSF space, rate of absorption and turnover
RESULTS: Clearance curve analysis gave the following results (mean ± standard deviation): estimated CSF space 3.97 ± 1.76 ml; turnover rate 33.4 ± 11.8 % ; CSF production: 13.2 ± 6.6 microliters/min
Visual analysis of the image sequence permitted visualization of both caudal and and rostral diffusion of the tracer, with early appearance of kidney activity and progressively increasing activity in the bladder.
CONCLUSION: CSF has a crucial role for the homeostasis of the CNS; abnormal production and clearance of CSF can be associated with several neurologic disorders. At present no standardized procedure is available for measurement of CSF clearance. The rapid reabsorption and clearance through the kidneys of ^{99m}Tc-DTPA permits to the use of a simplified bicompartimental analysis. Quantitative estimates of CSF production and turnover rate are in good agreement with published results using more invasive techniques such as ventriculo-cisternal perfusion; therefore the procedure could be used both in animals and in humans to assess CSF clearance.

OS_428

TUMOR TARGETING WITH RADIOLABELED ALFAVBETA3 INTEGRIN BINDING RGD PEPTIDES IN A NUDE MOUSE MODEL

O.C. Boerman (1), M. Janssen (1), C. Frielink (1), W. Oyen (1), S. Edwards (2), M. Rajopadhye (2), F. Corstens (1). (1) Nuclear Medicine, University Hospital Nijmegen, Nijmegen, the Netherlands; (2) Dupont Pharmaceuticals, N. Billerica, MA, USA.

Aim: The $\alpha v\beta 3$ integrin is expressed on newly formed endothelial cells and on various tumor cells. We aim to develop $\alpha v\beta 3$ integrin binding RGD peptides for peptide radionuclide targeting of tumors. Here we investigated the tumor targeting properties of a radiolabeled dimeric RGD peptide in a murine tumor model.
Methods: The dimeric peptide $[RGDfK]_2$-E, was derivatized with the macrocyclic chelator DOTA, enabling fast and efficient labeling with ^{111}In or ^{90}Y (15 min, 100 °C). Analogously, the peptide was derivatized with HYNIC, to allow rapid and efficient labeling with ^{99m}Tc. The radiochemical purity of the radiolabeled peptides was checked with ITLC and RP-HPLC. The biodistributon of the ^{111}In and ^{99m}Tc-labeled peptide (10 nmoles) was studied in nude mice with s.c. NIH:OVCAR-3 ovarian tumors (1, 2, 4, 8 and 24 h p.i.) (5 mice/group). To determine the specificity of the localization of the peptide in the tumor, the biodistribution of a peptide with a scrambled aminoacid sequence $[RGfDK]_2$-E was studied in the same mouse model. Furthermore, the biodistribution of the ^{111}In-labeled $[RGfDK]_2$-E peptide was studied at a receptor saturating peptide dose (30 µmoles). The therapeutic potential of _v_3 targeting was determined by monitoring the tumor growth after injection of the peptide labeled with a maximum tolerated dose of ^{90}Y (1 mCi).
Results: Biodistribution experiments showed that the ^{111}In and the ^{99m}Tc-labeled peptide preferentially localized in the tumor: tumor uptake 7.5 %ID/g and 6.0 %ID/g at 2 h p.i., respectively. Tumor-to-blood ratios reached values as high as 96 and 28 (24 h p.i.), respectively. The uptake of the radiolabel in the tumor was largely dependent on the interaction of the peptide with _v_3, as demonstrated by very low tumor uptake of the scrambled peptide (0.2 %ID/g, 2 h p.i.) and at a tumor saturating dose (0.2 %ID/g, 2 h p.i.). Tumor growth of small tumors (<250 mm^3) was significantly delayed after injection of 1.0 mCi ^{90}Y-labeled RGD peptide compared to untreated tumors (57 vs 29 days until tumor volume reached 2000 mm^3).
Conclusions: The dimeric RGD peptide derivatized with HYNIC or DOTA can be readily labeled with ^{99m}Tc or ^{111}In/^{90}Y, respectively. These radiolabeled peptides can localize specifically in tumors, and can potentially be used for peptide receptor radionuclide imaging and/or peptide receptor radionuclide therapy.

OS_429

YAP-(S)PET: A HYBRID PET-SPECT IMAGER FOR SMALL ANIMAL

G. Di Domenico (1), G. Zavattini (1), A. Motta (2), N. Sabba (2), A. Duatti (2), M. Giganti (2), L. Uccelli (2), A. Piffanelli (2), A. Del Guerra (3). (1) Dipartimento di Fisica, Università di Ferrara, Ferrara, Italia; (2) Dipartimento di Medicina Clinica e Sperimentale - Sezione di Medicina Nucleare, Università di Ferrara, Ferrara, Italia; (3) Dipartimento di Fisica, Università di Pisa, Pisa, Italia.

AIM: The need for tomographic scanners dedicated to experimental animal studies has been recognized by several groups and demostrated by the recent development of a number of specialised small animal imaging systems. Both PET and SPECT modalities provide a non-invasive method for performing in-vivo studies on new radiophamaceuticals and to evaluate molecular therapeutic agents.

METHODS: At Ferrara University, we have built the YAP-(S)PET tomograph: a hybrid PET-SPECT imager for performing in-vivo studies on small animals. The scanner is made up of four detecting heads on a rotating gantry. Each head consists of a scintillator matrix (4x4x3 cm^3) composed of 20x20 match-like crystals (2x2x30 mm^3 each), each viewed by a position sensitive photomultiplier (Hamamatsu mod. R2486-06). The gantry aperture is 15 cm, and the field of view in both PET and SPECT is 4 cm diameter by 4 cm axially. The scintillator used is YAP:Ce ($YAlO_3$ perovskite, doped with Cerium), with high density (5.37 g/cm^3) but medium/low Z (effective Z ~ 32). In PET configuration each opposite pair is put in coincidence. In SPECT mode 2 heads are equipped with a high resolution collimator (hole diameter 0.6 mm, septa 0.15 mm, thickness 20 mm). The SPECT modality was added at a later stage to the original PET scanner. Fast reconstruction algorithms have been implemented and they allow the intrinsic high spatial resolution properties of the system to be recovered. The performance of this scanner has been validated with standard phantoms and with experimental studies on rats in both PET and SPECT configuration.

In particular, we have compared the different properties of cardiac perfusion and uptake of three radio-pharmaceuticals, all tagged with ^{99m}Tc. The first one is ^{99m}Tc-SESTAMIBI, the second-one is ^{99m}Tc-NOET, the third one ^{99m}Tc-X whose name and formula are still under proprietor restriction.

RESULTS: The main performance parameters of the scanner for both PET and SPECT mode are shown in table I. In-vivo rat images will be presented in comparison to traditional in-vitro analysis.

Table I - Main performance of the YAP-(S)PET scanner

Mode	PET	SPECT
Energy Resolution (FWHM)	26% at 511 keV	32% at 140 keV with collimator
Spatial Resolution (FWHM)	1.6 mm	3.5 mm
Sensitivity	640 cps/μCi at center	4.2 cps/μCi

CONCLUSIONS: The YAPPET scanner is very versatile and appropriate for small animal PET and SPECT studies thanks to the YAP:Ce scintillator properties and the scanner's geometrical configuration.

OS_430

UPTAKE OF RADIOLABELED HERCEPTIN BY EXPERIMENTAL MOUSE MAMMARY TUMORS

M. Mirowski (1), R. Wiercioch (1), E. Balcerczak (1), J. Switalska (2), G. Birnbaum (2), E. Byszewska (2), D. Pawlak (2), R. Wierzbicki (1). (1) Department of Biochemistry, Faculty of Pharmacy, Medical University, Lodz, Poland; (2) Radioisotope Center POLATOM, Otwock-Swierk, Poland.

Recombinant humanized anti-c-$ErbB_2$ monoclonal antibody (herceptin) is new agent for the treatment of women with tumors that overexpress epidermal growth factor receptor 2 (c-$ErbB_2$). Aim of the present study was to determine biodistribution of ^{131}I-herceptin in experimental mammary carcinoma to predict the radiodiagnostic utility of this antibody.

Methods: Iodination of ^{131}I-herceptin was based on the chloramine T method. Biodistribution study of the radioactive compound was done in healthy and in tumor-bearing mice. Tumors were growth in C3H/Bi mice by injection of cell suspension prepared from spontaneously growing mammary tumors. Amplification of the *c-erbB$_2$* gene in experimental tumors was detected by the polymerase chain reaction technique and its protein product expression by Western blot analysis.

Results: The histological analysis by eosin and hematoxylin (E&H) method showed that above 90% of investigated tumors can be classified as adenocarcinomas. Most of the tumors after Western blot analysis revealed *c-erbB$_2$* oncogene protein products expression. In more than 50% of tumors the amplification of *c-erbB$_2$* gene was detected. Biodistribution study showed increased accumulation of ^{131}I-herceptin in time with the maximum at 48 hours since injection (7% ID/g). At this point tumor/muscle ratio was the highest (about 20). After 96 hours ^{131}I-herceptin accumulation in tumor tissue was 2.5 times higher than in the blood.

Conclusion: ^{131}I-herceptin has high affinity to the mouse mammary adenocarcinomas what might suggest their usefulness in imaging of c-$erbB_2$ expressing tumors in humans.

OS_431

A QUANTITATIVE METHOD FOR SIMULTANEOUS VENTILATION PERFUSION LUNG SPECT

A. Sanchez-Crespo (1), R. Hatherly (1), C. Jonsson (1), P.O. Schnell (1), H. Jacobsson (1), M. Pagani (2), J-O. Thorell (3), J. Pettersson (4), M. Mure (4), S.G.E. Lindahl (4), S.A. Larsson (1)(1) Section of Nuclear Medicine, Karolinska Hospital, Stockholm, Sweden; (2) Institute of Neurobiology and Molecular Medicine, CNR, Rome, Italy; (3) Karolinska Pharmacy, Stockholm, Sweden; (4) Department of Anestesiology and Intensive Care, Karolinska Hospital, Stockholm, Sweden

Aim: A major advantage of SPECT is its ability to visualise several biological functions simultaneously, in vivo, by using different radiopharmaceuticals. In an on-going project regarding basic human lung functional physiology, ^{99m}Tc technegas and ^{113m}In-MAA is used for simultaneous imaging of lung ventilation and perfusion. In order to assess the spatial ventilation perfusion ratio (V/Q), a method including correction algorithms for „spill-over", radioactive decay, photon scattering and attenuation as well as organ outline was developed and validated experimentally.

Methods: The method was based on a non-simultaneous emission-transmission acquisition procedure using a three-headed SPECT-system (Trionix). Patient examinations were performed after administration of about 100 MBq ^{113m} In-MAA (392 keV) and 100 MBq ^{99m}Tc-technegas (140 keV). In order to correct for the „spill-over" of scattered photons from ^{113m}In into the ^{99m}Tc windows and to correct for photon scattering, data acquisition was performed in four separate energy windows. The „spill over" correction was based on an empirical model of the multiple scatter distribution from phantom experiments under different geometrical conditions and activity concentrations. The scatter originating from the scintillator/collimator has been analysed separately from that obtained from the patients. The scatter correction utilises a theoretical model of the first order Klein Nishina function. A non-uniform iterative attenuation correction algorithm was applied utilising attenuation data obtained from transmission measurements using a ^{99m}Tc line-source. Finally an edge detection algorithm, operating on the reconstructed transmission scans was used for delineating the activity distribution in the lungs. The validation of the method was carried out using a scatter and attenuation „free" stack phantom system.

Results: Scattered high-energy photons in the collimator/scintillator unit represented less than 10% of the total scatter obtained from a patient in the 392 keV energy window. The influence in lower energy windows was negligible. The average difference between the regional activity concentrations assessed after correcting the SPECT-data obtained from the „tissue" version of the stack-lung phantom and those obtained from the corresponding „scatter and attenuation-free" version was 3.9%±4.2% for ^{99m}Tc and 0.6%±3.7% for ^{113m}In in various parts of the lungs.

Conclusions: This quantitative method represents an accurate, effective and non-invasive tool for quantifying regional V/Q distributions in-vivo. The use of two different short-lived generator produced radionuclides gives high examination flexibility without high radiation doses.

OS_432

MULTICENTRE EVALUATION OF LUNG PERFUSION AND VENTILATION IMAGING WITH AN ANATOMICALLY ACCURATE PHYSICAL PHANTOM

J. Heikkinen (1), J. Kuikka (2), P. Rautio (3). (1) Department of Nuclear Medicine, Etelä-Savo Hospital District/ Mikkeli Central Hospital, Mikkeli, Finland; (2) Department of Clinical Physiology and Nuclear Medicine, Kuopio University Hospital, Kuopio, Finland; (3) Department of Clinical Physiology, North Karelia Central Hospital, Joensuu, Finland.

Aims: Combined perfusion and ventilation lung radionuclide imaging offers a very high degree of sensitivity in the diagnosis of acute pulmonary embolism whereas its specificity is relative low. We compared the quality of lung perfusion and ventilation imaging in Finland.

Methods: Eighteen Finnish hospitals participated in the survey. The survey was organised by Labquality Ltd. (Helsinki). A medical physicist visited all laboratories with a new anatomic-physical lung phantom. The containers of the phantom were filled with activities that produced count rates close to clinical situations. The phantom simulated two patient cases (male and female) expressing a variety of diseases i.e. lung embolus and fibrosis. Each laboratory performed their acquisition, analysis, hard copying and reporting according to their local clinical routine. Two nuclear medicine specialists evaluated the anonymous reports and the images. Nine separate components were judged and scored from the reports and six from the image series. Points were summed and normalised to the value of 10. Score $\leq$ 6.0 was classified as inadequate for clinical use.

Results: Some of the reports and images were low-quality. The average scores for the reports were 7.2 * 1.7 (range from 4.7 to 10.0) and for the images 7.2 * 1.3 (4.8 – 9.7). Ten laboratories received at least one inadequate score (8 reports and 9 images).

Conclusions: There were large variations in lung radionuclide imaging protocols in Finland, as expected. We noted several pitfalls (limited number of projections, poor image contrast, low-quality printer etc.), which explained most of the low scores. Our specialists developed and shared as a feedback a national recommendation for lung imaging according to international publications and national circumstances. The recommendation was distributed to all participants with their personal evaluation scores.

OS_433

CROSS-REFERENCE MAXIMUM LIKELIHOOD RECONSTRUCTION FOR POSITRON EMISSION TOMOGRAPHY WITH EMPIRIC STUDIES

J. Chen (1), K. Tu (1), T. Chen (2), H. Lu (2), R. Liu (3), K. Chou (3), C. Chen (4). (1) Institute of Radiological Science, National Yang-Ming University, Taipei, Taiwan; (2) Institute of Statistics, National Chiao Tung University, Hsinchu, Taiwan; (3) National PET/Cyclotron Center, Taipei Veterans General Hospital, Taipei, Taiwan; (4) Institute of Biomedical Engineering, National Taiwan University, Taipei, Taiwan

Aim: Our study is to improve image quality of positron emission tomography (PET) using a new and efficient method to incorporate the correlated structural information obtained from magnetic resonance imaging (MRI)

Methods: A mean estimate smoothing the maximum likelihood estimate (MLE) locally within each region of interest is derived according to the boundaries provided by the structural information. Since the boundaries may not be correct, a penalized MLE using the mean estimate is sought. The resulting reconstruction is called a cross-reference maximum likelihood estimate (CRMLE). The CRMLE is obtained through a modified expectation maximization (EM) algorithm, which is shown to be effective by our phantom and clinical studiesWe use SIEMENS Vision plus 1.5-T scanner to obtain MRI images as the source to provide the prior information Scanditronix PC-4096-15 WB PET scanner is used to obtain the sinogramsThe image fusion technique is implemented first and the image segmentation is applied to extract the useful prior information by a variant of Forgy's method in cluster analysisThe original sinogram data is used to reconstruct images using MLE-EM and CRMLE-EM, respectivelyThe differences between the two images are compared by subtraction of these two images

Results: Figure 1 shows one of our results. This new method preserves the advantages of MLE-EM, including the proper modeling for PET, linear complexity, row operation, and monotonic convergence. The cross-reference methods are quite robust to the mis-registration of boundaries in our studies, which is achieved by the regularization of MLEMoreover, the CRMLE-EM does contain more structural information than MLE-EM does because the incorporation of structural information from the fused imageThe empirical studies confirm the advantages of this new method

Conclusions: It has been shown in this study that the proposed CRMLE can take advantage of prior information effectively, even in the case of incorrect boundary informationThis is verified by the phantom and clinical studies.

Figure 1 (A): 2D Hoffman brain phantom study

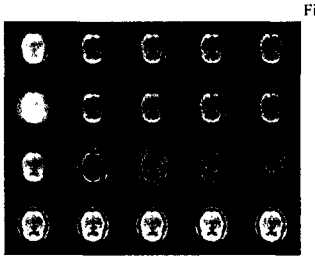

OS_434

QUANTITATIVE ANALYSIS OF DYNAMIC FDG-PET STUDIES RECONSTRUCTED BY ORDERED-SUBSETS-EXPECTATION-MAXIMIZATION (OSEM)

G. Meisetschläger, W.A. Weber, S.I. Ziegler, F. Munz, M. Schwaiger. Nuklearmedizinische Klinik, Technische Universität München, Deutschland.

Aim: It has been shown, that iterative reconstruction algorithms may improve image quality of oncological FDG-PET studies. But little is known about the effect of iterative reconstruction on quantitative analysis of dynamic studies. Thus, the aim of the present studies was to compare parameters derived from filtered back projection and ordered subsets expectation maximization reconstructed dynamic PET studies.

Methods: In 17 Patients (41 – 79 years, 45 – 96 kg, 3f, 14m) with malignant intrathoracic tumors an attenuation corrected, dynamic PET-Scan (duration 60 min , after injection of 250-350 MBq ^{18}F-FDG) was performed (ECAT EXACT 47, 32 frames, duration 5 sec to 5 min). Reconstruction was done by OSEM (5 iterations, 4 subsets) and filtered back projection (Hanning filter, cutoff 0.4 cycles/bin). The number of OSEM iterations was adjusted using high count statistic images of a body phantom , such that small lesions (10-38 mm) show the same image recovery as was found in FBP images. 32 tumors (1.0 –3.0 cm) with increased FDG-uptake were analyzed with Patlak-analysis. The input function was derived from ROIs placed in the descending aorta (0.8 cm Ø in 6 consecutive slices). The areas under the curve for blood (AUC_{bl}) and for tumors (AUC_{tu}) as well as the influx constants (K_i) for OSEM and FBP images were compared (linear regression, Wilcoxon-test). In addition the residual variance of the Patlak-analysis was measured by ANOVA.

Results: Both AUC_{bl} and AUC_{tu} were slightly but significantly higher for FBP than for OSEM (5.53E7±8.30E6 vs. 4.79E7±9.72E6 resp. 1.13E8±5.40E7 vs. 1.02E8±5.54E7, in Bq/ml, $p<0.05$, $r=0,78$ and $r=0,98$). K_i values were slightly lower for FBP than for OSEM (4,6±2,7 vs. 5.1±3.5, $p<0.05$). The maximum difference between the tumor values for all time points was 13%, for K_i 10%. A tendency to higher differences could be seen in the first frames because of low count statistics. The residual variance for Patlak-analysis was significantly lower for OSEM than for FB ($p<0.001$).

Conclusion: Even with carefully chosen reconstruction parameters, small systematic differences can be found in quantitative analysis of dynamic PET data reconstructed with FBP or OSEM. These are probably explained by the count level dependent convergence characteristics of OSEM. Nevertheless the lower residual variance of Patlak-analysis in OSEM reconstructed studies indicates a higher reliability of parameter estimation.

OS_435

THE ROLE OF REGRESSION MODELS IN THE LOGAN ANALYSIS OF NOISY PET DATA

J. Varga, ZS. Szabo. Department of Radiology, Johns Hopkins University, Baltimore, USA.

Logan analysis is a robust method for the estimation of the total distribution volume *(DVt)* of reversibly bound radiopharmaceuticals. However, it has been reported that the estimated values of *DVt* decreased with increasing noise. The aim of our work was to test whether applying a different regression model could reduce the noise dependence of the calculated *DVt*. Logan analysis transforms the measured data into a linear plot, and the slope is an estimation of *DVt*. The „classical" linear regression model minimizes the sum of the squared vertical *(Y)* differences between the points and the line. It is appropriate when the independent variable *(X)* is free of error, but with Logan analysis both variables *(X* and *Y)* are calculated from noisy measurements. Our hypothesis was that the noise dependence of the Logan slope can be decreased by using a linear regression model that minimizes the sum of the squared distances measured along line sections drawn from the data points perpendicularly, rather than vertically, to the fitted line.

Methods: *Experiment 1:* Six different levels of noise were added to simulated receptor binding data, and repeated 2000 times at each level. Logan analysis was performed in each case, applying both linear regression models.*Experiment 2:* Logan analysis with the „perpendicular" regression model was applied to real data from a dynamic brain transporter binding PET study, using two different approaches: *(a)* generating time-activity curves of large brain regions first, then creating their Logan plot; and *(b)* calculating the Logan slope from each voxel first, and then averaging over the same regions as in *(a)*.

Results: *Experiment 1:* While the average of *DVt* values calculated from the „classical" model decreased significantly with increasing noise levels (as reported previously), there was no noise dependence when applying the „perpendicular" model ($P>0.05$). *Experiment 2:* Using the „perpendicular" model there were no significant differences between the *DVt* values calculated for large brain regions or individual pixels (paired t-test).

Conclusions: Our experiments prove that the *DVt* calculated from the Logan plot is not noise dependent if the linear regression model accounts for errors in both the *X* and *Y* variables. Our second experiment showed that Logan analysis was also applicable on a voxel-by-voxel basis, and the *DVt* values were not changed, making it possible to create parametric images from dynamic PET studies.

OS_436

DICOM IMAGE ARCHIVING AND PRESENTATION OF NUCLEAR STUDIES IN A LARGE UNIVERSITY HOSPITAL

O. Nickel (1), C. Kadalie (1), P. Mildenberger (2), S. Walther (3), P. Bartenstein (1). (1) Department of Nuclear Medicine; (2) Department of Radiology; (3) Department of Electronic Data Processing, Klinikum der J. Gutenberg Universitaet, Mainz, Germany.

All image data (except PET) of our department are archived since 1999 in a central DICOM server (Image Devices), which stores all radiological data (MRT, CT, DR) as well. The practicability and usability of this system regarding archiving and image communication capabilities will be discussed in this presentation.

Methods: All data from 5 gammacameras (3 Siemens and 2 Marconi systems) are stored via DICOM storage on a central DICOM system, which is administered by the radiological department. A database of the nuclear medicine patients with image data references is maintained within the nuclear medicine department. A back transfer of all image data to the originating systems is possible without loss of proprietary data fields, which is important for, e.g., reconstruction of SPECT projection data. The transfer of CT and MRT data to the nuclear workstations for image fusion of the different modalities is possible as well. Image viewing and presentation is available in the whole hospital by a web server in the departments of radiology and nuclear medicine providing a Java-based viewer application. For the presentation of SPECT and PET volumes we developed a windows based application („Gammaview"), which is independent of the DICOM archive, but uses FTP file transfer for the reconstruced tomograms.

Results: The centralizing of the image archive has several benefits: The administration of the archive as well as the transfer of data between the different modalities is much easier than before. Image fusions can be performed on a routinely basis (now about 3-4 fusions per week). Online presentation of results in the clinical departments has been introduced within the last months with high acceptance of the referring physicians. Not all results can be presented up to now: The presentation of screen shots (preserving all contrast and color information) is not yet fully supported by all systems. The data transfer between the nuclear systems (Siemens/Marconi) is not quite satisfying due to different interpretation of certain DICOM objects.

Conclusions: Archiving of nuclear medicine images in a central DICOM system is possible and can be recommended. The benefits are: Easier administration, easy and fast data transfer between different modalities and the possibility of online presentation of results. The acceptance of nuclear medicine procedures can be improved by using this fast image communication provided by the central image distribution. The optimal use of the system, however, is not yet given and requires some additional efforts by the manufacturers.

OS_437

USING DICOM IN NUCLEAR MEDICINE FOR SCHEDULING, IMAGE ARCHIVING, REPORT AND DATA DISTRIBUTION

K. Jönsson, C. Abelson, L. Bertenstam, H. Carlsson. Center for Medical Imaging and Physiology, Lund University Hospital, Sweden

Aim: In our department some 6000 scintigraphic studies are performed per year using 4 gammacameras.As a fully digitized nuclear medicine department we are trying to streamline the data flow by implementing DICOM services according to the concept of IHE (Integrating the Healthcare Enterprise).

Methods: Examination requests from referring clinicians are transferred electronically to our department via a RIS (Radiological Information System) . After acceptance by our physician in charge the patient is scheduled for examination day and gammacamera. Every morning the gammacameras make requests to the RIS using the DICOM Modality Work List. The "schedule of the day" is downloaded to the gammacamera and patient name and other keys are loaded into the gammacamera database. After acquisition and processing by the technician final results and raw data are archived in the department PACS (Picture Archiving and Communication System) using DICOM Storage Class. The PACS system is also used for archiving all radiological images like MR, CT produced within the hospital. An "autorouting " function in the PACS is set up for immediate transferring (copying) of incoming images to predefined workstations, display stations and to a Web server using DICOM Storage Class. These stations are used by the physicians for image interpreting. In order to get access to images from previous examinations another PACS tool is used,"prefetching", using schedule information from RIS. Every night , all previously archived images, including MR and CT regarding the following days patients are read from archive and downloaded to predefined displaystations and Web server. After interpretation the report is either written into or dictated into the RIS.The Web server is also used for fast distribution of images and reports to referring clinicians in the hospital. The final reports can be transferred from RIS to the Web server using DICOM "Structured reporting". The web server application can be viewed on ordinary PC browsers without plug-ins. The system allows differentiated access control and the security level of the account and password defines the subset of studies one can access. High resolution image display are provided with interactive colour scaling, thresholding, zooming, cine, ROI, printing. Dual screens are supported for image comparison.

Conclusions: The system is running in routine within the department with most basic functions implemented. Pitfalls and problems will be reported. Most problems relate to manufacturers late DICOM implementation. Major advantages are safety in registration and fast access to images and reports for both department physicians and referring clinicians.

OS_438

AN OPEN SOURCE BASED APPROACH FOR NUCLEAR MEDICAL IMAGE ADMINISTRATION AND DISTRIBUTION

G. Dobrozemsky (1), H. Poetzl (2), T. Svizensky (2), J. Jank (3), P. Schaffarich (1). (1) Department of Biomedical Physics and Engineering, Vienna University, Vienna, Austria; (2) Department of Computer Languages, Vienna University of Technology, Vianna, Austria; (3) Department of Nuclear Medicine, Vienna University, Vienna, Austria.

Aim: To design and implement an inexpensive yet flexible, easy to maintain and scalable infrastructure for distributing nuclear medical images and reports, as a nuclear medical archive had to be prepared for transfer to a new archiving facility.

Methods: At the department of nuclear medicine of the Vienna General Hospital, a part of the Vienna University, the old imaging archive (consisting of image data in NEMA-Interfile format residing on some 90 MODs organized by means of a VAX 4000 based ORACLE-database) was restored to hard disk on a Personal Computer (Pentium III Coppermine, 600 MHz, 256MB) running Linux (SUSE 6.4). There a new database has been set up utilizing the Open Source components Postgres, Apache and Python as well as basic UNIX tools like awk and sed. For image viewing, an integrated image creation tool has been added, allowing for image preview before download/distribution. User access can be granted on several security levels, on authentification schemes presented by the webserver, restricting access to the web-based frontend to certain hosts as well as different users and user groups. As additional goodies, the system provides multi-language-support as well as the possibility of DICOM export utilizing PART 10 files.

Results: The access to the archive has become user-friendly, and fast. In a thorough test, the archive presented patient data according to complex search criteria in less than a second with more than 62,000 patient records in the database. We have also been able to set up the interface in a way that allows the non-expert user to easily search for studies of basic investigation types. The process of retrieval of archived studies and upload to processing workstations has been speeded up form an time-consuming, complex half-hour process to a mere one-minute task. We also have been able to recover major inconsistencies in the primary database due to erraneous patient administration, changing acquisition protocols as well as archiving errors of the old system.

Conclusions: The imaging database has proven as a fast and reliable means of nuclear medical image distribution. Its reliability, scalability and flexibility have saved us much time, as well as given the possibility of fast adaptation to new problems with old data. We will further adapt this tool, as well as expand it to further tasks, e.g. DICOM transfer and HL7 support.

PS_1

WHICH IS THE BEST INDICATOR OF ISCHEMIC VIABLE MYOCARDIUM, THE MARKER OF FATTY ACID METABOLIM, GLUCOSE METABOLISM OR HYPOXIA? EXPERIMENTAL STUDY USING A NEW RADIOLABELED 2-NITROIMIDAZOLE ANALOG AS A HYPOXIA MARKER

T. Kaneta (1), Y. Takai (1), Y. Kagaya (1), Y. Yamane (1), H. Wada (1), M. Yuki (1), R. Iwata (1), M. Tsujitani (2), T. Ido (1), S. Takahashi (1), S. Yamada (1)(1) Department of Radiology Cardiovascular medicine and Cyclotron & Radioisotope center, Tohoku University, Sendai, Japan ; (2) Pola Chemical Industries, Yokohama, Japan; (3) Hiraka General Hospital, Yokote, Japan.

Purpose: Fatty acid or glucose metabolism markers have been used for evaluating myocardial viability. But these metabolism markers are often influenced by the systemic metabolic state. Recently we have succeeded in labeling a new 2-nitroimidazole analog; RP170 (1-[2-hydroxy-1-(hydroxymethl)-ethoxy] methyl-2-nitroimidazole) with [^{18}F] to make [^{18}F]FRP170. RP170 was developed as a hypoxic radiosensitizer in Pola Chemical Industries. The purpose of this study is to compare the distribution of [^{18}F]FRP170 with that of [^{125}I] 15-(p-iodophenyl)-3-(R,S)-methylpentadecanoic acid (BMIPP) or [^{14}C]deoxygluxose (DG) in the ischemic myocardium using double-tracer autoradiography technique and to determine the best indicator for ischemic viable myocardium.

Methods: Rats were injected [^{18}F]FRP170 and [^{125}I]BMIPP or [^{14}C] DG 30min after the ligation of left coronary artery and were sacrificed 15min after this. In every autoradiogram, small circular regions of interest (ROIs) were placed throughout the left ventricular wall. The uptake in every ROI was normalized by the average uptake in the septum. We defined High-FRP as the area where FRP170 uptake is greater than 150% of the septum, and Low-FRP where FRP170 uptake is less than 50%.

Results: BMIPP uptake decreased gradually from the periphery region to the center of the ischemic myocardium. On the other hand, FRP170 accumulated significantly higher in the margin and lower in the center. The %BMIPP in High-FRP and Low-FRP are 42.7±3.9% and 3.1±0.6% respectively. DG images were similar to FRP170 images. The %DG in High-FRP and Low-FRP are 122.0±9.0% and 1.8±0.2% respectively. According to the circumferential profile curve, the increase of FRP170 uptake starts almost at the same position where DG uptake increases. But the decrease of DG uptake starts at the closer point to the septum than a point where FRP170 uptake starts decreasing. These findings indicate that the high FRP170 uptake areas are larger than the high DG uptake area, and this phenomenon was visually confirmed.

Conclusion: FRP170 and DG images were able to visualize ischemic viable myocardium better than BMIPP image. Moreover, FRP170 was more sensitive for detecting viable area than DG. FRP170 has a great possibility to detect the ischemic viable myocardium more sensitively than DG. FRP170 might be able to become a new gold standard for detecting the ischemic viable myocardium instead of fluorodeoxyglucose.

PS_2

DOSE CA CHANNEL BLOCKER IMPROVE MYOCARDIAL ISCHEMIA AND FATTY ACID METABOLISM ABNORMALITY IN PATIENTS WITH HYPERTROPHIC CARDIOMYOPATHY ?

T. Sakatani, H. Mani, T. Kawasaki, T. Kamitani, S. Kawasaki, H. Sugihara. Department of Cardiology, Matsushita Memorial Hospital, Sotojima-cho, Japan.

Aim: Myocardial ischemia and fatty acid metabolism abnormality may play an important role on natural history of patients with hypertrophic cardiomyopathy (HCM). It has been reported that Ca channel blocker prevents myocardial ischemia during short interval in patients with HCM. We investigated whether Ca channel blocker improves myocardial ischemia and fatty acid metabolism abnormality during long interval in patients with HCM.

Methods: The subjects were 20 patients with HCM who showed transient perfusion defects on exercise myocardial Tl-201 SPECT. They underwent exercise Tl-201 SPECT and I-123-BMIPP SPECT before and after 4-8 years after oral administration of verapamil or diltiazem. The SPECT image was divided into 17 segments and the severity of the defect was scored visually using defect score, a 4-point scoring system. Transient dilation index (TDI) was calculated as an index of subendocardial ischemia.

Results: The Tl-201 total defect score decreased significantly from 9.8±4.35 to 5.50±4.63 ($p<0.001$) after treatment of verapamil or diltiazem. TDI decreased from 1.20±0.12 to 1.08±0.09 ($p<0.001$). The I-123-BMIPP total defect score increased from12.52±7.4 to 14.8±7.8 ($p<0.01$).

Conclusions: Verapamil or diltiazem improves myocardial ischemia, but does not have an effect on fatty acid metabolism abnormality during long interval in patients with HCM.

PS_3

THE CORRELATION WITH TC-99M-MIBI MYOCARDIAL SCINTIGRAPHY AND MYOCARDIAL CYTOCHROME OXIDASE ACTIVITY IN HYPERTROPHIC CARDIOMYOPATHY

O. Satake (1), K. Masuyama (1), Y. Ishikawa (2), T. Ueda (3), S. Kanayama (1), T. Yamagata (1), S. Kanemitsu (1), H. Tsugawa (1), S. Matsui (1), N. Takekoshi (1). (1) Department of cardiology; (2) Department of pathology (II); (3) Department of anatomy, Kanazawa Medical University, Uchinada, Japan.

Aim: It was suggested that Tc-99m-MIBI (MIBI) was associated with mitochondrial function in myocardium. In hypertrophic cardiomyopathy (HCM), we examined how hypo-uptake on MIBI was affected mitochondrial cytochrome oxidase (MCO) activity of myocardium and how reflect the prognosis.

Methods: Eighteen patients with HCM were studied with MIBI and endomyocardial biopsy. SPECT images of MIBI at exercise and rest were analyzed with four scaled visual scores set in 17 segments. Biopsy specimens were prefixed with 2.5% glutaraldehyde for 30 minutes. After that staining of MCO activities were performed by 3-3'-diaminobenzidine, catalase and cytochrome c. Specimens stained with toluidine blue were observed at a magnification of x400 by light microscopy, and examined about the degree of these activity.Results: MIBI was divided between high defect score (I group) and low defect score (II group). MCO activities of I group (2.4 ± 1.2) were significant decreased than those of II group (3.4 ± 0.7). ($p = 0.04$) MIBI defect score showed a strong correlation with the degree of MCO activity in myocardium. ($y = -0.108x + 4.078$, $r = -0.622$, $p = 0.006$)

Conclusion: It was suggested that MCO activities were useful for the pathophysiology and the prognosis of HCM with combination of MIBI methods.

PS_4

PROGNOSTIC VALUE OF MYOCARDIAL VIABILITY RECOGNIZED BY THALLIUM SCINTIGRAPHY IN PATIENTS WITH PREVIOUS MYOCARDIAL INFARCTION: THE QUESTION OF REVASCULARIZATION OF PATIENTS WITHOUT SIGNS OF MYOCARDIAL VIABILITY

Z. Petrasinovic (1), M. Ostojic (1), B. Beleslin (1), S. Pavlovic (2), D. Sobic (2), A. Dikic (1), J. Marinkovic (3), A. Nedeljkovic (1), I. Nedeljkovic (1), J. Stepanovic (1), V. Obradovic (2)(1) Institute for Cardiovascular Diseases; (2) Institute for Nuclear Medicine, Clinical Center of Serbia.

Background: In patients (pts) studied early after myocardial infarction (MI), recognition of myocardial viability is associated with a better survival, but its prognostic significance in different patients subgroups is still unclear. Objective: The aim of the study was to assess the prognostic value of myocardial viability recognized by thallium-201(Tl)-scintigraphy in pts with previous (>3 months) myocardial infarction.

Methods: Myocardial viability was assessed in 95 pts consisting of 55 pts (50 male; mean age 58±9 years) by Tl rest-redistribution (after 4 hours) scintigraphy and in 40 pts (38 male; 56±8 years) by Tl stress-redistribution-reinjection scintigraphy (dipyridamole: 0,54mmg/kg over 4 min; redistribution after 4 and 24 hours; reinjection after 24 hours). There was no significant difference between 2 groups concerning data on clinical, angiographical, and echocardiographical characteristics of the pts (p=ns). All pts had angiographically documented significant CAD, with the mean ejection fraction of 43±10%. Dyssynergic segments were defined with Tl activity of <50%, whereas myocardial viability was defined with increase in Tl activity in those segments of >15%. Out of 95 pts, 36 were medically treated, and 59 were revascularized. All pts were followed up for 12 months, for adverse cardiac events (death and nonfatal myocardial reinfarction).

Results: Tl-rest and stress scintigraphy was positive for myocardial viability in 65 pts (68 %) and negative in 30 pts (32 %). During follow-up there were 11 adverse cardiac events (12%; 7 deaths, 4 reinfarctions) including 8 out of 36 medically treated pts (22%) and 3 out of 59 revascularized pts (5%, p=0.02). By Kaplan-Meier analysis in the 36 medically treated patients, the 12 months survival was 90% in pts with myocardial viability and 60% in pts without myocardial viability (p=0.06). In the 59 revascularized patients, the 12 months survival was 98% in pts with myocardial viability and 87% without myocardial viability (p=0,06). Using the Cox proportional hazards model, myocardial viability was the best predictor of adverse cardiac events (HR 0,22, p= 0,04).

Conclusions: In pts with previous MI and significant CAD the best survival and lowest incidence of adverse cardiac events was observed in viable pts, either medically or surgically treated patients. In addition, survival of revascularized patients without signs of viability was significantly better than in non-revascularized non-viable patients, representing therapeutical dilemma to accepted clinical indications for revascularization.

PS_5

DYSFUNCTION OF FATTY ACID METABOLISM IN THE CARDIOMYOPATHY IN PATIENTS WITH MUSCULAR DYSTROPHY

M. Ohyanagi, H. Naruse, T. Arii, M. Masai, K. Takahashi, T. Iwasaki. 1st.dept.int.med.Hyogo College of Medicine, Nishinomiya, Japan.

[Aim] Duchenne dystrophy (DMD) often associated with cardiomyopathy. Evaluation od myocardial dysfunction of these pateients were assessed using electrocardiogram, echocardiogram and thalium scintigram. Although I-123-BMIPP (BM), a beta-methyl-branched fatty acid, were used to evaluate fatty acid metabolism and to detecte myocardial injury, there has been a few reports of myocardial fatty acid metabolism in patients with DMD. We compared BM images with histological changes in animal dystrophy model and investigated whether BM could be used in the diagnosis of cardiac injury of patients with DMD.
[Method] [1] Experiment: 10 Ci of I-125-BMIPP (BM) were injected to J-2-N humster, muscular dystrophy model, associated with heart failure. Hearts were resected, and examined by autoradiography. Humsters were divided into 2 groups. A group was associated with heart failure (n=7, mean CPK=39696), which showed edema, pleural effusion and ascites. B group was not associated with heart failure (n=7, mean CPK=1285). We compared 2 gpoup with BM uptake, histological changes and ECG changes. [2] Clinical study: BM and Tl-201 (Tl) scintigraphy were performed to DMD 14 patients (muscular severity grade; 4-7). Intensity of uptake was assessed by the semiquantitative scoring method (normal = 27 points), and wall motion (WM) was assessed by same method with echocardiography.
[Result] [1] Abnormal ECG changes were observed in 5/7cases in A group, but not in B group. Dilated cardiac cavity and pathological changes (fibrosis et al) were shown in broup A but not B. BM uptake in A group (3.3±0.9 c/mm2) was lower than B group (10.8±5.9 c/mm2) (p=0.006). [2] Tl uptake score (21±3) was higher than BM score (17±4)(p=0.016) in Patients with DMD. There is a relation between BM and WM (R=0.71, p=0.005). However, there is no relation between stage of DMD and Tl, BM, and WM.
[Conclusion] The experimental data suggest that the damage of fatty acid metabolism occured in heart failure model. In clinically, since BM uptake was less than Tl uptake, dysfunction of fatty acid metabolism may also occure in patients with DMD. Since there was a good correlation between BM and WM, BM could be used in the diagnosis of cardiac injury of patients with DMD.

PS_6

INCREMENTAL VALUE OF REST-REDISTRIBUTION THALLIUM-201 SCAN IN ASSESSMENT OF VIABLE MYOCARDIUM IN FIXED 99MTC-TETROFOSMIN PERFUSION DEFECTS

K.C. Cheng (1), W.Y. Ho (1), E.Y.L. Leung (1), K.K. Wong (1), F.T.H. Ho (1), R.Y.L. Leung (1), M.W.M. Law (2), T.Y.C. Au (1), T.C. Chan (1), J.Y.C. Lui (1). (1) Nuclear Medicine Unit, Department of Radiology; (2) Medical Physics Unit, Queen Mary Hospital, Hong Kong.

Aim: This study assessed how frequent rest-redistribution thallium scans depict viable myocardium which appeared as fixed perfusion defects in tetrofosmin myocardial perfusion scans.
Methods: 2-days protocol of ^{99m}Tc-Tetrofosmin was performed after exercise or pharmacologic stress. Gated SPECT images were acquired 1 hour after 25 mCi tetrofosmin injection. Rest-redistribution thallium scans were scheduled for patients presented with large-sized fixed myocardial perfusion defects of marked decreased tracer uptake. 3 mCi thallium was injected at rest and SPECT images were acquired 30 minutes and 4 hours post-injection. Comparison was made with the tetrofosmin images. Reconstructed SPECT images were divided into 9 segments and analyzed qualitatively in a 4-point scale from normal to marked perfusion defect. Reversibility was graded qualitatively in a 5-point scale. The presence of a reversible perfusion defect was defined as definite perfusion defect with at least partial reversibility (predominantly fixed perfusion defect was considered as non-reversible).
Results: 8 patients (7 men, 1 woman; mean age 60.3, range 33-72) were studied with 7 patients had ischemic heart disease and one patient had history of myocardial infarction. 7 patients underwent persantin pharmacologic stress and 1 patient had exercise stress. 6 patients had gated SPECT images acquired while 2 patients had problems in gating. 33 fixed perfusion defects were identified with 28 marked perfusion defects and 5 moderate defects. For the marked perfusion defects, 14 lesions appeared fixed, 3 predominantly fixed, 9 partially reversible and 2 reversible. Gated SPECT images showed impaired wall thickening in those marked perfusion defects. For the moderate perfusion defects, 3 partially reversibie and 2 reversible defects were identified. Thallium scan demonstrated 39.3% (11/28) reversible perfusion defects in marked perfusion defects and in all moderate perfusion defects (5/5).
Conclusions: These findings suggest that when fixed tetrofosmin perfusion defect is present, rest-redistribution thallium scintiscan is helpful in identification of viable myocardium. A larger study is required to verify these preliminary findings.

PS_7

MYOCARDIAL VIABILITY ASSESSMENT WITH LATE REDISTRIBUTION OF THALLIUM-201 IN FIXED MYOCARDIAL PERFUSION DEFECTS IN 4 HOURS DELAYED REINJECTION IMAGES

K.C. Cheng (1), W.Y. Ho (1), E.Y.L. Leung (1), K.K. Wong (1), F.T.H. Ho (1), R.Y.L. Leung (1), M.W.M. Law (2), T.Y.C. Au (1), T.C. Chan (1), J.Y.C. Lui (1). (1) Nuclear Medicine Unit, Department of Radiology; (2) Medical Physics Unit, Queen Mary Hospital, HK.

Aim: This study evaluates how frequent the apparently fixed myocardial perfusion defects in 4 hours delayed reinjection thallium images demonstrate reversibility in 24 hours late redistribution images.
Methods: From 1997 to 2000, 79 patients (68 men, 11 women; mean age 65, range 34-79) with 51 known ischaemic heart disease, 24 myocardial infarction and 4 suspected ischaemic heart disease were referred for myocardial perfusion thallium scan. SPECT images were acquired immediate post-exercise/pharmacologic stress after injection of 2 mCi thallium-201 and 4 hours delayed with 1 mCi thallium-201 reinjection 10 minutes before the rest study. 24 hours delayed redistribution images were acquired if fixed perfusion defects were identified. Reconstructed SPECT images were divided into 9 segments and analyzed qualitatively in a 4-point scale from normal to marked perfusion defect. Reversibility was graded qualitatively in a 5-point scale. The presence of a reversible perfusion defect was defined as definite perfusion defect with at least partial reversibility (predominantly fixed perfusion defect was considered as non-reversible).
Results: 174 fixed myocardial perfusion defects after reinjection were identified, with 95 marked defects, 51 moderate defects and 28 mild defects. For marked perfusion defects, 30 segments (32%; 27 partially reversible and 3 near-completely reversible) demonstrated reversibility in 24 hours delayed images while 50 segments appeared fixed and 15 segments were predominantly fixed defects. For moderate perfusion defects, reversibility was noted in 30 segments (59%; 23 partially reversible, 6 near-completely reversible and 1 reversible); 11 segments were fixed and 10 segments were predominantly fixed defects. For mild perfusion defects, 20 segments showed reversibility (71%; 9 partially reversible and 11 reversible) and 8 fixed defects were identified in 24 hours delayed images. The overall reversibility rate is 46% (80/174).
Conclusions: Late (24 hours) redistribution imaging is promising in demonstrating reversibility of fixed myocardial perfusion defects observed in stress-reinjection imaging. It enhances the detection of viable myocardium.

PS_8

ASSESSMENT OF MYOCARDIAL VIABILITY BY NITRATE-TEST 99MTC-MIBI SPECT IN PATIENTS WITH PREVIOUS MYOCARDIAL INFARCTION: COMPARISON WITH NITRATE-ECHOCARDIOGRAPHY

Y. Lishmanov (1), V. Chernov (1), E. Makarova (1), K. Zavadovskiy (1), V. Bezlyak (2), I. Vorozcova (2), I. Bukhovets (2), V. Babokin (3), A. Evtushenko (3). (1) Department of Nuclear Medicine; (2) Department of Functional Diagnosis; (3) Department of Cardiac Surgery, Institute of Cardiology, Tomsk, Russia.

Purpose: Myocardial viability assessment is crucial in patients with acute myocardial infarction (AMI), to rule out therapy and prognosis. At the present the gold standard in adjectives of myocardial function is PET whit ^{18}F-FDG. But this method is very expensive and therefore not extends. Alternative strategy in diagnostic of viable myocardium is SPECT with 201-Tl or 99mTc-MIBI in combination with pharmacological tests. In ultrasound diagnostic used stress-echocardiography with nitrate.
Aim: The aim of the study was to compare 99mTc-MIBI SPECT (rest and nitrate) with nitrate echocardiography (NE) for the identification of viable myocardium.
Method/materials: Eighteen patients with previous myocardial infarction were studied with of rest and nitrate 99mTc-MIBI SPECT. Before nitrate 99mTc-MIBI SPECT patients also underwent nitrate echocardiography. All of the patients underwent coronary artery bypass surgery and postoperative echocardiography (rest) and rest-99mTc-MIBI SPECT was also obtained following three weeks of revascularization. Left ventricular wall motion analysed by dividing the left ventricle into 16 segments. All studies were analysed by semiquantitative visual scoring using the same four-grade scale for wall motion and perfusion abnormalities. Segments that improved at least one grade on the subsequent NE or images or uptake of nitrate 99mTc-MIBI more than ≥30% of peak were considered to represent viable myocardium.
Results: Basal echocardiography demonstrated 68 assynergic or dissynergic segments; 24 of those 68 (35%) showed functional recovery on nitrate. Echocardiography after bypass surgery showed 39 a/dissynergic segments. In that way sensitivity, specificity and overall predictive accuracy of NE for viable myocardium diagnosis were 69%, 90% and 81%. 99mTc-MIBI SPECT demonstrated 36 segments with uptake less 30% in 68 a/dissynergic segments; 6 of those 36 showed expansion of uptake more that 30% on nitrate. So the sensitivity of nitrate 99mTc-MIBI SPECT test for viable myocardium diagnosis was 93%, with specificity 72% and overall predictive accuracy 81%. Overall predictive accuracy SPECT in combination whit nitrate echocardiography was 91%.
Conclusions: Nitrate 99mTc-MIBI SPECT and nitrate echocardiography method is useful technique for the identification of viable myocardium. Thus 99mTc-MIBI SPECT has higher sensitivity, and NE has higher specificity. Joint usage of echocardiography and SPECT let increasing of overall predictive accuracy finding myocardial viability.

PS_9

USE OF TL-201 PROTOCOLS IN DETECTING VIABLE MYOCARDIUM AND PREDICTING RECOVERY OF REGIONAL VENTRICULAR DYSFUNCTION AFTER CORONARY ARTERY BYPASS

M. Koutelou (1), G. Athanassopoulos (2), A.P. Kouzoumi (1), V. Tsapaki (1), V. Cokkinos (2). (1) Department of Nuclear Medicine; (2) 1rst Cardiology Department, Onassis Cardiac Surgery Center, Athens, Greece.

Use of Tl-201 protocols in detecting viable myocardium and predicting recovery of regional ventricular dysfunction after coronary artery bypassThallium-201 (TL) scintigraphy and low-dose dobutamine echocardiography (LDDE) were performed in 49 patients (pts) (mean age 58 years) with chronic ischemic left ventricular dysfunction (IVD) to assess the effects of revascularizaiton on myocardial function.

METHODS: 49 pts with IVD (LVEF <40%) underwent stress-redistribution-reinjection and-24-hours redistribution scintigraphy before coronary artery bypass (CABG) and LDDE to study improvement regional abnormality. An increase in wall thickening and the presence of reversible or partial reversible defects on TL scintigraphy was considered as a sign of viable myocardium. All pts underwent an echocardiographic study post-CABG to assess the recovery of myocardium.

RESULTS: a. Pre-operatively, 140 abnormal segments were found in Tl scintigraphy (99 reversible and 41 fixed-non viable) and (65 hypokinetic and 31 dys and/or akinetic by LDDE). Concordance of the 2 techniques was 80%. Seventy pts had 3 vessel disease (VD), 34 pts with 2 VD and 4 pts had 1 VD. From the 116 diseased vessels 103 were revascularized (almost complete revascularization). b. Post-operatively, improvement in wall motion was noticed in 78 (79%) of the reversible segments, but only in 10 (25%) of the non-viable (fixed) segments (p =0.0001) The sensitivity and specificity of Tl-201 in predicting recovery of regional ventricular dysfunction were 90% and 61% respectively.

CONCLUSION: TL scintigraphy is documented as an accurate method in detecting viable myocardium and predicting recovery in IVD pts. These pts had a low mortality at 2 years.

PS_10

COMPARISON OF FDG SPECT AND CONTRAST ECHOCARDIOGRAPHY FOR MYOCARDIAL VIABILITY ASSESSMENT

O. Lang (1), H.R. Balon (2), R. Feuereisl (3), J. Sklenar (3), F. Melichar (1), M. Kaminek (4), M. Myslivecek (4). (1) Department of Nuclear Medicine, Charles University, 3rd School of Medicine, Prague, Czech Republic; (2) Department of Nuclear Medicine, William Beaumont Hospital, Royal Oak, Michigan, USA; (3) Kardiologie Ltd., Hospital Bulovka, Prague, Czech Republic; (4) Department of Nuclear Medicine, Palacky University, Olomouc, Czech Republic

Aim: Detection of viable myocardium (VM) is important before revascularization. It can be assessed by evidence of preserved glucose metabolism or by demonstration of contractile reserve. Another new method is imaging of intact capillary bed by myocardial contrast echocardiography (MCE). The goal of our study was to compare the results of FDG SPECT and MCE in patients after myocardial infarction.

Methods: We evaluated 8 men (mean age = 57 years, range 49-65) by both methods. MCE was performed with intravenous contrast medium Levovist using intermittent harmonic imaging. FDG SPECT was performed within 2 weeks of MCE with ^{18}F-FDG using a gamma camera equipped with an ultra-high energy all-purpose collimator, after patient metabolic preparation with insulin and glucose. The studies were evaluated blindly.

Results: On MCE, 4 pts had preserved capillary bed, 4 pts had defects (apex - 1 pt, inferior wall – 2 pts, apico-antero-septal wall – 1 pt). On FDG SPECT, 5 pts were normal (4 of these 5 had normal MCE), 3 pts had defects (apex - 1 pt, inferior wall – 1 pt, apico-antero-septal wall – 1 pt). The defect localization in these 3 pts was identical between the two methods. Both methods agreed in 7/8 pts (88%).

Conclusions: In this small group of pts there was good agreement between FDG SPECT and MCE in VM assessment. The main advantage of MCE is better spatial and temporal resolution, therefore it can depict transmural distribution of intact capillary bed. The main advantage of FDG SPECT is greater clinical experience.

PS_11

EVALUATION OF MYOCARDIAL METABOLISM AND LEFT VENTRICULAR FUNCTION FOLLOWING MYOCARDIAL INFARCTION

M. Nanasato (1), A. Ando (2), S. Isobe (2), M. Nonokawa (2), N. Tsuboi (1), T. Ito (1), M. Tadokoro (3), T. Ishigaki (3), M. Hirai (2), M. Yokota (4), H. Hirayama (1)(1) Cardiovascular Center, Nagoya Daini Red Cross Hospital, Nagoya, Japan; (2) First Department of Internal Medicine, Nagoya University, Nagoya, Japan; (3) Department of Radiology, Nagoya University, Nagoya, Japan; (4) Department of Clinical Laboratory Medicine, Nagoya University, Nagoya, Japan

It has been well established that myocardium alters the metabolic substrate from free fatty acid to glucose under ischemic condition. The course of myocardial metabolism after myocardial infarction, however, remains to be unknown. This study was sought to assess myocardial metabolism after myocardial infarction and the influence of myocardial metabolism on left ventricular function.

Method: Eleven patients (10 men, 1 women, mean age 60.3 +- 9.4 years) treated with reperfusion therapy underwent 201-thallium (Tl) single photon emission tomography (SPET) at exercise, 123I 15-iodophenyl-3-R,S-methyl pentadecanoic acid (BMIPP) SPET at rest, 18F-fluorodeoxy glucose positron emission tomography (FDG-PET), and left ventriculography (LVG) 3 months after myocardial infarction. FDG-PET was performed under fasting. Left ventricular myocardium was differentiated into 5 segments. The uptake of SPET and PET was graded visually in all segments of each patient. The 4-point scoring system was used to indicate the defect of segments on SPET and the accumulation of segments on PET. The severity score was defined as the summation of defect or accumulation scores on each patient. The regional wall motion was scored visually from 0 = normal to 3 = akinesis or dyskinesis. Left ventricular wall motion (LVWM) was calculated as the sum of regional wall motion score.

Results: No patients showed redistribution on Tl and significant stenosis on coronary angiography. Severity scores were 5.3 +- 3.4 on Tl, 7.8 +- 4.2 on BMIPP, and 5.7 +- 1.5 on FDG, respectively. Left ventricular ejection fraction and LVWM were 63 +- 11%, and 14.3 +- 2.7. The defected segments were found in nine patients on Tl, and in all patients on BMIPP. Ten patients had the accumulated segment of FDG. All discordant segments between Tl and BMIPP accumulated FDG. The severity score of FDG was significantly greater (p=0.01). The severity score of FDG correlated with the severity score of BMIPP (r=0.655), the number of discordant segments between two SPETs (r=0.742), LVEF (r=-0.549), and LVWM (r=0.642).

Conclusions: The accumulation of FDG has well correlation with the discordant segments between Tl and BMIPP. Metabolic alteration on myocardium after severe ischemia continues on the majority of patients and does not result from myocardial ischemia. Prolonged metabolic disorder on myocardium might be one of the factors deteriorating left ventricular function, as the segments FDG accumulated reduced on wall motion.

PS_12

DOBUTAMINE ECHOCARDIOGRAPHY AND FDG SPECT IN MYOCARDIAL VIABILITY ASSESSMENT - A COMPARISON OF PRINCIPALLY DIFFERENT METHODS

O. Lang (1), H.R. Balon (2), R. Feuereisl (3), F. Melichar (1), M. Myslivecek (4), M. Kaminek (4). (1) Department of Nuclear Medicine, Charles University, 3rd School of Medicine, Prague, Czech Republic; (2) Department of Nuclear Medicine, William Beaumont Hospital, Royal Oak, Michigan, USA; (3) Kardiologie Ltd, Hospital Bulovka, Prague, Czech Republic; (4) Department of Nuclear Medicine, Palacky University, Olomouc, Czech Republic

Aim: Detection of viable myocardium (VM) in pts with ischemic heart disease is important for guiding further therapy. There are two principally different modalities for assessment of VM in clinical practice. Dobutamine echocardiography (DE) demonstrates contractile reserve, while FDG scintigraphy (FDGS) demonstrates preserved glucose metabolism. Our goal was to compare the results of both methods in a retrospective study.

Methods: We evaluated 71 pts (58 M, 13 F, mean age=58 y). All pts had wall motion abnormalities on rest ECHO and resting perfusion defects on Tc-99m MIBI, none had clinical signs of heart failure. DE was performed with low dose Dobutamine (5-10 μg/kg/min), FDG SPECT with a dual-head camera with UHE collimators and 370 MBq ^{18}F-FDG. FDG SPECT and DE were perfórmed within 2 months of each other in clinically stable pts. Evaluation was blind. Criteria for VM by DE was improved wall motion, by FDG SPECT a perfusion/metabolism mismatch. The identification of VM and non-VM by vascular territory was compared in 34 pts.

Results: Of 71 pts, 21 were not evaluable by DE. Both methods agreed in 42/50 remaining pts (84% concordance), 28/42 had VM, 14/42 had non-VM. Of 8 discordant pts, 3 had VM by FDGS, 5 by DE. Localization of VM/non-VM by vascular territory agreed in 30/34 evaluated pts (88%).

Conclusions: VM assessment was similar with both methods, agreement in VM localization was also excellent. Both methods can be used interchangeably. We believe DE is the method of choice because of its lower cost and wider availability. Its main disadvantage in our series was the failure to evaluate 30% pts.

PS_13

GUIDE TO DECIDE THE PET ACQUISITION AND INCORPORATION IN THE VIRGEN DEL ROCIO UNIVERSITY HOSPITALS

I. Borrego, R. Vázquez, P. Gómez, J. López, R. Alvarez. Nuclear Medicine Diagnosis Unit. Virgen del Rocio University Hospitals. Sevilla. Spain.

OBJECTIVE: Presentation of GANT (New Technologies Acquisition Guide) to analyse cost and opportunity of introducing PET in the Virgen del Rocío University Hospitals.
METHOD: Thanks to GANT, decisions, strategy of programme and management are much easier when a new technology is incorporated. Taking into account the possible side effects produced by the use of PET, Virgen del Rocío Universities Hospitals is applying GANT, after checking the scientific literature and clinical, economic, social prospects as well.
RESULTS: Description: At present, PET is still in a diffusion stage. Though some indications are still discussed, its level of implantation is deficient in our area. Clinical Aspects: It is a diagnosis for patients treatment suffering from cancer, heart and neurological disease. Its indications will be specified in the document about the adequate use of PET, written by a group of experts coordinated by Andalucia Health Technology Evaluation Agency (AETSA). It is estimated that 1500 patients per year, could be treated, most of them included in the oncology field. It is a non-aggressive technique with the capacity of early diagnosis and with more sensitiveness than conventional techniques. This method avoids the use of aggressive techniques and surgery. Organization and Management: The PET unit of Virgen del Rocío University Hospitals will attend all patients from the western Andalucia provinces (Cádiz, Córdoba, Huelva, and Sevilla). Morphological techniques, as well as agressive studies and surgery will be reduced a 20 %. Time of hospitalization for lung cancer, colorectal, lymphoma and melanoma malignant diseases will also be reduced. Apart from the clinical tasks, the Unit will have to develop financed research and assess the usefulness of PET in connection with AETSA. Finally, it will carry out training programmes especially thought for specialists education. Financial Aspect: The economic assess backed the acquisition of two equipments, instead of out source contract for explorations.
CONCLUSIONS: The cost-opportunity analysis advised buying PET instead of the outsource services. Taking into account our community«s needs (7.5 million inhabitants), it was decided to buy two PET systems. The development of a guide for clinical know-how and for a rational use of PET in Andalucia was estimated necessary.

PS_14

THE TREND AND CURRENT DEMAND OF PET IMAGING IN A COMMUNITY HOSPITAL: THE FINANCIAL IMPACT OF ONCOLOGIC APPLICATIONS

C.Y.O. Wong, J.C. Hill, M. Gaskill, D. Fink-Bennett, D. Kondas, E.A. Hill, R. Sharma, R. Nunez, H. Balon, C. Dickinson, H. DworkinPET Center, Dept of Nuclear Medicine, William Beaumont Hospital, Royal Oak, USA.

Aim: To analyze the trend and current demand of clinical PET imaging in a large comprehensive community hospital, which has services in all major medical disciplines and assess the financial impact. Methods: The database containing clinical data and report of PET scans, including both the dedicated ring system PET camera and gamma camera positron coincidence imaging (PCI) was analyzed from Y92 to Y00. The PET procedures were grouped into oncology, cardiology and neurology. Results: The demand for oncologic PET increased exponentially from 1.3% of the total procedures in Y92, to 77.6% in Y00. The greatest amplitude of growth occurred after 1998 when medicare (a US government program) started to reimburse certain cancers. Among 1978 PET scans performed in Y99-00, 1242 (63%) was in oncology: single pulmonary nodule (SPN) and lung cancer (847/1242=68%), lymphoma (8%), melanoma (2%), colorectal (6%), esophageal (2%) and other (14%) cancers. A quarter (502/1978=25%) was in neurology: dementia (25%), CNS tumor (20%), epilepsy (9%) and trauma (10%). The rest (234/1978=12%) was in cardiology: 16% for perfusion vs. 84% for viability. Only 31 out of 1978 (1.6%) scans were performed by PCI. The revenue generated by PET imaging accounted for 40% of the total departmental income, which was roughly equal to that of myocardial perfusion imaging by SPET. Conclusion: There is high demand of oncologic PET imaging (68% of total PET scans) in a community hospital which impacts greatly in the running of Nuclear Medicine service, both financially and clinically. About half of the total PET scans is in lung cancer and SPN. This analysis is important to coup with changing medical environment and survival of clinical PET center. Due to great potential for future growth, the results of the analysis are also important in the reallocation of human resources in the Nuclear Medicine department.

PS_15

COMPARISON OF TWO-DIMENSIONAL AND THREE-DIMENSIONAL IMAGING IN THE CASE OF ONCOLOGICAL PATIENTS

M. Voth (1), T. Opfermann (1), S. Käpplinger (2), D. Gottschild (1). (1) Nuclear Medicine, Friedrich-Schiller-University, Jena; (2) Siemens, Erlangen, Germany.

In the present study, the clinical results in two-dimensional (2D) and three-dimensional (3D) aquisition mode were compared.
Methods: 30 oncological patients were observed with F-18-FDG in a 2D whole body routine scan (5 or 6 bedpositions), followed by one bedposition scan in 3D technique in a region with detected lesion. Data was aquired with a Siemens ECAT Exact PET Scanner. Both 2D and 3D data were reconstructed using iterative reconstruction (2 iterations with 8 subsets). A visual interpretation of contrast, identifiability, geometrical form and a quantitative evaluation (SUV and metabolic extention) was performed
Results: No clinically relevant differences in detection of lesions between 2D and 3D mode was found by the qualitative and quantitative analysis. The contrast, geometrical form and the SUV compared side by side showed small differences.
Conclusions: Based on this preliminary results, it seems that 3D technique is equal with 2D in clinical oncological PET.

PS_16

COMPARISON OF DUAL-HEAD COINCIDENCE DETECTION F-18 FDG PET WITH TC-99M MIBI PLANAR AND SPET TO EVALUATE SUSPICIOUS BREAST LESIONS

S.N. Yoon, C.H. Park, K.H. Hwang, C.W. Joh. Department of Nuclear Medicine, Ajou University School of Medicine, Suwon, Korea.

Recently PET study became possible using a hybrid SPET/PET system by adding coincidence module to a dual-head gamma camera and by using 18FDG.
Methods: We evaluated 28 patients with suspected breast cancer by MIBI planar, MIBI SPET and FDG gamma camera PET (CoDe PET). Pathologic results were reviewed to evaluate usefulness of different imaging protocols. Images were visually assessed.
Results: Histology revealed breast cancer in nineteen patients. Both F-18 FDG and Tc-99m MIBI SPET demonstrated focal uptake suggesting breast cancer in two lesions which MIBI planar image missed. With respect to nine benign lesions, both FDG CoDe PET and MIBI planar/ SPET yielded two false positive scans. MIBI planar, MIBI SPET and FDG CoDe PET revealed sensitivities of 81%, 94% and 93%, respectively for detection of primary breast cancer. MIBI planar, MIBI SPET and FDG CoDe PET revealed specificities of 75%, 78% and 78%, respectively.
Conclusion: It appears feasible to perform PET in patients with breast cancer cost effectively utilizing a hybrid SPET/PET gamma camera. Our results indicate that F-18 FDG CoDe PET and Tc-99m MIBI SPET showed improved sensitivity than planar MIBI scintimammography.

PS_17

RECENT FEMORAL ARTERIAL CATHETERISATION IS ASSOCIATED WITH INCREASED FDG UPTAKE IN THE GROIN

T. Akhurst (1), Y. Fong (3), L.A. Brody (2), G. Getrajdman (2), K.T. Brown (2), H.W.D. Yeung (1), S.M. Larson (1). (1) Nuclear Medicine Service, Department of Radiology; (2) Department of Radiology; (3) Department of Surgery, MSKCC, New York NY, USA.

Aim: Patients with low rectal cancers may present with metastases in the inguinal regions as the venous and probably lymphatic drainage of the low rectum is via the "systemic" rather than the "portal" route. We investigated the hypothesis that femoral catherisation prior to FDG PET scanning could conceivably interfere with staging the groin in such patients.
Methods: 97 patients with colorectal cancer metastatic to the liver were studied with FDG PET as part of a prospective trial examining the efficacy of FDG PET scanning in staging patients prior to hepatic resection. All patients were studied on a dedicated BGO based PET system, with all studies attenuation corrected and iteratively reconstructed. Of these 97 patients, 35 were studied post right femoral puncture for CTAP, with the remainder (n=61) being studied prior to femoral catheterization. One patient's groin was not included in the field of view.
Results: In those patients studied after femoral catheterization there were a number of patterns of FDG uptake seen, the first being diffuse arterial uptake, the second being uptake along the catheter track and the final pattern being focal uptake in the region of the track. In all cases the pattern of uptake was able to be distinguished from a pattern of uptake seen in malignant inguinal or femoral adenopathy as may be seen with low rectal cancers. The patients with the highest degree of uptake were studied with PET between 5 -10 days post arterial catherisation (see scatter plot). The mean differences in the SUV from the right to the left groin within those patients studied post catheterization were statistically significantly different mean left groin 1.463 +/-0.378, mean right = 3.43+/-1.77. By paired t test, the difference of the means was 1.967, t=6.6, p<0.0001. In those patients studied prior to catherisation there was a minor difference in uptake from the right to left leg, mean right = 1.546 mean left=1.424 differences of the means 0.122 t=2.662 p=0.01.

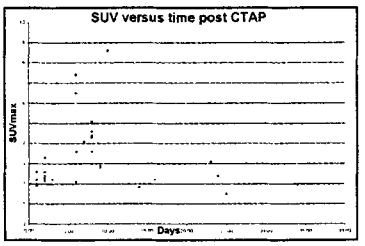

Conclusions: Groin hypermetabolism is to be expected after femoral arterial catheterization. In those patients in whom groin metastases could be expected, an FDG PET scan should where possible precede the CTAP. Clinical history is helpful in distinguishing between arterial puncture and pathological FDG uptake, and the pattern of uptake is also suggestive. Although the numbers are small peak uptake appears to occur around days 5-10 post catheterisation.

PS_18

RISING TUMOR MARKERS IN CANCER PATIENTS - THE ROLE OF COMBINED CAMERA-BASED PET/CT USING F-18 FLUORODEOXYGLUCOSE (FDG)

O. Israel, M. Mor, R. Bar-Shalom, J. Sachs, N. Yefremov, Z. Keidar. Department of Nuclear Medicine, Rambam Medical Center and Faculty of Medicine, Technion, Haifa, Israel.

Aims: To assess the role of a new imaging camera-based PET and CT technology (Hawkeye VG, Elgems, GEMS), which uses combined transmission and emission tomography (TET) in the evaluation of cancer patients (pts.) with rising serum tumor markers and normal or inconclusive imaging studies.
Methods: Combined PET/CT was performed after injection of 10 mCi F-18 FDG, in 23 pts. with known malignancies. Twelve pts. had GI tract tumors, three pts. each had carcinoma of the breast and pancreas, two pts. each had carcinoma of the ovary and lung and one patient had a prostate carcinoma. All pts. were referred for evaluation by TET due to rising values of serum tumor marker and no definite evidence for metastases or recurrence on anatomic imaging modalities. Results of FDG-TET were correlated to biopsy results, or imaging and clinical follow up. Differential diagnosis of FDG uptake, the precise localization of lesions and detection of previously unknown sites of disease were recorded.
Results: Sixteen pts. had a positive FDG-TET study. In nine of these pts. FDG-TET provided additional information of clinical value. In four pts. TET allowed for retrospective lesion identification as cancer-related pathology by better definition of inconclusive CT findings with congruent FDG uptake. Final diagnosis of active cancer was made by biopsy (2 pts.) or clinical follow up (2 pts.). In three pts. TET allowed for precise localization of PET findings on a normal CT as a guide for further imaging or invasive procedures. Cancer was proven in these cases by clinical follow up (2 pts.) and biopsy (1 pt.). In 2 pts. TET allowed for better assessment of inconclusive PET findings by excluding the presence of cancer in areas of FDG uptake unrelated to disease (post-surgical scar tissue and physiologic excretion in colon).
Conclusions: Present data demonstrate the clinical value of TET in 39% of pts. evaluated for rising tumor markers and normal or inconclusive imaging studies. In this selected group of pts. TET provided additional information, improved the accuracy of both the PET and CT studies and guided further diagnostic procedures.

PS_19

THE CLINICAL VALUE OF MOLECULAR COINCIDENCE DETECTION IMAGING WITH [18]F-FDG IN THE DIAGNOSIS OF TUMOR

R.F. Wang, H.X. Hu, Y. Fan, Z.L. Fu, C.L. Zhang, G.Y. Zhao, Y.F. Wang, J.H. Lin. Department of Nuclear Medicine, Peking University First Hospital, Beijing, China.

Aim: To validate the application of 2-[fluorine-18]-fluoro-2-deoxy-D-glucose (FDG-18F) molecular coincidence detection (MCD) in tumor metabolism imaging and evaluate its clinical value.
Methods: One hundred and seventy-nine patients with suspicious of primary or recurrent cancer from out or in-patients were studied using FDG-18F MCD imaging. The images with attenuation correction (AC) and without AC (NAC) were reconstructed iteratively, and the ratio of tumor-to-background (T/B) was calculated in both AC and NAC images. Sixty-six patients with cancer and 10 patients with benign lesions determined histopathologically were analyzed.
Results: FDG-18F imaging results in 63 of 66 patients with cancer showed one or more abnormal radioactivity concentrated regions with T/B>2.0. but in 3 cases with lung adenocarcinoma, rectal and hepatic carcinoma didn't demonstrate abnormal FDG uptake. The sensitivity was 95.5%. In 10 patients with benign lesions, FDG-18F images of 7 cases showed no abnormal radioactive accumulation and 3 cases including 2 cases of inflammatory lesions and 1 case of tuberculosis focus showed abnormal high glucose uptake. Both false positive and false negative cases were 3. The specificity was 70%, with positive predictive value of 95.5% and negative predictive value of 70%, and the diagnostic accuracy was 92.1%. The treatment project of thirty-seven patients with tumor in this study was changed according to FDG findings.
Conclusion: FDG-18F MCD/AC imaging is a high technique and new imaging modality which has distinctive advantages in obtaining tumor cell metabolism statue information, differentially diagnosing malignant from benign lesion, tumor staging and grading, predicting therapeutic efficacy and prognosis.

PS_20

DO THE SERUM GLUCOSE LEVELS AFFECT THE NON-SPECIFIC COLONIC ACTIVITY IN WHOLE BODY FDG-PET?

N.V. Ghesani, H.M. Zhuang, F. Ponzo, A. Alavi. Hospital of the University of Pennsylvania, USA.

Non-specific colonic activity in whole body FDG-PET can sometimes interfere with optimal interpretation in certain circumstances such as in the setting of abdominal lymphoma and colon cancer. Unfortunately, it is common to observe colonic activity in FDG-PET imaging and the mechanism of colonic activity is less clear. Several reports have indicated that gastric uptake in FDG-PET is correlated with serum glucose level. The **aim** of this study was to assess whether the non-specific colonic activity is also correlated with serum glucose level at the time of FDG injection.
Methods: 177 patients who had FDG-PET for evaluating lung nodules and had no history of diabetes or inflammatory bowel disease were retrospectively reviewed. All patients had their serum glucose determined just before intravenous injection of FDG. FDG-PET images were obtained using a C-PET camera (ADAC). The degree of colon uptake was scored as 0 to 3 with hepatic uptake as internal standard (0: no uptake; 1: uptake less than hepatic uptake; 2: uptake equals to hepatic uptake; 3: uptake more than hepatic uptake).
Results: 121 patients had colonic activity while 56 patients did not have colonic activity. The average serum glucose level in patients with colonic activity was 95.2 mg/dl, which was not statistically different (P=0.95) from that of (94.3 mg/dl) the patients without colonic activity. In patients with colonic activity, 60.3% (n = 73) had FDG uptake in the ascending colon, 41.3% (n = 50) the transverse colon, 69.4% (n = 84) the descending colon and 32.2% (n = 39) the sigmoid colon. The ascending colon received the highest average score (1.18) with the sigmoid colon the least score (0.49). However, none of the scores from any segment of colon correlated with the serum glucose level (p >0.1 for all groups).
Conclusion: Different from FDG uptake by stomach, serum glucose level at the time of FDG injection is not a significant factor contributing to non-specific colonic activity in FDG-PET imaging.

PS_21

QUANTITATIVE ACCURACY OF PET IMAGES OF SHORT ACQUISITION TIME OBTAINED BY SEGMENTED ATTENUATION CORRECTION AND ITERATIVE RECONSTRUCTION

K. Sugimoto (1), S. Nishizawa (2), T. Tsuchida (1), H. Ito (1), Y. Yonekura (2). (1) Department of Radiology; (2) Biomedical Imaging Research Center, Fukui Medical University, Fukui, Japan.

Segmented attenuation correction with iterative reconstruction (SAC/IR) yields better image quality from the PET data of short acquisition time. Quantitative accuracy of SAC/IR applied to 2D FDG-PET data of short acquisition time was investigated by comparing SAC/IR with measured attenuation correction and filtered back-projection (MAC/FBP).

Methods: Quantitative accuracy of SAC/IR images of 2-min emission and 1-min transmission scans (fast SAC/IR) was evaluated in relation to the number of subsets (from 7 to 56, iteration 2). Quantitative values of fast SAC/IR were compared with those of standard MAC/FBP images of 10-min emission and 10-min transmission scans (Hanning filter, cutoff: 0.5 cycles /pixel). For this purpose, both phantom and clinical studies were performed. By means of phantom study, signal to noise ratio (SNR) in fast SAC/IR image was compared with that of standard MAC/FBP in relation to the number of subsets. Quantitative accuracy of SAC/IR in cold areas was also assessed by using NEMA phantom with three cold areas (air, water and Teflon). In clinical studies performed in 10 patients with lung tumors, SUVs were obtained from lung tumors (hot spot), muscles (intermediate) and lung fields (cold area) and were compared between fast SAC/IR and standard MAC/FBP.

Results: With the number of subsets smaller than 21, % noise obtained from the fast SAC/IR of the uniform phantom was identical to or less than that of standard MAC/FBP. Errors of quantitative values in the cold areas decreased as the number of subsets increased. Although the cold area of Teflon had negative values in MAC/FBP images, SAC/IR images always kept positive values and an error was less than 5% with the number of subsets larger than 28. In the analysis of SUV, the number of subsets that yielded minimal errors including lung tumors, muscles and lung fields was 21.

Conclusion: By choosing the optimal number of subsets, fast SAC/IR images keep the quantitative accuracy identical to standard MAC/FBP images.

PS_22

FACTORS AFFECTING NON-PATHOLOGICAL GASTRIC UPTAKE IN WHOLE BODY FDG-PET IMAGING

T. Tomemori, M. Kitagawa, T. Nakahara, K. Nakagawa, K. Uno, J. Wu, K. Abe, K. Tomiyoshi, M. Kawano. Nishidai Clinic Diagnostic Imaging Center, Itabashi-Ku Tokyo, Japan.

Positron emission tomography (PET) using 2-deoxy-2-[^{18}F]-fluoro-D-glucose (FDG) is very useful for the detection and staging of tumors. However it is known that FDG uptake also occurs the normal tissue in various degrees and this physiologic FDG uptake can be often confused with malignant tumor. The aim of this study was to identify factors influencing physiologic FDG uptake in stomach.

Methods: A total of 136 persons who underwent staging of tumors except for gastric cancer or cancer screening using FDG whole-body PET was examined (mean age 55.6 yrs). All subjects fasted for at least 4 hours before the PET study and were administrated with FDG intravenously (mean FDG dose 308.9 MBq). Emission images were acquired on a whole-body PET scanner and images were reconstructed without attenuation correction. The intensity of gastric uptake of FDG whole-body PET image was visually classified into 3 grades; grade 2 = the intensity of gastric uptake more than pulmonary uptake, grade 1= the intensity of gastric uptake equal to or less than pulmonary uptake, grade 0 = no contrast between gastric uptake and background.

Results: Twenty-eight subjects (20.6%) were classified into grade 2, 42 subjects (30.9%) were grade 1 and 66 subjects (48.5%) were grade 0. Subject's age, fasting time, FDG dose, serum glucose level, free fatty acid level and insulin level were not significant correlated with the intensity of gastric uptake. But the subjects with higher gastric uptake tended to be positive anti-Helicobacter pylori (H. pylori) antibodies. The positive rate of anti-H.pylori antibodies in the cases with grade 2 of gastric uptake is significantly higher than grade 1 (85.7% vs. 69.0%, $p<0.05$), and that in the cases with grade 1 is significantly higher than grade 0 (69.0% vs. 40.9%, $p<0.01$).

Conclusion: Gastric uptake was detected in about half of subjects. Especially, high gastric uptake was seen in 20%. High gastric uptake was associated with H.pylori infection. It was suggested that the subjects with high gastric uptake have gastritis, gastric ulcer and so on. So it is important that these subjects were diagnosed with endoscopy and treated for H.pylori infection.

PS_23

QUANTITATIVE POSITRON EMISSION TOMOGRAPHY (PET) WITH FDG IN MALIGNANT TUMORS AND CORRELATION TO GENE EXPRESSION

L.G. Strauss (1), R. Koomägi (1), A. Dimitrakopoulou-Strauss (1), T. Heichel (2), T. Lehnert (3). (1) German Cancer Research Center, Heidelberg, Germany; (2) Dept. of Orthopedic Clinics, Univ. of Heidelberg, Heidelberg, Germany; (3) Dept. of Surgery, Univ. of Heidelberg, Heidelberg, Germany.

Aim: Association of quantitative PET data and expression of genes in malignant tumors.

Methodology: PET examinations with FDG were performed in 42 patients with malignant tumors (soft tissue and bone sarcomas, breast ca.) prior to treatment. Data were acquired dynamically for 60 min following the intravenous application of FDG using a PET ring system (ECAT HR+, Siemens Co.). Cross sections were iteratively reconstructed and quantitatively evaluated with volume-of-interests (VOIs). A two compartment model was used to assess the FDG kinetics. Furthermore, a non-compartment model was used to calculate the fractal dimension from the dynamic data. Tumor specimen were obtained when the patients were directed to surgery. Quantitative RT-PCR was used to quantify the expression of mdr1, mrp, cyclin A and gst. Furthermore, the HC-G110 and HU-95A chip (Affymetrix Co.) were used in selected patients to assess the expression of a variety of genes in the tissue samples.

Results: The FDG uptake, as measured by SUV, demonstrated a broad overlap for the different tumor tissues. However, the kinetic parameters (K1-k4, distribution volume) provided more detailed information regarding histology and grading. Fractal dimension was increased as compared to reference data, giving evidence for a more "chaotic" distribution of the FDG metabolism in the malignancies. An inverse association was observed for the expression of mdr1 and the FDG uptake in the tumors. We noted a nonlinear correlation between the kinetic FDG data and the quantitative expression of mdr1 and cyclin A. The gene chip data revealed an increase in a variety of cancer genes: human interferon-inducible protein 9-27, c-myc, v-fos, brca2.

Conclusions: The full kinetic analysis of dynamic PET data provides additional information for the biological characterisation of malignant tumors. The use of gene expression data gave evidence for an association of quantitative FDG kinetic parameters and the expression of resistance and cell cycle genes.

PS_24

HEAD-TO-HEAD COMPARISON OF FULL RING AND GAMMA CAMERA BASED PET SCANNERS: A SYSTEMATIC REVIEW

L.M. Haslinghuis-Bajan (1), L. Hooft (2), A. Van Lingen (1), M. Van Tulder (2), W. Deville (3), G.S. Mijnhout (1), O.S. Hoekstra (1). (1) Department of Nuclear Medicine, Free University Medical Center, Amsterdam, The Netherlands; (2) Department of Clinical Epidemiology & Biostatistics, Free University Medical Center, Amsterdam, The Netherlands; (3) Institute for Research in Extramural Medicine, Amsterdam, The Netherlands.

Aim: While clinical oncology gradually accepts FDG PET, the role of dual-head coincidence gamma camera systems (DHC) is less clear. The optimal design to assess the relative merits of systems with similar physiological basis is to compare the alternative scan technique (DHC) with the reference method (PET) in the same patient. To summarize the available evidence on this issue we performed a systematic review of such studies.

Methods: Using a validated search algorithm (Haslinghuis et al. Eur J Nucl Med 2001) nine studies were identified. Two independent observers assessed the methodological quality using the criteria of the Cochrane Methods Group on Screening and Diagnostic Tests (levels of evidence 1- 4), and extracted relevant data (type of tumor, size, location in the body, imaging modality, uptake intensity).

Results: Level 2 evidence was provided by 3 studies, versus level 4 by 6 (level 1 highest, level 4 lowest). Methodological limitations were especially related to blinding and standardization. Five studies provided detailed data on individual malignant lesions: 134/159 (84%) were detected with either modality. Lesion diameters (CT based) were mean=2.9 cm (sd=1.8 cm), with 25% ≤ 1.5cm. The observed contrast at DHC was 64±24% of the non-attenuation corrected PET signal (n=73, $p<0.001$). Quantitative analysis of data on individual malignant lesions (provided in 5 studies) showed that, as expected, contrast at PET and DHC-PET concordance were positively related. Multivariate logistic regression showed that PET-DHC concordance could be predicted ($p<0.001$) as a function of lesion size (OR 3.7, 95% CI 1.8-7.6) and location in the body (OR 0.14, 95% CI 0.04-0.43, abdomen=1, chest=0). The model was correct in 86% of the published lesions.

Conclusions: If applied in a relevant patient spectrum, head-to-head studies can help to provide diagnostic algorithms using DHC as a filter for PET. Knowledge about lesion size and location, can predict the difference in diagnostic performance between the two devices. Furthermore, we conclude that proper blinding and standardization is essential for a meaningful head-to-head comparative study.

PS_25

AN ATTEMPT TO REDUCE PHYSIOLOGICAL FDG ACCUMULATION IN THE HEART AND STOMACH USING HEPARIN

Y. Nakamoto, Y. Nakamoto, E. Tadamura, S. Saga, M. Ishimori, H. Mamede, J. Konishi. Department of Nuclear Medicine, Kyoto University, Kyoto, Japan.

Aims: In interpreting metabolic images obtained by positron emission tomography (PET) using F-18-fluoro-2-deoxy-D-glucose (FDG) for oncological patients, intense physiological uptake is sometimes cumbersome. A reverse correlation has been observed between the FDG uptake in the heart and stomach, and serum free fatty acid (FFA) concentration. The aim of this study is to investigate the feasibility of heparin pretreatment for reduction of physiological uptake in these organs.

Methods: Ten healthy male volunteers (age, 23-38; mean 30.5 y.o.) underwent PET scan twice, one with heparin infusion (2500IU), the other with saline infusion. Heparin infusion 30 min prior to FDG injection caused significant elevation of serum FFA (3045.3±1606.8 mEq/L), compared to control study with saline (609.3±316.2 mEq/L). FDG uptake in the heart and stomach was evaluated visually using 4 grading scores (0 = negative, 1 = weak, 2 = fair, and 3 = intense) with a consensus of 2 nuclear medicine physicians. For a quantitative analysis of the heart, the metabolic rate of glucose (MRG) (mmol/min/g) and K complex (/min) were calculated for both studies.

Results: Qualitative analysis demonstrated myocardial uptake was lower in heparin study than in control study, which was not statistically significant (p=0.06). In the stomach, uptake was diminished in 3 of 5 cases, but no significant difference was found (p=0.25). MRG of the septum, anterior wall and lateral wall of the heart were 0.15±0.08 vs 0.08±0.07 (p=0.02), 0.14±0.06 vs 0.08±0.07 (p<0.01), and 0.16±0.08 vs 0.09±0.07 (p=0.01), respectively. Likewise, K complexes were 0.032±0.016 vs 0.020±0.017 (p=0.02), 0.031±0.012 vs 0.019±0.015 (p<0.01), and 0.034±0.015 vs 0.021±0.016 (p=0.02), respectively.

Conclusion: Our preliminary data suggest that simple heparin infusion has a potential to decrease the physiological uptake in the heart, although it did not show sufficient effects for reducing the tracer activity in the stomach. Further investigations may be needed to determine optimal dose and the mode of administration.

PS_27

INFLUENCE OF THE SIZE OF THE LESIONS FOR THE DETECTION WITH [18F]-FDG OF COLORECTAL CANCER RECURRENCES USING A HYBRID CDET GAMMACAMERA

F. Montravers, D. Grahek, K. Kerrou, V. de Beco, C. Colombet-Lamau, Y. Petegnief, O. Vandici, N. Younsi, J.N. Talbot. Service de Médecine Nucléaire, Hôpital Tenon, Paris, France.

Our objective was to determine if FDG scan performed on a CDET gammacamera was efficacious in detection of small colorectal recurrences as compared with histology and measurement of the size of the resected sites.

Methods and patients:

After fasting for 6h or more, 3-5 MBq/kg of [18F]-FDG were injected i.v. and imaging (whole-body scan and at least a tomoscintigram) was started 45 min. later, using a dual-head MARCONI gammacamera with sodium iodine crystal 19 mm thick. Iterative reconstruction was used and no attenuation correction by an external source was applied. Among 98 examinations followed by surgery, performed between July 1997 and January 2001, we considered only the 41 cases with measurement, by the anatomopathologist, of the size of the malignant lesions.

Results:

Final histology with size measurement was available on 76 malignant lesions in these 41 patients. Of 76 measured malignant lesions, 45 were > 1 cm and 31 were < 1 cm. FDG-CDET correctly detected 39/45 supracentimetric recurrences (Se = 87 %) and 8/31 centimetric or infracentimetric recurrences (Se =26 %). (Table details the results according to the topography of the lesions).

	Lung	Liver	Lymph node	Peritoneal or abdominal nodules
> 1 cm	10 TP	14 TP	2 TP	13 TP
	1 FN	3 FN	1 FN	1 FN
< 1 cm	2 TP	5 TP	1 TP	0 TP
	11 FN	5 FN	1 FN	6 FN

The smallest size of the detected lesion was 0.8 cm in the thorax and 0.8 cm in the abdomen.

Conclusion: These results show that it is possible to detect centimetric or infracentimetric recurrences of colorectal cancer both in the abdomen and in the thorax when using a CDET gammacamera. As for dedicated PET systems, the sensitivity of detection of these small lesions significantly decreases compared to the sensitivity of detection of larger lesions.

PS_26

CLINICAL ONCOLOGY IMAGING WITH THE ECAT EXACT HR+ OPERATED IN 3D

T. Beyer (1), R. Nicoletti (2), T. Bruckbauer (1), D. Rocak (3), R. Aigner (2). (1) CTI PET Systems Inc., Knoxville, USA; (2) Karl-Franzens-University, Department of Radiology, Graz, Austria; (3) Technical University, Institute of Technical Physics, Graz, Austria.

Aim. While Positron Emission Tomography (PET) is intrinsically a volume imaging technique, most PET exams in clinical oncology today are performed in 2D. Retraction of the inter-plane septa, and subsequent 3D acquisition mode offer higher sensitivity, which can be translated into lower injected doses *or* shorter emission scan times while maintaining image quality. We report on our experience with the introduction of 3D PET imaging protocols for clinical oncology exams using the ECAT EXACT HR+.

Methods. Standard 2D PET protocols at the PET center in Graz involve a 370MBq injection of FDG followed by a 45-60min uptake period. Whole-body (WB) FDG-PET studies are performed over six to eight bed positions scanned in 2D emission (Em) and 2D transmission (Tx) mode for 6min and 3min, respectively, thus yielding a total scan time of one hour and more per patient. Daily throughput is limited to six WB patients. To validate potential 3D acquisition protocols we have performed a series of single-bed patient studies at comparable activity levels.

Following the standard 2D WB protocol a lesion site was chosen from the reconstructed WB image, and the patient was repositioned in the scanner, such that the chosen lesion was located in the center of the FOV (for maximum sensitivity). A 2D Em scan of 6min was followed by a dynamic 3D Em scan (6x1min), and a 3min post-injection 2D Tx scan. Em images were reconstructed using AW+OSEM with 2 iterations and 8 subsets. We compared the corrected emission images for the following combinations of Tx/Em scan time [min]: 3/6min for 2D, and 3/2, 3/3, 3/4, 3/5, and 3/6 for 3D. The images were validated visually, and ROI analysis was used to estimate the lesion contrast in 2D and 3D for different scan time combinations.

Results. In a preliminary series of 10 patients we found that similar image quality was achieved in 2D and 3D with a 3D Em scan of half the 2D Em scan time. For very thin patients Em scan time could be reduced to 2min without sacrificing diagnostic utility. By optimizing the processing of the attenuation data Tx scan time could also be reduced.

Conclusion. Operating this state-of-the-art PET tomograph in 3D brought about a reduction in WB scan time of at least 30% at no cost to the image quality but to much relief of the patient.

DIAGNOSTIC ONCOLOGY 2

PS_28

THE USE OF 18F-FDG PET IN THE STAGING OF PATIENTS WITH MALIGNANT LYMPHOMA: COMPARISON WITH CONVENTIONAL STAGING

K. Taborska (1), J. Slaby (2), O. Belohlavek (1), D. Janeba (1), M. Trneny (2), P. Klener (2). (1) Dept.of Nuclear Medicine, Na Homolce Hospital, Prague, Czech Republic; (2) 1-st Dept. of Medicine, Charles University General Hospital, Prague, Czech Republic.

Aim: Accurate assessment of disease extension in patients with malignant lymphoma is important for therapy management. This study was undertaken to compare the results of initial conventional staging in patients with Hodgkin disease (HD) and non-Hodgkin lymphoma (NHL) to those with 18F-FDG PET imaging.

Methods: We studied 40 consecutive patients (16 men, 24 women, age range 17-71 y.); 27 patients at diagnosis and 13 patients at relapse; 27 NHL (20 aggressive, 7 indolent) and 13 HD. Conventional staging included physical examination, CT of thorax, abdomen and pelvis and bone marrow biopsy. Attenuation corrected PET imaging was performed by dedicated ECAT EXACT PET scanner from the base of the skull to the upper thighs 1 hour after intravenous administration of 18F-FDG (7,6 ± 1,3 MBq/kg). For purpose of this study PET scans were evaluated visually by one observer without knowledge of any clinical data and were classified as positive, equivocal or negative for disease. The sites of disease were assessed for each patient at the following regions: neck, axilla, groin, bone marrow, lung, mediastinum, liver, spleen, retroperitoneum and abdomen.

Results: PET imaging identified 96 positive sites of lesions compared with 85 ones identified by conventional procedures, discordance was detected at 58 sites (most results were not checked by other methods). The highest number of discordance (11) was identified in bone marrow: PET was false negative in 7 of 9 patients at sites confirmed by biopsy; vice versa only PET was positive in 4 additional patients (1 confirmed by MRI, 1 by clinical follow up, 2 unresolved). Considering only PET, 3 patients would be free of disease (2 indolent NHL, 1 MH), 8 patients would be downstaged (7 due to false negative bone marrow finding) and 7 patients would be upstaged in comparison to conventional staging. In our series PET initiated real changes of staging in 5 patients (3x from stage II to IV, 2x from stage I to stage II) resulting in changes in therapy.

Conclusions: 18F-FDG PET scans give additional information for staging of patients with malignant lymphoma. In our series PET changed therapy in 12,5 % (5/40) patients. PET has complementary role to bone marrow biopsy and both methods seem to be necessary for appropriate staging.

PS_29

DETECTION OF TUMOR PROGRESSION IN THE FOLLOW-UP OF IRRADIATED LOW GRADE GLIOMAS: COMPARISON OF 18F-FLUORODEOXYGLUCOSE PET, 123I-[ALPHA]-METHYL-L-TYROSINE SPECT AND 99M TC-SESTAMIBI SPECT

M. Henze (1), A. Mohammed (1), W. Mier (1), H. Schlemmer (3), K. Herfarth (4), J. Debus (4), M. Eisenhut (1,2), U. Haberkorn (1,2). (1) Dept. of Nuclear Medicine, University of Heidelberg, Germany; (2) Clinical Cooperation Unit Nuclear Medicine; (3) Division Oncological Diagnostics and Therapy; (4) Clinical Cooperation Unit Radiation Oncology, German Cancer Research Center, Heidelberg, Germany

Aim: MRI often fails to distinguish progressive tumor from radiation injury because both types of lesion can show a Gd-DTPA enhancement. A known drawback of FDG PET for the evaluation of malignant lesions in the brain is its limited sensitivity due to high cortical uptake. Our aim was to assess the potential of alternative SPECT tracers in the same patients.
Methods: 35.3 ± 21.0 months after stereotactic radiotherapy (59.0 ± 4.4 Gy) of low grade gliomas (LGG; median WHO II), 17 patients presenting 26 Gd-DTPA-enhancing lesions on MRI were examined by PET and SPECT. Lesions were classified as progressive tumor (PT, n = 17) and non-PT (NPT, n = 9, including radiation injury and stable disease) based on prospective follow-up (clinically, MRI, ^{1}H MR spectroscopy) for 28.1 ± 10.0 months after PET / SPECT. In all patients, PET scans 60 min after injection of 209 ± 40 MBq ^{18}F-2-fluoro-2-deoxy-D-glucose (FDG) were acquired. Lesion to normal ratios (l/n) were calculated based on standard uptake values of the lesion and the contralateral gray- ($l/n_{FDG\ gm}$) and white-matter ($l/n_{FDG\ wm}$). In 15 patients, two SPECT scans were started 15 and 60 min after injection of 694 ± 67 MBq ^{99m}Tc-hexakis-2-methoxyisobutylisonitrile (^{99m}Tc-sestamibi). ^{123}I-α-methyl-L-tyrosine (IMT) SPECT was acquired in all patients 15 min after injection of 285 ± 59 MBq. For SPECT examinations, l/n-ratios for IMT (l/n_{IMT}) and sestamibi (l/n_{MIBI}) were calculated using a reference region mirrored to the contralateral hemisphere.
Results are given in the table. Sensitivities and specificities are based on the following cut-off values: $l/n_{FDG\ gm}$ 0.6, $l/n_{FDG\ wm}$ 1.4, l/n_{IMT} 1.3 and l/n_{MIBI} 1.3. For FDG and IMT, significantly higher ratios were found in PT as compared to NPT ($l/n_{FDG\ gm}$, $l/n_{FDG\ wm}$ and l/n_{IMT}: $p<0.001$). Using sestamibi, there was no statistically significant difference (l/n_{MIBI} $p=0.21$) between PT and NPT.

	FDG PET (gm)	FDG PET (wm)	IMT SPECT	MIBI SPECT
Sensitivity	83%	83%	94%	53%
Specificity	78%	89%	100%	75%
PT-group : l/n (mean ± s.d.)	1.1 ± 0.5	2.4 ± 1.0	1.8 ±0.4	3.7 ± 2.8
NPT-group: l/n (mean ± s.d.)	0.5 ± 0.1	1.1 ± 0.3	1.1 ± 0.1	1.8 ± 1.8

Conclusion: Contrasting to sestamibi SPECT which showed a wide overlap between the PT and NPT group, the sensitivity as well as the specificity of IMT-SPECT was even higher as compared to FDG-PET. IMT is considered to be a useful tracer for differentiating PT from NPT in the follow-up of irradiated Gd-DTPA enhancing LGG.

PS_30

FDG-PET HAS A HIGHER SENSITIVITY THAN CT FOR DETECTING NODAL DISEASE IN STAGING LOW-GRADE LYMPHOMA

L. Kostakoglu (1), J.P. Leonard (2), M. Coleman (3), H. Zoe (1), S. Vallabhajosula (1), S.J. Goldsmith (1). (1) New York Presbyterian Hospital Weill Cornell Medical Center Divisions of Nuclear Medicine; (2) Hematology/oncology; (3) The Center for Lymphoma And Myeloma, New York, NY, USA.

FDG-PET is highly sensitive in identifying disease sites in aggressive non-Hodgkin's lymphoma (NHL), its value in low-grade NHL, however, has not been studied with a large number of patients. The aim of this study was to compare the findings of FDG-PET (dual-head camera with attenuation correction) and CT for identification of nodal disease sites in low-grade NHL at initial diagnosis or at clinical relapse.
Methods: Thirty-two contemporaneous FDG-PET and CT were performed on patients with low-grade NHL (16 follicular lymphoma-mixed cell type, 9 follicular lymphoma-small cleaved cell type, 7 follicular lymphoma-small lymphocytic type). All patients underwent staging with CT of the chest, abdomen and pelvis and whole-body FDG-PET. Disease sites were correlated on a site-by-site basis on both FDG-PET and CT. Discordant FDG-PET and CT findings were confirmed by clinical evaluation and repeat FDG-PET and CT.
Results: FDG-PET detected a total of 219 disease sites. There was discordance in the number of disease sites between FDG-PET and CT in 11 patients. In 10 of 11 patients, FDG-PET detected more disease sites than CT at 33 sites (15%) (5 head/neck, 19 chest, 11abdomen/pelvis). CT detected one additional site of disease not detected by FDG-PET (iliac;1.5 cm;small lymphocytic type). In the discordant group, FDG-PET detected 52% more nodal disease sites in mixed cell lymphoma group, 50% more disease in small cleaved cell group, and only 14 % more in small lymphocytic cell group than CT. According to the disease location, sensitivity of FDG-PET was better than CT mostly in the chest; 32% more nodal sites were detected by FDG-PET as compared to CT. In the head/neck and abdomen/pelvis, FDG-PET detected 10% more nodal sites for each location and missed one site in the pelvis. In this group, FDG-PET findings did not change staging of disease.
Conclusions: FDG-PET has significantly greater sensitivity than CT (99.5% vs. 85%, respectively) in detecting nodal disease in low-grade NHL. Although FDG-PET did not affect disease staging, evaluation of response to therapy is primarily dependent on accurate pre-therapy assessment of extent of disease.

PS_31

CAMERA-BASED WHOLE TRUNK FDG PET IN THE STAGING OF MALIGNANT LYMPHOMAS

K.H. Hwang (1), C.H. Park (1), S.N. Yoon (1), H.C. Kim (2), H.S. Kim (2), C.W. Joh (1), J.S. Jang (1). (1) Department of Nuclear Medicine; (2) Department of Hematology-Oncology, Ajou University School of Medicine, Suwon, Korea.

Objectives : This study was performed to evaluate the clinical usefulness of whole trunk F-18 FDG coincidence PET (CoDe-PET) imaging in the staging of malignant lymphomas.
Materials and methods : Thirty-four patients with histologically proven malignant lymphoma underwent F-18 FDG CoDe-PET using a dual-head gamma camera equipped with coincidence detection circuitry for staging before treatment. Histological subgroups included low (3), intermediate (14), high (3), undetermined (8) grades non-Hodgkins' lymphoma and Hodgkins' disease (6). 30 CoDe-PET studies were done for initial staging and 4 for re-staging after relapse. The entire trunk from the cervical to the inguinal regions were scanned. Attenuation correction was not made and image reconstruction was done using filtered back-projection. CoDe-PET images were compared with corresponding CT or MRI and the lymphomatous involvements identified by both CoDe-PET and CT/MRI were regarded as actual locations of disease. Discordant results were verified with biopsy or clinical follow-up.
Results : A total of 68 lymphomatous involvements were noted on both CoDe-PET and CT. CoDe-PET detected 19 additional lymphomatous lesions not identified by CT or MRI. Of them, three were true-positive (extra-nodal involvements), two false-positive. CT or MRI demonstrated 9 more lymphomatous lesions not shown on CoDe-PET and only one was confirmed positive. Four of 9 were small intra-abdominal nodal lesions less than 1.5 cm. Staging was changed from _ to _ in three patients by CoDe-PET by depicting extra-nodal involvements and from I to II in one by detecting nodal involvement.
Conclusion : Camera-based whole trunk FDG PET without attenuation correction is clinically acceptable for staging malignant lymphomas especially in the assessment of extra-nodal involvement. However, in the detection of nodal involvement, it should be used in conjunction with CT or MRI.

PS_32

EVALUATION OF BONE MARROW INFILTRATION IN LYMPHOMA PATIENTS WITH FDG PET

L.Y. Zhang, G. Chen, X.F. Jiang, H. Wang, P.Y. Li. Department of Nuclear Medicine, Ruijin Hospital, Shanghai Second Medical University, Shanghai, China.

Purpose: To investigate the efficacy of FDG PET whole body scan as a alternative method to evaluate bone marrow infiltration in patients with malignant lymphoma.
Method: 28 patients with either non-Hodgkin's lymphoma (NHL; n=18) or Hodgkin's disease (HD; n=10) were studied FDG PET scan following injection of 0.065mCi/kg body weight 18FDG. Attenuation correction was performed in all cases. Visual analysis was used to detect lymph node and to evaluate the uptake of FDG at liver and marrow. Unilateral iliac crest marrow aspirates and biopsies were performed on all patients. Bone marrow that involved by the disease was represented by the increased marrow uptake of FDG and graded as normal or abnormal using visual grading system through comparing the FDG uptake at marrow and liver.
Results: PET scan showed 17/28 patients had FDG uptake at their lymph node. FDG bone marrow grading and marrow histology agrees in 24/28 patients, being concordant positive in 7 and concordant negative in 17 patients. In 2 patients the FDG uptake at marrow were inhomogeneous with focal FDG hot spots but staging biopsy was negative. In 2 patients the marrow biopsy specimen was positive but the marrow grading by FDG uptake was negative. These two patients had NHL whose malignant cells did not take up FDG at lymph node.
Conclusion: Marrow FDG uptake showed by PET study can correctly assess marrow disease status in a high proportion of lymphoma patients. PET has the potential to reduce the need for staging marrow biopsy.

PS_33

COMPARISON OF FDG PET AND GALLIUM SCINTIGRAPHY IN LYMPHOMAS

D. Huglo (1), A. Delcourt (1), F. Morsschauser (2), E. Hector (1), T. Prangere (1), M. Steinling (1). (1) Department of Nuclear Medicine; (2) Department of Haematology, Hopital Huriez, CHU of Lille, Lille, France.

Aim: As we had access to a dedicated PET scanner for several months only 80 km from our hospital, we evaluated the results of PET clinical examinations for patients with lymphomas and those by gallium scintigraphy and compared the two methods wherever this was possible.
Method: The haematologists were free to prescribe the examination that seemed most appropriate. Because of administrative procedures and the timetable for PET use, 4 weeks were needed to obtain an appointment and accordingly the indications were restricted to an evaluation of the response to treatment. The PET was conducted using a Siemens CTI ECAT scanner 1 hour after intravenous injection of 370 MBq of Fluorodeoxyglucose, without transmission scan. The gallium scintigraphy was performed using a DST XLI (SMV) gamma-camera 48 or 72 hours after injection of 185 MBq of gallium citrate. A bone scintigraphy was sometimes performed before this scintigraphy.
Results: Twenty four PET were conducted since June 2000 on 23 patients. Fourteen of these 23 patients had received from 1 to 5 gallium scintigraphies (1 in 8 patients, 2 in 2 patients, 3 in 2 patients and 5 in 2 patients). Comparisons between the two methods were possible for 10 examinations in 9 patients : 6 Hodgkin's lymphomas and 3 non-Hodgkin's. A difference in favour of the FDG was obtained in 2 patients (a residual sub-clavicular mass in 1 case, a mediastinal in another, with normal gallium scintigraphies). There was agreement in 6 cases (normal examinations in 3 patients, abnormal ones at the same site in 3 other cases for 2 patients). There was partial agreement in 2 patients (a 4th site detected with FDG not seen with gallium in 1 case, 5 additional sites with FDG in the other case). All the sites were more clearly visible and easier to locate with FDG. There were no false positives with gallium.
Conclusion: Only 60 % of the patients who were given a PET also received a gallium scintigraphy. Prescriptions for the PET therefore seemed to be more frequent that those of gallium scintigraphy. The results of FDG in the evaluation of the response to therapy were better than those of gallium, but in a situation where access to PET is limited, gallium could be used as a first resort and FDG could be used only when the gallium scintigraphy is negative.

PS_34

RADIONUCLIDE IMAGING OF HODGKIN'S DISEASE: A PROSPECTIVE COMPARISON OF 18FDG-PET AND 67GA-SPECT FOR MONITORING RESPONSE TO TREATMENT

J.N. Rini (1), E.Y. Manalili (1), G. Karayalcin (2), M.B. Tomas (1), M.A. Hoffman (3), B. Mehrotra (3), C.J. Palestro (1). (1) Division of Nuclear Medicine, Long Island Jewish Medical Center, New Hyde Park, New York, USA; (2) Division of Pediatric Hematology Oncology Schneider Children's Hospital, Long Island Jewish Medical Center, New Hyde Park, New York, USA; (3) Division of Hematology Oncology, Long Island Jewish Medical Center, New Hyde Park, New York, USA.

Aim: We compared the efficacy of ^{18}FDG-PET and ^{67}Ga SPECT imaging for assessing response to treatment in 22 patients with Hodgkin's disease (HD). Methods: 22 patients (12-56 years old (mean age 26); 12 male, 10 female) with previously untreated Hodgkin's disease (19 nodular sclerosing, 2 mixed cellularity, and 1 lymphocyte-depleted) are included. Stages of disease include Stage IA=1; IIA=7; IIB=3; IIIA=3; IIIB=3; IVB=5. Imaging was performed before and after chemotherapy (2-7 month interval between baseline and follow-up studies). All 22 patients had baseline studies demonstrating ^{18}FDG and ^{67}Ga avid disease. All patients received GCSF. For ^{18}FDG-PET, patients fasted $\geq$6 hours. Imaging was performed from head to upper thigh 1 hour after injection of 150-220 MBq ^{18}FDG. After ^{18}FDG-PET, patients were injected with 250-370 MBq ^{67}Ga citrate and imaged 72 hours later. Whole body images and SPECT were performed from head to mid thigh. A single reader independently reviewed the ^{18}FDG-PET and ^{67}Ga SPECT studies blinded to all others results. Studies were classified as positive, equivocal, or negative for disease in the following sites: head/neck, thorax, axilla, abdomen and pelvis. Results of scan interpretations were correlated with outcome. Results: Clinical follow up performed up to 24 months after diagnosis showed all patients in remission with no evidence of relapse. 17/22 had negative ^{18}FDG-PET and ^{67}Ga SPECT follow-up studies (true negative (TN)); 2/22 had abnormal uptake of both tracers in the thorax and 1/22 in the spleen (false positive (FP)); 1/22 had abnormal ^{18}FDG uptake in the thyroid (FP) and negative ^{67}Ga scan (TN), and 1/22 had ^{67}Ga uptake in the right groin (FP) and a negative ^{18}FDG-PET study (TN). The overall accuracy of both tracers was 81%. Conclusion: These data indicate that in Hodgkin's disease, ^{18}FDG-PET is comparable to ^{67}Ga SPECT for diagnosis and monitoring response to treatment. The advantages of ^{18}FDG-PET, including shorter time period between injection and acquisition and improved visualization of abdominal disease, make this the radionuclide imaging procedure of choice in Hodgkin's disease.

PS_35

PREDICTION OF I-131 THERAPEUTIC RESPONSE BY F-18 FDG PET IN PATIENTS WITH RECURRENT OR METASTATIC THYROID CANCER AND NEGATIVE IODINE SCAN

B.I. Kim, G.J. Cheon, W.I. Yang, J.S. Lee, C.W. Choi, S.M. Lim, S.W. Hong. Department of Nuclear Medicine, Korea Cancer Center Hospital, Seoul, Korea.

F-18 FDG PET and iodine scan have a complementary role in detection of recurrent or metastatic thyroid cancer. According to the dedifferentiation of differentiated thyroid cancer, there are discrepancies between the findings of F-18 FDG PET and Iodine scan. In the patients with suspected recurrent thyroid cancer and iodine negative scan, we are in a dilemma to decide further treatment plans. The aim of this study was to evaluate the ability of F-18 FDG PET to predict the therapeutic response of high dose I-131 therapy in the patients with recurrent or metastatic thyroid cancer and negative iodine scan.
Methods: 15 patients with suspected recurrent or metastatic papillary thyroid cancer and negative iodine scan underwent F-18 FDG PET (4 men and 11 women, mean age: 51±10). The tumor-to-background ratio (TBR) was measured for the lesions that were positive for FDG uptake. After I-131 high dose therapy (dose 176 mCi in 9 patients, 200 mCi in 6 patients), F-18 FDG PET, sTg, and measurement of tumor size were performed (mean follow-up period: 13.6±5.3 months) to evaluate the therapeutic response (improved/ stationary/ aggravated). Correlation between TBR and therapeutic response was evaluated by Spearman rank correlation.
Results: Three patients improved, 10 patients were stationary, and 2 patients aggravated after I-131 therapy. TBR of each therapeutic response group (improved/ stationary/ aggravated) was 5.1±0.24, 7.3±3.27, and 14.5±3.59, respectively and there were a tendency of difference between the groups (p=0.06 by Kruskal-Walis one-way ANOVA test). There were a statistical tendency in counter-correlation between TBR and therapeutic response (rho= –0.393, p=0.08 by Spearman rank correlation), which means that patients with low TBR on F-18 FDG PET had a possibility of I-131 high dose therapeutic response.
Conclusions: F-18 FDG PET could have a possibility to predict I-131 therapeutic response of patients with differentiated thyroid cancer and negative iodine scan. However, statistical significance and optimal cut-off value of FDG uptake should be determined in further study.

PS_36

THE IMPACT OF NON-DEDICATED POSITRON EMISSION TOMOGRAPHY (NPET) ON THE TREATMENT STRATEGY OF CANCER PATIENTS

F. Giammarile, C. Desuzinges, P. Chauvot. Department of Nuclear Medicine, Centre Léon Bérard, Lyon, France.

OBJECTIVE: T evaluate both the accuracy of a coincidence gamma camera (NPET) using 2-[F18] fluoro-2-deoxy-D-glucose (FDG) and the impact of FDG imaging on the treatment strategy of cancer patients.
METHOD: In our institution, between January and December 2000, 186 patients (113 male and 73 female, mean age 47.5 years), underwent 198 examinations for malignancy by means of FDG imaging. 36 patients presented colon cancer, 30 patients lung cancer, 28 patients (33 examinations) malignant lymphoma, 28 patients (35 examinations) germ-cell tumor, 19 patients thyroid cancer, 14 patients breast cancer, and 31 patients others solid tumors.
The NPET studies were performed after intravenous administration of 2 MBq/kg of FDG, using a three-head gamma camera (coincidence detection working on two heads, for the first 123 examinations) IRIX GAMMA PET 2 (MARCONI MEDICAL SYSTEMS)
Validation of the FDG imaging findings has been carried out by histopathologic examination and/or clinical follow-up longer than 6 month. Clinical strategy decisions were then taken on the basis of the validated NPET findings.
RESULTS: 82 observations could not be taken into account for this study due to the lack of gold standards. NPET correctly identified the majority of the lesions previously assessed by conventional imaging (US, CT, MRI). FDG imaging provided 4 false positive cases, due to inflammatory diseases and 13 false negative cases, mostly because of non detectable lesions (<15 mm). According to the histopathologic and clinical findings, sensitivity, specificity and positive predictive value of NPET in detecting malignant lesions were 84%, 88% and 95%, respectively. NPET provided additional information on patients' clinical status in 25 cases. This result modified the treatment strategy in 19 cases (over 116). In 9 cases unnecessary surgery was avoided; in 7 cases the effectiveness of non considered surgical treatment was proved; in the latter 3 cases chemotherapeutic strategy was modified.
CONCLUSION: NPET is an accurate diagnostic tool that provides additional information and can affect clinical decision strategy in the treatment of cancer patients.

PS_37

FDG-PET ASSESSMENT OF THE TIME SCHEDULE OF EVALUATION OF THE THERAPEUTIC EFFECT OF CHEMO-RADIATION THERAPY FOR PATIENTS WITH MALIGNANT TUMORS OF THE HEAD AND NECK REGION

K. Torii, T. Okamura, K. Koyama, J. Kawabe, H. Sakamoto, H. Ochi, R. Yamada. Department of Radiology, Osaka City University, Osaka, Japan.

Aim: In our hospital, chemo-radiation therapy is usually performed initially for patients with malignant tumors of the head and neck region. After evaluation of therapeutic effect, the next treatment is determined. In addition to CT examination, FDG-PET studies are performed to evaluate changes in glucose metabolism of malignant tumors before to after chemo-radiation therapy. However it is not established when post-treatment FDG-PET should be performed.
Methods: Eight patients with malignant tumors of the head or neck region underwent FDG-PET before and after chemo-radiation therapy. (1: pharyngeal carcinoma, 3: tongue carcinoma, 1: oral floor carcinoma, 1: maxillary sinus carcinoma, 1: oropharyngeal carcinoma, 1: hypopharyngeal carcinoma). FDG-PET was performed a total of 3 times; the first examination was carried out within 10 days before the start of irradiation, the second examination 2 weeks after irradiation (shortly after irradiation in 2 cases), and the third examination 4 weeks after irradiation. On the images obtained as described above, a region was established in the area of the primary focus, the standardized uptake value (SUV) was obtained, and values were compared. To compare the degree of decrease in SUV between the 1st-2nd measurements and the 1st-3rd measurements, the slope of decrease for each [(2nd SUV-1st SUV)/interval (days), (3rd SUV-1st SUV)/interval (days)] was obtained.Results: SUV was 9.15±2.89 before treatment, 5.17±2.04 at 2 weeks after the end of irradiation and 4.10±1.83 at 4 weeks after the end of irradiation. In all cases but one, SUV decreased in order of examination time. Regarding the rate of this decrease, the slope of decrease for the 2 week period after irradiation exhibited a good correlation with that for the 4 week period after irradiation (n=8, R=0.974).Conclusions: Evaluation of efficacy of radiotherapy combined with chemotherapy by FDG-PET has to date been performed at 4 weeks after the end of irradiation. The present examination, however, showed that the therapeutic effect at 4 weeks after irradiation could be estimated based on the results obtained at 2 weeks after irradiation, indicating that earlier decision concerning subsequent treatment is possible.

PS_38

PROGNOSTIC VALUE OF FDG PET AND COMPUTED TOMOGRAPHY (CT) AFTER 3 AND 6 CYCLES OF CHEMOTHERAPY IN PATIENTS TREATED BY ADDITIONAL HIGH-DOSE CHEMOTHERAPY FOR HIGH-GRADE NON-HODGKIN'S-LYMPHOMA (NHL)

U. Cremerius (1), U. Fabry (2), J. Wildberger (3), M. Zimny (1), B. Nowak (1), P. Reinartz (1), K. Setani (1), W. Schaefer (1), R.W. Guenther (3), R. Osieka (2), U. Buell (1)(1) Department of Nuclear Medicine; (2) Department of Internal Medicine IV; (3) Department of Radiology, Technical University, Aachen, Aachen, Germany.

Aim: Comparison of FDG PET and CT for assessment of therapy response in patients with high-grade NHL in whom additional high-dose chemotherapy (HDChx) with autologous stem cell transplantation (ASCT) was performed.
Methods: Included were 10 consecutive patients aged 27-64 yrs., who were studied by whole-body PET and CT of neck, chest and abdomen before therapy, after 3 and after 6 cycles of conventional chemotherapy. The lesion with highest FDG-uptake was taken as a reference and the standardised uptake value (SUV) was quantified using the maximum pixel value. Disappearance of all hypermetabolic foci was termed complete metabolic response (CMR), SUV reduction >50% partial metabolic response (PMR). Tumor response in CT was classified complete remission (CR), complete remission unconfirmed (CRu), partial remission (PR), stable disease (SD) or progressive disease (PD) according to recent international guidelines for NHL (Cheson et al. 1999). Progression-free survival (PFS) was chosen as end point. Kaplan-Meier analysis and log-rank test were performed to evaluate the impact of PET and CT findings on PFS.
Results: 5 patients relapsed after a median interval of 5 months (range 2-9), while 5 patients remained in stable remission for 15 months (range 7-23). Therapy response assessed by PET after 6 therapy cycles predicted the final outcome ($p<.05$; CMR vs. less than CMR), while CT was not predictive ($p=.39$; CR/CRu vs. less than CRu). After 3 therapy cycles neither PET ($p=.14$; CMR/PMR vs. less than PMR) nor CT ($p=.34$; CR/CRu/PR vs. less than PR) were predictive. All patients with stable remission after HDChx and ASCT had reached PMR (or CMR) after 3 cycles and CMR after 6 cycles.
Conclusions: FDG PET after 6 cycles of chemotherapy for high-grade NHL has a higher prognostic value than CT. HDChx and ASCT may not be an effective additional treatment in patients, who had not reached a complete metabolic response before.

PS_39

COMPARISON OF F-18 FLUOROETHYL-L-TYROSINE AND F-18 FLUORODEOXYGLUCOSE TRANSPORT KINETICS WITH RADIO SENSITIVITY OF DIFFERENT CARCINOMA CELLS IN VITRO

J. Förster (1), T. Held (1), T. Renné (1), M. Kunkel (2), R. Jacob (2), A. Enk (3), J. Brockmann (4), F. Rösch (4), M. Schreckenberger (1), P. Bartenstein (1). (1) Department of Nuclear Medicine; (2) Department of Maxillofacial Surgery; (3) Department of Dermatology; (4) Institute of Nuclear Chemistry, University Mainz,Germany

Aim: It is well known that fast tumor progression often correlates with radio sensitivity. Metabolic activity of tumors mirrors growth and can be quantified using uptake of PET-tracers as F-18 fluoroethyl-L-tyrosine (FET) or F-18 fluorodeoxyglucose (FDG) that resemble amino acid or glucose metabolism, respectively. However, prediction of radio sensitivity in early tumor stages is difficult. For the in vitro correlation between of radio sensitivity and the surrogate markers amino acid or glucose metabolism, we established cell culture models based on different tumor entities.
Methods: Human cell lines derived from squamous cell carcinomas PCI13, A549 and melanoma Mel624 were cultured. Confluent cells were radiated with doses of 25, 50, 75, and 100 Gy. Following incubation for 48 hr, total protein concentration of survived cells was determined. Tracer uptake of untreated cells was measured by gamma counting after incubation with 0.5 MBq/ml FET or FDG in the supernatant for 1, 3, 8, 15, 30 or 5, 10, 20, 30, 60 min, respectively, and standardized to identical protein concentration. Specific uptake inhibitors served as negative controls.
Results: Radio sensitivity was cell type specific and correlated to the radiation dose. Survival after 48 hr following 100 Gy was 23, 68 and 90% for PCI13, Mel624, and A594, respectively. For both tracer, all tested cell lines has a specific uptake that followed an exponential kinetic and depended on the cell number. For FET A549 had maximum uptake (arbitrarily set to 100%) followed by Mel624 (44%), and PCI13 (43%). In contrast, order of FDG tracer uptake was PCI13 (100%), Mel624 (52%), and A549 (16%).
Conclusion: For the investigated cell lines, uptake kinetics for amino acid and glucose metabolism showed no correlation. High FDG uptake paralleled with high radio sensitivity whereas FET showed no concordance. Our data support in vivo observations that glucose is a better marker for radio sensitivity compared to amino acid metabolism.

PS_40

A HEAD TO HEAD COMPARISON BETWEEN LEUKOSCAN AND TC-99M-LEUKOCYTES IN THE ASSESSMENT OF INFLAMMATORY BOWEL DISEASE

M.P.M. Stokkel, H.I.E. Reigman, E.K.J. Pauwels. Department of Nuclear Medicine, Leiden University Medical Center, Leiden, The Netherlands.

Ulcerative colitis (UC) and Crohn's disease (CD) are the most important chronic inflammatory bowel diseases (IBD). Assessment of IBD is based on the patient's clinical condition, on laboratory parameters, radiological examinations and endoscopy. In this respect, however, Tc-99m white bloodcell scintigraphy (WBS) is highly accurate and the most patient-friendly diagnostic procedure. A main disadvantage of WBS is the time-consuming aspect. The aim of the present study was to evaluate the role of Tc-99m LeukoScan in the assessment of IBD.
Methods: All patients with an exacerbation of IBD and at least a grade II disease activity in 2 bowel segments on WBS were included in the present pilotstudy. The interval between WBS and imaging with LeukoScan ranged from 2 to 7 days, while no medication was initiated during this interval. Up to 5 hours after the injection of 500 MBq of Tc-99m Leukoscan acquisition was performed. Planar images were performed at 1,3 and 5 hours p.i., whereas whole body scintigraphy and SPECT were performed only at 3 hrs. p.i. All patients underwent endoscopy with an interval of 14 days. A relative sensitivity of at least 90% was agreed upon to accept LeukoScan for further studying. Subsets of 3 patients were evaluated each time to decide wether to continue or to stop the pilot-study. The maximum number of patients that could be included in the present studied was 15.
Results: In six patients included in the present study, WBS clearly demonstrated increased activity in at least two segments. In three out of six patients studied, slightly increased uptake was seen intraabdominal 3 hours after the administration of LeukoScan. Since these sites did not correspond with the sites of infection, it was assessed to be excretion by the liver. The overall quality of the LeukoScan images was good, whereas the whole body images demonstrated a normal, physiologic distribution pattern. Nevertheless, WBS was better than imaging with LeukoScan in the assessment of IBD.
Conclusion: Tc-99m LeukoScan is no alternative radiopharmaceutical in the assessment of IBD. A prospective study is not justified due to the false negative results

PS_41

COMPARISON OF SULFUR COLLOID AND LABELED RBC METHODS IN DETECTING LOWER GASTROINTESTINAL BLEEDING IN PRACTICAL PRACTICE

F. Ponzo, L.B. Lacorte, H.M. Zhuang, M. Pourdehnad, F.M. Liu, A. Alavi. Hospital of the University of Pennsylvania, USA.

Background: Nuclear medicine study is more sensitive than angiography for detecting lower GI bleeding. However, controversy exists over which nuclear medicine imaging technique to use in this setting. The objective of this study was to assess whether labeled RBC method has practical advantages over sulfur colloid (SC) method in a busy clinical situation.
Methods: 338 continuous GI bleeding studies in our center from 1996-2000 were retrospectively reviewed. Among them, there were 174 Tc-99m SC scans, which lasted 30 minutes, and 137 RBC scans which lasted 60 minutes. In addition, there were 27 scans started with 30 minute SC method followed by up to several hour RBC methods. The relation of the methods and the findings were analyzed.
Results: Among 174 scans using SC method, 46 (26.4%) successfully identified the location of bleeding. Among 137 scans using RBC method, 37 (27.0%) were successful. The difference in the proportion of positive studies between SC method and RBC method is not statically significant (p=0.92). For 27 scans started with SC method and followed by RBC method, 4 (14.8%) positive bleeding were identified in prolonged period. Among these 4 positive results, only one of them was identified within 1 hour of the beginning of the study.
Discussion: Although RBC method has a theoretical advantage over SC method, in reality it is difficult to keep patients under the camera for indefinite time in a busy practice. In addition, RBC method involves extra steps to handle the patient's blood and increases chances of iatrogenic errors. The reason for the further identification of bleeding site in the studies using SC followed by RBC is likely due to prolonged imaging time but not method used per se.
Conclusion: the simpler SC method is as efficient as RBC method if the scanning time is not further prolonged.

PS_42

OESOPHAGEAL TRANSIT AND DISINTEGRATION OF PLACEBO TABLET FORMULATIONS

A.C. Perkins (1), M. Frier (1), R.M. Vincent (1), P.E. Blackshaw (1), R.J. Dansereau (2), R.C. Spiller (1). (1) University Hospital, Nottingham, UK; (2) Procter and Gamble Pharmaceuticals, Cincinnati, USA.

Introduction: Bisphosphonates are a class of synthetic compounds used in the treatment of osteoporosis and Pagets disease. There have been clinical reports of adverse events including pill-induced oesophagitis, ulceration and dysphagia, following impaired swallowing of bisphosphonate formulations[1]. In this study scintigraphy was used to compare the esophageal transit of two different shaped (oval and round) tablets used for bisphosponate therapy, when swallowed with minimal volumes of water (30 and 50 mL).
Methods: Placebo tablets were manufactured to contain 5mg Sm oxide and placed in a nuclear reactor for 48h to produce 1MBq Sm-153 at time of dosing. 31 healthy postmenopausal women mean age 63 years (range 55 - 74 years) were randomized into a four-way crossover study. Subjects swallowed the tablets with 30 or 50 ml of water and dynamic images acquired.
Results: The mean oesophageal transit time of the oval tablet was significantly shorter than that of the round uncoated tablet for both volumes of water. In 3 subjects who swallowed the round tablet with 30 mL of water, the esophageal transit was greater than 10 minutes.

Oesophageal transit as a function of formulation and volume of water swallowed

Esophageal transit	30 mL Water		50 mL Water	
	Oval Tablet (N = 28)	Round Tablet (N = 30)	Oval Tablet (N = 29)	Round Tablet (N = 30)
Mean ± SEM, (sec)	3.2 ± 0.3	65.2 ± 32.8	2.3 ± 0.2	3.4 ± 0.4
Min Max (sec)	0.5, 6.5	1.5, 596	1.0, 5.5	1.0, 10.0

Conclusion: This study demonstrates how scintigraphy can be used to examine the effects of shape and dosing parameters on tablet swallowing. Additional information such as time of disintegration, gastric emptying and reflux can also be measured.

.[1] deGroen, P. C., *et al.*, 1996. Esophagitis associated with the use of alendronate. New England Journal of Medicine, 335(14), 1016-1021.

PS_43

COMPARATIVE STUDIES OF THE GALLBLADDER (GB) MOTILITY BY BOLUS (BC) AND INFUSION (IC) CHOLESCINTIGRAPHY

V. Artiko (1), V. Obradovic (1), M. Petrovic (2), N. Petrovic (1), M. Milicevic (2), M. Matovic (1), K. Kostic (1), V. Bosnjakovic (1). (1) Institute for Nuclear Medicine; (2) Institute for Digestive Diseases, Clinical Center of Serbia.

The aim of the study is the estimation of the GB motility parameters before and after stimulation. MATERIAL AND METHODS: BC was performed with 185 MBq 99m-Tc-EHIDA (CCK-OP 30 ng/kg i.v. in 60th min). IC (150 MBq, 99m-Tc-EHIDA, 0.25 mg/ml) lasted 3h (10ml/h), preceeded by a loading dose (two eggs in 120th min).
RESULTS: In the controls with stimulation (BC/IC;n=10/8) appearance time (AT) was registered earlier with BC (X=9.80+/-5.1 min) than with IC (X=23.38+/-16.3 min) (p<0.05). Also, in comparison to BC (X=30.50+/-12.77 min),filling time (FT) was prolonged with IC (X=74.5 +/-18.4 min)(p<0.01). However, ejection fraction (EF) didn't depend upon the method performed (BC:X= 75.58+/-8.31%; IC:X=76.7+/-11.9)(p>0.05). Emptying time (ET) was shorter (X=17.10+/-6.33) and ejection rate (ER) faster (X= 4.82+/-1.85%/min) with BC comparing to IC (X=37.8+/-11.4 min; X=2.32+/-0.8%/min).During ICH, spontaneous EF and ER (n=13) are X=42.1+/-7.2% and X=1.97+/-1.22%/min. After stimulation (n=8) these values are higher (p <0.05) (X=76.7+/-17.9% and X=2.32+/-0.81%/min). ET shortens (p <0.01) after stimulation from X=56.8+/-26.0 min to X=37.8+/-11.4 min. However, AT and FT didn't differ in response to stimulation (p>0.05). In the 15 patients with chronic cholecystitis and calculosis examined with BC EF and ER were lower (X=22.44+/-17.71% and X=2.24+/-1.88%/min) than in the controls after stimulation (p<0.01). EF and ER obtained by IC in 6 patients were also decreased (p<0.01) (X=47.2+/-6.9% and X=1.05+/-0.41%/min).
CONCLUSION: EF is the only parameter that does not depend upon the method performed in the controls and patients. Among the parameters studied, EF and ER are significantly decreased in patients with altered GB contractile function comparing to the controls. BCH is a feasible and reliable method, but ICH is carried out in more physiological conditions: the steady state of the 99m-Tc-EHIDA in hepatocytes and GB is achieved.

PS_44

COMPARISON OF TWO SAMPLE AND CONVENTIONAL MULTIPLE SAMPLE METHODS IN THE DETERMINATION OF GASTRIC EMPTYING

T.Y. Erdil (1), F. Dede (1), T. Ones (1), O. Noshari (1), N. Imeryuz (2), T. Turoğlu (1). (1) Department of Nuclear Medicine, Marmara University Hospital, Istanbul, Turkey; (2) Nephrology Section, Department of Internal Medicine, Marmara University Hospital, Istanbul, Turkey.

Since solid phase gastric emptying is linear, solid phase half-life of gastric emptying (T1/2) is usually calculated by processing protocols applying linear fit. The aim of our study is to determine the best time for two sample method for the calculation of gastric emptying using multiple sample method as a reference. Methods: The study was performed in 26 patients (aged 20-56 years) after a 12 hour fasting. Patients ingested a Tc-99m tin colloid labelled egg meal cooked to a firm consistency. Scintigraphic acquisitions were obtained every 5 min for 30 min and every 10 min thereafter in anterior and posterior projections until we reached the 10% of the initial activity. The patient was in the sitting position during acqusition. T1/2 of gastric emptying was calculated from the geometric mean of the anterior and posterior counts of the stomach. T1/2 was determined by multiple sample method and by two sample method from 60 min, 90 min, 120 min, 150 min counts (two sample formula: $T\ 1/2 = (T/2)\ X\ [C_0 / (C_0 - C_T)]$). The mean difference (systemic bias) between multiple sample and two sample studies were expressed as a percentage of the mean value of the two studies, and the standard deviation of these percentages represented the accuracy. Results: The mean of T1/2 of multiple sample and 60. min, 90 min, 120 min, 150 min was found to be 99.42 ± 28.9, 111.21 ± 43.55, 105.45 ± 32.6, 104.16 ± 29.03 and 104.84 ± 23.43 min respectively.

	Correlation (r)	Regression line (y=)	Accuracy (%)	Systemic bias (%)
60 min	**0.938**	**1.41x-29.3**	**14.2**	**9.99 (-12 to 44)**
90 min	**0.935**	**1.05x+0.65**	**11.3**	**6.57 (-3 to36)**
120 min	**0.938**	**0.94x+10.5**	**15.8**	**6.83 (-9 to 52)**
150 min	**0.882**	**0.71x+33.8**	**22.4**	**9.85 (-13 to 75)**

Conclusion: The best sampling time for two sample method in determining the T1/2 of gastric emptying was found to be 90 min. It might be related to mean T1/2 of our group (99.42 ± 28.9); therefore the sampling time should be selected according to mean T1/2 of gastric emptying for the patient population of each laboratory.

PS_45

DIAGNOSTIC SCINTIGRAPHY FOR BILIARY ATRESIA

F. Chehade (1), M. Habli (1), M. Abou Alfa (1), W. Dayeh (1), A. Zaatari (1), Z. Hammoud (1), F. Fakih (1), E. Hindie (2), C. De Labriolle-Vaylet (2). (1) Hammoud Hospital, Sidon, Lebanon; (2) Hopital Saint Antoine, Paris, France.

Introduction : The biologic liver function tests do not accurately differentiate between neonatal hepatitis and biliary atresia. Hepatobiliary scintigraphy is a non-invasive test that can play an important role in early diagnosis of biliary atresia and other causes of cholestasis. The presence of radiotracers in the intestines rules out biliary atresia and may thus avoid the need of exploratory laparotomy. The rapid extraction of the radiotracer by the liver and the long parenchymatous stasis without excretion in the intestines are observed in biliary atresia. The weak extraction of the radiotracer by the liver without excretion in the intestines reflects the deterioration of the hepatocellular function secondary to either hepatitis or prolonged stasis of biliary atresia.

Materials and Methods : Between 1997 and 2000, 12 hepatobiliary scintigraphies using technetium 99m-labeled mebrophenine (TBIDA) were performed in 10 newborns, aged between 2 weeks and 2 months, with cholestatic jaundice and suspected to suffer from biliary atresia.

Results : Hepatobiliary scintigraphy suggested the diagnosis of biliary atresia in 2 cases, eliminated atresia in 6 cases, and suggested hepatitis in the last 2 cases. A control scintigraphic test done after surgery on a patient with biliary atresia has shown a weak excretion of the tracer in the intestines with stasis and dilatation of the intrahepatic biliary tree (biliary insufficiency). In another newborn, the second scintigraphy confirmed the diagnosis of neonatal hepatitis suspected during the first scintigraphy. These scintigraphic results correlate well with the clinical follow-up and, when performed, subsequent hepatic biopsies, and macroscopic examination of the hepatobiliary tree during laparotomy.

Commentary : The sensitivity of the hepatobiliary scintigraphy using the TBIDA in the diagnosis of biliary atresia was 100 % and the specificity was 75%. In trying to differentiate between biliary atresia and neonatal hepatitis, this test has succeeded to avoid laparotomy in 80% (8 cases out of 10) of newborns who were not all in favorable conditions for surgery.

PS_46

PROGNOSTIC VALUE OF GASTRO-ESOPHAGEAL SCINTIGRAPHY IN YOUNG CHILDREN WITH RESPIRATORY SYMPTOMS

A. Bestetti, S. Fracassi, C. Di Leo, F. Carola, L. Tagliabue, S. Pajoro, G.L. Tarolo. Department of Nuclear Medicine, University of Milan-S.Paolo H., Milan, Italy.

The **aim** of this study was to evaluate the prognostic value of gastro-esophageal reflux in young children with respiratory symptoms with the use of gastro-esophageal scintigraphy.

Methods: A total of 34 children (16 females and 18 males), with a mean age of 26 months (range: 2-156 months) were studied. Twenty one (62%) patients had both respiratory tract symptoms and vomiting, while 13/34 (38%) had only vomiting and regurgitation episodes. After a 4-hour fasting 18/34 children underwent gastro-esophageal scintigraphy via the administration of 15 ml/kg of orange-juice labeled with 2 mCi ^{99m}Tc-sulfur colloid, and the remaining 16 patients underwent gastro-esophageal scintigraphy via the administration of 15 ml/kg of milk labeled with 2 mCi ^{99m}Tc-sulfur colloid. Twenty children (58%) underwent clinical follow-up: the mean duration was 18 months, ranging from 2 months to 40 months.

Results: Eighty-five percent of patients (29/34) were found to have positive gastro-esophageal reflux scan, of these 9 (31%) had positive distal reflux (GER-pd) and 20 (69%) positive proximal reflux (GER-pp). The frequency, duration and degree of reflux episodes were significantly greater in patients with proximal as compared to those with distal reflux ($p < 0.05$). Patients with proximal reflux had significantly prolonged gastric emptying times compared to those with distal reflux. Among 21 patients complaining of respiratory symptoms, 14 (67%) showed GER-pp, 2 GER-pd (10%) and 5 (23%) no reflux. Five of seven (71%) patients with proximal reflux who received oral antacid and prokinetic treatment were asymptomatic at follow-up.

Conclusions: Most young children with respiratory disease had detectable proximal gastro-esophageal reflux. Acid exposure of the proximal part of the esophagus, by setting the stage for micro-aspiration of gastric material into the larynx , remains one of the major causes of damage to bronchial mucosa. Slowed gastric emptying time might be a predisposing factor. These patients should be orally treated with antacid and prokinetic therapy.

PS_47

IMPROVED DETECTION OF INTRAHEPATIC CHOLESTASIS BY DYNAMIC HEPATOBILIARY SPECT WITH OSEM RECONSTRUCTION ALGORITHM

J. Sato (1), N. Shuke (1), Y. Ishikawa (1), A. Okizaki (1), A. Kashiba (1), S. Kasai (2), T. Aburano (1). (1) Department of Radiology; (2) Department of Surgery 2, Asahikawa Medical College, Asahikawa, Japan.

The purpose of this study was to assess the utility of ordered subset expectation maximization (OSEM) reconstruction algorithm in dynamic hepatobiliary SPECT for detecting intrahepatic cholestasis by phantom and clinical studies.

Methods: To compare OSEM and conventional filtered back projection (FBP) algorithms, a phantom study was carried out assuming intrahepatic cholestasis near the high radioactive structures such as gallbladder. Two cylindrical phantoms of 3 cm in diameter, filled with ^{99m}Tc in the several radioactivity ratios (2:1, 5:1, 10:1, 20:1, 50:1), were placed closely in the air and projection data were acquired on a 3-headed digital gamma camera system. The projection data were reconstructed using both FBP and OSEM algorithms. On the reconstructed transaxial SPECT images, delineation of the hot phantoms was compared between FBP and OSEM algorithms. In the clinical study, eight patients with suspected intrahepatic cholestasis (primary sclerosing cholangitis, 1; primary biliary cirrhosis, 1; intrahepatic stone, 4; jaundice of unknown etiology, 1; biloma, 1) were studied. Immediately after an intravenous injection of 185 MBq of Tc-99m-pyridoxyl-5-methyltryptophan (PMT), dynamic SPECT data acquisition was started in a continuous rotation mode with an acquisition time of 60 sec/rotation for 60 minutes. Transaxial SPECT images were reconstructed with OSEM and FBP algorithms and coronal SPECT images were generated. By merging coronal SPECT images, merged anterior projection, equivalent for planar image, were generated for each rotation. SPECT images with OSEM algorithm were compared with those with FBP and also with the anterior projections.

Results: Two cylindrical phantoms in the activity ratios greater than 10 could not be delineated as separated two objects because of streaks artifact with FBP algorithm, but those were delineated well with OSEM algorithm. In the clinical study, detection and localization of intrahepatic cholestasis were obviously improved in dynamic hepatobiliary SPECT with OSEM, compared to those with FBP and to the anterior projection images.

Conclusion: Dynamic hepatobiliary SPECT with OSEM algorithm could delineate the hepatobiliary system without significant artifacts, facilitating the detection of intrahepatic cholestasis.

PS_48

HEPATOBILIARY SCINTIGRAPHY FOR THE COMPARISON OF ORTHOTOPIC AND AUXILLIARY LIVER TRANSPLANTS

A. Aktaş (1), S. Ayaz (1), N. Yoloğlu (1), H. Karakayalı (2), M. Haberal (2). (1) Department of Nuclear Medicine; (2) Department of General Surgery, Başkent University, Ankara, Turkey.

Liver transplants are either orthotopic with the entire donor liver or segments of the donor liver, or auxilliary in which native liver remains and a portion of donor liver is added. The aim of this study was to compare the function of orthotopic and auxilliary liver transplants by the use of hepatobiliary scintigraphy.

Nine patinets with orthotopic and 9 patients with auxilliary liver transplants were included for this study. Scintigraphies obtained 2-3 months after surgery were evaluated and at the time of scintigraphic examination no complication was present. Hepatobiliary scintigraphy was performed after intravenous bolus injection of 185 to 330 MBq Tc-99m mebrofenin. A large field of view camera with low energy all purpose collimator was used for the acquisition. For the evaluation of parenchymal function, data was acquired at every 30 sec for 40 minutes. Hepatocyte extraction potential was calculated by comparing the count rates measured in the liver and in the left ventricle at 5 min after injection. For this, equally sized region of interests were drawn over the left ventricle and over the liver. Mean hepatocyte extraction value for orthotopic and auxilliary liver transplants were 4.15±1.43 and 3.95±1.85, respectively. Although the mean extraction was slightly better for orthotopic than for auxilliary liver transplants, the difference was statistically insignificant.

In conclusion, our results have shown that orthotopic and auxilliary liver transplants demonstrate similar hepatocyte extraction function on hepatobiliary scintigraphy.

PS_49

CCK AUGMENTED CHOLESCINTIGRAPHY. A STUDY TO ASSESS NATIONAL UK PRACTICE AND THE RESULTS OF OUR LOCAL TECHNIQUE

R.H. Ganatra, P. Facey, L. Bartley, J. Jones, J.I.S. Rees. Department of Nuclear Medicine, University Hospital of Wales, Cardiff, UK.

Porcine cholecystokinin (CCK) was a reliable and accepted agent used to measure the gallbladder ejection fraction (GBEF). This measurement is important in the assessment of patients with suspected acalculous cholecystitis. Since the withdrawal of CCK from the UK market in December 1998, many centres have ceased to perform augmented HIDA scans. Sincalide is a synthetically prepared C-terminal octapeptide of cholecystokinin. When injected intravenously it causes gallbladder contraction similar to that which occurs in response to endogenous CCK. However, the use of sincalide has been limited by the lack of knowledge of its existence and by the variety of administration protocols in the literature.

The purpose of this study was twofold. Firstly we wanted to assess a long sincalide infusion technique to measure the GBEF. Secondly we conducted a national postal survey to assess the performance of augmented cholescintigraphy.

We evaluated the GBEF using a continuous sincalide infusion in a series of 20 patients with clinically suspected acalculous cholecystitis. Ultrasound scan was normal in each case. After a four hour fast, sincalide infusion (0.02 mcg/kg diluted in 250 mls. saline) was commenced 60 minutes following injection of Tc^{99m} BRIDA. The infusion was continued for 45 minutes, and dynamic images were acquired for 60 minutes. The calculated GBEF in the 20 patients ranged from 26-97% with a mean GBEF of 73%. Only 2 patients had a GBEF of <35%, (considered to be abnormal). There were no side effects.

Questionnaires were sent to 240 nuclear medicine departments throughout the UK. To date, 140 replies (58%) have been received. Of these 140 centres, 88 had never performed HIDA scans to measure the gallbladder ejection fraction (GBEF) and 38 had stopped performing the study since the withdrawal of porcine CCK. Only 12 centres used sincalide to calculate the GBEF. Twenty-nine centres did not measure the GBEF but used a fatty meal (such as chocolate, milk or Calogen) to assess gallbladder contractility. There was a wide variation in the dose of sincalide (0.009mcg/kg – 0.12mcg/kg), volume of administration (1.4ml – 200 ml), and rate of infusion (0.23ml/min – 6.7ml/min). Many centres were unaware of the existence of sincalide.

We conclude that this infusion protocol gives a good GBEF and we recommend its use. The results of our survey indicate that there is national under-performance of this investigation due to a lack of knowledge of the existence of sincalide and the variety of administration protocols in the literature.

PS_50

FEASIBILITY EVALUATION OF NEW TC-99M-GSA INDEX TO ESTIMATE LIVER FUNCTION WITH A SHORT-TERM ACQUISITION

K. Fujimori, N. Yama, M. Takeda, M. Hareyama. Department of Radiology, Sapporo Medical University, Sapporo, Japan.

Galactosyl human serum albumin (GSA) is an analog of asialo-neoglycoalbumin which binds asialogalactosyl protein receptors only expressed at hepatocytes and Tc-99m-GSA scintigraphy is useful method to evaluate liver function. It usually takes 15 minutes to perform a dynamic acquisition to calculate two standard indexes, a blood clearance index (HH15) and a receptor index (LHL15). Although these indexes are easy to calculate and very useful for patients with sever condition, e.g. with an artificial respirator, it is often difficult to perform 15 minutes dynamic study. We calculated new parameters with early 5-minutes acquisition to evaluate feasibility of liver function estimation with a short-term acquisition.

Methods: Tc-99m-GSA studies were performed in 60 patients with normal liver function to sever liver damage. 185 MBq/3mg of Tc-99m-GSA was injected intravenously and 10 seconds/frame, 64x64 matrix data were acquired to 18 minutes to calculate the receptor amount (Ro) with a non-linear three-compartment model. Five new indexes were calculated with first 5 minutes data: 1) a forward rate constant with Patlak's plot (k-value), 2) a clearance rate of the blood pool activity with mono-exponential fitting (crH), 3) an activity index of the cardiac pool (H5/H1, which is the ratio of the cardiac pool activity at 5 miutes over one minute), 4) an uptake rate of the liver with a reverse mono-exponential fitting (urL), and 5) an activity index of the liver uptake (L5/L1, which is the ratio of the liver uptake at 5 miutes over one minute). These new indexes were compare to the receptor amount (Ro) in the liver estimated with a non-linear three-compartment model.

Results: Linear regression and multiple correlation coefficients (r^2) to Ro were calculated.

	Linear regression	r^2
k-value	y=0.38x+0.64	0.845
crH	y=0.91x+3.69	0.910
H5/H1	y=-0.018x+0.87	0.851
urL	y=0.34x+0.36	0.791
L5/L1	y=0.043x+1.5	0.459

Since r^2 of standard indexes (HH15, LHL15) between Ro were 0.784, 0.696, respectively, new early phase indexes seem to be useful except L5/L1.

Conclusions: It seems to be possible to estimate liver function with 5-minute acquisition even though full time acquisition needs to be given up.

NEUROLOGY / PSYCHIATRY 1

PS_51

BRAIN PERFUSION TC-99M ECD SPECT IN DEMENTIA WITH LEWY BODIES COMPARED TO DEMENTIA OF ALZHEIMER TYPE

J. Pasquier (1), B.F. Michel (2), B. Dedienne (1), I. Brenot-Rossi (1), R. Sauvan (1), J.L. Gastaut (2). (1) Département de Médecine Nucléaire, Institut Paoli-Calmettes, Marseille, France; (2) Unité de Neuro-Gériatrie, Service de Neurologie, Hôpital Sainte Marguerite (CHRU), Marseille, France.

Dementia with Lewy Bodies (DLB) is the second most common senile degenerative dementia after Dementia of Alzheimer Type (DAT). DLB is principally characterized by a progressive and fluctuating cognitive decline, visual hallucinations and spontaneous parkinsonism. The aim of this study was to evaluate if the pattern of regional cerebral perfusion studied by SPECT may contribute to distinguish DLB from DAT.

Methods: Brain perfusion with Tc-99m ECD was performed in 62 patients (pts). Thirty-four pts were considered to have a probable DLB (mean age: 74±8 years - M: 18, F: 16 - visual hallucinations: 25, parkinsonism: 29) and 28 pts a probable DAT (mean age:76±7 years - M: 15, F: 13 - no visual hallucination). The difference was not significant between both groups for age, gender and symptom duration. After reconstruction by backprojection, 11 regions of interest were drawn manually on the main cerebral areas; tracer uptake was expressed as a corticocerebellar activity ratio (CCr).

Results: In DLB, uptake was significantly lower than in DAT for right occipital area (ROc) ($p<0.01$), left occipital area (LOc) ($p<0.01$) and right posterior temporal area ($p<0.05$). Statistical signification was borderline for the left posterior medial temporal area higher in DLB than in DAT. Using CCr<0.95 in uptake of ROc and LOc associated for diagnosis of DLB versus DAT, sensitivity (Se) was 44.1% (15/34 pts; all 15 pts had visual hallucinations) and specificity (Sp) 85.7% (24/28 pts). In DCL without visual hallucination (9/34), all CCr of ROc and LOc were both ≥0.95. Using ROc + LOc with the same uptake threshold associated to right posterior temporal area hypoperfusion (CCr<0.85), Se was 41.2% (14/34 pts) and Sp 94.4% (17/18 pts). Finally, when the same decrease uptake in ROc and LOc were associated with left posterior temporal mesial area ≥0.60, Se was 32.4% (11/34 pts) and Sp 89.3% (25/28 pts).

Conclusions: These findings show essentially a good specificity for DLB of bilateral hypoperfusion in visual cortex; that suggests a close connection with visual hallucination. The specificity for DLB was improved by the association of occipital hypoperfusion with right posterior temporal hypoperfusion or normal left posterior medial temporal uptake. Thus, this pattern may offer the possibility to distinguish DLB from DAT in some cases where the clinical diagnosis is not easy.

PS_52

PREDICTORS OF COGNITIVE-BEHAVIORAL RESPONSE TO CHOLINESTERASE INHIBITORS IN ALZHEIMER'S DISEASE: EVIDENCE FROM BRAIN PERFUSION SPECT

D. Volterrani (1), G. Manca (1), R. Ceravolo (2), S. Suriano (1), G. Tognoni (2), G. Dell'Agnello (2), G. Boni (1), M. Grosso (1), L. Murri (2), R. Bianchi (1). (1) Division of Nuclear Medicine; (2) Division of Neurology, University of Pisa, Pisa, Italy.

Cholinesterase (ChoE) inhibitors are effective drugs for symptomatic treatment of cognitive impairment in mild-to-moderate Alzheimer's Disease (AD) patients. Also the behavioral disorders AD-related might be improved by ChoE inhibitors. However a proportion of AD patients do not show a positive response on cognition and/or on behavior after ChoE inhibitors, and the characteristics of the responders are still unclear. Aim of the study was to identify a perfusional pattern predictor of a positive cognitive and behavioral response to ChoE inhibitors.

Methods: The functional imaging profile as assessed by ^{99m}Tc-ECD SPECT at baseline, was retrospectively explored in 48 AD patients presenting with behavioral disorders. All the patients fulfilled the diagnosis of probable AD according to NINDS-ADRDA criteria. On the basis of the clinical assessment performed by means of Neuropsychiatric Inventory (NPI) and Mini Mental State Exmination (MMSE) at baseline, and after 1 and 3 months of ChoE inhibitors therapy, the patients were divided into two groups (Responders, Nonresponders). SPECT acquisitions were carried out by using a dual head gamma camera equipped with LEHR collimators about 30 min. after i.v. tracer injection (740 MBq). FBP and a Butterworth prefiltering (cut-off 0.50 cycles/cm, order 10) were used for images recontruction. Uniform attenuation correction was also applied. Cerebral regions of interest were symmetrically defined in each hemisphere and cortical-to-cerebellar perfusion ratios were semiquantitatively established.

Results: No significant difference of regional cortical perfusion pattern was found between AD cognitive responders (n=32) and nonresponders (n=12). A significant hypoperfusion was observed in AD behavioral responders (n= 23) with respect to nonresponders (n=25) in bilateral cingulate gyrus, superior, inferior, medial frontal gyrus ($p<0.05$). Moreover the severity of the behavioral disorders as evaluated by NPI scores strictly correlates with such regional hypoperfusion ($p=0.02$, stepwise regression analysis).

Conclusions: ^{99m}Tc-ECD SPECT seems to be a predictor of response to ChoE inhibitors. Our findings suggest that a pretreatment cingulate and frontal hypoperfusion may predict behavioral response to ChoE inhibitors in AD.

PS_53

VOXEL-BASED COMPARISON OF 99MTC-HMPAO SPECT IMAGES IN ALZHEIMER AND FRONTO-TEMPORAL DEMENȚIA REVEALED DISTINCT PATTERNS OF CBF ALTERATIONS

S. Pappatà (1), A. Varrone (2), C. Caracò (3), A. Soricelli (1.2), A. Brunetti (1), G. Milan (4), A. Postiglione (4), B. Alfano (1), M. Salvatore (2).
(1) Centro C.N.R. per la Medicina Nucleare, Napoli, Italy;
(2) Dipartimento di Scienze Biomorfologiche e Funzionali, Università ;
(3) IMSEB C.N.R., Cosenza, Italy; (4) Dipartimento di Medicina Clinica e Sperimentale, Università

Voxel by voxel analysis using Statistical Parametric Mapping (SPM) was successfully applied to PET images of brain perfusion and metabolism at rest to identify specific patterns of cerebral dysfunction in dementia without a priori hypotheses. This highly sensitive approach was less applied to SPECT-CBF images and never used to compare frontotemporal dementia (FTD) to Alzheimer's disease (AD). In this study we used SPM and a high resolution SPECT brain camera to assess whether different specific patterns of rCBF decrease may characterize FTD and AD on a voxel by voxel basis.

Methods: 18 patients were studied with diagnosis of probable AD (n=10) and FTD (n=8). Patients were matched for age and severity of dementia (FTD: mean age 67 ± 9 yr, MMSE score 13.8 ± 9.6; AD: mean age 65 ± 7, MMSE score 14.7 ± 5.3). Perfusion images were obtained after the injection of 99mTc-HMPAO using a brain-dedicated device (CERASPECT). The SPECT images were spatially normalised to a PET CBF template in the MNI space and smoothed with 8-mm FWHM filter. Statistical analysis was performed between groups using an ANCOVA design. The effect of global perfusion was removed by using proportional scaling. Two contrasts were tested: FTD versus AD and AD versus FTD. Significance for rCBF decreases was settled at a cluster level (voxel size $p<10^{-3}$, cluster $p<0.05$ corrected) and/or at a voxel level ($p<0.05$ corrected). Regions of activation were reported as Brodmann areas (BA).

Results: When FTD patients were compared to AD patients a relative CBF decrease was found in the fronto-polar region bilaterally (BA 10; x,y,z 28 50 8, -28 42 -6), in the right ventral prefrontal cortex, (BA 11; x,y,z 12 48 –10) and in the right anterior superior temporal gyrus (BA 38; x,y,z 56 8 -12). The reverse contrast showed that in AD there was a preferential reduction of rCBF in the left posterior cingulate gyrus (BA 31; x,y,z –10 – 40 38) and the parietal cortex, bilaterally (BA 7/40; – 40 – 66 46; 52 –36 46).

Conclusions: This study shows that a voxel by voxel statistical analysis applied to SPECT-perfusion images allows to detect distinct and precisely located patterns of perfusion alterations in FTD and AD patients. The sensitivity of this method at individual level should be evaluated in a larger series of patients in view of potential clinical applications.

PS_54

PET WITH 18FDG: THREE PATIENTS WITH SUSPECT CREUTZFELDT-JAKOB'S DISEASE SHOWED AN UPTAKE CONSISTENT WITH ENCEPHALITIS

H. Engler, C. Trampal, I. Savitcheva, J. Sörensen, M. Bergström, B. Långström. Uppsala University PET Centre, Uppsala, Sweden.

PET with ^{18}FDG: three patients with Suspect Creutzfeldt-Jakob's disease SHOWED AN UPTAKE pattern consistent with Encephalitis

Aim: Three patients with clinical symptoms of Creutzfeldt-Jakob's disease (CJD) were examined with ^{18}FDG-PETat the Uppsala University PET Centre. Because we have examined 10 patients with CJD, and found a pattern of general hypometabolism, the proposal of the new examinations was to compare the pattern of glucose uptake in those three patients with that obtained in the patients with confirmed CJD.

Method: Three female patients in the age 64, 53 and 70 years, with symptoms of rapid onset dementia (suspect CJD) were examined. The examination of the brain was performed with ^{18}FDG and the glucose consumption in micromoles by minute by 100 ml was calculated.

Results: The pattern of uptake in those patients was not compatible with the hypometabolic pattern previously seen in cases of the prion disease, but areas of hypermetabolism were detected in the medial part of temporal lobes, the anterior cingulis and basala ganglia. In the three cases, our first diagnosis was suspect Limbic Paraneoplasic Encephalitis (LPE), but we recommended other investigations to exclude autoimmune or virus diseases that could give a similarly pattern in the uptake with ^{18}FDG.

In the 1st case, the physicians found Sjögren's disease as cause of the disease and after treatment with corticosteroids and cyclophosphamide the patient recovered completely.

In the 2nd case, no ethiology was found, but the patient became spontaneously better after three months and feels still all right. We suspect virus infection.

In the 3rd case no reasons for the patient symptomatology were found, and seven month later, after a new MRI examination, the physicians proposed again the diagnosis Creutzfeldt-Jacob's disease.

We sustained our first diagnosis and performed a whole body examination to locate the primary tumour founding a rounded focus of uptake measuring 3 cm in diameter in the right hemithorax at parahiliar level.

CT of the thorax couldn't confirm the presence of a tumour in the right lung and the patient died short time after those examinations.

The autopsy confirmed the presence of an adenocarcinoma in the right lung.

Conclusions: In the case of rapid onset dementias, PET may play an important roll in the differentiation of LPE, autoimmune encephalitis and virus encephalitis from Creutzfeldt-Jakob's disease. In the case of LPE, PET may help to localise the primary unknown tumour earlier than conventional methods.

PS_55

METABOLISM IN BRAIN AREAS NOT USUALLY INVOLVED IN ALZHEIMER'S ARE ASSOCIATED WITH NEUROPSYCHOLOGICAL DEFICITS

A. Newberg, A. Cotter, G. Glosser, A. Alavi, C. Clark. University of Pennsylvania, Philadelphia, USA.

Aim: This study was designed to determine whether semiquantitative metabolic measures in areas not typically believed to be involved in Alzheimer's Disease (AD) actually were associated with neuropsychological impairment. Methods: FDG PET scans on 40 patients with AD were acquired on the PET HEAD scanner 40 minutes following the intravenous administration of 115μCi/Kg of FDG. All FDG-PET scans were analyzed blindly by using a region of interest (ROI) template with regions for the primary visual cortex (PVC), secondary visual cortex (SVC), cerebellum, and basal ganglia (BG). Counts from all ROIs were normalized to whole brain activity and the results were compared to psychometric and neuropsychological measures. Results: A number of significant correlations were found between these structures and various neuropsychological measures. Specifically, there were significant correlations between clock drawing and the cerebellum activity ($R=0.40$, $p=0.02$); memory and activity in the PVC ($R=0.35$, $p=0.03$), SVC ($R=0.40$, $p=0.01$), and cerebellum ($R=0.43$, $p=0.006$); social score and activity in the PVC ($R=0.40$, $p=0.01$) and left cerebellum ($R=0.43$, $p=0.01$); judgment and activity in the right SVC ($R=0.36$, $p=0.02$) and right PVC ($R=0.34$, $p=0.03$); and the overall mini mental state exam and activity in the PVC ($R=0.54$, $p=0.001$), and cerebellum ($R=0.39$, $p=0.01$). Conclusion: The results of this study suggest that metabolism in areas not typically involved in the pathology of AD, such as the PVC, SVC, and cerebellum, is significantly correlated with deficits in neuropsychological function. This may have important clinical and pathophysiological implications in the study of Alzheimer's and other dementing illnesses.

PS_56

EFFECT OF DONEPEZIL HYDROCHLORIDE ON BRAIN PERFUSION IN PATIENTS WITH DEMENTIA OF ALZHEIMER TYPE, EVALUATED BY I-123-IMP SPECT

Y. Ogura (1), I. Narabayashi (1), K. Utsunomiya (1), T. Komori (1), M. Sugino (2), M. Tagami (2), T. Seo (3), J. Sakai (3). (1) Department of Radiology; (2) 1st. department of internal medicine; (3) Department of Psychiatry, Osaka Medical College, Takatsuki, Japan.

Aim: To examine the effects of donepezil hydrochloride on brain perfusion in patients with dementia of Alzheimer type.
Methods: I-123-IMP SPECT was performed on 12 healthy volunteers (controls: 5 males and 7 females, mean age 69.7±6.4) and 15 consecutive patients with dementia of Alzheimer type (DAT group: 6 males and 9 females, mean age 71.0±5.1) to get regional brain blood flow (BBF) in the frontal, parietal, temporal, occipital, cerebellar hemisphere, and etc. using the I-123-IMP-ARG method. All 15 patients were diagnosed as having DAT by Diagnostic and Statistical Manual of Mental Disorders, Fourth Edition (DSM-_) criteria in a two-step diagnostic procedure. These 15 patients received 5 mg/day of donepezil hydrochloride after breakfast. Treatment was continued for 3 to 12 months. At 3~6 and/or 6~12 months after the start of the treatment, I-123-IMP SPECT was performed again to obtain the regional BBF in the areas.
Results: There is no significant difference in mean age and gender between controls and DAT group. No laterality of the regional BBF between controls and DAT group can be seen in any areas. BBF in the frontal, parietal, and hippocampus of DAT group {mean of left and right; 28.1±7.5, 23.5±7.9, 22.1±5.6 (ml/100g/min)} are significantly lower than those of controls {mean of left and right; 38.7±11.7, 35.0±10.6, 33.6±11.1 (ml/100g/min)}. Before and after the treatment for 3 to 6 months, right hippocampal perfusion has tendency to decrease from 22.2±6.1 to 19.6±5.5 ml/100g/min (p=0.092) although no tendency to increase or decrease the BBF in any other regions. However, donepezil hydrochloride has significantly improved the BBF in the frontal, parietal, and occipital after more than 6 months treatment from 25.7±8.7, 20.6±7.9, 27.2±6.0 to 29.3±6.9, 24.9±6.2, 35.0±7.6 ml/100g/min respectively although no tendency to increase or decrease the BBF in any other regions.
Conclusions: Donepezil hydrochloride did go up the BBF of DAT, which suggests it should be efficacious against DAT whose BBF reduction is usually progressive.

PS_57

FRACTAL ANALYSIS OF STRIATAL DOPAMINE REUPTAKE SITES USING I-123 BETA-CIT SPECT IN PATIENTS WITH PARKINSON'S DISEASE

J.-.K. Chung (1), J.S. Yeo (1), J.I. Hwang (1), S.I. Cho (1), D.S. Lee (1), J.C. Paeng (1), Y.K. Kim (1), H.J. Jeong (1), B.S. Jeon (2), M.C. Lee (1). (1) Department of Nuclear Medicine; (2) Department of Neurology, Seoul National University College of Medicine, Seoul, Korea.

Heterogeneity in dopamine reuptake receptor density within the brain is measurable with SPECT using iodine-123 labelled 2beta-carbomethoxy-3beta-(4-iodophenyl)tropane ([123I]beta-CIT). It has been previously shown that the observed variance increases with increasing number of subregions in the /tissue studied (Fractal Analysis). It was well known that Parkinson's disease(PD) is associated with decreased dopaminergic transmission but less was known about heterogeneity of dopaminergic system in PD . We studied if heterogeneity of dopamine reuptake was also changed in Parkinson's patients.
Methods: Forty-seven patients with PD (age 56.8±12.3 years,15 male and 32 female) and 6 controls were enrolled this study using [123I]beta-CIT SPECT. We acquired striatum specific uptake ratio after normalization with cerebellum uptake count; specific uptake ratio=(mean striatum uptake count - mean cerebellum uptake count)/mean cerebellum uptake count. And we calculated fractal dimensions for each side of striatum using ROI.
Results: Striatum specific uptake ratio was significantly low in patients with PD than controls (Rt: 2.87±1.19 vs 5.82±1.55 , Lt: 3.02±1.09 vs 5.91±1.51, p<0.005). But fractal dimensions in patients with PD was not significantly different from controls (Rt: 1.46±0.16 vs 1.49±0.07 , Lt: 1.40±0.12 vs 1.46±0.06, p>0.1). Striatum specific uptake ratio was not correlated to fractal dimension (p>0.1). Age and sex had no correlation with fractal dimension of patients with PD.
Conclusion: We found fractal dimension of striatal uptake of [123I]beta-CIT was not decreased in patients with PD. This result indicate that [123I]beta-CIT distribution was not significantly more or less heterogeneous in the striatum of patients with PD than in healthy controls, even though striatal uptake itself was significantly decreased in patients with PD.

PS_58

STRIATAL AND EXTRASTRIATAL DYSFUNCTION IN PARKINSON'S DISEASE WITH DEMENTIA. A 6-[18F]FLUORO-L-DOPA PET STUDY

K. Ito (1), A. Nagano-Saito (1), T. Kato (1), Y. Arahata (1), A. Nakamura (1), Y. Kawasumi (1), K. Hatano (1), Y. Abe (1), T. Yamada (2), T. Kachi (2), D.J. Brooks (3,4)(1) Department of Biofunctional Research, National Institute for Longevity Sciences, Obu, Japan; (2) Department of Neurology, Chubu National Hospital, Obu, Japan; (3) MRC Clinical Sciences Centre, Imperial College School of Medicine, Hammersmith Hospital, London, UK; (4) Institute of Neurology, Queen Square, London, UK

We investigated relative differences in striatal and extrastriatal dopaminergic function between Parkinson's disease without (PD) and with dementia (PDD) with ^{18}F-dopa PET.
Methods: The 10 PD and 10 PDD patients were equivalently disabled having a mean score of around 3 on the Hoehn and Yahr rating scale. ^{18}F-dopa influx constant (Ki) images of those patients and 15 age-matched normal subjects were transformed into standard stereotactic space. Between group significant differences in mean regional Ki values were localized with statistical parametric mapping (SPM) on a voxel-by-voxel basis. To clarify the regional association of ^{18}F-dopa uptake, significant correlations between striatal and extrastriatal Ki values in 20 patients combining both PD and PDD were also localized with SPM.
Results: Compared with the normal group, SPM localized declines of the ^{18}F-dopa Ki bilaterally in the putamen, in the right caudate nucleus, and in the left ventral midbrain for the PD group ($p < 0.01$, corrected). Compared with the normal group, the PDD group showed reduced ^{18}F-dopa Ki bilaterally in the striatum, midbrain, and anterior cingulate area ($p < 0.01$, corrected). A relative difference in ^{18}F-dopa uptake between PD and PDD was the decline bilaterally in the anterior cingulate area and in the right caudate nucleus in the latter ($p < 0.01$, corrected). The mean Ki values for the caudate nucleus and putamen significantly correlated each other and also positively correlated with the Ki values bilaterally in the midbrain and anterior cingulate area and in the left amygdala ($p < 0.01$, corrected).
Conclusions: In this study we have demonstrated a significant dysfunction in both striatal and extrastriatal regions in PD patients with superadded dementia. These findings are consistent with the hypothesis that impairment of mesofrontal dopaminergic function plays an important role in the dementia of PD.

PS_59

DIFFERENTIAL DIAGNOSIS BETWEEN CORTICOBASAL DEGENERATION AND PARKINSON'S DISEASE ASSESSED BY HMPAO SPECT

P. Charpentier (1), A. Kreisler (2), L. Defebvre (2), P. Lecouffe (1), A. Destee (2), M. Steinling (1). (1) Nuclear Medicine: Functionnal Brain Imaging Unit; (2) Dpt of Neurology, University Hospital, Lille cedex, France.

INTRODUCTION: Corticobasal degeneration (CBD) is a rare parkinsonian syndrome. Its diagnosis is difficult despite the existence of some typical clinical features. Few previous studies of Single Photon Emission Computerised Tomography (SPECT) data describe an original pattern with asymmetric hypoperfusion in pre and retro-rolandic regions.
OBJECTIVE: To compare the regional cerebral blood flow measurements studied by SPECT with 99m-Technetium HMPAO in CBD and Parkinson's disease (PD), using a discriminant analysis applied to different regions of interest (ROI).
METHODS: Fifteen patients with probable CBD (ten women; mean age: 66.1 years; mean disease duration: 4 years) and 15 patients with PD (nine women; mean age: 65.5 years; mean disease duration: 5.6 years) underwent brain SPECT imaging after intraveinous injection of 740 MBq of ^{99m}Tc HMPAO. The relative fixation and the fixations asymmetry indexes of 13 pairs of regions of interest (ROI) drawn on two transverse slices (orbito-meatal plane + 5 cms and + 8 cms) were studied by Wilcoxon rank test and by a stepwise discriminative analysis. In order to classify automatically the patients, a predictive score was established.
RESULTS: There was a decrease of HMPAO uptake in medial frontal regions in the CBD group when compared to the PD group. Among the 30 patients, 27 [14/15 (93%) of DCB and 13/15 (87%) of PD] were correctly classified by the score.
CONCLUSIONS: A medial frontal hypoperfusion on upper slices allowed separating the CBD group from the PD group. We estimate that this semi-automatic classification can be a precious tool to comfort clinical differential diagnosis between CBD and PD.

PS_60

DISTURBED HMPAO CELLULAR TRAPPING AND BLOOD FLOW-METABOLISM DISSOCIATION AND ACUTE DOPAMINERGIC NIGRO-STRIATAL DAMAGE IN A SURVIVAL OF AN ACUTE CYANIDE INTOXICATION

J. Zaknun (1), H. Rieck (1), K. Stieglbauer (1), J. Trenkler (2), W. Langsteger (3). (1) Div. of Neuronuclear Medicine / Dept. of Neurology, Wagner-Jaureg Hospital, Linz, Austria; (2) Dept. of Neurology; (3) Institute of Radiology; (4) Dept. of Nuclear Medicine, St. Vincent Hospital, Linz, Austria

Cyanide, an inhibitor of cytochrome oxidase disrupts the respiratory chain and leads to apoptosis or severe neuronal damage due to cellular energy depletion.
A 35years old right handed female survived a suicide attempt by cyanide after a prompt i.v. antidote therapy with 2,5gr dimethyl aminophenole. After 1 week at the ICU she was transferred to the dept. of neurology. On admission she presented with agitation, involuntary movements of the trunk, upper and lower extremities which subsided to a state of akinetic mutism during the 2nd-3rd week. On day 9 a quantitative perfusion study by 99mTc-HMPAO RN-Angiography followed by SPECT and quantification of mean hemispheric blood flow (mhBF) using patlak and Lasson's transformation, β-CIT SPECT (day 18), MR (day 11) and 18FDG-PET (day 19) were conducted. SPECT and MR image registration was done.
Results : MR revealed Gd-uptake in the corpus striatum and pre-central frontal regions (Brodmann 4,6). HMPAO revealed inhomogeneous pattern. Frontal regions with Gd-enhancement showed increased uptake similar to that seen in subacute infarction. Reduced uptake was found bilaterally fronto-basal and left frontal and in both anterior and lateral temporal lobes. In addition significantly reduced uptake in the basal ganglia especially the left nucleus caudatum, left G. pallidus and left thalamus with a consistent mild left cerebellar diaschisis were found. Paradoxically, mhBF values were within normal range for age (R=55, L=53 ml/min/100gr). FDG-PET (day 19) during the akintic mutistic phase revealed bifronto-temporal, striatal and thalamic hypometabolism. β-CIT indexes were markedly reduced, tracer distribution indicated a diffuse reduction of dopamine reuptake-site density.
Conclusion: In Brain region with normal MR-pattern during the sub-acute phase following cyanide intoxication, quantitative data indicate a dissociation between blood flow and HMPAO trapping possibly due to reduced or depleted cellular glutathion. Regions with damaged blood-brain-barrier may show hypo- or hyperfixation as in ischemic insults. Fronto-temporal and basal ganglia hypometabolism by FDG-PET correlated well with the clinical state of akinetic mutism. An acute dopaminergic dysfunction occurs early in the course of cyanid intoxication. Left lateralization of neuronal damage may indicate a higher susceptibility of the dominant hemisphere.

PS_61

TC-99M ECD BRAIN SPECT IMAGING IN TOURETTE'S SYNDROME AND CHRONIC TIC DISORDER: QUANTITATIVES ANALYSIS USING STATISTICAL PARAMETRIC MAPPING

J.S. Jang (1), S.N. Yoon (1), C.H. Park (1), I.S. Hwang (2), E.Y. Oh (2). (1) Department of Nuclear Medicine; (2) Department of Psychiatry, Ajou University School of Medicine, Suwon, Korea.

Aim: We assessed regional cerebral blood flow(rCBF) in children with tourrett's syndrome and chronic tic disorder using statistical parametric mapping.
Methods: 30 patients (M:F=24:6, mean age=10.23±2.87y) with chronic tic disorder, 27 patients(M:F=23:4, mean age=10.78±3.18y) with tourrette's syndrome and 7 normal control subjects(M:F=6:1, mean age=10.28±4.07y) underwent a Tc-99m ECD brain SPECT. Chronic tic disorder group is divided into two groups, one is attention deficit hyperactivity disorder(ADHD) with chronic tic disorder(M:F=10:2, 10.00±2.79y), and the other is pure tic patients(M:F=14:4, 10.39±2.99y). Tourrette's syndrome group is divided into two groups, one is ADHD with tourrette (M:F=7:2, 9.78±2.91y), and the other is pure tourrette patients(M:F=16:2, 11.28±3.31y).Using a statistical parametric mapping, we compared SPECT images of our patients with those of 7 normal control subjects. Evaluation was made to detect areas with significant hypoperfusion($p<0.001$).
Results: Chronic tic disorder group (n=30) had a significant hypoperfusion in the right parietal and left temporal lobes when compared with normal control subjects (n=7)($p<0.001$). Left frontal lobe, insular, basal ganglia and left temporal lobe revealed significantly decreased rCBF in torrette's syndrome group (n=27) in comparison to the normal control subjects (n=7). Statistical parametric mapping depicted that, compared with normal control subjects, ADHD with chronic tic disorder group had a significant hypoperfision in the both frontal and left temporal lobes and pure tic group had a significant hypoperfusion in the both parietal and left frontal lobes. ADHD with tourrette's syndrome group had a significant hypoperfusion in the both frontal lobes and basal ganglia and pure tourrette's syndrome group had a significant hypoperfusion in the temporal, left frontal, right parietal lobes, basal ganglia and insular, as compared with the normal control subjects. Compared with tourrette's syndrome, chronic tic disorder had significantly decreased perfusion in the temporal lobe.
Conclusion: In comparison to the normal subjects, regional cerebral blood flow in basal ganglia was decreased in tourrette's syndrome group whether subjects have comorbidity or not. SPM analysis demonstrated the chracteristic rCBF pattern in chronic tic disorder and tourrette's syndrome in children.

PS_62

DECREASED DOPAMINE TRANSPORTER BINDING IN ASYMPTOMATIC MACHADO-JOSEPH DISEASE GENE CARRIERS

T.C. Yen (1), K.Y. Tzen (1), C.S. Lu (2), S.P. Wey (3), G. Ting (3). (1) Department of Neurology, Chang-Gung Memorial Hospital and University; (2) Department of Nuclear Medicine, Chang-Gung Memorial Hospital and University; (3) Institute of Nuclear Energy Research, Taiwan; (4) Institute of Nuclear Energy Research, Taiwan

Aim: The aim of this study was to extend our previous research (J Nucl Med 2000; 41: 994-998) for further investigating changes in this binding for asymptomatic MJD gene (aMJD) carriers and to compare the results with MJD patients and healthy controls. Methods: Imaging of dopamine transporter (DAT) concentration in the striatum region, using ^{99m}Tc-TRODAT-1/single photon emission computed tomography (SPECT) was performed on 5 aMJD gene carriers, 10 age-matched MJD patients and 10 age-matched healthy controls. Brain SPECT images were acquired at 4 h after intravenous injection of 25 mCi of ^{99m}Tc-TRODAT-1, which is known to bind specifically to DAT on nigrostriatal terminals. Results: By fusing the SPECT images with striatal atlas obtained from MRI, binding of this tracer in the entire striatum was measured and the uptake values in bilateral striatal areas were compared among these 3 groups. The uptake values in both aMJD gene carriers ($p = 0.000$) and MJD patients ($p = 0.000$), displayed a significant reduction as compared to those of controls. The reduction was more severe in the MJD patient group ($p < 0.05$). Bilateral putamen/caudate ratios were significantly lower in both aMJD gene carriers and MJD patients groups ($p < 0.001$). The dopamine neuronal activity as represented by the tracer binding was more prominently affected in the putamen in these patients. Conclusions: We conclude that ^{99m}Tc-TRODAT-1 brain SPECT is capable of detecting early alteration of dopamine neurons in the striatal region. Significantly, the results suggest that this impairment of presynaptic dopamine function actually occurs at an earlier stage, which is previously unrecognized in these asymptomatic MJD gene carriers.

RADIONUCLIDE THERAPY / DOSIMETRY 1

PS_63

TREATMENT AND PROGNOSIS OF THYROID MICROCARCINOMA: AN EXPERIENCE ON 320 PATIENTS

L. Pedrazzini, M. Andruccioli, A. Baroli, G. Calcagno, G. Lomuscio, L. Mazzucchelli, L. Colombo. Ospedale di Circolo, Nuclear Medicine, Busto Arsizio, (VA), Italy.

The aim of this study was to evaluate retrospectively the treatment and the prognosis of thyroid microcarcinoma.
Methods: From 3093 pts. treated for differentiated thyroid carcinoma in the period 1964-1996 in our Dept., we selected 320 consecutive pts.with thyroid microcarcinoma (tumor ≤ 1 cm.Ø) with follow-up ≥ 2 yrs. (71 males and 249 females, mean age at the time of first diagnosis 43,8±14,8 yrs. range 16-77 yrs.).
Results: Initial stage of tumor was: T1N0M0 for 228 pts.(71,2%), T1N1M0 for 90 pts. (28,2%), T1N0M1 for 2 pts. (0,6%), both follicular carcinoma. Histological diagnosis was papillary carcinoma in 303 pts. (94,6%) and follicular carcinoma in 17 pts. (5,4%). Tumor diagnosis was incidental in 202 pts. (63,2%) and non incidental in 118 pts.(36,8%) (first manifestation: palpable metastatic lymph nodes in the neck 72 pts. (61,1%); palpable nodal thyroid in 44 pts. (37,2 %); distant metastasis in 2 pts. (1.7%).
Characteristics of pts.treated nor treated with 131-I for ablation of thyroid's remnant:

	TYPE OF SURGERY	ISTOTYPE	STAGE	MULTI FOCALITY	DIMENSION = 1 CM.	INVASION OF THYROID'S CAPSULAR
131-I treated (ablation of remnant) 170 pts.	136 tot.thyroid. 33 sub.thyroid. 1 lobectomy	166 papillary 4 follicular	83T1N0M0 85 T1N1M0 2 T1N0M1	70	58	16
131-I non treated 150 pts.	31 tot.thyroid. 66 sub.thyroid. 52 lobectomy 1 enucleation	137 papillary 13 follicular	145 T1N0M0 5 T1N1M0	28	22	0

16 pts.(5,0%) had a total of 22 sites of recurrence or distant metastases; 131-I therapy was given to 15 pts.:

None patient has died nor has shown tumors activity at mean follow-up of 8,91±4,82 yrs. (range 2-35 yrs.).

Pts	Age	Type of Surgery	Istotype	Stage	Multi focality	Sites of local recurrence	Sites of lymph node metastases	Sites of distant metastates	131-I treated (ablation of remnant)	Follow-up (after initial treatment)
16	37± 15 yrs. (range 18-71)	8 tot. thyroid. 3 sub. thyroid. 5 lobectomy	16 papillary	5 T1N0M0 11T1N1M0	7	6 (5 in controlateral lobe after lobectomy)	13	3 lung	11	5,26 ± 5,37 yrs. (range 0,4-16)

Conclusions: Thyroid microcarcinoma has very good prognosis, even when there is recurrence of disease. We use to treat with 131-I only pts. who have initial signs of potential future extention of disease. Total thyroidectomy is the best surgical approach when the tumor is discovered pre-operatively. Lobectomy increases the risk of recurrence (9,4% in our study). However there isn't strong indication to perform completion thyroidectomy if the tumor is incidental.

PS_64

THERAPEUTIC EFFICACY OF IODINE-131-THERAPY IN THYROID CANCER PATIENTS WITH POSITIVE THYROGLOBULIN BUT NEGATIVE IODINE-131 WHOLE BODY SCANS

C.-O. Sahlmann (1), J. Meller (1), K. Lehmann (1), K. Schreiber (1), I. Meyer (1), G. Altenvoerde (1), W. Becker (1). (1) Department of Nuclear Medicine; (2) Department of Internal Medicine, University, Goettingen, Germany.

Aim: The indication for an Iodine-131 (I-131) therapy in thyroid cancer patients with elevated serum thyroglobulin (hTg) but negative I-131- whole body scan is under discussion. This retrospective study was performed to evaluate the therapeutic efficacy of an I-131 therapy in these patients.

Methods: 115 patients with differentiated thyroid cancer were treated with iodine-131 (1,8 GBq to 9,2 GBq) between 1995 and 2001. In seven patients hTg was positive and the postherapeutic scan was negative. In all these patients total thyroidectomy, neck-dissection and iodine-131-ablation had been performed previously. 6 patients had papillar thyroid cancer, one a follicular cancer. In all patients Tg-levels (SELco®Tg with functional sensitivity <0,5 ngTg/ml) were measured in hypothyroidism (TSH>30) before and 3 – 24 months following treatment.

Results: Pretherapeutic Tg-levels (median 8,6 ng/ml, range 7,8 to 98,2 ng/ml) decreased in 6 from 7 patients during follow up (median 8,0 ng/ml, range 2,6 to 42,1 ng/ml), in one patient Tg increased from 6,4 to 11,1 ng/ml.

Conclusion: There is enough evidence (6 from 7 patients) that I-131 therapy is effective in thyroid cancer patients with positive hTg but negative whole body scan. Further studies have to exam the final outcome and the dose regiment for these patients.

PS_65

THE DEPENDENCE OF DISTANT METASTASES APPEARANCE AND THE FURTHER DISEASE COURSE IN RELATION TO PATHOHISTOLOGIC TYPES OF DIFFERENTIATED THYROID CARCINOMAS

LJ. Stefanovic, M. Malesevic, J. Mihailovic, D. Srbovan, J. Vojicic. Department of Nuclear Medicine, Institute of Oncology, Sremska Kamenica, Yugoslavia.

Aim: To determine the frequency of distant metastases appearance in relation to pathohistologic types of differentiated thyroid carcinomas and investigate the influence of pathohistologic types on the outcome of patients with metastases.

Patients and methods: The 65 follicular and 254 papillary carcinomas were observed and treated. All patients underwent three kind of treatment: surgery, radioactive iodine and l-thyroxin; external radiotherapy was implemented in some of them, and polychemotherapy only in 4 patients with distant metastases. The differences were compared by t-test of proportions, the treatment outcomes (remission, stable disease, deterioration and death) in relation to pathohistologic types were tested using regression analysis and Kaplan & Meier's method determined survivals.

Results: Metastases were detected in 32.3% patients with follicular and in 12.6% with papillary carcinomas; the difference was very highly significant ($p<0.001$). The mean age of patients with metastases at the moment of diagnosing thyroid malignancy was very significantly higher in follicular carcinomas ($p<0.01$). Lung metastases were very significantly more frequent in papillary ($p<0.001$) and bone metastases in follicular carcinomas ($p<0.001$); the other systems were involved rarely in both types of carcinoma. The difference of radioactive iodine accumulation in metastases between papillary and follicular carcinomas was not significant ($p>0.3$). The female to male ratio was not significantly different between metastatic papillary and follicular carcinomas ($p>0.2$). The general outcome was significantly better in patients with metastatic papillary carcinomas ($p<0.05$), particularly with regard to get remissions. But, the probability of 10 years cumulative survival between papillary and follicular carcinomas with metastases was not significantly different ($p>0.4$), although papillary carcinomas had the tendency of longer survival.

Conclusion: The metastases of follicular carcinomas were significantly more frequent. Bone metastases were more frequent in follicular and lung metastases in papillary carcinomas. The general outcome of patients with metastatic papillary carcinomas comparing to follicular carcinomas was significantly better, but the difference was not significant with regard to the survival.

PS_66

WHAT IF MOM WAS PREGNANT DURING TREATMENT WITH IODINE-131

J. A. K. Blokland (1), E.K.J. Pauwels (1), W.H. Thomson (2), L.K. Harding (2). (1) Nuclear Medicine, Leiden University Medical Centre, Leiden, The Netherlands; (2) Physics and Nuclear Medicine, City Hospital, Birmingham, UK.

The treatment of benign thyroid disease and differentiated carcinoma through radiotherapy with iodine-131 (I-131) is an effective therapy with minimal side effects. In women between 15 and 45 years of age, thyroid cancer is the most commonly diagnosed cancer of head and neck. Before treatment of these women in childbearing age they should undergo a pregnancy test. However, this test is not always carried out and the patient may not be aware of their gestation in the early stage. Little has been published in literature about the absorbed dose by the foetus and its thyroid. Most authors suggest that it may be extremely high. The radiation dose to the foetus and especially to its developing thyroid may lead to tissue malformations and tumour induction. Therefore, it is useful to estimate the dose to the foetus when such a patient is accidentally treated with a high dose I-131.

Some radiopharmaceuticals, e.g. I-131, can easily cross the placenta. Then, the radiation dose to the foetus consists of two components: external radiation from the activity in the mother, and internal radiation from the radiopharmaceutical that crossed the placenta. During the first two months the foetal thyroid does not accumulate iodine. So, during this period the radiation dose to the foetus is mainly determined by activity in the mother (e.g. bladder) and will be more or less equal to the dose to the uterus. Depending on the mother's thyroid uptake and the administered amount of ^{131}I the absorbed dose will be in the range of tens of mGy per 750 MBq I-131. At 70–90 days after conception the foetal thyroid starts to accumulate iodine. Also the weight of the thyroid is increasing rapidly. The dose to the foetal thyroid depends on its uptake and weight. Using the model published by Johnson (*Health Phys* 1982; 43(4): 573-582) we have calculated for a woman receiving 600 MBq ^{131}I at 15 weeks pregnancy an absorbed dose by the foetal thyroid equal to 450 Sv. In the recently published *Annals of the ICRP* on pregnancy and medical radiation (Publication 84, Vol. 30(1), 2000) a similar dose is given: 375-875 Gy on the foetal thyroid.

Despite the high dose it appears that in the majority of patients given radioiodine therapy the baby will be normal, thus a decision about abortion will largely depend on social factors.

PS_67

THE EFFECTS OF RADIOIODINE THERAPY ON PERIPHERAL BLOOD LYMPHOCYTES SUBPOPULATIONS IN PATIENTS WITH GRAVES' DISEASE. PRELIMINARY REPORT

M. Turowska (1), D. Turowski (2), J. Wysocka (2), F. Rogowski (1). (1) Department of Nuclear Medicine; (2) Department of Laboratory Diagnostics, Medical University, Bialystok, Poland.

Aim: Treatment of Graves' disease patients with radioactive iodide (I-131) becomes the standard therapy in a rising group of cases but can induce alterations in immune response like increasing in levels of autoantibodies, and in part, exacerbation of opfhtalmopathy.
The aim of this study was assessing the changes in peripheral blood (PB) lymphocytes subpopulations after I-131 treatment of patients with Graves' disease.
Methods: The study was carried out in a group of 30 patients with Graves' disease (f:23; m:7) 49,5±10,0 years of age, 26 with different subjective ocular signs like gritty sensation, increased lacrimation, orbital pain, and exophtalmos. PB lymphocyte subsets analysed by cytofluorometry (Coulter Epics XL), serum concentration of TSH and fT4 (RIA, IRMA Polatom Świerk, Poland) were evaluated before and 6 weeks after radioiodine treatment (average dose 505,3±113,9 MBq of I-131).
Results: After I-131 treatment significant increase in CD3+, CD4+, CD3+HLA-DR+ and decrease in CD19+ percentages of lymphocyte subsets were found in comparison to the initial evaluation, respectively: median (p25-p75), 69,8 (67,9-73,7%) vs. 74,2 (71,7-75,8%), p<0,0001 for CD3+, 44,6 (38,7-47,4%) vs. 48,5 (44,6-51,6%), p<0,00001 for CD4+, 3,5 (1,9-5,9%) vs. 5,3 (3,5-7,2%), p<0,005 for CD3+HLA-DR+ and 13,3 (10,3-15,7%) vs. 9,3 (7,9-13,0%), p<0,00001 for CD19+. No significant changes in percentage of CD8+ and NK (CD3-CD16+CD56+) cells were observed during this study. Significant increase in TSH and slight decrease in fT4 concentration took place in 6th week after I-131 application, respectively: 0,62 (0,09-2,39µIU/ml) vs. 0,15 (0,002-0,41µIU/ml), p<0,02 for TSH, and 15,5 (9,5-25,1pmol/ml) vs. 11,5 (7,2-14,9pmol/ml), p=0,16 for fT4.
The patients with subjective improvement of ocular signs during the therapy initially had percentage of CD3+, CD8+ lymphocytes significantly increased compared to those with no changes observed after I-131 treatment.
Conclusions: The changes in PB lymphocyte subsets caused by I-131 treatment of Graves' disease confirm involvement of acquired cellular immunity after radiation damage of thyroid gland. The decreased percentage of CD8+ and CD3+ lymphocytes at the beginning of the study can make a prediction of ocular symptoms persisting after radioiodine treatment in some patients with ophtalmopathy.

PS_68

ACUTE EFFECT OF I-131 TREATMENT ON CHROMOSOMES

T. Erselcan (1), S. Sungu (2), S. Özdemir (1), D. Doğan (1), O. Özdemir (2). (1) Department of Nuclear Medicine; (2) Department of Medical Biology and Genetics, Cumhuriyet Univ., School of Med., Sivas, Turkey.

Although chromosomal abberative effect of ionizing radiation is well known, it is not well documented in I-131 treatment receiving patients with sister chromatide exchange method (SCE). There are quite a few study on the subject with the contradictory results.The aim of the on going study was to investigate probable effect of I-131 treatment on chromosomes, by means of SCE method. We report here the preliminary results of 10 patients (mean age±SD = 48.0±17.6), either received 3700 MBq of I-131 for the ablation purpose (3 patients) or various doses (259-740 MBq) with the aim of the thyrotoxicosis treatment (toxic nodular goitre or Grave's disease). Pre-treatment mean serum levels of T_3, T_4 and TSH in ablation dose receiving and in thyrotoxicosis patients were 0.73±0.46 pg/ml, 0.31±0.19 ng/ml, 61.67±43.75 µIU/ml and 2.97±1.15 pg/ml, 3.08±5.10 ng/ml, 0.54±0.91 µIU/ml, respectively. Chromosome analysis was performed to determine SCE frequency in cultured peripheral lymphocyte cells of patients, before and 72 hours post-treatment with I-131. Pre-treatment and post-treatment SCE frequencies were 3.02±1.04 and 9.76±1.22, respectively (p<0.001). On the other hand, although escalating trend in SCE frequency with the higher doses of I-131 was observed, it was not statistically significant. Also, no statistically significant relationship found between SCE frequency and thyroxinemia, serum level of TSH or with the pre-treatment thyroid Tc-99m uptake (in thyrotoxic patients).
The preliminary results of the present study, although with the limited number of I-131 treatment receiving patients, suggest a significant increase in the SCE frequency in short term.

PS_69

RADIOIODINE THERAPY OF UNIFOCAL OR MULTIFOCAL TOXIC AUTONOMOUSLY FUNCTIONING THYROID NODULES LARGER THAN THREE CENTIMETER IN DIAMETER

B. Değirmenci (1), C. Taşcı (1), A. Çomlekci (2), O. Özdoğan (1), S. Yeşil (2). (1) Department of Nuclear Medicine; (2) Department of Endocrinology, Dokuz Eylül University, Izmir, Turkey.

There is controversy about the treatment of large toxic autonomously functioning thyroid nodules (TAFTN). In large TAFTN, the surgery may be preferred because radioiodine treatment (RT) may not eliminate thyrotoxicosis in first therapy and the second or third therapy may be required. The aim of this study was to investigate the effectiveness of RT in unifocal and multifocal TAFTN larger than 3 cm in diameter and the effect of radioiodine uptake (RU), the presence of suppression of the extranodular tissue , the dose given to patient, the antithyroid drug (ATD) using before RT on the effectiveness of RT. We also investigated the relationship the occurrence of early (first to third month) and delayed (sixth months or later) hypothyroidism and the same parameters mentioned above.
Methods: Twenty patients (12 female and 8 men) with a mean age of 65.75±4.8 were included in the study. All patients had unifocal or multifocal TAFTN larger than 3 cm in diameter (3- 6 cm) and were in thyrotoxic status with suppressed TSH. To reduce the iodine pool a low iodine diet for 15 days before planned RT and ATD were discontinued 5 days before RT. We used standard dose regimen. The mean dose of iodine 131 given to patients was 20 mCi±3.8 (15-25 mCi). The patients were followed up a mean interval 9.1±5.6 months.
Results: All patients were cured by RT. Single- dose cure rate was 90%. Second-dose RT was needed in two patients. Two (10%), 7 (35%) and 7 (35%) patients were euthyroid and first, third and sixth months after RT, respectively. Permanent hypothyroidism was occurred in 4 patients (20 %). There was no any other complications and side-effect were developed. We did not find any statistically difference between the cure rate with RT and RU, the presence of suppression of the extranodular tissue , the dose given to patient, the ATD using before RT. There was also no statistically difference between the occurrence rate of hypothyroidisim and the same parameters.
Conclusion: Our study suggests that radioiodine therapy may be preferred in patients with TAFTN as an effective and safe therapy method. The further study with a large number of patients in this selected group are needed.

PS_70

CLINICAL EFFICACY OF A SIMPLIFIED METHOD TO DETERMINE THE THERAPEUTIC RADIOACTIVITY OF I-131 FOR HYPERTHYROIDISM

J. Sequeira (1), D. Passos (2), P.A. Santos (1,3), S. Carmona (1), M. Filipe (1), M.J. Carapinha (1), B. Abrantes (1), A. Quintal (1), P. Almeida (1,3), J. Portugal (2), A.I. Santos (1)(1) Serviço de Medicina Nuclear; (2) Serviço de Endocrinologia; (3) IBEB-FAC. Ciências Da Universidade De Lisboa, Almada, Portugal.

Aim: The purpose of our study was to evaluate the clinical efficacy of a simplified, gamma camera (GC) based, method used to calculate the iodine-131 therapeutic radioactivity (TR) for the treatment of hyperthyroidism.
Methods: Fifty-nine patients (pts), 48 females and 11males, <age>=58.2 ±11.9 years, with a minimum follow-up of 6 months, were studied. The aetiology of the hyperthyroidism was: 29 pts with Grave's Disease (GD), 14 pts with Toxic Multinodular Goitre (TMG) and 16 pts with Toxic Adenoma (TA). To determine the I-131 TR all patients were administered I-131 capsules with a radioactivity's of 1,5MBq. The pts Iodine-131 uptake (Up) at 24 h was determined on a GC using a standardized method. A planar image of the thyroid was also obtained, at that time, to determine the mass (M) of that gland, based on its area. The TR values were calculated as follows:

$$TR(MBq) = M(g) \times SR(MBq/g) \Big/ Up(24) \times 100$$

where SR means Specific Radioactivity. SR considered was 3,7MBq/g of thyroid tissue for GD and TMG and 9,3 MBq/g for AT. The majority of pts did not receive anti-thyroid drugs after Iodine-131 treatment.
Follow-up was done every 6 months (mth) and pts clinical status was classified as: Hyperthyroidism (Hyper), sub-clinical Hyperthyroidism (scHyper), Euthyroidism (Euth), sub-clinical Hypothyroidism (scHypo), Hypothyroidism (Hypo). Two other parameters were calculated: remission rate (RR) – percentage of pts without Hyper – and hypothyroidism rate (HR) – percentage of pts with scHypo and Hypo.
Results: There were no pts lost to follow-up. The TR administered ranged from 104 to 555MBq, with an average of 303MBq. The clinical results were:

	n	Hyper		scHyper		Euth		scHypo		Hypo		RR	HR
		n	%	n	%	n	%	n	%	n	%	%	%
6mth	59	20	34	10	17	16	27	3	5	10	17	49	22
12mth	44	14	32	3	7	20	45	1	2	6	14	61	16
18mth	28	3	11	1	3	17	61	0	0	7	25	86	25
24mth	18	1	5,5	1	5,5	9	50	0	0	7	39	89	39
30mth	10	0	0	0	0	5	50	0	0	5	50	100	50

Conclusions: Therapeutic activity of iodine-131 can be easily quantified with a gamma camera and a simple calculation method. Clinical application of this method, results in high remission rates, similar to those derived from different and more complicated methods.

PS_71

RADIOIODINE ALONE VERSUS COMBINATION OF PERCUTANEOUS ETHANOL INJECTION AND RADIOIODINE IN TREATMENT OF LARGE TOXIC THYROID NODULES NOT ELIGIBLE FOR SURGERY

M. Zingrillo (1), S. Modoni (2), G. Valle (2), V. Trischitta (1), V. Frusciante (2). (1) Department of Endocrinology; (2) Department of Nuclear Medicine, Casa Sollievo della Sofferenza, San Giovanni Rotondo, Italy.

Aim: The commonest therapeutic option for large toxic thyroid nodules (TTN) is surgery. Some patients, however, may be at high surgical risk. Their treatment is therefore a choice between radioiodine (RAI) and percutaneous ethanol injection (PEI).
Methods: Eighteen informed consent patients with single „hot" nodule, larger than 4 cm, with suppression of extranodular tissue, with clinical and biochemical hyperthyroidism and high surgical risk or refuse of surgery, were randomly assigned to two different treatments.
Group A: in 9 patients, RAI was administered at the dose of 12,580 kBq/mL of nodular volume (NV), measured by ultrasound by ellipsoid formula and corrected for 24-h 131-I uptake (RAIU). Group B: in 9 patients RAI was preceded by 2-4 PEI sessions (mL ethanol injected = 30 % NV), at weekly intervals, without relevant side effects. NV re-evaluation, 24-h RAIU and RAI treatment were performed two months after last PEI.
Local symptoms (neck pressure, dysphagia, aesthetic complaint), were evaluated by an arbitrary score (0=absent; 1=moderate; 2=severe). Sum of symptoms score (SYS) was then calculated. FT4, FT3 and TSH were also measured. Methimazole was stopped 15 days before 24-h RAIU and RAI treatment. TSH values were < 0.1 mU/L at RAI administration. Data (mean ± SD) were compared by Student's *t*-test .
Results: Nodule volume at baseline were respectively 56.8±21.1 mL (range 36.0-103) and 57.8±26.8 mL (33.5-112). Two months after PEI, group B patients showed a NV reduction: 32.6±19.6 mL ($p<0.05$)
Their 24-h RAIU was not different from that of group A patients: 51.2 ± 1.6 % vs. 59.1 ± 10.1 %. Administered RAI dose (on the basis of NV and 24-h RAIU) was consequently lower ($p < 0.05$) for group B (707 ± 229 MBq; 444 - 1110) vs. group A (1110 ± 414 MBq; 740 - 2035). Six months after RAI, percentage of NV reduction was, respectively, 45.7±12.9% (28.5-64.8) and 72.8±17.7% (47.0-95.8) for group A and B. Group B patients showed a greater reduction ($p < 0.05$) of both NV and SYS; 3 patients from group A were subclinically hyperthyroid (i.e. normal FT4 and FT3 and suppressed TSH values), while 1 patient in both groups showed a slight increase of TSH with normal FT4 and FT3.
Comment: when surgery is not applicable in large TTN, RAI dose may be reduced when it is preceeded by few sessions of PEI, allowing, despite this, a greater NV shrinkage and amelioration of local symptomatology. This combined treatment is, at least, similarly effective than RAI alone in treating hyperthyroidism., suggesting its use as treatment of choice for large TTN.

PS_72

131I-LIPIODOL THERAPY: INFLUENCE OF POTASSIUMIODIDE ON THYROIDAL UPTAKE AND DOSE

K. Bacher (1), B. Brans (2), A. Troisi (3), M. Monsieurs (2), L. Defreyne (4), P. Vanlangenhove (4), I. Colle (3), B. de Hemptine (3), H. Thierens (1), R.A. Dierckx (2). (1) Departement of Medical Physics; (2) Division of Nuclear Medicine; (3) Gastro-enterology and Surgery Departments; (4) Division of Interventional radiology, Ghent University Hospital, Ghent, Belgium

Aim: In 131I-Lipiodol therapy, 131I-iodide may be released causing undesirably irradiation the thyroid gland. Although generally no special precautions are advocated, some authors have reported uptake in the thyroid. Aim of this study was to evaluate the potential benefit of potassium-iodide (KI) pre-medication.
Methods: Between June 1999 en March 2001 we gave 66 treatments in 41 patients for hepatocellular carcinoma (HCC). 131I-Lipiodol was given as a slow bolus through a hepatic catheter non-selective in the hepatic artery propria (n=36) or selective in the right and/or left hepatic artery (n=30). The mean activity we used was 1828 MBq (49.4 mCi) in a volume of 2 (n=19) or 4 (n=47) ml. The effect of KI, given in a dose of 100 mg per day one day before 131I-Lipiodol until 2 weeks after therapy, was studied prospectively and randomized: 35 treatments were associated with ("KI") and 31 treatments without KI pre-medication ("non-KI"). Thyroidal uptake was assessed by the percentage of activity measured on scintigraphy 7 days after 131I-Lipiodol (n=44); thyroidal dose was assessed by scintigraphy after 7 and 14 days using a mono-exponential fitting model and MIRD dosimetry (n=26).
Results: Thyroidal uptake was lower in the KI group (n=24), being 0.23 +/- 0.08 % of injected activity compared to the non-KI group (n=20) being 0.44 +/- 0.23 %. Consequently, KI pre-medication resulted in a lower mean thyroidal dose with decreased standard deviation: 5.6 +/- 1.6 Gy in the KI group (n=16) versus 11.5 +/- 4.9 Gy in the non-KI group (n=10). Thyroidal uptake was in all cases higher on the early scan after 7 days as compared to 14 days after therapy. An effect of amount of added cold Lipiodol (2 versus 4 ml total volume) or selectivity of 131I-Lipiodol administration was not evident.
Conclusions: KI pre-medication is associated with a lower thyroidal uptake and dose in 131I-Lipiodol therapy causing a consistently lower dose range as compared to patients without KI in whom a higher variability is observed, possible caused by other factors being different inter-individually.

PS_73

I-131 THERAPY OF GRAVES DISEASE: THE RESULTS OF OUR 40-YEAR EXPERIENCE

G. Ronga (1), M. Filesi (1), A.R. Vestri (2), T. Montesano (1), A. Annovazzi (1), A. Di Nicola (1), L. D'Ignazio (1), F. Fiore Melacrinis (1), A. Signore (1). (1) Nuclear Medicine, Department of Clinical Sciences; (2) Department of Experimental Medicine, University, Rome. Italy.

The aim of our study was to evaluate the results of I-131 treatment in patients with Graves disease during a long term follow-up.
Methods: We considered 364 pts with Graves disease observed in our department from 1960 to 2000 (M/F ratio 1:11.6, mean age at diagnosis 34.7±12.7 yrs, range 15-49 yrs). The diagnosis was performed by clinical, scintigraphic and hormonal data. In 162 pts as well as an increase of thyroid size, cold nodules were also found. All patients were first treated with antithyroid drugs (methimazole or propylthiouracil) and thyroid extracts or Levo-thyroxine for at least 18 months. Only in 99 pts (27.2%) the complete recovery was obtained, while in 21 the surgical therapy was recommended for the young age. In the remaining 245 radioiodine therapy followed medical therapy. The I-131 dose administered was between 5.2 and 18.5 mCi and was based on the weight of thyroid (45-115 g) and I-131 uptake at the 24th hour.
Results: In 187 pts (76.3%) we obtained remission of disease after the first dose, while in 50 (20.2%) a second dose was administered and in the remaining 8 (3.5%) three or more administrations were necessary to obtain the remission of disease. In 59 pts (24.1%) hypothyroidism, clinical (TSH values >10 µU/ml) or subclinical (TSH values 5-10 µU/ml), occurred within 6-12 months from the last I-131 administration. In the following years the rate of new hypothyroidism was about 2% per year, lower after 10 yrs. In all treated cases a remarkable decrease of the thyroid size was obtained (mean 22.7%) but this result was more evident when the initial weight was less than 50 g. No correlation was observed with the initial presence or absence of cold nodules that did not change their sizes after therapy. During a 40-year observation no pathological consequences of therapy were found. Ophthalmic disease very often improved after I-131 therapy.
Conclusions: In our experience, Graves disease is well cured with a single I-131 dose. After a long term follow-up hypothyroidism was about 4%. We consider it a unwanted effect but it is must be accepted as a "natural" and often unavoidable consequence of I-131 therapy.

PS_74

EVALUATION OF THE EFFECT OF VARIOUS PARAMETERS ON THE AMOUNT OF RADIATION DOSE RECEIVED BY HOMEMATES OF I-135-THERAPY PATIENTS

S. Sarkar (1), M. Dehghanpour (1), M. Saghari (1), M. Ghiasinezhad (2). (1) Tehran University of Medical Sciences; (2) Tarbiat Modarres University, Teheran, Iran.

The main concern with respect to discharge of ^{131}I-therapy patients from hospital is the contamination of their surroundings and exposure of people in close contact with them. We have measured and evaluated the effects of various parameters on the dose absorbed by homemates of these patients within one week after being discharged from hospital.
Methodes: The absorbed dose to 100 individuals including: patients with thyroid cancer (23), their family members (70), patients suffering from hyperthyroidism (2) and their family members (5), were measured. The measurements were performed by TLD. The hospitalization period for those patients suffering from thyroid cancer, varied between 2-3 days, whereas hyperthyroidism patients were treated as out-patients. The patients were discharged from hospital according to ICRP-60.
Results: Even though hyperthyroidism patients received much less activity in comparison to those with thyroid cancer, due to slow iodine discharge rate from their bodies, they radiated more to the surroundings. For patients having thyroid cancer, as the activity given to them increased from 100 mCi to 150 mCi the average dose absorbed by their homemates increased by a factor of 3. The duration of hospitalization (2 or 3 days) as well as the amount of activity (100 or 150 mCi) given to the patients had a significant effect (up to 6.5 times) on the amount of radiation dose received by their homemates.
Increasing the size of the patient's home from 45-50 m to 75-100 m and to 120-400, reduced the average radiation dose received by their homemates by a factor of 4 and 6 respectively. The average dose received by the members of the family who were at home for less than 10 hours a day was about 5 times less than that of those who spent more time at home. The average absorbed dose by children was 9 times bigger than that of spouses.
Conclusions: For deciding the discharge of the ^{131}I-therapy patients from the hospital, parameters such as: the amount of activity received, the type of disease, the size of home, presence of children at home, and the time spent with homemates are suggested to be taken into account.

PS_75

123-IODINE IN FOLLOW-UP OF PATIENTS WITH DIFFERENTIATED THYROID CANCER: OUR EXPERIENCE

L. Dell'Erba (1), G. Calò Gabrieli (2), R. Golia (1), G. Squame (1).
(1) Medicina Nucleare, Università Federico II, Napoli, Italy; (2) Medicina Nucleare, P.O. Di Venere, Bari, Italy.

It is common knowledge that 123-iodine is an ideal tracer for imaging with scintillation cameras due to its physical characteristics (pure gamma emitter, 159 keV primary emission, T/2 = 13.3 hr). Moreover, it does not reduce subsequent uptake of 131-iodine administered for therapeutic use (thyroid stunning). Nevertheless, high cost and cumbersome supply reduce the use of this tracer.
Methods: In 1999 and 2000, we studied 8 patients (6 women and 2 men, age range 26-70 years), affected by differentiated thyroid cancer, with 123-iodine whole body scan. They underwent previous thyroid surgery (between 1990 and 1997) and ablation for thyroid remnants with 131-iodine. Clinically, they were disease free and no one had a previous positive 131-iodine whole body scan. After 30-35 days of withdrawal of the levotiroxine therapy they were subjected to whole body scan with 123-iodine (185-210 MBq e.v.) and static views of the neck area. Imaging was performed at 2, 6-8 and 24 hours.
Results: In 7 patients (TSH > 50 mU/ml, hTG < 0.8 ng/ml) we found a negative whole body scan. One patient (woman, 45 year old, TSH = 24 mU/ml, hTG = 0.7 ng/ml) had a jugular area of iodine uptake and ultrasonography demonstrated an oval formation (7x4 mm) with blurred edges (lymph node) at this point. After 3 weeks, she received 3700 MBq of 131-iodine. No uptake was seen in the same area, but a diffuse, tenuous liver activity appeared. This demonstrates the presence of at least one area of hormonal synthesis.
Conclusions: Our data seem to confirm a greater diagnostic value of 123 iodine versus131-iodine.

CARDIOVASCULAR 2

PS_76

MYOCARDIAL BLOOD FLOW AND CORONARY RESISTANCE DURING 'CARDIAC FATIGUE' AFTER PROLONGED EXERCISE

J. Knuuti (1), K.K. Kalliokoski (1), M. Laaksonen (1), M. Luotolahti (3), H. Laine (1,2), T.O. Takala (1), P. Nuutila (1,2). (1) Turku PET Centre; (2) Department of Medicine; (3) Department of Clinical Physiology, University of Turku, Finland.

Strenuous long-term exercise has shown to transiently decrease myocardial contractility, but the mechanisms have remained unclear. Insufficient myocardial blood flow possibly due to coronary dysfunction during prolonged exercise could be one of the factors behind myocardial fatigue. The purpose of this study was to investigate the effects of marathon running on cardiac function, myocardial perfusion, and perfusion reserve.
Methods. Myocardial blood flow and flow reserve (PET and ^{15}O-H_2O) of seven healthy marathon runners were measured before and 85-115 min after marathon running. Echocardiography studies to measure myocardial contractility and blood sampling to measure indices of myocardial damage were performed before and 10 min, 150 min and 20 h after marathon running.
Results. Rate-pressure corrected resting myocardial blood flow was increased by 35 % (0.88 ± 0.14 vs 1.16 ± 0.21 mL · min^{-1} · g^{-1}, p<0.05) and blood flow during adenosine stimulation by 48 % (3.67 ± 0.81 vs 5.14 ± 0.76 mL · min^{-1} · g^{-1}, p<0.05) after marathon running, but flow reserve remained unchanged (4.3 ± 1.4 and 4.6 ± 1.0, p=NS). Coronary resistance was lower after running both at rest (106 ± 15 vs 59 ± 13 mmHg · min · g · mL^{-1}, p<0.05) and during adenosine stimulation (26 ± 6 vs 18 ± 3 mmHg · min · g · mL^{-1}, p<0.05). Stroke volume, ejection fraction, and fractional shortening were significantly lower at 150 min after marathon running, but relative plasma volume was unchanged at the same time compared to pre-running values. Both systolic blood pressure/end systolic diameter –ratio and meridional wall stress tended to be lower compared to pre-running values. No evidence of myocardial cell damage was found, since serum troponin-I was unaltered after marathon running.
Conclusions. The results of the present study show that, despite of evidence of decreased myocardial contractility after strenuous exhausting exercise, resting myocardial blood flow and blood flow in response to exogenous adenosine are not reduced, but rather improved. Thus, cardiac dysfunction after prolonged exercise is not accompanied with coronary dysfunction.

PS_77

MYOCARDIAL PERFUSION IMAGING AFTER PERCUTANEOUS TRANSLUMINAL CORONARY ANGIOPLASTY (PTCA) IN DIABETIC PATIENTS

O. Lang (1), H.R. Balon (2), L. Treslova (1), M. Andel (1), R. Feuereisl (3), B. Kallmüntzer (3), P. Jebavy (3), M. Kaminek (4), M. Myslivecek (4).
(1) Department of Nuclear Medicine and Internal Medicine, Charles University, Prague, Czech Republic; (2) Department of Nuclear Medicine, William Beaumont Hospital, Royal Oak, Michigan, USA; (3) Kardiologie Ltd., Hospital Bulovka, Prague, Czech Republic; (4) Department of Nuclear Medicine, Palacky University, Olomouc, Czech Republic

Aim: To evaluate prognostic value of myocardial perfusion imaging (MPI) in diabetic patients after acute myocardial infarction treated by coronary angioplasty.
Methods: We have retrospectively evaluated 77 patients (18 female and 59 male) of mean age of 59 years (45-76). All were after acute myocardial infarction treated by coronary angioplasty with stenting, patency of infarct related artery was verified by coronary angiography. Left anterior descending coronary artery was treated in 36%, left circumflex in 26% and right coronary artery in 38%. Myocardial perfusion imaging was performed with one-day stress-rest protocol using Tc-99m MIBI in the fourth week after procedure. Results were divided into positive (reversible and/or fixed perfusion defects) and negative (without any perfusion defect). Patients were divided into two groups. Diabetic patients had diabetes mellitus as at least one risk factor, non-diabetic were the others. Patients were followed for 16 to 30 months and cardiac events – death, myocardial infarction, revascularization or new angina - were monitored. Frequency of cardiac events were compared by contingency cross tabulation and chi-square test, p-value and Fischer exact test.
Results:

All patients				
		MPI		
		positive	negative	Total
Cardiac events	yes	27	9	36
	no	3	38	41
	total	30	47	77
p-value < 0,01				

Diabetic patients				
		MPI		
		positive	negative	Total
Cardiac events	yes	8	3	11
	no	1	8	9
	total	9	11	20
Fischer < 0,01				

Other patients				
		MPI		
		positive	negative	total
Cardiac events	yes	19	6	25
	no	2	30	32
	total	21	36	57
p-value < 0,01				

Conclusions: Myocardial perfusion imaging is a useful method for prognosis assessment in diabetic patients with acute myocardial infarction treated by primary angioplasty with stenting. Its value is the same as in non-diabetic patients even if it is performed early (during the fourth week) after procedure.

PS_78

PREDICTIVE VALUE OF MYOCARDIAL SCINTIGRAPHY WITH IODINE-123 LABELED BMIPP IN PATIENTS WITH ACUTE MYOCARDIAL INFARCTION TREATED WITH PRIMARY PERCUTANEOUS TRANSLUMINAL CORONARY ANGIOPLASTY

M. Nanasato (1), A. Ando (2), S. Isobe (2), M. Nonokawa (2), N. Tsuboi (1), T. Ito (1), Y. Kinoshita (3), I. Nanbu (3), M. Hirai (2), M. Yokota (4), H. Hirayama (1); (1) Cardiovascular Center, Nagoya Daini Red Cross Hospital, Nagoya, Japan; (2) First Department of Internal Medicine, Nagoya University, Nagoya, Japan; (3) Department of Radiology, Nagoya Daini Red Cross Hospital, Nagoya, Japan; (4) Department of Clinical Laboratory Medicine, Nagoya University, Nagoya, Japan

Primary percutaneous transluminal coronary angioplasty (PTCA) is not only treatment for patients with acute myocardial infarction (AMI) but also depicts the severity of coronary artery disease and left ventricular function. Although the predictive value of thallium-201 (Tl) after AMI has been well established, it is unclear whether iodine-123 labeled 15-iodophenyl-3-R,S-methyl pentadecanoic acid (BMIPP) imaging following AMI treated with primary PTCA is useful to predict future cardiac events in addition to the variables obtained from cardiac catheterization.

Methods: One hundred fifty-nine patients (122 men; age 62.5+-10.3 years; Max CPK 2943+-2172 IU) with AMI treated with primary PTCA underwent left ventriculography (LVG) at the admission, Tl and BMIPP myocardial scintigraphies at rest before the discharge. Scintigrams were visually assessed. Left ventricular myocardium was divided into 17 segments and each segment was scored from 0 (normal uptake) to 3 (defect). Defect score (DS) was calculated as the summed score of each segment. Mismatch was defined as the visual discordance between Tl and BMIPP. Major cardiac adverse event (MACE) was defined as cardiac death including sudden death, congestive heart failure, and recurrence of acute coronary syndrome. Left ventricular ejection fraction (LVEF) was measured from LVG by area length method. Percent diameter stenosis more than 75% on coronary angiography by visualized assessment was defined significant.

Results: One hundred fifty-nine patients were followed up for a mean interval of 34.5 months. Twenty-six patients had MACE and ten patients died during the follow-up. Kaplan-Meier analysis indicated that patients with the larger half of BMIPP-DS had significantly higher cardiac event rate on MACE (p=0.009) and cardiac death (p=0.03). Patients with mismatch also had significantly more MACE (p=0.04) and cardiac death (p=0.04). On the prediction of MACE, global chi-square value was 5.2 (p=0.001) by mean of LVEF (< 45%) and number of diseased vessels (2 or 3). Adding BMIPP-DS to these variables improved the global chi-square value (x^2=6.7). Adding BMIPP-DS and mismatch improved it more (x^2=7.2). Global chi-square value with the variables from cardiac catheterization was 2.1 on the mortality. The global chi-square value was made better by supplementing BMIPP-DS and mismatch (x^2=4.2).

Conclusions: Myocardial scintigraphies using Tl and BMIPP predict future cardiac events in patients with AMI treated with primary PTCA and provide the additionally predictive value to the variables obtained from primary PTCA. Myocardial scintigraphies are of use to diagnose the prognosis accurately even in patients underwent primary PTCA.

PS_79

NO-REFLOW PHENOMENON AFTER TROMBOLYTIC THERAPY IN ACUTE MYOCARDIAL INFARCTION: A COMPARISON OF TC-99M TETROFOSMIN REST SPECT AND CORONARY ANGIOGRAPHY IN THE EARLY PHASE

F. Canbaz (1), T. Başoğlu (1), M. Elcik (2), B. Kirtiloğlu (1), M. Sahin (1), S. Aibayrak (1), O. Yapıcı (1). (1) Department of Nuclear Medicine; (2) Department of Cardiology, Ondokuz Mayıs University Hospital, Samsun, Turkey.

Assesment of early myocardial perfusion in infarct related regions has clinical importance in the management of patients. Angiographic reflow in the infarct related artery (IRA) after trombolysis does not always rule out perfusion anomalies in the related myocardial tissue. The aim of our study was to compare scintigraphic (SNRP) and angiographic no-reflow phenomenon (ANRP) in patients with acute myocardial infarction (AMI) after trombolytic therapy.

Methods: Eighteen patients (4 F, 14 M; Mean age 56,4 ± 11 yrs.) with AMI were included in the study. The patients underwent echocardiography (ECHO) and hereafter coronary angiography (CA) within 4-10 days following trombolytic therapy. Rest myocardial perfusion SPECT using 740 MBq Tc-99m Tetrofosmin was performed the day after CA. The ECHO wall motion score (ECWS) was determined by dividing the sum of segmental motion scores (normal, hypokinesis, akinesis, dyskinesis, aneurism) by 16 in each patient. The blood flow in the infarct related artery was evaluated using the TIMI grading system (Trombolysis In Myocardial Infarction). TIMI-flow grade (TFG) and TIMI-frame count (TFC) regarding the IRA were determined during CA. Scintigraphic perfusion was scored using a 4-grade system (normal, mild hypoperfusion, moderate or severe hypoperfusion and defect) in 20 left ventricular segments. A defect score (DS) was determined as the sum of the perfusion defects and a defect score index (DSI) was calculated as DS divided by the number of segments supplied by the infarct related artery.

Results: In six patients meeting the ANRP criteria (TFG ≤ II without mechanical obstruction after recanalization), SNRP (perfusion defect) was also observed. Five of 18 (28 %) patients having TFG III (re-flow) had SNRP. Both DS and DSI did not correlate with angiographic and echocardiographic parameters. Presence of SNRP and ECWS (r=0,6 and p<0,05) as well as TFC and ECWS (r=0,7 and p<0,05) were moderately correlated.

Conclusion: SNRP occur despite angiographic re-flow in a non-negligible number of patients who undergo recanalization. Early reperfusion decreases infarct size and improves survival. Thus, myocardial SPECT should be part of the standart investigations in the assesment of AMI patients after recanalization therapy to obtain a maximum of diagnostic data. Long term angiographic and scintigraphic studies are valuable to confirm the final perfusion status.

PS_80

COMPARISON OF THALLIUM-201/IODINE-123-BMIPP MYOCARDIAL SINGLE-PHOTON EMISSION TOMOGRAPHIC FINDINGS WITH ELECTROCARDIOGRAPHY AND CARDIAC FUNCTION IN PATIENTS WITH ACUTE ANTERIOR MYOCARDIAL INFARCTION

S. Isobe (1), M. Okada (2), A. Ando (1), M. Nanasato (1), M. Nonokawa (1), M. Hirai (1), M. Yokota (3). (1) First Department of Internal Medicine, Nagoya University School of Medicine, Nagoya, Japan; (2) Nagoya Ekisaikai Hospital, Nagoya, Japan; (3) Department of Clinical Laboratory Medicine, Nagoya University School of Medicine, Nagoya, Japan.

Aim: No study has been attempted to investigate the relationship among scintigraphic findings, time course of changes in electrocardiography (ECG), and that in cardiac functional in patients with acute myocardial infarction (MI). The purpose of this study was to determine whether thallium-201 (Tl) and iodine-123-β-methyl-p-iodophenyl pentadecanoic acid (BMIPP) myocardial single-photon emission tomographic (SPET) images were clinically useful for evaluating changes in ECG in addition to changes in cardiac function of patients with acute anterior MI.

Methods: Seventy-four patients were subjected to Tl and BMIPP SPET 1 week after the onset of MI and to ECG and echocardiography both 1 and 4 weeks after the onset. The mean defect ratio on Tl [(%) defect on Tl] and that on BMIPP [(%) defect on BMIPP] derived from circumferential profile curve analysis were calculated. The percentage defect-discordant ratio of both SPET images [(%) discordance on Tl/BMIPP] was obtained. The total sum of ECG R wave voltage on each chest lead was calculated. The percentage increase ratio of ECG R wave voltage on chest leads [(%) increase of R wave] and the increase of the left ventricular ejection fraction from 1 to 4 weeks (delta-EF) were obtained.

Results: There was a significant high correlation between the (%) defect on Tl and that on BMIPP ($r = 0.88$, $p < 0.0001$). There were significant correlations between the (%) discordance on Tl/BMIPP SPET images and the delta-EF and between the (%) increase of R wave and the delta-EF ($r = 0.43$, $p < 0.01$; $r = 0.46$, $p < 0.005$, respectively). Moreover, there was a significantly good correlation between the (%) discordance on both images and the (%) increase of R wave ($r = 0.71$, $p < 0.001$). In follow-up study (n = 15, 190 ± 89 days after the onset of MI), patients with the discordance on Tl/BMIPP showed cardiac functional recovery at follow-up compared with 4 weeks after the onset.

Conclusion: The discordance on Tl/BMIPP SPET images, with larger defect on BMIPP compared to Tl (perfusion-metabolism mismatch), may be related not only the recovery of cardiac function but also to that of R wave voltage in ECG. Combined examinations of Tl/BMIPP SPET tracers are clinically useful not only to evaluate the infarct size but also to follow up patients with acute anterior MI.

PS_81

EVALUATION OF MYOCARDIAL PERFUSION IN LEFT-SIDE BREAST CANCER TREATED WITH ADJUVANT RADIOTHERAPY

J. Drac-Kaniewska (1), M. Olszewska (2), I. Kozlowicz-Gudzinska (1), J. Galecki (3), A. Niwinska (3). (1) Department of Nuclear Medicine; (2) Internal Medicine Consulting Group; (3) Breast Cancer Department, The Maria Sklodowska-Curie Memorial Cancer Center, Warsaw, Poland.

The purpose of the study was to evaluate myocardial perfusion damage in left-side breast cancer patients after adjuvant radiotherapy using photons- or electrons-beam.

Methods.49 patients with left-side breast cancer aged 36-69 , with no clinical signs of coronary artery disease and negative ECG were recruited. They underwent left mastectomy or tumor excision, chemotherapy and adjuvant radiotherapy or left mastectomy (or tumor excision) and adjuvant radiotherapy. All of them were irradiated with photons or electrons; the standard dose was 45-50 Gy divided into 20-25 fractions. Each of patients underwent dipyridamol-stress scintigraphy before, 3 months and at least 12 months after radiotherapy; 2-day protocol was applicated. G-SPECT aquisition was performed 60 min after IV injection of 740 MBq 99mTcMIBI with dual-head gamma camera;image was reconstructed by filtered back-projection. Image analysis was performed qualitatively and quantitatively on 13 segments polar maps. Perfusion defects were classified as no defects (> 75% activity), moderate (65%-74% activity) and severe(50%-64% activity).Deterioration of perfusion was defined if moderate or severe defects appeared after radiotherapy in at least 2 segments of polar maps.

Results.Among 49 evaluable patients 38 (77%) were no new perfusion defects at control perfusion scintigraphy 12 months after radiotherapy. 11 of 49 pts (23%) had new perfusion defects after 12 months follow-up; in 3 of them deterioration of perfusion appeared 3 months after treatment, in 8 – after 12 months. 8 of 49 investigated pts demonstrated transient perfusion defects 3 months after radiotherapy.These observed perfusion defects were moderate or severe, but they were never below 50% activity; defects were located mainly in segments of anterior and inferior wall, rarely at lateral wall and septum.

Conclusions. An adjuvant radiotherapy using photons- or electrons beam seems to protect the myocardium from harmful irradiation, as majority of patients presented no perfusion deterioration 12 months after treatment. Nevertheless some patients demonstrate moderate segmental perfusion defects and they may need further cardiological follow-up.

PS_82

PERFUSION DEFECT PATTERNS HELP DISCRIMINATE PATIENTS WITH PROXIMAL FROM DISTAL LEFT ANTERIOR DESCENDING ARTERY STENOSIS ON THALLIUM MYOCARDIAL SPECT

J.K. Yoon, K.H. Lee, J.M. Park, Y. Choi, Y.S. Choe, S.E. Kim, B.T. Kim. Nuclear Medicine, Samsung Medical Center, Seoul, Korea.

Purpose: In patients with left anterior descending artery stenosis (LAD), those with proximal disease have a poorer prognosis and generally require intervention compared to those with distal disease. We investigated whether patterns of perfusion defects (PD) in the LAD territory may help discern patients proximal from those with distal stenosis.

Methods: Among patients who underwent coronary angiography (CAG) and thallium SPECT with adenosine (or dipyridamole) stress within 1 month of each other, 90 patients with a significant single vessel LAD stenosis (>50%) and a reversible PD were included. Size and severity of PD as well as presence of apical LV dilatation on apex, anterior and septal wall were visually graded from inspection of tomographic images and Bull's eye displays.

Results: CAG revealed the locations as proximal LAD (n=51, including 4 os lesions) and mid LAD (n= 39, including 2 distal lesions). Patterns of PDs were categorized as type I (n=20, PD on apex, apical anterior wall and septum), type II (n=25, PD on apex and septum), type III (n=20, diffuse PD on most of LAD territory displayed as wedge shape on Bull's eye), type IV (n=17, PD confined to apex) and the others (n=8, PD confined to anterior wall or anteroseptal wall). Patients with type I and III had a higher proportion of proximal LAD stenosis (75% and 90%), while those with type II and IV patterns were more likely to have mid LAD stenosis (68% and 71%). The 8 cases with other patterns showed PD confined to part of anterior wall (n=4) or mild anteroseptal wall (n=4). Most of the former cases (3/4) had a combined significant stenosis (>75%) on 1st diagonal branch and the latter cases had less severe proximal LAD stenosis (about 80%, n=3) or subtotal stenosis of 1st septal branch (n=1). The proportion of the presence of transient apical LV dilatation was not different between the patients with proximal LAD stenosis (n=9) and mid LAD stenosis (n=8).

Conclusion: Specific defect patterns on myocardial perfusion SPECT can aid in differentiating patients with high likelihood of proximal LAD from those with mid LAD stenosis. Such patterns may help select patients in whom coronary angiography is required to evaluate the need for revascularization.

PS_83

LEFT VENTRICULAR MASSES MEASURED AT STRESS AND REST MYOCARDIAL PERFUSION SPECT IN PATIENTS WITH PERFUSION DEFECT

B.C. Ahn, S.W. Lee, J. Lee, K.B. Lee. Department of Nuclear Medicine, Kyungpook National University Hospital, Taegu, South Korea.

Left ventricular mass(LVM) can be used as prognostic marker in patients with hypertension or heart disease. We measured LVM using quantitative gated myocardial perfusion SPECT(QGS) to evaluate the difference between LVM measured at stress(S-LVM) and that measured at rest(R-LVM) in subjects with perfusion defect.

Methods: Forty-six subjects(M/F=34/12, ranged 43 to 84 yrs, mean age 64yrs) with myocardial perfusion defect underwent QGS with ^{99m}Tc-MIBI at rest and 1 hour after stress. LV volume was measured from AutoQuant program (Pegasys, ADAC) and LVM was calculated by multiplying the volume by the specific gravity of myocardium.

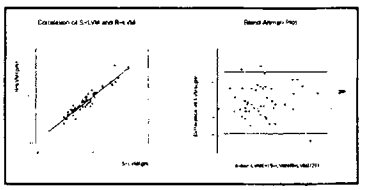

Results: There was good correlation between LVMs measured at stress and rest QGS(138.7±27.1 vs 138.9±26.7, r=0.945, p<0.01). Higher correlation was found at subjects with fixed defect or small defect extent(lesser than 20%) or lower ejection fraction(lesser than 50%). LVM measured by AutoQuant program at stress and rest QGS in subjects with perfusion defect

subjects with	S-LVM (gm)	R-LVM (gm)	Cor
Reversible defect(n=41)	134±22	135±23	r=0.920, p<0.01
EF?50%(n=30)	130±19	129±18	r=0.874, p<0.01
Extent?20%(n=17)	140±27	143±30	r=0.943, p<0.01

subjects with	S-LVM (gm)	R-LVM (gm)	Cor
Fixed defect(n=6)	167±39.7	165±34.	r=0.993, p<0.01
EF<50%(n=17)	154±32	155±31	r=0.970, p<0.01
Extent<20%(n=22)	134±27	133±25	r=0.960, p<0.01

Cor=correlation, r=correlation coefficient, Extent=extent of perfusion defect, EF=ejection fraction at rest QGS.

Conclusion: LVMs measured at stress and rest myocardial perfusion SPECT are good correlated in subjects with perfusion defect, especially in patients with fixed or small perfusion defect.

PS_84

IMPROVED PERFUSION AND INCREASED REVERSIBILITY WITH SUBLINGUAL NITROGLYCERIN BY REST THALLIUM-201 MYOCARDIAL PERFUSION SPECT

T W. Wen. Department of Nuclear Medicine,Tzu-Chi General Hospital, Hua-Lien, Taiwan.

The objective of the study is to determine whether sublingual nitroglycerin given at rest improves perfusion and increases reversibility by Tl-201 myocardial perfusion SPECT in patients suspected of coronary artery disease.

Methods: Sixty-nine consecutive patients (Mean age 60±2, 38 males) referred to our nuclear cardiology laboratory underwent exercise or dipyridamole stress Tl-201 myocardial perfusion SPECT according to standard stress/redistribution protocol. 92.5 MBq of Tl-201 chloride was injected at peak stress and delayed imaging was obtained at 3-4 hours post injection. Immediately following the redistribution imaging, patients were given nitroglycerin 0.6 mg sublingually, and a third set of myocardial SPECT was performed. SPECT images were processed by Xpert software (GEMES, Ltd).

Results: Sublingual nitroglycerin improved perfusion and increases reversibility in 65% (45/69) of patients; among them, 49% (22/45) and 42% (19/45) had reversible defects and normal perfusion respectively. In those who had fixed defects, only 9% (4/45) were found to benefit from sublingual nitroglycerin with improved reversibility.

Myocardial Perfusion SPECT	NTG Effects	
	Increased Reversibility	No Change
Total	45/69 (65%)	24/69 (35%)
Reversible Defect	22/45(49%)	3/24(13%)
Normal	19/45(42%)	7/24(29%)
Fixed Defect	4/45(9%)	14/24(58%)

Conclusion: Sublingual nitroglycerin improves perfusion and increases reversibility by Tl-201 myocardial perfusion SPECT, the effects are more evident in patients with myocardial ischemia and normal coronaries, than in patients with fixed defects.

PS_85

MULTICENTER CLINICAL EVALUATION OF GATED BLOOD POOL SPET FOR THE ASSESSMENT OF VENTRICULAR FUNCTION

M.W. Groch (1), W.D. Erwin (1), E.G. DePuey (2), A. Belzberg (3), M. Kamran (2), A. Ali (1), R.C. Hendel (1), C.A. Barnett (4), R.C. Marshall (4), M. Kiess (3). (1) Departments of Nuclear Medicine, Northwestern Memorial Hospital; Northwestern University and Rush Presbyterian St Lukes Medical Center, Chicago, Il, USA; (2) Department of Nuclear Medicine, Roosevelt-St Lukes Hospital, New York, NY, USA; (3) Department of Nuclear Medicine, St Paul's Hospital, Vancouver, BC, Canada; (4) Department of Nuclear Medicine, VA Medical Center, Martinez, CA, and University of California, Davis, CA, USA

Gated blood pool SPECT (GBPS), inherently three-dimensional (3D), has the potential to replace planar gated blood pool (PBP) imaging for computation of left ventricular ejection fraction (LVEF) and analysis of regional wall motion (RWM). With SPECT scanning and dual-headed cameras, functional imaging can be accomplished in less time than a 3-view planar study with a 3D perspective to isolate cardiac chambers. The purpose of this study was to evaluate GBPS vs. PBP imaging in a large cohort of patients from a multicenter, multi-national environment for assessment of left ventricular function. **Methods**: Patients normally referred to nuclear medicine in 5 institutions underwent conventional PBP imaging followed by GBPS. Each of the clinical sites followed an acquisition (ACQ) protocol which included 180^0 rotation, 32 views @1 min/view or 64views @ 30 sec /view in a 64^2 matrix for dual-head cameras (ACQ time = 16 min); or with single-head cameras, 32 views, 1 min/view (ACQ time = 35 min). Transverse GBPS images were reconstructed with a Butterworth filter 0.55 Nyquist cut-off, 7th order, and short axis images were created. All GBPS studies were processed with a new GBPS program, (NUMUGAS), and LVEF was computed from the isolated LV chamber and compared to the standard PBP LVEF method of each site. Using GBPS, RWM and image quality from 3-D surface shaded and volume rendered cine displays were evaluated qualitatively in a subset (n=30) of the patients. **Results**: LVEF was evaluated in 201 cases from the participating institutions. The correlation between GBPS LVEF and PBP LVEF was excellent, r= 0.90, p<0.01. Mean GBPS LVEF was 62.3 %+/-17.1 % vs. 53.9 %+/- 15.6 % for PBP, p<0.001. The line of linear regression was: GBPS LVEF = (1.035 * PBP LVEF) + 5.9. Bland-Altman analysis revealed an increasing bias in GBPS LVEF with increasing LVEF value (mean difference = 8 % +/- 6.2 %). In the subset of the patients evaluated qualitatively, RWM assessment was enhanced using 3D cine display in 30 % of the studies, equivalent in 56 % and PBP analysis was better in 14 %, largely in the septal area (2 patients). Conclusions: GBPS LVEF correlated well with PBP LVEF values. GBPS LVEF values were somewhat higher, likely due to exclusion of the left atrium. Three dimensional GBPS may become a practical replacement for planar gated blood pool imaging, with a concomitant increase in magnitude of LVEF, perhaps reflecting true ejection fraction.

PS_86

COMPARATIVE PROGNOSTIC VALUE OF SA-ECG AND RADIONUCLIDE ANGIOGRAPHY IN PATIENT WITH ARRYTHMOGENIC RIGHT VENTRICULAR CARDIOMYOPATHY

D. Le Guludec (1), R. Porcher (1), D. Daou (1), F. Harel (1), M. Faraggi (1), L. Sarda (1), R. Lebtahi (1), M. Slama (2). (1) Department of nuclear medecine, Bichat Hospital, Paris, France; (2) Department of cardiology, Antoine Béclère Hospital, Paris, France.

Aim: The prognosis of patients with right ventricular (RV) arrhythmias remains uncertain. We prospectively compared the prognostic value of right (RV) and left ventricular (LV) involvement assessed by radionuclide angiography (RNA) and signal average ECG (SA-ECG) as risk factors for sudden death.

Methods: 153 patients evaluated for severe arrhythmias originating from the RV were followed for a mean of 45 ± 34 months. Patients were classified as Group I (n=49) with a normal RNA or Group II (n=104) with an abnormal RV suggestive of arrhythmogenic right ventricular cardiomyopathy (ARVC), classified as diffuse or localized disease, with or without associated LV abnormalities. SA-ECG was considered positive if at least two out of three following abnormal criteria were present: (respectively with 25 Hz and 40 Hz filters): QRS duration >120 or 114 msec; LAS > 40 or 38 msec; RMS < 25 or 20 μV.

Results: During the follow-up period, 14 patients died suddenly, all in Group II. None of the clinical and electrical data, especially SA-ECG, were predictive of death. An abnormal RV at RNA study was the only highly predictive factor for death (p< .005) as well as the presence of LV abnormalities (p<.01). Abnormal SA-ECG were significantly associated to diffuse forms of RV disease.

RNA	QRS (msec)			LAS (msec)			RMS (μV)		
	mean	SD	P	mean	SD	P	mean	SD	P
normal	112.7	24		41.8	34.2		32.1	29.7	
localized	111.8	20		43.1	16.7		27.0	27.0	
diffuse	148.0*	44	<.0003	63.2	30.7*	<.001	12.0	10.6*	<.01

Conclusions: The study confirms that ARVC is a severe disease with a high risk for cardiac death. The evidence of RV abnormalities is highly predictive for sudden death, as well as association with LV involvement, while SA-ECG is only the reflect of disease extension.

PS_87

SIGNIFICANCE OF REINJECTION OR LATE REDISTRIBUTION THALLIUM-201 IMAGING AFTER REST-REDISTRIBUTION IMAGING IN DETERMINING MYOCARDIAL VIABILITY

T. Erdil, F. Dede, O. Noshari, T. Ones, S. Inanır, T. Turoğlu. Department of Nuclear Medicine, Marmara University Hospital, Istanbul, Turkey .

The aim of this study was to determine the whether reinjection after rest-redistribution imaging, or late redistribution after reinjection or without reinjection would provide further information in identifying myocardial viability over conventional rest-redistribution Tl-201 imaging.

Methods: Thirty patients (pts) (24M, 6F, mean age:58.29±9.96, range 40-72 yrs) with chronic coronary artery disease and left ventricular dysfunction underwent rest-redistribution Tl-201 imaging. Reinjection image after rest-redistribution was performed in 19 pts one hour after injection of 1 mCi of Tl-201. Seventeen of these pts were further studied with late redistribution (24-hr) imaging. Late redistribution imaging without reinjection was performed in 11 pts. All pts underwent coronary arteriography within one month before or after Tl-201 study. In each pt, myocardial Tl-201 activity was measured in 9 myocardial segments over polar map on stress, redistribution, reinjection and late redistribution images. An abnormal segment required to have a regional activity of less than 75% of peak activity. An abnormal segment was considered to be reversible if the regional activity increased by ≥ 10% from rest to early redistribution, reinjection or 24 hr image, whereas a segment was considered to be irreversible if the change in regional activity was < 10%.

Results: Of the 135 abnormal myocardial regions (50%) on the rest images, 104 (77%) had persistent defect on redistribution images by quantitative analysis, of which 31 (23%) demonstrated improved ^{201}Tl uptake after early redistribution, 8 (8%) showed improved uptake after reinjection, and 22 (23%) after late redistribution (10 segments (45%) after reinjection, 12 segments (55%) without reinjection. The mean normalized Tl-201 activity in regions with rest perfusion defect for rest, redistribution, reinjection and 24-hr images was 54.2%±14.9%, 54.3%±14.4%, 55.5%±13.7%, 57.9%±13.3% respectively.The improvement from redistribution to rest and from reinjection to redistribution and rest images and from 24-hr to reinjection was insignificant, but it was significant from 24-hr to rest and early redistribution (p<0.03) images. If regions with less than 60% of peak activity was considered to be nonviable, in 20 segments, only 24-hr image demonstrated more than 60% of peak activity all of these regions showed more than 10% improvement compared with stress images.

Conclusion: Late redistribution image gave clinically relevant information on myocardial viability compared with rest-redistribution and reinjection images.

DIAGNOSTIC ONCOLOGY 3

PS_88

COMPARATIVE STUDY OF ENHANCED X-RAY COMPUTED TOMOGRAPHY AND DUAL-HEAD TOMOGRAPHY WITH COINCIDENCE IN DIAGNOSIS OF SMALL LUNG CANCER

R.F. Wang, N.S. Qing. Department of Nuclear Medicine, Peking University First Hospital, Beijing, China.

Aim: To investigate enhanced x-ray computed tomography (CT) scanning and dual head tomography with coincidence (DHTC) imaging in detection of small lung cancer.

Methods: Eighteen patients (male 11, female 7) aged 19 ~ 71 years (median 51.7 years) with ϕ < 3 cm of soldiery pulmonary nodules were enrolled in this study. All patients were performed using enhanced CT scanning (Siemens Plus 4) after injection of 100 ml iodinated contrast medium to observe the enhancement degree and using DHTC imaging (ADAC Epic Vertex plus MCD/AC) following injection of 129.5 ~ 166.5 MBq of FDG-18F, respectively. The images of DHTC with attenuation correction (AC) and without AC (NAC) were reconstructed iteratively, and the ratios of tumor-to-background (T/B) were calculated.

Results: The imaging findings obtained from both enhanced CT and FDG-18F DHTC showed that 11 of 18 patients with soldiery pulmonary nodules had small lung cancer (squamous cell carcinoma of lung: 2 case, alveolar cell carcinoma: 3 cases and adenocarcinoma: 6 cases) histopathologically confirmed. CT detected the mediastial lymph node metastasis in 6 of 11 patients with small lung cancer, and DHTC noted 5 cases. In 5 cases with inflammatory lesions (inflammatory nodule: 4, pulmonary abscess: 1) and 2 cases with pulmonary tuberculoma, one inflammatory nodule was misdiagnosed as small lung cancer by enhanced CT, and 1 tuberculoma was misdiagnosed by FDG-18F DHTC with 4.23 of T/B ratio.

Conclusion: The results suggested that the enhanced chest CT scanning and DHTC with FDG-18F imaging had no difference in diagnosis small lung cancer, but the combination with the results of the two examinations could give more help to improve the diagnostic accuracy of small lung cancer.

PS_89

USEFUL PATTERNS OF ABNORMAL FDG UPTAKE BY VARIOUS HISTOLOGIC TYPES OF NON-SMALL CELL (NSC) LUNG CANCER AT INITIAL STAGING BY PET

C.Y.O. Wong, R. Nunez, P. Bohdiewicz, R. Welsh, G.W. Chimielweski, D. Fink-Bennett, K.P. Ravikrishnan, J.C. Hill, S.E. Pursel, H. Balon, H. Dworkin PET Center, Dept of Nuclear Medicine, William Beaumont Hospital, USA.

Aim: To identify useful patterns of abnormal FDG uptake by different types of NSC lung cancer and to assess their clinical implications. Methods: 103 sequential pts with newly diagnosed, pathology proven NSC lung cancer were included. The FDG PET images were acquired by dedicated PET scanner 1 hr after iv injection of 10 mCi F-18 FDG. There were 35 squamous cell (SQC), 17 large cell(LGC), 38 adenocarcinoma (ADC), 1 bronchioalveolar (BAC) and 12 non-classified NSC. The analysis of PET images were categorized into detectable patterns of necrotic center in the primary tumor, satellite lesions (T4), hilar lymph nodes (N1), N2, N3 and M1 lesions by visual interpretation of PET images for SQC, LGC and ADC(90 pts in total). BAC was excluded because of known low FDG uptake and hence few referrals. 12 non-classified NSC were also excluded. The PET lesions were later correlated with surgical pathology, and CT for inoperable cases. Results: The frequency of each pattern was tabulated. Necrosis was present more commonly in the primary tumors of LGC(53%) and SQC(43%) than those of ADC (26%) ($p<0.0001$ and <0.01 resp). The frequencies of nodal uptake in ADC, SQC and LGC were similar (71, 60, 59% resp). However, M1 lesions were present significantly more in LGC(41%) and ADC(34%) than SQC(3%) (both $p<0.0001$). There were significantly more surgically inoperable pts determined by PET (T4, N3, M1) in ADC(50%)and LGC(41%) than SQC(26%)($p<0.001$ and <0.02 resp). Conclusion: Results suggest wide variations of PET findings for different NSC lung cancers. Identification of these patterns are useful in clinical PET reading for initial staging and planning management by checking against the most probable association between PET patterns and the histologic type.

Total=90	Necrosis	Satellite	Hilum	N2	N3	M1
SQC(N=35)	15	7	8	5	8	1
LGC(N=17)	9	2	4	5	1	7
ADC(N=38)	10	10	7	6	14	13

PS_90

CLINICAL IMPACT OF ABNORMAL FDG UPTAKE IN PULMONARY NODULES DETECTED BY CT IN PATIENTS WITH ONLY HISTORY NON-LUNG CANCERS

C.Y.O. Wong, R.J. Welsh, G.W. Chmielewski, D. Fink-Bennet, R. Nunez, J.C. Hill, E.A. Hill, K.P. Ravikrishnan, S.E. Pursel, H. Balon, H. Dworkin PET Center, Dept of Nuclear Medicine, William Beaumont Hospital, Royal Oak, USA.

Aim: To assess the clinical impact of positive FDG uptake in single (SPN) or multiple (MPN) pulmonary nodules detected by CT in pts with known past history of non-lung cancers (but no known lung cancers). Methods: 28 sequential pts with non-lung cancers (15 breast, 8 colon, 5 prostate) referred for evaluation of SPN or MPN by PET over a period of 2 years were included. PET images were acquired by a dedicated PET scanner 1 hr after injection of 10 mCi of F-18 FDG with pts fast for 4 hrs prior to the scan. PET images, covering chest and upper abdomen, were interpreted blindly and then correlated with CT findings for the precise location of abnormal FDG uptake in the chest. Results: There was a significant number of abnormal FDG uptake in both SPN or MPN as tabulated. Positive abnormal uptake suggestive of malignancy was found in 25% of SPN and 39% of MPN($p<0.03$). All positive cases were followed by tissue diagnosis and/or surgical attention. The negative cases were followed clinically. Of the 11 positive cases of MPN, 2 pts (18%) showed only abnormal FDG uptake in just one of the nodules, which was later confirmed at surgery to be a primary cancer of lung in both pts. Conclusion: Results suggest that: (1) PET scan would be just as useful in pts with SPN and known non-lung cancers as other pts with no history of any cancers; (2) Not all pts with non-lung cancers and MPN have pulmonary metastasis by PET criteria; (3) PET may single out a primary lung malignancy in pts with non-lung cancer and MPN. PET has thus great clinical impact in the evaluation of single or multiple pulmonary nodule(s) in pts with known non-lung cancers as the management would otherwise be completely different in all situations revealed by the study.

Cancer	SPN	+ve in SPN	MPN	+ve in only 1 nodule of MPN	+ve in >1 nodules of MPN
breast (N=15)	8	5	7	1	5
colon (N=8)	5	1	3	1	2
prostate (N=5)	2	1	3	0	2

PS_91

F-18-FDG SCAN ON A DUAL HEAD GAMMA CAMERA WITH COINCIDENCE DETECTION IN THE EVALUATION OF SOLITARY PULMONARY NODULE

J. Soares Jr. (1), M. Izaki (1), E.T.P. Albuquerque (1), A. Osawa (1), M. Terra-Filho (2), V.L. Capelozzi (3), M.C.P. Giorgi (1), G.G. Cerri (4), J.C. Meneghetti (1). (1) Department of Nuclear Medicine, Heart Institute (InCor); (2) Division of Respiratory Diseases, Heart Institute (InCor); (3) Division of Pathology; (4) Division of Imaging Diagnosis, Heart Institute (InCor),University of Sao Paulo Medical School, Sao Paulo, Brazil

An accurate diagnosis of pulmonary cancer represents a clinical challenge. The first radiological alteration consists of a pulmonary nodule detected during routine chest radiographs with multiple differential diagnoses and clinical implications. The aim of this study was to evaluate the usefulness of F-18-FDG on a dual head gamma camera with coincidence detection (CDET) in characterizing pulmonary nodules as benign or malignant.

Methods: We evaluated 31 patients (26 male, 38-78y) with unclear diagnoses of solitary pulmonary nodules (SPN) after conventional radiological screening. The mean size of pulmonary nodules by computed tomography (CT) was 2.1cm (range 1.0-3.0 cm). CDET was performed on a dual head gamma camera (MCD Vertex-plus Adac) after injection of 18-F-fluorodeoxyglucose intravenously . Image acquisition began after 1 hour. Qualitative analysis of the images was performed by visual identification of areas of increase or absence of FDG uptake.

Results: Seven patients (23%) showed a marked increase in FDG uptake and underwent surgery. Histopathological evaluation revealed malignant disease in five of these patients and benign nodules in two of them (positive predictive value = 71%). 24 patients (77%) showed absence of FDG uptake. 9/24 underwent surgical procedure. Malignancy was found in only one. 15 patients with negative FDG studies are being followed up with a CT scan every 4 or 6 months. None of them has shown any changes in morphological characteristics of the nodule so far. One patient was dismissed after two years of clinical follow-up. The negative predictive value of F-18-FDG imaging for SPNs was 96%.

Conclusion: This study suggests that F-18-FDG CDET may help to differentiate malignant SPN from benign SPN. Therefore, it can avoid unnecessary procedures, reducing morbidity/mortality and costs.

PS_92

18F-FDG HYBRID PET FOR LOCOREGIONAL STAGING OF PATIENTS WITH NON-SMALL CELL LUNG CANCER, COMPARISION WITH CONTRAST ENHANCED SPIRAL CT

H. Everaert, N. Walgraeve, T. Lahoutte, C. Vanhove, L.O. Dierickx, V. Caveliers, P.R. Franken, A. Bossuyt. Free University Brussels (AZ VUB), Brussels, Belgium.

Aim: To investigate the potential of hybrid PET in mediastinal stagxing of pts with non-small cell lung cancer (NSCLC).Methods: Thirtythree consecutive pts with histologically proven NSCLC underwent 18F-FDG imaging using a hybrid PET camera (E.CAM+, Siemens), starting 90min. after tracer administration (260MBq) in fasting state. Emission data were recorded over 35 min., no correction for attenuation was made, OSEM (3 iterations, 10 subsets) was used for reconstruction. Results: Primary lesions were visualized in all patients. Compared to contrast enhanced spiral CT, the nodal (N) status determined by hybrid PET was identical in 20 (61%) pts: 13 N0, 1 N1, 6 N2 and 13 N3. In 10 (30%) pts the N status with hybrid PET was higher; in 3 (9%) pts it was lower. This resulted in upstaging from potentially surgical (< stage III according AJCC-guidelines) to inoperable status in 5 (15%) pts; while 2 (6%) pts were downstaged from inoperable to operable. Of pts that were upstaged 4 had surgery, in 3 mediastinal involvement was confirmed (true positive), 1 pt had a false positive PET scan (anthracosilicosis), 1 pt was medically inoperable. Of the pts that were downstaged one was staged as N1 peroperatively, 1 pt was medically inoperable.Conclusion: Hybrid PET has important consequences on the therapeutic management of pts with NSCLC. As for dedicated PET, positive results should be confirmed if possible by histology.

PS_93

18 F-FLUORODEOXYGLUCOSE POSITRON EMISSION TOMOGRAPHY IMAGING IN RADIOLOGICALLY UNDETERMINATE PULMONARY LESIONS

G. Ruiz-Hernández (1), R. De Juan (1), R. Delgado (1), I. Otero (2), H. Verea (2), M.J. Pérez-Castejón (3), R. Montz (3), C. Bernal (1), J.L. Carreras (1,3). (1) Nuclear Medicine Department, San Carlos University Hospital, Madrid, Spain; (2) Neumology Department, Juan Canalejo Hospital, La Coruña, Spain; (3) PET Institute Dr. Carreras, Madrid, Spain.

Aim: Throughout our daily clinical experience we frequently find pulmonary lesions which are considered radiologically indeterminate after conventional imaging investigations such as thoracic radiography or computed axial tomography. The aim of our study was to evaluate the diagnostic accuracy of 18 F-fluorodeoxyglucose positron emission tomography (FDG-PET) in the differential diagnosis of radiologically indeterminate pulmonary lesions.
Methods: 45 patients (33 men, 12 women; age range 23-78; mean age 60,5) underwent whole body FDG-PET imaging. All patients, with or without previous malignancy (13 and 32 respectively) had single pulmonary lesions of unknown origin. Lesion size ranged from 1 to 4 cm across the main axis in 43 cases (nodules) and was above 4 cm in two patients (masses). Confirmation diagnosis was based on pathology findings or clinical and imaging follow-up (minimum 6 months). Imaging was performed with photon attenuation correction using a dedicated ADAC tomograph.Prior to the FDG-PET scan all patients fasted for at least six hours, had their baseline glucose checked, were hydrated and orally sedated with 10 mg diazepam. After intravenous injection of 74–185 MBq (2-5 mCi) of FDG patients rested for 40 to 60 minutes before image acquisition. Images were analyzed semiquantitatively by determining the standardized uptake value (SUV) and then calculating sensitivity (Se), specificity (Sp), positive predictive value (PPV), negative predictive value (NPV) and accuracy (A).
Results: Confirmation diagnosis showed 25 patients with malignant lesions and 20 cases of benign nature. These data were obtained after surgery (42%), clinical and conventional imaging follow-up (49%), fine needle aspiration biopsy (5%), bronchoscopy washings and sputum cytology (4%). After receiver operating characteristic (ROC) curves analysis, the optimal SUV threshold value for distinguishing benign from malignant lesions was found to lie within the 2.5-3 range, obtaining the following results for SUV = 2.5 : Se = 91%; Sp = 90%; PPV = 90%; NPV = 90%; A = 90.7%
Conclusions: FDG-PET imaging allows discrimination between benign and malignant lesions with high diagnostic accuracy while optimizing therapeutic management in most cases.

PS_94

FIRST RESULTS OF A NEW PET CENTER IN DIAGNOSIS OF MALIGNANCY IN SOLITARY PULMONARY NODULES WITH F18DG -PET

A. Castagnoli (1), L. Vaggelli (1), V. Briganti (1), A. D' Agata (1), E. Costanzo (1), P. Ferri (1), C. Gallini (1), A. De Francisci (2), A. Grosso (3), P. Gigli (4), C. Pieroni (1)(1) UO Medicina Nucleare 2; (2) Uo Radiodiagnostica; (3) UO Pneumologia 1; (4) UO di Chirurgia Toracica, Azienda Ospedaliera Di Careggi, Firenze, Italy

Several reports in the literature show that F^{18}DG -PET performs well in diagnosis of malignancy in solitary pulmonary nodules indeterminate origin (SPN), selecting patients for surgery or biopsy. As a matter of fact F^{18}DG -PET is a novel diagnostic tool and even a skilled nuclear medicine team must face new problems both from technical and clinical point of view.
Aim of the study: to assess if the limited experience of a new PET Center may affect F^{18}DG -PET diagnosis of malignancy in SPN.
Material and methods. Ninety-one consecutive patients with SPN have been referred since August 1998 to November 2000. Twenty patients were lacking of final clinical data and have been excluded. Seventy-one patients (22 female and 49 male, age between 23 and 82, median 64) form the present series. Patients were studied with 370 MBq of F^{18}DG after 45-60 minutes of delay. Patients were fasting since at least 6 hours and their blood glucose, tested just prior the injection, was always below 130 mg/dl. PET Scans were acquired with a dedicated PET scanner (GE PET Advance) with emission (first) and transmission (later) scan for correction of attenuation. Studied were processed with filtered back projection. Final clinical judgement as positive, negative and indeterminate for malignancy was obtained after visual inspection of reformatted images, in clinical setting, knowing clinical and radiological findings.
Results: Upon final diagnosis, obtained with surgical specimen (n=33) and with clinical and radiological data with at least 6 months of follow up, we had the following results: TP 30 , TN 34, FN 2 (bronchioloalveolar carcinoma in both cases), FP 2 (nodule stable after 6 and 11 months) and 3 indeterminate (in one case with progression while two others are stable after 6 months). If we exclude indeterminate cases, we obtained a sensitivity of 93 %, specificity of 94 %, PPV of 93 %, NPV of 94 % and overall accuracy of 94 %.
Conclusions: from our data we can say that F^{18}DG -PET performs well in diagnosis of malignancy in SPN even if the team has limited experience .

PS_95

THE EFFECT OF PRE-SCAN PERCEPTION ON THE ACCEPTANCE OF FDG-PET RESULTS IN PATIENTS WITH PULMONARY NODULE BY REFERRING PHYSICIANS

F. Ponzo, H.M. Zhuang, L.B. Lacorte, B. Moussavian, N.V. Ghesani, A. Alavi. Hospital of the University of Pennsylvania, Philadelphia, USA.

FDG-PET is effective in differentiating malignant from benign lesion in patients with pulmonary nodules. The **aim** of this study was to assess if referring physicians have accepted this modality as part of their routine practice.
Methods: 161 patients referred for evaluating pulmonary nodules by FDG-PET were retrospectively reviewed. Among them, 64 had high pre-scan suspicion of malignancy (based on referring physician's impression and recent CT findings), 97 had low or indeterminate suspicion. Post-PET management was surveyed to assess if PET results were used to guide management decisions.
Results: A. In patients with high pre-scan suspicion, FDG-PET was positive in 34 and negative in 30. Following PET, all except 2 patients with positive PET and 10 patients (32%) with negative PET underwent an invasive study (bx, mediastomy or lobectomy). Among those 10 patients with negative FDG-PET results in this group, 9 proved to be true negative and one was false negative (brochochoalveolar carcinoma). B. In patients with low or intermediate pre-scan suspicion, FDG-PET was negative in 59 positive in 38. Among these patients, none with negative PET was subjected to invasive study but also 7 patients (18%) with positive PET results did not undergo further evaluation because of refusal by patient. It was conceivable that patient's decision was partially based upon referring physician's pre-PET opinion. Of these 7 patients with positive PET study without further invasive investigations, 4 proved to have malignancy in follow-up, 1 proved to have benign lesion and 2 were lost for following-up. Overall, 97.8% (87 of 89) of PET results were accepted when they corroborated the pre-PET impression. In contrast, only 76% (55 of 72) of PET results were accepted when they were different from the pre-PET perception.
Conclusion: These results clearly demonstrate that clinicians rely heavily upon the results of FDG-PET in patients with lung nodules. However, this reliance varies depending on the pre-test estimates for a malignancy. Further education is required to influence optimal utilization of FDG-PET results.

PS_96

VALUE OF F-18-FDG POSITRON EMISSION TOMOGRAPHY IN MEDIASTINAL TUMORS

B.I. Kettner (1), V. Ivancevic (1), J.C. Rueckert (2), D.L. Munz (1). (1) Clinic for Nuclear Medicine; (2) Clinic for Surgery, University Hospital Charité, Berlin, Germany.

Aim: Mediastinal tumors are rare and encompass different tumor entities. At present diagnostic procedures lack sensitivity and specificity. Aim of this study was to assess the diagnostic value of F-18-FDG PET in these patients prior to surgery.
Method: Fiveteen patients (10 f, 5m; age: 48±16 years) with mediastinal tumor in computed tomography underwent F-18-FDG PET under fasting conditions. FDG PET was performed 1 h after i.v. injection of 370 MBq F-18-FDG (ECAT Exat 921/47, Siemens/CTI) with a spatial resolution of 6.5 mm, followed by iterative reconstruction. Analysis was performed visually and quantitatively by SUV value.
Results: In 14/15 patients thoracic surgery was performed and the suspected diagnosis of mediastinal tumor was proven histologically. In 6/14 patients thymic tissue was found (thymic hyperplasia n=4, thymoma n=1, thymic carcinoma n=1). In these patients median SUV value was 3.0 (2.2-4.3), but thymic carcinoma had a SUV value of 2.7. Other histologically proven malignant tumor entities (lymphoma n=3, carcinoma unknown origin n=2, bronchial carcinoma n=2, pleural mesothelioma n=1) SUV values were higher with 6.2 (2.6-18.2). No other sites of abnormal uptake were found outside the mediastinum (concordant with other imaging modalities). In one patient, negative on PET, surgery was not indicated because of a pericardial cyst without evidence of malignancy in all imaging modalities and confirmed by follow up.
Conclusion: In this limited number of patients with mediastinal tumors F-18-FDG PET seems to be useful for differentiation of benign and malignant mediastinal tumors.

PS_97

CHARACTERIZATION OF MEDIASTINAL FDG UPTAKE USING SIMPLIFIED TISSUE RATIO IN PATIENTS WITH EXTRATHORACIC CANCER

J. Park (1), J.J. Min (2), J.K. Yoon (1), H.J. Jang (1), Y.H. Kim (1), Y. Choi (1), Y.S. Choe (1), K.H. Lee (1), S.E. Kim (1), B.T. Kim (1), J.K. Chung (2)(1) Department of Nuclear Medicine, Samsung Medical Center, Sungkyunkwan University, Seoul, Korea; (2) Department of Nuclear Medicine, Seoul National University Hospital, Seoul, Korea.

It is difficult to distinguish between malignant and benign mediastinal lymph node FDG uptake using PET not corrected for attenuation in patients with extrathoracic cancer.
Purpose: The purpose of the present study was to characterize FDG uptake in metastatic mediastinal lesions using a simplified tissue ratio in FDG PET not corrected for attenuation.
Methods: The population of this study consisted of 54 cancer patients underwent FDG PET for primary foci other than lung, esophagus including breast(n=13), colorectal(n=9), ovary(n=6), cervix(n=5), head and neck(n=12), others(n=9). Fourteen of these patients proved to have mediastinal lymph node metastases in pathology(n=6) and chest CT(n=8; 6/8 in 3 mo later), while there was no evidence of metastasis in the other 38 patients in average 1 yr follow-up. Other 2 patients were proved to multiple lung metastasis in chest X-ray. Mediastinal and lung ratios(M/L ratios) were calculated using images not corrected for attenuation.
Results: M/L ratios in the metastatic mediastinal lesions were significantly higher than those in the non-metastatic lesions(9.6±3.9 vs. 4.3±2.2, $p<0.001$). When M/L ratio of 6.0 was applied as a cut-off value for distinguishing between metastatic and benign lesions, negative and positive predictive values were 94.4%(34/36) and 85.7%(12/16), respectively. Among 38 patients with mediastinal lymph node uptake proved to be normal, M/L ratios of 22 patients with radiological abnormalities suggesting pulmonary tuberculosis, bronchiectasis, or emphysematous changes were higher than that of 16 patients with normal chest finding($p<0.001$).
Conclusion: The result suggests that a simplified FDG PET tissue ratio may be useful to distinguish between metastatic and benign mediastinal lesions in patients with extrathoracic cancer.

PS_99

PET WITH 11C-METHIONINE IN THE ASSESSMENT OF SUSPECTED RECURRENT BRAIN TUMORS AND IN FOLLOW-UP OF THERAPY

T. Skvortsova, M. Roudas, Z. Brodskaja, S. Medvedev. PET Lab, Institute of the Human Brain, St.Petersburg, Russia.

Aim: to assess the clinical value of PET with 11C-methionine for diagnosis of recurrent brain tumors and for monitoring of disease progression.
Method: we studied 56 patients with suspected recurrent brain tumor using PET with 11C-methionine (PET-Met). 21 patients were examined repeatedly. There was 86 PET studies. Recurrent tumor was excluded in 13 patients. The analyzing population comprised 41 patients suffering from gliomas (15 low-grade and 11 high-grade), meningiomas (n=10) and other types of tumor (n=5). PET findings were correlated with surgery in 21 patients and with the outcomes of MR or CT imaging and clinical follow-up studied in others. Visual analysis included the determination of focal increase 11C-methionine uptake, its extent and borders. Tumor uptake of the tracer was assessed semiquantitatively using tumor to normal contralateral cortex uptake ratio (T/C).
Results: PET-Met clearly delineated the extend of recurrent brain tumor as single or multiple focal areas of increased accumulation of 11C-methionine (T/C varied from 1,5 to 6) in 41 patients. In follow-up studies it was noted the increase of extent of high 11C-methionine uptake area in 11 patients and in 6 ones from them T/C ratio also increased. Additionally metastatic growth in other parts of the brain was detected in 1 patients with recurrent medulloblastoma. Malignant transformation of the tumor was confirmed in 5 patients of this group. These changes in the tumor extension and metabolic activity correlated with negative dynamics of neurological symptoms. In other 10 patients follow-up PET-Met showed stable or decreased extend and level of 11C-methionine accumulation that corresponded stable clinical conditions. In 7 from 10 patients with meningiomas PET-Met allowed to detect the appearance of new small meningiomas other localization which were not diagnosed before surgery.
Conclusion: PET-Met seems to be a valuable tool for evaluation of recurrent brain tumors and for monitoring of tumor metabolic activity during therapy.

DIAGNOSTIC ONCOLOGY 4

PS_98

COMPARISON OF 18F-FDG AND 11C-METHIONINE PET IN PATIENTS WITH SUSPECTED GLIOMAS

M. Roudas, T. Skvortsova, Z. Brodskaja, S. Medvedev. PET Lab, Institute of the Human Brain, St.Petersburg, Russia.

Aim. Both tracers have advantages and limitations and have been used for detection of a tumor, histologic grade evaluation, prediction of prognosis. The aim of this study was to evaluate diagnostic usefulness of FDG and Methionine (Met) and to choose optimal tracer.
Methods. 30 patients with suspected brain gliomas were studied with 18F-FDG and 11C-Met PET. Results of visual analysis using 5grade Schifter scale (for FDG) and three tumor/referent region ratios were compared with histological data and survival time.
Results. Positive FDG correlation with histological data was shown by visual analysis ($r=0.73$, $p<0.05$) as well as tumor/contralateral cortex uptake ratio (T/CC, $r=0.71$, $p<0.05$). Schifter scale correlated with T/CC ratio ($r=0.92$, $p<0.05$) and easily used visual analysis might be the most favorable grading criterion. Mean Met T/CC uptake for astrocytoma was 1.85 ± 0.61, for anaplastic astrocytoma 2.71±0.54, for glioblastoma 3.6±1.87. However there was considerable overlap between the three groups. So far Met uptake didn't correlate with histological grading but correlated with survival time. It was shown in our study that in 15 patients out of 30 Met was better than FDG demonstrating increased uptake in the lesion that confirmed low-grade glioma or deliniated high-grade tumor, located in the cortex.
Conclusion. Met gives a possibility for easily tumor detection, it's extension, prediction of prognosis and seems to be the preferred tracer for glioma evaluation.

PS_100

IS CAMERA BASED FDG PET USEFUL IN PATIENTS WITH PAPILLARY THYROID CARCINOMA?

C.H. Park, K.H. Hwang, J.S. Jang, S.N. Yoon, C.W. Joh. Department of Nuclear Medicine, Ajou University School of Medicine, Suwon, Korea.

Objectives: Recently fluonine-18 fluorodeoxy glucose (F-18 FDG) positron emission tomography (PET) is effectively used in the detection of differentiated thyroid cancer that fails radioiodine uptake. The purpose of this study was to assess clinical applicability of more widely available camera based (CB) FDG PET in the evaluation of patients with papillary thyroid carcinoma (PTC).
Methods: Twenty patients with PTC (15 females, 5 males, mean age 45 (range:24~17)) were underwent FDG PET of the neck and chest using a dual-head SPET/PET hybrid camera (Elscint's Varicam). Scan was done 1 hr following IV injection of 111~185 MBq FDG after 6~12 hour fasting. Image processing was done without attenuation correction and using a filtered back projection. The mean thyroglobulin (Tg) level after discontinuation of L-thyroxine was 123 ng/ml (range <0.75 ~ >600). There were 18 patients with elevated Tg levels and negative I-131 scan after the ablation therapy. One had only lobectomy and the other had preoperative FDG PET for neck node evaluation. Focal hypermetabolic areas above the regional background are considered abnormal and FDG PET abnormality was compared with US/CT, clinical exam and post-radioiodine therapy scan if performed.
Results: FDG PET was positive in 10 of 18 patients with negative I-131 scan and elevated Tg levels. There were 2 cases whose Tg level less than 0.75 ng/ml. FDG PET was positive in 1(FP) and negative in the other. There were 8 TP, 10 TN, 1 FP and 1 FN. Two patients with milliary pulmonary metastases failed to concentrate FDG but neck diseases were detected.
Conclusion: In a limited number of patients studied thus far, CB FDG PET appears to be useful in the management of PTC. On going study to include more number of patients is in progress.

PS_101

LOCALIZATION OF RECURRENCES IN MEDULLARY THYROID CARCINOMA: ROLE OF F-18-FDG PET

A. Bruno (1), M. Castellani (1), U. Verga (2), R. Leo (1), P. Beck Pecoz (2), F. Voltini (1), P. Gerundini (1). (1) Department of Nuclear Medicine; (2) Department of Endocrinology, Ospedale Maggore-IRCCS, Milano, Italy.

Medullary thyroid carcinoma (MTC) shows an elevated incidence of recurrences, but preoperative localization of the tumor, although essential, is always difficult. Over the years, various imaging techniques were used, but clinical results are still unsatisfactory. A more sensitive imaging technique, capable of identifying the sites of disease is needed to improve the patient management.
The aim of this study is to demonstrate the usefulness of FDG-PET for the detection of recurrent MTC.
FDG-PET images of 8 pts. (5F; age range: 34-69 yrs.) with recurrent MTC after thyroidectomy were compared with images obtained with ultrasound, CT, and 111In-Octreoscan. Two of pts. had familial MTC; six pts. were affected by sporadic MTC. Identified metastatic lesions were assessed directly by surgery or indirectly by follow-up data (change or persistence of laboratory findings).
RESULTS: The calcitonin levels ranged from 31 to 38000 pg/ml and CEA levels from 5 to 412 ng/ml. No correlation was found between PET and serum tumoral markers level. PET was able to identify 50% of local recurrencies, as well as the other imaging techniques considered (echo, CT and Octreoscan). One false negative result was recorded with PET and CT; one false positive was observed with echo. In one subject, PET was the only method capable to differentiate an enlarged loco-regional but not metastatic lymphnode. Echo plus PET correctly detected 62.5% of relapses.
In conclusion PET-FDG may be considered an useful technique for identifying MTC recurrences particularly when elevated blood markers are elevated and ultrasonography is negative.

PS_102

FDG PET FOR THE DETECTION OF METASTATIC THYROID CANCER: IN EUTHYROID OR HYPOTHYROID STATE?

P.L. Jager, K.M. van Tol, T.P. Links, D.A. Piers. PET Center, University Hospital, Groningen, The Netherlands.

Aim: to determine whether FDG PET for the detection of metastatic thyroid cancer should be performed in euthyroid or in hypothyroid state.
Methods: Eight patients suspected of having recurrent or metastatic differentiated thyroid cancer because of persisting elevated thyreoglobulin levels, were sequentially studied: first in euthyroid state (euPET) and secondly in hypothyroid state (hypoPET), after stopping T3 hormone suppletion therapy for 2 weeks. Median interval was 35 days (range 21-49 d). Within one week after hypoPET, a therapeutic I-131 dose was administered with post treatment scans obtained 10 days later. Uncorrected whole body PET images were acquired using a Siemens ECAT HR+, 90 min after i.v. injection of 400 MBq FDG. HypoPET and euPET images were compared with each other and with I-131 post-treatment scans by two independent observers. Findings were verified using other imaging modalities or biopsies.
Results: Median TSH was 0.04 (range 0.01-2.4) in euthyroid state, and 64 mU/l (range 16-160) in hypothyroid state. EuPET showed abnormalities in 4 patients, hypoPET in 5 patients: one patient (with a confirmed pulmonary metastasis) was only positive on hypoPET. In two other patients hypoPET clearly identified more lesions. In all positive patients lesion contrast was better for hypoPET. All hypoPET findings were confirmed using CT, MRI or biopies. In three patients both PET studies were negative. I-131 studies were negative in 3 patients (2 with positive PET). In general I-131 findings were disconcordant with FDG PET in 6/8 patients. In two patients, hypoPET findings led to a significant management change as compared to euPET findings.
Conclusion: The performance of hypoPET was either superior or equal to euPET, but never inferior. To detect metastatic or recurrent differentiated thyroid cancer FDG-PET should be performed in the hypothyroid state.

PS_103

18F-FDG PET FOR THE DETECTION OF RECURRENT THYROID CANCER IN PATIENTS WITH NEGATIVE IODINE SCAN

M. Yun (1), L. Eldeiry (2), N. Alnafisi (1), A. Alavi (1), S. Mandel (2). (1) Department of Radiology; (2) Department of Internal Medicine, University of Pennsylvania Medical Center, Philadelphia, PA USA.

Aim: FDG PET has shown its potential value in patients with iodine-negative thyroid cancer and elevated serum thyroglobulin. This study was undertaken to evaluate the value of FDG PET for the detection of recurrent thyroid cancer in patients with negative iodine scan.
Methods: Sixteen patients with suspected recurrent papillary thyroid cancer were included in this study. All had FDG-PET and iodine scans (13 patients with ^{123}I and 3 patients with ^{131}I). Indications for PET were high clinical suspicion for recurrent disease with negative diagnostic iodine scans. Final conclusions were based on ultrasonography (US) guided biopsy, operative pathology, post-treatment ^{131}I scan, other imaging studies, clinical follow up or combination of these modalities.
Results: Eight of 16 patients were proved to be disease free. FDG PET showed one false positive lesion in these 8 disease free patients. In the remaining 8 patients, a total of 13 recurrent lesions were confirmed by US (5), CT (3), post-treatment ^{131}I scan (3), bone scan (1), operative pathology (1). FDG PET correctly detected 5 lesions and the rest 8 lesions were not identified. Four of 18 patients had ^{131}I treatments and 5 iodine-avid lesions in 3 patients were identified on post-treatment ^{131}I scan. Two of these 5 lesions on post-treatment ^{131}i scan showed positive FDG uptake on PET. Eight lesions that were false negative on both iodine and PET scans appeared as recurrent disease in other modalities, 4 on US, 1 on CT, 1 on operation and 2 on post-treatment ^{131}I scan. Three of 16 patients had lung metastasis, 2 of which were seen on PET scans.
Conclusions: PET detected recurrent tumors in 5 of 13 false negative lesions on diagnostic iodine scans. Tumors detected on PET were not necessarily iodine-negative on post-treatment scans. US was useful for detecting recurrence in the neck when iodine and PET scans were both negative. PET combined with US seems to detect majority of the recurrent thyroid cancer in patients with negative iodine scans.

PS_104

FDG PET FOR DETECTION OF RECURRENCES FROM MALIGNANT PRIMARY BONE TUMORS: COMPARISON WITH CONVENTIONAL IMAGING

C. Franzius (1), H.E. Daldrup-Link (2), A. Wagner (3), J. Sciuk (1), H. Jürgens (3), 0. Schober (1). (1) Department of Nuclear Medicine; (2) Department of Clinical Radiology; (3) Department of Paediatric Haematology and Oncology, Münster University, Münster, Germany.

Purpose: The aim of this study was to assess the diagnostic ability of positron emission tomography using F-18-flourodeoxy-glucose (FDG PET) in the detection of recurrences from malignant primary osseous tumors compared with conventional imaging.
Patients and Methods: In 27 patients (7 osteosarcomas, 20 Ewing's sarcomas; 9 femal, 18 male; age 8 – 35 years, median 17 years) 41 FDG PET examinations (ECAT EXACT 921/41, CTI/Siemens) performed for diagnosis or exclusion of recurrent disease were evaluated. Conventional imaging techniques consisted of local magnetic resonance imaging (MRI), thoracic computed tomography (CT), and Tc-99m methylene diphosphonate (MDP) bone scintigraphy. The reference methods were the histopathologic analysis and/or the clinical and imaging follow-up.
Results: In 25 examinations reference methods revealed 52 sites of recurrent disease (local n=7, osseous n=22, pulmonary n=13, soft-tissue n=10). On an examination based analysis FDG PET had a sensitivity of 0.96, a specificity of 0.81, and an accuracy of 0.90. Comparable values for conventional imaging were 1.0, 0.56, and 0.82. On a lesion based analysis sensitivity values of FDG PET and conventional imaging were 0.92 and 0.88, respectively. There were 11 false positive findings using FDG PET and 16 false positive lesions using conventional staging.
Conclusion: The sensitivity, specificity and accuracy of FDG PET in the detection of recurrences from osseous sarcomas are high. There is a slight inferiority of FDG PET in the sensitivity on an examination based analysis in comparison with conventional imaging. However, the smaller number of false positive findings resulted in superior specificity and accuracy values in FDG PET as compared to conventional imaging. The main advantage of FDG PET is the fact, that a whole-body information is gained in one single examination.

PS_105

COMPARISON OF FDG-PET, BONE SCINTIGRAPHY AND MAGNETIC RESONANCE IMAGING (MRI) FOR THE DETECTION OF OSSEOUS METASTASES

J.W. Sam, M. Yun, N. Alnafisi, L.B. Lacorte, S. Jang, A. Alavi. Department of Radiology, University of Pennsylvania Medical Center, Philadelphia PA USA.

Aim: To compare the accuracy of FDG-PET, ^{99m}Tc-MDP bone scintigraphy, and MRI in the detection of osseous metastases from various malignancies.
Methods: A retrospective review of patients with known or suspected malignancies (31 lung, 15 lymphoma, 4 colon, 4 breast, and 14 others) who had FDG-PET imaging and either bone scintigraphy, MRI, or both within a four month period was performed. The sensitivity, specificity, and accuracy of each modality were calculated using biopsy results or, in the case of true negative studies, clinical follow-up for a period of time not less than six months, as the standard of truth. Both the imaging studies and follow-up results were considered positive or negative based on the patient as a whole, i.e. positive if there was one or more skeletal metastases and negative if there was none.
Results: Sixty-eight patients met our inclusion criteria, with 35 and 48 of these patients having undergone MRI or bone scintigraphy, respectively. FDG-PET was the most accurate modality with a sensitivity, specificity, and accuracy of 78% (18/23), 82% (37/45), and 81% (55/68), respectively. In comparison, ^{99m}Tc-MDP bone scintigraphy had a sensitivity, specificity, and accuracy of 83% (10/12), 64% (23/36), and 69% (33/48), respectively, whereas MRI had a sensitivity, specificity, and accuracy of 74% (14/19), 56% (9/16), and 66% (23/35), respectively.
Conclusions: FDG-PET is more accurate than either bone scintigraphy or MRI in the detection of skeletal metastases. Although all three modalities have a similar sensitivity, FDG-PET is the most specific for neoplastic involvement.

PS_106

FDG CDET IS ALSO ABLE TO DETECT THE RECURRENCE OF BREAST CANCER!

D. Grahek, F. Montravers, K. Kerrou, N. Younsi, L. Mabille, F. Achaibou, Y. Petegnief, V. De beco, C. Colombet, JN. Talbot. Service de Médecine Nucléaire, Hôpital Tenon, Paris.

Aim : Few studies have evaluated the potential role of FDG TEP performed with dedicated cameras to detect the recurrence of breast cancer. Their results showed a high sensitivity compared to conventional imaging. In our study, we have evaluated the performances of FDG 2D-CDET performed with „ hybrid " gamma cameras in this indication.
Methods : The patients, fasted for 6 hours or more, and 1 hour after IV injection of 150-250 MBq of [18F]-FDG, the acquisition of images started. A whole body scan and at least a tomoscintigram were acquired, using a PICKER Prism XP 2000 or a MARCONI Irix. The tomographic slices were reconstructed using an iterative algorithm (OSEM or EM ML) and without attenuation correction by an external source. The images were displayed without any pre or post-filtering. The interpretation was visual. CDET FDG findings were confirmed by guided imaging or by biopsy or by follow up over a period of at least 12 months.
Results : Results were obtained in 20 pts with an „ occult disease " i.e.a raise of tumour marker levels with negative conventional imaging. Sensitivity was 100% (13/13) and specificity was 85.7% (6/7). In 4 cases FDG CDET showed a multifocal recurrence. The false positive result corresponded to a muscular uptake.
Results were also obtained in 21 pts suspicious of recurrence at physical examination or conventional imaging. Sensitivity was 88% (15/17) and specificity 100% (4/4). In 9 cases, FDG CDET showed a multifocal recurrence versus only 3 cases with conventional imaging. The two false negative results corresponded to a 5 mm pulmonary metastasis and a recurrence in the lung and the liver, that appeared 11 months after FDG CDET.
Conclusions : The performances of FDG CDET to detect the recurrence of breast cancer were similar to that of FDG PET. This technique has a potential impact on patient management and survival, since it allows the detection of recurrence in occult disease and of multiple metastases.

PS_107

CLINICAL VALUE OF 18F-FDG-PET WITH A DUAL HEAD CAMERA USING COINCIDENCE DETECTION IN BREAST CARCINOMA

H. Erler (1), G. Windbichler (2), E. Donnemiller (1), C. Bacher (1), D. Kendler (1), R. Moncayo (1), G. Riccabona (1). (1) Department of Nuclear Medicine; (2) Department of Gynecology, University of Innsbruck, Austria.

The usefulness of 18FDG-PET in breast carcinoma, not only visualizing the primary tumor but also lymph node or distant metastases, is well known. But dedicated PET cameras are, however, still expensive and therefore not available in many centres even if ^{18}FDG supply would be possible. Aware of the lower resolution of dual head cameras with coincidence mode in comparison with dedicated PET cameras we tried to define the clinical value of our system in breast carcinoma.
Methods: 18FDG-PET was performed in 28 patients (mean age 58y ± 13) with breast carcinoma. 7 women were investigated because of suspicion of local recurrence or lymph node metastases, in 12 cases distant metastases were suspected and 9 studies were done due to high levels of tumor markers or for restaging. PET was carried out with a double-head gamma camera (ADAX VERTEX), equipped with molecular coincidence detection (MCD), 60 minutes post injection of 148-185 MBq of 18F-deoxyglucose. The obtained results were compared with CT, MRT, conventional radiology, histology, surgical notes, autopsy reports and follow-up informations.
Results: ^{18}FDG imaging could visualize lesions in 17 patients in a correct way (true positive), whereas in 8 studies no uptake was seen (true negative). In 3 cases the pathological tracer accumulation seen with our camera system could not be verified (false positive), but there was no false negative result. So sensitivity, specificity and accuracy for all investigations were 100%, 73% and 89%, respectively.
Conclusions: Our data show that the performance data regarding specificity and sensitivity for this camera system are similar to those reported for dedicated PET cameras. The diagnostic value of ^{18}FDG-PET with a dual head camera using coincidence detection in the patients with breast carcinoma seems acceptable for clinical routine.

PS_108

PREOPERATIVE ASSESSMENT OF ADNEXAL TUMORS BY [18-F]-FDG PET PERFORMED ON A HYBRID GAMMA CAMERA WITH COINCIDENCE DETECTION EMISSION TOMOGRAPHY (CDET)

K. Kerrou, D. Grahek, F. Montravers, N. Younsi, C. Colombet-lamau, V. De beco, Y. Petegnief, JN. Talbot. Service de Médecine Nucléaire, Hôpital Tenon, Paris, France.

Aims: The aim of this prospective study was to evaluate the role of [18-F]-FDG PET performed on a hybrid gamma camera with CDET in preoperative assessment of adnexal tumours for tissue characterisation and staging.
Methods: After a 6 hour fast, the patient (pt) was injected I. V. with 150-250 MBq of [F-18]-FDG and imaging (whole-body scan and at least a tomoscintigram) was started 60 min. later, using MARCONI Prism XP 2000 dual-head or Irix 3000 triple-head CDET gamma cameras. Between May 2000 and January 2001, 17 pts were prospectively studied for preoperative assessment of adnexal tumours. All pts had an adnexal mass discovered with ultrasonography (size range : 15 to 40 mm) and subsequent conventional imaging consisting in CT and/or MRI. All patients are currently evaluable with histology after surgery.
Results : The mean age of the 17 pts was 58 years (range 28 to 87). [F-18]-FDG was true positive in 2 pts. In the first one, [F-18]-FDG was taken-up by the pelvic mass and by multiple foci of peri-hepatic and peritoneal carcinomatosis (size less than 10 mm). In the second patient, [F-18]-FDG showed intense uptakes by the ovarian mass and by a focus of uterine secondary deposit of 10 mm size. For both patients, [F-18]-FDG scan detected more lesions than ultrasonography, CT and MRI.
One patient corresponded to a false positive result related to stage IV endometriosis.
The remaining 14 patients corresponded to true negative results, benign tumours being confirmed by histology.
The overall sensitivity and specificity on a per patient basis were respectively 2/2 and 14/15. The negative predictive value (NPV) was 14/14. More patients are needed to accurately estimate the positive predictive value.
Conclusion: This clinical setting was not evaluated previously using CDET gamma cameras. CDET was able to detect pelvic and abdominal lesions of a size equal to or less than 10 mm size.
Our preliminary results seem very promising in order to avoid unnecessary surgical interventions (high NPV) or to prepare for adequate surgical procedure (positive [F-18]-FDG).

PS_109

LOCALISATION OF RECURRENCES OF MELANOMA BY [18F]-FDG ON A 2D-DUAL HEAD GAMMACAMERA IN COINCIDENCE MODE (CDET)

N. Younsi, K. Kerrou, F. Montravers, D. Grahek, V. De beco, J.N. Talbot. Medecine Nucleaire, Hopital Tenon, AP-HP, Paris, France.

Recently, [18F]-FDG was registered in France. The primary staging of melanoma was included among several clinical indications. The present study aimed both to establish the feasibility of FDG scintigraphy in the particular case of melanoma which requires an extended field of imaging and to evaluate another clinical setting in melanoma : localisation of recurrences.
Material and methods : In patient fasting for 6 hrs or more, 150-250 MBq of [18F]-FDG were injected IV. After a delay of 60 min, the examination began on a "hybrid" Picker Axis gamma-camera. It consisted of a whole body acquisition by scanning (PT 511") and one or two tomoscintigrams (60s per 6° step over 180°) depending on the abnormalities suspected on whole body CDET or on conventional imaging (CI). Tomoscintigraphic reconstruction was performed without any pre or post filtering.
Results : 14 examinations have been performed in 13 patients suspected of recurrent melanoma - either CI showed an equivocal aspect (5 cases) - or CI showed a lesion which appeared isolated and resectable (4 cases) – or lymph nodes were palpable (5 cases). FDG showed **less** lesions than suspected at CI in 7 cases including one patient with modification of management after both FDG examinations and 3 cases with histologic evidences : 1 TP, 1 TN and one patient whose CT lesion corresponded to a carcinoid tumour which did not take-up FDG. FDG showed **more** lesions than suspected in 4 cases, including 1 TP on histology and 1 FP of both FDG and CT in parasitic lesions of the liver. In 3 cases, FDG **confirmed** the known lesions (1 TP on histology).
In conclusion, FDG scintigraphy could be performed with this 2D CDET camera in a reasonable time (max 2h), including whole body images that permit to study arms and legs. Our experience is currently limited to a small number of patients, but, to the best of our knowledge, no other data have been published using CDET in melanoma, a potentially extensive cancer that challenges coincidence imaging. 2D FDG-CDET appeared able to detect foci which were not known or suspected and conversely to classify as probably benign several lesions seen at CT, with the well known limitation of sensitivity in neuroendocrine tumours, such as carcinoid tumours. Globally, a modification in the number of suspected foci occurred in 11/14 cases.

PS_110

NON-DEDICATED POSITRON EMISSION TOMOGRAPHY (NPET) DETECTION OF COLORECTAL METASTASES OF THE LIVER: CORRELATION WITH ANATOMIC IMAGING AND HISTOPATHOLOGIC FINDINGS

F. Giammarile (1), M. Rivoire (2), P. Kaemmerlen (3), M.C. Blanchet (2), P. Meuus (2), C. Desuzinges (1), P. Chauvot (1). (1) Department of Nuclear Medicine; (2) Department of Surgery; (3) Department of Radiology, Centre Léon Bérard, Lyon, France.

OBJECTIVE: To compare the performance of a coincidence gamma camera (NPET) using 2-[F18] fluoro-2-deoxy-D-glucose (FDG), with conventional imaging techniques for the diagnosis of colorectal cancer metastases to the liver.METHOD: In our institution, between January and December 2000, 20 patients (10 male and 10 female, mean age 55 years), underwent FDG imaging for suspected hepatic metastases from colorectal cancer.Anatomical resecability of liver metastases was assessed by computed tomography during arterial portography (CTAP) and magnetic resonance imaging (MRI). The NPET studies were performed after intravenous administration of 2 MBq/kg of FDG, using a IRIX three-head gamma camera (MARCONI MEDICAL SYSTEMS).In the 19 patients who underwent resection of hepatic metastases, imaging findings were correlated with the results of intraoperative ultrasound (IOUS). The final diagnosis was obtained by histopathologic examination of all lesions.RESULTS: No extrahepatic abnormalities were detected, and in no case surgical plans were modified. A total of 95 suspicious intrahepatic lesions were identified (67 by IOUS, 49 by ND-PET, 60 by CTAP, and 60 by MRI). Of the 95 suspicious lesions, only 64 were malignant. NPET correctly identified the majority of CTAP or MRI false positive lesions. However, NPET was negative in 17 small metastasis (<15 mm). According to the histopathologic findings, the sensitivity, specificity and accuracy in detecting metastatic disease to the liver of IOUS were respectively 100%, 90% and 96%, of NPET 73%, 94% and 96%, of CTAP 77%, 65% and 82%, of MRI 83%, 68% and 83%.CONCLUSION: The NPET imaging appears to be superior to CTAP and MRI in characterising suspected colorectal liver metastasis. The limitation of this method is related on detecting small metastases. However, the results of our preliminary study were in agreement with those of previous reports, obtained with dedicated PET. Further prospective studies are needed to determine the role of PET in diagnosis and clinical management of colorectal cancer metastases to the liver.

PS_111

F-18-FDG DIAGNOSIS OF PANCREATIC CARCINOMA WITH A DUAL HEAD CAMERA/MCD

A. Kroiss (1), A. Kroiss (1), CH. Auinger (1), K. Rettensteiner (1), M. Gschwandtler (2), R. Roka (3), W. Weiss (2). (1) Institute of Nuclear Medicine; (2) 4th Medical Department; (3) 1st Surgical Department, KA Rudolfstiftung, Vienna, Austria.

The aim of the study was to evaluate the fole of F-18-FDG for differentiating malign from benign pancreatic disorders, in particular scar tissue and chronic inflammatory signs. A dual head camera with molecular coincidence detection (MCD) was used for this purpose since even endo-sonography, ERCT, spiral-CT and biopsy did not show conclusive results.
Method: 26 patients were invetigated (9 female, 17 malge, age 50.9± 13.5 a). At an average,k 148 MBq (4 mCi) F-18-FSG (FZS Seibersdorf, BSM) were applied i.v. after control of blood sugar content. After 1 hr, the abdominal region was imaged with an ADAC Vertex, MCD.
Results: From 17 patients with a histological confirmed pancreatic carcinoma, and 9 patients with a benign disease, the F-18-FDG showed a sensitivity of 88% and a specificity of 89%, as to the pancreatic carcinoma. One false negative results related to a patient with hyperglycaemia, another to a patieht with a 2 cm tumor in CT. One false positive result occurred at a patient in an acute phase of chronic pancreatitis. All results were confirmed by operation and/or biopsy.
Conclusion: F-18-FDG investigations with a dual head camera/MCD offer a concenient, non-invasive diagnostic tool for iffrerentiating malign from beinign pancreatic tumor. This method is strongly recommended in all cases where morphological investigations of pancreatic tumors show unclear results, in particular if tumormarkers are increased.

PS_112

IMAGING OF EXTRACRANIAL TUMORS WITH F-18-FLUOROETHYL-L-TYROSINE (FET)

W.A. Weber, H.J. Wester, M. Herz, M. Schwaiger. Department of Nuclear Medicine, Technische Universität, München, Germany.

Aim: The amino acid analog ^{18}F-Fluoroethyl-L-tyrosine (FET) has shown promising results for imaging of brain tumors. In this study we evaluated the feasibility of PET imaging using FET in patients with extracranial tumors.
Methods: 7 patients (2f, 5m, age 61± 9 years) with histopathologically proven primary or metastatic malignant tumors were studied (histopathological diagnosis: 2 non-small cell lung cancer (NSCLC), breast cancer, renal cell carcinoma, pancreatic cancer, malignant melanoma, and prostate cancer). The primary tumor was evaluated in 4 patients (NSCLC, prostate, breast and pancreatic cancer). In 3 patients (melanoma, renal cell carcinoma and NSCLC), metastatic lesions in the lungs (n=2) and in the liver (n=1) were studied. For PET imaging patients were injected with 250-350 MBq ^{18}F-FET. In 4 patients an attenuation corrected dynamic emission scan of the primary tumor was acquired (total acquisition time 60 min). In the 3 patients with metastatic lesions a static whole body emission scan was performed 40 min after tracer injection. For quantitative assessment of tracer uptake tumor/background ratios were calculated. In attenuation corrected studies standardized uptake values (SUV) were determined for tumor tissue, muscle, liver (n=3), and lung (n=2).
Results: The whole body studies demonstrated renal excretion of the tracer and showed no retention of FET in any organ system. Focal tumor uptake of FET was noted in two patients with intrapulmonary lesions (NSCLC and metastatic melanoma, size: 4 and 2 cm, respectively). In these lesions the relative uptake of FET compared to normal lung (tumor/lung ratio) was 3.5 and 2.5, respectively. All other tumors were not visible in the FET-PET studies (SUV ≤ 2.6, tumor/bloodpool and tumor/muscle ratio ≈ 1). Uptake of FET by muscle tissue, liver and lung was 1.4±0.1, 2.4±0.2, and 0.5 SUV. Blood pool activity showed a SUV of 2.0±0.1.
Conclusions: In this preliminary study of extracranial tumors FET-PET demonstrated only a low image contrast. If these findings are confirmed in larger series of patients the use of FET for staging of extracranial tumors may be limited.

PS_113

EVALUATION OF HEAD AND NECK CANCER WITH F-18 FDG PET. A COMPARISON WITH CONVENTIONAL IMAGING METHODS

E. Kresnik (1), P. Mikosch (1), H.J. Gallowitsch (1), S. Wieser (2), M. Heinisch (1), O. Unterweger (1), G. Kumnig (1), I.,. Gomez (1), G. Grünbacher (1), P. Lind (1). (1) Dept.of Nuclear Medicine and Endocrinology - PET Center, Klagenfurt, Austria; (2) Derpt. Of Otolaryngology, LKH Klagenfurt.

Aim: Evaluation of F-18 FDG PET in diagnosing and staging of primary and recurrent malignant head and neck tumors in comparison to conventional imaging methods.
Patients and methods: A total of 54 patients were investigated retrospectively.
Results: Unknown primary cancers (CUP). In 11/15 cases the primary cancer could be found with F-18 FDG. The detection rate was 73.3%. One patient revealed breast carcinoma that could not be detected with F-18 FDG PET, but was detected by CT. In three cases the primary cancer could not be found with any imaging method. Staging. 24 patients were investigated . A total of 13 local and three distant lymph node metastates could be detected by F-18 FDG PET, whereas the conventional imaging methods detected 9 local and one distant metastatic lymph node in these patients. The results of F-18 FDG PET therefore led to an upstaging in 5/24 (20.8%) patients. The conventional imaging methods were false positive in 4/24 (16.6%). Restaging. A total of 15 patients with suspected recurrence after RCT were investigated. F-18 FDG was true positive in 7/15 (46.6%) and true negative in 4/15 (26.6%). The conventional imaging methods were true positive in 5/15 (33.3%) and true negative in 4/15 (26.6%). One false negative (6.6%) and three false positive findings (20%) in F-18 FDG PET were due to inflammated tissue. The conventional imaging methods were false positive in three (20%) and false negative in three cases (20%).
Conclusion: In comparison to conventional diagnostic methods F-18 FDG PET provides additionally and clinically relevant information in patients to detect primary and metastatic carcinomas as well as in early detection of recurrent or persistent head and neck cancer after RCT. F-18 FDG PET compares favorably with conventional imaging methods and therefore should be early performed, before CT or MRI is done, in clinically routine.

PS_115

QUANTITATIVE ANALYSIS OF BASAL AND POST CAPTOPRIL 99MTC-DMSA SCINTIGRAPHY IN THE DIAGNOSIS OF ISCHEMIC NEPHROPATHY

M. Sapienza, H. Sado, F. Kiy, C. Ono, J. Praxedes, J. Santello, T. Watanabe, P. Aguirre Costa, C. Buchpiguel. Centro de Medicina Nuclear, University of São Paulo, Brazil.

INTRODUCTION: Renal artery stenosis (RAS) clinical features include renovascular hypertension (RV) and ischemic nephropathy (IN). Renogram with angiotensin-conversion enzyme inhibition, although sensitive to RV, has unsatisfactory results in IN, mainly due to renal basal dysfunction. Captopril is also known to decrease ^{99m}Tc-DMSA uptake in RV.
AIM: The purpose of this study was to evaluate the quantitative analysis of basal and post captopril ^{99m}Tc-DMSA scintigraphy in the diagnosis of IN.
METHODS: Absolute uptake of ^{99m}Tc-DMSA (DMSAUp) was calculated before and after captopril in 10 patients with unilateral renal dysfunction. The patients were also evaluated by basal and post captopril ^{99m}Tc-DTPA, Doppler and renal angiography. Severe artery stenosis was associated to renal dysfunction in 5 patients (group A: 35±17 year old, 2 male) and it was not present in the remaining 5 pts (group B: 46±11 year old, 2 male).
RESULTS: DTPA was inconclusive in all patients. Group A showed a higher drop in mean blood pressure (BP) after captopril than group B (27 mmHg x 9 mmHg). DMSAUp decreased from 4.5±3.4% to 3.6±3.7% after captopril at the side of RAS and from 30.4±13.0% to 21.7±11.0% at the contra-lateral kidney. Group B showed a bilateral increase in DMSAUp with captopril (mean: 10.0±5.7 to 14.2±8.8).
CONCLUSION: A decrease in DMSAUp induced by captopril suggests IN, however the similar response of the contra-lateral kidney might reflect a secondary effect of BP drop or other systemic haemogram dynamic factors.

OTHER CLINICAL SCIENCE. NEPHRO-UROLOGY 1

PS_114

DUAL ENERGY WINDOW ACQUISITION FOR SCATTER AND RENAL DEPTH CORRECTION IN RENAL COUNTING METHOD FOR TC-99M MAG3

H. Hirota (1), N. Shuke (1), W. Yamamoto (1), A. Okizaki (1), J. Sato (1), Y. Ishikawa (1), T. Aburano (1), S. Kaneko (2), S. Yachiku (2), T. Sasajima (3), K. Kikuchi (4)(1) Department of Radiology; (2) Department of Urology; (3) Department of Surgery 1; (4) Department of Internal Medicine 1, Asahikawa Medical College, Asahikawa, Japan

The aim of this study was to examine the influence of scatter and renal depth correction with dual energy window acquisition in the renal counting method for estimating Tc-99m MAG3 clearance.
Methods: Sixty-nine patients with renal dysfunction were studied. After an intravenous injection of Tc-99m MAG3 (185 MBq), dynamic images were recorded at 2 sec/frame for 3 min, then at 10 sec/frame for 27 min using main photo-peak and sub-peak windows (140+-14 and 123+-3 keV). Based on the triple energy window method proposed by Ogawa, scatter correction was done. Scatter fraction (SF) in the main photo-peak window was also calculated to estimate renal depth. Renal uptake was calculated from integrated renal counts (1 to 2 min) and injected dose determined by syringe counting, with and without scatter correction. As for the renal depth estimation, conventional tønnensen's method (Rt), estimation from scatter fraction based on a theoretical formula (Rs=exp ((SF-C1)/C2), C1-2= constants) and a weighted sum of tønnensen's renal depth and scatter fraction (Rts=C1Rt+C2SF, C1-2=constants) were tried. Using reference clearance calculated according to a single sample method proposed by Russell and an attenuation coefficient (0.153/cm), necessary constants for the renal depth estimation were determined by regression analysis. Renal uptakes after scatter and renal depth correction were compared with the conventional renal uptake in correlation to the reference clearance.
Results: correlation coefficients (r2) were summarized in the table. Scatter-corrected renal uptake with renal depth correction using Rts showed best correlation.
Conclusion: Dual energy window acquisition could improve estimation of Tc-99m MAG3 clearance by renal counting method.

PS_116

COMPARISON OF 99MTC-DMSA, 99MTC-MAG3 AND ULTRA-SOUND IN DETECTION ACUTE PYELONEPHRITIS

A. Şahin, M. Yıldırım, H. Uslu, H. Akyazı, C. Ak, E. Varoğlu. Atatürk University Medical Faculty, Depts of Nuclear Medicine, Erzurum, Turkey.

We compared the effectiveness of 99mTc-DMSA, 99mTc-MAG3 and ultrasonography in the detection of acute pyelonephritis.
Metods: Thirty children (9 boys, 21 girls; aged between 1- 18 years) were included in this study, All patients were admitted during the acute phase of acute pyelonephritis. The diagnosis of acute pyelonephritis was based on clinical and biochemical findings including fever (>38.5 °C) and positive urine culture. 99mTc-DMSA, 99mTc-MAG3 and ultrasonography study performed during the acute phase (1-5 days after onset of symptoms) of acute pyelonephritis.Ultrasonography assessed the parenchymal echogenicity hyper - or hypoechoic focal lesions, calyceal dilation, scarring and renal size. Gamma camera assessed parenchymal uptake (presence or absence uptake, hypoactive areas, single or multiple defects).
Resuls: While in study cortical defects were seen in 23 (76.6 %) and 21 (70 %) in DMSA and MAG3 studies, respectively. cortical defect were seen in 21 (70 %) patients. Ultrasonography showed abnormal finding in 14 (46.6 %) patients.
Conclusion: Two tracers showed excellent matching in demonstrating parenchymal lesions. Morever, 99mTc-DMSA show more lesions than 99mTc-MAG3 in detection of acute pyelonephritis, and in the diagnosis of acute pyelonephritis 99mTc-DMSA and 99mTc-MAG3 imagings were more useful than ultrasonography.

PS_117

ESTIMATION OF OIH CLEARANCE FROM TC-99M MAG3 SINGLE BLOOD SAMPLE

N. Shuke (1), W. Yamamoto (1), A. Okizaki (1), J. Sato (1), Y. Ishikawa (1), K. Usui (1), S. Kaneko (2), S. Yachiku (2), K. Kikuchi (3), T. Sasajima (4), T. Aburano (1); (1) Department of Radiology, Asahikawa Medical College, Asahikawa, Japan; (2) Department of Urology, Asahikawa Medical College, Asahikawa, Japan; (3) Department of Internal Medicine 1, Asahikawa Medical College, Asahikawa, Japan; (4) Department of Surgery 1, Asahikawa Medical College, Asahikawa, Japan

The objective of this study was to determine an empirical formula for directly converting Tc-99m MAG3 (MAG3) concentration at certain time to I-131 OIH (OIH) clearance based on the Russell's single sample method ('96).
Methods: Sixty-four patients with various degrees of renal dysfunction were studied. After simultaneous bolus injection of MAG3 (185 MBq) and OIH (3.7 MBq), 8-point venous blood sampling was performed from 2 to 44 min. By fitting time-concentration profile to 2-exponential function, plasma clearance was calculated. Using OIH 8-point clearance and plasma distribution volume of MAG3 at 30 and 44 min, necessary constants (P_{1-4}) for the Russell's formula ($Ct/W=P_1+P_2X+P_3X^2+P_4X^3$, $X=\ln(pW)$, C=OIH clearance in ml/min, t=sampling time in min, P_{1-4}: constants, W: weight in kg, p= fraction of the injected dose/ liter of plasma)were determined by regression analysis.
Results: Calculated 8-point clearances of MAG3 and OIH ranged from 17.2 to 539.2 and from 110.5 to 756.8 ml/min/1.73m^2. Determined constants, correlation coefficients (r) and standard errors of estimate (SE) from the regression analysis were summarized in the table.

Time (min)	P_1	P_2	P_3	P_4	r	SE (ml/min/1.73m^2)
30	330.8	-200.1	24.76	5.01	0.921	58.8
44	350.8	-225.4	64.42	-8.53	0.922	58.1

Conclusion: Using these constants and Russell's formula, OIH clearance could be directly determined from Tc-99m MAG3 single blood sample.

PS_118

CORRELATION OF PLASMA CYSTATIN C, B-2 MICROGLOBULINE AND CREATININE CLEARANCE TO TC-99M DTPA CLEARANCE IN ADULTS

I. Uslu (1), H. Uzun (2), M. Halaç (1), C. Türkmen (1), S. Aydın (2), L. Kabasakal (1), B. Yıldırım (2), E. Uslu (2), S. Kaya (2). (1) Department of Nuclear Medicine; (2) Department of Biochemistry, Cerrahpasa Medical Faculty, Istanbul University, Turkey.

Serum creatinine is commonly used for monitoring renal function. Beta 2 microglobulin is a potentially amyloidogenic low molecular weight protein. Increased serum levels are seen in renal diseases that decrease glomerular filtration and/or tubular reabsorption. Recently, serum cystatin C, a cysteine protease inhibitor, has been suggested to be a new marker of glomerular filtration rate (GFR). In order to evaluate the usefullness of cystatin C as a marker of renal function this study is carried out. For this purpose 105 subjects, age ranged from 24 to 65 years (mean age 43.3±8.3), were included to the study (56m, 49f). Serum creatinine, beta-2 microglobulin and cystatin C levels were determined using commercially available methodologies. GFR was determined as a reference, by using single or two blood sample methods with Tc-99m DTPA. Plasma creatinine levels were ranged from 0.6 mg/dl to 8.7 mg/dl with a mean value of 2.3 ±1.7 mg/dl. Plasma cystatin C levels ranged from 0.5 mg/l to 4.9 mg/l with a mean value of 2.00±1.27 mg/l. The correlation coefficient between creatinine clearance and cystatin C levels was 0.82 (Pearson's correlation) ($p<0.001$ for the difference). Tc-99m DTPA GFR values were ranged from 10 ml/min/1.73 to 173 ml/min/1.73 with a mean value of 71.0±37.7 ml/min/1.73. The correlation between creatinine clearance levels was better than the correlation between plasma cystatine C levels and reference GFR method with the correlation coefficients of r=0.96 and r=0.79, respectively. The correlation coefficient between beta-2 microglobulin values and DTPA GFR was r=0.72 ($p<0.05$). When we conclude that for the evaluation of renal function Tc-99m DTPA clearance study can not be replaced by measurement of plasma cystatine C or creatinine levels.

PS_119

ASSESSMENT OF THE OPTIMAL TIME INTERVAL AND BACKGROUND REGION OF INTEREST IN MEASUREMENT OF RELATIVE RENAL FUNCTION IN TC-99M EC RENOGRAPHY

AF. Yapar (1), M. Aydın (1), N. Yoloğlu (1), H. Yalcın (1), Z. Yapar (2). (1) Department of Nuclear Medicine, Başkent University, Adana Hospital, Adana, Turkey; (2) Department of Nuclear Medicine, Cukurova University School of Medicine, Adana, Turkey.

Measurement of relative renal function (RRF) is one of the main parameter of the radionuclide renography, for this measurement, several time intervals and different types of background region of interests (BGROI) have been used.
Aim: To determine the optimal time interval and the type of BGROI for the calculation of RRF in Tc-99m-ethylenedicysteine (EC) studies. For this purpose, using different time intervals and types of BGROIs various RRF values were calculated from EC renographies and these values were compared with those obtained from DMSA studies as reference.
Methods: Twenty patients (13 F, 7 M; age range: 0.2-60 yrs; mean age: 13±18 yrs) were studied. All patients underwent both of EC and DMSA scans in the same week, and the second study was performed at least 2 days later from the first one. For determination of RRF in EC renography the selected time intervals were 0.5-1.5; 0.5-2; 1-2; 1.5-2.5; 2-3 min and the BGROI types were inferolateral crescent, lateral crescent, and perirenal shaped. RRF calculation was based on the integral method and for this calculation all types of BGROIs were used for each time interval. The reference RRF was obtained from DMSA study, using inferolateral crescent BGROI and geometric mean of anterior and posterior views. For each patient with the low functioning kidney, relative uptake differences between the DMSA and EC were calculated. Then the mean differences and the standart deviation were found. Standart deviation of these differences represented the precision of the technique.
Results: When compared with DMSA scan, RRF values obtained from EC renography, using inferolateral crescent shaped BGROI within 1.5-2.5 min time interval had the lowest error (3.24%) and the highest correlation coefficient (r=0.98).
Conclusion: Our findings indicate that the optimal combination is inferolateral crescent shaped BGROI within 1.5-2.5 min time interval. Using this combination, the calculated RRF values from EC renography showed the best correlation with the RRF values obtained from DMSA studies.

PS_120

DIFFERENTIAL RENAL FUNCTION: A COMPARATIVE STUDY OF DTPA AND DMSA RENAL SCAN

S.R. Zakavi, K. Ariana. Nuclear Medicine Department, Imam Reza Hospital, Mashad university of medical sciences, Mashad, Iran.

AIM:Renal scan has important role in diagnosis of renal disease. Measurement of differential renal function (DRF) is very important in clinical decision of unilateral nephrectomy in a patient with a poor functioning kidney. DRF can be measured using DTPA or DMSA renal scan. This study tries to compare the results of DRF measurement in these two kinds of renal scans.
METHODS: We studied retrospectively, 56 patients who referred for both DTPA and DMSA scan. DRF was calculated using semilunar (Method1) and circumferential(Method 2) background subtraction in DTPA scan and using geometric mean (from anterior and posterior views) without background subtraction in DMSA renal scan.
RESULTS: Fifty six patients were studied (22 Female, 34 Male) with the mean age of 28.2 years and age range of 0.08 -85 years. The mean time span between the two scans were 4.13 days (range=1-11 days). The calculated DRF using multiple methods and radiotracers were highly correlated (r>0.95).
Using DTPA, mean DRF for the right kidney were 59.1% and 57.7% in method 1 and 2 respectively. The same mean was 56.8% in DMSA renal scan. Mean difference between method 1 and DMSA scan was 1.44% with 95% confidence interval of 0.125%-2.77%. Mean DRF for the right kidney using method 2 and DMSA scan were 57.7% and 56.8% respectively. Using paired t-test mean DRF were compared in different methods. Right kidney has generally lower DRF in method 2 compared to method 1 in DTPA renal scan (P=0.03). This is due to liver background effect, which is subtracted only in method 2. The calculated DRF using DMSA renal scan has no significant difference with DRF measured using method 2(p=0.519). However it was significantly lower for right kidney when compared to method 1(P=0.05).
CONCLUSION: 1) Semilunar background subtraction in DTPA renal scan significantly overestimates right kidney contribution in DRF while circumferential background subtraction is more concordant with DMSA results. So circumferential background selection may be the preferred method in calculating DRF using DTPA renal scan. This is more important when working with poor functioning kidneys. 2) There was excellent correlation of DTPA and DMSA renal scans in measuring DRF which suggests interchangeable use. 3) DMSA scan is not necessary, if DRF measurement is the only indication and the result of DTPA renal scan is available.

PS_121

THE COMPARISON OF RELATIVE RENAL FUNCTIONS IN TC-99M DMSA SCINTIGRAPHY MEASURED FROM POSTERIOR VIEWS AND GEOMETRIC MEAN

A.F. Yapar (1), M. Aydın (1), N. Yoloğlu (1), H. Yalcın (1), Z. Yapar (2).
(1) Department of Nuclear Medicine, Baskent University Adana Hospital, Adana, Turkey; (2) Department of Nuclear Medicine, Cukurova University School of Medicine, Adana, Turkey.

In the measurement of relative renal functions (RRF) in Tc-99m dimercaptosuccinic acid (DMSA) scintigraphy, posterior images or the geometric mean of the counts from the anterior and posterior (AP) images can be used. The aim of this study was to evaluate the importance of geometric mean of the counts obtained from AP views to calculate the RRF for both children and adults.

Methods: 123 children (75 F, 48 M, mean age 6.1±5.5 yrs) and 28 adults (15 F, 13 M, mean age 48.2±13 yrs) were studied. DMSA scans were performed 4 hour after injection of 1-5 mCi (37-185 MBq) Tc-99m DMSA, and eight planar images were obtained with a dual head gamma camera. RRF values were calculated for each patient from both posterior images and geometric mean of AP images by using inferolateral background region of interest. For each patient, the differences and correlation coefficient between the relative functions of the low functioning kidney determined from both the posterior view and the geometric mean of anterior and posterior views were calculated. The mean and the standart deviation of the differences were calculated and Student's t test was performed on the differences.

Results: In adults, only 4 of 28 patients (14.2%) showed important differences (3 of them >5%, one of them >10%) (r=0.98) that was not statistically significant (p>0.05). In children, 15 of 123 (12.1%) patients showed important differences (10 of them >5%, 5 of them >10%) (r=0.96) that had statistical significance (p<0.01).

Conclusions: The results of the present study suggest that the accurate RRF calculation in adults may be done from the posterior view only, but in children the RRF may be calculated more sensitively from the geometric mean of anterior and posterior views.

PS_122

51CR-EDTA CLEARANCE: THE INFLUENCE OF THE TIMING OF THE FIRST BLOOD SAMPLE. IS KIDNEY FUNCTION DIMINISHED OVERNIGHT?

E. Petursson. Department of Nuclear Medicine - Isotopastofa, Landspitali - University Hospital, Reykjavik, Iceland.

51Cr-EDTA clearance is conventionally measured by drawing 3 blood samplesafter 2, 3 and 4 hrs from the injection. Single sample clearance methods have also been advocated. When clearance is suspected to be low it has been recommended that a late blood sample be drawn, even as late as 24 hrs post injection (for clearance < 15 ml/min).

Methods:During the interval June 1999 to October 2000 we have done 93 evaluations (79 pts) of 51Cr EDTA-clearance by drawing 5 blood samples at 2, 3, 4, 5 and 24 hrs post injection and compared the results obtained from all five samples (1-5) to those obtained from sample (1-3), (1-4), (2- 4) and (3-5) respectively. A paired t-test was used for the comparison.

Results: 20 measurements on 18 pts gave clearance values between 2.6 and 15 ml/min/1.73 m2 by the 1-3 sample method (1-3). There was good correlation between all methods. The mean values declined slightly from method (1-3), which gave 10.2, through (1-4), (2-4), (1-5) and (3-5), which gave 9.1 ml/min/1.73 m2. There was significant difference at the 5% level between method (1-3) vs (1-5), (1-3) vs (3-5), (1-4) vs (1-5), (1-5) vs (3-5), and (1-4) vs (3-5).

Conclusions: The results could indicate that 1) when 51Cr-EDTA clearance is evaluated the 1st blood sample should be drawn no earlier than 3 hrs post injection. 2) kidney function is diminished during the night.

PS_123

OPTIMIZATION OF GATE'S TECHNIQUE FOR SIMULTANEOUS RENAL SCAN AND GFR MEASUREMENT

S.R. Zakavi, M. Momen Nezhad. Nuclear Medicine Department, Imam Reza Hospital, Mashad university of medical sciences, Mashad, Iran.

AIM: Using Gate's technique for GFR measurement with γ-camera and without plasma sampling, 3mCi of Tc-99m-DTPA is usually injected. This low injected dose precludes optimal renal scanning. This study tries to optimize Gate's technique, for GFR measurement during routine renal scan (i.e.: with doses of more than 10 mCi).

Methods and Materials: Increasing amounts (3,9,12,15 and 18 mCi) of ^{99m}Tc, in a 2ml syringe and 30cm away from the detector, were imaged for 60 seconds with a γ-camera. A 12mCi sample was imaged for 5,10,15,20 and 30 sec with the same condition. Also the same sample was again imaged for 10 sec, in different distances (10,20, 30 and 40 cm) from the detector. Acquisitions repeated 10 times for each sample and recorded in 256 x 256 matrices. Maximum count/pixel as well as total counts in each image were obtained using a rectangular ROI. After optimization of the technique, nine patients were studied. We performed renal scan with injection of 10-15mCi of ^{99m}Tc -DTPA. Pre and post-inject syringe and injection site, were imaged for 15 sec using 256 x 256 matrix, and 30cm away from detector. GFR was calculated using renal scans and compared with creatinin clearance, which is measured using 24 hours urine collection.

Results: With 60 sec acquisitions, mean total counts were increasing from 397498.8 for 3mCi sample to 1131203.1 for 15 mCi and decreasing to 1126232.5 for 18mCi. Maximum counts/pixel was 26577 with 3mCi and 32767 in all other samples. (32767 equal to 2^{15}-1 = maximum capacity of each pixel using word mode acquisition.) This finding suggests count loss, in all 60 sec images except 3mCi sample. Mean maximum count/pixel for 12mCi sample were 8996.2, 17690, 26407.5, 32767 and 32767 for 5,10,15,20 and 30 sec acquisitions respectively. So using 12mCi and counting 15 sec or less, no count loss was noted. Mean maximum counts/pixel for 12mCi sample, using 10 sec/image, were 32767,24950, 16465.6 and 11014.3 for 10, 20, 30 and 40 cm distances respectively. So for accurate counting, syringe distance from the detector should not be less than 20cm. In our patients, mean GFR was 83.34 ml with scintigraphy and 84.88 ml with creatinin clearance methods (P=0.88). Correlation coefficient also was 0.83(P=0.005).

Conclusion: With minimal modification of Gate's technique, GFR can be measured during routine renal scan with significant correlation with laboratory creatinin clearance.

PHYSICS / INSTRUMENTATION 1

PS_124

USE OF REFERENCE TISSUE MODELS WITH BINDING IN THE REFERENCE REGION

G. Blomqvist, G. Hagberg, P. Meractsaki, P. Hartvig, B. Långström. Uppsala University PET Centre, UAS S_75185 Uppsala, Sweden.

Reference tissue methods have become widely used in analyzing PET data, especially data from ligand-receptor interactions. Often it is known that the reference region is not perfect but has specific binding. If this binding is estimated in one study (with the aid of models using input function), the result can provide an "offset value" which can be used in other studies where the input function is not measured. This procedure can be useful when a region is known to have the same binding in two groups being compared. In the present work the effect of irreversible transfer in the reference tissue is addressed.

Methods: With irreversible transfer between two tissue compartments both in the target- and reference regions, the operational equation becomes:

$$C_{targ}(t) = R\,C_{ref}(t) + K_1 \int_0^t C_{ref}(x)dx + k_2\left(k_2/(k_2+k_3) - R\right) \int_0^t \{(k_2+k_3)(x-t)\}\, C_{ref}(x)dx$$

$$- l_3[K_1 \int_0^t (l_3,x)dx + k_2^2/(k_2+k_3) \int_0^t [(k_2+k_3)(x-t)]\, g(l_3,x)dx\,],$$

$$\text{where } g(l_3,t) = \int_0^t l_3(x-t)\, C_{ref}(x)dx$$

$$\text{and } K_1 = k_2k_3/(k_2+k_3).$$

Here C_{targ} and C_{ref} are the time-activity data in the target and reference regions, respectively, R is the ratio between the K_1 values in the target and reference regions and k_2 is the rate constant for transport from the brain in the target region. k_3 and l_3 are the rate constants for the irreversible transfer in the target and reference regions, respectively. The model contains three unknown parameters, R, k_2, and k_3. The model was applied to 12 examinations of healthy volunteers with [^{11}C]-5-hydroxy-L-tryptophan, a tracer for measurement of serotonin synthesis rate. The cerebellum was taken as reference region. The used value of l_3, 0.018 min^{-1}, was obtained from fit of the uptake in cerebellum with the corresponding model using a plasma input function.

Results: The following regional values for the macro-parameter K, were obtained (in min^{-1}):

region	Putamen	Caudate	Thalamus	Occip. cortex	Pons	White matter
mean	0.0169	0.0157	0.0064	0.0033	0.0037	0.0016
standard dev	0.0028	0.0020	0.0033	0.0017	0.0014	0.0010

With I_3 equal to zero substantially smaller Ki values were obtained, which often became zero in regions with low synthesis rate.
Conclusions: The results illustrate that the applied model with irreversible transfer in the reference region provides an index for the transfer, Ki, which gives good discrimination between regions and good precision in regions with high transfer rate.
(1) Hagberg G et al, manuscript 2001

PS_126

GENERATION OF FUNCTIONAL IMAGES OF THE TISSUE TRAPPING CONSTANT FOR -[11C]METHYL-L-TRYPTOPHAN USING CONSTRAINED LINEAR REGRESSION AND VENUS SINUS NORMALIZED INPUT FUNCTION

Y. Kumakura, J. Natsume, P.J. Toussaint, P. Rosa, A. Nakai, S. Mzengeza, E. Meyer, M. Diksic. Montreal Neurological Institute, McGill University, Montral, QC, Canada.

-[11C]methyl-L-tryptophan (-MTrp) has been developed as a tracer to measure brain serotonin (5-HT) synthesis in humans with positron emission tomography. To be able to utilize more powerful statistical methods like statistic parametric mapping one needs to have parametric (functional) images of the brain trapping constant (K; ml/g/min) for _-MTrp. We and others have been utilizing the Patlak approach because of its high computational speed in generating parametric images of K defined in terms of the model parameters as: K= (K1*k3)/(k2+k3) in the analysis of PET data obtained with _-MTrp. However, estimates of K derived from the linear regression of the Patlak plots might be biased because of possible uncertainty of which part of the curve could be assumed to be linear, especially for tracers with slow kinetics. To eliminate this problem, we have adopted an approach, originally proposed by Blomqvist (1) for the pixel-by-pixel calculation of K, or from it 5-HT synthesis rates (R; pmol/g/min). To avoid non-physiological solutions, non-negative constraints were added to the calculation of the macro-parameters, K1, K1*k3 and k2+k3, by the linearized equation describing a 3-compartment model: Ci(T) = K1*I1(Cp) + K1*k3*I2(Cp) - (k2+k3)*I1(Ci); where Ci(T), Cp and In(f) indicate the instantaneous tissue activity, the plasma input function and the nth integral of the function f up to time T, respectively. This input function used in this calculation was as the one described by Nishizawa et al.(2). The K images generated by this approach were compared to those obtained from the Patlak method. The ratios of K-s in the grey (GM) and white matter (WM) for 8 regions (4 lobes, bilaterally), using MRI-based automatic segmentation, were compared between the two methods. The K images generated by the constrained linear algorithm using the venous-sinus-derived input function resulted in about 5% overestimation of the absolute K values when compared to those calculated with the arterial input function. Furthermore, the constrained linear calculation resulted in higher GM/WM ratios of K (1.40_0.07) than with the Patlak approach (1.16_0.04). This improvement in the contrast is statistically significant ($p<0.008$). In conclusion, this new constrained linear algorithm, paired with a less invasive input function, produces K or R images which give better GM to WM contrast than those using the Patlak approach. The proposed approach results also in a reduction of time required for the generation of 5-HT functional images in PET studies. Supported by MT13368 and RO1-NS-29629.

1) G. Blomqvist. J Cerebral Blood Flow Metabol 1984; 14:629-632.
2) S. Nishizawa et al. J Cerebral Blood Flow Metabol 1998; 18:1121-9.

PS_125

EFFECT OF REGION OF INTEREST DEFINITION ON THE BINDING PARAMETERS OF [11C](+)MCN5652

T.K. Owonikoko (1), J. Varga (1), M. Chen (1), U. Scheffel (1), W.B. Mathews (1), H.T. Ravert (1), J. Hilton (1), R.F. Dannals (1), G. Ricaurte (2), Z. Szabo (1). (1) Division of Nuclear Medicine, Department of Radiology; (2) Department of Neurology, Johns Hopkins University, Baltimore, Maryland USA.

Aim: The radioligand [11C](+-)McN5652 has been used for assessment of the deficits of the serotonin transporter (SERT) in animals and humans. The purpose of this study was to investigate the effect of regions of interest (ROI) drawing on the binding parameters of [11C](+-)McN5652.
Methods: Six dynamic PET studies were performed, three in a control and three in an MDMA (serotonergic neurotoxin) treated baboon. In the images, two types of ROIs were drawn: 1) a series of circular regions (ROIs) of equal size over cortical and subcortical brain areas, guided by peak activities of the PET scans and 2) volumetric regions of interest (VOIs) of irregular shapes by utilizing coregistered MR images. Regional distribution volumes (DVs) were determined from a three-parameter, single tissue compartment model in 12 brain areas, 6 with high specific binding (pons, midbrain, hypothalamus, thalamus, caudate, putamen) and 6 with low specific binding (cerebellum, frontal, parietal, occipital, cingulate and temporal cortex).
Results: The magnitude and reproducibility of the two sets of DV was comparable (in the control baboon DVVOI = 12 - 30; DVROI = 13-36; CV = 8 % for both parameters). The two parameters correlated well (r = 0.88), however, DVVOI was 4 - 9 % higher than DVROI in the cingulate gyrus, caudate and frontal cortex and 3 - 38 % lower in the remaining brain areas. The two techniques resulted in comparable differences between the control and MDMA treated animal (average DVROI difference 44 %; average DVVOI difference 43%, correlation of parameter differences r = 0.80). Differences between the two animals were more significant using anatomically based VOIs in the caudate and putamen due to a homogeneous distribution of the SERT. In brain areas with inhomogenous distribution of the SERT, such as the midbrain and pons, activity based ROI analysis provided better separation.
Conclusion: The data demonstrate that the shape of regions of interest may influence the absolute values of radioligand binding parameters. The shape of the regions of interest does not change the overall conclusion concerning the effects of the serotonergic neurotoxin MDMA. Supported by grants AG14400 and AA11653.

PS_127

DETECTION OF LOCAL DOPAMINE RELEASE DURING ACTIVATION USING A SINGLE BOLUS-INFUSION SCAN : A FIRST STUDY

M.C. Gregoire (1), V. Frouin (2), J.B. Poline (2), C. Comtat (2), S. Pappata (3), J. Delforge (2). (1) URA 2210, CEA, SHFJ, Orsay, France; (2) SHFJ, DSV, CEA, Orsay, France; (3) INSERM U334, SHJF, CEA, Orsay, France.

PET and 11C-raclopride has been recently proposed to assess using two studies, one at rest and one during activation, the endogenous dopamine release induced by cognitive activations. However, this method requires two injections, and is limited by individual variability of endogenous dopamine baseline level. We propose here to use a single bolus-infusion acquisition protocol in conjunction with compartmental modelling information and statistical analysis. This work aims at exploring dedicated regressors in a statistical general linear model and validating this approach using simulated data.
Methods : (i) Generalised Linear Model: We use the GLM and statistical inferences implemented in the SPM software. Four regressors are considered in the model, three for baseline and one for activation. The baseline regressors are orthogonalised, and a noise model is inserted. The goodness of the model is assessed with the residual sum of squares and F-statistics.
(ii) Modelling regressors : Using a full compartmental model approach, including both endogenous and exogenous systems, we simulated dopamine release during different periods of activation. The 11C-raclopride rate constants and the input function were derived from a former modelling study which involved full characterisation of the model with a multi-injection protocol. The endogenous dopamine rate constants were derived from the literature, and dopamine release was supposed to be correlated in time with the activation paradigm. Bolus-infusion acquisition parameter Kbol was calculated from former bolus data. Three characteristic kinetics were derived, representing large functional areas at rest : striata, cortex and cerebellum.
(iii) Simulations : In order to mimic a PET acquisition, we started from real segmented MRI volumes. Ten compartments were identified and associated to specific baseline time-activity curves. We study the detection capability by inducing various dopamine release amplitudes in areas of different sizes and location : putamen, accumbens, and caudate nucleus. Bolus-infusion realistic acquisitions were simulated using an analytical simulator of the ECAT HR+ PET camera, and statistics taken from real scans.
Results : Preliminary results on noiseless data show that a 100% endogenous dopamine increase during 10 minutes induces a 13% change in PET signal. Results of realistic simulations will focus on the impact of the choice of appropriate regressors on the detection efficiency, depending on the amplitude and spatial extend of dopamine release. We will also present the effects of a bias in the Kbol estimate.

PS_128

INTRA- AND INTEROBSERVER VARIABILITY OF SEMI-AUTOMATICAL ANALYSIS OF I-123 JOFLUPAN RECEPTOR STUDIES

J. A. K. Blokland, P. Dibbets, M.P.M. Stokkel, E.K.J. Pauwels. Nuclear Medicine, Leiden University Medical Centre, Leiden, The Netherlands.

I-123 joflupan can be used to image the receptor density in the striatum. Quantitative assessment of the density requires the outlining of the left and right nucleus caudate and the putamen, as well as a reference region in the occipital area of the brain. So, several regions of interest (ROIs) must be drawn by hand. In earlier studies it has been shown that differences in shape and size of the ROIs, even drawn by one person, will result into a more significant error than the use of ROIs with a fixed shape and size. In this study we present a semi-automatically procedure to analyse these receptor studies.

To start the program the user has to select an I-123 joflupan study. The program automatically finds the transaxial slices with the highest count density in the central region of the brain. In general, in this slice the striatum is at least partially visible. Next the operator can move two predefined ROIs to include the striatum and another ROI to assign a background/reference ROI. These ROIs can only be translated; they cannot be rotated. Then the program finds the slice with the highest count density within the ROIs. The program calculates the minimum number of slices that should be analysed to encompass a total slice thickness of at least 10 mm. The slice with the highest count density will be the central slice of the set. Then, for each slice in the set the operator can adapt the position the ROIs around striatum. Finally the uptake ratios of the activity in the nucleus caudate and the putamen to the occipital region of the brain are calculated. To be able to compare the obtained ratios with normal values and with measurements from other departments the ratios are multiplied with recovery coefficients, which are obtained from phantom studies with known activity distributions.

To assess the intra- and inter-observer variabilities 32 patient studies were analysed three times by two operators. For each study the deviations from the mean value were calculated. Finally the mean deviation and its standard deviation were calculated over all studies. Using this procedure in 32 patient studies we obtained very low intra- and inter-observer variabilities: 0.14 ± 0.13 respectively 0.19 ± 0.18 (CV: 2.4% resp. 3.1%).

We conclude that this semi-automatically procedure to analyse I-123 joflupan studies of the brain results in very low operator variations.

PS_129

IMPROVEMENT OF QUANTITATIVE DEFECT DETECTION IN TL-201 MYOCARDIAL SPECT USING SCATTER AND ATTENUATION CORRECTIONS

A. Kojima (1), S. Tomiguchi (2), N. Katsuda (2), M. Matsumoto (3), M. Takahashi (2), N. Motomura (4). (1) Radioisotope Research Center, Kumamoto University, Kumamoto, Japan; (2) Department of Radiology, Kumamoto University School of Medicine, Kumamoto, Japan; (3) Department of Radiological Technology, College of Medical Science, Kumamoto University, Kumamoto, Japan; (4) Medical Engineering Laboratory, Toshiba Corporation, Tochigi, Japan

Scatter and attenuation in the body cause significant distortions in SPECT images and limit quantitative measurement of absolute radioactivity. The aim of this study was to investigate how both scatter and attenuation corrections can quantitatively improve lesion detectability under the condition that there are various activity distributions around the myocardium in Tl-201 myocardial SPECT study using a sophisticated phantom.

Methods: In this study, we performed Tl-201 myocardium SPECT imaging using a dual-head gamma camera SPECT system and an anthropomorphic torso phantom with a cardic insert. Attenuation correction (AC) using an asymmetric fan-beam collimator and Tc-99m external source specially designed for the SPECT system and scatter correction (SC) by the triple energy window (TEW) method was performed. A fillable defect were placed in the inferior wall of the cardiac insert and the radioactivity concentration ratio of the defect to the myocardial wall was 0.5 : 1. ECT projection data were acquired for three different Tl-201 distributions: the myocardium activity only (M), the myocardium and liver activities (M + L), and the myocardium, liver, and background activities (M + L + B). Four ECT image reconstructions were performed for each activity distribution: without both SC and AC (SC-/AC-), with SC and without AC (SC+/AC-), without SC and with AC (SC-/AC+), and with both SC and AC (SC+/AC+).

Results: The 50% defect-to-normal wall SPECT image-count ratios (D/N ratios) were calculated and compared among three activity distribution and four image reconstructions. Furthermore, the ratios (R ratios) of the D/N ratio-value for the M + L or the M + L + B and the D/N ratio-value for the M were also obtained. The SC+/AC+ images showed the closest ratio to the true ratio (0.5) and a small influence on the activity distributions around the myocardium as the following table.

Tl-201 Activity distribution	SC-/AC-		SC+/AC-		SC-/AC+		SC+/AC-	
	D/N ratio	R ratio	D/N ratio	R ratio	D/N ratio	R ratio	D/N ratio	R ratio
Myocardium (M)	0.41	1	0.34	1	0.53	1	0.45	1
M + Liver (L)	0.47	0.87	0.35	1.03	0.62	1.17	0.47	1.04
M + L + Background (B)	0.54	1.32	0.39	1.15	0.67	1.26	0.48	1.07

Conclusion: Quantification in Tl-201 myocardial SPECT study can be improved using both scatter and attenuation corrections.

PS_130

CLINICAL INTERESTS OF THE SCATTER CORRECTION PER(TM) TECHNIQUE FOR PLANAR TC99M-SCINTIGRAPHIES

C. Billotey (1), C. Salvat (1), J. Mas (2), S. Vinot (3), P. Girard (3), J.D. Rain (4), P. Hannequin (5). (1) Dpt of Nuclear Medicine, Saint-Louis Hospital, Paris, France; (2) Dpt of Nuclear Medicine, Clinique le ligne bleue, Epinal, France; (3) GEMS-SMVI Society, Buc-sur-yvette, France; (4) Dpt of Nuclear Medicine, Centre d'imagerie, Paris, France

Clinical interests of the scatter correction PER™ technique for planar Tc99m-scintigraphies.

Objectives :

Photon Energy Recovery (PER™) technique was developed to remove scatter. It enables to select the photons according to their true energy and to separate the unscattered from the scattered events. The aim of this study is to report clinical interests of this technique with several examples of various 99mTc-scintigraphies.

Methods :

All static planar images were acquired (DST-XL camera, SMV) and processed with PER™ software. Acquisition parameters (matrix size and counts statistics) depended on type of exams. Scatter corrected (Col) and no corrected (Unl) images were performed. We measured counts statistics in ROIs corresponding to cold or hot spot and adjacent area on Col and Unl. We calculated contrast for Col (CRCo) and Unl (CRUn), and enhancement contrast ratio (ECR) defined as [(CRCo - CRUn) / CRUn]x100. We calculated these values on images of bone lesions (BL) (cold or hot focus), melanoma sentinel node (SN), intestinal hemorrhage (IH), and abnormal parathyroid gland (APG).

Results :

Table presented some values of CR and ECR for cases of hot or cold focus lesions. The enhancement of contrast given by PER™ was very important (46 to 413 %). Cervical SN(2) was only detected on Col.

	Cold BL (1)	Cold BL (2)	Hot BL (1)	Hot BL (2)	SN (1)	SN (2)	IH	APG (mediastinal)	APG (cervical)
CRCo(%)	37.2	16.9	32.8	30	77	44.9	31.7	119	105
CRUn(%)	25.4	10	21.2	11	15	≤ 0	21.3	73.7	71.4
ECR(%)	46.5	69	54.7	173	413	+++	48.8	61.5	47.1

Conclusion :

PER™ appears useful and efficient for various types of Tc99m-scintigraphies. Especially cold bone lesions, SN located near the primary lesion (*i.e.* the injection sites), small and/or posterior APG, could be more easily detected. The site of IH is better localized because the shape of extra-vascular activity is better defined.

PS_131

USE OF GADOLINIUM-153 TRANSMISSION ATTENUATION MAPS FOR QUANTITATIVE I-131 SPECT WITH DUAL WINDOW SCATTER CORRECTION

A.J. Green, S. Baig, R.H.J. Begent. CRC Targeting and Imaging Group, Royal Free and University College Medical School, London, UK.

The dosimetry of directed anti-cancer therapies requires quantification of radionuclide images of the directing agent. Radioimmunotherapy and Antibody Directed Enzyme Prodrug Therapy both rely on antibodies and antibody-like molecules which have relatively long half lives so that long-lived radionuclides are employed to follow their distribution. In this work we have investigated the use of a commercially available scanning line source system (ADAC Vantage) to produce standard ^{99m}Tc attenuation maps and the transformation of these maps for use in the reconstruction of ^{131}I images.

A phantom was constructed from an elliptical Perspex cylinder with the inclusion of cylinders containing a model lung tissue volume and a cold volume. The body of the phantom was filled with ^{131}I solution; a solution of the same specific activity was used to fill the interstices in the lung volume; the cold volume was filled with nonradioactive water. Data were acquired into 64 projections each of matrix size 128 x 128. The phantom was imaged with a range of acquisition times to produce a range of image count densities. Images were acquired with 20% windows for the 364 keV peak of ^{131}I and the 100 keV peak of ^{153}Gd, and an ^{131}I scatter window set at 30 percent and abutting the lower edge of the peak window. 100 keV gadolinium peak transmission data is automatically generated by the system with reference to a daily blank scan. Standard (^{99m}Tc) transmission images were reconstructed using filtered back projection (default) and OSEM; the reconstructed transmission images were rescaled to account for the difference in attenuation factor between technetium and iodine photon energies. Standard dual window scatter correction was applied to the iodine data . The scatter corrected iodine data were reconstructed by OSEM using the derived attenuation map, and a uniform ellipse attenuation map.

The total acquired counts in the ^{131}I window ranged from 3.2×10^6 to 7.1×10^7.

At low count densities the reconstructed images were dominated by statistical noise, this noise was seen to reduce with increasing count density. At high count densities the lung to background activity ratio was estimated correctly using the measured attenuation map; at low count densities and with the uniform attenuation map the estimation of this ratio was poor.

Attenuation maps acquired with ^{153}Gd transmission sources can be used to improve quantification of ^{131}I SPECT images. Further work is needed to investigate the use of the technique with low count density images.

PS_132

SEMI QUANTITATIVE ANALYSIS OF F18-FDG IMAGING USING A HYBRID CAMERA FOR THE ASSESSMENT OF TUMOUR RESPONSE TO THERAPY

A.J. Green, S. Baig, R.J. Francis, R.H.J. Begent. CRC Targeting and Imaging Group, Royal Free and University College Medical School, London, UK.

The assessment of response to therapy of solid tumour masses, in the clinic and in clinical trials, is an application ideally suited to ^{18}FDG imaging with a hybrid camera. The problem is to assess the intra-patient changes in FDG uptake when the size and avidity of uptake by the lesions may change with treatment.

We have developed an analysis method based on simple segmentation for adaptively growing a tumour volume of interest (VOI) from a seed point together with a normal tissue volume of similar size. Count density histograms are plotted for the VOIs and statistical comparisons made.

In a longitudinal study patients underwent FDG imaging and conventional response assessment:

	Baseline assessment	Early Assessment	Conventional assessment
2 weekly regimens	FDG and CT Within 2 weeks prior to commencement	FDG After 2 cycles 3-4 weeks	FDG and CT After 6 cycles 12 weeks
3 or 4 weekly regimens		FDG After 1 cycle 2-4 weeks	FDG and CT After3 cycles 9-12 weeks

The FDG imaging protocol was strictly standardised to minimise the effect of any non-linearity in the camera response. Patients were fasted for 5 hours prior to administration of 150 MBq ^{18}FDG i.v. and asked to rest for 90 min before emission and transmission images were acquired (ADAC MCD system) in 2 or 3 bed positions.

Images were reconstructed by OSEM utilising transmission attenuation maps and normalised for any deviations from the protocol. VOIs were grown from different seed points within the tumour and background to test the sensitivity of the method to seed point position. Background and tumour histograms were generated and compared at each scanning time; background histograms and tumour histograms were compared longitudinally for each patient.

Tumour VOI were insensitive to choice of seed point, background VOI position was sensitive to seed point however the histogram generated from the VOI was insensitive to VOI position within the same tissue type. Tumour histograms were significantly different from the adjacent normal tissue histograms. Background tissue histograms were not significantly different at different imaging times. In general tumour histograms changed significantly over time, changes in the height and position of the median were both seen, the change at the early assessment time being a good predictor for the change at the conventional assessment time. The response to therapy predicted by the change in tumour histogram correlated well with conventional response assessment.

^{18}FDG PET by hybrid camera shows promise in this application.

PS_133

STATISTICAL UNCERTAINTY IN GATED BLOOD POOL SPET IMAGING

M.W. Groch, W.D. Erwin. Department of Nuclear Medicine, Northwestern University and Northwestern Memorial Hospital, Chicago, Il, USA.

The objective of this study was to evaluate the statistical requirements for quantification of ejection fraction (EF) from gated blood pool SPET (GBPS) studies. Due to the nature of SPET imaging, simple Poisson statistics do not apply in the reconstructed images.

Methods: The statistical uncertainty in GBPS was determined empirically using a non-beating GBPS phantom consisting of a cylindrical chamber 6cm in diameter and 10cm long, mounted at 60¡ from the vertical axis in a 40cm water bath. Phantom studies were acquired with the same acquisition parameters as patient GBPS studies (64x64 matrix, 180° arc, 32 projection (PROJ); however, the computer was set up to acquire 32 identical views at each of the 32 PROJs. Each data set represented 32 identical studies of the same phantom volume, thus, any variation from one study to the next would be due to the statistical uncertainty of the data. Regions of interest (ROI) were used to determine the counts in each of the 32 identical reconstructed data sets. The size of the region was varied so that the standard deviation (SD) as a function of region counts, could be studied. The variation in counts for a given ROI was used to empirically determine the statistical uncertainty of the EF calculation by plotting a histogram of the counts versus acquisition set and computing the percent CD. Additionally, reconstruction parameters were varied to determine the effect of filter selection and interpolation on the noise properties of the data set.

Results: The relationship between percent SD and counts was determined by fitting the data to an equation of the form: $y = a \times 1/\sqrt{x}$. The value of a, is affected by the matrix size, convolution kernel, angular sampling of the projection data and the attenuation properties of the medium. Percent SD was determined for oblique data reconstructed from 32 PROJ with a Butterworth filter 0.5/10; reconstruction zoom of 2. The percent SD obtained by fitting the data using the method of least squares was found to be = 128 x $1/\sqrt{}$counts.

Conclusions: The statistical uncertainty of quantitative calculations from GBPS data was empirically determined for typical patient acquisitions and can be used to assess the statistical errors in GBPS imaging.

PS_134

DETECTION OF SMALL LEFT-TO-RIGHT CARDIAC SHUNTS BY RADIONUCLIDE ANGIOCARDIOGRAPHY

A. Stanicic (1), R. Jakl (2), D. Ivancevic (3), S. Popovic (3), Z. Milas (4), V. Capkun (1). (1) Department of Nuclear Medicine, Clinical Hospital, Split; (2) Department of Pediatrics, Clinical Hospital, Split; (3) Department of Nuclear Medicine and Radiation Protection, University Hospital, Zagreb; (4) Faculty of Engeneering, Split, Croatia

Sensitivity and precision of methods for evaluation of left-to-right cardiac shunts are of utmost importance in clinical practice for patient planning. If the first pass radionuclide angiocardiography is routinely performed with bolus of good quality, the radionuclide method can offer high quality data.

Methods: We analyzed lung curves obtained from 31 patients aged 1 week to 28 years (mean 14.5 years). The diagnosis of a left-to-right cardiac shunt was established by cardiac catheterization. We also analyzed 20 normal curves, obtained from a similar age group of patients without left-to-right shunt. Good boli could be obtained even in small crying children by injections during expirium.

In order to allow comparison, lung curves were standardized by plotting count rate values, expressed as percent of the first peak, against times, expressed in standard deviations of the first gamma variate fit. Normal values were established from data obtained in 20 patients without left-to-right shunt. The analysis of standardized curves was focused on the interval between the first pass and the systemic recirculation components where the first shunt recirculation appears. Normal variations in this segment were low. Small left-to-right shunts were detected by the type of deviation from mean normal values. An elevation above normal values during the first shunt recirculation with successive return to normal values before a significant systemic recirculation appears is a characteristic of a small left-to-right shunt. The influence of successive shunt recirculations is insignificant.

Results: In shunts as low as 9% of pulmonary flow the standardized curves clearly declined from normal values for the level of significance of 95%, while shunts as low as 3% could be detected by deviations from the mean normal values. The low variations in normal values can also explain the precision of the radionuclide method in quantitative analysis of left-to-right cardiac shunts.

Conclusions: Lung curves obtained by radionuclide angiocardiography can provide high quality data regarding the presence of small left-to-right cardiac shunts. No false positive findings are expected above the level of 3% of pulmonary flow.

Company	Model	Sensitivity Z = 0 cm (cps/kBq)	Ang.res. Z = 1 cm (deg)	G Z = 1 cm (cps/kBq)	Ang.res. Z = 4 cm (deg)	G Z = 4 cm (cps/kBq)
Care-Wise	C-Trak Automatic	31.6	84	26.6	55	6.3
Care-Wise	C-Trak Automatic 1 coll.	29.1	77	29.8	49	7.8
Care-Wise	C-Trak	28.7	82	27.1	50	7.8
Care-Wise	C-Trak 1 coll.	19.8	68	33.4	44	9.4
Care-Wise	C-Trak 2 coll.	6.3	90	8.1	50	4.3
Eurorad	Europrobe CsI	10.8	81	16.3	54	5.4
Eurorad	Europrobe CsI 1 coll.	4.3	62	12.9	43	4.6
Eurorad	Europrobe CdTe	6.2	87	8.8	64	1.6
Eurorad	Europrobe CdTe 1 coll.	2.3	64	4.5	41	1.2
Gammasonics	SRP MKIII	11.6	88	-	54	-
Neoprobe Corp.	Neoprobe 2100 14 mm	25.6	100	11.4	72	1.6
Neoprobe Corp.	Neoprobe 2100 14 mm 1 coll.	3.7	62	7.8	44	2.1
Neoprobe Corp.	BlueTip 12 mm (intern. coll.)	2.5	73	3.8	38	1.9
Neoprobe Corp.	BlueTip 12mm (intern. coll.) 1 coll.	1.2	41	7.1	31	2.0
Neoprobe Corp.	BlueTip 12mm (not intern. coll.)	12.2	98	9.4	67	2.1
Neoprobe Corp.	BlueTip 12mm (not intern. coll.) 1 coll.	2.3	62	4.8	41	1.4
Neoprobe Corp.	BlueTip 19mm (not intern. coll.)	38.6	123	32.5	83	24.7
Neoprobe Corp.	BlueTip 19mm(not intern. coll.) 1 coll.	8.2	98	10.8	58	5.1
Pol.hi.tech.	11C	7.7	70	10.1	36	5.0
Pol.hi.tech.	11L	9.1	75	14.9	47	4.5
Pol.hi.tech.	15-3	24.7	84	32.5	48	11.4
Pol.hi.tech.	15 LVR 0*	31.2	97	25.3	68	6.0
Pol.hi.tech.	15 LVR 1*	16.8	88	18.1	62	4.3
Pol.hi.tech.	15 LVR 2*	10.2	87	12.3	56	4.4
Pol.hi.tech.	15 LVR 3*	7.3	83	10.9	42	6.6
Pol.hi.tech.	18LVR 0*	17.1	103	14.0	71	4.1
Pol.hi.tech.	18LVR 1*	10.8	90	11.6	58	4.6
Pol.hi.tech.	18LVR 2*	7.4	89	8.9	58	3.5
Pol.hi.tech.	18LVR 3*	5.3	87	7.1	53	3.3
Pol.hi.tech.	22 LVR 0*	31.3	111	35.8	69	11.6
Pol.hi.tech.	22 LVR 1*	18.8	103	21.3	66	7.6
Pol.hi.tech.	22 LVR 2*	12.4	100	14.8	63	6.0
Pol.hi.tech.	22 LVR 3*	8.7	88	13.0	52	7.5
USSC	Navigator	3.6	84	3.7	61	0.8

Conclusions: physical performances of the most common commercial probes were determined under the same experimental condition. Probes with larger crystal diameter (usually conceived for medium or high energy photons) show higher G values because of their high sensitivity, but they have very poor spatial resolution, so they may make difficult an accurate sentinel node localization. It goes without saying that the G parameter classifies probes on the basis of their physical performances only. Of course the choice of whichever model may be leaded by several other criteria (costs, reliability, weight, sound, options, service contract).

* Variable callimator position; 0 = minimum callimation; 3 = maximum callimation

PS_135

INTRAOPERATIVE GAMMA PROBES: SYSTEMATIC INTER-COMPARISON OF 14 COMMERCIAL DEVICES UNDER IDENTICAL EXPERIMENTAL CONDITIONS - INTRODUCTION OF A SIMPLE PHYSICAL FIGURE OF MERIT

C. Chiesa (1), F. Toscano (2), M. Mariani (2), E. Bombardieri (1). (1) Istituto Nazionale Tumori, Unità Operativa Medicina Nucleare, Milano, Italy; (2) Politecnico di Milano, Dipartimento di Ingegneria Nucleare, Milano, Italy.

Aim: Our goal was to accomplish an inter-comparison between the most common commercial devices under the most homogenous experimental condition. Besides that, a simple physical figure of merit is proposed, easily deducible from acceptance tests results.

Materials and methods: methods are described in the Italian Protocol for intraoperative probes quality control. It is important the definition of the "standard energy window", centered on the peak and twice the energy resolution wide. Such a width includes the same portion of energy spectrum for different detectors, and only in this condition sensitivity comparisons are meaningful. Sensitivity measurements were performed at contact of the same ^{57}Co point source ($S(0; {}^{57}Co)$). Its activity was decay corrected. Spatial resolution, defined as $2X_{1/2}(Z)$ = FWHM of the point spread function for a ^{99m}Tc source, was determined at depth Z = 1, 2, 3, 4 cm in plexiglass, as well as the $S(Z, {}^{99m}Tc)$ relative to $S(0; {}^{99m}Tc)$. According to common sense, a probe is better the higher its sensitivity and narrower its aperture cone. Given the well known trade off between these two parameters, the G (goodness) figure of merit was introduced, defined as $G(Z) = S(Z) / F(Z)$, where F(Z) is the fraction of solid angle subtended by the cone of semi-aperture (half angular resolution) $\theta_{1/2}(Z) = \text{arctg}[X_{1/2}/Z]$.

Results are reported below for 1 and 4 cm depth only.

RADIOPHARMACY / RADIOCHEMISTRY 1

PS_136

IMAGING AND QUANTIFICATION OF TUMOR APOPTOSIS USING 99MTC-EC ANNEXIN V

E. Kim (1), D. Yang (1), A. Azhdarinia (2), D.F. Yu (1), D.A. Podoloff (1). (1) The University of Texas, M.D.Anderson Cancer Ctr; (2) The University of Texas Medical School, Houston, USA.

Aim: Assessment of apoptosis would be useful to evaluate the efficacy and mechanisms of cancer therapy and also its progression or regression. Annexin V has been used to measure an apoptosis both in vitro and in vivo. This study was to report an imaging technique to measure and monitor tumor cells undergoing programmed cell death caused by radiation and chemotherapy using 99mTc-EC-annexin V.

Methods: Ethylenedicysteine (EC) was conjugated to annexin V using carbodiimide as a coupling agent. The yield of EC-annexin V was 100%. In vitro cellular uptake, pre and post-radiation (10-30 Gy) and paclitaxel treatment was quantified using 99mTc-EC-annexin V. Tissue distribution and planar imaging of 99mTc-EC-annexin V were determined in breast tumor-bearing rats at 0.5, 2, and 4 hrs. To demonstrate in vivo cell apoptosis that occurred during chemotherapy, a group of rats was treated with paclitaxel and planar imaging studies were conducted at 0.5-4 hrs. Computer outlined region of interest (ROI) was used to quantify tumor uptake on day 3 and day 5 post-treatment. 99mTc-EC was used as a control.

Results: In vitro cellular uptake showed that there was significantly increased uptake of 99mTc-EC-annexin V after irradiation (10-30 Gy) and paclitaxel treatment. In vivo biodistribution of 99mTc-EC-annexin in breast tumor-bearing rats showed increased tumor-to-blood, tumor-to-lung, and tumor-to-muscle count density ratios as a function of time. Conversely, tumor-to-blood count density ratios showed a time-dependent decrease with 99mTc-EC in the same time period. Planar images confirmed that the tumors could be visualized clearly with 99mTc-EC-annexin. There was a significant difference of ROI ratios between pre and post-paclitaxel treatment groups at 2 and 4 hrs post injection.

Conclusion: The results indicate that tumor apoptosis can be imaged and also quantified using 99mTc-EC-annexin.

PS_137

PROPERTY OF IODIDE UPTAKE AND EFFLUX IN SODIUM/IODIDE SYMPORTER GENE TRANSFECTED HUMAN CANCER CELL LINES

J.H. Shin, J.K. Chung, Y.J. Lee, J.J. Min, J.M. Jeong, D.S. Lee, M.C. Lee. Department of Nuclear Medicine, Seoul National University College of Medicine Seoul, Korea.

Aim : Radioiodide uptake in differentiated thyroid carcinoma cells depend on sodium-iodide symporter(NIS). To apply this property for nonthyroid carcinoma and anaplastic thyroid carcinoma, we transfected hNIS gene to several human cancer cell lines, and investigated the property of iodide uptake and efflux in these cell lines.

Methods :. With liposome, hNIS gene and geneticin resistance gene were transfected into human cancer cell lines, SNU-449 (hepatocellular carcinoma cell), SNU-C5 (colon carcinoma cell), ARO (anaplastic thyroid carcinoma). To select of hNIS expessing cells geneticin is treated. After incubation, uptake and efflux of ^{125}I were measured in the transfected and wild type cell lines . We treated these cell lines with 1mM/L potassium perchlorate, 100 or 300 μmol/L of the anion channel blocker 4,4'-diisothiocyano-2,2'-disulfonic acid stilbene(DIDS), and lithium chloride and evaluated the effect on uptake and efflux of iodide.

Results : The hNIS gene transfeted SNU-449N, SNU-C5N, ARO-NIS accumulated up to 13, 7 and 109 times more iodide than did non-transfected cells, respectively. Treatment of DIDS increased iodide uptake 27%, 167%, 42% in transfected cell lines, and potassium perchlorate and lithium chloride inhibited iodide uptake significantly. In iodide efflux study, 70% (SNU-449N, SNU-C5N) and 40%(ARO-NIS) of radioactivity flowed out during the first 10min. In SNU-449N, DIDS hold 10% more iodide at 10min than not treated, whereas the effect of DIDS was not significant in SNU-C5N and ARO-NIS. Lithium chloride increased efflux of iodide, especially in ARO-NIS.

Conclusion : Transfection of hNIS gene induces accumulation of iodide. Retention of iodide in hNIS transfected thyroid cancer cell was higher than other cancer cells. DIDS increased uptake and decreased efflux of iodide in hNIS transfected human cancer cells.

PS_138

RETINOIC ACID INCREASES IODIDE UPTAKE IN A HUMAN SODIUM/IODIDE SYMPORTER GENE TRANSFECTED ANAPLASTIC THYROID CARCINOMA CELL LINE

J.H. Shin, J.K. Chung, Y.J. Lee, J.J. Min, J.M. Jeong, D.S. Lee, M.C. Lee. Department of Nuclear Medicine, Seoul National University College of Medicine, Seoul, Korea.

Aim : Decreased iodide uptake in anaplastic and poorly differentiated thyroid cancers impedes radioiodide therapy. Retinoic acid was reported to increase Sodium/Iodide Sympoter (NIS) mRNA in thyroid cancer cells. We investigated the effect of retinoic acid on iodide uptake and expression of hNIS mRNA in a hNIS transfected human anaplastic thyroid carcinoma cell line.

Methods :. We transfected hNIS genes into a human anaplastic thyroid carcinoma cell line (ARO) by liposome. hNIS expressing cell lines were generated by geneticin. After incubation of ARO, transfected ARO and rat thyroid cell line FRTL-5 with ^{125}I, the uptake and efflux of iodide were determined. To corroborate the expression of hNIS, the inhibition study was examined with 1 mM perchlorate. After 3 days treatment of 1 mM all-trans retinoic acid (RA) on transfected cell lines, ^{125}I uptake was measured and the expression of mRNA was evaluated using RT-PCR.

Results : The expression of hNIS genes transfected cell lines (ARO-NIS) was certified by RT-PCR. Iodide uptake of ARO-NIS cells was 109 times higher than ARO cells. Perchlorate (1 mM) completely inhibited the uptake of iodide in ARO-NIS and FRTL-5. Iodide efflux of ARO-NIS cells was slower ($T_{1/2}$ = 12 min) than that of FRTL-5 thyroid cells ($T_{1/2}$ = 8 min). After RA treatment, ARO-NIS took up iodide 11 times higher than did untreated ARO-NIS (446.1±26.2 vs. 39.9±2.0 pmole/10^6 cells). The expression of mRNA was higher in RA treated ARO-NIS cells than in untreated ARO-NIS cells.

Conclusions : Our data show that RA increased iodide upatake in a hNIS transfected human anaplastic thyroid carcinoma. RA might be a useful adjuvant for radioiodide therapy using hNIS gene.

PS_139

99MTC-LABELED CHONDROITIN SULFATE: A NEW APPROACH TO TARGET OSTEOARTHRITIS. - BINDING AND UPTAKE OF THE TRACER

G. Sobal (1), J. Menzel (2), H. Sinzinger (1). (1) Department of Nuklear Medicine; (2) Institut of Immunology, University of Vienna, Austria.

This study was undertaken to investigate in-vitro interaction of cultured human chondrocytes with chondroitin sulfate (CONDROSULF (CS), (Sanova Pharma, Vienna). This substance is used in the treatment of human osteoarthritis as a slow acting symptomatic drug.

Methods: Radiolabeling of CS was performed using $^{99m}TcO_4^-$/stannous chloride in 0.50 M sodium acetate buffer at pH 5.0. Human chondrocyte cultures were established in monolayer as well as suspension cultures. For binding studies using ^{99m}Tc-labeled CS, monolayer cultures containing 27,000 cells per well were incubated with increasing amounts of labeled CS at 4°C for two hours. Uptake studies were performed in monolayer and in suspension cultures at 37°C. Uptake was monitored for a total of 120 minutes, samples being drawn every 10 minutes. To verify the degree of CS-internalisation, cell CS-coatings were digested with 1000 I.U. hyaluronidase/well for 30 minutes at 37°C. Supernatants and washed cells were counted before and after hyaluronidase treatment.

Results: A saturation-type binding curve was obtained. Scatchard analysis of binding data obtained in two different independent assays revealed a very high affinity of CS for the receptors, as indicated by a Kd of $5.6x10^{-9}$M. Number of CS-molecules maximally bound per cell was found by extrapolation to amount to $3.8x10^8$ per chondrocyte. These results were obtained when using the theapeutically administered CS preparation containing Ca-stearate, 25 percent per weight. After extensive dialysis of CS to remove the detergent, the respective data were $8.3x10^{-9}$M and $1.2x10^8$ CS molecules per cell. Thus, not only the resorption of the drug is enhanced by Ca-stearate, but binding data are also much better in presence of this additive. Viability of chondrocytes after incubation with either CS-preparation was found by trypan blue exclusion to be above 90 %. Uptake studies performed in monolayer and in suspension cultures giving a maximal uptake of 0.5 and 5.0 %, respectively. The cells were saturated already after an incubation interval of 10 minutes. Dialysed CS showed a signifiantly reduced uptake by suspension cultures, namely 1.0 %. The data reveal that after 90-120 minutes of uptake, only 5-7 % of total cellular radioactivity could be liberated by the enzyme, indicating that most of the CS is indeed taken up by the chondrocytes via receptor-mediated pinocytosis.

Conclusions: We therefore conclude, that radiolabeled chondroitin sulfate could be a promising agent to target osteoarthritis, due to its simple radiolabeling procedure, high stability and its incorporation into the cartilage.

PS_140

URINARY IODINE DETERMINATION BY A SIMPLE READY-TO-USE ANALYTICAL KIT

A. F. Sedda (1), G. Rossi (1), C. Cipriani (2). (1) ENEA Casaccia ,Triga Reactor, Rome, Italy; (2) Nuclear Medicine Dept., S.Eugenio Hospital, Rome, Italy.

The analytical determination of iodine in biological fluids, and particularly in urine, is the most important parameter to ascertain a pathological deficiency or eccess in iodine uptake. The importance of analytical determination of iodine in urine is also present in nuclear medicine, particularly in connection with the ^{131}I ablation therapy of thyroid tumors. In many cases the iodine content of the metabolic pool in eligible patients is found increased, due to the use of iodine containing drugs or, more frequently, to the use of iodinated contraste media in radiological examinations. In such cases the fraction of ^{131}I fixed in the thyroid is greatly reduced in comparison with a patient with normal iodine intake. This fact account for the need of a routinary analytical screening of I^- content in the urine of the patients before the ^{131}I administration. The determination of the I^- content of the urine is usually performed in chemical laboratories by a spectrofotometric or a potentiometric technique. This determination requires the use of relatively complex analytical instrumentations, usually not present in a Nuclear Medicine Division.

Methods: in order to ascertain the amount of I^- in the urine of the patients before the ^{131}I administration a new simple, ready-to-use, commercial, analytical kit was tested.

Results: the results showed a good reproducibility of results, and a satisfactory precision, when certified analytical standards of I^- were analyzed. A skilled tecnician was able to affordably perform a great number of determination per day without problems.

Conclusion: the reproducibility of analytical results, coupled with the semplicity of the analytical procedure and the low cost of the kit, render this technique attractive as routinary analytical determination for all patients recruited for ^{131}I diagnostic or therapy.

PS_141

INTERACTION OF TC-99M (V) DMSA WITH PLASMA PROTEIN IN HUMAN BLOOD

N. Chiu, B. Lee. Department of Nuclear Medicine, National Cheng Kung University Hospital, Tainan, Taiwan.

Background: As a crucial step toward the understanding of the localization of Tc-99m (V) DMSA, we investigated its binding and transport in blood.
Methods: The studies were performed to assess the relationship between Tc-99m (V) DMSA and plasma protein by ultrafiltration, electrophoresis, gel filtration chromatography, and affinity chromatography.
Results: By ultrafiltration, electrophoresis and gel filtration chromatography, plasma samples showed 70 - 80% protein binding, whereas dialysis indicated considerable non-protein-bound Tc-99m (V) DMSA, the amount depending on the dialysis medium. Electrophoresis showed 23.8% unbound to plasma protein, and 76.2% of Tc-99m (V) DMSA to be bound to plasma protein, including 58.9% albumin,¡@4.4% bound to α1-globulin, 4.6% bound to α2-globulin, 4.0% bound to β-globulin, and 4.3% bound to γ-globulin. The figures of Ga-67 are 22.9%, 77.1%, 5.5%, 3.5%, 3.8%, 61.1% and 3.2% respectively. According to affinity chromatography, Tc-99m (V) DMSA did not bind to transferrin unlike Ga-67.
Conclusion: This study demonstrates that Tc-99m (V) DMSA at the tracer level in blood is mainly bound to albumin, not transferrin.

PS_142

INFLUENCE OF PROPANOLOL, CYCLOSPORINE, ADRIAMICINE AND NIFEDIPINE ON THE IN VITRO LABELLING OF RED BLOOD CELLS WITH 99MTC

V. Cardoso (1), M. Roca (2), J. Martin-Comin (2). (1) Faculdade de Farmacia. Universidade Federal de Minas Gerais, Brasil, Capes; (2) Servicio de Medicina Nuclear, Hospital de Bellvitge, Spain.

Technetium-99m-labelled red blood cells (RBC) have been widely used in nuclear medicine. Although the labeling efficiency of these procedures is high, possible interferences of drugs have been reported in the RBC labeling with technetium-99m (^{99m}Tc).
Objectives: To evaluate the possible influence of Propanolol, Ciclosporine, Adriamicine and Nifedipine on the labelling ***in vitro*** of red blood cells.
Methods: Eighteen ml of blood were withdrawn of healthy volunteers that haven«t used drug seven days before of experiments. The samples (2,0ml) were incubated at 37°C for 30 min with differents concentrations of drugs. Two labelling methods were employed: in the simple method 60µl of stannous chloride solution (10,2 µg/ml) were added and the samples centrifuged at 1000g for 5 min and plasma and blood cells were isolated. After that, 2,0ml of saline, 0,2 ml of EDTA (2,2%) and 7,4 MBq of 99mTc were also added. The samples were centrifuged and yield labelling was calculated. In the hypochlorite method the blood samples were incubated with $SnCl_2$ (10,2µg/ml) for 5 min. After this period of time, 40µl of NaClO solution (1%) and all the reagents mencioned to simple method were added
Results:

	Propanolol			
Methods	Control	50 ng/ml	100ng/ml	200ng/ml
Simple	96,09±1,79	95,35±1,34	95,27±1,59	95,41±1,88
Hypochlorite	96,01±1,76	95,73±1,95	94,83±2,00	94,94±2,08
	Ciclosporine			
Methods	Control	250 ng/ml	500ng/ml	1000ng/ml
Simple	96,14±1,39	96,25±1,36	96,39±1,34	96,42±1,28
Hypochlorite	96,23±1,81	96,61±1,55	96,17±1,68	95,81±1,64
	Adriamicine			
Methods	Control	50 ng/ml	100ng/ml	200ng/ml
Simple	95,70±1,22	95,79±1,18	95,80±1,29	95,78±1,34
Hypochlorite	95,38±1,03	95,68±1,74	95,93±1,68	96,00±1,09
	Nifedipine			
Methods	Control	100 ng/ml	250ng/ml	500ng/ml
Simple	94,79±2,18	95,00±2,08	95,11±2,02	95,22±1,96
Hypochlorite	94,35±2,38	94,50±2,34	94,60±2,35	94,50±2,30

The values are expressed as mean ± sd (n=10)

Conclusions: The analysis of the results shows that using the two methods described there are no alterations on the labelling **in vitro** of RBC with ^{99m}Tc to the employed concentrations of all of these studied drugs. We can speculate that the interferences observed in vivo may be due the presence of actives metabolites or interactions among different drugs.

PS_143

MECHANISM INVOLVED IN TC-99M (V) DMSA UPTAKE BY HUMAN NEOPLASTIC CELL LINES

N. Chiu, B. Lee. Department of Nuclear Medicine, National Cheng Kung University Hospital, Tainan, Taiwan.

Background: The aim of this study was to determine the uptake mechanism of Tc-99m (V) DMSA uptake by HeLa cells, K562 cells, and Raji cells.
Methods: Uptake kinetics of Tc-99m (V) DMSA by HeLa cells, K562 cells, and Raji cells were studied. The effect of transferrin, metabolic inhibitors, trypsin and various concentration of Tc-99m (V) DMSA on uptake by HeLa cells, K562 cells, and Raji cells were studied. The relationship was studied between the number of non-viable HeLa cells, K562 cells, and Raji cells and Tc-99m (V) DMSA uptake by HeLa cells, K562 cells, and Raji cells. Because studies have reported tumor tissue to be more acidic than normal tissue, acidification might be related to the Tc-99m (V)-DMSA localization in tumor tissue. Thus, in the present study, a working hypothesis drew to test the acidification as a plausible factor, and an in vitro cellular system using HeLa cells, K562 cells, and Raji cells implemented. A parallel experiment for determining the uptake of Ga-67 by the same cell lines was carried out using the same procedures.
Results: The evidence suggests that Tc-99m (V) DMSA uptake by HeLa cells, K562 cells, and Raji cells is linear as a function of Tc-99m (V) DMSA concentration. Uptake by HeLa cells, K562 cells, and Raji cells was not inhibited by metabolic inhibitors. Their binding to HeLa cells, K562 cells, and Raji cells could be removed by trypsin. In non-viable HeLa cells, K562 cells, and Raji cells, the plasma membrane diffusion barrier no longer exists and Tc-99m (V) DMSA uptake increases markedly. There were similar results with Ga-67 uptake. With addition of transferrin to the HeLa cells, K562 cells, and Raji cells, the cellular uptake of Tc-99m (V) DMSA did not increase but Ga-67 uptake by HeLa cells, K562 cells, and Raji cells did. Acidification alone showed no effect on the radioactivity accumulation in HeLa cells, K562 cells, and Raji cells; nevertheless, if accompanied by a pre-dilution of the Tc-99m (V)-DMSA sample added into the cell incubation media, cellular radioactivity accumulation was observed.
Conclusion: Acidification as a mediator for the Tc-99m (V)-DMSA accumulation in tumoral cells, concurrently with dilution as the promoter of the process, constituted the foundation for Tc-99m (V)-DMSA uptake by HeLa cells, K562 cells, and Raji cells.

PS_144

HIGH EFFICIENCY IN LABELING OF RBC WITH TC-99M IN IN VITRO CONDITIONS

T. Ertay (1), R. Bekis (1), C. Taşcı (1), E. Bilgin (2), H. Durak (1). (1) Department of Nuclear Medicine, Dokuz Eylül University, Izmir, Turkey; (2) Department of Nuclear Medicine, Celal Bayar University, Manisa, Turkey.

It is a major problem to obtain sufficient labeling efficiency (LE) in labeling of RBC's with Tc-99m with most of the commercial radiopharmaceuticals (RF) in in vitro conditions. The RF's that provide high labeling efficiency are very expensive.
Aim: The aim of this study was to label RBC's with Tc-99m in high LE by modification in in vitro conditions.
Materials and methods: 30 microgram (0,5 mL) stannos cloride in medronate was used for labelling RBC's, pH was adjusted to 7 with 1 N NaOH and 1 mL anticoagulated blood was mixed with the solution. The mixture was incubated for 5 minutes. 0-5 mL NaOCl as oxidant was added to the solution in order to inactivate stannos ions in extracellular enviroment. 1mL(5mCi) Tc-99m was added to the cell solution and the solution was incubated for 20 minutes. For quality controls 200 microliters of RBC solution and 2 mL saline were mixed. The mixture was centrifuged in 4250 rpm for 5 minutes. Supernatant and cell activities were measured. LE was found as 95±3 %. Imaging was performed in 4 rabbits and in a human volunteer. The planar images were visually compared with images obtained using our routine RF. The image quality was found superior to routine images. In our study pH was adjusted to 7 instead of 5, and low amount of stannos ions and NaOCl as antioxidant were used. These modifications brought about high LE of RBC with Tc-99m.
Conclusion: We suggest that this modified method for labeling of RBC's with Tc-99m is very easy and cheap and can be used in each nuclear medicine lab in routine conditions.

PS_145

LABELING OF GLY-GLY-L-ALANINE WITH TECHNETIUM-99M AND THE ASSESSMENT OF IT'S RADIOPHARMACEUTICAL POTENTIAL

M.S. Taner (1), D. Özdemir (2), K. Köseoğlu (1), M. Argon (1), A. Dirlik (1), Y. Duman (1). (1) Department of Nuclear Medicine, Ege University, Izmir, Turkey; (2) Izmir Institute of Technology Department of Chemistry, Urla, Izmir, Turkey.

Recently, labeling of small (molecule) peptides with radionuclides, which can be used in tumor and infection imaging, has gained enormous importance and become a very intensive research area. Although Technetium-99m (^{99m}Tc) labeled Monoclonal Antibody (Mab) and their fragments (Fab, Fab_2) have been known and used for tumor and infection imaging for the last 10 years, their blood clearance and target organ accumulation rates are limited. In the diagnosis phase, the need for the agents with better blood clearance and target organ accumulation rates has been indicated by the clinicians. It is possible to obtain quality imaging with high accuracy, better target specific accumulation behavior and rapid clearance with radiolabelled small peptides compared to all other known agents.
In this study, Gly-Gly-l-Alanine (GGA) was selected to investigate its potential as a radiopharmaceutical after labelling with ^{99m}Tc by direct labelling method. Gly-Gly-l-Alanine was labeled with a yield that is close to the USP acceptance criteria's. In all these labeling studies, quality control has been performed by reverse phase HPLC analysis method with the use of a Beckman-Gold R-HPLC system. Latter on, radiopharmaceutic distribution and organ uptake characteristics of this labeled peptide (^{99m}Tc-GGA) on rabbits were studied by using gamma camera imaging technique. In direct radiolabeling method developed for the small molecule peptides, retention time and labeling yield for ^{99m}Tc-GGA radio-complex were 78.98 % at 12 minute, respectively in reverse phase Radio-HPLC analysis system (Beckman-Gold system). Toshiba GCA602A gamma camera imaging studies have indicated that the peptide GGA have demonstrated remarkable rapid blood clearance and dynamic discharge through kidneys.
In biodistribution studies on rabbits, in terms of radio-peptide retention, the most important organ and body fluid samples were taken and then counted with Tennelec well type detector system. When compared to the other body organs, it was observed that kidneys showed the most active retention and the most of the applied radio-peptide were thrown out through urine. The results indicated that ^{99m}Tc-GGA can be a potential kidney agent in nuclear imaging applications.

PS_146

EVALUATION OF TWO CHROMATOGRAPHIC METHODS FOR RADIOCHEMICAL QUALITY CONTROL OF 99MTC-ALBUMIN NANOCOLLOID AND 99MTC-COLLOIDAL SULPHIDE

N. Urbano, S. Modoni, G. Martino, F. Dicembrino, G. Palladino, V. Frusciante. Department of Nuclear Medicine, Casa Sollievo della Sofferenza, San Giovanni Rotondo, Italy.

Aim: 99mTc-nanocolloids are routinarily used in clinical nuclear medicine practice for diagnosis of pulmonary embolism, bone marrow, lymphatic and inflammations scanning.
Two chromatography methods for radiochemical quality control of 99mTc-albumin nanocolloid (<=80 nm) and 99mTc-colloidal sulphide (<=50 nm) preparations, were developed and compared with the recommended manufacturer's method.
Methods: 99mTc-nanocolloids (VENTICOLL and NANOCOLL, Nycomed, Amersham Sorin Srl) and 99mTc-sulphur colloid (LYMPHOSCINT, Nycomed, Amersham Sorin Srl) were prepared according to manufacturer's methods. It recommends the use of ITLC-SG paper (Gelman Instruments, Ann Arbor, MI, USA) developed in a solvent system of methanol:water (85:15). Following strip development, free pertechnetate migrates to the solvent front and 99mTc-bound remains at the origin.
The radiochemical analyses and purity determinations of these radiopharmaceuticals were performed comparing three techniques: the manufacturer's system (ITLC-SG/methanol:water) and other two systems using the same support (ITLC-SG) and Methyl-Ethyl-Ketone (MEK) and NaCl 0.9% (according to X Pharmacopoeia) as solvents, respectively. The strips were cut into 1,5x20 cm, with the origin and solvent front drawn 2 and 17 cm from strip origin, respectively. Chromatography developing tank was initially satured by the required solvent system The strip was spotted (5µl) and immediately placed in developing tank. When the solvent migrated to the solvent front line, the strip was removed from the tank, dried and counted for activity by using a scanning radio-chromatography detection system for thin layer chromatography. (Mini-Scan. Bioscan, Inc. Washington, DC).
The Retention factor (Rf) value, that is relative solute/solvent migration, was calculated for each radiochemical species.
Results: The manufacturer's procedure was completed in 30-35 min, while other two alternative techniques required 12-15 min only.
The Rf ranges of both 99mTc-albumin nanocolloid and 99mTc-colloidal sulphide were 0,0-0,05 for all three solvent systems; Rf range of $99mTcO_4^-$ was 0.9-1.0, 0.75-1.0 and 0.95-1.0 with, respectively, Methanol/Water, MEK and NaCl 0,9%.
There were not significant differencies among three techniques regard to percent labelling efficiency. NaCl and methanol/water mixture, showed a narrow peak of $99mTcO_4^-$ in despite of MEK.
Conclusions: The recommended procedure for radiochemical purity calculation requires almost 30 min for completion and is, therefore, more time-consuming as compared to other two.
Moreover, we point out that Methanol is a toxic solvent: its contact and, especially, inhalation are very dangerous and its use is forbidden without appropriate tools.
In conclusion, radiochromatography by MEK and NaCl is a more rapid and safe technique than methanol-water.

PS_147

CHARACTERIZATION OF MONOCLONAL ANTIBODY CG250 LABELED WITH 88/90-Y AND 177-LU

J. van Eerd (1), A.H. Brouwers (1), E. Oosterwijk (2), W.J.G. Oyen (1), F.H.M. Corstens (1), O.C. Boerman (1). (1) Department of Nuclear Medicine; (2) Department of Urology, University Medical Center Nijmegen, Nijmegen, The Netherlands.

Aim: Until now, the chimeric monoclonal antibody G250 (cG250) directed against the G250 antigen expressed on most clear cell renal cell carcinoma's (RCC) was labeled with ^{131}I for radioimmunotherapy (RIT) purposes. Since ^{131}I is not the most optimal β-emitting radionuclide for RIT, we have explored labeling cG250 with $^{88/90}$Y and ^{177}Lu using 3 chelators: cyclic DTPA anhydride (cDTPA), isothiocyanato-benzyl-DTPA (ITC-Bz-DTPA) and 1,4,7,10-tetraazacyclododecane tetra acetic acid (DOTA).
Methods: The $^{88/90}$Y and ^{177}Lu labeling procedure of cG250 conjugated with either cDTPA, ITC-Bz-DTPA and DOTA was optimalized and characterized. The labeling efficiency and the maximum specific activity of the preperations were assessed. Furthermore, the immunoreactivity of the conjugates was determined. For ^{88}Y and ^{177}Lu the stability of the labeled conjugates in serum at 37 ¡C (up to 21 days) was assessed using ITLC and FPLC aanalysis. The biodistribution of the radioimmunoconjugates was studied in nude mice with SK-RC-52 human RCC xenografts (1, 3 and 7 d p.i.).
Results: All three conjugates of cG250 could be efficiently labeled with $^{88/90}$Y and ^{177}Lu. The highest specific activity was obtained with ITC-Bz-DTPA: 10 and 5 TCi/Tg for ^{90}Y and ^{177}Lu, respectively, vs 3 TCi/Tg for the DOTA-conjugate. The immunoreactivity of ^{177}Lu-cG250 labeled via ITC-Bz-DTPA, cDTPA and DOTA was 82%, 88% and 87%, respectively. The in vitro stability analyses using FPLC demonstrated that ^{177}Lu-cG250-ITC-DTPA and ^{88}Y-cG250-ITC-DTPA showed less than 5 % release of the radiolabel during 14 d of incubation. ^{88}Y-cG250-DOTA and ^{177}Lu- cG250-DOTA showed less than 5 % release during 21 d post-labeling. The biodistribution studies demonstrated relatively rapid blood clearance for cDTPA-cG250 (6 % ID/g) and relatively high bone uptake (11 % ID/g) for both ^{88}Y and ^{177}Lu at 3 d p.i. Both ITC-Bz-DTPA and DOTA radiolabeled cG250 showed high uptake in the tumor and slow blood clearance (90 ± 20 %ID/g ± SD and 13 ± 0.5 %ID/g ± SD, respectively). Bone uptake was similarily low at 3 d p.i. (1.1 and 1.5 % ID/g for ^{88}Y-ITC-Bz-DTPA-cG250 and ^{88}Y-DOTA-cG250) and (1.3 and 0.5 % ID/g for ^{177}Lu- ITC-Bz-DTPA-cG250 and ^{177}Lu-DOTA-cG250).
Conclusions: The in vitro stability was highest for the DOTA conjugated radiolabeled antibody. However, the labeling efficiency and specific activity were highest for ITC-Bz-DTPA, while the biodistribution experiments gave similar results. Therefore, for further RIT trials using cG250 labeled with various radionuclides ITC-Bz-DTPA appeares to be the most suitable chelator.

PS_148

WASHOUT RATE OF TC-99M SESTAMIBI INDICATES SEVERITY OF HEART FAILURE IN PATIENTS WITH DILATED CARDIOMYOPATHY

T. Tomonori (1), H. Takase (1), T. Toriyama (1), T. Goto (1), Y. Hikita (2), H. Ishikawa (2), T. Kagohashi (2), Y. Dohi (3). (1) Department of Internal Medicine, Enshu General Hospital, Hamamatsu, Japan; (2) Department of Radiology, Enshu General Hospital, Hamamatsu, Japan; (3) The Second Department of Internal Medicine, Nagoya City University Hospital, Nagoya, Japan.

Aim: Tc-99m sestamibi scintigraphy has been used for the diagnosis or evaluation of myocardial viability in patients with ischemic heart disease. The tracer is known to bind to mitochondria and the image reflects mitochondrial function in myocardial cells which may be impaired in heart failure. Therefore, this study was designed to investigate whether the WR of sestamibi can be used for evaluating the severity of heart failure in patients with dilated cardiomyopathy. Methods: We studied 16 patients (male/female=11/5, 64.4±2.8 year-old; mean±SEM), who had been diagnosed as dilated cardiomyopathy (DCM), with stable condition at least for recent 6 months (ejection fraction: EF; 11.0 to 52.0%). They underwent resting sestamibi single photon emission computed tomography (SPECT) as well as quantitative gated SPECT (QGS). Before the injection of the tracer their blood samples were taken and SPECT imaging was performed 1 hour (early image) and 3 hours (delayed image) after the injection. WR was manually calculated using both early and delayed images. The same procedure was performed in normal subjects for reference (n=12). Results: The patients were older than the normal subjects (44.5±4.5 year-old; $p<0.001$). Blood pressure or heart rate in the both groups was not different. In patients with stable condition of DCM, WR was higher (30.7±1.5%) than that in the normal subjects (23.7±1.6%; $p<0.05$), but heart to mediastinum (H/M) ratio was similar in the both groups. In the patients, levels of atrial and brain natriuretic peptide and left ventricular end-diastolic and end-systolic volume index (by QGS) were increased (ANP; 102.6±33.5 vs 14.8±1.7 pg/ml, BNP: 320.3±94.4 vs 5.0±0.9 pg/ml, LVEDVI; 103.4±13.6 vs 52.2±3.1 ml/m^2, LVESVI; 73.5±13.3 vs 21.5±2.4 ml/m^2), and EF (by QGS) was decreased (33.1±2.9 vs 60.5±2.8%) as compared with normal subjects ($p<0.05$). In the patients, WR was positively correlated with ANP or BNP levels ($r=0.707$ and $r=0.805$, respectively) and negatively correlated with H/M ratio ($r=-0.574$) without any correlation with LVEDVI, LVESVI or EF. In contrast, there was no correlation between WR and other parameters in the normal subjects. Conclusions: In stable condition of DCM, WR is related to ANP or BNP levels or H/M ratio. Since ANP or BNP reflects severity of heart failure, WR of sestamibi is useful for evaluating the severity of heart failure in patients with DCM.

PS_149

TIME COURSE EVALUATION OF MYOCARDIAL PERFUSION AND CARDIAC FUNCTION USING TC-99M SESTAMIBI GATED SPECT BEFORE AND AFTER REPERFUSION THERAPY IN PATIENTS WITH ACUTE MYOCARDIAL INFARCTION

R. Tanaka (1), T. Nakamura (2), H. Kumamoto (2), J. Simokawa (2), M. Miura (2), K. Seino (1), N. Nomura (1), K. Fujita (2). (1) Department of Radilogy; (2) Department of Circulator, Kushiro-ishikai Hospital, Kushiro, Japan.

Tc-99m Sestamibi(MIBI) SPECT was performed to obtain a image before reperfusion therapy using freeze method and early, delayed images on 1,4,7 and 20 days after reperfusion therapy in 20 patients with the first acute myocardial infarction. I-123 BMIPP(BM) image on averaged 7 days was also obtained in the same patients. The data were assessed quantitatively, and analysis of cardiac function by Gated SPECT using QGS program was also performed.

The time-related changes in the number of abnormal area (NAA) which was defined the number of segments less than 60% of percent uptake improved significantly on the early images from pre-reperfusion to 7 days after reperfusion therapy, but no significant difference was observed on the images from 7 days to 20 days with a plateau of improved myocardial perfusion on 7 days after reperfusion therapy.

NAA on the delayed images from 1 day to 20 days after reperfusion therapy, on the other hand, showed large constant values in comparison with early images ($p<0.01$). The NAA correlations between the pre-image and the post-7d-delayed image, the pre-image and the BM image, and the post-7d-delayed image and the BM image were very close ($r = 0.828$, $r = 0.861$, and $r = 0.985$, respectively). Although no significant improvement was observed in LVEF(%) for evaluation of cardiac function, regional wall motion showed a significant improvement on 20 days in comparison with the images on 1 day after reperfusion therapy($p<0.05$).

These results suggested that MIBI SPECT images on more than 7 days after reperfusion therapy might be appropriate for evaluation of salvaged area and both MIBI delayed images and BM images might be useful for estimating the risk area.

PS_150

INITIAL INFARCT SIZE AND PLASMA BRAIN NATRIURETIC PEPTIDE LEVEL ARE USEFUL INDICATORS FOR LEFT VENTRICULAR REMODELING AFTER MYOCARDIAL INFARCTION

S. Kanayama, S. Fujino, K. Masuyama, O. Satake, M. Kitayama, S. Ohkubo, T. Asaji, S. Kanemitsu, H. Tsugawa, S. Matsui, N. Takekoshi. Department of Cardiology, Kanazawa Medical University, Ishikawa, Japan.

Aim: We investigated the relations among risk area, infarct size, plasma BNP and subsequent LV dilatation in patients undergoing direct PTCA for AMI using MIBI gated SPECT.

Methods: Twenty five patients with first AMI were studied. Before revascularization MIBI was injected and gated SPECT was performed immediately after PTCA. Subsequent gated SPECT were performed 24 hours and 1 month after PTCA. LVEF, LVEDV and LVESV were measured by QGS program and risk area and infarct size were measured by threshold method. Plasma BNP level was determined on admission and 1 month after .

Results: According to increase of LV volume in 1 month after AMI, patients were divided into two groups; with remodeling group, R(+), n=9, defined EDV increased greater than 120% of pre-PTCA, and without remodeling group, R(-), n=16. In all phase, EF was significantly lower and defect size was significantly higher in R(+) than R(-). In R(-) group, EF and defect size improved 24 hours after PTCA. In R(+) group, they were not changed 24 hours after PTCA, and significantly improved 1month after PTCA. EDV of R(+) was similar as R(-) before PTCA, but it significantly 24hours after PTCA, and resulting in the significant difference as compared to R(-). ΔEDV (EDV in 1 month after – EDV before PTCA) and risk area showed significantly correlation ($r=0.50$), but ΔEDV and infarct size on 24 hours after PTCA showed excellent correlation ($r=0.61$). BNP level of R(+) significantly increased during 1 month (115 to 317pg/ml), whereas those of R(-) remained unchanged (65 to 53pg/ml). ΔEDV and BNP on 1month after PTCA were significantly correlated ($r=0.67$).

Conclusions: Infarct size measured by MIBI gated SPECT 24 hours after revascularization predicts early LV remodeling after myocardial infarction. Plasma BNP may be useful marker for LV remodeling.

PS_151

VALUE OF NUCLEAR MEDICINE DIAGNOSIS IN MYOCARDIAL IMPAIRMENT DUE TO IMMUNOSUPPRESSANTS

K. Takahashi (1), M. Ohyanagi (1), H. Naruse (1), M. Masai (1), T. Sakaki (1), T. Iwasaki (1), M. Fukuchi (1). (1) 1st.Dept.Internal Medicine; (2) Dept.of Nuclear Medicine, Hyogo College of Medicine, Nishinomiya, Japan.

[Aim]

Cyclosporin (CY) and tacrolimus (TA) used as the main postoperative immunosuppressive drugs have been reported to cause myocardial impairment. The time of onset and clinical profile of the impairment induced by these drugs differ. We investigated with a nuclear medicine approach using an animal model whether the characteristics of myocardial impairment due to immunosuppressive drugs were clarified and whether the impairment was reversible, in comparison with pathological findings.

[Methods]

With administration of CY or TA, rabbits were assigned to the control group (N), one-week administration group (1W), two-week administration group (2W), and group subjected to one-month withdrawal following two-week administration (1M). The heart weight and cardiac hypertrophy in these groups were determined. After administration of 201Tl (TL) and 123-I-BMIPP (BM), their accumulation rates per gram of the myocardium were compared. The results were compared with the pathological findings. In the kidney transplant patients who received TA, the pre- and postoperative TL and BM accumulation findings were compared.

[Results]

The nuclear medicine findings revealed no difference between the TL and BM accumulation rates in the CY groups. Regarding the nuclear medicine findings of the TA groups, no difference was observed in the TL accumulation rate in the groups. However, the BM accumulation rate decreased significantly in the 1W and 2W groups than in the N group (N : 1W : 2W = 0.44 ± 0.03 : 0.32 ± 0.01 : 0.33 ± 0.03, $p<0.05$ vs. N), whereas no differences in the BM accumulation rate (0.50 ± 0.14) were observed. The pathological findings showed no marked myocardial impairment in any of the CY treatment groups. Those for the TA treatment groups showed myocardial interstitial edema and cellular infiltration in the 1W and 2W groups and only slight myocardial interstitial edema in the 1M group. The comparison of TL and BM accumulation findings in the kidney transplant patients indicated that the single patient with cardiac symptoms exhibited a reversible reduction only in the BM accumulation.

[Conclusion]

Myocardial impairment caused by administration of TA was grasped using BM. It was suggested that this impairment was reversible.

PS_152

COMPARISON OF LOW-DOSE DYPIRIDAMOLE RADIONUCLIDE VENTRICULOGRAPHY AND LOW-DOSE DIPYRIDAMOLE STRESS ECHOCARDIOGRAPHY FOR IDENTIFICATION OF MYOCARDIAL VIABILITY

Z. Petrasinovic (1), M. Ostojic (1), B. Beleslin (1), S. Pavlovic (2), D. Sobic (2), A. Dikic (1), J. Marinkovic (3), A. Nedeljkovic (1), I. Nedeljkovic (1), J. Stepanovic (1), V. Obradovic (2)(1) Institute for Cardiovascular Diseases, Clinical Center of Serbia; (2) Institute for Nuclear Medicine, Clinical Center of Serbia; (3) School of Medicine, Belgrade, Yugoslavia.

Background: It has been shown previously that low dose dipyridamole (Dipy) stress echocardiography (ECHO) may identify myocardial viability. However, diagnostic potential of Dipy-ECHO has not been compared to the other techniques for viability detection.
Objective: The purpose of the study was to compare diagnostic value of low dose dipyridamole radionuclide ventriculography (Dipy-RNV) and low dose dipyridamole echocardiography (Dipy-ECHO) for the prediction of functional recovery of viable myocardium in the medium term follow up.
Methods: Twenty patients (18 male; 51±10 years) with previous myocardial infarction and resting wall motion dyssynergy were studied before angioplasty of infarct related artery (IRA), by RNV and ECHO at rest, as well as during dipyridamole infusion (0,28 mcg/kg/min over 2min). RNV as well as ECHO was repeated at rest, 12 weeks after successful angioplasty. Five percent increase of regional ejection fraction (REF) by RNV was used as criterion for functional improvement of infarcted regions. By ECHO, viability was defined as improvement of wall thickening or contractile improvement of >1 grade, utilizing wall motion score index (WMSI).
Results: Out of 180 examined (20x9) segments by RNV, 51 were dyssynergic and they had abnormal REF (<50%). Out of 51 segments, functional improvement was documented in 33 on low Dipy-RNV. Sensitivity for predicting functional recovery after 12 weeks follow up was 63%, and specificity was 77%. WMSI assessed by ECHO was 1.35±0.22, 1.16±0.20 and 1.13±0.14 for rest, low Dipy and rest follow up, respectively ($p<0.05$ vs. resting echo). Sensitivity of low Dipy-ECHO for predicting functional recovery was 80%, and the specificity was 90% (p=ns vs. low Dipy-RNV).
Conclusion: Both techniques, RNV and ECHO are comparable diagnostic predictors of myocardial viability in medium term follow up, with Dipy-ECHO having even stronger diagnostic potential.

PS_153

ANALYSIS OF CHANGES OF OUTCOME OF MYOCARDIAL PERFUSION SCINTIGRAPHY IN TIME

J.J.J. Borm (1), R.P. de Haan (1), E.E. van der Wall (2), E.K.J. Pauwels (1). (1) Nuclear Medicine; (2) Cardiology, LUMC, Leiden, The Netherlands.

Aim: To assess the cause for observed major changes in the observed monthly percentage of normal myocardial perfusion studies {MPS} over the period August 1995 and April 1998.
Methods: During the trial period, results from consecutive MPS studies were prospectively entered in the Leiden Tetrofosmin Database. As part of a follow-up study this database was expanded with extensive data on clinical history, risk factors, interventions and outcome results. Changes in referral pattern, clinical data and results from MPS were visualised by plotting monthly frequency of occurence over time. To distinguish a gradual shift due to changes in reporting from a shift due to changed referral pattern, a step-wise logistic regression model was built, to predict perfusion outcome, based on all clinical and historic data. This model was then used to predict perfusion outcome for all individual cases.
Results: During the recruitment period 1269 consecutive patients underwent their first MPS study. Patient characteristics: males: 65%; age: 61 ± 11 year, diabetes: 16%; hypercholesterolaemia 54%; previous myocardial infarction 29%, PTCA 17%, bypass surgery 18%. Percentage normal perfusion studies: 42 %. This percentage varied widely. The 5-month average percentage normal perfusion studies varied from 28 to 45 %. Similar wide variation was also seen for most risk factors and for historic data. Logistic regression resulted in a model, that included diabetes, hypercholesterolaemia, previous infarction, revascularization, age and gender. Using this model, it was possible to correctly classify 74% of all perfusion studies. Time of recruitment was used as an independent variable, but did not contribute to the model, even when used in a 2nd or third order model, or a cyclic model. The supervising physisian was also not predictive for outcome using this model.
Conclusions: -1- Outcome of myocardial perfusion scintigraphy can show wide variation, even within a single institution; -2- Such outcome variation should be evaluated before data on the prognostic value of perfusion scintigraphy can be assessed, as it can result in biased prognostic models.

PS_154

INFLUENCE OF A NEGATIVE INOTROPIC ACTION BY ANTI-ARRHYTHMIC DRUGS IN PATIENTS WITH CHRONIC HEART FAILURE

S. Isobe (1), M. Okada (2), A. Ando (1), M. Nanasato (1), M. Nonokawa (1), M. Hirai (1), M. Yokota (3). (1) First Department of Internal Medicine, Nagoya University School of Medicine, Nagoya, Japan; (2) Nagoya Ekisaikai Hospital, Nagoya, Japan; (3) Department of Clinical Laboratory Medicine, Nagoya University School of Medicine, Nagoya, Japan.

Aim: Although patients with chronic heart failure (CHF) indicating ventricular arrhythmias are often treated by anti-arrhythmic drugs, it is possible that left ventricular (LV) function may be more deteriorated because of their negative inotropic action. Therefore, we focused whether 3 anti-arrhythmic drugs (mexiletine, disopyramide, and pilsicainide) which are often used at present can be relatively safe to use for patients with CHF.
Methods: Twenty-five patients with CHF and ventricular arrhythmias [19 men_6 women, mean age 60_±_9 y_LV ejection fraction (LVEF) < 45%] were studied. Patients were classified into 3 groups; patients who orally received a single dose of 4 mg/kg mexiletine (n = 8, mean LVEF 36_±_7%), those who received a single dose of 6 mg/kg disopyramide (n = 8, mean LVEF 38_±_4%), and those who received a single dose of 6 mg/kg pilsicainide (n = 9, mean LVEF 37_±_5%). All patients were performed equilibrium 16 frames per cardiac cycle gated cardiac-pool scintigraphy with Tc-99m-HAS of 740 MBq at both of baseline rest and peak exercise. On a separate day, they had drugs once and were subsequently performed equilibrium gated cardiac-pool scintigraphy at both of rest and peak exercise. Blood concentration of each drug was examined. We compared LVEF between at baseline and after drug administration.
Results: The plasma level of each drug was effective value. There was no significant difference between baseline rest LVEF and rest LVEF after administration as well as between baseline rest LVEF and baseline exercise LVEF among the 3 groups. Although exercise LVEF after administration showed significantly lower than rest LVEF after administration in addition to baseline exercise LVEF in both of disopyramide and pilsicainide groups (disopyramide: 34_±_4%_vs. 37_±_4%, $p < 0.05$; 34_±_4%_vs. 42_±_5%, $p < 0.005$; pilsicainide: 32_±_4%_vs. 36_±_5%, $p < 0.05$; 32_±_4%_vs. 41_±_6%, $p < 0.05$, respectively), no significant change was recognized in mexiletine group.
Conclusions: Caution is necessary to treat by disopyramide or pilsicainide for patients with CHF because these drugs induce more cardiac functional decline during exercise. On the other hand, mexiletine can be safely used for patients with severe LV dysfunction. Patients with severe LV dysfunction should be treated using anti-arrhythmic drugs with less inotropic action.

PS_155

ENHANCED DETECTION OF MYOCARDIAL DEFECT REVERSIBILITY BY TL-201 INFUSION STUDY

O. Yapıcı, M. Sahin, T. Başoğlu, S. Albayrak, F. Canbaz. Department of Nuclear Medicine, 19 Mayıs University, Samsun, Turkey.

The underestimation of myocardial viability noted with traditional stress / redistribution and rest / redistribution Tl-201 imaging has lead to the development of alternative protocols. The aim of our study was to compare the method of bolus injection and infusion of Tl-201 in the identification of reversibility of the defects.
Methods: Eighteen patients with documented CAD were divided into two groups. Stress / redistribution / reinjection / 24-hr SPECT images in group 1 (10 patients) and rest / redistribution / 24.hour SPECT images in group 2 (8 patients) were obtained. All patients underwent Tl-201 infusion study in a separate day. SPECT was performed following two hours infusion of 3 mCi Tl-201 in 100cc normal saline solution. Short axis slices were grouped as apical, midventricular and basal and divided each of them into 8 segments. Apex was divided into 2 segments in vertical long axis. Total of 26 segments for each patient were semiquantitatively evaluated by using a 10 colour scale. Values equal or less than 80% in myocardial segments were accepted as decreased perfusion. At least 10% increase in relative Tl-201 uptake was considered reversible. Non-reversible defects of ≥50 of peak activity were accepted as viable. Differences between studies in each group were compared by paired-t test.
Results: Defect reversibility in group 1 was detected in 31 of 116(%26), 30 of 116(%25), 49 of 116(%42) and 65 of 116(%56) segments on redistribution, reinjection, 24.hour and infusion images respectively. In group 2, defect reversibility was detected 14 of 73(%19), 12 of 73(%16) and 13 of 73(%17) segments on redistribution, 24.hour and infusion respectively. The degree of defect severity and reversibility in myocardial segments with initial defects were shown in table.

Group 1 (n=123)	mean±s.d. (% of peak)	Group 2 (n=82)	mean±s.d. (% of peak)
Stress (S)	52.9± 18.8	Rest (R2)	65.7±13.7
Redistribution (RD)	55.3±19.4	Redistribution (RD2)	66.0±14.2
Reinjection (RI)	54.4±18.7	24.hour (24H2)	63.7±12.8
24.hour (24H)	57.2±20.2	Infusion (INF2)	67.1±14.9 #, ##
Infusion (INF)	58.1±18.3 *,**		

* p=0.000 INF vs RD, INF vs RI ; ** p>0.05 INF vs 24H # p<0.05 INF2 vs R2; ## p<0.000 INF2 vs 24H2

Conclusions: Infusion of Tl-201 improves uptake in jeopardized myocardial segments in comparison with redistribution, reinjection and late studies. Infusion seems the most appropriate protocol between Tl-201 studies in the myocardial viability evaluation. Further work is necessary with larger patient populations.

Poster presentation

PS_156

EARLY REST THALLIUM/BMIPP IMAGING PREDICTS POST MYOCARDIAL INFARCTION EVENTS

S. Fukuzawa, S. Ozawa, M. Inagaki, K. Shimada, J. Sugioka, S. Okino, A. Ikeda. Divion of Cardiology, Funabashi Munnicipal Medical Center, Chiba, Japan.

BMIPP has been most widely used for assessing myocardial metabolism, particularly in Japan and some European countries. On the other hand, low-intensity exercise testing immediately (five to ten days) after acute myocardial infarction (AMI) is a typical noninvasive risk stratification approach. This single center study is undertaken to investigate the prognostic values of rest dual thallium(Tl)-201/BMIPP single photon emission computed tomography (SPECT) for earlier risk stratification after AMI compared to predischarge exercise Tl-201 imaging.
Methods: 86 patients presenting with their first AMI underwent an early (day 2 to 5) rest dual Tl-201/BMIPP SPECT study and a predischarge (day 7 to 14) submaximal exercise Tl-201 study. We have now completed three-year follow-up on all 86 patients.
Results: Defect size of Tl-201 did not differ between the rest Tl-201 image of dual SPECT study and the redistrbution image of exercise study. But the rest BMIPP defects of dual SPECT study were larger than exercise Tl-201 defects. For rest dual Tl-201/BMIPP testing, multivariate predictors of post-discharge death or myocardial infarction (7%) were anterior location of AMI and nuclear imaging valuabies (BMIPP defects size and discordant defect size by BMIPP and Tl-201). The stress defect size on Tl-201 imaging was the only multivariate predictor of the death or myocardial infarction for the predischarge exercise Tl-201 study. Better stratification of patients into low- and high- risk groups was possible with the immediate rest dual Tl-201/BMIPP image compared with the predischarge exercise Tl-201 imaging.
Conclusion: Rest dual Tl-201/BMIPP tests may allow early after AMI predicted post discharge cardiac events as well as the more traditional submaximal exercise imaging. We suggests that rest dual Tl-201/BMIPP imaging may allow earlier management decisions, thereby potentially reducing the number of early events in high-risk patients and decreasing hospitalization time for low-risk patients.

PS_157

HOW TO BEST JUDGE ADEQUACY OF EXERCISE TESTS AS PART OF MYOCARDIAL PERFUSION SCINTIGRAPHY ? .

J.J.J. Borm (1), E.E. van der Wall (2), E.K.J. Pauwels (1). (1) Nuclear Medicine; (2) Cardiology, LUMC, Leiden, The Netherlands.

Aim: To evaluate which method is best suited to judge the adequacy of exercise tests, as done as part of myocardial perfusion scintigraphy [MPS]
Methods: MPS studies were performed as previous described. Betablockers were discontinued whenever the clinical conditions permitted so. Various parameters, including maximum heart-rate, highest systolic bloodpressure and the physical validity were recorded for each stress test. Physical validity [PV] was based on published normal values for attainable exercise levels, taking into account age, gender, weight and length, and expressed in a percentage of the corresponding reference value. The age-normalized maximum heart-rate [NHR] was expressed as a percentage of the value obtained by the formula [220 - age]. The product of maximum systolic bloodpressure and maximum heart-rate [BPHR] was evaluated as the a third parameter. The adequacy of each parameter was evaluated by means of receiver operator characteristic analysis [ROC] and by evaluation of its prognostic value in a step-wise proportional hazards model. In both analyses, the endpoint was all-cause-death.
Results: Patients were recruited between August 1995 and April 1998. A total of 799 patients out of a cohort of 1269 consecutive subjects underwent their first MPS using a bicycle exercise test. Patient charachteristics: males: 68%; age: 59 $\pm$ 11 y; NHR 88 $\pm$ 13 %; PV 97 $\pm$ 16 %; BPHR 25638 $\pm$ 6225. Normal myocardial perfusion: 43%, reversible defects: 33% and irreversible defects: 24%. Follow-up was over 96% complete [patient-years]. A total of 31 subjects died. Average censored follow-up was 2.31 year, with a minimum of 1 year for survivors versus 1.56 year for the 31 subjects who died during follow-up. The area-under-the-curve [AUC] for the ROC-analysis of PV was 0.634, for NHR 0.608 and for BPHR 0.653. Stepwise Cox' regression analysis using clinical data only [proportional hazards model] showed age, previous myocardial infarctions and PV to have the best predictive power [chi-square 39.4, P < 0.00005]. NHR did not even contribute in the univariate model, but BPHR did [chi-square 11.3, P = 0.0008].
Conclusions: It is concluded that adequacy of an exercise test as part of perfusion scintigraphy is best judged based on the exercise level reached, using published normal values for age, gender, length and weight. The use of the bloodpressure-heartrate product is an acceptable alternative, but age-normalized maximum heartrate is not.

PS_158

ASSESSMENT OF MYOCARDIAL PERFUSION BY HARMONIC POWER DOPPLER IMAGING AT REST AND DURING ADENOSINE STRESS: COMPARISON WITH TC-99M SESTAMIBI SINGLE PHOTON EMISSION COMPUTED TOMOGRAPHY AND CORONARY ANGIOGRAPHY

H. Palmedo (1), M. Bangard (1), A. Manka-Waluch (1), S. Kuntz-Hehner (2), K. Tiemann (2), H. Becher (2), MJ. Reinhardt (1), HJ. Biersack (1), T. Krause (1). (1) Department of Nuclear Medicine; (2) Department of Cardiology, University of Bonn, Bonn, Germany.

The aim of this study was to compare myocardial perfusion assessed by harmonic power doppler imaging (HPDI) to that obtained by MIBI-SPECT during rest and adenosine stress.
Methods: HPDI was performed in 18 consecutive patients (mean age 60y +/- 12.6) using Levovist as a contrast agent (Schering; 400mg/ml;1.5 ml/min). HPDI images were obtained at baseline and during adenosine infusion (140µg/kg/min, 6 minutes; HDI 5000 ATL-Ultrasound) performing the apical four and two chamber view. In 11 patients, MIBI-SPECT was done using the one-day protocol (rest:300 MBq imaging 60 min p.i.; stress: 900 MBq, imaging 45 min p.i.). HPDI and MIBI-SPECT was graded visually and blinded for each coronary territory (CT) by two cardiologists and two nuclear medicine physicians, respectively. (normal perfusion=NP; perfusion defect=PD). Results were compared to coronary angiography.
Results: In the HPDI group (18 pts.), 40 out of 54 CT were assessable. PD were observed in 13/17 assessable CT with significant stenosis (>70%), whereas 23/26 CT with coronary stenosis less than 70% showed a NP (p=0.001). In the subgroup of 11 patients with both MIBI-SPECT and HPDI, 26 out of 33 CT (79%) were assessable. Out of these 26 CT, MIBI-SPECT and HPDI both demonstrated a NP and a PD in 8 and 10 territories, respectively. In 8 CT, MIBI-SPECT and HPDI indicated discordant results with MIBI-SPECT demonstrating 3 false positive results in the inferior wall and with HPDI showing 3 false negative results in the lateral wall region.
Conclusions: Initial results show that also myocardial contrast echocardiography using HPDI is able to detect relevant perfusion abnormalities during adenosine stress test. One disadvantage of HPDI was that 20% of coronary territories were not assessable.

PS_159

IS PERFUSION SCANS WITH NITRATE ENHANCEMENT A MARKER OF COLLATERAL DEPENDENT MYOCARDIUM?

R.H. Ganatra, H.L. Blundell, G.W. Middleton, M.I. Robinson, A.C. Tweddle. Department of Nuclear Cardiology, University Hospital of Wales, Cardiff, UK.

The mechanism of action of oral nitrate in the relief of angina is unclear. Evidence suggests it may have a predominantly peripheral effect, with reduced myocardial flow in collateralised myocardium. If this hypothesis is correct, it would have implications for nitrate enhanced rest perfusion imaging, which is frequently used in the identification of hibernating myocardium. This study compares the perfusion Thallium SPECT images following nitrate administration with the redistribution images.
Fourteen patients with poor left ventricular function (LVEF < 35%) due to documented coronary artery disease, underwent rest perfusion imaging. The patients were given 0.8 mg (2 puffs) of sublingual nitrate followed (after 5 mins) by 80 MBq of Thallium intravenously. SPECT Images were acquired at five minutes after injection of Thallium with redistribution images at 3-4 hours. Imaging was performed using an Elscint SP4 and reconstructed using a Butterworth filter. The scans were analysed visually and semi-quantitatively using polar plots and 'difference' plots for each of the major coronary artery territories. Coronary angiograms were scored for presence and adequacy of collaterals using TIMI grading.
Overall, in 9 of the 14 patients, the nitrate enhanced scans showed 'less' perfusion in comparison to the redistribution image in at least one major coronary distribution.
Collateral flow (TIMI 2+) was identified in 8 patients by angiography. In 7 of these 8, patients, the nitrate enhanced image demonstrated decreased segmental perfusion in comparison to the redistribution image.
In the remaining 6 patients, where no collateral flow had been demonstrated at angiography, the nitrate enhanced images showed a decrease in perfusion in 2, in comparison to redistribution.
In summary, these results suggest that nitrate enhanced imaging should include a redistribution image when used for the identification of hibernating myocardium, especially where the myocardium may be supplied by collateral flow.

PS_160

DIPYRIDAMOLE TC-99M SESTAMIBI MYOCARDIAL SPECT IN THE ASSESSMENT OF CAD RISK IN NON CARDIAC VASCULAR SURGERY

M.L. De Rimini (1), M. Catalano (1), A. Scalzone (2), R. Merenda (2), M. De Angelis (3), V. Ippolito (1), P. Muto (1). (1) Department of Nuclear Medicine; (2) Cardiovascular Department; (3) Vascular Surgery Division, A.O. Monaldi, Naples, Italy .

Coronary Artery Disease (CAD), the most frequent cause of perioperative and late mortality and morbidity after non cardiac vascular surgery, suggests the utility of presurgical cardiac risk stratification.

Aim of the study was to assess prognostic value of myocardial perfusion imaging (MPI) in patients (pts) undergoing abdominal aorta aneurysm surgery.

Methods: Tc-99m Sestamibi myocardial Gated-SPECT, two-day dipyridamole (Dip.) - Rest protocol was performed in 45 pts (mean age 63), 60% of them without pain or CAD and 40% with history of stress induced angina or previous myocardial infarction. Tc-99m stestamibi myocardial uptake was quantified in 990 segments (S) as % of peak in a 4 points scale (from 0 as normal to 3 as severe defect), using a 22 segment scheme. Defects were classified as fixed (F) or as reversible (Rev.>60% of peak) or partially reversible (PRev.>50% of peak)., in presence of 10% uptake increase at rest with respect to Dip.

Results: No angina Dip. induced; in 3 pts ECG abnormal changes were detected. MPI showed: 6 pts (Gr.1) with Score 3-PRev defects in 45S/132S; 39 pts (Gr.2) with:

Tot. S	Score 0 (%)	Score 1 - Rev	Score 2 - Rev	Score 3 - F
858	725 S (84.%)	48 S (5.%)	75 S (8.%)	10 S (1.%)

G-SPET analysis confirmed rest akinesia corresponding F-defects S (% thickness range: 0 - <10%) and LVEF >50%. Gr.1 pts underwent angiography and revascularization before surgery. Gr.2 pts underwent surgery without subsequent events; to reduce cardiac events 19 pts of them received beta-blockers treatment respectively: before / after surgery in 12 pts with Score1-Rev and/or Score3 F defects, and before / during / after surgery in 7 pts with Score 2-Rev defects.

Conclusion: Our data confirm the high negative predictive value of MPI, in cardiac risk stratification before abdominal aorta aneurysm surgery, the incremental prognostic value of GSPET and the role of MPI in predicting pre-surgical therapeutic strategies suggesting myocardial rivascularization choice in severe ischemia, or beta-blockers and anesthetic strategies in low or moderate myocardial hypoperfusion.

PS_161

CARDIAC PERFORMANCE AND EXERCISE TOLERANCE IN NEVER-TREATED HYPERTENSIVE FEMALE - AN ASSESSMENT WITH RADIONUCLIDE VENTRICULOGRAPHY

N. Topuzovic (1), J. Djurijancek (2), A. Rusic (1), B. Krstonosic (1), I. Karner (1). (1) Department of Nuclear Medicine; (2) Department of Cardiology, Osijek Universitiy Hospital, Osijek, Croatia.

Aim: The aim of this study was to investigate left ventricular function and exercise capacity in never-treated female hypertensive patients.

Methods: Seventeen female patients with newly established, uncomplicated essential hypertension (aged 25 to 57 years) were examined by means of maximum physical exercise testing and radionuclide equilibrium ventriculography, and were compared to 23 female normotensive volunteers of comparable age.

Results: Mean blood pressure were significantly higher in patients at rest and during exercise than in controls (121±13 vs. 89±7 mm Hg, and 143±11 vs. 122±9 mm Hg, respectively, p<0.001). At peak exercise patients achieved a similar workload and exercise duration. Increase in heart rate during exercise was similar in patients and controls (from 72 ± 8 to 142 ± 16 vs. 75 ± 10 to 138 ± 14 beats/min, respectively). At rest, there were no significant difference in end-diastolic (EDV), end-systolic left ventricular volume (ESV) and cardiac output (CO) between two groups. During stress, EDV and CO were significantly higher in patients (91 ± 13 vs. 68 ± 11 ml/m^2; and 6.8 ± 2.2 vs. 4.7 ± 1.6 l/min/m^2, respectively, p<0.01), while ESV was similar in both groups. Ejection fraction (EF) at rest and stress did not differ significantly (54 ± 10 vs. 55 ± 8%, and 70 ± 10 vs. 66 ± 8%, respectively), but % rise in EF during exercise was significantly higher in patients.

Conclusions: Female patients with newly diagnosed, never-treated hypertension have preserved maximal exercise performance and systolic function, but they have significant enlargement of EDV and elevated cardiac output during exercise.

PS_162

SEGMENTAL PATTERN OF MYOCARDIAL SYMPATHETIC DENERVATION IN IDIOPATHIC DILATED CARDIOMYOPATHY. RELATIONSHIP TO REGIONAL WALL MOTION AND MYOCARDIAL PERFUSION ABNORMALITIES

V. Prassopoulos, F. Parthenakis, S. Koukouraki, M. Kanakaraki, E. Skalidis, A. Velidaki, P. Vardas, N. Karkavitsas. Heraklion University Hospital, Crete, Greece.

AIM: Idiopathic dilated cardiomyopathy (ID) is a primary myocardial disease of unknown origin with a major defect in myocardial contractility that leads to progressive enlargement of cardiac chambers. Cardiac I-123-MIBG uptake has been reported to be reduced in patients (pts) with congestive heart failure and not only global, but also regional reduction has been demonstrated, the degree of each being positively correlated to markers of severity of heart failure. This study aimed to assess the regional pattern of cardiac autonomic innervation using I-123-MIBG as a marker for pre-synaptic neuronal uptake activity, and to address its relationship both with echocardiographic regional wall motion abnormalities and myocardial perfusion using Tc-99 Sestamibi scintigraphy in patients with ID.

METHODS: We studied 24 pts (55,5±13 years), with angiographically proven ID, (group A), and 10 healthy age-matched individuals (group B). Both groups underwent planar and SPECT myocardial imaging 10 min and 4 hours after intravenous injection of 5mCi I-123-MIBG. The heart to mediastinum (H/M) ratio was calculated to quantify cardiac MIBG accumulation, while SPECT study was performed to investigate the regional distribution of adrenergic innervation. A four point score system was used to determinate the I-123-MIBG accumulation (0-3 mormal-absence of uptake). All pts underwent Tc-99m-MIBI SPECT and echocardiographic study. WMSI was assessed using a four point scoring system (1-4 normal-diskynesia). Interpretation of myocardial adrenergic innervation, myocardial perfusion and regional wall motion was performed, using a 5-segment model (IVS, apex, anterior, lateral, posterior).

RESULTS: H/M_{groupA} ratio in 10 min and 4 hours <H/M_{groupB} (1,6±0,18 vs 2,08±0,2 and1,43±0,19 vs 2,05±0,34 respectively, p=0,001). There was significant correlation between H/M and LV EF, cardiac index, NYHA , WMSI (p<0,01,p<0,05,p<0,01,p<0,01)in group A. 14(11.7%) out of 120 segments had normal wall motion, 7(65%) hypokinetic, 28(23.3%) akinetic and1dyskinetic. In MIBG study, 11(9.2%), 75(62.5%), 33(27.5%) and 1(0.8%) segments presented normal, mild reduced, moderate reduced and absent uptake respectively. In Tc-99m-MIBI SPECT analysis 25(20,8%),82(68,3%) and 13(10,9%)segments showed normal, markedly reduced and definitely reduced activity respectively. A significant correlation was found between ECHO and MIBG uptake in the apex, septum and anterior wall.

CONCLUSION: I-123-MIBG reduction in patients with idiopathic dilated cardiomyopathy is related to the severity of LV wall motion abnormalities. Microvascular alteration in the regions of reduced adrenergic innervation may be responsible for the wall motion abnormalities in those patients.

CORRELATIVE IMAGING

PS_163

TC99M SESTAMIBI MUSCLE SCINTIGRAPHY TO ASSESS THE RESPONSE TO ELECTRICAL STIMULATION AND ISOMETRIC EXERCISE OF QUADRICEPS FEMORIS MUSCLE

Y. Pekindil (1), M. Birtane (1), A. Sarıkaya (2), A. Salan (2), S. Kokino (1). (1) Department of Physical Therapy and Rehabilitation; (2) Department of Nuclear Medicine, Trakya University, Edirne,Turkey.

Background: Neuromuscular electrical stimulation (NMES) and isometric exercises (IE) are widely used for improving muscle strentgh by simultaneous contraction in prevention of muscle atrophy. Although there exist many clinical methods for evaluating therapheutic responce of the muscles, Tc99m sestamibi which is a skeletal muscle perfusion and metabolism agent has not previously been used for this purpose.

Purpose: The aim of our work was to ascertain whether Tc-99m sestamibi muscle scintigraphy is useful in the monitoring of therapeutic response of NMES and IE in cases with knee osteoarthritis.

Materials and methods: The study included 20 women with bilateral knee ostoearthritis (age 41-62 yrs).Both QFMs of the same patients were studied. After the randomization to remove the effect of dominant side, one QFM of each case was subjected to the procedure of NMES whereas the other side was applied IE for a period of 20 days. NMES was performed with alternating biphasic rectangular current (50 Hz frequency) using a computed electrical stimulator daily for 23 min. IE was performed for 9.5 min per day. Lequesne index and thigh circumference measurements were assessed in pts before and after the training programmes . 60 min after injections of 555 MBq Tc-99m sestamibi anterior static images over the thigh were obtained for 5 min. The thigh-to-knee uptake ratio was calculated by semiquantitative analysis and normalized to body surface area (NUR=normalized uptake ratio).

Results: For the pre- and post-theraphy NURs values were:

	Pre-therapy	Post-therapy	p value
NMES	1.64±0.41	1.99±0.47	<0.0001
IE	1.65±0.46	1.90±0.38	<0.0001

Statistical analysis of the pre- and post-therapy NURs showed significant increases with respect to both NMES and IE groups. Although there was an increase in post-theraphy values of both group, it was not significant statistically. NURs values for both group also well correlated with Lequesne indices. Significant increases were found in thigh girth values for both groups with a higher mean increase in NMES group.

Conclusion: These results indicated that Tc-99m sestamibi muscle scintigraphy as a new tool may be useful in evaluation of therapeutic responses of both NMES and IE.

PS_164

THE COMPARISON OF 99MTC MIBI AND MAGNETIC RESONANCE IMAGING IN THE EVALUATION OF MUSCULOSKELETAL TUMORS

K. Özuğur (1), F. Güngör (1), A. Yıldız (1), U. Şenol (2), A. Demiral (3), A.T. Aydın (4), I. Gürer (5), V. Hazar (6), A. Boz (1), B. Karayalcın (1).
(1) Department of Nuclear Medicine; (2) Department of Radiolgy; (3) Department of Radiation Oncology; (4) Department of Orthopedics Surgery, Akdeniz University, Antalya, Turkey

Objectives: We performed a prospective study to evaluate the imaging potential of ^{99m}Tc MIBI as compared with magnetic resonance imaging (MRI) in patients with musculoskeletal tumors.
Methods: Five primary and 15 recurrent/residual lesions (RL's) were evaluated in 18 patients (12 male, 6 female; age range 11-81 years) by ^{99m}Tc MIBI scintigraphy and MRI within 2 weeks of each study. Four patients were with liposarcoma, 3 with malignant fibrous histiocytoma, 2 with osteosarcoma, 2 with Ewing sarcoma, and the rest of them with chondroblastoma, chondrosarcoma, fibrosarcoma, synovial sarcoma, alveolar rhabdomyosarcoma, dermatofibroma, and malignant mesenchimal tumor. Planar and SPECT imaging was performed 15 min after the injection of 740 MBq ^{99m}Tc MIBI.
Results: While the final diagnosis in all of the primary lesions and 11 of 15 RL's was achieved histopathologically, in the rest of 4 RL's was by long-term clinical follow-up. MIBI imaging and MRI were true positive in all primary lesions. In the 15 RL's, while there were 7 true positives (TP), 6 true negatives (TN), 2 false negatives (FN), and no false positives (FP) in MIBI imaging; 8 TP, 1 TN, 2 FP, 4 equivocal findings and no FN in MRI. MIBI was TN in three and TP in one of the four equivocal MRI.
Conclusion: It was concluded that MIBI imaging could be a valuable complementary method in the evaluation of musculoskeletal tumors especially in the case of equivocal findings in MRI.

PS_165

99MTC SESTAMIBI MUSCLE SCINTIGRAPHY TO ASSESS THE RESPONSE TO NEUROMUSCULAR ELECTRICAL STIMULATION OF NORMAL QUADRICEPS FEMORIS MUSCLE

Y. Pekindil (1), A. Sarıkaya (2), M. Birtane (1), G. Pekindil (3), A. Salan (1).
(1) Department of Physical Theraphy and Rehabilitation; (2) Department of Nuclear Medicine; (3) Department of Radiology, Trakya University, Edirne,Turkey.

Neuromuscular electrical stimulation (NMES) is widely used for improving muscle strength by simultaneous contraction in prevention of muscle atrophy. Although there exist many clinical methods for evaluating therapheutic responce of the muscles, ^{99m}Tc-sestamibi which is a skeletal muscle perfusion and metabolism agent has not previously been used for this purpose. The aim of our work was to ascertain whether ^{99m}Tc-sestamibi muscle scintigraphy is useful in the monitoring of therapeutic response of NMES in healthy women. The study included 16 women aged between 21 and 45, with the mean age of 32.7±6.4. Both quadriceps femoris muscles (QFM) of the same patients were studied. After the randomization to remove the effect of dominant side, one QFM of each case was subjected to the procedure of NMES for a period of 20 days. NMES was performed with alternating biphasic rectangular current, using a computed electrical stimulator daily for 23 minutes. After measurement of skinfold thickness over the thigh, pre- and post-NMES girth measurements were assessed in centimeters. Sixty minutes after injections of 555 MBq ^{99m}Tc- sestamibi anterior static images over the thigh were obtained for 5 minutes. The thigh-to-knee uptake ratio was calculated by semiquantitative analysis and normalized to body surface area (NUR=normalized uptake ratio).The difference between the pre-NMES NUR values versus post-NMES was significant (1.76 ± 0.31 versus 2.25 ± 0.38, p=0.0000). Percentage (%) increase of NUR values also well correlated with the % increase of thigh girth measurements (r=0.89, p=0.0000). These results indicated that ^{99m}Tc-sestamibi muscle scintigraphy as a new tool may be useful in evaluation of therapeutic responses to NMES.

PS_166

SCINTIGRAPHY WITH SOMATOSTATIN ANALOGS DEPICTS THE IMMUNOLOGICALLY COMPETENT STRUCTURES OF THE ORO-PHARYNX

R. Moncayo (1), M. Hamm-Pauler (2), R. Bale (3), R.A. Sweeny (4), C. Decristoforo (1), E. Donnemiller (1), M. Wenger (1), K. Seydl (1).
(1) Dept. of Nuclear Medicine; (2) Dept. of ENT; (3) Dept. of Radiology; (4) Dept. of Radiotherapy, University of Innsbruck

Aim: To define the anatomical structures being depicted by somatostatin analogs in the oropharyngeal region. Specific uptake of somatostatin analogs, e.g. octreotide uptake, in inflammatory processes has been a debated issue. The majority of authors have interpreted this uptake as an expression of increased blood pool. Evaluation of OctreoScan images alone does not allow to recognise exactly the anatomical structures involved thus leading to inconclusive results. In order to settle this issue we analysed octreotide scans together with the corresponding morphological data obtained by CT.
Methods: A series of 12 patients referred to octreotide scanning were analysed. The underlying diseases were: meningioma, ocular tumor metastasis, unilateral or bilateral exophthalmos and brain tumors. An in-house tracer, ^{99m}Tc-HYNIC-TOC tracer (Eur.J.Nucl.Med. 2000; 27: 1318-1325), was used. A conventional CT examination without contrast media was conducted 2-3 days before or after the scan. Both studies were aligned for image fusion by means of external markers. The threshold settings for the scans were set in such a way as to increase signal/background ratio, e.g. the pituitary appeared larger as the sella turcica.
Results:

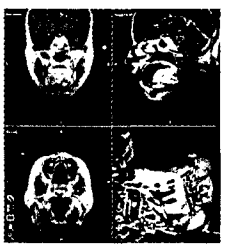

The Figure shows a representative image fusion analysis of the oro-pharynx region in the transversal, the coronal and sagittal planes. Tracer uptake can be seen in the tonsils, nasal mucosa and tongue. In one case, an unsuspected chronic tonsillitis was identified primarily by the scan as a band-like uptake on the dorsal part of the tongue. Diagnosis was confirmed by then ENT specialist.

Conclusions: Somatostatin analogs posses the ability to image resident immune cells in the oro-pharynx. Image fusion leads to improved visualisation of physiological structures.

PS_167

DIAGNOSIS AND MANAGEMENT OF UNEXPLAINED LOW BACK PAIN USING BONE SPECT

B. Kanmaz (1), O. Özmen (1), M. Hallaç (1), L. Kabasakal (1), H. Sayman (1), H. Koyuncu (2), K. Kanberoğlu (3), K. Sönmezoğlu (1), C. Önsel (1), C. Nisli (1), İ. Uslu (1); (1) Department of Nuclear Medicine; (2) Department of Physical Therapy; (3) Department of Radiology, I.U. Cerrahpasa Medical Faculty, Istanbul, Turkey.

Aim: Low back pain is a common, usually self limiting complaint. A variety of imaging modalities such as planar x-ray, CT and MRI including bone scintigraphy have been recommended as appropriate for the investigation of chronic low back pain. The aim of this study was to evaluate the role of bone SPECT in patients with x-ray findings which can not explain low back pain and correlate the results with CT findings.
Methods: 29 patients 11 male and 19 female aged between 17 and 62 years with a mean age of 36,2 years were included in the study. Conventional planar radiography was performed in all patients. Patients with normal planar x-ray or with x-ray abnormalities, which could not explain low back pain, underwent bone scintigraphy and computer tomography of lumber spine. CT images was displayed with bone and soft tissue windows.
Results: SPECT showed increased activity in 14 facet joints, in 2 vertebral bodies and in one patient in sacrum. CT identified 9 hypertrophic facet joints, 10 disc bulging, 5 disc prolapse, 2 spondylolysis and 1 posterior arch lesion. SPECT was able to detect more facetal joint lesions compared to CT. Out of 13 patients with facet joint arthropathy in 5 patients both SPECT and CT could detect facet lesions. In 7 patients only SPECT could show facet joint disease. In 1 patient CT showed facet joint hypertrophy but SPECT was normal. CT was able to show disc degenerations such as disc bulging and disc prolapse. Out of 15 disc degenerations without any facet joint arthrophaty in CT, SPECT identified additional facet joint uptake at the same level in 5 patients.
Conclusions: We conclude in our study that SPECT has superiority to CT in detecting facetal joint lesions. Additional to CT findings such as disc prolaps and bulging, metabolic active bony lesions can be detected by SPECT, which are clinically significant. In patients with low back pain without neurological deficit and with a planar x-ray finding, which can not explain the cause of low back pain, bone SPECT of lumbar region should be performed.

PS_168

CORRELATIVE TC-99M ANTIGRANULOCYTE FAB(LEUKOSCAN)/NANO COLLOID BONE MARROW SCANS VS MAGNETIC RESONANCE IMAGING IN OSTEOMYELITIS SUPERIMPOSED CHARCOT JOINT

G. Limouris (1), G. Petrikos (2), V. Voliotopoulos (1), C. Alexandropoulos (3), E. Matsouka (2), A. Stavraka-Kakavaki (1), E. Dounis (3), N. Dimitropoulos (1), L. Vlachos (1). (1) Areteion University Hospital,Nuclear Medicine Dept.; (2) Laikon General Hospital,Internal Medicine Dept.; (3) Laikon General Hospital,Orthopedic Surg Dept., Athens, Greece.

Objectives: An approximately 6% to 7%of pts with diabetes mellitus develop neuropathic (charchot) joint.usually in the foot. A superimposed ostemyelitis is very difficult to defferantiated.Eventhough MR imaging as well as radiolabelled leukocytes are reported having increased sensitivity, comparative data are lacking. The aim of this study was to compare leukocyte scan and bone marrow scintigraphy to MRI for differentiating osteomyelitis superimposed on neuropathic(charcot) joint.

Methods: Fourteen diabetes pts,6 men and 8 women aged 51-72 yr. underwent Tc99m labeled leukocyte scintigraphy (750 MBq Leukoscan, Immunomedics) Tc99m nano-colloid bone marrow scintigraphy (750 MBq Nanocis, CIS) and MRI. Leukocyte scans were interpreted as positive for osteomyelitis when focally increased osseous uptake was shown. Bone marrow leukocyte scintigraphies was observed without corresponding activity on the marrow scan. MRI was classified positive for osteomyelitis when bone marrow exhibits low T1 and highT2 signal intensity.

Results: Osteomyelitis was present in 6 out of 14 charcot joints. Leukoscan scintigraphs correctly identified osteomyelitis in both cases, but was false positive in 8 of 14 unaffected joints. Leukoscan/bone marrow scintigraphy was true positive in both osteomyelitis cases and true negative in all uninfected joints. MRI was false positive in 2 uninfected joints and false negative in both osteomyelitis cases.

Conclusion: Correlative leukocyte/bone marrow/MRI imaging in charcot joints can differentiate the superimposed osteomyelitis leukocyte/bone marrow imaging seems to be the procedure of choice for the differential diagnosis.

PS_170

TC99M MIBI SCINTIGRAPHY IN METASTATIC BONE INVOLVEMENT OF BREAST CANCER

G. Durmus Altun (1), C. Uzal (2), S. Hacımahmutoğlu (1), G. Pekindil (3), A. Sarıkaya (1). (1) Department of Nuclear Medicine; (2) Department of Radiation Onkology; (3) Department of Radiology, Trakya University Medical Faculty, Edirne, Turkey.

Technetium-99m methoxyisobutylisonitrile (MIBI) breast imaging might provide additional information in the differentiation of malignant pathologies from benign lesions in patients with palpable breast anomalies The aim of this study was to investigate the possible role of Tc99m MIBI scan in metastatic bone involvement of breast cancer.

METHODS: Twelve women (mean age: 51.7±11.8 y) with metastatic breast cancer were evaluated with Tc99m MIBI imaging for metastasis. All patients were underwent Tc99m MDP and Tc99m MIBI scintigraphy. The diagnosis of metastatic bone involvement was based on radiographic, scintigraphic, or pathologic data. Scintigraphic images were evaluated by visually.

RESULTS: Tc99m MIBI scintigraphy found abnormalities in 16 of 31 (51%) foci detected by Tc99m MDP scan, additionally 3 lytic bone lesions which without Tc99m MDP uptake and two pathologic fracture zone, and one local soft tissue recurrent lesion had visible Tc99m MIBI uptake. The sensitivity of Tc-99m MIBI scintigraphy for the identification of the metastatic lesion was 57.1%.

CONCLUSION: According to our finding, we concluded that Tc99m MIBI scintigraphy might be a valuable new tool for detecting metastatic bone involvement of breast cancer, especially diagnosis of lytic bone lesion due to metastatic involvement or suspecting pathologic fracture.

DIAGNOSTIC ONCOLOGY 5

PS_169

SCINTIMAMMOGRAPHY: DOES SIZE MATTER?

J.R. Buscombe, J.B. Cwikla, A. Kolasinska, S.P. Parbhoo, T. Davidson, B. Holloway, N. McDermott, A.J.W. Hilson. Royal Free Hospital, London, UK.

One of the major factors which determine the accuracy of breast imaging is the size of the detected lesion. This may be a particular issue in those women with dense breast in whom a small lesion may be difficult to see on mammography. The aim of this study was to review the results of Tc-99m MIBI scintimammography and x-ray mammography and compare these results with lesion size. Comparisons in accuracy were performed by comparison of area under ROC curve analysis.

Data from 273 women were reviewed. The mean age of the women studied was 52 with a range of 26-84 years. All patients underwent x-ray mammography, Tc-99m MIBI scintimammography and had definitive biopsy of any suspicious site. Results of the imaging were then compared to the final histology in three size groups. Firstly in the 74 cancers of less than 2cm the sensitivity of mammography was 51% and scintimammography 70%. In the 104 cancers sized 2-4 cm the sensitivity of mammography was 70% and scintimammography 87%. In the 52 cancers greater than 4cm mammography found 88% of cancers and scintimammography all cancers.

Both methods have an improved sensitivity with increasing lesion size. Scintimammography was always more sensitive than mammography, however the biggest difference was in tumours of less than 2cm when the sensitivity of scintimammography was significantly better than mammography ($p<0.05$). Therefore scintimammography may be of help in all women with breast cancer irrespective of tumour size but offers the biggest advantage in the smallest cancers.

PS_171

THE COMPARISION OF TC-99M MIBI AND TC-99M MDP SCINTIMAMMOGRAPHY IN DETECTION OF BREAST LESIONS

M. Atalay (1), E. Uluc (2), M. Polat (1), S. Gür (3), A. Çökmez (3). (1) Department of Nuclear Medicine; (2) Department of Radiology; (3) Department of Surgery, Atatürk State Hospital, Izmit, Turkey.

MIBI is a lipophilic cationic myocardial perfusion imaging agent. It has also uptake in varöous tumors including significant uptake in Breast lesions. MDP is a bone scaning agent. And it has also been used in diagnosis of breast lesions in same examination. The aim of the study was to compare the value of MIBI and MDP scintimammography in patients with breast lesions.

Methods: Twety- one patients with 34 suspicious breast lesions, aged between. 25-44 were studied. All of them underwent ultrasonography, MDP-SMM(scintimammography) and MIBI-SMM. The results were compared with histopathology. MDP-SMM was performed10-20 min. after injection of 15-20 mc Tc- 99 m MDP. MIBI-SMM was perfomed 20 min.and 2 hours after inj ection of 10.-15 Tc 99 m MIBI. The results were evaluated by two nuclear medicine physicians independetly. Semiquantative analysis was done. By drawing ROI over lesion and contral tõssue on contra side. Ratio of average counts/ pixel from areas of lesion and non lesion were calculated.

Results: The sensitivity of MIBI-SMM for defection of malignant lesions was %80 ad its spesificty %82. MDP-SMM had %78 sensitivity and %70 spesificity for detecting malignant lesions.

Conclusions: We have found no significant difference in detecting malignant lesions with MIBI-SMM and MDP-SMM. However, specificity of MIBI-SMM was higher than MDP-SMM. On the otherhand the bone scan can be done immediately following MDP-SMM Additionally the cost of MDP-SMM is significantly lower than MIBI-SMM.

PS_172

UTILITY OF 99MTC-SESTAMIBI PRONE SCINTIMAMMOGRAPHY FOR THE CHARACTERIZATION OF ISOLATED CLUSTERS OF MICROCALCIFICATIONS

M. Grosso, D. Volterrani, G. Boni, G. Manca, F. Bianchi, S. Suriano, R. Bianchi. Department of Nuclear Medicine, University of Pisa, Pisa, Italy.

In recent years a great part of the oncological research concerned with the non-palpable breast cancer. The presence of microcalcifications (MC) can be the only indication of a carcinoma. Mammography (MRx) is the accepted diagnostic technique to detect MC. It has a great sensitivity in the detection of breast anomalies, but a low specificity in the diagnosis of breast cancer.

Aim of the study was to evaluate the contribution of ^{99m}Tc-Sestamibi scintimammography (SMM) to the diagnosis of benign or malignant isolated clustered of MC previously detected by MRx. One hundred fifty-one women (mean age 49±11 years) with MC on mammograms were submitted to SMM. Scintigraphic images were acquired 10 minutes after i.v. injection of ^{99m}Tc-SESTAMIBI (740 MBq). Planar images of both breasts were simultaneously obtained in lateral prone position and in the anterior and oblique projections using a dual head camera. One hundred twenty-three women underwent surgery, whereas the remaining 28 had a negative follow-up up to three years as a 'gold standard'. Histology demonstrated 41 primary breast cancers (prevalence of disease: 27%) and 82 benign lesions. SMM was positive in 30/41 breast cancers and negative in 93/110 benign breasts leasions, whereas MMx was positive in 35/41 breast cancers, but negative in 81/110 benign lesions. Moreover, the association of MMx and SMM findings provided a significant improvement of negative predictive value (up to 100% for MC with low suspicion of malignancy at MMx).

In conclusion, this study confirms the good diagnostic specificity of SMM, as previously reported, suggesting the complementary role of this technique with MMx. Because of the relevant improvement of negative predictive value, SMM seems to be especially useful to reduce the number of negative breast biopsies or surgical interventions.

PS_173

CORRELATION AND MULTIVARIATE REGRESSION ANALYSIS BETWEEN TC-99M (V)DMSA AND TC-99M MIBI UPTAKE AND STEROID RECEPTORS, PROLIFERATION INDEX, TUMOR SIZE, AGE, MALIGNANT GRADE, P53 AND C-ERBB-2 IN PRIMARY BREAST CANCER

V. Papantoniou (1), L. Nakopoulou (2), J. Christodoulidou (3), E. Papadaki (1), M. Souvatzoglou (1), A. Stipsaneli (1), D. Lazaris (4), M. Sotiropoulou (2), A. Keramopoulos (4), S. Michalas (4), C. Zerva (1) (1) Department of Nuclear Medicine; (2) Department of Pathology; (3) Department of Radiology; (4) Department of Obst. and Gyn. Alexandra Hospital University of Athens, Athens, Greece

The scope of this study was to identify the relationship between the uptake of both traces and the presence or absence of each parameter separately and further isolate by multivariate regression analysis these factors witch can independently affect (V) DMSA and/or MIBI uptake in primary breast cancer.

Material-Methods: Twenty nine patients with histologically confirmed breast carcinoma underwent preoperatively scintimammography (SMM) with (V) DMSA and MIBI in consecutive sessions (48h intervall) 10 and 60 min after administration of 25-30mCi (740-925 MBq) of each tracer. Semiquantitative analysis (T/B ratio) was performed and correlated with the presence of steroid receptors (ER, PR), proliferation index (Ki-67) tumor size, grade of malignancy p53 and C-erbB-2. ER-PR receptors, p53 and C-erbB-2 were determined by immunohistochemical method (AB complex). Step wise multivariate regression analysis included T/B of (V) DMSA and MIBI as dependent and all the others as independent variables.

Results: Positive correlation was found between Ki-67 and (V) DMSA ($rKi\text{-}67_{10min}$=0,492 p<0,001 $rKi\text{-}67_{60\ min}$=0,634, p<0,001) and negative (inverse) between ER, PR and (V) DMSA (r $ER_{10\ min}$=-0,320, p<0,05, r ER_{60min}=-0,350, p<0,05, rPR_{10min}=-0,413, p<0,03, rPR_{60min}=-0,378, p<0,05). Multivariate analysis demonstrated positive correlation of the independent variable Ki-67 and (V) DMSA at 10 and 60 min (p<0,05). Tumor size and Ki-67 (10min) were positively correlated with MIBI. ER and PR had negative but not significant correlation with MIBI. (r tumor $size_{10min}$=0,455, p<0,03, r tumor $size_{60min}$=0,533, p<0,008, $rKi\text{-}67_{10min}$=0,406, p<0,05). Multivariate analysis found independent significant correlation of MIBI only with tumor size (p<0,05). Ki-67 was negatively correlated with ER and PR receptors. Grade of malignancy and p53 were negatively correlated with ER receptors.

Conclusions: Proliferation index seems to constitute the major independent factor affecting (V) DMSA uptake in breast cancer. Tumor size was the only independent parameter influencing MIBI uptake in breast cancer. The negative correlation between ER, PR receptors and (V) DMSA can be interpreted as indirect, based on the negative correlation between Ki-67 and ER, PR. (V) DMSA seems to have the advantage over MIBI to visualize tumors with intense proliferating activity and consequently tumour aggressiveness.

PS_174

99MTC-MIBI UPTAKE AND BCL-2 OVEREXPRESSION IN UNTREATED BREAST CANCER PATIENTS

S. Del Vecchio (1), A. Zannetti (1), A. Ciarmiello (2), L. Aloj (1), R. Fonti (1), C. Caracò (1), M. Salvatore (3). (1) CNR-Centro Medicina Nucleare; (2) Istituto Nazionale Tumori; (3) Università Napoli, Italy.

Lack of 99mTc-MIBI uptake is consistently reported to predict poor response to subsequent chemotherapy in a variety of human malignant tumors.

Aim. Since 99mTc-MIBI accumulates within mitochondria which play also a central role in apoptosis through the integration of death signals by Bcl-2 family members, we tested whether initial 99mTc-MIBI uptake is affected by the expression of anti-apoptotic Bcl-2 protein and pro-apoptotic Bax protein.

Methods. Thirty-three untreated breast cancer patients were i.v. injected with 740 MBq of 99mTc-MIBI and planar images were obtained 10 minutes post-injection with the patients in prone lateral position. The tumor-to-background (T/B) ratio was obtained by region of interest analysis on 99mTc-MIBI positive lesions. Tumor specimens were then obtained at surgery and processed for the determination of Bcl-2 and Bax levels by immunoperoxidase staining. The apoptotic index and the rate of tumor cell proliferation were also determined in all specimens.

Results. Thirty out of 33 breast carcinomas showed focal uptake of 99mTc-MIBI and 10 min. tumor-to-background ratios varied between 1.14 and 6.93. Bcl-2 and Bax expression was graded from 0 to 3 when no reaction, faint, moderate or intense staining were observed, respectively. In 99mTc-MIBI positive lesions, we found an inverse significant correlation between T/B ratios and Bcl-2 levels (r= -0.52 p< 0.01) whereas no correlation was found between early uptake ratio and Bax expression. After multiple regression analysis by the backward stepwise procedure, among the variables (Bcl-2, Bax, apoptotic index and proliferation) potentially affecting 99mTc-MIBI uptake, only Bcl-2 levels showed significant correlation with tumor-to-background ratios (r = 0.52, F=10.5, p<0.01). In the three 99mTc-MIBI negative lesions (diameter >1.8 cm), we found a marked overexpression of Bcl-2. To confirm this observation, we retrieved from our archive 5 additional breast cancers (diameter > 2 cm) which had failed to accumulate 99mTc-MIBI. All negative 99mTc-MIBI lesions showed a dramatic reduction of the apoptotic index and a marked overexpression of Bcl-2 independently of Bax levels and rate of proliferation.

Conclusion. Our findings indicate that initial uptake of 99mTc-MIBI in breast carcinomas is affected by Bcl-2 levels. High levels of Bcl-2, despite the stabilization of mitochondrial membrane potentials, prevents permeabilization of mitochondrial membrane and accumulation of 99mTc-MIBI in tumor cells.

PS_175

99MTC-MIBI UPTAKE IN BREAST CANCER CELLS DURING EARLY PHASES OF APOPTOSIS INDUCTION WITH STAUROSPORINE

L. Aloj (1), A. Zannetti (1), C. Caracò (1), R. Fonti (1), S. Del Vecchio (1), M. Salvatore (2). (1) CNR-Centro Medicina Nucleare; (2) Università Napoli, Italy.

99mTc-MIBI is reported to accumulate within normal and cancer cells in response to plasma membrane and mitochondrial inner membrane potentials. Apoptosis, or programmed cell death, is caused by a cascade of molecular events which ultimately cause permeabilization of the mitochondrial membrane, disruption of mitochondrial membrane potentials and nuclear DNA fragmentation. Staurosporine, a protein kinase inhibitor, is a strong inducer of apoptosis in cultured cells.

Aim. As mitochondria play a key role in both apoptosis and 99mTc-MIBI uptake, we evaluated the early effects of apoptotic activation by Staurosporine on 99mTc-MIBI uptake.

Methods. First, we studied the ability of well established cultured human breast cancer cells (T47D, MCF-7, MDA-MB-231 and SK-BR3) to accumulate 99mTc-MIBI. Cells in multiwell plates were incubated with 1x10E6 counts of 99mTc-MIBI for different times up to 1h at 37¡C. After several washes in cold PBS, cells were lysed in 1M NaOH, the whole lysates were counted and the activity specifically associated to cells was expressed as the percentage of total added radioactivity per mg of protein content. Pretreatment with 1.5 μM Staurosporine was performed for 5 min up to 4.5 h before adding 99mTc-MIBI. Following apoptosis induction, annexin V binding and DNA laddering determinations were also performed at different times.

Results. The cell lines tested showed a range of different absolute uptake values. In all cell lines, 99mTc-MIBI uptake reached a plateau between 30 and 60 min of incubation. Treatment with Staurosporine determined a 2- to 5-fold increase of 99mTc-MIBI uptake which was observed as early as 5 minutes after Staurosporine addition and continued to be detected up to 4.5 hours of treatment. The enhancement of 99mTc-MIBI uptake was paralleled by an increase of annexin V binding whereas DNA laddering became evident only after 4.5 h indicating that the time window explored did not include the degradative phases of the apoptotic process.

Conclusion. 99mTc-MIBI uptake is dramatically increased in the early phases of apoptosis induced by Staurosporine, when mitochondrial transmembrane potentials are presumably maintained. Our findings indicate that clinical studies with 99mTc-MIBI shortly after chemotherapy, may be able to identify early phases of drug-induced apoptosis through enhanced tumor uptake.

PS_176

CORRELATION OF TC-99M MIBI UPTAKE WITH ESTROGEN RECEPTOR, PROGESTERONE RECEPTOR, HISTOLOGICAL GRADE, NUCLEAR GRADE AND MITOTIC INDEX IN INVAZIVE DUCTAL BREAST CANCER: PRELIMINARY RESULTS

R. Bekis (1), E. Derebek (1), S. Özkal (2), M.A. Koçdor (3), T. Canda (2), H. Durak (1). (1) Department of Nuclear Medicine; (2) Department of Pathology; (3) Department of Surgery, Dokuz Eylül University, Izmir, Turkey.

AIM: Ten patients (pts) with invazive ductal breast cancer (age 54±10) in order to investigate the correlation between the degree of accumulation of Tc-99m MIBI and estrogen receptor, progesterone receptor, histological grade, nuclear grade and mitotic index in tumor tissues.
METHOD: All of patients underwent scintimammography. Anterior, left and right prone lateral images were obtained 20 minutes and 2 hours after the injecting of 740MBq Tc-99m MIBI. Tumor and background activity ratios (T/BG) are calculated from lateral projection. T/BG activity ratios are classified as equal (1pts), greater (6 pts) or lesser (3 pts) than 1,5. A pathologist determined the estrogen receptor, progesterone receptor expression by immunohistochemical method as well as histological grade, nuclear grade and mitotic index. Estrogen receptor and progesterone receptor expressions are reported as negative(4 pts, 3 pts respectively), <75% positive(5 pts, 3pts resp.) and >75% positive(1 pts, 4 pts. resp.). Histological grades were evaluated according to the ratio of solid and tubular structures, nuclear grades nucleus charecteristics, existence of nucleoli, Mitotic index is expressed on number of mitosis in 10x microscopic field. Both histological grade, nuclear grade and mitotic index were classified into 3 groups (1,2,3).
RESULTS:

T/BG	Histological Grade			Nuclear Grade			Mitotic Index		
	1	*2*	*3*	*1*	*2*	*3*	*1*	*2*	*3*
≤1,5	2	1	—	—	2	1	—	1	2
≥1,5	—	4	3	1	—	6	—	1	6

All of the pathological data were seperately compared with T/BG activity ratios of Tc-99m MIBI. The statistical evaluation was performed using spearman correlation test and chi-square analysis (Fisher exact test). No statistical difference was found (p>0,05) between T/BG activity ratios of Tc-99m MIBI and estrogen receptor, progesterone receptor, histological grade, nuclear grade and mitotic index.
CONCLUSION:According to our preliminary results there seems to be no correlation between Tc-99m MIBI uptake ratios and tumor aggressiveness, though the number of patients are limited.

PS_177

CORRELATION BETWEEN 99M-TC TETROFOSMIN UPTAKE AND P-GLYCOPROTEIN EXPRESSION IN BREAST CANCER

E. Yücesoy (1), G. Çekin, M. Atalay, Ö. Gür, S. Gür. (1) Department of nuclear medicine; (2) Department of nuclear medicine; (3) Department of nuclear medicine; (4) Atatürk Stata Hospital, Department of General surgery, Izmir, Turkey

The aim of this study was to invastigate the relationship between Tecnetium-99m tetrofosmin accumulation- washout in the tumor and the expression of P-glycoprotein. (Multidrug resistance mediated MDR 1)
Methods:16 breast cancer patient were made Tc-99m tetrofosmin scintigraphy before biopsy and operation. _mages were taken immediately after the intravenogeus enjection as dynamic ,and after 20 minutes and 2 hours. Scans were interpreted both visually and quantitatively. Washout degrees were calculated between 20.minutes and 2 hours images. Tumor P-glycoprotein (Pgp) quantity was analysed with immunohistochemical methods because of its practical use and the ability to detect Pgp in a single cell.
Results: We found all patients with breast cancer Pgp's (-) except one . Only one patient's Pgp 's was found (+). There were not any different uptake level between first pass and 20 minutes images. There were modarete activity washout in all patient between 20.minutes and 2 hours images but it was prominent in the Pgp (-) patient
Conclusions: Our study is continuoning now and we have got few patient yet .As far our data we can say Pgp owerexpression in breast cancer is not very usuall or may be immunohistochemical methods isnt enough to detect through amount of Pgp. We can expect prominent washout in Pgp (+) patient with tetrofosmin . There can be inverse correlation between Pgp quantity and tetrofosmin uptake like MIBI.But we need more study and more data to say this conclusion. There is not any necessary to take first pass dynamic images for this purpose.

PS_178

SCINTIMAMMOGRAPHY WITH 99M TECHNETIUM TETROFOSMIN IN BREAST CANCER DETECTION

L.J. Jaukovic (1), N. Stankovic (2), S. Dimitrijevic (3), M. Strbac (4), R. Spaic (1), S. Markovic (1). (1) Institute of Nuclear Medicine, Military Medical Academy, Belgrade; (2) Clinic of Surgery; (3) Institute of Radiology; (4) Institute of Pathology, Belgrade, Yugoslavia

Routine mammography is a method for screening breast cancer patients. Abnormal or inconclusive mammograms need the further investigation for final diagnosis, especially in patients with dense breast.
AIM: The aim of this study was to compare the results of mammography (MM) and scintimammography with 99m Technetium- Tetrofosmin (SMM) in detection of primary breast cancer.
METHOD: Twenty six patients with twenty eight lesions suspicious for malignancy were studied. All of them had clinical investigation , MM, SMM and surgical biopsy for final histological diagnosis. An amount of 600 MBq 99m Tc-Tetrofosmin was injected intravenously in the arm opposite to the side of breast lesion. Ten minutes after injection planar breast 7-minutes scans were performed in supine (anterior) and prone (left and right lateral) position.
RESULTS: Out of 28 lession breast cancer was histologicaly confirmed in 19 (15 ductal invasive, one lobular, one colloid, one papillar carcinoma and one case of cystosarcoma phylodes- malignant tipe.) For MM sensitivity of 84%, specificity of 55% and accuracy of 75 % were obtained. At SMM 19/ 19 malignant lesions were detected. The smallest detectable carcinoma measured 0.6 cm. At patohistology nine lession presented benign. Four false positive results (two fibroadenomas, one lipogranuloma and one case of fibrocystic disease) were observed, five true negative results in three cases with fibrocystic disease and two fibroadenomas. The overall sensitivity of scintimammography was 100%, specificity 55% and accuracy 86%.
CONCLUSION: We concluded that sensitivity of 99mTc-Tetrofosmin scintimammography in detection of breast cancer is superior to that of mammography . Our results suggest that 99mTc-Tetrofosmin is a suitable tumor seeking agent for breast cancer imaging.

PS_179

COMPARISON OF SCINTHIGRAPHY OF THE BREAST WITH 99MTC MDP AND WITH 99MTC TETROFOSMIN IN PATIENTS SUSPECTED TO SUFFER FROM BREAST TUMOUR

P. Alves (1), P. Lourenco (1), A. Rodrigues (1), F. Botelho (2), J. Lima (2). (1) Laboratório de Radioisótopos; (2) Departamento de Biofísica, Faculdade de Medicina, Universidade de Coimbra, Portugal.

Introduction – Morbidity and mortality of breast tumours continue to be of high clinical importance. This fact is as well due to the frequency of the disease as to the difficulty in making an early diagnosis.
The accumulation of 99mTcMDP in soft tissues in bone scans realised for purposes of staging has been the subject of various studies, especially in the context of breast tumours. The high vascularisation of tumour tissue seems to be of importance in the scintigraphic appearance of malignant lesions.
Several publications have mentioned the annormal captation of 99mTc tetrofosmin in patients with breast tumours submitted to myocardial scintigraphy.
Objective – To evaluate the diagnostic efficiency of breast scintigraphy during traditional bone scans realised in patients with malignant breast tumours and to compare the results with those of breast scintigraphy realised with 99 mTc tetrofosmin. We evaluate the results in context with the clinical apresentation, laboratory results and histology.
Material and Methods – Seventy females were included in the study, thirty-five suspected of breast tumour and thirty-five without suspicion of oncologic disease. All patients were submitted to bone scans with 99mTc MDP with planar and tomographic image acquisition (GE Starcam AC/T 64f, 64x64). Fifteen days later breast scintigraphy with 99 mTc tetrofosmin with tomographic image acquisition was realised.
The tomographic and planar scintigraphies were evaluated concerning their morphology and degree of fixation of the radioactive marker. In the patients suspected to suffer from malignant disease laboratory exams and histologic evaluation were done, too.
Results – In the group of patients with breast tumour the mean age was 54,63 years; of the 35 scintigraphies with 99mTcMDP 31 showed a lesion, two were negative and two inconclusive. In the control group (mean age 52,05 years) seven exams showed a lesion, 28 did not. Using 99mTcTetrofosmin, in the patient group 22 scans showed a lesion, 10 were negative and three inconclusive; in the control group five scans were positive and 30 negative.
Conclusions – 99mTcMDP is more sensitive than 99mTcTetrofosmin in detecting nodular breast lesions, presenting also better image quality, especially when using coronal images, as these do not suffer interposition of other body parts that capture the radioactive marker.
The traditional bone scan realised in several clinical situations may serve as a tool for detecting breast pathology, if a tomographic study of the thorax is done after administration of 99mTcMDP.

PS_180

SCINTIMAMMOGRAPHY WITH TC99M MDP IN BREAST CANCER

S. Mihajlovska, N. Kosturski, Z. Petrovski, J. Gorgievski. Department of Nuclear Medicine, Medical Center, Bitola, Mazedonia.

The aim of the study was to assess the value of Tc99m MDP scintimammography in the detection of breast carcinoma.
Forty-nine patients (30-71 years, mean 49) were included into the study. There were 28 patients with diagnosed malignant lesions, 12 patients with mastectomy and 9 normal patients.
All women were injected with 555-74MBq of Tc99m MDP and double phase (15 min. and 2 h.) breast imaging was made. Whole body scans and lateral views of both breasts were obtained in prone position with elevated arms.
Focal accumulation of MDP uptake in tumor localization was considered positive.
Results: A clear uptake of Tc99m MDP was evident in 25 of 28 malignant lesions individuated (sensitivity 94.5, specificity 100 %). No false positive results were observed. 11 out of 12 patients presenting lymph node metastases (sensitivity 93.7%).
Radioactivity accumulations were detected on contralateral nonoperated gland in two of 12 patients who had masteclomy .
For detection malignancy mammography, ultrasonography and biopsy were performed but they were negative. Definitive diagnosis were made base on the histopathologic results and showed malignant lesions.
Our study suggests that scintimammography with Tc^{99m} MDP seems to be a highly sensitive and specific method in the differentiation of breast lesions. This method can be added to routine presurgical bone scinyigraphy as a diagnostic tool.

PS_181

GASTRIN RELEASING PEPTIDE RECEPTOR IMAGING IN HUMAN BREAST CARCINOMA USING TC-99M RP527 VERSUS IMMUNO-HISTOCHEMISTRY

C. Van de Wiele (1), K. Dhaene (2), R. Vandenbroeke (3), V. Cocquyt (3), F. Dumont (4), F. De Winter (1), G. Slegers (4), R.A. Dierckx (1).
(1) Department of Nuclear Medicine; (2) Department of Anatomopathology; (3) Division of Oncology; (4) Department of Radiopharmacy, Ghent University, Belgium

Aims : In vivo visualisation of gastrin releasing peptide receptor (GRP-R) status by means of 99mTc RP527 could predict or rapidly assess respons to treatment modalities targeting GRP-R. We report on the relationship between breast tumour uptake of 99mTc RP527, a 99mTc chelated peptide which binds to GRP-R, and GRP-R expression as measured by immunohistochemistry (IHC).
Methods : Nine patients referred because of a clinical diagnosis suggestive for breast carcinoma, four patients suffering from tamoxifen resistant bone mestastasised breast carcinoma and one patient presenting with a local breast carcinoma recurrence invading the sternum underwent 99mTc RP527 scintigraphy. Results obtained were compared to routine staging examinations in all patients and to routine histopathologic analysis and IHC GRP-R staining in the first nine patients.
Results : All 9 patients with suspected breast lesions were tumour positive on histology. Uptake of 99mTc RP527 was clearly depictable in the primary tumour of 8 out of 9 patients and in involved lymph nodes and part of the distant metastasis limited to the bone (occurring in only one patient) when present. In 5 patients, IHC was negative whereas 99mTcRP527 uptake was positive. In none of remaining patients, 99mTc RP527 uptake was found.
Conclusions : The different incidence GRP-R number found between 99mTc RP527 imaging, and IHC likely relates to differences in methodology. In the near future, 99mTc RP527 imaging might be helpful to further elucidate the role of GRP-R in human malignancies and to allow prediction or monitoring of therapy responsiveness to recently developped GRP-R antagonists.

PS_182

COMPARISON OF PLANAR AND SPECT SCINTIMAMMOGRAPHY WITH 99MTC-MIBI IN THE DIAGNOSIS OF BREAST CARCINOMA AND AXILLARY LYMPH NODE INVOLVEMENT

M. Myslivecek (1), M. Kaminek (1), P. Koranda (1), V. Husak (1), M. Hartlova (2), M. Duskova (3), K. Cwiertka (4). (1) Dept. of Nucl. Med. ; (2) Dept. of Radiolofy; (3) Dept. of Pathology; (4) Dept. of Oncol., University Hospital, Olomouc, Czech Republic

Aim: To compare SPECT and planar ^{99m}Tc-MIBI scintimammography (SMM) in the detection of primary breast cancer and axillary lymph node involvement, and to compare the scintigraphic results with the histopathological findings obtained after surgery.
Methods: 308 breast lesions with mammographically suspicious and indeterminate findings were studied. 740 MBq of ^{99m}Tc-MIBI was injected intravenously. Anterior supine, right and left lateral planar images were acquired in prone position at 10 minutes post injection. After this a SPECT study (60 projections, 64x64 matrix, 30sec/frame, 360 degrees arc) was acquired in supine position in the same patient. Filter Hanning, order 5, cut off 2.3 was applied for reconstruction with filtered backprojection. A final histopathological diagnosiss was chieved after surgery.
Results: Planar imaging missed 15 malignant lesions while SPECT missed only seven. 21 benign lesions showed uptake of MIBI on planar imaging while only 19 showed uptake on SPECT. In patients with breast cancer, the sensitivity was 92% (78/85) for SPECT and 82% (70/85) for planar imaging, respectively ; specificity was 91% (204/223) for SPECT and 91% (202/223) for planar scans; accuracy was 92% and 88% respectively. Metastatic axillary lymph node involvement was seen in 35 patients: the sensitivity was 66% (23/35) for SPECT and 54% (19/35) for planar images; specificity was 76% (38/50) and 86% (43/50) and accuracy 72% and 73% respectively. The comparison of our results with those published in literature has been discussed.
Coclusions: Our results confirm the high diagnostic accuracy of SMM in the diagnosis of breast cancer, and suggest that SPECT is more sensitive than planar images, especially in detecting malignant breast lesions. SPECT provides additional information to planar SMM with respect to localization of MIBI uptake and tumor extent and improves diagnostic certainty. Our experience suggests the routine use of SPECT combined with planar SMM.

PS_183

IODINE-LABELLED TAMOXIFEN UPTAKE IN HUMAN BREAST CARCINOMA

C. Van de Wiele (1), V. Cocquyt (2), R. Vandenbroecke (3), F. De Vos (1), F. De Winter (1), S. Van Belle (2), G. Slegers (4), R.A. Dierckx (1).
(1) Division of Nuclear Medicine; (2) Division of Medical Oncology; (3) Division of Oncological Gynaecology; (4) Department of Radiopharmacy, Ghent University, Gent, Belgium

AIMS : As the mainstay of hormonal treatment for breast cancer patients (bcp) is tamoxifen (TAM), assessing uptake, retention and eventually efflux of 123Iodine-labelled tamoxifen (ITX) in vivo by means of scintigraphy could help to increase our understanding of tamoxifen's action and the mechanisms involved in resistance to the drug. This in turn could provide new targets for the design of therapeutic agents which can both effectively antagonise the alpha-estrogen receptor (α-ER) dependent growth pathway, as well as circumvent or prevent the emergence of inevitable resistance to the drug.
METHODS :17 bcp were included in the study and divided in 2 groups. Group 1 (n, number of patients = 7) included untreated, histologially confirmed primary bcp, group 2 (n = 10) included TAM-resistant metastatic bcp, off hormonal treatment for at least 6 months. All bcp underwent whole body planar and tomographic (SPECT) imaging 30 min and 4-5 h pi. of 185 MBq ITX. Processed images were reviewed for the presence or absence of focally increased uptake at sites of known lesions from clinical or radiological findings. ITX uptake was quantified as the ratio of tumour lesion uptake to non-specific, contralateral breast or axillary uptake (T/N) on SPECT images. αER and progesteron receptor (PR) status was determined using immunohistochemistry.
RESULTS : In 4/7 bcp of group 1, all α-ER +ve/PR+ve, ITX uptake was clearly depictable. In 2 of these patients, involved axillary lymph nodes were also visualised. T/N ratios consistently increased over time. The remaining α-ER +ve/PR-ve and α-ER -ve/PR-ve tumours failed to show ITX uptake. In bcp of group 2, known tumour lesions in bone (n = 6), lung (n = 2) liver (n = 1) or liver and bone (n = 1) failed to take up ITX.
CONCLUSIONS : As PR positivity, reflecting α-ER functionality, in addition to α-ER positivity increases the likelihood of response to endocrine treatment, the lack of ITX uptake in α-ER +ve/PR-ve and α-ER -ve/PR-ve tumours may prove advantageous for predicting response to TAM treatment. The data presented further favor decreased intra-tumoral tamoxifen accumulation as a pathway for acquired resistance to tamoxifen in patients suffering from breast carcinoma.

PS_184

ROLE OF 99MTC-SESTAMIBI SCINTIMAMMOGRAPHY IN PATIENTS WITH INDETERMINATE MAMMOGRAPHY

A. Bagnato (1), R. Pellegrini (2), R. Tavolaro (1), A. Lanzillotta (1), G. Giannotta (3), A. Scarpelli (2), GB. Gallippi (3), P.C. Loizzo (1). (1) Department of Nuclear Medicine; (2) Department of Surgery; (3) Department of Pathology, Annunziata Hospital, Cosenza, Italy.

The aim of this study was to assess the value of the scintimammography (SMM) with 99mTc sestamibi in the detection of breast cancer in patients whit suspicious mammography (MMx) and ultrasound (US).

Methods: we report 41 patients (39 female and 2 male) with suspected breast cancer to MMx and US. The patient's age ranged from 28 to 67 years, with an average of 47±11 years. They, after routine analysis, were examined by SMM and undergone surgery. In all patients the histopathologic analysis was performed.

Results: the SMM was positive in 33 patients; the histopathologic analysis revealed 27 invasive ductal carcinomas, (20 **T1b N0**, 7 **T2 N0**), 3 lobular carcinoma (**T2 N0**) and one multifocal infiltrating (lobular carcinoma and invasive ductal carcinoma). We also examined two male patients, one of them showed a positive SMM that revealed an invasive ductal carcinoma, the second one carried a pace-maker near to the left breast. He presented with a node in the ipsilateral breast difficult to study by MMx, the SMM was negative and the histopatologic evaluation confirmed that it was a benign lesion. In one of the two patients with clinical suspicion of recurrence, the SMM revealed an ipsilateral axillary node involvement (1,1cm) identified by histopathologic examination as metastatic lymph node. The other patient was normal. The SMM was very useful in a patient with bilateral calcifications, some of them were very suspected with the MMx. The SMM revealed normal breasts and normal axillary nodes, but it showed a parathyroid adenoma; the laboratory analysis revealed a hyperparathyroidism clarifying the presence of calcifications. We obtained only one false positive in a patient with benign lesions.

Conclusions: this study confirms the high diagnostic accuracy of scintimammography with 99mTc-MIBI in the diagnosis of breast cancer.

PS_186

THE CONTRIBUTION OF LYMPHOSCINTIGRAPHY IN SENTINEL NODE BIOPSY IN BREAST CANCER

R.H. Ganatra (1), D. Clarke (2), W. Evans (3), J. Rees (1), R. Mansell (2). (1) Department of Radiology; (2) Department of Surgery; (3) Department of Medical Physics, University Hospital of Wales, Cardiff, UK.

The axillary lymph node status is one of the most important predictors of survival in breast cancer. Conventionally, women with breast cancer undergo axillary sampling or axillary clearance, both of which have associated morbidity. The sentinel lymph node (SLN) is the first draining lymph node from the primary tumour and SLN biopsy is becoming established as an accurate predictor of axillary lymph node status.

In a pilot study of 79 patients, the SLN was localised following a peritumoral injections of ^{99m}Tc nano-colloid, (Nanocoll, Nycomed Amersham UK), and patent blue dye. The preoperative injection of Nanocoll is followed by lymphoscintigraphy and marking of the SLN on the skin surface. At surgery, patent blue dye is injected around the tumour. The SLN is identified by tracing blue lymphatic vessels to a blue lymph node and also by using a hand held gamma-detecting probe. Once localised, the SLN is removed, followed by primary surgery for the breast cancer and subsequent axillary lymph node clearance.

This procedure has identified the SLN in 76 of the 79 patients (96.2%) in our study. Fifty-eight out of 75 patients (77.3%) had a hot node on preoperative lymphoscintigraphy, 65 out of 76 patients (85.5%) had a hot node ineraoperatively and 67 of 76 patients (88.2%) had a blue node. The SLN contained tumour in 27 out of 76 patients (35.5%). In 9 of these 27 patients, the SLN was the only positive node. The SLN was not detected in 3 out of 79 patients (4.0%). Two of these three were node negative and 1 had a single positive node on axillary clearance resulting in a false negative rate of 4.0%.

We conclude from our early results that the SLN in breast cancer can be accurately localised using a combination of lymphoscintigraphy and patent blue dye and that SLN biopsy is an accurate predictor of the axillary node status. Based on these results, a randomised UK trial, the Axillary Lymphatic Mapping Against Nodal Axillary Clearance (ALMANAC) trial is underway. The aims of the trial are to: (1) standardise SLN sampling, (2) assess arm and axillary morbidity and patient quality of life and (3) review cost implications.

DIAGNOSTIC ONCOLOGY 6

PS_185

RADIOGUIDED OCCULT LESION LOCALIZATION (ROLL) IN PATIENTS WITH NONPALPABLE BREAST CANCER: TECHNICAL ASPECTS AND CLINICAL RESULTS

P. Marinelli (1), P. Burelli (2), D. Dalla Libera (3), A. Spina (1), M. Caruso (4), P. Pianca (1), N. Borsato (1). (1) Servizio di Medicina Nucleare; (2) Divisione di Chirurgia; (3) Servizio di Anatomia Patologica; (4) Servizio di Radiologia, Ospedale di Conegliano, Treviso, Italia

ROLL is a promising technique for intraoperative localization of nonpalpable breast cancer (BC) with the aim of performing a conservative surgery. We reported here our experience in ROLL utilization in a group of 57 consecutive patients affected by a nonpalpable suspicious breast lesions preoperatively visualized at mammography or ultrasound (US). In particular, a nodule less than 1.5 cm was depicted in 16 cases and microcalcifications in 41 cases. Four MBq of 99mTc-macrocolloids (99mTc-MAA) were injected within the lesion under stereotactic-mammography guidance or US guidance. In addition, 5 of these patients with a needle cytology positive for BC, were contemporary injected both with 99mTc-MAA to localize the breast lesion and with 99mTc-nanocolloids to visualize the sentinel node. At surgery, performed 18-24 hours after injection, the breast hot spot was easily and quickly localized by an held-hand gamma probe in all cases, and an excisional biopsy of the primary tumor was performed. X-ray check of the excised specimen was also obtained. Pathologic examination revealed benign lesion in 30 patients, while BC was found in 27 patients. Considering the group of BC patients, in 19 cases the BC was found to be located in the middle of the excised surgical specimen and, thus, no further surgery was given. In the other 8 cases (29.6% - all microcalcifications), the lesion was located near the margins of the surgical specimen and, thus, a wide re-operation was required. In 26 patients, axillary lymphoadenectomy was also performed: histological examination revealed metastatic nodes in 5 cases whereas nodes were negative in 21 cases. Interestingly, concerning the group of 5 patients in whom both 99mTc-MAA and 99mTc-nanocolloids were injected, both the primary tumor and the sentinel node were correctly visualized and excised in the same surgical session. Complessively, in 19/27 patients (70.4%) ROLL permitted to perform a conservative breast surgery. On the basis of our data, ROLL proved to be an easy and sensitive technique for the intraoperative localization of occult breast lesions. Moreover, ROLL can be used with therapeutic purposes in patients with a clearly depicted nodular lesion at mammography and/or US examination, and it can play a diagnostic role in BC patients with microcalcifications. Lastly, in our preliminary experience, the contemporary injection of 99mTc-MAA and 99mTc-nanocolloids appears to be an useful procedure to remove both the primary tumor and the sentinel node in the same surgical session.

PS_187

LYMPHOSCINTIGRAPHY (LS) IN COMBINATION WITH PEROPERATIVE BLUE DYE AND GAMMA PROBE TO IDENTIFY SENTINEL NODE (SN) IN BREAST CANCER

N. Besseghir (1), J.F. Delaloye (2), C. Antonescu (1), J.P. Willy (1), A. Bischof Delaloye (1). (1) Department of Nuclear Medicine; (2) Department of Gynecology,CHUV,University Hospital,Lausanne,Switzerland.

Aim : To investigate prospectively if the combined approach using preoperative LS together with intraoperative probe and blue dye detection was necessary for SN identification.

Methods : From January 1998 to December 2000, 105 patients (mean age: 60 years, range: 33 to 88y) with operable pTis-T2 (< 3cm) breast cancers underwent LS the day (16-20h) before surgery with 3 peritumoral and one subdermal injections (70 MBq of ^{99m} Tc- nanocolloidal albumin particles) or with 2 subdermal (20 MBq) injections around the scar when lumpectomy had already been performed. Early dynamic views of the breast and late images were obtained in various projections, starting with the anterior oblique view. A mark was placed on the skin in projection of the detected SN. Then a gamma probe was used to quantify the radioactivity of the SN in comparison with background. Peritumoural and subdermal injection of blue dye (2ml Patent-V) was performed at surgery in 53 patients. A complete axillary dissection was performed after the SN biopsy in our first 40 patients.

Results :LS revealed 1 to 4 SN in 104/105 patients (99%). SN was shown within 90' in 101 patients, it appeared very quickly (< 5') in 15, quickly (< 30') in 18 of them and was delayed (up to 17 hours) in 3 patients. Ipsilateral axillary drainage was present in all 104 SN positive patients. One patient presented in addition a controlateral axillary SN; in 6/24 patients, whose tumour was located in an internal quadrant, visualisation of internal mammary node(s) occurred.Overall detection rate in the operative room was 99% (104/105), 95% (100/105) for the gamma probe, 87% (47/53) for the blue dye. In one patient with a non palpable tumour, the SN could not be identified with either technique. In 4 patients, the SN identified by LS was no longer active (> 19h post injection) at operation or could not be differentiated from tumour activity in the upper external quadrant. 6/7 blue negative SN were detected by the gamma probe.

Conclusions : LS allowed to sensitively follow drainage in one or more lymphatic basins. Peroperatively, addition of blue dye was able to identify all but one probe negative nodes. The 3 methods together shorten the operative procedure and insure reliable SN detection.

PS_188

SENTINEL LYMPH NODE (SN) DETECTION IN PATIENTS WITH BREAST CANCER. INFLUENCE OF TUMOUR SIZE AND AGE OF THE PATIENT

M. Cortés (1), A. Fernández (1), E. Benito (2), D. Azpeitia (2), L. Prieto (2), A. Moreno (2), Y. Ricart (1), A. Escobedo (2), J. Martín-Comín (1).
(1) Department of Nuclear Medicine, Hospital de Bellvitge. L'Hospitalet de Llobregat, Spain; (2) Unitat Funcional de Mama. Hospital Duran i Reynals, L'Hospitalet de Llobregat, Spain.

The aim of the study was to analyse the influence of the age of the patient and tumour size on the accuracy to identify SN in patients with breast cancer.
Material and methods: 165 patients (p) with breast cancer were examined. 16 p. aged under 40, 83p. between 40-60 and 57p. over 60 years. The size of the tumour was classified (in mm) as: 24p. <10, 54p. between 10-20, 55p. between 20-30, and 34p. >30. 81 p. were treated with primary chemotherapy.
All the patients received a dose 3mCi de 99mTc-colloidal albumin in the peritumoral area. 2h after tracer injection scintigraphyc images were obtained. When the SN was detected by lymphoscintigraphy, it was marked on the skin with permanent ink. At surgery SN was localised using a gammaprobe. Histopathologic analysis of SN was done with Hematoxilin-Eosine and inmunohistochemical techniques.
Results: SNs were identified on lymphoscintigraphy in 148 out of 165 patients (90%). 144 of them (97%) were localised in axilla. At surgery axillary SN were localised in 131 cases (3 of them have not been identified on lymphoscintigraphy)

Size (mm)	NLSD %	NSD %	FN %	Age (years)	NLSD %	NSD %	FN %
<10	4	13	0	<40	6	6	0
10-20	2	7	9	40-60	6	10	8
20-30	7	14	11	>60	13	10	10
>30	23	1	6				

NSD: no surgical detection; NLSD: no lymphoscintigraphic detection.

Conclusion: The age of patients and the size of the tumour seem to influence on the SN detection rates and false negative rate seems to be higher in older patients.

PS_189

AFFECT OF EXCISIONAL BIOPSY (BX) OF BREAST MASS ON NEGATIVE PREDICTIVE VALUE (NPV), ACCURACY (ACC) OR SUCCESS RATE (SR) OF SENTINEL NODE (SN) LOCALIZATION

S. Jana (1), M. Dakhel (1), D. Axelrod (2), B. Siegel (2), S. Bhaskaran (1), C. Mills (3), S. Heiba (1), M. Wallack (3), J. Luo (1), S. Sadek (1), H. Abdel-Dayem (1)(1) Nuclear Medicine Service, Department of Radiology, St. Vincent's Catholic Medical Centers of New York; (2) St. Vincent's Comprehensive Cancer Center; (3) Department of Surgery, St. Vincent's Catholic Medical Centers of New York.

AIM: The regular belief is, lymphatics are disrupted during prior surgery leading to diversion of lymphatic channels thereby causing either failure to localize SN or localization of lymph node(LN) which may not be the real SN. So, we are evaluating if prior excisional Bx of the breast mass significantly lowers the Success Rate, Sensitivity, ACC and NPV of SN localization. METHODS: 45 patients(pts) had SN localization 2-8 weeks following excisional Bx of the breast lump. Of these pts, 34 had SN localization by both Radio Colloid(RC) & Blue Dye(BD), and 9 pts had RC alone. 31 pts had axillary LN dissection irrespective of the pathology results of the SN. Approximately 10MBq ^{99m}Tc unfiltered sulfur colloid in 0.3-0.4ml was injected intra/subdermally above and below the breast scar 2-4hrs before surgery. Dynamic & static images were interpreted by 2 observers. At surgery BD was injected intraparenchymally, 4-6 places around the cavity. All LNs having counts >10 times of back ground activity, whether BD+ve or not, and all BD+ve LNs whether RC+ve or not were excised and labeled accordingly. All LNs were sent for frozen section, H&E and immunohistological(Cytokeratin) staining. RESULTS: The Avg. age was 51yrs. The concordance rate of RC&BD was 85%(29/34), of these pts, 3 were both RC&BD-ve (1 had hematoma after excision), all these 3 pts underwent axillary LN dissection and found to have no axillary LN metastases. The discordance was 15%(5/34), of these 3pts were BD-ve RC+ve and 2 were RC-ve BD+ve. In the 31 pts who had axillary LN dissection the success rate, Sensitivity, NPV and ACC using different methods are compared in the Table. CONCLUSIONS: BD method performs better than RC after excisional Bx, however, best results are achieved by the combined method using RC&BD. BD had no false negatives most likely because of intraparenchymal injections. In our study, SN approach preserved a high NPV even after excisional Bx contrary to the regular belief of excisional Bx as one of the causes for false negative results.
Comparison of Success Rates, Sensitivity, NPV and Accuracy

PRIVATE Method	Success Rate	Sensitivity	NPV	Accuracy
Radio-Colloid	84%(38/45)	89%(8/9)	94%(17/18)	96%(25/26)
Blue Dye	82%(28/34)	100%(5/5)	100%(16/16)	100%(21/21)
Combined	91%(31/34)	100%(7/7)	100%(16/16)	100%(23/23)

PS_190

RADIATION EXPOSURE TO THE PERSONNEL DURING RADIO-GUIDED SENTINEL LYMPH NODE (SLN) SURGERY IN DIFFERENT TUMOR TYPES

W. Brenner (1), H. Ostertag (2), S. Hoeft (3), C. Muhle (1), S. Maune (3), S. Lieschner (4), A. Hauschild (4), J. Luettges (1), N. Czech (1), W.U. Kampen (1), E. Henze (1)(1) Clinic of Nuclear Medicine; (2) Clinic of Gynecology; (3) Clinic of Otorhinolaryngology; (4) Clinic of Dermatology, Christian-Albrechts-University, Kiel, Germany

The aim of this study was to assess the radiation exposure to the personnel in the operating room (OR) and in the pathology work area caused by radioguided SLN detection in breast cancer, head and neck tumors, and melanoma patients.
Methods: In a total of 33 patients with either breast cancer (n = 15), head and neck tumors (n = 7), or melanoma (n = 11) undergoing tumor resection and radioguided SLN surgery after injection of 30 MBq Tc-99m-nanocolloid dose rates were obtained at the beginning of the operation 1-4 h p.i. and during the subsequent pathological work-up at various distances from the tumor: at 2.5 cm (finger dose), and 30 cm (whole-body dose) for the surgeon, and at 100 cm for the OR nurses. For the pathologist distances of 2.5 cm and 30 cm from the tumor specimens were used.
Results: In the OR the mean dose rates [_Gy/h] irrespective of the tumor type were 85.5 ± 42.1 at 2.5 cm, 3.37 ± 2.49 at 30 cm, and 0.88 ± 0.59 at 100 cm. Pathology work area: 43.5 ± 25.9 at 2.5 cm, and 1.66 ± 1.49 at 30 cm. From these data whole-body and finger doses were calculated for 100 operations per year assuming a mean radiation exposure time of 30 min for the breast and melanoma teams, 300 min for the head and neck team, and 20 min for the pathologist. Under these conditions the mean finger dose is 4.28 / 4.28 / 42.8 mGy for the surgeons of the breast / melanoma / head and neck team, respectively, and 1.45 mGy for the pathologist. Whole-body doses are 0.17 / 0.17 / 1.7 mSv for the surgeons, and 0.04 / 0.04 / 0.4 mSv for the OR nurses of the breast / melanoma / head and neck teams, respectively, and 0.06 mSv for the pathologist.
Conclusions: For staff members of the breast and melanoma teams and in the pathology a classification as radiation exposed workers (whole-body dose > 1 mSv per year) according to the Euratom guidelines is not necessary under the given conditions. However, surgeons of the head and neck team are to be classified as occupational radiation exposed workers due to the significantly longer operation time when performing tumor resection and neck dissection.

PS_191

THE VALUE OF VERTICAL ANGLE DUAL-HEAD GAMMA CAMMERA IMAGING TECHNIQUE IN THE PRE-OPERATIVE SENTINEL LYMPH NODE SCINTIGRAPHIC MAPPING

Y. Chen, M. Ho. department of gastrointestine surgery, Chou-Ho memorial hospital, Kaohsiung, Taiwan, China.

Intra-operative gamma probe detection of previous administered sulfur colloids allows the surgeon to identify localization of the initial incision. However, it is time-waste seeking procedure and may be interfered with scattering radioactivity from original injected point or breast soft tissue attenuation. In this article, we will introduce the pre-operative vertical angle dual-head camera scintigraphic mapping technique to assist intra-operative gamma probe detection in quick and accurate localization of sentinel lymph nodes.
Methods: We collect 36 female patients who were diagnosed as malignant breast tumors with or without previous cytological /pathologic result. The average age of our patients is 42 year-old. The pre-operative lymphoscintigraphic mapping was performed thirteen to fifteen hours before surgery. Tc99m labeled sulfur colloid, without filtration was administered around four corners of the breast lump by intradermal and peritumor injection techniques. Each corner of injected point was received 0.2 mCi Tc99m sulfur colloid with 0.9cc in volume. Supine and both hand-raised above head position was required. Image acquisition was performed by vertical angle dual-head gamma camera (LEHR collimator, Siemens E com) for anterior and lateral images. When the radioactivity of SLNs in two directions was identified on the monitor, we use point source to localize the related position and two points of skin marker were drawn. The central focus between these two projective skin markers was indicated point for initial detection or incision.
Results: There are total 18 in the right breast and 22 in the left, respectively. The numbers of tumors, which distribute in the different location of breast, are shown as: UOQ (30), UIQ (3), IOQ (1), IIQ (2) and nipple (4). Among detected SLNs in our cases, the axillary direction of lymphatic drainage is mostly found. Multiple clusters of SLNs are seen in two cases. Due to elder age, only one case can't be detected SLN after 2hr images. There is nearly 100% correlation between the localization of previous scintigraphic mapping and results of intra-operative gamma probe detection.
Conclusions: The vertical angle dual-head camera images simultaneously reveal the clear distribution and correct depth of SLNs from both anterior and lateral projection. Because the pre-operative mapping by this technique provides exact localization of SLNs, the detection of gamma probe becomes more quick and accurate during operation.

PS_192

PROSPECTIVE INTRAINDIVIDUAL COMPARATIVE STUDY FOR ASSESSMENT OF PERITUMORAL AND SUBAREOLAR APPLICATION OF TC-99M-NANOCOLLOID IN SENTINEL NODE DETECTION IN BREAST CANCER

S. Maza (1), K.J. Winzer (2), L. Geworski (1), A. Zander (1), J. Mueller (2), D.L. Munz (1). (1) Clinic for Nuclear Medicine; (2) Clinic for Surgery, Charite, Berlin, Germany.

Aim: The scintigraphic detection of sentinel nodes (SN) in breast cancer (BrCa) is widely accepted, the application mode (intratumoral (IT), peritumoral (PT), subcutaneous (SC), subareolar (SA)) is still discussed controversially. Difficulties due to anatomic condition (breast and tumor size, non-palpability, and sonographically not precisely locally defined or multifocal/centric tumor) might be avoided by SA-injection. Aim of this prospective intraindividual study was to evaluate whether lymph nodes detected after PT-injection are identical with those identified after quadrant related subareolar (QSA) and circum/subareolar (CSA) injection.

Methods: 28 women (32-76 years) with BrCa, palpable or assessed by sonography, without clinical suspicion of lymph node metastases were investigated on two subsequent days. On the first day, 140 MBq Tc-99m nanocolloid were injected at a distance of 1 cm along peripheral tumor margins, in non-palpable tumors guided by sonography. On the following day, 10 MBq were SA injected in the area of the quadrant related to the tumor location (3 QSA-deposits). Immediately thereafter, 30 MBq were SA administered in the remaining quadrants (3 deposits/quadrant). After each application dynamic and static lymphoscintigraphy of corresponding axillary, thoracic and cervical areas were performed in various views with a gamma camera. The results of each phase of investigation were compared with regard to numbers and location of SNs.

Results: In 25/27 patients the injection techniques performed revealed identical SNs (number and location). In 2/27 patients the PT-injection showed an additional SN in the mammaria interna group. After QSA- and CSA-injection SNs appeared within 10 min compared to 1 h on average after PT-injection. In 9/27 patients lymph node metastases could be detected histologically in the SNs: in 2 patients all SNs were positive, in 3 one out of three SNs was positive, in 2 two out of three SNs were positive, in 1 one out of two SNs was positive and in 1 two out of four SNs were positive.

Conclusion: Concerning the axillary nodes SA-injection visualises identical SNs which show up more rapidly than after PT-injection. Additional parasternal nodes can appear following PT-injection but, if regarded as therapeutically irrelevant, the tracer can be applied by simple QSA-injection.

PS_193

IDENTIFICATION OF SENTINEL LYMPH NODE IN BREAST CANCER BY SURGICAL GAMMA PROBE WITH PERITUMORAL TC 99M MIBI AND TC 99M SULFUR COLLOID INJECTION

P. Arıcan (1), E. İbiş (1), G. Aras (1), R. Çam (2), N.Ö. Kücük (1), S. Koçak (2), A. Soylu (1). (1) Department of Nuclear Medicine; (2) Department of Surgery, Ankara University, Ankara, Turkey.

Aim: To evaluate the efficacy of intraoperative gamma probe (IGP) with peritumoral injection of ^{99m}Tc MIBI and filtered ^{99m}Tc sulfur colloid in sentinel lymph node (SLN) detection in breast cancer for the deciding of axillary dissection.

Material-Method: 30 patients with T1/T2 breast cancer had peritumoral injection of ^{99m}Tc MIBI (74MBq/0.2ml at 4 different locations) and 42 patients had peritumoral injection of filtered ^{99m}Tc sulfur colloid (lymphoscint, Amersham, UK) (50 MBq/0.2ml at 4 different locations) 18-20 hrs before the surgery. Anterior, anterolateral and lateral spot images were taken at 10, 45, 60, 120 minutes and 24 hrs. Counts were later collected from the injection site, affected breast tissue, internal mammaries, axillary and supraclavicular regions and contralateral side by using the gamma probe during the operation. Peritumoral blue dye was also injected at surgery. The first lymph nodes with counts twice the background tissue and/or with blue dye uptake were surgically isolated, modified radical mastectomy and axillary dissection were performed; histopathological and immunohistopathological evaluations were made on SLN and other exciced tissues.

Results:

In the ^{99m}Tc sulfur colloid study, after demonstration of lymphatic drainage by lymphoscintigraphy in 42 patients, SLN was detected by IGP in 35/42. In 19/35 metastasis was histopathologically identified, axillary metastasis was also observed in 17/19. The correlation of IGP and histopathology was 95.2% in this group. In the study with ^{99m}Tc MIBI lymphatic drainage was demonstrated by lymphoscintigraphy in 30 patients. In 25/30 SLN was detected by IGP, metastasis was histopathologically demonstrated in 14/25 and axillary metastasis was observed in 14/14. There was a 100% correlation between IGP and histopathology.

Conclusion: In the demonstration of lymphatic drainage and detection of SLN by IGP in breast cancer, similar results were obtained with ^{99m}Tc MIBI and ^{99m}Tc sulfur colloid.

PS_194

DETECTION OF SENTINEL NODES WITH AN IMAGING PROBE IN PATIENTS WITH BREAST CANCER

P.G.H.M. Raijmakers (1), N.M. Bruin (1), A. Van Lingen (1), E. Baumann (2), R. Pijpers (1), T. Ijbema (3), G.J.J. Teule (1). (1) Department of Nuclear Medicine, Free University Medical Center, Amsterdam, The Netherlands; (2) Eurorad, CIT, Strassbourg, France; (3) PI-Medical Diagnostic Equipment Bv, Joure, The Netherlands.

New developments in probe guided surgery include the design of hand held imaging devices. Currently hand held gamma probes are frequently used to localise sentinel nodes (SN) in patients with breast cancer. A hand held imaging probe might add additional information about the exact location of SN('s) during surgery.

Aim: We studied the physical and clinical properties of a prototype of an imaging probe consisting of a 16x16 array of CdTe elements with a field of view of 5x5cm.

Methods: One day prior to surgery 18 patients with breast cancer were injected peritumourally with 100 MBq 99mTc-colloidal albumin. Gammacamera images and probe images were obtained about 4 hours after injection. The imaging probe was placed at the lateral side of the axilla and images of 60 or 120 seconds were obtained. During acquisition only unprocessed images were available. We used Matlab 5.3 (SE) for image processing. We scored the number of axillary foci in probe and gammacamera images without knowledge of the clinical data. During surgery only the data of the gammacamera images were available.

Results: Conventional imaging revealed a total of 21 SN's and 15 second echelon lymph nodes while the probe images revealed 19 SN's and 11 second echelon lymph nodes. In 1 patient the imaging probe failed to detect a single SN seen on the gamma camera (1 SN found during surgery). In 2 patients the gammacamera revealed 2 SN's while the probe detected only 1 SN (during surgery in both patients only 1 SN was found). In 1 patient the probe detected 2 SN's while the gammacamera detected only 1 SN (during surgery 2 SN's were found).

Conclusions: Image quality of the probe images was less than camera images. The majority of the SN's found with a gamma camera were also detected with this imaging probe. However, discordant results were obtained in 4 of the 18 patients (the probe image predicted in 3 of these 4 patients the number of SN's found during surgery, but missed 1 SN). After technical improvements of the imaging probe further study of this device during surgery is necessary.

PS_195

IN VIVO EVALUATION OF DIFFERENT RADIOCOLLOIDS USED FOR SENTINEL LYMPH NODE DETECTION

G. Andocs (1), I. Sinkovics (2.), L. Balogh (1.), K. Bodo (1.), A. Polyak (1.), G. Janoki (1.). (1) National Research Institute for Radiobiology and Radiohygiene; (2) National institute of Oncology, Budapest, Hungary.

Various colloidal radiopharmaceuticals are widely used for imaging and intraoperative identification of the sentinel node in carcinoma of breast and melanoma.Particle size of the colloid is a primary consideration when a radiocolloid is chosen for clinical use.

Aim of this study was to compare the connection of the particle size and the migration rate in the lymphatic system in case of different radiocolloids, in animal model.

Materials and methods. Four different 99mTc labelled radiocolloids were examined: NanoCIS, NanoColl, Nano-Albumon and Senti-Scint. For the particle size determination a DynaPro dynamic laser light scattering device was used. All colloid was labelled in the same condition: 450 MBq 99mTc in 3 ml and Beagle dogs were used for the animal study. From all colloids 0,1 ml/15 MBq was administered subcutaneously to the Beagle dogs near to the second thoracal mammary gland to both sides. Imaging study was done by a Mediso Nucline X-Ring digital gamma camera. Pictures were taken 5min, 30 min, 1h, 3h, 6h and 24h after the injection. ROI technique was used for follow the uptake and migration. The nodal retention efficiency was calculated.

Results. To order of particle sizing were NanoColl, Nano-Albumon, NanoCIS and Senti Scint and ranged between 10-300 nm. In the animal study NanoColl and Nano-Albumon showed very fast migration rate with high nodal uptake.1-2 node(s) were visualised in the late images. Senti-Scint showed the slowest migration rate, but the nodal uptake was relatively high in late images and always 1 lymph node was visualised.

Conclusion. All the examined radiocolloids are suitable for the sentinel node imaging, but compounds with smaller particle size are better for 1 day sentinel node imaging and surgery protocol , while colloids with larger particles can be suitable for 2 days protocols. Evaluation of currently used radiocolloids may help to develop new and ideal radiopharmaceutical for sentinel node imaging and surgical identification.

PS_196

PREOPERATIVE LYMPHOSCINTIGRAPHY IN THE LOCALISATION OF THE SENTINEL LYMPH NODE IN BREAST CANCER

R.H. Ganatra (1), D. Clarke (2), W. Evans (3), J. Rees (1), P. Facey (1), R. Mansell (2). (1) Department of Radiology; (2) Department of Surgery; (3) Department of Medical Physics, University Hospital of Wales, Cardiff, UK.

Sentinel lymph node (SLN) biopsy is a recognised technique in the management of patients with breast cancer. However, many centres using this technique omit pre-operative lymphoscintigraphy.
In a pilot study of 79 patients, the SLN was localised preoperatively by lymphoscintigraphy and intra-operatively using both a gamma detector and patent blue dye. Once localised, the SLN was excised, followed by primary surgery for the breast cancer and axillary lymph node clearance.
Using a combination of all 3 technique the SLN was identified in 96.2% of patients (76 of 79 cases). Preoperative lymphoscintigraphy identified a hot node in 77.3% and the intra-operative gamma detector probe identified a hot node in 85.5%. Of the 17 patients who were negative on lymphoscintigram, 7 had a hot node intra-operatively using the gamma probe. Of the 17 patients who did not have a hot node detected by a gamma probe, 6 were found to have a hot node on preoperative lymphoscintigraphy. Using a combination of preoperative lymphoscintigraphy and the intra-operative probe, we were able to localise the SLN in 89.5%.
We conclude that both the preoperative lymphoscintigram and the intra-operative gamma probe are complimentary and a combined technique using both in addition to blue dye should be used for the detection of the SLN in breast cancer.

PS_197

COMPARISON OF SUBDERMAL AND PERITUMORAL INJECTION TECHNIQUES OF LYMPHOSCINTIGRAPHY FOR SENTINEL LYMPH NODE IN BREAST CANCER: EARLY RESULTS

A. Eroğlu (1). (1) Department of Nuclear Medicine; (2) Department of Surgery, Faculty of Medicine, Istanbul University, Istanbul, Turkey.

Aim: Recently, sentinel lymph node (SLN) biopsy has gained importance for axillary staging in patients with breast cancer. Lymphoscintigraphy and intraoperative gamma probe are important guides for sentinel lymph node biopsy. In this study, we investigate the role of two different lymphoscintigraphic injection techniques in the same patient group to determine the SLN in patients with early breast cancer.
Methods: Ten women (mean age:48.7) with stage 1 or 2 breast cancer were prospectively studied. For lymphoscintigraphy, both peritumoral and subdermal injections were performed on each patient with an avarage of 4 days apart. Lymphoscintigraphy with peritumoral injections were obtained about 1-8 days before the surgery. Tc99m-rhenium sulfide colloid (20 MBq/1ml total) was injected into four quadrants around the tumor and 2 hour-delayed static images of anterior and lateral chest of all patients were obtained with a dual head gamma camera. On operation day the lymphoscintigraphy was repeated with 20 MBq /ml Tc99m-rhenium sulfide colloid which was injected subdermally over the breast mass. Dynamic 45 minutes of images and later 5-minute static images of anterior and lateral chest were obtained. After each imaging the SLN(s) were marked on the skin with a indelible marker. All patients had blue dye injections perioperatively, and had breast surgery and axillary curage. The axillary SLNs were found with intraoperative gamma probe and evaluated with histopathology.
Results: In 9 of 10 patients (90%) both injection techniques gave the same axillary drainage pattern (only in 2, the number of SLNs were different). In 6/10 the whole lymphatic drainage patterns were completely identical (i.e. axillary, internal mammary and other routes). In one patient while there was no drainage with peritumoral injection, subdermal injection revealed one axillary SLN. This patient had axillary metastases. There were internal mammary drainage in 3/10 with peritumoral injections and 1/10 with subdermal injections. In both techniques, the visualization rate of infraclavicular or intramammarial lymph nodes was high (4/10).
Conclusions: These preliminary findings show that the visualisation of sentinel lymph node patterns were identical in 60% of patients and similar drainage routes were observed in 90 % of the patients with peritumoral and subdermal injection techniques. The visualization rates of internal mammary lymph nodes were higher in peritumoral techniques. Further studies needed to confirm the results.

PS_198

A NEW METHOD FOR SENTINEL NODE INVESTIGATION : GAMMA DETECTING PROBE ASSOCIATED WITH SPECT EXAMINATION FOR DEPTH

G. Ascoli, D. Fornarelli, S. Piomboni, C. Giambartolomei. Nuclear Medicine - I.N.R.C.A. IRCCS - Ancona, Italy.

AIM : aim of tis study is to magnify the lymphoscintigraphy examination by gamma probe with SPECT acquisition for very accurate detection of depth of axilla node in patients affected by melanoma.
METHODS : according to physiological peculiarities the lymphatic system plays a very important role and represents the most important barrier to neoplastic cells spreading. The "sentinel node" is the first lymph node draining the affected area. The surgical tendence is a "preventive" axillary dissection, even in presence of a clinically negative examination. In fact a hight percentage of clinically negative limph node shows a positive histology (presence of metastatic cells). The nuclear medicine method for researching "sentinel node" is represented by a regional lymphoscintigraphy with normal gamma camera with a large field of view followed by examination with gamma detecting probe and, in following day, controlled in operating room to confirm the presence of the node early identified. We have complete this protocol with SPECT examination of affected axilla by use of injected laboratory capillary around axilla to perform an exact investigation of node depth.
DISCUSSION : Our experience in 150 cases in 18 months shows 100% of axilla "sentinel node" detection, 25 cases with positive hystologic examination and subsequently axillary dissection.
CONCLUSIONS : In conclusion the scintigraphic examination with lymphoscintigraphy represents a good tool for management of patient with melanoma and the use of "targeting" with collimated SPECT represent a very aid for the surgeon in reduction time for detection and dissection of lymph node, with hight reduction of anesthesia duration.

OTHER CLINICAL SCIENCE. GASTROENTEROLOGY 2

PS_199

FUNCTIONAL MAPPING OF REGIONAL LIVER ASIALOGLYCOPROTEIN RECEPTOR AMOUNT FROM SINGLE BLOOD SAMPLE AND SPECT

N. Shuke (1), W. Yamamoto (1), A. Okizaki (1), J. Sato (1), Y. Ishikawa (1), S. Kino (2), K. Nakamura (3), S. Kasai (2), I. Makino (3), T. Aburano (1). (1) Department of Radiology; (2) Department of Surgery 2; (3) Department of Internal Medicine 2, Asahikawa Medical College, Asahikawa, Japan.

The objective of this study was to validate a method for estimating regional liver asialoglycoprotein (ASGP) receptor amount from single blood sample and static SPECT with Tc-99m GSA. Methods: Based on a 2-compartment nonlinear model, regional ASGP receptor amount could be calculated from total liver ASGP receptor amount (Ro) and regional GSA uptake at certain time. Since Ro could be estimated from single blood sample using an empirical formula previously determined ($Ro=P1+P2 \cdot lnVd + P3 \cdot Vd$, P1-3: constants, Vd: plasma distribution volume), regional GSA uptake obtained as SPECT voxel count could be converted to regional ASGP receptor amount by solving the nonlinear model equation. To validate this method, data from 62 patients with chronic liver disease, who underwent dynamic SPECT (30-rotation/30 min) and simultaneous multi-blood sampling, were analyzed by this method. Ro was calculated as the sum of voxel values of parametric receptor image generated from plasma concentration of GSA at 20min and static SPECT image generated by merging dynamic SPECT data (12-20 min). Ro was also estimated by fitting time activity-curves (4-30 min) of plasma and whole liver to the nonlinear model using nonlinear regression method. Ro obtained from the receptor image was compared to that from curve fitting in relation to the results of hepatic function tests (ICG R15, hepaplastin test and branched-chain amino acids/tyrosine plasma concentration ratio) and the Child's classification. Results: Ros from two methods showed a significant linear correlation ($r^2=0.938$, $p<0.0001$, slope=0.90, y-intercept=1.5). Both Ros had significant correlations with the results of hepatic function tests ($p<0.001$) and differed significantly among the three groups of Child's classification ($p<0.0001$). Conclusion: The present method could provide a quantitative ASGP receptor image without dynamic data acquisition. This approach could be useful for quantitative evaluation of regional liver function and estimation of residual liver function in case of hepatectomy.

PS_200

QUANTITATIVE HEPATOBILIARY IMAGING IN EVALUATION OF RESERVED HEPATIC FUNCTION IN PATIENTS WITH HEPATOCELLULAR CARCINOMA BEFORE TRANSCATHETER ARTERIAL EMBOLIZATION

D.L. You (1), Y.M. Lin, V.P. Chuang. (1) Department of Nuclear Medicine; (2) Department of Internal Medicine, Koo-Foundation, Sun Yat-Sen Cancer Center, Taipei, Taiwan; (3) Department of Radiology, Koo-Foundation, Sun Yat-Sen Cancer Center, Taipei, Taiwan.

The purpose of this study is to use quantitative hepatobiliary scintigraphy(QHS) to evaluate reserved hepatic function(RHF) in patients with hepatocellular carcinoma(HCC) before transcatheter arterial embolization(TAE).

Methods: Eighty-two patients(M:F = 63:19 ; age range = 23-72 y/o , mean = 49.6 y/o) with HCC were included in this study. All of patients underwent 15-min retention rate of indocyanine green(ICG-15) and conventional hepatic function tests(HFTs), including total bilirubin (T-Bil), asparatate aminotransfertase(AST), alanine aminotransfertase(ALT), albumin, alkaline-phosphatase(Alk-P), prothrombin time(PT). QHS was done within 2 days after ICG-15 and HFTs and was performed after intravenous injection of 222MBq of Tc-99m diisopropylphenyl imino diacetic acid with 60 secs/frame for 60 mins. The hepatic extraction fraction(HEF), peak time of uptake(PTU) and clearance half time(T1/2) were calculated. The correlation analysis between HEF, PTU and T1/2 and ICG-15 and HFTs were studied using Pearson correlation method. The value of P<0.05 was considered significant.

Results: There was significant correlation between HEF and ICG-15, T-Bil, AST, ALT, albumin, Alk-P, and PT(Table). There was also significant correlation between PTU and T1/2 and ICG-15, T-Bil and Alk-P. Discrepancies between ICG-15 and HFTs occurred in 8 patients; however, the values of HEF in these 8 patients correlated well with HFTs.

	HEF		PTU		T1/2	
	r	P<	r	P<	r	P<
ICG-15	0.463	0.001	0.464	0.03	0.457	0.03
T-Bil	0.402	0.0001	0.457	0.0001	0.343	0.001
AST	0.397	0.002	0.180	NS	0.098	NS
ALT	0.413	0.002	0.054	NS	0.006	NS
Albumin	-0.369	0.005	-0.166	NS	-0.172	NS
Alk-P	0.433	0.02	0.305	0.01	0.321	0.009
PT	0.236	0.02	0.182	NS	0.118	NS

Conclusion: HEF, PTU and T1/2 are potential indicators for RHF in patients with HCC before TAE, and HEF could be a single indicator for RHF. HEF, reflecting true RHF more closely, could be used as a final arbitration when discrepancy between ICG-15 and HFTs occurs.

PS_201

TL-201 PER RECTUM SCINTIGRAPHY IN CHRONIC LIVER DISEASES: PROPER HEPATIC LOCALIZATION OF HEPATIC REGION OF INTEREST (ROI) IN PATIENTS WITH INHOMOGENEOUS HEPATIC UPTAKE PATTERN

Y.Y. Choi (1), S. Cho (1), M.H. Lee (2). (1) Department of Nuclear Medicine; (2) Department of Internal Medicine, Hanyang University Hospital, Seoul, South Korea.

Aim: Heart to liver uptake ratio(shunt index) on Tl-201 per rectum scintigraphy(PRS) is one of the useful indices in assessment of portal systemic shunt. However, hepatic uptake of Tl-201 is inhomogeneous in many cases, and therefore hepatic ROI selection can affect the value of shunt index. The purpose of this study was to choose the proper location of hepatic ROI whose shunt index best correlate with histopathologic diagnosis.

Methods: Eighty patients with biopsy-proven chronic liver disease(35 chronic hepatitis and 45 LC) showed inhomogeneous hepatic uptake pattern on PRS. After instillation of 18.5MBq of Tl-201 into upper rectum, sequential images(30sec/frame) and time-activity curve were obtained for 25 minutes. Shunt indices were calculated from three ROIs [increased uptake zone(IUZ), porta hepatis zone(PHZ), decreased uptake zone(DUZ)], and correlation between shunt index and disease severity (histopathologic diagnosis) was evaluated using Spearman's rho test.

Results: The shunt indices showed different values according to the location of hepatic ROIs in each disease group(p<0.01), respectively. The shunt index from hepatic ROI in PHZ showed strongest positive linear correlation with the disease severity(from CPH to LC) (Speaman's rs=0.511)

Diagosis	Shunt index in each of hepatic ROIs			T-test
	IUZ	PHZ	DUZ	CPH(n=6)
CAH, mild(9) CAH, moderate(13) CAH severe(7)	0.19 (n=22)	0.20 (n=35)	0.38 (n=28)	*p = 0.000*
LC (n=45)	0.29 (n=33)	0.45 (n=45)	0.50 (n=29)	*p = 0.000*
T-test	*p = 0.018*	*p = 0.000*	*p = 0.053*	
Spearman's rs	*0.257 (p=ns)*	*0.511(p=0.001)*	*0.256 (p=ns)*	

Conclusion: Proper localization of hepatic ROI is important for correct calculation of shunt index. In our study, shunt index obtained from the hepatic ROI in PHZ best correlated with the histopathologic diagnosis in patients with inhomogeneous hepatic uptake pattern on Tl-201 PRS.

PS_202

THE ROLE OF THE HEPATIC RADIONUCLIDE ANGIOGRAPHY IN THE PORTAL PERFUSION ASSESSMENT IN CIRRHOSIS AND LIVER TUMOURS

V. Artiko (1), V. Obradovic (1), M. Petrovic (2), N. Petrovic (1), M. Perisic (2), S. Janosevic (3), K. Kostic (1), V. Bosnjakovic (1). (1) Institute for Nuclear Medicine, Clinical Center of Serbia; (2) Institute for Digestive Diseases, Clinical Center of Serbia; (3) School of Medicine, Belgrade.

Aim: The aim of the study is the examination of the relative portal blood flow, by assessment of the hepatic perfusion index (HPI) in different degrees of hemodynamic alterations related to liver cirrhosis and some focal liver diseases.

Methods: Hepatic radionuclide angiography (HRA) was performed with bolus injection of 740 MBq- 99m-Tc-pertechnetate, during one minut (1f/sec), using ROTA scintillation camera and Micro Delta computer Siemens). HPI was estimated using Sarper's method of slope analysis.

Results: In 10 controls (C), HPI was 0.68+/-0.06; it was significantly decreased (p<0.01) in 5 patients with chronic active hepatitis (HAH, 0.57+/-0.03), 13 with liver cirrhosis without (LC, X=0.49 +/-0.13) and 18 with esophageal varices (LCEV, X=0.32+/-0.19), as well as in 4 patients with LC and sclerosated esophageal varices (LCSEV, X=0.16+/-0.11). Comparing to HAH and LC (HAH-LC, p>0.05), HPI values were significantly lower in LCEV (p<0.01) and LCSEV (p<0.05), while the values between the last two groups didn't differ (p> 0.05). In 22 patients with liver hemangiomas (LH, X= 0.64 +/-0.08) HPI values were physiological (C-LH, p>0.05). However, in 4 patients with hepatocellular carcinoma (H, X=0.26+/-0.20), and 8 with liver metastases (LM, X=0.40 +/-0.28), HPI values were significantly decreased (p<0.01), but they didn't differ between themselves (H-LM, p>0.05).

Conclusion: Portal liver perfusion decreases in respect to the portal hypertension and collateral circulation development. Thus, significant difference is proved between HPI values in cirrhotic patients with and without esophageal varices, while after sclerotherapy, HPI remains very low. Considering that in patients with hemangiomas, HPI values are normal, which is not the case in those with primary carcinomas and metastases, HRA is an useful method for the differential diagnosis of hemangiomas and primary liver carcinomas, together with ultrasonography and blood pool scintigraphy.

PS_203

DIAGNOSTIC VALUE OF BLOOD POOL SPECT EXAMINATION THE EVALUATION OF LIVER HEMANGIOMAS AND ITS COMPARISON OTHER RADIOLOGICAL METHODS

M. Atalay (1), D. Özer (2), E. Uluc (2), M. Can (2), G. Cekin (1), A. Çökmez (3). (1) Department of Nuclear Medicine; (2) Department of Radiology; (3) Department of Surgery, Atatürk State Hospital, Izmir, Turkey.

The aim of this study is to differentiate hemangiomas using liver blood pool SPECT studies with Tc99 m labeled enrythrocytes,MRI and dynamic C.T in the hyperechogenous masses established in USG examination and to compore the efficiency of these methods.

Methods: 32 masses have been studied in 22 cases, ranging from 19 to 80 in age.

Results: Hemangioma diagnosis have been established in 19 masses out of 12 cases. We have found that USG has %58 specificity, CT has %75,MRI and SPECT have %83 specificities respectively.USG specificity has been found to be lover than those of other methods. In view of detecting liver hemangiomas.Although CT specificity has increased in determining hemangiomas, other methods have needed to be resorted for the purpose of establishing definitive diagnosis in most cases. In our study MRI and SPECT have shown almost egual specificties. However both methods have proved unsuccessful in differentiate cases.The liver hemangiomas cases which MRI failes to detect are those which show no diagnostic findings in examinations. Those which can not be detected during SPECT examinations are lesions which are localized near or close to vascular structures and less than 2 cm in diameter.

Conclusions: The blood pool SPECT can be tolereted by cases easily, has lover cost, and shows higher specificity, it is a method which must be preferred before MRI in cases of liver hemangiomas suspected by other radiolgic examinations.

Poster presentation

PS_204

ACCUMULATION DYNAMICS OF 99MTC LABELLED RED BLOOD CELLS IN LIVER HEMANGIOMA

N. Petrovic, V. Obradovic, V. Artiko, K. Kostic, V. Bosnjakovic. Institute of Nuclear Medicine, Belgrade, Yugoslavia.

AIM: The aim of the study was to examine the dynamics of acumulation of ^{99m}Tc labelled red blood cells (RBC) in liver hemangioma by means of early dynamic blood pool scintigraphy as well as delayed sequential blood pool scintigraphy.
PATIENTS AND METHODS: Eleven patients (8 females, 3 males) with total number of 14 liver hemangiomas have been examined. Nine patients had solitary lesions, one patient had two hemangiomas and another one three hemangiomas. In nine patients with solitary liver hemangioma a 30 min dynamic acquisition (15 frames/min) have been initiated at the same time as intravenous injection of ^{99m}Tc pertechnetate (last step of in vivo RBC labelling). After regions of interest delineation, corresponding hemangioma, liver tissue and heart time-activity curves have been generated, back-ground subtracted and filtered. The last 10 min portions of each curve have been fitted to linear equation and the slopes of the portion have been determined.
In all patients planar blood pool scintigrams 40, 60, 120 and 180 min after in vivo ^{99m}Tc labelling of RBC have been performed. Following back-ground subtraction and ^{99m}Tc decay correction, we calculated blood pool index of hemangioma and liver, as counting rate ratios: hemangioma/heart and liver/heart. These indexes have been calculated for each visualisation time.
RESULTS: The mean slope (0.90) of the hemangioma early blood pool time-activity curve was significantly higher ($p<0.01$) than that of liver curve (0.34). There has been no significant difference ($p>0.05$) between mean slopes of the time-activity curves of liver and heart (0.42). (Wilcoxon)
Within the interval 40-180 min after in vivo RBC labelling both blood pool index of hemangioma (mean = 0.84-0.86) and that of the liver (mean = 0.55-0.58) varied insignificantly ($p>0.05$). Blood pool index of hemangioma was much higher than that of liver in every single time of the interval ($p<0.01$).
CONCLUSION: Obtained results indicate that the maximal RBC concentration in hemangioma is not reached within the first 15 min following in vivo ^{99m}Tc RBC labelling. In most hemangioma patients this is accomplished within first 40 min of examination. This is the interval needed for establishing a plateau of labelled RBC concentration in hemangioma. Liver blood pool scintigrams acquired after this period do not contribute significantly to the diagnostic value of the method.

PS_205

TECHNETIUM-99M RED BLOOD CELL SCINTIGRAPHY IN DIFFERENTIAL DIAGNOSIS OF LIVER HEMANGIOMAS AND HEPATIC METASTASES

S. Sergieva (1), G. Kirova (2), V. Ivanov (2), I. Gergov (2), A. Tzonevska (1), A. Chakarova (3). (1) Department of Nuclear Medicine; (2) Department of Radiology; (3) Department of Radiotherapy, National Centre for Active Cancer Treatment, Sofia, Bulgaria.

Purpose: Hemangionas are the most common benign tumours with an incidence amounting to 7%. Many of them are asymptotic and discovered incidentally. What is more, liver is the usual site of metastatic disease from various malignant tumours. The purpose of this work was to determine diagnostic relevance of Tc-99m red blood cell scintigraphy with Tc-99m MDP-RBC in distinction between liver hemangiomas and hepatic metastases in patients with oncologic diseases.
Patients & Methods: Thirty - seven patients (pts), 26F/11M, 33-76 ages with various oncologic diseases were studied for a total of 46 liver lesions, detected by abdominal CT and/or US. Tc-99m MDP-RBC scintigraphy was performed dynamically under gamma - camera collimator within 20 min. after application and 2h later using SPECT. Clinical diagnosis was proved by biopsy, laparotomy and pt follow-up.
Results: A total of 33 hepatic „hot" spots was visualised in 27 pts. Comparative assessment of the CT, US and scintigraphic results with the histopathology test showed 2 false positive results in 2 pts with breast cancer liver metastases with size of 18 and 23 mm. Gigantic cavernous hemangiomas ranged from 50 to 70 mm were detected in 6 cases; multiple lesions were imaged in 8 pts; single lesions with the least size of 17 mm were scanned in 11 pts. Scintigraphic results were negative in 10 pts with liver metastases. Sensitivity, specificity and accuracy of this method were 91%,83% and 89% respectively. SPECT application improved image quality for lesions with size under 25 mm.
Conclusion: Blood pool and liver perfusion scintigraphy with Tc-99m MDP-RBC are non-invasive techniques for visualisation of hepatic hemangiomas, necessary for differential diagnosis with metastatic lesions of the liver.

PS_206

EFFECT OF THE LAPAROSCOPIC FUNDOPLICATION ON GASTRIC EMPTYING IN PATIENTS WITH GASTRO-ESOPHAGEAL REFLUX DISEASE

G. Boni (1), M. Anselmino (2), S. Suriano (1), M.G. Bellomini (2), G. Manca (1), M. Grosso (1), D. Volterrani (1), A. Gennai (2), B. Solito (2), R. Bianchi (1), M. Rossi (2)(1) Division of Nuclear medicine, Department of Oncology, University of Pisa, Pisa, Italy; (2) Chirurgia generale IV, Azienda Ospedaliera Pisana, Pisa, Italy.

The effect of fundoplication on gastric emptying is not well investigated, and literature shows contradictory results. Gastring emptying study using radioisotope technique is at present considered the best method for evaluation of stomach kinetic in patients with foregut symptoms. We studied twenty-four patients (17 males and 7 females, median age 48 years, range 21-72) with gastro-esophageal reflux disease detected by esophageal manometry and 24-hour pH-monitoring. All the patients were treated with laparoscopic anti-reflux surgery. There were 12 floppy total (360¡) posterior wraps (Nissen) with complete gastric fundus mobilization obtained with short gastric vessels section, and 12 partial (270¡) posterior fundoplications (Toupet) with partial section of the spleno-gastric ligament. A gastric emptying study was performed before and 9-12 month after operation administering to patients a solid meal (700 Kcal) labelled with colloidal ^{99m}Tc-albumine (18.5 MBq) and recording anterior and posterior images of the stomach up to three hours to calculate the emptying half time (t1/2).
None of the patients had symptoms of delayed gastric emptying such as nausea, post-prandial gastric distension or vomiting before or after operation. A good control of gastroesophageal reflux symptoms was obtained in all patients after fundoplication. Persistent flatulence and need to evacuate after meal was detected in 8 patients after the Nissen procedure and in none of patients who had the Toupet operation. Overall the pre-operative gastric emptying t1/2 was 97±23 min which is similar to our asymptomatic controls (93±21 min, $p<0.01$). This acceleration of the gastric emptying was particularly significant in patients who had total Nissen fundoplication (115±25 min pre-op. and 63±18 min post-op., $p<0.01$) compared to those who had partial Toupet fundoplication (90±12 min pre-op and 74±18 min post-op., $p<0.05$). The subset of patients who had post-operative flatulence and need to evacuate after meal had a further significant decrease in their gastric emptying t1/2 after operation (108±19 min pre-op and 49±18 min post-op., $p<0.01$).
Fashioning of a wrap using the gastric fundus accelerates the gastric emptying in patients with gastroesophageal reflux disease due to lower esophageal sphincter deficiency and without pre-operative delayed gastric emptying. This is true independently from the type of wrap, even if patients who have Nissen procedure experience a greater acceleration of their gastric emptying. Symptoms such as post-operative flatulence and post-prandial need to evacuate are greatly correlated with a further decrease in gastric emptying time.

PS_207

DIAGNOSTIC VALUE OF DETECTION AND QUANTIFICATION OF ENTEROGASTRIC REFLUX BY DYNAMIC SCINTIGRAPHY

V. Obradovic (1), V. Artiko (1), M. Petrovic (2), N. Petrovic (1), H. Chebib (1), V. Bosnjakovic (1). (1) Institute for Nuclear Medicine; (2) Institute for Digestive Diseases, Clinical Center of Serbia.

Aims and material: We investigated 162 patients with: duodenal (21) and gastric (15) ulcer, after Billroth I (12) and II (7) surgery, with gastroesophageal reflux (GER, 46), after cholecystectomy(28), with cholecystitis (20), with chronic duodenal diseases (13), as well as 10 controls.
Method: Dynamic acquisition was performed after i.v. application of 185 MBq 99m-Tc-EHIDA during 90 min (1f/min), anterior view, with test-meal stimulation in 30th minute. Gaster was labelled with 18 MBq 99mTc-S-colloid in 100 ml of water. According to the maximal and minimal activities of 99m-Tc-EHIDA in hepatobiliary system and gastric region, index of enterogastric reflux (EGR%) and reflux duration were calculated.
Results: Reflux was registered in the controls in small quantity (EGR%=4,4+/-4,2%) exclusively postprandially, lasting shortly (4.3+/-2.0 min). The obtained values were significantly ($p< 0.001$) increased in patients after Billroth II resection(68.8+/-43.7%; 58.4+/-4.0min), with duodenal ulcer (36.6+/-33.0%; 40.3+/-22.2 min), cholecystitis (31.0+/-8.7%; 26.5+/-6.8 min), after Billroth I (28.2+/-22.7%; 34.1+/-12.4 min), postcholecystectomy (27.1+/-17.2%; 37.6+/-19.7 min), with gastric ulcer (24.5+/-13.6%; 21.9+/-10.2 min) with GER (24.5+/-14.9%; 29.6+/-19.5min) and chronic duodenal disease (17.2+/-5.6%; 27.3+/-8.0 min). Quantity of reflux was highly correlated ($r=0.580$, $DF=75$, $p < 0.01$) with its duration. Fasting reflux was detected in 28 out of 75 (37.3%) refluxers in average quantity of 41.0+/-29.7% which was significantly different ($p < 0.01$) from those postprandially detected (23.26+/-16%). Increased values of EGR index are found in 75 (46.3%) patients: 85.7% and 75% after BII and BI gastrectomy, 60% with gastric and 52.4% with duodenal ulcer, 46.1% with chronic duodenal disease, 41.3% with GER, 39.3% with cholecystectomized patients and 20% in those with cholecystitis.
Conclusion: The obtained results prove clinical value of dynamic scintigraphy, as a noninvasive physiological method, in EGR detection and estimation of its quantity and duration.

PS_208

111-IN LABELLED ANTIBODIES IN THE DETECTION OF COLORECTAL CARCINOMAS

V. Obradovic (1), V. Artiko (1), M. Petrovic (2), N. Petrovic (1), B. Davidovic (1), Z. Krivokapic (2), D. Kecmanovic (2), V. Bosnjakovic (1), G. Adanja (1), R. Rebic (1). (1) Institute for Nuclear Medicine; (2) Institute for Digestive Diseases, Clinical Center of Serbia.

Aim: The aim of the study is detection of the recurrences and metastases of colorectal carcinomas using 111-In labelled antibodies B72.3.
Material and method:14 patients has been examined (13 with adenocarcinomas of caecum, colon and rectum and one with squamocellulare colonic carcinoma) from 4 months till two years after surgery, two of them after two months after the end of radiotherapy. Radiochemical purity of the radiopharmaceutical was over 97%. Planar anterior, lateral and posterior scintigrams of thorax, abdomen and pelvis are done after 10 min, 24h, 72 and 96h after i.v. injection of Oncoscint CR-103, containing monoclonal antibodies B72.3 labelled with 150MBq 111-In while tomographic scintigrams of the pelvis are done after 72h.
Results: In 12 patients recurrences of carcinomas (5-12 cm), in 6 recurrences with liver metastasis, and in two only liver metastases were detected and confirmed by surgery. Planar immunoscintigraphy was positive in 8/8 patients with liver metastases and 9/14 patients with recurrences while in 5/14 recurrences were detected only by tomography. US was positive in all patients with liver metastases, CT finding was false negative in two patients with recurrences, while MRI in one. In three patients with recurrences, CEA was not increased. In 4 patients intensive accumulation of labeled antibodies was observed in colostomas, in one with granuloma, as well as in one with recurrence of squamocellulare carcinoma.
Conclusion: With tomography, we can access better distinction of tumour in comparison to other structures and estimation of its size. Other imaging methods (CT,US) have advantage in detection of liver metastases, while immunoscintigraphy is more specific for the assessment of malignant abdominal tumors and extrahepatic metastases. The first results point out that Oncoscint CR-103 can be useful in diagnosis of recurrences and metastases of colorectal carcinoma, viability assessment after radiotherapy and in the choice of the adequate surgical treatment in dependence of the spread of the disease.

PS_209

INCREASED INTESTINAL PERMEABILITY IN PATIENTS UNDERGOING CARDIOPULMONARY BYPASS: 51CR-EDTA EVALUATION

L. Romano (1), V. Valenza (1), M. Rossi (2), M. Mazzone (3), F. Reale (1), A. M. Samanes Gajate (1), S. Guarneri (2), N. Gentiloni Silveri (3), R. Schiavello (2), M. L. Maussier (1). (1) Institute of Nuclear Medicine; (2) Department of Anaesthesiology; (3) Institute of Internal Medicine, Catholic University of Rome, Italy.

Introduction: In patients underwent open-heart surgery with cardiopulmonary bypass (CPB) is well known a splanchnic hypo-perfusion (intestinal blood flow decreases to maintain preferential perfusion of the heart and brain) with increase of gut permeability; this phenomenon interferes with mucous barrier function, allowing translocation of intestinal flora and bacterial products (especially endotoxines).
Aim of the study is to evaluate extent and duration of the gut ischemic damage consequent to cardiac surgery, studying gut permeability (with ^{51}Cr-EDTA) and gastric pH (with naso-gastric tonometer).
Materials and Methods: Ten uncomplicated patients (M/F = 9/1) operated of coronary artery bypass grafting (CABG) under normothermic CPB, were enrolled following informed consent. All patients were underwent this protocol: 1) ^{51}Cr-EDTA test (an oral dose of 80 µCi administered after an overnight fast, followed by fractioned urine collection) was performed a) three days before surgery (basal study) and b) during surgery and following 48 hours; 2) gastric tonometric pH and PCO_2 and gastric PCO_2-$PaCO_2$ (Pg-$PaCO_2$) gradient, were performed during the operation and until the 1th postoperative day.
Results: The percentage (expressed as median value ± standard deviation) of the ^{51}Cr-EDTA recovered in the urine, every six hours, is reported in Table I with the results of tonometry test.

Table I

	Basal	Pre-CPB	6 hours Post- CPB	12 hours Post- CPB	18 hours Post- CPB	24 hours Post- CPB	42 hours Post- CPB
51Cr-EDTA (%)	6.7 ± 4.3	6.5 ± 4.0	12.1 ± 4.8	11.3 ± 5.8	9.5 ± 6.2	3.7 ± 3.7	1.5 ± 1.9
PCO_2- $PaCO_2$ (mmHg)	1.7 ± 1.1	8.6 ± 1.2	18.6 ± 7.0	22.5 ± 8	21.8 ± 8		

In particular, we found a significant increased value of ^{51}Cr-EDTA absorption after 24 hours from CPB (39.1 ± 16.4 %) if compared with basal value, that decreased in the 2th postoperative day (9.99 ± 9.6 %).

Discussion: We collected fractioned urine to test the ^{51}Cr-EDTA absorption and we observed an increased post-surgical gut permeability. This alteration was detected earlier during surgical procedure and it became more relevant in first 24 hours after surgery. A keen physiological recovery of intestinal permeability was found between 24 and 48 hours after surgery so that we described this phenomenon as acute but transient. The behaviour of gastric tonometric data confirmed the gut functional failure in the first post-CPB hours.
Conclusion: The ^{51}Cr-EDTA test has been a useful, easy and reliable tool to investigate post-surgical gut injury.

OTHER CLINICAL SCIENCE. LUNG

PS_210

REST AND EXERCISE QUANTITATIVE LUNG PERFUSION SCINTIGRAPHY IN PATIENTS AFTER SINGLE LUNG TRANSPLANTATION (SLT) FOR IDIOPATHIC PULMONARY FIBROSIS (IPF) AND EMPHYSEMA

A.P. Steinmetz (1), D. Starobin (2), G. Fink (2), M.D. Kramer (2), R. Hardoff (1). (1) Department of Nuclear Medicine, Rabin Medical Center; (2) Pulmonary Institute, Rabin Medical Center, Beilinson Campus, Petah Tikva, Israel.

Introduction: Most of the pulmonary perfusion and ventilation are shifted towards the transplanted lung following successful SLT. This study investigated lung perfusion changes occurring during maximal exercise in patients after successful single lung transplantation.
Patients and Methods: Patient population consisted of 12 stable patients after successful transplantation (52±16 months after surgery). Six patients were transplanted for emphysema and six for IPF. Patients were injected with 0.3 mCi Tc99m-MAA at the peak of upright cycloergometric cardiopulmonary exercise test. Anterior and posterior lung views were obtained 15-30 minutes after the exercise. Following this, patients were injected with 3 mCi Tc99m-MAA in sitting position and resting lung scans were performed in anterior, posterior, right- and left posterior oblique views. Regional lung perfusion was assessed for the upper, middle and lower thirds of each lung.
Results: At rest, total perfusion to the transplanted lung was 76±12% and 24±12% in the native one. Mean perfusion of transplant was higher (83.3±8%) in the emphysema group than in IPF (68.7%±12%; p=0.028). At peak exercise perfusion shifted by 1.42% (95% CI 0.4-2.4) from the transplant to the native lung (p=0.0095); 1.5% in the emphysema group and 1.3 % in the IPF group respectively. Regional quantification analysis showed most of the change in the transplant was a shift away from the lower third (from 30.5 % to 28.9%; p=0.037) to the middle and upper thirds.
Conclusions: Following successful SLT, most of the perfusion is directed towards the transplanted side. During exercise there is a small shift towards the native lung. The proposed explanation is that vascular bed of the transplant is fully dilated, possibly due to denervation. At increased cardiac output during exercise the native lung is recruited to accept the additional load.

PS_211

I-123 MIBG SCINTIGRAPHY IN THE DETECTION OF AMIODARONE INDUCED PULMONARY TOXICITY

G. Durmus Altun (1), A. Altun, Y.S. Salihoğlu, A. Sarıkaya, G. Özbay, S. Berkarda. (1) Department of Nuclear Medicine; (2) Department of Cardiology, Trakya University Medical Faculty, Edirne, Turkey.

Amiodarone (AM) is a potent antidysrhythmic agent that is limited in clinical use by its adverse effects, including potentially life-threatening AM-induced pulmonary toxicity (AIPT). The lung plays an important role in the metabolization of the circulating vasoactive substance noradrenalin (NA). Iodine-123 metaiodobenzylguanidine (MIBG), radio-iodinated analogue of the adrenergic neurone-blocking agent guanethidine, shares the same uptake and metabolic pathways with NA. The aim of this study was to evaluate the potential of MIBG scintigraphy as a diagnostic tool for the assessment of AIPT.

Methods: Fifteen White New Zeland rabbits with initial mean body weight 4.1±0.2 kg were divided into two groups. AIPT group (n=10) was administered AM (20 mg/kg BW) ip as a 5% aqueous solution for 6 week. The control group (n=5) was administered the same amount of 0.9% saline. I-123 MIBG scintigraphy and Tc-99m DTPA radioaerosol inhalation lung scintigraphy was performed all subject. Histopathologic (HP) evaluation of the lung was performed and AIPT group was divided into two subgroups according to HP. AIPT-I had interstitial pneumonitis (n=4) and AIPT-II had interstitial fibrosis (n=6).

Results:

Group	DTPA-lung clearance (min)	I-123 MIBG early lung-to-background ratio	I-123 MIBG lung clearance
(%) ABAT-I (n=4)	40±13	1.75±0.4	37±16
ABAT-II (n=6)	115±27	1.50±0.2	53±12
Control (n=5)	54±7	1.27±0.08	37±4
P	0.02	0.03	0.04

Conclusion: We concluded that Tc-99m DTPA radioaerosol inhalation lung scintigraphy is valuable for diagnosis of AIPT histopathologic subtype, and I-123 MIBG scintigraphy can be demonstrated in amiodarone induced interstitial fibrosis, but not demonstrated interstitial pneumonitis.

PS_212

COMPARISON WITH CLEARANCE OF TC-99M DTPA AEROSOL, AND CO DIFFUSING CAPACITY, AND LUNG FUNCTION TEST IN HOUSE PAINTERS

M. Kaya (1), A. Salan (1), E. Tabakoğlu (2), N. Aydoğdu (3), M. Yüksel (1), Y.S. Salihoğlu (1), O.N. Yiğitbaş (1), S. Berkarda (1). (1) Department of Nuclear Medicine; (2) Department of Chest Disease; (3) Department of Physiology, Trakya University, Edirne, Turkey.

An increased risk of airway problems have been shown in the house painters.The objectives of this study were as follows: (1) to investigate changes in lung permeability in house painters using the rate of inhaled Tc-99m DTPA as a permeability index; and (2) to compare with CO diffusing capacity, and lung function test in house painters.

Methods: 10 non-smoking house painters (28,8 ± 8,76 yrs) and 10 healthy voluntary non-smoking subjects carried out Tc-99m DTPA aerosol scintigraphy. After inhalation of radiotracer through a nebulizer for 5 minutes, dynamic scintigrams (1 frame/min, up to 10 min) were taken from both lung. ROI's were drawn over the both lung area, and time-activity curves were obtained and half-time ($T_{1/2}$) of DTPA was measured from the curves. CO diffusing capacity was measured in all house painters.

Results: The mean $T_{1/2}$ values (min ± SD) were calculated to be 93,74 ± 32,79 for house painters, and 90,96 ± 40,02 for control group, respectively. There was no significantly differences between house painters and control groups. We found a positive correlation between the mean $T_{1/2}$ and duration of working (mean; 14,9 ± 8,2 yrs), and also a negative correlation to CO diffusing capacity (mean; 35,25 ± 9,64 ml/min/mmHg) (r=0,78, p=0,007; r=0,82, p=0,006), respectively. We did not found any correlation between the mean $T_{1/2}$ and the other spirometric measurement.

Conclusion: Our preliminary findings indicate that lung epithelial permeability in house painters is normal when using Tc-99m DTPA aerosol scintigraphy.

PS_213

WATER-PIPE (NARGHILE) SMOKING EFFECTS ON PULMONARY PERMEABILITY COMPARED TO PASSIVE SMOKERS

A. Aydın (1), G. Kiter (2), H. Durak (1), E.S. Ucan (2), G. Çapa Kaya (1), E. Ceylan (2). (1) Department of nuclear medicine; (2) Department chest disease,Dokuz Eylül University School of Medicine, Izmir, Turkey.

Harmful effects of cigarette smoking on respiratory system and health have been investigated widely. But water-pipe smoking (narghile,hubble-bubble) effects have not been investigated enough. The aim of our study was to search the effects of water-pipe smoking on pulmonary function and respiratory system. Because water-pipe smoking habit needs a special instrument, it is smoked in some definite cafes. At that point water-pipe smokers become passive smokers at the same time, so we selected our control group from passive smokers. Technetium-99m diethylene triamine penta-acetate (99mTc-DTPA) inhalation scintigraphy technique was used for local and global evaluation of lungs.14 water-pipe smoker volunteers (all men, mean age 53.7±9.8) and 11 passive smoker volunteers (1 women ,10 men ,mean age 43.8± 12) were included in this study. 40mci Tc-99mDTPA was inhaled for 3 minutes in supine position using Ventiscan Biodex III nebulizer. Lung images were obtained from posterior projection for every one minute during 30 minutes. Regions of interest were drawn around the periphery of the lungs ,on the major airways and upper,middle and low zones of the lungs.Time activity curves were obtained with decay correction for Tc-99mDTPA. Clearance half-time was calculated by placing a monoexponential fit on the curves. Penetration index was also calculated by dividing the peripheric counts to the sum of the peripheric and central counts. Student's t-test was used for statistical analysis.

Tc-99mDTPA and pulmonary function results	Water-pipe smokers	Passive smokers	P value
Total penetration index	58 ± 14	50 ± 12	insignificant
Total central clearance (min)	55.8 ± 23.5	80.1 ± 35.2	0.025<p <0.05
Total peripheral clearance(min)	57.3 ±12.7	64.6 ± 13.2	0.025<p <0.05
FEV1/FVC	81.6±8.51	87.7±6.52	0.025<p< 0.05

According to our findings, FEV1/FVC ratio and peripheral clearance were significantly decreased in water-pipe smoking group. Compared to passive smokers, increased central mucociliary clearance in water-pipe smoking may be due to increased humidity of the airway tracts.

PS_214

EVALUATION OF ALVEOLO-CAPILLARY MEMBRANE PERMEABILITY AND PULMONARY PERFUSION ABNORMALITIES IN PATIENTS WITH TYPE II DIABETES MELLITUS

G. An (1), Ö. Özdoğan (2), B. Değirmenci (2), O. Itil (1), A. Çömlekçi (3), H. Ellidokuz (4). (1) Department of Chest Disease; (2) Department of Nuclear Medicine; (3) Department of Endocrinology; (4) Department of Public Health, Dokuz Eylül University, Medical School, Izmir, Turkey

Diabetes Mellitus (DM) is a chronic, systemic, metabolic disease that affects pulmonary system secondary to diffuse microvascular disease. The aim of this prospective study was to evaluate the alveolo-capillary membrane permeability changes, pulmonary perfusion abnormalities, pulmonary function tests (PFT). To define the relations of the results with the duration of DM, the presence of microvascular disease and the degree of diabetic control in patients with DM.

Methods: 25 patients (5 women, 20 men) with type II DM were included in the study. The mean duration of disease was 9.4±7.5 (0-30) years. 10 healthy individuals (6 women, 4 men) were included in the control group. The mean ages both groups were 55.6±9.9 (33-68) and 46.8±10.4 (33-65) respectively. Tc-99m DTPA aerosol inhalation scintigraphy, Tc-99m MAA lung perfusion scintigraphy, PFT, ophthalmoscopic eye examination, determination of HbA1C levels, determination of creatinine, protein and microalbumin levels in 24-hour urine sample were obtained. The perfusion scintigraphy was evaluated qualitatively and the aerosol inhalation scintigraphy was evaluated qualitatively and quantitatively by calculating peripheric penetration indexes and alveolo-capillary clearence time of whole lungs and upper, middle and lower zones.

Results: Microvascular disease was detected in 12 (48%) and diabetic control was poor in 6 (24%) patients. There was no statistical difference in clearence time and peripheric penetration indexes between DM patients and control group although the clearence time of both upper zones is longer in DM patients than in control group and in patients with microvascular disease. The duration of DM and the level of diabetic control (HbA1C) had no affect on clearence time, peripheric penetration indexes and pulmonary perfusion abnormalities. Small subsegmenter and nonsegmenter perfusion defects were observed in 6 out of 12 patients (50%) with microvascular disease and 3 out of 13 (23%) patients without microvascular disease.

Conclusion: DM affects pulmonary system to a lesser extend than the other systems. Perfusion abnormalities are common in DM patients having microvascular disease.

PS_215

REGIONAL PULMONARY VENTILATION FUNCTION IN PATIENTS WITH LUNG CANCER: QUANTITATIVE EVALUATION WITH MAXIMAL INSPIRATION AND EXPIRATION XE-133 EQUILIBRIUM IMAGES

H. Hirota (1), Y. Ishikawa (1), J. Sato (1), N. Shuke (1), A. Okizaki (1), T. Aburano (1), A. Yatsuyanagi (2), T. Sasajima (2), N. Yazaki (3), Y. Ohsaki (4), K. Kikuchi (4)(1) Department of Radiology; (2) Department of Surgery 1; (3) Clinical Laboratory; (4) Department of Internal Medicine 1, Asahikawa Medical College, Asahikawa, Japan

For quantitative evaluation of regional pulmonary ventilation (RPV) function in patients with lung cancer, a simple method is proposed.
Methods: Ventilation scan with Xe-133 was performed on 20 patients with lung cancer before and after lobectomy. In the equilibrium phase, lung spot images at maximal inspiration and expiration were acquired with an acquisition time of 10 seconds each. Regions of interest (ROIs) were drawn over right and left lungs separately on these spot images. Using the counts in the lung ROIs at maximal inspiration and expiration (Cinsp, Cexp), an index of lung residual volume fraction (XRV) was calculated by dividing Cexp by Cinsp (XRV = Cexp / Cinsp). XRV was calculated for total lung and separately for the unresected and resected sides before and after lobectomy. XRV was compared between before and after lobectomy in relation to the changes in vital capacity (VC) and forced expiratory volume in 1 second (FEV 1) for references. Mean transit time (MTT) from the washout phase was compared with XRV in relation to the changes in VC and FEV 1.
Results: Total XRV showed significant correlations with VC (-0.359, $p<0.03$) and FEV1 ($r=-0.502$, $p<0.03$) before lobectomy, but MTT did not. VC and FEV 1 after lobectomy showed significant differences from those before lobectomy ($p<0.0001$, $p<0.002$). XRV of the resected side showed significant decrease after lobectomy ($p<0.0008$), but XRV of the unresected side showed no significant difference. On the other hand, MTT showed no significant difference between before and after lobectomy on either side.
Conclusion: These results suggested that XRV could be better than MTT in reflecting RPV function. This method could be useful for preoperative evaluation of RPV function in patients with lung cancer.

PS_216

RELATIONSHIPS BETWEEN HYPOXEMIA AND VENTILATION-PERFUSION RATIO DISTRIBUTION STUDIED WITH 99MTC-MAA/81MKR DUAL ISOTOPE PLANAR LUNG IMAGING

D. Vilain (1), M. Stern (2), D. Daou (3), P. Puyo (4), S. Friard (2), C. Tainturier (1). (1) Department of Nuclear Medicine, Foch Hospital, Suresnes, France; (2) Department of Pneumology, Foch Hospital, Suresnes, France; (3) Department of Nuclear Medicine, Antoine-Béclère Hospital, Clamart, France; (4) Department of Thoracic Surgery, Foch Hospital, Suresnes, France

Dual isotope planar lung scintigraphy (DIPLS) realized with ^{99m}Tc-macroaggregated albumin (^{99m}Tc-MAA) and ^{81m}Kr may be useful for the characterization of the regional distribution of lung ventilation-perfusion ratio (VA/Q). The aim of our study was to evaluate whether quantitative variables derived from the lung VA/Q distribution histogram calculated with DIPLS correlate to the severity of arterial hypoxemia.
Methods: The population studied consisted of 42 consecutive patients investigated for suspected pulmonary embolism (n=32) or lung cancer (n=10) who had arterial blood gases and ^{99m}Tc-MAA / ^{81m}Kr DIPLS and 10 asymptomatic patients (control group), with normal ^{99m}Tc-MAA/^{81m}Kr DIPLS and no known pulmonary disease. Lung regions of interest (ROI) were drawn manually on posterior view of the ventilation - perfusion scans and a corresponding VA/Q functional image reflecting a pixel-by-pixel VA/Q ratio was computed. Two VA/Q lung distribution histograms were computed by plotting the percentage of overall perfusion or ventilation counts against VA/Q on a log scale abscissa and corresponding standard deviations were calculated from both the %perfusion-VA/Q (sdP) and %ventilation-VA/Q (sdV) distribution histograms. The standard deviation of VA/Q value below (sdP-, sdV-) and above (sdP+, sdV+) the mean of %perfusion-VA/Q and %ventilation-VA/Q distributions, the % of perfusion with VA/Q<0.5 (P%v/q<0.5) were also computed. Quantitative parameters of VA/Q lung distribution histogram below mean+3sd of control group values were considered normal.
Results: 25/42 patients had at least one abnormal quantitative parameter derived from their VA/Q lung distribution histogram and all parameters showed significant correlation with arterial PO_2 ($p<0.001$). The best correlation ($p<0.05$) with arterial PO_2 was encountered with SdP- ($r=-0.72$) as compared to the other parameters (r=-0.59, -0.55, -0.55, -0.50,-0.50, and -0.44 for respectively sdP, P%v/q<0.5, sdV-, sdP+, sdV, sdV+). P%v/q<0.5 was significantly higher for the 15/42 patients with abnormal sdP- (9.4±10.8% versus 0.12±0.2%, $p<0.0001$). PO_2 values were significantly lower for these 15/42 patients (61±8 mmHg versus 76±9 mmHg, $p<0.0001$). The good correlation between sdP- and P%v/q<0.5 with hypoxemia underlines the major role of low VA/Q regions in the generation of arterial hypoxemia.
Conclusion: The above quantitative parameters derived from DIPLS are moderately to well correlated with arterial PO_2. In particular, sdP- presents the best correlation because it reflects the importance of low VA/Q area. These parameters derived from DIPLS provide an interesting unique way for the evaluation and quantification of hypoxemia generated by regional VA/Q distribution abnormalities.

PS_217

A QUANTITATIVE STUDY OF THE DIFFERENCE IN PULMONARY PERFUSION IN DIFFERENT RESPIRATORY PHASES

S. Yoshida (1), W. Don (1), M. Fukumoto (2), N. Akagi (2), H. Seguchi (1). (1) Department of Anatomy and Cell Biology; (2) Department of Radiology, Kochi Medical School, Nangoku, Japan.

Pulmonary perfusion scintigraphy with Tc-99m MAA can demonstrate the exact distribution of pulmonary perfusion in differentposition of the subject during the tracer injection. It is influenced by many correlated factors. One of them is physiological gravity. This study is aimed at investigating the physiological pulmonary perfusion in different maximum respiratory phases with using quantitative analysis.
Methods: 4 nonsmoking healthy volunteers underwent SPECT after the injection of Tc-99m MAA in a dose of 185 MBq in each maximum respiration phase at a week's interval. The tracer was injected while the subject was in a supine position and holding breath for 20 seconds at each maximum inspiration phase and expiration phase. Quantitative analysis by calculating the normalized center of perfusion intensity were performed, that was originally devised for this study.
Results: Quantitative measurement, normalized center of perfusion intensity, certified that the average of normalized Y (ventrodorsal component) values transfer from 51.4 to 44.8 (shift : 13%) in the upper part of the lung, from 54.6 to 48.5 (shift : 10.5 %) in the middle part and from 63.5 to 52.6 (shift : 17 %) in the lower part. These indicated that the pulmonary perfusion activity in the maximum expiration phase moved towards ventral direction compared to that in the maximum inspiration phase. The average of normalized Z (craniocaudal component)values ranged from 57.0 to 58.6 (shift : - 3 %)in the upper part of the lung, from 47.8 to 49.5 (shift : - 3.6 %) in the middle part and from 41.9 to 41.4 (shift : 1.3 %) in the lower part. These values indicated that the pulmonary perfusion activity in the maximum expiration phase moved towards caudal direction compared that in the maximum inspiration phase in both the upper and middle parts of the lung, while in the lower part it moved slightly towards cranial direction. In X(horizontal component) direction, pulmonary perfusion activity indicated no agreement in movement direction. The values are all within the range of (1,100).
Conclusion: We found change pattern of pulmonary perfusion between maximum expiration phase and inspiration phase, as well as in different parts of the lung, by quantitatively measuring the normalized center of perfusion intensity.

PS_218

VENTILATION/PERFUSION SCAN IN PULMONARY EMBOLISM: STILL THE BEST SCREENING TEST?

S. Carmona (1), J. Sequeira (1), M. Filipe (1), M.J. Carapinha (1), B. Abrantes (1), A. Quintal (1), L. Vieira (1), M.J. Furtado (2), A. Tomaz (3), A.I. Santos (1). (1) Serviço de Medicina Nuclear; (2) Serviço de Radiologia; (3) Serviço de Medicina, Hospital Garcia de Orta, Almada, Portugal.

The aim of this study was to evaluate the clinical impact of lung scans for the diagnosis of pulmonary embolism, on a hospital within a community of 350 000 inhabitants, with a nuclear medicine department equipped with a single headed gamma camera (10 hours/day, 5 days/week) and a radiology department with Spiral CT (24 hours/day, 7 days/week).
Methods: Between 01-January-1999 and 31-December-2000, 230 ventilation/perfusion lung scans (V/QS) were performed in 199 patients: 192/230 (83,5%) for suspicion of first episode of Pulmonary Embolism (PE); 38/230 (16,5%) for follow up of previous episodes of PE. In 21/230 exams, there was also a Spiral CT (sCT) with a delay < 12 days from the V/QS. On the first group of 192 V/QS, 72 (37,5%) had COPD (11/72) and/or cardiopathy (65/72). The following risk factors were identified: previous surgery – 29 (15,1%); hormonal therapy - 4 (2,0%); cancer – 12 (6,3%); puerperium - 2 (1,0%); and vein thrombosis - 29 (15,1%). The V/QS was performed with inhalation of 99mTc-Technegas and infusion of macroaggregated albumin labelled with Tc-99m. They were classified as: normal; low probability (LP) – 1 or less segments (or equivalent) mismatch ventilation/perfusion; high probability (HP) – 2 or more segments (or equivalents) mismatches ventilation/perfusion; and medium probability (MP) - > 1 and < 2 segments (or equivalent) mismatches.
Results: We have found 44/192 (22,9%) V/QS normal; 51/192 (26,6%) HP exams, 11/192 (5,7%) MP exams, 86/192 (44,8%) LP exams. In this last group, 67/86 (77,9%) V/QS showed other pathologies. On the 21 studies which could be correlated with sCT, we have found: 1 with both studies normal; 17 HP V/QS vs 12 positive sCT and 5 negative sCT; 1 MP V/QS with a non diagnostic sCT; 2 LP V/QS vs 1 sCT non diagnostic and 1 negative sCT.
Conclusions: The role of lung scans for screening of pulmonary embolism still persists, which makes clinicians ask for it, even in hospitals with low nuclear medicine resources. We have found very few non diagnostic or medium probability studies. Although the number of studies evaluated is small, the accuracy of Spiral CT for the diagnosis of pulmonary embolism doesn't seem higher than the one of lung scans.

PS_219

THE SCINTIGRAPHIC PULMONARY PERFUSION ABNORMALITIES DO NOT REFLECT THE HEMODYNAMIC SEVERITY OF CHRONIC POST EMBOLIC PULMONARY HYPERTENSION

D. Daou (1), C. Coaguila (1), O. Sitbon (2), F. Parent (2), B.O. Helal (1), M. Humbert (2), G. Simonneau (2). (1) Department of Nuclear Medicine; (2) Pneumology Department, Antoine Beclere Hospital, AP-HP, Clamart, France.

Aims: The value of pulmonary perfusion scintigraphy for the differential diagnosis of chronic post embolic pulmonary hypertension (CPE-PH) is widely admitted. However, whether the extent of pulmonary perfusion abnormalities evaluated with pulmonary perfusion scintigraphy reflects the severity of the disease is not well defined. We aimed to evaluate the correlation between the pulmonary vascular occlusion evaluated with pulmonary perfusion scintigraphy and the severity of pulmonary hypertension as reflected with total pulmonary resistance (TPR).
Methods: Twenty-eight patients with CPE-PH were studied. Mean age was 55±15 years, and 16/28 were males. Nineteen patients had pulmonary thrombo-endarterectomy. All 28 patients had pulmonary perfusion scintigraphy before PTE and the 19 patients with PTE had perfusion scintigraphy at 3 months after operation. The pulmonary vascular obstruction (PVO) score was calculated as previously reported: each lobe assigned a weight based on the regional distribution of pulmonary blood flow, and for each lobe a semi-quantitative perfusion score from 0 to 1 was estimated from the film density (0, 0.25, 0.5, 0.75, 1) by comparison with an apparently normally perfused area. Then, a PVO score was calculated as (1-overall perfusion score)x100.
Results: Preoperative and post-PTE PVO scores were 68±14 and 55±18 % with an absolute paired difference of 12±17 %. The preoperative and post-PTE TPR were 31±11 and 13±7 UI.m2 with an absolute paired difference of 19±11 UI.m2. No correlation was found between preoperative, postoperative and paired difference of respectively PVO score and TPR.
Conclusion: Pulmonary perfusion scitntigraphy may be valuable for the etiologic diagnosis of pulmonary hypertension but it is not correlated to the hemodynamic severity of the CPE-PH neither preoperatively nor post-PTE. Moreover, the PVO score variation between preoperative and post-PTE levels is not correlated to the variation in the hemodynamic severity of the CPE-PH.

PS_220

DO PATIENTS RECEIVE NECESSARY SCINTIGRAPHIC FOLLOW-UP AFTER PULMONARY EMBOLISM? CLINICAL EXPERIENCES FROM A GERMAN UNIVERSITY HOSPITAL

M. Gotthardt, M. Schipper, H. Hoeffken, D. Brandt, U. Welcke, K. Joseph, T.M. Behr. Department of Nuclear Medicine, Philipps-University, Marburg, Germany.

Aim: Little is known about the rate of persisting perfusion defects after pulmonary embolism (PE). We determined the number of persisting perfusion defects in pulmonary perfusion scintigraphy (PPS) in those patients diagnosed to have pulmonary embolism (PE). We also investigated how many of our patients received scintigraphic follow-up after the diagnosis of PE had been made by PPS.
Methods: Between 1991 and 1999, a total number of 3640 patients received PPS in our department. We included those patients into our study, that had perfusion defects (or persisting perfusion defects, respectively) in PPS meeting the PIOPED criteria of an „intermediate" or „high probability" lung scan. A persisting perfusion defect had to be unchanged over a time period of more than one year.
Results: From 3640 patients, 451 (12.4%) had intermediate or high probability perfusion scans. Of those, 119 (26.4%) received a scintigraphic follow-up. 19 of these patients (16%) had persisting perfusion defects. In 62 patients (52.1%), a reperfusion of the defects was found. In 38 patients (31.9%), the defects persisted within a follow-up period of up to 12 weeks but no PPS was performed after a year. Out of the 119 patients receiving a scintigraphic follow-up, only 26 (21.8%) had a follow-up over more than one year, 19 of those had persisting perfusion defects.
Conclusions: Only a limited number of patients diagnosed with PE received a scintigraphic follow-up. Of those who did, nearly three quarters were found to have persisting perfusion defects. In many cases, there was no follow-up even if no reperfusion of the defects had been visible in early follow-up perfusion scans. Our data show an inadequate scintigraphic follow-up of patients with PE. Patients and referring physicians should be made aware of the necessity of scintigraphic follow-up as persisting perfusion defects mimicking fresh PE may lead to unnecessary treatment possibly causing severe side-effects.

PS_221

ALVEOLAR TO BLOOD CLEARANCE OF INHALED TC-99M DTPA IN PRIMARY PULMONARY HYPERTENSION (PPH)

M. Sofia (1), M.L. De Rimini (2), M. Catalano (2), A. Stanziola (1), V. Ippolito (2), P. Muto (2). (1) Dpt Respiratory Disease, University Federico II, A.O. Monaldi; (2) Department of Nuclear Medicine, A.O. Monaldi,Naples, Italy .

PPH is a rare and progressive disease which is characterized by unexplained severe pulmonary hypertension associated to remodelling of pulmonary vascular bed. Impairment of alveolar diffusion to inhaled gases has been reported in PPH but it is unknown if alveolar-capillary permeability to inhaled solutes is affected.
Aim: Nuclear Medicine contribute in evaluating alveolar-capillary permeability to inhaled solutes compromission in PPH.
Methods: we performed ventilation lung scan (Tc-99m DTPA nebulization) in two patients affected with PPH and normal lung function test. Overall and regional T/2 in minutes were calculated as an index of alveolar to blood clerance and they were compared to perfusion images. The effect of the inhaled prostacyclin stable analogue Iloprost on 99mTcDTPA T/2 was also assessed.
Results: Delayed T/2 DTPA clerance resulted in one case matching decreased perfusion in the same lung. Inhaled Iloprost at doses of 25 to 100 mcg was associated to a significant decrease of prolonged T/2 DTPA in the same lung. In the other case where disomogenous perfusion pattern was present, T/2 DTPA clearance resulted within the control values recorded in 5 non smocking subject.
Conclusion: This report shows that alveolar to blood clearance of inhaled solutes could be delayed in PPH in lung zones with decreased perfusion. This finding could be relevant when the effect of inhaled pulmonary vasodilators and/or follow-up non invasive studies are scheduled for PPH patients.

PS_222

DOES THE CLINICAL PROBABILITY OF PULMONARY EMBOLISM (PE) DETERMINE WHETHER PATIENTS HAVE FURTHER INVESTIGATION FOLLOWING NON-DIAGNOSTIC VENTILATION PERFUSION (V/Q) LUNG SCAN

M. D. Stewart (1), P. Kemp (2), V. Lewington (2), H. H. Gray (1). (1) Wessex Cardiothoracic Centre; (2) Department of Nuclear Medicine, Southampton General Hospital, Southampton, United Kingdom.

Introduction: Accurate assessment of the importance of a non-diagnostic ventilation perfusion scan requires prior assessment of the clinical probability of PE. We present evidence that inadequate clinical assessment and failure to integrate clinical probability into the interpretation of these scans results in subsequent under investigation of patients
Method: Over a six-month period the medical records of 284 in-patients referred for V/Q scanning were reviewed, and the clinical probability of PE, as documented by the admitting medical team was recorded. Where this was not recorded a retrospective assessment of the clinical probability was made using an established scoring system. Referral for further investigation after the V/Q scan was recorded.
Results: Of the 284 scans, 151 were felt to be diagnostic (94 normal, 57 high probability) and 63 patients had both a low V/Q and low clinical probability. None of these patients were considered to require further investigation by existing protocols. 25 patients had an intermediate or indeterminate probability V/Q scan, only 12 (46%) of these underwent further investigation to exclude PE. An intermediate or high clinical probability was identified in 14 patients with a low probability V/Q scan, with only 5 (35%) of these undergoing further investigation. In the remaining 31 patients, with low V/Q probability, the clinical probability was not documented by the referring medical team and could not be determined due to inadequate clinical information. 4 of these 31 (13%) underwent further investigation. 70% of patients with a non- diagnostic V/Q scan, and high, intermediate or undetermined clinical probability, had no further investigation to exclude PE.
Conclusion: Our results show that, following an inconclusive V/Q scan, relatively few patients were referred for further investigation. Clinical probability is poorly utilised in the determining the requirement for further investigation and highlights the potential for under-diagnosis of PE. These findings may indicate that referring clinicians mis-understand the reporting of this investigation.

PS_223

ONE MORE REASON FOR LUNG VENTILATION STUDIES

I. Bofilias. Clinic of Nuclear Medicine, Technical University, Munich, Germany .

A renaissance in Lung Ventilation Studies (LV) is unavoidable; if a subtle identification of the regional extent of the various syndromes in their pure and mixed forms of obstructive, restrictive and hyperinflate is possible in assessment of follow up examinations. The realization of the „Three Phases Bolus Inhalation Scintigraphy" (3P-BIS, single breath (SB), equilibrium (AE) and wash out (WO)), with a γ -Camera and ^{133}Xe is sensitive enough to distinguish clearly pure and mixed components in both groups of patients suffering of emphysema and sarcoidosis *II* and *III* degree.

Method. The patient was sitting in front of the γ-Camera rebreathing into a spirometer. The ^{133}Xe was inhaled as bolus at the maximal expiration level, so that the SB-Phase corresponds to the Vital Capacity (VC). The AE-Phase was found to be proportional to the Actual Lung Volume (ALV) and the Intrapulmonary Transit Time Constant (ITTC) quantified the WO-Phase. These parameters were always evaluated for 6 lung regions. Physiological values of ITTC has been found to lie in 20 healthy patients between 0.18 and 0.22, whereas values greater than 0.24 describe the degree of the obstructive component. The total acquisition time was 320 s by 80 frames and 4 s per frame. Pure restrictive and hyperinflated lung regions was defined by %VC < 80% and %VC > 120% respectively by normal values of ITTC, whereas mixed types was accompanied by delayed WO-Phase with ITTC > 0.24.

Results. In 30 patients suffering from COLD hyperinflation was observed in 23% of all the lung regions with mean values of %VC greater than 130%±15% relative to the normal region and in 42% of all regions the %VC has been found lower than 70%±10% by ITTC > 0.24 and by relative homogeneous ALV in the AE-Phase. Normal values of VC, AE and ITTC were found in the rest of the regions. In 17 patients with sarcoidosis *II* and *III* the most characteristic features were the multifocal regions in which elevated values of more than 120% of VC accompanied by retention with ITTC > 0.40 by inhomogeneous ALV. In 61% of all the other regions show low mean values of %VC (63%±15%) by increased ITTC and inhomogeneous ALV. In 11 patients following anti-obstructive medication a slightly normalization in LV was observable of a reduction of the hyperinflated component (%VC< 110%) and retention (ITTC=0.26±10%) in obstructive areas.

Conclusions. The 3P-BIS differentiate quite sensitively among the various pure and mixed components in COLD associated with parenchyma destruction or airspace enlargement and safe assess the course of therapyÉ renaissance in LV.

PS_225

EFFECTS OF ACUTE TREATMENT WITH COCAINE AND GBR 12909 ON THE IN VIVO BINDING OF D1 AGONIST R-[C-11]SKF 82957 IN RAT BRAIN

J.N. DaSilva, V. Sanci, S. Houle. Centre for Addiction and Mental Health PET Centre, University of Toronto, Toronto, Canada.

Dysregulation of the dopamine (DA) system with changes in endogenous DA concentration has been implicated in a number of neuropsychiatric disorders. Previous PET studies revealed no difference in striatal binding of D_1 antagonist radioligands compared to controls, following treatment with amphetamine. In theory, D_1 receptor (D_1R) high-affinity state (D_1^{HIGH}) is functionally coupled to the G_S protein, and only an agonist tracer is capable of selectively assessing in vivo D_1^{HIGH} using PET. Maximal internalization of cell surface D_1R into intracellular endocytic vesicles occurs in vivo in rats within ~20 min after agonist treatment and intracellular D_1R are still detectable after 5 h (Dumartin et al., J Neurosci 18:1650, 1998). This study was carried out to determine the effects of increased endogenous DA on D_1 agonist R-[^{11}C]SKF 82957 binding following cocaine or GBR 12909 treatments, before, during or after maximal internalization of D_1R. Both cocaine and GBR 12909 are DA transporter blockers, and increase extracellular DA levels.

Methods: Rats were injected with R-[^{11}C]SKF 82957 at time (T) =0. Cocaine (30 mg/kg, i.p., 20 min prior, n=7-17 per group) or GBR 12909 (7 mg/kg, i.v., 30 min prior, n=6-9 per group) were administered at T=-24h, -6h, -20min, 0, or +20min. Animals were killed 45 min after radioligand injection and various brain regions were dissected.

Results: The region-to-cerebellum binding ratios of R-[^{11}C]SKF 82957 showed no significant difference compared to controls (received vehicle, combined group n=51), except cocaine pretreatment (T=-24h) which caused a significant increase in the striatum (n=17 rats).

Conclusions: Except for striatal increase following cocaine treatment at T=-24h, these results indicate that R-[^{11}C]SKF 82957 is not sensitive to competition from acute increases in synaptic DA levels for binding to D_1R, which are either partly internalized (T=-20min, and possibly -6h, -24h) or on the cell surface (T=0). R-[^{11}C]SKF 82957 agonist binding, which should produce receptor internalization, was also not affected by increased endogenous DA (T=+20 min). These results are similar to those reported using the DA releasing agent amphetamine (Soc. Nucl. Med. Annual Meeting 2001). (Supported by the MRC/CIHR of Canada #13258)

NEUROLOGY / PSYCHIATRY 2

PS_224

A FULLY VALIDATED SIMPLE METHOD FOR IN VIVO QUANTIFICATION OF STRIATAL DOPAMINERGIC D2 RECEPTOR DENSITY IN BABOON, USING PET

M. Bottlaender, C. Loc'h, F. Dollé, H. Valette, C. Fuseau, C. Coulon, M. Ottaviani, J. Delforge. Service Hospitalier Frederic Joliot, DRM, DSV, CEA, Orsay, France

The follow up of the dopaminergic D2 receptor density in the striatum is of great interest in progressive neurodegenerative disorders such as Parkinson and Huntington diseases. The interaction between FLB-457, a D2 specific antagonist, and receptor sites has been previously studied using a multi-injection approach (Delforge et al, 1999). Due to the very high affinity of FLB457, all model parameters (including receptor concentrations) have been estimated in vivo using PET in baboon. However, this method, using data from a multi-injection protocol, is complex and difficult to perform routinely. Thus, we propose a method that allow the quantification of the D2 receptor concentration in the striata using a simple experimental protocol suitable for repeated measurements.

Methods:

Simulations, performed using the parameters from the multi-compartmental modelisation, demonstrate that the D2 receptor density can be obtained directly by measuring the PET concentration after injection of a single saturating dose of FLB-457 (>40 nmol). This simplified protocol was tested using FLB-457 labeled in two different positions, with bromide-76 or with carbon-11. D2 receptor concentrations obtained using this method were compared with the receptor concentrations determined by the reference method. Four experiments were performed in baboons with each tracer with injected mass ranging from 58 to 88 nmol (67 ± 13 and 79 ± 10 nmol for bromide-76 and carbon-11 labeled FLB-457, respectively).

Results:

PET concentrations of FLB-457 measured in caudate nucleus and putamen during 20 minutes (4 frames of 5 min each) showed a good stability with both tracers (2% variability in both structures). Values in caudate and putamen are 37.0 ± 1.2 and 41.6 ± 1.1 pmol/ml with 76Br-FLB and 45.4 ± 2.2 and 54.9 ± 2.0 pmol/ml with 11C-FLB. These values do not differ significantly from the values of the D2 receptor density obtained with the multi-injection method (44.0 ± 12.8 et 44.7 ± 12.6 pmol/ml in caudate and putamen, respectively). Moreover, the measurement obtained with the simplified method is robust since the concentrations are independent of the injected dose and of the time of measurement.

Conclusion:

The extreme simplicity of this method, could allow to perform the follow up of the striatal D2 receptor density in animal model of neurodegeneratives diseases by monitoring the disease progression and the effects of neuroprotective treatments

PS_226

GBR12909 DOPAMINE TRANSPORTER OCCUPANCY: ARE 11C-COCAINE AND 11C-WIN35,428 PET MEASUREMENTS COMPARABLE?

A.M. Catafau (1), C.J. Endres (1), O. Gay (1), A.S. Dogan (1), J. Hilton (1), S. Cherstniakova (2), R.B. Rothman (2), K.C. Rice (3), L. Shin (3), L.R. Cantilena (3), D.F. Wong (1). (1) Johns Hopkins Medical Institutions, Baltimore, MD, USA; (2) Uniformed Services University of the Health Sciences, Bethesda, MD, USA; (3) IRP, National Institute On Drug Abuse, Nih, Baltimore, MD, USA.

GBR12909 (GBR) is a dopamine transporter (DAT) binding drug that can potentially be used for treatment of cocaine addiction. PET imaging can be used to assess drug-induced DAT occupancy. However, the choice of the PET ligand may be critical, since kinetics of the ligand might influence PET measurements.

Aim: To compare PET measurements of GBR DAT occupancy at steady state using a rapidly reversible binding DAT ligand such as 11C-Cocaine (COC), and a slowly reversible binding DAT ligand such as 11C-WIN35,428 (WIN).

Methods: Two baboons were treated with GBR (2mg/kg/day i.m.). Each baboon underwent both COC and WIN PET scans at baseline (before treatment) and after 16 days of GBR treatment. GBR plasma levels (GBRpl) were measured from day 10 to day 16 of treatment and during the GBR PET scans. Binding potential (BP) measurement was obtained from a two-tissue compartmental modeling with a blood input function after metabolite correction for both ligands. DAT occupancy was calculated as %BP change from baseline to GBR PET scans.

Results: GBRpl were stable in both baboons prior to the PET scans (baboon#1: 33.4±9.9 ng/ml, baboon#2: 35.7±3.1 ng/ml). Baboon#1 presented stable GBRpl during the two PET scans (33.2±2.3 vs. 31.1±1.1 ng/ml) and similar %DAT occupancy measured with both COC (22.7 %) and WIN (28.5 %). In baboon#2, GBRpl increased during the PET scans, and was highest during the WIN scan (59.0±6.8 vs. 78.0±5.7). Consistent with this change in GBRpl, a higher DAT occupancy was measured with WIN (41.4 %) than with COC (25.9 %) in baboon#2.

Conclusion: PET measurement of DAT occupancy using the slowly reversible ligand WIN is comparable to that of the more rapidly reversible compound COC under equilibrium of chronic GBR dosing. Therefore, when steady state of the inhibitor drug is achieved, results obtained with these two PET ligands may be comparable.(Grant DA09482)

PS_227

DOES MRI-PET COREGISTRATION INFLUENCE MEASUREMENT OF AMPHETAMINE INDUCED STRIATAL DOPAMINE RELEASE?

A.S. Doğan, A.M. Catafau, Y. Zhou, A.H. Crabb, D.F. Wong. Department of Radiology, Johns Hopkins Medical Institutions, Baltimore, MD, USA.

D-amphetamine (AMP) is known to decrease the binding potential (BP) of D2 receptor antagonist 11C-raclopride by increasing endogenous dopamine levels in the synaptic cleft, which can be measured by PET indirectly. However, MRI-PET co-registration (CRG) has not been consistently used for measuring AMP induced dopamine release.

Objective: To investigate if CRG would influence measurement of AMP induced dopamine release in striatum.

Methods: Five healthy adult volunteers (33±11 yrs.) underwent two high specific activity 11C-raclopride PET studies before and after iv. administration of AMP (0.3 mg/kg). Anatomic ROIs on caudate, putamen and cerebellum were drawn blindly both on PET directly (without CRG) and on MRI images after CRG with PET. Two tissue compartmental modeling with equilibrium volume (Ve) constraint ($Ve=K_1/k_2$, estimated from reference tissue cerebellum) was applied to obtain BPs for caudate and putamen. Percentages of BP change between baseline and AMP PET scans were used to assess AMP induced dopamine release.

Results: As seen on Table, no significant differences were found in the decrease of BP when the studies were analyzed with and without CRG (Wilcoxon U-test).

Conclusion: 11C-raclopride PET measurement of amphetamine induced dopamine release in striatum is not influenced by the use of CRG. This study may validate previous data on AMP challenge PET studies performed without using CRG. These results need to be confirmed with a larger sample size.

Table: Percent BP change with AMP

	CRG	no CRG	
caudate	-22.1±27.3%	-20.7±26.8%	NS
putamen	-29.9±22.2%	-28.6±21.9%	NS

NS: not significant

PS_228

HOW RELEVANT IS THE RECONSTRUCTION-FILTER FOR THE SENSITIVITY AND SPECIFICITY OF I-123-IBZM-SPECT?

H. Hoeffken (1), A. Gerstner (2), W.H. Oertel (2), T.M. Behr (1). (1) Dept. clinical nuclear medicine; (2) Dept. Neurology, Hospital of the Philipps-university Marburg, Marburg, Germany.

I-123-IBZM-SPECT has been reported to be able to distinguish between Parkinson«s disease and other nigro-striatal degenerations like MSA or PSP. In order to optimize the differential diagnosis of the Parkinson«s syndromes, we studied 59 patients with I-123-IBZM using different filters for the reconstruction of the transverse images.

Methods: The age of the 59 patients, 23 females and 36 males, ranged between 30 and 73 years with a mean age of 51.5 years. According to the clinical diagnosis 25 patients suffered from Parkinson«s disease, 22 from MSA and 12 from PSP. 90 minutes after intravenous injection of 185 MBq I-123-IBZM, SPECT-studies were acquired into 128x128 pixel matrices using a triple-headed gamma camera equipped with LEHR-collimators. Transverse slices were reconstructed using Butterworth filters with an order of 10, and 3 different cut-off frequencies of 0.22, 0.28 and 0.32 Nyquist frequency. For semiquantitave analysis of orbito-meatal parallel slices corrected for **attenuation,** striatal and frontal region templates were used. The shapes of the striatal region templates were derived from 15 normal persons. The striatal region templates were fitted to the striatum individually by rotating, shrinking and expanding, respectively. Striatum to frontal cortex ratios were calculated and compared to the clinical diagnoses and the apomorphine test by ROC-analysis.

Results: Using a cutoff frequency of 0.28, the best results in distinguishing Parkinson«s disease from MSA or PSP were obtained: MSA or PSP were diagosed with a sensitivity of 0.708 and a specificity of 0.733. A lower threshold for the striatal to frontal ratio of 1.53 was determined. Compared to a negative apomorphine test, sensitivity and specificity were reduced to 0.700 and 0.722. Cutoff frequencies of 0.22 and 0.32 led to a sensitivity of 0.692 and 0.533 with a specificity of 0.700 and 0.520, respectively.

Conclusions: This study shows that sensitivity and specificity for the diagnosis of MSA or PSP is strongly dependent upon the filter beeing used for reconstruction. In this preliminary study the best results were obtained using a Butterworth filter with a cut-off frequency of 0.28 and an order of 10.0. Further optimization may be possible in testing more different cut-off frequencies and orders as well as in generating separate region templates for the Nucleus caudatus and the putamen.

PS_229

REPRODUCIBILITY OF SEMIQUANTITATIVE I-123-IBZM SPECT INVESTIGATIONS

E. Ambrus (1), G. Szekeres (2), T. Sera (1), Z. Janka (2), P. Laszlo (1). (1) Department of Nuclear Medicine; (2) Department of Psychiatry, University of Szeged, Szeged, Hungary.

Several methods are known for the semiquantitative evaluation of I^{123}-IBZM-SPECT. The most frequently applied procedure is based on the calculation of the striatum/cortex activity ratio. The aim of the present study was to examine the reproducibility of a semiquantitative evaluation method. Method: Twenty-three I^{123}-IBZM-SPECT examinations were performed in 13 chronic schizoprenic patients (10 patients underwent control examinations). Two independent observers drew an ellipse to the striatum, and then mirrored it to the frontal and occipital cortex. From these data, activity ratios were calculated for both hemispheres. Results: One observer's data, on the right (R) side were as follows: striatum (S)/frontal cortex (F) activity ratio: 1.62±0.1, S/occipital cortex (O) activity ratio: 1.66±0.15. On the left (L) side, S/F was 1.64±0.11, and S/O was 1.71±0.15. The other observer's activity ratios were: R S/F: 1.63±0.12, R S/O: 1.65±0.13, L S/F: 1.64±0.1, and L S/O: 1.73±0.1. There were no significant differences between the two observers data (R S/F: p=0.57, R S/O: p=0.65 L S/F p=0.85, L S/O p=0.71). The correlation coefficients were as follows: R S/F: r=0.87, JS/O: r=0.77, B S/F: r=0.61 and BS/O: r=0.82. Conclusion: The reproducibility of our semiquantitative evaluation of I^{123}IBZM-SPECT is good. This method can readily be applied for determination of the D2 receptor density.

PS_230

IS THE RELIABILITY OF I-123-FP-CIT-SPECT DEPENDENT ON RECONSTRUCTION TECHNIQUE?

H. Hoeffken (1), A. Gerstner (2), W.H. Oertel (2), T.M. Behr (1). (1) Dept. clinical nuclear medicine; (2) Dept. Neurology, Hospital of the Philipps-university Marburg, Marburg, Germany.

Due to its high binding potential to dopamine transport proteins, I-123-FP-CIT-SPECT was reported to provide a powerful tool in the diagnosis of Parkinson«s syndrome even by visual assessment without using semiquantitative evaluation techniques. But there are only poor data on the influence of the filter used for reconstruction. In order to study the influence of the filter, we studied 51 Patients and 10 normal subjects with I-123-FP-CIT using two different filters for the reconstruction of the transverse data sets.

Methods: The age of the 10 normal subjects and 51 patients, 19 females and 42 males, ranged between 25 and 80 years. According to the clinical diagnosis, 46 patients suffered from Parkinson«s syndrome and 5 from essential tremor. 3 hours after intravenous injection of 185 MBq I-123-FP-CIT SPECT-studies were acquired into 128x128 pixel matrices using a triple headed gamma camera equipped with LEHR-collimators. Transverse slices were reconstructed using Butterworth filters with an order of 10, and 2 different cut-off frequencies of 0.4 and 0.5 Nyquist frequency. For semiquantitave analysis of orbito-meatal parallel slices corrected for attenuation, striatal and occipital region templates were used. The shapes of the striatal region templates were derived from 10 normal patients and 5 patients with essential tremor. The striatal region templates were fitted to the striatum individually by rotating, shrinking and expanding, respectively. Striatum to occipital ratios were calculated and compared to the clinical diagnoses by ROC-analysis.

Results: Using a cut-off frequency of 0.4, the best results in distinguishing between Parkinson«s syndrome and normal subjects or essential tremor were obtained, respectively: Parkinson«s syndrome was diagosed with a sensitivity of 0.913 and a specificity of 0.900. A lower threshold for the striatal to occipital ratio of 3.17 was determined. A cut-off frequency of 0.5 led to a sensitivity of only 0.826 and a specificity of 0.800.

Conclusions: According to our results, the sensitivity as well as specificity for the diagnosis of Parkinson«s syndrome is influenced by the filter beeing used for reconstruction of I-123-FP-CIT images. According to these preliminary data the best results were obtained using a Butterworth filter with a cutoff frequency of 0.4 and an order of 10.0. Further optimization is necessary by testing a greater number of sets with different cut-off frequencies and orders.

PS_231

NON-INVASIVE METHODS FOR ABSOLUTE CEREBRAL BLOOD FLOW MEASUREMENT USING 99M-TC-ECD : A CORRELATION STUDY

K.J. Van Laere (1), M. Koole (2), F. Dumont (3), J. Versijpt (1), G. Slegers (3), R. Dierckx (1). (1) Department of Nuclear Medicine; (2) Medical Image Processing; (3) Radiopharmacy Department, Ghent University, Ghent, Belgium.

Aim: Radionuclide angiography with ^{99m}Tc-ethyl cysteine dimer (ECD) allows non-invasive estimation of absolute cerebral blood flow (CBF), either by graphical Patlak-Gjedde analysis (PGA) or by spectral analysis (SA). Other methods have estimated CBF by means of single arterial or venous sampling. The aim of this study was to evaluate radionuclide scanning and single-point venous sampling as potential clinical methods for CBF determination in a large set screened healthy volunteers over the adult age range.
Methods: 83 healthy volunteers (20-81 years, 43 M, 40 F) underwent planar radionuclide angiography with 925 MBq ^{99m}Tc-ECD. After correction for camera deadtime loss, hemispheric CBF was calculated from brain perfusion indices (BPI) : BPI^G for the PGA, and BPI^S from SA. Of the volunteers, 49 also underwent venous sampling 6 minutes postinjection from which the lipophilic octanol extraction fraction and hemispheric brain fractionation index (BFI) was determined. All datasets were correlated and evaluated as a function of age and gender. Intrasubject variability for the BPI measurements was assessed in 11 volunteers by repeat study within 2 weeks of the first acquisition.
Results: Graphical and spectral analysis BPI were strongly correlated ($R = 0.849$, $p < 0.00001$). The BFI was weakly correlated to both BPI indices (BPI^G : $R = 0.34$, $p = 0.02$; and BPI^S : $R = 0.31$, $p = 0.04$).
The right hemisphere showed significant asymmetry for BPI^S (AI = 2.7 ± 4.3 %, $p<0.001$). All three indices were inversely related to age, with an increased gradient after the age of 55 years, while there was no significant gender difference. The ratio of BPI^G/BIP^S, which is a measure of the cerebral extraction fraction for ^{99m}Tc-ECD, was not dependent of age. Intersubject variability was 15.5 % in both radionuclide scanning based methods and 18.2 % for venous sampling, all independent of age. A much lower intrasubject variability was observed for BPI^S (7.2 %) versus BPI^G (12.6 %).
Conclusion: This study provides reference values for normal perfusion indices assessed by graphical and spectral analysis. The results also infer that spectral analysis allows the most reproducible estimate related to hemispheric perfusion by an operator-independent and objective approach. Whereas accurate calibration of normal BPI^S values to CBF with established methods needs to be performed, this method may allow non-invasive absolute quantification of cerebral blood flow by means of ^{99m}Tc-ECD with direct applicability in clinical routine settings.

PS_232

THE EFFECT OF ACETAZOLAMIDE ON BRAIN PERFUSION IN RIGHT-HANDED SUBJECTS: ANALYSIS WITH SPM

S.H. Kim (1), Y.A. Chung (1), I.R. Yoo (1), E.N. Kim (1), H.S. Sohn (1), Y.H. Park (1), S.K. Chung (1), Y.W. Bahk (2). (1) The Catholic University of Korea; (2) Sung Ae Hospital, Seoul, Korea.

Objectives: The purpose of this study was to investigate the effect of acetazolamide on ^{99m}Tc-HMPAO uptake pattern in brain perfusion SPET of right-handed normal volunteer by means of statistical parametric mapping (SPM) analysis.
Materials and Methods: The study populations were 9 right-handed matched healthy volunteers (male: 3, female: 6, age range: 24~52 years). We performed baseline brain perfusion SPET using 20 mCi of Tc-99m HMPAO. Two days later, acetazolamide brain perfusion SPET was obtained. All of the SPET images were spatially transformed to standard space, smoothed and globally normalized. The differences between the baseline and acetazolamide SPET images were statistically analyzed using SPM-99 software. The difference between two sets of brain perfusion SPET was considered significant at a threshold of uncorrected *P* values less than 0.001.
Results: The perfusion was definitely increased in left frontal and basal ganglia areas on subtracted images in 7 out of 9 subjects. SPM analysis revealed significantly higher uptake in left inferior frontal cortex in acetazolamide SPET compared with baseline SPET.
Conclusion: The results suggest that brain perfusion is increased in the left cerebral hemisphere, especially frontal region of right-handed persons on acetazolamide SPET. This study would helpful in understanding of neurophysiology.

PS_233

EFFECT OF GENDER ON CEREBRAL 18FDG AND 11C-METHIONINE UPTAKE: A DIRECT COMPARATIVE PET STUDY

M. Lacic (1), G.J.R. Cook (2), P.K. Marsden (2), I. Fogelman (2), M.N. Maisey (2). (1) Department of Oncology and Nuclear Medicine, University Hospital ; (2) The Clinical PET Centre Guy's and St. Thomas' Hospital Trust, London, UK.

Aim: The aim of this study was to evaluate the effect of gender on regional and global cerebral uptake of 2-deoxy-2-^{18}fluoro-D-glucose (^{18}FDG) and L-methyl-^{11}C- methionine (^{11}C-MET) in a direct comparative positron emission tomography study (PET).
Methods: Thirty-five patients (20 male, 15 female) aged between 3 and 61 years (mean 32) with suspected brain tumour were studied. All patients underwent a ^{11}C MET and ^{18}FDG PET scan and at least one anatomical brain scan (CT or MRI). Regional and global cerebral uptake of ^{11}C-MET and ^{18}FDG were measured semi-quantitatively.
Results: There was no significant difference between the uptake of ^{18}FDG in female and male patients population in any of evaluated cerebral regions ($p>0.05$). When the cerebral uptake of ^{18}FDG were compared between female and male patients in the group of patients older than 18 years, statistically significant difference in all evaluated regions has been achieved ($p<0.05$). The group of female patients had significantly higher uptake of ^{18}FDG in comparison to the group of male patients in all evaluated regions. The difference in global cerebral uptake of ^{18}FDG between female and male patients was statistically significant ($p<0.05$). The global cerebral uptake of ^{18}FDG was significantly higher in the female group of patients in comparison to male one. The regional ^{11}C-MET cerebral uptake did not differ significantly between female and male patients ($p>0.05$). In the group of adult patients (older than 18 years) female patients had significantly higher uptake of ^{11}C-MET in all evaluated brain regions ($p<0.001$). The difference in global cerebral uptake of ^{11}C-MET between female and male patients was statistically significant ($p<0.05$). The global cerebral uptake of ^{11}C-MET was significantly higher in the female group of patients in comparison to male one.
Conclusion: We concluded that gender-related changes in regional and global cerebral uptake of ^{11}C-MET and ^{18}FDG could be observed in the patients population older than 18 years. Higher regional and global cerebral uptake of ^{18}FDG and ^{11}C-MET could be measured in adult female patients.

PS_234

AGE-DEPENDENCE OF SEROTONIN TRANSPORTER DENSITY MEASURED BY IODINE-123-β-CIT-SINGLE PHOTON EMISSION COMPUTER TOMOGRAPHY (SPECT)

S. Hesse (1), H. Barthel (1), T. Murai (2), U. Müller (3), D. Sorger (1), R. Kluge (1). (1) Department of Nuclear Medicine, Leipzig University, Leipzig, Germany; (2) Department of Neuropsychiatry, Faculty of Medicine, Kyoto University, Kyoto, Japan; (3) Psychiatry, University Hospital, Leipzig University, Leipzig, Germany.

Objectives: The central neurotransmitter serotonin plays a major role in a number of neuropsychiatric disorders. To understand mental disorders in different life-conditions the dependence of age on the central serotonin transporter (SERT) density has to be evaluated.
Aim of this study was to investigate age-related changes of SERT density.
Methods: SERT density was analyzed in control patients without evidence of neuropsychiatric disorders as well as in healthy control subjects (n=22, 14 female, 8 male, age range 18-83 years) using [^{123}I]-2β-carbomethoxy-3β-(iodophenyl)tropane ([^{123}I]β-CIT) and a brain dedicated single photon emission computer tomography (SPECT) system (Ceraspect, DSI, Waltham, USA). The radiotracer uptake in SERT-rich brain areas was quantified using a semi-automatic quantification system (Hermes software, Nuclear Diagnostics, London, Canada).
Results: SERT density and age showed a significant inverse correlation ($y = -0.03518x+4.786$, $r = -0.688$, $p = 0.01$, hypothalamic region). Mean difference of values of one experienced investigator (intra-rater variability) was 0.3% with a standard deviation of 21.5%. SERT density declined 55% within the age range of our patients (11.5% per decade).
Conclusion: The data indicate a relevant age-dependence of SERT density, which must be considered in future clinical studies.

PS_235

DIFFERENT UPTAKE OF 99MTC-ECD AND 99MTC-HMPAO IN THE NORMAL BRAINS: ANALYSIS BY STATISTICAL PARAMETRIC MAPPING

H.S. Sohn, E.N. Kim, S.H. Kim, Y.A. Jung, I.R. Yoo, S.K. Chung. Departments of Nuclear Medicine, College of Medicine, St. MaryÁøs Hospital, The Catholic University of Korea.

Aim: This study investigated the differences between technetium-99m ethyl cysteinate dimer (99mTc-ECD) and technetium-99m hexamethylpropylene amine oxime (99mTc-HMPAO) uptake in the normal brains by means of statistical parametric mapping (SPM) analysis.
Methods: We analyzed retrospectively age- and sex matched 53 cases of normal brain SPECT. Thirty-two cases were acquired with 99mTc-ECD and 21 cases with 99mTc-HMPAO. No one had abnormal finding on brain MRI. All of the SPET images were spatially transformed to standard space, smoothed and globally normalized. The differences between the 99mTc-ECD and 99mTc-HMPAO SPECT images were statistically analyzed using statistical parametric mapping (SPM) 99 software. The difference between two groups was considered significant at a threshold of corrected P values less than 0.05.
Results: SPM analysis revealed significantly different uptake of 99mTc-ECD and 99mTc-HMPAO in the normal brains. On the 99mTc-ECD SPECT images, relatively higher uptake was observed in the frontal, parietal and occipital lobes, in the basal ganglia and thalamus and in the superior region of the cerebellum. On the 99mTc-HMPAO SPECT images, relatively higher uptake was observed in subcortical area of frontal region and medial temporal lobes.
Conclusion: Uptake of 99mTc-ECD and 99mTc-HMPAO in the same normal-looking brains was significantly different on SPM analysis. The selective use of 99mTc-ECD or 99mTc-HMPAO in brain SPET imaging appears especially valuable for the interpretation of cerebral perfusion. Further investigation is necessary to determine which is more accurate for diagnosing different clinical conditions.

PS_237

DETECTION OF LOCAL INFLAMMATION FOCI WITH 199TL-CHLORIDE SCINTIGRAPHY

V. Zavadovskaya (1), O. Kilina (1), V. Skuridin (1), V. Tchernov (2), Y.U. Lishmanov (2), K. Zavadovskiy (1). (1) Siberian State Medical University, Tomsk, Russia; (2) Institute of Cardiology, Tomsk, Russia.

Adequate delineation of variety of inflammatory conditions, including abdominal or lung abscess and bone infections, is an important, clinically relevant issue. One of the newer agents suggested for scintigraphic evaluation is 199Tl-chloride.
Aim. The aim of the study was to evaluate usefulness of 199Tl-chloride in detection of inflammation foci of various location.
Material and methods. 24 patients (10 males, 14 females, aged 39±7 years) with suspected inflammatory disease of skeleton (n=9), abdomen (n=13) and lung (n=2) were included. The 199Tl-chloride imaging was performed 20 and 60 min after injection of 150 MBq. Diagnosis was verified by x-ray, morphological tests and clinical follow-up.
Results. Results of scintigraphy were reported as positive if local uptake of 199Tl-chloride was observed. 199Tl-scan showed 20 true-positive (TP), 2 true-negative (TN) and 2 false-negative (FN) results. TP results were observed in 2 pts with infected diabetic foot, in 2 pts with frostbite, in 3 pts with osteomyelitis and in 13 females with salpingitis. The absense of FP scans resulted in a specificity of 100%. Sensitivity and accuraricy were 90,2% and 91,6% respectively. The highest degree of 199Tl-chloride uptake was seen in 20 min after injection and moderately decreased on 60 min after scan. TN results were revealed in 2 pts with hip prosthesis locking. Two lung inflammation cases showed FN patterns.
Conclusion. 199Tl-scan is a safe and reliable method and can be suggested as an alternative to labelled leucocytes techniques to reveal both bone and abdominal inflammatory foci and to assess results of treatment.

TECHNOLOGY PROGRAM 1

PS_236

ACCURACY OF CPU VERSUS VECTOR PROCESSOR BASED RECONSTRUCTIONS OF 2D AND 3D PET SCANS WITH THE ECAT HR+ PET SCANNER

S.C.M. Balen, R. Boellaard, A.A. Lammertsma. Clinical PET Center, Free University Medical Center, Amsterdam, The Netherlands.

Purpose: To determine the quantitative accuracy of CPU based reconstructions using FBP and iterative reconstruction (OSEM) of 2D and 3D scans as compared with reconstructions using dedicated 'vector processor' hardware (VP).
Methods: 30 min 2D and 3D 30min emission scans were acquired with an ECAT HR+ PET scanner for three phantoms, each filled with 74MBq F-18 : (1) a 5cm diameter phantom; (2) a 20cm diameter phantom and; (3) a NEMA phantom with cold air, water en Teflon inserts. Transmission scans of 30min were performed after a 12 hr interval. FBP (Hanning 0.5) and OSEM (2 iterations with 16 subsets) reconstructions included measured attenuation correction, decay and scatter correction. Reconstructions were performed both on the VP and CPU. Regions of interest (ROI) analysis was performed to determine the average pixel value or activity concentration (Ct) within each compartment of the phantoms. The average Ct derived from CPU reconstructed images were compared with those obtained from VP reconstructions. In addition, for the NEMA phantom the effects of CPU and VP reconstruction on the ratio between the average pixel value within each insert and the background region was studied. Analysis was performed for both 2D and 3D data.
Results: For 2D scans agreement within 2% between VP and CPU reconstructed Ct was found for all phantoms. OSEM reconstructions yielded higher average pixel values within the NEMA inserts than FBP reconstructions. These results were consistent for VP and CPU data. 3D CPU reconstructed images yielded 6% and 13% higher Ct for the 5 and 20cm diameter phantoms, respectively, compared with VP data. VP reconstructed data were within 2% of the Ct derived from samples counted using a calibrated well counter. The ratio of the Ct within the Teflon (bone) insert and background region of the NEMA phantom was 0.20 and 0.09 for the CPU and VP reconstructions respectively. For the air insert these ratio's equalled –0.03 and 0.07.
Conclusion: For 2D acquisitions CPU and VP reconstructions have comparable accuracy for both FBP and OSEM. The higher pixel values within the NEMA inserts observed for OSEM are explained by the non-negativity constraint applied with OSEM. Differences in pixel value within the NEMA insert between 3D CPU and VP reconstructions are probably caused by the different 3D scatter correction models implemented for both reconstructions.

PS_238

A STUDY OF MULTIFOCAL FLAT PHANTOM FOR BETTER UNDERSTANDING OF SENTINEL NODES DETECTION IN SCINTIGRAPHY

H. Sayman, M. Demir, S. Ahmed, C. Nisli, E. Dirlik, I. Uslu. Department of Nuclear Medicine, Cerrahpasa Medical Faculty, Istanbul University, Istanbul, Turkey.

Background. Lymphoscintigraphy being an emerging branch of nuclear oncology, highactivityat the injection-site is still of a great concern nowadays. Sometimes, it's also confusing to differentiate two nearby sentinel nodes because of star/ flashing effects due to high nodal activity.
Aim. The object of this study is to choose most proper collimator and its dependence to different depths for any particular medium.
Method. We performed our study with a multifocal flat phantom made out of plexiglass with point holes in it. The center point contained 100 µCi Tc-99m and other 10 points contained 1µCi each. All the points were arranged in a helical way at distances of 1cm, 2cm, 3cm.....10 cm within a background medium containing 10µCi/5 lt. We used three types of collimators: Low energy high resolution (LEHR), low energy all purpose (LEAP) and medium energy all purpose (MEAP). Entire study was performed by Siemens Digitrac 75 Planar Camera. We placed the phantom at three distances from the collimator: i) Surface position ii) 5 cm depth of water iii) 10 cm depth of water. In static mode, we acquired 170,000 counts in 256x256x16 matrix.
Results and discussions. We normalized all the readings with respect to the background for three collimators at different depths individually and determined the ratio of point counts and background. The value shows maximum variation at LEAP and minimum at LEHR collimator. The variation is reasonable for MEAP collimator. The images with MEAP at surface position and at 5 cm depth are free of flashing and star effects. All other images show more or less both of the effects with highest intensity at images acquired using low energy high resolution (LEHR) collimator. Furthermore, These images (LEHR), at different depths show a lack of spatial resolution which is very significant to be considered in practice.
Conclusion. Medium energy all purpose (MEAP) collimator seems to provide better delination of injection sites that most concerned with sentinel nodes detection.

PS_239

MEASUREMENT OF DOPAMINE TRANSPORTER (DAT) DENSITY IN HUMAN STRIATUM BY PET WITH 11C ALTROPANE

S.A. Barrow, A.A. Bonab, E. Livni, B.K. Madras, P. Meltzer, A.J. Fischman. Department of Nuclear Medicine, Massachusetts General Hospital, Boston MA.

Aim: ^{123}I labeled Altropane (E ^{123}I-2β-carbomethoxy-3β- (4-fluorophenyl)- N-(1-iodoprop-1-en-3-yl)nortropane is a new radiopharmaceutical with high affinity and selectivity for dopamine transporter (DAT) sites in the striatum. Recently, dynamic SPECT studies demonstrated the utility of this reagent for DAT imaging in healthy volunteers and patients with early Parkinson's disease (Synapse 1998;29:128-141). Since maximal striatal accumulation of ^{123}I labeled Altropane occurs within 30 min. after injection, we hypothesized that ^{11}C labeled Altropane would be useful for PET imaging of the DAT.

Methods: The precursor for preparing ^{11}C Altropane was synthesized by acid hydrolysis of ^{127}I Altropane. This compound was then methylated with $^{11}CH_3I$ and purified by HPLC. Healthy human subjects were injected with ~15 mCi of ^{11}C Altropane and dynamic PET images were acquired over 90 minutes using a PC-4096 PET camera. The images were reconstructed using a standard filtered back projection algorithm to an in-plane resolution of 6 mm FWHM. Arterial blood was sampled in parallel with imaging and metabolite analysis was performed by HPLC. The PET and metabolite corrected arterial blood data were used to calculate k_3/k_4 by a linear graphical method for reversible ligands.

Results: The PET images showed superb striatal definition, with clear separation of caudate nucleus and putamen. In addition, there was minimal accumulation of tracer in brain regions with high 5HT transporter density. Striatial time-activity curves displayed the pattern characteristic of a reversible tracer and metabolite analysis demonstrated that at 60 minutes after injection, approximately 80% of circulating radioactivity eluted with intact ^{11}C Altropane. The average value for k_3/k_4 was greater than 3.5.

Conclusions: These results indicate that ^{11}C Altropane is a useful PET tracer that combines the favorable characteristics of: 1) rapid and specific striatal binding; 2) reversible binding kinetics and 3) high selectivity for DA vs. 5-HT transporter sites. These properties will almost certainly make ^{11}C Altropane an important PET ligand for quantitative measurements of DAT density in Parkinson's disease and other neurological disorders.

PS_240

PC BASED DATA ACQUISITION SYSTEM FOR ANGER SCINTILLATION CAMERA

M. Petrovic (1), N. Stojanova (1), D.B. Popovic (1), V. Artiko (2), V. Obradovic (2), V. Bosnjakovic (3). (1) Faculty of Electrical Engineering, University Of Belgrade, Yugoslavia; (2) Nuclear Medicine Institute, CCS, Belgrade, Yugoslavia; (3) Center for High Technology, CCS, Belgrade, Yugoslavia.

Aim: The design of a modular, adaptable to clinical needs, ready for integration in the PACS and HIS information systems PC based data acquisition system for Anger scintillation camera.
Methods: A high-performance analog to digital (A/D) PCI card (National Instruments, Austin, TX) was selected as an interface between a standard PC computer and Anger scintillation camera. The manufacturer guarantees the linearity, sampling rate and other technical performances of the A/D board. The device is CE certified. The three outputs from the Anger camera (X and Y co-ordinates, and the summing up Z signal) were connected to the three inputs of the high speed A/D card. The Z signal was also used as a trigger for starting the A/D conversion. Windows NT operating system and LabVIEW 4.1/5.0 (National Instruments, Austin, TX) provided the basic tools for the development and testing of the software, and the system as a whole.
The system is designed for planar (static, dynamic) and SPECT studies (including the gated studies), using the multiple energy windows. The software supports different recording protocols developed by almost any institution or manufacturer of Anger camera. The data acquisition system supports image formats used by the leading manufacturers of nuclear medicine instrumentation, yet it primarily supports the DICOM standard.
Results: The system was experimentally tested using the phantoms (e.g., dead time < 3μs, bar phantom spatial resolution < 3 mm, no constraints to the SPECT system). The computer system was clinically evaluated by examining the consecutive 159 clinical static and dynamic studies in 112 subjects. The evaluation was blinded; the clinical expert evaluators of the acquired images were not aware which system was used for data capturing. The same images were captured in parallel with both new PC based computer system and Siemens, „Microdelta" system at the Clinical Center of Serbia. The three blinded clinically experienced observers have found the present system diagnostically more efficient in 94%, 91% and 87% of the analysed studies, respectively.
Conclusions: A new PC based computer system for real-time image capturing and later analysis of the data from an Anger scintillation camera was developed. This development follows the world trend of designing medical instrumentation: use of general-purpose PC computer or workstation with a high quality interface. The novel system improves, and facilitates diagnostics in numerous nuclear medicine units and maximise the performance to cost ratio.

PS_241

GENDER VARIATIONS IN GASTRIC EMPTYING RATE: ARE SEPARATE NORMAL RANGES NECESSARY?

N. Storry, I. Jones. Southern Derbyshire Acute Hospitals NHS Trust, Nuclear Medicine Service, London Road, Derby, UK.

The aim was to determine if a significant variation existed between the sexes in gastric emptying rates and, if so, was there a need for different normal ranges to be applied.
A proprietary available cottage pie was used as a semisolid meal. The potato layer was labelled with 12 MBq of $^{99}Tc^{m}$ labelled DTPA. Imaging was commenced immediately upon completion of the meal. Anterior and posterior projections of the stomach were recorded for thirty seconds using a 128 matrix at 0,5,10 and 20 minutes and then every 15 minutes up to 125 minutes. Exact time of acquisition, referenced to meal completion, was recorded.
Gastric counts in each projection were analysed using an Excel spreadsheet. For each time interval, the data was decay corrected and a geometric mean value calculated. These values were then expressed as percentage of meal remaining in stomach.
Variation in gastric emptying with gender was investigated retrospectively in 110 patient datasets (55 female, 55 male). Mean and standard deviation values for each gender dataset and the whole population were determined at each time interval (+/- 2 minutes). Appropriate t-testing was performed to compare male-female, male-total and female–total populations.
The result of this analysis showed male gastric emptying to be significantly faster than female for a semi-solid meal. However, this gender difference is not significantly great to necessitate separate normal ranges.

PS_242

FROSTBITE INJURY: SCINTIGRAPHIC PREDICTION OF SOFT TISSUE AND BONE VIABILITY

V. Zavadovskaya, O. Kilina, I. Sinilkin, S. Ekimov, O. Shulga, L. Ekimova. Siberian State Medical University, Tomsk, Russia.

Frostbite injuries occur in extremely cold climates during cold periods, lead in many cases to soft tissue and bone infarction that required amputation. The major obstacle is the difficulty in estimating the extent of dead tissue early after the cold injury but before the development of gangrene.
Aim. The aim of the study was to assess value of 2-phase scintigraphy in detection of soft tissue and bone necrosis during deep frostbite.
Material and methods. 11 pts (10 males, 1 female) aged 40±6 years, having frostbite (3 pts of both hands, 3 pts of both feet, 5 pts of both hand and feet) were scanned in 3 to 20 days from the onset of cold injury during winter 2000-2001 using 370MBq of 99mTc-MDP .
Results. 9 pts studied revealed 4-th degree frostbite which pattern included „cold" areas both in bones and soft tissues for equal distance. 2 pts with the 3-rd degree of frostbite revealed „cold" area in the soft tissue and preserved visualization of bones. Scintigraphic border of „silent" area coincided with clinical demarcation line (DL) in 6 pts who were investigated later than 10 days after frostbite. Scintigraphic DL was established in 5 pts 3 days after cold injury and was verified later by clinical follow-up, surgical inspection and by microscopic pathology. DL was revealed scintigraphically in the projection of distal interphalangeal joints of hands and feet (n=5), of middle third of feet (n=4), of radiocarpal joints (n=1) and of mean third of crus (n=1).
Conclusion. 2-phase scintigraphy is a safe method for early prediction of bone and soft tissue necrosis degree and allows to work out optimal ways to treat deep frostbite.

PS_243

DEVELOPMENT OF A NEW WHOLE BODY TABLETOP: GAINING IMAGE QUALITY BY DECREASING DISTANCE BETWEEN PATIENT AND GAMMACAMERA DETECTOR

N.J. Mijnders (1), I.M.A. van Rooijen Beuman (1), C.J.H. Smits (1), G. van der Wilt (2). (1) Dept. of Nuclear Medicine, Amphia Hospital, Breda, The Netherlands; (2) Kokke van der Wilt Contracting, Boxtel, The Netherlands.

Aim: Modern gammacameras are well suited to perform all kinds of examinations in just one hardware set-up. The patient tabletop is optimised for SPECT acquisitions. The design is narrow, curve shaped and often uncomfortable for obese patients (often with pain) undergoing whole body scanning. We developed a tabletop for whole body scanning and spot imaging to decrease distance between patient and detector and hence to gain image resolution and contrast.
Methods: A removable tabletop was designed with a maximum of patient area to fit within the gammacamera gantry, as thin as possible, maximum bend of 18 mm when loaded with 100 kg in the centre, maximum weight allowance of 180 kg. Four candidate materials were tested for the least mass (total weight!) and the least attenuation for 140keV. The current and new tabletops were tested for sensitivity and resolution for 99mTc. Ten patients, injected with a standard dose of 550 MBq 99mTc-HDP, were scanned twice approximately 3 hours post injection with the current and the new tabletop. The used gammacamera was a Toshiba GCA 7100pi equipped with a low energy high resolution (LEHR) collimator. Scanspeed was 10 cm / min. Scintigrams were reported blindly.
Results: A 2 mm thick aluminium alloy with a specific gravity of 2.64 g/cm3 was used to construct a flat, cone shaped table top. Measured system sensitivity was 79.0 (no tabletop installed), 73.5 (current) and 75.8 cnts/sec/MBq (new). Resolution at 10 cm from the collimator surface was 8.31 (no tabletop installed), 8.40 (current) and 8.38 mm (new). Contrast and image quality dramatically increase in all ten patients. Especially in areas where the distance between patient and detector was decreased, like spine, limbs and hands. All patients preferred the new tabletop for its comfort, as they weren't tied up.
Conclusions: The maximum of image quality can be achieved when the gammacamera detector is placed closest to the patient. This is a major basic principle in nuclear medicine imaging. Curve shaped tabletops are ideal for SPECT acquisitions but deteriorate whole body imaging. A flat table top with more patient comfort increases image contrast just by decreasing the distance between patient and gammacamera detector.

PS_244

PROBLEM BASED LEARNING IN NUCLEAR MEDICINE

A.W.M. Tops, W. Hoorn van, M. Weberink. Fontys University of Professional Education, Department MBRT, Best, The Netherlands.

Aim
At this poster the twelve years of experience that now exist with this problem based curriculum for teaching nuclear medicine will be highlighted. An introduction will be given to the program, the choice for Problem Based Learning (PBL) will be explained and motivated and some figures about student in-and output will be shown.
Methods
When the curriculum was designed, the profession was analyzed not only with regards to it's contents, but also to the circumstances of practice and to some meta-skills that are being demanded by the employers to be. By designing the curriculum it was a must that this new curriculum had to exist next to the other hospital based, inservice curriculums for each Diagnostic Imaging and Radiation Therapy separately.
Results
As a result of that analysis the new program was based upon the didactical concepts of Problem Based Learning. Among other things this means that the program is integrated, teacher extensive, theme centered rather than subject centered and relying heavily on self study, on groupwork by the students and on in-school skills traning in a specially designed skills lab. These practical tranings at school are completed by periods of practical training in hospital departments.
Conclusions
In 1989 the Dutch started a universitary based combined BSc-curriculum in all Diagnostic Imaging modalities and Radiation Therapy. Graduates are licensed to work as technologist in Radio Diagnostics including CT and MRI, and in Ultrasound, Nuclear Medicine and Radiation Therapy. The objective is to bring forth graduates who are trained in a wide variety of skills, at entry level.

PS_245

CENTRAL BENZODIAZEPINE RECEPTORS IN DEMENTIA OF VASCULAR AND ALZHEIMER'S TYPE

A. Panzacchi (1), G. Rizzo (1), C. Messa (1), C. Gobbo (1), RM. Moresco (1), G. Frisoni (2), M. Alberoni (3), C. Mariani (3), A. Carpinelli (1), G.B. Rossini (2), F. Fazio (1). (1) LNB-CNR, Universitá Milano – Bicocca, Scien. Inst. h San Raffaele; (2) IRCCS Fatebenefratelli, Brescia; (3) IRCCS Don Gnocchi, Milano, Italy.

Aim In a previous study, no significant differences in [^{11}C]flumazenil (FMZ) binding between patients with dementia of vascular type (VD) and with Alzheimer's disease (AD), were observed. To understand the possible impact of this finding on disease classification, we now report the PET results in a slightly larger group of VD patients compared with the same AD patients and their relationship with the severity of disease.
Methods 14 patients, 6 with AD and 8 with VD diagnosed according to NINCDS-ADRDA and NINDS-AIREN, were recruited. Age and severity of disease assessed by MMSE score were 73±5 and 15±5 in AD and 73±2 and 20±5 in VD. Images of BDZ distribution in the brain were acquired dynamically with a 4.5 mm resolution PET camera (GE Advance) after i.v. injection of 3.7MBq/Kg of [11C]flumazenil. Blood arterial samples were collected from a radial artery for calculation of metabolite corrected plasma input function. ^{11}C-flumazenil delivery to brain tissue (K1), which depends on blood flow and the tissue distribution volume (DV), which is a measure of tracer binding to benzodiazepine (BDZ) receptors, were obtained using a two compartment model. Images were normalised into the MNI space (SPM96) and, using a basis function, transformed into parametric normalised images of K1 and DV. Regional values of K1 and DV were obtained with ROIs and compared a) between AD and VD patients and b) between patients with MMSE scores lower (n. = 6) or greater (n. = 8) than 18, using repeated Student's t-tests.
Results: No significant differences in K1 or BDZ binding between AD and VD patients could be found in any of the regions examined. On the other hand, when patients were regrouped according to the MMSE scores, a significant difference ($P<0.05$ uncorrected) in the parietal and lateral temporal cortices was found for DV only, being these values lower in the more severely affected patients (2.9 ± .7 in MMSE<18 vs. 4 ± 1.1 in MMSE>18 for the parietal cortex).
Conclusions: A reduction in BDZ binding but not in K1 values was found only when demented patients were grouped according to the severity of cognitive decline and not to the standard clinical-anatomical classification. Such finding may represent a pure neuronal regional loss related to the severity of disease and it is independent on blood flow changes.

PS_246

A SUGGESTED PANEUROPEAN IMPLEMENTATION MODEL FOR RADIOPHARMACIES FOR RADIOPHARMACEUTICAL RECONSTITUTION PRACTICES

D. O'Leary (1), J. McCavana (2), L. Rainford (1). (1) School of Diagnostic Imaging, UCD, Herbert Avenue, Elm Park, Dublin 4, Eire; (2) Nuclear Medicine Department, St Vincent University Hospital, Elm Park, Dublin 4, Eire.

AIM: The European Guide to Good Manufacturing Practice and the UK Audit documents for Radiopharmacy provide established methods of evaluation, enable investigation of current standards and facilitate recommendations for acceptable levels of practice in Radionuclide departments. These recognised European guidelines suggest that reconstituted products not manufactured according to the guidelines may leave the radiopharmacies open to legal challenge. The aim of this work is to examine awareness of these guidelines and to establish the extent of their implementation into Radiopharmacy reconstitution workstations and work practices.
METHOD: Following visits to various European and UK radiopharmacy locations, to access the compliance of these with recognised guidelines, the questionnaire format for use in a full Irish survey was completed. Visits and structured interviews in all Irish radiopharmacies were undertaken. Direct comparisons are currently being made between radiopharmacies in the Irish Republic, the UK, and other European centres and the results will be judged in light of recommendations in the published literature.
RESULTS: Preliminary results indicate that many radiopharmacies in Ireland and some centres in Europe are open to legal challenge as the radiopharmaceutical reconstitution methods do not follow European Good Manufacturing Practice Guidelines. Remaining data is currently being analysed and it is anticipated that results will be presented at this meeting.
CONCLUSIONS: Preliminary data from this investigation provides evidence that guidelines are not being adhered to. A panEuropean model for a dedicated radiopharmacy, which reconstitutes radiopharmaceuticals beyond legal challenge, is recommended. By assessing any shortfall in the existing radiopharmacy service, these issues will be open for further debate and findings of this work will facilitate change in radiopharmacy standards.

PS_247

DUAL ENERGY X-RAY ABSORPTIOMETRY (DXA) AND TOTAL HIP PROSTHESES: METHODOLOGICAL PROBLEM

G. d'Arnaud, R. Kingma, I.C. Heyligers, J.C. Roos. Nuclear Medicine Vrije Universiteit Medical Centre, Amsterdam, The Netherlands.

Aim. We use DXA for follow up of bone mineral density (BMD) measurements in patients with a total hip prostheses. We noticed that the total area of the „Global Region" (GR), meant to correct for soft tissue, influences BMD in the chosen subregions of interest around a prosthesis. The only instruction given by the manual about this GR is that it „should be large enough to contain enough soft tissue". We investigated the influence of GR size in 7 subregions medial of the prosthesis (R1, the upper part of the minor trochanteric area; R7, an area just below the stem of the prosthesis) in 8 patients.
Methods. All patients had an uncemented total hip prosthesis (type Meridian; Stryker/Howmedica/Osteonics). The DXA scans were performed on a Hologic QDR 2000plus. BMD in R1 – R7 was analysed with the standard software for prosthetic hip implants with metal removal option. We varied the GR size from maximal (the scanned area) to minimal (the area just around the 7 subregions) and analysed the effects on area, bone mineral content (BMC) and BMD in R1 – R7).
Results. Irrespective of the chosen subregion, the change in GR area resulted in a change of – 15 to + 35 % for the area of the subregion, - 22 to + 41 % in BMC and – 13 to + 5 % in BMD. The mean percentage change (+/- standard deviation) decreasing the GR from maximal to minimal is given for the area, BMC and BMD per subregion in the Table.

% change +/- SD	Area	BMC	BMD
R1	11.0 +/- 12.7	8.5 +/- 15.7	-2.2 +/- 4.6
R2	2.2 +/- 4.1	1.1 +/- 5.4	-1.1 +/- 2.5
R3	-0.5 +/ - 2.6	-2.1 +/- 3.5	-1.5 +/- 2.6
R4	-1.7 +/- 3.6	-3.9 +/- 5.6	-2.1 +/- 2.9
R5	-3.5 +/- 6.0	-7.9 +/- 8.9	-4.7 +/- 3.8
R6	-4.6 +/- 6.6	-9.9 +/- 10.1	-5.7 +/- 5.1
R7	0,0 +/- 1.5	-1.0 +/- 2.7	-1.0 +/- 1.5

Conclusion. The GR size chosen during analysis of BMD around a hip prosthesis influences the outcome in BMD substantially. Further research is warranted to investigate the optimal GR size in relation to accuracy.

PS_248

PROTOCOL FOR INTRAOPERATIVE MEASUREMENT OF RENAL BLOOD FLOW

U. Dopichaj-Menge, H. Müller, D. Sandrock, D. L. Munz. Clinic for Nuclear Medicine, University Hospital Charité, Berlin, Germany.

Aim: During cardiac surgery there is an altered circulation situation (volume and blood pressure, flow instead of pulse wave circulation), especially, if the heart-lung machine (HLM) is in use. This often results in a decrease of the urine excretion during the intervention. Hence, it was the aim of this study to develop an adapted protocol for measuring the renal blood flow and proof its feasibility and suitability under intraoperative conditions.
Methods: Based on calculated compartment assumptions, the following protocol was created: i.v. injection of 10 MBq I-123-orthoiodohippurate (OIH) 30 min before start of HLM; blood sampling 15 min before and at least three times during HLM. After the end of HLM, again i.v. injection of 10 MBq OIH (for better count statistics) was done and at least one blood sample was drawn until 15 min p.i.. The detailed surgical procedure, HLM-protocol, and exact time points of blood drawings were tried to be obtained from the perfusionist and anesthesiologist. Additionally, sex, age, and hematocrit were noted. The protocol was tested in 37 patients (pts., 11 women, 26 men; aged 41-84 years).
Results: In four pts. (11 %) it was not possible to obtain a blood sample *before* start of HLM. *During* HLM running (41-181 min, mean 88 min) seven pts. (19 %) had three blood samples, 23 pts. (62 %) had four, five pts. (14 %) had five, and two pts. (6 %) had six samples. There was only one pt. without any sample *after* the end of HLM. 24 pts. (65 %) had one sample, ten pts. (27 %) had two, and two had three samples, respectively. The exact documentation of the sampling times, surgery and HLM-protocol could be achieved in all pts.
Conclusions: This protocol is feasible under surgical conditions in most cases. Communication with the anesthesiologist and perfusionist and exact documentation are indispensable.

CARDIOVASCULAR 4

PS_249

PROGNOSTIC VALUE OF COMBINED MYOCARDIAL PERFUSION SPECT IMAGING AND TL-201 LUNG UPTAKE

M. Kaminek (1), M. Myslivecek (1), M. Skvarilova (2), V. Husak (1), P. Koranda (1), I. Metelkova (1), O. Lang (3). (1) Department of Nuclear Medicine, University Hospital, Olomouc; (2) Department of Internal Medicine, Universisty Hospital, Olomouc; (3) Dept. of Nucl. Med., Univ. Hospital, Prague-Vinohrady, Czech Republic.

Aim: It is generally accepted that Tl-201 lung uptake has an important prognostic value in patients (pts) with coronary artery disease. The use of Tc-99m-MIBI SPECT imaging for risk stratification has also been reported and validated; however, the pulmonary uptake of this radiopharmaceutical has usually not been calculated. The aim of our study is to explain in which group of pts assessed by exercise SPECT the quantification of Tl-201 lung uptake helps to evaluate the prognosis.
Methods: 149 pts - 74 after myocardial infarction (MI) - underwent exercise Tl-201 SPECT. The SPECT patterns were divided into normal (n=45), fixed defects (n=29) and inducible ischemia (n=75). Anterior planar image was performed before SPECT acquisition to calculate the lung-to-heart ratio (L/H). L/H<0.5 was considered as a normal result. An average follow-up of pts was 20±9 months and a cardiac event was defined as either cardiac death or nonfatal MI.
Results: We registered cardiac events in 21 pts (8 deaths and 13 nonfatal MI). L/H ratio was higher in pts with cardiac event (average value 0.57) than in those without it (0.45); L/H ratio depended on the severity of the cardiac event: average value 0.54 in nonfatal MI and 0.7 in cardiac death. Among 45 pts with normal SPECT, no hard event was observed and L/H ratio (average value 0.36; range 0.22-0.58) was not helpful for risk stratification. In 29 pts with the presence of fixed defects, we registered four cardiac deaths (all in pts with L/H>0.5), annual event rate being 21.1% for L/H>0.5 versus 0% for L/H<0.5; P < 0.05. Pts with ischemia had 17 events, annual event rate being 15.4% for L/H>0.5 versus 13% for L/H<0.5; P = not significant.
Conclusions: Our results suggest the benign prognosis in all pts with normal SPECT. Conversely, pts with ischemia are at high risk for future cardiac events (irrespective of L/H ratio). The quantification of the Tl-201 lung uptake helps to predict future cardiac events in pts with fixed defects (significantly higher risk in pts with L/H>0.5). Therefore, for assessment of the prognosis in pts after MI we prefer Tl-201 instead of MIBI.

PS_250

DUAL ISOTOPE IN CHRONIC CORONARY ARTERY DISEASE. INCREMENTAL VALUE OF STRESS G-SPECT

M.L. De Rimini (1), M. Catalano (1), A. Scalzone (2), R. Merenda (2), V. Ippolito (1), P. Muto (1). (1) Nuclear Medicine Dpt; (2) Cardiovascular Dpt, A.O. Monaldi, Naples, Italy.

In patients (pts) affected with chronic CAD and Left Ventricular (LV) dysfunction, Rest Thallium-201 has high prognostic value. Stress-SPECT myocardial imaging can provide enhanced risk stratification and Gated-SPECT yield greater incremental prognostic value for prediction of hard event than stress perfusion SPECT alone.
Aim of the study was to verify the extension of myocardium viability with a Dual Isotope myocardial scintigraphy in chronic CAD, by combining assessment of post-stress LV function and regional myocardial thallium activity?
Methods: Dual Isotope (Tl-201 SPET Rest 20' – Rest 24h; Stress-Gated-SPET-Tc-99m Sestamibi) protocol was performed in 12 pts affected with chronic dysfunctional CAD. Combined assessment of of LV function was given from GATED-SPET scan. Tracers myocardial uptake was quantified in 264 segments (S) as % of peak in a 4 points scale (from 0 as normal to 3 as severe defect), using a 22 segment scheme. Defects were classified as fixed (F) or as reversible (Rev.>60% of peak) or partially reversible (PRev.>50% of peak)., in presence of 10% uptake increase at rest with respect to stress. Threshold uptake for viability criteria was 50%. LV Rest Ejection Fraction and regional wall motion as % of thickening (%T) were obtained from Gated data at Emory analysis.
Results: Preserved Rest-thallium and Stress-Sestamibi uptake were found in 192 segments; in pathological S, Stress-Sestamibi defects showed an incremental prognostic value for ischemic extension than comparated each-other thallium 20' and 24h scan.

Tot.S SPET-		Score 1	Score 2	Score 3
Sestamibi-Stress Defect :	tot. 72 S	18 S (25.%)	24 S (33. %)	30 S (41.%)
Tl 201 - 20' Defect:	tot. 57 S	27	18	10
Tl 201 - 24h Defect:	tot. 30 S	12	11	7

Stress-G-SPET-Sestamibi, in corresponding defects areas showed: %T: <- 10 as dyskinesia in 3 S; %T = 0-10 in 30 S; %T = 20 – 30 in 28S. Post stress global dysfunction in 8 pts: LVEF < 37%.
Conclusion: In patients with chronic CAD and Left Ventricular dysfunction, our data confirm that Stress-G-SPECT myocardial imaging can provide enhanced risk stratification and the high role of rest-redistribution thallium SPET.

Poster presentation

PS_251

INTERPRETIVE REPRODUCIBILITY OF STRESS THALLIUM 201 SPECT PERFUSION IMAGING IN OBESE PATIENTS

P. Lecouffe, P. Tellier. Department of Nuclear Medicine, Clinique Ste Catherine, Arras, France.

Aim : In routine clinical practice, cardiac thallium 201 SPECT images are of poor quality in obese patients. So, the aim of this study was to assess the reproducibility of their clinical interpretation.
Methods : 100 patients (61 men, 39 female), with a body mass index > 30 kg/m2 were prospectively included. Two experienced readers interpreted stress (58 treadmill exercise and 32 dipyridamole) and rest thallium 201 SPECT images. A first interpretation was done without any clinical data. A second reading was performed using all clinical and stress data. Images were classified as normal or abnormal for ischemia. Reproducibility was assessed by use of percent agreement and Kappa statistic.
Results : Without clinical data, agreement was mild (75 %, Kappa = 0.34). Addition of clinical data significantly increased agreement (86 %, Kappa = 0.59, $p < 0.05$). Discrepancies concerned both inferior and anterior wall in female, but were highly more frequent in inferior wall in male patients. No difference was observed between dipyridamole and treadmill exercise tests.
Conclusion: As expected interpretive reproducibility of thallium 201 SPECT perfusion images is mild in obese patients. Nevertheless, this study point out that clinical data are of importance in interpretation of perfusion images, especially in obese patients, leading to an acceptable interpretive reproducibility in clinical routine practice.

PS_252

IS REST-REDISTRIBUTION THALLIUM TOMOSCINTIGRAPHY A PREDICTOR OF LONG TERM CLINICAL OUTCOME OF PATIENTS WITH ACUTE MYOCARDIAL INFARCTION?

E. Tran-ngoc (1), P. Martin (1), B. Peperstraete (2), N. Dumarey (1), J. Devriendt (2), J. Paternot (1), R. Gheldof (1), P. Decoodt (2), M. Verhas (1). (1) Nuclear Medicine CHU Brugmann; (2) Cardiology CHU Brugmann, Brussels, Belgium.

Aim : to assess if the presence or absence of 201 Tl redistribution (R) in recent acute myocardial infarction (AMI) could predict favourable or unfavourable late clinical outcome of the patient (reinfarction, death).
Methods : from 01 1996 to 05 1997, 65 patients (64 +/-13y) with AMI had 201 Tl rest-redistribution (R-R) myocardial tomoscintigraphy (180¡ acquisition, Sopha DSX rectangular tomocamera, late acquisition without reinjection 3 hours later). 58 pts. had a clinical follow-up until september 2000 (16 non Q wave AMI and 42 Q wave AMI). Coronal slices were divided into 3 or 4 segments whom activity was normalized to peak activity, to which a 100% value was assigned. R was considered + in case of a gain > 10% of activity with initial value of <75%.
Results : according to this, R+ was 29% (12/42) in Q wave AMI (19% inf. AMI and 44% ant. AMI) and R+ was 69% (11/16) in non Q wave AMI. The clinical outcome was more favourable in 34/42 (81%) Q wave AMI (92% inf. AMI and 81% ant. AMI) than non Q wave AMI 8/16 (50%). 100% of Q wave AMI with R+ had a favourable evolution in regard with 55% of R+ non Q wave AMI. We also found a high percentage of favourable clinical outcome in Q wave AMI with R- 25/30 (83%) in regard with 2/5 (40%) of non Q wave AMI independently of localisation. According to this, the sensibility and specificity of R+ to predict late clinical evolution was 40% and 62% respectively. Positive predictive value was 78,3% and negative predictive value was 23%.
We conclude that taken separately, R- in Q wave AMI did not predict a bad evolution. For Q wave AMI, R+ was associated with favourable outcome but this trend is not significant as compared with R- Q wave AMI, from a statistical point of view (Chi2 test p=0,13, n.s.). Half of the patients with non Q wave AMI, independently of R+ or R-, had an unfavourable outcome : this is in accordance with the literature data which predict a worse outcome for these patients. The higher % of favourable clinical outcome in inferior AMI in spite of a higher rate of R- could be due to a more limited functional consequence of inf. AMI.

PS_253

ASSESSMENT OF THE EFFECTS OF ATENOLOL-INDUCED HEART RATE DECREASE ON MYOCARDIAL PERFUSION AND CONTRACTILITY IN PATIENTS WITH CORONARY HEART DISEASE USING 99MTC-MIBI GATED SPECT

L. Samoylenko , E. Safonova, V. Mikheev, E. Zharova, V. Sergienko. Department of Nuclear Medicine, Cardiology Research centre, Moscow, Russia.

Aim: To assess the effects of atenolol-induced heart rate decrease on myocardial perfusion (MP), systolic and diastolic function in patients with chronic coronary artery disease (CAD) and mildly depressed myocardial contractility.
Methods: 17 males (mean age 51±3 yrs) with stable angina (10 pts with CCS functional class II and 7 pts with CCS functional class III), angiographically confirmed CAD (10 pts with 3-vessels disease, 7 pts with 2-vessels disease, and 11 pts with previous myocardial infarction) and mildly depressed systolic function (mean LVEF 44.4%) were underwent rest/stress 99mTc-MIBI gated SPECT before and after 10 days administration of atenolol (mean dose 100 mg/day) (12 pts) or placebo (5 pts). Atenolol dose was titrated to reach decrease in the heart rate at least by 20% from the baseline. The results were processed using Siemens Quantification and GS Quantification program.
Results: After 10 days atenolol treatment course the heart rate decreased from 79±8 to 58±5 bpm (p=.01), whereas in placebo group there were not significant changes. Myocardial perfusion improvement was shown in all patients treated with atenolol. 10 days treatment course with atenolol compared with placebo was associated with significant decrease in the ischemic score (25.7±5.0 to 18.0±2.4 [p<.01] vs 23.6±4.6 to 21.3±5.1 [NS]) and increase in LVEF (43.8±10 to 50.8±8 [p<.01] vs 45.0±7 to 43.1±7 [NS]). LVEDV decreased from 147±46 ml to 139±48 ml in atenolol group (p<.05). Diastolic time lengthened from 465±186 ms to 632±145 ms (p<.01) in the atenolol group and did not significantly changed in placebo group (430±150 to 440±145; NS). In addition, there was improvement in the symptoms and increase in the total workload time in the atenolol group.
Conclusion: Heart rate decrease by 20% on atenolol is associated with the myocardial perfusion improvement as well as systolic and diastolic function in patients with chronic CAD.

PS_254

EARLY REST AND LATE STRESS - REST 99MTC - TETROFOSMIN SPECT AFTER ACUTE MYOCARDIAL INFARCTION, IN IDENTIFYING MYOCARDIUM AT RISK AND EXERCISE-INDUCED ISCHAEMIA

L. Petrovici (1), R. Capalneanu (1), C. Medrea (1), C. Sfangeu (2). (1) Department of Nuclear Cardiology, Heart Institute ; (2) Department of Nuclear Medicine, County Hospital Cluj-Napoca, Romania.

PURPOSE: As myocardial infarction is often due to haemodynamical insignificant coronary lesions, myocardium at risk and exercise -induced ischemia may differ. The objective was to compare early and late rest SPECT with late exercise SPECT, to identify myocardium at risk and ischemia.
METHODS:28 patients (19 men, 9 women) were examined at rest in the first two weeks after a first acute Q-wave MI (17 anterior, 12 trombolysed and 11 inferior, 5 trombolysed). All of them were reexamined later (42-124 days) with a two-day rest-stress protocol. All studies were performed at 1 hour after the i.v.administration of 740 MBq 99m-Tc tetrofosmin. All studies were imaged on the same one-head camera, Philips ARC 3000 with ADAC Pegasys X workstation. The myocardium was divided in 19 segments, uptake was scored from 0 (absent) to 3 (normal). All patients underwent coronary angiography. There were 14 univascular, 6 bivascular and 9 multivascular patients.
RESULTS: From 134 segments (25%) with an uptake of 0-1 at early rest, only 85 (16%) were present at late rest There were 51 (10%) segments with an uptake of 0-2 at exercise, reversible at late rest. From these segments with reversible defects 26 (5%) had an uptake of 0-1 at early rest, normal at late rest and 25 (5%) were normal at booth rest studies. From the 26 partially reversible segments at early rest and reversible at late rest, 15 were in univascular patients, 3 in bivascular patients, 8 in multivascular patients. From the 25 reversible segments at booth rest studies, 3 were in univascular patients, 4 in bivascular patients, 18 in multivascular patients.
CONLUSIONS: After acute myocardial infarction, early rest even at 2 week late rest-exercise 99m-Tc tetrofosmin can differentiate myocardium at risk from exercise-induced ischemia. Differences between them are quite common. Myocardium at risk and exercise-induced ischemia in the same segments are more often in univascular patients, in different segments more often in multivascular patients.

PS_255

Abstract withdrawn

PS_256

THE ROLE OF RFS (RADIONUCLIDE FRACTIONAL SHORTENING) IN QUANTITATIVE EVALUATIONS OF MYOCARDIAL INFARCTIONS

M. Atalay (1), Y. Duman (2), A. Altıntığ (3), E. Teber (1), H. Akın (1).
(1) Department of Nuclear Medicine, Atatürk State Hospital;
(2) Department of Nuclear Medicine, Ege University Hospital;
(3) Department of Cardiology, Ege University, Izmir, Turkey.

The aim of the study is to evaluate the relationships between RFS (Radionuclide fractional shortening) values, first pass radionuclide angiography, LV(Left ventricule) ejection fraction LVEF values, SPECT examination (to determine the site and the size of infarcted area) and gated perfusion examination findings in patients with myocardial infarction based on clinical, enzymatic or electrocardiographic criteria.

Methods: All the patients were performed with first pass radionuclide angiography of Tc-99m MIBI, rest SPECT and gated perfusion studies. The sizes of defected areas were determined(%) in SPECT examinations. Gated cardiac examination was end diastol (ED) and sistol (ES) visions were obtained left anterior oblique projection. Vertical and horizantal axis were drawn in their anteroposterior wall(ap) and septum-lateral(sl) positions. The lenght of each axis was calculated by the formula below.

$$\text{Global RFS}(\%) = \frac{(EDap + EDsl) - (ESap + ES\,sl)}{EDap + EDsl} \times 100$$

Results: Linear correlation was found between LVEF and global RFS values. It was found that there were opposite correlation between % defectiveness with LVEF and global RFS.

Conclusions: Global RFS seems to be good parameter showing left ventricular function capacity.

PS_257

PROGNOSTIC VALUE OF MYOCARDIAL TC-99M TETROFOSMIN GATED-SPET IN PATIENTS UNDERGOING THORACIC SURGERY

M.L. De Rimini (1), M. Catalano (1), A. Scalzone (2), R. Merenda (2), A. D'Amico (3), V. Ippolito (1), P. Muto (1). (1) Department of Nuclear Medicine; (2) Cardiovascular Department; (3) Anesthesiology Service, A.O. Monaldi,Naples, Italy .

Patients (pts) undergoing major surgical procedures with scintigraphic evidence of stress induced ischemia have a significantly higher incidence of perioperative cardiac events. However, it is also well demonstrated that poor left ventricular function places pts at increased jeopardy of perioperative events.

Aim of the study was to evaluate prognostic value of Myocardial Gated-SPECT in presurgical assessment of cardiac risk in high risk pts.

Methods: we enrolled 12 pts, all male, mean age 66 years, affected with lung carcinoma undergoing to surgery, 5 of them with history of CAD and previous myocardial infarction over one year. Double-day Tc-99m Tetrofosmin Dipyridamole and Rest myocardial Gated-SPECT were performed during beta-blockers therapy. A 22 segment (S) model, with a total of 264 (S), was used to analyse Tetrofosmin myocardial perfusion uptake. LV Rest Ejection Fraction and regional wall motion as % of thickeness (%T) were obtained from Gated data at Emory analysis.

Results: Severe reversible defects, corresponding areas: %T< 10-20% and Rest LVEF < 40% were found in 1 pts; moderate but extense reversible defect with abnormal %T and LVEF > 50% in 2 pt. All of them underwent angiography and planning for simultaneous myocardial riperfusion and lung carcinoma surgery was programmed. Low-Moderate reversible defects, LVEF >50% and no severe abnormalities of %T were found in 4 pts, suggesting beta-blockers treatment before, during and after lung surgery. No myocardial perfusion abnormalities or LV function in 5 pts were found.

Conclusion: Our data suggest that Dipyridamole test can better reproduce stress surgery induced and showed the incremental prognostic value provided from Gated Perfusion SPECT data to perfusion study

PS_258

IMPORTANCE OF PHASE ANALYSIS IN EARLY ASSESSMENT OF SEGMENTAL CONTRACTILITY IN PATIENTS WITH ACUTE MYOCARDIAL INFARCTION

A. Cickusic (1), N. Latic (2), Z. Kusljugic (3). (1) Deparment of Nuclear Medicine Cantonal Hospital Zenica, Bosnia and Herzegovina; (2) Deparment of Nuclear medicine Cantonal Hospital Zenica, Bosnia and Herzegovina ; (3) Department of cardiology, Internal Clinic UKC Tuzla Bosnia and Herzegovina.

Myocardial infraction impairs the heart muscle contractility. Regional disorders of the heart walls motions are very characteristic and sensitive indicators of the left ventricle function after AIM.

The aim of this study is to establish the frequency and the level of the segmental contractility disorder in the early stage after AIM by means of a phase analysis of radionuclide ventriculography .

Forty two subjects have been analyzed, 36 males and 6 females of an average age of 51.31 ± 11.28. The study has encompassed 23 subjects with AIM of the front and 19 subjects with AIM of the lower wall.

Method: Radionuclide ventriculography in equilibrium has been carried out on 4.33 ± 0.25 day from the onset of symptoms. Contrast ventriculography with selective angiocardiography has been carried out on 28.08 ± 21.19 day in relation to the onset of symptoms. In 42 subjects 462 segments have been assessed. Out of that 56.56% of segments have been dysinergic. The greatest frequency of dysinergy has been observed in the septal and apical region and the lowest one in the lateral region of the LV.

Result: Using contrast ventriculography as a golden standard, sensitivity and specificity of our method have been determined with regard to the level and localization of the segmental contractility disorder. The sensitivity of our method in determination of the level of the segmental contractility disorder amounts to 89%, specificity 93% and predictive value 89%. The sensitivity of our method with regard to the segmental disorder localization amounts to 89%, specificity 89% and predictive value 86%.

RNV is a very important non-invasive method in determination of the level and degree of the segmental contractility disorder in an early phase of acute myocardial infarction what is an important predictor of prognosis as well as in decision making with regard to the choice on further therapeutic treatment in an early phase of acute myocardial infarction.

PS_259

THE ACCURACY OF ST CHANGES DURING TREADMILL EXERCISE IN PREDICTING OF LOCALISING REGIONAL MYOCARDIAL ISCHAEMIA

N.W. Garvie, C. .J. Cooke, F. Salehzahi. Royal London Hospital, Nuclear Medicine Department, London E1 1BB, UK.

Aim

Despite the increasing clinical acceptance of stress myocardial perfusion imaging (MPI) in the diagnosis and management of ischaemic heart disease (IHD), the Exercise Tolerance Test (ETT) remains the most popular technique employed by cardiologists. This paper examines the significance of ST changes developing during ETT procedures, performed as part of a stress MPI protocol.

Methods

212 patients with clinically - suspected IHD underwent MPI, using a 2 day MIBI protocol. ETT was used as the stress procedure. All patients attained their target heart rate before isotope injection. ST depression, when present, was graded minor (1mm) significant (2mm) or marked (>2mm), and the location was charted.

Results

37 patients were found to have ischaemia on the basis of the subsequent MPI images.

16 of this group (43%) showed ST depression, of which 7 (19%) were minor, 5 (14%) were significant, and 4 (11%) were marked. In 11 instances (69%) the location the ST changes matched the site of ischaemia on MPI. Of the 175 normal patients 50 (29%) showed ST depression, of which 34 (19%) were minor, 15 (9%) significant and 1 (~ 0.0%) marked.

Six of the patients with proven ischaemia (16%) developed angina - type symptoms (ATS) during ETT, compared to 36 (21%) of the normal group.

Conclusions

Minor (1mm) ST depression occurred equally amongst patients with proven IHD and normal patients (19%). This feature is, however, frequently regarded by cardiologists as 'borderline', and therefore an indication for stress MPI. Significant (2mm) depression was slightly more predictive of I.H.D (PPA, 60 %), but only marked ST depression appeared to adequately discriminate, (although the number in this group (5) is really too low for analysis). The presence of ATS was of no predictive value.

The absence of ST changes during ETT does not reliably exclude IHD. Conversely ST changes, even if significant, are not a reliable guide to the existence of disease.

PS_260

BRAIN NATRIURETIC PEPTIDES (BNP): RELATION WITH SLEEP-RELATED BREATHING DISORDERS (SRBD) IN PATIENTS WITH STABLE HEART FAILURE (SHF)

J. López (1), M. Villa (2), E. Quintana (3), R. Álvarez (1), P. Gómez (1), D. G Solís (1), F. G Pesquera (1), A. Martínez (2), A. Cayuela (4), A. Ramos (1), R. Vázquez (1)(1) Department of Nuclear Medicine; (2) Department of Cardiology. HUV Rocío, Sevilla, Spain; (3) Medical-Surgical Unit of Respiratory Diseases. HUV Rocío. Spain; (4) Supportive Research Unit. HUV Rocío. Sevilla. Spain

Aim: Brain natriuretic peptides (BNP) are markers of several heart diseases. We wanted to analyze if their levels have a relation with the presence of sleep-related breathing disorders (SRBD) in patients with stable heart failure (SHF).

Methods: We have consecutively studied 19 patients with left ventricular ejection fraction <45% who were clinically stable (symptoms or signs of heart failure had not changed in the previous 4 weeks) and had received standard therapy. Baseline assessment included determination of BNP (quantitative determination by immunoradiometric assay: SHIONORIA BNP), and isotopic ventriculography. All patients underwent a full-night polysomnography. SRBD was defined with an apnea-hipopnea index (AHI) >10.

We used U-Mann-Whitney test to analyze the results.

Results: 6 patients had SRBD (group 1) and there were 13 patients without SRBD (group 0). There were no significant differences between both groups in age, sex, body mass index and left ventricular ejection fraction. BNP median was 37.3 in group 1 (Percentil 25: 14.3; Percentil 75: 227.72) and 17.1 in group 0 (Percentil 25: 17.1; Percentil 75: 42.75); p 0.32.

Conclusions: Although there were no significant differences in BNP between both groups, our results show higher levels in group 1 (SRBD present). The correlation of this finding with the prognostic of these patients, it would be determined.

PS_261

THE NITRATE ENHANCED TC-99M MIBI SPECT IN DETECTING VIABLE MYOCARDIUM IN PATIENTS WITH CORONARY ARTERY DISEASE AND LV DYSFUNCTION

M. Kostkiewicz, W. Tracz, M. Olszowska, T. Przewlocki, P. Podolec. Department of Nuclear Cardiology, Jagiellonian University, Cracow, Poland.

In patients with chronic coronary artery disease and the depressed left ventricular function, assessment of residual viability in akinetic myocardium is vital for therapeutic management. In the present study a direct comparison between perfusion imaging with nitrate enhanced Tc 99mMIBI imaging and wall motion pattern in echocardiography was carried out, as well as the usefulness of this modality for detecting myocardial viability was assessed.

Methods and Results: Twenty-four patients with coronary artery disease underwent Tc 99m MIBI imaging during intravenous nitroglycerine infusion. Eighteen patients had their echocardiograms repeated after revascularization. Perfusion and wall motion scored from 1 to 3 (absent to normal). The sensitivity for the rest –nitroglycerine perfusion scan was 87%. The specificity for this procedure was down to 55%. Positive predictive value achieved 89% while the negative predictive value did not exceed 40%.

Conclusions: Nitroglycerine enhanced Tc99m MIBI imaging is a useful technique for detecting underperfused, viable myocardium. There is high concordance between perfusion and echocardiographic imaging. The ultimate selection of therapy should ideally be based on a comprehensive range of complementary methods.

PS_262

PROGNOSTIC VALUE OF SIZE AND SEVERITY OF PERFUSION DEFECTS IN PATIENTS AFTER ACUTE MYOCARDIAL INFARCTION

V. Chernov (1), S. Salpagarova (2), J. Vesnina (1), Y.U. Zayblov (2), Y.U. Lishmanov (1). (1) Nuclear Medicine Laboratory; (2) Out-patient Department, Institute of Cardiology, Tomsk, Russia.

Aim: The aim of this study was to estimate the prognostic value of size and severity of perfusion defects in patients (pts) after acute myocardial infarction (AMI) by adenosine (A) – rest (R) Tc-99m MIBI SPECT.

Methods: 155 CAD pts (all males, mean age 52±4) were underwent A-R Tc-99m MIBI SPECT, echocardiography and bicycle test 3-4 weeks after AMI. The next indices were assessed: A (ADS) and R perfusion defect size (RDS), integral indices of A (IIAD) and R (IIRD) perfusion defect, as well as ejection fraction (EF) and exercise tolerance (ET). A cardiac event was defined as either cardiac death (CD), nonfatal AMI, unstable angina requiring further revascularization (UA).

Results: During an average follow-up of 18±6 months all pts were divided into two groups: Gr.1 (105 pts) with benign current of disease and Gr.2 (50 pts) with cardiac events (5 - CD, 12 - AMI and 33 - UA).

The myocardial perfusion parameters in these patients are presented in the Table.

Indices	1 Gr. M±m	2 Gr. M±m		F	R^2
ADS (%)	23,9±1,1	32,7±2,2	0,001	16,53	0,10
RDS (%)	18,0±1,0	27,2±2,1	0,0000	26,3	0,15
IIAD (%)	10,5±1,0	16,5±2,1	0,01	6,25	0,05
IIRD (%)	5,7±0,5	9,3±1,1	0,001	11,11	0,07

The low level of EF and ET had own prognostic value, but did not add prognostic value to 99mTc-MIBI SPECT.

Conclusion: The extensive sizes of perfusion defects at rest and at peak of adenosine test was shown to predict future cardiac events.

PS_263

A WASHOUT RATIO OF 123I-15-(P-IODOPHENYL)-3-R,S-METHYL PENTANOIC ACID (BMIPP) AS A GOOD PREDICTOR OF MYOCARDIAL FUNCTIONAL RECOVERY AFTER THE FIRST ACUTE ANTEROSEPTAL MYOCARDIAL INFARCTION

H. Yamawaki (1), M. Ueeda (1), K. Takeda (1), K. Kono (1), M. Obika (1), Y. Nagano (1), M. Imai (1), S. Kusachi (2). (1) Division of Cardiology, Mitoyo General Hospital, Kagawa, Japan; (2) Department of Medical Technology, Okayama University Medical School, Okayama, Japan.

Aim: The preserved free fatty acid metabolism in an infracted myocardium is an evidence for viability. We conducted this study to clarify whether a washout ratio of ^{123}I-BMIPP could use as an indicator of preserved free fatty acid metabolism and a predictor for myocardial functional recovery.
Methods: The study population was 23 patients with first acute anteroseptal myocardial infarction. All patients received a successful direct percutaneous coronary intervention within 12 hours after the onset. A resting ^{201}Tl _ ^{123}I BMIPP dual SPECT study was conducted at the 7-10th day. Fifteen minutes and three hours after the injection of both radioisotopes, we collected SPECT data as early and delayed images, respectively. The Bull's eye maps were automatically divided into 25 segments, and we picked up percent uptakes and washout ratios of thallium and BMIPP in both infracted and control area. A coronary angiography and a left ventriculography (LVG) were performed at the 3rd week, and several functional data were compared to SPECT data.
Results: Significant correlations were observed between global LVG ejection fraction (LVG-EF) and Tl %uptake in the infarct area ($r=0.72$, $p<0.01$), BMIPP %uptake in the infarct area ($r=0.71$, $p<0.01$) and washout ratio ob BMIPP in the infarct area ($r=0.71$, $p<0.01$). A washout ratio of thallium had no relation to LVG-EF ($r=0.22$). A washout ratio of BMIPP was also well correlated to the segmental ejection fraction (segment 2, $r=0.69$, $p<0.01$, segment 3, $r=0.56$, $p<0.05$) and the systolic left ventricular volume index ($r=0.71$, $p<0.01$). These data indicated that an infracted area with less reduction of % uptake and more accelerated washout of BMIPP showed better functional recovery with minimum expansion of a left ventricle.
Conclusions: A washout ratio and percent uptake of BMIPP in an infracted area could be a good predictor for functional recovery and remodeling of a left ventricle at chronic phase.

PS_265

THE ROLE OF INTRASURGICAL GAMMA PROBE COMBINED WITH LYMPHOSCINTIGRAPHY IN IDENTIFICATION OF SENTINEL NODE IN MELANOMA AND BREAST CANCER

S. Koukouraki (1), E. Sanidas (2), A. Velidaki (1), I. Askoxilakis (2), T. Tsagatakis (2), D. Tsiftsis (2), N. Karkavitsas (1). (1) Department of Nuclear Medicine; (2) Department of Surgical Oncology, University Hospital,Crete, Greece.

Purpose: The purpose of this study is to evaluate the potential of the gamma ray detecting probe (GDP) in combination with lymphoscintigraphy, to detect sentinel nodes in patients with melanoma and breast cancer.
Methods : 60 patients with operable palpable breast tumour and 30 patients with melanoma were estimated before and during surgery using a gamma ray detecting probe (Neoprobe 1500) and a lymphoscintigraphy before surgery. 2-4 hours before surgery, 1-1.5mCi 99mTc-Re(SC) was injected intradermally around the lesion . A ? camera GE Millenium provided with a LEGP collimator was used. Planar views were taken at 10', 30' and 2 hours p.i. In the same time the GDP was used to locate the node emitting the greatest activity, before and during the surgery. Isosulfan was also used during surgery.
Results: Both techniques revealed one or more lymphonodes within the first 30 min in all cases. Axillary nodes were revealed in 60/60 patients(100%) with breast cancer. In 1/20 an internal mammary node was also revealed. In all cases of melanoma the localization of SN was succesful . Lymphoscintigraphy, GDP and isosulfan showed the same nodes in all patients (the node in the internal mammary chain was revealed by lymphoscintigraphy and GDP only)
Conclusion: The use of lymphoscintigraphy which allows accurate preoperative localization of the SN in association with the use of GDP which identify the SN before the incision, maximise the success of sentinel node localization.

DIAGNOSTIC ONCOLOGY 7

PS_264

RADIOGUIDED BIOPSY OF SENTINEL NODE IN MALIGNANT SKIN MELANOMA

L. Feggi (1), G. Soliani, L. Bergossi, S. Panareo, E.F. Jorizzo, N. Prandini, A. Ciprian, U. Maestroni, W. Pagani, P. Carcoforo. (1) Nuclear Medicine , St. Anna Hospital; (2) Dermatology Unit, Hospital of Rovigo; (3) Nuclear Medicine , University of Ferrara; (4) Clinical General Surgery, University of Ferrara, Italy

The biopsy of the first tumor-draining lymph node (sentinel node, SN) is bound to become the procedure of choice in regional staging of skin melanoma patients. A tumor-negative SN virtually excludes lymphatic metastases and obviates the need for lymph node dissection; a therapeutic dissection is then performed only in patients with proven nodal disease. *Material and methods:* The study, began in November 1997, comprised 87 patients aged between 31 and 82 years (mean 59) with histologically proven cutaneous melanoma stages I and II (according to the American Joint Committee on Cancer staging criteria) located on the neck in 6 cases, on the trunk in 43 cases, in the upper limbs in 7 cases and in the lower limbs in 31 case. The Breslow thickness ranged from 0.81 to 3.94 mm. All patients underwent preoperative lymphoscintigraphy to demonstrate the lymphatic basins at risk for metastatic disease. The injection of 99m-Tc nanocolloid (10MBq) was performed in 4 intradermally spots around the surgical scar of the primary tumour in the morning of the surgery: the scintigraphy was then performed within 1 hour. In all the cases of our series we utilized a probe (Pol.hi.tech. srl) specific for collimation for the intraoperative detection of SN. After induction of general or local anesthesia, Isosulfan blu vital dye was also injected around the excision scar. *Results:* Identification of one or more SNs was possible for 86 patients of the 87 patients (98.86%); in only one case it was not possible to identify the SN because the lymphatic mapping was dramatically modified by radical excision of melanoma. The accuracy of lymphatic mapping was examined by comparing the histopathology of SN and non SN specimens and the result was 100%: i.e. we didn't find any false negative. In 1 patient the SN was identified only by probe and not with lymphoscintigraphy. *Conclusion:* The experience indicates that preoperative lymphoscintigraphy and intraoperative mapping can accurately identify the SN in skin melanoma. The SN biopsy is a cost-effective procedure because reflect the status of the regional nodal basin and represent a minimally invasive and highly accurate screening technique often possible in local anesthesia saving discomfort, time and money.

PS_266

ACTIVITY-DEPENDENT IMAGING OF AFFERENT LYMPH VESSELS IN SENTINEL-NODE SCINTIGRAPHY

G. Altenvoerde (1), J. Meller (1), M. Funke (2), K. Lehmann (1), D. Hempel (1), W. Becker (1). (1) Department of Nuclear Medicine, Georg-August-University, Göttingen, Germany; (2) Department of Radiology, Göttinge, Germany.

Aim: Sentinel-node scintigraphy imaging of the afferent lymph vessels can supply important anatomical informations to the surgeon. Aim of the retrospecive study was the evaluation wether the imaging of lymph vessels depends on the activity given.
Methods: We performed dynamic sentinel-node scintigraphy in 42 patients (age 58y ± 14y, range 31y – 84y, median 62y, 23 male, 19 female) with malignant melanoma. Malignant melanoma were localised at the head (n=1), at the upper limbs (n=8), at the upper part of the body (n=10), abdominally (n=5) and in 18 patients at the lower limbs. We injected 0.1ml Tc-99m-NANOCOLL (NYCOMED AMERSHAM SORIN) intracutaneous peritumorally. Planar acquisition with one-headed-camera (Marconi SX 100, LEHR-collimator, 30 minutes, 15s/frame) was performed. In 18 patients we injected <50MBq activity (38.3MBq ± 1.9MBq, range 37MBq – 43MBq, median 37.5MBq), 24 received >50MBq activity (98.3MBq ± 18.0MBq, range 58MBq – 119MBq, median 102.5MBq).
Result: In 40 (90%) of the patients the sentinel lymph node could be identified. The afferent lymph vessels could be imaged in only 3 (16.7%) of the patients with activities <50 MBq. Conversely the afferent lymph vessels were seen in 23 (95.8%) of the patients with higher activities >50MBq.
Conclusion: In sentinel-node scintigraphy the use of higher activities (>50 MBq) is necessary for the identification of the afferent lymph vessels, without a significant increase of the patients radioactive burden. This can be helpful if an en-bloc-resection of tumor and lymph vessel is planned.

PS_267

ACCURACY ENHANCEMENT OF LYMPHOSCINTIGRAPHIC IDENTIFICATION AND LOCALIZATION OF SENTINEL NODES (SNS) OF CUTANEOUS MALIGNANT MELANOMA (MM) BY TEMPORARY SHIELDING OF HOT SPOTS

S. Maza (1), L. Geworski (1), V. Ivancevic (1), A. Zander (1), E. Dräger (2), H. Winter (2), W. Sterry (2), D.L. Munz (1). (1) Clinic for Nuclear Medicine; (2) Clinic for Dermatology, Charite, Berlin, Germany.

Aim: The sentinel lymph node mapping offers a minimally invasive way of assessing the regional lymph node basins draining a cutaneous melanoma. The detection of the „true" SN(s) and, hence, the staging of regional lymph nodes is essential for management and prognosis in MM. In this study it was prospectively evaluated whether simple temporary shielding of hot spots could improve the accuracy of SN diagnostics.
Method: In 100 consecutive MM-patients (45 women, 55 men; age, 11-91 years) dynamic and static lymphoscintigraphy in various views was performed after strict intracutaneous application of Tc-99m-nanocolloid (40-150 MBq; 0.05 ml/deposit) around the tumor (31x) or the biopsy scar (69x, safety distance 1 cm) (gamma camera, LEAP collimator, 256x256 matrix). The images were acquired up to 2 hours p.i. with and without temporary lead shielding of the most prominent hot spots (injection site, drainage area (DA).
Results: In 33/100 patients 1-2 additional less tracer accumulating or smaller (<1.5 cm) SNs were detected after shielding of the prominent hot spots in the DA. In 4/33 patients metastases were found even in the less accumulating/smaller SNs, the non-SNs removed in the subsequent elective lymph node dissection were tumor negative. In 3/100 patients hot spots in the DA proved to be lymph vessels (LV), intersections or vessel ectasies after temporary shielding, hence, the node interpreted secondary at first glance proved to be the real SN. In 2 of these patients lymph node metastasis was histologically confirmed, the non-SNs were tumor free. In 7/100 patients the exact course of LV could be mapped after shielding, in one of these patients 2 additional SNs (with metastasis) could be detected. In total, 43/100 patients the temporary shielding of hot spots in the DA showed an improvement of the accuracy of lymphoscintigraphy.
Conclusion: The temporary shielding of prominent hot spots in the DA of a MM leads – in combination with dynamic acquisition in various views – to accuracy improvement of the identification and localization of SNs by lymphoscintigraphy.

PS_268

LYMPHATIC MAPPING AND SENTINEL LYMPH NODE BIOPSY IN MELANOMA

G. Çivi (1), H.B. Sayman (1), Y. Aydın (2), H. Arslan (2), K. Özcan (1), B. Kanmaz (1), L. Kabasakal (1), I. Uslu (1). (1) Department of Nuclear Medicine; (2) Department of Plastic Surgery, I.U. Cerrahpasa Medical Faculty, Istanbul, Turkey.

Aim: Lymphatic mapping with selective lymphadenectomy is an attractive approach in melanoma patients to avoid unnecessary elective lymph node dissection (ELND). We performed lymphoscintigraphy (LS) in 20 patients with strong clinical suspection of melanoma (13) or diagnosed as melanoma by biopsy preoperatively (7). 8 patients had melanoma of the extremities (1 upper, 7 lower), 4 patients had melanoma of the trunk and 8 of the neck.
Methods: Prior to surgery, 37 MBq Tc- 99m tin colloid in 1cc was injected ID in 4 quad. of lesion in equal doses to define the regional lymphatics and sentinel lymph node (SLN). Following injection, 3 min dynamic images were acquired until any SLN(s) appeared. In all cases, a CdTe gamma probe (GP) was used to skin-mark the SLN in accordance with the peak count rate observed and vital blue dye (VBD) was also used during surgery. After wide excision of the primary lesion, investigation of the SLNs were also continued intraoperatively and the operation was completed by SLN(s) excision. The pathology of the primary lesion and SLN(s) were defined by HEO staining.
Results: In 1 patient the primary lesion was found to be a basal-cell carcinoma with a metastatic SLN. Preoperatively in all cases at least 1 SLN could be detected by LS and GP. In 1 case, while only 1 SLN was detected by LS and GP preoperatively, it is found to be a pack of SLNs intraoperatively and pathologically. Each SLN which was detected preoperatively could be verified intraoperatively by GP and VBD except 2 cases. One of them was unable to be detected intraoperatively despite it was visualized preoperatively, because of a timing problem. The other was detected pre and intraoperatively by GP but could not be visualized by VBD. In one case intraoperative mapping also revealed additional SLN sites. In 13 cases, SLN(s) were invaded by malignant cells. These patients underwent axillary LND (1), inguinal LND (3) and radical neck dissection (2) by reoperation. SLN(s) were the only malignant LNS in 5, while in 1 case 2 more LNS other than SLN were found to be invaded by malignant cells pathologically. No distant metastases were found in any of the cases.
Conclusion: These results demonstrated that lymphatic mapping and SLN biopsy using a GP is an attractive approach in melanoma to avoid morbidity and mortality caused by unnecessary ELND.

PS_269

THE NUCLEAR MEDICINE GLOBAL APPROACH TO SENTINEL NODE (SN) TECHNIQUE IN PATIENTS WITH BREAST CANCER AND CUTANEOUS MELANOMA

S. Severi, F. Matteucci, C. Corbelli. Nuclear Medicine Dpt, Faenza, Italy.

INTRODUCTION: the SN technique has been largely developed in recent years and great will be the request of lymphoscintigraphy in the future also from outlying centre. In our department we cover four different hospital and deal with 13 different surgeons at least. In this conditions it is important to offer a complete assistance from the SN localization to the surgical excision, in order to ensure an high exam sensibility.
MATERIALS: in the last two years we performed 140 SN procedure; 110 were done for breast cancer and 30 for melanoma. As a standard we did a subcutaneous injection of 17 MBq 99mTc Nanocoll in 0,2 ml, in melanoma and superficial breast cancer. In breast cancers distant more than 1,5 cm from the skin we did a deep injection with the same radioactivity in 0.5ml under echography control. In deep breast tumours we had sometime (10%) the necessity to perform a second superficial tracer injection due to a lack of SN localization. Dynamic and static view were acquired with particular attention to the lateral and oblique projections to get either the marker of the SN projections on the skin and the identification of possible secondary sentinel lymphnodes involved.
RESULTS: thanks to the mentioned procedure we had a 100% SN localization and also a 100% SN surgical excision with a plateau learning curve of all the 13 surgeons involved. The effectiveness of the SN excision was made by probe measure and, when ever possible, gamma camera images. The number of double SN is about 15% and we also had, in one melanoma of the back, 3SN. The mean number of lymph-nodes exceeded was 4 standing the very little wound performed in patients that were generally awake.
CONCLUSIONS: the necessity to perform an high number of procedure for SN detection schould not cause a lack of Nuclear Medicine personnel presence also considering the high number of surgeon frequently involved. Moreover the complexity of the procedure, number of SN involved and differentiation between the lymph-node exceeded, require the presence of well trained operators in order to avoid false negative results.

PS_270

SONOGRAPHIC CARACTERISTICS OF SENTINEL LYMPH NODES IN PATIENTS WITH MALIGNANT MELANOMA

M. Lacic (1), M. Stanec (2), M. Ivkic (3), Z. Stanec (4), Z. Kusic (1).
(1) Department of Oncology and Nuclear Medicine, University Hospital ;
(2) Department of Surgery, Cancer Institute, Zagreb, Croatia;
(3) Department of Head and Neck Surgery, University Hospital ;
(4) Department of Surgery, University Hospital, Zagreb, Croatia

Aim: The aim of this study was to evaluate the sonographic characteristics of the sentinel lymph nodes (SLNs) in patients (pts) with malignant melanoma (MM).
Methods: Sentinel lymph node scintigraphy was performed in 124 pts, 57 female and 68 male, aged from 12 to 80 years (mean 49 years). Up to 74 MBq of Tc-99m nanocolloid were injected intradermally around the skin lesions (4 pts) or the biopsy scar (120 pts), followed by dynamic planar imaging until the SLNs became visible. The SLNs were marked on the skin using an external radioactive marker. Gray-scale sonography, followed by Color and Power Doppler analyses have been done using a 10 MHz linear probe. A hand held gamma probe and/or a blue dye technique were used for intra-operative mapping of SLN.
Results: SLNs were successfully detected in 123 from 124 pts on scintigraphy. 199 SLNs (1.6 per pts) were visualized on scintigraphy in 162 lymphatic basins (1.4 per pts). Among the 53 operated pts. 13 (25%) had positive SLN for MM. In 7 (54%) of these 13 pts SLN was the only metastatic node. 131 regional lymphatic basins in 94 pts were evaluated sonographicaly. Sonography was unable to differentiate SLNs from surrounding fatty tissue in 34(36%) pts. In 49(52%) pts SLNs had benign sonographic appearance. SLNs changes suspected to be metastatic lesions were detected in 11 (12%) pts on sonography. In 9(82%) of these 11 pts suspected metastatic lesions were histologically confirmed. Four (31%) of 13 pts with histologically proven SLNs metastasis had no sign of disease on sonography. A signal of increased blood flow within SLNs was detected in 7/94 (8%) pts on Color and Power Doppler sonography.
Conclusion: Scintigraphically guided, preoperative, sonographic evaluation of drained lymphatic basins seems to be a reasonable diagnostic approach to the management of pts with MM.

PS_271

GAMMA-PROBE-GUIDED SENTINEL LYMPH NODE BIOPSY IN MELANOMA PATIENTS

M. Papos (1), J. Varga (2), T. Sera (1), M. Lazar (1), K. Kapitany (2), J. Olah (2), I. Korom (2), G. Mohos (2), A. Dobozy (2), L. Pavics (1). (1) Department of Nuclear Medicine; (2) Department of Dermatology, University of Szeged, Szeged, Hungary.

Correct sentinel node (SN) localisation plays a crucial role in the planning of the surgical approach in melanoma patients. The value of preoperative and intraoperative SN localisation techniques is analysed. Forty-three patients (25 males, 18 females, mean age: 52 years, range: 30-77 years) with malignant melanoma (MM) were investigated. The localisations of the MM were as follows: trunk: 20, extremities: 23. On the Clark classification: I: 7, II: 25, IV: 11). Twenty-four hours before surgery, the SN was localised visually by a gamma camera technique. For intraoperative localisation of the SN, the gamma-probe and blue dye methods were applied. Preoperatively, SNs were detected in all patients (43/43, 100%). One SN was detected in 35 cases (81%) and two SN were verified in 8 cases (19%). The preoperative localisation of the SNs matched with the intraoperative gamma-probe findings in 39 patients (90%), wheeas there was a mismatched localisation in 4 patients (10%). The gamma-probe and blue dye techniques gave identical SN localisation in 38 cases (88%). In 2 cases, the SNs were not stained, and in another 3 patients the blue SNs could be found only with the help of the gamma-probe. The SNs were found to be positive for MM involvement by histology in 11 cases (25%). Block dissection was carried out only in these patients. Histological analysis of the removed lymph nodes revealed MM involvement in 2 cases.
Conclusion:
Preoperative SN localisation is helpful for the planning of the surgery.
The intraoperative gamma-probe technique is the most accurate method for the localisation of SN.
The biopsy of SN can reduce the number of unnecessary lymph node dissections.

PS_272

CLINICAL ROLE OF SENTINEL NODE BIOPSY IN SKIN MELANOMA

J. Sequeira (1), A.I. Santos (1), C. Martins (2), A. Paraés (3), V. Farricha (3), S. Carmona (1), M.J. Brito (4), J. Gíria (3). (1) Serviço de Medicina Nuclear; (2) Serviço de Dermatologia; (3) Serviço de Cirurgia; (4) Serviço de Anatomia Patológica, Almada, Portugal

Introduction. Elective lymph node dissection (ELND) for patients with malignant melanoma of the skin (MM) was classically indicated in patients with primary lesions ≥ 3mm of thickness. At present, although ELND is still controversial, the majority of the authors proposes the biopsy of the first tumour draining lymph node, sentinel node (SN), which can be identified by means of radionuclide techniques.
Aim of the study. To demonstrate that, in patients with MM, the sentinel node biopsy is a much more accurate method for selection of candidates for ELND.
Patients and Methods. We have selected 28 patients with MM with primary lesions ≥1 mm of thickness and without clinical suspicion of lymph node involvement (10 with MM of the legs, 9 of the trunk, 6 of the arms and 3 of the head and neck). 26/28 patients had melanoma < 3 mm thickness. A lymphoscintigraphy (LS) was performed, using planar acquisitions (Matrix 128), beginning immediately after pericicatricial or peritumoral i.d. injection of colloidal (Re) sulphide labelled with Technetium-99m, to define the regional lymphatic basin and identify the sentinel node. In the same day, biopsy of the sentinel node was performed with per-operatory (PO) detection using a surgical gamma probe in all patients and, in 17 patients, also with patent blue (PB) dye injection. The pathological examination of the sentinel node included examinations of hematoxilin-eosin staining and immunohistochemistry for S-100 and HMB-45 MoAB.
Results. The sentinel node (SN) was detected in a total of 28/28 (100%) patients (LS+PO+PB); LS+PO correctly localized SN in all (100%) patients, although PB only localized 10/17 (59%) SN. Five SNs of the retrieved were positive for metastases. Three patients with metastases found in SN had tumours with thickness of 5 mm, 3 mm and 1,1 mm; the other two had unknown thickness. These patients were submitted to elective lymph node dissection; in 2/5 cases SN was the only positive node.
Conclusions: Lymphoscintigraphy and gamma probe are useful for identification of SN, allowing for biopsy to be performed. This technique is a more reliable method for selecting patients for lymphadenectomy than the thickness of the primary lesion.

PS_273

THE USE OF PREOPERATIVE LYMPHOSCINTIGRAPHY AND INTRA-OPERATIVE GAMMA PROBE GUIDANCE IN THE DIAGNOSIS OF SENTINEL NODE IN MALIGNANT MELANOMA

V. Voliotopoulos (1), G. Limouris (1), A. Stavraka-Kakavaki (1), I. Ioannovits (2), D. Tsoutsos (2), L. Vlachos (1). (1) Areteion University Hospital, Nuclear Medicine Dept; (2) G.Genimatas General Hospital, Plastic Surg.Dept, Athens, Greece.

Purpose: The detection of the sentinel node (SLN) in patients with malignant melanoma is of considerable prognostic value. Aim of this study was to localize the sentinel node either with lymphscintigraphy or using intraoperatively gamma probe guidance.
Methods:120 patients, in three years, with histologically proven malignant melanoma were preoperatively examined with lymphoscintigraphy using 300 ? Ci Tc-99m-nanocolloid intradermally around the primary lesion. The first lymph node identified was marked on the skin of the patient. After that the patient was reffered to the operation room,were using the gamma probe the surgeon was guided towards the site with high uptake of the previously administrated radiotracer. After excision of the node, SLN, the lympatic basin was cheked for radioactivity.
Results: The 'hotest'lymphonode was found in all patients in the preoperativelly marked lymph node. Histolically in 20 patients metastatic involvment of the lymph node was found and the surgeons proceed in radical lymph node excision.
Conclusion: The preoperative lymposcintigraphy and the intraoperatively mapping with the gamma probe is of a great importance for the exact localization of the SLN.

PS_274

DIAGNOSTIC VALUE OF DELAYED SCANS IN THE DETECTION OF SENTINEL NODES IN PATIENTS WITH MALIGNANT MELANOMA

P. Koranda (1), M. Mysliveèek (1), P. Benes (2), S. Pallová (3), M. Kohoutek (2), V. Huák (1), M. Kamínek (1). (1) Dept. of Nuclear Medicine; (2) Dept. of Oncology; (3) Dept. of Plastic Surgery, Palack University, Olomouc, Czech Republic.

Aim: Delayed scans are considered to be an essential part of lymphoscintigraphic detection of sentinel lymph nodes (SN) in patients (pts) with malignant melanoma (MM). The purpose of this study was to evaluate the diagnostic impact of these scans.
Methods: 61 consecutive pts with 62 MM were studied using the lymphoscintigraphy (LS). 80 MBq of 99mTc-nanocolloid in 0.5 ml was administered in six to eight small portions intracutaneously around the melanoma or on both sides of the scar after diagnostic excision. The initial study (IS) was started immediately after administration of radiopharmaceutical. Dynamic scintigraphy was performed for 6 min acquiring 1 frame/20s. Subsequently, a series of static scintigrams (100s acquisition time) in anterior and posterior and lateral projections was made 5-45 min p.i.; patient's body contour was outlined by moving a 57Co marker. The delayed scan (DS) was acquired 2-3 hours p.i. All scans were performed using a dual-head gamma camera equipped with parallel-hole HR collimator.
Results:

Localization of MM	trunk	extremities	total
Nr. of MM	40	22	**62**
Nr. of lymphatic basins on IS	66	23	**89**
Nr. of lymphatic basins on DS	67	23	**90**
Nr. of SN on IS	86	41	**127**
Nr. of SN on DS	87	42	**129**
Better visualization of nonsentinel lymph nodes on DS than on IS	21	13	**34**

SN were detected in all MM during IS, mean time of SN visualization being 7.3 min (median 5 min). 2 additional SN and 1 lymphatic basin were found on DS but these findings did not change the staging of MM in our study.
Conclusions: Our results indicate that the most important part of lymphoscintigraphic detection of SN is IS enabling precise differentiation between SN and early imaged second- and third-echelon lymph nodes (LN). Delayed scans detect unknown SN relatively seldom, however, they give often more information about nonsentinel LN. In spite of the former fact we consider DS to be an integral part of lymphoscintigraphic detection of SN.

PS_275

SENTINEL NODE DETECTION WITH TC99M - DEXTRAN IN MALIGNANT SKIN LESIONS

S. Neubauer (1), I. Mena (1), R. Schwartz (2), J.C. Acevedo (2), R. Iglesis (2), L. Gomez (2), A. Leon (2). (1) Department of Nuclear Medicine; (2) Department of Surgery, Clinica Las Condes, Santiago, Chile.

Purpose : The aim of this work is to evaluate the ability of lymphoscintigraphic sentinel node identification with Tc99m – Dextran node in skin lesions.

Materials and Methods : Forty four consecutive patients, 23 women and 21 men, 48 ± 17 years, (mean age ± SD), (range 5 – 79 years), had perilesional intradermal injection of Tc99m-Dextran 2 hours before surgery. Gammacamera serial images and gamma detection with a handheld probe were used to direct sentinel node biopsy pre and intraoperatively. The skin lesions were 41 melanomas , 2 Merkel cell tumors and 1 squamous cell tumor. The lesion was located in the limbs in 21 cases, in thorax and pelvis in 19cases, in the head and neck in 4 cases.

Results : In 42/44 patients lymph channels and a total of 56 sentinel nodes (one to three sentinel nodes/patient) could be demonstrated. In two patients, one with melanoma of the dorsum and one with melanoma of the face, lymphoscintigraphy failed to show lymph channels or sentinel nodes.

All 56 sentinel nodes could be found and excised at surgery. They were submitted to microscopic analysis.

In our study group 8 sentinel nodes had metastasis corresponding to five patients with melanoma graded as Breslow 4, one patient with melanoma graded as Breslow 3 and two patients with melanoma of unknown original thickness.

Conclusion : lymphoscintigraphy with Tc99m-Dextran provides satisfactory definition of lymph channels and sentinel node localization to direct surgery by means of a handheld probe. Unexpected drainage sites and more than one lymphatic channel draining the tumor bed demonstrated by lymphoscintigraphy directed the surgeon in patients with skin lesions to a rational lymph node excision.

DIAGNOSTIC ONCOLOGY 8

PS_276

USEFULNESS OF A SIMULATION MODEL COMPARING THE PHYSICAL CHARACTERISTICS OF 6 GAMMA PROBES

S. Messina (1), R. Tarducci (2), I. Palumbo (1), B. Palumbo (1), T.O. Moschini (1), S. Ricci (2), R. Palumbo (1). (1) Dept. of Nuclear Medicine, University of Perugia; (2) Unit of Biochemical Physics, Perugia General Hospital, Italy.

Aim: The aim of our study was to perform a simulation model with 6 different gamma probes able to reproduce an idealised form of the clinical situation.

Methods: The probes studied are: Neoprobe 1000 (Neoprobe Corporation), Europrobe (Eurorad), Scintiprobe MR100 (Polytech), Neoprobe 2000 (Neoprobe Corporation), Crystal Probe (Crystal GmbH), Navigator (United States Surgical Corporation). Scintiprobe MR100 and Europrobe are equipped with a CsI(Tl) detector, while all the other probes have a Cd-Te(Zn) detector (with a diameter of 12 mm for Neoprobe 1000, of 14 for Neoprobe 2000 and Navigator). Measurements were performed in a water bath (2/3 filled) being the source (37 MBq of ^{99m}Tc) positioned in a box of lead with a hole of 1 mm of diameter. The source block was placed either at 1 cm or at 3 cm of depth, in order to better simulate the injection site and node position. The probe held perpendicular to the water surface by a clamp was mechanically moved for a frame of 1 mm. Data acquired (Cps/MBq) were organized in order to obtain a simulation process. The position of injection site and of the node was reconstructed by overlapping measurements carried out with the source either at 1 cm of depth or at 3 cm of depth. The data obtained with the source at 3 cm of depth were reduced of a factor of 1/10 (to simulate the ideal node uptake) and moved along the axis of abscissas.

Results: In our study the different probes show similar characteristics in the common practical, except Scintiprobe MR100 that, being equipped with a dedicated software, allow a management by computer. The probes provided with a CsI(Tl) detector are confirmed to be more sensitive with respect to probes with a Cd-Te(Zn) detector. Among the last mentioned is the most sensitive was Neoprobe 2000, probably for the type electronic equipment associated with detector. Furthermore about the spatial resolution, reported as the FWHM, Neoprobe 2000 with a 14 mm detector, Scintiprobe MR100 with a 18 mm detector and Navigator with a 14 mm detector disclosed the best results, while Neoprobe 1000 showed the worst resolution, as evidenced in the table.

Probe	Neoprobe 1000	Neoprobe 2000	Scintiprobe	EuroProbe	Navigator	Crystal Probe
Detector	Cd-Te(Zn)	Cd-Te(Zn)	CsI(Tl)	CsI(Tl)	Cd-Te(Zn)	Cd-Te(Zn)
Diam detector	12 mm	14 mm	18 mm	14 mm	14 mm	14 mm
FWHM	3.6	1,6	1,8	2,4	1,5	1,8

Conclusions: In our opinion, considering the actual use of the probes, the simulation technique is very useful to correctly evaluate the typical characteristics in a standard situation specifical for a sentinel node localization.

PS_277

INSTITUTIONAL LEARNING CURVE FOR SENTINEL LYMPH NODE BIOPSY IN BREAST CANCER: A STEP TOO FAR FROM VALIDATION ISSUES?

S. Drago (1), M. Catarci (1), G. D'Errico (2), L. Marino Cosentino (1), G. Longo (1), M. Remedi (1), S. Negrini (1), G. Ricci (1), G.B. Grassi (1). (1) Surgical Oncology, San Filippo Neri Hospital, Rome, Italy; (2) Nuclear Medicine, Catholic University, Rome, Italy.

Aims: To assess the learning curve and institutional validation series of sentinel lymph node biopsy (SLNB) in breast cancer in a prospective study on 30 consecutive cases carried out in a major community hospital. The main aim of this evaluation was the validation of the center for enrolling patients in an ongoing multicenter national trial.

Methods: Over a twelve months period, thirty consecutive patients with preoperative evidence of T1-2 breast cancer and clinically negative axillary nodes were enrolled in the study upon agreement to an informed consent on the investigational purposes of the study. They were all submitted to preoperative lymphoscintigraphy, intraoperative injection of a vital dye (Blu Patent V 2,5%) and scanning with a hand-held gamma probe (Navigator®, U.S.S.C., Norwalk, U.S.A.) performed by one of four surgeons in close cooperation with the nuclear medicine specialist. Axillary lymph node dissection was completed in all cases. No case was excluded and final analysis was carried out on an intention-to-treat basis. Main outcome measures were length of the procedure, rate of visualization of the sentinel node, overall accuracy and false negative rate.

Results: We recorded no toxicity from the injection of the tracer or the vital dye. Overall length of the procedure (mean ± sem) was 16.4 ± 5.8 minutes. It was significantly higher in the first five cases (24.2 ± 2.7) than in the last five ones (9.7 ± 2.1). One or more sentinel node(s) were identified using all the three methods in all but two cases (93.3 %). Accuracy in detecting axillary metastasis was 86.6% (13 out of 15 cases). Overall accuracy rate was 92.8% (26 out of 28 cases). We recorded two false negatives (6.6%).

Conclusions: We accepted a close cooperation with the nuclear medicine specialist and followed the guideline to use both vital dye techniques and nuclear medicine imaging in order to enhance the accuracy rate during the learning curve. Thirty consecutive cases were sufficient to acquire the technical skills in order to successfully perform the procedure, but overall accuracy did not match the recommendations of a national scientific board. Nonetheless, every day many surgeons are becoming eager to perform SLNB in breast cancer without axillary dissection beyond any trial, often under the pressure of patients aware of the procedure and media advertising, without any consideration of the risk of disreputing the technique by adversely affecting the prognosis of their patients. It appears more logical and appropriate to separate the two issues by overtaking the learning curve and then proceeding to the evaluation of institutional series for validational purposes.

PS_278

THE SMALL BREAST CANCER TREATMENT WITH COMPLETE SENTINEL NODE (SN) PROCEDURE: LOCAL VERSUS GENERAL ANAESTHESIA

S. Severi, F. Matteucci, C. Corbelli. Nuclear Medicine Dpt, Faenza, Italy.

INTRODUCTION: although the definitive results of the trials performed to verify the accuracy of the SN procedure are not published, many patients (pt) are conscious of the possibility to avoid axillary dissection in case of SN negativity and ask to be treated in this way. We tested the feasibility to operate small breast cancer in general and local anaesthesia in a group of voluntary pt, in order to verify which is the more comfortable, practical and economic approach.
MATHERIALS: we studied pt with proved monofocal invasive breast cancer smaller than 1,5 cm., never operated before, with clinically and ecographically negative axilla, who subscribed a detailed informed consensus. Our population was divided in two group of 25 pt each (G1 and G2) afferent from two different hospitals. In G1 pt were operated in general anaesthesia with frozen sections study either of the tumour and of the SN. The axillary dissection was performed in positive SN. In (G2) pt were treated in local anaesthesia with quadrant or nodulectomy of the tumour and SN excision. A delayed axillary dissection was performed for SN positivity. The lympho-scintigraphy was performed the day before surgery injecting 99mTc 18MBq Nanocoll superficially (in 0,2 ml) or deeply (in 0,4 ml) according to the tumour distance from the skin (cut off 1,5 cm). Dynamic and late static view were acquired also comprehensive of lateral and oblique. In the second day the pt was operated after a probe mapping and with a superficial reinjection of the unfound SN deeply injected.
RESULTS: all the SN were found with 10% reinjection of the cases deeply injected. The Excision of the SN was always effective and in 12% we had a double SN. Of the G1 pt 6 had the SN positive and were treated with axillary dissection that showed a complete negativity of all the lymphnodes. In 1 case the frozen sections of the SN exam were negative and the final diagnosis positive. This pt had a delayed dissection. Of the G2 pt 2 had the SN positive and had a delayed axillary dissection with negative axillary lymphnodes. The mean length of the G1 procedure was 90-120 min whereas the G2 mean duration was 45 min. All the pt were included in an accurate follow up.
CONCLUSIONS: in our opinion the complete SN procedure may be applied only after a specific pt request and in small breast cancer. In these cases the operation may be performed in local anaesthesia to have tumour quadrantectomy and SN excision all together. This kind of procedure offers minor invasivity, secure diagnosis, lower morbidity, fast recover and economic gain

PS_279

MISTAKES IN DETECTING THE SENTINEL LYMPH NODE. WHO IS RESPONSIBLE FOR THEM?

F. Pons, S. Vidal-Sicart, F. Martín, M. Ortega, J.J. Mateos, D. Fuster, F.J. Setoain, A. Muxí, F. Lomeña. Department of Nuclear Medicine, Hospital Clínic, University of Barcelona, Spain.

Sentinel lymph node (SLN) technique has led to the rebirth of lymphoscintigraphy as well as having provided an opportunity for nuclear medicine physicians to take part in surgical operations. However, when a SLN is not found or it is erroneously identified, nuclear medicine physicians are blamed.
AIM: To try to explain the reasons for erroneous SLN identification based on our experience.
METHOD: We retrospectively reviewed our first 500 patients who had undergone the SLN technique. Three hundred and forty five melanoma patients (Breslow > 0,76 and AJCC I/II stage), 140 breast cancer patients (65 T1 and 75 T2) and 15 vulvar squamous cancer patients (8 T1, 4 T2 and 3 T3 tumours) were studied. Lymphoscintigraphy was performed on all of them the day before surgery by injecting 74-111 MBq of nanocolloid-Tc99m. After radiotracer administration, dynamic and static images were acquired. The SLN location was marked externally on the skin. On the day of surgery, blue dye was injected about 15 minutes before surgical incision. A hand-held gamma probe was used to precisely localise the SLN.
RESULTS: In melanoma patients SLN identification was incorrect in 2.9% (10 patients). Out of the 10 patients, SLN was not identified in 3 cases (2 of them with a conclusive lymphoscintigraphy), in 2 cases the surgeon decided not to harvest the SLN (to avoid facial nerve damage) and in the remaining 5 the SLN was a false negative finding (in three of them the pathological molecular studies showed a positive result for metastases). In breast cancer patients the SLN identification was not correct in 10.7% (15 patients). From this group, SLN was not identified in 9 cases (in 5 of them the surgeon/nuclear medicine specialist team was not the regular SLN surgical team) and in the remaining 6 a false negative result was observed (immunohistochemistry studies showed micrometastases in 4 of them). In the vulvar squamous cancer patients SLN was not detected in one case (6.6%) which was a T3 tumour.
CONCLUSIONS: SLN identification needs the implementation and collaboration of several physicians of diverse specialities. This particular point can imply a number of mistakes in the SLN identification (surgical team changes, absence of thorough histologic study). However, SLN technique allows performing a correct stagement and avoids considerable morbidity in these patients. However, it is not possible to completely explain why, in a very small percentage of cases, the SLN was erroneously identified.

PS_280

RADIOGUIDED SURGERY: A NOVEL APPROACH IN PATIENTS WITH MALIGNANT GLIOMA

G. Boni (1), G. Parenti (2), G. Manca (1), S. Suriano (1), B. Lenzi (2), G. Grossi (2), M. Grosso (1), D. Volterrani (1), F. Bianchi (1), R. Bianchi (1). (1) Division of Nuclear Medicine, Department of Oncology; (2) Division of Neurosurgery, Department of Neurosciences, University of Pisa, Pisa, Italy.

Surgical cytoreduction is the first step in the treatment of cerebral gliomas. Although the advancement of neuro-imaging facilitates the surgical approach and the preservation of functional brain areas, radical tumor removal is still a problem. In order to obtain a better localization and extension of the tumor during surgery, we developed a novel radioguided surgical technique. It is based on the use of a gamma-probe for the intraoperative detection of the cerebral neoplastic tissue, which was previously labeled with an oncotropic radiopharmaceutical. The protocol consisted of two steps. In the preoperative phase, the mapping of the proliferative areas of the tumor was obtained by the i.v. injection of 740 MBq of ^{99m}Tc-tetrofosmin. A SPET scan of the brain was performed 30-60 min after the injection to check the presence and the distribution of the radiopharmaceutical within the tumor. Finally, the surgical procedure was performed within 24 hours from the scan. We used a 10 mm diameter-collimated probe connected to a gamma ray detector (Scinti Probe MR 100 - Pol.hi.tech., Aquila - Italy) to scan the neoplastic lesion. The counts were recorded on the neoplastic area and on the normal brain tissue and a tumor-to-background ratio was calculated. Then the surgeon started to remove the neoplasm and used the gamma probe to check the radioactivity on the resection margins and estimate the tumor remnants. The removed specimens of the tumor were counted with the probe and analyzed histopatologically. We studied 16 patients (10 men and 6 women, age range 35-76 years) affected by malignant gliomas (tumor size range 15-80 mm). There were five patients with recurrent neoplasms.
A good uptake of the tracer was demostrated in all the tumors by scintigraphy and by the intrasurgical gamma-probe measurements. The tumor-to-background ratio ranged from 1.4 to 3.7. Scintigraphic and gamma-probe data regarding tumor localization and extension were correlated with the radiological imaging and the surgical findings. The intraoperative detection by gamma-probe was easy to perform and useful to localize the tumor remnants. In conclusion, these preliminary data suggest that this radioguided surgical technique could help the neurosurgeon to distinguish the neoplastic tissue from the macroscopically intact brain tissue and to perform a better resection of the tumor.

PS_281

RADIOGUIDED SURGERY IN PRIMARY HYPERPARATHYROIDISM

N.Ö. Küçük (1), S. Koçak (2), P. Arıcan (1), G. Aras (1). (1) Department of Nuclear Medicine; (2) Department of Surgery, Ankara University, Ankara, Turkey.

Surgical neck exploration is usually made in primary hyperparathyroidism (PHPT). Localisation of the adenoma or detection of hyperplasia may reduced the operation period and limit the extention of the surgery.
In this study the efficacy of preoperative Tc-99m MIBI scintigraphy and intraoperative gamma probe was evaluated.
Material-Method: 6 patients with PHPT preoperative Tc-99m MIBI parathyroid scintigraphy and intraoperative gamma probe (IGP) was used surgical neck exploration.
Results: Parathyroid adenoma was observed in 2/6 patients in the scintigraphy (the right retroclavicular region and the left lobe of the thyroid). Both of them were clearly detected by IGP during the surgery and easily removed by the surgeon in a short time (35 min) with a small incision. Pathologic examination confirmed to the parathyroid adenoma.
Abnormal MIBI uptake was not observed in scintigraphy in 4/6 patients. Parathyroid hyperplasia was identified with IGP in two of these patients and removed then.
Conclusion: Preoperative Tc-99m MIBI scintigraphy and use of IGP may limit the exploration and then operation time and surgical complications reduce.

PS_282

LYMPHOSCINTIGRAPHY AND DETECTION OF SENTINEL NODES WITH SURGICAL GAMMA PROBE IN HEAD AND NECK CARCINOMA

N.Ö. Küçük (1), P. Arıcan (1), A. Demireller (2), G. Aras (1).
(1) Department of Nuclear Medicine; (2) Department of Otorhinolaryngology, Ankara University, Ankara, Turkey.

The prognosis in patients with head and neck cancers due to lymphatic metastasis. In the presence of micrometastasis in the first draining lymph node, the surgical exploration must be extended to the contrlateral and ipsilateral lymph nodes. Lymphoscintigraphy and surgical gamma probe to detect lymphatic drainage and sentinel lymph node has been commonly used in breast cancer and melanoma.
Aim: The aim of this study was to evaluate the efficiency of lymphoscintigraphy to show lymphatic drainage and the value of surgical gamma probe to detect sentinel lymph node in head and neck cancers.
Material-Method: 8 patients with head and neck cancer were included in the study (2 larynx cancer, 2 parotid carcinoma, 1 gingiva cancer, 2 tongue cancer, 1 tonsillar cancer). In all patients, USG, CT and/or MRI demonstrated no signs of lymph node metastasis.
148 MBq Tc99m filtered sulfur colloid was injected peritumorally (37 BMq/01ml each at 4 different locations) all the patients except two larynx ca patients. Planar images were obtained of 30, 45, 60 and two and four hours from anterior, right lateral, left lateral if necessary oblique views. 2 patients with larynx ca were evaulated only with surgical gamma probe without lymphoscintigraphy because of the necessity of general anesthesia for injection. During the operation, the lymph nodes which were detected with surgical gamma probe were explorated and histopathalogical examinations were made.
Results: The lymphatic drainage were clearly demonstrated with lymphoscintigraphy in all patients, especially cross drainage, ipsilateral and contrlateral drainages were shown. They were also identified with surgical gamma probe. Histopathological examinations were made and metastasis were detected in 6/8 patients.
Conclusion: Lymphoscintigraphy combined with surgical gamma probe is feasible method to detection of lymphatic drainage and sentinel lymph node(s). This technique may guide the surgeon to decide the extent of resection when micrometastasis is observed in sentinel lymph node in the patients with head and neck cancers.

PS_283

SENTINEL LYMPH NODE BIOPSY IN SQUAMOUS CELL CARCINOMA OF THE ORAL CAVITY AND THE OROPHARYNX: A PRELIMINARY EXPERIENCE

L. Feggi (1), G. Turetta, A. Tarabini, D. Turetta, N. Prandini, P. Carcoforo, A. Pastore. (1) ENT Clinic and Clinical General Surgery, University of Ferrara, Italy; (2) ENT Division, Hospital of Rovigo, Italy; (3) Nuclear Medicine Dpt., St. Anna Hospital, Ferrara, Italy.

The presence of regional metastatic lymphnodes (N+) is one of the most important prognostic factors in cervico-facial carcinomas. Accurate neck staging is therefore fundamental for planning a therapeutic strategy. In spite of this, 30% of cases clinically N0 present occult metastasis diagnosable only after comprehensive (I-V levels) or selective neck dissections, that are the current gold standard treatment. Nevertheless neck dissection becomes over-treatment for 70% of patients: the aim of this study is to valuate the application of the Sentinel Node (SN) biopsy strategy, in the therapeutic approach of head and neck carcinomas, in order to avoid unnecessary lymphadenectomy.
Materials and methods: The study comprised 11 patients aged between 58 and 75 years (mean 65) affected by T1 (seven patients) and T2 (four patients) carcinomas, clinically N0, of the oral cavity and oropharynx: five patients with tongue edge cancer, two with tonsillar cancer, three with retromolar region cancer and one with inferior alveolar process cancer. In the afternoon before the surgery we inject a nanocolloid (Nanocoll", Amersham) at the four poles of the primitive neoplasm and within 30 minutes we perfom the scintigraphy. The dose is calculated in order to have 10 MBq of 99mTc at the moment of the surgery the day after. In all the cases we utilized a probe collimated for intraoperative detection of SN (which is examined separately from the remaining lymph nodes): Isosulfan Blu vital dye was also injected around the neoplasm intraoperatively. Functional comprehensive neck dissection was always performed.
Results: SN was always shown at the scintgraphy. In eigth cases the SN resulted negative for metastatic infiltration at the histologic examination like the remaining lymph nodes. In three cases the SN presented micrometastasis where the remaining lymph nodes were negative: we never had false negative SN. In all cases the SN was located ipsilateral to the lesion.
Conclusions: The application of the SN technique in the carcinoma of the oral cavity and the oropharynx is easy and repeatable. An important factor is selection of the patient (clinical N0, no past surgery or radiotherapy of the neck) and good multidisciplinary collaboration between sugeon, nuclear medicine and pathologist. The possibility of introducing the management of patients affected by carcinoma of the oral cavity with neck N0 into clinical practice would lead to a reduction in the morbidity: a fundamental condition for the success of this project is the application of this experimental phase in other centers in order to enlarge the group.

PS_284

DEPICTION OF SENTINEL LYMPH NODES IN GASTRIC AND RECTAL CANCERS

K. Yokoyama (1), S. Kinami (2), S. Kinuya (1), K. Nakajima (1), G. Nishimura (2), T. Kobayashi (2), K. Miwa (2), T. Michigishi (1), N. Tonami (1). (1) Department of Nuclear Medicine; (2) Second Department of Surgery, Kanazawa University, Kanazawa, Japan.

Sentinel lymph node biopsy has provided less invasive surgery for breast cancer and melanoma. We have attempted to apply the sentinel node concept to gastrointestinal (GIT) cancers, which are the major cause of cancer death in Japan. Moreover, it is favorable for the patients' quality of life after surgery to optimize extent of node dissection.
Methods: Twenty-four cases consisted of 11 gastric and 13 colorectal cancer patients were enrolled in this study after obtaining the informed consent. Using a fiber endoscopy, 111-148 MBq of Tc-99m-phytate was injected into the submucosa of the peritumoral areas. Although there is no approved radiopharmaceuticals in our district suitable for lymphoscintigraphy, Tc-99m-phytate is reported to form particles when interacted with cationic calcium ion. Moreover, our previous study on sentinel lymphoscintigraphy of breast cancer has confirmed the applicability of this radiopharmaceutical. Lymphoscintigraphy was performed at 15, 60 min and 3 hr and the patients were operated upon the following day. The surgical gamma probe and patent blue dye were used for sentinel node mapping. In some cases, a hand-held palm-sized gamma camera equipped with the CZT semiconductor detector was utilized to obtain the intraoperative lmyphoscintigrams. All the resected lymph nodes was measured in a well-type scintillation counter and pathologically examined.
Results: The mean numbers of hot nodes detected intraoperatively for gastric and colorectal cancers were 4.6 and 3.8, respectively. These numbers were not significantly different from those detected by the dye for colorectal and gastric cancers: 5.2 and 4.0. In case of the tumors located in the inferior part of the colon, the dye method could not find the sentinel nodes because of the surgeon's field of view. All of the nodes with micrometastases from 4 cases showed higher radioactivity than the rest of the regional nodes. Although the lymph nodes scintigraphyically imaged were less in number, those gave better navigation for surgeons to search the appropriate area including the sentinel node. The surgical palm-sized gamma camera helped investigate broader area than the pinpoint view with a gamma probe.
Conclusions: The sentinel node concept could be applied to the gastric and rectal cancers when Tc-99m-phytate was administered via an endoscopy.

PS_285

FEASIBILITY OF LYMPHOSCINTIGRAPHY OF THE GASTRO-ESOPHAGEAL JUNCTION

G.W. Sloof (1), J.M. Klaase (2), P. Fockens (3), J.J.B. Van Lanschot (2). (1) Department of Nuclear Medicine; (2) Department of Surgery; (3) Department of Gastro-Enterology, Academic Medical Center, Amsterdam,NL.

The surgical approach of carcinoma of the gastric cardia (gastro-esophageal junction) is controversial because of its borderline location. A total gastrectomy may be performed when the tumor is limited to the cardia. Some argue in favour of an esophagectomy with proximal gastric resection because of epidemiological and histological similarities with esophageal cancer. Further, metastatic spread to the paraesophageal lymph nodes is found in approximately 20% of patients. However, morbidity and mortality rates are higher for esophagectomy compared to gastrectomy. This study was undertaken to assess the feasibility of lymphoscintigraphy of the cardiac area and the detection of paraesophageal lymphatic drainage.
Methods: eight patients elected for esophagectomy with proximal gastric resection because of esophageal cancer located at least 3 cm above the Z-line were enrolled in this study. On the preoperative day an endoscopy was performed and 100 MBq 99m-Technetium labelled nanocolloid (n=5) or sulphur colloid (n=3) was injected submucosally in the cardia, which was free of tumor. Lymphoscintigraphy, including SPECT, was obtained 30 minutes, 4 and 20 hours after injection. Surgery was started shortly after the last acquisition. Just preoperative, blue dye was injected at the same site of the radiolabelled tracer, again using an endoscopic procedure. After resection of the esophagus-cardia including the site of injection, locoregional lymph node stations were measured systematically for radioactivity by a gamma probe. Thereafter, the resection specimen itself was measured for radioactivity, both by gamma probe and camera, and investigated on the presence of blue nodes.
Results: In each patient at least 1 radioactive lymph node was detected. In total 21 lymph node drainage areas were detected: 2 left paracardial, 4 right paracardial, 6 lesser curvature, 4 celiac trunc , 3 radix mesenterica, 3 splenic artery and 1 paraesophageal . Detection of preoperative scintigraphy and per operative gamma probe measurements were similar, except for one, obese patient in which a radioactive lymph node was detected by the gamma probe but was missed by gamma camera acquisition. In only about half of the radioactive nodes, blue nodes could be clearly detected.
Conclusions Lymphoscintigraphy of the gastric cardia is feasible. The scintigrams can accurately determine the location of radioactive lymph nodes in the mediastinum and upper abdomen. Paraesophageal drainage was present in 1 out of 8 patients; further studies are warranted to assess the clinical utility of lymphoscintigraphy of the upper digestive tract.

PS_286

SENTINEL LYMPH NODE IDENTIFICATION IN VULVAR SQUAMOUS CANCER

F. Martin (1), S. Vidal-Sicart (1), L.M. Puig-Tintore (2), M. Ortega (1), J.J. Mateos (1), J.A. Lejarcegui (2), F. Pons (1,3). (1) Department of Nuclear Medicine, Hospital Clínic, University of Barcelona; (2) Department of Gynaecology, Hospital Clínic, University of Barcelona; (3) IDIBABS, University of Barcelona, Spain.

AIM: Sentinel lymph node (SLN) biopsy is a new technique that represents a considerable improvement in our ability to evaluate the tumour status of the regional lymph nodes and could be useful in selecting patients for adjuvant therapy. Our goal is to describe our initial experience in SLN identification in vulvar squamous carcinoma and its relationship with regional lymph nodes, in order to, in the future, to perform the regional lymphadenectomy only on patients with metastatic SLN.
MATERIAL AND METHOD: We studied prospectively 20 patients with vulvar squamous carcinoma. Seventeen of these patients had T1 or T2 tumours. The remaining three presented a T3 tumour. A lymphoscintigraphy was performed on all of them the day before surgery by injecting 74-111 MBq of nanocolloid-Tc99m. After radiotracer administration, dynamic and static images were acquired. The SLN location was marked externally on the skin. On the day of surgery blue dye was injected about 15 minutes before surgical incision. A hand-held gamma probe was used to precisely localise the SLN. After SLN identification a standard inguinal lymphadenectomy was performed. All surgical samples were referred for pathological study.
RESULTS: SLN was localised by lymphoscintigraphy and a hand-held gamma probe in all but one patient (19/20 = 95%). SLN was not identified in the patient with T3 tumour. Blue dye stained SLN in 15/20 patients (75%). A total amount of 36 SLNs were harvested, two of them being metastatic (2 patients). In these two patients a total amount of 13 regional lymph nodes were harvested, only one of them being positive for metastases. In SLN negative patients all regional lymph nodes removed were negative for metastases.
CONCLUSIONS: This short series of patients indicates to us that SLN identification of vulvar malignancies is a simple and reliable method for selecting patients for lymphadenectomy. Its accuracy improves in small tumours (T1 or T2) with minimal misidentification.

PS_287

SENTINEL LYMPH NODE (SLN) DETECTION IN CERVICAL CANCER

J. Grimm (1), C. Kujat (1), T. Lantzsch (2), J. Buchmann (3), H. Koelbl (2), T. Mende (1). (1) Department of Nuclear Medicine; (2) Department of Gynaecology; (3) Institute of Pathology.

Aim: The SLN-biopsy is an international established method in patients with melanoma or breast cancer. The purpose of the study is to verify the feasibility of the SLN-procedure in patients with evidence of cervical cancer.
Methods: We explored 17 women with early stage cervical cancer (T1/T2). One day before surgery a lymphoscintigraphy was done. We injected subepithelially on average 88 MBq ^{99m}Tc-labelled human colloides (Albu-Res®) in the cervix at 3, 6, 9 and 12 o'clock. The volume was about 0,2 ml NaCl each. The colloid was filtered before to obtain the small particle fraction between 200-450 nm. Images were recorded immediately after injection (dynamic scintigraphy from anterior view with 28 images, 1 minute per frame). Additional we made static images, 5 minutes per image, 30 and about 120 minutes after injection from anterior, right and left lateral view. The SLN locations were marked on the skin. The SLN were intraoperatively identified using a hand-held gamma probe. In all cases a complete pelvic lymphadenectomy was done.
Results: Imaging was in 15/17 cases successful. In 7/15 cases lymph channels have been visualized. We found in 13/15 cases intraoperatively one or more radioactive lymph nodes (on average 2 SLN). In all cases of detected SLN we found no lymph node metastases at all (SLN and other lymph nodes tumor-free). In the 2 cases of no presentability of SLN, which should always result in a complete lymphadenectomy, we found lymph node metastases. We did not found any tumor-positive non-SLN in case of tumor-negative SLN.
Conclusion: We need larger studies to evaluate the accuracy of the selective SLN-biopsy in patients with cervical cancer. After this study with 17 patients we have no reasonable certainty if the detected SLN is the real first-tumor-draining lymph node. What is with women, who had a conization before lymphoscintigraphy (injection site is not equal to the tumor site)? Is the lymphdrainage of the ectocervix equal to the endocervix (injection site ectocervical, tumor sometimes endocervical)? However 15/17 patients underwent a lymphadenectomy with no benefit for survival and with a high rate of morbidity. In future we have to estimate the reliableness of this method to avoid radical lymphadenectomy in patients with tumor-free SLN.

PS_288

IS THERE A "SENTINEL LYMPH NODE" FOR THE PROSTATE? LYMPHOSCINTIGRAPHIC PATTERN IN PROSTATE CANCER

O. Örömy (1), I. Balogh (1), J. Varga (2), B. Ruszinkó (2), Z. Tóth (2), K. Pócza (3), GY. Jánoky (4). (1) Dpt. of Nuclear Medicine, Uzsoki Hospital, Budapest, Hungary; (2) Urological Dpt,Uzsoki Hospital, Budapest, Hungary; (3) Pathological Dpt., Uzsoki Hospital, Budapest, Hungary; (4) OSSKI, Budapest, Hungary

Patients with early stage (T1NxM0) prostate cancer are mostly asymptomatic. Elevated PSA blood level on screening can be the only sign of the disease. If there is no contraindication of operation, after staging examinations the patients undergo suprapubic radical prostatectomy with ablation of external iliacal and obturator lymph node basins.
Aim: We would like to evaluate the lymphatic drainage of prostate with scintigraphic method, to find out: is there any well repeatable, characteristic, preferred draining lymph node(s) of the prostate, and how can
we help to find them easily and quickly during operation.
Patients: We examined 6 patients with early stage of prostate cancer, before suprapubic radical prostatectomy. Methods:We did lymphoscintigraphy with bone marrow SPECT and blood pool scintigraphy before the operation. The radiopharmakon was injected transperineally into the prostate in two depots. 2-3 hours and 24 hours later we did lymphoscintigraphy. The 2 hours lymphoscintigraphy was combined with one marrow SPECT. We performed blood pool scintigraphy as well to identify the relation of lymph nodes to blood vessels. We repeated the perineal injection and lymphoscintigraphic procedure the day before the operation. During the operation we searched the radioactive lymph node with intraoperative gamma probe (Navigator). After ablation of radioactive lymph node the surgeon removed non-radioactive lymph nodes of the region as well. The harvested lymph nodes were evaluated for metastases by the pathologist.
Results: We could find radioactive lymph nodes on the scintigram in every case. The pattern of radioactive lymph nodes were the same on both lymphoscintigraphy. In these cases the surgeon could find radioactive lymph
nodes during the operation as well. In 4/6 cases the radioactive lymph nodes were outside the routinely harvested lymph node basin. One of the radioactive lymph node was metastatic, it would not be removed without intraoperative gamma detection.
Conclusions: The number of the cases is low so we need further evaluation. Preoperative lymphoscintigraphy combined with bone -marrow SPECT, blood-pool scintigraphy and intraoperative radiodetection can identify draining lymph nodes of prostate cancer. Instead of routine ablation of statistically stated lymph node basin this method can „lead the hand of the surgeon" to a patient-specific draining lymph node.

PS_289

LYMPHOSCINTIGRAPHY IN A PATIENT WITH NON-HIV KAPOSI SARCOMA

T.A. Balcı (1), H. Komek (1), Z. Aytuğ (1), H. Kaya (1), N. Kılınc (2). (1) Department of Nuclear Medicine; (2) Department of Pathology, Dicle University Medical Faculty, Diyarbakır, Turkey.

Kaposi sarcoma is an uncommon, opportunistic, multisentric, vascular neoplasm characterised with the proliferation of a mixed cell collection included endothelial cells. It is usually associated with AIDS and HIV positivity; but it can be occur in every immunosupressive situations. It can be in the form of fulminant disseminated visseral involvement and besides it can also show benign skin involvement merely. Lymphedema can be occur by the involvement of the lymphatic vessels. The patient (70 years-old, male) diagnosed as Kaposi sarcoma by skin biopsy refered us with mild lymphedema of the lower limbs, and the disseminated, purple-red plaques on the legs. Skin of these areas was very tough. He was HIV (-) and had no known immunosupressive situation except his old-age. Doppler ultrasonography of the lower extremities were normal. There was no significant abnormality in the laboratory findings. However he had a story of upper gastrointestinal system bleeding and the diagnosis of prepyloric ulcer. We performed lymphoscintigraphy by injecting intradermal 500 µCi (17 MBq) Tc-99m sulphur colloid to the first interdigital spaces of the feet bilaterally. We obtained static images from the lower extremities and the pelvic region on the 2nd, 4th and 24th hours. We visualised focal radiotracer accumulations on the right leg (bigger plaques than the others), no accumulation on the right pelvic region, and delayed and decreased visualisation of the left pelvic lymph nodes.

PS_290

PEROPERATIVE RADIOISOTOPIC EVALUATION OF OSTEOID OSTEOMA

G. D'Errico (1), V. Valenza (1), M. Galli (2), M.A. Rosa (2). (1) Nuclear Medicine Institute, Catholic University of Rome; (2) Orthopaedic Institute, Catholic University of Rome, Italy.

Introduction: drawback of surgery of osteoid-osteoma, a benign but painful and small size bone lesion, may be an incomplete excision of the „nidus", and recurrences, rare complication, may be the result of a partial excision of osteoid-osteomas. Since osteoid-osteomas concentrate ^{99m}Tc-methylene-diphosphonate (MDP), radionuclide imaging has become an established technique for the localisation of these tumours. aim: the Authors report on the use of peroperative radionuclide localisation of osteoid-osteoma performed to evaluate the clinical efficiency of this technique. Material and methods: approximately three hours before surgery fourteen young patients (9 osteoid-osteoma of femoral diaphysis, 3 of femoral condyle, 1 of ulna and 1 of talus) were injected intravenously with ^{99m}Tc-MDP at dose of 740 MBq to perform three-phase scintigraphy. Bone scan showed increased uptake of the bone seeker in the „nidus" and in the perilesional sclerosis; anterior, lateral or oblique views were acquired to better define the position of the „nidus-within-the-sclerosis". With a fine radioactive marker the region of focal abnormality was localised and the skin was marked at that precise site by pen. ROIs were plotted out the hot-spot-area and adjacent bone region (background) to calculate the „ratio" between target/background. A preoperative detection, using a handheld _-probe, was performed to localise the „hot-spot-area" compared to an adjacent control region. In the operative field measurements of radioactivity were carried out by means of the same sterilised _-probe guiding the surgeon to determine the orientation of the nidus.
Results: high activity at „nidus-within-the-sclerosis" was found in all the intraoperative measurements; the preoperative detection was useful to correctly approach, at surgery, the bone lesion and to guarantee complete removal of the lesion. In fact, because the closer collimation and the ability to respond in a directional manner of the _-probe, the nuclear physician was able to show to the surgeon the exact localisation of the nidus deep. In order to detect possible pathological residual activity on bone after removal of osteomas the nuclear physician rescanned the cavity after curettage verifying the residual radioactivity. About 20 days after surgery all the patients underwent three-phase scintigraphy to confirm the complete removal of osteoid osteoma.
Conclusions: the Authors conclude that the peroperative nuclear medicine, e.g., the preoperative localisation of the „nidus" and of the active surrounding part of the osteoid osteoma and next successful detection of lesions at surgery can represent an effective aid for conservative surgical excision assuring a complete removal of lesions.

PS_291

LYMPHOSCINTIGRAPHY IN NON SMALL CELL LUNG CANCER

F. Scopinaro (1), O. Bagni (2), R. Salvatori (2), G. Baiano (2), R. Massa (1), M. Carletti (2), A. Saltarelli (2), M. Iozzino (2), O. Schillaci (3). (1) University ; (2) General Hospital, University of Rome, Rome, Italy.

Aim: Surgery is the best choice for curing patients with non small cell lung cancer (NSCLC). The status of hilar and mediastinal lymph nodes is of primary importance for selecting surgical candidates and for prognosis; moreover, radical lymphoadenectomy improves survival. The aim of this study was to develop a new scintigraphic technique to evaluate the lymphatic drainage in NSCLC. Methods: Eight male patients (age range: 53-72 years) were considered; in all of them a CT-scan guided double perilesional injection of about 0.3 ml of Tc-99m labelled sulfur colloid particles (≅ 17 MBq) was made. Multiple planar static images of the chest were obtained at 15, 30, 60 and 120 minutes postinjection in various projections, using a large field of view gamma-camera. An intraoperative gamma-detecting probe was used in 6 patients during surgery, performed 3-6 hours after lymphoscintigraphy. Results: In 6 patients images demonstrated ipsilateral both hilar and mediastinal drainage, whereas in the other two patients only ipsilateral hilar drainage was observed. In one case an atypical drainage from a NSCLC in the right superior lobe to a lymphnode in the right triangularis ligamentum was revealed. During surgery, the lymphatic drainage patterns were easily detected. Conclusions: Our preliminary results suggest that this new lymphoscintigraphic technique is useful in patients with NSCLC. It allows an accurate lymphatic mapping of possible tumour spreading, with a better staging of the disease, and can help and guide the surgeon in the resection.

GENERAL TOPICS

PS_292

PATIENTS' AND PERSONNEL'S PERCEPTIONS OF SERVICE QUALITY AND PATIENT SATISFACTION IN NUCLEAR MEDICINE

S. De Man (1), P. Gemmel, P. Vlerick, R. Dierckx. (1) Faculty of Economics and Business Administration, Ghent University, Belgium; (2) Faculty of Psychology and Educational Sciences, Ghent University, Belgium; (3) Division of Nuclear Medicine, Ghent University Hospital, Belgium .

Aim: SERVQUAL, the most commonly used service quality measurement scale, has been used in a department of Nuclear Medicine. The aim of this paper is to demonstrate the use of SERVQUAL for measuring patients' perceptions of health care quality in an ambulatory care clinic, the link between service quality and patient satisfaction, the relationship between perceptions of service quality and patient satisfaction of patients and personnel.
Method: 75 patients visiting the department of Nuclear Medicine filled in a self-administrated patient questionnaire. The questionnaire included demographic questions, SERVQUAL for measuring service quality perception and a question about overall patient satisfaction. The personnel of the Nuclear Medicine department filled in a similar self-administrated questionnaire.
Results: The results indicate that SERVQUAL appears to be a reliable scale to measure health care service quality. However, the proposed five dimensions (Tangibles, Assurance, Responsiveness, Reliability and Empathy) of SERVQUAL are reduced to four. Tangibles and Assurance are perceived as one dimension of service quality, where the other factors are Responsiveness, Reliability and Empathy. The results also indicate that perceived health care service performance by patients is associated with patient satisfaction (r=.756). The factor Reliability correlates strongest with overall patient satisfaction (r=.729), which means that Reliability has the strongest effect on patient satisfaction. Patients and personnel did not differ significantly in service quality perception (t=-.993, p>.01) . Only for the Tangibles-Assurance factor, there is a different perception of patients and personnel (t=3.181, p<.01), where the personnel perceives the Tangibles and Assurance dimension less good ($\bar{x}$ = 5.42, s.d. = .59) than the patients ($\bar{x}$ = 5.88, s.d. = .95). Health care personnel seem to estimate very well the overall patient satisfaction (t=-1.444, p>.01).
Conclusion: SERVQUAL appears to be a reliable instrument to measure service quality perceptions in Nuclear Medicine. Patients and personnel of a Nuclear Medicine department seem to have a similar perception of service quality. Only Tangibles and Assurance is perceived significantly different by the personnel what is an illustration of the deficiency in patient knowledge to evaluate the technical quality of the service. Management must be aware that investments in Tangibles-Assurance will not have higher service quality perceptions of patients as result. The SERVQUAL instrument can be used as a management tool to recognize areas to improve in order to build a more patient-focused attitude towards service delivery.

PS_293

NUCLEAR MEDICINE SERVICES IN THE KINGDOM OF SAUDI ARABIA

R.Y. Al-Mazrou (1), J. Prince (2), A. Arafah (3). (1) Biomedical Physics Department, King Faisal Specialist Hospital and Research Center, Riyadh, Saudi Arabia; (2) Physics Department, University of North Texas, Denton, Texas, United States; (3) Nuclear Medicine Section, Radiology Department, King Faisal Specialist Hospital and Research Center, Riyadh, Saudi Arabia.

A postal survey was distributed to the 29 nuclear medicine departments existing in the Kingdom of Saudi Arabia asking for details of current practice and technology in nuclear medicine. The aim of the survey is to create a complete database of available equipment, quality control and clinical procedures performed in these departments during the years 1997, 1998 and 1999. From this database, the level and sophistication of nuclear medicine services in the Kingdom will be known.
Method: The survey form was sent to the Heads of the 29 nuclear medicine departments in the Kingdom. A covering letter accompanied the form explaining the objectives and the importance of the questionnaire. Three months later a reminding letter was sent to non-responding departments. This was further followed up by telephone and fax.
Results: Data were received from 27/29 (93%) departments. These departments have 44 gamma cameras, 12 of these cameras are dual headed and 2 are triple headed. A total of 49638 procedures were performed in year 1997, while 55399 procedures in year 1998 and 50763 procedures in year 1999. Imaging procedures composed 94.7%, 93.1% and 93.5% for the years 1997, 1998 and 1999 respectively. While non-imaging procedures composed 4.1%, 5.5% and 5.2% for the same years and therapy procedures composed 1.2%, 1.4% and 1.3% for the same years. Number of scans performed per camera are 1069, 1172 and 1079 for the years 1997, 1998 and 1999 respectively. Bone scan was the most frequent imaging procedure performed in all years with percentages of 17.0, 16.1 and 16.5 of the imaging procedures for 1997, 1998 and 1999 respectively. Myocardial Perfusion scan came as second for all years with percentages of 13.5, 13.9 and 14.8. This survey also showed that only few centers performed acceptance testing on their cameras and few of these centers perform the minimum required periodic quality control procedures for their gamma cameras.
Conclusion: number of nuclear medicine procedures performed in the Kingdom of Saudi Arabia is below the average numbers in the European countries. Policy makers should plan to educate the users of these cameras on the importance of quality control procedures. The nuclear medicine services in the Kingdom do need a lot of efforts from its community to improve this specialty and educate the referral physicians about the importance and ability of this modality.

PS_294

MAJORITY OF EANM MEMBER SOCIETIES AIM AT EANM-GUIDELINES

J.D. Kuyvenhoven, E. Busemann Sokole, P.P. van Rijk, A. Plachcinska, M. Clausen, S. Steien, H. Sayman, R.A. Dierckx. EANM Task Group on Quality Assurance and Standardisation.

Background: The various efforts undertaken in the past towards management of quality in nuclear medicine were mainly national initiatives on an ad-hoc basis. Some degree of harmonisation to assure the quality of radiopharmaceuticals and the performance of nuclear medicine instrumentation existed in 1996. In EANM member societies, nationally accepted procedures existed in 6 of 23 and 18 of 23 had set up a quality assurance committee. However, nationally accepted guidelines reflect differences in legislation, available equipment, customs and reimbursements. Supranational guidelines and standards that gradually cover the entire nuclear medicine service could be a possible strategy to implement a systematic quality management in nuclear medicine. Aim: To achieve insight in the current status of guidelines in EANM member societies and their future plans.
Methods: A postal questionnaire was addressed to the national delegates of the EANM member societies in July 1999. This questionnaire focussed on:
- Current status of national guidelines
- Specification of the cover and the level of national guidelines
- Future plans for national, EANM and SNM guidelines
Results: Complete response rate was 96% (n = 27). Guidelines are required by 19 member societies, initiated by the member societies in 16 and provided by 13, of which 12 in the national language. In 10 societies, staff other than nuclear medicine physicians take the lead on some guidelines, in particular physicists in 7 and radiopharmacists in 5 societies. Active collaboration with other medical societies in developing guidelines exists in 9 societies, of which 7 with cardiology societies. Currently, only 18% of the items of necessary procedure guidelines are covered. A commitment for future development of guidelines is shared by 26 member societies. 25 indicate a high priority need for guidelines and 21 prefer EANM guidelines to national guidelines.
Conclusions: Two thirds of EANM member societies require guidelines and half of them currently provide them. Various professional groups are involved in setting up guidelines. Most of procedure items are left uncovered. Compared with 1996, the relative proportion of societies that provide guidelines has doubled, indicating progress. Almost all member societies share a commitment for future development of guidelines and the majority prefer the EANM route at present.

PS_295

THE DYNAMIC RELATIONSHIP BETWEEN WORK PRESSURE, PRODUCTIVITY, WORK INTENSITY AND SERVICE QUALITY IN NUCLEAR MEDICINE

S. De Man (1), P. Gemmel, P. Vlerick, R. Dierckx. (1) Faculty of Economics and Business Administration, Ghent University, Belgium; (2) Faculty of Psychology and Educational Sciences, Ghent University, Belgium; (3) Division of Nuclear Medicine, Ghent University Hospital, Belgium.

Aims: The financial pressure to reduce labor costs, combined with a cyclical shortage of health care labor might lead to higher work pressure. Work pressure can be defined as the relationship between the amount of work and the available labor capacity. There are several different strategies to deal with high work pressure:
Obtaining additional resources through investment in capital or labor
Increasing the work intensity (available labor works more hours than agreed in the contract).
Increasing productivity (one is spending less time to the patients).
The aim of this research is to investigate the relationship between work pressure, work intensity, productivity and service quality in a dynamic way and from a combined economic and psychological point of view. We formulate the following hypotheses:
Pressure to increase the work intensity and/or the productivity (following a situation of continuous high work pressure) leads to the erosion of service quality if insufficient capacity is available.
In personal-interactive services the patient will use the perceived time of contact as compared with the expected time as an important determinant of service quality. In task-interactive services (Nuclear Medicine) the service quality is determined by other factors. Consequently hypothesis 1 is not longer valid in task-interactive services.
Many different variables will further have an impact on this relationship:
Service quality is a subjective concept and is measured as the gap between perception and expectations. This also means that evaluating quality is a subjective process. Different agents involved in the hospital (such as management, personnel and patients) perceive quality in a different way and react differently on changes in the level of quality. There exists different 'gaps' between how quality is understood by the customer, personnel and management. In health care special attention must also be paid to how physicians perceive the level of quality. There are many structural and organizational factors that determine how fast the service quality is eroded following high work pressure. Such factors are technology, professional quality standards, trainingÉ
Methods: We set up a longitudinal study in which different operational measures (work pressure, quality, structural and organizational factors) of a department of Nuclear Medicine are tracked. The process of this longitudinal study will discussed on the congress.

PS_296

THE RELATIONSHIP BETWEEN PERCEPTION OF SERVICE QUALITY AND WAITING TIME IN NUCLEAR MEDICINE

S. De Man (1), P. Gemmel, P. Vlerick, R. Dierckx, M. Decoussemaker. (1) Faculty of Economy and Business Administration, Ghent University, Belgium; (2) Faculty of Psychology and Educational Sciences, Ghent University, Belgium; (3) Division of Nuclear Medicine, Ghent University Hospital, Belgium; (4) Faculty of Economy and Business Administration, Ghent University, Belgium

Aim: Service quality is an overall judgement similar to an attitude and related, but not equivalent to consumer satisfaction (Parasuraman Zeithaml and Berry, 1988). Service quality is a subjective concept and is measured as the gap between perception and expectations (Parasuraman et al., 1985). This also means that evaluating quality is a subjective process. In literature, waiting time is supposed to have a significant influence on service quality perception (Mowen, Licata and McPhail, 1993). Because the specific nature of Nuclear Medicine, departments of Nuclear Medicine are usually confronted with long waiting times.
Method: 192 patients visiting the department of Nuclear Medicine filled in a self-administrated patient questionnaire. The questionnaire included demographic questions, questions about subjective waiting time and waiting time behavior, SERVQUAL for measuring service quality perception and a question about overall patient satisfaction. Different waiting times (before injection, before scan and total waiting time) for the patients were registered.
Results: The subjective waiting time for scanning is significant smaller than the objective waiting time for scanning ($t = -3.054$, $p < .01$). Although patients must wait longer than expected ($t=-2.843$, $p<.01$), most patients are satisfied with the waiting time ($\bar{x} = 5.21$, s.d. = 1.4). Only 6.3% did not know to that they had to wait between injection and scanning. Age (_=.209, p<.05)) and objective waiting time for injection (_=-.036, p<.05) have a significant influence on the perception of service quality (R_= .185).
Conclusion: Patients perceive waiting time shorter than the objective waiting time. Almost all patients are informed about the waiting time between injection and scanning. Older patients with a shorter objective waiting time for injection perceive service quality higher.

PS_297

WATING PERIODS OF PATIENTS REFERRED TO NUCLEAR MEDICINE DEPARTMENT

F. Sakar, H. Durak. Depertmant of Nuclear Medicine, Dokuz Eylül University, Medical School, Izmir,Turkey.

There is a rising demand for continuous improvement of health services due to the increased needs and expectations of patients. Patients expect to be diagnosed and treated with novel techniques in the shortest time with accuracy. The aim of this survey was to analyze the waiting time of the patients and the effective factors in order to minimize the patient discomfort in nuclear medicine.
Methods: A flow chart was created for each patient starting from the appointment time until receiving the final report for 10 consecutive working days. The time elapsed between each unit was calculated. Total of 200 patients (53 thyroid, 38 bone, 25 DMSA, 26 myocardial perfusion, 9 parathyroid scintigraphies, 49 miscellaneous scintigraphies) were followed. History taking which lasted for 9 minutes occurred 23 minutes after the admission of the patient. Intravenous injection of the radiopharmaceutical happened 75 minutes after admission. The reason for this delay was using a single vial for more than one patient, and waiting for all the appointed patients to arrive before preparing the radiopharmaceutical. A mean of 2 hours and 11 minutes elapsed between injection and imaging. Routine imaging lasted 27 minutes, but 19 minutes were spent for additional views. The patients waited between the routine imaging and additional views, for decision making for the necessity of these extra views and they left the imaging unit 2 hours and 32 minutes after their first enterance to the camera room. The patients spent 4 hours and 11 minutes in the nuclear medicine department. This period was 6 hours and 22 minutes for parathyroid scintigraphy, 6 hours and 2 minutes for thallium tumor imaging, 5 hours and 30 minutes for bone imaging. The shortest residence time was for lung scintigraphy (1 hour).
Conclusions: Nuclear medicine imaging seems to take more time than other modalities related to the nature of the radiopharmaceutical used. This may cause a disadvantage when compared to other modalities. We need to decrease the waiting times in order to minimize the patient discomfort. New radiopharmaceuticals with shorter localization times and effective instruments to improve the counting rate need to be developed to provide a better health service for the patients.

PS_298

DESIGNING A NUCLEAR MEDICINE DEPARTMENT FOR OPTIMUM PERFORMANCE IN THE 21ST CENTURY

E.D. Williams (1), M.P. Bewick (1), R. Blair (2), A.C. Knight (1).
(1) Regional Medical Physics Department, Sunderland Royal Hospital, Sunderland, UK; (2) Regional Medical Physics Department, Newcastle General Hospital, Newcastle upon Tyne, UK .

The expectations of both patients and staff are continually rising, concerning their experiences when using clinical departments, and present a challenge when providing efficient, safe services. Nuclear Medicine is a particularly complex operation, where the needs of radiation safety rules and radiation-sensitive equipment can be in conflict with the demands of a clinical environment. Our aim in developing design guidance for nuclear medicine was to meet these challenges.

Methods: The approach employed was to describe design needs based on expertise gained from many years' experience in building and operating nuclear medicine departments at 13 hospitals over our region. This experience, including the results of patient surveys, was used to develop principles and features which could be applied to designing a nuclear medicine department.

Results: The resulting principles govern the layout of the department. The main point is separation between 'patient' and supporting 'staff only' areas, which enables both groups to feel comfortable. Other significant areas include the working and usage relationships between different functional areas (imaging rooms, dose administration etc), and the overall ambience of the environment, including colour, furnishings, lighting and noise level. Features developed were a large number of specific points, including details within each special purpose room to provide safety and comfort in use, and optimisation of the design of specialised areas: the radiopharmacy is a particularly difficult area to design for efficiency of use and economy of floor space while meeting regulatory specifications. The range of radionuclides expected to be used was also considered, and allowance made for some future development. The results of applying these principles in practice to a newly constructed department, within the constraints of a larger building scheme, showed that they could largely be achieved.

Conclusions: We conclude that these principles should be generally applicable to new building schemes for nuclear medicine, and are important not only for service efficiency, but also for the well-being of patients and staff.

PS_299

AMIFOSTINE (AF) AND RADIOTHERAPY (RT): PHASE III STUDY

D. Di Gennaro (1), M. Alfieri (2), B. Curcio (1), G. Scimone (1), C. Bianco (1), A. Losco (1), E. Falcone (1), S. Di Fiore (1), R. Pacelli (3).
(1) Department of Radiation Therapy Salerno Hospital; (2) Pharmacy Mercatosanseverino Salerno Hospital; (3) Department of Radiological Science Federico II Naples University.

Purpose: to evaluate the tolerance and efficacy of Amifostine (WR-2721) as a radioprotector
Methods: in 1999 we began a clinical study to evaluate AF as radioprotector; till now we have used in n¡24 patients, with an age varying from 16 to 36 (median age 25), affected by n¡18 Hodgkin Limphomas (HL) (mantle field - dose: 30Gy/20 fract.), n¡6 Non-Hodgkin Linphomas (NHL - Neck field - Dose: 41.4 Gy/ 23 fract.), and 1 patient, age 53 years, affected by a pelvic mass from a cervix ca. (dose:61 Gy), already surgically treated (ureteral-bladder-ileotomy) for iatrogenic toxicity (bilateral ureteral necrosis) caused by cisplatin. The bladder was created from an ileal loop, and was highly prone to radiation necrosis. AF was used: a)in young patients treated to Head and Neck (to prevent xerostomia) b)in young patients treated with mantle field (to prevent xerostomia, esofagitis and second chemo-radiation tumours) c) in patients already treated (higher risk of radionecrosis). AF was given at a dose of 500 mg. diluted in 5 cc of fisiologic solution, s.c., in two different subministrations 15 m' before RT. We always gave antiemetic profilaxis with serotinin – antagonists. Subcutis way was more useful, for our department (100 patients/day).
Results: We did not notice bad effects caused by subcutis subministration of AF; we noted 4/18 acute radiation toxicities (Grade 2 esophagitis), but no acute xerostomia, and a complete compliance to radioprotector and radiotherapy schedule.
Conclusion: AF is safe and useful, and now is routinely given in our department to this subgroups of young patients.

OTHER CLINICAL SCIENCE. NEPHRO-UROLOGY 2

PS_300

EVALUATION OF ESOPHAGEAL SCINTIGRAPHY IN CHRONIC RENAL FAILURE AND THE ROLE OF HEMODIALYSIS TREATMENT

B. Okudan (1), B. Okudan (1), Y. Üstündağ (2), N. Gülçelik (3), M. Kayatas (3). (1) Department of Nuclear Medicine; (2) Department of Gastroenterology; (3) Department of Nephrology, Numune Research and Training Hospital, Ankara, Turkey.

Aim: Foregut motor dysfunction especially in the esophagus has been commonly reported in uremic patients. However, as far as we know there is scarce data on esophageal motor functions in uremia. Esophageal scintigraphy provides a non-invasive demonstration of gastrointestinal motor abnormalities. In this study, we investigated esophageal motor functions by using scintigraphic method.

Method: Twenty-six patients chronic renal failure and 10 healthy subjects were enrolled into the study. Male to female ratio was 13/13 in patients and 4/6 in controls. Mean age of the patients and the controls were 45.58±13.52 yrs (range; 29-77) and 38.8±16.68 yrs (range 19-67) respectively. Fifteen of 26 patients were being on regular hemodialysis treatment and the rest were terminal renal failure patients who were in predialysis period. The age and sex distributions were similar in both groups. Neither of the patients had amiloidosis, diabetes mellitus or collagen vascular disease, nor was using drugs, which can affect gastrointestinal motility. Esophageal scintigraphy was made using an Elcint SPX-6 Gamma camera with low energy-multipurpose, parallel hole collimator. The radiopharmaceutical is 200-400 µCi of DTPA in 15 ml of water. With the patient supine the liquid is taken into mouth through a straw and then a single swallow is performed. Rapid sequential images (2 per second) are acquired for 1 minute. Dry swallows follow this at 15 seconds intervals for up to 10 minutes. Computer analysis is performed using a region of interest over the esophagus and used to evaluate the progression of the bolus.

Results: Esophageal residual activity (RA) is that is defined as percentage of liquid bolus left the esophagus within 10 seconds of time measured in each patient and controls. The mean RA was 84.1±13.1 % (49-98 %) in patients and 81.63±17.52 % (53-98 %) in controls. The difference was not significant statistically (p>0.05). The hemodialysis group has mean RA of 89.01±7.5 (70-96.6) and, the rest of patients had mean value of RA 76.78±15.65 (49-97.8 %). The difference was found to be significant (p<0.05).

Conclusion: As a conclusion, we believe that esophageal motor functions are abnormally affected in predialysis chronic renal failure patients possibly due to neuropathy or myopathy in association with uremia and, this abnormality can be corrected by hemodialysis treatment.

PS_301

COMPARISON OF DIFFERENT DIURETIC RENAL SCINTIGRAPHY PROTOCOLS (F+20, F+0 AND F-15) IN PATIENTS SUSPECTED OF URETEROPELVIC OBSTRUCTION

S. Türkölmez (1), T. Atasever (1), K. Türkölmez (2), O. Göğüs (2).
(1) Department of Nuclear Medicine, Gazi University, Ankara, Turkey; (2) Department of Urology, Ankara University, Ankara, Turkey.

The aim of this study was to compare three different diuretic renal scintigraphy protocols (F+20, F-15, F+0) for evaluation of suspected upper urinary tract obstruction.
Methods: A total of 22 patients (28 kidneys) suspected of ureteropelvic junction obstruction were performed three diuretic protocols. Twenty of the patients were adults and 2 were infants, their ages ranged from 3 to 43 (mean 28). The three protocols were identical, except for the time of injection of furosemide. In the F+20 study, furosemide was given 20 minutes after the injection of Tc-99m MAG3. In the F-15 scan, furosemide was injected 15 minutes before the injection of radioactivity. In the F+0 scan, furosemide and radioactivity were injected simultaneously. F+0 protocol could not be performed in one and F-15 in two of the patients. Each of the three protocols were performed for the rest of the patients.
Results: The results were classified as nonobstructive, equivocal and obstructive according to the renogram images and curves. None of the patients showed equivocal results in both F+0 and F-15 protocols. In the F+20 studies, 9 of the 28 kidneys were evaluated as equivocal. Of these, 6 kidneys showed nonobstructive and 3 kidneys obstructive renogram patterns with the other two protocols (F+0 and F-15). Moreover, one of the 14 kidneys which was evaluated as nonobstructive in F+20 protocol showed obstructive pattern in both F+0 and F-15 protocols. All of the kidneys that showed obstructive pattern in F+20 study also revealed obstruction in F+0 and F-15 investigations. We could not find difference between the renogram patterns of F+0 and F-15 investigations.
Conclusion: As a conlusion, there is no need for further investigation when obstruction is determined by F+20 protocol. F+0 and F-15 protocols allow clarification in cases of equivocal F+20 studies. We suggest F+0 protocol when equivocal results are obtained by F+20 study since it is more practical and shorter.

PS_302

COMPARATIVE STUDY OF CAPTOPRIL RENOGRAPHY / CR/ IN CHILDREN AND IN ADULTS WITH HYPERTENSION

I. Kostadinova (1), A. Simeonova (1), R. Krasteva (2), V. Petrova (3), A. Gadavelov (4), B. Deliiska (2). (1) Departments of nuclear medicine; (2) nephrology; (3) paediatrics, Medical University; (4) Department of electronics, University of Chemical Technology,Sofia

The aim of the study was to apply CR in children and in adults with hypertension in order to compare the obtained results, regarding the age of the patients /Pts/. CR was performed in 20 children with mean age 10.2 years, mean blood pressure 160/106mmHg and in 38 adults with mean age 40.4 years, mean blood pressure 165/104mmHg. According to the weight, 37-74 MBq 99mTc-MAG3 was administered during basal study and 1h after oral intake of 12.5-50mg Captopril. Different qualitative / shape of the curves/ and qualitative criteria / divided renal function, Tmax., Retention index /were considered. For making final diagnosis, renal angiography was performed in 21 Pts with positive result from CR for renal vascular hypertension /RVH/ and /or high renin level / more than 2.8ng/ml / and/or positive result from Duplex Doppler sonography. As a clinical background, we have found that only 20% of children had essential hypertension and in the rest-75% had kidney etiology of the disease. In the adults, essential hypertension was revealed in 51% of them and in the rest - kidney etiology in 53% of Pts. In the children /n=20/, CR gave rightly positive result in 6 of the cases, rightly negative - in 13, with a sensitivity of 100%, specificity-92,8% and accuracy-95%. In the adults /n= 38/ CR gave rightly positive result in 10 of the cases, rightly negative - in 21with a sensitivity of 71,4%, specificity- 87,5% and accuracy-81,5% These results show that the stenosis of renal arteries in children is more often haemodinamically significant, which explains higher sensitivity of CR in children than in adults and predicts better clinical outcome after eventual revascularization. The less accuracy of CR in adults could be explained with more long-lasting hypertension with microangiopathy which hinders the evaluation of the exact influence of Captopril on renography. Conclusions: 1.CR for a detection of RVH in children has a higher sensitivity than in adults.2. Hypertension in children is often associated with kidney's etiology, which in addition necessitates performing renography.

PS_303

RADIONUCLIDE EVALUATION OF RENOVASCULAR HYPERTENSION USING RENAL SCINTIGRAPHY WITH 99M TC-DMSA BEFORE AND AFTER CAPTOPRIL

M.J. Acosta-Gómez, A. Rodríguez, J.M. Llamas, J.M. López, M. Gómez, A. Moral, M.A. Muros, A. Ramirez, G. Sabatel, S. Ortega. Department of Nuclear Medicine, Virgen de las Nieves Hospital, Granada, Spain

Aim: Value the utility of studies with ^{99m}Tc-DMSA with captopril (scintigraphy imaging and unilateral renal function) in identifying renovascular or renal disease in hypertension patients with high probability of renovascular hypertension.
Methods: We studied 27 hypertension patients (12 males, 15 females) mean age 49 years, SD: 9.46, with high probability of renovascular disease. General analysis and radiology was made to all of them including renal arteriography as gold standard. Two renal scintigraphy with ^{99m} Tc-DMSA were made to all of them, baseline study and one hour after administration of 50 mg of captopril, a week between both studies. Renal scintigraphy (anterior and posterior images) was obtained 4 hours after the administration of 111 MBq (3 mCi) of ^{99m} Tc-DMSA and results were evaluated quantitatively and qualitatively calculating unilateral renal function. We considered positive for renovascular hypertension studies with impaired of more than 5% in unilateral renal function or a new defect absent in baseline study. Scintigraphic results were compared with arteriography to determine sensitivity, specificity and predictive values.
Results: Arteriography demonstrated significant renal artery stenosis in 18.5% of patients. Renal scintigraphy with captopril using ^{99m} Tc-DMSA demonstrated sensitivity of 60%, specificity of 91%, positive predictive value of 60% and negative predictive value of 91%. Were identified 3 patients with segmental defects of uptake consistent with chronic pyelonephritis scarring.
Conclusions: Studies with ^{99m} Tc-DMSA using captopril present high specificity and are useful in patients with high clinical probability of renovascular hypertension, identifying high number of patients with significant renal artery stenosis. The possibility of DMSA in identify renal abnormalities, as specially pyelonefritis scarring, add value to renal studies with captopril using others tracers. May identify renal etiologies of renovascular hypertension different to renal artery stenosis.

PS_304

SCINTIGRAPHIC EVALUATION OF THE ALLOGRAFTED KIDNEYS TRANSPLANTED FROM THE SAME CADAVERIC DONOR

A. Aktaş (1), G. Moray (2), H. Karakayalı (2), M. Haberal (2). (1) Department of Nuclear Medicine; (2) Department of General Surgery, Başkent University, Ankara, Turkey.

This study was designed to compare the early postoperative course of allografted kidneys transplanted from the same cadaveric donor by the use serial renal scintigraphy.
Fifteen pairs of recipients were being evaluated by serial radionuclide imaging during the early post-transplant period. For scintigraphic imaging, every patient was administered with 7 mCi of Tc-99m DTPA. Images were acquired at every second for the first one minute , and at every 30 sec during the rest of the study (20 minutes). Scintigraphic perfusion index was calculated by the method described by Hilson. Functional parameter of scintigraphy included the calculation of uptake (the ratio of peak kidney activity to background activity). Patients were imaged on the second and fifth post-operative days and as required thereafter.
Although, on perfusion, 3 pairs of recipients and on function, 4 pairs of recipients had discordant pattern; no statistically significant difference has been observed for recipients of the same donor for perfusion and function. The pairs having an abnormal scintigraphy on the first study demonstrated a similar course of recovery.
In conclusion, our results have shown that allografted kidneys transplanted from the same cadaveric donor demonstare similar perfusion, uptake and recovery function on renal scintigraphy obtained during the early transplant period.

PS_305

THE ROLE OF INFLAMMATORY MARKERS IN SELECTION OF UTI CHILDREN INDICATED FOR 99MTC DMSA SCINTIGRAPHY

S. Bykov (1), V. Smolkin (2), I. Garty (1), R. Halevi (2), A. Klimov (1). (1) Nuclear Medicine Department; (2) Pediatric B Department, Haemek Medical Center, Afula,Israel.

Non specific signs and symptoms in infants and low age children make the clinical differentiation of lower urinary tract infection (LUTI) and acute pyelonephritis (APN) very difficult. At present time the 99mTc DMSA scintigraphy is considered the most reliable technique in the diagnosis of APN. However, the indications for this study still remain debatable. The aim of this study is to assess the role of infectious markers for selection of patients indicated for 99mTc DMSA scintigraphy.
Methods: A prospective study was conducted in 56 infants and young children (2 months – 3 years of age, mean 16 months, 41 females and 15 males) admitted with a first episode of high fever and bacteriuria, suspected for APN. All children were investigated by 99mTc DMSA scintigraphy, procalcitonin (PCT), c-reactive protein (CRP) and white blood cells blood counts (WBC), within first 7 days after admission and 6 months later for control. Patients, who had pathological findings on both first done and control 99mTc DMSA scintigraphies (cortical scarring) were excluded from the study.
Results:

DSMA scintigraphy	PCT normal	PCT Elevated	CRP normal	CRP elevated
Normal (n=40)	36	4	7	33
APN (n=16)	1	15	-	16
Total (n=56)	37	19	7	49

PCT showed 90% and 94% specificity and sensitivity respectively. CRP showed 17.5% and 100% specificity and sensitivity respectively. There was no significant difference between WBC in APN and LUTI.
Conclusions: This study shows a significant correlation between positive 99mTc DMSA scintigraphic findings (APN) and elevated plasma concentration of PCT. Since PCT plasma level is considered as a reliable adjuvant for the diagnosis of APN, we suggest that elevated plasma PCT may be successfully used for selection of patients with UTI indicated for subsequent 99mTc DMSA scintigraphy.

PS_306

REPRODUCIBILITY OF TC-99M MAG3 CLEARANCE IN PATIENTS WITH IMPAIRED RENAL FUNCTION

T.Y. Erdil (1), F. Şen (1), S. Tuğlular (2), F. Dede (1), O. Noshari (1), C. Özener (2), E. Akoğlu (2), T. Turoğlu (1). (1) Department of Nuclear Medicine; (2) Section of Nephrology, Department of Medicine, Marmara University Hospital, Istanbul, Turkey.

The aim of this study was to test the reproducibility of the mercaptoacetyltriglycine (MAG3) clearance determinations in patients with impaired renal function.
Methods: Seven male and five female patients (mean age: 55.9yr ± 7.53 yr, range 45 yr- 68 yr) with a history of chronic renal failure (plasma creatinine levels = 3.33 mg/dl ± 0.79 mg/dl, range: 2.1mg/dl-4.6 mg/dl) were included in the study. The patients were not yet on dialysis during the study. Two seperate multiple sample clerance studies were performed in each patient within a week under similar physiologic conditions. After intravenous injection of the tracer, 10 blood samples were taken between 5 to 180 minutes. The clearances were calculated according to Sapirstein and corrected for body surface area. The mean difference between two studies were expressed as a percentage of the mean value of the two studies, and the standard deviation of these percentages represented the precision.
Results: The plasma clearances of first studies ranged from 26.5 ml/min to 93 ml/min with a mean of 59.4 ± 24.7 ml/min. The clearances of the second studies ranged from 22.4 ml/min to 125 ml/min with a mean of 60.8 ± 29.2 ml/min. There was no statistically significant difference between the two clearance studies (p = 0.69). The mean difference (systematic bias) between the first and second measurements was 1.11% (in six patients, the differences were 29.3%, 20%, 16.7%, 15.3%, 14.5% and 13.1%, in other six patients it was less than 10 %) and the precision was found to be 15.6%.
Conclusion: We did not observe a very good precision of MAG3 plasma clearance in patients with poor renal function; therefore, it should be interpreted cautiously in daily routine practice.

PS_307

THE EFFECT OF FUROSEMID ADMINISTRATION ON THE ACCURACY OF DMSA SPLIT RENAL FUNCTION DETERMINATION IN PATIENTS WITH PELVIC RETENTION

C. Türkmen, O. Özmen, N. Alan, M. Halaç, K. Özcan, C. Önsel, L. Kabasakal, K. Sönmezoğlu, I. Uslu. Department of Nuclear Medicine, Cerrahpaşa Medical Faculty, Istanbul University, Turkey.

It has been proposed that split renal function determination using Tc-99m DMSA (DMSA) may overestimate differential renal function in patients with excretion abnormalities due to pelvic retention of DMSA. It is also recommended that furosemid injection may be useful in these particular patients to calculate differential renal function.
Aim: The aim of the present study was to evaluate the effect of diuretic administration in determining differential renal function using DMSA scintigraphy.
Methods: For this purpose 19 patients, ages ranged from 1 month to 64 years (12.1±13.3 years, 15 m, 4 f) who had documented pelvic retention were included to the study. DMSA scintigraphies were performed to all patients 2 hours after injection and 6 planar images were obtained. Right after the standard study the furosemid was injected to all patients and same number of images were also obtained. DMSA split renal function was calculated for each patient and from each study by using arithmetic mean method. The precision of split renal function determinations were estimated by calculating the difference between the corresponding DMSA split renal function for the kidney with the lowest uptake. The mean of differences represented the systemic bias and the SD of the mean of the differences represented the precision of the technique.
Result: We did not observe any significant difference between the split renal function values obtained before and after diuretic administration (p>0.5). The values of split renal function ranged from 8.3% to 49.5% and from 7.7% to 49.2% in before and after diuretic administration respectively. Differences between values of the lowest split renal function obtained before and after diuretic administration varied from 2.6% to 0.2%. When we compared DMSA split renal function values the mean of the differences was only 0.2% and the SD was only 0.9%.
Conclusion: In conclusion we did not observe interference from pelvicalyceal activity in these patients who had documented pelvic retention and diuretic administration may be a useless intervention for improving the accuracy of split renal function determination.

PS_308

ALGODISTROPHY AND AVASCULAR NECROSIS OF HEAD FEMORAL IN THE POST-RENAL TRANSPLANT: DIFFERENCIAL DIAGNOSIS BY TRIPHASE BONE SCINTIGRAPHY

A. Bagnato (1), R. Bonofiglio (2), R. Tavolaro (1), A. Lanzillotta (1), N. De Napoli (2), PC. Loizzo (1). (1) Department of Nuclear Medicine; (2) Department of Nephrology, Annunziata Hospital, Cosenza, Italy.

Algodystrophy and avascular necrosis of head femoral represent two distinct complications in the transplanted patients receiving CsA and steroids. The exact prevalence in transplanted patients is unknown and several factors can determine influence its development, such as immunosuppressive therapy, steroids and diagnostic criteria. The symptomatology , characterized by pain of the hip , is common of the two entities and only a correct diagnosis permits the differencial diagnosis . The aim of our study was to evaluate the diagnostic value of the bone thiphase scintigraphy in the differencial diagnosis between algodystrophy and avascular necrosis of head femoral.
Methods: In a group of 98 patients with renal transplant we have selected 14 pts (M 10 ; F 4) age raging from 35 to 58 years and with transplant age raging from 3 to 60 months, admitted in our ward for pain of the hip and for functional limitation. All patients were in triple therapy (CsA / or Tacrolimus, Azathioprine or Mycophenolate, Steroids). In all patients, bone triphase scintigraphy were performed after suitable position under gamma camera and after injection of 550 MBq of 99mTc- MDP.
Results: 6 patients (M 4; F2) did not show mark of bone pathology of the head femoral; in the remaining 8 patients (M 5; F 3) we made diagnosis of algodistrophy in 5 (M 3; F2) and of avascular necrosis in 3 (M 2; F1). In the group of patients with algodystrophy, the bone triphase scintigraphy showed on the head femoral an increased periarticular radionuclide activity during the vascular and parechymal phases. In the patients with avascular necrosis of the head femoral , the bone scintigraphy showed a reduction of blood flow on the epiphyseal region, while during blood pool and retarded phases we showed an area of uptake that surrounded the ipoactive head femoral.
Conclusions: Bone triphase scintigraphy represents a useful, non invasiv tool for the differencial diagnosis between algodystrophy and avscular necrosis of head femoral.

OTHER CLINICAL SCIENCE. PEDIATRICS

PS_309

QUANTITATIVE ANALYSIS OF 99MTC-DMSA DURING ACUTE PYELONEPHRITIS (APN) FOR PREDICTION OF LONG TERM RENAL SCARRING

A. Hitzel (1), A. Liard-Zmuda (2), A. Manrique (1), I. Gardin (1), J.F. Ménard (3), F. Gutman (1), A. Sanson (1), J.N. Dacher (4), P. Véra (1). (1) Service et GIE de Médecine Nucléaire, CH Becquerel et CHU Charles Nicolle, Rouen, France; (2) Service de Chirurgie Pédiatrique, CHU Charles Nicolle, Rouen, France; (3) Service de Biostatistiques, CHU Charles Nicolle, Rouen, France; (4) Service de Radiologie, CHU Charles Nicolle, Rouen, France

Aim. To evaluate whether ^{99m}Tc-DMSA renal planar scintigraphy (DMSA) performed during APN could discriminate kidneys that would develop scarring (ie remain abnormal) from those that would not (ie normalize).
Methods. DMSA was performed in 43 children (85 kidneys) at acute phase (DMSA1) and 7±2 months after APN (DMSA2). All DMSA were graded using a 9 point-semi-quantitative uptake score (each kidney divided in 3 thirds graded from 0 (no uptake) to 3 (normal uptake)) considered to be gold-standard. Renal scarring was defined as a score <7 on DMSA2. A comparison between the scores of DMSA1 and DMSA2 leaded to classify each kidney as: normal stable (NS) when scores on DMSA1 and DMSA2 were >7, abnormal improved (AI) when score was <7 on DMSA1 and had improved by 2 points or more on DMSA2 and abnormal stable (AS) when score was <7 on DMSA1 but improved by less than 2 points on DMSA2. For quantitative analysis of DMSA1, successive thresholds (20, 30, 40, 50, 60, 70 and 80%) were automatically applied to the posterior view of each kidney. For each threshold, the number of pixels and the count rate were expressed as a percentage of the total number of pixels and the maximal count rate over each kidney respectively. The ANOVAs and ROC curves analyses were performed.
Results. The distribution of kidneys was NS= 59, AI= 14 and AS= 12. Scarring was better predicted by the count rate ratio than that of the number of pixels ratio. Using ANOVA, it was possible to discriminate the NS, AI and AS kidneys by the count rate ratio (F =14.6, p <.0001). For the count rate ratio, a 70% threshold best isolated the AS from the AI kidneys (p =.004) and the NS from the AI kidneys (p <.0001). On ROC curve analysis, this 70% threshold provided the best AUC for prediction of renal scarring. Using a cut off value of .45 the sensitivity, specificity, positive and negative predictive values of the 70% threshold count rate ratio to predict scarring were .78, .83, .84 and .77 respectively.

Conclusion. A .45 cut-off value for the 70% threshold count rate ratio calculated on 99mTc-DMSA scintigraphy performed during acute pyelonephritis may help to predict renal scarring. Patients with a value > .45 did not develop renal scarring after their pyelonephritis.

PS_311

PROGNOSTIC VALUE OF DMSA SCINTIGRAPHY IN CHILDREN WITH ACUTE PYELONEPHRITIS: FIRST RESULTS FROM A PROSPECTIVE STUDY

V. Roelants (1), D. Tuerlinckx (2), T. Vander Borght (1), G. de Binderling (2), E. Bodart (2). (1) Department of Nuclear Medicine; (2) Department of Pediatrics, Yvoir, Belgium.

Aim: The aim of this prospective study was to report the evolution of various dimercaptosuccinic acid scintigraphy (DMSA) patterns observed in children with acute pyelonephritis (APN) and to evaluate the ability of DMSA to identify patient at risk for renal scarring.
Methods: The study group included 21 children with no previous history of APN (15F/6M; mean age: 44 months; range: 3-168 months) who presented with an APN as defined by a rectal temperature >38¡, ± flank pain or non specific symptoms and a positive urine culture. All patients underwent a DMSA within 2-3 days of admission and 6.8±1.1 months later and were treated with the same antibiotic regimen for 15 days followed by prophylactic antibiotherapy until DMSA was repeated. Scans were performed 4 hours after IV injection of a weight adjusted dose of Tc-99m-DMSA and at least 4 planar views were obtained (anterior, posterior, right and left posterior oblique; 200-300 kcounts/view). Images from both scan sessions were visually interpreted according to a 5-grade scale (grade 0: normal; grade 1: moderate hypoactive cortical area without outline deformation; grade 2: severe hypoactive cortical area without outline deformation; grade 3: wedge-shaped cortical defect and grade 4: deformed outline = scar) and compared together. Differential renal function was calculated using the geometrical mean method (a relative uptake between 45 and 55 % was considered as normal).
Results: Initial DMSA was abnormal in 16/21 patients (76%) and 29 lesions were observed (grade 1: n=16, grade 2: n=8; grade 3: n=3; grade 4: n=2). No patient suffered a second APN before the repeated DMSA. At 7 months, all normal DMSA remained normal, 9/16 patients (56%) normalized their scan while 4/16 (25%) demonstrated an improved pattern and 3/16 (19%) had a grade 4, consistent with scar. 23/29 lesions (79%) either improved or normalized, whatever their grade at the first scan. An altered initial differential renal function (n=3) was always associated with at least one lesion which severity remained unchanged 7 months later, whatever its grade. So far, none of the other non scintigraphic reported risk factors for scar was confirmed by this study.
Conclusions: These results suggest that differential renal function could be a reliable scintigraphic parameter to predict which patient with APN will develop persistent renal damage at 7 months. They also suggest that cortical retraction may not always correspond to renal scar and that 7 months may be insufficient for complete recovery of cortical function.

PS_310

STUDY OF THE RELATIONSHIP BETWEEN RECURRENT LOWER RESPIRATORY TRACT INFECTION, GER AND BRONCHIAL ASTHMA IN CHILDREN

L. Kabasakal (1), N. Alan (1), O. Özmen (1), M. Halaç (1), H. Cokugras (2), Y. Camçoğlu (2), C. Önsel (1), I. Uslu (1). (1) Department of Nuclear Medicine ; (2) Department of Pediatrics, Cerrahpaşa Medical Faculty, Istanbul University, Istanbul, Turkey, Istanbul, Turkey.

Gastroesophageal reflux (GER) has been suggested as a cause of recurrent respiratory infections, bronchial asthma and sudden death syndrome. GER scintigraphy has been shown to be a sensitive, noninvasive and a simple test in detection of GER. The aim of the present study which is a part of CRP conducted by IAEA, was to evaluate the relationship between GER and respiratory disorders using the outcome of therapy as final diagnosis. For this purpose 41 patients, mean age 48.3±28.3 months, 23 f, 37 m, who had recurrent respiratory infections were included to the study. All patients were followed clinically for 3 to 6 months to evaluate the outcome of medical antiacid therapy. All patients underwent GER scintigraphy using Tc-99m labeled colloid and up to 24 hours images were obtained from all patients. The number and the severity of GER episodes were evaluated visually and by generating the time activity curves of esophageus as well. All patients who had scintigraphic GER were treated using a standard antiacid treatment. Results: GER was determined in 68% of patients (n=28). GER was observed 82% of patients who had vomiting as primary symptom (n=11) and 40% of patients who had bronchial asthma as primary symptom. Antiacid treatment was given 86% of patients(n=24) who had GER. Among patients who received antiacid treatment 83% (n=20) of patients have demonstrated clinical improvement. Surgical treatment was performed in 1 patient and 3 patients were died due to severe broncopulmonary insufficiency. Among the patients who did not show GER and who received only symptomatic treatment for pulmonary diseases 70% (n=10) have demonstrated clinical improvement. In conclusion, GER scintigraphy is a noninvasive and sensitive test in the evaluation of patients with recurrent respiratory infections and may be useful in the management planing of these patients.
This study is a part of Coordinated Research Program conducted by International Atomic Energy Agency.

PS_312

QUANTIFICATION OF LEFT-TO-RIGHT CARDIAC SHUNTS BY EXPONENTIAL EXTRAPOLATION OF SHUNT ACTIVITY IN LUNG CURVES

A. Stanicic (1), R. Jakl (2), D. Ivancevic (3), S. Popovic (3), Z. Milas (4), V. Capkun (1). (1) Department of Nuclear Medicine, Clinical Hospital, Split; (2) Department of Pediatrics, Clinical Hospital, Split; (3) Department of Nuclear Medicine and Radiation Protection, University Hospital, Zagreb; (4) Faculty of Engeneering, Split, Croatia

Radionuclide methodology offers the data for quantification of left-to-right cardiac shunts as good as those from dye curves obtained during cardiac catheterization. Therefore it still deserves efforts for improvements. The possibility to separate the shunt activity from the systemic recirculation activity in lung curves is expected to give data for a more precise quantitative analysis.
Methods: A hydrodynamic model of left-to-right without systemic recirculation was used to analyze the time relationships between the single passes of radionuclide. An exponential decline of shunt activity was observed, as in left-to-right shunts a constant fraction of indicator leaves the central pool in each circulation. Pulmonary time-activity curves obtained by radionuclide angiocardiography from 31 patients aged 1 week to 28 years (mean 14.5 years) were analyzed. The diagnosis of a left-to-right cardiac shunt was established by cardiac catheterization. We also analyzed 20 curves obtained from patients without shunting.
Results: After subtraction of normal activity between the first pass and systemic recirculation components, a logarithm of the difference curve (i.e. of the shunt activity) could be fitted with a straight line for an interval comprising almost the entire three initial passes of activity through the lung, and with coefficients of correlation higher than 0.98. By extrapolation of the straight line, the systemic recirculation activity could be separated from shunt activity. The Qp/Qs ratio obtained by the standard method was tested using the extrapolation data. Gamma variate curves for successive shunt recirculations were added at time intervals which were based on the data from the hydrodynamic model and the data from the two first gamma variate fits. In the successive step changes in the second downslope of the second gamma variate fit were made. The Qp/Qs ratio which could reproduce the experimental curve with the lowest coefficient of variation was accepted. A good correlation with oximetry data was found with the regression line close to the line of identity. The errors in the computed shunt size would be within ±4% of pulmonary flow.
Conclusions: Radionuclide method can be easily applied in all age groups and data acquisition last for a short time. The error in the computed left-to-right shunt size is significantly lower than the reported values obtained by other methods.

PS_313

URINARY N-ACETYL-BETA-GLUCOSAMINIDASE IN CHILDREN WITH UPPER URINARY TRACT INFECTION, IN RELATION TO TC-99M DMSA SCINTIGRAPHY

G. Çapa Kaya (1), Y. Taşkıran (2), M. Bak (2), A. Aydın (1), O. Toksavul (2), Y. Uslu (2), E. Öztürk (2), H. Durak (1). (1) Department of Nuclear Medicine, Dokuz Eylül University Medical School, Izmir, Turkey; (2) Behçet Uz Children's Hospital, Izmir, Turkey.

N-acetyl-beta-glucosaminidase (NAG), a lysosomal enzyme, is located in the renal proximal tubule cells. In recent studies, urinary NAG levels has been used to localize urinary tract infection (UTI) and demonstrate epithelial necrosis of proximal tubule cells. The aim of this study was to investigate the relationship between Tc-99m DMSA scintigraphy and urinary NAG and NAG/creatinine in acute pyelonephritis.

Methods: Hundred children with the mean age of 5.1 ± 3.0 were included in this study. All children had positive urine culture. Tc-99m DMSA scintigraphy was performed within 3 days after the diagnosis of UTI. Plasma C reactive protein (CRP), erythrocyte sedimentation rate (ESR), leucocyte count, urinary NAG levels and NAG/creatinine ratios were also obtained. Thirty children had focal or diffuse decreased uptake, segmental cortical thinning and cortical irregularity in Tc-99m DMSA scintigraphy (Group 1). DMSA scintigraphy was normal in 70 children (Group 2).

Results: CRP, ESR and leucocyte count in group I (7.9±8.1 mg/lt, 56±26 mm/h, 15277±9162, respectively) were significantly higher than Grup 2 (1.0±1.8 mg/lt, 24±15 mm/h, 9626±3833, respectively). Urinary NAG levels and NAG/creatinine ratios are shown in the table.

	Group 1 Tc-99m DMSA (+)	Group 2 Tc-99m DMSA (-)	P values
NAG (U/L)	11.7 ± 2.5	2.6 ± 2.4	? 0.05
NAG/creatinine(U/gr)	16.6 ± 5.6	3.6 ± 3.3	? 0.05

In the localization of UTI, cut-off value was found as 5 U/L for NAG, 7 U/gr for NAG/creatinine ratios. There was a significant correlation between Tc-99m DMSA scintigraphy and urinary NAG (r = 0.864, p = 0.01) and NAG/kreatinin (r = 0.863, p = 0.01). Urinary NAG and NAG/creatinine had a sensitivity of 100 %, specificity of 94 %, positive predictive value of 88 %, negative predictive value of 100 % for acute pyelonephritis.

Conclusion: In this selected group of patients, urinary NAG and NAG/creatinine can be used to localize upper UTI when compared to Tc-99m DMSA scintigraphy.

PS_314

DOPPLER US IN THE DIAGNOSIS OF ACUTE PYELONEPHRITIS: COMPARISON WITH TC-99M DMSA SCINTIGRAPHY

G. Çapa Kaya (1), Y. Göktay (2), A. Aydın (1), M. Seçil (2), I.Y. Taşkıran (3), M. Bak (3), H. Durak (1). (1) Departments of Nuclear Medicine, Dokuz Eylül University Medical School, Izmir, Turkey; (2) Radiology, Dokuz Eylül University Medical School, Izmir, Turkey; (3) Behçet Uz Children's Hospital, Izmir, Turkey.

The appropriate treatment of urinary tract infection requires to assess the localization of infection. Tc-99m DMSA scintigraphy is considered as a gold standard in the diagnosis of acute pyelonephritis. The aim of this study was to compare Tc-99m DMSA scintigraphy with Doppler US (DUS) in children with clinically suspected acute pyelonephritis.

Methods: Eighty seven children (mean age: 5.1 ± 3.1, 72 girls and 15 boys) with the first episode of urinary tract infection and positive urine culture were included in this study. In all children, Tc-99m DMSA scintigraphy and DUS were performed within 3 days after the diagnosis of urinary tract infection. Focal or diffuse decreased uptake, segmental cortical thinning and cortical irregularity in Tc-99m DMSA scintigraphy were interpreted as an abnormal. Evaluation was performed both for each kidney (total of 169 kidney) and for each region as the upper, middle and lower regions separately (total of 522 regions).

Results: 25 of 169 kidneys were evaluated as an abnormal on planar images of Tc-99m DMSA scintigraphy. 14 of 25 kidneys were abnormal in DUS. Sensitivity (SEN), specificity (SPE), positive predictive values (PPV) and negative predictive values (NPV) were 56%, 88%, 45% and 92% for DUS, respectively. For each kidney, SEN and PPV were 64% and 47% for left kidney, 45% and 39% for right kidney. When the evaluation was performed according to regions, DUS was positive in 19 of 30 regions with abnormal DMSA scintigraphy and SEN, SPE, PPV and NPV were 63%, 96%, 48% and 98% for DUS, respectively. Upper region of the right kidney had the lowest SEN (33%) and middle region of the left kidney had the lowest PPV (48%).

Conclusions: We concluded that the sensitivity of DUS is relatively low in the diagnosis of acute pyelonephritis and sensitivity rate can be changed according to the kidney and region in which the lesion is localized.

PS_315

RADIONUCLIDE ASSESSMENT OF GLOMERULAR AND TUBULAR FUNCTION IN CHILDREN WITH PRIMARY VESICOURETERAL REFLUX

M. Vlajkovic (1), M. Bogicevic (1), M. Rajic (1), S. Ilic (1), G. Lilic (1), D. Mitic (1), A. Slavkovic (2), V. Artiko (3). (1) Department of Nuclear medicine, Clinical Center, Nis,Yugoslavia; (2) Clinic for Pediatric Surgery, Clinical Center, Nis, Yugoslavia; (3) Institute of Nuclear Medicine, Clinical Center Serbia, Belgrade, Yugoslavia.

OBJECTIVES:The purpose of this study was to investigate whether the glomerular and tubular renal parameters are in concordance in children with primary vesicoureteral reflux (VUR).

MATERIAL AND METHODS: A total of 94 children with 117 refluxing nefroureteric units (NU) were grouped according to the International Reflux Study Committee grading system as follows: Group I (VUR grades I, n=17), Group II (VUR grades II-III, n=70) and Group III (VUR grades IV-V, n=30). Findings were compared with those obtained in 64 healthy children. Overall and single kidney function was assessed using 99mTc-DTPA dynamic and clearance studies and 99mTc-DMSA static and uptake (2h and 24h) studies, respectively.

RESULTS: Significant correlation was found between relative function of kidneys in children with VUR obtained using 99mTc-DTPA of 50.0±7.0% and both 99mTc-DMSA uptake after 2h of 50.0±7.9% (R=0.906, p<0.0001) and 99mTc-DMSA uptake after 24h of 49.8±7.9% (R=0.899, p<0,0001). Regarding to the control value of 100%, absolute kidney uptake of 99mTc-DMSA after 24h was found 93% in Group I, 75% in Group II and 60% in Group III. However, single clearance 99mTc-DTPA values of kidneys with VUR were significantly less impaired in respect of control, being 93% in Group I, 86% in Group II and 66% in Group III, respectively. Overall 99mTc-DTPA clearance rate was reduced in 38%, while absolute 24h 99mTc-DMSA uptake was reduced in 61% children with VUR. In 55% of children with reduced overall absolute 24h 99mTc-DMSA uptake values, overall clearance 99mTc-DTPA values were within normal limits.

CONCLUSION: Relative renal function of kidneys in children with primary VUR can be reliably assessed either by dynamic 99mTc-DTPA or static 99mTc-DMSA study. However, overall glomerular and tubular function in children with VUR are not equally deteriorated, with more pronounced impairment of tubular function.

PS_316

SCINTIGRAPHIC SUPRANORMAL DIFFERENTIAL RENAL FUNCTION IN THE FIRST YEAR OF LIFE

A. Biyi (1), H. Lottmann (2), G. D'Amore (1), Y. Aigrain (2), B. Bok (1), F. Bonnin (1). (1) Department of Nuclear Medicine, Beaujon Hospital, Clichy, France; (2) Department of Surgery, Robert Debre Hospital, Paris, France.

In neonates with unilateral hydronephrosis, a supranormal differential renal function (DRF) can be seen on the side of the dilatation. The aim of this paper was to assess whether kidneys with normal and supranormal DRF have the same scintigraphic evolution during the first year of life.

Methods: 131 consecutive cases with unilateral hydronephrosis detected before birth by ultrasound were reviewed. The surgical management was identical for all children. In each case, one renal scintigraphy (RS) was performed at 3 months of age (range: 1-6 months), and one 6 months later using the same protocole (mercaptoacetyltriglycine labelled with 15 MBq of 99mTc; standardized hydratation). The DRF (area method) and a ratio S (surface of the dilated kidney divided by the surface of the normal kidney) were derived from all RS using regions of interest which were manually drawn on images taken 2 to 3 minutes after the tracer injection. DRF values and S values were compared using ANOVA and paired t tests.

Results: At the first RS, 24 neonates (18%) had a supranormal DRF (14 cases -group 1- underwent surgery and 10 -group 2- were not operated) and 107 cases had a normal DRF (16 -group 3- underwent surgery and 91 -group 4- were not operated). Between the two RS, 23% (30/131) of the children were operated including 46% (14/30) of cases with supranormal DRF. At the second RS, the variations of DRF and S values were different in the 4 groups ($p<0.05$). In group 1, the values of DRF decreased from 57±2% to 52±4% ($p<0.05$) and the values of S decreased from 48±33 to 15±19 ($p<0.05$). In group 2, the DRF values were unchanged and the S values increased non significantly. In group 3 and 4, the DRF and the S values were unchanged.

Conclusion: In the first year of life using the same criteria for surgical decision for all kidneys, the post-surgical changes of DRF and size of the dilated kidneys are different whether the DRF is normal or supranormal.

PS_317

COMPARISON OF SINGLE INJECTION RADIONUCLID METHODS WITH CLASSICAL CREATININE METHOD FOR CLEARANCE DETERMINATION IN CHILDREN ON PERITONEAL DIALYSIS (PD)

A. Bogdanovska (1), S. Kuzmanovska (2). (1) Department of Nuclear Medicine; (2) Pediatric Clinic, Medical Faculty, Skopje, Macedonia.

51 Cr-EDTA is very suitable radiopharmaceutical for GFR determination as a substitute for inulin clearance . The single injection method and monoexponential expression of plasma disappearance rate is well established in nuclear medicine. The idea was to use the method in patients undergoing PD in order to simplified the cumbersome procedure for creatinine clearance with fluid collection.
Six children aged 9.6 (6-14) years on PD were studied in hospital .51Cr-EDETA (3MBq) And 99m Tc-DTPA (200MBq) were injected simultaneously after the filling of peritoneal cavity with dialysate fluid.Blood samples were drawn at 4,24, and 48 hours after injection.Samples of 2 ml plasma and standards were counted on scintillation counter.
Peritoneal clearance was calculated taking the necessary data from the fitted monoexponential curve. There is high correlation between 51Cr-EDTA and 99mTc-DTPA clearance (r=).985,r+0.995)for any combination of two plasma samples, so the number of plasma sample could be reduced on two . We tried to obtain peritoneal clearance with single injetion method using one plasma sample.For that purpose we correlated the activity ration of the given dose and plasma sample (D/P) with clearance calculated with three plasma samples.The following coefficient of correlation were obtained : r= o.751 for 4h , r=0.986 for 24h and r=0.974 for 48h.The regression equation for 24h sample clearance =1.111+0.278(D/P) may be used for injection of clearance with one plasma sample , withdrawn 24 hours after injection of radiopharmaceutical.Mean error for clearance calculated in this way is 3.0% CONCLUSION: The single injection radiotraser method can be used for clearance estimation in patients on PD. Number of plasma samples may be reduced in one with most appropriated time after 24 hours.

PS_318

PROGNOSTIC VALUE OF THE ACUTE DMSA SCAN IN CHILDREN AT FIRST URINARY TRACT INFECTION

A. Biggi (1), G. Pomero (1), P. Cussino (2), L. Dardanelli (1), GF. Camuzzini (1). (1) S.Croce e Carle Hospital, Cuneo, Italy; (2) Ss. Annunziata General Hospital, Savigliano, Italy.

The recognition of a group of patients at risk to develop sequelae among children with urinary tract infection (UTI) in order to modulate the treatment and the radiological investigation is of great clinical importance.
Aim. In this prospective study we attempted to verify in 101 children at first UTI if it is possible to identify groups of patients with different risk of developing renal scarring, by taking into account both the extent of kidney involvement documented in the acute phase of infection using DMSA scan, and the presence or absence of vesicoureteral reflux (VUR).
Methods. We included only children at first symptomatic UTI, in whom the interval between the onset of symptoms and the diagnosis of UTI was less than 6 days and in whom DMSA scan was performed no later than 15 days following the presentation, the others being excluded. This study design consists of performing an acute DMSA scan (acute scan) for the detection of renal parenchymal involvement in the acute phase of infection, cystourethrography for vesicoureteral reflux detection and grading, and a follow-up scan (late scan) performed if the acute scan was abnormal. 101 children, 60 females and 41 males were inlcuded in the study. The mean age was 18 months (range 1 month - 13 years).
Results. Of the 101 children included, 31 had normal kidneys; 9 of the 70 children with pyelonephritis had bilateral disease. A follow-up scan was available in 59 of 79 kidneys with positive acute DMSA scan. 16/59 (27%) of abnormal kidneys had persistent lesion. The frequency of persistent lesions in kidneys with mild-moderate lesions (less than 50% of kidney involvement) in presence of VUR or in non-refluxing kidneys was similar (p=0.1447), while the frequency of persistent lesions in kidneys with severe lesions in presence of VUR was significantly higher than the frequency of persistent lesions in non-refluxing kidneys (p=0.0089).
Conclusions. The extent of kidney involvement and the presence of VUR make possible the identification of different categories of risk of scarring: in the „low risk group" (normal kidney with/without VUR) the risk of scarring is 0%; in the „intermediate risk group" (mild lesions with/without VUR; extensive lesions without VUR) the risk of scarring is between 14% and 38%, while in the „high risk group" (extensive lesions with VUR) the risk of scarring is 88%. Quantifying the risk of scarring could help in planning the treatment or in modifying later strategy.

PS_319

THE CLINICAL USEFULNESS OF TC-99M ECD BRAIN SPECT IN MEASLES ENCEPHALITIS

S.T. Lim (1), M.H. Sohn (1,3), J.C. Kim (2). (1) Department of Nuclear Medicine; (2) Department of Pediatrics; (3) Clinical Medical Reserch Center, Chonbuk National University Hospital, Chonbuk National University Medical School, Chonju, Korea.

Purpose: Since the prognosis of measles encephalitis is poor, early diagnosis and proper management are very important to improve clinical outcomes. We compared Tc-99m ECD brain SPECT (SPECT) with MR imging (MRI) for the detection of mesles encephalitis. Materials and Methods: Eleven patients (M:F=4:7, age range 18 months-14 yrs) with measles encephalitis were enrolled in this studies. All of them underwent both MRI and SPECT. The results of SPECT were scored from 0 (normal) to 3 (defect) according to perfusion state. We compared two image modalities for the detection of brain abnormality in measles encephalitis. Results: Seven of 11 patients (63.6%) revealed high signal intensity in the white matter on T2WI of MRI, on the other hand all patients (100%) showed hypoperfusion on SPECT. Severe perfusion deficits above score 2 were located with decreasing frequencies in the frontal lobe (81.8%), temporal lobe (72.7%), occipital lobe (27.3%), basal ganglia (27.3%), and parietal lobe (9.1%). Conclusion: We conclude that SPECT is more useful than MRI for the detection of brain involvement in patients with measles encephalitis.

PS_320

BONE SCINTIGRAPHY AND SPINE INJURY IN CHILDREN

E. Urbanova (1), J. Preis (2), J. Vizda (1), P. Kafka (1), M. Netikova (1). (1) Department of Nuclear Medicine; (2) Department of Pediatric Surgery, University Hospital, Hradec Kralove, Czech Republic.

Children with a suspicion of bone damage mostly after sport, or home accident were admitted to the hospital. They were referred for bone scintigraphy. The most common reason for referral were the exclusion of spine occult fractures or infractions. The aim of this study was to assess the role of bone scintigraphy in comparison with X-ray investigation.
Methods: We evaluated 58 children during seven years. Bone scintigraphy and SPECT scanning were performed 2h after intravenous injection of 99mTc-MDP. The interval from injury to scintigraphy was 5-14 days. The mean time between bone scintigraphy and X-ray investigation was 3 days (range 2 - 8 days)
Results: Normal results in both methods were in 23 of the 58 patients. The pathological findings were identical in 16 pts. In 19 from all investigated pts. bone scintigraphy concurred with X-rays as to the number and localisation of abnormalities. For 13 pts. bone scintigraphy proofed new or additional foci when compared with X rays and in 6 pts. only bone scintigraphy showed foci of spine.
Conclusions: Bone scintigraphy has a significant role in the investigation of spine pain after injury. The wider availability of SPECT has increased the number of clinical applications and enhanced sensitivity and specificity compared with planar imaging. Nuclear medicine provides information to identify the significance of structural changes found on anatomical imaging. Some of them may be asymptomatic.

PS_321

MYOCARDIAL SPECT IN CHILDREN WITH SICKLE CELL ANEMIA

C. Maunoury, P. Acar, I. Hallaj, L. Barritault. Hopital Necker-Enfants Malades, AP-HP, Paris, France.

While cerebral and bones strokes are well documented in children with sickle cell anemia (SCA), impairment of myocardial perfusion is an unknown complication. Conventional techniques such as exercise testing and echocardiography have a low sensitivity and specificity to detect myocardial ischemia in patients with SCA. The aim of this prospective study was to assess myocardial perfusion with Tl-201 SPECT in children with SCA.

Methods: Thirteen patients, aged 12±4 years, were included. Myocardial perfusion was assessed by Tl-201 SPECT after stress and 3 hours later after reinjection on a single head gammacamera equipped with a LEAP collimator (64x64 matrix size format, 30 projections over 180$_i$, 30s per step). Left ventricular ejection fraction (LVEF) was assessed by equilibrium radionuclide angiography at rest on the same day.

Results: Myocardial perfusion was impaired in 6/13 patients: 3 had reversible defects and 3 had fixed defects. The left ventricular cavity was dilated in 7/13 patients. The mean LVEF was 62±9%. There was no relationship between myocardial perfusion and left ventricular dilation or function.

Conclusion: Myocardial perfusion is frequently impaired in children with SCA. Prospective studies with a larger number of patients could assess the incidence and potential complications of myocardial ischemia in patients with SCA.

PS_322

EVALUATION OF GASTRIC EMPTYING SCINTIGRAPHY AND 13C-BREATHING TEST IN PEDIATRIC PATIENTS

N. Hamscho (1), J.H. Risse (1), B. Braden (2), P. Ahrens (3), M. Diehl (1), F. Grünwald (1). (1) Dept. of Nuclear Medicine; (2) Dept. of Internal Medicine; (3) Center of Pediatric Medicine, University of Frankfurt, Germany.

Gastric emptying scintigraphy has been predominantly described in adult patients. The aim of this study was to evaluate gastric emptying scintigraphy on pediatric patients who presented with bronchopulmonary diseases and to define typical gastric emptying curve patterns in correlation to the ^{13}C-acetate- breathing test.

Methods: We performed gastric emptying scintigraphy on 32 patients aged between 4 and 16 years with recurrent bronchopulmonary infections which were thought to be due to gastro-esophageal reflux. A semiliquid test meal was applied (rolled oats 5g, milk 75ml, sugar 3g, 40-60 MBq ^{99m}Technetium-Nanocoll, ^{13}C-acetate). This was followed by dynamic images over 60 min. The results of the scintigraphy were correlated with motility examinations and with the results of the ^{13}C-breathing test. The scintigraphic reference range of the gastric emptying was adopted from adult patient populations ($t_{1/2}$=60 min) because of the lack of reliable pediatric references.

Results: Out of 32 children 23 showed physiological, 7 obvious pathological and 2 borderline gastric emptying time ($t_{1/2}$=60 min). The comparison with the ^{13}C-breathing test showed a strong correlation between the half-life ranges of gastric emptying and those of the ^{13}C-breathing test ($t_{1/2}$=90 min).

Conclusions: Our data may help to improve the standards of gastric emptying scintigraphy in pediatric patients. We could show a strong correlation between the gastric emptying scintigraphy and the ^{13}C-breathing test in both pathological and physiological curve types.

RADIOPHARMACY / RADIOCHEMISTRY 2

PS_323

RGD-DTPA-OCTREOTATE, AN ANALOGUE FOR TUMOUR IMAGING AND RADIONUCLIDE THERAPY

M. De Jong (1), H.F. Bernard (1), A. Capello (1), W.A.P. Breeman (1), A. Srinivasan (2), M. Schmidt (2), E.P. Krenning (1), P.M. Van Hagen (1). (1) Erasmus University Medical Center Rotterdam, The Netherlands; (2) Mallinckrodt Medical Inc., St Louis Mo, USA.

Introduction and Aim: receptor-targeted scintigraphy and radionuclide therapy using radiolabelled somatostatin analogues are successfully used to detect and treat somatostatin receptor-positive (mainly subtype 2 (sst_2)) tumours. Also interesting for these purposes are RGD(Arg-Gly-Asp) peptides as they can antagonise tumour angioneogenesis, e.g. by binding to alpha$_v$beta$_3$ receptors on newly formed blood vessels, and induce apoptosis.

Methods and Results: we evaluated Tyr^3-octreotate, chelated with DTPA or DOTA, and found very high affinity binding to sst_2, leading to high uptake of ^{177}Lu-DOTA-Tyr^3-octreotate in sst_2-positive tumours in patients and rats. Radionuclide therapy in rats using the latter compound resulted in dose dependent responses with up to 100% cure after 555 MBq, showing its great promise.

Moreover, we introduced the RGD analogue c(Arg-Gly-Asp-D-Tyr-Lys)chelated with DTPA. In vitro and in vivo the analogue appeared to bind with high affinity to alpha$_v$beta$_3$ receptors on blood vessels and tumour cells in different rat and human cancers.

To combine tumour uptake via sst_2 and alpha$_v$beta$_3$ receptors, we synthesized an RGD-DTPA-Tyr^3-octreotate hybrid peptide. Labelling studies showed good labelling with ^{111}In. In vitro binding studies showed that the radiolabelled compound had retained affinity for both sst_2 and alpha$_v$beta$_3$ receptors, binding could be blocked with an excess of the different competing analogues. In animal studies, the high uptake found in the (sst_2- and alpha$_v$beta$_3$ receptor-positive rat pancreatic CA20948) tumour was mainly via sst_2 targeting, presumably because of the higher affinity of Tyr^3-octreotate for sst_2 than that of RGD for the alpha$_v$beta$_3$ receptor.

The therapeutic effects of DTPA-Tyr^3-octreotate, RGD-DTPA-Tyr^3-octreotate and DTPA-RGD labelled with the Auger electron emitter ^{111}In, were evaluated in vitro in a single cell, colony forming assay (100 cells/well in 6-well plates, 1 h incubation with ^{111}In-labelled peptide, 10 days colony growth) using CA20948 cells. These cells showed relative radioresistance in external beam radiation studies (survival after 1 and 2 Gy was 70% and 50% of control). In our in vitro system, all analogues were able to control tumour growth (0% survival), the effects were dependent on radiation dose, incubation time and specific activity used.

Conclusion: this hybrid peptide radiopharmaceutical is suitable not only for tumour scintigraphy, but it has potential for radionuclide therapy as well.

PS_324

VENTRICULAR NATRIURETIC PEPTIDE (BNP) IN HEART TRANSPLANTATION. CORRELATION OF PLASMA CONCENTRATIONS OF BRAIN NATRIURETIC PEPTIDE AND ENDOMYOCARDIAL BIOPSY

I. Hervás (1), L. Almenar (2), P. González-Cabezas (1), A. Saura (1), J. Osca (2), P. Bello (1), J.L. Pérez-Pastor (1), J.F. Martí (1), A. Mateo (1). (1) Department of Nuclear Medicine; (2) Depratment of Cardiology, University Hospital, Valencia, Spain.

Aim: Ventricular natriuretic peptide (BNP) is a novel cardiac hormone that may play a pathophisiologyc role in cardiac disorders. High levels of plasma ventricular natriuretic peptide have been identified after standard orthotopic cardiac transplantation. The aim of this study was to determine whether elevated plasma BNP levels observed after cardiac transplantation are related to the severity of rejection on the endomyocardial biopsy (EB).

Methods: We have studied 80 consecutive heart transplant patients (11 women and 69 men). In all of them we have determined the BNP levels using a radioimmunometric assay at the moment of the heart transplantation and the same day that were admitted to perform an EB. We have compared 223 BNP levels in serum with the grade of rejection on the EB (graded according to the International Society of Heart and Lung transplantation Standarized Grading System). For comparing that we have divided the patients in four groups according to the results on the endomyocardial biopsy: The first group (n=56) were the EB graded 0. The second (n=77) graded 1 A and 1 B. The third (n=60) graded 2. The fourth (n=30) graded 3 A, 3 B and 4. As statistical tool we have used the student's t test.

Results: The first group presented a mean BNP value = 171.8 pg/ml, the second a mean BNP value = 182.38 pg/ml, the third a mean BNP value = 263.69 pg/ml and the fourth a mean BNP value = 391.56. The fourth group (with suspicion of cardiac allograft rejection on the EB) had significant increased BNP levels ($p<0.05$) comparing with the other groups (with no suspicion of cardiac allograft rejection).

Conclusion: Mean BNP levels increased according to the increase of degree on endomyocardial biopsy. The group with suspicion of cardiac allograft rejection on the EB presented significant increased BNP values. These data suggest that BNP plasma levels could form the basis for a new, non-invasive screening test to predict acute cardiac allograft rejection.

PS_325

PREPARATION OF THE LIPOSOME ENCAPSULATED PLATINUM-[125I]IODOHISTAMINE COMPLEX. PRELIMINARY RADIOCHEMICAL AND BIOLOGICAL STUDY

P. Garnuszek, I. Liciñska, A.P. Mazurek. Drug Institute, Warsaw, Poland.

It has been demonstrated both in laboratory and in clinical trials that application of multifactorial cancer therapy, e.g. by combination of an ionising radiation and chemotherapeutic agents, enhance anticancer potency of the treatment. In a previous work we synthesised the platinum-[*I]iodohistamine complexes possessing cytostatic activity both in vitro and in vivo. The present work aims to study the potential use of liposomes for specific targeting of the radioactive platinum-iodohistamine complex.

Methods: Liposomes with positive surface charges were formed in the presence of stearylamine (18 mmoles), phosphatidylcholine (63 mmoles), and cholesterol (9 mmoles) (Sigma kit L4395). Encapsulations of the Pt-[^{125}I]iodohistamine (specific activity ca. 0.5 MBq/mmol of Pt) were studied using a different molar ratio of the complex and lipid, likewise various incubation procedures. The yield of the complex entrapment into liposomes was monitored by TLC and RP HPLC. The comparative biodistribution study in healthy Wistar rats was done after intravenous administration of the encapsulated and free Pt-[^{125}I]iodohistamine.

Results: The highest yield of the encapsulation (ca. 80%) was achieved after mixing the complex solution in DMSO with the freeze-dried liposomes in the molar ratio of the lipid to Pt 1.5:1, following by rehydration with saline and incubation for 1 hr at 50°C with shaking and occasional sonication. There were significant differences in the organ distribution between of the two preparations of the radioactive platinum complex (table 1). The concentration of the activity in blood after 2 hrs p.i.v. was two times lower for the encapsulated complex, and uptake of the radioactivity by liver, spleen, and lungs were more than twice that obtained with the free Pt-[^{125}I]iodohistamine preparation.

Table 1. Comparison of tissue uptake of the two preparations of platinum-[^{125}I]iodohistamine in rats (2 hrs p.i.v., %ID/g , mean and SD, N = 4)

Tissue	Pt-[^{125}I]IodoHistamine	Liposome-Pt-[^{125}I]IodoHistamine
Blood (1ml)	1.16 ± 0.14	0.54 ± 0.07
Heart	0.46 ± 0.09	0.41 ± 0.05
Thyroid gland	0.80 ± 0.40	0.21 ± 0.06
Lung	0.60 ± 0.02	1.82 ± 0.19
Liver	1.86 ± 0.27	4.42 ± 0.31
Spleen	1.00 ± 0.33	2.47 ± 0.44
Kidney	2.37 ± 0.37	1.33 ± 0.37
Stomach	2.03 ± 0.77	0.90 ± 0.26
Intestine	0.71 ± 0.03	0.52 ± 0.10

Conclusion: The results of present study indicate that platinum-[^{125}I]iodohistamine can be efficiently incorporated into cationic liposomes. However, evidently uptake of the encapsulated complex by the liver and spleen macrophages demands further modification of the lipid membrane. A variety of the existing protocols for coating of liposomes surface make possible an optimisation of the specific system for targeting of the platinum-radiopharmaceutical.

PS_326

PRECLINICAL COMPARISON OF FOUR YTTRIUM LABELLED SOMATOSTATIN RECEPTOR-SPECIFIC PEPTIDES AS CANDIDATES FOR CANCER TREATMENT

A. Laznickova (1), M. Laznicek (1), F. Trejtnar (1), H. Maecke (2), K. Eisenwiener (2), J. C. Reubi (3), S. Wenger (3). (1) Faculty of Pharmacy of the Charles University, Hradec Kralove, Czech Republic; (2) Nuclear Medicine Department, University Hospital, Basel, Switzerland; (3) Institute of Pathology, University of Bern, Switzerland.

Visualization of somatostatin receptor-positive tumours with the employment of In/111/-DTPA-octreotide indicates potential applications of octreotide analogues labelled with a suitable therapeutic radionuclide (such as Y-90) for cancer treatment. The purpose of the present study was to compare biodistribution characteristics and to analyze elimination mechanisms of two octreotide analogues, namely Y-DOTA-octreotide (Y-DOTA-OC) and Y-DOTA-Tyr/3/-octreotide (Y-DOTA-TOC), and two octreotate derivatives, namely Y-DOTAGA-Tyr/3/-octreotate (Y-DOTA-GATATE) and Y-DOTAtGA-Tyr/3/-octreotate (Y-DOTA-t-GATATE), in rats.

Methods: Radiolabelled peptides were prepared by adding an acidic yttrium/88/ chloride solution to the peptide in acetate buffer with gentisic acid. After incubation at 90-95¡C for 25 minutes, radiochemical purity was determined by gradient RP-HPLC analysis. Y/88/ isotope instead Y/90/ was used as a label because of its more suitable physical characteristics for preclinical experiments. For biological experiments, male Wistar rats were used. For the analysis of elimination mechanisms, the perfused rat liver and the perfused rat kidney were employed.

Results: Radiochemical purity of the peptides under study was higher than 98%. Biodistribution studies showed a similar radioactivity-time decrease in the blood and most organs in interdrug comparison. Binding to plasma proteins and blood cell accumulation were negligible for all agents. Radioactivity concentrations in organs with a high density of somatostatin receptors (the adrenals and pancreas) increased in the order Y-DOTA-OC < Y-DOTA-TOC < Y-DOTA-t-GATATE < Y-DOTA-GATATE and radioactivity excretion by faeces also increased in the same order. The main elimination pathway was urine excretion of radioactivity in all peptides. Perfusion experiments confirmed that the peptides were eliminated in the kidney mostly by glomerular filtration. Bile clearance in the perfused rat liver was very low for all agents. The main obstacle for therapeutic applications of radiolabelled peptides under study was high and long-term radioactivity uptake in the kidney.

Conclusions: Radiolabelled peptides under study represent new drugs targeted for the radiotherapeutic treatment of somatostatin receptor-expressing tumors. The most promising candidate in this field is probably Y-DOTA-GATATE.

The study was partly supported by the Grant Agency of Charles University - Grant No. 264/2001, and partly by the Czech Ministry of Education – Project No. J13/98:11600002

PS_327

TC(99M)-EDDA/HYNIC-TYR(3)-OCTREOTIDE: PHARMACOKINETICS IN RATS AND COMPARISON WITH IN(111)-DTPA-OCTREOTIDE

M. Laznicek (1), A. Laznickova (1), C. Decristoforo (2), S. J. Mather (3). (1) Faculty of Pharmacy, Charles University, Hradec Kralove, Czech Republic; (2) Nuclear Medicine Department, University Hospital Innsbruck, Austria; (3) Nuclear Medicine Research Laboratory, St. Bartholomews Hospital, London, UK.

For the detection of somatostatin receptor positive tumours, Tc(99m)-labelled HYNIC-Tyr(3)-octreotide (HYNIC-TOC) using ethylene diamine diacetic acid (EDDA) as the co-ligand appears to be a promising agent to replace currently used octreotide derivatives labelled with In(111). The aim of this study was to determine biodistribution and elimination characteristics of the agent in rats in comparison with that of In(111)-DTPA-octreotide (DTPA-OC).

Methods: Tc(99m)-EDDA/HYNIC-TOC was prepared by a kit procedure with high specific activity and purified with the use of a SepPak mini cartridge. Radiochemical purity of the labelled peptide, determined by HPLC, was greater than 98%. Male Wistar rats were used for biological experiments. Distribution in 22 selected organs and tissues was determined 5 min, 1 hr, 2 hrs, 24 hrs, and 48 hrs after administration of the peptides.

Results: Distribution profiles of radiolabelled peptides under study in rats were very similar. Both agents exhibited rapid clearance from the blood and most organs, and the activity was eliminated mostly by urine. The fraction bound to plasma proteins was 0.15 for In(111)-DTPA-OC and 0.36 for Tc(99m)-HYNIC-TOC. High (but comparable) and long-term kidney uptake of radioactivity in both peptides was determined. On the other hand, radioactivity concentrations in somatostatin receptor-rich organs (the pancreas and adrenals) were significantly higher after Tc(99m)-HYNIC-TOC when compared with In(111)-DTPA-OC. Radioactivity elimination into urine was somewhat slower and radioactivity excretion by faeces was higher (more than twice) after Tc(99m)-HYNIC-TOC in comparison with In(111)-DTPA-OC. Bile clearance of both agents, determined in the perfused rat liver, was very low and comparable.

Conclusions: The results indicate similar pharmacokinetics of Tc(99m)-HYNIC-TOC and In(111)-DTPA-OC in rats and confirm that Tc(99m)-HYNIC-TOC seems to be an excellent candidate for visualization of somatostatin receptor-positive tumours.

The study was partly supported by the Grant Agency of Charles University - Grant No. 34/99/C, and partly by the Czech Ministry of Education – Project No. J13/98:11600002

PS_328

NEW PEPTIDE CONJUGATES AS LIGAND FOR CHOLECYSTOKININ RECEPTOR LABELLED WITH RHENIUM

C. Pedone (1), G. Morelli (1), S. De Luca (1), A. Dolmella (2), U. Mazzi (2), M. Saviano (1), D. Tesauro (1), R. Visentin (2). (1) Centro Interuniversitario di Ricerca sui Peptidi Bioattivi, Università degli Studi di Napoli ; (2) Dipartimento di Scienze farmaceutiche, Università di Padova, Padova, Italy.

Several human tumors overexpress receptor of cholecystokinin (CCK). For these reason in the last years in nuclear medicine the interest to use as scaffold CCK_8 is increased. *Aim* Based on the structural NMR characterization of the interaction between the type A cholecystokinin receptor and CCK_8 ligand we synthetized a new peptide conjugate covalently bond to a new chelating system to bind Rhenium and Technetium (CCK10PRe). We have also tried to assess at the MM and QM level: (*i*) if the modified ligand CCK10PRe is a stable structure compared to CCK8; (*ii*) the details of the interaction between CCK_A-R and CCK10PRe. *Methods:* CCK-8 was synthesized according to standard solid-phase schemes. This compound was covalently coupled to the ligand by adding a Cys protected, a Gly and the phosphine $PPh_2(CH_2)_2COOH$, to the NH_2 free terminus of the peptide anchored to the solid support; acid treatment allows peptide cleavage from the resin and deprotection of amino acid side chains. The conjugate was coupled to metal treating in acetonitrile with $ReOCl_3(PPh_3)_2$. The identification were performed using spectroscopic methods. The modeling of the $PPh_2(CH_2)_2$-CO-Gly-Cys- modified dipeptide has been made using the molecular templates available in the PC Spartan Pro software. The most obvious distortions of the resulting arrangement have been removed by running a MM (molecular mechanics) minimization; a full geometry optimization has then been performed at the QM (semiempirical quantum mechanics) level, and the fragment has been stored for further calculations. MM calculations have been performed with the MMFF94 force field; QM work has been made at the PM3-RHF level. *Results:* The IR , UV spectrum and mass analysis confirm the coordination of the metal centre The theoretical studies highlight two different effects which follow the modification of the CCK8 peptide: the MM work suggests that the elongation of the peptide chain enhances the internal strain, while QM data indicate that the stabilizing charge interactions lower the energy of the system. In addition, the modified ligand substantially preserves the most important binding interactions, especially those involving Tyr^{27}-Met^{28} and W39-Q40. *Conclusion:* CCK-8-PN_2S appears to be a good candidate to label with Rename complex and potentially technetium also. The MM and QM calculations suggest that the modified ligand CCK10PRe is a stable molecule and that the interaction of CCK10PRe with the receptor is substantially similar to the one made by the natural substrate CCK8.

PS_329

LABELING METHOD STUDY AND BIO-ACTIVITY EVALUATION ON RE-188-ANTI BLADDER CANCER MONOCLONAL ANTIBODY BDI-1

R.F. Wang, C.L. Zhang, L.Z. Yu, Y. Bai, Y.F. Guo. Department of Nuclear Medicine,Peking University First Hospital, Beijing, China.

Aim: To prepare Re-188-BDI-1 suitable for radioimmunotherapy (RIT) of bladder cancer, and investigate the optional labeling method and bio-activity of Re-188-BDI-1.

Methods: BDI-1- an anti-bladder cancer antibody provided by Peking University Immunology Department was reduced by 2-mercaptoethanol Two labeling methods including ligand exchanging and direct labeling method were used to prepare Re-188-BDI-1. The influence of pH, reaction time and $SnCl_2$ concentration on the labeling yield was studied. Biodistribution and radioimmunoimaging were performed in nude mice bearing human bladder carcinoma at different time points following injection of 629 KBq and 111.1 MBq of Re-188-BDI-1, respectively. The ratio of tumor to background (T/B) was calculated.

Results: The optium labeling condition was at pH 4.4 ~ 5.0, reaction time 2 h for ligand exchanging method and $SnCl_2$ concentration of 4.17 ~ 8.33 mg/ml, pH 4.4 ~ 5.0, reaction time 1 h for direct labeling method and the maximum labeling yields were 31.2 % and 90.8 % respectively. The Re-188-BDI-1 obtained from two labeling methods showed high T/B ratio of greater than 2.0 %ID/g 24 h postinjection, and the T/B ratio of Re-188-BDI-1 from ligand exchanging (tumor/muscle 16.9%ID/g) showed higher than that of Re-188-BDI-1 from direct labeling method (tumor/muscle 5.52%ID/g). Both of them had excellent tumor locating property on scintigram.

Conclusion: Re-188-BDI-1 with good bioactivity could be obtained by both ligand exchanging and direct labeling method. Direct labeling method could obtain high labeling yield of Re-188-BDI-1, and was easy to perform and more available.

PS_330

LABELING OF THE ANTI-MELANOMA 14F7 MONOCLONAL ANTIBODY WITH RHENIUM-188 USING A PRE-LABELED MAG3 CHELATE: OPTIMISATION, IN VITRO, AND IN VIVO ANALYSIS

J.L. Crudo, M.M. Edreira, E.R. Obenaus, S.G. de Castiglia. División Radiofàrmacos, Comisión Nacional de Energia Atómica, Buenos Aires, Argentina.

The aim of the present study was to optimise the procedure for labeling the anti-melanoma 14f7 monoclonal antibody (MoAb 14f7) with 188 Re, using an active ester of S-benzoyl-mercaptoacetyltriglycine (S-benzoyl-MAG_3). Quality assurance tests were performed during the entire labelling procedure and on the final radiolabeled antibody. Stability studies in saline and human serum were also performed and the biodistribution of the labelled antibody was evaluated in C57 mice with a solid tumour.

Methods: This was a preconjugate approach with 3 steps. 1st step: labeling of S-benzoyl-MAG_3 with a fresh elution of a $^{188}W/^{188}Re$ generator (^{188}W $T_{1/2}$=69.4/^{188}Re $T_{1/2}$=17) in saline (370 MBq approximately). 2nd step: esterification of the S-benzoyl-MAG_3-^{188}Re with 2,3,5,6-tetrafluorophenol (TFP) in order to obtain ^{188}Re-MAG_3-TFP active ester. 3rd step: conjugation of the active ester with amines of monoclonal or polyclonal antibodies maintaining its biological activity. The labeled conjugated protein was purified and controlled by HPLC using a Protein Pack SW300 (Waters) column and the eluent was phosphate buffer at 1ml/min.

Results: Yields of more than 95% were obtained when the ratio of $SnCl_2.2H_2O$ to 188 Re activity was higher than 3.13μg/MBq and nearly quantitative yields were obtained when the ratio of S-benzoyl-MAG_3 to 188 Re activity exceeded 0.81μg/MBq. This was a solid phase reduction of perrhenate by the stannous ion, with citrate used as transfer ligand. The maximum labeling efficiency (46.9%) was obtained when the molar ratio of ester to protein was 333:1, in which case the specific activity of labelling was 90.3 MBq/mg antibody.

In vitro stability assays showed that 80.0% and 70.3% of the activity remained bound to MoAb14f7-MAG_3 after incubation in saline and serum at room temperature respectively.

Uptake of the antibody in the tumour amounted to 8.80±1.51and 7.23±1.30 %ID with a tumour-to-blood ratio of 0.55 and 0.68 for 24 and 48 hs respectively.

Conclusions: The indirect method of labeling antibodies using a 188Re-labeled via the active ester MAG_3 produced a 188 Re-MAG_3-MoAb 14f7 complex of high specific activity and in vitro stability, and significant uptake by the tumour.

PS_331

FIBRIN BINDING PEPTIDES FOR DETECTION OF PULMONARY EMBOLISM

M. Rusckowski (1), G. Liu (1), C. Wescott (2), A. Sato (2), N. Liu (1), S. Gupta (1), D.J. Hnatowich (1). (1) Department of Radiology, University of Massachusetts Medical School, Worcester, MA, USA; (2) Dyax Corp., Cambridge, MA, USA.

By phage display, low molecular weight peptides have been identified which show high specificity for human fibrin.

Aim: The intent of this study was to investigate the in vitro and in vivo properties of two dodecapeptides selected for high binding affinity to human fibrin for their potential as pulmonary embolism imaging agents.

Methods: The peptides, DX-180 and DX-328 (MW~2kDa), were synthesized with HYNIC on the N-terminus via a hexanoic spacer for Tc-99m labeling. The peptides were labeled using either tricine or EDDA as coligand.

Results: By SE-HPLC of serum (37°C) incubates, the radiochromatographic profile was virtually unchanged at 3hr using EDDA, whereas with tricine as coligand, about 50% of the activity was on serum proteins. This difference in serum binding influenced the biodistribution results in normal mice. At each time point, differences in organ activity levels among the peptide/coligand complexes were evident. With tricine, both peptides showed higher organ and blood activity. For DX-180, total organ activity at 3 hrs was 45% with tricine vs. 10% with EDDA while for DX-328, these values were 33% vs 6% respectively. Liver, kidney and blood accounted for the major differences. Of the four peptide/coligands investigated, DX-328/EDDA showed the highest excretion and lowest whole body activity. Using a rabbit model consisting of a human fibrin clot in one femoral artery retained by an embolization coil, all four peptide/coligand complexes were investigated along with AcuTect as a control. Animals were imaged for 2 hrs and then sacrificed for dissection. As in the mouse, DX-328 with EDDA showed the lowest levels of activity in tissues. For example, liver was 4.6-fold lower than with tricine, and 2.6-fold lower than AcuTect. The excised clotted artery to normal artery radioactivity ratio with DX-328/EDDA was 6:1 vs. 2:1 for AcuTect.

Conclusion: These data, showing low background and high target to non-target ratios, suggest that peptides can be selected by phage display as potential detection agents for pulmonary embolism.

PS_332

CLINICAL APPLICATIONS OF ANTI-TSH RECEPTOR AND ANTI-THYROPEROXIDASE ANTIBODIES RADIOMETRIC ASSAYS IN GRAVES' DISEASE

L. Giovanella, L. Ceriani, S. Garancini. University Hospital, Varese, Italy.

The detection of autoantibodies to the TSH-receptor (TRAb) and anti-thyroperoxidase (AbTPO) are largely requested in clinical practice for the diagnostic work-up of Graves' disease.

Aim: Aim of our work was the comparative evaluation of the diagnostic performance of TRAb and AbTPO in diagnosis of Graves' disease.

Method: We evaluated the diagnostic performance of a newly developed 2nd generation TRAb assay (DYNOtest TRAb human™, BRAHMS GmbH, Germany), a 1st generation TRAb assay (TRAK assay™, BRAHMS GmbH, Germany) and an AbTPO assay (DYNOtest AbTPOn™, BRAHMS GmbH, Germany) in 124 patients affected by Graves' disease, 156 patients affected by Hashimoto's thyroiditis and 188 patients affected by euthyroid nodular goiter.

Results: The 2nd generation TRAb assay showed a better diagnostic sensitivity in Graves' disease (97%) respect the 1st generation assay (85%) and AbTPO assay (64%). The AbTPO assay was positive in 94% patients affected by autoimmune thyroiditis while the 1st and 2nd generation TRAb assays were positive in 7% and 13% of patients affected by autoimmune thyroiditis, respectively. No patients affected by nodular goiter showed positive 1st and 2nd generation TRAb assay (specificity 100%) while AbTPO levels were positive in 9% of patients (specificity 91%).

Conclusions: TRAb assay by 1st and 2nd generation methods is clearly more sensitive and specific than AbTPO assay in diagnosis of Graves' disease. Consequently, AbTPO assay should be not performed, never alone or in association with TRAb, in Graves' disease diagnostic work-up. Finally, the 2nd generation TRAb assay is clearly more sensitive than the 1st generation test and should be used in clinical practice to minimize the incidence of TRAb-negative Graves' disease.

PS_333

RADIOCHEMICAL CHARACTERISTICS AND BIOLOGICAL TESTING OF TECHNETIUM-99M LABELLED ANTIMICROBIAL CATIONIC PEPTIDES FOR INFECTION DETECTION

S. Mongera (1), M.M. Welling (1), A. Lupetti (2), P.H. Nibbering (2), U. Mazzi (3), E.K.J. Pauwels (1). (1) Department of Nuclear Medicine, Leiden University Medical Center, Leiden, The Netherlands; (2) Department of Infectious Diseases, Leiden University Medical Center, The Netherlands; (3) Department of Pharmaceutical Sciences, University of Padua, Italy.

Recently we introduced ^{99m}Tc labelled synthetic cationic antimicrobial peptides, i.e. ubiquicidine (UBI) and human lactoferrin (hLF) derivatives, for the detection of infections in mice and rabbits. Specific tagging of bacterial surfaces with these peptides allowed us to discriminate between infections and sterile inflammatory processes. The labelling mechanism of this direct method has been the subject of an interinstitutional study, revealing that reduction of ^{99m}Tc pertechnetate is accomplished by stannous ion, whereas borohydrate maintains the ^{99m}Tc in the reduced oxidation state.

We report on our experiments regarding radiochemical analysis and stability testing of the peptides using ITLC and HPLC techniques, as well as on the *in vivo* scintigraphic imaging and *ex vivo* analysis of activity distribution in mice injected with these radiolabelled peptides. A scrambled peptide containing the same amino acids as one of the antimicrobial peptides (UBI 29-41), but in a different sequence, was used as a control agent for these studies.

Using ITLC and HPLC we assessed high yields of labelling (>95%) already 10 min after initiation of the labelling reaction. Until 24 h after starting the labelling the complex maintained stable under various challenging circumstances. Also, we studied the in vivo characteristics of the labelled peptides in healthy mice and observed fast clearance via kidneys and bladder as determined by scintigraphy and *ex-vivo* countings. Besides, we observed a good correlation ($r>0.844$, $p<0.01$, $n=5$) between these two methods of analysis until 1 hr post injection. Unless the radioactivity was not accumulating in liver and intestines both methods of measure the biodistribution remained in concordance.

In conclusion, direct labelling of synthetic antimicrobial peptides with ^{99m}Tc is a highly efficient and reliable method to study these agents for scintigraphic detection infection.

PS_334

CHROMOGRANIN-A AND NEURON-SPECIFIC ENOLASE IMMUNORADIOMETRIC ASSAY IN DIAGNOSIS AND FOLLOW-UP OF NEUROENDOCRINE TUMOURS

L. Giovanella, L. Ceriani, S. Garancini. Department of Nuclear Medicine, University Hospital, Varese, Italy.

Immunohistochemical detection of chromogranin-A (CgA) and neuron-specific enolase (NSE) is a very useful tool for diagnosis of neuroendocrine tumours (NET). Immunoradiometric assay (IRMA) methods to measure both serum NSE and CgA are available in clinical practice.

Aims: Aims of our work were: 1) to compare the sensitivity and specificity of serum CgA and NSE in NET patients and controls, 2) to investigate the relationship between serum markers and disease extension, 3) to compare serum expression of both markers with immunohistochemical findings and 4) to evaluate the role of both markers in the follow-up of the disease.

Methods: We enrolled 124 patients affected by NET: all diagnosis were histologically confirmed and serum samples were obtained before surgery or other therapies. Evaluation of tumor extension was performed using ^{111}In-pentetreotide scintigraphy and helical CT. Immunohistochemical stains were performed using avidin-biotin-complex and monoclonal antibodies against CgA and NSE. Serum CgA and NSE were measured by two-site IRMA methods (NSE Prolifigen™, Byk Sangtec, Sweden and CgA RIA CT™, Cis BioInternationale, France). A group of 142 healthy blood donors was evaluated as control. A sub-group of 55 patients with one or both markers elevated at diagnosis was followed-up by serial markers assay and imaging methods for 12-48 mounths.

Results: Basal CgA a nd NSE were elevated in 75 (60%) and 29 (33%) of the NET patients. CgA levels were significantly higher in NET patients than controls (U-test $p<0.0001$) and in limited versus extensive disease (U-test $p<0.01$). We found a significant overall positive correlation between serum and tissue CgA (linear regression R^2 0.896 $p<0.01$) while no differences were found in serum NSE levels. The use of markers and particularly of CgA in the follow-up showed a positive lead time of 5-23 mounths and can be employed to rule out unnecessary imaging tests or invasive procedures. The patients with basal elevation of NSE generally showed a more aggressive tumoural phenotype and a poor prognosis.

Conclusions: Serum CgA is a reliable marker of NET and reflects both tumour burden and CgA granular content in tumoural tissue. Serial evaluation of CgA is useful to predict the relapse of the disease and to avoid other procedures if marker is negative. Serum NSE should be employed to identify poorly differentiated tumours but is not accurate in diagnosis of NET.

PS_335

NEURON SPECIFIC ENOLASE (NSE), BETA-AMYLOID AND TAU PROTEINS AS MARKERS OF DEMENTIA

B. Palumbo (1), A. Bianchi (1), D. Siepi (1), V. Gallai (2), A. Lanari (2), S. Amici (2), S. Messina (1), I. Sabalich (1), L. Parnetti (2). (1) Dept. of Nuclear Medicine, University of Perugia; (2) Dept. of Neuroscience, University of Perugia, Italy.

Aim: The identification of biochemical markers able to contribute to the diagnostic accuracy of dementia disorders represents a relevant issue. Cerebrospinal (CSF) levels of beta-amyloid $_{(1-42)}$ protein (Abeta42), the main component of brain beta-amyloid plaques, appear significantly reduced in Alzheimer's disease (AD), while CSF concentration of the microtubule-associated protein tau, a constituent of neurofibrillary tangles, is increased. Neuron Specific Enolase (NSE) levels in CSF are increased in several neurological diseases and represent an index of organic neuronal damage; a NSE conformational epitope cross-reacts with a monoclonal antibody raised against beta/A4-protein of AD brain. We measured CSF concentration of NSE, Abeta42 and total tau in patients with different dementia disorders.

Methods: We studied 66 patients, 37 affected by probable AD according to NINCDS-ADRDA criteria, 9 by Age-Associated Memory Impairment (AAMI) according to Crook's criteria, 11 by Fronto-temporal dementia (FTD) according to Lund and Manchester criteria, 9 by vascular dementia (VaD) according to DMS-IV R criteria. NSE was also measured in 15 controls referred to Urology Department for minor surgical problems requiring spinal anaesthesia. NSE was measured by a solid phase two-site immunoradiometric assay (ELSA-NSE, CIS bio International-Schering), while Abeta42 and tau were dosed by ELISA assay (Innogenetics, Gent, B).

Results: NSE levels were significantly higher in AD (mean±SD: 23.14±7.9 ng/ml) vs controls (mean±SD: 7.8±2.4 ng/ml, $p<0.001$), FTD (mean±SD: 15.45±6.6 ng/ml, $P<0.05$) and VaD (mean±SD: 14.77±5.8 ng/ml, $p<0.05$); NSE was also significantly increased in AAMI (mean±SD: 21.38±8.8 ng/ml) vs controls ($p<0.001$). On the other hand Abeta42 was significantly lower in AD than in AAMI ($p<0.05$), while tau was significantly higher in AD than in FTD ($p<0.005$). NSE was significantly correlated with P-tau ($p=0.000$, $r^2=0.592$).

Conclusions: Our results show that CSF NSE, likely other well established biological markers, is altered in dementia, thus supporting the clinical accuracy of diagnosis. Finally it is worth of note that NSE is significantly increased not only in overt dementia but also in AAMI; this finding seems to support the hypothesis that AAMI might represent an early monosymptomatic phase of AD.

PS_336

BACHELOR OF MEDICAL LABORATORY TECHNOLOGY, THE NEW TITLE FOR TECHNOLOGIST IN DENMARK

L. Kragh, L. Larsen, J. Lohse. Department of Nuclearmedicine/physiology, Rigshospitalet, Copenhagen University Hospital, Denmark.

In Denmark there has been no special education for technologists who work in nuclear medicine.
In 1996 a new 3-years education for technologists started, including nuclear medicine (and clinical physiology). The first students graduated July 1999.
The structure of the training was classified in 7 modules.

U 1	: 1 month	Introduction in the Hospital
U 2 + 5 + 6	: 4 + 6 + 1 months	School periods 1 + 2 + 3
U 3 + 4 + 7	: 6 + 6 + 18 months	Laboratory period

(e.g. Clinical Chemistry, Clinical immunology, Nuclear medicine)

In the last period the students make a theoretical and practical 4-weeks project with essay and oral examination.

With the new education of technologists (in Danish „bioanalytiker") the theoretical and practical skills in nuclear medicine have been much improved.
From year 2001 the education has been changed to a more international system, with the introduction of European Credit Transfer System (210 ECTS points):
- The school period will be 2 years and give 135 ECTS points
- The Laboratory period will be 1_ years and give 75 ECTS points
- The students will be graduated as „Bachelors of Medical Laboratory Technology".

PS_337

EVALUATION OF BONE MINERAL DENSITY BETWEEN SPINE AND HIP IN DIFFERENT AGE POPULATION

K. Chun (1), M. Doonan (1), R. Goldfarb (2), K. Byun (2), L. Blunt (1), L. Freeman (1). (1) Montefiore Medical Center, Dept of Nuclear Medicine; (2) Beth Israel Medical Center, Dept of Radiology, Albert Einstein College of Medicine, New York, NY, USA.

Aim: To evaluate whether BMD measurement by T-score in the spine would correlate with the hip bone loss.
Methods: Using DEXA (Hologic 4500C) in the spine and the hip, which were obtained in the same day, we compared BMD test results of 1049 women. 985 females were mostly peri/postmenopausal (45-92 y.o.) and 64 females (<44 y.o.) were mainly with endocrine disorders, including secondary amenorrhea or long-term steroid treatment. Data were classified according to the WHO criteria (T-score). A-P lumbar spine included L1-L4 vertebrae. Total hip BMD data was used instead of other hip region data for greater precision and higher reproducibility. 577 cases were 45-64 y.o., 251 cases were 65-74 y.o., and 157 cases were above 75 y.o.
Results: In this studied population, 64 women (<44 y.o) showed spine BMD worse or equal to hip BMD in 62 cases. In 577 females (45-64 y.o.), 554/577 (96%) cases had the spine T-scores worse (320/577) or equal (243/577) to hip T-scores. Of 190/577 with N-hip, 149/190 had E-spine, 37/190 had O-spine. 134/577 had E-hip but O-spine. (N-normal, E-osteopenia, O-osteoporosis). Older patients (>65 y.o.) trended to have worse hip T-scores than spine T-scores (6% in 65-74 y.o., 21% in 75-84 y.o., 50% in >85 y.o.). Degenerative changes with osteophytes and/or collapsed vertebra may have been the influencing factors.

Age (yrs)	Osteopenic spine	Osteoporotic spine	Decreased S/H ratio*	S = H**	Increased S/H ratio***	# of pts
< 44	33	17	37 (58%)	25 (39%)	2 (3%)	64
45-64	241	194	320 (56%)	243 (42%)	14 (2%)	577
65-74	94	109	125 (50%)	110 (44%)	16 (6%)	251
75+	51	49	33 (21%)	87 (55%)	37 (24%)	157

*↓S/H ratio: spine BMD score worse than hip (E-spine/N-hip, O-spine/N-hip, O-spine/E-hip)
**S=H: congruent spine and hip BMD scores (N-spine/N-hip, E-spine/E-hip, O-spine/O-hip)
***↑S/H ratio: spine BMD score better than hip (N-spine/E-hip, N-spine/O-hip, E-spine/O-hip)
Conclusions: 96% of the patients (<65 y.o.) showed greater (56%) or equal (40%) bone mineral loss in the spine compared to the hip. The findings could be related to earlier bone mineral loss in the metabolically active spine (predominantly trabecular bone) than hip (predominantly cortical bone). The spine BMD information in this relatively younger age group (<65 y.o.) can predict possibly less severe disease in the hip, potentially guiding prophylactic therapy for prevention of serious and costly hip fracture, while hip BMD measurement alone may underestimate the severity of spine BMD loss.

PS_338

FOUR IMPORTANT TERMS OF RADIATION PROTECTION: DOSE, DISTANCE, DURATION, SHIELD

T. Arnold (1), E. Mörl (2). (1) Nuclear Medicine, Radiologische Gemeinschaftspraxis Drs. Bader/Correll/Heim/Thiel, Göppingen, Germany; (2) Nuclear Medicine, Radiologische Praxis Dr. Klimeck, Ludwigsburg, Germany.

The harmonizing of the radiation protection in Europe makes it necessary to think about the possibilities of how to minimize radiation exposure.
On the one hand there are new tasks for the staff in Nuclear Medicine, for example to the quality controll measures, whereas on the other hand you have to realise the new limit values for staff.
To reduce the radiation to a minimum, itws necessary to know these four terms of radiation protection.
Let's take a closer look:
Dose: The Euratom-Guideline from June 1997 fixed under the catchword „optimisation" that there must be reference-values for examinations with radiation. These are not only dose-values, but also in case of radionuclide activity-values. In the case of children-examinations there exist recommendations of the Paediatric Task Group of the EANM.
Distance: the rule of the half dose as the square of the distance is one of the most important rules to limit radiation exposure. Several studies in diagnostical Nuclear Medicine came to the conclusion, that the radiation exposure can be limited to a dose which is far below the dose set by the radiation protection regulations.
Duration of stay: It is noticable, that the individual studies bring varied radiation doses for the technologists. This is not only a problem of the administered dose, but also of indigent patients. If a patient required continual assistance, the radiation exposure would be higher, of course.
Shield: leaded hot cells, shielded containers for transport and storage of syringes, mobile leaded shield
These criteria should be respected in all categories of Nuclear Medicine, in quality assurance and especially in the daily work with patients.

PS_339

ONE-YEAR EXPERIENCE ON THE UTILIZATION OF FDG PROVIDED BY EXTERNAL RADIOPHARMACY

M. Schiavini, R. Casati, A. Bruno, M. Castellani, R. Leo, A. Cascio, P. Cau, G. Maiocchi, F.R. Colombo, P. Gerundini. Department of Nuclear Medicine, Ospedale Maggiore-IRCCS, Milano, Italy.

At our department the installation of a PET camera has been accomplished in large advance compare to the Cyclotron and related Radiopharmacy. Infact there was the need to use the PET camera without an internal production of FDG; it was verified that Switzerland was the only country in 1988 from where FDG could be imported (following the procedure indicated by the law of 11 February 1997). After obtaining the authorization from the Italian authorities, a one-year experience of 152 shipments from Zurich to Milan has been carried out (4-5 hours transport time). This allowed 850 patient examinations
The delivery has been done on the scheduled time 42% times, with a delay lower than 90 minutes 32% times, with a delay higher than 120 minutes 22% times and 2% times before the scheduled time. The arrived activity was 46% times on the range of ± 10%, 39% times lower and 15% times greater than the ordered one. Concerning the management of patient examinations: in 55% times the schedule has been in agreement, 28% times the number of examinations was less than schedule and 17% times one additional examination has been performed. The average of the cost per shipment (FDG + transport) was about 5000 Euro. In conclusion, this experience demonstrated that the clinical use of a PET scan in a center not equipped with a cyclotron could be possible by supplying the FDG within 3-4hr delivering. However a less restrictive law that allows delivery from Italian producers to an Italian users is needed for reducing the drawbacks due to the long route and the costs of transportation.

PS_340

OPERATOR DEPENDENT VARIABILITY IN LVEF MEASUREMENTS FROM GATED SPECT

L. Åkesson. Dept. of Clinical Physiology, Lund University, Lund, Sweden.

Aim. Left ventricular ejection fraction (LVEF) can be assessed using gated myocardial perfusion SPECT imaging. The processing from raw images to the final LVEF calculations is to a great extent an automated process, but a few manual steps remain. The aim of this study was to evaluate the variability in LVEF measurements for different experienced operators.

Methods. Thirteen patients who underwent a gated SPECT using ^{99m} Tetrofosmin were selected. The material included three patients with normal perfusion, five with large fixed apical defects and five with reversible defects in the apical area.
Eight experienced medical laboratory technologists (MLT) processed the post stress studies, starting from the raw projection data, creating short axis slices and finally using the Cedars Sinai quantitavive gated SPECT (QGS) program for calculation of LVEF. The studies were presented in a random order without any clinical information of the patients. The QGS program uses as input the short axis slices. For creation of short axis slices the operator has to define two alignment axes parallel to the long axis of left ventricle (in the transaxial- and obique plane).

Results. The LVEF measurements ranged from 8.9% to 66.1% (normal patients 59.3%- 66.1 %, fixed apical defects 8.9–40.4 %, and reversible apical defects 41.6%-66.0%).
Eight different LVEF measurements (one for each operator) were obtained for each patient. In three of five patients with a fixed apical defect the differences in LVEF between the operators were 4%. In two of five patients with a reversible apical defect the differences in LVEF between the operators were 3%. For the remaining patients the differences were 2% or less.
For each patient the eight operators defined two alignment axes. In 6 of the 13 patients the variability for one of the two axes was at least 10 degrees.

Conclusions. The reproducibility of the calculated LVEF between different operators was very high, even in patients with low LVEF%. The variability in definition of alignment axes between the observers did not have a major impact on LVEF.

PS_341

THE PRACTICAL USE OF AN IMAGING PROBE IN NUCLEAR MEDICNE

N.M. Bruin (1), A. Van Lingen (1), E. Baumann (2), P.G.H.M. Raijmakers (1), T. Ijbema (3), G.J.J. Teule (1). (1) Department of Nuclear Medicine, Free University Medical Center, Amsterdam, The Netherlands; (2) Eurorad, CIT, Strassbourg, France; (3) PI-Medical Diagnostic Equipment Bv, Joure, the Netherlands.

Aim:We investigated the physical and clinical use of a prototype device consisting of a 16x16 array of CdTe elements (2.83x2.82x2.0 mm) with an effective field of view (FOV) of 49x49 mm and a tungsten collimator (15 mm thick, 7.7 mm^2 holes and 0.3 mm septa), weighing 1995 gram. Since this device was a prototype, proper certification and technical refinements were not undertaken until the significance of the performance is clarified.
Methods: The detector unit was interfaced to an electronic read-out for 256 channels and coupled to a PC through a serial line. At this moment simple on-line imaging software shows the acquired data in colour, both the persistence and the accumulated image. Persistence rate can be set from 0.5 to 20 sec. Currently a display matrix of 16x16 pixels is used. The energy window can be selected between 30 and 200 keV. Extensions (larger matrix size, smoothing and interpolation software) are under development. The image data is stored on disk as ASCII text files and can be analysed with any software available. We used Matlab 5.3 (SE) for the image analysis, to evaluate the physics tests and for image processing.
The prototype was applied to image sentinel nodes (SN's) of 18 breast cancer patients. As a reference, gamma camera images were obtained for initial localisation. The area around the SN was then examined with the imaging probe. Furthermore, in 8 (of these 18) patients we evaluated the optimum imaging time (2, 5, 10, and 60 sec).
Results: The system was physically characterised by a spectral resolution of 6% FWHM per pixel (12% FWHM, if averaged over 256 pixel spectra) at 120 keV, 10% image uniformity (with correction), a spatial resolution of 6 mm (FWHM) on the collimator face and a counting sensitivity for 99mTc of 833 cps/MBq (30-200 keV) and 318 cps/MBq (100-200 keV).
In 17 of 18 patients a SN was found with the imaging probe. In addition, 10 sec of acquisition time proved sufficient.
Conclusions: The physical performance is suitable for imaging sentinel nodes. Our experience so far was that the device still needs further technical developments, such a more on-line image processing. The largest impact may be in the operating theatre to confirm complete removal of the (multiple) nodes. Although the FOV is sufficient for SN imaging, for other applications it may be enlarged.

PS_342

THE EFFECT OF EXREMELY LOW FREQUENCY ELECTRO-MAGNETIC FIELD (ELF) ON ROTAT_NG GAMMA CAMERA

M. Demir (1), A. Sabbir (1), T. Kalkan (2), H. Sayman (1), I. Uslu (1). (1) Department of Nuclear Medicine; (2) Department of Biophysics , Cerrahpasha Medical Faculty, University of Istanbul, Turkey.

One of the physical factors affecting SPET's images is the extremely low frequency electromagnetic fields (ELF) radiated from electrical devices.

Aim: The object of this study is to investigate the effects of extremely low frequency (50 Hz) electromagnetic fields on rotating gamma cameras.

Method: In these experiments a Siemens Orbiter 7500 digitract gamma camera system and LEAP collimator were used. To create ELF we connected 8 serially combined solenoids to the mains supply (220 V, 50 Hz) with 4 ampers current flowing through them. The solenoids were moved along the vertical plane below the face and 30^0, 45^0, 60^0 laterally of the detector to change the ELF intensity. Magnetic flux density of the created ELF was found to be between 0.05 mT and 1.2 mT at the center of the detector. For measuring the magnetic flux density of ELF, teslameter was used.

Results: We optained the countrates of ELF, applied to the center of the detector, in the 50-80 keV energy scale. We found that ELF had exponentially decreased the count rates of a ^{99m}Tc point source. There was a complete loss of the counts as well as the individual photopeaks under the influence of the magnetic field. Homogenity and spatial resolution tests were taken under costant ELF (~1.2 mT) and at the same time the homogenity and resolutions were distorted.

Results: According to our observations in these experiments magnetic fields higher than 0.4 mT cause serious defect in the field of view.

PS_343

PARTIAL RIB DISSECTION BY USE OF SURGICAL PROBE

C. de Haan (1), T. van Mesdag (2), G.M.M. Gommans (1), R.O. Boer (1), A. van Dongen (1), J.W.D. de Waard (2). (1) Department of Nuclear Medicine; (2) Department of Surgery, Westfries Hospital, Hoorn, The Netherlands.

Partial rib dissection of a scintigraphical marked hot spot often failed due to the fact that the patient at the operating theatre is not positioned in the same way as marked during the scintigram.
The aim of this study was to investigate whether radioguided biopsy of a scintigraphical hot spot can improve the localisation during surgery.
Patients and methods: In eleven patients (5 male and 6 female) with previous anamnesis of carcinoma a scintigraphical solitaire hot spot in one rib was found. No other pathology in this group of patients was found. In a twelfth patient (female) without prior history of malignancy a solitaire hot spot was found in one rib. All twelve patients underwent surgical biopsy by using the probe.
Three hours before surgery all patients were injected with 500 MBq 99mTc HDP. Thirty minutes after injection a local scintigram was performed and the hot spot was marked on the skin. Three hours after injection just before the start of operating, above the hot spot, determination and adjusting of the probe settings took place. Using the radioguided probe, by minimal invasive surgical procedure all hot spots quickly were localised and removed or biopted.
Results: All 12 procedures were successful. In five patients a metastasis was found. In five patients rests of fracture were found and in two patients an osteoid osteoma was found. Using minimal invasive surgery by probe all procedures took place within 10-15 minutes.
Conclusion: Although our series of twelve patients is small, it seems to be a reliable and useful procedure for partial rib localisation, dissection or biopsy.
Advantage of this method is a quickly diagnosis with less morbidity, reduced OR time and short recovery.

Poster presentation

PS_344

CHAYOTTE EXTRACT EFFECT ON THE LABELING OF RED BLOOD CELLS AND PLASMA PROTEINS WITH TECHNETIUM-99M: IN VITRO AND IN VIVO STUDIES

M. Bernardo-Filho (1), G. Dire (1), E. Lima (1), D.M. Mattos (1), M.L. Gomes (1), M.V. Castro-Faria (2). (1) Department of Biofísica e Biometria; (2) Department of Biologia Celular e Genética, Instituto de Biologia Roberto Alcantara Gomes, Universidade do Estado do Rio de Janeiro, Rio de Janeiro, RJ, Brasil.

The biodistribution of the radiopharmaceuticals can be altered by therapeutic drugs as the labeling of red blood cells with technetium-99m (^{99m}Tc) has been influenced by patient medications or the labeling conditions or the presence of extracts of plants. Chayotte (*Sechium edule*) is used as food or as medication in popular medicine. AIM: We evaluated the influence of chayotte on the labeling of blood elements with ^{99m}Tc.
METHODS: In *in vitro* study, blood was incubated with chayotte macerated, (100% v/v). In *in vivo* study, the animals were treated with chayotte macerated, (100% v/v), as drinking water (15 days) and samples of blood were withdrawn. The blood samples were incubated with stannous chloride and with ^{99m}Tc. Plasma (P) and blood cells (BC) were isolated, also precipitated with trichloroacetic acid and soluble (SF) and insoluble fractions (IF) separated.
RESULTS: The fixation of the radioactivity on the blood elements isolated from samples of whole blood (from animals that have received normally water) which were treated with chayotte *in vitro* did not decrease ($p>0.05$) on the labeling of the blood elements. The distribution of the radioactivity on blood cells and in insoluble fractions of plasma and blood cells isolated from whole blood withdrawn from animals that have received chayotte (15 days), as drinking water decreased slightly ($p<0.05$) in RBC (from 98.16 ± 1.57 to 90.35 ± 5.04) and strongly in the insoluble fraction of the plasma proteins.(from 83.96 ± 4.28 to 53.26 ± 6.69). The presence of toxic compounds was tested and we did not find them in the preparations of chayotte used in our experiments.
CONCLUSION: The chemical agents present in the extracts obtained from *Sechium*, could, depending on the metabolization *in vivo* can induce the generation of active metabolites that could, (i) bind (chelating action) to stannous and pertechnetate ions and/or (ii) bind to the binding sites of ^{99m}Tc in plasma proteins. chayotte would be capable to generate reactive oxygen species (ROS), these could to oxidize the stannous to stannic ion. Then, this fact could explain the decrease on the labeling of red blood cells and plasma proteins with ^{99m}Tc in the presence of chayotte, when the referred drug is administered *in vivo*.

PS_345

IFOSFAMIDE EFFECT ON THE BIODISTRIBUTION OF THE RADIOPHARMACEUTICAL TECHNETIUM-99M-MDP IN MALE C57BL/6J MICE

M. Bernardo-Filho (1), R.O. Aguiar (2), J.K. Kwee (2), E.F. Paula (2), N.M. Fonseca (2). (1) Department of Biofísica e Biometria, Instituto de Biologia Roberto Alcantara Gomes, Universidade do Estado do Rio de Janeiro, Rio de Janeiro, RJ, Brasil ; (2) Serviço de Pesquisa Básica, Instituto Nacional de Câncer, Rio de Janeiro, RJ, Brasil.

The biodistribution of radiotracers used in diagnostic imaging can be grossly and recognizably altered by a wide variety of factors. The knowledge of such altered biodistribution is important in making diagnostic inferences from scans. Altered biologic behavior may also be due to interferences caused by pharmacodynamic effects of drugs. When, the altered behavior is desired, the alteration is used for diagnostic intervention or drug therapy monitoring. However, when, it is undesired, it may due to toxicity in the organs or direct reaction with the radiopharmaceuticals and it can lead to misdiagnosis. Ifosfamide, an analog of cyclophosphamide, also is activated in the liver and present some toxic effects (leukopenia, hemorrhagic cystitis, nephrotoxicity, central nervous system disturbances). Ifosfamide is a chemotherapeutic drug that is used in combination with other drugs for germ cell testicular cancer and is widely used to treat pediatric and adult sarcomas. AIM: As a drug can interfere in the biodistribution of the radiopharmaceuticals, we decided to investigate the effect of the ifosfamide in the biodistribution of 99mTc-MDP radiopharmaceuticals in mice. METHODS: Ifosfamide (150mg/kg) was administered by ocular plexus via into male isogenic C57Bl/6j mice (8-12 week-old) per day for three days. One hour after the last dose, 99mTc-MDP (7.4 MBq) was injected and after 0.5 hour the animals (n=15) were sacrificed. The organs were isolated, the radioactivity uptakes determined in a well counter and the percentages of radioactivity (% ATI) in the organs were calculated. The results were compared with the control group (n=15), without ifosfamide and statistical analysis were performed. RESULTS: The results have shown that the treatment with ifosfamide: (i) decreased significantly (t test, $p<0,05$) the uptake of the 99mTc-MDP in bone, (ii) increased the radioactivity in the whole blood (t test, $p<0,05$) and (iii) did not alter the uptake of the radiopharmaceutical in inguinal lymph node, prostate, pancreas, testis, seminal vesicle, bladder, kidney, stomach, small intestine, spleen, thymus, heart, lung, brain, and muscle. CONCUSION: In conclusion, the effects of ifosfamide in the uptake of the 99mTc-MDP in bone and in blood, could be due to specific toxic effects as already reported. Moreover, although our results were obtained with animals, we suggest to take care with the interpretation of the bone scan obtained from patients submitted to the treatment with ifosfamide.

PS_346

THE USEFULNESS OF PRONE LATERAL BREAST IMAGING IN THE SENTINEL NODE PROCEDURE

S. Baank (1), P.A. Doodeman (1), I.J. van den Heuvel (1), C.M. Bauhuis (1), B. Pool (1), P.J. Tanis (2), R.A. Valdés Olmos (1). (1) Department of Nuclear Medicine; (2) Department of Surgery, The Netherlands Cancer Institute, Amsterdam, The Netherlands.

AIM: The prone lateral breast technique also called hanging breast (HB)- technique, was originally developed for the scintimammography with ^{99m}Tc-sestamibi . We evaluated this technique in order to proof its usefulness in the sentinel node (SN)- procedure, especially for the detection of intramammary lymph nodes.
METHODS: We used an ADAC dual-head gamma camera. Following a 5-min anterior image performed 15 min after a single injection of ^{99m}Tc nanocolloid, the camera is put in lateral position and the usual mattress is replaced with the mattress for prone acquisition of a lateral 5-min image. Both anterior and lateral images, are performed with a ^{57}Co flat-source for simultaneous transmission imaging and repeated after 2 and 4 hours.
RESULTS: The evaluation concerned 400 patients (mean age 55y, range 27y-85y) with T_1-T_3 N_0 breast cancer referred to the nuclear medical department for a mammary SN lymphoscintigraphy between January 1997 and November 2000. Scintigraphy showed 29 patients (7,3%) with drainage to intramammary SNs (Fig. 1), in 28 of them accompanied by axillary and/or internal mammary drainage. At histopathology isolated intramammary SN metastases were found in 2 patients and in another 3 patients together with axillary SN metastases.
CONCLUSION: The HB-technique can provide information about the presence of intramammary lymph nodes which may be overlooked using the supine lateral breast imaging technique. The HB-technique can also be useful to detect SNs located close to the injection site if the tumour is in the upper outer quadrant of the breast.

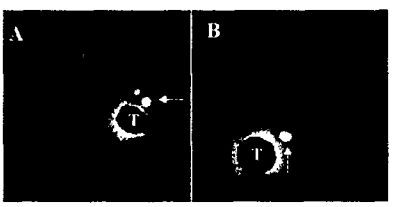

Fig. 1. A) Anterior image of a patient injected in the left breast (T) showing lymphatic drainage to SN (horizontal arrow) and second echelon lymph nodes in the left axilla. B) Prone left lateral image of the same patient showing the SN (vertical arrow) as an intramammary lymph node.

PS_347

EFFECT OF INTRA-GASTRIC POLYETHYLENE GLYCOL-ELECTROLYTE SOLUTION (GOLYTELY) ON GASTROINTESTINAL DISTRIBUTION OF 18FDG IN RATS

S.A. Barrow, M. Burker, C.D. McCusker, E.A. Carter, A.J. Fischman. Department of Nuclear Medicine, Massachusetts General Hospital, Boston MA, USA.

Aim: Interpretation of ^{18}FDG-PET studies of the abdomen is frequently complicated by accumulation of ^{18}FDG in normal gastrointestinal tract. Several anecdotal reports have suggested that bowel preparation with agents such as GoLYTELY™ may alleviate this problem. In this study we evaluated the effect of intra-gastric polyethylene glycol-electrolyte solution (GoLYTELY™) on gastrointestinal distribution of ^{18}FDG in rats.
Methods: After 2 hrs of fasting, GoLYTELY™ was administered intragastrically (60 ml/kg) to a group of 6 male Sprague-Dawley rats (~150 g). Six untreated animals served as controls. Both groups of rats were fasted over night with free access to water. On the following morning, each animal was injected i.v. with 0.5 mCi of ^{18}FDG-PET. One hr later, the animals were sacrificed and biodistribution was determined. Results were expressed as % injected dose/gram (%ID/g) and % injected dose/organ (%ID/o), mean ± SD.
Results: The animals in the treatment group demonstrated marked diarrhea. No other adverse effects were observed in either group of animals. As indicated in the table, the biodistribution study demonstrated remarkably similar levels of ^{18}FDG accumulation in both stomach and bowel (small plus large intestine). Similarly, GoLYTELY™ treatment did not affect tracer accumulation in any other tissues of the rat.

	Stomach (%ID/g)	Stomach (%ID/o)	Bowel (%ID/g)	Bowel (%ID/o)
Treatment	0.57±0.18	0.68±0.16	0.96±0.41	3.99±1.05
Control	0.56±0.05	0.66±0.10	0.81±0.09	4.58±0.42

Conclusion: These results clearly demonstrate that bowel treatment with GoLYTELY™ does not alter ^{18}FDG accumulation in the GI-tract of rats.

PS_348

FDG PET AND BONE MARROW SCINTIGRAPHY IN PRIMARY HYPEROXALURIA TYPE 1

C.T. Kadalie (1), M. Schreckenberger (1), O. Schreiner (2), E. Bayer (2), P.R. Galle (2), M. Otto (3), P. Bartenstein (1). (1) Department of Nuclear Medicine; (2) Department of Internal Medicine; (3) Department of Pathology,University, Mainz, Germany.

The case of a 29 year old woman with a history of renal failure at the end-stage renal disease is described. In the course of her illness she developed clinical signs consistent with a paraneoplastic syndrome.
A bone marrow scintigraphy with Technetium-99m labelled leucocytes (Tc-99m WBC) showed extensive homogeneous symmetrically distributed tracer uptake almost along the full length of the long bones of the limbs and a reduction of nuclid accumulation in the axial skeleton.
F-18-fluorodeoxyglucose (FDG) PET images showed no signs of a malignant tumor, but increased, symmetrically distributed FDG activity in the bony-chondral junction of the ribs. Either focally or diffusely increased tracer uptake was seen in the sternum, the scapulae and both the hip and sacroiliac joints.
Finally primary hyperoxaluria type 1 was diagnosed, a rare genetic disorder due to a reduced activity of the liver enzyme alanine/glyoxylate aminotransferase (AGT).
The systemic manifestation of the disease is called oxalosis. Affected patients may present in a clinical variable form. Since the only curative therapy is a combined liver-kidney transplantation, early diagnosis is important.
Nuclear medicine imaging modalities contributed towards reaching the diagnosis:
Tc-99m WBC findings indicated an underlying metabolic disease with bone marrow involvement. F-18-fluorodeoxyglucose (FDG) PET helped to rule out a malignant neoplasia as the cause of a potential paraneoplastic syndrome. Furthermore the differential diagnosis of the distribution pattern of FDG activity pointed towards the skeletal manifestation of a metabolic disorder. This report is one of the few published cases of primary hyperoxaluria type 1 with skeletal involvement documented by bone marrow scintigraphy and represents the first publication of a proven case of oxalosis in the field of PET.

PS_349

99MTC-MDP BONE SCINTIGRAPHY AND GLOBAL SKELETAL UPTAKE CORRELATION WITH MARKERS OF BONE METABOLISM IN ADVANCED PROSTATE CANCER PATIENTS

G. Rubini (1), A. Fontana (2), D. Rubini (1), A. Niccoli-Asabella (1), J. Bagnoli (1), N. Pansini (2), A. D'Addabbo (1). (1) Department of Nuclear Medicine, University of Bari, Italy; (2) I Department of Clinical Patology, University of Bari, Italy.

Aim: To correlate and integrate biphasic bone scintigraphy data with dosage of biochemical markers of bone metabolism (neoformation and riabsorption) in pts with advanced prostate cancer.
Material and Methods: 25 pts with prostate adenocarcinoma (Gleason degree >8), without metabolic bone disease, and free from therapy affecting bone metabolism and normal kidney function were enrolled. 99mTc-MDP biphasic whole body bone scintigraphy (BS) was used to detect the presence, site and number of bone metastases (BM) and to evaluate the radiopharmaceutical global skeletal up take at 4 hours after injection (4-h-GSU). In all pts, the serum dosage of Osteocalcin (OS) (n.v. 1-25 mg/l), as a marker of bone neoformation, bone isoenzyme of alkaline phosphatase (B-ALP) (n.v. 12-26 U/l) (ALKAPHASE - B; METRA BYOSISTEM) as a marker of bone neoformation and N-Telopeptide of type 1 collagen urinary escretion (n.v. 14-87 BCE/mM creat) (OSTEOMAK; OSTEX BOUTY) as a marker of bone riabsorption were performed.
4h-GSU evaluation was performed as follows: after i.v. injection of 99mTc-MDP (740 MBq), two whole body scans (anterior and posterior view), were performed after 30 sec and 4 hours. Comparison of counts in the whole skeleton region of interest at 4 hours with those of whole body in early scan gave the 4h-GSU as a percentage of injected dose.
Results: In 11 pts BM were detected by BS (group A), 12 BM in 1 pt, 10 BM in 1 pt, 7 BM in 2 pts, 5 BM in 2 pts, 3 BM in 3 pts and 2 BM in 3 pts, in another 14 pts BS resulted negative (group B). In group A the B-ALP dosage was more than normal range, while OS dosage was higher than group B but within normal range.
In group A OS, B-ALP, N-Tx and 4h-GSU resulted respectively 16,7±5,1; 99,9±59,6; 92,3±31,1; 45,8±3; in group B respectively 13,3±4,2; 26,2±10,1; 86,2±17,6; 32,9±4,3. In group A, a significant (p<0,01), higher value of B-ALP, OS and 4h-GSU (p>0,001) was found.
A good correlation between 4h-GSU and B-ALP (Speraman test p<0,01) was found.
Conclusions: In pts with osteolithic and osteosclerotic BM due to advanced prostate cancer markers of bone neoformation, B-ALP and OS, resulted significantly increased, and permit to distinguish pts with or without BM, give information about the grade of skeleton involvement but do not detect the number and sites of BM. The NTx serum dosage in pts with osteoblastic and osteolithic simultaneously BM can not be clinically useful.

PS_350

EVALUATION OF RECONSTRUCTION TECHNIQUES AND SCATTER CORRECTION IN BONE SPECT OF THE SPINE

S.Å. Starck (1), S. Carlsson (2), J. Ohlsson (3), M. Areskog (3), M. Fjälling (2), S. Sandström (4). (1) Department of Hospital Physics, County Hospital Ryhov, Jönköping, Sweden; (2) Department of Radiology, Uddevalla Hospital, Uddevalla, Sweden; (3) Department of Clinical Physiology, County Hospital Ryhov, Jönköping, Sweden; (4) Department of Radiology, County Hospital, Skövde, Sweden

A tomographic nuclear medicine examination can be reconstructed in several ways. Hitherto the most common technique involves two-dimensional pre-filtering of acquisition data followed by a reconstruction using filtered back-projection (FBP). Fast computers and efficient algorithms have made the iterative reconstruction technique (ITR) possible. Furthermore, attenuation and scatter correction can be applied as well as three-dimensional post-filtering of reconstructed data. The aim of this study was to compare the effect of filtered back-projection and iterative reconstruction technique, different types of filters and scatter correction on bone SPECT using the concept of visual grading.
Methods: Twenty-eight consecutive bone SPECT examinations were used in the study. The acquisition was made in 64 frames (360°), 20 s per frame and in 128x128 matrix using a single-head gamma camera with a high resolution collimator ($FWHM_{10cm}$=16.6 mm). Three energy windows were used in order to perform the scatter correction. Each study, with and without scatter correction, was reconstructed using FBP and ITR and 3D post-filtering. The filters used were Butterworth filters with a cut-off of 0.85-0.90/cm and Metz filters with filter factors 6-7. Each study was also reconstructed using the current technique in routine use in the department. This technique includes a 2D pre-filtering using a Metz-filter and FBP. These images were used as references.
A total of 224 images of coronal and sagittal slices were analysed by 5 experienced observers. Visualisation of vertebras, spinal canal and vertebral processes together with an overall impression of the image was ranked on a scale –2 to +2 (clearly worse to clearly better) compared to the reference image graded as zero.
Results: Combined mean scores for each technique averaged over all observers and the significance of the differences from the reference image.

itr, metz no tew	itr, but. no tew	fbp, metz no tew	itr, but. tew	itr, metz tew	fbp, but. no tew	fbp, metz prefilter	fbp, metz tew	fbp,but tew
0,638	0,369	0,342	0,246	0,093	0,012	0	-0,001	-0,125
p<0,01	p<0,01	p<0,01	p<0,01	n.s.	n.s		n.s	p<0,05

(0,638–0,369, p<0,01)
Conclusions: This study shows that scatter correction does not improve image quality due to the reduced number of counts and hence the increased noise. A contrast enhancing Metz filter together with iterative reconstruction is preferable to use in bone SPECT using a gamma camera of specified type.

PS_351

SENSITIVITY AND SPECIFICITY OF DEXA METHOD IN OSTEOPOROTIC VERTEBRAL FRACTURES

T. Erselcan (1), V. Nacitarhan (2), D. Doğan (1), O. Sumengen (3), S. Özdemir (1). (1) Departments of Nuclear Medicine,; (2) Physical Therapy and Rehabilitation; (3) Radiodiagnostics, Cumhuriyet Univ., School of Medicine, Sivas,Turkey.

The aim of the present study was to evaluate sensitivity and specificity of the fracture risk score (T) in DEXA method in osteoporotic vertebral fractures (wedge, biconcave or compression). 74 women (mean age±SD=54.9±10.8) were randomly included into the study from the out patient clinics, in whom anterior and lateral radiogram of the lumbar region by conventional radiology and bone mineral density measurement (L1-L4) by DEXA method (Hologic, 4500W, USA) were obtained. Three vertebral fracture index (wedge, biconcave or compression) were generated according to Eastell method by measuring anterior, posterior and middle heights in 294 vertebrae in lateral radiogram. Any of the fracture index < -3 SD in any vertebra was defined as fracture positive (37 vertebrae; 56 % wedge, 22 % biconcave and 22 % compression fractures). Increased fracture risk level in any vertebra was defined as T score < -2.5 SD in DEXA method. Results; sensitivity, specificity, positive and negative predictive values in the fracture risk estimation by DEXA method were 32%, 74%, 15% and 88%, respectively. On the other hand, if increased fracture risk level defined as T score < -1.5 SD then, above mentioned values were as follows; 57%, 47%, 13% and 88%, respectively. Meanwhile, DEXA was least sensitive to the biconcave type vertebral fractures.
In conclusion; Vertebral fracture risk assessement by T score < -2.5 seem to be an insensitive parametre. One of the reason would be the ready-to-use (foreign) reference values that we used in the study. But even so, lowering the T score by 60% did not helped to make the test much more sensitive. We believe that the 2 dimentional vertebral surface measurement, as commonly used in DEXA devices is not a suitable technique.

PS_352

BONE GEOMETRY, BIOMECHANICS AND MINERAL DENSITY ASSESSED BY PERIPHERAL QUANTITATIVE COMPUTED TOMOGRAPHY IN PATIENTS WITH PRIMARY HYPERPARATHYROIDISM SUBMITTED TO PARATHYROIDECTOMY

C. Di Leo (1), A. Bestetti (1), A. Bastagli (2), L. De Pasquale (2), L. Tagliabue (1), G.L. Tarolo (1), L. Pepe (3). (1) Department of Nuclear Medicine, University of Milan - HSPaolo - Italy; (2) Clinical Surgery Division, University of Milan - HSPaolo - Italy; (3) L'ACN-Laboratori Scientifici, Milan - Italy.

Aim: non-invasive measurement by peripheral quantitative computed tomography (pQCT) of bone geometry, biomechanics, and mineral content in patients (pts) with primary hyperparathyroidism (PHPT) enrolled to perform parathyroidectomy.
Materials and methods: total, trabecular and cortical mineral density (totBMD, cortBMD, trabBMD), bone geometrical properties (total area, trabecular area, cortical area, trabecular area/cortical area) and biomechanical parameters (cortical thickness and strength-strain index), were assessed by pQCT at distal radius, in 17 (14 F; 3 M) consecutive pts with PHPT (mean age: 59 yrs; range: 30-77) enrolled to perform parathyroidectomy.
Results: serum biochemical characteristics were: iPTH (407±317 pg/ml; range: 107-1438, normal: 30-65), Calcium (11,6±1,1 mg/dl; range: 10,6-13,5, normal: 8,1-10,4) and Alkaline Phosphatase (388±272 U/L; range:173-1174, normal: 98-279).
Surgery and histology revealed fifteen solitary adenomas; the weight varied from 0,64 to 71 g (mean of 9,2±19) and the size from 1,2 to 5,5 cm (mean of 2,7±15).
Compared with 50 healthy age-matched subjects, total, trabecular and cortical bone densities were reduced in all pts (TotBMD: 229 mg/cm^3 vs ctr 343, -33%, p<0,02; TrabBMD: 80 mg/cm^3 vs ctr 146, -45%, p <0,003; CorBMD: 689 mg/cm^3 vs ctr 793, -13%, p <0,02), such as cortical thickness (0,145 cm vs ctr 0,159, -9%, p<0,04) and strength-strain index (576 mm^3 vs ctr 787, -27%, p<0,02). Geometrical parameters were not different in the two groups. The weight of parathyroid adenomas, showed a strong positive correlation with serum PTH levels (r=0,92 p<0,01).
Conclusion: pQCT measurements in PHPT showed: 1) osteopenia in all bone compartments, grater at trabecular site; 2) reduced cortical density and cortical thickness consistent with „cancellization" of the inner cortex and b) lower ability of bone to absorb loading forces; 3) reduced strength-strain index, indicatives of inadequate ability to adapt to mechanical use and augmented risk for fracture. In these series, serum PTH levels were not associated with preservation of trabecular bone.

PS_353

QANTITATIVE EVALUATION OF SACROILIITIS IN THE PATIENTS WITH BRUCELLOSIS

H. Kaya, A. Cobaner, T.A. Balci, S. Çerçi. Department of Nuclear Medicine, Dicle University Medical Faculty, Diyarbakir, Turkey.

Brucellosis is an infectious disease with multiorgan involvement, especially the musculoskeletal system. We aimed to show the sacroiliac joint involvement in the patients with brucellosis presenting with back pain and to evaluate the value of the sacroiliac index (SI) by means of radionuclide imaging. With this purpose we performed Tc-99m MDP bone scintigraphy to 56 patients and to the 15 control patients with no complaint of back. We obtained spot images from the lumbosacral region on the posterior projection and whole-body images. We drew ROI's with the same pixel over the sacroiliac joints and over the sacrum on the spot images and calculated SI by using the formula of [SI= Sacroiliac joint count/Sacrum count]. All images also evaluated visually. Mean SI was 1.52±0.03 and 1.13±0.25 in the patient group and the control group, respectively. There was a statistically significant difference between the groups (p<0.05). We concluded that SI was a useful parameter for the evaluation of sacroiliac joint involvement, namely sacroiliitis, in brucellosis.

PS_354

CONSECUTIVE QUANTITATIVE SPECT STUDIES IN CEMENTLESS TOTAL HIP ARTHROPLASTY. 5-YEAR FOLLOW-UP

E. Zouboulis (1), P. Megas (2), D. Apostolopoulos (1), C. Giannakenas (1), T. Spiridonidis (1), A. Kaisidis (2), E. Lambiris (1), P.J. Vassilakos (2). (1) Department of Nuclear Medicine, University Hospital of Patras, Greece; (2) Orthopaedic Department, University Hopsital of Patras, Greece.

Aim: Midterm fixation of cementless total hip implants and prognostic value of Q-SPECT analysis of periprosthetic ^{99m}Tc-MDP uptake are evaluated.
Material-Methods: 31 patients (33-76 years), scheduled for a total hip arthroplasty due to primary osteoarthritis were divided into 2 groups. Group A (n=18), where a proximal porous coated and B (n=13), where a smooth tapered design cementless prosthesis, was implanted respectively. The choice of implant was made using a CAD/CAE technique. Patients were imaged 1 week pre-operative, and 2, 8, 36, 60 weeks and 4 years post-operative. Clinical and x-ray follow-up was performed accordingly. Quantitative measurements were performed with a Region Of Interest (ROI) technique by using the mean counts for each ROI and the the ratio of normal bone concetration. Q-SPECT analysis of the radionuclide uptake was performed in coronal, transaxial and sagittal projections, where the slice thickness was four (4) pixels, for image matrix size 128X128 pixels. Elliptical angular analysis in the two latter was also included.
Results: Elliptical angular analysis serves for the in vivo estimation of the biomechanical behavior of the cementless implant and the type of fixation achieved. Qualitative criteria of the design characteristics of each implant are presented. Q-SPECT analysis of periprosthetic ^{99m}Tc-MDP uptake serves as an early prognostic tool for the final implant fixation. Correlation of the imaging findings with the clinical and x-ray follow-up is presented. Four distinct types of ^{99m}Tc-MDP uptake, which correspond to different biomechanical and clinical performance of each implant, are obtained, - Type I: adequate initial stability, Type II: secondary fixation, Type III: response to anelastic implant (excessive thigh pain) and Type IV: failure of initial stability.
Conclusions: Consecutive Q-SPECT studies in cementless total hip arthroplasty offers the ability to assess in vivo the biomechanical properties of the cementless implants, as well as to establish early prognostic signs for the final implant outcome. Failure of achieving a „steady-state" condition of periprosthetic metabolism until the 60th post operative week is considered as a failure of achieving initial stability of the implant, probably leading to early aseptic loosening.

PS_355

COMPARISON OF TC 99M MDP, TC 99M HIG, TC 99M WBC SCINTIGRAPHY FOR THE DIAGNOSIS OF INFECTED JOINT PROSTHESIS

S. Ünal (1). (1) Department of Nuclear Medicine; (2) Department of of Ortophedics, Istanbul Faculty of Medicine, Istanbul,Turkiye.

Aim: The aim of this study was to investigate the role of Tc 99m methylene diphosphonate (MDP), Tc 99m human immunoglobulin (HIG), Tc 99m leukocytes (WBC) for the diagnosis of infected joint prosthesis.
Methods: Thirty two patients (5 men, 27 female, mean age 59.4 year) with suspected infection of a hip or a knee prosthesis were studied prospectively. All the patients had undergone Tc 99m MDP (3 phase), Tc 99m WBC scintigraphy (42 prosthesis). Tc 99m HIG scintigraphy could be performed only in 21 patients (30 prosthesis)
These scintigraphic examinations were completed within 7 days. Focal or diffuse tracer uptake was scored visually according to 4 point scale for HIG and WBC scintigraphy. The pattern of uptake was also correlated with bone scan findings.
Results: There were 42 prosthesis in 32 patients (3 bilateral hip, 6 bilateral knee, 4 unilateral knee and 20 unilateral hip). Final diagnosis was based on operative findings, culture, and clinical outcome. False positive HIG scans (7) were due to loosening of the prosthesis. There was only one false positive scan for WBC.

%	S	Sp	P pv	N pv
Tc MDP	87	79	50	96
Tc HIG	83	71	42	94
Tc WBC	89	97	89	97
Tc MDP+ Tc HIG	83	71	42	94
Tc MDP+ Tc WBC	89	97	89	97

S: Sensitivity, Sp: Specificity, P pv: Positive pv, N pv: Negative

Conclusion: These results indicate that high false positive scans and low specificity of Tc HIG scan eliminates its use. On the other hand Tc WBC can be used safely for the diagnosis of infected hip prosthesis.

PS_356

COMPARISON OF TC-99M HIG SCINTIGRAPHY AND THREE PHASE TC-99M MDP BONE SCINTIGRAPHY FOR EVALUATING THE EFFICACY OF YTTRIUM-90 SILICATE THERAPY IN RHEUMATOID KNEE SYNOVITIS

A. Gençoğlu (1), G. Aras (1), O. Küçük (1), S. Ataman (2), A. Soylu (1), N. Söğüt (1), E. Ibis (1). (1) Department of Nuclear Medicine; (2) Department of Physicial Therapy and Rehabilitation, Ankara University Medical Faculty, Ankara, Turkey.

The aim of this study was to compare the value of quantitative Tc-99m human polyclonal immunoglobulin G (HIG) scintigraphy to the value of quantitative three-phase Tc-99m methylene diphosphonate (MDP) bone scintigraphy for evaluating the efficacy of yttrium-90(Y-90) silicate therapy in rheumatoid knee synovitis.

Materials and Methods: 24 knee joints with chronic persistent synovitis in 15 rheumatoid arthritis patients (13 F and 2 M, mean age 53.5 ± 8.4 years) were treated with 185 MBq Y-90 silicate. The patients were examined before and at 3, 6, 9, and 12 months after Y-90 therapy using clinical evaluation, Tc-99m HIG scintigraphy and three-phase Tc-99m MDP bone scintigraphy. Each scan was evaluated quantitatively and the index of tracer uptake was calculated. The scintigraphic findings were then compared to clinical results at each subsequent assessment.

Results: In the 14 knee joints that exhibited excellent or good clinical response to Y-90 therapy, the Tc-99m HIG index values at 3 months after radionuclide synovectomy were significantly lower than the pretreatment index figures ($p<0.001$). In 13 of these 14 joints, these values remained low throughout the study. 1/14 joint that showed recurrent arthritis at 9 months, the HIG index value was increased at this stage compared to the findings at 3 and 6 months, and it remained high at 12 months. In these 14 joints, the Tc-99m MDP index values (vascular and late phases) were statistically similar before and at 3 months after Y-90 therapy. At 6 months, the MDP index values were diminished in both the vascular ($p<0.01$) and late phases ($p<0.05$) in all 14 joints, and these low values continued to be observed in 13/14 of the joints at 9 and 12 months. In the one joint which developed recurrent arthritis at 9 months, MDP index value rose at this stage compared to the value at 6 months, and this was also true at 12 months. In the 10 knee joints that failed to respond to treatment, the MDP and HIG index values were statistically similar before and after the Y-90 therapy .

Conclusion: The study showed that quantitative Tc-99m HIG scintigraphy is a valuable method for evaluating the efficacy of Y-90 silicate therapy in rheumatoid knee synovitis, starting from the early post-treatment period. Quantitative three-phase Tc-99m MDP bone scintigraphy may be useful for evaluating the efficacy of radionuclide synovectomy only in the late period.

PS_357

ROLE OF THREE PHASE BONE SCINTIGRAPHY IN THE EARLY DIAGNOSIS OF REFLEX SYMPATHETIC DYSTROPHY OF THE HAND

A. Kumar (1), A. Pankaj (2), P.P. Kotwal (2), R. Mittal (2), K.K. Deepak (3), C.S. Bal (1). (1) Department of Nuclear Medicine; (2) Department of Orthopaedics; (3) Department of Physiology, All India Institute of Medical Sciences, New Delhi, India.

Aim: Post-traumatic reflex sympathetic dystrophy (RSD) of the hand can lead to severe physical disability, if not diagnosed and treated early. RSD is usually diagnosed on high clinical suspicion along with relevant history. However, early diagnosis is sometimes difficult because of paucity and variability of signs and symptoms and plain x-ray is usually non-contributing. Therefore, there is a need for a reliable diagnostic modality to diagnose it early. We tried to assess the role of three-phase bone scintigraphy and sympathetic skin response (SRS) in the early diagnosis of RSD. **Methods:** After complete clinical evaluation, three-phase bone scan and SRS was performed in 30 patients with clinical suspicion of RSD. Bone scan was done after injecting 20 mCi of Tc-99m MDP, and taking immediate blood flow images, blood pool images and static images after 2-4 hours. SRS was measured in both the hands after fixing electrodes to the palm and the dorsum of both hands and applying electrical stimuli of single square wave pulses of 0.1 msec duration and 1-2 mA intensity. **Results:** Mean age of the patients was 42.6±12.3 years with equal numbers of male and female. In most of the patients, right hand was affected (77%). The commonest preceding event leading to the development of RSD was a simple fracture (67%), that too colles fracture (53%). Crush injuries and compound fracture, history of a surgical procedure and soft tissue injuries of the upper extremity were responsible for 7%, 10% and 16% of cases, respectively. Pain was the most disabling symptom and along with loss of motion was present in all cases, though with varied severity. The delayed phase of bone scan was positive in all cases, blood pool phase in 93.3% and blood flow phase in 90% cases, showing increased multiple periarticular tracer uptake in the affected limb. All patients with negative blood flow and blood pool images had > 3 months duration of illness. SRS was found abnormal in only 8 cases (27%) and in only 4 cases (33%) of < 3 months duration. **Conclusion:** Three-phase bone scintigraphy is a very sensitive corroborative test to confirm the clinical diagnosis of RSD, particularly during its early stage.

PS_358

ALVEOLAR CAPILLARY MEMBRANE PERMEABILITY IN THE PATIENTS WITH RHEUMATOID ARTRITIS

H. Kaya, T.A. Balci, M. Polat, S. Erdoğan, O. Gülen. Department of Nuclear Medicine, Dicle University Medical Faculty, Diyarbakır, Turkey.

Rheumatoid artritis (RA) is a chronic nonspesifik systemic disease characterised by the inflammation of the peripheral joints. It causes progressive destruction on the joints. Because it is a systemic disease it may involve the lungs and especially interstitial pulmonary disease occurs in the course of time. The goal of this study is to evaluate if an alteration occurs on the pulmonary epithelial permeability in the patients with RA. Thirty patients had normal pulmonary function test and no pathological appearance on their chest x-rays. All of them were non-smoker. We constituded a healty control group (15 subjects) with the similar pulmonary properties of the patient group. We carried out Tc-99m DTPA inhalation scintigraphy and just after that we obtained dinamic images on the posterior projection of the lung regions during 10 minutes. We draw 6 ROI's on the both lungs and calculated percentage of decreasing activity over the lungs and so we obtained capillary epithelial permeability values. CEP values of the patient group were lower than the normal group, and 0.827±0.34% and 1.282±0.27% in the patients group and control group respectively. The difference between the groups was also significant statistically ($p<0.001$). Pulmonary epithelial membrane permeability decreases in the patients with RA, and there was a relationship between the age of the disease and the reduction of the CEP values. CEP values can be used for follow up the deterioration of the disease in the patients without clinical findings of pulmonary involvement.

PS_359

ANALYSIS OF UPTAKE PATTERNS IN METASTASIS AND BENIGN DISEASES ON SPINE SPECT: DIFFERENTIAL DIAGNOSIS IS POSSIBLE IN CANCER PATIENTS?

Y.Y. Choi, S. Cho. Department of Nuclear Medicine, Hanyang University Hospital, Seoul, South Korea.

Aim: One or more abnormal vertebrae detected at bone scintigraphy is a common finding in clinical practice, and it could pose a diagnostic dilemma especially in cancer patients, as either metastasis or benign disease may cause the scintigraphic abnormality. The purpose of this study was to determine whether additional spine SPECT has a role in differentiating malignant from benign lesions in cancer patients.

Methods: We reviewed spine SPECT studies obtained over a 3-year period in 108 patients. Among them, fifty-two patients with abnormal SPECT and with clinically followed records were evaluated (20 cancer patients were included). Uptake patterns on SPECT images were classified as follows: 1. Body ① diffusely increased uptake(DIU), ② linear increased uptake of end plate(LIU), ③ segmental increased uptake(SIU), ④ cold defect and/or surrounding increased uptake(CD), 2. posterior element ① posterior to body(PB): lamina ② posterior to intervertebral disc space(PD): facet joint ③ spinous process(SP). Lesions were correlated with radiologic findings and with final diagnosis.

Results: Seventy-six bone lesions were detected on SPECT images.

		Metastasis (18)	Degenerative (28)	Compression Fracture (21)	Failed back syndrome (9)
Body	DIU	4		9	
	LIU		12	6	
	SIU	5		1	
	CD	6			
Posterior element	PB	2		2	4
	PD		15		3
	SP	1	1	3	2

Conclusion: Cold defect and segmental increased uptake of body were characteristic findings of bony metastasis, but care should be taken because compression fractures showed segmental increased uptake in some cases. Degenerative diseases were easily diagnosed due to typical finding of linear increased uptake of end plate and facet joint uptake. Therefore, additional bone SPECT after planar bone scan would be helpful for differentiating metastasis from benign condition in cancer patients.

Poster presentation

PS_360

RELATIONSHIP BETWEEN 99MTC-HDP PETROSA BONE SPECT FINDINGS AND SENSORINEURAL HEARING LOSS IN PATIENTS WITH OTOSCLEROSIS

D. Volterrani (1), S. Berrettini (2), F. Ravecca (2), G. Boni (1), M. Grosso (1), S. Sellari Franceschini (2), G. Manca (1), F. Bianchi (1), R. Bianchi (1). (1) Division of Nuclear Medicine; (2) Division of Otorhynolaryngoiatry, University of Pisa, Pisa, Italy.

Otosclerosis (OS) is a primary disease characterized by bilateral hearing loss (HL) and by the progressive replacement of the normal bone of the ossicles and otic capsule with a disorganized fibrous and osseus tissue. The diagnosis is usually based on family history, progressive HL, absence of stapedial reflex, on-off effect on impedance tympanometry. Although CT and HR-CT are reported to be useful, both false positive and false negative results can occur. In this study we evaluated diphosphonate bone SPECT findings in relation to the presence of OS and the degree of the sensorineural HL

Methods: Thirty-six patients (72 ears) with surgically confirmed OS, affected by mixed (conductive and sensorineural) HL, and 12 normal hearing subjects free of any otoiatric disease, underwent a bone SPECT of the skull with ^{99m}Tc-HDP. SPECT studies were carried out by using a dual head gamma camera equipped with LEHR collimators. FBP and a Butterworth prefiltering (cut-off 0.50 cycles/cm, order 10) were used for images recontruction. Attenuation correction was not applied A scintigraphic uptake index (UI) value was calculated by dividing the mean activity of the ROIs drawn along the petrosa bones by the mean activity for the occipital bone.

Results: A statistically significant increase of diphosphonate uptake was found when comparing the scintigraphic UI values of the patients affected by OS with controls (2.21±1.70 vs 1.13±0.26; $p<.0001$). An inverse relationship ($p<.005$) between patients age and petrosa UI values was observed. A stright relationship was found between UI and the severity of sensorineural HL, revealing a statistically significant difference among UI values of patients with mild, moderate and severe sensorineural HL, especially when only younger (≤ 45 yrs) patients were considered.

Conclusions: Petrosa bone SPECT seems to be an useful tool for the assessment of OS. Moreover, SPECT could be a predictor for medical treatment efficacy with diphosphonates of patients with a more severe sensorineural HL by directely visualizing those active lesions which much more accumulate diphosphonate.

PS_362

DYNAMICS OF MYOCARDIAL PERFUSION AND FUNCTION IN PATIENTS WITH ACUTE MYOCARDIAL INFARCTION: EVALUATION BY GATED SPECT (G-SPECT) WITH 99MTC-MIBI

E. Egorova, E. Khodareva, M. Ruda, V. Sergienko. Department of Nuclear Medicine, Cardiology Research centre, Moscow, Russia.

Aim: to assess the dynamics of myocardial perfusion and function for 6 months in patients (pts) with acute myocardial infarction (AMI) after reperfusion therapy (6 month follow up).
Materials and methods: 29 pts with AMI were studied. All pts underwent reperfusion therapy (RT): systemic thrombolysis in 26 and PTCA in 3. Gated -SPECT (G-SPECT) with 99mTc-MIBI was performed in each case before the onset of RT (area of risk), 24 hours later, before the discharge (10 days), 1 and 6 months after the development of AMI. Results were analyzed by ejection fraction (EF %) and the size of perfusion defects (DP, % LV).
Results: Depending on the RT efficacy all pts were divided into 2 groups: those with the infarct-related artery reperfused (1st gr., n=19) and those with no evidence of reperfusion (2nd gr., n=10). Results in 2 gr. of pts. are presented in the table.

		Before RT	24 h.	10 days	1 mnth	6 mnths
DP(%)	1 gr.	31±10,0	25±10,2***	21±9,7***	20±8,7	20±9,6
	2 gr.	35±9,3	33±9,0	29±8,0**	29±7,6	26±8,5*
EF (%)	1 gr.	43±10	43±10	46±7,1*	46±6	47±8
	2 gr.	41±9	38±10	43±8	42±7	43±10

***-P<0.001, **-P<0.01, *-P<0.05, ^{n}-P>0.05 (paired t-crit).

There was no initial difference in the extent and EF between the two groups. Pts with effective RT exhibited a decrease in the extent by 20% ($p<0.05$) 24 hours following the onset of AMI and by 32% ($p<0.002$) in 10 days; followed by EF increased by 3% ($p<0.05$) on the 10th day of the disease. No subsequent changes in perfusion or global LF function occurred in this group of pts. In ineffective RT there were no changes in the size of DP and EF within 24 hours. A decrease in the extent by 17% ($p<0.006$) on the 10th day and by 26% in half a year ($p<0.02$) was noticed. EF failed to demonstrate any changes throughout the period of observation in this group of pts.
Conclusions: successful RT is denoted by accelerated and better-pronounced restoration of myocardial perfusion, followed by improvements in contractility.

CARDIOVASCULAR 5

PS_361

SYSTOLIC AND DIASTOLIC STUNNING 30 MIN AFTER EXERCISE IN PATIENTS WITH ANGINA PECTORIS: EVALUATION WITH GATED TC -99M-TETROFOSMIN SPECT

T. Kawasaki, T. Sakatani, H. Mani, T. Kamitani, S. Kawasaki, H. Sugihara. Depertment of Cardiology, Matsushita Memorial Hospital, Sotojima-cho, Japan.

Aim: We investigated whether systolic and/or diastolic dysfunction persists even 30 min after exercise-induced ischemia in patients with angina pectoris (AP).
Methods: Twenty patients with AP and 15 controls(C) underwent exercise/rest Tc-99m-tetrofosmin (TF) gated SPECT 30 min after injection. Data acquisition was gated for 16 frames / cardiac cycle. Left ventricular (LV) volume curves were generated using QGS program and four harmonics of Fourier series was retained for the analysis. From this curve and its first derivative curve, we derived ejection fraction (EF) as systolic index and peak filling rate (PFR), time to PFR (TPFR) and 1/3 filling fraction (1/3FF) as diastolic indices.
Results: Post exercise EF did not differ from resting EF in C. In 8 of 20 patients with AP, post exercise EF was > 5 % lower than the resting value. There were no difference in PFR, TPF and 1/3 FF between post exercise and rest in C. Both post exercise PFR(%/sec) and 1/3 FF(%) were less than the resting values in patients with AP (PFR 195.6±48.4 vs 225.0±40.2, 1/3FF 37.5±18.0 vs 42.5±14.0, $p<0.01$). Post exercise TPF was more prolonged than resting values in patients with AP (203.0±35.1 vs 185.0±28.3, $p<0.01$).
Conclusions: Post exercise stress LV systolic and diastolic dysfunction was often found 30 min after exercise in patients with AP.

PS_363

ROLE OF THE 99M TC-SESTAMIBI G-SPECT IN THE EVALUATION OF SEPTAL DYSFUNCTION AFTER CORONARY ARTERY BY-PASS SURGERY

P. Sullo (1), E.M. Covelli (1), G. Mazzarella (1), A. Cardillo (2), A. Natale (2), C. Formato (1), F. Boccagna (1), C. Chieffo (2), G. Belfiore (1). (1) Diagnostic Imaging Department - Caserta Hospital; (2) U.O. Cardiologia Riabilitativa, Caserta Hospital, Italy.

Abnormal septal wall motion is a possible complication due to pericardiotomy after coronary by-pass surgery (CABG) and traditional noninvasive techniques evaluating LV regional function are not reliable to assess this condition. Gated-SPECT (G-SPECT) with Tc99m labeled perfusion tracers allows simultaneous assessment of cardiac regional function and perfusion. Aim of our study was to investigate septal dysfunction and corresponding perfusion in patients with previous CABG.
Methods: Thirty-nine patients (28M, 11F; mean age 60±12 years) with CABG for multivessel disease underwent rest Tc99m-sestamibi (925 MBq) G-SPECT using a 90; dual-detector camera (Vertex, ADAC) and 2D-echocardiography within 1 week. According to the standard QGS and QPS protocol, septal wall was divided in 6 (2 para-apical, 2 medial and 2 para-basal) of 20 segment model. Septal wall motion (SWM) was scored in corresponding segments from 1 (normal) to 3 (a-dyskinesia) on both G-SPECT and 2D-echocardiography. Segmental Tc-99m sestamibi uptake was quantitatively measured and expressed as percentage of normal region activity in reference population database.
Results: Of the 234 septal wall-related segments, 92 (40%) were a-dyskinetic, 127 (54%) hypokinetic and 15 (6%) normal on G-SPECT study; 2D-echocardiography revealed 90 (38%) segments with a-dyskinesia, 121 (52%) with hypokinesia and 23 (10%) with normokinesia. Agreement between G-SPECT and 2D-echocardiography was observed in 193/234 (82%, k=0.66) segments. No statistically significant different sestamibi uptake was found in normal (65±4), hypokinetic (63±5, p= n.s.) and a-dyskinetic (62±4, p= n.s.) segments, indicating normal perfusion stastus in all segment groups.
Conclusions: These results suggest that Tc99m-sestamibi G-SPECT can reliable discriminate dysfunctional but normoperfused septal wall due to CABG and it might be accurate technique in the noninvasive evaluation of this patient population.

PS_364

ASSESSMENT OF RESIONAL LEFT VENTRICULAR PERFUSION AND FUNCTION WITH GATED-SPET IN PATIENTS WITH SURGICALLY REPAIRED TERALOGY OF FALLOT

T. Higuchi, J. Taki, K. Nakajima, H. Sumiya, S. Kinuya, N. Tonami. Kanazawa University, Department of Nuclear Medicine, Kanazawa, Japan.

[Purposes] Intracardiac repair of teralogy of Fallot (TOF) may result in abnormal septal perfusion and function. The aim was to evaluate regional perfusion and function by ECG-gated perfusion SPECT (G-SPECT) in TOF. [Methods] Eight patients with TOF (aged 15±4) who had undergone intracardiac repair (TOF group) and ten age-matched normal control subjects (aged 14±4) (control group) were enrolled. The average interval between the operation and postoperative G-SPECT in TOF group was 9±3 years. Tc-99m-MIBI (740 MBq) was injected at rest, and G-SPECT was performed. We evaluated left ventricular ejection fraction (EF), inward regional wall motion (WM), systolic % wall thickening (WT) and % tracer uptake with QGS program. Regional parameters were obtained in 20-segments model based on the functional polar map. [Results] There were no differences between TOF and control groups in global EF, regional % tracer uptake and WT in all segments. However, WM (unit: mm) in the 4 septal segment decreased compare with normal group (1.9±1.8 mm vs. 6.0±1.4 mm, $p<0.01$). [Conclusion] WM and perfusion in the septal segments show mismatch, indicating pseudoparadoxical motion after surgery. Thus, systolic wall thickening analysis is preferred to evaluate regional function in repaired TOF.

PS_365

CORRELATION BETWEEN POST-STRESS AND REST GATED MYOCARDIAL PERFUSION IMAGING : AN APPROACH TOWARDS THE BEST METHOD FOR MEASURING LEFT VENTRICULAR FUNCTION

A.M. García Vicente, S. Rodado, V. Poblete, A. Soriano. Department of Nuclear Medicine, Alarcos Hospital, Ciudad Real, Spain.

The ventricular function data obtained by gated SPECT reflect the condition at the time of acquisition while the perfusion data are dependent on conditions at the time of injection. **Aim** : to compare post-stress and rest ejection fraction, thickening and wall motion in patients with coronary artery disease and investigate the relationship between the development of perfusion abnormalities and the changes in left ventricular ejection fraction (LVEF) measurements. **Methods**: A same day post-stress and rest gated SPECT with 740 MBq and 1110 MBq of Tc 99m-tetrofosmin respectively was performed on 28 patients (average age:57). 16 underwent an exercise test and 12 a pharmacologic stress test. All patients had known ischaemic cardiopathy (21 with previous myocardial infarction). Post-stress and rest tomograms were qualitatively analysed by using a 13 segment model. The perfusion images were interpreted independently by two experts assessing reversible and fixed defects. The data were analysed using a comparative analysis of independent variables (t-student).

Results: The average LVEF for post-stress was 36,5 % and for the rest:37,6 %. These values did not show significative statistical differences (p=0,586).

3 of 9 patients (group 1) with LVEF higher in post-stress, showed significative statistically differences (>5%); 1 patient did not show any differences and 18 patients (group 2) showed lower LVEF in post-stress gated images compared with rest gated images (9 of them significative).

A total of 100 perfusion defects , 59 reversible and 41 fixed, were detected. 20 reversible defects showed thickening in rest gated and 10 in post-stress gated. The group 2 (18 patients) had more reversible defects (average: 2,8 segments) than group 1 (9 patients) who showed an average of 1 segment. There were no significative statistical differences (p=0,646) between the number of fixed defects in group 1 (average: 1,5 segment) and group 2 (average: 1,3 segments).

Motility alterations showed concordance between both methods in 24 patients. 10 of them showed agreement with perfusion abnormalities and 14 showed discrepancy, 9 were septal dyskinesia in 5 patients with left bundle branch block.

Conclusions: Patients with more reversible defects showed lower LVEF in post-stress gated compared with rest gated but without statistical differences. The thickening of reversible defects was more evident in rest gated. The post-stress gated underestimated the viability determined by thickening but had a prognostic value, as a lower LVEF showed a great number of reversible defects and therefore myocardial in risk.

PS_366

EVALUATION OF DIFFERENCES BETWEEN POST STRESS AND REST LEFT VENTRICULAR EJECTION FRACTION ASSESSED WITH GATED MYOCARDIAL PERFUSION SPECT

H.J. Verberne (1), M.G.W. Dijkgraaf (2), B.L.F. van Eck - Smit (1). (1) Department of Nuclear Medicine; (2) Department of Clinical Epidemiology & Biostatistics, Academic Medical Center, University of Amsterdam, The Netherlands.

Aim. Gated SPECT has an additional value to routine myocardial perfusion imaging. The purpose of the study was twofold: 1) to determine the reproducibility of gated SPECT assessed left ventricular (LV) ejection fraction (EF) and 2) to determine patient characteristics correlating to differences in LVEF assessed directly post-stress and at rest.

Methods. In 229 randomly selected patients gated SPECT was performed post-stress and at rest. Reproducibility of LVEF measurement was determined in 22 patients by comparing two consecutive gated acquisitions at rest after patient repositioning. Data acquisition was performed 1 hour after administration of 500 MBq ^{99m}Tc-Tetrofosmin with a 3-headed SPECT system. The Germano Quantitative Gated SPECT (QGS) software was used to calculate LV dimensions and EF. Reproducibility of the repeated rest measurement was expressed as a mean difference and 95% confidence interval (95% CI). Multivariate regression analysis was used to correlate the difference between post-stress and rest LV-measurement (delta EF) and items concerning patient characteristics, clinical history, stress related factors and scintigraphic findings.

Results. The mean difference between two consecutive measurements at rest was 0.09% EF-units with a 95%CI from − 4 to 5% EF-units. Independent predictors of delta EF were the presence of scintigraphically proven ischemia (standardized coefficient: 0.173, p= 0.009) and differences in heart rate (HR) during acquisition (standardized coefficient: 0.203, p= 0.005). End-diastolic volume, maximal HR during stress, scintigraphically proven infarct and stress-type (adenosine vs. ergometry) were no independent predictors of delta EF.

Conclusions. Gated SPECT assessed LVEF is reproducible under standard clinical conditions. However, differences in LVEF between rest and post-stress assessment can be expected if HR has changed between two measurements and in patients with scintigraphically proven ischemia.

PS_367

LEFT VENTRICULAR EJECTION FRACTION (LVEF), END DIASTOLIC VOLUME (EDF) AND END SYSTOLIC VOLUME (ESV) BY QUANTITATIVE GATED MYOCARDIAL PERFUSION SPECT (QGS). COMPARISON WITH ECHOCARDIOGRAPHY (ECHO) IN ACUTE CORONARY SYNDROME

M.D. Marin (1), A. Gonzalez (2), M. Coronado (1), I. Roldan (1), R. Couto (1), T. Navarro (1), G. Riesco (1), R. Plaza (3). (1) Servicio Medicina Nuclear, Hospital; (2) Servicio Cardiologia, Hospital; (3) Servicio Radioproteccion, Hospital, Hospital Universitario, Madrid, Spain.

The objective of this study is to evaluate left ventricular function and volumes measured by rest QGS and its correlation with echocardiography and equilibrium ventriculography techniques.

MATERIAL AND METHODS

A total of 48 patients from 41 to 77 years old (men age 59.9 ± 9.3, 46 males and 2 females), with non complicated acute myocardial syndrome (16 patients without ST segment elevation and 32 with ST segment elevation) were evaluated retrospectively by means of gated ventriculography, two dimensional echo and ^{99m}Tc-sestamibi gated SPECT stress/rest. A total of 46 underwent exercise test and 2 of them underwent pharmacological test. Abnormal perfusion defects were found in 67% of patients and abnormal segmental wall motion were found in 62% of patients. These techniques were performed 5 days to 30 days after presentation of acute coronary syndrome. LVEF, EDV and ESV were assessed with Echo, automatic QGS and equilibrium ventriculography (LVEF only)

RESULTS

	LVEF	EDV	ESV
QGS	54.4% ± 11.5	107.3± 28.9 ml	50.8 ± 23.8 ml
ECHO	51.9% ± 10.4	110.6 ± 34 ml	55.2 ± 28.3 ml

EQUILIBRIUM VENTRICULOGRAPHY LVEF: 51.8 ± 8.9 ml.

Pearson correlation was used to compare the results between echo and QGS for LVEF (r=0.68); EDV (r=0.75) and ESV(r=0.82). This coefficient was also used to compare equilibrium ventriculography with echo and QGS for LVEF (r=0.68 and r=0.72 respectively).

CONCLUSIONS

All QGS cardiac SPECT parameters correlated well with echocardiography and equilibrium ventriculography. Besides, it is a fast, objective and reproducible method and provides additional information about myocardial perfusion. The echocardiography, on the other hand, has the disadvantage of being an observer dependent method and slower to perform.

PS_368

CORRELATION BETWEEN LEFT VENTRICULAR EJECTION FRACTION (LVEF) CALCULATED FROM TC-99M TETROFOSMIN GATED SPECT (GS) AND ECHOCARDIOGRAPHY (EC)

A. El-Shirbiny (1), M. Islam (2), I. Seo (1), J. Luo (3), C. Homs (1), R. Kappas (1), W. Sy (1). (1) Nuclear Medicine Department, The Brooklyn Hospital Center; (2) Department of Cardiology, The Brooklyn Hospital Center; (3) Nuclear Medicine Service, Department of Radiology, St. Vincent's Catholic Medical Centers of New York, USA.

Aim: Evaluation of accuracy of LVEF from Tc99m Tetrofosmin (TF) GS SPECT as compared to the commonly used EC .
Method: We retrospectively compared LVEF form GS, using the commercially available Cedars Quantitative Gated SPECT software and EC using modified Simsons method within 15 days of each other in 199 patients.
Results: Normal perfusion was found in 109, inferior wall perfusion defect in 40 and multiple perfusion defects in 12 patients.
The results of comparison are shown in the following table and graphs.

	Whole		EF < 50		EF > 50	
	GS	ECHO	GS	ECHO	GS	ECHO
Max	87	86	50	72	87	86
Min	16	15	16	15	51	39
Average	53.21	57.66	36.94	47.26	58.27	62.02
SD	14.95	13.52	10.01	14.28	7.61	8.70
t-Test	0.002		0.000		0.277	
Correlation	0.697		0.691		0.218	
Intercept	8.750		14.044		50.298	
Slope	0.771		0.485		0.191	

Conclusion: LVEF calculated from Tc99m TF GS has overall acceptable correlation with EC (r = 0.69). However, EC overestimates LVEF at lower GS EF values < 50% and underestimates LVEF at GS EF values > 60%. Inferior wall and multiple perfusion defects had no effect on the correlation values.

PS_369

LEFT VENTRICULAR EJECTION FRACTION DETERMINED BY GATED-SPECT MYOCARDIAL PERFUSION IN CORONARY PATIENTS.COMPARISON WITH EQUILIBRIUM ISOTOPIC VENTRICULOGRAPHY

I. Casáns-Tormo (1), A. Llácer (2), J.A. Ferrero (2), J. Ciudad (1). (1) Nuclear Medicine; (2) Cardiology Departments. Hospital Clínico Universitario. Valencia. Spain.

To assess the accuracy of left ventricular ejection fraction (EF) measurement by gated SPECT (GSPECT), we have studied 34 coronary patients proven by coronary angiography, 17 of them with EF≤40% and the other 17 with EF>40%.
Methods: SPECT myocardial perfusion was obtained with 99mTc-Tetrofosmin (2 day-protocol), with gated acquisition always 1 h after tracer injection, administered at peak exercise in 19 patients and at rest in 15 patients (8 frames/cycle, 180°, 64x64, 30 images, 45 s/image) and EF measurement by QGS program. An equilibrium isotopic ventriculography (EV) was obtained 48 h later, with EF determination by usual non-geometric semiautomatic method. All studies showed suitable quality for quantification. We have assessed differences in mean EF values, correlation and agreement (Bland-Altman analysis) between the two methods.
Results: Considering all patients, we have found high correlation in EF determination between GSPECT and EV (r: 0.96, p: 0.0001), although mean EF by GSPECT was 37.8±18.4%, and 40.8±19.3% by EV (p: 0.0001). Mean difference between both methods was 3.0±4.9, with limits of agreement from –6.8 to 12.8. In patients with EF>40%, the correlation was good (r: 0.82, p: 0.0001), with mean EF values of 53.8±9.4% (GSPECT) and 58.0±8.9% (EV), p: 0.007
Mean difference between methods was 4.1±5.5, with –6.8 to 15.2 as limits of agreement. In the group with EF≤40%, the correlation was higher (r: 0.87, p: 0.0001), mean EF values were 21.8±8.1% by GSPECT and 23.7±7.9% by EV, p: NS. Mean difference between methods was lower: 1.8±4.1 and narrower the agreement limits: -6.4 to 10.0.
Conclusion: Mean EF values obtained with gated SPECT were lower than the mean values determined by equilibrium ventriculography in the group of patients with higher EF, without significative differences in the lower EF group. Good correlation and agreement was found between both methods in EF determination in patients with higher EF and even better in patients with lower EF. So, gated SPECT provides suitable accuracy in quantification of EF in coronary patients with as without ventricular dysfunction.

PS_370

RELIABILITY OF 201-TL ECG-GATED SPECT VERSUS PLANAR RADIONUCLIDE VENTRIVULOGRAPHY FOR THE MEASUREMENT OF LEFT VENTRICULAR EJECTION FRACTION

D. Daou (1), C. Coaguila (1), B.O. Helal (1), I. Ponturier (1), T. Fourme (2), S. Dinanian (2), R. Lebtahi (3), M. Faraggi (3), M. Slama (2), D. Le Guludec (3). (1) Department of Nuclear Medicine, Antoine Beclere Hospital, AP-HP, Clamart, France; (2) Cardiology Department, Antoine Beclere Hospital, AP-HP, Clamart, France; (3) Department of Nuclear Medicine, Bichat Hospital, AP-HP, Clamart, France.

Objectives: Coupling myocardial perfusion to function is interesting. Good correlation between left ventricular ejection fraction (LVEF) calculated with ^{201}Tl ECG-gated SPECT (GSPECT) versus other modalities has been reported. But, its reliability for the study of LVEF has not been studied with ^{201}Tl GSPECT. Moreover, this reliability has not been compared in the same patients to that of planar equilibrium radionuclide angiography (RNA). We aimed to compare the reliability of GSPECT and planar left anterior oblique (LAO) RNA for the measurement of LVEF.
Methods: Nine patients with coronary artery disease had both rest ^{201}Tl GSPECT and planar LAO RNA. The rest ^{201}Tl GSPECT consisted of 2 acquisitions (8 frames/RR) realized at 15 min (Technician 1) and 4h after injection (Technician 2). This was followed by a planar LAO RNA (Technician 2). Then, the patient was allowed to rest in the waiting room for at least 15 min and a second planar LAO RNA acquisition was realized (Technician 1). The LAO acquisitions were processed at 8 frames/RR with a widely validated software. The GSPECT were processed using 2 different softwares: QGS (Cedars-Sinai) and SU (Stanford University). Processing was realized twice by 2 different observers with a one-week interval. The % variation between 2 measurements was calculated as the % of their difference normalized to their average. The intra and inter observer and interstudy % variabilities and paired absolute difference of LVEF were calculated and compared between planar LAO, QGS and SU.
Results: The intra-observer, inter-observer and inter-study % variation for LVEF calculated with LAO, QGS and MD were respectively (0±7 %, 0±5 % and -5±13* %; (*) p<0.05 for the variance), (0±11 %, 1±7 % and -3±23* %;(*) p<0.05 for the variance) and (2±10* %, -6±27 % and -6±30 %;(*) p<0.05 for the variance). The corresponding absolute paired difference were respectively (0±2 %, 0±2 % and -2±5 %), (0±3 %, 1±3 % and -2±11 %) and (2±3 %, -4±10 % and -3±9 %).
Conclusion: The reliability for LVEF is best with planar LAO RNA as compared to rest ^{201}Tl GSPECT. It should remain the preferred technique for the measurement of the temporal evolution of LVEF in a given patient.

PS_371

DETECTION OF TRANSIENT ISCHEMIC MYOCARDIAL STUNNING FROM EARLY AND DELAYED GATED SPECT THALLIUM-201 MYOCARDIAL PERFUSION IMAGING BY AUTOMATED QUANTITATIVE ANALYSIS

M. Mirzaitehrane (1), S. Heiba (2), F. Dede (3), J. Santiago (2), S. Jana (2), H. Abdel-Dayem (2). (1) Department of Cardiology, St. Vincent's Catholic Medical Centers of New York; (2) Nuclear Medicine Service, Department of Radiology, St. Vincent's Catholic Medical Centers of New York; (3) International Research Fellow, Turkish Science Foundation, Marmara University, Turkey.

AIM: We investigated the feasibility of automated quantitative analysis in detecting post ischemic myocardial stunning from immediate post stress and delayed gated SPECT imaging with Thallium-201.
METHOD: We studied 1640 myocardial segments in 82 patients (52 men), average age of 60, who underwent treadmill exercise (n: 57) or dobutamine (n: 25) stress test with both early and delayed gated SPECT Thallium-201 myocardial perfusion imaging using a commercially available software (autoQUANT™). Perfusion score, % wall thickening and degree of wall motion for each segment were derived from automated quantitative analysis. A scale of 5 points was used in the automated segmental summation perfusion score. Stunning was identified by increase in % wall thickening or degree of wall motion at delayed as compared to early images.
RESULTS: There was good correlation between wall thickening and wall motion in post stress and delayed images in ischemic (Pearson correlation = .728 & .739) fixed defect (.652 & .695) and normal perfusion segments (.529 & .585). Of 1640 segments studied (in the 20 segment model), there were 482 segments with abnormal perfusion. Out of those abnormal segments, there were 338 ischemic and 144 fixed defect segments. In the 338 ischemic segments the mean wall thickening increased from 25.33 to 29.33% (p <0.001) and mean wall motion score increased from 4.69 to 5.19 mm (p <0.001) between the immediate post stress and delayed images indicating transient stunning. When mild ischemic segments (only 1 score improvement at delayed images) were excluded, the mean wall thickening score in the remaining segments (120) increased from 24.4 to 29.4% (p <0.001) while the mean wall motion increased from 4.3 to 5 mm (p <0.005). These changes were also more significantly noticed in moderate or severely ischemic segments than mildly ischemic ones. No significant differences, however, were seen in the wall motion and thickening measurements between early and delayed images in segments with fixed perfusion abnormalities.
CONCLUSION: In the post stress and delayed gated SPECT Thallium-201 studies, wall thickening and wall motion measurements derived from automated quantitative analysis correlate well in all types of myocardial perfusion. Both quantitative measurements can be used in the detection of post ischemic myocardial stunning and show significant relationship to the severity of myocardial ischemia.

PS_372

IMPROVEMENT IN ESTIMATION OF LEFT VENTRICULAR FUNCTION WITH TC-99M TETROFOSMIN GATED-SPECT : A MULTIVARIATE ANALYSIS

A. Okizaki, N. Shuke, H. Hirota, J. Sato, Y. Ishikawa, W. Yamamoto, K. Kikuchi, T. Aburano. Department of Radiology, Asahikawa Medical College, Asahikawa, Japan.

Aim: The purpose of this study was to improve accuracy in estimating the quantitative parameters related to left ventricular function from Gated-SPECT through an empirical approach by multivariate analysis. **Methods:** Ninety-six patients with various cardiovascular diseases were studied. After an injection of Tc-99m Tetrofosmin (740MBq), Gated-SPECT was performed on a three-headed digital gamma camera system. Left ventricular ejection fraction (EF), end-diastolic volume (EDV) and end-systolic volume (ESV) were calculated from the gated SPECT data with the QGS program. Left ventriculography (LVG) was performed within 2 weeks after the SPECT. EF, EDV and ESV were also calculated from LVG by area-length method for references. Multivariate analyses were performed with EF, EDV and ESV from LVG as dependent variables and height, heart rate (HR) , age and EF, EDV, ESV obtained by the QGS program as explanatory variables to determine empirical formulas for predicting these parameters. The predicted values of EF, EDV and ESV by the determined empirical formulas were compared with those obtained directly from the QGS program in correlation with the results of LVG. **Results:** Multivariate analyses could improve accuracy in estimation of EF, EDV and ESV. Results were summarized in the table. Statistically significant improvement was seen in EF. Although not statistically significant, improvements in correlation coefficients were seen in EDV and ESV.
Conclusion: The empirical approach by multivariate analysis could improve the accuracy in estimating EF from Gated-SPECT.

	Multivariate Analysis		QGS	
	R^2	SE	R^2	SE
EF	0.65504*	8.94763	0.48512	10.63666
EDV	0.33670	40.71570	0.32418	40.94073
ESV	0.57285	27.38880	0.51825	28.61870

R^2: correlation coefficients
SE: standard errors of estimates
* $p<0.05$

PS_373

GATED 201-TL PLANAR PERFUSION IMAGING FOR SIMULTANEOUS EVALUATION OF PERFUSION AND LEFT VENTRICULAR FUNCTION

D. Sobic-Saranovic, S. Pavlovic, N. Kozarevic. Institue of Nuclear Medicine, CCS, Belgrade.

SPET and planar ECG-gated 99mTc-MIBI scintigraphy has been used during the past few years for the simultaneous evaluation of myocardial perfusion and left ventricular ejection fraction (LVEF).
Aim: The aim of this study was to evaluate the feasibility of planar ECG-gated 201-Tl scintigraphy (GTL) in the assessment of resting LVEF at the same time as evaluation of myocardial perfusion.
Methods: Seventeen coronary patients, 14 with angina pectoris and 3 with previous myocardial infarction were studied. 201-Tl was administered at dose of 150MBq at the end of submaximal exercise, and stress SPET perfusion images, and 4 hours later redistribution images were performed. After stress perfusion images acquisition, eight frames per cardiac cycle studies were performed in LAO 45 view. After digital smoothing, regions of interest were drawn in all frames along the endocardial border of the left ventricle. LVEF was computed from time-activity curve. The results were correlated with LVEF determined in all patients by equilibrium radionuclide ventriculography (ERNV) performed within 1 week of the 201-Tl study.
Results:LVEF determined by GTL ranged from21% to 82% (mean+/-S.D.:55+/-14%), while the mean LVEF assessed by ERNV was 59+/-12% ($p>0.05$). Correlation between these two methods foe LVEF was r=0.88. Inter-observer variability for GTL LVEF was r=0.81, while intra-observer reproducibility was r=0.86. In 2 of 17 patients determination of LVEF was impossible because of left ventricular obliteration.
Conclusions:Using gated planar 201-Tl imaging, left ventricular function can be evaluated at the same time as myocardial perfusion, with the same dose of 201-Tl, but care is needed to obtain reproducible results.

PS_374

LEFT VENTRICULAR FUNCTION EVALUATED WITH REST 201TL NON-GATED SPECT AS COMPARED TO ECG-GATED SPECT

D. Daou (1), C. Coaguila (1), B.O. Helal (1), T. Fourme (2), I. Carel (2), R. Lebtahi (3), M. Faraggi (3), M. Slama (2), D. Le Guludec (3). (1) Department of Nuclear Medicine, Antoine Beclere Hospital, AP-HP, Clamart, France; (2) Cardiology Department, Antoine Beclere Hospital, AP-HP, Clamart, France; (3) Department of Nuclear Medicine, Bichat Hospital, AP-HP, Clamart, France.

Aims: Left ventricular (LV) function evaluated with ^{201}Tl ECG-gated myocardial perfusion SPECT (GSPECT) is valuable. It allows the estimation of LV end-diastolic volume (EDV), end-systolic volume (ESV) and ejection fraction (EF). These parameters have been largely validated, particularly with the QGS software. For different reasons gating may not be realized in some studies. We simulated this situation by summing a GSPECT study into a non-gated study (sSPECT). This reduces the LV function information available with GSPECT into only one measure of LV volume (sV). We aimed to quantitate the amount of information provided by the sV measured with QGS on a sSPECT study as compared to LV function information provided by the corresponding GSPECT study (EDV, ESV, EF).
Methods: Ninety patients with CAD having both a rest ^{201}Tl GSPECT study and a planar left anterior oblique equilibrium radionuclide angiography (RNA) were studied. 48/90 patients had also radiological LV angiography (Rx). Using the QGS software, LV EDV, ESV and EF were calculated on the GSPECT. Then, a sSPECT study was generated from each GSPECT study and a corresponding LV sV was calculated with the QGS software. Were compared the correlations of sV and GSPECT EDV, ESV, and EF with respectively the EDV-Rx, ESV-Rx and planar RNA LVEF. The correlations of sV versus respectively GSPECT EDV, ESV and EF were also studied.
Results: The sV presents high correlation with the GSPECT EDV and ESV; similar good correlation to EDV-Rx and ESV-Rx as GSPECT EDV and ESV; good correlation with GSPECT LVEF. However, as compared to GSPECT, sV presents a lower correlation to planar RNA LVEF.

LV r/ser	Planar EF	EDV-Rx	ESV-Rx	sV
SV	-0.69 / 13	0.77 / 40	0.86 / 27	-
EDV-QGS	-	0.79 / 38	-	0.99 / 12
ESV-QGS	-	-	0.87 / 26	0.99 / 11
EF-QGS	0.84 / 10	-	-	-0.77 / 10
p=0.001 for all linear regression correlations				

Conclusion: Because of better evaluation of LV function, gated ^{201}Tl SPECT should be preferred to non-gated SPECT. In non-gated SPECT studies, sV presents good correlation with LV function and should be realized routinely.

PS_375

DETERMINATION OF LEFT VENTRICULAR EJECTION FRACTION BY GATED 99MTC-MIBI SPECT ON THE BASIS OF OUR EXPERIENCE. CORRELATION WITH ANGIOGRAPHY

M. Kobylecka (1), A. Rak (2), J. Kunikowska (1), L. Krolicki (1), G. Opolski (2). (1) Department of Nuclear Medicine, Medical University; (2) Chair and Department of Cardiology and Internal Medicine, Medical University, Warsaw, Poland.

Left ventricular ejection fraction (LVEF) is one of the most powerful predictors of prognosis. There are several techniques providing the ejection fraction information used in clinical practice. However the concordance between them is various in different medical centres. Aim of this study was the comparison between Gated 99mTc-MIBI SPECT LVEF and LVEF obtained from contrast ventriculography in our hospital.
Method: 28 patients (9 women 19 men) aged 34-68 (mean age 52, SD 9,43) with established CAD, reported for coronary angiography were included. All patients underwent the contrast ventriculography and the MIBI-perfusion study using a standard two days stress/rest MIBI SPECT protocol with G-SPECT at rest.
Ejection fraction (EF) was calculated from G-SPECT resting perfusion images using the commercial software (QGS-SPECT). A standard technique was used for EF calculation during contrast ventriculography.
Results: EF obtained from G-SPECT ranged from 28% to 68% with a mean value 54.30 (SD 11.04)
EF calculated from contrast ventriculography ranged from 54% to 86% with a mean value 73.00 (SD 11,70) The differences between G-SPECT EF and contrast ventriculography EF were significant ($p<<0,05$), mean value 18,72 (SD7,10).The correlation coefficient calculated for EF between both modalities was 0,81
G-SPECT tend to underestimate LVEF compared to contrast ventriculography. It is important to use only one technique for EF measurement for patients follow up studies. However if comparison of different modalities EF data is necessary, the calculated correlation coefficient would be helpful.

PS_376

A NONINVASIVE METHOD TO DIAGNOSE MDR RELATED PGP EXPRESSION BY PARALLEL ADMINISTRATION OF 18FDG AND 99MTC-MIBI

T. Márián (1), N. Szincsák (2), H. Nagy (3), L. Galuska (4), K. Goda (3), K. Bálint (2), L. Balkay (1), L. Trón (1), Z. Krasznai (3). (1) PET Center; (2) Department of Dermotology; (3) Department of Biophysics and Cell Biology; (4) Center of Nuclear Medicine, University of Debrecen, Hungary

To detect the presence of Pgp in the tumours of patients several assays have been worked out on the mRNA or Pgp protein level. However, these methods do not provide information about the dynamic function of the Pgp drug efflux pump. It was reported recently that ^{99m}Tc-hexakis-2-methoxybuthyl isonitrile (MIBI) uptake is drastically reduced in cancer cells that expresses the multidrug resistance (MDR) product, Pgp 170 kDa (Pgp), suggesting that ^{99m}Tc-MIBI is a transport substrate for this transmembrane glycoprotein. The success of tumour imaging with PET and 2-deoxy-2-fluoro[^{18}F]-D-glucose (^{18}FDG) is based on preferential accumulation of ^{18}FDG in tumours. The ^{18}FDG uptake is metabolic rate dependent. In our recent study, we explored if the Pgp substrate modulator verapamil modifies ^{18}FDG and/or ^{99m}Tc-MIBI accumulation in tumour tissues similarly to that of measured in vitro in cell culture, enable us better in vivo visualization of tumours and provide non invasive method for the prediction of overexpression of the drug efflux pump P-glycoprotein. *Methods:* In a SCID BC-17 mice model, the drug-sensitive KB-3-1 human epidermoid carcinoma tumour and the KB-V1 Pgp expressing human carcinoma tumour were grown in opposite flanks. In vivo visualization of multidrug resistance was done in a pinhole collimator equipped gamma camera. For validation, in vitro and biodistribution studies with ^{99m}Tc-MIBI and ^{18}FDG were carried out using gamma counter. The expression of the MDR product was proved by immunohistochemistry. *Results:* ^{99m}Tc-MIBI uptake was significantly lower in KB-V1 Pgp expressing human carcinoma tumours compared to the KB-3-1 human carcinoma tumours MDR+/MDR- = 0.61±0.13, while the ^{18}FDG uptake was 1.38±0.06 times higher in the MDR+ tumours (n=4). When the animals were preincubated for 30 min with verapamil (0.1 mg/kg) the ^{99m}Tc-MIBI ratio of the MDR+/MDR- tumours decreased to 0.38±0.05 while ^{18}FDG uptake increased to 2.08±0.33. *Conclusions:* Since verapamil treatment increases the ^{18}FDG uptake with simultaneous decrease of the ^{99m}Tc-MIBI accumulation of MDR+ tumours, the parallel application of the drugs and verapamil treatment seems to be a good candidate for a noninvasive marker to diagnose MDR related Pgp expression in tumours.

PS_377

TISSUE-SPECIFIC HSV THYMIDINE KINASE (HSVTK) GENE TRANSFER ON GANCICLOVIR UPTAKE AND PROLIFERATION IN MEDULLARY THYROID CARCINOMA

S. Jiang (1), A. Altmann (1), S. Sieger (1), F. Schönsiegel (1), J. Kleinschmidt (2), U. Haberkorn (1). (1) Clinical Cooperation Unit Nuclear Medicine; (2) Applied Tumor Virology, Cancer Research Center, Heidelberg, Germany.

The calcitonin (CT) gene is expressed in thyroidal C-cells and in neoplastic cells derived from them and could be used for tissue specific expression of therapeutic genes. However, the regulatory elements of the CT gene are weak in rAAV-mediated transgene expression. Therefore, we investigated the effects of viral vectors with enhancer amplification on the expression of the HSVtk gene in medullary thyroid carcinoma (MTC) cells.

Methods: Three CT enhancer fragments and tissue-specific elements (EtsE2) were linked to the CT promoter upstream of the HSVtk gene (rAAV3×CTenhCTHSVtk). At 44 h after infection of HeLa cells and rMTC 6-23 cells (rat medullary thyroid carcinoma) with this construct and a construct bearing a single CT enhancer element (rAAVCtenhHSVtk) the cells were pulsed with ^{3}H-GCV for 6 h. Furthermore, a ^{3}H-thymidine (^{3}H-TdR) incorporation assay was performed after treatment with 12.5 µM GCV for 2 h. The radioactivity in the acid-insoluble fraction of the cells was counted and normalized to the viable cell number.

Results: The ^{3}H-GCV uptake in rMTC 6-23 cells infected with rAAVCtenhHSVtk was 2.4-fold higher than that in HeLa cells. After infection of rMTC 6-23 cells with rAAV3×CTenhCTHSVtk the ^{3}H-GCV uptake increased up to 17-fold of that in HeLa cells, whereas no significant difference between both tissue specific constructs was observed in infected HeLa cells. ^{3}H-TdR incorporation in rMTC 6-23 cells infected with rAAV3×CTenhCTHSVtk decreased to 2% of cells without infection whereas the ^{3}H-TdR incorporation in cells infected with rAAVCtenhHSVtk decreased to 79.4% of the controls.

Conclusion: The multi-enhancer elements of calcitonin not only significantly enhance HSVtk gene expression but also maintain a high tissue-specificity as shown by their effects on ganciclovir and thymidine uptake. These tissue specific effects should be detectable in vivo using the corresponding radiolabeled compounds.

PS_378

CORRELATION OF TC-99M (V) DMSA AND TC-99M MIBI WITH CALCITONIN GENE RELATED PEPTIDE (CGRP) AND CALCITONIN (CT) IMMUNOHISTOCHEMISTRY IN INVASIVE AND PREINVASIVE BREAST LESIONS

V. Papantoniou (1), L. Nakopoulou (2), J. Christodoulidou (3), E. Papadaki (1), V. Valotassiou (1), M. Souvatzoglou (1), A. Stipsaneli (1), A. Louvrou (4), A. Keramopoulos (4), S. Michalas (4), C. Zerva (1) (1) Department of Nuclear Medicine; (2) Department of Pathology University of Athens ; (3) Department Radiology; (4) Department of Obst. and Gyn. Alexandra Hospital University of Athens , Greece

The purpose of this study was to derermine immunohistochemically the presence or absence of CGRP and Ct in invasive and preinvassive breast lesions and further to investigate their correlation with tumour Tc-99m (V) DMSA and Tc-99m MIBI uptake by scintimammography.

Material and Methods: 29 patients with histologically proven breast cancers have been submitted to Tc-99m (V) DMSA and Tc-99m MIBI scintimmamography in separate sessions before surgery, 10 and 60 min after administration of 25-30 mCi (740-925 MBq) of each tracer. Immunohistochemistry for CGRP and Ct was performed on the surgical specimens. (V) DMSA and MIBI T/B ratio and retension ratio (RR=T/B delayed-T/B early) were calculated and correlated (t-test) with CGRP and Ct expression in invasive (I.C.) and invasive carcinomas associated with preinvasive lesions as DCIS or epithelial hyperplasia (I.C. + DCIS or E.H.). Linear regression analysis was also performed between (V) DMSA and MIBI retention ratio and CGRP and Ct concentrations in the invasive and the preinvasive component of the tumors associated with. The presence or absence of microcalcifications was studied in relation to CGRP and Ct expression.

Results: Histology confirmed 15 I.C. and 14 I.C. associated with DCIS or E.H. 7/15 (46%) I.C. and 10/14 (71,4%) I.C.+DCIS or E.H. were CGRP positive. T-test showed statistically significant difference between CGRP concentration in I.C. and I.C.+DCIS or E.H. (I.C. = 12,3±7,8 , I.C.+DCIS or E.H = 20±10 , p<0,05). Ct positivity was found only in 2 cases where CGPR was also increased. All CGRP positive I.C.+DCIS or E.H. were grade I or II and all CGRP negative were grade III. (V) DMSA retention ratio demonstrated positive correlation with CGRP in the preinvasive component (r=0,600, p<0,05) MIBI retention ratio did not show a positive correlation. CGRP and Ct positivity was not observed to be related to the presence or absence of microcalcifications.

Conclusion: CGRP is more frequently found than Ct in breast cancer cells. Its cellular concentration seems to be enhanced in cancers with DCIS or epithelial hyperplasia this is associated with the tendency of (V) DMSA to concentrate in such lesions and indicates a possible functional relationship between the two substances. The presence of CGRP in low grade cancers may reflect its precocious role in the process of cancerous cellular deformation, in view of its known relationship with the blood flow rate in breast vessels and its participation in neoangiogenesis.

PS_379

NON-INVASIVE IMAGING OF AD-VECTOR-TRANSFECTED OVARIAN XENOGRAFTS

T.R. Chaudhuri (1), B.E. Rogers (2), J.M. Mountz (1), E.E. Partridge (3), K.R. Zinn (1). (1) Department of Radiology, Division of Nuclear Medicine; (2) Department of Radiation Oncology; (3) Department of Obstetrics and Gynecology, Gynecologic Oncology, University of Alabama at Birmingham, AL 35294, UK.

Aim: The purpose of the present study was to develop a light-based non-invasive imaging method to assess ovarian tumor during therapy in live mice.

Methods: Ovarian tumor cells SKOV3 were transfected with adenoviral vector encoded for GFP. GFP-positive SKOV3 cells were implanted intraperitonealy (i.p.) in 4 groups of six athymic nude mice. The sensitivity of the light-based imaging approach was evaluated by introducing only $1x10^6$ GFP-positive cells, and by conducting imaging early after implantation. In the first experiment, the images were collected at 1 hour after i.p. implantation and after 4 days. Second experiment was conducted to test if the effect of adriamycin therapy could be visualized by light-based imaging in live animal. This included 2 groups of mice (6/group). The first group was injected i.p. with adriamycin (50 µg /mouse) at 24 h after the implantation of the GFP-positive SKOV3 cells. The second group received 0.5 ml of normal saline i.p. For imaging, the mice were maintained under Enflurane anesthesia. Images were collected at 1 hour, day 3 and 5 using a fluorescence stereo microscope. In both experiments GFP-positive cells, tumor nodules and peritoneal wash were collected in sterile media for culture, viability tests and cell counts.

Results: In the first experiment, at 1 hr *in vivo* images showed multiple regions of green fluorescence outlining the intestine in all mice. From 4 day images, i.p. tumors were detected externally in all live mice by light-based imaging. This experiment averaged 3.4+0.5 tumors/mouse. The size of tumors ranged between 0.2-1.5 mm in diameter from 4mm depth. In the second experiment, GFP-positive SKOV3 cells were killed by adriamycin *in vivo* and the green fluorescence was diminished with time. By using special filters, GFP and orange fluorescence of adriamycin were simultaneously imaged in the same field without interfering each other. Day 2 images showed the tumor color to be orange-green. In addition, a region in the same abdominal field was orange. The orange color was due to uptake of adriamycin. It was obvious that in the adriamycin-treated mouse the green fluorescence was greatly decreased, while the tumor region in the control mouse still retained the original brilliant green fluorescence. Day 4 images showed complete disappearance of green fluorescence and appearance of bright orange fluorescence. Cell viability test showed that adriamycin treatment

resulted in significantly fewer GFP-positive cells on days 2, 4, and 5. On day 2, 2.2% GFP-positive viable tumor was measured from the adriamycin-treated mice. On day 4, only 0.03% GFP-positive viable tumor cells was measured. *In vivo* imaging on day 5 showed no GFP-positive region and viable tumor cells were not detected.
Conclusions: The present study demonstrated that light-based imaging is a highly sensitive *in vivo* tool for the early detection and monitoring of human ovarian tumors in mice models. This provides valuable information for evaluation of anti cancer therapy. This would be of great diagnostic utility to gynecologists, especially in detecting primary and recurrent i.p. tumors at an early stage.

PS_381

IODIDE UPTAKE IN CARCINOMA CELLS AFTER TRANSFER OF THE HUMAN THYROID PEROXIDASE GENE

U. Haberkorn (1), A. Altmann (1), S. Jiang (1), I. Morr (1), M. Mahmut (1), M. Eisenhut (2). (1) Clinical Cooperation Unit Nuclear Medicine; (2) Dept. of Nuclear Medicine, Cancer Research Center, Heidelberg, Germany.

The human thyroperoxidase (hTPO) is critical for the accumulation of iodide in thyroid tissues. Poorly differentiated and anaplastic thyroid tumours which lack thyroid specific gene expression fail to accumulate iodide and, therefore, do not respond to ^{131}I therapy. We, therefore, investigated, whether the transfer of the hTPO gene is sufficient to restore the iodide trapping capacity in undifferentiated thyroid and non-thyroid tumour cells.
Methods: The human anaplastic thyroid carcinoma cell lines C643 and SW1736, the rat Morris hepatoma cell line MH3924A and the rat papillary thyroid carcinoma cell line L2 were used as *in vitro* model systems. Employing a bicistronic retroviral vector based on the myeloproliferative sarcoma virus for the transfer of the hTPO and the neomycin resistance gene the C643 cells and SW1736 cells were transfected while the L2 cells and MH3924A cells were infected with retroviral particles. Seven recombinant C643 and seven SW1736 cell lines as well as four recombinant L2 and four MH3924A cell lines were established by neomycin selection. They were studied for hTPO expression using an antibody based luminescence kit followed by the determination of the enzyme activity in the guaiacol assay and of the iodide uptake capacity in presence of $Na^{125}I$.
Results: Genetically modified cell lines expressed up to 1800 times more thyroperoxidase as compared to wild type tumour cells. The level of hTPO expression varied significantly between individual neomycin resistant cell lines suggesting that the recombinant retroviral DNA was integrated at different sites of the cellular genome. The accumulation of iodide, however, was not significantly enhanced in individual recombinant cell lines irrespective of low or high hTPO expression. Moreover, there was no correlation between hTPO expression and enzyme activity in individual cell lines.
Conclusion: The transduction of the hTPO gene per se is not sufficient to restore iodide trapping in non-iodide concentrating tumour cells. Future studies have to concentrate on the possible expression of enzymatically active proteins or the transfer of multiple genes involved in iodide trapping.

PS_380

CORRELATION BETWEEN IN VIVO AND IN VITRO DETECTION OF PROGRAMMED CELL DEATH IN AN INTRACARDIAC TUMOR

P.W.L. Thimister (1), L. Hofstra (2), E. Dumont (4), H. Boersma (1), A. DeBruine (3), TH. Elenbaas (2), G. Kemerink (2), C. Reutelingsperger (4), G. Heidendal (1). (1) Department of Nuclear Medicine, University Hospital Maastricht, The Netherlands; (2) Department of Cardiology, University Hospital Maastricht, The Netherlands; (3) Department of Pathology, University Hospital Maastricht, The Netherlands; (4) Department of Biochemistry, Cardiovascular Research Institute, University of Maastricht, The Netherlands

Aim: In vivo detection of cell death may aid the diagnosis and therapy selection in localized malignant tumours. Because high proliferation and apoptotic indices have been reported in rapid growing malignant tumours, information about the extent of cell death in the tumour may give insight into the biology of the process. This report describes the case of a 65 year old male patient with a large intra-cardiac tumour in which cell death was monitored both in vivo (by using 99mTc-Annexin V) and in vitro (immuno-histochemical analysis and post mortem investigation).
Methods: The tumour was localized by echocardiography. One day prior to surgery, approx. 800µg of Annexin V, (Apomate, Theseus Imaging Cambridge, MA, U.S.A.) labelled with 744 MBq of 99mTc was given intravenously. In order to correctly localize the heart, 201 Tl was injected 4 hours after the injection of Annexin V. Single photon emission computerized tomography (SPECT) was performed 10 hours after the injection of Annexin V, using a dual emission protocol. After removal of the tumour, immuno-histochemical analysis was performed for the detection of Annexin V and characterization of the tumour.
Results: A large area of 99mTc-Annexin V uptake was seen, localized within the left ventricle cavity as observed with Thallium perfusion scintigraphy. Immuno-histochemical analysis of the tumour showed a high-grade sarcoma, containing a high frequency of apoptotic cells as evidenced by the presence of active Caspase 3, correlating well with the scintigraphic results. Post mortem analysis showed a large tumour mass, which almost occluded the left ventricle.
Conclusion: These data demonstrate the feasibility of the 99mTc-Annexin V imaging protocol to obtain non invasively information of cell death in malignant (cardiac) tumours, and the excellent correlation between in vivo and in vitro detection. This could be of importance for the evaluation of malignant tumours, especially in diagnosis and selection of the most appropriate therapy.

PS_382

RADIOIODINATED BMIPP AS LIPOSARCOMA IMAGING AGENT IN TUMOR BEARING NUDE MICE

T.S. Lee, Y.S. Suh, K.S. Woo, W.S. Chung, S.J. Lim, S.J. Lee, C.W. Choi, S.M. Lim. Cyclotron Application Lab., Korea Cancer Center Hospital, Seoul, Korea.

Objectives ^{123}I labeled fatty acids are used for evaluation of the extent of regional myocardial metabolism. This study was aimed to evaluate the possibility of radioiodinated BMIPP as liposarcoma imaging agent. We compare *in vitro* uptake between liposarcoma(HTB-92) and glioma(9L) cell lines and examine biodistribution and *in vivo* images of ^{123}I-BMIPP in liposarcoma bearing nude mice.
Methods Glioma and liposarcoma cells were harvested and counted with _ counter after incubation of 5, 10, 15, 30, 60, 120, 180 mins with medium containing ^{123}I-BMIPP. The difference of biodistribution was determined between non-feeding(water only) group for 18 hr and feeding group in normal mice(n=3 / group) at 0.5, 2, 24 hr. For liposarcoma bearing nude mice model, liposarcoma, HTB-92, cell lines injected S.C. into left thigh of nude mice. The biodistribution of ^{123}I-BMIPP was evaluated at 0.5, 2, 24 hr (n=5 / group) and *in vivo* image of ^{123}I-BMIPP was obtained with _ camera at 2, 24 hr in liposarcoma bearing nude mice.
Results HTB-92 cell line showed increased uptake than 9L with 1.5 times at 180mins. The uptake of ^{123}I-BMIPP in liver, heart, muscle and fat tissues was higher in non-feeding group than in feeding group, especially at delayed time(24 hr) in the biodistribution of normal mice. In liposarcoma bearing nude mice, T(tumor)/ B(blood) ratio of ^{123}I-BMIPP was 0.94, 0.75, 1.38 and T(tumor)/ M(muscle) ratio was 0.66, 1.53, 1.11 at 0.5, 2, 24hr, respectively. ^{123}I-BMIPP was selectively localized in liposarcoma at 2, 24 hr image.
Conclusions The ratio of tumor to background was the highest at 24 hr in biodistribution studies. The localization of ^{123}I-BMIPP was clearly defined in tumor in liposarcoma bearing nude mice at 24hr. ^{123}I-BMIPP may be used for the diagnosis of liposarcoma.

PS_383

DIFFERENTIAL ROLES OF OSTEOTROPIC TC-BISPHOSPHONATES (TC-BP) AND TC(V)-DMS IN BIOLOGICAL AND PATHOLOGICAL ANIMAL MODELS AND BONE CELL CULTURE

K. Horiuchi-Suzuki (1), S. Fukuda (2), A. Konno (1), Y. Fukuda (1), H. Kobayashi (3), H. Saji (1). (1) Pathofunctional Bioanalysis, Kyoto University, Kyoto, Japan; (2) International Space Radiation Lab., National Institute of Radiological Sciences, Anagawa, Chiba, Japan; (3) Diagnostic and Interventional Imagiology, Kyoto University, Kyoto, Japan.

During past decades, bone scintigraphy has been the most sensitive imaging method for detecting skeletal metastases but low specificity in suspected malignancy has decreased its oncological use. Bone scintigraphy has relied on Tc-BP agents with great affinity for the mineral phase, the hydroxyapatite. On the other hand, the pentavalent technetium complex of dimercaptosuccinic acid, Tc(V)-DMS, has been known for its osteotropic character in pathological bone (osteosarcomas, bone metastasis, Paget"s disease) and in non-mature bone (children, rodents) but absent in normal adult bone. Aims: Studies on the osteotropic affinity of Tc-BP and Tc(V)-DMS in various biological (aging) and pathological (OVX, low phosphate diet) animal models and in bone cellular system. Methods: As Tc-BP agent, Tc-MDP and Tc-HMDP kits, and Tc(V)-DMS are used. Mice of different ages (5, 7, 9, 11, 23 wk), ovariectomized (OVX) rats and hypophosphatemic mice (low Pi diet, 5 d) (HypoP) are comparatively screened. Moreover, in bone cellular studies, osteoblastic (OB) cells isolated from neonatal mouse calvaria by enzymatic digestion and cultured at 37ûC (6-8 d) until confluency and osteoclastic (OC) cells harvested by co-culture of OB cells with mice (6 wk) bone marrow and isolated by Percoll fractionation were used. The differential OB and OC cells uptake of Tc-agents carried out at 37ûC using HEPES buffer at pH 7.4, at various incubation time. Results: Aging induced great decrease in mice bone accumulation of both Tc-agents but reduction was more dominant with Tc(V)-DMS. Only this agent showed an increased bone accumulation in OVX and HypoP groups, both pathological models of increased OC activity. Moreover, in cellular studies, differential OC accumulation of Tc(V)-DMS were clearly detected, differing 40 to 50 times over the OB cells; OB cells showed preferential uptake of Tc-BP agents. Conclusion: The osteotropic character of Tc(V)-DMS associated with pathological bone status of animal models with accelerated OC activity. Moreover, in cellular studies, accumulation of Tc(V)-DMS by OC rather than OB cells was clearly detected . Meanwhile, since in clinical studies, Tc-BPs are rather associated with OB cells activity (osteoblastic type metastases), consequences of this differential character of Tc(V)-DMS from Tc-BP in clinical diagnosis will be discussed.

PS_384

A SIMPLIFIED PROCEDURE FOR CONTINUOUS INTRAOPERATIVE EXTERNAL MONITORING OF SYSTEMIC LEAKAGE DURING ISOLATED LIMB PERFUSION CANCER THERAPY

D. Casara (1), D. Rubello (1), P.L. Pilati (2), R. Scalerta (2), C.R. Rossi (2). (1) Servizio di Medicina Nucleare 2, Azienda Ospedaliera di Padova, Padova, Italy; (2) Clinica Chirurgica 2, Università di Padova, Padova, Italy.

Regional isolated perfusion using high doses of chemotherapy has been proposed in patients with loco-regional cancer. A critical step for isolated limb perfusion (ILP) is the accurate monitoring of systemic leakage with the aim of avoiding chemotherapy toxic effects. In the present study we reported our experience in monitoring systemic leakage during ILP in a group of 113 patients affected by a limb cancer: 54 melanoma, 44 sarcoma, 3 squamous cell carcinoma, 1 lymphoma. The majority of patients were treated during ILP with thermotherapy / chemotherapy alone or in combination with tumour necrosis factor (TNF). Regarding ILP technique, cannulas were placed in either external iliac / axillary artery and vein and connected with an extra-corporeal circuit. We used 99mTc-human serum albumin (99mTc-HSA) with 3 different techniques in monitoring the perfusate leak during ILP: the target was to limit the systemic leakage within 10% of the total dose infused in the isolated circuit. Initially, we used the traditional procedure based on radioactivity measurement by means of gamma counter of systemic blood samples drawn from a peripheral vein every 5 min, and compared with samples obtained from the isolated circuit. The second procedure used was based on the measurement of radioactivity counts of the 99mTc-HSA dose before infusion in the isolated circuit, and on the continuos monitoring of systemic radioactivity leakage through an external detector positioned over the hearth. The last procedure we have developed and we currently use, consists of following steps: 1) the 99mTc-HSA dose to be infused during ILP is calculated as 0.5 MBq/kg/b.w.; 2) 72 hours before ILP, a simulation test is obtained injecting the patient with a 99mTc-HSA dose corresponding to 10% of total dose; 3) during the simulation test, radioactivity counts are continuously registered by means of an external hand-held probe positioned over the hearth, and mean counts are calculated during a 30 min time-interval. One of the major advantage of the simulation test is that it allows to depict the precordial area with the highest count-rate activity. This area is marked on patient skin and, the day of ILP, it allows to locate the probe in the same position of simulation test. Another advantage of this procedure is that physicians can know before the infusion therapy, the acceptance limit of systemic count-rate activity. In our experience, this procedure seems to be simple and accurate enough in monitoring systemic leakage during ILP.

PS_385

BONE MARROW SCINTIGRAPHY USING TC-99M MONOCLONAL ANTIGRANULOCYTE ANTIBODIES IN DETECTING BONE METASTASES FROM BREAST CANCER

J. O. Prior (1), G. Storto (1), G. Barghouth (1), A. Boubaker (1), J.-F. Delaloye (2), S. Leyvraz (3), A. Bischof Delaloye (1). (1) Department of Nuclear Medicine; (2) Department of Gynecology; (3) CePO Oncology Center, CHUV University Hospital, Lausanne, Lausanne, Switzerland.

Purpose: To prospectively evaluate bone marrow scintigraphy (BMS) in detecting bone metastases from breast cancer when performed as a complement to conventional bone scan (BS).

Methods: We studied 60 women aged from 37–84 years (*mean±std*: 58±9.6y) with breast cancer (stage I:25, II:27, III:5, IV:4) who underwent conventional Tc-99m-DPD bone scan with a Tc-99m bone marrow scan, 1–35 days (9±7d) later. Anterior and posterior whole-body scans were performed on a dual-head gamma camera (Biad, Trionix, USA). Patients had neither chemotherapy nor radiotherapy in the 6 months preceding imaging. Bone marrow scan was performed 4-6 hours after a 0.5–1mg *i.v.* injection of BW250/183 antigranulocyte antibodies directed against the non-specific cross-reacting antigen NCA-95 labeled with 370MBq/70kg. Metastases on BMS were defined as photopenic lesions concordant to BS lesions or isolated focal lesions in the axial skeleton. Two-experienced nuclear medicine physicians interpreted BS and BMS images and classified observed defects as indicative of benign or metastatic disease. Extension of bone marrow in long bones was also assessed. Results were compared to a gold standard composed of subsequent CT, MRI, X-rays, BS examinations and/or at least a 6-month follow-up.

Results: Metastases were present in 9 out of 60 patients (15%). Sensitivity, specificity, positive predictive value (PPV), negative predictive value (NPV) and accuracy were calculated for BS and BS+BMS on a per patient basis (Table) and are statistically different ($p<0.01$), except for NPV. Bone marrow extension in long bones was observed in 57 patients (95%).

Scintigraphy *(n=60)*	True Negative	True Positive	False Negative	False Positive	Sensitivity	Specificity	PPV	NPV	Accuracy
BS	36	7	1	16	88%	69%	30%	97%	72%
BS+BMS	44	8	0	8	100%	85%	50%	100%	87%

Conclusion: BMS supplements BS by improving sensitivity, specificity, positive predictive value and accuracy in detecting breast cancer bone metastases. BMS may thus be useful in patients with positive or equivocal BS for metastases. Like BS, this method is limited by its inability to show micro-metastases and by its modified distribution after radiotherapy and/or chemotherapy thus possibly masking bone metastatic disease.

PS_386

PROGNOSTIC VALUE OF FLOW CYTOMETRIC DNA MEASUREMENTS IN INDIAN PATIENTS WITH THYROID CANCER

G.V. Punjabi (1), A. Kumar (1), A. .K. Karak (2), S. Das (3), C.S. Bal (1). (1) Department of Nuclear Medicine; (2) Department of Pathology; (3) Department of Biotechnology, All India Institute of Medical Sciences, New Delhi, India.

Aim: It is an well-accepted feature of carcinomas that they have a higher mitotic rate than normal, and they have an increased incidence of karyotypic abnormalities. The available data suggests that the nuclear DNA content of neoplasms reflect their biological behavior and diploid tumors in particular carry a better prognosis. However, no study has been carried out in Indian patients to evaluate ploidy as a prognostic factor in thyroid carcinoma.

Methods: Cellular DNA content was measured using flow cytometric method to analyze paraffin embedded tissue blocks from 74 patients with thyroid cancer. Mean age of the patients was 35.93±13.97 years (range 8-66 years). There were 32 males and 42 females (M: F 1:1.3). There were 18 (24.3) cases of follicular, 46 (62.2%) cases of papillary, 5 (6.75%) cases of medullary, 2 (2.7%) cases of Hurthle cell and 3 (4.0%) cases of Undifferentiated carcinoma thyroid.

Results: DNA histograms were classified as diploid in 31 cases (41.9%) and aneuploid in 43 cases (58.1%). DNA aneuploidy was found in 9 (50%) of 18 follicular, 26 (56%) of 46 papillary, 4 (80%) of 5 medullary, 1 (50%) of hurthle cell and 3 (100%) of 3 undifferentiated carcinomas. Among patients with tumor recurrence, 14 out of 18 had aneuploidy. Local/distant metastases were seen in 42 cases (56.75%) (20 males and 22 females) with mean age of 36.23±15.13 years. Thirty (71.4%) of these cases had aneuploidy. On univariate analysis, aneuploidy ($p=0.03$), male sex ($p=0.01$), and presence of local invasion ($p=0.007$) and metastasis ($p=0.007$) at the time of diagnosis were significant predictors of a shortened disease free survival. However, it was not significantly related to tumor histology, patient age or tumor size. On multivariate analysis, only local invasion (RR – 4.80) and male sex (RR – 4.59) were found to be significant predictors of a shortened disease free survival.

Conclusions: DNA aneuploidy is common in thyroid cancers in Indian population. It is associated with aggressiveness of the tumor, with the presence of metastasis, tumor recurrence and a shortened disease free survival.

PS_387

ENHANCED EXPRESSION OF HSV THYMIDINE KINASE AND HUMAN SODIUM IODIDE SYMPORTER AFTER CHEMO- GENE THERAPY WITH GEMCITABINE AND ADENO ASSOCIATED VIRUS (AAV) VECTORS

S. Jiang (1), A. Altmann (1), J. Kleinschmidt (2), U. Haberkorn (1).
(1) Clinical Cooperation Unit Nuclear Medicine; (2) Applied Tumor Virology Cancer Research Center, Heidelberg, Germany.

Induction of stress e.g. by co-infection with helper virus or by treatment with genotoxic agents results in induction of expression of AAV genes responsible for viral replication. Since the chemotherapeutic drug gemcitabine leads to DNA chain termination these reactions are expected after treatment with gemcitabine and may result in enhancement of suicide gene expression for gene therapy.

Methods: Infection experiments were done in different cell lines (HeLa, MTC, MH3924A, NIH3T3) with and without pretreatment with increasing doses of gemcitabine using vectors bearing the genes for the enhanced green fluorescence protein (EGFP), the sodium iodide symporter (hNIS) or the HSV thymidine kinase (HSVtk). EGFP activity was determined using fluorescence microscopy and quantified with fluoroscan and FACS analysis. The hNIS gene expression was evaluated by iodide uptake. HSVtk activity was determined by the uptake of ^{3}H-ganciclovir or by growth inhibition and inhibition of ^{3}H-TdR uptake after treatment with ganciviovir.

Results: Gemcitabine treatment resulted in a dose-dependent enhancement (up to 21-fold) of transgene expression as measured by all transferred genes. The expression after gemcitabine treatment was equivalent to that obtained after helper virus infection. Labeling of rAAV particles with Cy3 showed no difference between treated and untreated cells in their kinetics of internalization and transport to the nucleus. Furthermore evidence was found that rAAV integration to cell genome is elevated by gemcitabine.

Conclusion: Gemcitabine treatment enhances AAV-mediated transgene expression, which may be measured in vitro using EGFP or in vivo with the HSVtk or the hNIS gene as in vivo reporter genes.

PS_388

SIGMA RECEPTOR SCINTIGRAPHY WITH N-[2-(1'-PIPERIDINYL) ETHYL]-3-[123I]IODO-4-METHOXYBENZAMIDE, P[123I]MBA, IN PATIENTS WITH SUSPECTED PRIMARY BREAST CANCER

V. Caveliers (1), H. Everaert (1), C.S. John (2), A. Bossuyt (1).
(1) Department of Nuclear Medicine, Free University Hospital, Brussels, Belgium; (2) Department of Radiology, George Washington University, Washington DC, USA.

Aim. To visualise in vivo accumulation of a radioiodinated benzamide, P[^{123}I]MBA, in primary breast cancer patients. Uptake of benzamides in breast cancer is based on a preferential binding to sigma receptors that are overexpressed on the tumour cell membrane. The expression and density of sigma receptor sites has been shown to correlate with tumour proliferation.

Methods. Ten patients with a newly diagnosed breast mass and two control patients were included in the study. Radiosynthesis of P[^{123}I]MBA was achieved by iododestannylation of its trimethyltin derivative using chloramine-T as oxidising agent. Approximately two hours after administration of 148-185 MBq P[^{123}I]MBA, whole body and lateral images of both breasts were obtained. Images were interpreted visually and quantified by ROI analysis. Final diagnosis of breast cancer was made based upon histological examination.

Results. All of the patients were ultimately diagnosed with breast cancer. An increased focal tracer uptake within the suspected breast was demonstrated in eight out of ten patients. One patient presented a lesion in the contralateral breast that could not be confirmed as malignant. ROI analysis showed a mean tumour-to-background ratio of 2.04. The two control patients with benign breast conditions presented a normal scan.

Conclusions. Uptake of P[^{123}I]MBA was demonstrated in 80% of the patients with primary breast cancer. If a relationship between in vivo uptake and sigma receptor density can be established, P[^{123}I]MBA scintigraphy may offer a powerful tool to non-invasively assess tumour proliferation.

PS_389

SYNTHESIS AND FIRST IN VIVO EVALUATION OF [I-123]AZA-RGD-1: A RADIOLABLED RGD-MIMETIC FOR THE NONINVASIVE DETERMINATION OF ALPHA(V)BETA3 INTEGRIN EXPRESSION

R. Haubner (1), G. Sulyok (2), W. Weber (1), W. Linke (1), C. Bodenstein (1), H.J. Wester (1), H. Kessler (2), M. Schwaiger (1). (1) Department of Nuclear Medicine, Technische Universität München, Munich, Germany; (2) Institute of Organic Chemistry and Biochemistry, Technische Universität München, Garching, Germany.

The _v_3 integrin plays an important role in tumour metastasis and tumour-induced angiogenesis. Recently, we demonstrated that RGD-containing peptides can be used for selective determination of _v_3 expression using SPECT and PET. Here we describe the synthesis and biological evaluation of 5-[*N'*-(3-guanidinobenzoyl)-hydrazino]-3-(4-hydroxy-3-[^{123}I]iodo)-5-oxopentanoic acid ([^{123}I]Aza-RGD-1) the first radioiodinated RGD-mimetic and compare the in vivo characteristics with the previously described glycopeptide [^{125}I]cyclo(-RGDyK(SAA1)-) ([^{125}I]Gluco-RGD).

Methods: Synthesis of the RGD-mimetic was performed by coupling of different building blocks using solid phase synthesis. Treatment of 3-methoxybenzaldehyde with ethyl acetoacetate and subsequent hydrolysis resulted in the glutaric acid derivative, which was coupled with protected hydrazine, and 3-aminobenzoic acid on the solid support. After guanylation and cleavage from the resin the methylether moiety was cleaved using borontribromide. Labelling of the precursor was carried out using the IodoGen™ method.

Melanoma M21-bearing nude mice were used for the in vivo studies. Planar _-camera images were obtained 2h after simultaneously injecting 7.40MBq [^{123}I]Aza-RGD-1 and 1.85MBq [^{125}I]Gluco-RGD. Imaging time was 10min. Subsequently, animals were sacrificed and biodistribution studies were carried out.

Results: Biodistribution 3h after simultaneous tracer injection showed an approximately 1.6-fold higher uptake of [^{125}I]Gluco-RGD (0.96±0.22%ID/g) in the tumour than of [^{123}I]Aza-RGD-1 (0.60±0.19%ID/g). Activity concentration in blood and muscle was 0.05±0.01%ID/g and 0.13±0.05%ID/g for [^{125}I]Gluco-RGD and 0.08±0.02%ID/g and 0.12±0.04%ID/g for [^{123}I]Aza-RGD-1, respectively. This results in lower tumour/blood (7.4 vs 19.2) and tumour/muscle (5.0 vs 7.4) ratios for [^{123}I]Aza-RGD-1. However, distribution of [^{123}I]Aza-RGD-1 in most of the other organs was lower compared to [^{125}I]Gluco-RGD (e.g. kidney: 0.28±0.09%ID/g vs 0.89±0.31%ID/g; liver: 0,23±0.09%ID/g vs 0.38±0.09%ID/g; lung: 0.17±0.04%ID/g vs 0.32±0.02%ID/g; skin: 0.31±0.08%ID/g vs 0.89±0.14%ID/g). This led to improved tumour/organ ratios for [^{123}I]Aza-RGD-1 (e.g. kidney: 2.1 vs 1.1; liver: 2.6 vs 2.5; lung: 3.5 vs 3.0; skin: 1.9 vs 1.1). Activity concentration in the intestine and thyroid was comparable for both tracer. Planar _ -camera images using [^{123}I]Aza-RGD-1 confirmed the biodistribution data and showed a clearly contrasting tumour. Higher activity concentrations were found in intestine and thyroid only.

Conclusions: Compared to [^{125}I]Gluco-RGD accumulation of [^{123}I]Aza-RGD-1 in the _v_3-expressing tumour is somewhat lower. However, the small non-peptide tracer [^{123}I]Aza-RGD-1 showed further improved elimination kinetics compared with the glycopeptide and is a promising tracer for the noninvasive determination of _v_3 expression using SPECT. Moreover, this readily available precursor also allows labelling with ^{11}C-carbon and introduction of ^{18}F-fluorine.

Poster presentation

PS_390

TENASCIN-C INHIBITS §1 INTEGRIN-DEPENDENT CELL ADHESION BY A DISIALOGANGLIOSIDE-MEDIATED SIGNALING MECHANISM

P. Pesheva, R. Probstmeier, H.-J. Biersack. Department of Nuclear Medicine, University of Bonn, Bonn, Germany.

A characteristic event following neoplastic transformation is often the upregulation of tenascin-C (TN-C) expression thus implying the modulatory role of this extracellular matrix protein in oncogenesis. We have previously shown that TN-C inhibits §1 integrin-dependent cell adhesion to fibronectin (FN) by its interaction with an RGD-independent cellular receptor. The aim of this study was to identify this TN-C receptor on tumor cells and to elucidate the molecular mechanism of inhibitory action induced by TN-C binding.

Methods: Cell adhesion and protein kinase C assays using different tumor cell lines and activators, inhibitors or modulators.

Results: We could demonstrate that the inhibitory effect of TN-C on §1 integrin-dependent cell adhesion on FN is mediated by the interaction of the protein with membrane-associated disialogangliosides which interferes with protein kinase C-related signaling pathways. The following experimental data support these findings. (1) In substrate mixtures with FN, an RGD sequence-containing FN fragment or synthetic peptide, TN-C inhibited tumor cell adhesion by a disialoganglioside-dependent, sialidase-sensitive mechanism leading to an inhibition of protein kinase C. Similar to TN-C, immobilized antibody to GD2 (3F8) or sphingosine, a protein kinase C inhibitor, strongly inhibited RGD-dependent focal cell adhesion. (2) The interaction of intact or trypsinized, i.e. cell surface glycoprotein-free, cellswith immobilized TN-C was strongly inhibited by gangliosides or antibodies to gangliosides and TN-C. (3) A preincubation of immobilized TN-C with soluble disialogangliosides resulted in a delayed cell detachment as a function of time. (4) The degree of TN-C-induced inhibition of cell adhesion was proportional to the degree of disialoganglioside levels of expression by different tumor cells.

Conclusions: In the present study, we describe a novel mechanism of inhibition of RGD-dependent tumor cell adhesion to FN by TN-C which may play a crucial role in the molecular control of cell-matrix interactions during metastasis of highly malignant cells (i.e. neuroblastoma, glioblastoma, melanoma and breast carcinoma cells which express considerable amounts of disialogangliosides). Our findings thus provide a valuable tool towards the possible clinical application of radioactively labeled disialoganglioside-binding TN-C fragments to tumor diagnostics and therapy.

PS_391

GLUT-1 IS OVER EXPRESSED IN HYPOXIC REGIONS OF HUMAN COLORECTAL LIVER METASTASES

T. Akhurst (1), C. Hedvat (2), T. Kates (4), M. Mazumdar (3), I. Linkov (2), S. Mastorides (2), D. Klimstra (2), S.M. Larson (1), Y. Fong (4). (1) Department of Nuclear Medicine; (2) Department of Pathology; (3) Department of Biostatistics; (4) Department of Surgery, Memorial Sloan Kettering Cancer Center, New York, New York, USA

Glut1, Glut3 and Hexokinase over-expression are all thought to play a role in FDG uptake into human colorectal cancers. The distribution of Glut-1 expression in colorectal liver metastases has not yet been described.

Objective: To investigate the distribution of Glut-1 staining in colorectal cancer metastases to the liver.

Methods: Histopathological samples from resected liver metastases of human colorectal cancer were obtained from sections of the tumor that looked grossly viable. Standard tissue fixation was then performed and immunohistochemical staining for Glut 1 transporter expression was performed using the streptavidin peroxidase technique. Blinded readings of the transporter expression were obtained in a four-point scale. 2 Data points were captured for each slide namely the degree of staining in perinecrotic areas („N") and the degree of stain in microscopically viable areas („V").

Results: From 24 patients, 69 specimens were available. The distribution of staining was as follows

	Viable & Scored 0	V& Scored 1	V& Scored 2	V& Scored 3
Peri-necrotic N & scored 0	9	0	0	0
N & Scored 1	3	1	0	
N & Scored 2	2	**11**	5	0
N & Scored 3	4	**20**	7	7

Due to the presence of clusters within ordinal data, a Mcnemar's test with correction for clustering was performed for the presence of any staining versus no staining (Chi-square of 8.555 with p=0.003).

Conclusions: Glut-1 staining in liver metastases is largely seen in peri-necrotic areas, and attempts at correlation with other markers of malignancy may be overwhelmed by this fact. Correlations of HIF-1 and Glut-1 expression in colorectal cancer metastases remain to be investigated.

DIAGNOSTIC ONCOLOGY 10

PS_392

AUTORADIOGRAPHIC IN VIVO DISTRIBUTION OF 111IN-PENTETREOTIDE IN NEUROENDOCRINE GASTROENTEROPANCREATIC (GEP) TUMOURS AND COMPARISON WITH SCINTIGRAPHY

Y. Petegnief (1), R. Lebtahi (2), C. Vissuzaine (2), J.P. Marmuse (2), I. Sobhani (2), M. Mignon (2), D. Le guludec (2). (1) Service de Médecine Nucléaire Hôpital TENON, Paris; (2) Service de Médecine Nucléaire Hôpital Bichat, Paris.

The in vivo distribution of ^{111}In-pentetreotide in neuroendocrine GEP tumours of patients scheduled for surgery was prospectively studied by autoradiography (AR) and compared to scintigraphic findings. Twenty patients (19 adults: mean age 52 ± 7yr and 1 child) were i.v. injected with 135 ± 30 MBq of ^{111}In-pentetreotide: 10 Zollinger Ellison syndrome (ZES), 5 carcinoids tumours (CT), 5 nonfunctioning neuroendocrine tumours (NET). Planar scintigrams (SRS) at 4 and 24 hr post injection and SPECT at 24 hr were obtained at the day before the surgery. Sections from 33 verified tumours (diameter: 1.8 to 50 mm, mean:17 mm) were analyzed by quantitative AR (20-µm thickness) and by immunohistochemistry (3-µm thickness). SRS tumour-to-background ratio (T/B), AR tumour uptake per unit mass of tumour (%IA/kg) were calculated. Intratumoral distribution of both activity and immunohistochemical expression of tumour markers of neuroendocrine differentiation were compared. SRS visualized 30/33 tumours (91%) with variable T/B (2.2 ± 1.5, range 1.05-10). SRS missed 3 tumours with diameter of 3, 8, and 8 mm, and respectively uptake of 5, 2.4, 42 %IA/kg. AR confirmed a tumoral uptake in all 33 tumours with high variations among patients (2.4 to 150 %IA/kg). Uptake was higher for ZES tumours than for CT and NET (35.5 ± 19.2 %IA/kg vs 12.1 ± 5.8 %IA/kg, $p<0.005$). In 5 cases, intratumoral activity patterns were heterogeneous. This was not correlated with the immunohistochemical distribution of neuroendocrine markers. Uptake of ^{111}In-pentetreotide was confirmed in 100% of GEP tumours studied by AR with highly variable uptake, significantly higher for ZES tumours than CT or NET. Intra-tumoral heterogeneous distribution was sometimes found. SRS tumour-to-background findings did not directly reflect the density of somatostatin receptors. Autoradiographic results are more appropriate and confirm the potential of ^{111}In-pentetreotide for therapy specially for ZES tumours.

PS_393

111IN-DTPAOC SCINTIGRAPHY: PLANAR IMAGES VERSUS SPECT IN DIAGNOSIS OF CARCINOID TUMOR AND PANCREATIC NEUROENDOCRINE TUMORS

J. Banzo (1), M.D. Abós (1), E. Prats (1), P. Razola (1), E. Freile (2), S. García (3), F. Gomollón (3), F. García (1), T. Escalera. (1) Nuclear Medicine Department, University Hospital, Zaragoza, Spain; (2) Radiology Department, University Hospital, Zaragoza, Spain; (3) Gastroenterology Department, Miguel Servet Hospital, Zaragoza, Spain.

Somatostatin receptor scintigraphy (SRS) is the first line diagnostic tool for staging neuroendocrine tumors. Nevertheless, there is only slight information about the diagnostic influence of the SRS-SPECT .

The aim of our study was to compare the sensibility of planar scintigraphy and SPECT images in the detection of the primary tumors and metastases in patients with carcinoid tumors (CT) or pancreatic neuroendocrine tumors (PNT),.

Matherials and methods.- We have evaluated using SRS 33 patients, studied for disease staging (n=19) or for post-therapy follow-up (n=14). The patients evaluated for staging were 6 insulinomas, 4 bronchial carcinoids, 2 pancreatic CT, 2 gastrinomas, 2 non-functioning PNT, 1 carcinoid of unknown origin, 1 glucagonoma and 1 somastostatinoma. In the group of patients evaluated in post-therapy follow-up we included 4 bronchial CT, 3 ileal CT, 2 appendix CT, 1 ovarian CT, 1 thymic CT, 1cecal CT, 1 stomach CT and 1 non-functioning PNT. Definitive diagnosis was performed by way of biopsy in all cases. We have compared planar images with SPECT study, 24 abdominal and 10 thoracic, obtained 24 h post ^{111}In-DTPAOC injection (184 MBq)

Results.- The sensibility of planar images in detection of primary tumors was 43,3% (9/19), whereas the sensitivity of SPECT study was 63,1% (12/19). Three primary tumors were demonstrated only with SPECT: 1 bronchial CT, 1 insulinoma and 1 glucagonoma. The sensitivity in the detection of metastases, hepatic and extrahepatic, was 77,7% (13/17) for planar images and 88,2% (15/17) for SPECT.

Conclusions.- In patients with neuroendocrine tumors, abdominal and/or thoracic SPECT increases the sensibility of planar images in the detection of primary tumor and their metastases. Therefore SPECT must be included in the SRS protocols.

PS_394

111IN-OCTREOTIDE BONE METASTASES DETECTION IN CARCINOID TUMORS AND PANCREATIC NEUROENDOCRINE TUMORS

J. Banzo (1), M.D. Abós (1), E. Prats (1), P. Razola (1), S. García (2), F. Gomollón (2), F. García (1), E. Freile (3), T. Escalera (1). (1) Department of Nuclear Medicine, University Hospital, Zaragoza, Spain; (2) Department of Gastroenterology, Miguel Servet Hospital, Zaragoza, Spain; (3) Department of Radiology, University Hospital, Zaragoza, Spain.

There is slight information about the usefulness of somatostatin receptor scintigraphy (SRS) for bone metastases detection in neuroendocrine tumors.
The aim of the study was to retrospectively assess the usefulness of SRS in the detection of bone metastases in patients with carcinoid tumor (CT) or neuroendocrine pancreatic tumor (NPT).
Material and Methods. We included 48 patients whom we classified in two groups according to the request of the clinicians: Group A.- Staging of a known or a clinically or biochemically suspected CT or NPT(n=28): 13 CT, 6 insulinomas, 4 non-functioning NPT, 2 glucagonomas, 2 gastrinomas, 1 somatostatinoma, and Group B.- Follow-up studies (n=21): 20 CT and 1 glucagonoma. One patient was included in the two groups. In all patients the final diagnosis was established by way of biopsy. SRS images were obtained at 4 and 24 h post ^{111}In-DTPAOC injection (184 MBq). Bone scans using ^{99m}Tc-MDP were performed when SRS demonstrated bone metastases or when the patient showed bone pain.
Results. Five patients, 2 of group A and 3 of group B, showed bone metastases (prevalence: 10.41%) located generally in the axial skeleton. The bone metastases were multiple and symptomatic in 3 patients, multiple but asymptomatic in one patient and simple and asymptomatic in the other patient. Bone metastases were associated with liver metastases in all patients. Bone scan detected higher number of metastases than SRS. SRS false negative results corresponded with lesions located in ribs and dorsal-lumbar region, masked by ^{111}In-DTPAOC physiologic activity in liver, spleen and kidneys.
Conclusions. The SRS usefulness in the staging of CT and NPT is increased by its capacity in bone metastases detection. Nevertheless, SRS and bone scan must be considered as complementary techniques, and a normal SRS does not exclude performing a bone scintigraphy.

PS_395

SOMATOSTATIN RECEPTOR SCINTIGRAPHY IN THE FOLLOW-UP OF PATIENTS WITH BRONCHIAL CARCINOID

S. Fanti (1), G. Savelli (2), A. Chiti (3), M. Salgarello (1), G.C. Montini (1), A. Fraternali (1), E. Del Giudice (1), C. Pettinato (1), E. Bombardieri (2), N. Monetti (1). (1) UO Medicina Nucleare, Policlinico S.Orsola-Malpighi, Bologna, Italy; (2) Medicina Nucleare, Istituto Tumori, Milano, Italy; (3) Medicina Nucleare, Istituto Clinico Humanitas, Milano, Italy.

Somatostatin receptor scintigraphy (SRS) has been employed for the diagnosis of neuroendocrine chest tumors, such as bronchial carcinoids (BC), and resulted to be a valuable tool for an accurate staging of BC.
Aim: aim of this study was to evaluate the role of SRS in re-staging and follow-up of patients with BC.
Methods: 25 patients (pts) with BC consecutively referred to the Nuclear Medicine Labs were reviewed (13 males 12 females). Overall, 36 SRS scans were obtained for patients re-staging and follow-up (28 scans in pts already treated with radical surgery and no evidence of secondary lesions; 6 scans in pts already operated on with known secondary lesions; 2 scans in surgically unoperable pts at follow-up). Pts were also studied with chest x-ray (28 scans), chest and/or abdominal CT (18 scans), chest MR (3 scans), liver sonography (6 scans). SRS was carried out at 4 and 24 hours after iv. administration of 250 MBq of 111In-Pentetreotide; all cases were investigated with both total-body scan and SPECT.
Results: out of 25 pts, secondary lesions were demonstrated in 14 and SRS was positive in 13 pts (19 scans). The remaining 11 pts had no evidence of disease, and SRS was negative in all of them (16 scans). Overall, in 16 pts SRS confirmed the information obtained by other diagnostic procedures (11 negatives and 5 positives with same number and site of lesions); in 7 pts SRS showed focal lesions not previously demonstrated; in 1 pt SRS showed less lesions as seen at CT (2 out of 4 hepatic lesions); in one patient SRS failed to show lung metastases suggested by CT and confirmed by pathology (metastatic diameter between 4 and 10 mm).
Conclusions: our results indicate that SRS could be considered as the main follow-up procedure in pts with BC.

PS_396

IMAGING WITH TECHNETIUM-99M SESTAMIBI DOES NOT PREDICT DRUG RESISTANCE OR OUTCOME IN CHILDHOOD NEUROBLASTOMA

C. Van de Wiele (1), B. De Moerloose (2), G. Laureys (2), C. Dhooge (2), K. Swerts (3), Y. Benoit (2), J. Philipp? (3), R.A. Dierckx (1). (1) Department of Nuclear Medicine; (2) Departments of Pediatrics; (3) Clinical Chemistry, Microbiology and Immunology, Ghent University Hospital, Gent, Belgium.

Aims : Tc-99m-sestamibi, a radiopharmaceutical used in tumor detection, has been shown to be a transport subtrate recognised by P-gp and MRP1. Hence, imaging studies using Tc-99m-sestamibi became attractive to evaluate in vivo transport activities of P-gp or MRP1, and to predict drug resistance and therapeutic outcome.
Methods : We evaluated Tc-99m-sestamibi imaging in children suffering from a neuroblastic tumor. These imaging results were compared with expression of P-gp and MRP1 and with the clinical outcome. Twenty children (mean age : 39.5 months) with the diagnosis of neuroblastoma (14), ganglioneuroblastoma (1) and ganglioneuroma (5) were evaluated by Tc-99m-sestamibi imaging at presentation. Scintigraphy was performed 20-30 minutes and 3.5-4 hours after injection of 740 Mbq/1.73 m2 Tc-99m-sestamibi. P-gp expression and activity were determined flow cytometrically. An immunocytochemical APAAP assay was performed to evaluate P-gp and MRP1 expression. The median follow-up was 30.5 months.
Results : Two patients were Tc-99-sestamibi positive. This correlated with the absence of P-gp in vitro but not with the clinical outcome of one of the patients who died from resistant disease. Sixteen others had no Tc-99m-sestamibi uptake in the tumor, which is suggestive for the presence of functional P-gp or MRP1. This was confirmed in 13 of 15 patients tested in vitro. However, 12/16 Tc-99m-sestamibi negative patients are alive without evidence of disease. The others died from resistant disease but had other tumor characteristics associated with bad prognosis. In the remaining 2 patients, Tc-99m-sestamibi scans could not be interpreted because of overlapping physiological tracer uptake.
Conclusions : Tc-99m-sestamibi scanning in neuroblastoma is not useful in tumour detection or stagin. Absence of radionuclide uptake at the tumor site does reflect the presence of functional P-gp but does not contribute of clinical drug resistance in neuroblastoma patients and hence does not give practicle information concerning response to chemotherapy and outcome of the patients.

PS_397

GLUCAGON-LIKE PEPTIDE-1 (GLP-1) RECEPTOR TARGETING: A NEW DIAGNOSTIC OPTION? INITIAL EXPERIMENTAL RESULTS

M. Gotthardt, I. Naeher, M. Fischer, J.-B. Holz, H. Jungclas, M. Béhé, K. Joseph, T.M. Behr. Department of Nuclear Medicine, Philipps-University, Marburg, Germany.

Aim: The problem of non-invasive detection of insulinomas is not appropriately solved by somatostatin receptor scintigraphy as its sensitivity is only about 50%. We investigated the biokinetics and specificity of the uptake and degradation of the incretin hormone Glucagon-Like Peptide-1 (glp-1) in a rat insulinoma cell line (RINm5F) *in vitro* and *in vivo* in order to demonstrate whether radiolabeled glp-1 may be suitable for visualization of insulinomas *in vivo*.
Methods: The iodogen method was used for radioiodination of glp-1 (7-36)amide. The specificity of the I-125-glp-1(7-36)amide uptake into RINm5F-cells was investigated as well as the lysosomal degradation. Degradation products of glp-1 (7-36)amide in the cell medium were purified by HPLC, and their masses and amino acid sequences were subsequently determined by Cf-252-plasma-desorption mass spectrometry. The amount of radiotracer incorporated into lysosomes was measured after differential centrifugation. Biodistribution studies were performed in a rat insulinoma model (NEDH rats and RINm5F-cells) with I-123-glp-1(7-36)amide and its more stable analog I-123-exendin 3. The same model was used for the scintigraphic visualization of insulinomas *in vivo*.
Results: The uptake of radiotracer into insulinoma cells reaches a maximum after a few minutes and is inhibited by an excess of unlabeled peptide. Degradation products of the peptide are found in the cell medium after incubation; we were able to determine their mass and to derive their amino acid sequence. I-125-glp-1(7-36)amide accumulates in the cells if lysosomal degradation is inhibited. Radiolabeling of exendin 3 was more difficult than in the case of glp-1 because of the lack of tyrosin in its primary structure. The His moiety had to be used instead. Biodistribution studies showed rapid blood clearence and an uptake of the radiotracer into the tumor and the pancreas. We were also able to detect insulinomas in an animal model by external scintigraphy using radiolabeled glp-1 (7-36)amide and exendin 3.
Conclusion: Glp-1 (7-36)amide is specifically internalized into insulinoma cells by a receptor-mediated mechanism. Our results demonstrate that glp-1-receptor-directed scintigraphy may be a new method for the detection of insulinomas *in vivo*. Due to the short half-life, its more stable analog exendin 3 may better suit this purpose *in vivo*. Labeling with radiometals is desirable in order to extend the methods clinical potential.

PS_398

SOMATOSTATIN RECEPTORS SCINTIGRAPHY AND CHROMOGRANIN A(CGA) SERUM LEVELS IN NEUROENDOCRINE TUMOURS

M. Cimitan (1), E. Borsatti (1), A. Buonadonna (2), R. Cannizzaro (3), R. Ruffo (1), V. Canzonieri (4), L. De Apollonia (4), N. Dal Bò (3). (1) Department of Nuclear Medicine National Cancer Institute CRO Aviano - Italy; (2) Department of Medical Oncology B; (3) Department of Gastroenterology; (4) Department of Pathology and Clinical Chemistry

A high density of somatostatin receptors has been found in many neuroendocrine tumours and the serum level of CgA has been recently validate as tumour marker in the clinical evaluation of the neuroendocrine disease. In this work we report the results of somatostatin receptors scintigraphies and serum CgA levels of 47 patients with histological evidence of neuroendocrine tumours.

Materials & Methods. We have evaluated 14 GEP carcinoid tumours, 12 GEP neuroendocrine carcinomas, 9 extra-pulmonary small-cell carcinomas, 3 bronchial carcinoids, 3 Merkel-cell carcinomas, 1 medullary thyroid carcinoma, 1 pulmonary and 1 mediastinal neuroendocrine tumours. Three others patients had histological diagnosis of metastatic disease from unknown neuroendocrine tumours. In our series a total of 29 (62%) patients showed clinical evidence of distant metastases (stage IV).

All patients underwent to somatostatin receptor scintigraphies 4 h and 24 h after i.v. injection of 185Mbq of (111)In-pentetreotide (Octreoscan) with whole body and tomographic acquisition. The CgA assay (DAKO ELISA with normal value < 30 U/L) was carried out within a week.

Results. Positive somatostatin receptors scintigraphies were found in 28 of the 47 (60%) patients examined and elevated serum CgA levels (ranged between 36 and > 450 U/L) were measured in 24 (51%). 20 (43 %) patients had both positive octreoscan scintigraphy and high CgA serum levels. However eight (26%) patients with positive octreotide scans had normal CgA serum levels (4 with GEP carcinoid tumours, 2 with pancreatic neuroendocrine carcinomas, 1 with a bronchial carcinoid and 1 patient with Merkel-cell carcinoma). Among the 29 patients with distant metastases (stage IV) 21 (72%) had octreotide scan findings positive and 20 (69%) had high CgA levels.

Discussion. In our series of patients high serum levels of CgA often co-occurred with a positive octreotide scintigraphy (83% of cases). Therefore serum assay of the CgA in patients with neuroendocrine tumours may be used for planning the scintigraphic evaluation of somatostatin receptors.

PS_399

CLINICAL ROLE AND ECONOMICAL ANALYSIS OF 111-IN-OCTREOTIDE IN GEP TUMORS

R. Sciuto (1), S. Rea (1), A. Festa (1), A. Tofani (1), S. Bergomi (1), P. Perri (2), C.L. Maini (1). (1) Dpt. of Nuclear Medicine, ; (2) Dpt. of Oncological Surgery, Rome, Italy.

The aim of the study was to clarify both the clinical and the economical role of receptorial scintigraphy with 111-In-Octreotide (OCT) in the management of gastro-entero-pancreatic (GEP) tumors considering the elevated costs of the study.

Methods: 150 scintigraphic studies were performed in 135 patients with suspected or proved GEP tumors coming to our Institution with different research questions (primitive localization, staging, receptorial characterization). All the studies were performed with the followings methods: i.v. injection of 111-222 MBq 111In-octreotide (Octreoscan" Byk-Gulden, Milan –Italy) with imaging at 24 hrs and 48 hrs including whole-body, a minimum of two planars acquisitions of the thorax and abdomen and relative SPECT. Patients were followed 1 year after the scan to evaluate the clinical impact of the OCT studies on decision making and final outcome. Cost/benefit analysis was employed considering the costs and the benefits related to all the performed scintigraphies. Costs analysis included both direct costs (radiotracer) and indirect costs (time and work costs); benefits were evaluated considering the costs of avoided octreotide therapy cycles. **Results:** Overall sensitivity for study was 80% and sensitivity for metastatic tumor sites was 90%. The clinical impact of the studies according to the research question resulted as follows: 40% in promoving early surgery of primitive tumor, 20% in modifying therapeutic strategy because of tumor staging change; 50% in selection for medical treatment with octreotide, 100% in identifying negative follow-up. Economical analysis identified the costs of the study (Û =167.640) and the benefits (Û = 215.362) associated with the 150 studies with a cost/benefit ratio = 0.77.

Conclusions: 111-In-Octreotide scintigraphy is a reliable imaging technique in GEP tumors because is: - *effective* in the pre- and post-surgery staging; - *useful* in improving quality of life and survival; - *economically sound* as it has a favourable cost/benefit ratio.

PS_400

INTRAINDIVIDUAL COMPARISON OF IN-111 LANREOTIDE AND IN-111 OCTREOTIDE SCINTIGRAPHIES

V. Ivancevic (1), H. Gerl (2), H. Lochs (2), D.L. Munz (1). (1) Clinic for Nuclear Medicine, University Hospital Charité, Humboldt University, Berlin, Germany; (2) Medical Clinic, University Hospital Charité, Humboldt University, Berlin, Germany.

Aim: At present In-111 octreotide is the standard tracer in somatostatin receptor scintigraphy of neuroendocrine tumours. Promising results have been obtained with In-111 lanreotide, another somatostatin receptor analogue which, due to its receptor affinity profile, might also be valuable in non-neuroendocrine tumours, especially pancreatic cancer. We investigated the diagnostic performance of lanreotide and octreotide in an intraindividual comparative study.

Methods: In 16 patients (9 women, 7 men; age range, 31-82 years) somatostatin receptor scintigraphies with both In-111 octreotide (Mallinckrodt Medical, Petten, NL) and In-111 lanreotide (OEFZ Seibersdorf, A) were performed in planar spot and whole-body as well as SPECT techniques. There were 10 patients with verified gastrointestinal neuroendocrine tumours, two without signs of relapse on follow-up, one patient with an ectopic corticotropin producing tumour and one with an unknown primary. Another two patients presented with liver metastases of a pancreatic and renal cell carcinoma, respectively.

Results: Lanreotide and octreotide scintigraphies were true positive in 4/10 and 8/10 patients with verified neuroendocrine tumours, respectively. Vice versa, there were 6/10 and 2/10 false negatives, respectively. There was only one patient with a true positive lanreotide but false negative octreotide scan. Both modalities were true negative in the two patients in follow-up of neuroendocrine tumours. Lanreotide and octreotide were false negative in the patient with ectopic corticotropin production which turned out to be located in the left lung and right adrenal gland, and in both patients with liver metastases. In the patient with unknown primary both methods were negative, and the primary remained unknown. With regard to comparative analysis, concordant scintigraphic results were obtained in 10/16 patients. Of these, 7 were concordantly negative and 3 positive. In two of the 3 concordantly positive patients octreotide uptake in the lesions was much more intense than that of lanreotide.

Conclusion: Lanreotide scintigraphy displayed a markedly higher rate of false negative findings than octreotide in patients with gastrointestinal neuroendocrine tumours. In positive cases, lesion uptake of octreotide was mostly higher than that of lanreotide. Both methods seemed not to be helpful in primarily non-neuroendocrine tumours. In spite of the small number of patients investigated, we conclude that lanreotide scintigraphy offers no advantage over octreotide in patients with gastrointestinal neuroendocrine tumours.

PS_401

FUNCTIONAL IMAGING OF METASTATIC NEUROENDOCRINE TUMORS

C. Cheze - le rest, J. Bomanji, D.C. Costa, D. Visvikis, P.J. Ell. Institute of Nuclear Medicine, UCL, London, UK.

Introduction: To optimize the prognosis and management of neuroendocrine tumors, an efficient staging procedure is mandatory. For this purpose, the best imaging strategy using either conventional radiology, functional imaging, or a combination of the two has not as yet been defined.

Objective: To investigate the use of different imaging procedures for staging neuroendocrine tumors, including the use of somatostatin receptor scintigraphy, MIBG scintigraphy and ^{18}FDG PET imaging.

Methods: We retrospectively compared all three investigations in patients with metastatic neuroendocrine tumors. Twenty patients (14 carcinoids, 6 paragangliomas) underwent all three studies within a period of one month. In the case of scintigraphy, planar images were acquired 1, 4, 24, and 48 hours following injection of ^{111}In-DTPA-octreotide (mean activity of 150MBq) /^{123}I-MIBG (200MBq). Whole body 2D PET scans were carried out between 45-60 minutes following injection of 370MBq of ^{18}FDG. PET images were corrected for attenuation effects.

Results: Somatostatin receptor scintigraphy was positive in 14/20 patients (56 lesions), MIBG was positive in 10/20 patients (80 lesions), while FDG PET was positive in 15/20 patients (145 lesions). All studies were negative in one patient, and all 3 studies were positive only in 2 patients (both of which were carcinoids). No single imaging procedure identified all metastatic sites.

Conclusions: Our results demonstrate that the affinity of neuroendocrine tumors for octreotide, MIBG, and FDG is variable. Even a single tumor may have a different affinity for any of these tracers. A complete staging should therefore include all 3 studies. The imaging results may also be used to explain the partial response that can be achieved by using ^{131}I MIBG, ^{111}In octreotide, or ^{90}Y DOTATOC for therapy.

PS_402

OPTIMIZED FUSION OF ABDOMINAL MORPHOLOGIC AND FUNCTIONAL IMAGING WITH A SIMPLE TOOL

C. Laumann (1), G.J. Foerster (1), M. Engelbach (2), K. Schunk (3), O. Nickel (1), P. Bartenstein (1). (1) Department of Nuclear Medicine; (2) Department of Internal Medicine; (3) Department of Radiology, University of Mainz, Germany.

Objectives: Because neuroendocrine tumors often are very small exact correlation of somatostatin receptor binding abnormalities with the morphological correlate is important for the planning of the surgical intervention. Problems in image fusion of abdominal datasets result from different positions of the patient and differences in investigation techniques. Aim of this study was to evaluate the quality of image fusion after standardization of patient position with a vacuum cushion.
Methods: 5 hr p.i. of 110 MBq ^{111}In-Octreotide, 7 patients with metastases of a carcinoid tumor were fixed in a vacuum cushion (MED-TEC, Vac-Loc) and investigated with helical-CT in middle breath position (Siemens, Somatom Emotion). Directly following the CT, a SPECT study (SPECT1) (Marconi, IRIX) of the abdominal region was performed without changing the position of the patients. 24 hr p.i. a second SPECT study (SPECT2) was done with the patients repositioned in their individually preformed vacuum cushion. A total of 8 markers suitable for imaging with CT and SPECT were fixed on the cushion. Datasets of CT/SPECT1 and CT/SPECT2 were fused by means of internal landmarks (e.g. metastases or margin of abdominal organs) or of the external markers using commercially available software (Image Volume Registration, Marconi).
Results: Image fusion using external markers was fast and easy to handle compared to the use of internal landmarks (fusion time: 3-5 vs 10-15 min). Using this technique, all lesions (n=15) detectable by SPECT appeared exactly superpositioned on the respective CT morphology by visual inspection. Geometry of markers remained almost identically between both SPECT investigations. Image fusion of CT/SPECT1 and CT/SPECT2 showed a mean deviation of the external markers smaller than the voxelsize of 4.67 mm: 4,15mm (CT/ SPECT1; SD 0.71) and 4,65mm (CT/SPECT2; SD 1.93), respectively. Using internal landmarks the mean deviation of the chosen landmarks was 6,17mm (SD 1,71) and 7,71mm (SD 1,56). Image quality of CT and SPECT was not affected by the vacuum cushion.
Conclusion: The use of the vacuum cushion results in a high quality of image fusion of SPECT to a CT in middle breath position regardless whether the patients were repositioned or not. Thus the proposed technique is able in a simple and cost effective way to generate abdominal datasets suitable for image fusion. External markers positioned on the cushion allow for a rapid and robust overlay even if no internal landmarks are detectable. This technique is in principle also suitable for MRI /SPECT fusion.

PS_403

NON-INVASIVE DUAL MODALITY IMAGING OF OVARIAN CANCER IN MICE

T.R. Chaudhuri (1), B.E. Rogers (2), K.R. Zinn (1). (1) Department of Radiology; (2) Deparment of Radiation Oncology; (3) Department of Radiology, University of Alabama at Birmingham, Birmingham, AL 35294, USA.

Aim: The purpose of the present study was to develop a non-invasive combined imaging method of gamma camera and fluorescence stereomicroscopy to assess ovarian tumor in nude mice. Gamma camera imaging offered high quantitative analysis and simultaneous fluorescence stereomicroscopic imaging offered high spatial resolution.
Methods: Ovarian tumor cells SKOV3ip.1 were implanted intraperitonealy in 2 groups of six athymic nude mice. After 15 days, a replication defective adenoviral vector (Ad-GFP-hSSTR2) encoding the genes for both green fluorescence protein (GFP) and human type 2 somatostatin receptor (hSSTR2) was injected intraperitonealy ($1x10^6$ pfu) in one group of mice and 0.5 ml of saline in control group of mice. Two days after viral transfection, the mice were intravenously injected with Tc-99m-labeled somatostatin peptide (P2045, Diatide, Inc)(23 MBq). The mice were imaged simultaneously (initial and 5 h) with an Anger gamma camera equipped with pinhole collimator for nuclear imaging and with a fluorescence stereomicroscope for GFP imaging. Following 5 h imaging mice were terminated for biodistribution analysis. Additional stereomicroscopic images were collected after removing the abdominal wall.
Results: Expression of hSSTR2 was detected in intraperitoneal tumors of all mice as indicated by imaging at 5 h after injection of the radiotracer. Expression of GFP was clearly visualized *in vivo* at 5 h by fluorescence stereomicroscopy and imaged simultaneously in the same mice with high spatial resolution of small intraperitoneal tumor lesions. Nuclear images showed the uptake of radiotracer by all peritoneal tumors. In the same location of same mouse, GFP-positive tumors were visualized in live animals in non-invasive way. After removal of abdominal wall, the GFP-positive tumors were visualized more clearly including single cell. Under bright field microscope, tumor as small as 0.2mm diameter from 4mm depth was not possible to be detected. However, by fluorescence stereomicroscopy, this small size tumor due to green fluorescence contrast, was visualized *in vivo*. GFP-positive cells were recovered from peritoneum and cultured in tissue culture media and SKOV3 cells grew. All GFP-positive tumor cells were radioactive as confirmed by gamma counter. Control mice did not have expression of either hSSTR2 or GFP. Imaging and cell count data indicated that GFP-positive cells were mainly cancer cells. Gamma camera and light-based imaging were complementary to each other.
Conclusions: The present study demonstrated that simultaneous dual modality imaging of light-based and gamma camera offered a highly sensitive *in vivo* tool for the early detection and monitoring of human ovarian tumors in mice.

PS_404

SKULL-BASE MENINGIOMAS: PROGNOSTIC VALUE OF 111IN-DTPA-OCTREOTIDE/99MTC-DTPA INDEX (OCT/DTPA) IN LONG TERM FOLLOW UP AFTER GAMMA-KNIFE RADIOSURGERY

D. Grigolato (1), A. Nicolato (2), M. Zuffante (1), M. Cavaggioni (1), P. Braggio (1), I.P. Pasquin (1), M. Gerosa (2), P.G. Giorgetti (1). (1) Department of Nuclear Medicine; (2) Department of Neurosurgery-University, Verona, Italy.

AIM: Our previous experiences showed that OCT/DTPA index is useful for differential diagnosis between skull-base tumours (meningiomas versus other lesions), the decreasing of OCT/DTPA index after γ-knife radiosurgery (GKR) treatment revealed to be positive prognostic factor of a favourable outcome at short follow up. With this review we investigate the impact of OCT/DTPA index in long term follow up.
METHODS: SPET is performed with multiple peak acquisition 4 hours after OCT and 2 hours after DTPA injection by means of a double-head gamma-camera (Elscint Helix; UHR collimators; 64 matrix; 10% window for 3 peaks; 60n steps of 60 sec. each). The OCT/DTPA index was calculated combining the uptake ratio obtained from the somatostatin receptor scintigraphy and DTPA brain scintigraphy of the lesion/controlateral occipital skull on the same transverse slice for each isotope. All patients were evaluated with double tracer SPECT before and 6 months after GKR, with MRI and neurological evolution before treatment and after 6, and from 12 to 36 months after.
RESULTS: We prospectively studied 10 patients (pts) with diagnosis of meningioma from December 1997 to February 2001. 8/10 pts had an early neuroclinical improvement stable in time and a decreased OCT/DTPA index. Among them, only one pt experimented a RMI shrinkage above 50%, obtained at 21 months after GKR, four pts showed a decreased MRI volume below 50% (only one pt 7 months after GKR, the others after 18 months). Three pts had a stable disease on MRI imaging with a follow up of 18 months. 1/10 pt had no clinical changes despite of a reduction of OCT/DTPA index and a MRI shrinkage below 50%, reached 12 months after GKR. 1/10 pt was clinically asymptomatic also before radiosurgery treatment and had no change of OCT/DTPA index but MRI imaging revealed a decreased volume below 50%.
CONCLUSION: In agreement with previous reports, the decreasing of OCT/DTPA index after GKR is predictive of a positive evolution, allowing better correlation with clinical and neurological improvement despite no or low evidence of tumour shrinkage obtained with RMI. Thus, for the high prognostic value, the OCT/DTPA index points out patients with meningioma with a favourable outcome both at short and long follow up after GKR .

PS_405

IN111-OCTREOSCAN AND F18-DG PET IN NEUROENDOCRINE TUMORS (NETS) OF ABDOMINAL ORIGIN: WHICH ROLE FOR BOTH?

F. Chierichetti (1), C. Pasquali (2), C. Sperti (2), P.L. Zanco (1), A. Fini (1), B. Saitta (1), M. Marcolin (1), S. Pedrazzoli (2). (1) U. O. Medicina Nucleare - Centro PET, Castelfranco Veneto, Italy; (2) Patologia Speciale Chirurgica, Università di Padova, Padova, Italy.

AIM OF THE STUDY: in our PET center we studied many patients with NETs. In this report, we considered a group of selected subjects with abdominal masses to evaluate the role of nuclear medicine in the final diagnosis of NET.
METHODS: 50 patients (mean age 62 years) among whom 10 cases of MEN where submitted to F18-DG PET with a dedicated tomograph. Scintigraphy (planar and SPECT) with In111-Octreoscan was performed in 46 out of them with a double head camera. At the radiological examinations 49 had an abdominal mass (pancreatic in over than 90%) and 23 presented liver and or nodal metastases, too. In one case liver metastases without primitive tumor radiologically localized. At the final diagnosis, surgically or clinically proved, and by a 2 years follow up, the patients were divided into two groups: 25 were affected of aggressive NETs, according to the size of primary lesion and to the presence of spread disease (among whom 3 out of 10 cases of MEN), and 25 of non aggressive tumors (comprising 5 insulinomas, the smallest one 1 cm diameter). In the first group In111-Octreoscan was performed in 24 and in the second one in 22.
RESULTS: the overall results are reported in the table below. In the 25 cases of aggressive tumors, F18-DG PET identified both primary and secondary (lung metastases in 2 and mediastinal nodes in 1, too) lesions in 20 patients including the primary lesion in breast in a woman with liver metastases. PET was positive in a larger number of aggressive NETs than receptor scintigraphy but, this last technique localized a greater number of metastases in 4 cases (abdominal nodes). In the group of 25 non aggressive lesions In111-Octreoscan correctly identified every site of tumor in 11 out of 22 the examined patients, among whom the one affected of the smallest insulinoma. We had no false positive lesions for both methods.

	PET positive	PET negative	Octreoscan pos.	Octreoscan neg.
Aggressive (25)	20	5	16	8
Non aggres. (25)	5	20	11	11

CONCLUSIONS: a common opinion is that F18-DG PET is a powerful mean to localize malignant lesions but, in our patients, it was negative in 20% of aggressive tumors. In111-Octreoscan was negative in 50% of non aggressive lesions and positive in 66% of aggressive tumors. Our results show that the contemporary use of F18-DG PET and receptor scintigraphy are useful to assess the extension of disease and to select patients for surgery and/or for further medical treatments: both of them must be recommended when abdominal NET is clinically suspected. Our data are based on a short term follow up and a longer one is required to better understand if F18-DG PET may be a marker of prognosis rather than malignancy.

PS_406

SOMATOSTATIN RECEPTOR SCINTIGRAPHY IN PARAGANGLIOMAS

M.D. Abós (1), J. Banzo (1), E. Prats (1), E. Freile (2), J. Velilla (3), P. Razola (1), T. Escalera (1), F. García (1). (1) Department of Nuclear Medicine, University Hospital, Zaragoza, Spain; (2) Department of Radiology, University Hospital, Zaragoza, Spain; (3) Department of Internal Medicine, Miguel Servet Hospital, Zaragoza, Spain.

Paragangliomas are relatively infrequent neuroendocrine tumors that express somatostatin receptors. There is little information about the role of the ^{111}In-DTPAOC scintigraphy, or somatostatin receptor scintigraphy (SRS), in the management of these tumors.

The aim of this study was to assess the utility of the SRS in the diagnosis, staging and follow-up of patients diagnosis from paraganglioma.

Material and Methods: We included 7 patients (5 females, 2 males) with histologic diagnosis of paraganglioma (4 quemodectomas, 2 extra-adrenal paragangliomas and 1 syndrome of Carney). In these patients we performed 8 SRS (148 MBq), 4 ^{123}I-MIBG scans (370 MBq) and 3 ^{99m}Tc-MDP bone scans (740 MBq). In two patients the SRS was performed for the staging of a known or suspected tumor, whereas in the other 6 patients the SRS was performed during the post-therapy follow-up: embolization or surgery associated with radiotherapy or metabolic therapy. One patient was explored twice, before and after surgery.

Results: SRS was positive in 6 patients. In two of them (1 jugulo-tympanic paraganglioma and 1 extra-adrenal paraganglioma) the SRS demonstrated an unsuspected metastatic dissemination, whereas in other patient (syndrome of Carney) the SRS scan detected multiple unsuspected paragangliomas. Of the 4 patients studied with both, ^{111}In-DTPAOC and ^{123}I-MIBG scans, similar information was provided in 2 patients with both explorations (1 metastatic extra-adrenal paraganglioma and 1 quemodectoma), in one patient the SRS was normal (bone metastases of an extra-adrenal paraganglioma) and in the other one the ^{123}I-MIBG scan was normal (1 carotid quemodectoma). One patient with local recurrence and metastatic dissemination of an extra-adrenal paraganglioma was treated with ^{131}I-MIBG.

Conclusions: SRS permits to detect, to stage and to assess the therapeutic response in patients with paraganglioma. The ability of obtaining whole body images provides the detection of unsuspected lesions. SRS and ^{123}I-MIBG scan are complementary techniques, particularly in the study of metabolic therapy candidate patients.

PS_408

IS IT SAFE TO OMIT I-131 UPTAKE MEASUREMENTS WHEN TREATING BENIGN THYROID DISEASE WITH RADIOIODINE?

T. Buhl, P. Hansen, W. Christensen, B. Hesse. Dept. of Clinical Physiology and Nuclear Medicine, Rigshospitalet, University Hospital of Copenhagen, Copenhagen, Denmark.

It has never been documented that determination of the iodine uptake ratio improves the long-term clinical outcome for patients treated for benign thyroid diseases (toxic and non-toxic goiter). On the other hand it is imperative not to treat patients with a very low iodine uptake. Determination of iodine uptake is time consuming and usually closely related to pertechnetate uptake, which is much quicker and less expensive.

Aim: To investigate whether a Tc-99m-pertechnetate (TcO_4^-) scintigraphy can replace the I-131 iodine uptake measurement prior to radioiodine treatment of patients with benign thyroid disease.

Methods: In a retrospective series of 100 patients with toxic (N=87) or non-toxic (N=13) goitre Tc-99m (TcO_4^-) scintigraphy was visually graded in 3 degrees (low, intermediate and high) by two experienced specialists and compared with the 24 h I-131 iodine uptake grouped in intervals (< 30 %, ≥ 30 % - < 60 %, and ≥ 60 %). In 13 of the patients it was still possible to calculate a semi quantitative score by drawing ROIs around the thyroid gland, a salivary gland, and the background. Count ratios between the thyroid gland and the salivary gland and the background, respectively, were calculated.

Results:

N = 100		Tc-99m TcO_4^-	Tc-99m TcO_4^-	Tc-99m TcO_4^-
		LOW	INTERMID.	HIGH
I-131 uptake	**< 30 %**	4	2	0
I-131 uptake	**≥ 30 % - < 60 %**	2	20	10
I-131 uptake	**≥ 60 %**	0	17	45

There is a good correlation between I-131 iodine uptake and visual evaluation of Tc-99m (TcO_4^-) scintigraphy (see table.

Semi-quantitation in 13 patients showed a good correlation between I-131 uptake and Tc-99m (TcO_4^-) thyroid gland/salivary gland or Tc-99m (TcO_4^-)/background ratios being R = 0.87 and 0.88, respectively, and the correlation to I-131 uptake compared with the visual evaluation was improved.

Conclusion: It seems acceptable to calculate I-131 iodine doses from estimation of the size of the thyroid gland and a Tc-99m scintigraphy. In particular, the risk of treating patients with low iodine uptake seems negligible.

OTHER CLINICAL SCIENCE. ENDOCRINOLOGY 1

PS_407

DOES THE ORBITAL 111IN-OCTREOTIDE UPTAKE DEMONSTRATE THE ACTIVE DISEASE IN PATIENTS WITH GRAVE'S OPHTALMOPATHY:ITS RELATION WITH CLINICAL ACTIVITY SCORE

İ. Ak (1), N. Ün (2), E. Zor (1), E. Vardarel (1), N. Yıldırım (2). (1) Department of Nuclear Medicine; (2) Department of Ophtalmology, Eskişehir, Turkey.

Accumulation of the 111In-Octreotide in patients with Grave's Ophtalmopathy (GO) is most probably due to the presence in the orbital tissue of activated lymphocytes bearing somatostatin receptors. Alternative explanations are binding to receptors on other cell types such as myoblasts, fibroblasts or endothelial cells or local blood pooling due to venous stasis by the autoimmune orbital inflammation. Clinical Activity Score (CAS) is a classification based on the classical signs of inflammation such as pain, redness, swelling, and impaired function in patients with GO. In this study, we assessed the correlation between CAS and Somatosatin Receptor Scintigraphy (SRS) with 111In-Octreotide in patients with GO.

Methods: Thirty five patients with GO and 8 control subjects were included in this study. After the clinical examination CAS of each patients were determined, ranging from 0 to 10 points. According to CAS (>/= 4/10 and <4/10), patients were classified as clinically active GO (n=12) and clinically inactive GO (n=23). Planar imaging was obtained at 4 and 24 hr after intravenous injection of 111 MBq of 111In-Octreotide. Orbital uptake was assessed by the ROIs generated for both orbits and brain. Using the mean counts an uptake ratio between the orbits and the brain was determined.

Results: The results of SRS showed an increased orbital accumulation of 111In-octreotide in patients with clinically active GO compared to patients with inactive GO and controls (orbit-brain-ratio: 2.35 ± 0.75, 1.25 ± 0.20, 1.29 ± 0.29, respectively, $p<0.05$). Patients with clinically inactive GO show a similar orbital accumulation of radioactivity compared to controls ($p>0.05$). We found a significant correlation between the CAS and SRS ($p<0.01$).

Conclusion: SRS with 111In-labeled octreotide correlates with Clinical Activity Score in patients with clinically active GO. The value of SRS lies in its ability to act as a measure of inflammation and may be useful as an activity parameter when planning therapeutic procedure as well as for GO follow-up.

PS_409

THE RESULTS OF RADIOIODINE THERAPY IN PATIENTS WITH HYPERTHYROIDISM AFTER ONE YEAR FOLLOW UP

M. Argon, O. Özyurt, K. Kumanlioğlu, H. Özkılıc. Department of Nuclear Medicine, Ege University, Izmir, Turkey.

Radioiodine (I-131) is one of the accepted forms of treatment for thyrotoxicosis. The aim of this retospective study was to evaluate the results of radiodine theraphy in patients with hyperthyroidism.

Methods: 132 Pts were (44 Graves' disease, 43 toxic adenoma and 45 toxic multinodular goiter) (85 female 64%-47 male36%) analyzed who were treated with radioiodine from 1997 to end of 1999 and still on follow up. Graves' disease Pts.' ages ranged from 30 to 74 (main 50±10,4), (28 female, 16 male). The doses ranged from 6 to 20 mCi (mean 12.3±4.2), 27 Pts recieved single dose, 17 needed 2 doses. Toxic adenoma Pts.' ages ranged from 30 to 78 (main 56.8±11.1)(22 female, 21 male), the doses ranged from 8 to 30 mCi (mean 18±5.6), 32 Pts received single dose, needed 2 doses, 2 needed 3 doses. Toxic multinodular goiter Pts.' ages ranged from 36 to 75 (main 60±10.5), (35 female, 10 male), the doses ranged from 8 to 30 mCi (mean 20.8±6.1), 33 Pts received single dose, 12 needed 2 doses.

Results: After one year follow up in Graves' disease; 15 Pts were euthyroid (34%), 25 Pts were hypothyroid(57%), 4 Pts were persistently hyperthyroid (9%). In toxic adenoma; 29 Pts were euthyroid (67%), 12 Pts were hypothyroid(28%), 2 Pts were persistently hyperthyroid (5%). In toxic multinodular goiter 34 Pts were euthyroid (75.5%), 7 Pts were hypothyroid (15.5%), 4 Pts were persistently hyperthyroid (9%). There was not any complication of I-131 treatment.

Conclusions: The main problem of raioiodine treatment was hypothyroidism and this was easily treated with L-thyroxine. Hypothyroidism was noted most commonly in Graves' disease Pts. Euthyroid state was obtained mostly in toxic multinodular goiter. The ranges of adminestered second or more doses were low. The radioiodine treatment was prefered in elderly patient rather than young Pts.

PS_410

DETERMINATION OF THYROID VOLUME PRIOR TO RADIOIODINE THERAPY: ULTRASONOGRAPHY VS MRI

P. Reinartz, M. Zimny, O. Sabri, B. Nowak, U. Cremerius, K. Setani, W. Schäfer, P. Meyer, U. Buell. Department of Nuclear Medicine, University Hospital, Technical University Aachen, Germany.

Aim: For radioiodine therapy, thyroid volume is one of the most significant factors in calculating the individual delivered activity. Method of choice for the exact determination of the thyroid volume is ultrasonography using the formula 0.5 x length x width x depth for each lobe separately. Aim of the study was to ascertain how exact the results of this technique are in comparison to MRI.
Methods: In 50 patients with confirmed Graves« disease (n=24) or multinodular toxic goiter (n=26) ultrasonography (Hitachi LSC 7500, 7,5 MHz) was performed by two experienced referees (US-Ref-1, US-Ref-2). Additionally, a 3D fast field echo MRI sequence (Philips Gyroscan NT, 1,5 Tesla) of the neck area was acquired with a voxel size of 3 mm. Acquisition time was four minutes each. Thyroid volume was assessed by using the formula mentioned above for ultrasonography as well as for MRI (MRI-e). Standard of reference was the thyroid volume determined by a region of interest technique applied to the MRI data set which calculates the exact volume after encircling the thyroid gland in each slice (MRI-r).
Results: Mean measured thyroid volume was 55.9 ± 39.4 mL for MRI-r, 51.4 ± 36.6 mL for MRI-e, 44.0 ± 29.3 mL for US-Ref-1, and 43.1 ± 29.6 mL for US-Ref-2. The table shows the mean absolute and relative difference as well as the standard deviation (sd) and the level of significance p (Wilcoxon test) between the different techniques.

	mean absolute Δ ± sd [mL]	mean relative Δ ± sd [%]	p
MRI-r vs MRI-e	7.8 ± 10.1	13.2 ± 8.4	0.30
MRI-r vs US-Ref1	14.0 ± 15.8	22.6 ± 15.1	< 0.01
MRI-r vs US-Ref2	14.3 ± 13.1	25.8 ± 14.8	< 0.01
US-Ref1 vs US-Ref2	7.0 ± 7.3		0.47

Conclusions: While there is a high level of agreement between the MRI-techniques on the one hand and the ultrasonographic results of the referees on the other hand, a significant difference could be found between the thyroid volume determined by ultrasonography and MRI with a mean difference of approximately 14 mL (>20%). It seems advisable to perform the short MRI sequence especially in patients with large or irregular shaped goiters in order to ensure a correct individual delivered activity.

PS_411

TECHNETIUM-99M METHOXYISOBUTYL ISONITRILE SCINTIGRAPHY IN VISUALIZATION OF SUPPRESSED THYROID TISSUE

M. Yıldırım (1), H. Uslu (1), F. Akçay (2), R. Bayrakdar (1), N. Ünüvar (3), E. Varoğlu (1). (1) Atatürk University Medical Faculty, Depts. of Nuclear Medicine; (2) Atatürk University Medical Faculty, Depts. of Biochmistry; (3) Atatürk University Medical Faculty, Depts. of Endocrinology, Erzurum, Turkey.

We studied the significance of Technetium – 99m Methoxyisobutyl Isonitrile (MIBI) scintigraphy in patients with nonvisualized thyroid tissue. The thyroid tissue was suppressed depending on various drugs and salt containing iodine.
Methods: Forty patients (30 women, 10 men; age range, 10-72 yrs; average age: 43.6 yrs) visualized on pertechnetate scanning were included in this study. Markedly reduced pertechnetate uptake was seen in all patients. At the same time, MIBI scanning was performed without thyrotropin (TSH) stimulation. Images of the neck were recorded at 30 min, 1h and 2 h after intravenous injection of Tc99-MIBI 5mCi (185MBq). The results were correlated with neck ultrasound, serum TSH, TT3, TT4, FT3 and FT4 levels. Images were recorded with a small field of view camera (GE Starcam 4000), equipped with a parellel-hole, all-purpose collimator, adjusted to record a photopeak of 140 keV with a 20% window. The MIBI scanning was analyzed both visually and semiquantitatively. For the semiquantitative analysis, regions of interest (ROIs) were generated over the right and left lobes of the thyroid gland. Mean counts in every ROI were calculated for MIBI.
Results: The technique identified the following conditions: normally sized thyroid (n = 2), diffuse goiter (n = 7) and multinodular goiter (n = 28). Moreover, substernal goiter was identified in 3 patients.The MIBI uptake ratios were 166.73 ± 158.2 at 30th min, 131.13 ±117.7 at the 60th min and 114.08 ± 110.4 at the 120th min.
Conclusions: Our results suggest that Tc99m-MIBI scintigraphy may contribute to the diagnosis of thyroid pathology and planning of the treatment in patients with suppressed thyroid tissue in pertechnate scintigraphy.

PS_412

EFFICACY OF 131-I TREATMENT IN PATIENTS WITH GRAVES-BASEDOW DISEASE

A. Saura, I. Hervás, P. González-Cabezas, A. Rivas, J. Alonso, P. Bello, A. Mateo. Department of Nuclear Medicine, University Hospital, Valencia, Spain.

Aim: To assess in our Hospital the efficacy of 131-I in patients with Graves-Basedow disease.
Methods: We have studied all the patients with Graves-Basedow disease (thyroid scintigraphy showing diffuse goitre, without nodules confirmed by ultrasonography and with thyroid hyperfunction) with no definitive control of the disease with the oral treatment with antithyroid drugs (ATD), treated in our Department since June-1998 until march-2000. We have studied 126 patients, 36 males and 90 females: age 20-81 years (average age 49 years approximately). All of them were treated with ATD: Carbimazol (average dose 20mg/day). 4% of patients left the oral treatment 30 days before treatment with 131-I. The other 96% left the oral treatment in the habitual period (7-10 days). The administered activity of 131-I was calculated depending on the glandular size (scintigraphy and palpation) and the hormonal state. The activity administered varied between 6,2 mCi-16,3 mCi (229 MBq- 603 MBq). The average dose was 10,63 mCi (393 MBq).
Results: At 01/March/ 2001: 77% of patients were controlled with one dose of I-131 and 11% needed a second dose of 131-I. None of them needed a third dose.51% presented hypothyroidism in 1-12 months (average 4 months), needing an average dose of 100µg of thyroid hormone (Levotroid®) interval (50-150). 26% of patients remained with euthyroidism. 23% of patients presented a relapse of the hyperthyroidism, and 11% of them were treated again with 131-I (second 131-I dose). The following table contains the dose of ATD, gender, age and hormonal state after the first dose of 131-I.
RESULTS

	EUTHYROIDISM	HIPOTHYROIDISM	HIPERTHYROIDISM
	Male/Female	Male/Female	Male/female
Number of Patients	11/22	12/52	13/16
Average age (years)	47/47	45/54	56/44
Average dose of ATD	3.75/3.25 mg/day	3.5/3.7 mg/day	3.75/4.75 mg/day
Average activity of 131-I (mCi)	10.1/9.97	10.2/11.1	11.1/10.4
Average activity (mCi)	10	10.9	10.6

Conclusions: We did not found statistical differences between patients who developed hypo/hyper or euthyroidism in relation with: dose of ATD previous to the 131-I treatment, age, average activity of 131-I; It seems that males have more tendency to remain with normo/hyperthiroydism. The activity of 131-I administered have been effective in the control of Graves-Basedow disease in a high percentage of cases.

PS_413

THYROGLOBULINE AND PEROXIDASE AUTOANTIBODIES IN THE FOLLOW-UP OF SEQUENTIAL HORMONE-IODINE GOITER THERAPY

M.J. Reinhardt (1), D. von Mallek (1), H. Palmedo (1), U.J.T. Kuehr (1), A. Manka-Waluch (1), F. Gruenwald (2), H.J. Biersack (1), T. Krause (1). (1) Dept. of Nuclear Medicine, Univ. Hospital Bonn, Germany; (2) Dept. of Nuclear Medicine, Univ. Hospital Frankfurt, Germany.

Aim: It is well known that iodine therapy may induce an increase of thyroglobuline (TG-ab) and thyroid peroxidase (TPO-ab) autoantibodies. The course of TG-ab and TPO-ab after switching from thyroid hormone to iodine therapy is currently unknown. Thus, the study retrospectively analysed the course of TG-ab and TPO-ab after changing thyroid hormone therapy of several years' duration to low-dose iodine therapy.
Methods: 79 patients (51 women, 28 men; aged 39±13 years; 40 diffuse goiter, 39 nodular goiter) in whom thyroid hormone therapy was changed to iodine therapy were included in the study. Mean thyroid hormone therapy lasted 85±64 months and mean iodine therapy lasted 59±33 months. TG-ab and TPO-ab were determined with CentAK?-Anti-TG and CentAK?-Anti-TPO kit from Medipan, Germany. Thyroid sonography and measurement of serum thyroid hormones and TSH were performed additionally. Suppression-scintigraphy was performed prior to the change to iodine therapy for exclusion of functional thyroid autonomy.
Results: Data were analysed in 3 groups. Group A (N=38) was treated exclusively with thyroid hormones and served as control. Group B (N=41) was treated with thyroid hormones followed by 100-200 µg iodine daily. Group C (N=22) was a subgroup to group B and covered all patients with repeated follow-up measurements of TG-ab and TPO-ab during thyroid hormone and iodine therapy. In group A, TG-ab and TPO-ab were increased in 13% and 20% of patients, respectively. In group B, the frequencies were 18% and 23%. These differences were not significant. The intraindividual course showed a tendency towards increasing TG-ab during iodine therapy, while TPO-ab decreased.
Conclusion: Application of 100 to 200 µg iodine daily did not induce a significant change of TG-ab and TPO-ab. This may be due to a possible immune-suppressive effect of the foregoing thyroid hormone treatment, which has been observed in patients with Hashimoto thyroiditis.

PS_414

THE RELATIONSHIP OF PYRAMIDAL LOBE WITH THYROID DISEASES

M. Yıldırım (1), H. Uslu (1), R. Bayrakdar (1), C. Ak (1), B. Erdoğmuş (2), F. Akçay (3), E. Varoğlu (1). (1) Atatürk University Medical Faculty; (2) Atatürk University Medical Faculty, Depts.of Radiology; (3) Atatürk University Medical Faculty, Depts. of Biochmistry, Erzurum, Turkey.

We aimed to investigate the relationship of pyramidal lobe with thyroid diseases by retrospectively evaluating 4834 thyroid scintigraphies.

Methods: 4834 patients visualized on pertechnetate scanning were included in this study. The results were correlated with neck ultrasound, serum TSH, TT3, TT4, FT3 and FT4 levels. Images were recorded with a small field of view camera (GE Starcam 4000), equipped with a parellel-hole, all-purpose collimator, adjusted to record a photopeak of 140 keV with a 20% window.

Results: Of 4834 patients, 534 (11 %) had pyramidal lobe: 62 % were localised in isthmus, 20 % were closer to the left lobe and 16.8 % were localized right side. Of 534 cases, 109 had nodular goiter, 96 diffuse goiter and 53 hyperthyroidism. The remaining ones had goiter with one nodule.

Conclusions: It was concluded that pyramidal lobe was seen in approximately 11 % of thyroid diseases and patients with noduler goiter were higher in number than ones with hyperthyroidism.

PS_415

A LONG TERM FOLLOW-UP IN PATIENTS AFFECTED WITH GRAVE'S DISEASE TREATED WITH RADIOIODINE

B. Santaniello (1), F. Schenone (2), G. Curti (1), M. Carletto (1), H. Rouhanifar (1), A. Piccardo (1), L. Tommasi (1). (1) Nuclear Medicine Service, DiMI - University of Genoa, Genoa, Italy; (2) Nuclear Medicine Service, IST - University of Genoa, Italy.

From 1954 to 1976, 1778 pts affected with Grave's disease were treated with ^{131}I. The aim of the study is to evaluate the results of therapy after a long period of time: from 23 to 46 yrs as in a previous evaluation where our incidence of hypothyroidism resulted quite different from other reports. Before the therapeutic dose the maximal thyroid uptake of ^{131}I tracer dose was calculated after 2h, 6-8h, 24h and 48h. The therapeutic dose was included within 80-120 nC/g of thyroid tissue. The first control of therapy effect was performed on 428 pts; actually we have studied 85 pts (medium age 68.3 yrs). The mean time (MT) between the actual check and the last therapeutic dose was 32 yrs. Our controls included clinical examination, FT3, FT4, TSH determination. In the first control in 1977, 4% of the pts were still hyperthyroid, 42,2% were normal and 55.37 were hypothyroid. Actually, 42 pts (49,4%) are euthyroid, and 43 (50,6%) are hypothyroid. In the first group the mean global dose of ^{131}I was 8,45 mCi and the MT from the last dose was 26,45 yrs. In the second group 22 pts affected with a clear hypothyroidism received a MGD of 9,6 mCi; the MT from the last dose has been of 27,6 yrs. The remaining 21 pts showed a subclinical hypothyroidism. The MGD was 11,3 mCi and the MT from the last dose was 22 yrs. The life table study of our statistics showed 52,6 % of probable hypothyroidism after 3 yrs and a 57,2% after 44 yrs.

PS_416

LONG FOLLOW-UP-RESULTS OF NEARLY TOTAL THYROIDECTOMY IN EUTHYROID GOITER

P. Mariß (1), M. Thermann (2), G. Wolfes (1), O. Höner (3), D. Emrich (1). (1) Gemeinschaftspraxis Radiology/Nuclear Medicine Dr. Stuckenholz & Partner, Bielefeld, Germany; (2) Klinik für Allgemein- und Visceralchirurgie, Städtische Kliniken Bielefeld, Germany; (3) Institut für Sportwissenschaften, University Bielefeld, Germany.

Aims: Iodine deficiency is still an important cause of goiter in Germany. 20 – 30% of the population (82 millions) suffer from iodine-deficient goiter. TSH and various growth factors induce diffuse goiter developement followed by nodular degeneration. Because medical treatment may be unsuccessfull in nodular goiter still about 80,000 surgical operations of nodular goiter are performed in Germany annually. The surgical methods used are: nodule-oriented partial thyroidectomy and near total thyroidectomy (NTT). Criteria of surgical quality assurance are considered as goiter recurrence-rate, hypoparathyreoidism and cord paralysis. Reports on follow up after operation because of euthyroid goiter suffer from several items. Methods: Out of 263 pts with euthyroid nodular goiter (mean age 50,2 ± 13.2 yrs, thyroid volume 82,8 ± 56,7 ml) operated by NTT during one year (1992) using an uniform technique 216 (82%) were reinvestigated after 7 yrs (clinical investigation, thyroid volume by sonography, TSHb, fT4, fT3). Results: One had a relapse of goiter, none had a cord paralysis and 3 pts had hypoparathyroidism. 11 of the medicated pts were latent or overt hypothyroid with elevated TSHb (4,5 – 15,3 uU/l) due to insufficient medication. The remaining 205 pts were subdivided as follows: no medication: n=11, thyroxine < 1.1 ug/kg: n=27, thyroxine ?1.1 ug/kg: n=136. 3 pts received iodide supplementation alone and 28 pts a combination of thyroxine and iodide with different doses. The residual mean thyroid volume was higher in the non medicated group (8.1 ± 5.2 ml) compared to the thyroxine medicated pts (2.7 ± 2.0 ml, $p < 0.001$) and the mean TSHb was higher and the mean FT4 was lower (both $p < 0.001$). In pts under high thyroxine medication (? 1.1 ug/kg)) the residual thyroid volume was significantly lower (2.3 ± 2.0 ml) compared to those under low doses (?1.1 ug/kg) (4.3 ± 3.2 ml, $p < 0.01$) in combination with a higher TSHb ($p < 0.05$) and a lower FT4 ($p < 0.01$). In conclusion nearly total thyroidectomy prevented goiter recurrence in 215 of 216 operated pts after 7 years. T4 medication kept the residual thyroid volume significantly lower dependent on its dosage.

PS_417

THE STUNNING EFFECT IN GRAVE'S DISEASE: INFLUENCE IN THE COURSE OF RADIOIODINE THERAPY

I. Bofilias. Clinic of Nuclear Medicine, Technical University, Munich, Germany.

We examine the stunning effect in Grave's disease (GO) because a) stunning may influence the thyroid absorbed Dose (Dabs) during the course of therapy, and b) the recurrence rate of thyrotoxicosis in GO lies with (30-50%) quite higher than other hyperthyroid subgroups. The recent introduction of a thyroid stunning constant ($D_{1/2}$~100 Gy) allows easily a) the characterization of the thyroid radiosensitivity to the therapeutic absorbed Dose in thyroid benign diseases, b) a subtle comparison among our data and other published results, and c) among the various thyrotoxic subgroups. We retrospectively calculated the $D_{1/2}$ in 45 pts with Grave's disease, in which a second ^{131}I treatment was performed. Two different stunning constants have been significantly distinguished, indicating the existence of two different radiosensitive behavior follicular types. They are obviously related to the high or low degree of the thyrotoxicosis recommending a modification of the current therapy abs. Dose concept.

Method: Daily ^{131}I thyroid uptake measurements of first MFU and second MSU treatment and Dabs calculations in Grave's disease in the Acute Therapeutic Stage (ATS, D_{ATS}) show in 39 patients (20%, total n=195 pts) a reduction MSU relative to MFU depending on the D_{ATS} already induced during the ATS. Individual values for $D_{1/2}$ were calculated. Two dif. mean values were observed using the t-test as well as higher order polynomials.

Results: 18 (40%) of the 45 pts showed a significantly lower value of $D_{1/2,low}$ = 71± 15% Gy and in 11 pts (24%) the $D_{1/2,high}$ mean value was 113 ± 17% Gy ($p<.05$). Calculations could not be performed for the remaining 6 (13%) cases because inversion of the relation (MSU/MFU > 1) occurs due to the discontinuation of ATD during therapy. For low aggressive types a Dabs of 150-200 (175 ± 15%) Gy was derived, whereas for high aggressive the current Dabs value remains unchanged.

Conclusions: The derivation of the two different stunning constants in Graves' disease reflects the existence of two radiosensitive different follicular behavior types, according to the degree of their thyrotoxicosis. Keeping the actual abs. Dose concept for high aggressive unaltered and changing the Dabs to 150-200 Gy for low types, the hypothyroidism rate may be considerably reduced. A comparison with other published data revealed that stunning constants varied greatly to each other. Further developments are needed.

PS_418

RESULTS OF TREATMENT WITH CALCULATED DOSES OF RADIOIODINE DEPENDING ON GLAND SIZE AND MORPHOLOGY IN GRAVES«DISEASE, ANALYSIS OF VARIABLES

S. Rodado (1), A.M. García (1), V.M. Poblete (1), A. Soriano (1), C. Martinez (2). (1) Department of Nuclear Medicine, Alarcos Hospital, Ciudad Real, Spain; (2) Deparment of Investigation, Alarcos Hospital, Ciudad Real, Spain.

Aim: To assess the efficacy of administered doses of Radioiodine (RAI) in the treatment of patients with hyperthyroidism in Graves«disease calculated depending on gland size and morphology
(assessment by palpation and scintigraphy) , analyzing which variables influence on the final result (hypothyroidism , hyperthyroidism and euthyroidism) of our sample , and on the early development of hypothyroidism.
Methods:99 patients diagnosed of hyperthyroidism in Graves«disease and treated with RAI between April 1996 and November 2000 were evaluated retrospectively.77 females and 22 males, mean age 44 years (range :18-76).Sixty –seven patients received treatment with antithyroid drugs , which were stopped seven days prior to and after of the treatment with RAI .The doses were administered depending on gland size and morphology , which were determinated by palpation and 99mTc-pertechnetate scintigraphy (doses range:185-629 MBq).Success was defined as elimination of hyperthyroidism ; and early hypothyroidism which appeared in the six months after therapy.
Results:The distribution of results accompanied by mean dose in each case is shown below :

HYPOTHYROIDISM	EUTHYROIDISM	HYPERTHYROIDISM
53 (9)	30 (9.3)	16 (8.3)

84 % of patients were controlled with one dose of RAI and 90% with one or two doses . 43% developed hypothyroidism within the first year of follow up (30% within the first 6 months). By means of the Discriminant Analysis stepwise method we found that only the time of evolution influenced in the final results .The rest of the variables (gender , age , doses , treatment with antithyroid drugs) did not influence them .Using Logistics Regression we studied the relationship between the appearance of early /late hypothyroidism and the administered doses: there were no significant statistical differences . On the other hand we found a certain tendency for early hypothyroidism to appear in the youngest patients.(p=0.111).
Conclusions:-The administered doses in our Department have shown to be effective in controlling tyrotoxicosis .The high range of hypothyroidism in the first year strongly supports the need for frequent initial controls.
-In our sample, only the time of evolution influenced on the final results of the patients.
-The age was the only factor which showed a certain tendency in the evolution to early /late hypothyroidism.

OTHER CLINICAL SCIENCE. INFECTION AND INFLAMMATION 1

PS_419

INFECTON: 99MTC-LABELLED CIPROFLOXACIN IN THE DIAGNOSIS OF BACTERIAL INFECTION. THE ISRAELI EXPERIENCE

C.L. Ben - Horin (1), A. Altschuler (2), A. Raitblat (1). (1) Nuclear Medicine Department ; (2) Radiology Department, Barzilai Medical Center, Faculty of Health Sciences, Ben Gurion University of The Negev, Ashkelon, Israel.

The diagnosis of infectious diseases is still a serious problem despite the wide range of imaging techniques and new therapeutic approaches. Known imaging techniques can be grouped in 2 categories: 1) those able to demonstrate local changes in the anatomy due to infection, in example, computerized tomography and ultrasound; 2) examinations that can demonstrate physiologic changes like those performed in nuclear medicine.
Nuclear Medicine has an important role in the diagnosis of infectious diseases in the human body. Today there is a wide range of well-known examinations, like 99mTc-MDP-bone scan, 67Ga scan, or 111In labeled white cells. Each test has particular indications and the spectrum of differential diagnosis in the case of a positive study is large. We use, for the first time in Israel, a new radio pharmaceutical, 99mTc ciprofloxacin (Infecton) in order to imaging and diagnosis bacterial infections.
The aim of this study was to check the accuracy of Infecton related to other imaging techniques in the diagnosis of bacterial infections.
29 patients (30 scans) were included in the study. All of them had an Infecton scan performed according to manufacturer instructions. Other imaging techniques were 19 ultrasound, 13 computerized tomography, 5 echocardiography, 13 different scans (99mTc MDP bone and 67Ga scans). Blood culture was obtained in 16 patients.
From 30 studies, 17 cases (56%) were considered true positive for bacterial infection; 8 cases true negative (26.6%); 3 cases were summarized as false positive (10%) and 2 cases (6.8%) a false negative. Our sensitivity was 89.1% and our specificity 72.7%.
Conclusion: Infecton is a promising imaging technique to be used in the diagnosis of bacterial infections.

PS_420

TC-99M MIBI IN PULMONARY TUBERCULOSIS EVALUATION

V. Rusu (1), C. Stefanescu (1), D. Boisteanu (2), D. Simion (2), D. Diculencu (2), I. Raileanu (1), T. Mihaescu (2). (1) Department of Biophysics and Nuclear Medicine; (2) Department of Pneumology, UMF, Iasi, Romania.

Our **aims** were to assess the possible usefulness of Tc-99m MIBI for the: 1) scintigraphic evaluation of pulmonary tuberculosis (PTB); 2) scintigraphically evaluation of PTB treatment efficacy (at 6 and 10 months, which rest to be done); 3) finding of new sites of PTB (in relation with the radiologic sites).
Methods: We have studied 28 active pulmonary tuberculosis new diagnosticated patients, without treatment (11 women and 17 men, mean age 29 years, 22 BK positive microscopically, 6 BK negatif). Each of them had i.v. received 7.4 MBq (0.2 mCi)/kg of Tc-99m MIBI. Scintigraphic images have been realised as follows: an anterior planar 3 000 000 counts image on the thorax at 15 minutes, followed by a SPECT acquisition and another anterior planar (same number of counts, same region) image at 60 minutes after radiotracer administration. Two nuclear physicians have analised the images and indexes (counts/pixel) lesion/heart (I-1) and lesion/normal (I-2) were calculated.
Results: In all active PTB the images were positive with I-1 comprised between 1.3 and 4.2, with differences between 15 minutes and 60 minutes images, for the same patient. In 9 BK positive patients suplimentar images have been seen projected in the pulmonary hilar aria, more eviden at 15 minutes. From the 6 BK negatif patients, 4 had positive images (coresponding to macronodular radiologic lesions). In 5 cases new sites (nonrelated to radiologic sites) have been seen. 10 positives patients examined again 7 days after the beginning of the treatment had decresed lesions uptake.
Conclusions: 1) Tc-99m MIBI is usefull for the functional imagistic of PTB; the time interval and degree of positive images seems to depend on the constitution of the lesion. Images at 15 and 60 minutes have relative distinct significance, earlier images being more evident in high BK positive patients. 2) Tc-99m MIBI scintigraphy in pulmonary tuberculosis could be a very earlier marker for the efficiency of PTB treatment, the radiotracer uptake decreasing only in some days, also more evident on the 15 minutes images. 3) Tc-99m MIBI pulmonary scintigraphy can make evidence of new tuberculosis lesions (not evident on X-ray images).
These data suggest that the radiotracer uptake elements in the constitution of PTB lesion are different, and *Mycobacterium Tuberculosis* seems to have a great role, which can be understood by correlated *in vitro* studies.

PS_421

UTILITY OF 99MTC-LABELLED ANTIGRANULOCYTE FRAGMENTS (LEUKOSCAN®) IN JOINT PROSTHESIS INFECTION

S. Carluccio, L. Trombettoni, B. Palumbo, D. Siepi, G. Fiorucci, F. Giuffrida, R. Falchi, A. Bianchi, R. Palumbo. Dept. of Nuclear Medicine, University of Perugia, Italy.

Aim: To investigate the value of ^{99m}Tc-labelled antigranulocyte fragments (Leukoscan®) in our patients we performed immunoscintigraphy in association with three phase ^{99m}Tc-MDP bone scan in patients with infected prostheses.
Methods: We studied 40 patients with suspected infected joint prostheses (22 hip, 12 knee, 6 femur). All patients underwent Leukoscan® (740 MBq i.v.; image acquisition after 4 and 24 hours) and three phase ^{99m}Tc-MDP bone scan. Fifteen out of the 40 patients underwent a ^{99m}Tc-HMPAO-WBC-scan (740 MBq i.v.; image acquisition after 4 and 24 hours) carried out 2 months before Leukoscan® for the same clinical suspicion. In addition in 10 out of the 40 patients a three phase evaluation with Leukoscan® was carried out in order to compare the data obtained with the results of three phase ^{99m}Tc-MDP bone scan. Ten patients underwent again Leukoscan® 4-6 months after the first exam for monitoring the effectiveness of therapy or for a worsening of the clinical conditions.
Results: 31 pts (77.5%) had positive Leukoscan® suggestive for sepsis, while 9 (22.5%) negative. The diagnosis was later confirmed by clinical follow up and a positive correlation ($p<0.00$; $r^2=0.894$) was observed between Leukoscan® and follow up. The Leukoscan® technique in our subjects was sensitive and specific, showing 2.7% of false negative cases, 21.6% of true negative and 75.7% of true positive. No false positive cases were observed in our study. Patients with a second Leukoscan® presented results that were in agreement with the clinical situation. Previous ^{99m}Tc-HMPAO-WBC-scan data of the patients studied were well related with the subsequent Leukoscan® (8/10 had the same results, while 2 had an increased uptake at Leukoscan®), being the comparison possible because very short was the interval between the 2 exams for the reason of a persistent pathology. Furthermore three phase evaluation with Leukoscan® in our patients provided similar results of three phase ^{99m}Tc-MDP bone scan, although scarce is the number of patients studied with both the three phase scans and a statistical analysis is not actually possible.
Conclusions: In our study Leukoscan® is confirmed as a valid indicator of infection of prostheses, while particularly interesting in our opinion seems to be the three phase evaluation, might probably being able to represent an alternative choice to three phase ^{99m}Tc-MDP bone scan. Further studies with an increased number of patients are necessary to strengthen these data.

PS_422

TC-99M IGG SCINTIGRAPHY IN PATIENTS WITH BEHCET'S DISEASE WITH AND WITHOUT ACTIVE UVEITIS

E. Varoğlu (1), G. Güllülü (2), H. Uslu (1), I. Akyol (2), M. Yıldırım (1), C. Ak (1), M. Demirci (1), A.R. Odabaş (3), R.A. Sarı (3). (1) Atatürk University Medical Faculty, Dept. Of Nuclear Medicine; (2) Atatürk University Medical Faculty, Depts. of Ophtalmology; (3) Atatürk University Medical Faculty, Depts. of Internal Medicine, Erzurum, Turkey.

The purpose of this study was to evaluate the role of Tc-99m IGG scintigraphy in the differentiation of active uveitis from inactive uveitis in patients with Behcet's Disease.
Methods: This study included 15 Behcet's patients and 7 healthy volunter as a control group. Total 30 eyes of the patients with Behcet's Disease and 14 eyes of control subjects were studied with Tc-99m IGG scintigraphy. There were 4 Behcet's patients with bilateral and 2 with unilateral active uveitis. Thus, 10 eyes with active uveitis of 6 patients with Behcet's Disease were examined. Remaining 2 single eyes of these patients, 18 eyes of 9 patients with inactive uveitis and 14 eyes of control subjects were also studied. Four hours after I.V injection of 20 mCi Tc-99m IGG, anterior planar images were obtained. Semi-quantitative analyses were performed drawing ROI around both eyes and on the scalp. Eyes to background activity ratios expressed eye / scalp indices were calculated.
Results: The eye / scalp indices of 10 eyes with active uveitis, 20 eyes without active uveitis and 14 eyes of control group were 1.69 ± 0.20, 1.49 ± 0.18 and 1.52 ± 0.27 respectively. The eye / scalp indices of the patients with active uveitis significantly greater than those of the patients without active uveitis, and normal subjects as well ($p = 0.007$, $p = 0.01$, Mann-Whitney U test).
Conclusion: Our results indicated that Tc-99m IGG scintigraphy could accurately use to differentiate active from inactive uveitis in patients with Behcet's Disease

PS_423

THE USE OF 99MTC-WBC SPECT IN SEPTIC CARDIOSURGERY: CLINICAL EXPERIENCE

G. Khubulava (1), N. Fadeev (2), V. Soukhov (2). (1) Military Medical Academy, Saint Petersburg, Russia; (2) Central Research Institute of Roentgenology and Radiology, Saint Petersburg, Russia.

The risk of septic complications remains high in spite of cardiosurgery techniques development. This is really true for prosthetic valve endocarditis (PVE) which diagnosics is the most difficult up to day. The inadequacy of such diagnostic procedures as CT, MRI and transesophageal EchoCG required more informative survey for the detection of PVE signs. For the solving of this problem whole-body scans and thoracic SPECT with ^{99m}Tc-HMPAO (hexametylpropilenaminoxim) labeled autoleucocytes in patients with PVE were performed. WB-scans and tomographic slices of fifty nine patients (27 females and 32 males) aged 16-56 years were evaluated. In 1, 3 and 24 hours postinjection inflammatory foci within the heart were seen as the areas of pathogenic activity. To ensure topic diagnostics we use 201Tl-SPECT in the same position of the patient (Patetented 1998)
In 18 patients the circumscribed activity seen in relation to prosthetic heart valves convincingly demonstrated abscesses 8-15 mm in diameter, and in 29 – vegetations. Eighteen patients had the scintigraphic evidence of pancarditis. The remaining patients showed a negative scan over the heart correlated with echocadiographic data, but whole body scanning revealed extracardiac infection (frontitis, sphenoiditis, ulcerative colitis, cholecystitis, empyema of pleura, mediastinitis and septic complication of postpoperative wound).
The data demonstrated that ^{99m} Tc-leucocytes imaging is a feasibe method for the detection of PVE, other septic complications of cardiosurgery and also noncardiac infection.

PS_424

THE USEFULNESS OF NUCLEAR MEDICINE PROCEDURES IN THE DIAGNOSIS AND MANAGEMENT OF THE DIABETIC FOOT

F. Matteucci, S. Severi, C. Corbelli. Nuclear Medicine Dpt, Faenza, Italy.

Early and accurate diagnosis of infection in diabetic foot is the key to successful management: diagnosis is difficult because the clinical likelihood of OM often does not appear through radiographic imaging.
Objectives: the aim of our study was to evaluate the diagnostic value of 99m-Tc-HMPAO-leukocyte scan (WBS) in combination with 99mtc-MDP bone scintigraphy (BS) for detection OM in diabetic patients (pts).
Methods: we have studied 35 pts (14 male and 21 female) with mean-age 59 (range 22-74 yr) with insulin dependent-diabetes, foot ulceration and suspicion of OM; all pts were submitted to clinical examination, radiography, ultrasonography and bacterial colture. All pts underwent BS with 740 MBq Tc-99m-MDP while injected, five minutes and three hours after being injected; a week later they were submitted to WBS, 4 and 24 hours after the administration. BS and WBS images were compared and defined positive or negative for OM. The final diagnosis was established by clinical follow-up and histological findings.
Results: OM was confirmed in 18 cases with WBS and BS; in 9 pts WBS and BS were negative for OM, confirmed by clinical follow-up; in 3 pts who resulted affected by OM, BS was negative while WBS was positive. In 3 pts giving negative results, BS showed a false-positive pattern, while in 2 pts with OM and BS positives, WBS was false negative.
The sensitivity, specificity and accuracy resulted of 91%, 100% and 94% for WBS, while for BS, 87%, 75% and 83% respectively.
Conclusions: our study confirms the importance of the nuclear medicine procedures in the diagnosis of OM; compared with BS, WBS proved to be more sensitive, specific and accurate.

PS_425

SCINTIGRAPHIC EVALUATION OF ACUTE PANCREATITIS PATIENTS WITH 99MTC-HMPAO LABELLED LEUKOCYTES

H. Uslu (1), A. Balık (2), M. Yıldırım (1), R. Bayrakdar (1), I. Hacıbeyoğlu (1), B. Seven (1), E. Varoğlu (1), I. Yılmaz (2). (1) Atatürk University Medical Faculty, Dept. of Nuclear Medicine; (2) Atatürk University Medical Faculty, Dept. of General Surgery, Erzurum, Turkey.

Our purpose was to demonstrate the localization of leukocytes in the pancreas during acute pancreatitis and to evaluate the contribution of the 99mTc-HMPAO labelled leukocyte in the prognostic assessment of patients with acute pancreatitis.
Methods: The study was performed on 15 patients (9 females, 6 males, age range 26-86 yrs, mean age 55 yrs). Labelled leukocyte scintigraphy using planar imaging and single photon emission computed tomography (SPECT) were performed to all patients. According to Ranson criteria, 8 patients had mild (group A), 5 had severe (groupB) and 2 had necrotic (group C) pancreatitis. Ten patients had biliary pancreatitis and the other five patients had no obvious cause.
Results: All patients of group C, three of group B, one of group A had a positive leukocyte scan.The sensitivity of leukocyte scintigraphy for the detection of a lethal course of acute pancreatitis was 100 %, of a severe course 60 % and of a mild course 12.5 %. The results of leukocyte scintigraphy were compared with the those of CT. All the patients with pancreatic necrosis in CT had a positive leukocyte scan. But two of ten patients without detectable pancreatic necrosis in CT had a positive leukocyte scan.
Conclusions: There was a correlation between the severity of the disease and leukocyte infiltration.Considering these results, we believe that leukocyte infiltration in the acute pancreatitis can be demonstrated by noninvasive 99mTc-HMPAO labelled leukocyte scintigraphy.

PS_426

REFLEX SYMPATHETIC DYSTROPHY SYNDROME: DIAGNOSIS AND FOLLOW UP OF THE TREATMENT

G. Fountos (1), I. Schina (2), L. Disnitsas (3), E. Kounadi (4), G. Papadopoulos (3). (1) Department of Medical Physics. Pammakaristos General Hospital of Athens, Greece; (2) Department of Nuclear Medicine. University Hospital of Ioannina Greece; (3) Department of Anaesthesiology. University Hospital of Ioannina Greece; (4) Department of Medical Physics. Alexandra General Hospital of Athens, Greece

Reflex Sympathetic Dystrophy Syndrome (RSDS) is a malfunction of the sympathetic neural system causing movement dysfunction in acroteria. These symptoms are accompanying with pain, swelling in an extremity, vasomotor instability and dystrophic skin. Diagnosis of (RSDS) have difficulties despite that have described from the past century. The scintigraphy as a method of diagnosis rely mainly in enhanced periarticular radionuclide activity in affected extremity in three phase bone scan. Aim of this study is to investigate the sensitivity of the diagnostic method when using MDP-99mTc scintigraphy combined with NANOCOLL-99mTc scintigraphy instead of MDP-99mTc scintigraphy alone. Also the ability of the method to follow up treatment is investigating.

Method: The study was performed in seventy (70) patients ranging from 18 to 67 years. The average age was 42 years. These patients were examined with both scintigraphic methods, 53/70 were examined once only before treatment, 25/53 suffered from (RSDS) while 28/53 suffered from other disease. 17/70 were examined and after therapy. The scintigraphic diagnosis were based in each case by both 1) MDP-99mTc dynamic scintigraphy and 2) NANOCOLL-99mTc dynamic scintigraphy. The scintigraphy applied in the acroteria diseased area.

Results: 1) Three phase dynamic scintigraphy with MDP-99mTc: The increased blood flow in first and second phase was not observed in all patients with (RSDS) while in the third phase in all patients was observed increased uptake of the radionuclide periarticular in joints of the affected extremities. During and after treatment the changes in scintigraphic images were not usefull to following up treatment.

2) Three phase dynamic scintigraphy with NANOCOLL-99mTc: The increased blood flow in first phase was observed in all patients with (RSDS) while in second and third phase we observe that was unable to visualize the structure of vessels and in many cases increased diffusion of the radionuclide in the affected extremity was record. Also in all patients changes in scintigraphic images was observed during and after treatment.

Conclusions: The clinical diagnosis of (RSDS) was confirmed using three phase dynamic scintigraphy with MDP-99mTc in all patients while the combination of the two scintigraphic methods provide increased sensitivity in the diagnosis of (RSDS) and the ability to follow up treatment.

PS_427

COMPARATIVE STUDY OF MONOCLONAL ANTIBODY SCAN (LEUCOSCAN) WITH 99MTC MDP BONE SCAN AND GA 67 JN DIAGNOSING BONE AND JOINT INFECTION. PRELIMINARY RESULTS

S. Koukouraki (1), A. Velidaki (1), H. Vavouranakis (2), A. Hatzipavlou (2), N. Karkavitsas (1). (1) Department of Nuclear Medicine, Crete, Greece; (2) Department of Orthopaedics, Crete, Greece.

Aim : the accurate diagnosis of bone and joint infections is very important for the decision of the therapeutic procedures in many clinical conditions. The purpose of this study is to compare the diagnostic accuracy of a new radionuclide scan Leucoscan, with 99mTc MDP bone scan and Ga67 in bone and joint infections.

Methods : Twenty two patients with suspected bone and joint infection (10 with total hip prosthesis, 4 with knee prosthesis, 2 with vertebral infection and 6 with long bone infection) were included in this study. All patients underwent conventional Rx, bone scan, Ga67 scanning and Leucoscan. Three phase 99mTc-MDP and Ga67 were performed using standard procedures. The monoclonal antibody, Leucoscan was labeled with 25 mCi of 99mTc and was injected intravenously. Planar images were taken 1h and 2h p.i using a GE Millenium ? camera provided with a LEGP collimator. The images were evaluated as score 1 (no abnormal uptake in the region of interest), 2(probably positive), 3(definitely infected), according the intensity of abnormally increased uptake. Leucoscan results were compared with 99mTc MDP bone scan and Ga 67 scans. The final diagnosis was given by the surgical verification with histopathology or culture.

Results : Seventeen of 22 patients had surgically or pathologically proven infection. 5/22 patients were negative for infection .14/17 with proven bone or joint infection had positive Leucoscan, and 12/17 positive Ga67 scanning. 4/5 patients with proven absence of infection had negative Leucoscan and 3/5 negative Ga 67 . Leucoscan showed a sensitivity 90% and specificity 80%.and Ga67 87% and 75% respectively.

Conclusion: Radiolabelled monoclonal antibody scan (Leucoscan), despite the small number of patients seems to be more sensitive and specific than Ga67 in diagnosing bone and joint infections.

PS_428

POSTOPERATIVE FEVER: PROSPECTIVE EVALUATION OF 18 FDG-IMAGING WITH A DOUBLE HEAD COINCIDENCE CAMERA (DHCC)

J. Meller, G. Altenvoerde, K. Lehmann, C. Sahlmann, I. Meyer, M. Behe, H. Luig, W. Becker. Department of Nuklear Medicine, University of Göttingen, Germany.

Aim: [18F] 2α-deoxy-2-fluoro-D-glucose (FDG) has been shown to be an effective tracer in the diagnosis of malignant and inflammatory disease. The aim of our study was the prospective evaluation of FDG-imaging with a double head coincidence camera (DHCC) in patients with undetermined postoperative fever (POF). POF was defined as fever >38,3¡ C, with unset within the first two postoperative weeks.

Methods: This study is a prospective analysis of 15 POF-patients (18 investigations) who underwent transaxial F-18- FDG- imaging with a double head coincidence camera (DHCC). Imaging was performed one hour following the intravenous injection of 300 MBq FDG. The final diagnosis was established by clinical follow up, X ray studies including high resolution helical CT, magnetic resonance imaging, bacteriological cultures, biopsy and endoscopy. The FDG images were interpreted by two investigators both blinded to the results of other diagnostic modalities.

Results: Infection was present in 7 patients (47%; 10 investigations; Group A). In this group FDG-imaging revealed 9 foci outside the surgical wound (inflammation n= 8, malignant disease n=1) responsible for fever. 5 foci were restricted to the surgical wound but only two of these foci represented inflammation (duration of POF> 8 weeks). 3 foci were due to granulation tissue (duration of POF< 8 weeks). In one patient with urosepsis we found a false negative FDG-study.

Infection could subsequently excluded 8 patients (53%; 8 investigations; Group B). 7 of these patients had a negative scan. In one patient a FDG-accumulation was found within the surgical wound but again granulation tissue was present (duration of POF< 8 weeks). Overall sensitivity of FDG-imaging in detecting the focus of fever was 91% but specifity was only 64% respectively.

Conclusion: 1. In the context of POF FDG transaxial tomography performed with a DHCC is sensitive in the diagnosis of inflammation and malignant disease within and outside the surgical wound.

2. The specifity of the method of detecting the focus of fever within the surgical wound is poor and therefore In-111 white blood cell imaging remains the scintigraphic procedure of choice in the diagnostic work up of POF.

PS_429

DETECTION OF INFLAMMATORY LYMPH NODES BY TC99M-HIG IN RABBITS

EL. Ergün (1), MF. Bozkurt (1), M. Ercan (1), S. Ruacan (2), B. Şener (3). (1) Department of Nuclear Medicine; (2) Department of Pathology; (3) Department of Clinical Microbiology, Hacettepe University, Ankara,Turkey.

Aim: ^{99m}Tc-HIG is known to be useful in the detection of inflammatory lesions. It was also found to be a successful and promising new agent for the visualization of lymphatic system.Our aim was to investigate the feasibility of demonstrating inflammatory lymph nodes with ^{99m}Tc-HIG.

Methods: Ten adult New Zealand rabbits were used initially (Group A).In baseline study, 37 MBq ^{99m}Tc-HIG (0.1 ml) was injected in both hind legs of the rabbits and sequential posterior gamma imaging of the rabbits lying prone was performed at 5, 30, 60, 90 and 120 min. under a single-headed gamma camera (Toshiba GCA G01 E). One week later, microorganisms (Staph.aureus) were injected in 0.1 ml volume intradermally into the web space between the second and third toes in bilateral hind legs of each rabbit in order to obtain inflammation in the popliteal lymph nodes and after 4 days 37 MBq ^{99m}Tc-HIG (0.1 ml) was injected in hind legs of rabbits and sequential imaging was done as described (the second study). Another group of 10 adult New Zealand rabbits (Group B) was injected by the same microorganisms in the right hind legs only. After 4 days scintigraphic imaging was carried out in the same way as described above (the third study). Regions of interests were drawn over the.injection sites and popliteal lymph nodes on each image for semiquantitative analysis. Count rates for each were calculated and decay correction was applied. Time-activity curves were generated to show the percent retention of radioactivity in each region. After scintigraphic imaging, some of the Group B rabbits were killed by intravenous injection of pentobarbitone (100-150 mg/kg). Both left and right popliteal lymph nodes were removed for microscopic examination.

Results: The baseline study showed good visualization of lymphatic channels and nodes. In the second study, bilateral popliteal lymph nodes were visualized more prominently than the baseline study. The right popliteal lymph nodes of Group B rabbits were more dominantly and clearly imaged in the third study. Semiquantitative analysis showed higher percentage uptake of radioactivity in the right compared to the left popliteal lymph nodes in Group B rabbits. Microscopic examination demonstrated inflammation in the right popliteal lymph nodes of Group B rabbits.

Conclusion: This preliminary study showed that 99mTc-HIG is a new promising agent for demonstration and evaluation of inflammatory lymph nodes.

PS_430

TC-99M CIPROFLOXACIN IMAGING IN VARIOUS CLINICAL SETTINGS: EXPERIENCE AT INHA UNIVERSITY, SOUTH KOREA

W. Choe (1), D.Y. Chi (2), M.W. Im (3), M.H. Chung (4), J.S. Ryu (4), J.K. Suh (5), S. Kim (1). (1) Nuclear Medicine; (2) Chemistry; (3) Obstetrics-Gynecology; (4) Internal Medicine; and 5 Urology, Inha University, Inchon, South Korea

Tc-99m Ciprofloxacin imaging was initiated by Solanki et al (J Nucl Med 34:119p, 1993), and is an imaging method to differentiate infection from inflammation. Furthermore, it can visualize a focus of infection specific to bacterial infection. Interestingly enough, it also claims to show an area with viable, proliferating bacterial population that is actively using DNA gyrase, which the Ciprofloxacin inhibits. The aim of this study was to confirm these characteristics using our own custom-formulated Tc-99m Ciprofloxacin.

Methods:

Preparation of Tc-99m Ciprofloxacin: Two mg of Ciprofloxacin were mixed with 1 mg of formamidine sulfinic acid in a 10 ml sterile serum vial, and dissolved on a vortex-gene 2 for 3 minutes. Ten mCi of Tc-99m were added to the vial. The air from the vial was evacuated, and the vial was microwaved in a 1000W microwave oven for 12 seconds. It was then cooled at room temperature for 5 minutes. Distilled water was added and filtered prior to intravenous injection. For quality control, instant thin layer chromatography was performed.

Imaging: Immediate, 1, 4, and 24-hour (in some cases) images of the whole body and/or spot views in the anterior and posterior views were obtained. SPECT images were added when necessary.

We have imaged 70 patients in the following clinical settings: patients with 1) orthopedic surgical prosthesis with suspicious bacterial infection, 2) soft tissue infection, 3) female pelvic inflammatory disease (PID), 4) pulmonary tuberculosis, and 5) chronic prostatitis.

Results: We achieved a 94% labeling efficiency.

1) Excellent visualization of the peri-prosthetic infection and verification of the previous reports of others, 2) detection of bacterial infection of the soft tissue in bacteremic patients, 3) verification and localization of PIDs that corresponded to physical examination, 4) visualization of active pulmonary tuberculosis, and 5) more uptake in the area of the prostate in the patients compared with the normal subject were shown.

Conclusion: Our custom-formulated Tc-99m Ciprofloxacin is as valid and convenient to use as any other previously reported in visualizing bacterial infection. The data obtained in this study suggests further validation and application of this imaging method in verifying peri-prosthetic infection, soft tissue infection, PID, and exacerbation of the chronic prostatitis, and in following-up the active pulmonary tuberculosis biologically.

PS_432

EVALUATION OF PULMONARY ARTERIAL BLOOD FLOW WITH 99MTC-MACROAGGREGATE ALBUMIN FIRST-PASS SCINTIGRAPHY

M. Sapienza (1), F. Hironaka (1), T. Watanabe (1), C. Ono (1), P. Aguirre Costa (1), I. Endo (2), S. Lewin (2), M. Marone (2), C. Buchpiguel (1). (1) Centro de Medicina Nuclear, University of Sáo Paulo, Brazil; (2) Hospital Samaritano, Sáo Paulo, Brazil.

Pulmonary artery blood flow is pulsatile, with a systolic and a diastolic peak intervened with a low amplitude retrograde flow. Retrograde flow probably occurs due to wave reflection in arterioles, a level where the available techniques are limited in the evaluation of pulsatility.

AIM: The purpose of this study was to develop a scintigraphic method to detect pulsatile events in peripheric pulmonary arteries.

METHODS: 10 healthy volunteers (34±10 year old, 2 males) underwent a first-pass study using ^{99m}Tc-MAA, with high temporal resolution (16 frames/sec) and ECG coregistration. Systemic shunt was excluded by whole body images. A time-activity curve (TAC) was generated for the lateral third of the right lung, and 4 to 6 heartbeats were selected in the phase with the highest slope in lung activity. Lung activity variation during these heartbeats depends only upon arterial flow and, as a result, the first derivative of the TAC mirrors pulmonary arterial flow.

RESULTS: TAC derivative shows two positive peaks (anterograde flow) and a negative peak (retrograde flow) between them, that was statistically significant by Poisson based statistics. The retrograde flow in the lateral third of the lung is higher than that described in central vessels, and similar to the one calculated by mathematical models.

CONCLUSION: Although still under investigation, the method described can increase our understanding of pulmonary flow pulsatility in physiological and pathological conditions.

OTHER CLINICAL SCIENCE. MISCELLANEA 1

PS_431

GLUCOSE UPTAKE IS PERFUSION-INDEPENDENT IN RESTING SKELETAL MUSCLE

V. Oikonen (1), P. Peltoniemi (2), U. Ruotsalainen (3), P. Nuutila (1), J. Knuuti (1). (1) Turku PET Centre, University of Turku, Turku, Finland; (2) Dept. of medicine, University of Turku, Turku, Finland; (3) DMI/Tampere University of Technology, Tampere, Finland.

Aim: There is some controversy over whether insulin increases perfusion in skeletal muscle and to which extent the increased blood flow would affect muscle glucose uptake. The relations between perfusion and glucose uptake in resting skeletal muscle were studied using positron emission tomography (PET) and [^{18}F]fluoro-2-deoxy-D-glucose (FDG).

Methods: FDG PET data from healthy young men, five in fasting state and five during an euglycemic hyperinsulinemic clamp (1 mUá(kg body weight)$^{-1}$min^{-1}), were analyzed using a four-compartmental model with six rate constants k_1-k_6 and vascular volume fraction V_A. The three tissue compartments in this model are the concentrations of FDG in the extracellular space and in the intracellular space, and the intracellular concentration of phosphorylated FDG.

Results: The perfusion and endothelial permeability (k_1) was 27 % higher and FDG transport increased three-fold in the insulin studies. Phosphorylation rate (k_3) was too high to be reliably measured in the insulin studies. The FDG uptake constant K, calculated as $K = k_1k_3k_5 / (k_2k_4+k_2k_5+k_3k_5)$ increased six-fold from 0.0016±0.0003 min^{-1} to 0.0093±0.0038 min^{-1}.

Parameter	Fasting	Insulin
k_1	0.017±0.001	0.022±0.007
k_2	0.224±0.023	0.178±0.136
k_3	0.039±0.014	0.123±0.039
k_4	0.019±0.012	0.003±0.004
k_5	0.025±0.008	0.72±0.83
V_A	0.018±0.010	0.015±0.009

A simple simulation showed that in the fasting state even a 100 % increase in the two perfusion-dependent parameters, k_1 and k_2, causes only a 5 % increase in K, which is in direct relation to glucose consumption by the muscle. During hyperinsulinemia, the increase in K would be 25 %, if glucose transport and phosphorylation were not down-regulated subsequently.

Conclusions: The effect of insulin on perfusion to muscle is minimal when compared to its impact on glucose transport. Increased perfusion is not expected to markedly enhance glucose uptake in resting skeletal muscle in healthy and especially not in insulin-resistant subjects.

PS_433

PREFERENTIAL VAGINA TO UTERUS PHYSIOLOGICAL CONNECTIONS EVALUATED BY SERIAL RADIONUCLIDE SCAN

G. Rubini (1), E. Cicinelli (2), D. Rubini (1), A. Niccoli-Asabella (1), M. Mele (1), P. Galantino (2), A. D'Addabbo (1). (1) Department of Nuclear Medicine; (2) I Department of Gynecology and Obstetrics, University of Bari, Italy.

Aim: The aim of the study was to investigate in vivo and in humans preferential physiological connections between the vagina and uterus in post-menopausal woman by serial scintigraphic evaluation.

Material and Methods: In pre-surgical (hysterectomy for benign disease) assesment phase 5 postmenopausal women received one vaginal administration of 0,2 ml of 99mTc-Pertechnetate corresponding to 15 MBq. Before administering the radionuclide, in 2 pts, the cervical canal was sealed by means of surgical glue. The biodistribution and kinetics of the radionuclide were monitored from radionuclide administration for 6 hours. Anterior and right lateral views (128 matrix, pre-set time:300 sec) of the pelvis and anterior view of the neck and abdomen were collected every 30 min. Radionuclide distribution was assessed in the area of administration and in the whole body.

The biodistribution of intravaginal administration compared to intravenous injection was evaluated. As a control, uterine and extrapelvic organ uptake of the same radionuclide was evaluated after intravenous administration in 5 postmenopausal woman undergoing thyroid scintigraphy.

Results: After intavaginal administration radioactivity was found only at the injection site for 60min. After 60 min the uterine activity began to appear and gradually reached the maximum after 180 min. In 3 pts uterine activity was maximal at 180 and in 2 pts at 210 min, then gradually decreased. After 330 min no uterine uptake was detectable. The 2 pts with occluded cervical canal showed the same biodistribution and kinetics as pts in whom the cervical canal had not been occluded. Extrapelvic uptake in the thyroid, salivary gland and stomach was detected in all pts but with a delay of 30 min after uterine visualization. In thyroid the uptake started 210 min and reached the maximum at 360 and than decrease. A lower uptake was detected in salivary glands and stomach with same time course. I.v. administered radiopharmaceuticals showed no uterine uptake, while thyroid salivary glands and stomach uptake was rapid and massive after just 30 min.

Conclusions: This study demonstrates the possibility of vaginal absorption of 99mTc-Pertchnetate as well as other pharmaceuticals. It is mediated by vaginal absorption of substances and subsequent preferential transfer mechanism to the uterus and not simply by cervico-uterine canal passage. The results of the study demonstrate „in vivo" and in humans, and specifically in postmenopausal women that there are preferential vagina-to-uterus vascular connections and gives an insight in to the mechanisms underlying this phenomenon.

PS_434

SCINTIANGIOGRAPHY IN THE EVALUATION OF PERFUSION IN NECROTIC TOES

P. Ylikangas (1), T. Lantto (2), R. Mokka (3). (1) Department of Clinical Chemistry and Nuclear Medicine, Päijät-Häme Central Hospital, Lahti, Finland ; (2) Department of Laboratory Centre, Tampere University Hospital, Tampere, Finland; (3) Department of Surgery, Päijät-Häme Central Hospital, Lahti, Finland.

The aim of this study was to evaluate the perfusion in clinically necrotic or blue, cold toes by scintiangiography.
Method: 93 toes in 10 patients were imagined and the case records of the patients were studied retrospectively. 28 of 93 toes were clinically blue or in such necrosis that resulted into amputation within one month after the scintigraphy.
740 MBq 99m-Tc-pertechnetate was injected.into a superficial vein of arm. Potassium perclorate was given orally before the injection to inhibit the accumulation of radioactivity in thyroid gland. Dynamic imaging of feet was done during circulation, and a static image was taken patient's feet against the collimator. The heads of the toes were marked with cobolt pen.
Results: There was no perfusion in scintiangiography in 25 of 28 clinically necrotic toes (true positives). We did not find any clinically vital toe, which was not perfused in scintiangiography (no false positive findings). In 3 of 33 later amputated toes, perfusion was normal in scintigraphy (false negative findings). 2 of those 3 toes were blue, not necrotic. 65 of 93 toes were clinically normally perfused, and the perfusion in scintiangiography was normal too (true negatives). The sensitivity of scintiangiography in this study was thus 89% and the specificity was 100%.
In addition, we imagined a patient, who had serious ischemia in his foot. 4 of 5 toes were clinically black, but the perfusion in toe was normal in scintiangiography. The patient went through a vascular by-pass operation, which improved the circulation in his foot, and no amputation was done.
Conclusions: Scintiangiography is a simple, non-invasive method for evaluation of the peripheral perfusion in feet. If the toes look necrotic, but have some perfusion left in scintiangiography, a vascular by-pass operation may be considered to improve the circulation in a foot in some cases. No false positive scintiangiographic images were found.

PS_435

DACRYOSCINTIGRAPHY IN THE EVALUATION OF NASOLACRIMAL DUCT PATENCY

P.S. Sundaram (1), S. Padma (1), P. Ravi (2), N. Jaganath (3). (1) Nuclear Medicine, Amrita Institute of Medical Sciences & Research Centre, Cochin, India; (2) Nuclear Medicine, S V Institute of Medical Sciences, Tirupati, India; (3) Ophthalmology, S V R R Hospital, Tirupati, India.

PURPOSE: Dacryocystitis is a common ophthalmic clinical condition in certain parts of India which is due to inflammation of lacrimal sac. It is a chronic condition usually involving the lower strata of society which can be easily controlled on early diagnosis. Dacryoscintigraphy can be instrumental in the diagnosis of nasolacrimal duct obstruction which leads to dacryocystitis.It is a simple, easy to perform imaging modality which is an alternative to dacryocystography , an invasive non physiological radiological procedure .The purpose of presenting this study is to highlight ;
The extreme sensitivity & simplicity of this imaging modality.
The high incidence of dacryocystitis in low socio-economic segment of Indian population.
The physiologic basis of this investigation.
METHODS: A total of 55 patients were screened, of which 40 were symptomatic and the rest (15) constituted the control group.99m Technetium Pertechnetate (TcO4) was instilled at the lateral canthus simultaneously in both eyes.Dynamic and late static images were acquired using a single head Gamma Camera with High Resolution Collimator.
RESULTS: Bilateral obstruction were noted in 22 patients of whom 9 had clinically unilateral Presentation. Unilateral obstruction was seen in 18 patients (right = 8 & left = 10).
CONCLUSION: We inferred from our studies that; a) Number of cases of bilateral obstructions exceeded unilateral cases .b)Peak incidence was found in middle aged females. C) It was closely associated with low income group. d) Members of the same family should be closely assessed. e) Bilateral obstruction are prevalent in unilateral clinical presentation.
Time, manpower and equipment should not be a constraint in performing this simple inexpensive investigation. Dacryoscintigraphy is physiological, non-invasive and has better patient compliance. So, screening of families should be undertaken by dacryoscintigraphy to enable early diagnosis of this condition. During imaging high resolution collimator is an efficient substitute to conventional pinhole collimator & it is advantageous as both eyes can be imaged simultaneously.
It has also been found that image acquisition in sitting posture has an edge over supine position.

PS_436

EVALUATION OF EXTRAPULMONARY GA-67 UPTAKE IN SARCOIDOSIS-A RETROSPECTIVE ANALYSIS

N.Ö. Küçük, E. Özkan, B. Gulev, G. Aras, M.K. Kir. Department of nuclear medicine, Ankara University, Turkey.

Ga-67 whole body imaging is frequently used in the diagnosis and prognosis of sarcoidosis. According to the disease activity pulmonary involvement is most commonly seen but it can also involve other organs (%10-15).
Ga-67 scintigraphy at 47 patients with sarcoidosis was investigated to evaluate the extrathoracie involvement retrospectively. 10/47 (21 %) patients had normal Ga-67 whole body scintigraphy, 14/47 (30 %) had hilar and mediastinal uptake (ambda sign) and 15/47 (32 %) had only hilar uptake and 3/47 (6 %) had only mediastinal uptake, 5/47 (11%) had diffuse lung parenchymal uptake .
In the examination of extrathoracic involvement ; the most characteristic extrapulmonary uptake pattern was the 'panda sign' in 11 patients (23 %). The most common site of prominent extrapulmonary uptake was the lacrimal glands in 21 patients (45 %). The lymph node uptake was observed in 9/47 patients (3 inguinal , 3 supraclavicular , 1 axillary , 3 abdominal 19 %) 4/47 patients had articulary uptake (1 knee, 3 shoul- der , 9%). Breast uptake was seen in one patient and one had cranial uptake .
Ga-67 whole body scintigraphy demonstrates not only pulmonary but also extrapulmonary involvement , and helps the clinician to evaluate the extension and activity of the disease.

PS_437

BIOCHEMICAL AND DENSITOMETRIC EVALUATION OF POST-MENOPAUSIC OSTEOPOROTIC PATIENTS SUBMITTED TO ANTI-REABSORPTIVE TREATMENT DURING ONE YEAR

A. Rodrigues (1), P. Lourenco (1), P. Ferreira (2), A. Garrett (1), E. Moura (1). (1) Laboratorio de Radioisotopos, Faculdade de Medicina, Universidade de Coimbra; (2) Serviço de Medicina III, Hospitais da Universidade de Coimbra, Portugal.

Introduction: Osteoporosis is an important public health problem, especially among postmenopausic females due to its morbidity and mortality. Therapy has to be maintained over a prolonged period of time and its result can be verified only by radiologic densitometry after one or two years.
Biochemical markers permit the evaluation of bone metabolism and may therefore be useful in early monitoring of treatment in order to adjust doses and to promote compliance.
Methods: One hundred and three post-menopausic women referred from their GP, were randomly assigned to one of three therapeutic groups: 1 - calcium and vitamin D; 2 - calcium and calcitonin; 3 - calcium and alendronate.
Levels of bone alkaline phosphatase (BAP), osteocalcin (OC), deoxypyridinoline (Dpd) and cross-linked N-telopeptide (NTx) were determined at baseline and after three, six and twelve months of treatment. One year after starting therapy, the lumbar spine, proximal femur and distal forearm were evaluated by DEXA (Hologic QDR 4500 Elite).
Results: The patients treated with alendronate had a significant increase of bone mineral density (BMD) in the lumbar spine. After three months there was a statistically significant decrease of BAP and NTx levels in the group treated with alendronate. In these group there was also a statistically significant decrease in the level of all markers determined after twelve months.
Conclusions: The group treated with alendronate was the only one to show significant increase on BMD after one year of treatment. In this very group the determination of BAP and NTx levels after three months showed a biochemical profile consistent with a response to anti-reabsorptive treatment.

PS_438

CONTRALATERAL EFFECTS OF ACUPUNCTURE ON REGIONAL CEREBRAL BLOOD FLOW ELOW EVALUATED BY 99M TC-ECD BRAIN SPECT AND STATISCTICAL PARAMETRIC MAPPING

H.-C. Song (1), S.M. Kim (1), H.S. Bom (1), S.G. Ahn (2), H.J. Kang (3). (1) Department of Nuclear Medicine, Chonnam National University Hospital, Kwangju, South Korea; (2) Department of Acupuncture & Moxibustion, College of Oriental Medicine, Wonkwang University, Kwangju, South Korea; (3) Department of Circulatory Internal Medicine, College of Oriental Medicine Dong-shin University,Kwangju, South Korea.

Purpose: To study correlation of the brain areas with acupoints to evaluate the hypothesis that selecting acupoints on the left side to treat disorders on the right side and vice versa is known as the crossing combination of acupoints.
Methods: Rest/acupuncture-stimulation ^{99m}Tc-ECD brain SPECT using a same-dose subtraction method was performed on 13 normal male volunteers (age range from 20 to 32 years) at acupoint, LI. 4 on the right hand. And 5 normal male volunteers (age range from 27 to 30 years) using acupuncture at acupoint. LI. 4 located on the left hand. In the control study needle location was chosen on a non-meridian focus 1cm posterior to the right fibular head. All images were spatially normalized, and the differences between rest and acupuncture stimulation were statistically analyzed using SPM97 for Windows.
Results: Stimulation at LI. 4 located on the right hand increased rCBF in the left hemisphere, mainly the left parietal and frontal lobes, and a part of the left temporal lobe Stimulation at LI. .4 located on the left hand increased rCBF in the right hemisphere, mainly the right parietal lobe, and a part of the right temporal lobe. In the control stimulation, no significant rCBF increase was observed.
Conclusion: The results demonstrated rCBF increase in the contralateral cerebral hemisphere of acupoint. Therefore, this result suggests that the action mechanism of acupuncture have a neural basis operating through the ascending neural tract crossing the midline at a certain level.

PS_439

DETECTION OF HELICOBACTER PYLORI INFECTION USING 14-C UREA BREATH TEST

V. Obradovic (1), V. Artiko (1), M. Petrovic (2), N. Petrovic (1), B. Davidovic (1), V. Bosnjakovic (1), G. Adanja (1), T. Milisavljevic (1), D. Nastic (1). (1) Institute for Nuclear Medicine; (2) Institute for Digestive Diseases, Clinical Center of Serbia.

Purpose: Helicobacter pylori infection is supposed to be one of the major causes of digestive and other diseases. Among a lot of invasive and noninvasive methods for its detection, none is ideal. The aim is assessment of the Helocobacter pylori infection in stomach using breath test and comparison to other diagnostic methods.
Material and method: 62 patients underwent the breath test (BT) and endoscopy. Biopsy samples (B) were taken from antral gastric mucosa for histological analysis and rapid urease test. After ingestion of the ^{14}C-urea capsule, in the presence of enzyme urease from H.Pylori, it is broken down into $^{14}CO_2$ and NH_3. $^{14}CO_2$ is absorbed and is exhaled by the lungs. Radioactivity in the collected exhaled air is detected using beta counter before (background activity) and 30 min after ingestion of the capsule. Significant increase of the activity indicates the presence of this bacterium.
Results: According to our results, the rise of over 100% of activity over background was considered as positive. 17 patients were both B and BT positive, 41 both negative, one was breath test indeterminate and histology +, one was breath test indeterminate and histology - , while two were breath test positive and histology negative. Sensitivity was 94%, specificity 93%, positive predictive value 89%, while negative predictive value was 100%.
Conclusion: Breath test can be useful in diagnosis but is a method of choice in following up the patients after therapy for H.pylori infection, because it is nonivasive, fast and precise.

PS_440

GALLIUM-67 SPECT SCINTIGRAPHY IN THE DIAGNOSIS OF TEMPORAL ARTERITIS

C.L. Ben - Horin (1), T. Raitblat (2), A. Raitblat (1). (1) Nuclear Medicine Department; (2) Reumathologic Outpatients Clinics, , Barzilai Medical Center, Faculty of Health Sciences, Ben Gurion University of The Negev, Ashkelon, Israel.

Temporal arteritis (TA) is a common syndrome in the elderly, consisting of persistent pain in the temporal area, jaw claudication, sudden visual loss, high erythrocyte sedimentation rate and tenderness on palpation in the temporal area. The diagnosis of this condition is relatively straightforward when the typical symptoms and positive temporal biopsy are present. Only half of the patients have positive temporal biopsy. Other diagnostic procedures such as color Doppler sonography or superficial carotid angiography have been proven to be useful for the diagnosis of TA but these techniques do not discriminate between inflammatory and non-inflammatory temporal artery disease. Gallium-67 planar scan is known to be useful in the diagnosis of the disease. Quantitative Gallium-67 SPECT may rise the accuracy of the diagnosis. The aim of the study was to check the effectiveness and usefulness of Gallium-67 SPECT scintigraphy in the diagnosis of TA and to diminish the influence of surrounding areas on quantitative relative Gallium-67 uptake estimations.
Methods: 8 patients (5 male and 3 female; mean age 65 y) with diagnosed TA and 6 controls (2 male and 4 female; mean age 65 y) were included in the study. All of them received 370 MBq Gallium-67 IV 48 hours before the scan. Gallium-67 uptake ratios were calculated on transaxial and coronal slices for: (1) temporal region/out of temporal area bone (TR/Bone) and (2) temporal region/inside of skull region (TR/Bkg) Prednisolone treatment was started in the diagnosed patients after the Gallium-67 imaging was completed.
Results: All patients showed increased uptake in the temporal area compared to out of temporal area bone. The calculated ratio was significantly higher in the TA group than in controls:

		TA	Controls	P
Transaxial	TR/Bone (SD)	1.31(0.14)	1.04 (0.09)	<0.001
Slices	TR/BKG (SD)	5.46(1.08)	4.12 (0.47)	<0.001
Coronary	TR/Bone (SD)	1.47 (0.16)	1.11 (0.006)	<0.001
slices	TR/Bkg (SD)	5.71 (1.14)	3.86 (0.34)	<0.001

Conclusion: our data suggests that Gallium-67 skull SPECT may be useful in the diagnosis of TA especially if the uptake ratio in the area is calculated. Further studies are needed to confirm these data.

NEUROLOGY / PSYCHIATRY 3

PS_441

CEREBRAL BLOOD FLOW SPECT IN ELDERLY LATE-ONSET MAJOR DEPRESSIVE DISORDER. PRELIMINARY RESULTS

F. Martin (1), F. Lomeña (1,3), V. Navarro (2), J. Mateos (1), C. Gasto (2), J. Pavía (1,3), M. Ortega (1), F. Pons (1,3), T. Marcos (2). (1) Department of Nuclear Medicine; (2) Department of Psychiatry; (3) IDIBABS, Hospital Clínic, University of Barcelona.

AIM: Depression is the most prevalent psychiatric disorder among the elderly. Often it is difficult to differentiate clinically a progressive degenerative dementia from a depressive disorder combined with cognitive impairment. Our aim is to determine the changes in the regional cerebral blood flow in elderly patients with late-onset major depression and evaluate the utility of brain SPECT in the clinical management of these patients.
METHOD: We studied prospectively with Tc^{99m}-HMPAO SPECT 42 unmedicated patients over 60 years, presented consecutively at the Psychiatric Department of our hospital with late-onset unipolar major depression. All the patients fulfilled DSM-IV criteria for major depressive event for at least one month. No patient showed cognitive impairment (Mini-mental State Examination score >25). The severity of depression was rated using the Hamilton Depression Rating and Newcastle Scales. The SPECT was performed with a dual-head gammacamera (Helix, GEMS), with high resolution fan-beam collimators. A visual analysis was performed from the SPECT images. In the first 30 patients who responded to the antidepressive treatment, we performed retrospectively a semi-quantitative analysis using a template of anatomical ROIs placed over ten 7.8mm thick frontocerebellar slices to calculate regional uptake ratios (cerebellum as reference). We used as a control group, 20 sex-age-and vascular risk factor-matched healthy subjects.
RESULTS: The SPECT was visually normal in 18/42 and abnormal in 24/42 patients (frontal region lower uptake=9, basal ganglia lower uptake=6, frontal and basal ganglia lower uptake=9). The patients who responded to the antidepressive therapy showed statistically low uptake ratios only in the left anterior frontal region (94.84±3.52 vs 100.25±2.88; $p<0.001$) and in the right frontal region (98.03±3.12 vs 101.35±3.27; $p<0.001$). No correlation was found between the anterior frontal uptake ratios and the demographic and clinical characteristic.
CONCLUSIONS: Our results suggest that the patients with late-onset unipolar depression may have lower cerebral blood flow in the anterior frontal region that the elderly without depression. Nevertheless, brain SPECT was visually normal in 43% of depressive patients and this is a relevant fact for their clinical management.

PS_442

EFFECT OF MODIFIED GROUP PSYCHOTHERAPY AND FLUOXETINE TREATMENT ON SEROTONIN TRANSPORTERS IN OBESE BINGE EATING WOMEN

J.T. Kuikka (1), K. Bergstrom (1), L. Tammela (2), L. Karhunen (2), A. Rissanen (3), E. Vanninen (1), E. Repo (2), J. Hiltunen (4), H. Naukkarinen (3), J. Tiihonen (2), M. Uusitupa (2)(1) Clinical Physiology and Nuclear Medicine, Kuopio University Hospital, Kuopio, Finland; (2) Departments of Clinical Nutrition and Forensic Psychiatry, University of Kuopio and Kuopio University Hospital, Kuopio, Finland; (3) Department of Psychiatry, Helsinki University Hospital, Helsinki, Finland; (4) MAP Medical Technologies Oy, Helsinki, Finland

Aim: Serotonin transporter density has been shown to be decreased in obese women with binge eating disorder. In order to investigate the effect of treatment on serotonin transporters we performed SPET imaging with iodine-123 labelled nor-β-CIT with obese binge eating women before treatment and after the modified group psychotherapy and fluoxetine medication.
Methods: Five obese women with binge eating disorder were studied. Their mean age was 38 year (range 32 – 53 year). A dose of 180 – 210 MBq of I-123 nor-β-CIT, which can be used as a tracer for SPET to visualise serotonin transporters in the brain was intravenously injected into the subjects antecubital vein. Scans were performed using a Siemens MultiSPECT 3 gamma camera with fan-beam collimators. The specific binding was calculated from the 24 h images as (midbrain – cerebellum) / cerebellum. After the first study the subjects participated modified group psychotherapy and were treated with 40-60 mg/day fluoxetine for several months. The SPET study was repeated 9 – 18 months later. Fluoxetine medication was stopped 3 months before the second SPET study.
Results: There was a significant increase in I-123 nor-β-CIT specific binding for serotonin transporters after the modified group therapy and fluoxetine treatment when compared to the baseline (2.42 ± 0.46 vs. 1.92 ± 0.34; mean ± SD; $t = 2.24$, $p < 0.05$).
Conclusion: To our knowledge, this is the first time to show the effect of combined group psychotherapy and fluoxetine treatment on serotonin transporters in obese binge eating women. The results tentatively suggest that the serotonin transporter density can be effected and the specific binding for serotonin transporters increases in obese binge eating women after the treatment.

PS_443

ASSESSMENT OF CHANGES IN REGIONAL CEREBRAL BLOOD FLOW IN PATIENTS WITH UNIPOLAR AND BIPOLAR DEPRESSION USING TC-99M-HMPAO SINGLE EMISSION TOMOGRAPHY

M. Kula (1), A. Tutuş (1), E. Esel (2), T. Turan (2), AS. Gönül (2), M. Reyhancan (2), M. Baştürk (2). (1) Department of Nuclear Medicine; (2) Department of psychiatry, Erciyes University, Kayseri, Turkey.

The aim of this study was to compare regional cerebral blood flow (rCBF) in patients with unipolar and bipolar depression to that of healthy subjects and to examine the relationship between rCBF and depressive symptoms.
Method: Eleven patients (6 M, 5 F; 48.18±9.17 yr) who met the DSM-IV criteria for major depressive disorder (recurrent) and 8 patients (4 M, 4 F; 39.42±11.08 yr) diagnosed with bipolar I disorder-depressive episode were included in the study. Control group consisted of age and sex matched healthy volunteers (25.56±8.76 yr). To evaluate the severity of the clinical symptoms of the patients, Hamilton Rating Scale for Depression (HAM-D), Clinical Anxiety Scale (CAS), Mini Mental State Examination (MMSE), and Brief Psychiatric Rating Scale (BPRS) were performed. All the patients had been free of psychotrophic medications for at least 2 weeks before Tc-99m HMPAO brain SPECT study. The SPECT imaging was performed after 20 minutes following the injection of 550 MBq Tc-99m HMPAO. For the semiquantative analysis of the data, rectangular region of interest (ROI) drawn over upper and lower frontal, temporal, parietal and occipital regions were used to obtain activity ratios, taking cerebellum as reference. Mean cortical/ cerebellar ratios (C/c) calculated for each ROI in patient and control groups.
Results: We found that rCBF values decreased in bilateral frontal, left temporal and left parietal areas in the unipolar depressive patients compared to the controls. Bipolar patients exhibited lower rCBF values than those of the controls in all brain regions investigated except occipital cortices. No significant differences in rCBF emerged between the bipolar and the unipolar patients. Negative correlations were found between the right parietal rCBF and CAS scores ($r = -0.726$, $p < 0.05$), and between length of illness and the left parietal rCBF ($r = -0.720$, $p < 0.05$) in unipolar patients.
Conclusion: These data reveal that both the patients with unipolar and bipolar depression show reduced rCBF in frontal, temporal and parietal regions, and support the idea that this finding is a common feature of various depression subtypes.

PS_444

RELATIONSHIP BETWEEN CEREBRAL BLOOD FLOW AND GLUCOSE METABOLISM IN NORMAL SUBJECTS AND SCHIZOPHRENIC PATIENTS

S. Mizuno (1), T. Momose (1), A. Abe (1), S. Oku (1), Y. Kumakura (1), Y. Kojima (1), Y. Nakashima (2), K. Ohtomo (1). (1) Department of Radiology, University of Tokyo, Tokyo, Japan; (2) Department of Psychiatry, Mitsui memorial hospital, Tokyo, Japan.

Aim:_ Since Roy and Sherrington, relation between blood flow and metabolism is an important issue in neurological sciences. Although coupling between flow and metabolism in whole brain was demonstrated in animals, it remains unclear whether or not flow-metabolism coupling exists regionally in human. In this study, we performed positron emission computed tomography (PET) to determine the relationship of regional distribution between cerebral blood flow (CBF) and glucose metabolism in normal subjects and schizophrenic patients.
Methods: Ten normal subjects without any previous history of psychiatric disease and ten non-hospitalized medicated schizophrenic patients were studied. We obtained quantitative measures of regional cerebral blood flow (rCBF) and regional glucose metabolism (CMRglu), using water labeled with oxygen-15 (O-15 H_2O) and fluoro deoxy glucose (F-18 FDG) at rest under identical conditions and analyzed the distribution of CBF and glucose metabolism using statistical parametric mapping 99 (SPM99) in each group respectively. We also compared the results of this statistical analysis with regions of interest (ROI) studies.
Results: Glucose metabolism was statistically higher than CBF in the cerebral cortex and stratum ($p<0.01$) and lower than CBF in the hippocampus and cerebellum ($p<0.01$) in normal subjects and schizophrenic patients. The difference between the two groups studied was not significant. ROI studies confirmed these findings.
Conclusion: By using SPM99, we found there is, in the stereo tactic space, a mismatch between CBF and glucose metabolism in the brain that is statistically significant, but not adversely affected by the presence of schizophrenia.

PS_445

LOW STRIATAL DOPAMINERGIC D2 RECEPTOR OCCUPANCY: A MAIN DIFFERENTIAL CHARACTERISTIC OF ATYPICAL ANTI-PSYCHOTICS?

A. Tembl (1), I. Corripio (2), A. Catafau (1), Y. Aguilar (1), JC. Martín (1), D. Puigdemont (2), V. Camacho (1), E. Mena (1), V. Pérez (2), I. Carrió (1). (1) Department of Nuclear Medicine; (2) Department of Psychiatry,Hospital Sant Pau, Barcelona, Spain.

Mechanism of action of antipsychotics has been related to striatal dopaminergic D2 receptor (D2R) occupancy. A low incidence of extrapiramidal symptoms (EPS), which might be explained by a low D2R occupancy, has been proposed as the main differential characteristic of atypical antipsychotics in comparison to tipical antipsychotics. However, whether low D2R occupancy is a differential characteristic of atypical antipsychotics has still not been demostrated.
AIMS: 1) To compare D2R occupancy induced by different atypical antipsychotics with the typical antipsychotic haloperidol, using ^{123}I-IBZM brain SPECT. 2) To investigate the relationship between D2R occupancy and EPS.
METHODS: ^{123}I-IBZM SPECT was carried out on 39 patients diagnosed with psychotic disorder (DMS-IV), who were under treatment with stable doses of different antipsychotics (12 hours after the last dose): haloperidol (n = 8, 10-20 mg./d); risperidone (n = 18, 3-9 mg./d); ziprasidone (n = 8, 80-160 mg./d); olanzapine (n =3, 5-10 mg./d) and clozapine (n = 2, 200-250 mg./d). Percentages of D2R occupancy were calculated by means of basal ganglia/occipital (BGO) uptake ratios and applying the following formula: 100-(100*(BGO-1)/(1.84-1)), being 1.84 the average BGO value previously obtained from 9 drug-naive patients. EPS were evaluated using the Sympson-Angus scale.
RESULTS: Percentages of D2R occupancy were: haloperidol, 77.5±8.4%; risperidone, 61.6±16.4%; ziprasidone, 51.2±19.3%; olanzapine, 52.4±29.1%; clozapine, 22.0±4.2%. Significant differences between haloperidol-ziprasidone, haloperidol- clozapine and risperidone-clozapine (ANOVA, $p< 0.001$, post-hoc Scheff? $p< 0.05$) were found. No statistically significant differences were found between haloperidol and risperidone. Olanzapine showed highly variable percentages of D2R occupancy (22.6, 53.5 and 80.9%). Patients on atypical antipsychotics showed much less EPS than patients on haloperidol. Whereas EPS were present in all patients on haloperidol and in 2/3 patients on olanzapine, only 9 patients on risperidone, 2 on ziprasidone, and none on clozapine showed EPS. No relationship was found between D2R occupancy and EPS (Sympson-Angus scale scores), neither with haloperidol nor with atypical antipsychotics (Spearman correlations, p NS).
CONCLUSIONS: This study shows that not all atypical antipsychotics present a low degree of D2R occupancy, and that EPS are not dependent on the degree of D2R occupancy. Therefore, a low D2R occupancy seems not to be a main differential characteristic of atypical antipsychotics. These results suggest that the low incidence of EPS presented by atypical antipsychotics is not explained by a low D2R occupancy. Other recently proposed mechanisms, such as the kinetics of drug-receptor interaction, may account for the mechanism of action of atypical antipsychotics. (FIS 00/0335)

PS_446

CEREBRAL BLOOD FLOW CHANGES DURING RETRIEVAL OF TRAUMATIC MEMORIES BEFORE AND AFTER PSYCHOTHERAPY

A. Newberg (1), J. Peres (2), J. Campos (3), M. Peres (3), A. Magalhaes (2), M. Peres (3), R. Cavini (3), M. Simao (3), J. Moll Neto (2), R. Veras (2). (1) University of Pennsylvania, USA; (2) Instituto Nacional de Terapia Regressiva Vivencial Peres; (3) Departamento de Psiquiatria da Faculdade de Medicina da USP.

Aim: Exposure to stressful events often determines how people subsequently organize their perceptions of themselves and of others. Traumatic experiences have been linked to difficulties in emotional and psychological development. Exposure-based therapy for reduction of emotional response to traumatic memories is effective when the traumatic event is comprehended and in a new schematic representation of reality. However, no previous studies have investigated the neural substrates which mediate the psychotherapeutic process in the scope of the traumatic memories. In this study, ECD SPECT was utilized to determine if such therapy would alter cerebral blood flow associated with the retrieval of primary traumatic memories. Methods: Six patients with traumatic memories were examined with SPECT using equal doses of 99Tc-ECD in two studies, one during the first psychotherapy session while the patient retrieved the traumatic emotion-laden memory (emotion state). The second SPECT scan was done during the retrieval of the same traumatic memory after sixty days from the psychotherapy session (non-emotional state). Each of the brain scans were resliced in the same plane and regions of interest (ROI) were overlayed onto each scan. Values were generated for each ROI and normalized to the average whole brain activity. The percentage change between the baseline and activation state was calculated as well as correlations between changes in activity. Results: There was a significant decrease ($p<0.05$) in activity in the parietal lobes during the first memory retrieval (emotion condition) with the right decreased by a mean of 10% and the left decreased by a mean of 7%. There was also a significant decrease in the activity in the left hippocampus by 11% ($p<0.05$) during the emotional condition. There was also a significant positive correlation between the change in activity (between the two conditions) in the left prefrontal cortex and the change in the left thalamus ($R=0.92$, $p=0.01$); and also between the change in activity in the left prefrontal cortex and the change in the left parietal lobe ($R=0.88$, $p=0.02$). Conclusions: The present study demonstrated several changes in cerebral blood flow associated with the retrieval of traumatic memories before and after psychotherapy. These findings indicate that psychotherapy has an important role in revisiting painful, traumatic memories in order to restructure the basic beliefs about these memories for the patient regain a sense of control and safety. Furthermore, these effects are associated with a measurable change in cerebral function.

PS_447

STATISTICAL PARAMETRIC MAPPING ANALYSIS WITH 99MTC-ECD SPECT IN OBSESSIVE COMPULSIVE DISORDER PATIENTS

P. Li, X. Jiang, WAHUA Guo, LINGLI Zhang, CHENMO Zhu. Department of Nuclear Medicine, Ruijin Hospital, Shanghai Second Medical University, Shanghai, China.

This study is to investigate alternations in regional cerebral blood flow (rCBF) in obsessive compulsive disorder (OCD) patients using statistical parametric mapping (SPM). Method: rCBF measurements using ^{99m}Tc-ethyl cysteinate dimer (ECD) SPECT was performed on 14 OCD patients and 23 age-matched healthy volunteers. The rCBF distribution was compared in these two groups with SPM under the conditions of increased and decreased perfusion, and with regions of interest (ROIs) using cerebral template. P value was set at 0.01 lever. Result: SPM analysis showed that rCBF decreased in cerebral areas including bilateral putamen, superior temporal gyrus and precuneus, and right orbital gyrus, superior and middle frontal gyrus, and left temporo-occipital lobule and superior parietal gyrus, and vermis. rCBF was also increased in left inferior frontal gyrus and posterior corpus callosum. With ROIs method, rCBF was decreased in right anterior frontal and temporoparietal lobule, and left temporo-occipital lobule. Conclusion: Our study supported the viewpoint that rCBF abnormality of frontostriatal circuits was involved in OCD patients. SPM method is a forceful tool in analyzing cerebral regional character.

PS_448

ELEVATED BRAIN MONOAMINE TRANSPORTER AVAILABILITY (SEROTONIN) IN CHILDREN WITH ASPERGER SYNDROME

K.A. Ahonen (1), M. Dahlström (2), H. Ebeling (2), S.L. Linna (2), J. Heikkilä (3), M. Kielinen (2), P. Torniainen (3), E. Jansson-Verkasalo (3), T. Tapio (3), I. Moilanen (3). (1) Division of Nuclear Medicine, Helsinki University Central Hospital, Helsinki, Finland; (2) Department of Pediatrics, Clinic of Child Psychiatry, University of Oulu, Oulu, Finland; (3) Division of Nuclear Medicine, University of Oulu, Oulu, Finland.

Aim: Asperger syndrome has now been defined as a diagnostic entity, where genetic factors play a significant role. It is a form of pervasive developmental disorder (PDD), and has thus some common features with autistic disorder.
Methods: We examined 41 drug-naive children and adolescents (aged 7-17)with various neuropsychiatric disorders (non-PDD including 31 patient depression present and 10 without depression) and 12 children (aged 7-12) with Asperger syndrome using I-123 beta-CIT in SPET imaging of brain monoamine transporters. Imaging was carried out using a dual head gamma camera equipped with fan beam collimators. The first scans were taken at one and four hours (at peak value times) mainly revealing serotonin transporters (SERT) in thalamic (TH) and hypothalamic/midbrain regions (HMB). At one day after the tracer injection dopamine transporters (DAT) at equilibrium state in striatal regions (STR) were imaged. Occipital (OWM) and frontal (FWM) white matter regions were used as the reference regions (representing non-displaceable tracer uptake). The significances of the differences between the groups were tested using ANOVA and t-test with Bonferroni method.
Results: SERT binding ratios (HMB/OWM) at one hour in HMB were in Asperger syndrome 1.48±0.09 (mean+sd). Correspondingly, in non-PDD depressive pts revealed SERT ratio values 1.28±0.11 and pts without depression 1.18±0.12. Children with Asperger syndrome had highly significantly increased SERT values in comparison with depressive and nondepressive children and adolescents (ANOVA $F=20.34$, $p=0.000$). Also at four hours in HMB region differences in SERT values between previous groups were also statistically highly significant. Contrary to those results at one day in HMB region statistically significant difference could be found only between Asperger and non-PDD depressive pts, but surprisingly, SERT values were even lower in Asperger syndrome (1.94±0.19) compared with non-PDD depressive pts(2.27±0.33)! In TH region SERT ratios revealed no significant differences. DAT binding ratios (STR/OWM) at 24 h in STR were 9.1±0.7 in pts with Asperger syndrome and correspondingly in non-PDD pts; 9.15±1.25 in pts with depression and 9.11±1.24 without depression.
Conclusions: Our findings in Asperger syndrome suggest highly significant increase in SERT availability in HMB region at the optimal imaging times (at one and four hrs) compared to patients with non-PDD (both depressive and non-depressive children and adolescents). Our preliminary SERT imaging results are first ones published indicating the possibility of biochemical disturbances behind Asperger syndrome and supporting the idea of hereditary background of this disease.

PS_449

TC-99M-HMPAO SPECT FINDINGS IN DRUG ABUSE HEADACHE

T. Basoğlu, F. Canbaz, T. Özbenli, M. Şahin, S. Albayrak. Department of Nuclear Medicine Ondokuz Mayıs University Hospital, Samsun, Turkey.

Analgesic drug abuse is commonly observed in chronic headache patients. Abuse of various compounds frequently leads to a state of dependency.It has been suggested that the most frequent cause for the transformation of a periodic headache into a daily headache is drug abuse.Our aim was to evaluate the cerebral cortical perfusion in patients with drug abuse headache (DAH).
Methods : 30 patients (M/F = 3/27, 38 ± 8.9 years, drug abuse period =13 ± 5 months) with the diagnosis of DAH underwent SPECT imaging 30 minutes following i.v. administration of 555 MBq of 99mTc -HMPAO before and after prophylactic treatment. The second imaging was performed after ceasing the abused drug and treatment with propranolol or valpronat during one month.Counts were obtained from regions of interest drawn around a total of 45 brain regions and the ratios to cerebellar counts were calculated.
Results : In the initial study, no significant ($p > 0,05$) uptake asmmetry was found between the hemispheres, neither focal uptake anomalies were observed in the medial single regions. The global baseline / post-treatment comparison of the quantified results showed significant ($p <0,05$) decrement of tracer uptake in 12 of 45 brain regions .Visual evaluation showed regional post treatment hypoperfusion in 9/30 patients. Clinically,19 of 30 patients had a decreament of headache. 7 of 9 patients showing visually post-treatment hypoperfusion, presented also with clinical improvement after treatment.
Conclusions: No significant cortical Tc-99m-HMPAO uptake asymmetry and no focal uptake anomaly was observed during drug abuse. Treatment with propranolol or valpronat appears to have a positive clinical effect on DAH. A relation between rCBF and DAH could only be partially demonstrated. The finding of regional post-treatment hypoperfusion needs to be further clarified.

PS_450

ABNORMAL NEURONAL NETWORK IN ANOREXIA NERVOSA WITH I-123-IMP SPECT

T. Takano (1), T. Shiga (1), N. Kitagawa, T. Koyama, C. Katoh (1), E. Tsukamoto (1), N. Tamaki (1). (1) Department of Nuclear Medicine; (2) Department of Psychiatry, Hokkaido University School of Medicine, Sapporo, JAPAN.

The etiology of anorexia nervosa is not fully understood, but probably consists of multi factors, including biological factors. Aim: We assessed the brain perfusion SPECT findings in patients with anorexia nervosa and normal controls by statistical parametric mapping. Methods: Fourteen patients with anorexia nervosa and eight healthy female volunteers were enrolled. They underwent brain SPECT scans with Iodine-123- iodoamphetamine (I-123-IMP). The automatic voxel-based analysis on the CBF-SPECT images was carried out using Statistical Parametric Mapping software (SPM96 for windows). Statistics across the entire brain were displayed as Z scores (threshold: $p<0.05$). Results: The statistical parametric image of Z value indicated the patients with anorexia nervosa had hypoperfusion in the region including the medial prefrontal cortex and the anterior cingulate (Zmax= 3.19) and hyperperfusion in the thalamus and the amygdala-hippocampus region(Zmax= 3.50) when compared with healthy volunteers. Conclusion: The CBF abnormality in anterior cingulate and thalamus may be due to the dysfunction as neuronal network. These results suggest the dysfunction in the neuronal circuits may be related to the anorexia nervosa.

PS_452

IN VIVO EVALUATION OF SEROTONIN-2A RECEPTORS IN NORMAL CANINE BRAIN: A SPECT STUDY WITH A SELECTIVE 5-HT2A RECEPTOR LIGAND LABELLED WITH 123I

K. Y. Peremans (1), K. Peremans (1), K. Audenaert (2), P. De Bondt (3), C. Van de Wiele (2), F. Dumont (4), F. Jacobs (2), G. Slegers (4), F. Verschooten (1), H. van Bree (1), R. Dierckx (3). (1) Department of Medical Imaging, Faculty of Veterinary Medicine, University of Ghent, Belgium; (2) Department of Psychiatry and Medical Psychology, University Hospital Ghent, Belgiume; (3) Division of Nuclear Medicine, University Hospital Ghent, Belgium; (4) Laboratory of Radiopharmacy, Faculty of Pharmaceutical Sciences, University of Ghent, Belgium

Introduction: Serotonin (5-HT) is a central and a peripheral neurotransmitter. Impairments of the serotonergic neurotransmitter have been associated with a variety of human mental disorders, including psychotic disorders, mood and anxiety disorders, eating disorders and dementia. In aggressive, impulsive dogs a decrease in 5-HIAA, a metabolite of 5-HT2a, is detected in the cerebrospinal fluid. A highly selective radiolabelled 5-HT2a antagonist, 123I-5-I-R91150 was developed for single photon emission tomography (SPET). The feasibility of the tracer was tested in rats, non-human primates and humans.

Our aim was to study the feasibility of this ligand in the normal dog brain.

Methods: Nine healthy shepherd type dogs (4F, 5M), free of neurological disorders and behavioural problems, were included. Age varied between 1 and 9 years and weight between 23 and 41 kg. The injected activity ranged from 0.11-0.21 mCi/kg .The interval between injection and acquisition ranged from 100 to 120 minutes. Acquisition was performed with a triple head gammacamera (Toshiba GCA-9300A) equipped with high resolution fanbeam collimators. A 153-gadolinium transmission scan was acquired.

Images were reconstructed with FBP and a Butterworth-filter (cut-off 0.16 cycli/pixel, order 8). Sorensen attenuation correction with a uniform attenuation coefficient of 0.12 /cm and triple-energy window scatter correction were applied. Images were analysed with ROI's drawn around fronto-, temporo, parieto-, occipito-cerebral, thalamic regions and the cerebellum. The uptake in the cerebellum (a region free from 5-HT2A receptors) was used as a reference for non-specific binding in addition to free ligand. The binding index (BI) is defined as (target activity – background activity in brain) / (background activity) which was operationally estimated as (counts/pixel in regional cortex) / (counts/pixel in cerebellum).

Results: Highest uptake was noted in the frontal cerebral region (145%) followed by the temporal area (133% RT, 134% LT). The parietal, occipital and thalamic regions had a similar lower degree of uptake (RP,LP: 119%; RO: 120%, LO: 118%; Thalamic region: 121%). Dose and weight did not significantly influence distribution of activity, nor did gender and age.

Conclusions: The use of the specific 5-HT2a receptor ligand is feasible for SPECT brain imaging in the dog. This tracer is a tool to visualise the binding index of the specific 5-HT2a receptors and has the potential to be useful in work on canine brain disease attributed to serotonine deficiencies.

OTHER CLINICAL SCIENCE. PRECLINICAL STUDIES

PS_451

IN VITRO AND PRECLINICAL STUDIES OF TARGETED ALPHA THERAPY FOR HUMAN BREAST CANCER USING 213BI-LABELED-PLASMINOGEN ACTIVATOR INHIBITOR TYPE 2

B.J. Allen (1), Z. Tian (1), Y. Li (1), N.J. Andronicos (1), S. Rizvi (3), M. Ranson (1). (1) Department of Biological Science, University of Wollongong, NSW 2522 Australia; (2) St George Cancer Care Centre, Gray St, Kogarah, NSW 2217 Australia; (3) UNSW, Kensington, NSW Australia.

Many breast cancer patients receive minimal long-term survival benefit despite undergoing surgery and adjuvant therapy, indicating that micrometastases are not eradicated. We are developing a new adjuvant therapy for the control of metastatic breast cancer based on alpha-emitting nuclides. This therapy exploits the involvement of cell-surface receptor bound urokinase plasminogen activator (uPA) in the metastatic spread of breast cancer cells. Once bound to specific cell-surface receptors, uPA efficiently activates plasminogen to the broad-spectrum protease, plasmin. A large body of experimental and clinical evidence implicates the uPA system as a marker of malignancy and therefore a useful and accessible specific target for therapy.

We have successfully labeled recombinant human PAI2 with the alpha radioisotope ^{213}Bi to produce alpha-PAI2. Labeling efficiencies of up to 95% are obtained, the alpha-PAI2 is stable in serum and the uPA inhibitory activity is maintained as determined by complex formation with uPA and by inhibition of uPA activity. Low doses of alpha-PAI2 are highly cytotoxic towards breast cancer cell lines in vitro, whereas non-specific alpha-BSA had no cytotoxic effect. Furthermore, alpha-PAI2 was not found to be cytotoxic with freshly isolated, normal human leukocytes reflecting that non-targeted cells are immune from alpha-PAI2.

In vivo toxicity studies in nude mice show that up to 6 mCi/kg of alpha-PAI2 (ip) is well tolerated. In vivo efficacy experiments in nude mice demonstrate in 5/5 mice that a local injection of alpha-PAI2 can completely inhibit the growth of tumour at 2 days post-cell inoculation. Further, systemic (iv) administration of alpha-PAI2 at 2 days post-inoculation can also cause tumour growth inhibition in a dose dependent manner, with 3/5 tumours uncontrolled at 1.5 mCi/kg, 2/5 at 3 mCi/kg and 1/5 at 6 mCi/kg.

These results indicate the promising potential of alpha-PAI2 as a novel therapeutic agent for micrometastatic breast cancer.

PS_453

THE EFFECTS OF BOTULINUM TOXIN INJECTION INTO GASTRIC MUSCLE TO THE GASTRIC EMPTYING TIME IN RATS

M. Halaç (1), K. Sönmezoğlu (1); B. Apaydın (2), C. Nisli (1), L. Kabasakal (1), F. Aydoğan (2), I. Karabıçak (2), E. Altınlı (2), I. Uslu (1). (1) Department of Nuclear Medicine; (2) Department of Surgery, Cerrahpaşa Medical Faculty, Istanbul,Turkey.

Botulinum neurotoxin type A (Botox, Allergan Inc, USA) produces a temporary and ultimately reversible blockade of neuromuscular transmission. It also provokes autonomic dysfunction by blocking sympathetic and parasympathetic ganglion cells and postganglionic parasympathetic neurons. It can be hypothesized that Botulinium-toxin injection into gastric muscular layer in antro-fundal junction may create a model of truncal selective vagotomy. In this study we aimed to make an experimental model of pharmacological selective vagotomy by using Botulinium-toxin and to ascertain its effect to the liquid and solid gastric emptying times.

Methods: 31 male Wistar rats underwent Botulinium-toxin injection into gastric muscular layer during a standard laparotomy procedure. For control groups, 22 rats also underwent laparotomy with saline injection instead of Botulinium-toxin into the same gastric region. Liquid and solid gastric emptying studies were performed in two separate groups. For liquid phase study, 17 rats with Botulinium-toxin injection and 12 control rats with saline injection were used. 14 models and 10 controls were used in solid phase studies. Both liquid and solid phase studies were performed 10 days after the laparotomy procedure. 10 MBq Tc-99m DTPA within 1 ml milk and 15 MBq Tc-99m tin colloid within particulated scrambled egg were instilled intragastrically under ether anaesthesia for liquid and solid phase, respectively. After intragastric instillation of radioactivity, the animals were placed on a rat holder under a gamma camera and static images were acquired at the beginning and at 90 min for both liquid and solid emptying. To analyse the data, a region of interest was drawn around stomach outline on both images and the emptying ratios at 90 min for both liquid and solid phases were calculated.

Results: The liquid emptying rate was accelerated while solid emptying time was decreasing in the Botulinium-toxin injected rats comparing to controls (Table). These findings are similar to those seen after the surgical truncal selective vagotomy.

Group	Liquid emptying %	Solid emptying %
Control	20.4 ± 15.8	52.7 ± 21.6
BoNT/A injected	31.1 ± 22.1	21.2 ± 11.3
p	0.03	< 0.001

Conclusions: Botulinium-toxin injection into the gastric muscle may mimic the effects of surgical truncal selective vagotomy related to liquid and solid gastric emptying times.

Poster presentation

PS_454

STUDIES IN GENETIC MUTANT ANIMALS INDICATE THAT ABCB4 (MDR1) AND ABCB1 (MDR2) GENES REGULATE HEPATIC SESTAMIBI TRANSPORT

K. Bhargava (1), B. Joseph (2), J. Kandimalla (2), H. Malhi (2), M. Afriyie (1), M. Schilsky (3), C.J. Palestro (1), S. Gupta (2). (1) Division of Nuclear Medicine, Long Island Jewish Medical Center, New Hyde Park,USA; (2) Liver Research Center, Albert Einstein College of Medicine, Bronx, USA; (3) Division of Liver Diseases and Transplant Institute, Mount Sinai School of Medicine, New York, USA.

Aim: Recent studies suggested that the multidrug resistance (Mdr) gene regulated hepatic sestamibi excretion. Mdr 1 and 2 genes have been renamed Abcb4 (ATP-binding cassette, subfamily B [MDR/TAP] member 4) and Abcb1, respectively. Abcb4 gene may be upregulated in cancer, including hepatocellular carcinoma, whereas deficiency of Abcb1 gene product impairs biliary phospholipid excretion, which leads to progressive familial intrahepatic cholestasis. To understand regulation of hepatic sestamibi handling, we utilized inbred normal, as well as mutated mice and rats in genetically defined backgrounds.
Methods: Tc-99m sestamibi was injected as an intrasplenic bolus injection followed by imaging at 5 frames per min for 60 min. Blood, liver and bile samples were obtained for assays as appropriate.
Results: In normal FVB/N mice and Long-Evans Agouti (LEA) rats, sestamibi was incorporated in the liver rapidly and approximately 50% hepatic activity was excreted over 60 min. In knockout mice deficient in either Abcb4 or Abcb1 gene in the FVB/N background, Tc-99m sestamibi excretion was impaired similarly and twice as much activity was retained in the liver at 60 min compared with normal control mice, $p<0.001$. In double-knockout mice deficient in both Abcb4 and Abcb1 genes, Tc-99m sestamibi excretion was impaired much more and hepatic Tc-99m sestamibi excretion at 60 min reached only approximately 50% of that in mice deficient in Abcb4 or Abcb1 genes alone, $p<0.001$. To determine whether Tc-99m sestamibi excretion was affected by chronic liver disease, we studied Long-Evans Cinnamon (LEC) rats, which are syngeneic to LEA rats, but with mutated atp7b gene, copper toxicosis and significant hepatic injury, identical to Wilson's disease. The kinetics of hepatic sestamibi handling in LEC rats were similar to LEA rats, although in one LEC rat biliary Tc-9m sestamibi excretion was greater.
Conclusions: Abcb4 and Abcb1 genes both regulate hepatic sestamibi excretion. In chronic liver disease, sestamibi excretion was unaffected indicating that Abcb4 and Abcb1 gene function remained intact in this situation. Utilization of sestamibi for assessing Abcb gene function should take into consideration the relative contribution of subfamily gene members.

(This work was supported by the Grant Agency of Charles University, grant No. 17/1999/B and by the research project No. J13/98:11600002 of the Czech Ministry of Education)

PS_455

BIOELIMINATION OF NEW RECEPTOR-SPECIFIC PEPTIDES LABELED WITH INDIUM-111 AND YTTRIUM-88 IN THE KIDNEY

F. Trejtnar (1), M. Laznicek (1), A. Laznickova (1), H.R. Maecke (2), K. Eisenwiener (2), J.C. Reubi (3), S. Wenger (3). (1) Department of Pharmacology and Toxicology, Faculty of Pharmacy, Charles University, Hradec Kralove, Czech Republic; (2) Division of Radiological Chemistry, University Hospital, Basel, Switzerland; (3) Institute of Pathology, University of Berne, Switzerland.

Aim: Somatostatin receptor-specific peptides labeled with convenient radionuclides can be used for diagnosis or therapy of somatostatin receptor-expressing tumors. Renal excretion is the main elimination pathway of radiolabeled somatostatin analogues. Significant renal uptake of the octreotide analogs reduces the sensitivity of scintigraphy for detection of small tumors in the perirenal region and the renal radioisotope cumulation can result in radiotoxicological injure of the kidney. The aim of the study was to analyze excretion parameters, mechanisms of excretion, metabolism and retention of newly designed somatostatin receptor-targeted peptides ^{111}In-DOTA-GATATE, ^{111}In-DOTA-t-GATATE, ^{88}Y-DOTA-GATATE, and ^{88}Y-DOTA-t-GATATE in the rat kidney in vitro.
Methods: Renal handling of the peptides was studied using the methods of the perfused rat kidney. Instead for therapy useful beta-emitter ^{90}Y, the labeling with chemically equivalent gamma-emitter ^{88}Y was used, enabling simple detection of the peptide concentrations in biological samples. The isolated rat kidney was perfused with Krebs-Henseleit solution containing bovine albumin, washed rat erythrocytes (6 %) and a mixture of aminoacids in a recirculation regimen. To consider possible metabolism in the kidney by renal peptidases, an analysis of the urine by gel chromatography was performed.
Results: Only nonsignificant differences were found between renal clearances of the peptides in the perfused rat kidney. The clearances were lower than the values of glomerular filtration rate. The filtrated amount of the compounds was considerably higher than that excreted in urine. It means that some reabsorption of the peptide complexes in renal tubules may exist. However, the differences between total renal and filtration clearances were not significant. Ratio of radioactivity in the kidney and the perfusate at the end of the perfusion was higher in case of the peptides labeled with indium-111. The retention was relatively lower in ^{88}Y- and ^{111}In-DOTA-t-GATATE. The analysis of the urine did not show any significant presence smaller low-molecular metabolic products of the peptides under study. This fact can document no significant destruction of the peptides by the kidney or a relatively effective tubular reabsorption of possible metabolites in the kidney.
Conclusions: Somatostatin receptor-specific radiolabeled peptides ^{111}In-DOTA-GATATE, ^{111}In-DOTA-t-GATATE, ^{88}Y-DOTA-GATATE, and ^{88}Y-DOTA-t-GATATE were excreted in in the perfused rat kidney by glomerular filtration, almost in unchanged form. While the found renal excretion parameters were similar, the renal retention of DOTA-GATATEs was higher than that of DOTA-t-GATATEs.

PS_456

OPTIMIZATION OF [18F]FLUORIDE ION WHOLE BODY SKELETAL IMAGING IN MICE UTILIZING MICROPET AND MICROCAT

F. Berger (1), A. Loening (1), A. Chatziioannou (1), A. Zisman (1), C. Tso (1), T. Yoneda (2), J. Lieberman (1), C. Sawyers (1), S. Gambhir (1). (1) University of California at Los Angeles, Los Angeles, USA; (2) University of Texas Health Science Center at San Antonio, San Antonio, USA.

Objectives: Mouse models for studying fundamental cancer biology are needed for non-invasive and repetitive imaging of bone metastases in order to better understand underlying cancer biology and therapeutics. The aim of this study was to optimize the reproducibility of fluoride ion bone scanning in normal mice and in tumor models.
Methods: Eight Swiss Webster mice were tail-vein or i.p. injected with 750μCi [18F]Fluoride ion and repetitively imaged on a microPET over 4 weeks. Optimal tracer uptake time for whole body scans (wbs) (5 min/bed position) was determined by performing dynamic scans. Images were reconstructed using an iterative and a filter-back-projection method. Quantitative reproducibility of the bone signal was measured using ROI based counts normalized to the (a) injected dose, (b) area under the heart image time-activity curve, (c) ROI over the whole skeleton. Mouse models for traumatic, primary tumor and metastatic bone lesions were developed and imaged over time. Functional imaging results were correlated with a dedicated small animal CT scanner (MicroCAT, Imtek Inc, Knoxville, TN, USA) utilizing a 200 μm image resolution (8 min acquisition).
Results: Optimal peak and plateau of 18F-fluoride uptake for wbs was estimated to be 60 minutes after injection of the activity (for either i.p. and i.v. injection). The highest reproducibility was achieved by normalizing bone c/p/m to an ROI over the whole skeleton, with a mean variation in a given mouse of <15% over serial images. Primary osteolytic bone tumors, metastases and traumatic lesions as small as 2 mm were successfully repetitively imaged. Correlation of microPET with microCAT demonstrated the high sensitivity of the functional imaging approach; microCAT was especially helpful in detecting small osteolytic lesions.
Conclusion: We have studied Fluoride ion whole body bone imaging and shown that this approach is reproducible and can be used to serially monitor normal and pathological changes to the mouse skeleton. This work sets the foundation for quantitative, high-resolution functional bone imaging of mice, which will be useful for numerous applications in basic small animal research.

PS 457

UPTAKE OF RADIOLABELED HERCEPTIN BY EXPERIMENTAL MOUSE MAMMARY CARCINOMAS

M. Mirowski (1), R. Wiercioch (1), E. Balcerczak (1), J. Switalska (2), G. Birnbaum (2), E. Byszewska (2), D. Pawlak (2), R. Wierzbicki (1). (1) Department of Biochemistry, Faculty of Pharmacy, Medical University of Lodz ,Poland; (2) Radioisotope Center, Polatom, Otwock-Swierk, Poland.

Recombinant humanized anti-c-ErbB$_2$ monoclonal antibody (herceptin) is new agent for the treatment of women with tumors that overexpress epidermal growth factor receptor 2 (c-ErbB$_2$). Aim of the present study was to determine biodistribution of ^{131}I-herceptin in experimental mammary carcinoma to predict the radiodiagnostic utility of this antibody.
Methods: Iodination of ^{131}I-herceptin was based on the chloramine T method. Biodistribution study of the radioactive compound was done in healthy and in tumor-bearing mice. Tumors were growth in C3H/Bi mice by injection of cell suspension prepared from spontaneously growing mammary tumors. Amplification of the *c-erbB$_2$* gene in experimental tumors was detected by the polymerase chain reaction technique and its protein product expression by Western blot analysis.
Results: The histological analysis by eosin and hematoxylin (E&H) method showed that above 90% of investigated tumors can be classified as adenocarcinomas. Most of the tumors after Western blot analysis revealed *c-erbB$_2$* oncogene protein products expression. In more than 50% of tumors the amplification of *c-erbB$_2$* gene was detected. Biodistribution study showed increased accumulation of ^{131}I-herceptin in time with the maximum at 48 hours since injection (7% ID/g). At this point tumor/muscle ratio was the highest (about 20). After 96 hours ^{131}I-herceptin accumulation in tumor tissue was 2.5 times higher than in the blood.
Conclusion: ^{131}I-herceptin has high affinity to the mouse mammary adenocarcinomas what might suggest their usefulness in imaging of c-erbB$_2$ expressing tumors in humans.

PS_458

DETECTION AND IDENTIFICATION OF SENTINEL LYMPHNODE IN CANINE ONCOLOGICAL PATIENTS

L. Balogh (1), G. Andocs (1), D. Mathe (1), J. Thuroczy (2), E. Perge (3), I. Erdelyi (4), K. Bodo (1), A. Polyak (1), G. Janoki (1). (1) Department of Applied Radioisotopes; (2) Department of Gynecology and Obstretrics, Faculty of Veterinary Medicine, Szt Istvan University, Budapest, Hungary; (3) Department of Pathology, Central Institute of Animal Health, Budapest, Hungary; (4) Department of Pathology, Faculty of Veterinary Medicine, Szt Istvan University, Budapest, Hungary

Aim: Tc-99m HSA colloid lymphoscintigraphy is used for the detection and imaging sentinel lymphnodes in human breast cancer, melanoma and other soft tissue tumor patients. Different human protocols are available concerning the optimum particle size of applied colloids, the ideal time of imagination and intraoperative guiding after application. The aim of this study was to compare the effectivity of detection sentinel lymphnodes by injecting radioactive particles mixed with blue stain and blue stain alone in spontaneously occuring oncological dog patients.
Methods: Altogether 14 dog patients with the history of mammary tumors (11), skin tumor (1) or other soft tissue tumors (2) in the oral cavity and the neck underwent within 3 days fine needle biopsy, thoracal radiography and hematological examinations. Three-six hours before surgical removal of tumors 20-37 MBq/0,1mL Tc-99m HSA colloid (Senti-Scint', N.R.I.R.R.) mixed with blue stain (Patent blau) was injected subcutaneously. Gamma camera imaging (Nucline X-ring, Mediso Ltd) and intraoperative gamma probe (Europrobe, Eurorad) was used for localizing sentinel nodes. Another group of 16 dogs having mammary tumors was injected only with blue stain (Patent blau) and visual localization of sentinel lymphnodes was carried out 30-60 minutes later. Removed tumors and lymphnodes were investigated by pathologist.
Results: Eighttteen sentinel lymphnodes in the 14 oncological dog patients were localized by using the combined method. Thirteen of the nodes (72%) were found to be painted by the blue stain intraoperatively. Only 12 lymphnodes (67%) were clearly identified by gamma camera imaging and 10 (55%) were palpable before surgery. Fourteen sentinel lymphnodes in the 16 dogs were found by injecting only the blue stain. Forty % of all the excised lymphnodes found to be positive by histopathological examination.
Conclusions: Palpation, blue stain localizing method and gamma camera imaging alone resulted not satisfactory data on sentinel lymphnode detection. Intraoperative radioactive guided surgery combined with blue stain seems to be the superior method for localizing sentinel lymphnodes in dogs like in human beings.

PS_459

HISTOLOGICAL CHANGES IN THE RATÁøS TISSUES AFTER LOCAL APPLICATION OF THE HO-166-CHITOSAN COMPLEX ATTACHED TO BIODEGRADABLE SOLID MATERIAL

J.S. Lee (1), S.J. Lim (2), W.S. Jung (2), T.S. Lee (2), K.S. Woo (2), S.J. Lee (2), C.W. Choi (2), S.M. Lim (2). (1) Department of Orthopedic Surgery; (2) Laboratory of Cyclotron Application, Korea Cancer Center Hospital, Seoul, Korea.

The aim of this study was to find out a clinically applicable method to insert a biodegradable solid material containing holmium-166-chitosan complex into the surgical field, and to evaluate the histological changes in the normal tissues after irradiation from Ho-166 according to the dose, period and type of tissues.
Methods: 111 MBq, 50 μl of the liquid state Ho-166-chitosan complex was attached to the absorbable gelatin sponge, the size of which was 7 x 7 x 5 mm. After 24 hours in the sterile bench for drying up of the liquid Ho-166-chitosan complex, the radiation activity measured by dose calibrator was 56 MBq. These Ho-166-chitosan complex containing absorbable gelatin sponges were inserted into thigh muscles and over the femur bones of the Wistar rats, weighed by 300 grams. The control group was prepared by inserting only absorbable gelatin sponge. One control case and 10 radioactive absorbable gelatin sponge cases were evaluated at 2, 4, 6 weeks after insertion (total number; 33) with respect to the histological changes of the soft tissues, bones, the depth of the tissue necrosis, and the changes of the ^{166}Ho-chitosan complex containing absorbable gelatin sponges.
Results: The histological changes at 2 weeks after the Ho-166-chitosan complex insertion were as follows; In the muscle, coagulation necrosis, degenerating myocytes, regenerating myocytes, intermuscular edema, and inflammatory cells were observed. The average necrosis depth was 3.3 mm (range; 2.5-4.0, SD; 0.54). In the bone, there sere no osteocytes in the lacuna of cortex (empty lacuna), marrow fibrosis, inflammation, and the average necrosis depth was 2.9 mm (range; 2.0-4.5, SD; 0.82). At 4 weeks, in the muscle, calcification and increased fibrosis with average necrosis depth by 3.3 mm (range; 2.5-4.0, SD; 0.48) were found in addition to the findings of 2 weeks. In the bone, additional findings were, increased marrow fibrosis with necrosis depth by 3.3 mm (range; 1.5-5.0, SD; 1.0). At 6 weeks, soft tissue shrinkage, increased fibrosis and granulation tissue formation, and nearly resolving inflammatory reaction were the findings.
Conclusions: The local application of the Ho-166-chitosan complex attached to biodegradable gelatin materials with surgery in the laboratory animals resulted in no mortality, no wound complication, and satisfactory tissue necrosis was induced by β-ray irradiation.

PS_460

THE USE OF 99M-TC-CIPROFLOXACIN (INFECTON) IN THE DIAGNOSIS OF INFECTION IN THE DOG: 2 CASES

K.Y. Peremans (1), F. De Winter (2), F. Verschooten (1), H. van Bree (1), R. Dierckx (2). (1) Department of Medical Imaging, Faculty of Veterinary Medicine, University of Ghent, Belgium; (2) Division of Nuclear Medicine, Ghent University Hospital, Belgium.

Introduction: Infecton® is a ^{99m}-technetium labelled radiopharmaceutical based on the fluoroquinolone antibiotic ciprofloxacin.
The advantages of this radiotracer lie in the isotope used (technetium is widely available, cheap and has good characteristics regarding radioprotection) and in the fact that synthesis is quick and is available as a kit. The pharmaceutical has an antibacterial activity through binding and inhibiting bacterial gyrase. It does not target death bacteria and sterile inflammatory lesions.
One case included involved a complication after total hip replacement. The other was a case of chronic fistulation at the level of the metatarsal bones.
Materials and methods:
Case 1.: german shepherd, female, 2 years old. Total hip replacement with a non-cemented prosthesis was performed. Sudden lameness was noted two months post-operatively and radiographic examination was non-conclusive.
Infecton® was injected (10mCi) IV. The scan was taken 3 hours post-injection and at 24 hours. Increased activity in the region of the femoral prosthetic element and in the acetabular region was found.
Bacteriologic examination revealed resistant Pseudomonas Aeruginosa.
Case 2: greyhound, male, 6 years old. This dog suffered from two fistular tracts at the metatarsal region of unknown duration.
Radiographs showed minor periosteal reaction at the lateral side of the fourth metatarsal bone. Infecton® was injected (10mCi) IV. Acquisition was performed 3 hours and 24 hours post-injection. A hot spot was noted at the lateral side of the fourth metatarsal bone and one was located more centrally at the level of the second and third metatarsal bones.
Bacteriology from the bone curretage material rendered Streptococcus Canis.
Conclusion: In the first case the Infecton® scan rendered a clear differential diagnosis of aseptic loosening versus chronic infection. In the second case infectious bone involvement was demonstrated with this technique. It was shown in these two cases that Infecton® can be a valuable aid in the diagnosis of infection in the dog.

PS_461

CAN TC-99M-HL91 UPTAKES IN THE TUMOUR PREDICT THE RESPONSE OF RADIOTHERAPY

K. Nakamura, T. Suzuki, T. Kawase, A. Kubo. Department of Radiology, Keio University School of Medicine, Tokyo, Japan.

We previously reported that Tc-99m-HL91 (HL91) uptake reflected the hypoxia in tumours.
Aim: The aim of this study was to evaluate if HL91 can predict the radiotherapy response before and following radiation since a strong correlation between tumour hypoxia and poor response to radiotherapy is observed.
Methods: Athymic mice bearing human epidermoid carcinoma, KB-31 or lung adenocarcinoma, HLC in the flank underwent planar imaging before and every three days for 15 days after receiving radiotherapy. In the image at four hours after injection of HL91, ROIs were placed on the tumour in one flank and the muscle in another flank. The HL91 uptake was shown by the ratio of radiointensities in two ROIs.
Results: Before radiotherapy, the HL91 uptakes in tumour xenografts were 1.4-2.2 for small (less than 70 mm^3) KB-31, 2.1-3.4 for big (more than 150 mm^3) KB-31, and 2.1-3.0 for any size of HLC. The control group that did not receive radiation showed the increase in HL91 uptake to 4.0-7.7 and 6.5-7.0 for KB-31 and HLC, respectively. The HLC tumours did not show any response to radiotherapy and their HL91 uptakes kept increasing after the radiation. The KB-31 tumuors responded to radiotherapy and their HL91 uptakes did not increase for a few days after radiation. KB-31 tumour xenografts where HL-91 uptakes were reduced showed tumour shrinkage, and then some of them (HL91 uptakes were less than 1.0) disappeared 15 days later. The KB-31 tumours of which HL91 uptakes did not change after radiation showed the growth delay, but they were re-grown a few days after showing the increase in HL-91 uptakes.
Conclusions: The failure to respond to radiotherapy could be predicted by high HL91 uptake in the tumour. The increase in tumour HL91 uptake after radiation indicated the presence of hypoxic area, suggesting that radiation effect was not satisfactory. The decrease in tumour HL91 uptake after radiation indicated the reduction of viable cells, suggesting the success for response. The HL91 uptake could assess the response of the tumour to radiotherapy a few days before they show their clinical appearance.

PS_462

LABELING MONOCLONAL ANTIBODIES WITH TC-99M AND RE-186: A COMPARISON BETWEEN THE TRICARBONYL METHOD AND THE HYNIC METHOD

E.B. Koenders, O.C. Boerman, J. van Eerd, F.H.M. Corstens. Dept. of Nuclear Medicine, UMC St Radboud, Nijmegen, The Netherlands.

Aim: A new method for labeling proteins with Tc-99m has been developed recently (Waibel et al. Nature Medicine 2000). This tricarbonyl method comprises the synthesis of the tricarbonyltriaquaion complex $[Tc(CO)_3(H_2O)_3^+]$ as an intermediate, and the subsequent reaction of this aquaion with the antibody. This method can be used to label proteins and peptides not only with Tc-99m (I), but also with Re-186. In our department we have extensive experience using the bifunctional chelator S-HYNIC, for labeling antibodies with Tc-99m. Here, we compared both methods to label the anti-CEA antibody MN-14 with Tc-99m.
Method: The immunoreactivity and the in vitro stability of the both radiolabeled antibody preparations were determined. The in vivo tumor targeting potential of both antibody preparations was determined in athymic mice with LS174T tumors. Mice received 1850 kBq ^{99m}Tc-MN-14 i.v. and were dissected at 4, 24 and 48 h p.i.
Results: HPLC analysis indicated that the aquaion intermediate could be formed with an efficiency of up to 90%. The overall labeling efficiency, immunoreactivity and the in vitro stability of both ^{99m}Tc-labeled MN14 preparations are summarized in the table.
Summary of the characteristics of ^{99m}Tc-MN14 labeled according to the tricarbonyl and the HYNIC method.

	Tricarbonyl method	Hynic method
Labeling efficiency	60%	96%
Immunoreactive fraction	70%	62%
In vitro stability in PBS	88%	94%
In vitro stability in serum	95%	97%

The behaviour of the two ^{99m}Tc-MN-14 preparations differed markedly in nude mice with LS174T tumors. The preparation labeled according to the tricarbonyl method cleared more rapidly from the blood than the HYNIC preparation (blood levels at 48 h pi : 4 % ID/g vs 10 % ID/g) and showed a lower tumor uptake (15% ID/g vs 40% ID/g, 48 h p.i. Tumor-to-blood ratios of both preparations were similar at all time points and reached a value of 4 at 48 h p.i.
Conclusions: In summary, the MN14 antibody can be labeled with Tc-99m using the tricarbonyl method. The ^{99m}Tc-MN14 preparations are stable in vitro during at least 24 hours. The antibody labeled via the HYNIC method showed a higher tumor uptake in nude mice with LS174T tumor, most likely due to a better in vivo stability.

PS_463

BIODISTRIBUTION OF 99MTC-LABELLED LOW MOLECULAR PEPTIDES AND PROTEINS IN AN ANIMAL MODEL OF INFLAMMATION

P. Komarek (1), I. Kleisner (2), M. Konopkova (3), I. Komarkova (4).
(1) Department of Pharmaceutical Technology and Drug Control, Postgraduate Medical School, Prague, Czech Republic; (2) Department of Nuclear Medicine, Kralovske Vinohrady University Hospital, Prague, Czech Republic; (3) Department of Radioisotope Diagnostics, Institute for Clinical and Experimental Medicine, Prague, Czech Republic; (4) Department of Radiopharmaceuticals, State Institute for Drug Control, Prague, Czech Republic

Aim: To evaluate accumulation of the low molecular peptides and proteins labelled with 99mTc in rat inflammatory/infection foci.
Methods: Peptides (human leukocyte dialysate – HLD, thymosin fraction 5 – TF5, aprotinin – APT), proteins (human IgG – HIG) were labelled with 99mTc using a redox polymer [Nucl.Med.Rew. 3, 2000, 65-72]. The labelling efficiency was evaluated using paper, TLC and/or column chromatography and electrophoresis. The biodistribution of the labelled substances was evaluated in Wistar rats with Staphylococcus aureus infection or with sterile kaolin suspension-induced inflammation in the left inguinal region 24 h after abscess induction. Accumulation of 99mTc activity was determined both by external gamma camera imaging and by counting dissected tissues 1-4 hours after administration.
Results: The evaluated peptides and proteins show a high labelling efficiency (99mTc-HLD > 98%, 99mTc-TF5 > 95%, 99mTc-APT > 98%, 99mTc-HIG > 95%). Use of redox polymer for labelling raises the stability of 99mTc-labelled substances so that the labelling efficiency remains to be virtually the same (95-98%) after 8 hours at least. In experimentally induced inflammation, the amount of 99mTc-peptides and 99mTc-HIG activity accumulated is 2.5-6.5 and 5.3-10.6 times, respectively, that in control tissue. A comparison of two types of model inflammations (inflammation induced by kaolin and Staphylococcus-induced inflammation) revealed the values measured with 99mTc-peptides are more than a double that induced by kaolin suspension.
Conclusions: The studied low molecular peptides labelled with 99mTc allow rapid localisation of infection foci in the animal model. 99mTc labelled HIG seems to be useful for the detection of both infections and inflammatory lesions.
The study was supported by grant No.NL/6071-3, awarded by the Internal Grant Agency of the Ministry of Health, Czech Republic.

PS_464

VINCRISTINE EFFECTS IN MICE: EVALUATION OF THE MASS AND HISTOLOGICAL STUDY OF THE ORGANS AND OF THE DISTRIBUTION OF RADIOPHARMACEUTICAL

M. Bernardo-Filho (1), D. Mattos (1), M. Gomes (1), R. Freitas (1), A. Nascimento (2), J. Carvalho (2), E. Boasquevisque (1).
(1) Departamento de Biof'sica e Biometria; (2) Departamento de Histologia, Universidade do Estado do Rio de Janeiro, Rio de Janeiro, Brasil.

Unintended alteration of the biodistribution of the radiopharmaceuticals can lead to sub-optimal outcome of nuclear medicine procedure. Altered biologic behavior of an administered radiopharmaceutical may be due to interferences caused by pharmacodynamic effects of therapeutic drugs. The vinca alkaloids are
cell-cycle-specific agents. AIM: As chemotherapeutic drugs can alter the growth of child and present important toxic effects, we have studied the effect of vincristine on the mass of organs from female mice and are trying to develop a model to evaluate the action of chemotherapeutic drug on the biodistribution of radiopharmaceuticals. Vincristine was administered by ocular plexus via into Balb/c mice. METHODS: The organs were isolated and their mass determined in an analytical balance. To study the distribution 99mTc-DTPA, vincristine was administered by ocular plexus via into female Balb/c mice in three doses with a total interval of 96 hours. One hour after the last dose, 99mTc-DTPA were injected by the same via. After 0.5 hour the animals were sacrificed and the percentage of total radioactivity per gram (%ATI/g) in each organ were calculated. RESULTS: The results have shown that the mass has been decreased significantly (Wilcoxon test, $p<0.05$) in thymus, spleen, lymph nodes, ovary, uterus, kidneys, pancreas, and liver. The biodistribution
results have shown an increase of the %ATI/g to the radiopharmaceuticals in ovary, uterus, spleeen, thymus, lymph nodes, lungs, heart, liver, kdneys and bone. As 99mTc-DTPA is used to evaluate the renal function, we decided to study deeply the ultrastructure of the kidney. A fragment of the kidney isolated from the animals treated with vincristine was cut into strips and fixed with 2.5% glutaraldehyde and 0.25% tannic acid in phosphate buffer pH 7.2 overnight at 40C. The strips were washed in phosphate buffer pH 7.2 and
postfixed in 1% osmium tetroxide and potssium ferricianate 0.8% in phosphate buffer pH 7.2. After a second washing, the tissues was dehydrated in graded series of ethanol, and Epon embedded. Ultrathin sections were prepared and observed in transmission electron microscopy. The comparison between the electron photomicrographies of the kidney of the treated animal and the control revealed important alterations in the basal lamina of the capilar endothelium. CONCLUSION: In conclusion, we suggest that the modifications induced for the vincristine is capable to alter the uptake of the studied radiopharmaceutical in the kidney.

PS_465

COMPARISON OF THE PROTECTIVE EFFECTS OF DIMETHYL-SULPHOXIDE AND METHYLPREDNISOLONE AGAINST THE WARM ISCHEMIA ON LIVER PARENCHIMA USING HEPATOBILIARY SCINTIGRAPHY

M. Yüksel (1), A.R. Hatipoğlu (2), E. Temiz (2), Y.S. Salihoğlu (1), S. Berkarda (1), O.N. Yiğitbaş (1). (1) Department of Nuclear Medicine; (2) Department of General Surgery, Trakya University, Edirne, Turkey.

Warm ischemia due to Pringle maneuvre during liver operations leads to parenchymal damage as a result of ischemia/reperfusion injury (I/R-I) accomplished with the duration of ischemia on liver parenchym. Radical oxygen species, generated after reperfusion, play important role by this I/R-I. Dimethylsulphoxide (DMSO) and methylprednisolone are two radical scavengers, and are used to protect the liver parenchima against the I/R-I. We aimed to investigate, the role of hepatobiliary scintigraphy (HBSc) in detection of the protective effect of DMSO and methylprednisolone liver parenchymal damage.

Methods: Total of 18 rabbits (A:Control; B: DMSO+PM; C:Methylprednisole+PM; n=6 each group) were injected 37MBq Tc-99m-mebrofenin through the ear veins. Dynamic scintigrams were taken for 60 minutes (1frame/min). In group A, HBSc was performed without any surgical application. In group B DMSO and in group C mg/kg methylprednisolone are injected to every rabbit before PM-application. PM was applied in group B and C for 30 minutes and after 15 minutes of ending of PM, tissue specimens for electron microscopy were taken from liver parenchym. Then HBSc was performed in groups B and C. From dynamic images time-activity-curves (TAC) were obtained for each group and the time of peak uptake (TPU) and the time for half of the activity to clear from the liver ($T_{1/2}$) values were calculated.

Results: TPU and $T_{1/2}$ of the control group were significantly lower than group B and C; $p<0.0003$ and $p<0.002$, for TPU respectively, and $p<0.02$ and $p<0.005$, for $T_{1/2}$ respectively. However, there was no statistical significant difference between the groups B and C for TPU and $T_{1/2}$ values. Electronmicroscopic examination showed that there was no histopathological difference between the groups B and C.

Groups	TPU (min)	$T_{1/2}$ (min)
A	3.20±0.45	12.06±1.11
B	10.8±2.48	30.35±13.57
C	11.33±3.51	33.47±26.51

Conclusion: According to our results, we suggested that hepatobiliary scintigraphy might be used as an non-invasive imaging technique to evaluate the protective effect of DMSO and methylprednisole, and that the protective effect of DMSO is not different than methylprednisolone against the ischemia/reperfusion injury on liver parenchym.

PS_466

TUMOR UPTAKE AND TUMOR RETENTION OF A MONOMERIC AND A DIMERIC TC-99M-LABELED RGD-PEPTIDE

O.C. Boerman (1), M. Janssen (1), C. Frielink (1), W. Oyen (1), S. Edwards (2), S. Liu (2), M. Rajopadhye (2), F. Corstens (1). (1) Nuclear Medicine, University Medical Center Nijmegen, Nijmegen, the Netherlands; (2) Dupont Pharmaceuticals, N. Billerica, MA, USA.

Aim: RGD peptides selectively bind to the αvβ3 integrin expressed on newly formed endothelial cells and on various tumor cells. Because tumors have enhanced αvβ3 expression, radiolabeled RGD peptides localize preferentially in tumors. Theoretically, peptides with more than one RGD sequence could bind the target cell multivalently, and thus more avidly. Multivalent interaction could result in higher uptake and/or better retention in the tumor. Here we compared the tumor targeting characteristics of a monomeric RGD peptide with those of a dimeric RGD peptide in mice with human tumor xenografts.

Methods: The monomeric peptide (RGDfK) and the dimeric peptide ($[RGDfK]_2$-E) were derivatized with hydrazinonicotinamide (HYNIC). The molecular weight of the monomeric and the dimeric peptide was 841 Da and 1534 Da, respectively. Both peptides were radiolabeled with ^{99m}Tc (100°C, 15 min). Quality control was done with ITLC and RP-HPLC. Identical doses of the radiolabeled peptides (30 nmoles) were i.v. injected in nude mice with s.c. NIH:OVCAR-3 human ovarian carcinoma xenografts. The biodistribution of the radiolabel was determined at 10, 30 min, 1, 2, 4 and 24 h pi (5 mice/group).

Results: RP-HPLC indicated that the radiochemical purity of both peptides exceeded 90% (<2% colloid). Both peptides rapidly cleared from the blood: blood levels of the radiolabeled peptides decreased between 10 min and 24 hrs p.i. from 2.8 to 0.04 %ID/g (monomer) and from 2.2 to 0.05 %ID/g (dimer). The uptake of the monomeric peptide in the tumor showed a gradual decrease between 10 min and 4 h p.i. from 5.8 to 2.6 %ID/g, while the uptake of the dimeric peptide in the tumor was stable until 4 hrs p.i.. Maximum tumor-to-blood ratios were similar for both peptides: 60 and 65, respectively. Both peptides were excreted exclusively via the kidneys. Activity concentration in the other organs examined (lung, spleen, liver, kidney, intestine) decreased with time.

Conclusions: These two HYNIC-derivatized RGD peptides preferentially localized in the tumor in this tumor model. While the maximum uptake of the peptides in the tumor was similar for both peptides, the retention of the dimeric peptide was slightly better.

RADIONUCLIDE THERAPY / DOSIMETRY 2

PS_467

METHODS TO REDUCE RENAL TOXICITY DURING 90Y-DOTATOC THERAPY

M. Cremonesi (1), M. Ferrari (1), L. Bodei (1), L. Leonardi (1), M. Chinol (1), E. Sacco (1), M. Stabin (2), A. Holmerg (3), J. Hiltunen (3), G. Paganelli (1). (1) Divisions of Nuclear Medicine and Medical Physics, European Institute of Oncology, Milan, Italy; (2) Department of Radiology and Radiological Sciences Vanderbilt University, Nashville, TN, USA; (3) MAP Oy, Helsinki, Finland.

Dosimetric studies have shown that high activities of ^{90}Y-DOTATOC can be injected with low myelotoxicity, although the absorbed dose for kidneys raise concern on possible delayed nephrotoxicity.

Aim: The aim of this work was twofold: i) to investigate the absorbed dose sparing to kidneys with the infusion of suitable renal protective agents; ii) to recalculate the maximum injectable activity.

Methods: Fifteen pts (5 pts/group) were enrolled into the protocol in order to investigate the renal protective efficacy of three different agents available at our institute. Within 2 weeks, each patient underwent two dosimetric evaluations: the 1st basal, and the 2nd associated with the infusion of a protective agent. In both cases 185 MBq of ^{111}In-DOTATOC was administered as a bolus i.v. injection. The drugs under investigation were the following: LAL (mixture of Lysine and Arginine, 400 mg/kg), PCP-10 (Positively Charged Protein-10; 2 mg/kg); PLyCD (Poly-Lysine Compound D; 2 mg/kg). The MIRD formalism was used for dosimetric calculations. Kidney dose reduction after LAL, PCP-10, PLyCD was obtained with an intra-patient analysis, in order to avoid patient variability.

Results: The time-activity curves for kidneys showed the same trend, with and without protection. Mean kidney absorbed dose reduction (%) resulted: 31±25 after LAL, 50±13 after PCP-10, and 51±24 after PlyCD infusion. Side effects, mostly grade I-II gastro-intestinal, occurred with LAL and PCP-10. At present, PCP-10 and PLyCD seem to be the most effective protectors.

Conclusions: Co-infusion of positively charged molecules during ^{90}Y-DOTATOC therapy reduces kidney irradiation, enabling a 30-50% increase of cumulative injectable activity. Accepting 25 Gy as the renal dose limit, total activities up to 12 GBq of ^{90}Y-DOTATOC can be administered after PCP-10 and PLyCD protection.

PS_468

HIGH-DOSE 111-INDIUM-PENTETREOTIDE RADIOTHERAPY FOR METASTATIC NEUROENDOCRINE TUMOURS

E. Seregni, G. Savelli, A. Chiti, F. Pallotti, E. Bombardieri. Istituto Nazionale Tumori, Milano, Italy.

Aim ^{111}In-pentetreotide (^{111}In-OCT) has become the standard radiopharmaceutical for localization of neuroendocrine tumours that overexpress somatostatin receptors type 2 and 5. Experimental evidences demonstrated that this radioligand is partially internalized and it can induce cytotoxicity by emission of Auger electrons. Aim of the present study is to evaluate the feasibility of radiotherapy with high-dose of ^{111}In-OCT in patients affected by metastatic gastro-entero-pancreatic (GEP) neuroendocrine tumours.

Methods Four patients with metastatic and progressive GEP neuroendocrine tumours were enrolled in this study. All patients were refractory to conventional medical and hormonal treatment. Each patient received a 6 GBq ^{111}In-OCT therapy every month with a cumulative dose ranging from 48 to 72 GBq (8-12 cycles). The main characteristics of the examined patients are reported in the table. Patients were evaluated after 4 and 8 cycles by means of conventional imaging technique including computed tomography, abdominal ultrasound and bone scan. Toxicity and response to therapy were assessed according to the Common Toxicity Criteria and the WHO criteria, respectively.

ID	Gender	Age	Primary tumour	Disease extension	No. of cycles
1	M	55	Ileum	Nodes, skeleton	12
2	F	45	Pancreas	Liver, skeleton	8
3	M	52	Rectum	Liver, lung	8
4	F	71	Pancreas	Liver, skeleton	8

Results No major treatment-related adverse reaction was observed. Only 2 of 4 patients experienced a mild (Grade I-II) reduction of haemoglobin. Clinical benefit was observed in all the patients. In fact 1 patient achieved a partial response with a striking reduction of the skeletal and nodal metastases while the other 3 patients showed a stable disease. The time to progression were 18 and 12 months for patient 1 and 2 respectively, whereas patients 3 and 4 are still without any clinical signs of progression.

Conclusions. In spite of the small series of the treated patients, our study indicate that high dose ^{111}In-OCT radiotherapy could be effective in patients with advanced otherwise untreatable GEP neuroendocrine neoplasms. Indeed, the therapeutic dose is well tolerated and yield a noteworthy clinical benefit to the patients. In order to define the optimal dosing scheduled and the appropriate timing of the administration further investigation are needed.

PS_469

I-131-MIBG IN THE TREATMENT OF NEUROENDOCRINE TUMOURS: INDICATIONS AND PERSPECTIVES

V. Rufini (1), A. Tornesello (2), S. Mastrangelo (2), A. M. Samanes Gajate (1), M. Salvatori (1), R. Mastrangelo (2), L. Troncone (1). (1) Department of Nuclear Medicine; (2) Division of Pedriatic Oncology, Università Cattolica del Sacro Cuore, Rome, Italy.

Since its initial application, I-131-MIBG has been considered a potential therapeutic agent for neural crest tumours. Since 1984, 66 patients have been treated at our Institution: 51 neuroblastomas (NB), 7 malignant pheochromocytomas/paragangliomas (PHEOS), 5 medullary thyroid carcinoma (MTC) and 3 carcinoid tumours. The therapeutic procedure consisted of: a) evaluation of MIBG uptake and retention by scintigraphy; b) thyroid blockade; c) administration of high specific activity I-131-MIBG (3.7-9.5 GBq by i.v. infusion); d) monitoring of the patient during the infusion; e) post-therapy whole body scintigraphy; assessment of tumour response 4-6 weeks after therapy. 1) In PHEOS, MTC and carcinoids, MIBG was effective with persistent partial reduction of primary tumoral lesions and palliation in metastatic disease; in patients with less advanced stage it could eradicate the residual tumour. The overall results obtained in this group of patients were: 2 CR, 3 PR, 6 SD, 4 PD. 2) In NB, MIBG therapy was initially applied in patients with refractory or progressive disease; 18 cases of stage 3 and 4 refractory NBs were treated. Pain relief was observed in almost all cases; an objective long-lasting therapeutic response was obtained in 12 patients:1 CR, 4 PR, 7 SD. In 5 cases of stage 3 and 4 NB I-131-MIBG was used as a first-line therapy (objective responses in 3 cases). At present, experiences combining chemotherapy and MIBG therapy are in progress. So far, 28 patients were treated. In the first 7 patients, cisplatin and I-131-MIBG were combined. Later on cyclophosphamide (Cy) was added to cisplatin prior to a single dose of I-131-MIBG in 11 cases. An intensification of the chemotherapy regimen by adding VP16 and vincristine was applied in other 10 cases. The overall response rate of the last two regimens showed 1 CR, 2 VGPR, 14 PR, 1 mixed R, 3 SD. MIBG therapy was well tolerated. With the exception of hypertensive crises in one case of NB and leukaemia after 7 years from therapy in another case of MTC, the major side effect recorded was myelosuppression.
Conclusions I-131-MIBG is a treatment which is effective for a wide range of neural crest tumours. In metastatic disease MIBG therapy has an important palliative role. In early stage disease it can eradicate the residual/recurrent tumour. In NB, the innovative combination of MIBG therapy and chemotherapy may represent an important route of investigation to improve final outcome in patients with advanced disease.

PS_470

THE INHIBITORY EFFECT OF RADIOLABELLED OCTREOTIDE ON INTRAHEPATIC TUMOUR GROWTH AFTER PARTIAL HEPATECTOMY

W.A.P. Breeman (1), G.D. Slooter (2), R.L. Marquet (2), E.P. Krenning (1), C.H.J. van Eijck (2). (1) Nuclear Medicine; (2) Surgery, Erasmus University Medical Center Rotterdam, Rotterdam, Netherlands.

The inhibitory effect of radiolabelled octreotide on intrahepatic tumour growth after partial hepatectomy
Background: Most neuroendocrine tumours and several other tumours such as breast carcinoma and malignant lymphoma express somatostatin receptors. Lesions expressing these receptors can be visualised in vivo by receptor scintigraphy using low radioactive doses of the somatostatin analogue [^{111}In-DTPA^{0}]octreotide. The same agent given in a high radioactive dose can be used for peptide receptor radionuclide therapy (PRRT). The aim of this study was to evaluate whether PRRT with [^{111}In-DTPA^{0}]octreotide is able to reduce tumour growth even under tumour growth-stimulating conditions induced by partial hepatectomy. **Methods:** Rats underwent 70% partail hepatectomy (PHx) or sham-operation. The development of hepatic metastases was determined 21 days after direct injection of SS-R-positive or -negative tumour cells into the portal vein. Groups of typically 8-9 animals that underwent PHx or sham-operation were treated with octreotide 50μg/kg sc. twice daily or with 370 MBq [^{111}In-DTPA^{0}]octreotide iv. on day 1 and 8. Both treatments were compared to control treatment. Forty non tumour-bearing rats were used to determine the influence of PRRT on liver regeneration after PHx. **Results:** PHx induced an increase in tumour growth in all groups ($p<0.01$). Octreotide treatment did not influence tumour growth after PHx or sham operation. PRRT could effectively reduce tumour growth in the liver of SS-R-positive tumours also under conditions of increased tumour growth as generated by PHx ($p<0.01$). PRRT was also effective on SS-R-negative tumours after PHx ($p=0.01$) but not after sham-operation. Furthermore, PRRT did not influence liver regeneration or liver function after PHx. **Conclusions:** PRRT with 370 MBq [^{111}In-DTPA^{0}]octreotide is effective in SS-R-positive tumours. During liver regeneration also the growth of SS-R-negative tumours is reduced. This effect is not induced by impairment of liver regeneration or liver function. PRRT could therefore be a promising treatment modality for patients with symptomatic liver metastases of neuroendocrine tumours in combination with liver resection.
C:\napels2001\prrteanm2001.doc 13-3-2001

PS_471

MODULATION OF IODIDE UPTAKE IN RAT HEPATOMA

U. Haberkorn (1), A. Altmann (1), M. Henze (2), I. Morr (1), M. Mahmut (1), P. Peschke (3), M. Eisenhut (2). (1) Clinical Cooperation Unit Nuclear Medicine; (2) Dept. of Nuclear Medicine; (3) Clinical Cooperation Unit Radiotherapy, Cancer Research Center, Heidelberg, Germany.

The ability of thyroid cells to accumulate iodide is a prerequisite for successfull radioiodide therapy of benign thyroid diseases and differentiated thyroid carcinoma. The transport of iodide across the cell membrane is the first step in the iodide accumulation process which is mediated by the sodium iodide symporter (hNIS). We, therefore, investigated whether the accumulation of iodide may be induced by the retroviral transfer of the hNIS gene in non-thyroid tumor cells.
Methods: Employing a bicistronic retroviral vector for the transfer of the hNIS coding sequence and the hygromycin resistence gene rat Morris hepatoma (MH3924A) cells were infected with retroviral particles and 32 hNIS expressing cell lines were generated by hygromycin selection. After incubation of the genetically modified and wild type hepatoma cells as well as the rat thyroid cell line FRTL5 with Na^{125}I the uptake and the efflux of iodide was determined. In addition, the iodide distribution in rats bearing wild type and the genetically modified hepatomas was monitored.
Results: Genetically modified MH3924A cell lines accumulated up to 235 times more iodide when compared to non-infected hepatoma cells. The maximal iodide uptake in the cells was observed after 60 minutes incubation time. Competition experiments in the presence of sodium perchlorate revealed a dose dependent decrease of the iodide uptake (87% to 92%). Moreover, FCCP led to a loss of accumulated I^- (32%) whereas DIDS increased the I^- uptake into the cells (22%). However, a rapid efflux of the radioactivity (80%) was observed during the first 10 minutes after $^{125}I^-$ containing medium had been replaced by non-radioactive medium. In rats, the hNIS-expressing tumors accumulated six times more iodide when compared to the contralateral wild type tumor as monitored by scintigraphy. The *ex vivo* quantitation of the iodide content performed 1 hour after tracer administration in 1g tumor tissue revealed a 17-fold higher iodide accumulation in the genetically modified tumors. In accordance with the *in vitro* data we also observed a rapid efflux of the radioactivity out of the tumor *in vivo*.
Conclusion: The transduction of the hNIS gene per se is sufficient to induce $^{125}I^-$ transport in Morris hepatoma cells *in vitro* and *in vivo*. With regard to a therapeutic application, however, additional conditions need to be defined which inhibit the iodide efflux out the tumor cells.

PS_472

188-RE-LIPIODOL: PREDICTION OF THE PATIENT DOSE BASED ON 131-I-LIPIODOL BI-PLANAR SCANNING AND MONTE-CARLO SIMULATION

K. Bacher (1), H. Thierens (1), S. Van de Putte (1), B. Brans (2), M. Monsieurs (2), R.A. Dierckx (2). (1) Departement of Medical Physics; (2) Division of Nuclear Medicine, Ghent University Hospital, Ghent, Belgium.

Aim: In this study we consider the loco-regional targeted radionuclide therapy, using 131-I-lipiodol for the treatment of hepatocellular carcinoma (HCC). Because of his better physical properties (half-life: 17 hrs, max β-energy: about 2 Mev), 188-Re-lipiodol, would cause less radioprotection problems and a lower effective patient dose. We made a prediction of the patient dose based on 131-I-lipiodol bi-planar scanning.
Methods: After the intra-arterial administering of the 131-I-lipiodol (mean activity: 1850 MBq), the biological half-life of the 131-I-lipiodol in the body of 10 patients (especially in the liver, tumor, lungs and thyroid) was calculated, using bi-planar images made at different time points (one week and two weeks after the therapy). Therefore, appropriate regions of interest (ROI) were selected for the organs and for the background correction. For the liver and tumor an attenuation correction is made, using the patient geometry from CT images. Assuming an identical distribution when 188-Re-lipiodol would have been used, a patient dosimetry was performed by a Monte-Carlo simulation in an MCNP environment. A mathematical phantom of an average patient was generated by the computer. The tumor geometry (size and location in the liver) is calculated by using CT images of the patient and is also implemented in the computer phantom.
Results: For a same tumor dose, a significant lower patient dose was calculated in the case of 188-Re-lipiodol. The liver dose decreased with a mean of 19.1%. Heart and kidney dose decreased with a mean of 82.4%. Consequently, the effective dose decreased with a mean of 25%.
Conclusions: If the in-vivo distribution and stability is the same as 131-I-lipiodol, 188-Re-lipiodol would be an excellent radiopharmaceutical for the treatment of HCC. 188-Re-lipiodol would cause a lower patient dose and less radioprotection problems.

PS_473

TREATMENT OF NEUROENDOCRINE LIVER METASTASES WITH INTERVENTIONAL NUCLEAR MEDICINE

R. Buscombe, M.E. Caplin, A.J. Watkinson, J. Tibbles, A.J.W. Hilson.
NET Clinic, Royal Free Hospital, London UK.

Metastatic neuroendocrine tumours (NETs) can be limited to the liver. These patients are often symptomatic. If surgery and embobolisation cannot be offered, liver transplantation may offer help but outcomes can be poor and often there is a long wait for a liver. Therefore we have developed a new way with which to treat these patients.
7 patients with proven NETs (6 carcinoid, 1 islet cell tumour, 2 women youngest) within the liver only have been selected for the initial treatment 2 patients have had 2 treatments. In all patients 900-1000 MBq of I-131 Lipiodol (Lipocis-CISbio) was infused into right or left hepatic artery (depending on tumour site) using a 5 French catheter. Infusion was performed with fluoroscopic screening to ensure tumour filling and prevent reflux of Lipiodol up the gastro-duodenal artery. The patient was then nursed in an isolation bed for up to 96 hours.
One patients died of a pre-existing cardiovascular disease, another patient died of their tumour but the remainder are well with good symptomatic response with minimal post procedure side effects In the 4 patients secreting 5-HIAA there has been a drop in levels. Objective evidence has not shown a reduction of more than 50% in tumour size. No patient has shown any further progression
I-131 Lipiodol therapy of metastatic neuroendocrine appears to stop cancer growth in 5/7 (72%) and reducing excretory function of the cancer in 4/7 (58%) patients. It may not however result in significant tumour shrinkage.

PS_474

BORON DISTRIBUTION IN MALIGNANT BRAIN TUMOURS FOR BNCT

L. Menichetti (1), V. Calderone (2), D. Petroni (1), L. Cionini (3), P. Salvadori (1). (1) National Research Council - Institute of Clinical Physiology, Pisa, Italy; (2) Department of Psychiatry, Neurobiology and Farmacology , University of Pisa, Italy; (3) Department of Oncology , University of Pisa, Italy.

Boron Neutron Capture Therapy (BNCT) is a radiotherapy modality based on the side emission produced by the capture of epythermal neutrons by Boron-10 atoms and is under investigation for the treatment of brain Glioma and skin Melanoma. *p-boronophenylalanine* (BPA) is extracted in these tumours at concentration 2-3 times higher than in normal tissues. Increasing the delivery of Boron within the target tissues as well as the need of new methodologies for the quantitative determination in vivo and non invasively are the crucial aspect for a the development of BNCT.
A combined approach using Positron Emission Tomography (PET) and digital autoradiography on animal models has been adopted in order to evaluate both the cerebral extraction of BPA, thus covering the lack of methods to asses the biodistribution and the concentration of the boronated drug in target and non target tissues. To this purpose ^{18}F-BPA and ^{3}H-BPA are used and preliminary results of BPA biodistribution are given in the present work.
A tumour bearing animal model has been set up (the cellular line of Glioma C6 has been selected and implanted in rat brain) and used to develop a method for autoradiographic tumour imaging. Using the tritiated analogue of BPA, the microdistribution data have been evaluated. Typical values 3-4 times higher of BPA extraction have been detected in tumour and an ubiquitary extraction in control animals has been found. ^{18}F-BPA will be used to stady BPA pharmacokinetic in vivo. The study of tritiated F-BPA is ongoing and the extraction ratio within the region of interest will be compared to BPA. The fluorinated analog of BPA has been synthesised using acetyl hypofluorite and the procedure has been optimised for ^{18}F-BPA production: synthesis, separation and quality control techniques have been set up with a remote control approach.
The use of ^{18}F-BPA for both digital autoradiography and PET is in progress in order to a) monitor drug localization, b) calculate the ^{10}B tissue concentration, c) assess the extent and homogeneity of tumour uptake. Following this approach, in vivo behaviour and tumour extraction of BPA and its fluorinated analog have been clarified and some limitations in technology have been resolved: this will allow a better understanding of the efficacy of BNCT for human application.

PS_475

BIODISTRIBUTION OF 111 IN LABELED TUMOR ANTIGEN-ASSOCIATED MACROPHAGES IN A PHASE I OF IMMUNOTHERAPY IN METASTATIC MELANOMA

A. Moisan (1), E. Garin (1), C. Lesimple (1), A. Carsin (1), A. Devillers (1), V. Quillien (1), I. Ollivier (3), C. Leberre (2), J. Lecloirec (1), L. Toujas (1). (1) Department of Nuclear Medicine, Centre Eugène Marquis , Rennes, France ; (2) ETS, Rennes, France; (3) CHU Dermatology, Rennes, France.

Aim: Tumor antigen vaccination represents a newly-introduced treatment of malignant melanoma. Tumor cell antigens recognized by cytotoxic T lymphocytes have a well-defined peptidic structure. They can be associated for vaccination with antigen-presenting cells, either macrophages or dendritic cells. In this study, we investigated the biodistribution of 111 In labeled tumor antigen associated macrophages injected along various routes and specially into peripheral lymph vessels.
Methods: Seven HLA-A2 positive patients with metastatic melanoma expressing MAGE-3 mRNA were treated with autologous macrophages (AM) associated with a MAGE-3 peptide. At monthly intervals, six AM aliquots were thawed , exposed to MAGE-3 peptide and injected into each patient along various routes : intradermally (ID), subcutaneously (SC), into lymph nodes (IN) and into catheterized peripheral lymph vessels (IL). Thirty six AM injections were realized. Eleven 111In-radiolabeling of AM were performed. The biodistribution of labeled AM was investigated by scintigraphy 3 and 24 h post injection, at most twice, in a given patient (2 ID, 2 SC, 2 IN and 5 IL).
Results: 2,5 x 10^6 to 20 x 10^6(mean value:12.7 x 10^6) AM were labelled with 4 MBq of 111In oxine. Labeling efficiency was 69 +/- 20 %. The mean radioactivity injected was 2.8 +/- 0,4 MBq. Scintigraphic images and variation of radioactivity uptake between 3 and 24 hours at the injected site, suggested that macrophages injected ID, SC and IN did not diffused from the injection site. In contrast, those injected into a superficial lymph vessel of the dorsal region of the foot, migrated well to popliteal and inguino-crural lymph nodes and remained at 24 hours.No significant activity was found in bone marrow and liver at 24h, attesting of good binding of 111In to labeled cells. The treatment was well tolerated.
Conclusions: In a phase I of immunotherapy in metastatic melanoma , scintigraphy of 111In macrophages demonstrates that administration of labeled peptide-loaded antigen presenting cells through peripheral lymph vessels appeared feasible. 111In oxine labelled macrophages are a suitable tool for kinetics study of adoptive immunotherapy.

PS_476

REPEATED SM-153 EDTMP I.V APPLICATIONS IN REFRACTORY PAINFUL PROSTATE METASTASES FOR LONGER LASTING ANALGETIC THERAPY

N. Baziotis (1), V. Voliotopoulos (2), A. Zissimopoulos (1), A. Zafirakis (1), A. Stavraka-Kakavaki (2), G. Limouris (2). (1) St. Savvas Anticancer Hospital, Nuclear medicine Dept, Athens Greece; (2) Areteion University Hospital, Nuclear Medicine Dept, Athens Greece.

Management of metastatic pain becomes particularly important in patients with prostate cancer in whom overall survival may be relatively long even with advanced disease, while the quality of life is frequently poor. The aim of this study was to evaluate the efficacy of Sm-153 EDTMP in refractory painful bone metastases secondary to prostate cancer after repeatad injection strictly according to the developed myelotoxicity.
Materials/Methods: Thirty seven MBg/kg Bw of Sm-153 EDTMP (CIS Bio Intern Gif sur Yvette) were i.v. injected in 22pts (aged 54 to 81 yrs) with multiple painful sceletal metastases due to hormone resistant prostate cancer and maintained on analgetic medication, often including narcotics. The efficacy of the treatment was assessed by a pain and performance questionnaire that patients were asked daily to complete and by comparison of bone scans, CT or MRI images, Kamofski indexes and BSI, before and at least 9 months after the initialitation of the therapeutic shceme. Strict criterion to repeat the radionuclide injection was the developed mylotoxicity.
Results: 15 out of 22 patients responded (2 with moderate pain ,10 pain free) after the first injection. 4 out of the rest 7 patients responded (2 with moderate pain,2 pain free) after the 2 injection.It is worthwhile to point out that the moderate responds of the first injection became pain after the second one. Given that a third dose could lead to aplastic disorders and that already the 13 patients underwent blood tranfusion the therapeutic scheme was stopped. The accumulative radiation deposition of the repated scheme was calculated to be approximately 6700 and 1500mGy/MBq in bone surface and bone marrow respectively.
Conclusion: The sum of the radiation has been cinsidered as still paliative ruther than curative,although CT scans 9 months post treatment show recalcification of the lytic component interpreted as response to therapy.

PS_477

THE VIENNA-PROTOCOL ON REPEATED LOW-DOSE 153SM-EDTMP THERAPY INDUCES PAIN PALLIATION AND LESION REGRESSION / STABILISATION

H. Sinzinger (1), K. Weiss (2), S. Granegger (1), S. Ofluoglu (1), CH. Kratzik (3), CH. Hajek (2). (1) Department of Nuclear Medicine, University of Vienna, Vienna, Austria; (2) Department of Radiology and Nuclear Medicine, Hospital of Wiener Neustadt, Austria; (3) Department of Urology, University of Vienna, Vienna, Austria.

In order to achieve therapeutic effects beyond pain palliation we introduced the Vienna-protocol (30 mCi [1,1 GBq] ^{153}Sm-EDTMP, 5 times in 3-months intervals) in prostate and breast cancer patients with multiple bone recurrences on an outpatient base. We are going to present in a total of 50 patients (36 – 96 a) with prostate cancer, finishing this first part of the 1-year protocol, lesion regression documented by scintigraphy, and in part by radiography, CT and MR, as well as by a decrease (> 71 %) of PSA (in 64 % after a temporary increase). Bone uptake of ^{153}Sm-EDTMP ranged between 47 and 82 %, onset of pain palliation was after 3 to 15 days. 48 % had complete pain palliation, 40 % partial, 5 % showed minor improvement, the effect lasted for at least 9 weeks in all the responders. Quality of life significantly improved. No correlation between the pain palliating effect, the bone uptake or the flair phenomenon and the extent of regression was monitored. The drop in peripheral blood cells (platelets – 28 %, white blood cells – 23 %, red blood cells – 18 %) showed a nadir after 3 – 6 weeks. No significant cumulative bone marrow damage was noted after the fifth treatment. The Vienna-protocol looks promising to achieve beyond pain palliation lesion regression / stabilization with minimal bone marrow damage at low costs on an outpatient base.

PS_478

AMIFOSTINE (AF) AND RADIOTHERAPY (RT) : PHASE 1 STUDY

D. Di Gennaro (1), M. Alfieri (2), B. Curcio (1), G. Scimone (1), A. Losco (1), C. Bianco (1), E. Falcone (1), S. Di Fiore (1). (1) Radiotherapy Unit – A.O. „San Giovanni Di Dio E Ruggi d'Aragona" – Salerno, Italy; (2) Pharmacy Mercato San Severino Hospital (SA), Italy.

Purpose: to evaluate the tolerance and efficacy of Amifostine (WR-2721) as a radioprotector
Methods: in 1999 we began a clinical phase 1 study to evaluate AF as radioprotector; until now we have used AF in n¡25 patients, with an age varying from 16 to 36 (median age 25), affected by n¡18 Hodgkin Limphomas (HL) (mantle field - dose: 30Gy/20 fract.), n¡6 Non-Hodgkin Linphomas (NHL - Neck field - Dose: 41.4 Gy/ 23 fract.), and 1 patient, age 53 years, affected by a pelvic mass from a cervix ca. (dose:61 Gy), already surgically treated (ureteral-bladder-ileotomy) for iatrogenic toxicity (bilateral ureteral necrosis) caused by cisplatin. The bladder was created from an ileal loop, and was highly prone to radiation necrosis. AF was used: a) in young patients treated to Head and Neck (to prevent xerostomia) b) in young patients treated with mantle field (to prevent xerostomia, esofagitis and second chemo-radiation tumours) c) in patients already treated (higher risk of radionecrosis). AF was given at a dose of 500 mg. diluted in 5 cc of fisiologic solution, s.c., in two different subministrations 15 m' before RT. We always gave antiemetic profilaxis with serotonin – antagonists. Subcutis way was more useful, for our busy department (100 patients/day).
Results: We did not notice bad effects caused by subcutis subministration of AF; we noted 4/18 acute radiation toxicities (Grade 2 esophagitis), but no acute xerostomia, and a complete compliance to radioprotector and radiotherapy schedule.
Conclusion: AF is safe and useful, and now is routinely given in our department to this subgroups of young patients.

PS_479

RADIATION EXPOSURE IS VERY LOW TO THE FAMILY MEMBERS OF PATIENTS TREATED WITH YTTRIUM-90 ZEVALIN® ANTI-CD20 MONOCLONAL ANTIBODY THERAPY FOR LYMPHOMA

G. Wiseman (1), B. Leigh (2), T. Witzig (1), D. Gansen (1), C. White (2). (1) Mayo Clinic, Rochester, MN, USA, Department of Nuclear Medicine; (2) Idec Pharmaceuticals, Corp., San Diego, Ca, Usa, Department of Oncology & Hematology, Rochester, USA.

Aim: Yttrium-90 (Y-90) is a beta-emitting radioisotope used in clinical trials for the radioimmunotherapy of patients with cancer. Although Y-90 emits no penetrating gamma photons, low levels of bremsstrahlung radiation are expected. Our aim was to quantify the radiation absorbed dose received by family members following a single dose of Y-90 ibritumomab tiuxetan (Zevalin), an anti-CD20 radioimmunotherapy under development for patients with B-cell non-Hodgkin's lymphoma. Methods: B-cell lymphoma patients receiving a single intravenous dose of 14.8 MBq/kg Y-90 Zevalin were instructed to avoid body excretion contamination but were not advised to isolate or keep a distance from family members. The family member anticipated to have the closest contact with the patient during the seven days after the Y-90 Zevalin infusion was assigned to wear a DoseGUARD Plus electronic personal dosimeter (AEA Technology QSA, Inc., Burlington, MA). In addition, an ion chamber device was used to measure radiation exposure at a distance of 1 meter from the lower chest of patients immediately after the Y-90 Zevalin dose.Results: Radiation exposure was measured in 13 patient family members following Y-90 Zevalin therapy. All patients confirmed that the personal dosimeter was worn at all times (including at night) when in the same building, car or airplane as the patient. The median deep dose equivalent radiation exposure was 0.035 mSv total accumulation over seven days with a range of 0.014-0.079 mSv. The median radiation exposure at one meter from the patient immediately following the Y-90 Zevalin dose was 0.00295 mSv/hour with a range of 0.0024-0.0039 mSv/hour.Conclusions: In many medical centers, Y-90 radioimmunotherapy does not require hospitalization. Patients are treated as an outpatient to return home after receiving the radiopharmaceutical. We have found that, even without patient isolation or shielding, radiation exposure to family members during the seven days following Y-90 Zevalin is very low and in the range of background.

PS_480

USE OF RADIOLANREOTICE TO TREAT SOMATOSTATIN RECEPTOR POSITIVE TUMOURS

R. Buscombe (1), M.E. Caplin (1), J. Hepplewhite (1), G. Johnson (1), P. Bouloux (1), T. Meyer (1), D. Hochhauser (1), I. Virgolini (2), T. Ah Yong (3), A.J.W. Hilson (1). (1) NET Clinic Royal Free Hospital, London UK; (2) University of Lienz, Vienna, Austria; (3) Queen Elizabeth Hospital, Hong Kong, China.

Targeted therapy with Y-90 Lanroetide may be appropriate in patients who have tumours which express somatostatin receptors. Many of these patients, for example those with carcinoid, do not respond to chemotherapy or external radiotherapy. The aim of this study is to review our experience in using Y-90 Lanreotide on such tumours
A total of 53 cycles of Y-90 lanreotide have been given to 23 patients over an 18 month period. All patients had failed or found to be unsuitable for other cancer treatments. There were 15 patients with carcinoid, 5 with gliomas, 1 fibrolamellar cancer, 1 ACTH secreting cancer and one malignant histiocytoma. Patients were infused with 0.8-1.2 GBq on a 3-4 week basis for 3 treatments and if there was response this was repeated afer a 3 month gap. Those with intra-cerebral tumours were treated with 200-400 MBq Y-90 Lanreotide intra-arterially into the tumour bed.
Most patients had fatigue for 7-10 days post treatment. There has been mild bone marrow toxicity in 4 patients and no renal toxicity. Response as measured by >50 reduction in tumour size on CT has occurred in 6 patients, stability of previously growing disease in 8 patients. All the remaining 9 patients with progressive disease have died of their disease. Poor prognostic indicators are massive tumour bulk and bone or lung metastases.
Y-90 Lanreotide can induce stability or regression in 56% of patients but may not be appropriate for those with very advanced disease

PS_481

FEASIBILITY OF HIGH-ACTIVITY SAMARIUM-153-EDTMP THERAPY FOLLOWED BY AUTOLOGOUS PERIPHERAL BLOOD STEM CELL REINFUSION IN UNRESECTABLE OSTEOSARCOMA

C. Franzius (1), S. Bielack (2), S. Flege (2), J. Sciuk (1), H. Jürgens (2), O. Schober (1). (1) Department of Nuclear Medicine; (2) Department of Paediatric Haematology and Oncology, Münster University, Münster, Germany.

Aim: Sm-153-EDTMP (samarium-153 ethylenediaminetetramethylene phosphonic acid) has been introduced for palliative pain therapy of osteoblastic bone metastases. The distribution of Sm-153-EDTMP is comparable to that of Tc-99m-MDP in bone scintigraphy. Osteoblastic osteosarcomas producing abundant primitive bone matrix usually present as 'hot spots' on a diagnostic bone scan. Despite highly efficacious chemotherapy, patients with osteosarcomas still have a poor prognosis if adequate surgical control cannot be obtained. These patients may benefit from therapy with radiolabeled phosphonates.

Patients and Methods: 6 patients (4 male, 2 female; 7-41 yrs.) with unresectable primary osteosarcoma (n=3) or unresectable recurrent sites of osteosarcomas (n=3) were treated with high-activity of Sm-153-EDTMP (150 MBq/kg BW). Whole-body scans were acquired immediately after Sm-153-EDTMP application, 4h, and 24h later. In all patients autologous peripheral blood stem cells had been asservated before Sm-153-EDTMP therapy.

Results: No adverse reactions were observed in the 6 patients neither during the injections nor during the hours following the application. In one patient bone pain increased during the first 48 h after therapy. Another patient had complete pain relief within 48 h. Autologous peripheral blood stem cell reinfusion was performed on day +14 in all patients to overcome potentially irreversible damage of the hematopoietic stem cells. In one patient external radiotherapy of the primary tumor site was performed after Sm-153-EDTMP therapy and polychemotherapy was continued. 21 months later this patient is still free of progression. 1 patient died 6 months after therapy, the other 4 patients are still alive (follow-up 3-15 mo).

Conclusion: These preliminary results show that high-dose Sm-153-EDTMP therapy is feasible and warrant further evaluation of efficacy. The combination with external radiation, and polychemotherapy seems to be most promising. Although osteosarcoma is believed to be relatively radioresistant the total focal dose achieved may delay local progression or even achieve permanent local tumor control.

PS_482

ANALYSIS OF STRONTIUM-89 INDUCED REGRESS OF BONE METASTASES IN PROSTATE CANCER

YU. Ussov (1), E.V. Barysheva (1), V. Obradovic (2), V. Baltic (3), S.P. Selivanov (1), S.N. Isaeva (1), S. Regoe (3), V. Artico (2), J.E. Riannel (1), S.A. Velichko (1). (1) Tomsk Medical Research Center, Tomsk, Russian Federation; (2) Serbian Clinical Center, Belgrade, SR Jugoslavia; (3) Institute of Oncology, Sremska Kamenica, SR Jugoslavia.

Sr is now widely used as agent of choice for pain relief in extensive metastatic bone disease. Nevertheless the anatomic features of bone metastases (mts) in the course of ^{89}Sr-therapy remain not well studied. Here we aimed to analyse the clinical, bone scan and MRI data in prostate cancer patients with extensive spread of disease (No. of mts >10) and in patients with amount of metastases < 5, all of whom received ^{89}Sr therapy.

47 patients with bone metastatic spread of prostate cancer, already on antiandrogen therapy, were treated with ^{89}Sr (MedRadioPreparate Ltd.) and studied before, and in 3-6 months after injection of ^{89}Sr. In everyone whole-body ^{99m}Tc-MDP (4h post-injection of 370 MBq) and T1- and T2-weighted MRI scans were performed. Both ^{99m}Tc-MDP and MRI images were quantified as {Metastasis/Background} pixel count ratio. Patients were gathered into groups of persons with extensive disease (Gr.1, No. of mts >10, 31 pts), in whom severe pain syndrome was present in 26 of 31, and those who did have minimal bone involvement (Gr.2, No. of mts < 5, 16 pts) and obvious pain symptoms in 9 pts only.

Everybody demonstrated prominent improvement in severity of pain syndrome with full pain relief in 27 (21 of Group 1 and 8 of Group 2). Duration of pain-free period was 2,9 sd 0,8 months in Group 1 and exceeded 4 months in every patient of Group 2. The {Metastasis/Background} ratios have been changed by $^{89}SrCl_2$ as :

	Group 1 (n=31)		Group 2 (n=16)	
	^{99m}Tc-MDP	T1-w MRI	^{99m}Tc-MDP	T1-w MRI
before treatment	3,89 sd 2,75	0,51 sd 0,14	1,81 sd 1,57	0,81 sd 0,23
3-6 mnths after Sr-89 injection	1,84 sd 1,94 p<0,05	0,78 sd 0,23 p<0.05	1,39 sd 1,12 p<0,05	0,93 sd 0,16 p<0.05

The decrease in ^{99m}Tc-MDP uptake after ^{89}Sr treatment correlated significantly with pre-treatment uptake both in Gr.1 (as –0,63+0,36X, r=0.67) and Gr.2(as –0,49+0,47X, r=0,86).

Thus, ^{89}Sr induces substantial regress of osteoblastic bone metastases in prostate cancer, regardless extent of disease, more prominent and lasting longer in cases with small number of mets.

PS_483

RADIATION HAZARD FOR PATIENTS AND RELATIVES AFTER PAIN PALLIATION WITH 30 MCI 153SM-EDTMP

H. Sinzinger (1), S. Ofluoglu (1), E. Havlik (2), S. Granegger (1). (1) Department of Nuclear Medicine; (2) Institute for Biomedical Physics, University of Vienna, Vienna, Austria .

^{153}Sm-EDTMP is one of the radioisotopes of choice for treatment of painful bone recurrences. Radiation exposure data of staff, patients and their relatives after therapy of painful bone metastasis with ^{153}Sm-EDTMP are extremely rare. We determined radiation dose in 14 patients being treated for bone metastases after breast (n=6) or prostate cancer (n=8) receiving a single treatment with 30 mCi (1,1 GBq) ^{153}Sm-EDTMP. Radiation dose was also measured in the partners of 5 of the patients. Patients received 2,79 ± 0,87 mSv, their respective partners 0,24 ± 0,14 mSv. Female partners exhibited higher radiation dose (0,40 - 0,49 mSv) as their male counterparts (0,24 – 0,42mSv). Their dose was 16,26 % for female and 10,25 % for male partners from treated patients. Furthermore, we assessed the finger dosis of the staff (tracer preparing technician and applying physician) with and without lead shielding of the syringe containing the radioisotope. Shielding resulted in an increase of finger dose for the technician (+ 20 %) due to a longer preparation time, while the physicians one was decreased (to 20%). Our findings show, that family members are exposed to about one tenth of the patients exposure and that at least four treatments with a dose of about 30 mCi ^{153}Sm-EDTMP can be administered to a patient to keep his partner within the tolerated limits of 1 mSv/a.

OTHER CLINICAL SCIENCE. BONE AND JOINTS 2

PS_484

QUALITATIVE AND QUANTITATIVE ANALYSIS OF TC99M LABELED HUMAN IMMUNOGLOBULIN G (HIG) SCINTIGRAPHY IN SYSTEMIC RHEUMATIC DISEASE (SRD)

A. Leondi (1), M. Souvatzoglou (1), E. Papadaki (1), J. Datseris (1), E. Moulopoulou (2), CH. Zerva (1), CH. Kostopoulos (3). (1) Department of Nuclear Medicine, Alexandra Hospital Athens, Greece; (2) Department of Radiology, Aretaion Hospital, University of Athens, Greece ; (3) Therapeutic Clinic, Alexandra Hospital, University of Athens, Greece .

The aim of this study is to evaluate HIG Immunoscintigraphy by qualitative and quantitative analysis in the assessment of pulmonary involvement in patients with SRD.

Material and Methods: 42 patients (34 females, 8 males, mean age 55,9 ± 12,4 years, mean disease duration 8,5 ± 7,3 years), 23 systemic sclerosis, 13 rheumatoid arthritis, 3 lupus erythematosus and 3 CREST and without evidence of concomitant pulmonary infection or heart failure, underwent HIG scintigraphy (1mg polyclonal human IgG-HIG- labeled with 750 MBq 99mTc, 4h p.inj. ,high resolution collimator, 600kcts, matrix 256x256, sophy camera NXT), as well as High Resolution Computed Tomography (HRCT) of the lungs (gold standard). Ten control subjects were also studied with HIG, because of painful hips. Qualitative interpretation of the scans was done by two independent nuclear medicine physicians. Quantitative analysis was performed on the posterior view (3 ROIS at Right Lung, 3 ROIS at Left Lung compared to Left Ventricular ROI) and the Average Score for every scan was calculated.

Results: HIG scintigraphy revealed increased HIG uptake in the lungs (diffuse, focal or over the large pulmonary vessels) in 37/42 pts and in none of the controls. There was no statistically significant difference in the results between HIG and HRCT.

The quantitative analysis of the controls' scintigrams revealed a mean value of the av. Score 1,48 ± 0,09 (range 1,3- 1,58), of the patients' negative scintigrams 1,5 ± 0,08 (range 1,4- 1,57) and of the positive scintigrams 1,9 ± 0,23 (range 1,6- 2,61). Scans with a score ≥ 1,60 were considered as positive. The comparison between the qualitative and quantitative analyses showed that all scintigrams that were interpreted as positive had a score ≥ 1,60. There is a significant difference between the group with negative scans and the group with positive scans (p<0,001).

Conclusions: HIG immunoscintigraphy of the lungs represents a highly sensitive, non invasive method for the detection of the pulmonary involvement in SRD. Quantitative analysis could be an indicator of the activity of the disease. This could contribute to the better management of the patients.

Poster presentation

PS_485

ENHANCED EFFECT OF F6-1,25(OH)2D3 ON RADIOACTIVE CALCIUM DEPOSITION IN OSTEOBLASTS

H. Seto (1), Y. Kamisaki (1), N. Watanabe (1), M. Shimizu (1), T. Miyahara (2), T. Shimoura (2), N. Osafune (2). (1) Department of Radiology; (2) Department of Toxicology, Toyama Medical and Pharmaceutical University, Toyama, Japan.

Purpose: Bone-seeking radiopharmaceuticals have been used as the therapeutic agents to relief intractable bone pain in patients with metastatic bone disease, in which the greater the osteoblastic activity, the greater the concentration of the agents in and about the tumor. Until now, several pharmaceuticals such as vitamin D3, PTH or androgen have been tried to enhance the deposition of radioactive agents, no routine clinical use is, however, available. In this study we assessed the enhanced effect of 26, 27-hexafluoro-1α, 25-dihydroxy vitamin D3 (vitamin F-D3) on radioactive calcium deposition in osteoblastic cells as compared to the effect of vitamin D3.

Methods: Fetal osteoblastic cells (SV-HFO) were cultured for 3 days in a α-MEN medium with 10% fetal bovine serum. Then, β-glycerophosphate (β-GP) and dexamethasone were added to induce the development of ossification. Moreover, vitamin D3 or vitamin F-D3 were added to enhance the deposition of calcium in osteoblasts. The medium was changed every 2 days. After the observation of ossification, radioactive calcium (Ca-45) was added to the medium, and was cultured for 24 hours. Then, osteoblasts were separated from the culture and radioactivity of Ca-45 in the osteoblasts was measured.

Results: Ca-45 deposition in the osteoblasts increased as the β-GP concentration increased from 0 to 10 mM. Addition of vitamin D3 enhanced the deposition of Ca-45 about 1.4 fold as compared to β-GP only. Moreover, vitamin F-D3 showed a strong enhanced effect on the deposition of Ca-45 about 16.4 fold as compared to β-GP only.

Conclusions: A new pharmaceutical, 26,27-hexafluoro-1α, 25-dihydroxy vitamin D3 (vitamin F-D3) has a potential enhanced effect on the deposition of calcium in osteoblasts. This pharmaceutical might be effective in patients with metastatic bone disease and osteomalacia instead of vitamin D3.

PS_486

THE EVALUATION OF BONE MINERAL DENSITY IN EPILEPTIC CHILDREN RECEIVING VALPROIC ACID

M. Kaya (1), S. Karasalihoğlu (2), N. Öner (2), H. Carman (2), F. Üstün (1), C. Çeltik (2). (1) Deparment of Nuclear Medicine; (2) Department of Pediatrics, Trakya University, Edirne, Turkey.

Atraumatic fractures are often seen in epileptic children. Several factors including immobilization and antiepileptic treatment lead to osteopenia causing increased bone fragility. Antiepileptic drugs such as phenytoin, phenobarbital, primidone are established contributors to osteomalacia and rickets. Recently valproic acid-induced changes in bone mineral density have been reported. The aim of this study is to evaluate the relationship between the bone mineral density and the dosage and duration of valproic acid therapy. The relationship between the bone mineral density and biochemical parameters such as calcium, phosphorous, alkaline phosphates, vitamin D, osteocalcin and parathormone are also evaluated .

Methods: Bone mineral density was measured by dual-energy x-ray absorbtiometry at L2-L4 levels of lumbar vertebrae, the femoral neck and the greater trochanter in 27 children (mean age; 7.3 ± 3,5 yrs) with uncomplicated idiopathic epilepsy treated with valproic acid for more than 6 months.

Results: Mean serum levels of valproic acid was 60.57 ± 14.3 µg/mL and mean duration of treatment was 18.5 ± 12.6 months, respectively. Mean bone mineral density values at L2-L4 levels of lumbar vertebrae, the femoral neck, and the greater trochanter was calculated to be 0.55 ± 0.2 g/cm^2, 0.61 ± 0.2 g/cm^2, 0.53 ± 0.1 g/cm^2, respectively. We found a negative correlation between the dosage of valproic acid and the bone mineral density at lumbar vertebrae, the femoral neck and the greater trochanter (r=0.47, p=0.015, r=0.49, p=0.01, r=0.55, p=0,003, respectively). There was a positive correlation between the serum level of alkaline phosphates and the bone mineral density at the femoral neck and the greater trochanter (r=0.43, p=0.02, r=0.40, p=0.04, respectively). There was no correlation between bone mineral density and duration of valproic acid therapy and other biochemical parameters.

Conclusion: Based on these results, it is suggested that the measurement of bone mineral density and biochemical supervision of the patients is required during high-dose valproic acid therapy.

PS_487

PROGNOSTIC VALUE FOUR PHASE BONE SCINTIGRAPHY FOR REFLEX SYMPATHETIC DYSTROPHY SYNDROME IN HEMIPLEGIA

B. Okudan (1), S. Serttaş (2), C. Çelik (2). (1) Ankara Numune Training and Research Hospital Nuclear Medicine Department; (2) Ankara Physical Medicine And Rehabilitation, Ankara, Turkey.

Background: Reflex sympathetic dystrophy syndrome (RSDS) is a painful disabling problem, the diagnosis of which can be difficult to confirm by objective measures. Although the pathogenesis of RSDS remains unknown, most hypotheses are based on an event (stroke) that triggers an abnormal central reflex arc. Bone scintigraphy is frequently used to confirm the clinical suspicion of RSDS.

Aim: This trial was carried out to investigate the correlation between four phase bone scan (FPBS) and clinical manifestation of RSDS in upper extremity of hemiplegia.

Methods: We have investigated 34 pts. (17 males, mean age 64±8; 17 females, mean age 59±12; mean disease period, 2-12 weeks) with cerebrovascular accident {CVO} confirmed by head computed tomography (infarction or hemorrhage). All patients received four phase bone scintigraphy (perfusion, blood pool, late blood pool and osseous phase). We analyzed perfusion and exact site was obtained every second for 60 seconds followed by first immediate static (early blood pool), second static after 20 minutes (late blood pool) and third static images after 3 hours for 500.000 counts.

Results: All patients received four phase bone scans; 25 scans positive for RSDS. Nine patients with negative scans except one had no symptoms of RSDS. Eleven patients with positive scans had symptoms at the time of bone scanning. Eight out of 14 asymptomatic patients with positive scans developed symptoms following six months. We found a significant correlation between positive FPBS and positive clinical symptoms of RSDS ($p<0.05$). There was a significant correlation between positive FPBS and subsequent development of clinical RSDS in previously asymptomatic patients ($p<0.001$). The positive scan of FPBS demonstrated sensitivity 95%; specificity 57%; positive predictive value 76%; and negative predictive value 88%. The most significant correlation was found in early and late blood pool phase when correlated with clinical RSDS evaluation.

Conclusion: We concluded that four phase bone scintigraphy may be a good predictor of the future development of clinical RSDS after CVO.

PS_488

CORRELATION OF BONE MASS MEASUREMENT AMONG LUMBAR SPINE AND HIP

R. Garcia (1), J. Lopez (1), M. Gonzalez (1), J. Luis (2), R. Alvarez (1), P. Gomez (1), M. Herrador (2), R. Vazquez (1). (1) Department of Nuclear Medicine; (2) Department of Medical Physics, H.H.U.U.Virgen del Rocio, Seville, Spain.

Dual –energy x-ray absorptiometry (DEXA) allows non-invasive direct measurement of bone mineral density(BMD). Only few data are available comparing the results of BMD measurement among various sites.

The aim of our retrospective study is the assessment of the correlation of BMD among lumbar spine and hip.

METHODS: BMD of the lumbar spine and hip was studied in 2108 patients. Bone mass measurement was performed with dual energy x-ray absorptiometer (DEXA) Hologic QDR 4500W. Relationships were analysed using Pearson's coefficients of correlation and its statistical significance test.

RESULTS: The results revealed a significant high correlation of BMD of total hip and lumbar spine ($r=0.705$ $p<0.001$).Nevertheless BMD of the spine was mostly correlated with BMD of trochanteric site ($r=0.709$ $p<0.001$) and least correlated with BMD of intertrochanteric region ($r=0.651$ $p<0.001$).

CONCLUSIONS: BMD of spine and hip are highly correlated. Though there is some heterogeneity of bone mass density among different measurement sites practically with this good level of correlation , bone mass measurement of lumbar spine might be used to predict the BMD of the hip.

PS_489

MANAGEMENT OF CONDYLAR HYPERPLASIA ASSOCIATED WITH MANDIBULAR ASYMMETRY

A. Fawzy (1), B. Gamal (2). (1) Nuclear Medicine Department, Faculty of Medicine, Cairo University; (2) Surgery Department, Faculty of Oral and Dental Medicine, Cairo University, Egypt.

Condylar hyperplasia is a malformation of non-neoplastic origin involving the size and morphology of one or both mandibular condyles. Unilateral cases lead to facial asymmetry.
Aim: To evaluate the role of osseous scintigraphy in determining the metabolic status of the condyle and assessing the actively growing condyles in patients with unilateral facial asymmetry. Also, assessing the addition of SPECT and quantitation to the planar images in offering an objective response and hence diminishing the false positive and negative results.
Methods: The study included 25 adult patients, who were divided into 2 groups (15 with unilateral facial asymmetry and 10 control patients). Both clinical and conventional radiological evaluation confirmed the presence of unilateral hyperplasia and disturbed occlusion in the 1st group. All 25 patients were subjected to bone scan after the IV injection of 740 MBq Tc-99m MDP and the mandible was imaged 2 hours later, both planar and SPECT, as well as the lumbar vertebrae as a reference point. Quantitation of the right and left condyles as well as the lumbar vertebrae was evaluated. The 1st group patients were all subjected to a corrective surgery (condylectomy) via a periauricular approach, and the removed condyles were evaluated histopathologically.
Results: The mean age of the patients was 21.8±4.1 years while that of the controls was 21.6±3.6 years. In the patients group there were 10 females and 5 males, while in the control group there were 6 females and 4 males. In the patients group, there were 9 right and 6 left condylar hyperplasia. The mean count in right condyle of the patients group was 6859±971, in the left 5948±1197 and in the 4th lumbar vertebra was 4631±418. While, in the control groups it was in the right condyle 4729±531, in the left 4698±485 and in the 4th lumbar vertebra was 4697±452. The ratios right/left condyles, right/lumbar and left/lumbar in the patients were 1.18±0.29, 1.47±0.21 and 1.29±0.25 respectively, while, in the control group they were 1.01±0.06, 1.01±0.05 and 1.00±0.04 respectively. The histopathological diagnosis showed numerous hyperplastic osteocytes in the periphery of the condyle.
Conclusion: SPECT osseous scintigraphy is a useful indicator of continued bone activity. Also, osseous scintigraphy is of immense value in choosing the management of patients with mandibular asymmetry.

PS_490

THE VALUE OF BONE SPECT TO EVALUATE LOW BACK PAIN ETIOLOGY: IN COMPARISON WITH PLANAR BONE SCINTIGRAPHY

M. Aydın, A.F. Yapar, N. Yoloğlu, H. Yalcın. Department of Nuclear Medicine, Baskent University, Adana Hospital, Adana, Turkey.

Aim: The purpose of this study was to evalute the additional value of bone SPECT compared to planar images in the revealing cause of low back pain.
Methods: Twenty-two patients (7 M, 15 F, age range 19-74 yrs, mean age 53±14) who suffered from low back pain were studied. Nine of 22 patients had known primary malignancy (4 breast, 2 lung, 1 thyroid, 1 prostate, and 1 renal cell carcinoma). Whole body bone scan, spot images and lumbosacral SPECT (360°, circular rotation, 128x128 matrix, 64 frames with 20 seconds acquisition time) were performed 3 hours after the injection of 20 mCi (740 MBq) Tc-99m MDP with a dual head gamma camera (Siemens e-cam). All patients underwent X-ray, 8 patients MRI and 4 patients CT.
Results: Three patients had increased uptake only in sacroiliac joints in planar and SPECT images (group 1). The remaining 19 patients had abnormal tracer uptake in the lumbar vertebrae (group 2). All of the group 1 patients were diagnosed as sacroiliitis by radiological and clinical findings. In group 2, the vertebral lesions classified into anatomical regions in SPECT images as whole vertebra, vertebral body, pedicle, facet joint and spinous process. Seven whole vertebrae, 5 vertebral body, 7 pedicle (4 only in pedicle, 3 in pedicle+facet joint), 10 facet joints and 1 spinous process lesions were found. The lesions that were only in the pedicle (4 patients) were confirmed as metastases by radiological techniques.
Conclusion: Our findings indicate that SPECT had no superiority to planar images in sacroiliac joint lesions. On the other hand, in the evaluation of vertebral lesions, SPECT images can localize abnormalities to the vertebral body, pedicle, facet joints or spinous process and this can result in additional diagnostic information, and might be routinely used in the evaluation of low back pain etiology.

PS_491

ASSESSMENT OF BONE SCINTIGRAPHY AND SPET IN THE VIABILITY DIAGNOSIS OF MICROVASCULARIZED FIBULA GRAFT USED IN MANDIBULAR RECONSTRUCTION

I. Hervás (1), L.M. Floria (2), P. Bello (1), A. Saura (1), P. González (1), R. Pérez (1), M.C. Baquero (2), A. Mateo (1). (1) Department of Nuclear Medicine; (2) Department of Maxillofacial Surgery, University Hospital, Valencia, Spain.

Aim: Bone allografts are often used in reconstructive mandibular surgery, generally following extensive oncologic resections, posttraumatic pseudoartthrosis or osteomyelitis. Vascularized fibular bone grafts have the advantages over other bone grafts in the restoration of the contour and function of defective mandibles. Bone scintigraphy has often been used to assess revascularization of bone, because positive uptake of 99mTc-HMDP reflects patent anastomoses and viability of the grafted bone. Nuclear medicine techniques have the advantage , regarding the angiography, that they are bloodless. The aim of this study is to assess bone scintigraphy and SPET in the detection of viability of the grafts.
Methods: Mandibular reconstruction with a free fibula flap was done in 13 patients in the last four years. Bone scintigraphy and SPET was applied in the follow up of nine patients. For bone scintigraphy 740 MBq of 99mTc-HMDP was administered intravenously. We have considered the blood pool and late images (which were obtained two hours after the administration of the radiopharmaceutical). In each view (anterior and both lateral from the skull) until 400000 counts were reached. The study was carried out on the fifth day. Control scintigraphies were performed in two patients (at month 5 and 1 year). SPET studies were acquired immediately after planar imaging. Sixty frames of 30 s each were collected during a 360° rotation. The projections were reconstructed in a 64X64 matrix. Transaxial, sagittal and coronal mandibular tomograms were obtained and analyzed. Semiquantitative assessment of the grafts was done with a six-grade scoring system, based on comparison of tracer uptake in the graft and in the calvarium.
Results: Complications were observed in one graft. Planar scintigrams showed a tracer uptake higher than grade five in grafts with an uncomplicated course. SPET were performed in addition to planar imaging in three patients showing a higher graft uptake. A lack of tracer uptake was observed in the failed graft.
Conclusions: It is conclude that bone scintigraphy performed within the first week after the mandibular reconstruction is a useful tool to monitor the viability and early complications of microvascularized fibular grafts and plays an important role in the process of decision-making on surgical reexploration. SPET is more sensitive than planar imaging for the assessment of graft viability. The microvascularized fibula flap is optimal in mandibular reconstruction.

PS_492

LEUKOSCAN IN CLINICAL PRACTICE

P.J. Ryan. Department of Nuclear Medicine, Medway Maritime Hospital, Gillingham, U.K.

Aim: The imaging of orthopaedic infection with Tc 99m antigranulocyte Fab' fragments (leukoscan) has shown impressive results from the limited published studies. This method of imaging infection has advantages of being less labour intensive and enabling completion on a single day. Data for this technique remains limited and there is a need for further corroborative data. This study examined the success of Leukoscan in the detection of orthopaedic infection in routine clinical practice.
Methods: 35 adult patients were investigated using 750 MBq Tc 99m Leukoscan injected intravenously with planar imaging performed 2 aqnd 6 hours post injection. The results of the isotope studies were compared to the eventual orthopaedic diagnosis by review of patient medical records with information noted including ESR, WBC, correlative anatomical imaging, microscopy and culture from sites of infection and clinical judgement.
Results: Of the 35 patients, 19 were total knee replacements (TKR), 6 operative internal fixations, 2 total hip replacements, 3 septic arthritis, 2 chronic osteomyelitis, and 3 other. There were 15 positive infections and overall sensitivity, specificity, positive accuracy and negative predictive accuracy were 82 %, 75 %, 60 %, and 90 % respectively. For the TKR group with 6 cases of infection the respective results were 85 %, 67 %, 67 %, 85 %.
Conclusions: We conclude that Leukoscan can be used successfully to investigate suspected orthopaedic infection with its strength being a high negative predictive accuracy. Positive studies may require further imaging to establish the diagnosis.

PS_493

SCINTIGRAPHIC IMAGING OF HISTOLOGIC OTOSCLEROSIS

M.J. Reinhardt (1), U.H. Ross (2), H. Freudenberg (3), D. von Mallek (1), H.J. Biersack (1), T. Krause (1). (1) Dept. of Nuclear Medicine, Univ. Hospital Bonn, Germany; (2) Dept. of Oto-Rhino-Laryngology, Univ. Hospital Freiburg, Germany; (3) Institute of Pathology, Univ. Hospital Freiburg, Germany.

Aim: Detection of sclerotic fixation of the stapedial footplate by tympano-cochlear scintigraphy (TCS) in-vivo to identify patients with progressive hearing loss due to otosclerosis.
Methods: 44 patients with otosclerosis prior to stapes surgery were included in the study. TCS was performed on a Siemens Basicam equipped with a one-pinhole collimator. Ten-minute-images of the middle-/ inner ear were obtained 2.5 hours after i.v. injection of 700 MBq Tc-99m DPD in a modified Mayer-projection. Accumulation of radiolabeled diphosphonate was compared with histologic findings of the surgically removed material.
Results: Sclerosis of the stapedial footplate is characterized by an enlargement of the bony part and a concomitant reduction of the cartilage part (1). Thus, histologic changes of the stapedial footplate were classified in 3 groups according to bone/cartilage ratio: normal (1/3 bone, 2/3 cartilage), slight or moderate sclerosis (1/2 bone, 1/2 cartilage), and severe sclerosis (2/3 bone, 1/3 cartilage). While only 1 of 18 patients with a normal bone/cartilage ratio had a focal accumulation in TCS, 18 of 20 patients with slight or moderate sclerosis and 5 of 6 patients with severe sclerosis showed increased uptake on scintigraphic images. Sclerotic enlargement of the stapedial footplate could be scintigraphically detected with a sensitivity of 88.5 %, a specificity of 94.4 % and a diagnostic accuracy of 90.9 %.
Conclusion: Sclerotic enlargement of the stapedial footplate can be differentiated in-vivo by means of tympano-cochlear scintigraphy (TCS) with a high diagnostic accuracy. Because the definite diagnosis of otosclerosis is made histologically, TCS might be helpful in the differential diagnosis of progressive hearing loss.

Reference:
1) Damjanov & Linder (eds.). Anderson's Histology, 10th ed. 1994: 2894-95, Mosby press, St. Louis, Missouri

PS_494

COMPUTED TOMOGRAPHY AND TYMPANO-COCHLEAR SCINTIGRAPHY IN THE DETECTION OF FENESTRAL AND COCHLEAR OTOSCLEROSIS

M.J. Reinhardt (1), U.H. Ross (2), A. Berlis (3), D. von Mallek (1), H.J. Biersack (1), T. Krause (1). (1) Dept. of Nuclear Medicine, Univ. Hospital Bonn, Germany; (2) Dept. of Oto-Rhino-Laryngology, Univ. Hospital Freiburg, Germany; (3) Dept. of Diagnostic Radiology, Univ. Hospital Freiburg, Germany.

Aim: To compare sensitivity and specificity of computed tomography (CT) and tympano-cochlear scintigraphy (TCS) for detection of fenestral and cochlear otosclerosis in the differential diagnosis of progressive hearing loss.
Methods: 95 patients (54 women, 41 men; aged 43±13 yrs., range 15-72 yrs.) with progressive hearing loss in 120 ears were included in the study. Conductive hearing loss was present in 67 ears and sensoneurinal hearing loss in 53 ears. CT was performed on a Siemens Somatom AR in bone algorithm (70 mA, 3 sec. scanning time, 130 kV, window 3200, center 600-1000). Continuous 2 mm slices were obtained in a clivus parallel position. TCS was performed on a Siemens Basicam equipped with a one-pinhole collimator. Images of the middle-/ inner ear were obtained over 10 min. in a modified Mayer position 2.5 hours after i.v. injection of 700 MBq Tc-99m DPD. The findings of CT and TCS were compared on the basis of clinically diagnosed otosclerosis.
Results: Tone- and speech audiometric and ear microscopic findings and tuning fork tests and stapedius reflex measurements confirmed clinically-suspected otosclerosis in 76 ears. The otosclerotic process was confined to the oval window in 46 cases and to the cochlea in 30 cases. The comparison of CT and TCS is shown in table 1. Sensitivity of TCS was significantly higher for detection of fenestral otosclerosis than that of CT. The difference between sensitivity of CT and TCS for cochlear otosclerosis was not significant.

Oto-sclerosis	True pos.	True neg.	False pos.	False neg.	Sensitivity	Specificity
Fenestral						
CT	9	21	0	37	19.6 %*	100 %
TCS	27	21	0	19	58.7 %*	100 %
Cochlear						
CT	30	23	1	0	100 %	95,8 %
TCS	25	23	0	5	83.3 %	100 %

Table 1. Comparison of CT and TCS in the differential diagnosis of clinical otosclerosis.
* $p < 0.01$ (χ^2-test)
Conclusion: Tympano-cochlear scintigraphy proved to be a useful tool in the differential diagnosis of progressive hearing loss.

PS_495

DIFFERENT PERFORMANCES OF BONE DENSITOMETERS IN THE REGION OF NORTH HOLLAND

K.P. Staal (1), J.C. Roos (1), R.A. Manoliu (2), P. Lips (3), P.J. Kostense (4). (1) Nuclear Medicine; (2) Radiology; (3) Endocrinology; (4) Epidemics and Biostatics, Free University Medical Centre, Amsterdam, Holland

Objectives: After the introduction of dual X-ray absorptiometry (DXA) to measure bone mineral density (BMD) the differences between the machines have been recognised as a difficult problem. Differences in equipment, calibration and reference population cause variation in the diagnosis of osteoporosis.
Methods: In the region North Holland, including Amsterdam, we tested all the available DXA-machines (1 Norland, 2 Lunar DPX, 2 Lunar Experts, 1 Hologic 1000, 3 Hologic 2000 and 8 Hologic 4500). Two anthropomorphic phantoms (Hologic lumbar spine and hip phantom) and 1 semi-anthropomorphic geometrically defined phantom (European Spine Phantom (ESP)) were used. Every phantom was measured 5 times at baseline and after 2 months. Between every measurement the phantoms have been repositioned. The measured values were interpreted by the tested DXA-machines as if they were derived from a fictive caucasian male or female person of 40 years old, 70 kilograms weight and 170 cm height.
Results: There was no significant drift in the measured values after a 2 months period. The coefficients of variation over repeated measurements were below 1.0%, except in the femoral neck (between 1.6 and 4.6%) and in the high density region of ESP (between 0.9 and 3.7%). Interpretation of the measured values by the software of the tested machines (expressed in T-scores) shows more variation: in the lumbar spine region up to 0.8 SD for men and 0.9 SD for women and in the total hip region up to 1.5 SD for men and 0.8 SD for women. The variations in T-scores is for about two third caused by the different reference populations installed on the tested DXA-machines and for about one third by the differences in the measured BMD values. Five different reference populations were used in our region, as well for the lumbar spine as for the hip.
Conclusion: The observed differences in T-scores may cause a shift in diagnosis from normal to osteopenic and from osteopenic to osteoporosis from 10-20% between the different hospitals. Standardisation of reference populations is of utmost importance to achieve more uniformity in bone densitometry measurements and diagnosis of osteoporosis.

CARDIOVASCULAR 6

PS_496

MYOCARDIAL ADRENERGIC INNERVATION IN PATIENTS WITH NEUROCARDIOGENIC SYNCOPE MEASURED WITH 123I-MIBG UPTAKE

L. Galuska (1), I. Lõrincz (2), I. Garai (1), J. Varga (1). (1) Department of Nuclear Medicine; (2) First Department of Internal Medicine, University of Debrecen, Hungary.

Background. Neurocardiogenic (NCS) – vasovagal – syncope is one of the most common problems in clinical practice and it may result from various pathologic abnormalities or physiologic changes. There are data about biochemical abnormalities (catecholamines) during syncope, but it may be hypothetized adrenergic myocardial structural damage.
Aim: To study the global and regional adrenergic myocardial innervation in patients (pts) with NCS which was demonstrated by head up tilt table testing (HUTT).
Patients and methodes: 14 adult pts with NCS were studied. The avarage age of pts group was 42±11 years (17-68), 8 were female and 6 were male. According the HUTT result two pts had cardioinhibitory, 8 pts had vasodepressor syncope and 4 pts suffered from mixed type NCS. The average time of onset of positive reaction was: 18,5±12 minutes (1-45). The ischaemic heart diseases were excluded by normal 99m Tc-MIBI rest-stress dipyridamol SPECT results. To investigate cardiac sympathetic innervation 250-370 MBq 123I-MIBG was used. After 15 minutes of intravenous administration of 123I-MIBG early, and 3 hours later delayed myocardial planar scintigraphy and SPECT were performed. The heart to mediastinum count ratio (H/M) was calculated for both early and delayed images with normalised wash out rate (WR) too. The regional 123I-MIBG uptake was visualised on SPECT slices and polar map pictures. The regional uptake was registered pathological below the 50% comparing to normal uptake site.
Results: The mean value of late H/M ratios was 1,6±0.31 9 (Normal range (1,6-1,8) 9 from 14 pts the late H/M ratio was below the normal range. All pts. have regional uptake 123I-MIBG deficit in different regions: 5 in inferior, infero-septal and 9 in anteriolateral separately. The mean WR was 24±4,2% (normal: 20-30%).
Conclusion: In our NCS pts group the global 123I-MIBG deficit occured freqently, and all pts. have regional adrenergic nerve function deficit. This alterations may play role in clinical symptoms and have importancy in treatment planning. The 123I-MIBG scintigraphy and SPECT is usefull methode in the diagnostical algorythm of NCS pts.
This study was supported by a grant from the Health Science Council (ETT)

PS_497

99MTC LABELLED LIPOSOMES FOR DIAGNOSIS OF PULMONARY EMBOLISM IN RABBITS

S. Ninio (1), J. Palachev (2), S. Kovacheva (3), T. Nejcheva (1), D. Petkova (1). (1) Institute of Biophysics, Bulgarian Academy of Sciences ; (2) University Hospital ; (3) University Hospital , Sofia, Bulgaria.

The diagnosis of pulmonary embolism is a very complicate and hard assessment. In this study we have investigated the possibility of the application of multilamellar 99mTc labelled liposomes from phosphatydylcholine and cholesterol (2:1 molar ratio) for testing pulmonary perfusion and ventilation after embolism in rabbits.

Methods. Multilamellar liposomes were prepared by the method of the reversed phases and lyophilised in the presence of $SnCl_2$. Lyophilised liposomes were labelled with 2ml $NaTcO_4$ (250 MBq) for 15 min immediately before application. The labelling efficiency was determined by scanning column gel chromatography on Sephadex G-25 and was 68%.

Results. Pulmonary embolism was provoked by injection of 0.2 ml air into ear vein of rabbits. For testing the pulmonary perfusion after embolism we used 99mTc- Lyo MAA (130-160000 particles) or 99mTc labelled liposomes (5μm diameter). 200000 counts were obtained for each frame during scanning of four standard positions (AP, LPO, PA, RPO) 30 min after application of each radiopharmaceutical by spate gamma camera. The two images of pulmonary perfusion show that after application of 99mTc-liposomes the scanning demonstrated in more details changes in the affected lung compared to that of 99mTc Lyo MAA. Pulmonary ventilation was investigated as well by application of 99mTc- DTPA or 99mTc-liposome aerosol using nebulaizer equipment. The particle size was 1-2μm and the air flow was 9-11 l/min. The two images revealed that the central deposition into the main bronchi and trachea was more intensive after liposome application. The dynamic of the elimination of liposome radioactivity was also investigated. The calculated slopes of the curves describing the elimination of the radioactivity after application of 99mTc-liposomes or 99mTc- Lyo MAA were almost equal thus the rate of radioactivity release ought to be one and the same in the both cases.

Conclusions. These results allow us to conclude that 99mTc-liposomes might be used for clinical testing of pulmonary perfusion and ventilation since the scanning demonstrated in more details changes in the affected lung due to their smaller size compared to the particles of 99mTc- LyoMAA.

PS_498

PULMONARY EMBOLISM AND NATRIURETIC PEPTIDES

S. Cabezón (1), M. Villa (1), J.E. Morán (1), P. Gómez (2), J. López (2), R. Otero (4), A. Cayuela (3), F. G Pesquera (2), A. Ramos (2), R. Vázquez (2), A. Martínez (1)(1) Department of Cardiology; (2) Department of Nuclear Medicine; (3) Supportive Unit Research; (4) Medical-Surgical Unit of Respiratory Diseases, HUV Rocío, Spain

Natriuretic peptides (NP) have a role in left heart diseases prognostic. They have also high levels in chronic cor pulmonale.

Aim: Analyze if brain natriuretic peptides (BNP) play a role as marker of acute right ventricular pression overload.

Methods: We consecutively have studied 15 patients with clinical suspect of pulmonary embolism (PE). Diagnosis of acute pulmonary embolism was made by the evaluation of the clinical and laboratory findings and lung scan. We have excluded patients with left or right heart disease and also those with pulmonary hipertension. Baseline assessment have included signs and symptoms of PE, two-dimensional echocardiographic examination in the first day, ventilation/perfusion lung scan in the first 48 hours, and determination of brain natriuretic peptides (BNP; radioimmunoassay-RIA) in the times: 0, 72 hours and 168 hours. Our laboratory reference of normality is 18.5 ng/dl. Echocardiography may reveal dilatation of right ventricle, pulmonary hypertension (PAP above 30 mmHg), paradoxical septal encroachment (without left bundle branch block) and dilatation of supprahepatic venous. We have considered that right ventricular pression overload was present if the study had two of the previous findings.

Results: Pulmonary embolism was diagnosed in 10 patients (PE group), and was not diagnosed in 5 patients (Non PE group). 7 of 10 patients in the PE group had BNP high levels (>18.5 ng/dl) in time 0: median: 37.0 (Percentil 25: 16.7; percentil 75: 217.5). 0 of 5 patients in the Non PE group had BNP levels in time 0 above our reference: median: 16.8 (Percentil 25: 14.15; percentil 75: 17.5).

8 of 10 patients of PE group had echocardiographic RV pression overload; 7 of these 8 patients presented high BNP levels.

In the PE group BNP levels experimented a progressive reduction during the first week.

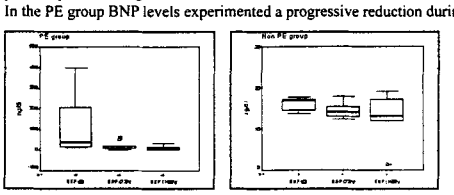

Conclusions: BNP can become biochemical markers of RV acute pression overload in PE. Future investigation may confirm this BNP test useful in the diagnosis of PE.

PS_499

USEFULNESS OF DUAL-ISOTOPE IMAGING WITH GA-67 CITRATE AND TC-99M MIBI FOR THE DIAGNOSIS OF CARDIAC SARCOIDOSIS

S. Tsuchimochi, M. Nakajo, D. Tanaka, H. Tanabe, M. Nakajo jr, T. Umanodan. Department of Radiology, Kagoshima University Hospital, Kagoshima, Japan.

Objectives: It is well known that Ga-67 citrate accumulates in the lesion of sarcoidosis. However, it is difficult to determine whether Ga-67 citrate accumulates in the heart or lung in the patients suspected of having cardiac sarcoidosis by Ga-67 citrate imaging alone. Therefore, we evaluated the usefulness of dual isotope imaging with Ga-67 citrate and Tc-99m MIBI, a myocardial perfusion imaging agent, for cardiac sarcoidosis. Methods: A total of 9 patients suspected of having cardiac sarcoidosis were included in this study: Sarcoidosis was finally diagnosed to involve the hearts in 5 patients and not to involve them in the remaining 4 patients. Ga-67 citrate SPECT was performed 48 hr after injection of 111 MBq of Ga-67 citrate (energy window for Ga-67; 93, 184 and 296 KeV + 10 %). Then dual-isotope SPECT was performed 15 min after injection of 740 MBq of Tc-99m MIBI (energy window for Ga-67; 184 KeV + 12.5 % and Tc-99m; 140 KeV + 5 %). Both Ga-67 and dual-isotope SPECT examinations were performed with 64 x 64 matrix, 6 degree x 60 steps and 25 sec/step. The crosstalk was estimated to be 1.40 - 3.45 % from Tc-99m to Ga-67 and 0.37 - 0.91 % from Ga-67 to Tc-99m. These examinations were also performed after steroid therapy in a patient with cardiac sarcoidosis. Results: The table shows the sensitivity, specificity and accuracy of Ga-67 SPECT, Tc-99m MIBI SPECT (obtained from the dual-isotope examination) and dual-isotope SPECT for cardiac sarcoidosis. Dual-isotope SPECT showed the accuracy of 100 %. Ga-67 citrate uptakes in the defect portions of Tc-99m MIBI cardiac SPECT images disappeared after steroid therapy in the treated patient. Conclusion: Dual-isotope SPECT with Ga-67 citrate and Tc-99m MIBI may be a useful means for the diagnosis of cardiac sarcoidosis.

	sensitivity (%)	specificity (%)	accuracy (%)
Ga-67 citrate	40 (2/5)	100 (4/4)	67 (6/9)
Tc-99m MIBI	80 (4/5)	25 (1/4)	56 (5/9)
Dual-SPECT	100 (5/5)	100 (4/4)	100 (9/9)

PS_500

EFFECTS OF STATINS ON LIPOPROTEIN METABOLISM IN HUMAN MAST CELLS AND BASOPHILS

S. Li (1), P. Valent (2), A. Kurtaran (1), E. Koller (3), M. Baghestanian (4), C. Novotny (1), E. Minar (4), R. Dudczak (1), I. Virgolini (1). (1) Department of Nuclear Medicine; (2) Department of Hematology and Hemostaseology; (3) Department of Physiology; (4) Department of Angiology, Internal Medicine I, University of Vienna, Austria

Statins, the inhibitors of 3-hydroxy-3-methylglutaryl coenzyme A (HMG CoA) reductase, are widely used to treat hyperlipidaemia. Recent studies suggest that not only the lipid-lowering potential of statins, but also other beneficial effects such as improved endothelial function of statins may contribute to the positive effects of statin treatment. Basophils and mast cells have been shown to play an important role in the lipid metabolism and atherogenesis. However, the effect of statins on lipoprotein binding to human mast cells and basophils is unknown. The aim of this study was to investigate the effects of statins on the interactions of ^{125}I-low-density lipoprotein (^{125}I-LDL) with human basophils (KU812 cell line) and a human mast cell line, HMC-1.

Methods: The metabolic fate of LDL in HMC-1 and KU812 was studied by radiolabeling the LDL with ^{125}I. Direct binding assay was performed. Binding data were calculated according to Scatchard analysis.

Results: Scatchard plots indicating two class of specific binding sites on KU812 cells and on HMC-1 cells, respectively. Exposure to HMG CoA reductase inhibitors, atorvastatin, simvastatin and cerivastatin increased significantly ($p<0.05$-0.01) the binding sites for ^{125}I-LDL on HMC-1 cells and KU812 cells in a dosis dependent manner. The rank order of potency for increase the binding sites for LDL on HMC-1 cells was cerivastatin > atorvastatin > simvastatin. The binding capacity of ^{125}I-LDL to KU812 was significantly incereased by pre-incubation with cerivastatin > semivastatin > atorvastatin. The statins - induced increase of ^{125}I-LDL binding sites was accompanied by increased ^{3}H-thymidine incorporation. However, no increase of adenosine 3«-5«cyclic monophosphate (cAMP) formation was found in human mast cells and basophils after treatment with statins. Furthermore, statin enhanced the cellular binding, uptake and degradation of LDL in HMC-1 and KU812 cells in a dose dependently fasion.

Conclusions: Our results provide evidence for the up-regulation of LDL binding sites on human basophils and HMC-1 mast cells through statins. The exact biological and pathophysiological roles of these regulative effects remain to be elucidated.

Poster presentation

PS_501

IS THE EFFECT OF SPINAL CORD STIMULATION IN PATIENTS WITH ANGINA AND NORMAL CORONARY ARTERIES RELATED TO AN IMPROVEMENT OF ADRENERGIC CARDIAC FUNCTION?

A. Giordano (1), G.A. Lanza (2), M.L. Calcagni (1), A. Sestito (2), F. De Seta (3), F. Pasutto (1), F. Reale (1), L. Romano (1), M. Massaro (4), F. Bellocci (2), L. Troncone (1)(1) Istituto di Medicina Nucleare, Università Cattolica del S. Cuore, Rome, Italy; (2) Istituto di Cardiologia, Università Cattolica del S. Cuore, Rome, Italy; (3) Medtronics Italia SPA, Italy; (4) Dipartimento di Medicina Interna, Università Tor Vergata, Rome, Italy

Spinal Cord Stimulation (SCS) is capable to significantly improve symptoms in patients with angina and normal coronary arteries (NCA). It can be hypothesized that this effect is due to the improvement of neuroadrenergic cardiac function which is often abnormal in these patients.

AIM of this study was to verify whether SCS improves neuroadrenergic cardiac function in patients with angina and NCA using I123-MIBG scintigraphy.

METHODS: we studied 7 patients (4 males, 3 females, 59 ±11 years old) with NCA, who underwent SCS device implantation because of anginal pain refractory to full medical therapy. Each patient underwent to MIBG-rest and Sestamibi-stress/rest scintigraphies both in basal conditions (SCS device switched off) and during active SCS (device switched on for 1 month). Overall, 28 scintigraphic studies were performed. I123-MIBG studies were done by early and delayed planar and SPECT acquisitions using 185 MBq of high-specific-activity agent. Global MIBG cardiac uptake was assessed by heart/mediastinum ratio (H/M ratio); regional MIBG uptake was assessed by an Uptake Defect Score based on the sum of the scores qualitatively attributed by 2 expert observers to 24 LV segments. Tc99m Sestamibi SPECT studies were performed within 2 days from MIBG studies, using single-day stress/rest technique. LV perfusion was qualitatively assessed in 24 LV segments.

RESULTS: in our pts the number of anginal episodes and nitrate consumption were both reduced by SCS, as compared to baseline conditions ($p<0.001$ and $p<0.004$, respectively). In 5/7 patients we found global and/or regional abnormalities of MIBG cardiac uptake; in all cases the scintigraphic pattern was unchanged in presence or absence of active SCS. The delayed H/M ratio in presence and absence of active SCS was 1.78±0.4 and 1.77±0.4, respectively (p=NS); similarly MIBG Uptake Defect Score was 18.6±26 and 18.4±25 (p=NS). Reversible exercise induced perfusion defects were detected in 4/7 patients in the absence of active SCS; in 2/4 patients perfusion defects improved during active SCS.

CONCLUSIONS: 1) our data confirm that MIBG cardiac abnormalities are frequent in pts with angina and NCA; 2) SCS does not significant affect MIBG abnormalities, thus its clinical benefit seems not related to the functional status of the cardiac neuroadrenergic system; 3) SCS caused an improvement of reversible perfusion defects in 2 pts, suggesting that its anti-ischemic effects can be scintigraphically verified, however the mechanisms of SCS clinical benefit and the non-constant correlation of its effects with myocardial perfusion remain to be clarified.

PS_502

THE ROLE OF I-131-MIBG AND TL-201 SCINTIGRAPHY IN THE EXAMINATION OF MALIGNANT VENTRICULAR TACHYARRHYTHMIAS

I. Balogh (1), I. Balogh (1), B. Merkely (2), E. Zima (2), L. Gellér (2), J. Környei (3). (1) Department of Nuclear Medicine, Uzsoki street Teaching Hospital, Budapest, Hungary; (2) Department of Cardiovascular Surgery, Semmelweis University, Budapest, Hungary; (3) Isotope Institute, Budapest, Hungary.

Aim: Investigating the pathomechanism of the malignant ventricular tachyarrhytmias (MVT) causing sudden death we studied the role of the sympathetic innervation (SI) of the heart in MVT. We examined the abnormalities of SI by MIBG scintigraphy (SC) and myocardial perfusion feature by myocardial perfusion scintigraphy (MSC) in patient (pts) with MVT having implantable cardioverter defibrillator (ICD) to prevent the dangerous complications. Seeking the correlation between the clinical and scintigraphic signs we compared the scintigraphic abnormalities with the frequency and severity of MVT on ICD registrations.

Patients and method: Rest MSC (with Tl-201 Chlorid) and MIBG SC (with high specific activity I-131-MIBG) were performed in 31 pts with MVT and ICD (14 myocardial infarction (MI), 11 dilatativ cardiomyopathy (DCM), 6 primer ventricular tachyarrhythmias (PVT)). We examined on MS the severity and extension of the perfusion abnormalities. On MIBG SC we calculated the diffuse MIBG uptake by measuring the mediastinum/heart ratio and analysed the severity and extension of regional MIBG uptake abnormalities.

Result: In the group of pts with MI, MIBG uptake decreased diffusely in 12/14 cases (in 3 cases severely) and comparing the regional MIBG abnormalities with the abnormalities on MS, the finding on MIBG was more severe and more extensive in every case. In the group of pts with DCM in addition to diffuse diminution of MIBG uptake (in 10/11 cases) we could find in all 11/11 cases severe regional abnormalities as well. The finding of MS scintigraphy was less positive than MIBG in 10/11 cases. In the group of pts with PVT the MIBG uptake decreased diffusely in 4/6 pts, and in 2/6 pts the inhomogenous uptake was the only abnormality on MIBG SC. The results of MS were better than the results of MIBG in every case. Among the pts with MVT registered on ICD (25/31) the most severe arrhythmias on ICD registration (repeated ventricular tachycardia and/or fibrillation) associated with the most severe MIBG abnormalities and with much better perfusion abnormalities on MS.

Summarizing our results: among the pts with MVT the MIBG SC was positive in every case. The diffuse decrease and / or regional abnormalities of MIBG uptake reflecting the damage of SI seems to be a characteristic sign in MVT (31/31). Because the most severe damage of it associated with the most severe clinical signs registered by ICD the SI may have a high prognostic value.

PS_503

THE CHANGE OF MYOCARDIAL SYMPATHETIC NEURONAL FUNCTION BEFORE AND IMMEDIATELY AFTER RADIATION THERAPY AND/OR SYSTEMIC CHEMOTHERAPY FOR LUNG CANCER

S. Tsuchimochi, M. Nakajo, D. Tanaka, H. Tanabe, M. Nakajo jr. Department of Radiology, Kagoshima Unversity Hospital, Kagoshima, Japan.

Objectives: Effect of radiation (RT) and systemic chemotherapy (SCT) on myocardial sympathetic neurons remains to be elucidated. Therefore we evaluated the change of myocardial sympathetic neuronal function before and immediately after RT and SCT by I-123 MIBG imaging. Methods: A total of 9 patient(pt)s with lung cancer (5 males and 4 females, age range; 52 - 75 yrs) were included in this study. None of them had cardiac diseases and cardiac involvement by cancer. RT of total doses of 50 - 60 Gy for the primary lesion including some part of the heart and SCT (cisplatin 80 mg/body and docetaxel 150 mg/body) were performed in 6 pts, and other 3 pts were treated with SCT (cisplatin 75 mg/m2 and docetaxel 90 mg/m2) alone. All pts were evaluated with ECG, UCG and I-123 MIBG planar imaging and 20 min and 4hr SPECT before and after therapy (within 1 week of the start and end of therapy). The whole myocardial % uptakes and washout rates of I-123 MIBG were calculated. Results: In the 6 pts treated with RT+SCT, some new abnormalities were detected after therapy on ECG in 4 pts (depression or inversion of T wave), and on UCG in 3 pts [mild valvular insufficiency (VI); 3 pts, and a small amount of pericardial effusion; 2 pts]. In the 3 pts treated with SCT, a pt showed mild VI on UCG, but no pts showed any new abnormalities on ECG. There was no significant changes before and after therapy in the whole myocardial % uptakes (RT+SCT: 5min; 2.57+0.14 vs 2.65+0.86, 20min; 2.38+0.10 vs 2.51+0.86 and 4hr; 1.80+0.18 vs 1.99+0.48, and SCT: 5min; 2.67+0.45 vs 2.48+0.67, 20min; 2.46+0.56 vs 2.30+0.67 and 4hr; 1.90+0.79 vs 2.04+0.75) and washout rates (%/hr) of MIBG (RT+SCT: from 5min to 20min; 28.9+9.0 vs 23.2+14.4, from 20min to 4hr; 6.7+1.7 vs 4.9+5.3, and SCT: from 5min to 20min; 35.0+22.6 vs 30.4+21.0, from 20min to 4hr; 6.8+3.8 vs 3.2+5.8). There was also no significant changes in the regional myocardial uptakes and washout rates before and after therapy in the patients with RT+SCT and SCT. Conclusion: Although new mild abnormalities are sometimes occurred on ECG and UCG, myocardial sympathetic neuronal function may not change immediately after RT and/or SCT.

PS_504

WHAT FACTORS DO RELATE WITH BNP CONCENTRATIONS? A STUDY BY NUCLEAR CARDIOLOGY

M. Sarai (1), T. Sato (1), K. Oshima (1), T. Kondo (1), S. Kakisawa (1), M. Tokuda (2), T. Furuta (1), H. Kurokawa (1), M. Nomura (1), H. Hishida (1), Y. Watanabe (1)(1) Department of Cardiology, Fujita health university, Aichi, Japan; (2) Department of Cardiology, Meitetsu hospital, Aichi, Japan.

Aim: Although plasma brain natriuretic peptide (BNP) concentrations correlate with left ventricular end-diastolic pressure, it is not defined weather BNP correlates with myocardial adrenergic activity or LV volumes. To investigate what factors correlate with BNP plasma concentrations, Iodine-123 metaiodobenzylguanidine (MIBG) and sesta-MIBI myocardial imaging were performed in various heart diseases.

Methods: 83 patients with various heart diseases (male/female; 57/26, mean age: 63.9±13.6 years, 22 OMI, 11 AMI, 5 AP, 14 DCM, 4 HCM, 2 RCM, 8 arrhythmia, 9 MR, 3 AS, 2 AR, 2 TOF, 1 ASD, 1 HT) underwent Iodine-123 metaiodobenzylguanidine (MIBG) and sesta-MIBI myocardial imaging. Plasma BNP levels were determined by commercial radioimmunoassays (Shionogi). Planar MIBG images and sesta-MIBI myocardial SPECT were obtained in a day in these patients. Myocardial uptake of MIBG was calculated as the heart/mediastinal activity ratio (H/M(early) and H/M(delay)) in early and delayed images. Storage and release of MIBG were calculated as percent myocardial MIBG washout from 15 min to 4 h after isotope injection. HR, BP and body mass index(BMI) were simultaneously measured. LVEDV, LVESV, LVEF, cardiac output (CO) and end-systolic pressure volume relation (ESPVR) were calculated using QGS program.

Results: In stepwise regression analysis, logBNP significantly correlated with H/M(delay)($F=17.1$, $P<0.0035$), BMI($F=21.6$, $P<0.003$) and ESPVR($F=12.1$, $P<0.0001$).

Conclusions: The present data suggest that BNP correlated with not only LVEDP but also myocardial adrenergic nerve activity (H/M delay), cardiac cachexia (BMI) and LV contractility (ESPVR).

PS_505

ASSESSMENT OF SYMPATHETIC INNERVATION IN PATIENTS WITH DILATED CARDIOMYOPATHY USING I123-MIBG AND THE CORRELATION WITH FUNCTIONAL PARAMETERS

M. Koutelou (1), A. Theodorakos (1), G. Athanassopoulos (2), V. Tsapaki (1), A. Kouzoumi (1), E. Nygaren (1), D. Cokkinos (2). (1) Department of Nuclear Medicine; (2) 1rst Cardiology Department, Onassis Cardiac Surgery Center, Athens, Greece.

In heart failure (HF) patients (pts) sympathetic dysfunction (SD) is associated with unfavorable prognosis. We assessed cardiac SD in pts with dilated cardiomyopathy (DCM).
METHODS: 123 I-metaiodobenzylguanidine (MIBG-123) single photon emission tomography (SPECT) was performed in 29 pts (18 male, 11 female) of DCM , mean age of 52.7±14.9 years. All were studied with early planar MIBG (10 min) and delayed MIBG SPECT acquisition; 15 pts underwent delayed planar acquisition and we calculated the washout (WO). Cardiac MIBG uptake was measured as the heart (H) to upper mediastinum (M) activity ratio (H/M). All underwent cardiac catheterization and echocardiography. Coronary arteriography did not reveal significant >50% coronary artery stenoses. Severity of HF was NYHA grade I 7 pts, grade II 9 pts, ,grade III 10 pts and 3 pts grade IV. Mean left ventricular ejection fraction (LVEF) was 28±7%. Fifteen underwent cardiopulmonary exercise tests. The reduction in MIBG uptake was evaluated visually. The myocardium uptake was studied in 6 segments (anterior, septum, posterior, inferior, lateral from the short axis and apex from long vertical axes) using a 4-point scale (0=normal, 1=moderately diminished, 2=severely diminished and 3=no uptake). Scores for all 6 segments (SG) was defect score (DS). We also calculated the mean counts/pixel of each segment.
RESULTS: The endiastolic (EDD) and endsystolic (ESD) diameter of LV were 71±10.5 mm and 59.7±11.2 mm respectively. The mean exercise time (mET) was 349±196.4 seconds and the peak oxygen uptake (VO2) was 15.3±4.8 ml/min/Kgr.
The H/M early and H/M delayed were 1.6±0.3 and 1.4±0.2 (p=0.03), the WO 37.7±9% (normal limits ≤20%) and the MIBG score was 8.5±2.5. Mean counts/pixel for SG was: anterior=59.4±93, septum=62.6±97, inferior=26.73±42, posterior=25.48±41, lateral=60.3±98.5 and apex=38.5±71. The reduction of counts/pixel in posterior and inferior SG was significant compared to other segments (p<0.00001). Delayed MIBG H/M correlated with LVEF (r=0.5, p=0.05) and with age (r=0.6, p=0.03). MIBG score correlated with age r=0.5 (p=0.005) and reduction in uptake in inferior and posterior SG with LVEF, EDD, ESD with r=0.5 (p=0.0002), 0.52(p=0.01) and 0.54 (p=0.007) respectively. There was no correlation between VO2 and the scintigraphic parameters nor with H/M and WO.
CONCLUSION: In DMC pts age, diminution of contractility and LV dilatation are correlated with sympathetic dysfunction.

PS_506

CARDIAC 123I-MIBG UPTAKE – WHAT IS NORMAL?

C. Novotny, G. Zettinig, A. Staudenherz, B. Fueger, A. Kurtaran, R. Dudczak. Department of Nuclear Medicine, General Hospital Vienna, Austria.

Aim: Reduced ^{123}I-Metaiodobenzylguanidin (MIBG) uptake in the heart is considered to be useful for the differential diagnosis of the parkinsonian syndromes. Reduction of cardiac ^{123}I-MIBG uptake is reported to occur only in Parkinsons disease but not in related neurodegenerative diseases with parkinsonism. However, cardiac ^{123}I-MIBG uptake is also hampered by cardiovascular disorders and several drugs, and the normal range of cardiac ^{123}I-MIBG uptake in the average population is not well defined. The aim of this retrospective study was to evaluate cardiac ^{123}I-MIBG uptake in a large cohort of patients who were all referred for ^{123}I-MIBG scintigraphy.
Methods: The scans of 149 patients (75 males / 74 females) who underwent ^{123}I-MIBG scintigraphy for evaluation of a adrenal tumor between 1 / 1998 and 12 / 2000, but were negative in this respect, were analysed retrospectively. None of the patients had medication known to affect ^{123}I-MIBG uptake. Planar images of the chest from an anterior view 20 hours after application of 350 MBq ^{123}I-MIBG were analyzed by 2 nuclear physicians. Cardiac uptake was interpreted visually and ranked in 3 categories (no, faint, clear cardiac uptake). All patients with absent or low cardiac uptake were further evaluated.
Results: In 7 / 149 individuals (5 %), tracer distribution in the heart region was absent, and 25 / 149 patients (17 %) showed a faint uptake in the heart equal to the mediastinum. In 117 / 149 patients (78 %), the myocardium was clearly visible. In 24 individuals of the 32 patients with low cardiac uptake, detailed evaluation was possible; from 7 outpatients, no clinical information could be obtained. Parkinsons disease known at time of scan was found in only 1 / 24 patients. None of the patients with lower cardiac uptake had angiographically documented coronary artery disease; 17 / 24 had hypertension, and in 2 / 24 individuals, a dilatative cardiomyopathy had been diagnosed.
Conclusion: These findings demonstrate low cardiac ^{123}I-MIBG uptake in 22 % of our patients, thus the diagnostic use of low cardiac ^{123}I-MIBG uptake is questionable.

PS_507

SYMPATHETIC INNERVATION IN PATIENTS WITH LBBB USING MIBG

M. Koutelou (1), A.T. Theodorakos (1), G. Athanassopoulos (2), V. Tsapaki (1), A. Kouzoumi (1), V. Cokkinos (2). (1) Department of Nuclear Medicine; (2) 1rst Cardiology Department, Onassis Cardiac Surgery Center, Athens, Greece.

INTRODUCTION: Patients with left bundle branch block (LBBB) frequently demonstrate left ventricular functional abnormalities. We assessed myocardial adrenergic activity using iodine-123 metaiodobenzylguanidine (MIBG).
METHODS: MIBG was performed in 17 patients(pts) with LBBB on ECG and all underwent coronary arteriography (CAR), echocardiocraphy and adenosine-thallium studies(AD-TL). Three pts had coronary artery disease and normal cardiac function (cad-group 1),13 pts dilated cardiomyopathy with normal coronary arteries (CA) and heart failure (group 2) and one patient valvular disease and normal CA (group 3). All underwent MIBG planar images 5 minutes after the injection of MIBG and single emission tomography (SPECT) 4-5 hours post injection. To evaluate the myocardial accumulation of MIBG the heart/mediastinal (H/M) activity ratio was calculated. MIBG and AD-Tl SPECT images were visually evaluated; We divided into 6 segments: anterior, septal, inferior, posterior, lateral and apical and graded as follows: o=normal uptake, 1=mildly reduced, 2=severe reduced uptake and 3=no uptake obtaining a global score. All pts had abnormal SPECT MIBG imaging. In group 1, H/M ratio was 1.7±0.3, the MIBG score was 7 ±1.5 and AD-TL was 3±1.5. Group 2 had H/M ratio 0.8±0.1 in pts with LVEF<30% and 1.9± 0.4 in pts with LVEF>30% (P<0.0005), the MIBG and AD-TL score was 6.6±1.2 and 0. 2 respectively and Group 3 (one patient with valvular disease) had H/M ratio 1.8, MIBG score 5 and normal AD-TL .
RESULTS: All pts with LBBB had multiple and extensive denervated segments independently of myocardial systolic function; diminished H/M was observed only in the patients with severe heart failure. The limitation of this study is that delayed planar images were not obtained to assess the MIBG washout into the 3 groups
CONCLUSION: _he major finding of this study is the extensive myocardium denervation in pts with LBBB regardless of the LVEF. The significant decrease of the H/M ratio only in severe cardiac systolic dysfunction can be attributed to the downregulation of neuronal receptors.

PS_508

THE EVALUATION OF CARDIAC SYMPATHETIC INNERVATION IN PATIENTS WITH DIFFERENT CARDIAC PATHOLOGY

I. Igor, V. Sergienko, V. Naumov, L. Samoylenko. Department of Nuclear Medicine, Cardiology Research centre, Moscow, Russia.

Aim: The aim of our investigation was to assess the cardiac sympathetic innervation disorders in patients with arterial hypertension (AH), hypertrophy cardiomyopathy (HCM) and coronary artery diseases (CAD).
Methods: We performed 123-J-metaiodbenzylguanidine (MIBG) scintigraphy in 9 pts with AH, 12 pts with HCM, 14 pts with CAD and 8 healthy volunteers. The sympathetic innervation was evaluated by using planar and SPECT scintigraphy. The heart/mediastinum ratio (H/M) was calculated for early (15 min) and delayed (4 h) planar images. Difference of MIBG uptake in anterior, posterior, lateral, septum and apex regions was detected by using semiquantitative SPECT analysis. We compared H/M ratio among all groups and among early and delayed images. Perfusion defects we evaluated by scintigraphy with 99m-Tc-metaiodbutilisonitril.
Results: There were significant differences between volunteers and patients in each group (P<0.001) but we could not find significant differences between AH, HCM and CAD group. Also there were no significant differences among early and delayed images – H/M ratio was 1.9±0.44 (early) and 2.0±0.52 (delayed) in pts with HCM, 1.6±0.44 (early) and 1.6±0.15 (delayed) in pts with CAD, 1.8±0.1 (early) and 1.9±0.3 (delayed) in pts with AH. The defects of MIBG uptake were found in 5 pts with AH (56%), 10 pts with HCM (83%) and in 11 pts with CAD (79%). Perfusion defects were found in 6 pts with AH, 11 pts with HCM and in all pts with CAD. All pts who has perfusion defects had also defects of MIBG uptake, there localization was congruent.
Conclusion: There is the decrease of MIBG accumulation in pts with AH, HCM and CAD. The reason of it's difference in pts with hypertrophy perhaps an accelerated washout of MIBG from sympathetic vesicules. Oppositely, the sympathetic innervation is absent in scar regions in pts with CAD.

PS_509

SERIAL CHANGE OF SYMPATHETIC NERVE ACTIVITY OF THE PATIENTS WITH HYPERTROPHIC OBSTRUCTIVE CARDIOMYOPATHY (HOCM) TREATED WITH PERCUTANEUS TRANSLUMINAL SEPTAL MYOCARDIAL ABLATION (PTSMA)

H. Matsuo, S. Watanabe, T. Yamaki, M. Iwama, T. Hirose, S. Tanaka, A. Murata, S. Miyata, T. Kadosaki, T. Segawa, M. TomitaDepartment of Cardiology, Gifu Prefectural Hospital, Gifu, Japan.

Background : PTSMA is a effective non-surgical technique for achieving the reduction of the pressure gradients of LV outflow and patients symptoms dramatically. However, the effect of this approach to the sympathetic activity is not well known. Purpose and methods: To investigate the time course of the sympathetic nerve activity, we evaluate the sympathetic activity by MIBG scintigraphy performed just before, 1week after, and 3 months after the procedure in 6 patients with severe HOCM. H/M ratio in early and delayed images and washout rate was used as the indexes showing sympathetic function. Results: The procedures were all successful without severe complications. CPK release ranged from 976 to 3642 IU. LV outflow PG decreased markedly from 110±16mmHg to 45±31mmHg and concomitant improvement of NYHA classification was evident (pre-PTSMA:2.5±0.8 post-PTSMA:1.2±0.4). MIBG demonstrates the transient increase of washout (pre:34±5% post:44±6%) and decrease of H/M ratio of delayed images (pre:1.9±0.8, post:1.7±0.2) at 1week after procedures. 3 months after procedure, significant decrease of washout(3M:30±8%) and increase of H/M ratio(3M:2.0±0.3) was observed. Conclusion: Transient overactivation of sympathetic nerve probably associated with iatrogenic infarction was observed early after PTSMA. However, sympathetic activity was gradually reduced at chronic phase suggesting the favorable effect of this therapy on loading conditions of the hypertrophied heart.

PS_510

ASSESSMENT OF CARDIAC ADRENERGIC NERVOUS SYSTEM WITH I-123-MIBG SPECT IN PATIENTS SUBMITTED TO TRANS-MYOCARDIAL LASER REVASCULARISATION. PRELIMINARY DATA

A. Teresińska (1), M. Œliwiński (2), S. Konieczna (1), M. Szymańska (2), P. Hendzel (2), Z. Juraszyński (2), A. Wojnowski (2), A. Dębski (3), B. Szumiłak (1). (1) Department of Nuclear Medicine; (2) Cardiosurgery Clinic; (3) General Cardiology Clinic, National Institute of Cardiology, Warsaw, Poland.

The aim of our program is to study the range of influence of the laser energy on cardiac adrenergic nervous system and to assess if disruption of this system can be one of the mechanisms responsible for clinical improvement observed after TMLR.

Methods: The patients with high pre-operative probability of having sole TMLR or TMLR combined with only 1 bypass are studied before the operation with Tc-99m-MIBI SPECT (perfusion test) and with I-123-MIBG SPECT (neuronal activity test). The patients (if they were operated according to the assumption) are studied postoperatively with I-123-MIBG SPECT as early as possible from clinical point of view and will be studied with Tc-99m-MIBI and I-123-MIBG SPECTs 6 months after operation. Up to now, in 14 patients the preoperative tests were performed and 3 patients had early postoperative (3-39 days) I-123-MIBG SPECT. The group characteristics: 8M and 6F; age: 54-69y, av. 63±5y; all the patients in III/IV CCS class; 8 patients after 1-4 MI (av. 1,1±1,2 MI per patient); 1 patient after earlier CABG. Registration of I-123-MIBG SPECT images was started 4 hrs after injection of the radiopharmaceutical. All SPECT studies were assessed in 17 segments (seg) of the LV.

Results: Preoperatively, there were 5-13 (av.9,5±2,5) underperfused segments per patient in Tc-99m-MIBI studies and 5-15 (av. 10,4±2,8) segments per patient with lowered I-123-MIBG uptake. On average, I-123-MIBG uptake deficiency was occupying more segments and was more severe in a patient than Tc-99m-MIBI deficiency. In 3 patients submitted to TMLR, postoperative I-123-MIBG uptake deficiency was occupying larger areas (1-3 segments more) and was more severe (in 3/34 segments uptake was the same, in 2/34 segments uptake improved, in 29/34 segments uptake decreased).

Conclusion: Our observations from all three studied patients support the hypothesis that TMLR reduces the activity of cardiac adrenergic nervous system, what can be one of the mechanisms responsible for clinical improvement noted after TMLR.

(supported by State Committee for Scientific Research, grant 4 P05B 02418)

DIAGNOSTIC ONCOLOGY 11

PS_511

MANAGEMENT OF DIFFERENTIATED THYROID CARCINOMA BY SERUM THYROGLOBULIN AND 131I SCINTIGRAPHY AFTER RECOMBINANT HUMAN TSH AND 99MTC-SESTAMIBI

G. Villa (1), M. Giusti (2), R. Zoccola (3), B. Guazzini (2), E. Molinari (1), F. Castagnola (1), L. Bertolazzi (3), F. Minuto (2). (1) Nuclear Medicine Service, DiMI - University of Genoa, Genoa, Italy; (2) DiSEM - University of Genoa, Genoa, Italy; (3) Nuclear Medicine Service, Civic Hospital, Alessandria, Italy.

AIM: Whole-body scan (WBS) and thyroglobulin (Tg) assay are methods of evaluating patients (pts) who have undergone surgery for well differentiated thyroid cancer (DTC). The use of recombinant human (rh)-TSH is a promising method in order to avoid LT4 discontinuation. We evaluated the sensitivity of Tg after rh-TSH versus WBS using both ^{131}I and ^{99m}Tc-Sestamibi in detecting residual thyroid cancer or normal tissue after surgery and radioiodine ablation.

SUBJECTS: Fifteen pts (29-78 yrs) on LT4 regimen were studied after 12 months (median) from primary treatments.

METHODS: Favourable results were considered: Tg levels <0.5 ng/ml after rh-TSH and negative scans after ^{131}I (185 MBq) and ^{99m}Tc-Sestamibi (740 MBq). Pts received rh-TSH (0.9 mg i.m., days 1 and 2); 24 h after the second dose, ^{131}I was administered and WBS was performed 48 h later. Serum Tg levels were evaluated on days 0, 3 and 6. WBS with ^{99m}Tc-Sestamibi were performed within 4 weeks.

RESULTS: In 12 pts Tg levels were <0.5 ng/ml in the first determination. In the other pts ranged from 0.8 to 28.0 ng/ml. A Tg change < 1 /ml ng was noted after rh-TSH in 10 pts, while in the 5 ranged from 1.8 to 803.9 ng/ml. 131I was positive in 3 pts and suspect in 2. WBS using ^{99m}Tc-Sestamibi was negative, suspect and negative respectively in 7, 4, 4. In all patients with positive ^{131}I WBS occurred unfavourable Tg results after rh-TSH and positive ^{99m}Tc-Sestamibi scans. Five pts, showing a positive or suspect ^{99m}Tc-Sestamibi scan, had an increased Tg after rh-TSH.

CONCLUSION: Undetectable Tg level followed by a Tg change <1 ng/ml after rh-TSH seems to be the best index on normality on follow-up in pts with a history of DTC. WBS with ^{99m}Tc-Sestamibi seems to be sensitive but not specific. Without LT4 discontinuation, Tg assay after rh-TSH seems to be more sensitive than ^{131}I-scan.

PS_512

99MTC-MIBI AND 201TL IMAGINGOF THYROID WITH COLD NODULE

Y.L. Yu, J.F. Yu, L.B. Chen, H. Ji, R.S. Zhu. Department of nuclear medicine,Shanghai 6th people's hospital, Shanghai, China.

The clinical value of ^{99m}Tc-MIBI and ^{201}Tl imaging of thyroid with cold nodule were assessed. Methods 87 patients with cold thyroid nodule were imaged with ^{99m}Tc-MIBI(early 15min, delayed 60min) and ^{201}Tl (early 15min, delayed 120min). Regions of interest(ROIs) were generated over the cold nodule and normal tissue on each image. The semi-quantitative analysis was performed by using a lesion to non-lesion ratio of early(ER) and delayed(DR) images. Retention index(RI) was calculated by dividing delayed-early subtraction to product ER. Results There was significant difference in the ER,DR and RI between malignant and benign lesions for ^{99m}Tc-MIBI and ^{201}Tl ($p<0.05$). The difference was no significant between carcinoma and inflammation($p>0.01$), but there was significant difference between carcinoma and cystic adenoma for ^{201}Tl imaging($p<0.01$).The sensitivity, specificity and accuracy using semi-quantification for both agents were significantly higher than visual method($p<0.01$), and DR,RI for both agents were higher than ER($p<0.05$).

Agents	Pathology	ER	DR	RI
^{99m}Tc	Tumor	1.08±0.25	1.22±0.16	0.08±0.09
-MIBI	Non-tumor	0.82±0.23	0.87±0.20	0.02±0.02
	Tumor	1.02±0.19	1.11±0.13	0.09±0.08
	Non-tumor	0.80±0.22	0.81±0.18	0.01±0.04
^{201}Tl Including	Cystic adenoma	0.65±0.18	0.79±0.11	0.01±0.02
	inflammation	0.82±0.17	0.80±0.15	0.03±0.02

		Sensitivity	Specificity	Accuracy
	ER	68.8%(5/8)	62.5%(24/47)	52.7%(29/55)
^{99m}Tc-MIBI	DR	87.5%(7/8)	55.3%(26/47)	60.0%(33/55)
	RI	75.0%(6/8)	68.8%(27/47)	60.0%(33/55)
	ER	68.8%(11/16)	57.7%(41/71)	59.8%(52/87)
^{201}Tl	DR	75.0%(12/16)	60.6%(43/71)	63.2%(55/87)
	RI	75.0%(12/16)	66.2%(47/71)	67.8%(59/87)

Conclusions ^{99m}Tc-MIBI and ^{201}Tl imaging of thyroid cold nodule using ER,DR and RI had higher clinical application value than visual method. ^{201}Tl delayed imaging had the possibility of identifying cystic adenoma from carcinoma.

PS_513

THYROID CARCINOMA FOUND AT PARATHYREOIDECTOMY : ASSOCIATION WITH PARATHYROID CARCINOMA. A CASE REPORT

A. Fotopoulos (1), S. Koukouraki (1), G. Schoretsanitis (2), A. Velidaki (1), D. Tsiftsis (2), N. Karkabitsas (1). (1) Department of Nuclear Medicine; (2) Department of Surgical Oncology, University Hospital of Crete, Greece.

Nonmedullary thyroid carcinoma is known to occur in association with primary hyperparathyroidism (PHPT). Parathyroid carcinoma is a rare cause for PHPT. A combination of parathyroid carcinoma and nonmedullary thyroid carcinoma is rare.
A retrospective review was performed, of patients who underwent surgery for PHPT between 1998 and 2000. Among 34 surgical patients with PHPT at this institution, four patients (12%) were found to have parathyroid neoplasms. Histological examination of parathyroid tumors revealed one parathyroid adenoma and three parathyroid carcinomas. In one case coexistence of parathyroid and papillary thyroid carcinoma was detected.
Therefore in the diagnosis of PHPT it is necessary to take into consideration association between malignant thyroid disease and hyperplastic or neoplastic parathyroid tissue

PS_514

TC99M PERTECHNETATE WHOLE BODY SCANNING IN DIFFERENTIATED THYROID CARCINOMA IN COMPARISON WITH I-131 WHOLE BODY SCINTIGRAPHY

A. Dirlik, M. Kayalıoğlu, S. Erhamamcı, O. Ömür, Z. Özcan, K. Kumanlıoğlu, H. Özkılıc. Department of Nuclear Medicine, Ege University Medical Faculty, Izmir, Turkey.

Aim: I-131 scintigraphy is sensitive and specific for the detection of functioning residual and metastatic tissue in patients with differentiated thyroid carcinoma (DTC). However, it has been reported that diagnostic whole-body I-131 scanning may impair subsequent the uptake of a therapeutic dose. The aim of this study was to investigate the value of Tc99m pertechnetate whole body scan (WBS) in comparison I-131 WBS prospectively.
Methods: Thirty-four patients (6 male, 28 female; range 12-67 y.o.) who had undergone total thyroidectomy for DTC (22 papillary and 12 follicular) were included in study population. Following thyroid surgery and during the clinical follow-up, all patients underwent Tc99m pertechnetate WBS with a dose of 10-20 mCi. Tc99m pertechnetate WBS preceded I-131 WBS while these patients were withdrawn thyroxine for at least 4 weeks. Tc99m pertechnetate WBS findings were evaluated comparatively with following posttherapeutic / postablative I-131 WBS findings. The number of foci of abnormal uptake was recorded for Tc99m pertechnetate and I-131 WBS.
Results: When I-131 WBS was taken as reference, Tc99m pertechnetate WBS detected lesions in thyroid bed 33/39 (84,6%), in pulmonary metastasis 13/29 (44,8%), in mediastinal metastasis 7/10 (70%), in lymph node metastasis 9/11 (81,8%), in bone metastasis 11/13 (84,6%). Interestingly diffuse lung infiltration confirmed with I-131 WBS could not be visualized on Tc99m pertechnetate WBS and lung CT. On the other hand, we obtained 4 false positive results (neck, mediastinum, lung, bone) with Tc99m pertechnetate WBS.
Conclusion: Although I-131scintigraphy is more sensitive in demonstrating residual and metastatic tissue than Tc99m pertechnetate scintigraphy, it may decrease subsequent iodine uptake and reduce therapeutic efficacy. Therefore, Tc99m pertechnetate WBS may be used as the first approach with its low cost and easy availability. In addition, positive Tc99m pertechnetate WBS may allow early detection and treatment of the disease in a subgroup of patients.

PS_515

ROLE OF MIBI-99MTC SCAN IN DETECTING LOCAL AND DISTANT METASTASES OF DIFFERENTIATED THYROID CANCER IMMEDIATELY AFTER TOTAL THYROIDECTOMY

S. Baldari (1), A. Campennì (1), M.A. Violi (2), G. Restifo Pecorella (1), F. Martino (1), D. D'Oppido (1), F. Trimarchi (2), F. Vermiglio (2). (1) Nuclear Medicine Unit, Department of Radiological Sciences; (2) Endocrinology Unit, Department of Experimental Medicine and Pharmacology,University of Messina, Italy.

The optimal management of primary brain tumor represents a significant challenge for clinicians and researches. Despite recent advances in neuroradiological imaging, neurosurgical treatment, neuroncological strategies, and nuclear medicine procedure, the preoperative assessment of cerebral lesions needs further noninvasive semiquantitative insights. 99mTechnetium-Sestamibi (MIBI) has been proposed as an useful radiopharmaceutical perfusion agent, which has been recently used as an imaging SPET agent for various neoplasms, including brain tumors. This technique can predict brain tumor grading and the behavior of glial tumors in terms of clinical aggressiveness. In addition, MIBI has been used in the differential diagnosis of some difficult cases. Aim of this study is to describe the experience obtained at our Institution in preoperative evaluation of 22 patients harboring a brain lesion, and evaluated during the last 18 months. They were 11 men and 11 females, ranging in age between 6 and 73 years (mean 47 yr.). Of these lesion, 21 (96%) were located in the supratentorial compartment, while in one pediatric case the lesion was located within the brain stem. Of these cases, 6 were low-grade glioma, 5 glioblastoma multiforme, 4 anaplastic astrocytoma, 2 meningiomas, 2 metastasis, and 1 epidermoid. Two additional cases were represented by benign nonneoplastic hemorrhagic diseases. SPET was performed within 10 minutes after intravenous injection of 10-20 mCi MIBI. The images were obtained with a dual headed-gamma camera using a high resolution collimator. Transverse, coronal, and sagittal views were reconstruced. MIBI uptake has been evaluated on the transverse slices, and expressed as tumor/background ratio. Two subgroups of patients were identified. MIBI uptake was found in 16 (72.7%) patients. The tumor/background ratio correlated with tumor histology, as proved from surgical or bioptical sample. In two patients of this group, a benign non-neoplastic disease has been detected, and proved on late neuroradiological observation. We found a marked difference ($p < 0.001$) between the MIBI uptake in non-tumor and low-grade lesions ($1.1 \pm 0,45$) vs high grade tumor (2.3 ± 0.14). According to our results, the specificity and sensitivity of MIBI brain SPET has been proved to be high. This tumor confirms the MIBI SPET as a valuable noninvasive semiquantitative tool, useful in the management of brain tumor patients, that offers clinically relevant pre-operative information in problem-solving session, such as differentiating neoplasms, and categorizing glial tumors in terms of clinical aggressiveness.

PS_516

THE VALUE OF 99MTC-GLUTATHIONE (GSH) IN DETECTION OF METASTASES OF DIFFERENTIATED THYROID CARCINOMA

M. Argon, O. Özyurt, O. Ömür, M.S. Taner, Y. Duman. Department of Nuclear Medicine, Ege University, Izmir, Turkey.

^{99m}Tc-Glutathione (^{99m}Tc-GSH) was used in many malignant tumours and metastases as a radiopharmaceutical. Recent studies has been showed that GSH was increased in adenomas and papillary carcinomas by 17% compared to normal thyroid while no changes were seen in goitres. In this preliminary study the aim was to test the feasibility of scintigraphic detection of metastases of differentiated thyroid carcinoma (DTC) with ^{99m}Tc-GSH.
Methods: 14 patients who had metastases of DTC, (5 follicular, 9 papillary) diagnosed with ^{131}I images and other radiological methods were studied. They were under T4 suppression and had several ^{131}I treatments. Their ages ranged from 40 to 61 years (mean 50.16, SD 5.1 years). GSH was labelled with ^{99m}Tc by Sn^{++} reduction method with an efficiency >97%. Following IV injection of 500MBq ^{99m}Tc-GSH, scintigraphic views were obtained at five minutes for imaging blood pool and 6 hours. Images were interpreted by visually .
Results: In all patients, there wasn't any ^{99m}Tc-GSH uptake at six hours images and any activity accumulation at five minutes blood pool images in metastases focus which were detected with I-131 images and other radiological method
Conclusions: Our preliminary results showed that ^{99m}Tc-GSH was not a potential radiopharmaceutical for detection of metastases of DTC. Despite high glutathione levels in thyroid carcinoma, ^{99m}Tc-GSH didn't accumulate in metastases of DTC

PS_517

A WARNING ABOUT USING ONLY OFF T4 SERUM HTG LEVELS IN FOLLOW-UP OF DIFFERENTIATED THYROID CANCER

D. De Palma (1), L. Giovanella (1), P. Vanoli (2), L. Ballada (1), L. Ceriani (1), A. Fachinetti (1), S. Garancini (1). (1) Department of Nuclear Medicine; (2) Department of Radiotherapy, Osp. di Varese,Italy.

AIM: Recently an interesting debate arouse about the true usefulness of a diagnostic radioiodine total body scan (DTBS) in patients that underwent total thyroidectomy and remnants ablation with 131I because of differentiated thyroid cancer (DTC) when serum hTG levels are undetectable (i.e. less than 2 ng/ml) after withdrawal of T4 treatment (offT4) in presence of normal levels of Ab against hTG. We actually performed routine DTBS one year after ablation (standard activity 3700 MBq) in all patients with previous DTC, independently from the results of post-ablation scan, if TG levels are undetectable during T4 therapy. We reviewed DTBS performed in the last two years (1999-2000) analysing the incidence of positive DTBS with undetectable hTG.

METHODS: DTBS and offT4 hTG assay were performed after four week withdrawal of the T4 therapy. DTBS was acquired 48 hour after oral administration of 185 MBq of 131I; a confirmation spot view was acquired 24 hours later in case of doubt. hTG assay was performed by an high sensitivity IRMA method (IRMA Tg-s, BRAHMS, Germany; functional sensitivity 0.3 ng /ml). The mean TSH level attained after T4 withdrawal was 65 mIU/ml, range 28-100.

RESULTS: 196 DTBS were reviewed. 11(5.6%) patients showed focal areas of abnormal iodine uptake in the cervical region, for a total of 15 foci, 6 from lymphonodal involvement and 9 from thyroid bed remnants/relapse. All patients had undetectable hTG and Ab against hTG levels. 6 patients had papillary DTC and 5 follicular variant of papillary DTC. All these patients underwent a new treatment with therapeutic activity of 131I (5550 MBq); the DTBS performed until now showed disappearance of the uptake in three cases and persistent nodal disease in a fourth.

CONCLUSIONS: OffT4 serum hTG levels showed indeed a negative predictive value of 94.4%. In deciding to do not perform DTBS with undetectable hTG we must be aware that this choice implies to leave some patients with residual disease. The prognostic implication of this fact remains unclear.

PS_518

EFFECTS OF RADIOIODINE THERAPY ON PULMONARY METASTASES WITH WELL-DIFFERENTIAL THYROID CANCER

Y.L. Yu, C.Q. Jin, L.B. Chen, H.K. Lu, R.S. Zhu. Depatment of Nuclear Medicine,Shanghai 6th People's Hospital, Shanghai, China.

The effects of radioiodine therapy on pulmonary metastases from well-differentiated thyroid cancer were investigated. Methods 85 volunteers(58 with pulmonary metastases, 19 without pulmonary metastases and 8 normal controls) were studied utilizing chest X-ray, pulmonary function test and ^{99m}Tc-DTPA aerosol clearance rates. Pulmonary function test determined vital capacity(VC), forced vital capacity(FVC), forced expiratory volume at 1 sec.(FEV_1) and maximum voluntary ventilation(MVV). The patient ^{99m}Tc-DTPA aerosol inhaled by tidal volume breathing. The data were acquired and analyzed for clearance half-time from the lungs with the SPECT. Results The data of pulmonary function test were no difference between various groups of cumulative radiation doses($p>0.05$). The difference of VC, FVC and FEV_1 was not remarkable between groups of sex($p>0.05$)but MVV($p<0.01$). ^{99m}Tc-DTPA aerosol clearance rates of between various groups were no difference($p>0.05$).

Tab1 Lung Function Test

	N	VC(%)	FVC(%)	FEV_1(%)	MVV(%)
< 300	24	93.08±20.30	87.50±23.19	86.70±23.33	89.83±32.25
301~650	8	100.18±13.41	86.53±14.55	78.13±23.76	78.83±29.56
651~1000	14	98.74±10.97	93.84±15.05	93.16±23.87	87.03±15.42
>1000	12	89.32±11.30	91.65±10.21	84.08±10.74	92.02±35.02
F		1.230	0.826	0.490	0.539
$F_{0.05(3,54)}$		2.78	2.78	2.78	2.78
P		>0.05	>0.05	>0.05	>0.05
Male	32	91.08±11.53	89.73±15.68	84.39±23.02	79.10±15.62
Female	26	99.03±19.19	95.23±19.01	91.40±21.71	100.31±38.54
F		1.633	0.631	2.788	13.446
$F_{0.05(1,56)}$		4.01	4.01	4.01	($F_{0.01(1,56)}$=7.12)
P		>0.05	>0.05	>0.05	(<0.01)

Tab2 ^{99m}Tc-DTPA Aerosol Clearance Rates

Metastases	<111GBq(n)	112~240GBq(n)	241~370GBq(n)	>370GBq(n)
Lung	51.8±5.3(24)	60.7±15.6(8)	54.9±13.2(14)	52.1±15.6(12)
Non-lung	55.3±9.9 (7)	55.2±19.1(6)	51.4±14.7(3)	50.3±18.5(3)
F	1.074	0.859	0.466	1.289
$F_{0.05(d0,df2)}$	4.18	4.75	4.54	4.67
P	>0.05	>0.05	>0.05	>0.05

Only one female, 43 years old, had received 518GBq(1400mCi) radioiodine over a 8-yr period. Pulmonary function test showed evidence of restrictive lung disease, chest x-ray showed haziness and DTPA half-time clearance was 26.4min,which is suggestive of interstitial fibrosis. Conclusion The effect of cumulative radio-iodine doses and sex had not statistics significance for pulmonary function. Interstitial fibrosis should appropriately be prevented when cumulative radioiodine doses were over 370GBq.

PS_519

THE INFLUENCE OF THE DELAYED 131-IODINE ABLATIVE THERAPY TO THE OUTCOME OF PATIENTS WITH DIFFENTIATED THYROID CARCINOMAS

A. Koutsioumpa, E. Trivizaki, S. Saranti, P. Natsis, L. Iordanidou, V. Babali, K. Pateniotis. Department of Nuclear Medicine, Piraeus, Greece.

This study aimed to evaluate the influence of the delayed ablative 131-iodine administration after the suggested two months interval from the surgery to the outcome of patients with DTC.

The reason for this possible delayed 131-iodine therapy was the small number of the dedicated beds in public Hellenic hospitals (only 17 for a population of 10 million) while there is a continuous increment of our needs (including a significant number of young people).

Material: Up to day we evaluated 91 patients (71 women, 20 men) with a follow- up time ranged from 8 to 173 months, mean 31.6 months. All studied patients had negative whole body scan and they were clinically free of disease.

The patients were divided in three groups.

Group A: 21 patients who received the ablation therapy within a period of two months after the surgery with a mean age of 39.6 years. Histologically there were 11 papillary, 9 mixed and 1 medullar-mixed carcinomas.

Group B: 35 patients with the ablation dose received 3-6 months after surgery, mean age 47.3 years (22 papillary, 1 follicular, 10 mixed and 2 Hurthle cell carcinomas).

Group C: 35 patients with the ablation dose received six or more months after the surgery, mean age 51.6 years (21 papillary, 2 follicular, 11 mixed and 1 Hurthle cell carcinomas.

All clinical and laboratory parameters were also evaluated for the studied population.

Results: In group A 9/21 pts. (45%) had negative whole body scan (WBS) after the ablation dose and 11/21 pts. (52,4%) after two therapeutical doses.

In group B 25/35 pts. (71,8%) had negative WBS after the ablation dose.

In group C 26/35 pts. (74,3%) had negative WBS after the ablation dose.

In 4/19 pts. who received two doses, the second dose was given because the Tg was elevated, while the WBS was negative after the ablation dose.

According to our data the administration of multiple therapeutical doses seemed to be related with the aggressiveness of the histological type and we believe there is a relative correlation with the size of the infiltered nodule.

Conclusion: According to our results we did not observe a negative influence on the outcome of the DTC patients when the ablation dose was administered in a period of time longer than two months after surgery. It should be mentioned that during the pretreated period the patients must have the appropriate follow up and the adequate suppression therapy, always under the condition that there isn't aggressive tumor pathology.

PS_520

RADIOIODINE IMAGING (WBS) AND SERUM THYROGLOBULIN(TG) IN MANAGEMENT OF THYROID CANCER (DTC): RANDOMISED STUDY WITH RECOMBINANT HUMAN TSH (RHTSH) AND WITHOUT THYROID HORMONE

L. Bertolazzi (1), R. Zoccola (1), M. Giusti (2), G. Villa (3), M. Scattina (1). (1) Department of Nuclear Medicine; (2) DISEM; (3) DIMI, University of Genoa, Italy.

Aim The purpose of this study is to prove if rhTSH, in patients after postsurgical radioablation of thyroid residue and treated with tiroxine (PtsT4), gives same outcomes in order to underline patologic values of Tg and thyroid tissue and/or metastasis with radioiodine imaging (185 MBq of 131 J) compared to patients in protracted hypothyroidism (Pts TH).
Methods During last year, we underwent 70 patients, with DTC and near-total thyroidectomy, to radiometabolic therapy (3700 MBq of 131 J) : 32 of them (all without metastasis in post-therapeutic WBS) were divided in two groups of 16 patients with same pathology (papillary cancer T1-T2), age and sex. In all patients no interference from anti-Tg antibody was present. After 4-5 months we treated the first group with rhTSH while second suspended the hormonal therapy to achieve hypothyroidism (>60 mU/ml).
Results The first group (11 F and 5 M age 29-78) presented 3 patients with at baseline detectable but low Tg (> 1.5 ng/ml) while after rhTSH the abnormal values of Tg were five. WBS was positive in six patients (3 thyroid tissue and 3 neck's nodes) : 4 with increased Tg and 2 with unchanged Tg after rhTSH . The negative WBS presented (after stimulation) a Tg value of 2.15 ng/ml.
The second group (12 F and 4 M age 29-74) presented 9 elevated Tg (5 at baseline). WBS was positive in all these patients and in one other patient with normal Tg (4 thyroid tissue, 3 neck's nodes and 3 pulmonary metastasis).
Both group stood WBS preparation without important upset.
Conclusions
rhTSH group
rhTSH increase the sensitivity of serum Tg in PtsT4
hypothyroidism group
we have average Tg higher than rhTSH group (respectively 45 and 32 ng/ml)
greater number of positive patients (on the whole 10 PtsTH vs 6 PtsT4)
C) in both group WBS underline the presence of thyroid tissue in more patients than Tg value
The our preliminary trial confirm that, after radiometabolic therapy, protracted hypothyroidism is best diagnostic approach. Only after negative results, we can continue patient follow-up with rhTSH.

PS_521

ROLE OF SCINTIGRAPHIC IMAGING IN METASTATIC MEDULLARY THYROID CARCINOMA (MTC): RESULTS ON 84 PATIENTS .

D. Casara (1), D. Rubello (1), G. Saladini (1), M.E. Girelli (2), B. Busnardo (2), P. Tamagnini (3), M.R. Pelizzo (3). (1) Servizio di Medicina Nucleare 2, Azienda Ospedaliera di Padova, Padova, Italy; (2) Servizio di Endocrinologia, Università di Padova, Padova, Italy; (3) Clinica Chirurgica 3, Università di Padova, Padova, Italy.

From 1991 to 2000, 84 MTC pts entered the study: 45 F, 39 M, mean age 53.7 yr; 37 of them had sporadic MTC, while in 47 pts MTC was associated to MEN. Nine pts were studied before surgery, whereas 75 during follow-up after first surgery because of elevated serum calcitonin and/or CEA levels. All pts were studied by 99mTc-MIBI scan, neck US, chest-abdomen CT, abdomen US; 99mTc-MDP scan was also performed in 56 pts, 111In-octreotide scan in 16 pts, 18FDG-PET in 7 pts. Surgical findings (n. 21), biopsy (n. 14) and/or clinical outcome were taken as gold standard. In 5/9 pts studied preoperatively, MIBI scan correctly visualized primary tumor and loco-regional lymph node mts (LNM); moreover, in 1 case MIBI scan revealed also bone mts (BM). Regarding the group of 75 pts studied during follow-up: cervical LNM were showed by MIBI scan in 34 pts (45.3%) and by US in 25 (33.3%); moreover, a complementary role between MIBI & US was found in 5 pts. Mediastinal LNM were showed by MIBI scan in 11 pts (14.7%), and by CT in 6 (8%). It is worth noting that in 3 cases with MIBI scan positive for loco-regional LNM, 111In-octreotide scan and 18FDG-PET were negative (1 case) or revealed less metastatic foci than MIBI scan (2 case). Conversely, in 2 MIBI scan negative cases, 111In-octreotide scan revealed the presence of mediastinal mts; thus, a complementary role between MIBI and 111In-octreotide scan was found in 5 pts. Pulmonary mts (PM) were detected both with MIBI scan and CT in 7 pts (9.3%). BM were detected by MIBI scan in 7 pts (9.3%), and by MDP scan in 11 (14.6%). Liver mts (LM) were showed by US/111In-octreotide/18FDG PET/ laparoscopy in 7 pts (9.3%), while MIBI scan was positive in only 1 of them (1.3%). In our experience, loco-regional LNM represent the most frequent site of mts in MTC, and MIBI scan associated with US and 111In-octreotide scan appears to be the most sensitive imaging protocol in visualizing this type of mts. Early detection of loco-regional mts is extremely important in MTC pts because they can be treated by surgery that is considered the most effective treatment for this type of tumor. Imaging modalities other than MIBI scan should be used to visualize MTC distant mts.

PS_522

ADDITIVE CLINICAL VALUE OF PINHOLE IMAGING IN FOLLOW-UP OF WELL DIFFERENTIATED THYROID CANCER AFTER SURGERY

S.T. Lim (1), S.A. Park (1), M.-.H. Sohn (1,2). (1) Department of Nuclear Medicine; (2) Clinical Medical Reserch Center, Chonbuk National University Hospital, Chonbuk National University Medical School, Chonju, Korea.

Purpose: It is well known that pinhole collimator (PH) has better resolution than high resolusion parallel-hole collimator (HRPH). We performed this study to compare PH with HRPH for the ability to differentiate of metastatic cervical lymphadenopathy (MCL) from remnant thyroid tissue (RT) after surgery for the treatment of thyroid cancer. Materials and Methods: One hundred forty three studies in 71 patients (M: F=12: 59, age 43.3±13.9 yrs) were analyzed. One hundred and eleven of 143 studies used 1110 MBq of I-131, HRPH and PH were performed 3 days after the radioiodine intake. PH images were obtained with 6 mm aperture for 10 minutes. Markers were placed to the submental and sternal notch regions. We compared two image modalities for the detection of MCL and RT in cervcal region. Results: All patients had well differentiated thyroid cancers (papillary:follicular=68:3). Sixty five of 111 studies (58.6%) showed concordant results but 46 of 111 (41.4%) discordant results. In the group showing discordant results, PH study was more useful for the detection of lesions with RT and MCL 25/46 (54.3%) and 29/46 (63%), respectively. Conclusion: In well differentiated thyroid cancer after surgery, we conclude that PH has more useful to monitor therapeutic response than HRPH, and provides additive information for the necessity of high dose radioactive iodine therapy in patient with MCL.

PS_523

DIAGNOSTIC ACCURACY OF RADIONUCLIDE IMAGING USING IODINE-131 NOR-CHOLESTEROL OR MIBG IN PATIENTS WITH HYPERSECRETING OR NON-HYPERSECRETING ADRENAL TUMORS

S. Maurea (1), M. Klain (2), R. Rossi (3), F. Izzo (4), M. Ziviello (1), M. Salvatore (2). (1) Medicina Nucleare e Radiodiagnostica, Istituto Nazionale Tumori, Napoli, Italy; (2) Centro per la Medicina Nucleare del CNR, Università Federico II, Napoli, Italy; (3) Endocrinologia, Universit" Federico II, Napoli, Italy; (4) Chirurgia C, Istituto Nazionale Tumori, Napoli, Italy

Aim: The aim of this retrospective study was to evaluate the diagnostic accuracy of nor-cholesterol and MIBG radionuclide imaging in two separate groups of patients with adrenal tumors to characterize lesions as adenoma or pheochromocytoma.
Methods: We studied 75 patients (22 M and 53 F, mean age 47±15 years) with hypersecreting (n=32) or non-hypersecreting (n=43) unilateral adrenal tumors detected by CT or MR scans. Iodine-131 nor-cholesterol adrenal scintigraphy was performed in 41 patients. Iodine-131 MIBG imaging was acquired in the other 34 patients. Pathology examinations (n=58) or CT follow-up studies (n=17) were obtained. Adrenal lesions were represented by 44 adenomas, 4 cysts, 1 myelolipoma, 1 pseudotumor, 1 ganglioneuroma, 16 pheochromocytomas, 3 carcinomas, 4 metastases and 1 sarcoma. Radionuclide studies were qualitatively evaluated and the corresponding results were classified as true-positive (TP), true-negative, false-positive (FP) and false-negative. Diagnostic sensitivity, specificity and accuracy as well as positive (PPV) and negative (NPV) predictive values were calculated.
Results: The diagnostic values of nor-cholesterol scintigraphy to identify adrenal adenomas were: sensitivity 100%, specificity 71%, accuracy 95%, PPV 94% and NPV 100%; of note, 2 FP cases were observed represented by a pheochromocytoma and a myelolipoma. The diagnostic values of MIBG scintigraphy to recognize pheochromocytoma were: sensitivity 100%, specificity 95%, accuracy 97%, PPV 94% and NPV 100%; only 1 FP case occurred consisting of a carcinoma.
Conclusions: In the large majority of cases, adrenal scintigraphy using nor-cholesterol or MIBG is able to characterize specific lesions such as adenoma and pheochromocytoma, respectively. These findings show relevant clinical impact particularly in patients with non-hypersecreting adenomas or pheochromocytomas. However, unusual findings may be rarely observed; nor-cholesterol uptake has been found in non-adenoma tumors such as myelolipoma and pheochromocytoma; similarly, MIBG accumulation may occur not only in lesions arising from medullary chromaffin tissue, but also in cortical adrenal carcinoma.

PS_524

Abstract withdrawn

PS_525

DIAGNOSIS, THERAPY, FOLLOW-UP AND SURVIVAL RATE OF PATIENTS WITH MEDULLARY THYROID CARCINOMA (MTC)

M. Malesevic (1), S. Popadic (1), J. Bogdanovic (2), N. Sljapic (3), LJ. Miljkovic (4), D. Savic. (1) Department of Nuclear Medicine; (2) Clinics for Oncology; (3) Department of Pathology; (4) Clinics for Internal Oncology, Institute of Oncology, Sremska Kamenica, Yugoslavia

In this paper we evaluated diagnosis, therapy, follow-up and survival rate of patients with MTC in the period from 30th January 1976 to 10th March 2001.

MATERIAL: There were 27 patients (pts) with sporadic MTC: 16 women (aged 29 to 73; mean age was 47.1 + 9.8) and 11 men (aged 39 to 75; mean age was 53.7 + 12.0).

METHODS: Diagnosis was done by the means of scintigraphy (99mTc or 131-I), ultrasonography, FNB, CIT analysis and ex-tempore biopsy of the nodular gland; follow-up and a therapy according to the Protocole for MTC of the Institute and the survival rate (SR) was determined according to Kaplan Meier's analysis together with Log rank programme.

RESULTS: Clear and suspect CIT findings for malignancy, in pre-operative diagnosis of the patients with MTC were 21(77.7%). All the pts were operated (total thyreoidectomy in 21(77.7%), lobectomy with isthmeoctomy in 4(14.8%) and nodulectomy in 2 (7.4%). The additional therapy was as follows: a radiological one in 5, polychemio in 4, radiological/ polychemio in 4 and reoperation LGN in 4 pts. All pts were under the substitution of L-thyroxine. There were 10(37%) pts in a stable remission, there were 10(37%) pts in a partial remission while 7(25.9%) died. According to pTNM there were Stage(St) I=2(7.4%), St II=9(33.3%), St III=11(40.7%) and St IV=5(18.5%). The pts were followed-up by the means of: thyrocalcitonin (TCT) (x=708.7 + 848.0), canceroembrionic antigen (CEA) (x=77.3+69.3), and the dg. whole-body scintigram with 99mTc DMS(v) (12(52.1%) with pathological, 11(47,9%) normal while in 4(14.8%) pts the scintigram was not done). Mediana of the follow-up was 5yrs and 11 days. The survival rate (SR) for women was 0.79 for 5.18 yrs; for men it was 0.38 for 8.5yrs (p=0.1). SR for all pts was 0.61 for 8.5 yrs. In St I and St II the pts were alive; in St III, SR was 0.44 for 8.5yrs and in St IV, SR was 0.40 for 5.18yrs (p=0.17).

CONCLUSION: Diagnosis should be fast obligatorily with FNB, CIT findings and ex tempore biopsy in pre-operative diagnosis. For better SR the total thyreodectomy with maximal disection of LGN is obligatory. The follow-up of pts with MTC is very convenient by the means of TCT, CEA and dg.sc. 99mTc DMS(v), because we can appropriately react by radiological therapy, polychemio therapy and reoperation of LGN. The SR of all the patients with MTC was very well and for pts in St III and St IV it is satisfying from the oncological point of view.

PS_526

MARROW TOXICITY ESTIMATES OF IODINE-131 THERAPY FOR THYROID CANCER

Y.L. Yu, L.B. Chen, Q.Y. Luo, H. Ji, R.S. Zhu. Depatment of Nuclear Medicine,Shanghai 6th People's Hospital, Shanghai, China.

The variance of peripheral blood cells in iodine-131 treatment of thyroid cancer was investigated to estimate marrow toxicity.

Methods: WBC,RBC,Hb and PLT of 177 patients with thyroid cancer were tested separately, investigating variance of peripheral blood cells in different sex, age, accumulative iodine-131 dose, cancer type and metastasis mode.

Results: WBC and PLT did not vary in sex (F_W=0.399, F_P=0.903_<$F_{0.05(175)}$=3.895_P>0.05), but RBC and Hb of female were markedly decreased (F_R= 25.217, F_H=30.895, >$F_{0.01(175)}$=6.785_P<0.01). The variance of blood cells had no statistics signification in age, cancer type and

Tab.1 Correlation between peripheral blood cell count and accumulative ^{131}I dose(n=177)

dose(MBq)	n	WBC(10^9/L)	RBC(10^{12}/L)	Hb(g/L)	PLT(10^9/L)
1480_9200	67	6.73±1.37	4.48±0.39	132.56±12.77	213.45±48.55
9201_18500	47	6.73±1.26	4.51±0.44	133.08±13.73	198.93±49.00
18501_27700	24	6.44±1.09	4.57±0.42	134.42±12.79	197.50±45.55
27701_37000	20	5.32±0.88	4.34±0.47	126.61±13.94	176.26±49.83
37001_46200	12	5.23±1.43	4.19±0.42	124.78±10.14	163.42±61.55
46201_53576	7	4.86±0.80	3.75±0.73	119.10±17.89	182.94±72.92
F		8.840	5.285	2.832	3.255
P		<0.01	<0.01	<0.05	<0.01

$F_{0.05(5,171)}$=2.265 $F_{0.01(5,171)}$=3.112

metastasis. The blood cells' mean of each group of iodine-131 dose was within ordinary range, but difference of within groups was very marked(F_{WBC}=8.84, F_{RBC}=5.285, F_{PLT}=3.255, >$F_{0.01(5,171)}$=3.112, P<0.01; F_{Hb}=2.832 >$F_{0.05(5,171)}$ = 2.265, P<0.05). The blood cells had a decreased trend while iodine-131 dose increased(r>$r_{0.01(175)}$= 0.195_t_b>$t_{0.01(175)}$= 2.576_P<0.01).

Conclusions: Though peripheral blood cell's counts were within ranges of normal value, it is certain for iodine-131 therapy to effect marrow toxicity. There were markedly negative correlation between peripheral blood cell's count and accumulative iodine-131 dose.

PS_527

99MTC-TETROFOSMIN AND 99MTC-MIBI WHOLE BODY SCINTIGRAPHY FOR DETECTING DISTANT METASTASES FROM DIFFERENTIATED THYROID CARCINOMA

J. Drac-Kaniewska (1), I. Kozlowicz-Gudzinska (1), H. Tomaszewicz-Kubasik (1), M. Kaniewski (2), P. Godlewska (2), M. Czetwertynska (2), A. Chaladaj-Kujawska (2). (1) Department of Nuclear Medicine; (2) Department of Brachytherapy,The Maria Sklodowska-Curie Memorial Cancer Center, Warsaw, Poland.

99mTc-Tetrofosmin (TF) and 99mTc-MIBI (MIBI) , non specific tumor-seeking tracers were evaluated for their ability to detect distant metastases from differentiated thyroid carcinoma (DTC) and reliability in the follow-up studies.

Methods. Whole body scintigraphy was performed 20-30 min after intravenous injection of 740 MBq 99mTcTF or 740 MBq 99mTcMIBI using dual-head gamma camera (followed by spot or SPECT if needed) in 108 patients with DTC ; 22 pts in clinical remission (no signs of neoplasm dissemination by imaging methods and thyroglobulin level within normal range units) and 86 pts with distant metastases in 131I whole body scintigraphy (53) or in other visual metods (rtg,CT,usg)(14) or with negative 131I whole body scan and elevated thyroglobulin level(19). Patients were randomized in two groups: 52 of them received TF, 34 – MIBI.

Results. ***TF.*** In group of 52 pts with signs of neoplasm dissemination 36 showed positive TF whole body scan (69%), 16 pts were TF negative (31%). 23 of 34 pts (68%) with 131I-positive whole body scan were also TF positive, 11 of 34 pts (32%) were TF negative. In a group of 7 pts with metastases in rtg,CT or other methods 4 were TF positive (57%), 3 were TF negative(43%). 9 of 11 pts with negative 131J whole body scans and elevated thyroglobulin level were TF positive (82%), while 2 were TF negative (18%). ***MIBI.*** Among 34 pts with distant metastases 21 (62%) presented positive MIBI whole body scans, while 13 (38%) were MIBI negative. 9 of 19 pts with positive 131I whole body scan were also MIBI-positive (47%); 10 were MIBI-negative (53%). In a group of 7 pts meta-positive in rtg,CT or others 5 demonstrated MIBI positive scan (71%), 2 were MIBI-negative (29%). 7 of 8 pts with negative 131I whole body scan and elevated thyroglobulin were MIBI-positive (87%) ; 1 was MIBI-negative. In a control group of 24 persons(22 with DTC in clinical remission, 11 TF and 11 MIBI , 2 disease-free) TF or MIBI scans were negative in all cases.

Conclusions: TF and MIBI are clinically useful for detecting distant metastases of DTC and deserve complementary clinical application in follow-up studies. TF and MIBI are highly satisfactory in patients with negative radioiodine whole body scan and elevated thyroglobulin level.

PS_528

THE PREOPERATIVE STAGING OF THE LARYNX CARCINOMA BY 99MTC-TETROFOSMIN SCINTIGRAPHY: A PRELIMINARY STUDY

M. Grosso, B. Fattori, F. Bianchi, G. Boni, G. Manca, D. Volterrani, A. Nacci, F. Ursino, R. Bianchi. Department of Nuclear Medicine, University of Pisa, Pisa, Italy.

Primary laryngeal carcinoma represents the most common malignancy of all tumors of the head and neck. The preoperative staging is usually performed with neck ultrasonography (US) and CT scan. Nevertheless, latero-cervical lymph node metastases can be observed in 60% of the patients (pts) at the time of diagnosis and can influence the surgery approach, the prognosis and the subsequent treatment. Aim of our study was to evaluate the utility of 99mTc-TETROFOSMIN in the preoperative staging of patients with larynx carcinoma.Twenty-two men patients (males, age 65-±9 yrs), with a diagnosis of carcinoma obtained by MLSD, underwent 99mTc-TETROFOSMIN scan (WBS and SPET study of the neck and chest 10 min. after iv injection of 740 MBq), neck US and CT scan. Ten of them underwent total laryngectomy and functional lymphoadenectomy, one patient total laryngectomy and total lymphoadenectomy, two patients partial laryngectomy and total lynphoadenectomy. Seven patient received radiotherapy and chemotherapy with extensive latero-cervical lymph node metastases. The remaining two are waiting for surgery. Pathologic results classified four lesions as well-differentiated squamous cell carcinomas (18.2%), sixteen as medium-differentiated (72.7%) and two (9.1%) as poor-differentiated. Cervical lymph node metastases were demonstrated by histological finding in 4 out 13 pts.
99mTc-TETROFOSMIN scintigraphy was positive for primary lesion in 21/22 patients and in 3 of 4 patients with latero-cervical lymph node metastases underwent surgery, while was positive in 1 of 7 patients underwent radio and chemotherapy. The specificity of lymph node metastases was 100% for Tc-99m-Tetrofosmin and 54% for CT, with a significant statistical difference (p=0.02). On the other hand the diagnostic sensitivity was highest for CT (89%) versus scintigraphy (44%) (p=0.06). In conclusion, on the basis of our experience, we believe that Tc-99m-tetrofosmin can be useful as a complementary imaging technique to CT scan for detecting primary disease and for a better application of the therapeutic and surgery protocols.

Patient	Sex	Age	Primary tumor	NCS	Bone SPET	MIBI SPET	MRI
1	M	34	Liposarcoma	Bilateral	Negative	Negative	Negative
2	M	41	Breast	Bilateral	Bilateral	Bilateral	Bilateral
3	M	48	Prostate	Bilateral	Bilateral	Bilateral	Bilateral
4	F	73	Breast	Bilateral	Right	Left	Bilateral
5	F	55	Breast	Right mandible	Right	Right	Right
6	F	35	Breast	Right mandible	Right	Negative	Negative
7	M	70	Larynx	Right mandible	Negative	Negative	Negative
8	M	69	NHL	Right mandible	Right	Pterigoyd area	Negative
9	F	61	Burkitt	Left mandible	Left	Left	Negative
10	F	55	Breast	Left mandible	Negative	Negative	Positive
11	F	29	Breast	Bilateral	Right	Mental	N.A.
12	M	65	Prostate	Left	Left	Left	Left

NCS is a rare condition, related to a dismal prognosis, which has a negative influence on the quality of life. Due to the complexity of skull base and mandible anatomy, it is difficult to obtain useful information concerning the aetiology of this condition. These first results suggest that these nuclear medicine procedures can play an important role in decision making concerning treatment.

PS_529

SESTAMIBI AND HMDP SPET FOR THE EVALUATION OF THE NUMB CHIN SYNDROME

G. Savelli (1), A. Caraceni (1), H. Dool (2), F. Simonetti (1), M. Maccauro (1), M. Testoni (1), E. Bombardieri (1). (1) Istituto Nazionale Tumori, Milano, Italy; (2) Leiden University Medical Centre, Leiden, The Netherlands.

Facial numbness restricted to the distribution of the mental nerve is called numb chin syndrome (NCS). This uncommon neuropathy may be caused by a number of conditions such as metastases involving the mental nerve, the trigeminal roots, the Gasserian ganglion and the meninges. The exact localization of these metastases is pivotal in the management of mental neuropathy.
Twelve patients with malignant disease and presenting with NCS were enrolled in this study. Imaging methods included magnetic resonance imaging (MRI), planar and Single Photon Emission Tomography (SPET) with ^{99m}Tc-HMDP and ^{99m}Tc-Sestamibi SPET of the skull.
Five patients had NCS involving both left and right mandible, 4 patients had NCS on the right side and 3 on the left. Bone SPET was performed 3 hours after the i.v. administration of 555 MBq of ^{99m}Tc-HMDP. Sestamibi SPET was performed 5 minutes after the i.v. administration of 740 MBq of ^{99m}Tc-Sestamibi. Both these examinations were performed using a Picker Prism 3000 triple-headed gamma camera, equipped with low-energy ultra-high resolution parallel-hole collimators. Images were reconstructed using filtered back-projection (Ramp/Wiener filter, 0.2-0.4). MRI was performed after the nuclear medicine procedures. One patient did not undergo MRI because of claustrophobia. All the examinations were reported independently by nuclear medicine physicians and radiologists.
In 9 patients ^{99m}Tc-HMDP SPET was able to identify the location of the metastasis. Moreover, ^{99m}Tc-Sestamibi SPET evidenced 8 areas of uptake suspicious for metastases. MRI correctly identified 6 metastases. ^{99m}Tc-HMDP SPET showed 3 metastases and Sestamibi SPET 2, missed by MRI. In one case MRI demonstrated a metastasis not evidenced by both the nuclear medicine procedures. The imaging procedures in combination identified 10 of the 12 metastases.

PS_530

THE ROLE OF 99MTC-SESTAMIBI SPET IN THE PREOPERATIVE MANAGEMENT AND DIFFERENTIAL DIAGNOSIS OF CEREBRAL LESIONS

S. Baldari (1), G. Restifo-Pecorella (1), F.F. Angileri (2), R. Lipari (1), A. Germanò (2), S. Cosentino (1), A. Herberg (1), D. d'Avella (2), N. Bonanno (1). (1) Department of Radiological Sciences - Nuclear Medicine; (2) Department of Neurological and Neurosurgical Sciences, University of Messina, Messina, Italy.

The optimal management of primary brain tumor represents a significant challenge for clinicians and researches. Despite recent advances in neuroradiological imaging, neurosurgical treatment, neuroncological strategies, and nuclear medicine procedure, the preoperative assessment of cerebral lesions needs further noninvasive semiquantitative insights. 99mTechnetium-Sestamibi (MIBI) has been proposed as an useful radiopharmaceutical perfusion agent, which has been recently used as an imaging SPET agent for various neoplasms, including brain tumors. This technique can predict brain tumor grading and the behavior of glial tumors in terms of clinical aggressiveness. In addition, MIBI has been used in the differential diagnosis of some difficult cases. Aim of this study is to describe the experience obtained at our Institution in preoperative evaluation of 22 patients harboring a brain lesion, and evaluated during the last 18 months. They were 11 men and 11 females, ranging in age between 6 and 73 years (mean 47 yr.). Of these lesion, 21 (96%) were located in the supratentorial compartment, while in one pediatric case the lesion was located within the brain stem. Of these cases, 6 were low-grade glioma, 5 glioblastoma multiforme, 4 anaplastic astrocytoma, 2 meningiomas, 2 metastasis, and 1 epidermoid. Two additional cases were represented by benign nonneoplastic hemorrhagic diseases. SPET was performed within 10 minutes after intravenous injection of 10-20 mCi MIBI. The images were obtained with a dual headed-gamma camera using a high resolution collimator. Transverse, coronal, and sagittal views were reconstruced. MIBI uptake has been evaluated on the transverse slices, and expressed as tumor/background ratio. Two subgroups of patients were identified. MIBI uptake was found in 16 (72.7%) patients. The tumor/background ratio correlated with tumor histology, as proved from surgical or bioptical sample. In two patients of this group, a benign non-neoplastic disease has been detected, and proved on late neuroradiological observation. We found a marked difference ($p < 0.001$) between the MIBI uptake in non-tumor and low-grade lesions ($1.1 \pm 0,45$) vs high grade tumor (2.3 ± 0.14). According to our results, the specificity and sensitivity of MIBI brain SPET has been proved to be high. This tumor confirms the MIBI SPET as a valuable noninvasive semiquantitative tool, useful in the management of brain tumor patients, that offers clinically relevant pre-operative information in problem-solving session, such as differentiating neoplasms, and categorizing glial tumors in terms of clinical aggressiveness.

PS_531

99MTC-TETROFOSMIN BRAIN SPECT VERSUS CT AND MRI IN ASSESSMENT OF OUTCOME OF TREATMENT OF BRAIN TUMORS

H. Moustafa (1), A. Fawzy (1), H. Nasr (1), E. El-Ghoneimy (2), M. Moustafa (2). (1) Nuclear Medicine Department; (2) Oncology Department, Faculty of Medicine, Cairo University, Egypt.

Anatomic imaging modalities, such as X-ray, CT and MRI are often unable to differentiate post radiation gliosis from residual or recurrent tumor. Physiological imaging methods, such as ^{18}F-FDG PET and SPECT (^{201}Tl, ^{99m}Tc-Tetrofosmin or ^{99m}Tc-MIBI) have become an increasingly important method in solving this problem.

Aim: To evaluate the role of ^{99m}Tc-Tetrofosmin brain SPECT imaging in diagnosis of patients with viable residual or recurrent astrocytoma versus post radiation gliosis during their post-operative therapy course.

Methods: The study included 55 patients (14 females and 41 males). Their mean age was 33.2 ±15.6 years with a range of 4-80 years. Thirty-one patients had astrocytoma while 24 patients had glioblastoma multiforme. All patients had performed prior surgical tumor excision followed by radical radiotherapy in the form of whole brain irradiation followed by localized radiotherapy or stereotaxy. Nine patients received chemotherapy as well. All patients were subjected to ^{99m}Tc-Tetrofosmin brain SPECT imaging using 740 MBq with imaging at 20 minutes. Also radiological brain imaging (CT and/or MRI) were performed for comparison. The total number of SPECT studies performed and compared to CT or MRI were 61 studies.

Results: Forty-seven SPECT studies were positive while 10 studies were false negative due to cystic or small lesions <1cm evident in CT or MRI. Four studies were equivocally diagnosed by CT or MRI and were found to be true negative by SPECT. The sensitivity, specificity, positive predictive value, negative predictive value and accuracy of SPECT to detect residual or recurrent lesions versus fibrosis as compared to CT or MRI was 82.5%, 100%, 100%, 28.6% and 83.6.1% respectively.

Conclusion: ^{99m}Tc-Tetrofosmin brain SPECT is an additional complementary valuable diagnostic method in assessment of residual or recurrent viable brain tumors, and could be of help in therapeutic decision-making.

PS_532

INTRAARTERIAL INFUSION OF 99M-TC-ALBUMINE MICROSPHERES FOR DEPOT EFFECT ASSESSMENT OF A REGIONAL CHEMOTHERAPY IN COLORECTAL CARCINOMA PATIENTS WITH LIVER METASTASES

E. Piperkova (1), G. Kurteva (2), P. Kurtev (3), M. Beeva (4), M. Dimitrova (1). (1) Department of Nuclear Medicine; (2) Department of Chemotherapy; (3) Department of Surgery; (4) Department of Radiology, National Hospital for Active Cancer Treatment, Sofia, Bulgaria

The failure of systemic chemotherapy in the treatment of colorectal cancer patients with liver metastases has led to considerable interest in regional chemotherapy administration. The aim of this prospective study is to estimate the radiolabelled albumine-micrispheres'distribution, administered into the hepatic artery infusion pump, their concentration and remains in the blood flow of the hepatic metastases for getting depot effect of following regional chemotherapy in colorectal cancer patients with liver metastases

Method:.Seven patients have been subjected to intraarterial application of the 99mTc-MacrotecMono (Sorin Biomedica), injected through „port-jet"into the hepatic artery before the intraarterial infusion of chemotherapy. Dynamic control of radiolabelled particles (diameter 10-90 micrometers, 3,5 MBq/kg activity) distribution has been carried out in two phases on a gamma-camera „DIACAM"(Siemens):the first 1000ms/frame (60 frames), the second - 30 000 ms/frame – 30 frames.

Results: Scintigraphic control, planar and SPET on the 2nd, 4th and 24 th hours showed that microspheres remain in the vascularised liver metastases more than 24 hours, resulting in prolonged local effect of the applied chemotherapeutic agents. Clearly good results have been established in five of the patients by CT and SPETmonitiring.

Conclusion: Embolizing, biodegradable particles can be coadministered with anticancer drugs to show temporarily the arterial blood flow and to increase drugs uptake within the metastatic-bearing liver.

PS_533

SERUM TUMOR MARKERS VERSUS IMMUNOSCINTIGRAPHY AND INTRAOPERATIVE RADIOIMMUNODETECTION IN COLORECTAL CANCER

J. Vizda (1), P. Hladik (2), E. Urbanova (1), E. Malirova (1), B. Dlabalova (1), P. Kafka (1), M. Netikova (1). (1) Department of Nuclear Medicine; (2) Department of Surgery, University Hospital, Hradec Kralove, Czech Republic.

Immunoscintigraphy of tumors makes non-invasive in vivo imaging of tumor antigens distribution in whole body possible. Intraoperative radioimmunodetection with a hand-held gamma-detector probe in addition to preoperative immunoscintigraphy finds a pathological tissue during operation (radioimmunoguided surgery = RIGS). The aim of the present study was compare immunoscintigraphic findings with following RIGS and three serum tumor markers in 121 patients with histologicaly verified colorectal cancer. Two radiopharmaceuticals were used.

Materials and methods: Immunoscintigraphy (2x whole body scans from two projections and single photon emission computed tomography of abdomen) and radioimmunoguided surgery were performed in 106 pts. with primary and 15 pts. with recurrent colorectal cancer. As radiopharmaceuticals were used monoclonal antibody against TAG72 labeled with ^{111}In (Oncoscint) in 56 pts. and fragments of monoclonal antibody against CEA labeled with ^{99m}Tc (CEA-Scan) in 65 pts. Prior to injection of radiopharmaceutical blood samples were taken for determination of tumor markers (CEA, CA72-4, CA19-9) and HAMA in all patients. Postoperative the activity of resected tissue was measured and histological examinated, in controversial cases immunohistochemistry was performed. The ratio of activity tumor/healthy tissue was determined intraoperative and postoperative.

Results: The tumor tissue was detected with Oncoscint by immunoscintigraphy in 93% pts. and intraoperatively in 98% pts., with CEA-Scan by immunoscintigraphy in 92% pts. and intraoperatively in 100% pts. Average ratios tumor/healthy tissue were 2.2 (intraoperative) and 2.9 (postoperative) in Oncoscint group, 3.3 and 3.5 in CEA-Scan group. Serum levels at least one of tumor markers were increased in 58% pts. studied with Oncoscint (CEA in 48%, CA72-4 in 31%, CA19-9 in 33%) and in 56% pts. studied with CEA-Scan (CEA in 35%, CA72-4 in 38%, CA19-9 in 26%).

Conclusions: The results show expressive lower sensitivity of serum tumor markers in comparison with immunoscintigraphy and intraoperative radioimmunodetection. The determination of a greater number of serum tumor markers is necessary. Patients with high level of some tumor marker in serum have a higher probability of cancer but on the contrary normal levels do not exclude malignant disease. There is no correlation between serum levels of tumor markers and the rate of radiopharmaceutical uptake in tumors.

(This study was supported by the grant No.45323 of Czech Ministry of Health)

PS_534

DUAL-PHASE ANGIOHEPATOSCINTIGRAPHY IN ESTIMATION OF HEPATIC TUMORS VASCULARITY AND ASSESSMENT OF CHEMOEMBOLIZATION EFFICACY

P. Fadeev, D. Granov, A. Ivanova, V. Soukhov, T. Dubrovina. Nuclear Medicine Dept., Central Research Institute of Roentgenology and Radiology, St-Petersburg, Russia.

Chemoembolization (CE) at present is the method of choice in patients with hepatic tumors (especially in cases of multifocal metastatic lesions). While the success of CE mainly depends on the obtaining of the objective information about vascularity of tumor.

The purpose of this study was to evaluate dual-phase angiohepatoscintigraphy (DP-AHSG) for estimation of vascularity and assessment of (CE) efficacy in patients with hepatic tumors.

Mateial and methods: Twenty five patients (middle age 42 yrs) with hystologicaly verified malignant lesions of the liver (hepato-cellular cancer – 5 pts, and metastatic tumors – 20 pts) were evaluated. 18 patients were studied before and 7 patients – after CE.

DP-AHSG using 99m__-colloids was performed on APEX SP-6 gamma-camera (Elscint) just after i.v. injection of bolus of tracer in dynamic mode: in early (angio) phase for the first 60 seconds and late (parenchimae) phase. The frames of each time interval were summarized and the sums of the second phase were subtracted from the first ones. The uptake of radiopharmaceutical at the resulting scintigrams noted the vascularity of hepatic lesions (Patent _ 2156112).

Results: In 22 of 25 patients the hypervascular foci were visualized: in 5 pts with HCC and in 17 – with hepatic metastases of different tumors. DP-AHSG data were compared with the angiography results in the same patients: in 88% there were concordance of the results, in 12% – DP- AHSG data were false-negative. 7 patients assessed by means of DP-AHSG before and after CE showed successful embolization and in one patient CE was ineffective.

Conclusion: DP-AHSG is non-invasive and safe method with low radiation dose that feasible for repeated studies and can be used in vascularity estimation and assessment of CE efficacy in patients with hepatic tumors.

PS_535

TECHNETIUM-99M SESTAMIBI BRAIN SPECT IN THE FOLLOW UP OF GLIOMA FOR THE RESPONSE TO CHEMOTHERAPY

F. Prigent (1), F. Dubois (2), S. Blond (2), M. Steinling (1). (1) Deprt of Nuclear Medicine; (2) Depart of Neurosurgery, Hospital R Salengro. Lille, France.

Aim : Standard treatment of glioma consists in surgery followed by radiation therapy. Chemotherapy is used in case of recurrence. Because of lots of potential considerable side-effects of chemotherapy , early tumor response evaluation is necessary for clinicians to adapt the treatment. However, the response monitoring with computed tomography or magnetic resonance imaging is often difficult. The aim of this study was to evaluated the interest of repeated ^{99m}Tc-MIBI SPECT for these patients.

Methods Fifteen patients treated for recurrent high grade glioma were followed during their chemotherapy. Different chemical protocols were used (PCV, T?mozolamide, Fot?mustine). SPECT was performed one hour after the injection IV of 555 MBq of ^{99m}Tc-MIBI, using a dedicated SPECT system (Tomomatic® 564. M?dimatic. Dk). A total of 57 investigations were performed. A MIBI uptake index was computed as the ratio of counts in the lesion to those in the controlateral region. Previous studies have shown a cut off value at 2.0. SPECT indexes were compared to neurologic evaluation, CT or MRI. This assessment was performed every four months during and after the treatment.

Results : Three types of response were observed, so we classify our patients into three groups. In the fisrt one, 6 patients showed an increased MIBI index associated with a clinical or radiological progressive disease during chemotherapy ; this demonstrated an immediate resistance to treatment. In the second one, after initial response to therapy, 3 patients showed an increased MIBI index despite chemotherapy, demonstrating a secondary resistance to therapy. In the third group, 6 patients showed decreased MIBI index, demonstrating a good response to therapy. There is no correlation between the initial MIBI index value and the disease progression. The 9 first patients died shortly after the last tomoscintigraphy (on an average : 7 months). The therapeutic protocol was modified in 6 cases, but only successfully in 2 cases. In 9 cases, the tumor evolutivity was diagnosed with the tomoscintigraphy earlier than with clinical signs and in 4 cases earlier than with MRI.

Conclusion : ^{99m}Tc-MIBI SPECT is able to predict an early response or a resistance to chemotherapy. So this functional brain tumor imaging could be considered in the case of patient treated for recurrent high grade glioma as a valuable tool to adapt the therapeutic protocol effectively, and also to stop the treatment after a return to normal index (group 3).

PS_536

USEFULNESS OF DIASTOLIC RADIONUCLIDE PARAMETERS FOR THE PREDICTION OF ANTHRACYCLINE CARDIOXICITY

K. Massaloux-tarozzi (1), D. Mestas (1), C. Thouly (1), P. Chollet (2), J. Maublant (1). (1) Department of Nuclear Medecine; (2) Department of medical Oncology, Centre Jean Perrin, Clermont-Ferrand, France.

Objectives : Diastolic parameters determined by gated blood pool scintigraphy (GBPS) were evaluated before treatment in cancer patients (pts) in an attempt to predict cardiotoxicity of anthracyclines.

Methods : From April 1998 to July 2000, we prospectively analyzed data of GBPS realized during cardiac follow-up of 50 cancer pts treated by polychemotherapy based on anthracycline. Twenty pts had cardiovascular risk factors (R+), 13 had formerly received anthracycline (A+). Left ventricular ejection fraction (LVEF), peak filling and ejection rates (PFR and PER, both expressed in end-diastolic volume per second), and time to PFR and PER were determined before and after a treatment with a mean cumulative dose of 500 mg/m_ doxorubicin equivalent. Results before treatment were compared with normal values established in a control group of 64 pts without any cardiac risk factor nor former anthracycline treatment.

Results : In the 50 cancer pts, significant differences of pre-treatment LVEF, PFR and PFR/PER were observed with controls. When considering pts history, differences were significant only for R+ .

	n	LVEF	PFR	PFR/PER
Controls	64	63.5 ± 5.5	3.0 ± 0.7	0.88 ± 0.2
Treated	50	61.4 ± 6.4 *	2.9 ± 0.8 *	0.91 ± 0.2 *
R+	20	58.0 ± 4.2	2.6 ± 0.7*	0.82 ± 0.4*
A+	13	63.3 ± 5.0	3.3 ± 0.6	0.93 ± 0.2

* p<0.05 ; p<0.01

In predicting a fall of LVEF of > 5% in the overall population, ROC analysis showed that the most efficient parameter was a pre-treatment PFR/PER < 1, with positive and negative predictive values of 52% and 78%, respectively, and sensitivity and specificity of 80% and 48%, respectively. When combined with HR ≥ 82 bpm (ROC analysis threshold), these values rose to 75%, 82%, 71% and 85%, respectively.

Conclusion : This study shows that PFR/PER combined with HR are very useful GBPS parameters to predict anthracycline cardiotoxicity.

PS_537

SERIAL INDIUM-111 CAPROMAB PENDETIDE (PROSTASCINT) IMAGING IN PATIENTS WITH RECURRENT OR LOCALLY ADVANCED PROSTATE CANCER (LAPC) UNDERGOING COMBINED MODALITY THERAPIES

I. Sarikaya (1), A. Hussain (2), N. Bacetti (1), E. Siegel (1), L. Holder (1), B. Line (1). (1) University of Maryland Medical Center, Division of Nuclear Medicine, Baltimore, MD, USA; (2) University of Maryland Medical Center, Greenbaum Cancer Center, Baltimore, MD, USA.

We have incorporated Prostascint imaging into two clinical trials that we are conducting in patients (pts) who (1) experience rising serum PSA after undergoing definitive therapies [radical prostatectomy (RP) or/and radiation (XRT)] for localized prostate cancer, or (2) who present with locally advanced disease. In one trial, we are combining weekly Taxol chemotherapy with concurrent XRT and hormone ablation (to date 18 pts), while in the second trial we are using single agent Taxotere for 4-6 cycles followed then by 1 year of hormone ablation (to date 26 pts). Pts entered onto either trial get a baseline Prostascint scan, and those who have positive findings on initial scanning undergo subsequent imaging at the completion of therapy. Our aim is to determine the potential role of Prostascint imaging in assessing baseline disease status as well as in response to combined modality therapy, and to possibly correlate such findings with clinical outcome. So far, we have obtained 44 baseline and 9 follow-up Prostascint scans. Of the 44 patients entered onto the two trials, 10 had LAPC from the very outset, 8 were status post definitive XRT, 15 had undergone prior RP, while 11 had salvage XRT after initial RP. Overall, 30 (median PSA 15.05 ng/ml) of 44 (median PSA 13.7 ng/ml) pts had positive baseline Prostascint scans: 7 had uptake in prostate/prostatic bed, 14 had uptake in regional/abdominal or thoracic lymph nodes, while 9 had uptake in prostate area plus lymph nodes. Nine of the 18 pts entered onto the Taxol/XRT/hormone ablation trial have completed initial therapy, and have had follow-up Prostascint scans: 7 of the 9 show partial (n=3) or complete (n=4) resolution in areas of increased activity identified pre-therapy. In these 9 pts, the median pre- and post-treatment PSA values are 23.7 and 0.22 ng/ml, respectively. Follow-up Prostascint scans on the other pts will be obtained as they complete their treatment programs. In addition to traditional imaging and biochemical parameters, serial Prostascint scanning may provide potentially relevant information with respect to clinical response and outcome.

OTHER CLINICAL SCIENCE. ENDORINOLOGY 2

PS_538

LONG-TERM FOLLOW-UP OF PATIENTS WITH BONE METASTASES FROM DIFFERENTIATED THYROID CARCINOMA - SURGERY VERSUS CONVENTIONAL THERAPY

B.J. Fueger (1), G. Zettinig (1), C. Passler (2), C. Pirich (1), I. Kaufmann (1), S. Meghdadi (1), A. Becherer (1), K. Kaserer (3), R. Dudczak (1), B. Niederle (2). (1) Dpt. of Nuclear Medicine; (2) Dpt. of Surgery; (3) Dpt. of Pathology, University of Vienna, Austria.

AIM: Surgery of bone metastases from differentiated thyroid carcinoma seems indicated in individual patients. This retrospective study was performed (1) to analyse patients with bone metastases from differentiated thyroid carcinoma and (2) to evaluate the impact of surgery of bone metastases on survival.

Patients and Methods: We analysed 41 consecutive patients with bone metastases from differentiated thyroid carcinoma who had thyroid surgery at Vienna University Hospital since 1966. Median follow-up time was 12 years. There were 24 female and 17 male with a mean age of 60 ± 12 years. The primary tumour was follicular in 35 and papillary in 6 patients. Radioiodine treatment was performed in 32 patients with a mean administered activity of 2.7 ± 2.4 GBq 131-I. Metastases restricted to the skeleton were found in 22 patients whereas in 19 individuals, additional extraskeletal distant metastases were seen. Twenty-seven patients had multiple bone metastases. In 21 individuals, up to 5 bone metastases were surgically removed with the intention to keep the patient free from bone metastases. Statistical analysis of age, sex, tumour stage, histology, thyroid and lymph node surgery, presence of extraskeletal metastases, and surgery of bone metastases was performed using a cox regression model. A p value < 0.05 was considered as statistically significant.

RESULTS: Univariate analysis identified total thyroidectomy (p 0.005), lymph node surgery (p 0.002), radioiodine therapy (p 0.046), and the absence of extraskeletal distant metastases (p 0.021) as significant predictors of survival. Yet, in that small collective, multivariate analysis failed to identify significant prognostic factors. In the subgroup of patients with distant metastases limited to the bones, univariate analysis identified in addition to thyroid and lymph node surgery also the surgical extirpation of the bone metastases as a significant prognostic factor associated with improved survival (p 0.038).

CONCLUSION: These findings indicate that in patients without additional extraskeletal distant metastases, the radical surgical extirpation of bone metastases from differentiated thyroid carcinoma is associated with improved survival.

PS_539

TC-99M SESTAMIBI PARATHYROID SCINTIGRAPHY IN PATIENTS WITH MULTINODULAR THYROID GLANDS

M.B. Tomas, T. Kalapparambath, G.G. Tronco, M.O. Afriyie, C.J. Palestro. Division of Nuclear Medicine Long Island Jewish Medical Center, New Hyde Park, NY, USA.

Aims: The sensitivity of preoperative ^{99m}Tc- Sestamibi parathyroid lesion localization in primary hyperparathyroidism is 90 – 95% and the specificity ranges from 85 – 90%. Coexisting thyroid nodules and cervical lymph nodes are the most commonly reported causes of false positive results. Although primary hyperparathyroidism and a multinodular thyroid gland may coexist in the same patient, there are limited data about the effect of thyroid multinodularity on preoperative parathyroid scintigraphy. This retrospective review was undertaken to evaluate the effect of concurrent multinodular thyroid glands on preoperative parathyroid lesion localization in patients with primary hyperparathyroidism.
Methods: Twenty-eight patients, 23 women and 5 men, 25 – 80 years old (mean age = 62 years), with primary hyperparathyroidism and multinodular thyroid glands were included in this review. All patients underwent surgical exploration within 2 weeks of parathyroid imaging. Pinhole neck imaging was performed 90 - 120 minutes after the intravenous injection of 555 – 925 MBq (15 – 25 mCi) of ^{99m}Tc-sestamibi followed by injection of 185 MBq (5 mCi) ^{99m}Tc-pertechnetate and thyroid imaging. Images were background subtracted and normalized and the thyroid image was subtracted from the sestamibi image. Focally increased uptake was considered positive for a parathyroid lesion.
Results: Thirty-two parathyroid lesions were excised from the 28 patients. Twenty-five patients had 1 lesion each, 2 had 2 lesions each and 1 patient had 3 parathyroid lesions. All lesions were in the neck; 11/32 lesions (34%) were ectopic in location. There were 30 adenomas and 2 hyperplastic glands, ranging from 100 – 9300 mg in weight (mean weight = 3461 mg). 31/32 lesions were correctly localized (Sensitivity = 97%). A 190-mg adenoma was not identified preoperatively. There were 6 false positives (Specificity = 79%); three of these occurred in patients with a dominant thyroid nodule in a multinodular gland. Two of these 3 false positives were on the contralateral side of the parathyroid lesion.
Conclusion: In summary, our data indicate that although the specificity of ^{99m}Tc sestamibi parathyroid imaging is lower in patients with multinodular thyroid glands, than in the general hyperparathyroid population, its sensitivity is preserved. Consequently, it is still useful because it is a localizing rather than a diagnostic procedure.

PS_540

STRATEGY OF INITIAL EVALUATION AND ONE YEAR FOLLOW-UP OF DIFFERENTIATED THYROID CARCINOMA

A. Blaimont (1), J. Benoliel (1), J. Darcourt (1), X. Fontana (1), F. Ettore (2), F. Demard (3), F. Bussière (1). (1) Department of Nuclear Medicine; (2) Department of Anatomopathology; (3) Department of Head and Neck Surgery, Centre A. Lacassagne, Nice, France.

The follow-up of differentiated thyroid carcinoma (DTC) is based upon the measurement of serum thyroglobulin levels (Tg) and I131 Whole Body Scan (WBS). There is no definitive agreement on the follow-up protocol. Recent publications have proposed to use Tg alone.
Aim; The aim of this study is double: 1/ to analyse the performances of Tg and WBS in detection of metastases immediately after radical thyroidectomy to determine the immediate strategy (follow-up alone, another surgery, second therapeutic dose of I131). 2/ to compare the performances of the measurement of Tg alone to the protocol including WBS + Tg after one year follow-up.
Methods: 112 patients (80 females, 32 males) were studied retrospectively between March 96 and December 98 (98 papillary, 13 follicular and 1 mixed papillary-medullary cancer). The protocol consisted (after thyroid hormone withdrawal): 1/ 4 to 8 weeks after surgery: measurement of Tg (Tg1), WBS 5 days after administration of the therapeutic I131 dose (3,7 GBq) (WBS1).2/ 8 to 12 months after ablative I131 therapy: clinical examination, Tg measurement (Tg2), WBS 72 hours after 185 MBq I131 (WBS2), neck ultrasound (US) and chest X rays. The results of the two year follow-up (clinical examination, US and Tg measurement with WBS and/or another diagnosis procedures if necessary) served as reference.
Results: On the first evaluation, 99 thyroid remnants and 13 cases of metastases were discovered. After one year, 75 patients had a complete remission, 6 benign local remnants, 12 malignant local remnants, 11 lymph node metastases and 8 distant metastases. ROC analysis showed that optimal Tg1 threshold was 15 ng/ml. The sensitivity and specificity for lymph nodes metastases detection were 43% and 81% for Tg1, 86% and 99 % for WBS1 and concerning pulmonary metastases 100% and 82% for Tg1 and 100 and 98,9% for WBS1. On the second evaluation one year later, the sensitivity and specificity were 51% and 95% respectively for Tg2 alone (Tg2 threshold=2 ng/ml) and 89% and 93% for Tg2 + WBS2.
Conclusions: We confirm the role of WBS and Tg measurement during the first year after surgery for the detection of metastases and patient management .We demonstrated the usefulness of WBS after one year of follow up and the advantage to combine Tg and WBS.

PS_541

THREE-DIMENSIONAL SPECT MAXIMUM INTENSITY PROJECTIONS (MIP) OF TL-201 SCINTIGRAPHY: A NEW APPROACH FOR DIAGNOSIS OF DIFFERENTIATED THYROID CARCINOMA

R. Nishii (1), S. Noguchi (2), S. Jinnouchi (3), S. Nagamachi (3), K. Kawai (4), T. Murakami (1), S. Tamura (3). (1) Department of Radiology, Noguchi Thyroid Clinic and Hospital Foundation, Oita, Japan; (2) Department of Surgery, Noguchi Thyroid Clinic and Hospital Foundation, Oita, Japan; (3) Department of Radiology, Miyazaki Medical College, Miyazaki, Japan; (4) Central Research Laboratories, Miyazaki Medical College, Miyazaki, Japan

Background: Due to the accumulation of normal tissue and inflammation, the conventional planar images often fail to depict tumors with thyroid malignancies in Tl-201 scintigraphy.
Purpose: The aim of this study was to assess the usefulness of the maximum intensity projection (MIP) method, three-dimensional projection image, for detection of differentiated thyroid carcinoma in Tl-201 scintigraphy.
Materials and Methods: Twenty-two patients with differentiated thyroid carcinoma had Tl-201 scintigraphy using a gamma camera. Patients were injected 74 MBq of Tl-201 chloride intravenously. A conventional planar image and SPECT image of neck and chest were acquired in early phase (10 min after the tracer injection) and in delayed phase (120 min), respectively, for 10 min each. We applied MIP algorithm to SPECT images, and compared this MIP images with the conventional planar images. Tumor location and tumor size detected were evaluated. Results: The scanning time of SPECT was only 10 min that was the same time of planar imaging. Three-dimensional MIP images were easily obtained because they can be added to SPECT with only a few minutes of additional post-processing time. Because of emphasis the hot uptake, MIP images could depict the cancer location better than the conventional planar images. There were no cases, which could be diagnosed by planar image in spite of failure in MIP images. Minimum tumor size clearly recognized on MIP images was approximately 1 cm, however, that was difficult to diagnose on the conventional planar images. One case had pulmonary metastases and could be detected a lung nodule on only MIP images.
Conclusions: MIP method is a promising technique for the easy preliminary assessment of tumor detection of differentiated thyroid carcinoma.

PS_542

DOUBLE-PHASE PARATHYROID 99MTC-MIBI UPTAKE CORRELATES WITH SERUM IPTH LEVELS IN URAEMIC PATIENTS

D. Fuster (1), J. Ybarra (2), M. Ortega (1), F. Martín (1), M.J. Martínez-Osaba (3), J.V. Torregrosa (2), F.J. Setoain (1), S. Fuertes (1), F. Pons (1). (1) Department of Nuclear Medicine; (2) Renal Transplant Unitin; (3) Hormonal Department, Hospital Clínic, Barcelona, Spain.

Aim: ^{99m}Tc-MIBI identifies the presence of hyperfunctioning autonomous glands in patients with Secondary Hyperparathyroidism (SHP). The objective of this study was to assess whether changing serum calcium, phosphorus, iPTH and vitamin D concentrations correlate with MIBI«s uptake.

Methods: Double-phase parathyroid ^{99m}Tc-MIBI and total serum calcium, phosphorus, iPTH, creatinine, 25-OH Vitamin D and 1,25 $(OH)_2$ Vitamin D_3 determinations were performed simultaneously in 74 SHP patients (36F, 38M). Planar images of the neck and upper portion of the chest were obtained in the anterior view, 15 min (early phase) and 120 min (late phase) after the injection of 740 MBq of ^{99m}Tc-MIBI. In each patient, a final Parathyroid/Thyroid (P/T) activity index was obtained by adding the results of P/T index of all parathyroid lesions.

Results: There were significant correlation between iPTH levels and late ^{99m}Tc-MIBI uptake (r=0.656;P<0.000). Among all the variables, multiple regression analysis identified iPTH as the only significant predictor of late ^{99m}Tc-MIBI uptake (P<0.000). On the contrary, neither calcium nor phosphorus disclosed a significant correlation with ^{99m}Tc-MIBI uptake.

Conclusions: ^{99m}Tc-MIBI«s uptake in SHP patients can be predicted from circulating iPTH levels. On the contrary neither calcium, phosphorus or Vitamin D display significant correlation with ^{99m}Tc-MIBI uptake.

PS_543

COMPARISON OF TC99M-MIBI AND TL201 / TC99M SUBSTRACTION SCINTIGRAPHY IN PATIENTS WITH HYPERPARATHYROIDISM

H. Uslu (1), M. Yıldırım (1), E. Varoğlu (1), R. Bayrakdar (1), F. Akçay (2), N. Ünüvar (3), M. Demirci (1). (1) Atatürk University Medical Faculty, Dept. Of Nuclear Medicine; (2) Atatürk University Medical Faculty, Depts. of Biochmistry; (3) Atatürk University Medical Faculty, Depts. of Endocrinology Erzurum, Turkey.

TL201 / Tc99m pertechnetate substraction scintigraphy is recognized as a useful procedure in the preoperative localization of parathyroid adenomas. Tc99m -MIBI has recently been introduced for parathyroid imaging. The aim of this study was to compare diagnostic accuracy of parathyroid scan performed with Tc99m-MIBI and TL201 / Tc99m pertechnetate substraction in patients with hyperparathiroidism

Methods: Twenty-one patients (17 F, 4 M, mean age: 50 yrs) with a clinical and laboratory diagnosis of hyperparathyroidism were included in the study. TL201 / Tc 99m pertechnetate substraction and early-delayed cervico-thoracic images of Tc99m -MIBI scans were performed in all patients . The results of parathyroid imagings obtained with Tc99m -MIBI were compared with those obtained with TL201 / Tc 99m pertechnetate substraction scintigraphy, ultrasonography and histopathological findings after surgical exploration of the neck

Results: Positive scans in the seven and negative scans in the twelve patients were showed in both imaging methods. In one case, Tc99m -MIBI scan was negative but TL201 / Tc99m pertechnetate substraction scan was positive. In another case, while Tc99m -MIBI scan was positive TL201 / Tc99m pertechnetate substraction scan was negative. Surgical exploration of the neck was performed in patients (n=9) with positive Tc99m -MIBI and TL201 / Tc 99m pertechnetate substraction scans. Parathyroid adenoma in 7 and hyperplasia in 2 patients were detected. Ultrasonography was also negative in 12 patients whose both scans were negative. There was one false negative in Tc99m -MIBI scan and one false negative in TL201 / Tc 99m pertechnetate substraction scan. . The sensitivity rate of the both scans was 88 %, the specficity rate of the both scans was 100 %.

Conclusions: Both Tc99m -MIBI and TL201 / Tc 99m pertechnetate substraction scans had the same sensitivity rate for the detection of pathological parathyroid tissue. Scintigraphy is simple, safe and first step imaging technique for the detection of hyperfunctioning parathyroid glands.

PS_544

USEFULLNESS OF ABLATION DOSE OF 131-I IN PATIENTS WITH DIFFERENTIATED THYROID CANCER WITH HIGH 131-I UPTAKE DUE TO SUBTOTAL THYROIDECTOMY

V. Prassopoulos, J. Elias, N. Sifakis, M. Alevizaki, S. Gerali. Nuckear Medicine IASO Hospital, Athens, Greece.

AIM : Patients with differentiated thyroid cancer undergo total thyroidectomy. Many of them, though, have a high postoperative 131-I uptake due to partial thyroidectomy.

Aim of this study is to present the results concerning the mode of administration of high doses to 131-I for total thyroid ablation

MATERIALS – METHODS: In the past 10 years 67 patients who underwent thyroidechomy due to differentiated thyroid cancer (52 females –15 males) (age : 16-70 years) presented a high postoperative 131-I uptake at 48 hours post-administration (range : 13%-32%).

All of them had a negative brain CT scan and 6/67 had a positive whole body scan (adm dose : 4 mCi 131-I) for metastastic disease (3/6 : lung, 3/6 : bone). The ablative dose of 131-I was 50±20 mCi, with no adverse reactions.

RESULTS : 51patients were re-evaluated 6 months after the initial dose of 131-I was administrated 17pts (33,3%) had 131-I uptake ≤ 2%. 1/17 received a second ablative dose.

34 pts (68,6%) received a second dose of 131-I. After a period of 6mo. 33/34 had a 131-I uptake < 2%. 1/6 pts with metastatic disease had a 131-I uptake

< 2% after the first administration of the ablative dose and 4/5 after the second one.

CONCLUSION: In most cases in postoperative 131-I uptake is ≥ 10%, total ablation is reached after the administration of 2 or more relatively low doses of 131-I.

In cases with metastatic disease the administration of high doses of 131-I (100-150 mCi) is mandatory.

PS_545

RESULTS OF A THERAPEUTICAL TRIAL OF THYROID EYE DISEASE USING THE LONG-ACTING SOMATOSTATIN ANALOG SANDOSTATIN LAR IN PATIENTS REFRACTORY TO PREVIOUS THERAPIES

R. Moncayo (1), C. Watfah (1), I. Baldissera (2), K. Petrova-Schumann (3), A. Sztankay (3), E. Donnemiller (1), H. Erler (1), C. Bacher Stier (1), E. Donnemiller (1), G. Riccabona (1). (1) Dept. of Nuclear Medicine; (2) Dept. of Ophthamology; (3) Dept. of Radiation Therapy, University of Innsbruck, Austria.

Aim: To evaluate the efficacy of a long acting somatostatin analog (Sandostatin LAR) in the therapy of thyroid eye disease in patients who had not responded adequately to previous treatments. Octreotide scanning is done routinely at our Institution in order to evaluate the degree of activity in thyroid eye disease. The uptake of Octreotide in the retrobulbar space is taken as a sign of immune activation which depends on the expression of specific somatostatin receptors. This receptor availability provide an ideal setting for the use of long acting analogues (Sandostatin LAR) as a therapeutic option.

Methods: Eight patients presenting with therapy resistant thyroid eye disease were included in this series. All of them presented tracer uptake of OctreoScan in the retrobulbar space. The therapeutic scheme contemplated a monthly dose of 30 mg i.m. over a period of 6 months. In 2 cases Sandostatin LAR was given parallel to external radiation therapy (single dose of 1 Gy/fraction, total dose 20 Gy, 8MV).

Results: The administration of Sandostatin was well tolerated in 7/8 patients. Clinical improvement of inflammatory eye signs was alredy seen after 3 days. Pressure sensation and eye pain showed an improvement during the first month of treatment. After 6 months of treatment a constant improvement remained in 6/7 patients. Hyperthyroidism and eye signs relapsed in one male patient (persistent smoker). In one female patient presenting GI side effects for more than 4 weeks, eye disease also relapsed. She was taken off the drug. The 2 patients receiving the combined treatment (Sandostatin and radiation) showed a clear improvement by the time the radiation cycle was finished. In 2 cases gallstones developed 2-3 months after therapy was finished.

Conclusions:Our observations show the positive effect of Sandostatin in the treatment of thyroid eye disease which has been resistant to previous therapies. GI side effects are usually mild. The efficacy of Sandostatin LAR in newly diagnosed cases of thyroid eye disease remains to be evaluated.

PS_546

THE DEPENDANCE OF THYROID HORMONE LEVELS ON GLOMERULAR FILTRATION RATE (GFR) IN PATIENTS WITH ACUTE RENAL FAILURE (ARF)

S. Ilic, M. Vlajkovic, M. Rajic, D. Mitic, M. Bogicevic. Department of Nuclear medicine, Clinical Center, Nis, Yugoslavia.

Thyroid hormone disturbances are well known to occur in various nonthyroidal diseases. This study was aimed to establish the relationship between thyroid hormones levels and GFR in ARF patients.

MATERIAL AND METHODS: RIA of thyroid hormones serum levels were performed in 32 oligoanuric patients within 7 days after ARF onset. The patients were divided into two groups according to the values of glomerular filtration rate. The first group included 17 patients with 99mTc-DTPA clearance values over 25 ml/min (35±8), while the second group consisted of 15 patients with the clearance mean value of 16±7 ml/min. The serum creatinine value of the first group was 326+ 68 µmol/l and that of the second group 676±162 µmol/l.

RESULTS: The comparison of patients hormones levels with those of 15 healthy subjects showed a significant decrease of total and free thyroid hormones levels in the first group (T4 90±17nmol/l, T3 1.3±0.12 nmol/l, FT4 15±2.5 pmol/l, FT3 4.1±0.9 pmol/l), and a more marked decrease in the second group (T4 50±9 nmol/l, T3 0,5±0,10 nmol/l, FT4 5.0±1.1 pmol/l, FT3 1.2±0.3 pmol/l). The fall of hormones levels was severely expressed for T3 compared to T4 as well as free hormones related to total hormones. Reverse T3 was found increased in both the studied groups of patients (41±10 and 35±9 pmol/l) while TSH values were within the normal range. Regression analysis indicated a significant correlation between thyroid hormones and GFR in both groups.

CONCLUSION: The presented data suggest that the level of thyroid hormone disturbances is in proportion with the impairment of renal function. These alterations could be induced by a body defence reaction to stress, with a higher production of the metabolically less active hormone. The effect of uremic toxins upon pituitary-thyroid axis with the consequent suppression of hormones synthesis should be also considered.

PS_547

PITUITARY-TESTICULAR AXIS IN MALE PATIENTS AT MAINTENANCE HEMODIALYSIS. THE EFFECT OF RESIDUAL RENAL FUNCTION

S. Ilic, M. Bogicevic, M. Rajic, M. Vlajkovic, D. Mitic, V. Stefanovic. Department of Nuclear medicine, Clinical Center, Nis, Yugoslavia.

The aim of this study was to show the effect of the residual renal function upon the pituitary-testicular axis in patients on maintenance hemodialysis.
MATERIAL AND METHODS: Follicle stimulating hormone (FSH), luteinizing hormone (LH), prolactin (Pr) and testosterone were determined by RIA in serum of 30 healthy persons and 39 male patients on maintenance hemodialysis. According to the residual renal function, estimated by 24 hr urine output, all hemodialysis patients were classified into three groups: 1st -urine output under 500 ml, 2nd - urine output 501-1000 ml and 3rd -urine output above 1000 ml.
RESULTS: In patients on maintenance hemodialysis the serum concentration of LH (19.8±2.0 mIU) and Pr (843±127 mIU/l) were found to be significantly higher ($p<0.001$), while testosterone concentration (5.0±0.3 ng/ml) was significantly lower ($p<0.001$). The comparison among the groups with various residual renal functions shows a significantly higher($p<0.001$) Pr concentration in patients with small urine output (1st- 1126±192 mIU/l, 2nd-893±233 mIU/l, 3rd-426±44 mIU/l). The testosterone concentration was significantly lower ($p<0.05$) in the first group (3.9±0.5ng/ml) than in the second group (5.58±0.5 ng/ml).
CONCLUSION: The obtained results show an the increase of LH and Pr and the decrease of testosterone level in male patients on maintenance hemodialysis. A dependence of the serum levels of Pr and testosterone from the residual renal function was also established.

PS_548

CORRELATION BETWEEN RETINOPATHY AND ISCHEMIC HEART DISEASE IN NON-INSULIN DEPENDENT DIABETES MELLITUS PATIENTS

A. Fawzy (1), M. Abo-Zeid (2), M. Thabet (2), N. Al-Sayed (2). (1) Nuclear Medicine ; (2) Internal Medicine Departments, Faculty of Medicine, Cairo University, Egypt.

Background: Retinopathy and coronary artery disease (CAD) may have similar pathophysiological background related to widespread vascular damage. The risk of CAD is higher in patients with non-insulin dependent diabetes mellitus (NIDDM) than in non-diabetic subjects.
Aim of the study: To correlate between different degrees of diabetic retinopathy changes and CAD events in Non-insulin diabetes mellitus.
Patients and Methods: 40 NIDDM patients were divided into 2 groups with retinopathy (n=30) and without (n=10). They were all normotensive, non-smokers, no history of anginal pains and normal lipid profiles. They were subjected to full laboratory evaluation, resting and exercise ECG, echo heart and Tc-99m Tetrafosmine myocardial perfusion SPECT scintigrams.
Results: Echo heart was negative in all group B patients and was only positive in only 2 patients in group A. Also, there was evidence of ischemia in the myocardial perfusion scintigraphy in 80% of patients of group A, out of those 43.3% were reversible and 63.7% were irreversible. Among group B patients, 40% were positive and reversible and 60% were normal. None of group B had irreversible ischemia ($p<0.05$).
Conclusion: Diabetic retinopathy was associated with higher incidences of CAD in NIDDM patients and should be considered as a landmark for CAD. Also, myocardial perfusion is more sensitive than ECG and Echo for identifying silent CAD in diabetic patients.

PS_549

COMPARISON OF CEREBRAL BLOOD FLOW AND MENTAL STATES BEFORE AND AFTER THERAPY IN PRIMARY ALDOSTERONISM

S. Tsuchimochi, M. Nakajo, M. Nakajo jr, H. Tanabe, T. Umanodan, Y. Nakabeppu. Department of Radiology, Kagoshima Unversity Hospital, Kagoshima, Japan.

Objectives: We often met with anxiety or depression in patients with primary aldosteronism. It was previously reported that depression returned to normal after removal of an adenoma in a patient with primary aldosteronism, or that abnormal regional cerebral blood flow (rCBF) was shown in major depressives. Therefore, we evaluated the correlation of rCBF with plasma aldosterone levels and mental states in patients with primary aldosteronism. Methods: This study was consisted of 6 patients with unilateral aldosteronoma. The measurements of plasma aldosterone levels, psychological tests (STAI for anxiety, SDS for depression and Y-G test for both depression and nervousness) and Tc-99m ECD SPECT were performed before and a month after therapy (2 patients received tumor resection and 4 patients received transcatheter adrenal arterial embolization). Comparison of the rCBF between pre- and post-therapeutic conditions was made using statistical parametric mapping (SPM '96). Results: There was a significant difference in the levels of plasma aldosterone before and after therapy (288 + 81 vs 87 + 69 pg/ml, $p < 0.05$). However, there were no areas which showed significant differences in rCBF before and after therapy. Before therapy, definite abnormal scores were obtained in 1 patient in SDS, in 2 patients for characteristic anxiety scores and in 5 patients for conditional anxiety scores in STAI and in 3 patients for depression scores and in 2 patients for nervousness scores in the Y-G test. After therpay, the scores improved in 3, 5, 1, 2 and 3 patients, respectively and worsened in 1, 0, 3, 1 and 1 patients, respectively. Conclusion: The plasma aldosterone levels do not affect rCBF and phychiatric changes may not be related to rCBF changes in primary aldosteronism.

OTHER CLINICAL SCIENCE. INFECTION AND INFLAMMATION 2

PS_550

FIVE YEARS EXPERIENCE WITH CIPROFLOXACIN-TC99M (INFECTON) IN THE BONE INFECTED PATIENT

V.E. Soroa (1), R.C. Cabrejas (1), C. Alonso (2), K.K. Solanki (3), K.E. Britton (3). (1) Centro de Medicina Nuclear. Htal.Clínicas, UBA/CNEA, Bs.As, Argentina; (2) Servicio de Traumatología- División Ortopedia Htal.Clínicas, UBA, Bs.As, Argentina; (3) Department of Nuclear Medicine -Division Radiopharmacy. St.Bartholomew's, London, UK.

The purpose of our work was the evaluation of the outcome of 99mTc-ciprofloxacin (*Infecton*) scans in suspected orthopedic infected patients, as well as the impact of follow-up scans in their clinical management.
Methods: Out of 258 patients (125 males, 160 females) 93 follow-up *Infecton* scans were performed (36%). Forty one percent were on antibiotics (including ciprofloxacine). Frequent pathologies were osteomyelitis, hip, knee & lumbar prosthesis (86%) while the other 14% were abscess, septic arthritis & cellulitis. Flow, 1, 4, 24h planar or Spect images were acquired with i.v. 444-518MBq. *Infecton*. Complimentary intra-comparison laboratory, anatomical and one other nuclear scans were provided (MDP, 99mTc-Leucocytes, 99mTc-Immunoglobulins, Gallium-67).
Results: Neither adverse reactions, nor any relation of the scan outcome with the use of antibiotics were found. Positive uptake, read in the 24h images, was considered as persistent infection. Eleven percent of follow-up patients had 3-4 *Infecton* scan before negative results were achieved. The re-scanning was obtained in 3-4 months time from the former. Absence or decreased uptake at 24h images was obtained in 30%. *Infecton* Negative scans were taken as cure, while positivity implied persistent infection and antibiotic treatment continuity. Late intestinal activity found in 60% of studied patients, was usually accompanied by positivity in stools, with no relation with clinical symptoms of local infection.
Conclusions: In our studied series the highest specificity (80%) was achieved by the *Infecton* scan with a sensitivity of 93%. *Infecton* scan needs no blood manipulation and is recommended as a safe specific bacterial detector technique for osteoarticular infection and its follow-up.

PS_551

THE STUDY OF BONE INFECTIONS WITH 99MTC-CIPROFLOXACIN

N. Prandini (1), L. Feggi (1), S. Panareo (1), A. Ciprian (1), L. Massari (2), A. Galla (2), M.C. Danzi (3), M. Solbiati (3), K. Britton (4). (1) Department of Nuclear Medicine, Azienda Ospedaliera Universitaria, Ferrara, Italy; (2) Department of Orthopedics, Azienda Ospedaliera Universitaria, Ferrara, Italy; (3) Department of Infective Disease, Ospedale Civile Verona, Italy; (4) Department of Nuclear Medicine, S.Bartholomew's Hospital, London, United Kingdom

The use of radiolabelled white blood cells has been studied and evaluated in several pathologies and is still the reference method in the study of bone infections. Moreover in central bone and in chronic infection WBC scintigraphy often results in unspecific „cold areas".
We report an experience with Technetium99m-Ciprofloxacin an antibiotic that represent a specific tracer of bacterial active infection. We performed 58 studies with 99mTc-ciprofloxacin for a suspicion of infections of the vertebral column (24), hip prosteses (13), leg fractures (16), knee (2), foot (1), shoulder (2), and 1 polithrauma in 46 patients. The scintigraphies were obtained 1 and 4 hours after injection: further imaging at 8 or 24 hours were used in doubtful cases. All vertebral infections underwent SPECT.
In 23 patients, and in all peripheric infections, the results were compared with a 99mTc-HMPAO WBC study. All patients but 9 resulted positive on 99mTc-Infecton study: the uptake of antibiotic was always higher and wider than WBC's. A ratio of target/normal uptake lower than 1.5, or an activity that significantly decreases in late imagings were considered a negativity criterion.
The results of Infecton were 45 TP, 8 TN, 4 FP and 1 FN with an accuracy of 91%, a sensitivity of 97,8% and a specificity of 67,7%. We found a concordance with WBC in 23 positive and 4 negative patients. In 3 cases the WBC study was doubtful and resulted FP in 2 and TN in 1 on Infecton. In 4 patients with spondilodiskytis, 1 with sterno-clavicular septic arthritis, and in 2 with hip prosteses WBC study showed a cold area not signicant for the diagnosis of infection. Only in a patients with suspect of leg osteomyelitis the study with infecton resulted false positive and only 1 year after bone resection become negatve. In spondylodiskytis the Infecton study was always conclusive in contrast to the low sensitivity of WBC, and the useless of MRI and CT to assess persistence of infection in alterated vertebral bone: 2 of these positive studies were resulted positive for tubercular diskitis.
In conclusion, the accuracy of Infecton is comparable to WBC in peripheric osteomyelitis but it is more effective than WBC in central bone infections such as spondilodiskytis.

PS_552

IMAGING OF FUNGAL INFECTIONS WITH 99MTC-LABELLED FLUCONAZOLE AND ANTIMICROBIAL PEPTIDES

A. Lupetti (1), M.M. Welling (2), S. Mongera (2), A. Paulusma-Annema (1), P.H. Nibbering (1), E.K.J. Pauwels (2). (1) Department of Infectious Diseases; (2) Department of Nuclear Medicine, Leiden University Medical Center, Leiden, The Netherlands.

Fungal infections are difficult to diagnose in immunocompromised patients and a tracer for such infections could be very instrumental in initiating the therapy in such patients with febrile episodes. In the search for such a tracer, accumulation of ^{99m}Tc-labeled fluconazole, ^{99m}Tc-labeled synthetic peptides derived from human lactoferrin (hLF 1-11) and ubiquicidin (UBI 18-35, UBI 22-35, UBI 29-41) in *Candida albicans* infections in immunocompetent mice and *Aspergillus fumigatus* infections in leukocytopenic mice was compared with that in bacterial infections and sterile inflammatory processes. The results showed that ^{99m}Tc-labeled fluconazole detects *C. albicans* infections, but not infections with *A. fumigatus*, bacterial infections, or inflammatory processes. Imaging of *C. albicans* infections in mice was already achieved within the first hr after injection of ^{99m}Tc-labeled fluconazole and maximal accumulation of the tracer, i. e. target-to-non-target (T/NT) ratios between 3 and 4, was reached at 2 hrs after injection of this tracer. Furthermore, a good correlation between T/NT ratios for this tracer and the number of viable *C. albicans* was found, indicating that radiolabeled fluconazole may be useful in monitoring the efficacy of antifungal therapy in *C. albicans* infections. Furthermore, radiochemical analysis of ^{99m}Tc-labeled fluconazole indicated that this tracer remained stable for 24 hrs at 37°C. Another finding of this study was that ^{99m}Tc-labeled peptides were able to distinguish fungal infections from sterile inflammations but not from bacterial infections. Together our observations suggest that the combination of radiolabeled UBI peptides and fluconazole can be a useful strategy since it allows discrimination between infections and inflammations while discriminating infections with *C. albicans* from infections with other micro-organisms.

PS_553

THE CLINICAL VALUE OF GALLIUM-67 SCINTIGRAPHY IN WEGENER'S GRANULOMATOSIS

R.H.J.A. Slart (1), P.L. Jager (1), L. Poot (1), D.A. Piers (1), JW. Cohen Tervaert (2), C.A. Stegeman (2). (1) Department of Nuclear Medicine; (2) Department of Internal Medicine, Division of Nephrology, University Hospital Groningen, Groningen, The Netherlands.

Introduction: Diagnosis of active pulmonary and para-nasal involvement in patients with Wegener's granulomatosis can be difficult, especially in case of unclear clinical presentation. Usual diagnostic tools like ANCA-levels, inflammatory blood parameters and biopsy are not always conclusive. Gallium scintigraphy is sometimes used in these difficult cases, but its diagnostic contribution is unclear.
Aim: to evaluate the added diagnostic value of gallium scintigraphy in patients with suspected granulomatous or vasculitic inflammation in para-nasal and chest region.
Methods: We retrospectively evaluated 40 chest- and 20 head planar gallium scans of 28 patients who were evaluated for possible Wegener's disease activity. Gallium scans were reviewed qualitatively and were grouped in normal or increased uptake for the chest and para-nasal region. True active pulmonary or para-nasal involvement was concluded if histologically proved or in case of clinical diagnosis with appropriate response to treatment. Active infection had to be excluded.
Results: Four (14%) patients had active pulmonary Wegener disease, 3 (11%) patients had active para-nasal activity and 1 (4%) patient had both. In all these patients, chest and para-nasal scans showed increased gallium uptake (sensitivity 100%). In the group of patients (n=20) without active Wegener's disease, gallium scans were negative for pulmonary activity in 23 out of 35 scans (specificity 66%), and negative for para-nasal activity in 12 out of 16 scans (specificity 75%). False positive findings were caused by bacterial or viral infections. Following treatment, a follow up scan showed normalisation of pulmonary or para-nasal gallium uptake in all patients (n=3) with a true positive chest or para-nasal scan at diagnosis.
Conclusion: Gallium scintigraphy of the chest and nasal region has a high sensitivity for the detection of disease activity in Wegener's granulomatosis. However, due to positive scans with bacterial or viral infections, specificity was considerably lower. Since detection of disease activity can be difficult, gallium scans may be clinically helpful as a negative scan virtually excludes active Wegener disease

PS_554

COMPARISON OF IN VITRO ANTIMICROBIAL ACTIVITIES OF 99MTC-INFECTON AND CIPROFLOXACIN

H.C. Song (1), S.M. Kim (1), H.S. Bom (1), J.H. Shin (2), H.J. Jeong (1), J.Y. Kim (1). (1) Department of Nuclear Medicine; (2) Department of Clinical Pathology, Chonnam National University Hospital, Kwangju, South Korea.

Objective: We hypothesized that antimicrobial activity of ^{99m}Tc-labeled amine-ciprofloxacin (Infecton) could be an indirect evidence of its specificity to bacterial infection. To evaluate the hypothesis we compared *in vitro* antimicrobial activities of Infecton and ciprofloxacin.
Methods: Minimum inhibitory concentration (MIC) and minimum bactericidal concentration (MBC) of Infecton and ciprofloxacin against three standard strains of bacteria, *Staphylococcus aureus* ATCC 29213, *Escherichia coli* ATCC 25922 and *Pseudomonas aeruginosa* ATCC 27853 were measured.
Results: MICs of Infecton and ciprofloxacin were 1.12±0.20 (0.8~1.6) μg/ml and 0.36±0.04 (0.2~0.4) μg/ml for *S. aureus*, 0.03±0.005 (0.025~0.05) μg/ml and 0.011±0.001 (0.006~0.012) μg/ml for *E.coli*, and 0.96±0.16 (0.8~1.6) μg/ml and 0.56±0.098 (0.4~0.8) μg/ml for *P. aeruginosa*, respectively. MBCs of Infecton and ciprofloxacin were 2.56±0.39 (1.6~3.2) μg ml and 0.88±0.2 (0.4~1.6) μg/ml for *S. aureus*, 0.04±0.06 (0.025~0.05) μg/ml and 0.02±0.01 (0.025~0.05) μg/ml for *E.coli*, and 2.24±0.39 (1.6~3.2) μg/ml and 1.44±0.16 (0.8~1.6) μg /ml for *P. aeruginosa*. respectively.
Conclusion: Although both MICs and MBCs of Infecton were higher than those of ciprofloxacin, all three standard bacterial strains were sensitive to Infecton. It is an indirect evidence of specificity of ^{99m}Tc Infecton to bacterial infection.

Poster presentation

PS_555

PLATELET GEL, AS A NEW METHOD TO IMPROVE WOUNDS' HEALING AND TISSUE RIGENERATION IN PATIENTS WITH STERNAL WOUNDS INFECTIONS (SWIS) AND 99MTC-HMPAO LABELLED GRANULOCYTES SCINTIGRAPHY AS A DIAGNOSTIC PROCEDURE

M.C. Sacchi (1), R. Zoccola (3), L. Bertolazzi (3), E. Cornaglia (1), M. Serra (2), D. Medici (2), A. Levis (1), L. Ressia (2), P. Scotti (2), G. Sinaccio (2). (1) Department of Hematology and Transfusional Medicine; (2) U.O.A. Cardiac Surgery; (3) Department of Nuclear Medicine.

Aim Clinical trials seem to reveal that platelet gel, a source of multiple autologous GFs, can be considered a useful and available tool to increase either the quality or the final quantity of new-conformed bone and to stimulate the healing of chronic wounds resulting in accelerated granulation tissue formation and epithelization. Surgical wound infections are a serious problem in openheart surgery despite continuing efforts to improve post-operative conditions. Early and accurate detection of SWIs is important because this complication performed by sternotomy carries high morbidity and mortality rates. The aim of this study is to assess the clinical use of scintigraphy with ^{99m}Tc-HMPAO-labelled granulocytes in the diagnosis of postoperative SWIs, before and after this innovative treatment.

Methods During last year, 454 patients underwent a cardiac surgery procedures, 333 of them coronary bypass. 11 patients developed SWIs post-operative. Bacteriological analyses of wound secretions were performed in all patients with SWIs. Platelet concentrated (PC), prepared starting from a low quantity of whole blood (60 ml), is activated by a Batroxabine-calcium gluconate blend to obtain a platelet gel. According to the clinical signs and microbiological findings we applied this gel to 5 patients (all were given informed consent before inclusion in the study) for a period of 1 month, twice a week, on lesion . We exposed all patients with suspected SWI to scintigraphy with HMPAO-Tc99m labeled granulocytic fractions: a) before the treatment with the aim to distinguish between superficial and deep SWI; b) after the treatment (1 month from the outcome) to evaluated the healing or the persistence of infection. The method used for the separation and labelling of granulocytes with 99mTc-HMPAO (Amersham) was as described by Ferrante et al. with some modifications. We obtained scintigraphy with acquisitions at 3 h and 20 h after injection in 3 projections (anterior, lat.right and left) planars and SPET.

Results The diagnosis of SWIs was obtained in all patients enrolled in this sperimental study before the treatment with platelet gel. The scintigraphic analysis, performed 1 month after the outcome, confirmed the recovery of all the patients treated.

Conclusion These preliminary data seem to demonstrate the effective of platelet gel to improve and accelerated the healing of SWIs, completely correlated by ^{99m}Tc-HMPAO-labelled granulocytes scintigraphy, in according to the extreme sensitivity of this nuclear methods.

Ethical aspects This study has been projected following the indications of Helsinki's Declaration , Good Clinical Practice's laws (GCP) and D.M. 18.3.1998.

PS_556

BIODISTRIBUTION AND DOSIMETRY OF F18 FDG LABELED LEUKOCYTES (F-18-FDG WBC) IN A NORMAL HUMAN SUBJECT

L. Forstrom, B. Mullan, J. Hung, V. Lowe, L. Thorson, W. Dunn. Nuclear Medicine, Mayo Clinic, Rochester, Minnesota, USA.

Aim: This study was performed for preliminary assessment of F18 FDG WBC dosimetry in man.

Methods: Using methods previously reported from our laboratory, a mixed cell suspension of autologous leukocytes in heparin-saline was labeled with F18 FDG by incubation at 37° for 20 minutes. After washing and re-suspension, 315 MBq F18 FDG WBC was administered by slow IV injection in a normal volunteer subject. A GE Varicam with 511 keV collimation was used for whole body imaging at _, 1, 2, 4 and 6 hours. Blood samples were obtained at corresponding times, as well as hourly urine samples.

Results: F18 FDG WBC uptake was seen predominantly within the RE system, consistent with physiologic leukocyte distribution. Urinary excretion (6.7 % at 6 hrs) and brain uptake (2.1% at 6 hrs) were consistent with minor elution of F18 FDG, likely due to intracellular dephosphorylation. Calculated organ dosimetry based on image analysis is as follows: 0.013 mGy/MBq to brain, 0.07 mGy/MBq to liver, 0.036 mGy/MBq to lungs, 0.405 mGy/MBq to spleen, 0.0708 mGy/MBq to red marrow, and 0.012 mGy/MBq to whole body.

Conclusions: Preliminary estimates of organ dosimetry using 315 MBq F18 FDG WBC in a normal subject are comparable with reported results for leukocytes labeled with 18.5 MBq In-111 oxine. Further studies of F18-FDG WBC as a potential agent for PET imaging of inflammation/infection appear warranted.

PS_557

POTENTIAL USEFULNESS OF TC-99M- HUMAN POLYCLONAL IMMUNOGLOBULIN G (HIG) SCINTIGRAPHY IN EVALUATION OF SJÖGREN'S SYNDROME

G. Karanikas (1), K. Bobacz (2), A. Becherer (1), K. Wiesner (1), R. Dudczak (1), K. Machold (2), K. Kletter (1). (1) Department of Nuclear Medicine; (2) Department of Rheumatology, University of Vienna, Vienna, Austria.

Sjögren's syndrome is an autoimmune disease that affects the salivary and lacrimal glands. It is characterized by lymphocytic infiltration and destruction of gland tissue. In the diagnosis and evaluation of Sjögren's syndrome, an objective examination is required, since patient complaints do not necessarily reflect the severity of salivary gland disease. Radiolabeled human non-specific polyclonal immunoglobulin G (HIG), is used for the diagnosis of inflammation/infection. In this study we evaluate the potential usefulness of Tc-99m- HIG scintigraphy in patients with Sjögren's syndrome.

Methods: Ten consecutive patients with verified secondary Sjögren's syndrome according to the Copenhagen criteria were included in this prospective study. The control group consisted of seven patients with Lupus erythematodes; none had clinical signs of Sjögren's syndrome. Planar and SPECT images of the head were performed six hours after i.v. administration of Tc-99m HIG (500-550MBq).

Results: Nine out of ten patients with secondary Sjögren's syndrome showed a positive result (sensitivity 90%) in planar as well as in SPECT images, while one of them was false negative according to the Copenhagen criteria. Tracer accumulation in patients with positive scintigraphy demonstrated a great variability. In five patients tracer accumulation was enhanced in the oral region, in four increased uptake was seen in the salivary gland and in one additionally in the lacrimal sinus. All patients of the control group showed a correct negative result.

Conclusions: Our data suggest that Tc-99m HIG scintigraphy is a modality with high sensitivity for the diagnosis of Sjögren's syndrome and can provide objective information on the severity of the disease.

PS_558

ROLE OF COMBINED 3-PHASE BONE SCAN & TC-99M LABELLED ANTI-GRANULOCYTE ANTOBODY FAB' IMAGING IN DIFFERENTIAL DIAGNOSIS OF INFECTED AND NON-INFECTED LOOSENED PROSTHESIS

D. Rubello (1), G. Saladini (1), A. Pellicanò (2), D. Casara (1). (1) Servizio di Medicina Nucleare 2, Azienda Ospedaliera di Padova, Padova, Italy; (2) Unità Operativa di Ortopedia e Traumatologia, ASL 16, Padova, Italy.

Twenty-one consecutive pts with painful loosened prosthesis (P) suspected to be infected on the basis on clinical and laboratory findings entered the study:19 of them had hip P (4 bilateral) and 2 knee P, implanted 5 mo. to 10 yr (median 3 yrs) before nuclear medicine evaluation. In all pts, Tc-99m-HDP 3-phase bone scan (BS) was followed by Tc-99m-labelled anti-granulocyte antibody Fab'-fragment (Tc-AGA) (LeucoScan", Immunomedics) imaging obtained 4 hrs and 18-24 hrs post-injection. The peri-prosthetic tracer uptake intensity was graded by means of a 4-point scale: normal=0, mild=1, moderate=2, intense uptake=3. Scintigraphies were blindly evaluated by two nuclear medicine physicians. Surgical findings were taken as gold standard in the 21 loosened P: 9 P were diagnosed to be infected, and 12 non infected. Moreover, in pts with bilateral hip P, the 4 painless P were taken as controls. BS was positive in all 21 cases of loosened P. Despite we did not observe a BS pattern specific for the infected vs non-infected P, however, it is worth noting that the BS flow-phase was positive in all 9 cases with infected P while in only 3/10 cases with non infected P. Tc-AGA scan was positive in all 9 cases with infected P (BS +, Tc-AGA +), whereas it was negative in 10/12 cases with non infected P (BS +, Tc-AGA -). False positive Tc-AGA results were recorded in 2 loosened non-infected P: in these pts the P was implanted 5 mo. and 7 mo. before, respectively, and in both cases a mild to moderate diffuse peri-prosthetic tracer uptake was recorded. On the other hand, both BS and Tc-AGA were correctly negative (BS -, Tc-AG -) in the 4 cases of asymptomatic hip P. On the basis of these preliminary data, we can conclude that: a) BS is a highly sensitive technique in differentiating loosened from asymptomatic P; b) BS is not able to differentiate infected from non-infected loosened P, even if a positive flow-phase has to lead the physician to suspect infection; c) Tc-AGA scan appears to be accurate enough to differentiate infected from non-infected loosened P, even if some false positive results can be observed when scintigraphic evaluation is performed in the first period following surgery.

PS_559

DETECTION OF FOCAL CARDIOVASCULAR AND SOFT TISSUE INFECTIONS WITH 99M-TC-LABELED ANTI-GRANULOCYTE ANTIBODY FRAGMENTS

U. Kampen, C. Jaekel, W. Brenner, M. Zuhayra, N. Czech, E. Henze.
Clinic of Nuclear Medicine, Kiel University, Germany.

Aim: Elevated inflammatory blood parameters without any distinctive focus or fever of unknown origin are still challenges in clinical diagnostics. These patients require a quick and easy-to-perform whole-body examination protocol for the detection of possible inflammatory foci which can not be achieved by conventional radiology. Application of an antibody fragment labeled with 99m-Tc and directed against surface antigens of human granulocytes (LeukoScan) is a promising method, although it is primarily approved for diagnosis of osteomyelitis. Therefore, the aim of our study was to look for the diagnostic impact of immunoscintigraphy with LeukoScan in patients with signs of inflammation but without any distinctive knowledge of the responsible focus.
Methods: A total of 36 patients (17 female, 19 male, aged 17-81 years) were enrolled into this retrospective study. Clinicians demanded immunoscintigraphy with LeukoScan because of suspected infections in the cardiovascular system (n=8), soft tissue involvement (n=16) or even without any idea of localization (n=12). Planar whole-body imaging was performed 3 hours after injection of 600MBq 99m-Tc-LeukoScan, completed by SPECT or delayed imaging after 24 hours whenever necessary. Scintigraphic data were compared to the final diagnoses, proven by histopathology or by carefully directed radiological diagnostics, e.g. CT, MRI or conventional tomography, guided by the LeukoScan images. In cases without any positive scintigraphic finding, clinical follow-up was taken for proof.

Results: Immunoscintigraphy showed the following results:

n	*Suspect of*	*true +*	*true −*	*false +*	*false −*	*Sens.*	*Spec.*
8	*Cardiovascular focus*	*6*	*1*	*0*	*1*	*0,86*	*1,0*
12	*Origin unknown*	*3*	*8*	*1*	*0*	*1,0*	*0,89*
16	*Soft tissue focus*	*6*	*3*	*1*	*6*	*0,5*	*0,75*

The over-all sensitivity and specificity was calculated as 0,68 and 0,86, respectively. A high number of false negative results in soft tissue infection, which accounts for the lower over-all sensitivity was possibly due to four cases with an abscess, known to have a significantly reduced blood supply resulting in a lack of local tracer deposition. Two other patients had a proven nephritis in which LeukoScan is known to be ineffective because of tubular stacking of the antibody fragments. False positive results were caused by both misinterpretation of unspecific tracer deposition in the gut and local granulocyte accumulation after surgery.
Conclusion: Immunoscintigraphy with LeukoScan showed encouraging results in patients with cardiovascular infection and fever of unknown origin. In case of soft tissue infection, its diagnostic impact is decreased by a high degree of false negative results.

PS_560

DIAGNOSTIC VALUE OF TC-99M-CIPROFLOXACIN (INFECTON) IN PATIENTS WITH PROSTHETIC IMPLANTS OF SUSPECTED INFECTION

K. Sönmezoğlu (1), M. Halaç (1), I. Akgün (2), C. Türkmen (1), C. Nisli (1), C. Önsel (1), N. Erdoğan (1), B. Kanmaz (1), I. Uslu (1). (1) Department of Nuclear Medicine; (2) Department of Orthopedics, Cerrahpaşa Medical Faculty, Istanbul University, Istanbul, Turkey.

Aim: In this prospective study we have evaluated the diagnostic value of Tc-99m-labelled ciprofloxacin (INFECTON), a new and bacteria specific infection localizing agent in the patients with prosthetic implant infections.
Methods: 21 patients with 26 prosthetic implants (11 total hip prosthesis, 11 total knee prosthesis, 3 intramedullary femoral nails and 1 hip screw) were referred to our department for the investigation and/or confirmation of clinically suspected infection. All patients underwent both Tc-99m-HMPAO WBC and INFECTON scans. Biochemical, radiological, microbiological data and clinical follow-up (at least 3 months) contributed along with the scintigraphic techniques in deciding on the presence or absence of infection. Scintigraphic images from the areas of interest were performed at 1 and 4 hr postinjection of 370-400 MBq of Tc-99m-INFECTON or 185-200 MBq of Tc-99m-HMPAO-WBC in at least two projections. There were at least 2 days and at most 7 days between two scintigraphic studies.
Results: 15 of 26 prosthetic implant sites of suspected infection were finally considered positive for osteomyelitis. In the remaining 11 sites, there was no proven evidence of infection. INFECTON scans gave positive results for 14 of 15 sites of infected implants. WBC imaging was positive in 11 of 15 sites with osteomyelitis. There were 14 true-positive, 1 false-positive, 10 true-negative and 1 false-negative results with INFECTON. With Tc-99m HMPAO WBC, the figures were 11, 2, 9, and 4, respectively. Values for sensitivity, specificity and accuracy are 93 %, 91 %, 92 % with INFECTON scan, and 73 %, 82 %, 77 % with WBC scanning. Differences between the two agents were statistically significant ($p < 0.05$)
Conclusion: We concluded that INFECTON is a better agent for detecting prosthetic implant infections comparing to Tc-99m HMAPO WBC scintigraphy. The lacking of bone marrow uptake of INFECTON makes it more powerful agent particularly in proximal extremities, mostly where prosthetic implants present

OTHER CLINICAL SCIENCE. MISCELLANEA 2

PS_561

SOMATOSTATIN RECEPTOR SCINTIGRAPHY AND BETA-2-MICROGLOBULIN IN THE DIAGNOSIS, STAGING AND FOLLOW-UP OF MALIGNANT LYMPHOMAS

D. Vassileva (1), S. Sergieva (2). (1) National Centre of Haematology and Transfusiology; (2) National Centre of Oncology, Sofia, Bulgaria.

Various tumours contain high number of somatostatin receptors, which enable the use of somatostatin receptor scintigraphy (SRS) for visualisation of these tumours. The purpose of this study was to assess the value of SRS, serum beta-2-microglobulin and the correlation between them for diagnosis and staging and follow-up of patients with malignant lymphomas. Forty-five patients with malignant lymphomas were investigated (20 with non-Hodgkin's lymphomas and 25 with Hodgkin's Disease). Planar and SPECT images were performed 24 hours and 48 hours after i.v.injection of 110-185 MBq 111-In labelled octreotide (Mallinckrodt, Petten) on the rotating gamma camera (Diacam, Siemens). SRS results were compared with the data of conventional methods (clinical examination, x-ray, CT, bone marrow biopsy). Beta-2-microglobulin levels were measured by radioimmunoassay using the Immunotech international microtest.
The SRS was true positive in 36 patients with malignant lymphomas. Ninety-two lesions were identified. Twenty-three of them were with extranodal localisation. Seven previously unknown localisations were visualised in 5 patients. Additional CT and ultrasound examinations confirmed the presence of a tumour tissue. Clinical staging of all these patients were changed. Significant correlation was found in patients with true positive SRS and higher serum beta-2-microglobulin in patients with an advanced disease. In 2 patients false positive results on the SRS were found. True negative scans were obtained in 7 patients.
These data indicate that malignant lymphomas express somatostatin receptors in sufficient quantity and density to allow a tumour visualisation with 111-In labelled octreotide. In conclusion, SRS provides a sensitive non-invasive diagnostic modality to localize a tumour tissue of malignant lymphomas and the positive scintigraphy shows a good correlation with the data of serum beta-2-microglobulin in different stages of the disease.

PS_562

DOES 111IN-OXINE PLATELET SEQUESTRATION PATTERN HAVE ANY IMPACT IN THE MANAGEMENT OF PATIENTS (PTS) WITH CHRONIC IDIOPHATIC TROMBOCYTOPENIC PURPURA (ITP)?

A. Sevilla, P. Colarinha, H. Camejo, T. Rézio, G. Ramos, M. Vieira.
Instituto Português de Oncologia F.G., Lisbon, Portugal.

In chronic ITP when corticosteroid therapy failed and splenectomy is considered necessary just 80% of patients will afford cure of disease.
The aim of this work is to assess the clinical impact of the platelet kinetic studies in the management of chronic ITP patients.
Method: It has been reviewed the management and treatment result of a group of 43 chronic ITP patients with platelet lifespan longer than 4 days and submitted to a platelet kinetic study. Abnormal platelet sequestration site (spleen, liver, spleen & liver) has been correlated with the management (proposed splenectomy vs. others therapeutic options). Therapy results have been checked (complete remission vs. trombocytopenic). Platelet sequestration site analysis was based on external probe spleen and liver counts. Each measure was acquired under identical conditions so that a day-to-day profile could be recorded (after ^{111}In decay correction).
Sequestration was analysed according to the following activity ratio: (Spleen at last day of platelet lifespan/Spleen at 30thmin=S) and (Liver at last day of platelet lifespan /Liver at 30th min. =L). Abnormal high platelet sequestration was considered when the ratio value was ≥1,20. Four different sequestration patterns have been found: Splenic (S≥1,2&L≤1,2), Hepatic (S≤1,2&L≥1,2), Mixed (S≥1,2&L≥1,2) and Absent (S≤1,2&L≤1,2).
Results: Splenectomy has been the therapeutic option for 24/31 pts with splenic sequestration and for 2/11 pts with hepatic and mixed. Up to now 19pts* have already been operated with complete remission for all except one** case of mixed sequestration.

Sequestration pattern	Splenic (n=31 pts)	Hepatic (n= 7 pts)	Mixed (n= 4 pts)	Absent (n=1pts)
Proposed splenectomy	24	1	1	0
Splenectomized *	17	1	1**	0
Others therap. options	7	6	3	1

Conclusion: The sites of abnormal platelet sequestration have been taken into account in the management of the disease concerning this group of 43 chronic ITP patients. Splenectomy is mainly considered in purely splenic sequestration and mainly avoided in hepatic and mixed sequestration pattern.

Poster presentation

PS_563

RADIONUCLIDE IMAGING OF ESOPHAGEAL AND PULMONARY INVOLVEMENT IN PROGRESSIVE SYSTEMIC SCLEROSIS

N. Prandini (1), R. La Corte (2), L. Feggi (1), A. Ciprian (1), S. Panareo (1), D. Santilli (2), F. Trotta (2). (1) Department of Nuclear Medicine; (2) Department of Rheumathology, S.Anna Hospital, Ferrara, Italy.

Esophageal transit scintigraphy and Tc99m-DTPA alveolar permeability seem to be valid methodologies to assess impaired esophageal motility and active alveolitis in systemic sclerosys (SS).

We compared the results of 126 esophageal scintigraphies and lung clearances performed in 114 SS patients (10 patients had 2 double studies and one 3 double studies).

After an overnight fast, all subjects underwent to repeated transit of single radionuclide swallows, using both liquid and semisolid boli (10 ml fruit puree) labelled with 99mTc-sulfur colloid, orally ingested in upright and supine positions. A visual analysis of condensed images and a calculation of mean transit time (integral method) were performed independently by two physicians: the patients were scored from 0 (all normal transit) to 4 (all pathological transit).

Within 2 weeks the same patients underwent to a measure of pulmonary epithelial permeability calculating the half time after ventilation of Tc99m-DTPA: an half time higher than 60 minutes was considered normal; values of half time between 40 and 60 minutes were considered mild accelerated and values lower than 40 minutes were considered highly pathological.

The table summarize our results comparing the two scores obtained with esophageal scintigraphy and lung clearance: only 9 patients resulted normal with both procedures. Most of the patients had alterations of either pulmonary alveolar permeability or esophageal transit time and 83 of both.

These findings indicate that in SS the visceral involvement of the disease is frequent. The radionuclide studies are useful methods to demonstrate the early involvement of both respiratory and digestive apparata.

PS_564

AN IMPROVED PROTOCOL FOR INCREASING THE POTENTIAL OF LYMPHOSCINTIGRAPHY IN PATINTS WITH PERIPHERAL LYMPHEDEMA

G. Taddei (1), F. Buffoni (1), P. Erba (1), M. Carletto (1), M. Bagnasco (1), G. Agnese (1), F. Castagnola (1), F. Boccardo (2), G. Villa (1), C. Campisi (2), G. Mariani (1)(1) Nuclear Medicine Service, DiMI - University of Genoa, Genoa, Italy; (2) Microsurgery Unit, University of Genoa, Genoa.

Objectives: To improve the conventional protocol of lymphoscintigraphy in patients (pts) with peripheral lymphedema, with the aim of increasing the diagnostic potential of this procedure in the characterization of both the Superficial Lymphatic Circulation (SLC) and Deep Lymphatic Circulation (DLC).

Methods: A total of 137 consecutive pts were evaluated, 90 women and 47 men with mean age 51.78±18.03 yr (median 53, range 0,33-86): lymphedema was primary in 31 and secondary in 108 pts, affecting the lower limbs in 106 pts, the upper limbs in 36 pts (about 50% of the pts had bilateral lymphedema). The DLC was evaluated first, by injecting ^{99m}Tc-nanocolloid albumin (most of the particles between 30-80 nm) in aliquots of 300-500 μCi (11-18 MBq) in the aponeurotic sites of the palms or soles using a 25G needle. The pt is then asked to exercise for 5 min, and gamma-camera images are recorded until complete visualization of regional draining lymph nodes (usually within about 10-15 min). The SLC is evaluated next, by injecting similar tracers doses intradermally at approximately the same sites and applying massage. Static scans are then recorded similarly as done for DLC, and superficial regional lymph nodes are usually visualized within 5-10 min (recording is continued until visualization of the liver).

Results: Based on semiquantitative evaluation, the lymph flow was found to be normal in 37% and, respectively, 37% for the DLC and SLC, while it showed mild delay in 51,7% DLC and 50,4% SLC, moderate delay in 26,6% DLC and 31,6% SLC, and severe delay in 21,7% DLC and 18% SLC (the latter was associated with dermal back-flow in 0.5% Dlc and 10.5% SLC). Correlation between the overall lymphoscintigraphic pattern and the site of obstruction was found in 98% of pts with monolateral and in 60% of pts with bilateral lymphedema. Instead, there were no differences between the DLC and SLC patterns in primary or secondary lymphedema.

Conclusion: Evaluating both the DLC and the SLC in the same scintigraphic session enabled to better classify the various pattern of abnormal lymph flow. In particular, knowledge of the DLC pattern increased sensitivity of the procedure by about 20%.

PS_565

CURRENT ROLE OF LYMPHOSCINTIGRAPHY IN THE STUDY OF CHRONIC LYMPHEDEMA OF THE LOWER EXTREMITIES

M. Mitjavila, M.A. Balsa, L. GªCañamaque, P. GªAlonso, F.J. Penin, V. Torres, C. Pey. Nuclear Medicine Department, H.U.Getafe, Medrid, Spain.

Patients: 31 patients (25F, 6M) complaining of swelling one or both lower extremities were studied. 9/31 patients had associated pathologies: 2 neoplasm, 4 venous pathology, 2 leg trauma and 1 retroperitoneal fibrosis.

Method: The lymphoscintigraphy (LS) studies were performed by interstitially injecting 111 MBq (3mCi) 99mTc-Sn sulphur microcolloid, divides into four equal portions of 0.1 ml, into the webbed spaces of both feet. Whole body images were obtained at 20 minutes and 2-4 hs after injection.

Qualitative assessment of images was performed: 1) presence of asymmetries of lymphatic vessels and groin nodes and 2) signs of imparied lymph flow (pooling of radionuclide, intradermal backflow and identification of collateral vessels). The diagnostic categories ranged from: normal, hypoplastic, aplastic, megalymphatics and dermal backflow.

ECO doppler of lower extremities was also performed on all patients, pelvic CT on 2 patients and MRI on other two.

Results: In 12 patients there were no signs of lymphedema. In 19 patients the presence of lymphedema was diagnosed, 5 of them secondary. In 12/19 patients hypoplastic or aplastic lymphedema was found and megalymphatics in 3. In 7/19 patients dermal backflow was observed whith or without other categories (hypoplastic 2, megalymphatic 1). In patients with vascular problem in lower extremities lymphatic involvement was showed by scintigraphy in 2.

Conclusion: In patients with limb swelling, lymphoscintigraphy is a noninvasive, simple and useful procedure in the differential diagnosis of lymphedema from other sources of edema.

PS_566

PLASMA VOLUME (PV) MEASUREMENT IN SUSPECTED POLYCYTHAEMIA - DIRECT MEASUREMENT OR INDIRECT MEASUREMENT?

N. Nagaraj (1), K. Shmueli (2), F. Nadir (3). (1) Department of Nuclear Medicine; (2) Department of Medical Physics; (3) Department of Haematology, Charing Cross Hospital, London, UK.

Although only red cell mass (RCM)measurement is required to evaluate pts with polycythaemia,

the additional measurement of PV helps in the interpretation of the results and subclassification of patients. Due to cost and limited shelf life I-131 HSA required for PV measurement may not always be available and PV is indirectly estimated from the measured RCM and venous Haematocrit (Hv) using the formula PV = RCM [1/ (0.91 x Hv)- 1]

To compare the two methods &determine the clinical relevance of differences if any, we indirectly estimated the PV of 60 consecutive pts with suspected polycythaemia whose PV & RCM were measured directly using I-125 HSA and 51-Cr respectively. The results were interpreted according to ICSH criteria based on surface area. The final diagnosis based on actual measured results and clinical follow up were True polycythaemia (TP) (28) and apparent polycythaemia(AP) (32).

Differences between the two methods was calculated as estimated- measured /measured and ranged from −24% to +28%. Although the indirectly estimated method demonstrated only <5% difference in 55% of the cases, there were larger discrepancies with >±10% difference in 25% of the cases of which 5 pts had differences >±25%.

Since the hallmark of TP is an elevated red cell mass, diagnosis was not affected in this group despite >±10% differences in the estimated PV. In AP gp, primary diagnosis was not affected by indirect method despite overestimation of PV in 4 pts and underestimation in 3 pts resulting in incorrect subcategory placement within the same group. However, incorrect subcategorisation did not affect the clinical management and the reasons for this will be discussed.

In conclusion, although direct measurement of PV in suspected polycythaemia is preferable, indirect estimation from actual measured RCM and venous haematocrit may be substituted effectively for routine clinical purposes.

PS_567

COMPARISON OF PENTETREOTIDE INDIUM 111 AND GALLIUM 67 SCINTIGRAPHIES IN LYMPHOMAS

D. Huglo (1), M. Nocaudie (1), B. Quesnel (2), F. Morscchauser (2), X. Marchandise (1). (1) Department of Nuclear Medicine; (2) Department of Haematology, Hopital C. Huriez, C.H.R.U. of Lille, Lille - France.

FDG uptake in lymphoma is usually compared to gallium 67 citrate (Ga67) uptake. The aim of this prospective study was to compare pentetreotide-indium 111 (OctreoScan, Mallinckrodt) and Ga67 uptakes in residual masses of lymphomas.
Methods : Patients with Hodgkin's disease or with intermediate-grade or high-grade of non-Hodgkin's lymphoma were considered before therapy. Patient was included if he had at least a superficial palpable mass or a mass bigger than 7 cm. Whole body study (8 cm/min.) and static images (600 s per frame) were acquired 24 hours after intravenous injection of 185 MBq of pentetreotide-indium 111 and 72 hours after injection of 260 MBq of gallium 67. A SMV DSX gamma camera equipped with a ME collimator was used. Scintigraphies and CT-scan were performed first at diagnosis before therapy (n = 9), then after 4 cycles of chemotherapy (n = 6) and finally at the end of therapy (n =5).
Results : Nine patients were included, 3 with Hodgkin's disease, 6 with non-Hodgkin's lymphoma. At diagnosis, all abnormalities were seen with both radiopharmaceuticals in 8 patients of 9, but there were differences between uptakes according to sites. The contrast was always higher with Ga67 but bone uptake of this tracer could be a real problem. For 1 patient with mantle cell lymphoma, no uptake of pentetreotide was registered on the sites positive with Ga67. After 4 cycles of chemotherapy, two other patients did not want to proceed ; all abnormal sites had decreased uptake or had no uptake. Two patients had no residual uptake. Residual uptake was seen either only with Ga67 (n = 2), or only with pentetreotide (n = 2). At the end of therapy (n = 5), one of these later patients could not be studied, the other showed again on the same site uptake of pentetreotide alone, in agreement with CT scan which evoked an active residual mass. The scans of the 4 other patients were normal (except in one case uptake of pentetreotide-indium secondarily to radiotherapy).
Conclusion : The weak number of patients did not allow to demonstrate greater performances of one tracer over the other, but our results show that pentetreotide and Ga67 scans are complementary rather than opposite. Differences between the uptakes of the tracers deserve more detailed cellular studies.

PS_568

NON-INVASIVE VERSUS INVASIVE METHOD OF PLATELET PRODUCTION ESTIMATION IN THROMBOCYTOPENIC PATIENT

M. Todorovic-Tirnanic (1), V. Obradovic (1), S. Pavlovic (1), M. Colovic (2), N. Suvajdzic (2), I. Elezovic (2), V. Starcevic (3), N. Milic (3), V. Bosnjakovic (1). (1) Nuclear Medicine Institute, Clinical Center of Serbia, Belgrade, YU; (2) Haematology Institute; (3) School of Medicine, Belgrade, YU.

The **aim** was to compare results of non-invasive (PI, platelet production index) and invasive (Mk, megakaryocyte abundance) method of platelet production estimation in thrombocytopenic patients.
Methods: PI was calculated on the basis of ^{111}In-oxinate labelled platelet life span (LS) and Pt blood count (BC) determination for subjects with linear platelet survival curve (formula I).

$$PI_l = (LS_h \times BC_i)/(LS_i \times BC_h) \quad (I)$$

$$PI_e = (R_i \times BC_i)/(R_h \times BC_h) \quad (II)$$

Formula II was used for PI calculation in the cases with exponential platelet survival curve. R is the platelet renewal; i, investigated person; h, healthy subject. Platelet renewal was calculated using the formula: $R=[\ln 2/(T/2)] \times 100 = (69,3)/(T/2)$, where T/2 is the labelled Pt half-life. Megakaryocyte abundance was graded as 1. numerous, 2. present, 3. poor Pt production, 4. rare megakaryocytes.Fifty-five persons were investigated: 49 TP, thrombocytopenic patients (40 ITPc, chronic idiopathic thrombocytopenic purpura; and nine MDS, myelodysplastic syndrome) and six C, control, healthy subjects. In TP both methods (PI and Mk) were applied, while in C only PI was determined.
Results: We obtained linear platelet survival curve in all MDS and C subjects. Mean value for LS in MDS was 8,2 days, while in C group it was 8,9 days. There was no significant difference in LS between MDS and C group. In ITPc patients we obtained exponential platelet survival curves and shortened platelet LS (mean LS value was 1,1 day). There was highly significant difference in LS between ITPc and C group, and also between the two TP groups: ITPc and MDS ($p<0,001$). The mean value for PI in C group was 1,0 (SD=0,2); in ITPc 1,2 (SD=0,5), while in MDS it was 0,2 (SD=0,2). Highly significant difference was noticed in PI between the two TP groups: ITPc and MDS ($p<0,01$), as well as between MDS and C group ($p<0,01$). PI was significantly lower in MDS than in ITPc or C group. Mean value for Mk in ITPc group was 1,0 (SD=0,8) and in the MDS group it was 1,0 (SD=1,4). There was no significant difference in Mk between ITPc and MDS group ($p>0,05$).
Conclusions: Non-invasive method of PI determination is better method for Pt production estimation than invasive megakaryocyte abundance determination. Together with Pt LS determination, PI non-invasively and reliably differentiates between thrombocytopenia caused by inadequate Pt production (MDS) and thrombocytopenia caused by increased Pt production (ITPc).

PS_569

THE BEHAVIOUR OF CONCENTRATIONS OF INTERLEUKINES IL-1BETA AND IL-6 IN PLASMA AND IN LYMPHOCYTES OF PATIENTS WITH B-CELL CHRONIC LYMPHOCYTIC LEUKAEMIA WITH REGARD TO DISEASE PROGRESSION

A. Parfienczyk (1), B. Kiersnowska -Rogowska (2), F. Rogowski (1), E. Jaroszewicz (1), A. Citko (1). (1) Department of Nuclear Medicine; (2) Department of Haematology, Medical University, Bialystok, Poland.

B-cell chronic lymphocytic leukaemia (BCLL) belongs to malignant lymphomas and originates from the immunological system. The etiopathogenesis of the disease has not been fully explained yet. Cytokines propably take part in the development and in the course of the BCLL.
Therefore **the aim** of the study was determination of the concentrations of IL-1β and IL-6 in blood plasma, culture supernatant and in isolated, ultrasonically broken lymphocytes obtained from patients with BCLL (12 individuals in I stage and 12 in III stage according to the Rai classification, aged 45-65 years) and from 10 healthy volunteers (staff members of Nuclear Medicine Department). The double two hour limphocyte cultures of each patient were conducted with and without mitogene (Neupogen, Roche) simultaneously.
Methods: The measurement of the concentrations of the interleukins mentioned above was made using immunoradiometric kits from Bioscource Europe, S.A. (Belgium). Mitogene was added to trigger blastic transformation and lymphocyte activation.
Results: A significant increase in IL-1β and IL-6 concentrations were found in blood plasma in I and in III stage of BCLL , before and after stimulation in the supernatant culture and in the isolated, broken lymphocytes in I and in III stage of BCLL. A significant difference was observed between the levels of cytokines in the nonstimulated and stimulated with Neupogene cultures at the same time. In most cases these concentrations were higher after stimulation.
Conclusions: Increased concentrations of IL-1β and IL-6 in the plasma and in the culture supernatant may indicate that leukaemic lymphocytes release these interleukines known as the stimulators of the leukaemic proliferation. Elevated concentrations of IL-1β and IL-6 in the broken lymphocytes may be characteristic feature of neoplasmatically changed lymphocytes.

PS_570

ROLE OF GFR AND ERPF IN PREDICTING RENAL DYSFUNCTION IN ANAEMIC PATIENTS WITH NORMAL SERUM BIOCHEMISTRY

C. .S. Bal (1), A. Ghosh (2), B.L. Jailkhani (2), A. Kumar (1). (1) Department of Nuclear Medicine; (2) Department of Laboratory Medicine, New Delhi, India.

Objective: Anaemia causes multisystemic functional changes, including that of kidneys. However, in early stages, biochemical parameters for renal function may remain within normal limit. We tried to find out the role of GFR and ERPF in such conditions. **Methods:** Seventy-six subjects were recruited in this study. They were divided into following groups: group A: patients with Hb ≤ 3 gm/dl (n=33); group B: patients with Hb ≤ 6 but > 3 gm/dl (n=33); group C: healthy controls with normal renal function and Hb > 12gm/dl. Thirty-six patients had iron deficiency anaemia (A=20, B=16), 24 had aplastic anaemia (A=11, B=13) and the rest 6 had megaloblastic anaemia (A=2, B=4). No subject had hypertension, diabetes, primary renal disease or any other systemic illness, affecting kidney. Various biochemical parameters for renal function along with GFR with Tc-99m DTPA and ERPF with I-131 OIH were calculated. **Results:** Average duration of anaemia was 3.5 months. Fourteen patients had mild to moderate pedal edema (A-10; B-4). Out of them, 8 had palpable liver and signs of systemic congestion. Signs of raised systemic venous pressure (raised JVP) were found in 7 patients from group A. Urine output was >600 ml/day in all cases. Demographic and clinical profile of all the subjects is given in the following table:

Table: Demographic and clinical profile

Diagnostic indices	Group A	Group B	Group C
Age	32.7±3.8	32.0±3	31±2
Sex (M:F)	3.1	0.94	4.0
Haemoglobin (mg/dL)	2.6±0.05	5.3±0.11	13.5±0.3
Blood urea nitrogen (mg/dL)	28±2.38	23+1.3	16.5+2.2
Serum Creatinine (mg/dL)	1.06+0.05	0.81+0.04	0.81+0.06
Serum Potassium (mEq/L)	4.49+0.09	3.67+0.09	3.8+0.12
Serum Calcium (mg/dL)	8.98+0.15	8.74+0.11	8.97+0.23
Serum Phosphate (mg/dL)	4.3+0.16	4.11+0.15	3.98+0.4
Routine Urine Examination	N	N	N
GFR (ml/min/1.73m^2 BSA)	60.0±0.71	72.0±1.43	109±2.9
ERPF (ml/min/m^2 BSA)	362±18.4	422±19	559±38.5

Values are expressed as mean ±1SEM; N= normal

Poster presentation

Although, Blood urea nitrogen, serum creatinine and serum potassium was relatively higher in severely anaemic patients, all biochemical parameters for renal function were within normal reference range, used in our laboratory. However, GFR and ERPF were significantly reduced among patients, indicating sub-clinical renal dysfunction; the reduction was correlating well with the severity of anaemia.
Conclusions: Anaemia leads to sub-clinical renal dysfunction. Though biochemical parameters for renal function may remain normal in early stages, GFR and ERPF are significantly reduced in such patients and can help in early diagnosis.

PS_572

DIPYRIDAMOLE STRESS TEST FOR EARLY EVALUATION OF CEREBRAL CIRCULATORY DISORDERS

T. Molnar (1), K. Zambo (2), E. Schmidt (2), E. Udvaros (2), L. Bogar (1).
(1) Department of Anaesthesia and Intensive Care; (2) Department of Nuclear Medicine, University Medical School of Pecs, Hungary.

Aim: The diagnosis of transient ischaemic attack (TIA) is mainly retrospective, based on the clinical symptoms presented by the patient. Professionals in nuclear medicine have made a successful attempt to detect TIA by single photon emission tomography (SPECT) imaging using stress test (e.g. acetazolamide) which is well known in literature. Dipyridamole stress test combined with SPECT imaging of patients with ischaemic heart disease is regularly performed in our department. After injecting dipyridamole intravenously we have found various forms of transient neurologic deficit.This is a retrospective study of SPECT brain scan using dipyridamole as a stress agent to assess transient cerebral circulatory disorders in patients with ischaemic heart disease.
Methods: The criterium of inclusion was transient neurological deficit during cardiac dipyridamole stress test. Selected TIA positive patients (23/100) were examined further on. We performed SPECT scanning of the brain with, and one week later, without dipyridamole stress. Dipyridamole was given intravenously according to the protocol (0.57mg/kg) before infusion of 99mTc-HMPAO. Patients were studied 30min later using a rotating gamma camera. Visual analysis of the scans was based on the consensus of two independent investigators. Neurological examination was also obtained before, during and after dipyridamole stress.
Results: The brain SPECT combined with dipyridamole stress was positive in all patients of the TIA positive group. Localizations of hypoactive foci were compared to the clinical topography based on neurological examination and good correlation was revealed. The brain SPECT imaging in resting condition showed variable regression (total, partial) of the perfusion abnormalities. However, permanent perfusion deficit in resting condition indicates subclinical lesion if the neurological status is negative.
Conclusion: The transient neurological deficit observed in 23% of the dipyridamole stressed patients with ischaemic heart disease is a considerably higher incidence than reported previously in literature (1.22/10,000). This test may be suitable to provoke TIA safely, therefore combined with brain SPECT it could play an important role in neurologic diagnostic procedures, stroke prevention and preoperative management of patients scheduled for cardiac surgery.

NEUROLOGY / PSYCHIATRY 4

PS_571

BRAIN SPECT IN ACUTE CRANIOCEREBRAL INSULT PATIENTS: COMPARISON WITH DIFFUSION AND PERFUSION MAGNETIC RESONANCE IMAGES

E.N. Kim, H.S. Sohn, S.H. Kim, Y.A. Jung, I.R. Yoo, S.K. Chung.
Departments of Nuclear Medicine, College of Medicine, St. MaryÂøs Hospital, The Catholic University of Korea.

Aim: In this study, we compared findings of brain SPECT with conventional T2- weighted magnetic resonance image, diffusion- and perfusion weighted brain MRI in acute craniocerebral insult patients. Methods: Seven acute craniocerebral insult patients were studied by Tc-99m HMPAO brain SPECT, conventional MRI, and diffusion- and perfusion brain MRI. Brain SPECT was obtained and processed using two head gamma camera (ECAM; Siemens, Erlangen, Germany), and MR images were obtained using 1.5 Tesla machine (Vision Plus; Siemens, Erlangen, Germany) and processed using home made software written in IDL and C^{++}. All images were taken within 3 days. We compared the findings of these modalities and clinical situations of patients.
Results: In all images except conventional T2 weighted image, insult-related changes were relatively well observed. The lesions on the brain SPECT were largest of all other modalities. On brain SPECT, insult-related changes of cerebral blood flow were well observed with higher signal to noise ratio (SNR) than cerebral blood flow map on perfusion MRI. However, with brain SPECT alone, we could not differentiate recent insult related changes from blood flow changes resulting from previous insult prior to recent insult. Diffusion weighted MRI demonstrated cytotoxic edema areas with highest SNR and shortest acquisition and post-processing time. Perfusion weighted images could demonstrate other information such as time to peak map, cerebral blood volume map, and mean transit time map in whole brain as well as cerebral blood flow map, but with relatively low signal to noise ratio and longest post-processing time. The findings of brain SPECT and diffusion weighted images showed better correlation with clinical situation of the patients.
Conclusion: Diffusion weighted MR and brain SPECT are more useful than conventional T2 weighted images and perfusion weighted MR in patients with acute craniocerebral insult patients due to their higher SNR and short post-processing time.

PS_573

REGIONAL CBF QUANTIFICATION IN ANEURYSMAL SUBARACHNOID HEMORRHAGE

M. Hosono, K. Machida, T. Matsui, N. Honda, T. Takahashi, A. Kashimada, H. Osada, Y. Shimizu, M. Ohmichi, S. Dei, T. Asano
Department of Radiology, Saitama Medical Center, Kawagoe, Japan.

Regional cerebral blood flow (rCBF) may variably change due to cerebral vasospasm as well as surgical invasion in aneurysmal subarachnoid hemorrhage (SAH). To date, cerebral perfusion imaging has been useful in monitoring patients (pts) with SAH. In this study, rCBF was quantified by using 99mTc-ECD to determine if rCBF changes were observed and if the rCBF measurement enabled the detection of symptomatic vasospasm.
Methods: Thirty-five consecutive pts with SAH (55±12 yo) who underwent clipping had 99mTc-ECD examinations at days 1 and 7 after surgery. mCBF was measured by Patlak plot analysis and then SPECT was performed with calculation of absolute rCBF values using Lassen's correction as previously reported. Regions of interests were placed at 12 regions on rCBF maps, that is, the bilateral cerebellar hemispheres, frontal, temporal, occipital lobes, basal ganglia, thalami. rCBF-change was calculated as (rCBFday1-rCBFday7)//rCBFday1.
Results: Nine of 35 pts had vasospasm confirmed by angiography, CT and/or MR. When decrease of more than 10 % in rCBF from days 1 to 7 was considered significant, numbers of regions showing significant perfusion-decrease were 6.8 ± 3.8 and 2.2 ± 2.6 (p=.002) for pts with or without vasospasm, respectively. In terms of ability of discriminating vasospasm and non-vasospasm, number of perfusion-decrease regions showed (with a cutoff of 4 regions) the sensitivity, specificity, positive predictive value, and negative predictive value were 88.9 (8/9 pts), 73.1 (19/26), 53.3 (8/15), and 95.0 (19/20) %, respectively. Moreover, the absolute rCBF values indicated no significant differences between vasospasm and non-vasospasm in any of the 12 regions at either days 1 and 7. On the other hand, there were significant differences in rCBF-changes between vasospasm and non-vasospasm in 6 of 12 regions (rt cerebellum p=.016, lt cerebellum p=.009, rt frontal p=.037, lt frontal p=.002, rt temporal p=.036, rt occipital p=.005).
Conclusion: Significant rCBF changes were observed extensively in the brain in the course of SAH. The rCBF-change from day 1 to day 7 after surgery may be more useful than the absolute rCBF values for the detection of vasospasm.

PS_574

DEVELOPMENT OF SUPER RAPID DYNAMIC SPECT, AND ANALYSIS OF 99MTC-ECD DYNAMICS IN ISCHEMIC LESION

A. Komatani, Y. Sugai, T. Hosoya. Department of Radiology, Yamagata University, Yamagata Japan.

Aim: Development of super rapid dynamic SPECT (single photon emission computed tomography) system, and analysis of early phase dynamics of 99mTc-ECD (ethyl cysteinate dimer) in ischemic lesion using the SPECT system.
Methods: We newly developed a super rapid SPECT system, which enabled to take a SPECT series every 2 seconds. Each SPECT series contain maximal 16 slices (6.6mm thickness) in matrix size of 32 x 32. This system was designed originally based on the „CERASPECT" (DSI, Inc, Waltham, MA, U.S.A).
Twenty patients with ischemic lesion that was detected clearly by 133Xe-rCBF (regional cerebral blood flow) SPECT but unclear on the static 99mTc-ECD SPECT were examined. For the dynamic SPECT, 700MBq of 99mTc-ECD were injected intravenously, and dynamic SPECT data was acquired every 2 or 3 second during 90 second or more. The serial dynamic SPECT and time-activity curves at some reduced lesion in rCBF and at the contra-lateral normal brain were analyzed. These dynamic SPECT data were compared with conventional static 99mTc-ECD SPECT and quantitative 133Xe-rCBF SPECT.
Results: The sensitivity of this system was 175 kcps/MBq/ml/cm slice thickness, and resolution was 17mm FWHM at the center of 20cm$B&U(B water phantom.
All of mildly or moderately reduced rCBF lesions on the 133Xe-rCBF SPECT were recognized as a low activity region only at the early phase (about 2-20sec.), and vanished the lesion gradually. These lesions were not recognized on the conventional static SPECT taken after the dynamic study.
Conclusions: This study suggests that the esterase activity participate in ECD retention is tolerated to the mild or moderate ischemia. The tolerance may be one of the most important causes of the non-linearity in correlation of ECD accumulation with the cerebral blood flow.

PS_575

ICTAL AND INTERICTAL TC-99M HMPAO BRAIN SPECT IN PEDIATRIC MIGRAINE WITH AND WITHOUT AURA

M. Sahin (1), T. Karslı (2), S. Uysal (2), T. Basoğlu (1). (1) Department of Nuclear Medicine; (2) Department of Pediatrics,19 Mayıs University, Samsun, Turkey.

The objective of this investigation was to evaluate changes in regional cerebral blood flow (rCBF) on pediatric patients suffering from migraine with aura (classic migraine) and without aura (common migraine).
Methods: Nine patients with aura (age ranges: 11-16, mean age±sd: 13.5±2) and 12 patients without aura (age ranges: 7-16, mean age±sd: 12.3±3) were studied. Tc-99m HMPAO study was performed during the headache- free (interictal) and headache periods (ictal). Transaxial slices parallel to orbitomeatal line (by adding 3 slices passing from the cerebellum, basal ganglia, supraventrikuler region and vertex) were used to determine the mean corticocerebellar ratio of total 17x2 brain regions. Paired-t test was used the compare the mean rCBF values in ictal and interictal period images of patients with aura and without aura. Student-t test was used to compare the mean rCBF for ictal images in patients with aura and without aura, as well as to compare interictal images.
Results: Ictally, decreased rCBF values were found in 8/9 patients with aura and 6/11 patients without aura. Decreased rCBF values were observed in 6/9 patients with aura and 2/11 patients without aura during the interictal period. Two patients without aura showed hyperperfused areas in addition to hypoperfused areas in ictal period. Any patient showed new lesion in interictal period. Significant differences were detected between patients with aura and without aura in ictal and interictal periods, as well as between ictal and interictal rCBF values in patients without aura. No significant difference was detected between ictal and interictal rCBF values in patients with aura. The distribution of hypoperfused brain regions in brain lobes was indicated in table.

	With Aura		Without Aura	
	Ictal	Interictal	Ictal	Interictal
Frontal	33 / 144 (%23)	19 / 144 (%13.2)	12 / 176 (%6.8)	2 / 176 (%1.1)
Parietal	15 / 72 (%21)	11 / 72 (%15.2)	14 / 88 (%15.9)	4 / 88 (%4.5)
Temporal	9 / 36 (%25)	6 / 36 (%16.6)	3 / 44 (%6.8)	1 / 44 (%2.2)
Oksipital	7 / 27 (%26)	2 / 27 (%7.4)	3 / 33 (%9)	1 / 33 (%3)

Conclusions: Migraineurs with aura revealed more prominent brain lesions than migraineurs without aura in both ictal and interictal period. _nterictal SPECT imaging alone underestimated number and extent of pathological areas. Therefore, ictal rCBF evaluation should be used to determine brain perfusion pattern.

PS_576

IMAGE-FUSION OF BENZODIAZEPINE RECEPTOR SPECT AND BRAIN MRI IN PRESURGICAL ASSESSMENT OF TEMPORAL LOBE EPILEPSY

M. Wissmeyer (1), R. Wiest (2), K. Schindler (2), J.P. Wielepp (1), L. Mariani (3), G. Schroth (3), B. Weder (4), F. Donati (2), D. Luescher (1), J.A. Kinser (1). (1) Department of Nuclear Medicine, University of Berne, Berne, Switzerland; (2) Department of Neurology, University of Berne, Berne, Switzerland; (3) Departments of Neurosurgery/Neuroradiology, University of Berne, Berne, Switzerland; (4) Department of Neurology, Cantonal Hospital, St. Gallen, Switzerland

Aim: The aim of this study was to evaluate the usefulness of the image-fusion of benzodiazepine receptor (BDR) SPECT using I-123-Iomazenil and brain MRI in the presurgical assessment of patients (pts) with therapy- refractory temporal lobe epilepsy (TLE).
Methods: We evaluated 21 pts with therapy-refractory TLE due to mesiotemporal sclerosis or other focal brain anomalies. 16 pts have been operated, 5 were inoperable due to the extent of the focal brain anomalies. To delineate the epileptogenic zone and to locate the presumed extent of resection, clinical evaluation, video-EEG recordings using scalp and semi-invasive foramen ovale electrodes, high resolution brain MRI, interictal CBF SPECT using Tc-99m-ECD and BDR SPECT were performed. Brain MRI and BDR SPECT were fused using a standardised computerised brain atlas (CBA).
Results: Of the 16 pts treated operatively, 10 pts had a 12-month outcome of Engel class I, 5 pts of Engel class II and 1 patient of Engel class III. Ictal semi-invasive foramen ovale EEG recordings located the epileptogenic focus in all pts in the temporal region. Reduced BDR density and correct delineation of the epileptogenic focus was shown in 20/21 pts. Brain MRI failed to detect morphological lesions in 2 pts, whereas BDR SPECT revealed a focal anomaly in both cases. There is a significant correlation between positive EEG/MRI findings and BDR SPECT with a sensitivity, a specifity and a positive predictive value of 0.94. The additionally performed interictal CBF SPECT localised the epileptogenic focus correctly in 16/21pts, corresponding to a sensitivity of 0.80, a specifity of 0.90 and a positive predictive value of 0.89.
Conclusion: BDR SPECT using I-123-Iomazenil fused with brain MRI is a non-invasive procedure that provides useful functional information in the delineation of temporal lobe epilepsy, especially in pts with negative morphological imaging techniques.

PS_577

ICTAL AND INTERICTAL SUBTRACTION CBF SPECT FUSED WITH HIGH RESOLUTION BRAIN MRI IN THE PRESURGICAL EVALUATION OF EPILEPSY: PRELIMINARY RESULTS

M. Wissmeyer (1), K. Schindler (2), R. Wiest (2), P. Ritter (1), K. Lövblad (3), B. Weder (4), F. Donati (2), K. Oswald (3), D. Luescher (1), J.A. Kinser (1). (1) Department of Nuclear Medicine, University of Berne, Berne, Switzerland; (2) Department of Neurology, University of Berne, Berne, Switzerland; (3) Department of Neuroradiology, University of Berne, Berne, Switzerland; (4) Department of Neurology, Cantonal Hospital, St. Gallen, Switzerland

Aim: The aim of this study was to determine the usefulness of the fusion of ictal and interictal subtraction CBF SPECT with high resolution brain MRI in the localisation of epileptogenic foci in patients with therapy-resistant epilepsy.
Methods: We evaluated 5 patients (2 male, 3 female; 30-37 years old) suffering from intractable epilepsy performing video scalp EEG registration and CBF SPECT using Tc-99m-ECD in the interictal state followed by an ictal CBF SPECT during a seizure with an injection on time (cutoff 30 seconds after EEG onset) in 3 cases and late injection in 2 cases. After normalisation of the SPECT data in all patients, interictal scans were subtracted from the ictal scans. All voxels with a difference of more than 3 standard deviations (SD) from the mean intensity of the subtraction scan were considered to truely delineate the epileptogenic focus. Additionally, both SPECT scans were compared with studies of healthy volunteers (n=16) in order to determine the extent (more than 3 SD) of the ictal hyperperfusion and interictal hypoperfusion. The results of this voxel-based statistical process were fused with high resolution MRI scans using the Brain Voyager software (Brain Innovation).
Results: The subtraction CBF SPECT scans located the epileptogenic focus correctly in circumscribed areas of the temporal lobe in all patients. The lateralisation to the right (n=4) and left (n=1) hemisphere corresponded with the video-EEG findings in all patients, whereas comparison with the MRI showed concordance in only 3/5 cases (1 patient with a normal MRI scan, 1 patient with a contralateral morphological abnormality). The fusion of the statistically processed subtraction CBF SPECT data with the high resolution brain MRI scans of the patients revealed involvement of the hippocampus in 2 patients, the insular cortex in 2 patients and the frontal pole of the temporal lobe in 1 patient. Subtracting only the ictal CBF SPECT data from the sampled normal scans of the healthy volunteers, we additionally found that the ictal hyperperfusion extended all over the temporal lobe ipsilateral to the presumed focus, affecting the mesial temporal lobe in each patient, and to distant areas corresponding to homotope areas of the contralateral hemisphere, which may correlate to the differing ictal injection times.
Conclusion: The fusion of ictal and interictal subtraction CBF SPECT with high resolution brain MRI provides independent functional information in the presurgical evaluation of epilepsy, especially in patients with normal or discrepant MRI findings.

PS_578

THE USEFULNESS OF REPEATED ICTAL SPET FOR LOCALIZATION OF EPILEPTIC FOCUS IN PATIENTS WITH NEOCORTICAL OR MULTIFOCAL SEIZURE: COMPARISON WITH IMAGING ANALYSIS BY SUBTRACTION AND ICTAL SPET SPM

M.C. Lee (1), Y.K. Kim (1), D.S. Lee (1), J.S. Yeo (1), J.S. Lee (1), S.K. Lee (2), C.K. Chung (3), J.K. Chung (1). (1) Department of Nuclear Medicine; (2) Department of Neurology; (3) Department of Neurosurgery, Seoul National University College of Medicine, Seoul, Korea.

Introduction: In neocortical or multifocal seizure, the ictal perfusion changes may be subtle or have complex pattern. It is particularly difficult to localize the epileptic focus by EEG, MR or conventional brain SPET. In this study, we investigated whether repeated ictal SPET during video-EEG monitoring could improve the sensitivity in localization of the epileptic focus. We compared the visual analysis of repeated ictal SPET with the results of the analysis using subtraction ictal image and ictal SPET SPM.

Methods: Twenty-two patients (8 FLE, 3 PLE, 2 lateral TLE, 1 OLE and 8 multifocal seizure) were included in this study. All patients got the unexpected or inconclusive results in first ictal SPET and performed repeated ictal SPET (second ictal SPET in 17 and more in five). Also, fourteen of these patients performed interictal SPET. After normalization using interictal SPET, subtraction images were acquired and co-registrated to standard MR. Using SPM analysis, the ictal perfusion in each scan was compared with the perfusion of 15 young healthy controls. Ictal image interpretation was performed independently and side-by-side analysis with interictal SPET.

Result: The first ictal SPET correctly lateralized seizure origin in 10 of all patients (45%), but localized epileptic focus in only 5. In another 12 ictal SPET (55%), no hyperperfusion area was founded. In second ictal SPET, ictal hyperperfusion localized correctly epileptic origin in additional 3 patients with single epileptic focus and the sensitivity improved from 29 % to 50 %. In cases of eight multifocal seizure, first ictal SPET indicated one seizure origin in 7. In second ictal SPET , another seizure focus was reveled in 5 (63%). SPM analysis with first ictal SPET gave the additional information for localization or lateralization in four, confirmatory information in five (corrected $p<0.01$) compared with visual analysis of repeated ictal SPET. However, SPM failed to show significant difference despite positive ictal SPET in three. Subtraction image analysis indicated additional epileptic zone in five scans that was not detected ictal hyperperfusion by visual analysis. Overall diagnostic sensitivity of subtraction image with first ictal SPET was higher than visual analysis of repeated ictal SPET (71.4 % vs. 50%).

Conclusion: Subtle ictal perfusion change in neocortical epilepsy could be found by repeated ictal SPET. Subtraction image analysis improved the diagnostic accuracy than visual interpretation or SPM analysis of ictal SPET. And repeated ictal SPET could indicate the different seizure focus suggested by ictal EEG in cases of suspected multifocal seizure.

PS_579

COMPARISON OF STATISTICAL PARAMETRIC MAPPING AND SUBTRACTION ICTAL IMAGE CO-REGISTERED TO MRI TEMPLATE: IN EVALUATION OF ICTAL BRAIN SPET

M.C. Lee (1), D.S. Lee (1), J.C. Paeng (1), J.S. Yeo (1), H.J. Jeong (1), Y.K. Kim (1), S.K. Lee (2), C.K. Chung (3), J.K. Chung (1). (1) Department of Nuclear Medicine; (2) Department of Neurology; (3) Department of Neurosurgery, Seoul National University College of Medicine, Seoul, Korea.

The subtraction ictal SPET has been reported to have improved diagnostic power with using co-registration to MRI. And meanwhile, statistical parametric mapping (SPM) was introduced and reported to be helpful to the performance of ictal SPET. In this study we compared the performance of these two methods.

Methods: Forty-nine patients with medically intractable epilepsy (age 26.9±8.8 years, 33 male and 16 female) and 15 normal volunteers were enrolled. All of the patients had surgically and pathologically proven diagnosis of epileptic focus. Thirty-five patients were diagnosed as temporal lobe epilepsy (TLE) and 14 patients, as neocortical epilepsy (NE). Ictal and interictal SPET were performed before operation in all patients and SPET was also performed in normal volunteers as the control group. Ictal SPET and SPET from normal patients were analysed using SPM99 software. The epileptic focus was localized by perfusion increase relative to normal control, with corrected threshold P value of 0.05 and 0.01. Afterwards, the subtraction ictal images were reconstructed and co-registered to MRI template for the better anatomical correlation. With this image, the epileptic focus was also localized by increased ictal perfusion relative to interictal one. The localizing power of these two methods were compared.

Results: In TLE patients, 27 were localized with SPM analysis (77%) and 21 of them were correct (78%). Subtraction and co-registration methods localized 26 (74%) patients and 24 of them were correct (92%). Among 8 patients who were unlocalized in SPM, 4 were additionally localized correctly in subtraction and co-registration method. In NE patients, 9 (64%) were localized and 8 of them were correct (89%) with SPM while 8 (57%) were localized and 5 (63%) of them were correct with subtraction and co-registration method. Among 6 patients who were unlocalized in SPM, no one was additionally localized with subtraction and co-registration method.

Conclusion: When the SPM was used in the interpretation of ictal SPET, the method of subtraction and co-registration to MRI template had some additive value in TLE. But the method did not have any additive value in neocortical epilepsy.

PS_580

INTERICTAL R-CBF BRAIN SPET, BRAIN MRI/CT AND EEG IN THE CLINICAL CHARACTERIZATION OF LESIONAL AND CRIPTOGENETIC PARTIAL EPILEPSY (PE)

R. Benti (1), E. Mariani (2), A. Antonini (2), F. Zito (1), M. Gasparini (1), C. Sdraiati (1), G. Pezzoli (2), P. Gerundini (1). (1) Department of Nuclear Medicine, Ospedale Maggiore-IRCCS, Milano, Italy; (2) Neurosciences Department,Istituti Clinici di Perfezionamento,Milano, Italy.

Ictal r-CBF SPET is an established adjunct to EEG in the pre-surgical localization of epileptogenetic zones unresponsive to medical treatment. However, the role of r-CBF SPET assessment in PE is still debated. Interictal SPET, routine EEG and MRI/CT brain studies were obtained in 28 PE patients diagnosed according to the ILAE criteria (age 45±8 ys; duration 17.7±5 ys). Clinical localization was temporal (15) occipital (6), frontal (4), parietal (1) and fronto-parietal (2). PE presented as secondary (SPE) to brain lesions (16 cases) or as cryptogenic partial epilepsy (CPE) with normal MRI. SPET was performed after Tc-99m ECD injection using a dedicated gamma-camera; after iterative reconstruction, focal ipoperfusions were assessed by visual analysis and quantitated by ROIs analysis vs. contralateral structures. EEG-Epileptifom Abnormalities (EA) where present in 20/28 cases: 16 consisting with the clinical seizure presentation (CSP) and in 4 patients consisting with a non-specific findings. SPET showed 29 focal defects (24 cortical, 5 subcortical) in 23/28 patients, mean r-CBF impairment in SPE and CPE foci detected was 27.1±10.8 % and 16.4±3.6 respectively. In the SPE group, SPET localization matched clinical seizure presentation (CSP) better than EA (9/16 vs 12/16 patients, $p=0.02$), whereas lesion location/extension assessement by MRI/CT was related to CPS in 6/16 cases only. Moreover EA, SPET and CPS matched in 4 extralesional foci showing normal MRI/CT findings. In CPE group, interictal EA was present in 6/12 and focal hypoperfusions in 9/12 patients. EA and SPET patterns in CPE positively matched CPS in 33% and 58% respectively ($p<0.05$), in 4/12 both EEG and SPET positively matched CPS. Interictal SPET pattern of focal hypoperfusion positively correlated with the presentation of seizure in SPE (75%) and CPE (58%), and localized clinical foci better than interictal EEG ($p<0.02$) and MRI/CTI ($p<0.001$) in PE patients evaluated.

PS_581

ICTAL AND INTERICTAL BRAIN SPECT IN CHILDREN WHIT ELECTRICAL STATUS EPILEPTICUS DURING SLOW SLEEP (ESES)

M. Dondi (1), G. Fagioli (1), S. Zoboli (1), M. Salgarello (1), S. Fanti (2), M. Farsad (1), A. Moretti (1), C. Pettinato (3), G. Montini (2), S. Meletti (4), C.A. Tassinari (4)(1) Department of Nuclear Medicine Maggiore Hospital Bologna; (2) Department of Nuclear Medicine S.Orsola-Malpighi Hospital Bologna ; (3) Department of Health Physic S.Orsola-Malpighi Hospital Bologna; (4) Department of Neurology Bellaria Hospital Bologna, Italy

Background: ESES is a neurological disease characterized by electrical status epilepticus in children which, if unrecognized, drives to aphasia, memory loss and other cognitive disorders. Nuclear medicine, either PET or SPECT studies, has been employed to evaluate brain perfusion in areas of possible epileptogenic activity.

Aim of the study: we aimed at evaluating the contribution of brain SPECT in detecting possible epileptogenic foci in patients with electrical epilepticus status during slow sleep. Studies were performed in children injected awakened (intercritical studies) and during sleep (critical studies).

Materials and methods: Three children (8, 8 and 9 years old) with diagnosis of ESES who underwent both ictal and inter-ictal brain SPECT have been enrolled in this study. Brain SPECT was carried out by means of a three-head variable angle system, equipped with ultra-high resolution collimators. For ictal studies (injection given asleep) children were prepared with a venous access placed on and then continuously monitored by experienced personnel until seizures appeared. Injection (Tc99m ECD at an amount adjusted for weight and age) was immediately carried out and imaging performed within 45-60 minutes. For interictal studies, injection was given with children awakened. Possible epileptic foci were identified from visual comparison of both ictal and interictal studies. SPECT results were compared to clinical, EEG and MRI findings. Localizations were considered true positive when SPECT results were congruent with at least two of the other findings.

Clinical results: on EEG and clinical data, we had 2 cases of temporal (right) and 1 case of parieto-occipital EEG localization of seizure. SPECT results: in case 1 and 2, SPECT showed a regional blood flow increase in the right temporal lobe and in case 3, where the EEG localization directed towards the right parieto-occipital lobe, SPECT showed a regional blood flow increase in the right temporal lobe.

Conclusions: Clinical characteristics of ESES (electrical activity detectable only during slow sleep and no typical MRI findings) brain SPECT performed with children asleep remains the only methods to investigate this rare disease.

PS_582

THE ROLE OF INTERICTAL SPECT IN MANAGEMENT OF PATIENTS WITH COMPLEX PARTIAL EPILEPSY ACCORDING TO EEG AND RESPONSE TO MEDICAL THERAPY

S. Crnkovic (1), R. Petrovic (1), S. Hajnsek (2), Z. Poljakovic (2), Z. Jurasinovic (1), M. Poropat (1), D. Dodig (1). (1) Clinical Department of Nuclear Medicine and Radiation Protection; (2) Clinical Department of Neurology, University Hospital Zagreb, Zagreb, Croatia.

Management of patients with complex partial epilepsy (CPE) is a significant neurological problem requiring interdisciplinary co-operation, because they are often medically resistant and consequently, surgery remains an important treatment option. The aim of our study was to evaluate the diagnostic usefulness of interictal SPECT and to correlate SPECT findings in these patients with clinical symptoms, EEG and response to therapy.
Methods: Interictal SPECT was used to examine regional cerebral blood flow (rCBF) in 21 patients with CPE (13 female, 8 male, median age 25 years, range 17-42), treated with different kind of antiepileptic drugs. Of them, 64% had temporal lobe epilepsy (TLE), and 36% experienced seizures of extratemporal origin (Ext). All patients underwent EEG monitoring as well as CT/MRIs for comparison. SPECT scans were acquired 20 minutes after injection of 740 MBq of Tc-99m-ECD by IRIX triple headed rotating gamma camera and analysed on Odyssey FX 820 workstation. Images were analysed visually and semiquantitatively.
Results: All of our patients had normal CT/MRI findings. In 8 patients SPECT failed to identify any perfusion abnormality and correlated with mild clinical symptoms, EEG (normal in 10 patients, asymmetric in 2 and diffusely paroxysmally dysritmic in 1) and good response to antiepileptic therapy. However, 13 patients had abnormal SPECT (temporal hypoperfusion in 3 patients, frontotemporal hyperperfusion in 5, basal ganglia hyperperfusion in 2, global hypoperfusion in 2). All of these patients had frequent seizure episodes, pathological EEG (diffuse paroxysmaly dysritmic, frontotemporal and temporoparietal focuses), and were refractory to medical treatment. Only in patients with TLE, SPECT lesions corresponded to EEG seizure focuses, while in patients with Ext focuses were difficult to localise. Pattern of hyperperfusion corresponded to particularly intractable CPE patients.
Conclusion: Although the SPECT brain imaging was performed on the patients during the interictal phase, there was a high correlation among SPECT findings, clinical diagnosis, EEG and response to medical therapy. We recommended it as a valuable diagnostic procedure, simultaneously with EEG monitoring, in medically refractory group of CPE patients with negative CT/MRIs, especially those undergoing surgical treatment. In a group of satisfactory treated patients interictal SPECT is of no particular clinical value, thus the performance of an ictal study is required.

PS_583

MALADAPTATION OF CEREBRAL PERFUSION IN THE SPINAL CORD INJURED INDIVIDUALS

I. Cho (1), K. Chun (1), K. Won (1), H. Lee (1), S. Ahn (2), K. Hayashida (3). (1) Department of Nuclear Medicine, Yeungnam University Hospital, Taegu, Korea; (2) Department of Rehabilitation, Yeungnam University Hospital, Taegu, Korea; (3) Department of Radiology, National Cardiovascular Center, Osaka, Japan.

Orthostatic hypotension is a common problem in the spinal cord injured (SCI) individuals with quadriplegia and paraplegia due to an impaired sympathetic nervous system. The aim of this study was to compare tilt-induced alteration of cerebral perfusion of spinal cord injured individuals with able-bodied (AB) individuals.
Methods: Supine and upright sitting brain-perfusion SPECT imaging was performed using a 1-day protocol and ^{99m}Tc-ethylcysteinate dimer (ECD) in 11 SCI individuals (2 women, 14 men; mean age, 32.6 y), with lesions between C3 and T4, and 5 AB individuals (2 women, 3 men; mean age, 31.4 y).
Results: In the SCI individuals, brain perfusion SPECT showed postural cerebral hypoperfusion in the frontal, temporal and parietal areas, of which the mean count ratio of the cerebral-to-cerebellar area between the upright and supine positions significantly changed. No postural changes in cerebral perfusion was evident in the occipital lobe, basal ganglia and thalamus in the SCI individuals. In the AB individuals, there were no such changes in cerebral perfusion during the upright test.

The mean count ratio of the cerebral-to-cerebellar area between the upright and supine positions in SCI individuals (n=14)

	Frontal area	Temporal area	Parital area	Occipital area	Basal ganglia	Thalamus
Upright	0.74±0.13	0.80±0.11	0.93±0.13	1.09±0.15	1.11±0.14	1.14±0.12
Supine	0.80±0.12	0.86±0.13	1.06±0.15	1.08±0.17	1.17±0.17	1.15±0.15
P	<0.01	<0.01	<0.001	>0.05	>0.05	>0.05

Conclusion: Postural cerebral hypoperfusion in the frontal, temporal and parietal areas in the SCI individuals might relate to maladaptation of the vascular response during the upright position.

PHYSICS / INSTRUMENTATION 2

PS_584

ACCEPTANCE TESTING OF HYBRID GAMMA CAMERAS USING THE NEW NEMA PET DRAFT STANDARD

G. Minear (1), G. Dobrozemsky (2,3), P. Schaffarich (2), H. Bergmann (2,4). (1) City Hospital, St. Poelten, Austria; (2) Department of Biomed. Eng. and Physics, University of Vienna, Austria; (3) Department of Nuclear Medicine, University of Vienna, Austria; (4) L. Boltzmann Institute of Nuclear Medicine, Vienna, Austria

Aim: Hybrid cameras when used in coincidence mode exhibit inferior image quality compared to conventional ring PET scanners. The new NEMA draft standard NU 2-2000 for performance measurements of PET systems accommodates both types of equipment and should emerge as a basis for comparison of performance parameters. Up to now no performance parameters were available from manufacturers.
Methods: Following the new protocols three hybrid cameras from 3 different manufacturers underwent a set of acceptance tests, including measurements of spatial resolution, scatter fraction, count losses and randoms measurements, system sensitivity and image quality. The measurements were made with the axial collimation, energy window(s) and reconstruction software recommended for routine use by the manufacturers. The phantoms specified in the standard were produced locally. Manufacturer independent software for the evaluation of the measurements was used. All cameras passed the planar and SPECT acceptance procedures.
Results: Tomographic spatial resolution in the center in air was 5.9, 6.2 and 6.3 mm FWHM for camera (1), (2) and (3) respectively. The scatter fraction was 46% for camera (1), 50% for camera (2) and 34% for camera (3). Count losses and randoms reflected by the NEC curves were measured for (2) only, since uncorrected raw data required for the calculations were not available on systems (1) and (3). System sensitivity was measured with the method of staggered sleeves of aluminium tubes. The axial sensitivity profiles showed essentially flat profiles on both 3-D and 2-D systems. Image quality was visually assessed from tomographic slices through the centers of the hot spheres, and quantitatively determined by contrast measurements. At a target to background ratio of 8:1 the smallest sphere that could be visualized on camera (1) was 13 mm, camera (2) 13 mm and camera (3) 10 mm.
Conclusions: Although we find the proposed draft of great value for camera-scanner intercomparison it is hard to strictly implement with current hybrid coincidence gamma cameras. Software and hardware requirements such as disabling random corrections and choosing the type of rebinning algorithm (SSRB vs. FORE) were not accessible for the end user on all systems. The main difference to NU 2-1994 is to use large phantoms that extend outside imager's axial field of view, which better simulates clinical imaging conditions. The effect was most clearly noted on relative high scatter fractions and lower peak NEC values than previously reported.

PS_585

A TRIPLE-HEADED-HYBRID GAMMA CAMERA: PRELIMINARY EVALUATION OF COINCIDENCE PHYSICAL PERFORMANCES

F. Zito (1), G. Tarantola (2), S. Arrigoni (2), A. Bruno (1), R. Secli (2), M. Rognoni (1), D. Locatelli (2), M. Gasparini (1), B. Gaggia (2), V. La Bella (2), P. Gerundini (1)(1) Nuclear Medicine Department, Ospedale Maggiore IRCCS, Milano, Italy; (2) Marconi Medical Systems Italia, Vimercate (MI), Italy.

Aim: The aim of this work was to evaluate the physical performances of a triple-headed coincidence gamma camera, in order to determine the best acquisition procedure and data processing for clinical applications.
Methods: All the studies were performed with the IRIX^{TM}-_PET^{AZ} (Marconi, Cleveland-OHIO-USA) having three _" NaI(Tl) crystals with a 480x390mm coincidence FOV. „U" shape configuration (180¡ between heads 2 and 3) and axial collimators were used. Sensitivity profiles and spatial resolution were assessed with a 260 kBq ^{22}Na point source, placed at different distances from the axis of rotation (off-axis). Tomographic studies were acquired in list-mode with 511 keV ±20% energy window at different radii of rotation (ROT=15, 20, 22, 29, 35.5 cm). Projection data were generated from 2D rebinning (transverse acceptance angle=32¡, axial acceptance angle=16¡). Spatial resolution in the three different directions (radial, tangential and axial) was measured in terms of FWHM of the point spread function on transaxial and sagittal slices more representative of the point source, reconstructed with FBP and RAMP filter.
Results: Spatial resolution. Fixed the source position, this parameter didn't depend on the radius of rotation, while moving the source off-axis it worsened tangentially and axially, as can be observed from the following data: (on-axis) radial=tangential=5.4mm, axial=6.2mm; (10 cm off-axis) radial=5.2mm, tangential=7.9mm, axial=13.5mm. Sensitivity. Keeping the point source on axis and varying the ROT from 15 to 29cm it had a constant value (≅0.8 cps/kBq), while it decreased of 8% using a 35.5cm ROT. For each radius of rotation, a uniform sensitivity profile was obtained moving the point source off-axis, showing that the third detector allowed the recovery of lines of response escaping from the two opposite heads which cause the typical linear decrease of double-headed coincidence systems.
Conclusions: These preliminary results pointed out that a triple headed coincidence gamma camera has a uniform sensitivity profile across the FOV, resulting into an effective increasing of sensitivity with extended radioactive sources. In order to better characterize this system and improve its clinical performances, further studies concerning noise-equivalent-count (NEC) and image quality analyses of anthropomorphic phantoms are under examination.

Poster presentation

PS_586

TRIPLE HEAD COINCIDENCE IMAGING ON GAMMAPET CAMERA – SOME CLINICALLY RELEVANT PERFORMANCE TESTS

D. Grosev, S. Loncaric, D. Dodig. Department of Nuclear Medicine and Radiation Protection, REBRO Hospital, Zagreb, Croatia.

Gamma cameras with the capability of coincidence imaging , when compared with dedicated PET scanners , have comparable spatial resolution but their sensitivity is still several times lower. Most currently available gammaPET cameras perform dual head coincidence with two opposite detectors. Adding additional detector would improve sensitivity of such systems. Our triple head gamma camera IRIX (Marconi Medical Systems, Inc. Cleveland Ohio, USA) is capable of performing coincidence imaging with all three heads. We present some test imaging performed to determine optimal parameters regarding clinical acquisition of gammaPET Tomo studies.

Methods: Count rate curves were obtained using two uniformly filled cylindrical phantoms: „short" (d=20 cm, h=20cm), and „long" (d= 15 cm, h=80 cm) with range of F-18 activity concentrations 2-37 MBq/L and 0.5-10 MBq/L respectively. Two tomographic phantoms, one cylindrical with cold rods and cold spheres segments, and one elliptical with cold rods segments, were filled with various amounts of F-18 activity to determine: 1) possible image degradation when random coincidences start to predominate; 2) optimal choice of energy windows during acquisition to improve sensitivity; 3) resolution limit by observing the smallest group of phantom objects that are visible on reconstructed slices.

Results: For maximum head radius of 35.5 cm, count rate curve for short phantom is linear up to activity concentration of 17 MBq/L . For long phantom linearity of response is preserved up to 6 MBq/L. For long phantom, decrease of head radius from 35.5 cm to 28 cm leads to increase in count rate by 20 kcps on linear part of the curve. Loss of image contrast on elliptical ECT phantom slices, for head radius 28 cm, is visible for concentration up to 8 MBq/L. Using two energy windows (Photopeak + Compton) leads to more than 30% increase in total events rebinned compared with Photopeak window only. Resolution limit for cold objects is 10 mm.

Conclusions: This investigation helped us to establish a preliminary clinical protocol: 1 hour after injection of 370 MBq of FDG the first acquisition is started with Photopeak+Compton window. Two consecutive tomographic acquisitions can be preformed within an hour, without significant loss in sensitivity.

PS_587

COMPARISON OF LINE PROFILE VS FWHM METHODS IN QUANTIFYING OBJECT VOLUME ABOVE & BELOW SYSTEM'S LEAST RESOLVABLE VOLUME IN HYBRID PET IMAGING

M.O. Afriyie, P.V. Pugliese, K.K. Bhargava, T.P. Kalapparambath, M.B. Tomas, C.J. Palestro. Division of Nuclear Medicine, Long Island Jewish Medical Center, New Hyde Park, NY. 11040, USA.

AIM: Accurate tumor staging, including differential imaging of metastatic vs recurrent tumors is dependent on the accuracy of volume detection in patient images. In volumetric imaging as in Hybrid PET, volume quantification depends on how faithfully the Apparent Volume (ApV) of the images data represents the object volume. Theoretical cutoff in volume resolution is defined as the Least Resolvable Volume (LRV) of a system, 6.3cc in our case. Object volume larger than LRV may be resolved & smaller than LRV may be overestimated. There are two methods frequently employed to estimate dimensions of an object. Using the dimensions so obtained, ApV of an imaged object can be calculated: Line Profile (LP) & FWHM methods are the commonly used methods by which dimensions of imaged objects are obtained from their images. This work compared the ApV (imaged volume) obtained by both methods to object's Actual Volume (AcV) to determine which method best restores volume of objects.

METHODS: 6 cylinders of axial diameter (d in cm) & known Volume (V in cc) of 3.2 &50,2.2 & 25,1.5 & 10, 1.0 & 5, 0.8 & 3, 0.5 & 1 were filled with ^{18}F-FDG solution of 0.74 MBq per cc. The cylinders were arranged in PET resolution phantom. Emission and transmission scans (^{137}Cs source) were acquired. The attenuation corrected Transaxial images were then reconstructed into 3D images, the ApV. The base radius r and height h in cm. of each imaged cylinder were estimated by two methods: LP method; a line profile was drawn on respective images, r & h were calculated. FWHM methods; Full Width at Half Maximum of the line profiles across the width and height were calculated, registered as r and h respectively. ApV was calculated mathematically using r & h in V(cylinder) = pi x r^2 x h & compared.

RESULTS: ApV calculated using data from FWHM methods agreed exactly with AcV for every AcV that was equal to or greater than the system's LRV. For AcV smaller than the system's LRV, FWHM methods overestimated ApV by 2x. ApV estimated by using data from LP methods, however, resulted in 2x overestimation for volumes larger than system's LRV, & 4x overestimation for volumes smaller than system" LRV.

CONCLUSIONS: Data show that for volumes above system's LRV, FWHM methods yield an ApV that is an accurate representation of the AcV, whereas LP overestimates AcV regardless of size of object volume.

PS_588

A PROGRAM CALCULATING NEMA RESOLUTION PARAMETERS IN GAMMA CAMERA SYSTEMS, BASED ON INTERFILE

H. Lønborg-Jensen. Dept. Nuclear Medicine, Glostrup University Hospital, Copenhagen County, Denmark.

Calculating NEMA resolution parameters in planar, SPECT or PET gamma camera imaging, during acceptance testing or routine quality assurance, requires analysis of thousands of line spread functions. The commercially available gamma camera systems seldom offer simple solutions to this problem, leaving a time consuming problem to the physicist testing the equipment.

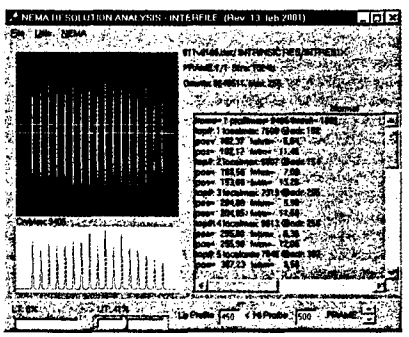

To assist in solving this problem a MS Windows based program has been developed, allowing analysis of resolution measurements converted to INTERFILE 3.3 format.

The program supports calculating FWHM and FWTM values from single or multiple slices of defined slice width in the following matrix formats: 128*128*2bytes, 256*256*2bytes and 1024*1024*1byte. Calculated parameters can be exported in various formats for further analysis.

The program has been tested on data from two gamma camera manufacturers.

PS_589

EVALUATION AND CORRECTION OF COUNT LOSSES RELATED TO DEADTIME DURING CLINICAL TRIALS OF RADIOIMMUNOTHERAPY WITH IODINE-131

L. Ferrer (1), G. Delpon (2), A. Lisbona (1), M. Bardies (2). (1) Department of Nuclear Medicine, Centre René Gauducheau, Nantes, France ; (2) Inserm Unit 463, Nantes, France.

Introduction: When dosimetric studies are performed during treatment (rather than after tracer injection), the high activities involved make quantification difficult because of gamma camera deadtime. This study in which count losses were considered in a realistic context proposes a correction method applicable to acquisitions during clinical trials (*i.e.* considering geometric and scatter conditions that influences count losses).

Materials and methods: An initial evaluation step consisted in estimating the number of counts observed as a function of the real count rate. Increasing iodine-131 activities (up to 2.22 GBq) were added in a water tank, while ensuring a uniform source volume. Images in list mode (energy: 0-750 keV) were acquired during 30s on a DST-Xli camera (SMVi-GEMS).

To study the spatial distribution of count losses, several list mode images were acquired, first a standard source (37 MBq) then this latter juxtaposed with sources of increasing activity (up to 740 MBq).

The acquisition of the standard allows the sensibility to be estimated without losses. The loss of sensibility on the standard on other acquisitions defines a correction factor that takes into account the geometric and scatter conditions.

This method was tested in air on the previous acquisitions, and in scattering conditions on acquisitions performed on an Alderson anthropomorphic phantom with liver containing 740MBq.

Results: Losses due to deadtime reached 20% for an observed count rate of 15 kcps on the 20% window (*i.e.* around 150 kcps for 0-750 keV). Our camera behaved like a paralysable system, with a maximum count rate of around 30 kcps on the 20% window.

Losses before correction reached 30% on the 740 MBq source and 22.5% on the standard. Acquisition from the 740 MBq source alone, together with spectral analysis, showed that this difference resulted from septal penetration through the collimator, which led to an underestimation of the correction factor. However, the method allowed quantitative error due to count losses to be reduced to less than 10% for acquisitions with the anthropomorphic phantom.

Conclusion: This study shows that count losses are high for 15 kcps on the 20% window. It is possible to use a known activity standard to estimate losses occurring in the sources to be measured. Septal penetration leads to a quantification bias, but the difference with the real count value is less than 10%. Improvement of method precision would require the use of a high-energy, high-resolution collimator (which would also reduce the sensitivity of the gamma camera).

PS_590

MULTICENTRIC COMPARATIVE EVALUATION OF ABSOLUTE CALIBRATION OF POSITRON EMISSION TOMOGRAPHS

L. Geworski (1), M. de Wit (2), V. Ivancevic (1), R. Bares (3), D.L. Munz (1). (1) Nuclear Medicine, Charite, Berlin, Germany; (2) Oncology, Hamburg, Germany ; (3) Nuclear Medicine, Tuebingen, Germany.

Aim of this study was to test the accuracy of the scanners' calibration by correlating the image-pixel values to the true activity concentrations [Bq/ml] in tissue represented by a suitable phantom. This has been done comparatively for all devices included in a multicenter study.
Methods: Measurements were carried out on a total of 23 tomographs of 7 different types. Of these, 16 were investigated in both 2D and 3D mode, while 4 and 3, respectively, could be operated in 2D or 3D mode only. Measurements were done with a cylindrical phantom of 20 cm diameter and 20 cm axial length. Three emission scans with adequate counting statistics were acquired for each acquisition mode. All data were corrected for attenuation (transmission scan) and scatter as implemented in the scanners' standard softwares. The scanners' absolute calibration was checked by comparing the activity concentration in the phantom, known from volume and activity as determined in the dose calibrator, with the ROI data derived from the image, and the cross calibration with two samples from the phantom and measured in a well counter. The dose calibrators were tested using always the same three Ge-68 standards containing 42 MBq, 4.03 MBq and 0.383 MBq, respectively.
Results: All of the PET scanners investigated were suitable for visual data analysis. Five sets of measurements had to be repeated due to incorrect scanner calibration. Three tomographs had to be cross calibrated again, because their errors were significantly higher than 10%. In 2D mode thirteen out of twenty (65%) scanners showed errors <5% and another 4 (20%) errors around 10%. The respective error ranges were found in 10 (53%) and 5 (26%) of the 19 scanners tested in 3D mode. All the other scanners had errors from 5% to 10%. Due to hardware and software problems the measurements performed on two tomographs could not be analysed adequately.
Conclusion: In multicenter studies merging quantitative PET data from different institutions, a thorough investigation of the absolute calibration of the tomographs used is mandatory.
(This research project was supported by the „Deutsche Krebshilfe" grant no. 70-2329).

PS_591

COUNTING SENSITIVITIES OF LOW ENERGY-COLLIMATORS IN I-123 IMAGING: DEADTIME COUNT LOSS MEASUREMENT

A. Kojima (1), M. Matsumoto (2), N. Katsuda (3), S. Tomiguchi (3), M. Takahashi (3), N. Motomura (4). (1) Radioisotope Research Center, Kumamoto University, Kumamoto, Japan; (2) Department of Radiological Technology, College of Medical Science, Kumamoto University, Kumamoto, Japan; (3) Department of Radiology, Kumamoto University School of Medicine, Kumamoto, Japan; (4) Medical Engineering Laboratory, Toshiba Corporation, Tochigi, Japan

Radiopharmaceuticals labeled with I-123 (159 keV) are employed in the SPECT studies for the brain and the myocardium. However, for quantitative I-123 SPECT imaging, adequate collimator selection should be considered because of scatter or collimator penetration of higher energy photons emitted from I-123. The aim of this study was to investigate counting sensitivities of low energy-collimators in I-123 imaging with measuring deadtime count loss.
Methods: Two low energy-collimators were investigated: a low-energy, high resolution (LEHR) collimator and a low-energy, general purpose (LEGP) collimator. Images and energy spectra for two low energy-collimators were acquired in air using a syringe containing I-123 (300 MBq) and a digital gamma camera. A Tc-99m syringe (5.67 GBq) was also counted in air as the comparative radioisotope. For I-123 and Tc-99m, counting rates were measured during about four days continuously and these time-decayed counting rates were correlated with counting rates by a radioisotope dose calibrator. Imaging energy windows were 159 keV ± 7.5% for I-123 and 140 keV ± 7.5% for Tc-99m, respectively. The source to camera distance was 10 cm for each measurement.
Results: For I-123, count loss occurred at 5.5 kcps (~45 MBq) for the LEGP collimator and 4.0 kcps (~37 MBq) for the LEHR collimator. For Tc-99m, however, count loss occurred at 55 kcps (~500 MBq) for the LEGP collimator and 55 kcps (~1000 MBq) for the LEHR collimator. For 111 MBq of I-123, count losses were ~3.5% and ~7% for the LEGP collimator and the LEHR collimator, respectively. For 222 MBq of I-123, count losses became greater, ~7.2% and ~17.3% for the LEGP collimator and the LEHR collimator, respectively. For other larger amount of I-123 , dead time count loss of the LEHR collimator became severer than one of the LEGP collimator.
Conclusion: For the low-energy collimators, higher energy photons (440 keV, 529 keV, and so on) emitted from I-123 cause deadtime count loss in the 159 keV imaging window at lower counting rate as comparing with Tc-99m and the count loss is affected by the amount of I-123. Therefore, suitable low energy-collimators with low septal penetration for higher energy-photons should be selected in quantitative I-123 imaging.

PS_592

A COMPARISON OF THE QUALITY OF THE THYROID SCANS OBTA_NED BY 5 MM AND 7 MM PINHOLE INSERTS

C. Taşci, G. Çapa Kaya, R. Bekis, Ö. Özdoğan, E. Demirtaş, B. Değirmenci, H. Durak. Department of nuclear medicine, Dokuz Eylül University School of Medicine. Izmir, Turkey.

Thyroid imaging using 5 mm pinhole insert (PI) increases the image quality but takes long time. The aim of this study was to compare the thyroid scans in quality and imaging time obtained from the same patient using 5 mm. and 7 mm. PI.'s.
Methods: Twenty nine patients (mean age = 43.1 ± 13.6) were included. All the patients had one or more thyroid nodules defined by ultrasonography. All the scans were 150.000 counts from ANT, RAO, LAO positions. After intravenous injection of 5 mCi Tc99m pertechnetate, imaging was started with 7 mm PI and continued with 5 mm PI. All the scans were evaluated by four Nuclear Medicine specialists independently and without knowing the imaging techniques. The specialists visually evaluated the scans from the aspects of the differentiation of the boundary of thyroid gland (first parameter) and the lesion detection from thyroid parenchyma (second parameter). They scored these two parameters (0: poor, 1: medium, 2: good, 3: high in quality) and noted the number of nodules as the third parameter. Student's t test for paired data and Pearson correlation test were used.
Results: The mean imaging time of ANT projections obtained using 5 mm PI (9.1 ± 4.3 minutes) was significantly longer than those using 7 mm PI (3.6 ± 1.6 minutes). The mean score of only one of the five observers for the first parameter was found meaningfully high in scans by 5 mm PI ($p=0.05$). The mean number of nodules counted by four of the observers were significantly high in scans by 5 mm PI ($p=0.001$, $p=0.000$, $p=0.046$, $p=0.030$ respectively). There was no difference between the mean scores of the second parameter of two techniques evaluated by each observer. The correlation between the mean number of nodules counted by each observer for each patient is found statistically meaningful (for 4 observers, $r = 0.88$, $r = 0.78$, $r = 0.76$, $r = 0.71$, respectively and $p = 0.01$).
Conclusions: While the mean imaging time using 7 mm PI is significantly shorter, the mean number of nodules observed in scans by 5 mm PI seems to be higher. If it is necessary to use 7 mm PI for thyroid imaging in local situations, it should be considered that there may be a risk of detecting lesser number of nodules.

PS_593

CHOICE OF OSEM PARAMETERS DEPENDING ON TOMOGRAPHY ACQUISITION CONDITIONS

D. Huglo, Y. Venel, A. Delcourt, H. Benticha, F. Lejeune-Prigent, S. Perez, Y. Djagba, G. Nemchi, E. Hector, T. Prangere, M. Steinling Department of Nuclear Medicine, Hopital Huriez, CHU of Lille, Lille, France.

Fast iterative reconstruction methods such as the ordered-subset expectation maximum (OSEM) usually provide better results in bone SPECT than filtered backprojection. With the OSEM no filters are chosen but two parameters have to be fixed : the subset number (S) and the number of iterations (I). In bone SPECT with 64 projections, 8 subsets and 2 iterations are recommended in the literature as being the best visual compromise. The aim of this study was to determine the best parameters in pulmonary SPECT and bone SPECT with 32 projections.
Method: All the tomography data were obtained with a Sophy DST-XLI (SMV) gamma-camera. For studies of pulmonary perfusion, after injection of 110-150 MBq of ^{99m}Tc-MAA, 64 projections (64x64, 20 seconds per projection) were recorded over 360¡. For the bone SPECT, 2 hours after injection of 740 MBq de ^{99m}Tc-DPD, 32 projections (128x128, 40 seconds per projection) were recorded in procubitus over 180¡. In each study, 12 reconstructions were produced using Vision's OSEM program (SMV), with I varying from 2 to 5 and S equal to 4, 6 or 8. The same slices, centred on anomalies when these existed, were printed out and examined separately by 6 nuclear medicine specialists. For each study, each observer chose 1 to 3 best reconstructions and ranked them in 1st, 2nd and 3rd order. For each reconstruction, the number of the choices were summed without weighting and then with weighting (3 for 1st choice, 2 pour 2nd and 1 for 3rd).
Results: Three patients were studied for the pulmonary perfusion SPECT. In decreasing order without (and with) weighting the choices were I3-S6 : 9 (23), I2-S8 : 9 (21), I3-S8 : 8 (8) and I4-S6 : 7 (14) then the other combinations. For the bone SPECT, 6 patients were studied. The choices were I2-S6 : 22 (57), I3-S6 : 15 (29), I3-S4 : 13 (20), I2-S8 : 11 (16) and I2-S4 : 9 (25) then the other combinations.
Conclusion: For the pulmonary perfusion SPECT (64 projections of 64x64), 2 iterations with 8 subsets or 3 iterations with 6 subsets were the best choice of OSEM parameters with very discrete visual differences. For bone SPECT, although only 32 projections were obtained because of a smaller number of projections per subset than with 64 projections, the best choice of OSEM parameters was clearly 2 iterations and 6 subsets.

PS_594

RADIOSYNTHESIS OF 4-[18F]FLUORO-H88, AN ANALOGUE OF H89, A POTENT CYCLIC AMP DEPENDENT PROTEIN KINASE INHIBITOR: REDUCTIVE AMINATION OF 4-[18F]FLUOROCINNAMALDEHYDE

K. Takahashi, S. Miura, M. Ibaraki, J. Hatazawa, E. Shimosegawa, H. Ito, H. Tamura, K. Okane, I. Kanno. Radiology and Nuclear Medicine, Reseach Institute for Brain and Blood Vessels -Akita, Akita, Japan.

For studying intracellular signal transduction system in the human brain, several radiolabeled compounds for positron emission tomography (PET) were investigated, for example, [^{11}C]diacylglycerol; a protein kinase C activator, and [^{11}C]rolipram; a phosphodiesterase-4 inhibitor. But it has not reported to label a cyclic AMP dependent protein kinase (PKA) inhibitor, such as H89 (N-[2-(4-bromocinnamylamino)ethyl]-5-isoquinoline-sulfonamide). Potent PKA inhibitors labeled with positron emitter would be useful for imaging cyclic AMP function in the living human tissue using PET. The aim of this study was to synthesize 4-[^{18}F]fluoro-H88 (N-[2-(4-fluorocinnamylamino)ethyl]-5-isoquinoline-sulfonamide) , a [^{18}F]-labeled analogue of H89, via a novel labeled precursor 4-[^{18}F]fluorocinnamaldehyde.

Methods: No-carrier-added [^{18}F]fluoride was produced by 18 Mev proton irradiation of [^{18}O]water. The [^{18}F]fluoride produced was activated by tetrabutylammonium carbonate under anhydrous condition. The nucleophilic aromatic substitution of 4-trimethylammonium-cinnamaldehyde triflate by the activated [^{18}F]fluoride was performed in DMSO at 120 °C for 10 min. The 4-[^{18}F]fluorocinnamaldehyde produced was isolated by SEP-PAK silica purification, and subsequently, was reductively aminated with H9 (N-(2-aminoethy)isoquinoline-5-sulfonamide), using sodium cyanoborohydride and acetic acid. Reaction was complete upon heating to 120 °C for 5 min in DMSO. The 4-[^{18}F]fluoro-H88 produced was purified by a preparative reversed phase HPLC system. After evaporation of solvent, the final product was dissolved in saline and passed through a sterile filter.

Results: The radiochemical yield of 4-[^{18}F]fluorocinnamaldehyde was typically 40-60 % based on [^{18}F]fluoride. The radiochemical yield of 4-[^{18}F]fluoro-H88 was 30-40 % based on 4-[^{18}F]fluorocinnamaldehyde, and the radiochemical purity was better than 95 % (HPLC: Inertsil-ODS2; 4.6 mm x 250 mm, 0.1M $AcONH_4/CH_3CN/AcOH$= 500/500/1, flow rate = 2 ml/min, retention time = 3.0 min). The over all time of synthesis including purification and sterilization was 80 min after end-of-bombardment. The formulated products, ready for biological studies, proved sterile and pyrogen-free.

Conclusions: 4-[^{18}F]fluoro-H88, a [^{18}F]-labeled analogue of H89, has been synthesized in a good yield under no-carrier-added condition. This radiolabeled tracer will provide further biological studies for clinical applications with PET. Both aromatic [^{18}F]-fluorination of cinnamaldehyde and reductive amination of 4-[^{18}F]fluorocinnamaldehyde gave good yields. The labeled cinnamaldehyde may be a useful synthetic precursor for the radiosynthesis of other complex radiotracers for use with PET.

PS_595

AUTOMATED FLT SYNTHESIS USING 3-N-BOC-1-(5-O-(4,4«-DIMETHOXYTRITYL)-3-O-NOSYL-2-DEOXY-§-D-LYXOFURANOSYL)THYMINE AS PRECURSOR

C. Mosdzianowski (1), M. Eisenhut, J. Martin, J. Eisenbarth, C. Korenjak, M. Nader. (1) Coincidence Technologies s.a., Liege, Belgium; (2) DKFZ Heidelberg, Abt. Radiochemie, Heidelberg, Germany; (3) Argos Zyklotron Gesmbh, Klagenfurt, Austria.

Aim: [^{18}F]FLT (3'-fluoro-3'-deoxythymidine) has been developed as a thymidine analogue for PET imaging in vivo. We investigated the use of a commercially available FDG synthesizer based on a disposable kit system for the synthesis of [^{18}F]FLT.

Methods: The automated [^{18}F]FLT synthesis was based on the method recently developed by Martin *et al.* The first steps of the synthesis are identical to the first steps of the [^{18}F]FDG synthesis: enriched water recovery through an anion exchange cartridge, elution of $^{18}F^-$ using 7 mg of K_2CO_3 and 22 mg of Kryptofix® 222, evaporation of the solvents before labeling and dissolving of the precursor in 3.5 ml of acetonitrile. After evaporation the precursor, 3-*N*-Boc-1-(5-*O*-(4,4'-dimethoxytrityl)-3-*O*-nosyl-2-deoxy-§-D-lyxofuranosyl)thymine was introduced in the reaction vessel containing the dried K222/$^{18}F^-$ complex. The labeling reaction was carried out at 105 ¡C within 4 minutes and at a temperature decreasing from 105 ¡C down to 85 ¡C within 3 minutes. The acetonitrile was then partially evaporated at 85 ¡C under argon flow during 4 minutes. Subsequently, 3 ml of 1 M hydrochloric acid were added to the remaining solution (about 0.5 ml). The hydrolysis was carried out within 10 minutes at 105 ¡C. The duration of synthesis was about 40 minutes. The analysis of the solution containing [^{18}F]FLT was done by Thin Layer Chromatography using the Instant Imager (Canberra Packard), an 254 UV lamp and Polygram SIL G/UV_{254} sheets (Macherey-Nagel). Methylene chloride/methanol 90/10 was used as mobile phase.

Results: Using increasing amounts of precursor the following decay corrected yields were obtained: 11.5 % with 10 mg, 23 % with 20 mg, 31.5 % with 30 mg and 33 % with 40 mg of precursor.

The R_f for $^{18}F^-$ was 0.00, the R_f for [^{18}F]FLT was 0.34 and the R_f for the labeled unhydrolyzed intermediate was 0.84. The main impurity was $^{18}F^-$. Only small amounts (< 5 %) of an unknown radioactive compound were found.

Conclusion: The promising results during these preliminary experiments lead us to improve the automated synthesis. Furthermore, we were able to use a commercially available sterile disposable kit system for the automated production of [^{18}F]FLT according to GMP regulations. Optimization of the synthesis parameters and implementation of a preparative HPLC for the purification of the final product is under progress. A HPLC system is easy to implement since there are 24 V signals available on the FDG-Synthesizer to start of the HPLC purification process.

PS_596

SYNTHESIS OF 2'-DEOXY-2'-(18F)-FLUORO-1-BETA-D-RIBOFURANOSYLURACIL

S.H. Ahn, Y.S. Cho, K.S. Chun, S.D. Yang, Y.S. Suh, C.W. Choi, S.W. Hong, S.M. Lim. Cyclotron Application Lab. Korea Cancer Center Hospital Seoul Korea.

Aim: ^{18}F labeled 2'-fluoro-1-β-D-ribonucleosides can be important candidates for cancer-related imaging tracer, especially in the field of the cancer gene therapy using herpes simplex type 1 virus thymidien kinase(HSV-tk) suicide gene as well as in cancer diagnostics. The presence of the 2'-fluoro-ribo substituent has been shown to confer biochemical stability to pyrimidine nucleoside as in the case of 5-(2-[^{125}I]iodovinyl)-2'-fluoro-2'-deoxyuridine(IVFRU). But the direct stereospecific introduction of radiofluorine at the 2'-position of the sugar moiety in pyrimidine nucleosides has not been tried so much. Here we report an synthetic method for [^{18}F]2'-deoxy-2'-fluoro-β-D-ribonucleosides from O-tetrahydropyranyl- precursor, useful in that its protecting group is easy to introduce and remove.

Methods: 3',5'-di-O-tetrahydropyranyl-1-β-D-arabinofuranosyluracil was converted to 2'-O-(trifluoromethane sulfonyl)-3',5'-di-O-tetrahydropyranyl-1-β-D-arabinofuranosyluracil (triflate) with 40% yield. Fluorination of the triflate with tetrabutylammonium fluoride in THF for several hours gave the desired product. It was also prepared from 3',5'-di-O-tetrahydropyranyl-1-β-D-arabinofuranosyluracil by the diethylaminosulfur trifluoride(DAST) and identified by ^{1}H NMR spectroscopy. For radiochemical synthesis, ^{18}F-fluoride was placed in a vial containing K_2CO_3/Kryptofix and evaporated to dryness. The dried fluoride was reacted with 2'-O-triflate in acetonitrile at 110°C for 20min, then followed by acidic hydrolysis for 20min. The crude product was purified by C-18 Sep-Pak cartridge and analyzed by HPLC.

Results: The radiochemical yield was 10-20% with >99% radiochemical purity in 3 runs. Synthesis time was 80-100min from the EOB.

Conclusion: 2'-O-(Trifluoromethanesulfonyl)-3',5'-di-O-tetrahydropyranyl-1-β-D-arabinofuranosyluracil was labeled with ^{18}F and deprotected easily in good yield. This method can be applied to preparation of new 2'-radiolabeled ribofuranosylnucleosides for PET studies.

PS_597

PREPARATION OF LIPIODOL SOLUTION OF 188RE-4-HEXADECYL-2,2,9,9-TETRAMETHYL-4,7-DIAZA-1,10-DECANEDITHIOL (HTDD) FOR TREATMENT OF LIVER CANCER

J.-K. Chung (1), Y.J. Kim (1), J.M. Jeong (1), Y.-S. Lee (1), D.S. Lee (1), Y.-G. Suh (2), M.C. L (1). (1) Department of Nuclear Medicine; (2) Pharmaceutical Manufacturing Chemistry, Seoul National University College of Pharmacy, Seoul, Korea.

It has been reported that lipiodol solution of ^{188}Re-2,2,9,9-tetramethyl-4,7-diaza-1,10-decanedithiol (TDD), a kind of N_2S_2 derivatives, accumulates in the liver cancer effectively if injected through the hepatic artery. However, its therapeutic effect might not be ideal as it diffuses out of the cancer tissue in several hours. To increase the retention of ^{188}Re-TDD in the liver cancer, we introduced long chain alkyl groups to TDD, which will increase van der Waals interaction with lipiodol molecules. Although the tissue uptake and retention increased as the introduced chain length become longer, labeling efficiency decreased in reverse. The low labeling efficiency is mainly related with the low solubility of the ligand. We tried to find out adequate condition for labeling ^{188}Re-HTDD-lipiodol.

Methods: 5-Hexadecyl-3,3,10,10-tetramethyl-1,2-dithia-5,8-diazacyclodecane was synthesized by *N*-alkylation with iodohexadecane in the presence of potassium carbonate in acetonitrile. HTDD was obtained by reducing 5-hexadecyl-3,3,10,10-tetramethyl-1,2-dithia-5,8-diazacyclodecane with zinc powder in concentrated hydrochloric acid. To 1 mg HTDD, tartaric acid (30–40 mg), $SnCl_2{\cdot}2H_2O$ (3 mg) and ^{188}Re-perrhenate (37–590 MBq/3 ml) were added. To adjust pH, adequate amount of 0.5 M trisodium phosphate, 2 M disodium phosphate and 10% sodium bicarbonate were added. After heating for 1 hr at 100°C, 10% sodium bicarbonate was added to adjust pH 8.5. Lipiodol (3~4 ml) was added to the reactant and mixed. Upper water phase was removed after centrifugation at 3000 rpm for 10 min. Radiochemical yield was determined by measuring the radioactivity of each phase. Radiochemical purity was checked by ITLC-SG/ethyl acetate or saline.

Results: At pH 4.5, 5.5, 6.5, 7.5, 8.5, and 9.5 radiochemical yields were 18.7 ± 10.9% (n=7), 6.7%, 23.1%, 46.2 ± 8.0 (n=7), 35.4%, and 33.9%, respectively, and radiochemical purities were 93.1 ± 2.5% (n=5), ND, ND, 96.2 ± 1.0% (n=6), 95.4%, and 95.5%, respectively. In the preparations using 2 M sodium phosphate for pH adjustment, a white-layer between aqueous and lipiodol phase was formed. Radioactivities of the white-layers were 35.5~69.7%.

Conclusions: We established an optimal condition to label ^{188}Re-HTDD-lipiodol that can be used for liver cancer therapy.

PS_598

EDTMP DRY KIT FOR TC-99M, SM-153, LU-177 AND OTHER LANTHANIDES LABELLING

R. Mikolajczak (1), D. Pawlak (1), P. Garnuszek (2), I. Licinska (2). (1) Department of Radiopharmaceuticals, Radioisotope Centre POLATOM, Otwock/Swierk, Poland; (2) Radioisotopic Drugs Department, Drug Institute, Warsaw, Poland.

The aim of our study was to develop the freeze-dried kit for preparation of EDTMP chelates with radio-lanthanides *e.g.*: Sm-153, Lu-177 or Ho-166, likewise with „diagnostic" Tc-99m a potential bone scanning radiopharmaceutical.

Methods: Stannous chloride and ascorbic acid were added to the kit. Low specific activity Lu-177 (1 and 7.6 GBq/mg of Lu) was used for formation of ^{177}Lu-EDTMP. Labelling yields of ^{177}Lu-EDTMP and ^{99m}Tc-EDTMP were investigated in function of ligand, stannous chloride and stabiliser concentrations. Stability, and biodistribution in healthy rats was compared to ^{153}Sm-EDTMP (EDTMP 17.5 mg/ml, $^{153}SmCl_3$ of spec. act. 35 GBq/mg Sm).

Results: Our previous studies on EDTMP complexes confirmed that stable chelates were formed easily, in the broad range of pH and stoichiometry. In present study, we observed that deposition of the ^{99m}Tc-EDTMP activity in femur increase with decreasing of the ligand concentration. Looking for compromise between yield and bone deposition, we used 15 mg of the ligand in the kit, which has been designed for total volume of 2 ml for lanthanides (spec. act. *min* 2GBq/mg), and of 5 ml for Tc-99m (total act. *max* 8GBq).

Addition of 0.2 mg of the stannous chloride was sufficient for ^{99m}Tc(VII) reduction and obtaining stable ^{99m}Tc-EDTMP complex. The same kit used for ^{177}Lu-EDTMP preparation showed good stability, especially when higher specific activity ^{177}Lu was used.

Biodistribution studies of ^{177}Lu- and ^{99m}Tc-EDTMP revealed similar tissue uptake and clearance to those observed with ^{153}Sm-EDTMP (see Table). The most significant difference was found in retention of activity in kidney, which in the case of ^{99m}Tc-EDTMP was the highest reaching ca. 6 % of the accumulated dose after 90 min *p.i.v.*

The normalised EDTMP chelate accumulation in the rats tissue 30 and 90 minutes p.i.v. (percent of accumulated activity in 1g of tissue × BW/100)

Tissue	^{153}Sm(III) (n = 15)		^{177}Lu(III) (n = 11)		^{99m}Tc(IV) (n = 9)	
	30 min p.i.v.	90 min p.i.v.	30 min p.i.v.	90 min p.i.v.	30 min p.i.v.	90 min p.i.v.
Lungs	0.67±0.23	0.07±0.04	0.44±0.14	0.10±0.05	0.69±0.17	0.20±0.18
Liver	0.27±0.11	0.13±0.01	0.21±0.07	0.10±0.04	0.38±0.18	0.20±0.09
Kidneys	4.05±2.05	0.84±0.13	3.31±1.34	1.29±0.52	7.36±2.03	5.98±3.25
Femur	7.43±0.22	11.05±1.27	8.15±0.95	10.83±1.10	7.78±0.93	9.55±0.69

Conclusions: The developed freeze-dried kit for EDTMP chelate formation can be utilised for preparation of bone-seeking radiopharmaceuticals *i.e.* ^{99m}Tc-EDTMP as well as ^{177}Lu-EDTMP, and due to similar chemistry, can be used for other „medical" radio-lanthanides. The kit content (15 mg EDTMP, 5 mg ascorbic acid, 0.2 mg $SnCl_2$) ensures a one-step radiopharmaceutical preparation of a high radiochemical purity, as well as sufficiently long shelf-life.

PS_599

STUDY ON A NOVEL POTENTIAL PERFUSION IMAGING AGENT

R.F. Wang (1), C.L. Zhang (1), S.L. Zhu (1), Y.B. Miao (2), Z.G. Tang (2), B.L. Liu (2). (1) Department of Nuclear Medicine, Peking University, Beijin, P.R.of China; (2) Department of Chemistry, Beijing Normal University, Beijing, P.R.of China.

Aim: To search for a novel potential SPECT cerebral blood flow perfusion imaging agent.

Methods: Tridentated MPBDA with N_2S obtained from chemical synthesis and characterized by IR spectrum, ^{1}HNMR, element analysis and MS was labeled with Tc-99m under optional conditions. Biodistribution in 25 mice was performed at different time points after intravenous injection of 100 μL 555 ~ 740 kBq Tc-99m-MPBDA. The dynamic imaging in 2 monkeys was immediately acquired following rapid injection of 218.3 ~ 333 MBq Tc-99m-MPBDA or Tc-99m-ECD, and monkey whole body imaging and cerebral tomographic imaging were performed at 70 min postinjection. Preclinical studies including toxicity and pyrogen tests in mice and rabbits were taken.

Results: The radiochemical synthetic yield and radiochemical purity of MPBDA labeled with Tc-99m were more than 95 %, 97 %, respectively. Biodistribution results of Tc-99m-MPBDA showed high uptake and good retention in mouse brain, and blood clearance half time was less than 15 min. The cerebral dynamic blood flow perfusion imaging in monkey demonstrated at 2 min after administration to attain the maximum radioactivity of Tc-99m-MPBDA in the brain (T_{max}). In comparison with activity at 2 min postinjection, 83 percents of initial activity remained in brain at 60 min images. It was showed that the brain uptake reached to 2.7 %ID at 70 min postinjection from the whole body imaging, which was slightly inferior to that of Tc-99m-ECD (2.9%ID). The tomographic images showed that the activity remained in gray matter was higher than that in white matter, with good contrast of imaging. No death, toxic and side-effects, pyrogen in mice and rabbits after injection of Tc-99m-MPBDA was found.

Conclusion: The results of this study revealed that Tc-99m-MPBDA possessing similar property of Tc-99m-ECD, and the initial high brain uptake and ideal brain retention in monkey was favorable for SPECT imaging. This proposed compound as a radiopharmaceutical showing safe and reliable in vivo appeared to be a novel potential cerebral flow perfusion imaging agent.

PS_600

SERUM CA 125 LEVELS VERSUS DISEASE CHARACTERISTICS IN PATIENTS WITH NHL

I. Zaharos (1), I. Ilias (2), E. Petreli (1), C. Batsakis (2), G. Panoutsopoulos (2), P. Roussou (1), I. Christakopoulou (2). (1) Third University Department of Medicine, ; (2) Department of Nuclear Medicine, Athens, Greece.

CA 125 is a glycoprotein expressed by epithelial ovarian tumors, pelvic inflammatory disease, hepatic disease and tuberculous effusions. Few studies have shown CA 125 to be also elevated in patients with non-Hodgkin«s lymphoma (NHL), especially in the presence of serosal involvement. The aim of the present study was to further evaluate CA 125 levels versus NHL characteristics in patients with and without pleural and/or peritoneal involvement.

We studied 21 men and 21 women (mean age±SD: 59±17 y.o.) at the initial diagnosis of the disease, as well as during treatment and/or at the end of therapy. The following clinical parameters were taken into consideration: sex, age, disease stage, presence of symptoms, disease localization as well as serum LDH. CA 125 levels were measured with IRMA (normal< 30 ng/mL) and assessed, using multiple correlation analysis – implementing Bonferroni«s correction – versus the above parameters. Variations in CA 125 levels versus disease course were assessed with the chi square test.

Fifteen patients showed complete and 22 partial remission; 7 patients died.

CA 125 levels were found to be more elevated in women, and correlated with disease stage and localization. No correlation of CA 125 was shown versus the patients«age, the presence of effusions and LDH levels. Normal CA 125 levels at the time of diagnosis or normalization of CA 125 levels after chemotherapy indicated a favorable prognosis ($p<0.05$, chi square).

In, conclusion CA 125 seems to be elevated in advanced NHL regardless of serosal involvement. Normal CA 125 levels after chemotherapy were associated with a favorable prognosis. The practical implication of these findings merits further evaluation.

PS_601

PERFORMANCE OF MYOVIEW KIT: HIGH SPECIFIC ACTIVITY AND SPLIT DOSES

R. Saponaro, G. Cannizzaro, C. Aprile. Nuclear Medicine Serv., Fond. S.Maugeri- Cl. Lav & Riab. IRCCS, Pavia, Italy.

AIM Although manufacturers discourage the adoption of any procedure other than strictly according to instructions, „in house" procedures, when supported by quality control and validation schemes performed in compliance with good radiopharmacy practice, may provide accurate and reliable products. In this work we have tried out an alternative method for the labelling of Myoview (Nycomed Amersham Sorin).

METHODS Eleven whole Myoview kits were reconstituted with the recommended volume of ^{99m}Tc but with an activity between 60 and 120 MBq/μg of tetrofosmin (TF), highly exceeding the upper limit of 39 MBq/μg specified by the manufacturer. As a second step we analyzed „in vitro" the effect of reconstitution, freezing and thawing of splitted Myoview kits on the labelling efficiency of the stored products. The kits were reconstituted with sterile nitrogen purged 0.9% saline and subdivided into fractions; 12 fractions were labelled immediately after reconstitution with saline, 12 were stored at –70¡C and thawed for labelling at different times up to 66 days. Radiochemical purity (RP%) was checked by the usual TLC method (Gelman ITLC-SG strips and acetone/dichloromethane as solvent) 30 minutes after labelling. Finally, 17 of the 35 Myoview preparations, after appropriate testing for stability and sterility, were used „in vivo", and a blind observer compared the clinical images provided by Myoview prepared as recommended with those provided by the alternative methods.

RESULTS The RP% of the 11 whole kits proved in all cases >90% and the labelled product was stable up to 6 hours.

No significant differences in RP% were found between fractionated Myoview and whole kit, as well as between freshly prepared and frozen fractions. Also, the labelling of all frozen doses did not seem to be affected by storage time at least up to 35 days, when a downward trend was observable. No significant differences could be detected in the „in vivo" biodistribution of Myoview prepared with the two labelling methods.

	n.	Activity MBq/μg TF		RP%	
		Mean	Range	Mean ± SD	range
Whole kit	11	104	60-120	96.8 ± 2.46	91-99
„Freshly prepared" fractions	12	187	57-330	96.6 ± 2.49	91-99
Frozen fractions	12	131	64-201	93.3 ± 4.11	87-98.6

CONCLUSIONS Myoview allows higher specific activity than recommended and the practice of „kit splitting". This approach offers advantages in terms of radiation dosimetry to the operator, reduces cost per patient/dose and optimizes work management, without significantly affecting „in vivo" test performance.

Poster presentation

PS_602

BIODISTRIBUTION OF GA-67-DOTA-LANREOTIDE IN ANIMALS

I. Szilvasi (1), J. Janoki (2), P. Angelberger (3), I. Virgolini (4). (1) Dept. of Nucl. Med., Semmelweis University, Budapest, Hungary; (2) FJC National Inst. For Radiobiology, Budapest, Hungary; (3) Research Center, Seibersdorf, Austria; (4) Dept. of Nucl. Med., University of Vienna, Austria

Lanreotide is a long-acting somatostatin analog wich binds to all 5 subtypes of somatostatin receptors. High affinity binding of Ga-67-DOTA-lanreotide to a variety of tumour cells has been previously found.

Aim of the present work was to study the biodistribution of Ga-67-DOTA-lanreotide in dogs and tumour-bearing nude mice.

Methods: 20 microgram of DOTA-lanreotide was labelled with 20-40 mCi of Ga-67-GaCl3 with high specific activity. Labelling efficiency was more than 92 per cent by ITLC and HPLC techniques. Gamma camera images were taken in 5 beagle dogs at 10 minutes, 2, 24 and 48 hours after i.v. injection of 2-4 mCi labelled substance. Activity of blood samples taken for 48 hours were also measured. Scintigraphy of 3-3 nude mice bearing MKN-45 and HT-29 tumours were performed. Organ distribution of activity in mice was measured ex vivo after 48 hours.

Results: scintigraphic images of Ga-67-DOTA-lanreotide were similar to In-111-octreotide images in normal dogs. Activity of the liver was high and a predominant renal excretion was found. Half-time of disappearance of activity from the blood was 98.5 minutes. 14.1 per cent of the activity – measured at 5 minutes - were present in the blood after 24 hours. 6.33 and 7.41 % per gram tissue of the injected activity were found in MKN-45 and HT-29 tumours respectively.

Conclusions: Ga-67-DOTA-lanreotide may provide the basis for producing a Ga-68 labelled somatostatin receptor imaging radiopharmaceutical.

PS_603

OPTIMIZING CONDITIONS FOR RADIOLABELLING DOTA-PEPTIDES AT HIGH SPECIFIC ACTIVITY

W.A.P. Breeman (1), M. de Jong (1), T.J. Visser (2), W. Goedemans (3), J.L. Erion (4), W.H. Bakker (1), E.P. Krenning (1). (1) Nuclear Medicine; (2) Internal Medicine; (3) Mallinckrodt Medical, Petten, NL; (4) Mallinckrodt, Discovery, St Louis, USA

Objectives: DOTA-conjugated peptides, such as [DOTA^0,Tyr^3]octreotate (DOTA-tate) and [DOTA-Pro^1,Tyr^4] bombesin, can be stably labelled with radionuclides such as ^{67}Ga, ^{90}Y, ^{111}In and ^{177}Lu. These radiolabelled peptides are nowadays in use in the field of Nuclear Medicine, including peptide receptor radionuclide therapy (PRRT). Radioligands for PRRT require high specific activities (SA), since the amount of ligand that can be administered is limited: A. an increase in ligand will also increase the competition between ligand and radioligand for the same receptor and B. in case the peptide is bioactive i.e. bombesin. Parameters influencing the reaction kinetics during radiolabelling were investigated, as well how to obtain the highest achievable SA with maximal radiochemical purity. Results: Reaction kinetics were optimal at pH 4-5, while pH ≤ 3 strongly slowed-down the kinetics. Above pH 5 reaction kinetics varied: the solubility of the radionuclide becomes uncertain, due to rapid formation of hydroxides. The reaction kinetics of labelling with the radionuclides were also found to be different. The reaction was complete for ^{90}Y and ^{177}Lu after 20' at 80? and for ^{111}In after 30' at 100?. Radiolabelling was performed at microscale: 1-10 mCi in 15-50 µL, and at macroscale: ≥ 500 mCi in ≥ 2 mL. ^{111}In-DOTA-tate was labelled up to SA of 25 mCi ^{111}In per nmoles, which is half of the theoretical maximum SA. Radiochemical purity of ≥ 98% directly after, and ≥ 90% 24 h after the start of the labelling, could only be achieved after additions of Na-ascorbate and/or gentisic acid (during the reaction) and even longer by further dilution, and/or the addition of ethanol directly post labelling. The additions proved to be very efficient to prevent radiolysis, as revealed by ITLC and HPLC. Conclusions: DOTA-peptides can be radiolabelled at very high SA with high radiochemical purity.

PS_604

TECHNETIUM LABELING OF SURFACTANT PROTEIN B (SP-B)

M. Wenger (1), R. Alberto, C. Decristoforo, A. Amann, R. Moncayo, G. Putz. (1) University Clinic of Nuclear Medicine; (2) University Clinic of Anaesthesiology, Insbruck, Austria.

Lung surfactant is a lipid (90%) - protein (10%) mixture, produced by lung alveolar cells type II, which lowers the surface tension of the lung under physiologic conditions. In acute respiratory distress syndrome (ARDS) the lung surfactant system is altered with respect to both composition and surface activity. Treatment by instillation of lung surfactant into ARDS lungs has lead to controversal results. Aim of the study was to develop a Tc-99m labeling technique of bovine surfactant for the scintigraphic observation of its spreading in vivo. Methods: Bovine surfactant was isolated according to the method of Van Eijk and directly incubated with $[Tc(CO)_3(H_2O)_3^+]$ at 65-70¡C under various conditions. Determination of radiochemical purity was performed with paper chromatography and size exclusion chromatography. The protein characterisation was done by means of silver staining and Western blot analysis combined with enhanced chemoluminescence using a SP-B antibody. Spreading experiments were performed in a rectangular 2-D glass trough filled with isotonic buffer. The spreading of the surfactant on the buffer surface was observed by 1) surface tension measurements (Wilhelmy technique), 2) Gamma camera imaging (Siemens ZLC, static [64 x 64 matrix, 1 s frames]and dynamic [256 x 256 matrix, 200000k]mode). Results: Tricine/SDS PAGE gel electrophoresis revealed no differences between labeled and unlabeled SP-B. The labeling yield in the organic phase was more than 70%. The labeled protein showed high stability. Only SP-B together with phosphlipids showed marked surface activity, the control runs were negative ([99mTc(CO)3 (H2O)3]+ or TcO4- mixed with natural surfactant extract; 99mTc-SP-B without other components). Conclusions: Direct and specific 99mTc-labeling of the hydrophobic surfactant protein B was achieved using the $[Tc(CO)_3(H_2O)_3^+]$precursor. This procedure can easyly be used to prepare specifically labeled surfactant mixtures with spreading properties that coincide with those of unlabeled surfactant, i.e. the presented labeling method does not diminish the biological activity.

CARDIOVASCULAR 7

PS_605

INTRACORONARY INJECTION OF TC-99M TETROFOSMIN IN INFARCT RELATED ARTERY: A COMPARISON TO IV INJECTION FINDINGS IN REST SPECT STUDIES AFTER ACUTE MYOCARDIAL INFARCTION

T. Başoğlu (1), F. Canbaz (1), M. Elcik (2), M. Şahin (1), S. Albayrak (1), O. Yapıcı (1). (1) Department of Nuclear Medicine; (2) Department of Cardiology, Ondokuz Mayıs University, Samsun, Turkey.

99m-Tc Sestamibi SPECT is a well accepted method in the measurement of the infarct size ,which is an important indicator of the efficacy of therapy in acute myocardial infarction (AMI).Clinical investigations regarding the diagnostic power of the more recent agent Tc-99m Tetrofosmin (TF) in this issue are necessary. Our objective was to compare the rest SPECT findings in AMI patients after selective intracoronary (IC) and intravenous (IV) injections of TF, that has a lower first-pass myocardial extraction fraction compared to 99m-Tc-Sestamibi.

METHODS: Sixteen patients 13 M, 3F (54±10 yrs) with AMI were examined . We performed two rest TF-SPECT acquisitions within 10 days after admission and trombolytic therapy (TT).Coronary angiograpy (CAG) was performed for all patients after TT. First SPECT was performed within 30 minutes following IC injection (IC-SPECT) of 74 MBq TF only in the infarct related artery (IRA) during CAG. Two days after CAG, second SPECT was acquired 45 min after IV injection (IV-SPECT) of 740 MBq TF. Regional TF defects of the infarct area were visually scored (DS) by a 4-point system. A score index (SI) was calculated in both studies (SI=DS/Number of infarct related segments).

RESULTS: Global correlation of SI values between IC-SPECT and IV-SPECT in all 16 patients was significant(R=0.75, P=0.001). No global correlation could be found between the degree of IRA stenosis and SI values in both studies. Statistical analaysis was repeated after exclusion of 6 patients with multivessel disease and 1 patient with single vessel disease having visible collaterals in CAG (Rentrop=2). Remaining 9 patients had single vessel disease and no visible colletarals on CAG (RENTROP=0). Correlation coefficient of SI between IC-SPECT and IV-SPECT in these 9 patients was higher (R=0,81,p=0,008). The degree of IRA stenosis and SA values were also correlated (R=0.67,p=0.047 for IC-SPECT and R=0.75,p=0.001 for IV-SPECT) in these patients.

CONCLUSION: The high correlation between IC-SPECT and IV-SPECT in a relatively standardized subpopulation indicates reliability of conventional TF-SPECT in infarct size determination. Further experimental and clinical studies, particularly from the acute or subacute to the chronic stage of AMI are necessary to confirm this finding.

PS_606

CORONARY RISK FACTORS AND ABNORMAL LONGITUDINAL BASE TO APEX PERFUSION GRADIENT BY PET BLOOD FLOW MEASUREMENTS

M. Hernandez Pampaloni (1), J. Sayre (2), F. Keng (1), T. Kudoh (1), H. Schelbert (1). (1) Division of Nuclear Medicine, Department of Molecular & Medcial Pharmacology, UCLA School of Medicine, Los Angeles, USA; (2) Department of Radiology, UCLA School of Medicine, Los Angeles, USA.

Aim: A longitudinal, base to apex, myocardial perfusion gradient has been described in patients with coronary artery disease (CAD) and was attributed to diffuse coronary luminal narrowing. We asked whether this abnormal perfusion gradient also exists in patients without CAD but with coronary risk factors as hypercholesterolemia or long-term smoking, assessing also if any of these risk factors is more related to its severity. Methods: Regional MBF was measured in absolute units with ^{13}N-ammonia and PET at rest and during dipyridamole hyperemia in 12 hypercholesterolemic (total cholesterol >240 mg/dl) patients (8 female, 57±9 years) and 11 long-term smokers (3 female, 49±10 years) without documented CAD or other coronary risk factors. Values obtained were compared to those of 12 age-matched participants without coronary risk factors (6 female, 53±10) and in 13 young (7 female, 25±5 years) normals to exclude an aging effect. MBF was determined globally, for each of the three coronary territories and in the mid and the apical sections of the left ventricle (LV). Results: Myocardial perfusion on qualitative analysis was normal at rest and during hyperemia and no flow defects were present. MBF in absolute units was similar in the three coronary territories. Hyperemic MBFs in the apical LV section were lower than in the mid LV section both in the hypercholesterolemic patients (1.89±0.57 vs 1.67±0.5 mL $\cdot g^{-1} \cdot min^{-1}$, $p<0.05$) and smokers (1.79±055 vs 1.61±052, mL $\cdot g^{-1} \cdot min^{-1}$ $p<0.05$) but not in the age-matched and young normals. However, the magnitude of the perfusion gradient was similar between the 2 groups (p=NS).Conclusions: The abnormal longitudinal perfusion gradient, observed during dipyridamole MBF in smokers and hypercholesterolemic patients suggests the presence of a functional and/or morphological alteration of the coronary circulation related to the presence of coronary risk factors. Smoking and hypercholesterolemia seem to equally account for the presence of this perfusion gradient.

PS_607

ATTENUATION CORRECTED STRESS MYOCARDIAL SPECT CAN REDUCE THE NUMBER OF UNNECESSARY REST INVESTIGATIONS

O. Belohlavek, K. Taborska, I. Kantorova, D. Janeba. Dept.of Nuclear Medicine, Na Homolce Hospital, Prague, Czech Republic.

Aim: Attenuation-corrected (AC) imaging shows frequently normal stress myocardial perfusion while non-corrected (NC) imaging shows hypoperfusion. It is unclear whether it is necessary to continue with resting examination in this situation or to leave it and save money and radiation burden. The aim of this work was to carry out retrospective evaluation of this situation.

Methods: Suspected ischaemia was found on AC and/or NC stress imaging in 121 consecutive patients, and therefore the rest examination was carried out. Emission and transmission data were acquired in the same time into 4 energetic windows by Siemens E.CAM camera equipped with Profile system. AC and also NC standard slices of the left ventricle were divided into 17 segments and retrospectively re-evaluated visually by an experienced physician.

Results: Stress AC imaging was normal in 29 patients, while hypoperfusion was found in at least one of the segments with NC imaging. At rest the AC and NC finding has not changed in 27 of this patients, which means that the stress ischaemia was not demonstrated. One female was normal AC finding both at rest and stress, but NC showed stress-induced ischaemia in the antero-septal segment. Subsequent coronarography was completely normal. A similar situation was detected in one male in the basal part of the posterior wall. The patient refused coronarography and remains under monitoring. Vice versa normal stress NC finding was present at one male only, while AC imaging revealed hypoperfusion of the anterior wall. At rest the AC and NC findings did not change in this case. The NC imaging in males showed hypoperfusion most frequently in the posterior segment (Fig.), in females in anteroseptal and posterior segments.

Conclusions: Additional resting examination add no information in 28 of 30 cases. In the remaining two patients NC in contrast to AC showed stress-induced ischaemia. In one case this was a false positive finding, in the other one there is no final conclusion. It means that the resting examination did not bring any benefits in 29 – 30 cases out of 30 (96.7 to 100.0 %). If the results of this study are considered accordingly, in our group approximately one fourth of the resting examinations (29 to 30 out of 121) could be saved.

PS_608

ATTENUATION CORRECTION IN 99M-TC SESTAMIBI STRESS/REST CARDIAC SPECT

R. Couto (1), M.D. Marin (1), M. Coronado (1), T. Navarro (1), R. Plaza (2), A. Gonzalez (3), G. Riesco (1), J. Coya (1). (1) Servicio Medicina Nuclear, Hospital; (2) Servicio Radioproteccion. Hospital; (3) Servicio Cardiologia. Hospital, Madrid, Spain.

BACKGROUND: The aim of this study is to evaluate the impact of attenuation correction (AC) on the diagnostic accuracy of conventional stress/rest ^{99m}Tc-sestamibi SPECT studies, which are often impaired by artefacts induced by nonuniform attenuation.

METHODS: We studied 34 patients (pts), 28 men and 6 women , ages from 22 to 91 years old(mean 61±13,9).They were remitted with suspected of acute coronary syndrome (CAD): 19 pts. with previous diagnose of CAD, and 3 with another associated cardiac disease.

Conventional exercise/rest perfusion SPECT was performed in 25 pts. and pharmacologyc /rest in 9 pts; all of them with AC and without (NAC), using a dual-head SPECT camera with a ^{133}Ba source.

The left ventricular myocardium was divided into 16 segments (seg), corresponding to: left anterior descending artery (LAD) territory (8 segments) ; right coronary artery (RCA) territory (5 segments); and circumflex artery (LCx) territory (3 segments) .

Qualitative analysis was performed by two nuclear medicine experts (NM), following the scale: Fixed defect-hipoperfusion (FD), reversible defect-hipoperfusion (RD), paradox defect-hipoperfusion (PD) and normal perfusion (N).

Coronary angiography was realised in 12 pts to establish diagnose of ischemia or infarction. We compared angyographic and SPECT findings on RCA with and without AC.

RESULTS:

LAD territory	1 NM , NAC N? seg / %	1 NM, AC N? seg / %	2 NM, NAC N? seg / %	2 NM, AC N? seg / %
FD	38 / 14	25 / 9,2	39 / 14,3	25 / 9,2
PD	2 / 0,7	2 / 0,7	2 / 0,7	3 / 1,1
RD	10 / 3,7	12 / 4,4	10 / 3,7	10 / 3,7
N	222 / 81,6	233 / 85,7	221 / 81,3	234 / 86
TOTAL	272 / 100	272 / 100	272 / 100	272 / 100

RCA territory	1 NM , NAC N? seg / %	1 NM, AC N? seg / %	2 NM, NAC N? seg / %	2 NM, AC N? seg / %
FD	61 / 35,9	26 / 15,3	78 / 46	30 / 17,7
PD	2 / 1,1	0 / 0	2 / 1,1	0 / 0
RD	22 / 13	20 / 11,7	13 / 7,6	15 / 8,8
N	85 / 50	124 / 73	77 / 45,3	125 / 73,5
TOTAL	170 / 100	170 / 100	170 / 100	170 / 100

LCx territory	1 NM , NAC N? seg / %	1 NM, AC N? seg / %	2 NM, NAC N? seg / %	2 NM, AC N? seg / %
FD	14 / 13,7	8 / 7,8	17 / 16,6	11 / 10,8
PD	0 / 0	0 / 0	0 / 0	0 / 0
RD	5 / 4,9	6 / 5,9	5 / 4,9	4 / 3,9
N	83 / 81,4	88 / 86,3	80 / 78,5	87 / 85,3
TOTAL	102 / 100	102 / 100	102 / 100	102 / 100

Findings of coronary angiography: Normal or insignificance disease: 4 pts; one vessel disease:1 pt (LAD);two vessel disease:4 pts (3 pts LAD and RCA; 1 pt LCx and RCA) ;three vessel disease :3 pt
(LAD, RCA and LCx).

Coronariography compared with SPECT on RCA: sensibility NAC:85% and AC: 72%.Especificity NAC 40% and AC 80% . Accuracy NAC:60% and AC :70%.

CONCLUSION: The results of our study indicate that AC reduce the number of FD due to attenuation artefacts, especially on RCA territory (40%). However, diagnostic accuracy presents no slight improvement in our serie.

PS_609

ITERATIVE RECONSTRUCTION AND FILTERED BACKPROJECTION OF 201-TL GATED SPECT PROVIDE SIMILAR ACCURACY FOR THE MEASUREMENT OF LVEF

D. Daou (1), I. Pointurier (1), C. Coaguila (1), B.O. Helal (1), T. Fourme (2), I. Carel (2), R. Lebtahi (3), M. Faraggi (3), M. Slama (2), D. Le Guludec (3). (1) Department of Nuclear Medicine, Antoine Beclere Hospital, AP-HP, Clamart, France; (2) Cardiology Department, Antoine Beclere Hospital, AP-HP, Clamart, France; (3) Department of Nuclear Medicine, Bichat Hospital, AP-HP, Clamart, France.

Objectives: Coupling myocardial perfusion to function with ^{201}Tl ECG-gated SPECT (GSPECT) is interesting. Previous studies have reported good correlation between LVEF calculated with ^{201}Tl GSPECT and other imaging modalities. All these studies have used filtered back-projection (FBP) reconstruction. We aimed to evaluate whether the use of iterative (I) reconstruction with ^{201}Tl GSPECT as compared to FBP may ameliorate the reliability of the measurement of LVEF.
Methods: Twenty-four patients having both rest ^{201}Tl GSPECT at 15 min and 4h (8 frames/RR) after injection and equilibrium planar radionulcide angiography (RNA) in the left anterior oblique projection (LAO) (processed at 8 frames/RR). FBP was done with a BW 5/0.25 filter and I reconstruction was done with the OSEM software (2 iterations, 8 subsets). Processing of GSPECT studies was done with the QGS software. Then, the correlation of LVEF provided with FBP and I at 15 min to LVEF provided by planar LAO RNA were compared. Then, the variance of the paired absolute difference between the 15min and 4h GSPECT studies with FBP and I were studied.
Results: Results are reported in the Table.

	Linear regression	r	ser	p	paired absolute difference
FBP	1.04*EF-QGS	0.99	7.27	0.0001	-2±13.4
I	1.03*EF-QGS	0.99	7.25	0.0001	-2.8±12

Conclusion: The use of I and FBP reconstruction with rest ^{201}Tl GSPECT studies provide similar correlation and reliability for LVEF as compared to planar LAO RNA.

PS_610

MYOCARDIAL SPECT WITH ATTENUATION CORRECTION IN THE DIAGNOSIS OF CORONARY ARTERY DISEASE. A PRELIMINARY STUDY

I. Banzo, J. Jimenez-Bonilla, C. Guede, F.J. Pena, R.H. Allende, R. Quirce, J.M. Carril. Servicio de Medicina Nuclear, HU Marqués de Valdecilla, Santander, Spain.

Aim: Attenuation correction (AC) has been proposed as a method to increase the specificity of myocardial SPECT in the diagnosis of coronary artery disease (CAD). The aim of this study was to evaluate preliminary and prospectively the diagnostic contribution of the attenuation correction with scatter compensation (AC+SC) in patients with suspicion of CAD.
Materials: We applied AC+SC on 202 patients in whom CAD was suspected. This study included the 24 firsts consecutives patients who underwent to coronary angiography. A conventional myocardial non-corrected SPECT (NC-SPECT) and myocardial corrected SPECT (AC+SC SPECT) were obtained using a one day protocol (stress / rest with 300 and 925 MBq of 99mTc-Tetrofosmin respectively) in a two head camera equipped with a multiarray line sources of 153Gd. The studies were evaluated by visual analysis, by consensus of 4 observers using a score 0-4 (0 = normal perfusion; 4 = defect of perfusion). A myocardial SPECT score degree ≥ 2 and a coronary angiography with stenosis ≥70% were considered pathologicals.
Results: Coronary angiography was normal in 12 patients, showed angiographic stenosis < 70% in 3 and angiographic stenosis ≥ 70% in 9; 3 one vessel, 4 two vessel and 2 three vessel. In the 9 patients with stenosis ≥ 70% NC-SPECT showed abnormalities in 8 (sensitivity 89%) and the AC+ SC SPECT in 7 (sensitivity 78%). NC-SPECT had false positive results in 11 of 12 patients with normal coronary angiography; AC+CS SPECT had false positive results in 5. For major coronary arteries, specificity of NC-SPECT was 33% for right coronary (RCA), 66% for circumflex artery (CX) and 50 % for left anterior descending artery (LAD). AC+SC SPECT had a specificity of 91% for RCA, 91 % for CX and 58% for LAD.
Conclusion: In clinical evaluation of CAD, myocardial AC+SC SPECT led to relevant increase of the specificity of NC-SPECT. This improvement in specificity was more important in RCA and CX territories.

PS_611

ATTENUATION CORRECTION OF THALLIUM MYOCARDIAL PERFUSION SPECT

P.J. Ryan, D. Hausenlot. Department of Nuclear Medicine, Medway Maritime Hospital, Gillingham, U.K.

Aim: The use of attenuation correction using a Gadolinium line source during scan acquisition was applied to routine clinical practice after phantom data indicated significant benefits. The accuracy of routine attenuation correction of myocardial perfusion thallium SPECT imaging was investigated in relation to angiographic findings.
Methods: A sample of 83 consecutive patients who underwent thallium myocardial stress redistribution perfusion SPECT and who also had coronary angiography within the subsequent 6 months were examined. Patients were of age 39 – 74 years and 61 male and 22 female. Stress modalities were treadmill exercise 38, adenosine 33 and dobutamine 13. For whole heart analysis coronary artery narrowing of 50 % in any artery was considered significant. For individual analysis the same criteria applied. 64 patients had angiographic demonstrated coronary artery disease and 78 had abnormal thallium scans. The 3 coronary artery territories were assigned as LAD – apex, anterior wall and septum, LCX – lateral wall and RCA – inferior wall. Both fixed and reversible defects were considered positive on thallium imaging.
Results: Results are displayed below.

	Whole Heart	LAD	LCX	RCA
Sensitivity	97 %	87 %	37 %	82 %
Specificity	11 %	90 %	89 %	70 %
Pos Accuracy	80 %	93 %	71 %	76 %
Neg Accuracy	60 %	77 %	71 %	79 %

Conclusions: Attenuation corrected SPECT thallium myocardial perfusion imaging produces good results in clinical practice and enables it to be used with confidence in a clinical setting. The results are particularly reliable for LAD and RCA disease.

PS_612

CORONARY CALCIFICATIONS IN CHRONIC RENAL FAILURE: CORRELATION WITH MYOCARDIAL BLOOD FLOW DETERMIED BY PET

M. Hernandez-Pampaloni (1), J. Goldin (3), I. Salusky (2), B. Gales (2), H.R. Schelbert (1). (1) Division of Nuclear Medicine, Molecular & Medical Pharmacology Department; (2) Division of Pediatrics; (3) Department od Radiology, UCLA School of Medicine, Los Angeles, USA.

Aim: Risk factors for development of coronary artery and end stage renal disease often overlap. We hypothesized that coronary calcifications may represent a more advanced stage of the atherosclerotic disease and that these calcifications might correlate with vasomotion coronary abnormalities. Methods: We measured myocardial blood flow (MBF) at rest and after dipyridamole induced vasodilation (DIP) by ^{13}N-ammonia and PET and the coronary calcifications by EBT, in 42 major coronary territories (defined by polar map approach) of 14 hemodialysis patients equally divided in 2 groups depending on their calcium score. Seven patients had coronary calcifications (357±34 Hounsfield units)±(6 female, 32±7 years) and 7 (2 female, 24±7 years) had not. We compared these findings with the same number of coronary territories of 10 age-matched healthy volunteers (6 female, 25±4 years) without coronary calcifications on the EBT. Results: All had normal and homogenous resting and DIP perfusion studies. MBF at rest was higher in hemodialysis (HMD) pts than in normals (1.15±0.38 and 1.01±0.35 vs 0.57±0.12 mL/min/g; P<0.01), regardless of the calcifications and proportionate to the rate pressure product (RPP) in HMD pts (RPP; 12.5±2.9 vs 6.0±1.5 mmHg/min · 10^3; P<0.05). However, MBF was higher in the territories with calcifications when compared to the territories without calcifications of the HMD pts (1.15±0.38 vs 1.01±0.35. p<0.05), with a higher RPP. (12.5±2.9 vs 10.5±2.0 mmHg/min · 10^3; P<0.05). Hyperemic MBF response to DIP reached normal values in both groups (2.23 vs 2.21 vs 2.08±0.41 mL/min/g in normals; NS). Minimal coronary resistances during hyperemia (calculated from the ratio of mean blood pressure to MBF) remained higher in the regions with calcifications, compared to the others (58±24 vs 47±16; P<0.05) and to normals (54±21 vs 49±10; P<0.05). Regions with calcifications showed a significantly lower flow reserve than the ones without calcifications (1.89±0.31 vs 2.27±0.43; P<0.05), in both cases reduced if compared to normals (3.5±0.59; P<0.05).
Conclusions: Coronary calcifications may correspond to a more advanced stage in the atherosclerotic process. Longitudinal studies would be required to completely define the role of coronary calcifications in the coronary vascular disease of chronic renal failure patients.

PS_613

COMPARISON OF GATED TL-201 SPECT WITH OR WITHOUT ATTENUATION CORRECTION AND CONTINUOUS ATTENUATION CORRECTED SPECT

H. Siljander, J. Heikkonen, M. Ventilä, K. Virtanen. Helsinki University Central Hospital, Division of Cardiology, P.O.Box 340, 00029 Helsinki, Finland.

The most pronounced factors affecting image quality in perfusion scintigraphy are attenuation, scatter and motion of the heart. The aim of this study was to compare the capability of three different algorithms of thallium scintigraphy to correctly identify diseased territories of left ventricular myocardium For this purpose gated SPECT was acquisited and reconstructed with (gt) and without (gc) attenuation correction and a separate acquisition of continuous SPECT with (ct) attenuation correction was done.

Methods: Ten patients (8 male and 2 female) were studied with Tl-201 (100 MBq) in stress and rest using double headed Toshiba 7200A/Dl gamma camera. In gated studies two energy windows were used and triple energy window (TEW) method was used in continuous SPECT study. For attenuation correction an uniform plate source filled with water containing 1.3 GBq Tc-99m was on the head of A-camera. Acquisition matrix size was 64x64 and sampling angle 6^0/step. Main window level was 20 % and lower sub window 7 %. The continuous rotational SPECT acquisition was performed immediately before or after gated study with TEW method (7, 20, and 7 %) as nongated. Images were displayed as normal tomographic planes, maps of myocardial SPECT results and as numeric data for each segment and were compared with coronary angiography.

Results: Ten patients had 15 diseased vessels in angiography. Six defects were in left artery (LAD), five in right coronary artery (RCA) and four in left circumflex artery (LCX). Attenuation corrected continuous SPECT detected all 15 diseased vessels and attenuation corrected gated SPECT study detected 14/15. Both methods showed two "false" defects not matching the coronary angiography. Gated SPECT study without correction detected 10/15 vessels but there were no false defects. The results are summarized in the table.

	ct	gt	gc
Correctly identified defects	15/15	14/15	10/15
"False" defects	2	2	0

Conclusions: This preliminary study shows that with attenuation correction results in better sensitivity as compared with diminution the effect of cardiac motion at the expense of slight loss in sensitivity. Attenuation corrected continuous SPECT study is a fast and useful method in myocardial scintigraphy but larger patient series should be studied before this issue can be settled.

PS_614

Abstract withdrawn

PS_615

SERIAL CHANGE OF FATTY ACID METABOLISM DURING ACUTE PHASE OF MYOCARDIAL INFARCTION ASSESSED BY 123I BMIPP

S. Watanabe, H. Matsuo, T. Yamaki, M. Iwama, T. Hirose, S. Tanaka, A. Murata, S. Miyata, T. Kadosaki, Y. Matsuno, M. Tomita Department of Cardiology, Gifu Prefectural Hospital, Gifu, Japan.

Background: Discrepancies between ^{123}I-labeled-15-iodophenyl-3-methyl- pentadecanoic acid (BMIPP) uptake and regional myocardial blood flow were reported in patients with myocardial infarction. Mismatched segments with relatively more reduced BMIPP uptake were observed more often in acute as opposed to chronic and more often in reperfused as opposed to non-reperfused myocardium. These mismatched area are assumed to represent the viable myocardium that is exposed to severe ischemia. But the relationship between the abnormal area with abnormal BMIPP uptake and the severity of ischemia at the time of hospital referral, and the time course of metabolical recovery of these myocardium has not been established.

Purpose: This study was designed to clarify the time course of abnormality in fatty acid utilization from acute to chronic (1M) phase in patients with acute anteroseptal infarction, and to determine if this time course may be influenced by the status of coronary reflow.

Study groups: Consecutive series of 28 patients with acute anteroseptal myocardial infarction, who were successfully recanalized (TIMI 3 flow) within 6 hours from onset, were divided into 2 groups (14 patients with TIMI 0 or 1 flow, and 14 patients with TIMI 2 or 3 flow at the time of emergency catheterization). All of patients had severe chest pain of at least 30 minutes in duration, typical ST elevation in at least 2 contiguous leads in V_1-V_4 and CPK elevation more than 600IU/ml (3 times the normal upper limit).

Conclusion: Metabolicaly abnormal area was smaller than area at risk and larger than infarct area. However the abnormal fatty acid utilization assessed by 123I-BMIPP showed drastic changes during the acute phase of myocardial infarction∞Cmetabolic abnormality in salvaged myocardium still persisted at least until 4 weeks after myocardial infarction. The severity of metabolic abnormality and the degree of this improvement was influenced by the severity of coronary obstruction (TIMI grade) at the time of emergency catheterization.

PS_616

DOES QUANTIFICATION CHANGES THE RESULTS OF MYOCARDIAL PERFUSION SPECT

R. Buscombe, G. Gopinathan, A.J.W. Hilson. Nuclear Medicine, Royal Free Hospital, London, UK.

Many gamma camera systems are now sold with cardiac quantification packages. These are said to increase the accuracy of reporting. However the use of such quantification packages may change the clinical report as read form the tomographic slices. The aim of this study was to quantify the differences between visual reporting and quantification.

The qualitative report of stress and rest myocardial perfusion scintigraphy was performed in 333 segments of the heart (9 segments/patient) in 37 patients imaged with a one day stress rest protocol using Tc-99m tetrofosmin. A defect was defined by a reduction in activity of >50% in each of the segments. on the tomographic slices reconstructed using interative reconstruction with a Wiener smoothing filter . Quantification used an Emory bullseye system with gender and age matched normal controls.

There were number of abnormal segments seen on the slices were 119 at stress and 79 at rest. For the bullseye plot 98 were seen at stress and 76 at rest. 33 segments (10% were abnormal on the slices alone and 7 (2%) were abnormal alone on bullseye. Of 55 segments reported as ischaemic on slices, 26 (48%) were normal on bullseye, 13 of these in the right coronary artery (RCA) territory segments. Of the 67 segments reported on the slices as an infarct 10 (13%) were normal on bullseye, 7 of these in the territory of the RCA segments.

Therefore there are significant differences in the results of reporting scans using a bullseye plot especially in identifying inferior ischaemia. Therefore before using such a quantification method a full assessment of the accuracy of each method should be performed.

PS_617

DETERMINATION OF INFARCT SIZE BY ENZYMATIC CRITERIA AND BY GATED-SPECT

S. Canclini, P. Rossini, A. Terzi, C. Pizzocaro, U. Pajoro, B. Panarotto, B. Paghera, R. Giubbini. Nuclear Medicine, Spedali Civili di Brescia, Italy.

Infarct size is a major prognostic determinant and influences LV remodelling after uncomplicated myocardial infarction. The infarct size may be determined by imaging procedures and estimated from EKG or enzymatic criteria. **Aim** of the present study was the comparison between infarct size determined by either Tc99m Sestamibi SPECT or enzymatic criteria peak CK-MB and cardiac.

Methods. 23 pts with acute MI were imaged by Tc99m Sestamibi SPECT within 96 hours from the onset of chest pain. The infarct size was quantified by comparison with a gender matched polar map. Peak CK-MB was calculated using a protocol with sample collection every 6h from pt admission; Troponin T(cTnT) concentration was measured in a single sample at day 3 after admission. Both tests were determined by Roche Elecsys system.

Results. A significant difference in plasma concentrations of CK-MB (164,3±150,5 vs 574,3±484,8 µg/l, p<0.005) and cTnT (1,6±1,26 vs. 3,4±2,04 µg/l, p<0.02) was found in pts with infarct size over or below 20%, respectively. However a weak correlation was found at linear regression analysis between blood concentrations of both enzymes and infarct size: cTnT vs infarct size: R2 = 0,3312, CK-MB vs infarct size: R2 = 0,2055.

In conclusion, although infarct size can be grossly estimated from peak CK-MB and cTnT release, imaging techniques are needed for a reliable quantification.

PS_618

DOES LONGTERM SMOKING INFLUENCE LUNG HEART RATIO (L/H) OF TC99M SESTAMIBI (MIBI) DURING ADENOSINE MYOCARDIAL PERFUSION IMAGING (MPI)?

N. Nagaraj, J.E. Prosser, J.S. Grime. Department of Nuclear Medicine, Royal Liverpool University Hospital, Liverpool, UK.

Aim: L/H ratio obtained during MIBI MPI is a recognised method of providing supplementary information of left ventricular function. The effect of smoking on pulmonary MIBI uptake is not well assessed. The aim of this study was to determine whether smoking increases the pulmonary MIBI uptake in the absence of significant CAD as this would affect the interpretation of L/H ratio of smokers.

Method: Quantitative assessment of L/H ratio of 39 patients with low pre-test likely hood of CAD and normal MPI was performed. Group A -21 non-smokers (mean age 59, 5M, 16F) & group B- 19 smokers of ? 20 pack years of cigarette smoking (mean age 59, 2M, 17F). Pts with hypertension, LBBB, AF, valvular heart disease, diabetes, renal failure, advanced COPD, abnormal baseline ECG, ECHO & MUGA were excluded. A 2 day adenosine stress/rest protocol was employed and SPECT acquisition at 60 minutes post injection performed (180-degree orbit, 32 angles, 45 sec/per projection). ROIs were drawn around the myocardium and a representative area of the left upper lung on summed anterior SPECT projections. L/H ratios were calculated for both stress and rest studies.

Results:

	Lung/Heart Ratio Smokers Mean SD	Non Smokers Mean SD	
Stress	0.40 ± 0.06	0.41 ± 0.05	P = NS
Rest	0.48 ± 0.08	0.47 ± 0.06	P = NS

Conclusion: In conclusion, long term smoking does not independently affect the L/H ratios obtained from anterior summed SPECT projections during adenosine stress MPI using Tc99m Sestamibi and L/H ratio interpretation remains valid in smokers.

PS_619

COMPARISON OF LEFT VENTRICULAR VOLUMES AND EJECTION FRACTION BETWEEN STRESS AND REST GATED PERFUSION SPECT IN PATIENTS WITH ISCHEMIC HEART DISEASE

J. Lee, B.C. Ahn, S.W. Lee, K.B. Lee. Deparment of Nuclear Medicine, Kyungpook National University Hospital, Taegu, South Korea.

The purpose of this study was to evaluate the differences of end-diastolic volume(EDV), end-systolic volume(ESV) and ejection fraction(EF) between stress and rest images measured by gated myocardial perfusion SPECT in subjects with ischemic heart disease.

Methods: Forty-seven subjects(M/F=34/12, ranged 43 to 84 yrs, mean age 64yrs) with myocardial perfusion defect were selected for this study. Dual head SPECT camera(Vertex plus, ADAC) was used to acquire ^{99m}Tc-MIBI myocardial perfusion SPECT and EDV, ESV and EF were measured by AutoQuant program(Pegasys X, ADAC). Acqusition of stress image was performed at 1 hour after iv administration of radiopharmaceuticals with myocardial stress.

Results: There were no significant differences in EDV and ESV, whereas EF was lower in stress gating SPECT. Excellent correlations of EDV, ESV, EF between stress and rest gating images(Pearson's correlation test, r=0.961, p<0.01, r=0.977, p<0.01, r=0.921 p<0.01, respectively).

EDV, ESV and EF measured by AutoQuant program at stress and rest gating myocardial perfusion SPECT in patients with perfusion defect

parameters	Stress gating	Rest gating	Correlation	paired T test(p)
EDV(ml)	105.2±35.5	105.7±37.0	r=0.961, p<0.01	ns
ESV(ml)	56.4±30.7	55.1±31.1	r=0.977, p<0.01	ns
EF(%)	48.6±11.2	50.3±11.4	r=0.921, p<0.01	p=0.014
ns means not significant				

Conclusion: EDV, ESV and EF are well correlated between stress and rest gating SPECT in subjects with perfusion defect. EDV and ESV measured by AutoQuant program are not different, but different EF was noted between stress and rest SPECT, probably due to stunning of ischemic myocardium.

DIAGNOSTIC ONCOLOGY 13

PS_620

THE ASSESSMENT OF MEDIASTINAL LYMPH NODES USING 99MTC TETROFOSMIN SPECT IMAGING IN PATIENTS WITH NON-SMALL CELL LUNG CANCER(NSCLC):COMPARING WITH CT

H. Wang (1), Q. Wei Chen (2), T.I.A.N. Wei Jia (1), P.A.N. Zhi Lai (3), Z.H.U. Cheng Mo (1). (1) Department of Nuclear Medicine; (2) Department of Surgery; (3) Department of Radiology, Rui Jin Hospital, Shanghai, China.

Aim: The preoperative accurate detection of mediastinal lymph nodes (MLNs) in NSCLC is very important In order to study the involvement of MLNs ,this work reported the clinical role of ^{99m}Tc-Tetrofosmin SPECT imaging in comparison with CT scan.

Methods: 76 patients (47 males, 29 females,age range 39-81 years) with suspected primary lung cancer were investigated. Staging procedures included radiography, CT scan and fiberoptic bronchoscopy. Both CT scan and ^{99m}Tc-Tetrofosmin imaging were performed within one week before surgery. in all patients.The metastatic involvement of mediastinal lymph nodes was assessed by histopathology after surgery and in 7 cases by mediastinoscopy. In this study,the results of ^{99m}Tc -tetrofosmin SPECT and CT were directly compared with surgical findings for evaluating the lung and mediastinal lymph node lesions.

Results: Primary NSCLC was confirmed in 64 patients (21 squamous cell cancers, 32 adenocarcinomas, 11 large cell carcinomas); in 4 patients we found 2 metastases and 2 tuberculoses. 8 pts were not submitted to surgery. MLN involvement was demonstrated in 31 of the 64 patients (48%) and ^{99m}Tc-Tetrofosmin SPECT imaging correctly staged 25 of 31patients and 29 of 33 patients without mediastinal nodes, with a diagnostic sensitivity of 80.6% and a specificity of 87.9%. We had 4 false positive result and 6 false negative results. CT scan gave 16 true positive, 10 false positive, 23 true negative and 15 false negative results, with a sensitivity of 51.6% and a specificity of 69.7%.

Conclusions: The study shows that ^{99m}Tc-tetrofosmin-SPECT is an accurate and useful tool to assess mediastinal lymph node involvement in NSCLC and its diagnostic accuracy is better than that of CT scan. This technique may play an important role in reducing the number of invasive staging procedures.

PS_621

TL-201 UPTAKE AND ITS RELATIONSHIP WITH CHEMO-THERAPEUTIC RESPONSE, METASTASIS, P53 STATUS, AND SURVIVAL IN PRIMARY LUNG CANCER

T.F. Çermik (1), M. Yüksel (1), C. Karlıkaya (2), L. Doğanay (3), E. Çakır (2), A. Salan (1), M. Ture (4), O.N. Yiğitbaşı (1), S. Berkarda (1). (1) Deparment of Nuclear Medicine; (2) Deparment of Chest Disease; (3) Deparment of Pathology; (4) Deparment of Statistic, Trakya University, Edirne, Turkey

Tl-201 scintigraphy has been used to detect malignant pulmoner disease. In this study, Tl-201 was used to clarify the relationship between Tl-201 uptake and response in chemotherapy and metastasis and survival.

Methods: 47 patients with lung cancer underwent Tl-201 SPET. From SPET images early (ER) and delayed (DR) tumour/normal lung ratios were obtained. In 19 patients p53 status were measured with immuno-histochemical staining. Patients were divided into subgroups according to change of the tumour size in CT scan taken after 4 cure of chemotherapy; responders [R(+)] and non-responders [R(-)], metastasis (+) and (-), and p53 (+) and (-).

Results: ER, DR and retention index were not different according to either response to chemotherapy or p53 status. While ER of patient with metastasis was significantly lower than those patients without metastasis, DR was slightly lower in patients with metastasis, but this difference was not different, significantly. Although there was no significant difference for ER and DR according to p53 status, we found a significant inverse correlation between Tl-201 uptake and p53 status, r=-0.48 and p=0.028 for ER, and r=-0.49 and p=0.027 for DR. The step wise regression analysis confirmed that the Tl-201 uptake ratio was an independent prognostic factor for survival.

	RESPONSE		METASTASIS		p53	
	(+)	(–)	(+)	(–)	(+)	(–)
No	15	15	18	19	11	8
ER	3.29±1.26	2.76±0.95	2.44±0.91	3.21±1.21*	2.72±0.92	3.45±1.15
DR	3.56±1.37	3.02±0.81	2.82±0.92	3.40±1.27	3.14±0.66	3.98±1.35
(+) vs (–): *:p<0.04;						

Conclusion: The inverse correlation between Tl-201 uptake and p53 status and the lower Tl-201 uptake values of patients without metastasis suggested that lung cancer patients with lower Tl-201 uptake tends to be more metastatic. Additionally, our results suggested that patients with higher Tl-201 uptake tend to response positive to chemotherapy

PS_622

QUANTIFIED 99MTC-TETROFOSMIN SPECT IN PREDICTING CHEMOTHERAPEUTIC RESPONSE IN NON-SMALL-CELL LUNG CANCER

D. Fuster (1), N. Viñolas (2), C. Mallafré (3), C. Falcón (4), F. Martín (1), F.J. Setoain (1), M. Ortega (1), J. Pavía (1), F. Pons (1). (1) Department of Nuclear Medicine, Hospital Clínic, Barcelona, Spain; (2) Department of Oncology, Hospital Clínic, Barcelona, Spain; (3)

Aim: To evaluate if tumour uptake of ^{99m}Tc-tetrofosmin can predict response to chemotherapy in patients with advanced non-small-cell lung cancer (NSCLC).

Methods: We prospectively studied nineteen men (mean age 57±9.9 years) suffering from advanced NSCLC cancer confirmed by histology. We included 11 cases of squamous cell carcinoma and 8 of adenocarcinoma. The mean size of tumour lesions was 5.1±1.1 cm. Thorax scintigraphy (SPECT) was performed 2 hours after an i.v. injection of 740 MBq of ^{99m}Tc-Tetrofosmin. The equipment consisted of a dual-head gamma camera fitted with a low energy, high resolution collimator. The tumoural uptake was quantified in SPECT images using the transversal slice where the tumour was best visualized. The response to chemotherapy was evaluated at three months upon completion of treatment. Based on computed tomography (CT) results, patients were classified as responders (significant size reduction by CT) or non-responders (no changes or size increase by CT).

Results: There was no relationship between the histologic type or tumour size and ^{99m}Tc-Tetrofosmin uptake. 12/19 patients responded to chemotherapy and 6/19 did not. One patient could not be evaluated because of premature death at 3 weeks after treatment administration. Those which responded to chemotherapy showed higher ^{99m}Tc-Tetrofosmin uptake (2.17±0.16) than non-responding patients (1.27±0.63) (p<0.001).

Conclusions: These results suggest that ^{99m}Tc-Tetrofosmin SPECT can be useful in the assessment of patients with NSCLC prior to chemotherapy treatment.

PS_623

THE RELATIONSHIP BETWEEN TC-99M MIBI UPTAKE AND CHEMOTHERAPEUTIC RESPONSE, METASTASIS, PGP, P53, AND PROGNOSIS IN LUNG CANCER

M. Yüksel (1), T.F. Çermik (1), L. Doğanay (2), C. Karlıkaya (3), A. Salan (1), E. Çakir (3), M. Ture (4), S. Berkarda (1), O.N. Yiğitbaşı (1). (1) Department of Nuclear Medicine; (2) Department of Pathology; (3) Department of Chest Disease; (4) Department of Biostatistic, Trakya University, Edirne, Turkey

Higher MIBI uptake in lung cancer is reported with positive response to chemotherapy. In various types of tumours, it was noted that Pgp expression had a negative correlation with MIBI uptake and it plays important role in chemotherapeutic failure. Additionally, p53 status may play important role in chemo- and radioresistance, metastasis and prognosis However, in lung cancer the results of published studies were conflicting. The aim of this study was to evaluate the relationship between MIBI uptake and Pgp, p53, metastatic status and prognosis.

Methods: Total of 56 patients with lung cancer underwent Tc-99m MIBI SPET before the chemotherapy. From SPECT images early (ER) and delayed (DR) tumour/normal lung ratios were obtained. In 26 patients P-glycoprotein expression and in 28 patients P53 status were measured with immuno-histochemical staining. Patients were divided into following subgroups; responders [R(+)] and non-responders [R(-)] according to change of the tumour size in CT scan taken after 4 cure of chemotherapy, metastasis (+) and (-), Pgp (+) and (-); and p53 (+) and (-).

Results: Patients had follow-up period 1-30 months with a mean value of 9.02±6.62 months. ER and DR of R(+) were significantly higher than those of R(-). Patients with metastasis had higher DR than those without metastasis, their ER was slightly higher. We found no significant difference between Pgp (+) and (-) group for ER and DR values. Interestingly patients with p53 (+) had significantly higher ER and DR values than those with p53 (-).There was no correlation between the uptake of MIBI and the degree of Pgp or p53 expression. Stepwise regression analysis showed that MIBI uptake did not effect the prognosis of patients.

	Response		Metastasis		Pgp		p53	
	(+)	(–)	(+)	(–)	(+)	(–)	(+)	(–)
n	19	22	29	27	18	8	19	9
ER	3.52±1.18	2.26±0.93*	2.33±1.06	2.91±1.18	2.62±1.01	2.64±1.29	2.21±081	3.26±1.29#
DR	3.58±1.43	2.52±1.08#	2.35±1.07	3.19±1.32#	2.66±1.02	2.79±1.28	3.26±0.71	3.34±1.37#
(+) vs (–): *:p<0.0005; #:p<0.02								

Conclusion: According to our results, in lung cancer we suggested 1.) that patients with higher MIBI uptake tend positive response to chemotherapy and tend to be less metastatic, 2.) that Pgp expression seems to play not an important factor for the chemotherapeutic response, and 3.) that patients with p53 (+) status have higher MIBI uptake than those of with p53(-).

PS_624

ASSESSMENT OF THYMIC ABNORMALITIES WITH TL-201 SCINTIGRAPHY IN PATIENTS WITH MYASTHENIA GRAVIS

T. Higuchi, J. Taki, S. Kinuya, H. Sumiya, K. Nakajima, K. Yokoyama, N. Tonami. Department of Nuclear Medicine, Kanazawa University, Kanazawa, Japan.

The preoperative evaluation of thymic status is important for the planning of the therapeutic strategy in patients with myasthenia gravis (MG). CT examination was reported to demonstrate insufficient results, therefore we aimed to determine the ability of thallium-201 (Tl) single photon emission computed tomography (SPECT) to evaluate thymic lesions, including lymphoid follicular hyperplasia (LFH) and thymoma, associated with MG.

Methods: Forty-six patients with MG who underwent thymectomy were included. Tl SPECT and computed tomography (CT) were performed preoperatively. Tl SPECT was performed 15 min (early image) and 180 min (delayed image) after the injection of Tl (111MBq). The results were visually assessed, and Tl uptake ratio (thymic lesional count density / lung count density) was obtained for quantitative analysis. Tl uptake was analyzed among three groups of normal thymus, LFH and thymoma. Diagnostic ability of Tl scintigraphy and CT were compared.

Results: In the histological examination, 19 had normal thymus, 16 had LFH_and 11 had thymoma. CT correctly diagnosed only 5 of 16 patients with LFH. The mean (95% CI) of uptake ratio in normal thymus, LFH and thymoma was 0.97 (0.90 – 1.03), 1.15 (1.04 – 1.32) and 1.94 (1.56 – 2.25) of the early image and 1.10 (1.00 – 1.18), 1.69 (1.48 – 1.85) and 2.12 (1.65 – 2.50) of the delayed image, respectively. On the early images, thymoma showed more intense Tl accumulation than normal thymus (p<0.01) and LFH (p<0.01). On the delayed images, both thymoma (p<0.01) and LFH (p<0.01) revealed more intense uptake than normal thymus. Tl SPECT, accurate diagnosis was obtained in 87.0% (40/46), and in contrast, 69.6% (32/46) with CT. Tl uptake ratio was more sensitive in detecting LFH than CT (13/16 vs. 5/16).

Conclusions: Tl SPECT can differentiate normal thymus, LFH and thymoma and has greater sensitivity for the diagnosis of LFH than CT in patients with MG. Tl SPECT is recommended as a preoperative examination of the thymus in patients with MG.

PS_625

ASSESSMENT OF CARTILAGINOUS TUMOR WITH TL-201 SCINTIGRAPHY

T. Higuchi, J. Taki, S. Kinuya, K. Nakajima, H. Sumiya, K. Yokoyama, N. Tonami. Department of Nuclear Medicine, Kanazawa University, Kanazawa, Japan.

Histological diagnosis and grading of cartilaginous tumor should be essential element, because it has an important bearing on its prognosis. We aimed to make clear the character of Tl-201 uptake in various histological types and grading of cartilaginous tumors and assessed its clinical values.

Methods: A total of 23 lesions of histologically proven cartilaginous tumors - 2 enchondroma, 16 conventional chondrosarcoma (low grade = 10, moderate grade = 6), 3 mesenchymal chondrosarcoma, 1 myxoid chondrosarcoma and 1 dedifferentiated chondrosarcoma - was assessed. Fifteen minutes after the intravenous injection of Tl-201 (111MBq), we recorded planar and SPECT images. Tl-201 uptake in the tumor lesion was evaluated visually using five-grade scoring system: 0 = equal to background activity, 1 = slight increase in uptake, 2 = moderate increase in uptake, 3 = strong increase in uptake and 4 = uptake stronger than heart uptake.

Results: Tl uptake scores were 0 in 2 / 2 lesions with enchondroma, 9 / 10 with low grade conventional chondrosarcoma and 4 / 6 with moderate graded conventional chondrosarcoma. Tl uptake scores were 1 in 2 / 6 lesions with moderate graded conventional chondrosarcoma, myxoid chondrosarcoma and 3 / 3 lesions with mesenchymal chondrosarcoma. Tl uptake score were 3 in dedifferentiated chondrosarcoma.

Conclusions: No Tl-201 uptake in cartilaginous tumor indicated enchondroma or low grade conventional chondrosarcoma. However, when the Tl-201 uptake was obvious, higher grade chondrosarcoma or other special types of chondrosarcoma should be considered.

PS_626

THE VALUE OF TC-99M-TETROFOSMIN SCINTIGRAPHY AS AN INDICATOR OF MALIGNANCY AMONGST BONE AND SOFT-TISSUE TUMORS

Z. Yapar (1), M. Kibar (1), S. Özbarlas (2), A. Uğuz (3), S. Zorludemir (3). (1) Department of Nuclear Medicine; (2) Department of Orthopedia; (3) Department of Pathology, Cukurova University School of Medicine, Adana, Turkey.

Tc-99m-tetrofosmin (TET) has been developed as a radiopharmaceutical for myocardial imaging. Recently, tumor uptake and prediction of multidrug resistance have also been reported regarding this tracer. In this study, TET was evaluated for its ability to detect malignant and benign lesions from bone and soft-tissue masses.

Methods: Thirty three patients (23 malignant, 10 benign lesions) with various bone and soft-tissue lesions were studied. Radionuclide angiography with TET was done except one patient, and planar images of the lesions were obtained at 30 min postinjection. The TET uptake ratio (UR) was calculated by dividing the lesion count by the background count. The planar images and the perfusion phase were also evaluated visually based on a scoring system. The lesions were resected by open biopsy to obtain a histopathological diagnosis.

Results: In visual analysis, twenty two of 23 (96%) malignant lesions and 4 of 10 (40%) benign lesions were visualized on TET images. On radionuclide angiography, 100% (22/22) of the malignant lesions and just 30% (3/10) of the benign lesions could be visualized. In quantitative analysis, the mean uptake ratio derived from malignant lesions was significantly higher than that of benign lesions (3.67 ± 2.47 versus 1.24 ± 0.42, respectively; $p< 0.001$). Among 10 benign lesions, there were 2 (20%) of which the UR exceeded the lower limit of malignant lesions' UR range. Among 23 malignant lesions, there were 3 (13%) of which the UR corresponded to the benign lesions' UR range.

Conclusions: According to our results, TET accumulation in malignant and benign bone/soft-tissue lesions differs significantly. In addition, blood flow could be assessed by radionuclide angiography with TET.

PS_627

THE ROLE OF BONE SCINTIGRAPHY AND TUMOR MARKERS IN THE ASSESSMENT OF BONE INVOLVEMENT IN MALIGNANT DISEASES

S.H. El-Haddad, A. Fawzy, W. Metnawy, M. Abo-Gabal. Nuclear Medicine and Clinical Oncology Department, Faculty of Medicine, Cairo University, Egypt.

Bone scan is the most sensitive complementary examination used to detect bone metastases. ICTP (type I collage telopeptide) is a new biochemical marker that has been introduced to assess bone resorption in different bone diseases including metastatic disease.

Aim: To evaluate the role of ICTP for the diagnosis and follow up of bone metastases.

Methods: The study included 80 patients having primary malignant. They were subjected to conventional whole body osseous scintigraphy following 740 MBq of Tc-99m MDP as well as measurement of serum ICTP level. They were divided into two main groups according to the results of the bone scan whether negative or positive. Furthermore, metastatic patients were classified according to the metastatic burden (number of metastases) into four grades.

Results: The mean serum ICTP level was higher than the reference interval (1.3-5.2 _g/L) in both the negative and positive groups (8.3+4.9 _g/L and 11.3+6.3 _g/L respectively). On correlating the ICTP level and bone scan results, 28 patients (73.7%) of the negative group (38 patients) had elevated ICTP levels and only 30 patients (71.4%) of the positive group (42 patients) had elevated ICTP level with no statistical significant difference in both ($P > 0.05$). In comparing the ICTP level with the bone scan results, it was found that ICTP had a reasonable sensitivity of 71%, a low specificity of 26% with a positive predictive value of 52%, a negative predictive value of 45% and 50% accuracy. On comparing the serum ICTP level with the metastatic burden of the patients, no significant statistical difference could be obtained between the ICTP level and the grade of bone deposits ($P > 0.05$). The positive finding in this study was the highly significant statistical difference that was obtained on correlating the complaint of patients with the bone scan results as 27 patients (71%) of the negative group were asymptomatic, while 32 patients (76%) of the positive group were complaining of bony pains ($P < 0.001$). An obvious finding that ICTP level was elevated on follow up of two cancer breast patients keeping with the progression state of their bone scans.

Conclusion: ICTP cannot replace bone scan in diagnosis and follow up metastasizing tumors but it may be used in the follow up of these tumors to monitor response to therapy in conjunction with bone scintigraphy.

PS_628

MARKED TL-201 UPTAKE IN GIANT-CELL TUMOR OF BONE

T. Higuchi, J. Taki, H. Sumiya, S. Kinuya, K. Yokoyama, K. Nakajima, N. Tonami. Department of Nuclear Medicine, Kanazawa University, Kanazawa, Japan.

Giant-cell tumor of bone (GCT) is a benign and a primary skeletal neoplasm. There are no reports that assess the precise features of Tl uptake in GCT lesion. We hypothesized intense Tl uptake in GCT lesions, because of their abundant blood flow and cell density. Accordingly, we aimed in this study to elucidate Tl uptake in GCT lesions, and discuss its clinical value.

Methods: Twenty-one patients with histopathologically proven GCT (22 lesions; 18 primary lesions and 4 recurrent lesions) underwent Tl scintigraphy. We also studied conventional osteosarcoma (10 lesions), a most common primary malignant bone tumor, and chordoma in the sacrum (4 lesions), an entity requiring differential diagnosis from GCT in the sacrum. Early and delayed planer imaging was performed at 15 min and 3 hr after the intravenous injection of Tl chloride (111MBq). Tl uptake ratio was calculated by dividing the count density of the tumor region of interest (ROI) by that of the background ROI.

Results: All GCT lesions showed increased Tl uptake in both early and delayed images. The mean Tl uptake ratios of primary GCT were 4.69± 2.67 in the early images and 2.19±0.66 in the delayed images, and those of recurrent lesions were 5.84± 3.97 in the early images and 2.71±1.09 in the delayed images. These values tended to be higher than those of osteosarcoma, 3.12±1.06 in the early images and 1.76±0.41 in the delayed images. Chordoma did not show appreciable Tl uptake; whose uptake ratio was 1.19±0.22 in the early images and 1.14±0.12 in the delayed images.

Conclusions: GCT, a benign lesion, shows intense Tl accumulation, probably reflecting abundant vascularity and viable cell number in the lesion. In the differential diagnosis, GCT can be excluded if Tl does not accumulate in the tumor lesion. It be also may helpful in diagnosing recurrent lesions on post-operative follow up.

PS_629

MONITORING THERAPY IN CHILDHOOD EWING'S SARCOMA WITH THALLIUM SCINTIGRAPHY AND MAGNETIC RESONANCE IMAGING

G. Vural (1), E. Özalp (1), S. Berberoğlu (2), N. Erçakmak (1), I. Ilhan (2), A. Cila (4), I. Pak (3), B. Turgut (1). (1) Department of Nuclear Medicine, Ankara Oncology Hospital, Ankara,Turkey; (2) Department of Pediatric Oncology, Ankara Oncology Hospital, Ankara,Turkey; (3) Department of Pathology, Ankara Oncology Hospital, Ankara,Turkey; (4) Department of Radiology, University of Hacettepe, Ankara, Turkey

Ewing's sarcoma is a highly malignant neoplasm. Magnetic resonance imaging (MRI) is the imaging modality to evaluate the extent of the primary lesion and to monitor the response to therapy.
Aim: The purpose of the study was to evaluate the value of Thallium (Tl-201) scintigraphy in monitoring therapy in childhood Ewing's sarcoma patients.
Methods: 10 patients (7 male, 3 female; mean age: 14 ± 4.6) with Ewing's sarcoma were evaluated with pretreatment and serial post-treatment MRI and Tl-201 scintigraphy (4 times). Lesion size, signal intensity relative to muscles (in T1w, T2w and STIR images) and enhancement patterns were evaluated in MRI. Tl-201 planar and whole body images were obtained at 10 minutes and 2 hours after iv injection of 2.5 mCi (92 MBq) of Tl-201. Thallium uptake was evaluated visually. All patients received chemotherapy according to the EICESS 92 protocol and radiation therapy. Four patients had surgical resection.
Results: In pre-treatment images all patients showed marked Tl-201 uptake in the affected sites. In 8 patients, Tl-201 uptake disappeared in the first scintigraphic evaluation after chemotherapy while MRI showed stable disease. Two patients showed decreased but still positive uptake in the first scintigraphic evaluation. They died because of metastases in follow-up. In one patient, Tl-201 uptake was re-observed at third scintigraphic evaluation and also MRI showed progression, and this patient was diagnosed relapse in primary tumor histopathologically. In MRI the earliest sign of therapy response was disappearance of edema in surrounding muscles. In 6 patients with good response to chemotherapy, regression of soft tissue component within 2 to 7 months was the most striking finding. Signal changes within the affected bone persisted even in patients who were considered to be in remission. Therefore STIR sequence was very sensitive but nonspecific for tumor versus post-therapeutic changes in the bone.
Conclusion: MRI and Tl-201 scintigraphy are sensitive methods for determining the tumor response to treatment, however Tl-201 determines the metabolic activation of the tumor tissue and viability more specifically and it provides also whole body evaluation which is especially important in patients with Ewing's sarcoma where skip metastases develop frequently. Therefore, we suggest that serial Tl-201 scintigraphy, especially the first evaluation, seems to be very valuable and can be sufficient in monitoring and planning therapy.

PS_630

COMPARISON OF 3-[123I]IODO-L-A-METHYL TYROSINE TRANSPORT IN HUMAN FIBROBLASTS AND EWING'S SARCOMA CELLS

C. Franzius (1), K. Kopka (1), F. van Valen (2), V. Eckervogt (2), B. Riemann (1), J. Sciuk (1), O. Schober (1). (1) Department of Nuclear Medicine; (2) Department of Orthopaedics, Münster University, Münster, Germany.

Aim: 3-[^{123}I]Iodo-L-α-methyl tyrosine (^{123}I-IMT) scintigraphy of extracranial malignant tumors has been described recently. But up to now, little is known about the transport characteristics of ^{123}I-IMT uptake into extracranial cells. Therefore, the aim of this study was to determine the transport systems of the ^{123}I-IMT uptake in extracranial tumor cell lines (human Ewing's sarcoma cell lines) in comparison to non-neoplastic extracranial cells (human fibroblasts).
Methods: The time course of [^{123}I]IMT uptake into human fibroblasts and the Ewing's sarcoma cell-lines VH-64 and CADO-ES-1 was examined between 1 and 60 min. [^{123}I]IMT uptake rates with varying concentrations of [^{123}I]IMT (5-300 µM) were determined to assess the precise kinetics of the [^{123}I]IMT transport. Furthermore, competition experiments of [^{123}I]IMT uptake with other amino acids were performed to determine the distinct transport systems involved in the [^{123}I]IMT uptake.
Results: The kinetic analysis of the [^{123}I]IMT uptake rates into the cells was concordant with the predominance of a single, sodium-independent transport system. The apparent Michaelis constants K_m were 116.2 ± 18.9 µM (fibroblasts), 46.3 ± 1.9 µM (VH-64), and 105.3 ± 21.3 µM (CADO-ES-1), respectively. The maximum transport velocities V_{max} amounted to 191.6 ± 13.9 pmol • 10^6 cells^{-1} • min^{-1} (fibroblasts), 270.4 ± 3.0 pmol • 10^6 cells^{-1} • min^{-1} (VH-64), and 351.9 ± 30.6 pmol • 10^6 cells^{-1} • min^{-1} (CADO-ES-1). Competitive inhibition experiments revealed solely a sodium-independent transport of [^{123}I]IMT into fibroblasts (79 ± 3 % via system L, 22 ± 4 % unspecific uptake). In the Ewing's sarcoma cells [^{123}I]IMT was mediated via system L (61 ± 1 % (VH-64), 67 ± 3 % (CADO-ES-1)) and via sodium-dependent systems A and/or $B^{0,+}/B^0$ (18 ± 1 % (VH-64), 17 ± 2 % (CADO-ES-1); unspecific uptake: 16 ± 3 % (VH-64), 14 ± 3 % (CADO-ES-1)).
Conclusion: While [^{123}I]IMT uptake into the human Ewing's sarcoma VH-64 and CADO-ES-1 cells is mediated mainly by the sodium-independent system L and to a minor extent by sodium-dependent systems A and/or $B^{0,+}/B^0$, [^{123}I]IMT is exclusively transported into human fibroblasts via system L. Furthermore, sodium-independent maximum transport velocities V_{max} are about 1.5 times higher in Ewing's sarcoma cells as compared with fibroblasts, suggesting a higher expression of amino acid transport systems in Ewing's sarcomas cells than in non-malignant fibroblasts.

PS_631

THE POSSIBILITY TO QUALIFY PATIENTS WITH CANCER FOR BONE SCINTIGRAPHY ACCORDING TO COLLAGEN TURNOVER MARKERS : PICP, PINP, ICTP, CTX.

M. Konieczna, G.W. Chmielowski, M. Dziuk. Department of Nuclear Medicine, Central Clinical Hospital Military Medical University , Warsaw, Poland.

Aim. It is known that bone metastases change bone metabolizm.Therefore the markers of collagen turnover (indicators of metabolic bone activity) can be helpful to determine patients who need scintigraphy.The aim of study was to asses the diagnostic efficacy of various bone formation and resorption markers in comparison to bone scintigraphy.
Methods:We enrolled 150 patients , 74 with prostate cancer, 61 with breast cancer, 10 with lung cancer and 5 with other type. According to results of bone scintigraphy they were divided into three groups.Group 0 - no change in bone scan, group 1 - single nonspecific hot spot, group 2 - multiple lesions. Bone scintigraphy was performed on the Aoex SP-6, Elscint gamma camera after intravenous injection of 925 MBqTc-99m MDP. As bone formation markers we evaluated amino- and carboxyterminal propeptides of procollage I type (PINP, PICP). The markers of bone resorption were: carboxyterminal telopeptide of collage I type (ICTP) and carboxy octapeptide (CTX).
Results:There was no significant difference between group 0 and 1. The levels of markers in group 2 are significsnt bigger. The Z scores for PINP, ICTP, PICP, CTX were 2.9, 1.56, 0.5, 0.46 respectively. In discriminant analysis PINP had best coefficient of corelation with discriminating function. The sensitivities were 96%, 69%, 27%, 56% for ICTP, PINP, PICP, and CTX respectively. The negative predictive values were 99%, 93%, 86% and 89% respectively.
Conclusions:PINP is best discriminating marker.The ICTP and PINP markers within reference limits may enable avoiding unnecessary bone scintigraphy

OTHER CLINICAL SCIENCE. GASTROENTEROLOGY 3

PS_632

POSTOPERATIVE DYSPHAGIA IN ORAL CANCERS: SCINTIGRAPHIC EVALUATION

F. Reale (1), J. Galli (2), G. D'Errico (1), L. D'Alatri (2), G. Almadori (2), V. Valenza (1). (1) Nuclear Medicine; (2) Otolaryngology, Catholic University of , Rome, Italy.

Oral cavity cancers need an aggressive surgery for the high local malignancy, so it follows a permanent damage with clinical findings linked to swallowing difficulties. The **aim** of this work is to study and evaluate the alterations of oral and pharyngeal swallowing phases complained about the patients (pts) underwent oral surgery, with great attention to dysphagia and aspiration, by oro-pharyngo scintigraphy (OPS).
Patient population: We studied 13 pts (12 males and 1 female, mean age 60, range 36-74), 4 with tongue cancer, 3 with palate cancer, 5 with tonsil cancer and 1 with jaw cancer respectively. We studied 17 healthy volunteers as control group.
Method: OPS was performed administering 10 ml of water with 37 MBq of 99Tc-SC and acquiring sequential images (0,125" frames for a total 60" examination) with patient standing in front of the gamma camera in a 80¡ right anterior oblique position. The study of the sequential scintigraphic images and of A/T curves permitted a qualitative (multiple deglutitions, nasopharinx refluxes, premature ingestion of the bolus) and quantitative analysis (oral and pharyngeal transit times and retention indexes, tracheal aspiration percentage) of swallowing disorders.
Results: OPS qualitative analysis showed: multiple deglutitions in 9 pts (69%), refluxes in nasal cavity in 5 (38%), premature ingestion of the bolus in 6 (46%). OPS quantitative analysis showed alterations of the following phases: oral transit time in 7pts (54%) and oral retention index in 9 (69%), pharyngeal transit time in 10 pts (77%) and pharyngeal retention index in 9 (69%); moreover 7 pts (54%) showed tracheal aspiration.
Conclusions: All patients except one showed one or more scintigraphic alterations. We demonstrated OPS is a sensible and simple technique to evaluate these disorders, it is well tolerated, with low irradiation dose for pts.

PS_633

A NEW EVALUATION METHOD USING LIVER ACCUMULATION RATE WITH 99M-TC-GSA SPECT : VERIFICATION OF BLOOD KINETICS AND CLINICAL UTILITY

Y. Sugai, K. Takahashi, A. Komatani, T. Hosoya. Department of Radiology, Yamagata University, Yamagata, Japan.

A new evaluation method using the liver accumulation rate with ^{99m}Tc-GSA SPECT was designed at our hospital. The aim of this study was to evaluate the accuracy and clinical utility of this easy to use method as a liver function index compared it with blood concentration change and conventional hepatic function tests.
Methods: One hundred and eighty-seven subjects were recruited from the total number of patients who underwent ^{99m}Tc-GSA SPECT between 1997 and 1999 at our hospital. Liver uptake ratio using SPECT (LUR15, %) is the added SPECT count in the whole liver slices divided by the whole SPECT counts of the syringe SPECT value. We compared the results of the conventional and clinical liver function indexes. The liver uptake rate 15 minutes after the injection of ^{99m}Tc-GSA (Liver Uptake Rate 15: UTR15) corresponding to the disappearance rate of ^{99m}Tc-GSA in the blood at 15 minutes postadministration, was calculated from a regression equation for 35 patients $\{100-(Y_0+Ae^{-15\cdot})\}$. The LUR15 and UTR15 values were compared to examine the relationships and the accuracy.
Results: LUR15 correlated well with every functional index, but a high correlation was found especially with cholinesterase, ICGR15, and KICG in particular. There was the extremely high correlation between LUR15 of the whole liver and UTR15 from the blood concentration ($Y=-7.179+0.966X$, $r=0.878$, $p<0.0001$).
Conclusions: The accuracy, reliability, and clinical utility of our new simple liver uptake ratio method using ^{99m}Tc-GSA SPECT was confirmed by comparison with the change in ^{99m}Tc-GSA concentrations in the blood and clinical hepatic function tests.

PS_634

GRAFT FUNCTION MONITORING IN LIVER TRANSPLANT RECIPIENTS USING QUANTITATIVE TC-99M MEBROFENIN SCINTIGRAPHY

A. Gençoğlu (1), H. Karakayalı (2), M. Haberal (2). (1) Department of Nuclear Medicine; (2) Department of Surgery, Başkent University Medical Faculty, Ankara, Turkey.

Liver transplantation is a successful treatment method for patients with end-stage liver disease. The post-operative follow-up is very important in liver transplant recipients, because various complications, which affected graft liver function, arise in this period. The aim of this study was to evaluate the efficacy of serial quantitative Tc-99m mebrofenin scintigraphy in the monitoring the graft function after the liver transplantation.
Materials and Methods: 8 orthotopic, 8 heterotopic total 16 liver transplant recipients (6 F,10 M, mean age 19.2± 2.9 years) were studied. The cause of liver failure was Wilson's disease in 6 patients, hepatitis B in 2, Alagille syndrome in 1, autoimmune hepatitis in 1, Byler's disease in 3, criptogenic cirrhosis in 3 patients. 9 patients recived cadaveric grafts and 7 patients recived grafts from living-related donors. The mean follow-up period after liver transplantation was 3.9± 0.6 years. Tc-99m mebrofenin scintigraphy and graft liver biopsy were performed at regulary intervals beginning with the early postoperative period. Hepatobiliary scans were evaluated quantitatively and hepatocyte extraction fraction (HEF), time to maximum activity (Tmax) and time to half of maximum activity (T1/2) parameters were used. Scintigraphic findings were then compared to biopsy results at each subsequent assessment.
Results: In the early post-transplantation period, 11/16 liver grafts had normal scintigraphy (HEF >%90,Tmax approximately 15 min,T1/2 approximately 30 min) and biopsy. The scintigraphic parameters of other 5 grafts were below the normal values in the early post-operative period. In these 5 grafts biopsy results were 2 acute rejection and 3 hepatocelluler damage. All of the 5 patients graft functions returned to normal levels after the episodes of acute rejection or hepatocellular damage. In the follow-up period, 1 graft had chronic rejection and 7 grafts had hepatocelluler damage episodes. During these episodes, grafts functions diminished and HEF, Tmax, T1/2 values were abnormal in all 8 patients. Scintigraphic parameters returned to normal values in the serial scintigraphies in 5 of these 8 grafts. In the other 8 grafts, scintigraphic findings and biopsy results remained normal throughout follow-up.
Conclusion: Serial quantitative Tc-99m mebrofenin scintigraphy is a sensitive and valuable method for the monitoring graft liver function in liver transplant recipients.

PS_635

ALTERATION OF INTESTINAL PERMEABILITY IN PATIENTS WITH GYNECOLOGIC CANCERS TREATED WITH PELVIC RADIOTHERAPY

A. Dirlik (1), M. Taner (1), S. Erhamamcı (1), Z. Özcan (1), I. Karadoğan (2), M. Esassolak (2). (1) Department of Nuclear Medicine; (2) Department of Radiation Oncology, Ege University Medical Faculty, Izmir, Turkey.

Aim: Pelvic radiotherapy (PRT) is an inevitable therapeutic modality in patients with cervix and endometrium cancer. However, PRT has known to cause intestinal adverse effects, which cannot be estimated beforehand. Additionally any objective test demonstrating intestinal injury occurring after pelvic radiotherapy has not been suggested yet. In the current study it is aimed to investigate the alteration of intestinal injury due to PRT in patients with gynecologic cancers.
Methods: The study group included 12 patients with cervix cancer and 13 patients with endometrium cancer in an age range of 42-75 yrs. Primary PRT was applied in 10 inoperable patients and postoperative PRT was applied in 15 patients. Pelvic radiotherapy doses were determined according to the patients' characteristics and ranged between 5040-6300 cGy. Clinical grading of acute and subacute toxicity was determined according to International Union Against Cancer criteria (grade 0-IV). Before and 1 week after therapy, patients received 0.5 mCi Tc-99m DTPA orally following an overnight fasting and urine samples were collected for 24 hrs. Urine samples and standards were measured in gamma counter and urine Tc99m DTPA excretion ratio was calculated.
Results: When the pre-therapeutic and post-therapeutic urine Tc99m DTPA excretion were compared a significant rise in intestinal permeability is noted following PRT (3,60±1,35% and 7,49±3,65% respectively; $p<0,001$). However, no significant change is found in patients with and without surgery and in patients with high and low dose PRT protocols ($p=0,764$ and $p=0,767$ respectively). Significant difference also could not be demonstrated in patients with grade 0-I and grade II-III toxicity ($p=0,196$)
Conclusion: Intestinal permeability seems to be significantly accelerated in patients receiving PRT. Therefore, this method can be suggested as a simple, objective and non-invasive test for the detection of intestinal injury. However, this alteration in intestinal permeability could not be found to correlate with the acute effects within these dose limits of PRT.

PS_636

PERFORMANCE OF SALIVARY SCINTIGRAPHY IN A SPANISH POPULATION WITH SJÖGREN'S SYNDROME DIAGNOSED BY THE EUROPEAN CRITERIA

R. Martínez-Lázaro (1), A. Cortés-Blanco (2). (1) Department of Nuclear Medicine, Hospital Universitario Miguel Servet, Zaragoza, Spain ; (2) Member of the Spanish Society of Nuclear Medicine, Zaragoza, Spain.

AIMS: 1) Evaluating the performance of the qualitative reading of salivary scintigraphy (SSC) for the detection of Sj?gren's syndrome (SS) based on the European classification criteria in a Spanish population. 2) Performing a clinical quantitation of this test in the Spanish population with SS according to the European criteria, xerostomic patients without SS as a control group and healthy participants as a normal group, and differentiating these three groups. 3) Establishing the most discriminatory scintigraphic parameters for the diagnosis of SS.
METHODS: This cross-sectional study included 76 patients diagnosed of primary or secondary SS on the basis of the European classification criteria and 61 xerostomic controls who did not fulfill those criteria, both groups referred for SSC since August 1998 in order to evaluate a suspicious or known SS, and 56 healthy volunteers. A 16-minute dynamic SSC with Tc-99m pertechnetate was done and it was interpreted by qualitative reading and clinical quantitation.
RESULTS: The qualitative reading demonstrated a normalcy fraction of 100%, sensitivity of 85.5%, specificity of 42.6% and accuracy of 66.4%. A normal database displayed a dispersion higher of 20% for function scintigraphic parameters. Normal area and function did not differ between right and left salivary glands. Normal uptake and excretion in parotid glands were significantly higher than in submandibular glands. SS patients showed significantly lower salivary gland areas, inferior parotid uptake and lower submandibular excretion than controls and normals. No optimal threshold of salivary gland area or function data, on an individual manner, had higher performance for the diagnosis of SS than the qualitative reading.
CONCLUSIONS: This is the first study which evaluates the performance of SSC for the detection of SS using the European classification criteria for diagnosing it. Qualitative reading of SSC shows high sensitivity and suboptimal specificity for the diagnosis of SS. Normal salivary gland function displays a wide standard deviation and higher values in parotid than in submandibular glands. There is not lateralisation right/left in normal salivary area and function. Salivary gland area, parotid uptake and submandibular excretion decrease in patients with SS. Clinical quantitation and qualitative reading of SSC appears to be complementary for diagnosing of SS.

PS_637

COLONIC TRANSIT DISORDERS IN PROGRESSIVE SYSTEMIC SCLEROSIS

S.J. Wang (1), J.L. Lan (2), D.Y. Chen (2), Y.H. Chen (2), T.Y. Hsieh (2), W.Y. Lin (1). (1) Department of Nuclear Medicine, Taichung Veterans General Hospital, Taiwan; (2) Division of Rheumatology, Taichung Veterans General Hospital, Taiwan.

Aim: Progressive systemic sclerosis(PSS) alters smooth muscle function throughout the gastrointestinal tract. The esophagus is the gastrointestinal segment most often involved. Involvement of the colon, though less common, may lead to life-threatenting complications. This study attempted to evaluate colonic transit in patients with PSS, using Tc-99m DTPA labeled charcoal in commercial enteric capsule.
Method: We studied 15 unselected patients with PSS and 20 age matched healthy controls using radionuclide colon transit study. The geometric center (GC) at 4 and 24 hours was used to summarize overall transit in the colon.
Result: In patients with PSS, colon trasit was delayed (GC4:0.42+/-0.58 vs 0.85+/-0.46; p=0.018) (GC24:1.65+/-1.10 vs 2.58+/-1.09; p=0.017). Abnormal geometric center values were observed in 10/15(66.6%) and 5/15(33.3%) PSS patients at 4 hours and 24 hours, respectively.
Conclusion: These findings suggest that delayed colon transit is common in patients with PSS. Radionuclide colonic trasit study is a valuable diagnostic tool for evaluating colonic transit in PSS.

PS_638

DETERMINATION OF INTESTINAL PERMEABILITY BY 99MTC-DTPA IN PROTOZOAN INFECTIONS

M.S. Taner (1), M. Argon (1), K. Köseoğlu (1), H. Dağcı (2), S. Üstün (3), S. Budak (2), Y. Duman (1). (1) Department of Nuclear Medicine; (2) Parasitology; (3) Gastroenterology, Ege University, Turkey.

Intestinal permeability (IP) studies using macromolecules have been assumed to demonstrate the intactness of intestinal mucosa. The aim of this study was to determine the IP, measured by oral ^{99m}Tc-DTPA in protozoan infections (PI) such as *Giardia intestinalis* (GI), *Blastocystis hominis* (BH) and *Entamoeba coli* (EC) and assess the applicability of this nuclear analysis technique.
Method: 39 patients with PI and 10 healthy volunteers were studied. IP was measured by orally administration of 0,5 mCi ^{99m}Tc-DTPA dissolved in 50 ml of water. All cases were asked to fast overnight and to empty their bladder prior to starting the test. 24-h urine collection was obtained. To calculate the percentage of urinary excretion of ^{99m}Tc-DTPA, 2 ml urine and 2ml of a 1/1000 solution of a standard dose of ^{99m}Tc-DTPA with the same activity of the administered dose were counted and used a formula as follows;
DTPA % = Urine cpm x Urine volume x 100 / Standard cpm x 1000.
Results: IP was increased in Pts with compared to the controls patients (7,20 ± 5,32 % vs 4,47 ± 0,65 % P= 0,0017). IP and P values were 9,91 ± 10,5 % , P = 0,0025 in GI Pts, 6,81 ± 2,25 % P= 0,00037 in BH Pts, 5,78 ± 2,84 %, P = 1,40 in EC Pts.
Conclusions: IP increases in patients with *G. intestinalis* and *B. hominis* but not in with *E. coli*. This finding supports that IP increases in PI which causes damage to the intestinal wall. Non pathogenic PI has no effect on IP in patients with *B. hominis* raises the idea that *B. hominis* can be a pathogenic protozoan. IP measurement by using oral ^{99m}Tc-DTPA is a non-invasive screening test and can be used in place invasive technique

PS_639

HAS SILDENAFIL A ROLE IN ACUTE DIABETIC GASTROPARESIS? TWO CASES EVALUATED WITH RADIONUCLIDE STUDY

V. Valenza (1), A. Bianco (2), G. D'Errico (1), A. Grieco (2), G. D'Andrea (1), B. Alfei (2). (1) Institute of Nuclear Medicine; (2) Institute of Internal Medicine and Gerontology, Catholic University of Rome, Italy.

Introduction and Aim: Sildenafil is a drug that modulates the Nitric Oxide dependent innervation of smooth muscle
fibers. On this basis the Authors supposed that the drug could affect neurotrasmission in the muscle layers of the stomach and, consequently, have a role in acute diabetic gastroparesis. Two patients, hospitalised for this pathology, were evaluated to assess the possible therapeutic effect of Sildenafil.
Methods: following informed consent 10 healthy volunteers were investigated to define normal patterns of gastric emptying scintigraphy, e.g., lag phase in minutes (LP), T 1/2 in minutes (T 1/2), and Residual Activity at 120' in percentage (RA% 120'). The gastric emptying scintigraphy was performed only one time: after an overnight fast each subject assumed, in five minutes, a solid meal of a sandwich with two ^{99m}Tc-MAA-scrambled eggs (74 MBq) and a glass of water. The acquisition started at the end of the meal in anterior view, followed 1 minute later by a posterior view; the frame of each acquisition was of 1 minute on a 64x64 matrix. Both anterior and posterior views were acquired every 15 minutes to 120 minutes. After an overnight fast two female patients, 45 and 40 years old, affected by acute diabetic gastroparesis, underwent three times specific radionuclide study. The gastric emptying scintigraphy was performed the first day to obtain a baseline study. The second and the third day the scintigraphy was taken 30 minutes after the oral assumption of two different drugs: Sildenafil (50 mg) and placebo (A vitamin) respectively, to evaluate the different effects of the drugs on gastric emptying.
Results: The results are reported in table I.

	Patient A			Patient B		
	LP	T 1/2	RA% 120'	LP	T 1/2	RA% 120'
Normal value	*< 30'*	*88' ± 16'*	*35 ± 10*	*< 30'*	*88' ± 16'*	*35 ± 10*
1) Basal Study	45'	94'	43	90'	213'	80
2) Sildenafil Study	30'	67'	27	30'	68'	25
3) Placebo Study	30'	97'	31	20'	548'	75

The studies showed that after Sildenafil there was an improvement of scintigraphic parameters in the two patients and relief of gastric symptoms.
Conclusion: the Authors suppose this new therapeutic approach as a useful aid to resolve acute diabetic gastroparesis. Due to the favourable results it would be advantageous to further evaluate Sildenafil and stomach motility considering the gastric scintigraphy a simple and well complying method to explore the effects of the drug on gastric emptying.

PS_640

CROHN'S ESOPHAGITIS VISUALISED BY ANTYGRANULOCYTE ANTIBODIES

D. Huiæ (1), D. Dodig (1), M. Premužiæ (2), Ž. Krznariæ (2), B. Vuceliæ (2). (1) Department of Nuclear Medicine and Radiation Protection; (2) Department of Gastroenterology, University Hospital, Zagreb, Croatia.

The involvement of the upper gastrointestinal tract has been considered to be a rare manifestation of Crohn's disease. We report herein the case of 49-year-old woman with 20 years history of Crohn's disease. The patient presented with progressive dysphagia, heartburn and weight loss. Esophagoscopy revealed diffuse erythema with mucosal inflammation. Endobiopsy specimens were described as esophagitis. Radiological studies showed normal small bowel transit and fistula between rectum and vagina.
With a view to estimate the spread of the disease the scintigraphic study with Tc-99m labelled anti-NCA 95 antigranulocyte antibodies (AGAb) was performed. Whole-body scans were obtained five hours after i.v. injection of 740 MBq AGAb. Very high uptake in thoracic and cervical esophagus was observed. Appearance of abdomen was normal without pathological AGAb accumulation.
To the best of our knowledge and according to MEDLINE base this is the first visualisation of Crohn's esophagitis by using AGAb and even the first with any scintigraphic method.
After the oral administration of metilprednisolone and mesalamine patient's symptoms were resolved.

PS_641

THE EFFECT OF PRESENCE OF ESOPHAGITIS AND HELICOBACTER PYLORI INFECTION TO THE GASTRIC EMPTYING TIME

K. Sönmezoğlu (1), O. Özlem (1), Z. Yüce (2), C. Nisli (1), A. Dobrucali (2), A. Çelik (2), I. Uslu (1). (1) Istanbul University; (2) Istanbul University, Cerrahpaşa Medical Faculty, Department of Gastroenterology, Istanbul, Turkey.

Aim: The aim of this study were to 1) investigate the relationship of the severity of esophagitis and gastric emptying time; 2) ascertain whether the presence of Helicobacter pylori infection affect gastric emptying time.
Methods: 37 patients (age range 17-80 years; mean age 47.3 ± 16.8) with subjective and/or objective evidence of esophagitis; and 14 normal volunteers (age range 25-72 years; mean age 49.2 ± 16.8) were included in this study. All participants underwent upper gastrointestinal endoscopy and radionuclide gastric emptying studies with both solid and liquid meals. According to esophagoscopic examination, the severity of esophagitis was graded into 4 scores. The presence and density of Helicobacter infection was confirmed by antral biopsies. Gastric emptying was measured using a Tc-99m sulfur colloid labelled scrambled egg for solid phase and a Tc-99m DTPA labelled orange juice for liquid phase using a double-head gama camera and gastric emptying time was expressed as T1/2 (time required for peak counts to decrease by half) for both liquid and solid phase studies. There was at least 2 days between two scintigraphic studies
Results: Comparing to control group, there was no statistically significant differences of both liquid and solid gastric emptying time in the patient group with no evidence of esophagitis (grade 0) and with mild esophagitis (grade I). However, there is a significant acceleration of solid emptying time in severe esophagitis group (Table 1). On the other hand, there was no significant relationship between the presence of Helicobacter pylori infection and gastric emptying time.
Conclusion: We concluded that while severe esophagitis accelerate the solid gastric emptying time, the presence of helicobacter pylori infection does not affect neither liquid nor solid gastric emptying time.

Table 1. Relationship of the severity of esophagitis and gastric emptying time

	Control group (n = 14)	No esophagitis Grade 0 (n=9)	Mild esophagitis Grade 1 (n=16)	Severe esophagitis Grade ≥ 2 (n=12)
Liquid phase (min)	35.7±15.1	49.2±38.9	50.6±28.8	38.1±20.0
Solid phase (min)	61.5±12.8	62.4±23.4	74.1±17.2	46.2±10.2*
* $p < 0.05$				

PS_642

99M-TC RED BLOOD CELL SCINTIGRAPHY (99MTC-RBC) PERFORMED WITH GAMMA CAMERA MOUNTED X-RAY TOMOGRAPHY IN A PATIENT WITH RECURRENT BLEEDING: A CASE REPORT OF AN INTESTINAL BLEEDING LOCALIZED WITH COMBINED CT/SPECT TECHNOLOGY IN A SINGLE DEVICE

A. Kurtaran (1), A. Staudenherz (1), G. Dobrozemsky (1), L. Öhler (2), S. Puig (3), W. Schima (3), F. Kainberger (3), G. Kornek (2), E. Wenzel (4), R. Dudczak (1). (1) Department of Nuclear Medicine; (2) Department of Internal Medicine I; (3) Department of Radiology; (4) Department of Surgery, University of Vienna, Austria

We report a case of upper intestinal bleeding that was diagnosed using 99mTc-RBC scan performed with combined CT/SPECT technology (GE Medical Systems, Millenium VG with Hawkeye) in a single device. To the best of our knowledge, this is the first case of localization of a gastrointestinal bleeding using such a system. The X-ray imaging system of this machine is composed of a low current X-ray tube and a set of detectors mounted on the camera's slip ring gantry rotating around the patient following SPECT acquisition.
A 74 year old women with severe anemia was referred to our hospital because of recurrent gastrointestinal bleeding. All routine diagnostic approaches including upper and lower endoscopy, CT and multisclice-CT as well as visceral angiography to localize the bleeding source were negative. Dynamic 99mTc-RBC demonstrated an active bleeding site in the left abdomen which was beleived to represent a bleeding in the descending colon, yet exact anatomical localization was not possible. In a repeated colonoscopy, however, no bleeding site in the colon could be detected. We hypothesized that a combined functional and anatomical study would help to localize the bleeding site. Thus, a 99mTc-RBC scan with a gamma camera-mounted anatomical X-ray tomography (GE MS Millenium VG with Hawkeye) was performed. With the help of the registered and fused anatomical/functional images, the bleeding site was shown to reside in the proximal intestine (duodenojejunal region). This precise anatomical information directed the surgeon to a selective surgical intervention. In the suspected region intraluminal-blood was found confirming the correct anatomical localization of preoperative diagnosis. However, also intraoperativelly no active bleeding source could be detected. Yet, since an upper gastrointestinal bleeding has been supposed, a devascularization (ligation of rigth gactric vessels, gastroduodenal vessels and right gastroepiploic vessels) and a highly selective vagotomy was performed. Postoperativelly the patient is free of bleeding and is clinically stable. This case report emphasizes the potential role of combining anatomical and functional imaging in a single device also in patients with obscure gastrointestinal bleeding, guiding selective surgical intervention.

NEUROLOGY / PSYCHIATRY 5

PS_643

ON THE TRANSPORT OF KETONE BODIES ACROSS THE BLOOD-BRAIN BARRIER

G. Blomqvist (1), M. Alvarsson (1), V. Grill (1), G. vonHeijne (2), M. Ingvar (2), J.O. Thorell (3), S. Stone-Elander (3), L. Wid?n (2), K. Ekberg (4). (1) Department of Endocrinology and Physiology, Karolinska Hospital; (2) Department of Clinical Neuroscience, Karolinska Hospital; (3) Karolinska Pharmacy; (4) Department of Physiology, Karolinska Hospital, S-17176 Stockholm Sweden

The cerebral utilization of ketone bodies at hyperketonemia (plasma concentration of §-hydroxybutyrate, [§HB], equal to 1.0±0.3 mmol/L) has been studied with PET using R-§-[1-^{11}C]hydroxybutyrate as tracer. In a Gjedde-Patlak plot the tissue uptake data fall along a straight line through the origin. Further, fit of a two tissue compartment model indicates that the transport across the blood-brain barrier (BBB) is irreversible during the scan time and that the volume of distribution of un-metabolized ketone bodies (DV_{free}) is compatible with zero. The previous interpretation of these results was that the transport across the BBB is the rate-limiting step. However, in a recent study using MR technique at hyperketonemia it has been shown that DV_{free} in the brain is substantial, close to 0.4, at [§-HB] equal to 1.0 mmol/L(1). Therefore we have re-examined our data to see if they are compatible with a high concentration of un-metabolized ketone bodies in the brain at hyperketonemia.
Methods: Six healthy subjects and six IDDM patients were included in the study. Infusion of §HB started one hour before the bolus injection of [^{11}C]-§HB (acquisition time 10 min in ECAT EXACT HR). The time course of tracer in arterial plasma was measured. A two tissue compartment model with three rate constants was applied to the average time-activity curves of the brain, with two constraints imposed on the rate constants. First, the constraint $DV_{free} = k_1/(k_2+k_3) = 0.4$ was imposed. Second, the constraint $k_2 < 100 \cdot k_3$ was imposed, forcing the y-intercept in the Gjedde-Patlak plot („apparent" DV) to be close to zero, even when DV_{free} is appreciable. Within the framework of the applied two tissue compartment model, the relationship between these two quantities is: $DV_{app} = DV_{free} \cdot k_2/(k_2+k_3)$.
Results: For both groups the constrained two tissue compartment model was found to give equally good fits to the data as the corresponding unconstrained model. According to this analysis there is a substantial concentration of ketone bodies in the brain tissue at hyperketonemia, and yet the transport across the BBB is essentially unidirectional.
Conclusions: The quoted MR and PET studies are compatible only if the transport across the BBB is not the rate limiting step, and if there is some mechanism that suppresses the transport of ketone bodies from brain back to the blood.
(1)Pans et al. J cereb Blood Flow Metab 20:1502-1507 (2000)

PS_644

ASSESSEMENT OF BLOOD-BRAIN-BARRIER INTEGRITY USING 99M-TC-DTPA SPECT IN PATIENTS WITH SEIZURES

H. Golan (1), A. Friedman (2), A. Korn (2), I. Shelef (3), I. Rachinsky (1), S. Lantsberg (1). (1) Departement of Nuclear Medicine, Soroka University Medical Center, Beer-Sheva, Israel; (2) Laboratory of Neurophysiology, Department of Neurosurgery, Soroka University Medical Center, Zlotowski Center of Neuroscience, Beer-Sheva, Israel; (3) Departement of Radiology, Soroka University Medical Center, Beer-Sheva, Israel.

Introduction: Electroencephalography and regional cerebral blood flow single photon emission tomography (rCBF-SPECT) have been shown to be useful diagnostic tools in identifying the pathological electroactivity and perfusion defects in patients with clinical seizures. ^{99m}-Tc-DTPA SPECT has the ability to evaluate the integrity of the blood-brain barrier (BBB). BBB disruption is present in infectious, vascular and degenerative diseases of the brain. The correlation of BBB pathology with ^{99m}-Tc-ECD rCBF SPECT and low-resolution electrotomography (LORETA) in patients with seizures is presented.
Objectives: To assess BBB integrity, brain perfusion and electrotomographic findings in patients with seizure disorders.
Materials and methods:
13 patients, age 15-54 years, presenting with partial or complex seizures were included, 5 were 6-12 months post brain surgery for removal of a benign meningioma, 5 post-closed head trauma, 2 with idiopathic seizures and one subject 36 month post-radiosurgery for arteriovenous malformation.
^{99m}-Tc-DTPA and ^{99m}-Tc-ECD SPECT studies were performed in all patients and LORETA was acquired in 6.
Results: 11 patients showed increased focal accumulation of ^{99m}-Tc-DTPA in the hypoperfused area identified on rCBF-SPECT with ^{99m}-Tc-ECD, one was normal in both studies and one was positive only on the DTPA study. All subjects who had LORETA studies showed localized elevation of EEG slow wave in the areas identical to the SPECT findings.
Conclusions: ^{99m}-Tc-DTPA SPECT can identify focal areas of BBB disruption that may alter neuronal activity and induce neurological symptoms including seizures.

PS_645

CHANGES IN RCBF DISTRIBUTION ASSOCIATED WITH MUSCULAR TENSION AND PSYCHASTHENIA. FIRST 99M-TC-HMPAO SPECT STUDY

M.M.E. Pagani (1), A. Gardner (2), D. Salmaso (3), G. Lindberg (2), C. Jonsson (4), R. Hatherly (4), M. Finnbogason (4), L. Johansson (4), H. Jacobsson (4), T. Hälström (2), S.A. Larsson (4)(1) Institute of Neurobiology and Molecular Medicine, CNR, Rome, Italy; (2) Neurotec, Section of Psychiatry And Department of Medicine, Karolinska Institute, Huddinge University Hospital, Stockholm, Sweden; (3) Institute of Psychology, CNR, Rome, Italy; (4) Section of Nuclear Medicine, Department of Hospital Physics, Karolinska Hospital, Stockholm, Sweden

Aim: Muscular Tension (MT), subjective muscular tenseness and aches, and Psychasthenia (PA), low mental energy and difficulties in compensating for energy consumption, show altered corresponding scores on the Karolinska Scale of Personality (KSP). This scale rates 135 items with a four-point response format summed up to 15 scales focused on personality traits that are thought to have biological correlates. This study aims to investigate for the first time the regional cerebral blood flow (rCBF) changes in patients with significantly increased KSP scores in either Muscular Tension or Psychastenia scales.
Methods: The rCBF distribution at rest in a group of 19 MT and in a second group of 19 PA patients was compared to that of 28 age-matched normal controls (CTR). 99mTc-HMPAO SPECT was performed using a three-headed gamma camera and intersubject group analysis was carried out by a Computerised Brain Atlas able to standardise brain anatomy in 3D space. The bilateral uptake in 27 functional subvolumes of the brain, including the most of Brodmann (B) areas, basal ganglia and thalamus, was analyzed by analysis of variance. The significance level was set at $p = 0.05$.
Results: Both patients to controls comparisons showed a significant global interaction ($p<0.03$). In the CTX/MT comparison group x VOI interaction was significant with increases in prefrontal cortex in B9 and B10 and decreases in posterior cingulate and parietal cortex in B31 and B39 respectively. Significant increases where found in the CTR/PA comparison in B9, B10 and in the putamen. In none of the 2 comparisons hemispheric effect was seen neither did the KSP scores correlate to rCBF in any of the analysed functional subvolumes.
Conclusions: rCBF changes in patients showing altered Muscular Tension and Psychastenia KSP scores were investigated for the first time. Prefrontal cortex, bilaterally, showed rCBF increase in both groups when compared to normal controls. Posterior cingulate and parietal associative cortex showed significant decreases in MT. These findings confirm that the symptoms reported by patients suffering of Muscular Tension and Psychastenia have an organic basis. They also suggest the usefulness of standardisation software and normal controls in reliably identifying both rCBF increases and decreases in psychiatric disorders.

PS_646

INCREASE IN CEREBRAL PERFUSION (CP) WITH GINKGO BILOBA (GB) LONG-TERM TREATMENT

A. Barbieri (1), R. Santos (2), M. Sevillano (1), M. Castiglioni (1), G. Alonso (1), L. Itaya (3), O. Bueno (2), J. Galduróz (2). (1) Dept. Diagnostico por Imagem - UNIFESP São Paulo, Brasil; (2) Dept. Psicobiologia - UNIFESP São Paulo, Brasil; (3) Dept. Medicina Nuclear - HIAE São Paulo, Brasil.

Introduction: CP alterations during normal aging could be explained by several mechanisms. A dry extract of *Ginkgo biloba* is one of the many attempts to minimize the aging effects.
Aim: GB long-term treatment effects on CP evaluated with ^{99m}Tc-HMPAO in an old age group.
Methods: Forty-eight right handed male between 60 to 70 years old, distributed randomly in two equal groups, received 80mg/day of GB or placebo for a 8 months period. CP was evaluated at the beginning and at the end of the treatment. CP was calculated by the difference between counts in 12 predefined regions of interest (ROI) and one in the cerebellum (*Value = ROI – cerebellum*) and another data (Table #1) showing the CP improvement was obtained subtracting the values post-treatment by pre-treatment.
Results: *Ginkgo biloba* group has had better perfusion than placebo showed by the decrease in the difference between ROIs and cerebellum. The inverse result was observed in the placebo group.

Table #1- CP improvement between pre and post treatment in the two groups.

ROI	Placebo	Ginkgo biloba
Pons	1,7±6,5*	6,3±7,5*
Frontal	-0,4±12,1	2,5±7,8
Temporal lateral	1,1±2,9	0,5±4,2
Temporal medial	3,8±6,4*	-0,4±7,5*
Upper basal ganglia	0,0±6,1*	-3,6±5,3*
Lower basal ganglia	2,0±6,3*	3,9±3,9*
Frontal	2,2±3,3*	-2,9±3,5*
Frontal-parietal	0,4±2,7*	-2,3±3,0*
Parietal	-0,2±2,0*	-3,3±2,6*
Temporal-parietal	0,6±3,3	-0,5±4,3
Temporal	0,8±2,7*	-0,9±1,9*
Occipital	3,8±3,6*	-0,7±2,4*

P=0,004 – Student „t" test with Bonferroni correction.

Conclusion: *Ginkgo biloba* promotes Cerebral Perfusion increase in several areas in both hemispheres.

PS_647

EFFECT OF TESTOSTERONE THERAPY ON CEREBRAL PERFUSION IN HYPOGONADAL MALES

N. Friedman (1), W.E. Barnes (1), N. Azad (2). (1) Dept of Nuclear Medicine; (2) Dept of Endocrinology, Hines VA Hopstal, Hines, Il, USA.

Aim: Testosterone replacement therapy is employed in adult males suffering from diminished libido and low testosterone levels. This study evaluated cerebral perfusion before and after testosterone therapy was initiated. Methods: 8 adult males with a mean age of 69 years (58 to 79), participants in an ongoing trial of testosterone replacement in documented hypogonadal males, were studied with SPECT perfusion imaging as part of an ongoing study. Each patient completed questionnaires during the study evaluating physical, sexual, memory and sleep performance and social interactions. Patients had a baseline cerebral SPECT scan performed with Tc99m HMPAO using a triple head gamma camera with ultra high resolution fanbeam collimation. Repeat scans were performed approximately one month and two months post initiation of testosterone therapy. Studies were analyzed visually and with statistical parametric mapping software (SPM96), comparing the difference between paired patient studies to the difference between 15 paired studies of normal subjects.
Results: Visual analysis of studies failed to demonstrate any consistent differences between individual scans. SPM grouped analysis of the change from baseline to one month post therapy indicated large clusters of activation in the left antero-medial frontal lobe (corrected p value 0.056) and the left posterior thalamus(0.061). A comparison of baseline to the two month study showed a similar but less significant activation. No significant group differences were identified between the two post therapy scans.
Conclusion: Testosterone replacement therapy in hypogonadal males appears to be associated with left frontal lobe and posterior left thalamic activation demonstrated by SPECT cerebral perfusion imaging. This change is associated with increased libido and sexual performance in most of the patients.

PS_648

TC-99M HMPAO BRAIN SPECT IN CHILDREN WITH DOWN'S SYNDROME

M. Kaya (1), S. Altay (2), A. Gültekin (1), S. Karasalihoğlu (2), O.N. Yiğitbaş (1), S. Berkarda (1). (1) Department of Nuclear Medicine; (2) Department of Pediatrics, Trakya University, Edirne, Turkey.

Down's syndrome is one of the most common chromosomal disorders (one in 800 births) and associated with developmental abnormalities of the central nervous system that result in mental retardation and age-dependent Alzheimer-type neurodegeneration. The aim of this (ongoing) study was to determine the regional cerebral blood flow alterations in children with down's syndrome, and to correlate IQ levels.
Methods: In this study; Tc-99m HMPAO brain SPECT was used to examine regional cerebral blood flow (rCBF) in 16 patients with Down syndrome (7 girl, 9 boys; mean age 6,84 ± 4,1 years). SPECT scans were acquired 20 minutes after injection of 18,5 MBq/kg Tc99m HMPAO in a quiet environment. All the children underwent detailed clinical examination, and IQ evaluation and/ or the Denver developmental screening test. SPECT images were analysed visually and semiquantitatively by defining side-to-side asymmetry index. The asymmetry indices was considered: < 6% as normal, between 6-12% as suspicious, > 12% as abnormal.
Results: Five children showed normal brain perfusion images. According to asymmetry indices, 4 cases showed abnormal cortical brain perfusion, and 3 cases showed abnormal perfusion on basal ganglia, and one patient had abnormal cerebellar perfusion. Suspicious perfusion abnormalities were determined in 4 patients. There was a positive correlation between IQ levels and right, and left frontal regions ($r=0,57$, $p=0.02$; $r=0,57$, $p=0.02$; respectively).
Conclusions: Tc-99m HMPAO brain SPECT can be helpful to assess the developmental brain abnormalities and understand which region in the brain related to mental retardation in children with Down's syndrome.

PS_649

STATISTICAL PARAMETRIC MAPPING IN BRAIN SPECT AFTER CARBON MONOXIDE INTOXICATION

N. Watanabe, H. Seto, K. Nouchi, M. Shimizu. Department of Radiology, Toyama Med. and Pharm. University, Toyama, Japan.

The purpose of this study was to assess regional cerebral blood flow (rCBF) in patients after carbon monoxide intoxication using brain SPECT and statistical parametric mapping (SPM 96).

Methods: Eight patients with delayed neuropsychiatric sequelae and ten patients with no neuropsychiatric symptoms after carbon monoxide intoxication were studied with brain single-photon emission tomography (SPECT) imaging with Tc-99m hexamethyl-propyleneamine oxime (HMPAO). 44 control subjects were also studied. We used the adjusted rCBF images in relative flow distribution (normalization of global CBF for each subject to 50 mL/100g/min with proportional scaling) to compare these groups with SPM.

Results: Using SPM, we revealed significantly decreased rCBF in the bilateral frontal lobes widly containing the bilateral insula and a part of the right temporal lobe in patients with delayed neuropsychiatric sequelae as compared with normal volunteers ($p<0.005$). In patients with no neuropsychiatric symptoms, significantly decreased rCBF in the bilateral frontal lobes particularly on the left side was detected. There was a significantly decreased rCBF in the right frontal and temporal lobes, and insula in patients with delayed neuropsychiatric sequelae as compared with no neuropsychiatric sequelae.

Conclusion: SPM is a useful technique for highlighting difference in rCBF in patients following carbon monoxide intoxication as compared with normal volunteers. The selectively reduced rCBF noted in this investigation supports the contention that brain damage following carbon monoxide intoxication may be prolonged and relapse particularly in the frontal lobe. In addition, the present study may help to clarify the characteristics of the pathophysiological alteration underlying delayed neuropsychiatric sequelae.

PS_650

99MTC HMPAO BRAIN PERFUSION IN FAMILY WITH CHOREA-ACANTHOCYTOSIS

T. Milanez (1), J. Kobal (2), M. Grmek (1), J. Fettich (1). (1) Department of Nuclear Medicine; (2) Department of Neurology,University Medical Centre,Ljubljana, Slovenia.

Chorea acanthocytosis (CA) is very rare autosomal recessive disorder characterised neurologically by involuntary movements and progressive neurodegeneration. Degeneration of the basal ganglia, closely resembling that seen in Huntington disease, results in atrophy of the putamen and caudate nucelus. Cerebral perfusion studies with positron emission tomography (PET) showed significant hypoperfusion of the frontal lobus, caudate nucleus, putamen and thalamus in patients with clinically expressed CA. Aim of this study was to assess cerebral perfusion with more available and less expensive 99mTc HMPAO SPECT in patients with clinically expressed CA as well as in asymptomatic siblings of these patients.

Patients and methods: Spect brain perfusion study with 99m Tc HMPAO was performed in four first degree relatives: two patients (age 48 and 46 years) with clinically expressed CA and two asymptomatic subjects (age 42 and 40 years) one with increased proportion of acantocytes and the other without acanthocytes in peripheral blood. Both patients with clinically expressed CA also underwent high-resolution MRI brain study. All examined subjects were free of other neurological disorders.

Results: 99m Tc HMPAO brain SPECT perfusion showed pathological decrease or lack of perfusion of the basal ganglia in both brain hemispheres and slightly decreased perfusion of right parietal lobe in patients with clinically expressed CA. Lack of basal ganglia perfusion in both brain hemispheres with 99mTc HMPAO SPECT were compatible with lesions found on high-resolution brain MRI. Decreased perfusion of left parietal lobe was found in one asymptomatic brother with increased proportion of acantocytes in peripheral blood and borderline decreased perfusion of putamen unilaterally in the asymptomatic subjects without acantocytes.

Conclusion: Our results of combined 99m Tc HMPAO brain SPECT perfusion/MRI are compatible to results of combined cerebral perfusion PET/MRI studies in patients with clinically expressed CA. Because of very high sensitivity of 99m Tc HMPAO brain SPECT scintigraphy it might be a useful tool to assess asymptomatic subjects with first degree family history of CA and increased proportion of acantocytes in perypheral blood.

PS_651

STRIATAL AND PONTO-CEREBELLAR HYPOPERFUSION IN HALLERVORDEN-SPATZ SYNDROM: A COMBINED PET AND MRI STUDY OF A CASE

M.J. Ribeiro (1), P. Castelnau (2), N. Boddaert (1,3), L. Hertz-Pannier (1,3), P. Evrard (2), M. Zilbovicius (1,4). (1) Service Hospitalier Frédéric Joliot, DSV-CEA, Orsay, France; (2) Service de Neurologie Pédiatrique, Hôpital Robert Debré, Paris, France; (3) Service de Radiologie Pédiatrique, Hôpital Necker-Enfants Malades, Paris, France; (4) Inserm U316, Chu Bretonneau, Tours, France

Aim: Hallervorden-Spatz syndrome (HSS) represent a group of rare and severe genetic disorders marked by optic atrophy extrapyramidal symptoms and iron accumulation in the pallidi usually visible on brain MRI („eye of the tiger"). The functional correlate of such structural abnormalities remains to be determined. Therefore, we have measured regional cerebral blood flow (rCBF) and dopaminergic function using positron emission tomography (PET), respectively with $H_2{}^{15}O$ and ^{18}F-L-DOPA, in a typical HSS case.

Methods: A 9 years old boy with a clinical and MRI diagnosis of HSS was examined in PET, using a 3D acquisition and a high-resolution tomograph . The relative rCBF was determined from the distribution of radioactivity after a bolus injection of $H_2{}^{15}O$. The rCBF images were analysed with the statistical parametric mapping software and compared to those obtained in 10 control patients (8.1 ± 2.1 years old). Comparisons between groups were performed with the t-statistic further transformed into Z statistic.

The dopaminergic function was assessed with ^{18}F-L-DOPA. The uptake constant (Ki, min^{-1}) of this radiotracer was calculated in the caudate nucleus and the putamen, using the occipital activity as a non-specific input function and compared to the corresponding mean values calculated in controls (n=8, 40.4 ± 14.9 years old).

Results: Voxel by voxel analysis of rCBF images revealed a significant hypoperfusion in the right caudate head, the pons and the cerebellar vermis compared to controls ($p<0.005$). No CBF abnormality was found in the pallidi. The Ki values measured for the four striatal structures (0.0122 and 0.0121, respectively for the right and the left caudate and 0.0119 and 0.0112, respectively for the right and the left putamen) were symmetrical and similar to those obtained for a control adults group (mean value ± standard deviation: 0.0127 ± 0.0014 and 0.0117 ± 0.0011, respectively for the caudate and the putamen).

Conclusion: To better define the pathophysiology of HSS, we performed a PET study using two different radiotracers. Our results indicate no metabolic variation in the pallidi where iron accumulates but a significant CBF decrease in the right caudate head, the ponto-cerebellum. Concerning the dopaminergic function, no visual localized abnormality was observed. However, the quantitative analysis was performed using the mean normal values obtained for a adult control group. These data support the notion that HSS pathogenesis is not restricted to the pallidi where iron accumulates and may provide elements to raise new pathogenic hypothesis.

PS_652

I-123 LABELED PYRIDINE BENZAMIDES AND THEIR DERIVATES AMINE PYRIDINES AS POTENTIAL NICOTINIC ACETYLCHOLINE RECEPTOR LIGANDS

H.-F. Li, F.-J. Gildhaus, K. Tatsch, K. Hahn. Department of Nuclear Medicine, University of Munich, Machioninistr.11, 81377 Munich, Germany.

Aim: Nicotinic acetylcholine receptors (nAChRs) are involved in a variety of neuropsychiatric disorders, such as Alzheimer's disease, Parkinson's disease, nicotine addiction and epilepsy. Until now, there is no nAChR ligand available which is suitable for clinical routine applications. Based on the structure of epibatidine, the aim of this work is to study the relationship between structure and brain uptake of different pyridine benzamides and their corresponding amine pyridine derivatives by synthesizing and radioiodinating these compounds and evaluating their biodistribution in rats.

Methods and results: Three pyridine benzamides and 3 amine pyridines were synthesized via two- and three-step-synthesis including the radioactive labeling with n.c.a. [^{123}I]NaI using the Iodogen method. The radiochemical yields ranged from 60% to 85%. The partition coeffiicients (logP) of these compounds were measured between 0.8 and 1.58. The biodistribution studies were carried out in male SD rats (n=3) at 2, 15, 60 120 min post injection. The brain uptake showed a considerable variation ranging from 0.11% ID/g for para-OH- ^{123}I-pyridine benzamide (p-OH-^{123}IPB) to 2.42% ID/g for ortho-OH-^{123}I-amine pyridine (o-OH-^{123}IAP) at 2 min p.i. The retention in brain with o-OH-^{123}IAP was distinctly longer than that of the other five compounds. The results of brain uptake (% ID/g) are summarized in the table below.

Compound	o-OH-^{123}IPB	m-OH-^{123}IPB	p-OH-^{123}IPB	o-OH-^{123}IAP	m-OH-^{123}IAP	p-OH-^{123}IAP
2 min	0.56	0.18	0.11	2.42	1.27	0.10
15 min	0.07	0.05	0.034	0.60	0.23	0.03
60 min	0.01	0.02	0.014	0.12	0.013	0.02
120 min	0.01	0.02	0.014	0.07	0.004	0.02
logP	***1.10***	***0.80***	***1.10***	***1.58***	***1.53***	***1.28***

Conclusions: The biodistribution data have shown that the brain uptake and the retention were not only related with the lipophilicity, but also with the position of the OH group on the aromatic ring. The compound o-OH-^{123}IAP had a significantly higher brain uptake than m-OH-^{123}IAP, although both had the similar lipophilicity. From the compounds tested, o-OH-^{123}IAP appears to be a potential radioligand for the nAChR. Binding, blocking and autoradiography studies are presently carried out to further characterize this promising ligand.

PS_653

THREE-DIMENSIONAL SURFACE PROJECTION PERFUSION IMAGES IMPROVE DIAGNOSTIC PERFORMANCES OF ECD-SPET STUDY FOR DETECTING ALZHEIMER'S DEMENTIA PATTERNS

T. Tang (1), T. Vander Borght (1), J. George (1), L. Robaye (2), V. Roelants (1), M. Ossemann (2), C. Swinne (3), C. Reynaert (4), P. De Coster (1), P. Laloux (2). (1) Nuclear Medicine Division; (2) Department of Neurology; (3) Department of Geriatrics; (4) Department of Psychiatry, UCL, Belgium

Brain perfusion study with Tc-99m ethylcysteinate dimer (ECD) is routinely used in the work-up of patients with cognitive impairment. In the current study, we evaluated the additional diagnostic value of fully automated stereotatic surface projection (3D-SSP) presentation to that of standard transaxial display in such clinical setting.

Methods: 72 patients (mean ± SD: 71 ± 9 y; range 43-86) with cognitive impairment underwent neuropsychologic testing, CTscan and/or MRI and brain SPET study, then were followed for 30 ± 7 months (range 20-48) for assessing the diagnosis. They were 27 patients with probable Alzheimer's disease and 45 with other disorders including Parkinson's diseases (PD: 6), probable fronto-temporal dementia (4), vascular dementia (3), chronic hydrocephalus (2), tumours (2), psychiatric diseases (21), and various pathological conditions (7). Brain SPET studies were acquired on a triple-head camera 1h after injection of 740 MBq ECD. Images were reconstructed by FBP, and displayed as transaxial section presentation. In addition, surface projection perfusion images were obtained by using a 3D-SSP technique (Minoshisma. *J Nucl Med* 1995;36:1238). Observers (#1 and #2) blinded to the diagnosis were asked to rate the degree of certainty of the diagnosis of AD pattern (grade 1: definite AD to 5: normal) on transaxial presentation alone or with 3D-SSP images. Area under the ROC curves as well as, by considering grade 1 and 2 as positive diagnosis of AD, intra- and interobserver reproducibilities and respective diagnostic performances were calculated.

Results: In comparison with transaxial section interpretation, 3D-SSP improved diagnostic performances as well as intra- and interobserver reproducibilities (see table).

	Area under the ROC curve		Sensitivity (%)		Specificity (%)		Accuracy (%)		Kappa Intra	Kappa Inter
Reader	#1	#2	#1	#2	#1	#2	#1	#2	#1	#1 *vs* #2
Transaxial	0.77 ± 0.06	0.84 ± 0.05	59	52	89	93	78	78	0.73	0.50
3D-SSP	0.92 ± 0.04*	0.91 ± 0.05*	81	70	93	98	89	88	0.88	0.84
Mean ± SD; two-tailed p value * <0.05.										

Conclusions: In the current series, visual analysis of ECD-SPET images has good overall accuracy in detecting AD patterns. However, fast automatic data processing for 3D-SSP presentation further improves the reproducibility and the diagnostic performances of ECD-SPET study for the clinical management of patients with cognitive impairment.

PS_655

RADIOSYNOVIORTHESIS WITH ERBIUM-169 (ER-169) CITRATE AFTER FAILURE OF LOCAL CORTICOSTEROID INJECTIONS IN PATIENTS WITH RHEUMATOID ARTHRITIS

L. Manil (1), A. Kahan (2), G. Mödder (3), J. Tébib (4), P. Verrier (2), A. Bonmartin (4), Y. De Rycke (1), F. Chossat (1), C.J. Menkes (2). (1) For CIS bio international, France; (2) Rheumatology A Dept, Cochin Hospital, Paris – France; (3) Köln-Marsdorf, Germany; (4) Rheumatology and Nucl Med Depts, CHU Lyon-Sud - France

Although Er-169 radiosynoviorthesis is an established local therapy in rheumatoid arthritis (RA), its effects have been less clearly demonstrated in corticosteroid-resistant joints. This double-blind, randomised, placebo-controlled, international study was designed to assess the efficacy of radiosynoviorthesis with Er-169 citrate after failure of local corticosteroid injections in RA patients.

Methods: 82 joints (46 metacarpophalangeal (MCP) and 36 proximal interphalangeal joints (PIP) in 43 RA patients) with failure of local intra-articular corticosteroid injections were randomised to receive within 6 months intra-articular injections of either Er-169 citrate (MCP: 30 MBq; PIP: 20 MBq) or placebo. Clinical assessment was performed before and 6 months after local therapy, using an visual analogue scale (VAS) and a 0 to 3 verbal rating scale (VRS) for pain, a 0-3 VRS scale for joint swelling and joint mobility.

Results: Improvement at 6 months in the Er-169 treated joints was statistically better than with placebo for pain (VRS: p=0.016; VAS: p=0.06 (tendency)), joint swelling (p=0.007), mobility (p=0.036), pain *and* swelling (p=0.002), pain *or* swelling (p=0.04). MCP joints presented higher Er/placebo ratios than PIP. Placebo effect was unexpectedly important, especially in the PIP.

Conclusions: These results confirm the clinical efficacy of radiosynoviorthesis with Er-169 citrate even after failure of local corticosteroid injections in RA.

RADIONUCLIDE THERAPY / DOSIMETRY 3

PS_654

PHYSICAL AND BIOLOGICAL DOSIMETRY IN PATIENTS UNDERGOING RADIOSYNOVIORTHESIS WITH ERBIUM-169 AND RHENIUM-186

L. Manil (1), P. Voisin (2), B. Aubert (3), D. Guerreau (1), P. Verrier (4), F. Chossat (1), J.M. Menkes (4), J. Tébib (5), J.Y. Devaux (4), A. Kahan (4). (1) For CIS BIO international, France; (2) Applied to Medicine Radiobiology Section, IPSN, France; (3) Physics Dept, IGR, Villejuif, France; (4) Rheumatology A and Nuclear Medicine depts, Hôpital Cochin, Paris, France

Physical and, for the first time, biological dosimetric studies were performed in rheumatoid arthritis (RA) patients (n=45) treated by radiosynoviorthesis (RSO) with Re-186 sulphide (medium sized joints) or Er-169 citrate (digital joints).

Methods: Biological dosimetry consisted in scoring dicentrics in lymphocytes, cultured from blood samples withdrawn just before and then 6h, 24h and 7 days after treatment. Physical methods included repeated blood samples counts and scintigraphy data. For Er-169 (pure beta emitter), only bremsstrahlung could be measured and solely in the injection area. For Re-186 (both beta and gamma emitter), whole body scans and static images of joints and locoregional lymph nodes were performed. Dosimetry calculations were in accordance with the MIRDOSE 3 software and tables. For Er-169 (21 patients), either metacarpophalangeal (30MBq) or proximal interphalangeal joints (20MBq) of the hands were treated (one joint per patient) ; 18 patients (out of 21) were interpretable for biological dosimetry, 10 (out of 11) for physical dosimetry and 6 (out of 10for both. For Re-186, 23 wrists, 9 elbows, 3 shoulders and 2 ankles were injected in 24 patients, with a maximum of 3 joints per patient (70MBq/joint); 20 patients/24 and 10/10 were interpretable for biological and physical dosimetry, respectively, and 8/10 for both methods.

Results: Er-169 biological dosimetry was negative in all interpretable patients, and physical dosimetry gave a blood dose of 15 ± 29 _Gy and an effective dose lower than 1 mSv/30 MBq. For rhenium-186, biological results showed negative results in 16 patients/20 but a blood irradiation around 200mGy in the last four. A significant cumulative increase of dicentrics 7 days after injection (16/10000 instead of 5/10000 prior to the treatment; p<0.04) was also noted. Gamma counts gave a blood dose of 23.9 ± 19.8 mGy/70MBq and the effective dose was found to be 26.7 ± 5.1 mGy/70 MBq, i.e. about 380 _Gy/MBq.

Conclusions: Er-169 RSO is very safe from both physical and biological dosimetry standpoints. Re-186 leak is greater, as demonstrated by the higher blood activity and the measurable, although limited, dicentrics induction in blood lymphocytes. However, the effective dose remains moderate, i.e. 30 times lower than in I-131 therapy in benign thyroid diseases.

PS_656

LONG TERM RESULTS OF YTTRIUM-90 RADIOSYNOVIORTHESIS IN CHRONIC KNEE SYNOVITIS OF DIFFERENT ORIGIN

M. Szentesi, M. Szentesi, S. Takacs. Semmelweis Univ., Chair of Rheumatology and Physiotherapy, Budapest, Hungary.

Authors report on the results of Yttrium-90 radiosynoviorthesis in chronic synovitis of the knee joint. Out of these 213 patients 122 suffered from rheumatoid arthritis, 17 ankylosing spondylitis,13 other seronegative spondylarthritis, 48 suffered from inflamed osteoarthritis , 1 hydrops articulorum intermitterns, 1 synovitis villonodularis, 11 from chronic traumatic synovitis .

Evaulation was based on the criteria as described by Müller, Rau and Scütte the score system was developed by the authors. In the first seven years excellent and good results were recorded in 71%. They achieved excellent as well as good results at 83% of patients with rheumatoid arthritis, at 50% of patients with ankylosing spondylitis and at 55% of patients with osteoarthritis. Seven years after radiosynoviorthesis 65% of patients did not need another punction.

Conclusion:

Radiosynoviorthesis is as effectiv method of treating chronic synovitis as surgical synovectomy.

Even after a seven-year period 71% the findings were rated as excellent or good.

72% of the patients do not need another punction even after a seven year period.

The effectiveness is worsened significantly by the stadium of the disorder and the local x ray phase and diagnosis. P 0.00001.

The treatment must be done in rheumatoid arthritis Steinbrocker stadium I-II, local stadium I-II.

PS_657

HISTOLOGIC STUDY OF EFFECTS OF RADIATION SYNOVECTOMY WITH RHENIUM-188 MICROSPHERE

S.J. Wang (1), W.Y. Lin (1), M.N. Chen (2), B.T. Hsieh (2), H. Huang (2), L.H. Shen (2), G. Ting (2). (1) Department of Nuclear Medicine, Taichung Veterans General Hosiptal, Taiwan; (2) Institute of Nuclear Energy Research, Taiwan.

Rhenium-188 microsphere is a relatively new radiation synovectomy agent developed for the treatment of rheumatoid arthritis. It has been shown that the levels of unwanted extra-articular radiation was negligible. A histologic study was conducted to assess the effect of radiation synovectomy on synovium and articular cartilage after intra-articular injection different doses of Re-188 microsphere into the knee joints of rabbits. Intra-articular injection of Re-188 microsphere into rabbit knee joints resulted in mild reactive inflammation and thrombotic occlusion of vessels which subsided rapidly. Sclerosis of subsynovium could be seen 12 weeks after injection. No evidence of damage to articular cartilage was noted. The comparison of the articular pattern after 0.3 and 0.6 mCi Re-188 microsphere failed to disclose any essential difference. This study suggests that a treatment dose of Re-188 microsphere cause transient inflammation of synovium without causing any detectable damage to the articular cartilage of knee joint.

PS_658

DISODIUM PAMIDRONATE/RE-186 HEDP COMBINED I.V APPLICATION FOR PALLIATION OF RECURRENT PAINFUL ENDSTAGE IDIOPATHIC OSTEOPOROSIS

G. Limouris (1), V. Voliotopoulos (1), A. Frantzis (1), S.K. Shukla (2), A. Stavraka-Kakavaki (1), L. Vlachos (1). (1) Areteion University Hospital, Nuclear Medicine Dept, Athens Greece; (2) CNR Collab Nucl Med Dept, St Eugenio Hosp, Rome, Italy.

The specificity and potency of pamidronate as an inhibitor of osteoclastic bone resorption provides the rationales for its therapeutic use in variety of conditions characterized by pathologically enhanced bone turnover,including idiopathic and steroid induced osteoporosis,as well osteolytic metastasis.Furthermore,in recent studies we assessed that the addition of pamidronate to conventional antiosteoporotic therapy not only arrests,but also reserves the loss of bone mass,a typical pathologic finding of idiopathic osteoporosis.Re-186-HEDP exclusively accumulates by chemisorption onto the surface of hydroxyapatite crystals of the osteosklerotic osseous lesion.an other characteristic of the collapsed vertebral bodies of the endstage idiopathic osteoporosis.

Three women aged 70 to yr. with long life history of painful idiopathic osteoporosis who were non-responsive to standard symptomatic therapies (sodium fluoride,calcitonine) were additionally treated with 180mg disodium pamidronate(Aredia,Ciba-Geigy Ltd. Basel) via i.v infusion at onset/monthly and for three months.In all 3 osteoporotic patients the initial dose was associated ,after a two week interval,by iv administration of 1400 Mbq of Re-186-HEDP. The follow-up period covered 16 weeks.The efficacy of the treatment was assessed by pain/performance questionnaire that the patients were asked to complete daily.A second technetium bone scan 12 weeks after therapy still showed the same activity.albeit the comparison of Karnofski Indexes,pain/performance questionnaires and bone densities assessed a satisfactory and statistical significant improvement.

Besides their main use in bone metastasis a cocktail disodium Pamidronate/Re-186-HEDP application appears to be very promising for palliation of recurrent idiopathic osteoporosis,where conventional treatment remains without beneficial effect.However any objective assessment of the place of pamidronate in osteoporosis is still not easy,since number of the enrolled patients is limited.On the other hand the applied new scheme prevents the development of hypercalcaemia,reduces bone pain,could prelude the risk of pathological fractures and increase mobility.

PS_659

RGD PEPTIDES LABELED WITH Y-86 AND IN-111: A COMPARATIVE DOSIMETRIC STUDY IN DOGS

W.C.A.M. Buijs (1), M. Janssen (1), O. Boerman (1), F. Roesch (2), F. Corstens (1), W. Oyen (1). (1) Department of Nuclear Medicine, University Medical Center, Nijmegen, The Netherlands; (2) Department of Kernchemie, University Mainz, Germany.

Aims: The pharmacokinetics and dosimetry of an ^{90}Y-labeled antibody can be estimated from the scintigraphic images of the ^{111}In-labeled antibody. Whether this holds for ^{90}Y-labeled peptides remains unclear. RGD peptides potentially target tumors by binding to the $\alpha_v\beta_3$ integrin, expressed on sprouting endothelial cells and on tumor cells. The objective of this study was to compare the pharmacokinetics and dosimetry of the ^{86}Y and ^{111}In-labeled analogues of a dimeric RGD-peptide in beagle dogs.

Methods: The DOTA derivatized dimeric RGD peptide $(RGDfK)_2$-E-DOTA was labeled with ^{86}Y or with ^{111}In. Quality control included RP-HPLC analysis and ITLC. Five beagle dogs were iv injected with 225 MBq ^{111}In-DOTA-E-$(RGDfK)_2$ and 74 MBq ^{86}Y-DOTA-E-$(RGDfK)_2$, respectively within a two-week period. The peptide dose was 315 µg in both cases. Whole body images were recorded with a dual head gamma camera (Siemens Multispect) and a PET camera (Siemens ART), respectively at one hour and at 1, 2 and 3 days post injection. ROIs were drawn, and the residence time of the radiolabel in the various organs was calculated after correction for transmission, scatter and build-up artefacts (gamma camera images) and transmission artefacts (PET camera). Using the MIRDOSE3 program the radiation dose of the ^{90}Y-labeled peptide to the relevant organs in a patient were estimated.

Results:

Dose (cGy/mCi)	^{111}Indium		^{86}Yttrium	
Organ	mean	SD	Mean	SD
Kidneys	5.4	1.7	4.2	0.9
Liver	2.8	0.4	2.4	0.4
Lungs	3.0	0.8	1.0	0.3
Red Marrow	2.5	1.1	2.0	0.2
Spleen	8.4	3.8	4.0	0.7
Bladder	4.0	0.8	3.8	0.9
Total body	0.6	0.1	0.6	0.1

Conclusions: The radiation dose of the ^{90}Y-labeled RGD-peptide can be estimated accurately based on the images of the ^{111}In-labeled peptide, although the radiation dose to the lungs is overestimated, significantly.

PS_660

THE EFFECT OF TARGETED THERAPY WITH RADIOLABELLED OCTREOTIDE ON COLON CARCINOMA CELLS TRANSFECTED WITH SOMATOSTATIN SUBTYPE 2 RECEPTOR IN A RAT LIVER METASTASIS MODEL

A.P. Breeman (1), A. Mearadji (2), L.J. Hofland (3), E.P. Krenning (1), C.H.J. van Eijck (2). (1) Nuclear Medicine; (2) Surgery; (3) Internal Medicine, Nuclear Medicine Erasmus University Medical Center Rotterdam, Rotterdam, Netherlands.

Introduction: Peptide receptor radionuclide therapy (PRRT) has proven to be a promising modality for tumours expressing somatosatin receptors (SS R). SS R are expressed in most neuroendocrine tumours and various other tumours, like breast cancer and malignant lymphoma. In previous studies we tested SS R-targeted therapy in a metastasised liver model with radiolabelled octreotide on SS R-positive and on SS R-negative tumours cells and found that SS R play a crucial role: PRRT was only successful in the SS R-positive model. The purpose of this study was whether the introduction of a SS R on SS R-negative tumour cells by transfection with a SS R subtype 2 gene will make these cells also feasible for this therapy. Therefore, SS R-negative colon carcinoma cells (CC531, p53 oncogene deleted) were transfected *in vitro* with a SS R subtype 2 gene (CC2B). The SS R status on the CC2B cells was confirmed *in vitro*: 12k per cell, with a high rate of specific internalisation of the radioligand, and confirmed in *vivo*: specific uptake and retention of the radioactivity in the CC2B cells. For *in vivo* therapy: 4 groups of male WAG/Rij rats (A-D, n=6-8) were formed. On day 0 CC531 cells (group A and B) or CC2B cells (group C and D) were injected into the portal vein. In addition, A and C were treated with 370 MBq [^{111}In-DTPA^0]octreotide on day 1 and 8. At day 28 the rats were sacrificed, the liver was weight and the tumour colonies scored. Results: no differences between A and B were found, ($p>0.05$), however, also no differences between C and D were found ($p>0.05$). Conclusion: Although the high expression of SS R on, and the uptake and retention of radioactivity in the SS R-positve tumour cells PRRT with radiolabelled octreotide did not have an antiproliferative effect on SS R-positive liver metastasis. Impaired efficiency of the p53-mediated cascade might explain the poor radiosensitivity of the SS R-positive CC2B cells in a rat liver model.

PS_661

BIODISTRIBUTION AND DOSIMETRY OF 99M TC-CIPROFLOXACIN, A PROMISING AGENT FOR THE DIAGNOSIS OF BACTERIAL INFECTION

F. De Winter (1), C. Van de Wiele (1), F. Dumont (2), J. Van Durme (2), K. Solanki (3), K. Britton (3), G. Slegers (2), R.A. Dierckx (1), H. Thierens (4). (1) Division of Nuclear Medicine, Ghent University Hospital, Belgium ; (2) Department of Radiopharmacy, Ghent University, Belgium ; (3) Department of Nuclear Medicine, St. Bartholomew's Hospital, London UK; (4) Department of Biomedical Physics and Radiation Protection, Ghent University, Belgium

This study reports on the biodistribution and dosimetry of 99mTc ciprofloxacin, a radioligand developed for the visualisation of bacterial infection.
Methods: Whole body scans were performed up to 24 h after intravenous injection of 370 MBq 99mTc ciprofloxacin in three male and three female volunteers. Blood samples were taken at various times up to 24 h after injection. Urine was also collected up to 24 h after injection, allowing calculation of renal clearance and interpretation of whole body clearance. Time activity curves were generated for the thyroid, heart, liver and whole body by fitting the organ-specific geometric mean counts, obtained from regions of interest. The MIRD formulation was applied to calculate the absorbed radiation doses for various organs.
Results: The images showed low to absent brain, lung and bone marrow uptake as well as rapid predominantly urinary, and to a lesser extent liver uptake and excretion of 99mTc ciprofloxacin, resulting in excellent imaging conditions for both the thoracic and abdominal regions, even at early time points (60 min) p.i. In none of the volunteers the gallbladder was visualised. Approximately 60% of the injected activity was recovered in urine by 24 h p.i. The highest absorbed doses were received by the urinary bladder wall, the thyroid, the upper large intestine, the lower large intestine and the uterus. The estimated mean effective dose for the adult subject, taking into account the weight factors of the ICRP60 publication, was 0.0083 mSv/MBq.
Conclusion: The amount of 99mTc ciprofloxacin required for adequate planar and tomographic imaging results in an acceptable effective dose to the patient.

PS_662

TUMOR SURFACE BINDING AS A FACTOR IN UPTAKE OF RADIOLABELED ANTIBODIES BY HUMAN TUMORS IN VIVO

R.P. Spencer. Division of Nuclear Medicine, Univ. Connecticut Health Center, Farmington CT, USA.

AIM. Multiple factors are likely involved in delivery and tumor uptake of radiolabeled antibodies which are administered intravenously. For example: perfusion, peritumor space , cell surface characteristics, and internalization may each play a role. To begin to analyze this, a conceptual model was utilized to examine cell surface effects.
METHODS. Cell surface area (A) can be approximated as a function of tumor volume (V). That is:
A = f(V). Volume depends on (assuming a sphere) tumor radius cubed, while surface area is approximated by radius squared. A logarithmic formulation is thus a reasonable initial step. A consequence is that, with a fixed number of acceptor sites on the tumor surface, relative uptake of radiolabeled antibody will fall with increasing tumor volume. Thus:

Log (Percent Uptake) = -k.Log (Tumor volume) + B

RESULTS. This formulation was utilized in assay of reported data on tumor uptake of radiolabeled antibodies given intravenously. For example, deBree and associates (Europ. J. Nucl. Med. 25:1562, 1998) assayed tumor uptake of 2 distinct labeled monoclonal antibodies in patients with head and neck
residual squamous cell carcinoma. In all 27 patients, tumor uptake was described by:

Log (Percent Uptake) = -0.34 Log (Tumor volume) + 2.66.

The p value was 0.0062. However, when results with the 2 antibodies were analyzed separately one had excellent correlation with the prediction, while the second did not. This suggests operation of additional factors such as antigenic modulation , loss of binding sites, induction of additional receptors, or changes in the quantity of radiolabeled antibody due to uptake by hepatic sites.
CONCLUSION. Assays of uptake of radiolabeled antibodies by tumors, versus size and/or external characteristics, may be of assistance in delineating the multiple biologic events involved.

PS_663

ASSESSMENT OF THE ERROR IN CELLULAR DOSE ESTIMATE DUE TO TRACING CUTOFF OF ELECTRONS AT 10 KEV IN THE EGS4 SIMULATION

E.H. Kim (1), C.W. Choi (2), S.M. Lim (2). (1) Lab. of Cyclotron Application, Korea Cancer Center Hospital; (2) Dept. of Nuclear Medicine, Korea Cancer Center Hospital, Seoul, Korea.

Aim: EGS4 is a code of popular choice for simulating the electron transport to estimate doses in cancer treatment using beta-emitting radioisotopes. In the EGS4 simulation scheme, the electrons are assumed to deposit their whole kinetic energy in the local volume where their kinetic energy becomes below 10 keV. The range of 10 keV electrons in the liquid water is ~2.6 _m. Since the cells, which are the critical targets responsible for radiation effect, are a few tens of micrometers in diameter at maximum, it is required to have the tracing cutoff energy for electrons much below 10 keV for accurate cellular dose estimation. In this study, we have assessed the error in cellular dose estimate caused by having the tracing cutoff energy for electrons at 10 keV.
Methods: The MCNP Monte Carlo code has been employed to calculate the linear energy transfer (LET) along the track for the electrons of initial kinetic energy ranging from 1 to 10 keV. The range of 1 keV electrons in the liquid water is ~0.068 _m and, therefore, we expect negligible magnitude of error in cellular dose estimate by assuming that the electrons deposit their whole kinetic energy in the local volume where they become below 1 keV. Using the LET data along the track, the energy deposited inside the cell has been calculated for a varying intracellular location where the electron becomes below 10 keV considering the direction of the electron track relative to the radial direction from the center of the cell. The calculation has been performed for the cells of 5, 10, 15 and 20 _m in diameter.
Results: The maximum energy loss by 10 keV electrons occurs at 1.5 _m from the starting point while it occurs at 0.4 _m by 5 keV electrons. Cellular dose is overestimated by 38, 22, 15 and 11 % for 5, 10, 15 and 20 _m-diameter cells, respectively, due to the tracing cutoff of the 10 keV electrons inside the cell. With 5 keV electrons stopped inside the cell, cellular dose is overestimated by 13, 6, 4 and 3 % for 5, 10, 15 and 20 _m-diameter cells, respectively.
Conclusion: The accuracy of cellular dose estimate should be improved by expanding the energy range for tracing electrons down to 1 keV.

PS_664

NEW COMBINED GENE-RADIONUCLEAR THERAPY WITH 125IVDU; INTRACELLULAR DISTRIBUTION OF 125IVDU IN HSV-TK EXPRESSED CELLS

S.J. Lee, K.S. Woo, E.H. Kim, W.S. Chung, S.J. Lim, T.S. Lee, C.W. Choi, S.M. Lim, S.H. Ahn. Cyclotron Application Lab. Korea Cancer Center Hospital, Seoul, Korea.

Objectives: ^{125}IUdR has been used in intraarterial cancer therapy with its low energy Auger electron.^{125}IVDU can be used as a substrate of HSV-tk gene in gene therapy monitoring. Viral thymidine kinase can phosphorylate ^{125}IVDU, and phosphorylated ^{125}IVDU can be incorporated into the nucleus. We investigated the intracellular distribution of ^{125}IVDU and ^{125}IUdR in HSV-tk positive (MCA-tk) cells and HSV-tk negative(MCA) cells and compared ^{125}IVDU with ^{125}IUdR for the selective localization in nucleus of the cells.
Methods: We synthesized ^{125}IVDU and ^{125}IUdR using TMS-VDU and UdR. MCA and MCA-tk cells were incubated with ^{125}IVDU and ^{125}IUdR in culture media. After 1hr and 4hr incubation, cells are washed and ruptured with sonication. Centrifugation of a cell extract at 700g for 15min downed nuclei, mitochondria at 7,000g, at 105,000g for 100min, cytosol remained the supernatant. Radioactivity of intracellular organelles was measured with gamma counter.
Results: The cellular uptake of ^{125}IVDU in MCA-tk cells was higher than that in MCA cells (45 times at 1hr, 100 times at 4hr). In MCA-tk cells, ^{125}IVDU was localized mainly in cytosol and mitochondria (46.7%, 27.1%) at 1hr incubation. However, the radioactivity was increased in nuclei (15.37% to 40.57%), and decreased in mitochondria (21.54%), in cytosol (29.84%) at 4hr. In MCA cells, ^{125}IVDU was localized 2.74% in nuclei, 1.59% mitochondria, 67.1% in cytosol. As time passed, intracellular distribution of ^{125}IVDU is unchanged. ^{125}IUdR showed similar intracellular distribution and localized 56.9% in nuclei, 9.26% in mitochondria, 34.68% in cytosol in 4hrs in both MCA and MCA-tk cells. Microdosimetry in the intracellular organelles predicted significantly high radiation dose to the nucleus of HSV-tk positive cells.
Conclusion: In MCA-tk cells, uptake of ^{125}IVDU was shifted from mitochondria and cytosol to nuclei. In MCA cells, uptake of ^{125}IVDU is negligible in nuclei. The shift of radioactivity into the nuclei is more cytotoxic to the HSV-tk expressed cells. We expect that the selective gene-radionuclear therapy with ^{125}IVDU can be applied.

PS_665

G2 ARREST AND APOPTOSIS OF CULTURED RAJI CELLS BY CONTINUOUS LOW DOSE RATE BETA IRRADIATION THERAPY WITH 188RE-PERRHENATE

S.J. Lim, K.S. Woo, E.H. Kim, W.S. Chung, S.J. Lee, T.S. Lee, C.W. Choi, S.M. Lim. Cyclotron Application Lab. Korea Cancer Center Hospital, Seoul, Korea.

Purpose : Beta emitting radionuclide therapy gives exponentially decreasing radiation dose rate and results in cell death presumably by apoptosis. We observed changes in DNA content and apoptosis in relatively low dose rate beta irradiation.
Methods : Raji cells were cultured and incubated with ^{188}Re-perrhenate (3.7MBq, 37MBq, or 370MBq/ml) for 4 hours to give irradiation dose of 0.4, 4, or 40 Gy. After changing the culture media, cells were cultured for 2, 4, 8, 16, and 24 hours. The cells were stained with Trypan blue, Annexin-V and Propidium Iodide (PI) to observe cell viability, cell membrane alteration by apoptosis and changes in DNA content respectively. Flowcytometry was done for Annexin-V and PI to quantitate apoptosis and necrosis in the irradiated cells. DAPI(4,6-diamidino-2-phenylindole) stain was also done to observe the damage in the nucleus.
Results : Cell viability decreased with an increasing radiation dose. Cells irradiated in 40 Gy showed early uptake of both Annexin-V and PI suggesting cell death by necrosis. Cells irradiated in 0.4 Gy showed delayed uptake of Annexin-V only, and later on PI uptake suggesting cell death mainly by apoptosis. The cells irradiated in 0.4 Gy showed G2 arrest in 16 hours after irradiation, but the cells irradiated in 40 Gy showed early DNA fragmentation within 2 hours after irradiation. In DAPI stain, early nucleus damage was observed in the cells irradiated in 40 Gy. On the other hand, slowly increasing apoptotic bodies were observed in the cells irradiated in 0.4 Gy.
Conclusion : These results suggest that continuous low-dose irradiation induces G2 arrest and progressive apoptosis in cells while continuous high-dose irradiation induces rapid necrosis. Therefore, we expect therapeutic effect by continuous low-dose rate irradiation with beta emitting radiopharmaceuticals.

PS_666

COMPARISON OF THE PREPARATION AND IN VITRO STABILITY BETWEEN 188RE-MAG3-LYM-1 AND 188RE-HYNIC-LYM-1 IMMUNOCONJUGATES FOR RADIOIMMUNOTHERAPY

T.S. Lee, S.H. Ahn, S.J. Lim, W.S. Chung, S.J. Lee, K.S. Woo, C.W. Choi, S.M. Lim. Cyclotron Application Lab. Korea Cancer Center Hospital Seoul Korea.

Objectives For Radioimmunotherapy, it is important that rapid labeling, high labeling yield and good stability. To prepare ^{188}Re immunoconjugates for radioimmunotherapy, monoclonal antibody was indirectly radiolabeled with ^{188}Re by MAG_3 chelate or HYNIC-lym-1 conjugate prepared radiolabeled with ^{188}Re-tricine. These ^{188}Re-lym-1 immunoconjugates were compared with the preparation and *in vitro* Stability.
Methods MAG_3 was radiolabeled with ^{188}Re using $SnCl_2$. ^{188}Re- MAG_3-TFP ester was prepared by EDC and tetrafluorophenol with ^{188}Re-MAG_3 and purified by Sep-pak C18. Purified ^{188}Re-MAG_3-TFP ester was conjugated with lym-1. For preparing ^{188}Re-HYNIC-lym-1 immunoconjugate, HYNIC-lym-1 was synthesized by HYNIC-NHS ester with lym-1 and its coupling ratio was determined. ^{188}Re-Tricine prepared using $SnCl_2$ was reacted with HYNIC-lym-1. ^{188}Re-HYNIC-lym-1 and ^{188}Re-MAG_3-lym-1 were purified by PD-10. ITLC and HPLC was used in each step. ^{188}Re-lym-1 immunoconjugates were allowed to stand at 4 for up to 16hr to estimate its stability in presence of Ascorbic acid.
Results . ^{188}Re-MAG_3 and ^{188}Re-MAG_3-TFP was radiolabeled with 98 % yield. Radiolabeling yield of lym-1 with ^{188}Re-MAG_3 was 23 %. ^{188}Re-Tricine was radiolabeled with 99 % yield. HYNIC coupling ratio to a molecule of lym-1 was 3.6. ^{188}Re-HYNIC-lym-1 was prepared by 20 % labeling yield and non-specific labeling of ^{188}Re-Tricine with lym-1 was < 1 %. Preparation time of ^{188}Re-MAG_3-lym-1 was 2 times higher than ^{188}Re-HYNIC-lym-1. Radiochemical purity of purified ^{188}Re-MAG_3-lym-1 and ^{188}Re-HYNIC-lym-1 were maintained at >80% after 16hr standing.
Conclusions Both ^{188}Re-MAG_3-lym-1 and ^{188}Re-HYNIC-lym-1 immunoconjugates showed 20% labeling yield and > 80% stability. Radiolabeling of lym-1 with HYNIC chelate than MAG3 was more simple and time-saving method. Antibody radiolabeling with ^{188}Re using HYNIC chelate can be used for the preparation of radioimmunoconjugate for radioimmunotherapy

PS_667

RADIATION SYNOVECTOMY WITH HOLMIUM-166 FERRIC HYDROXIDE - A FIRST EXPERIENCE

S. Ofluoglu (1), E. Schwameis (2), E. Havlik (3), A. Wanivenhaus (2), H. Sinzinger (1), C. Pirich (1). (1) Department of Nuclear Medicine; (2) Department of Orthopedics; (3) Department of Biomedical Engineering & Physics, University Hospital of Vienna.

Radiation synovectomy with tracers bound to ferric hydroxide particles has been shown to be effective and safe. Holmium-166 (^{166}Ho) offers promising physical properties for radiation synovectomy as does its carrier ferric hydroxide (FH) macroaggregates. ^{166}Ho FH is marketed for radiation synovectomy but there is a lack on clinical data.
Aim of the study: to evaluate the efficacy and safety of ^{166}Ho FH in a prospective clinical trial in 16 patients suffering from chronic synovitis.
Methods: Sixteen intra-articular injections were performed in 16 patients receiving a mean activity of 1.11 GBq (range: 1.0 ~ 1.24) ^{166}Ho FH. Blood activity measurements and monitoring of activity distribution by whole body gamma camera imaging were performed for control of leakage 3 and 24 hours after injection of ^{166}Ho FH. Doses to non-target organs were calculated. Clinically the patients were evaluated before radiation synovectomy, 1 week, 1 month and thereafter in 3 months intervals by the parameters joint effusion, pannus, local pain and range of motion and by the assessment of the patient«s satisfaction.
Results: In 12 of 16 treatments no leakage to non-target organs was visible while small amounts of activity could be detected in the local inguinal lymph nodes in four patients. Calculated maximum doses to the lymph nodes were 2.66 and 2.5 Gy, respectively. Leakage to the blood was negligible as was no leakage to other organs, either. Clinically 12 patients (75 %) exhibited a complete or partial response as defined by a reduction of the local clinical score by at least two points.
Conclusion: Radiation synovectomy with ^{166}Ho-FH was safe and effective in a small group of patients with chronic synovitis. Controlled clinical trials are necessary to evaluate the therapeutic efficacy and safety in comparison to other radionuclides and glucocorticosteroids.

PS_668

PHARMACOKINETIC EVALUATION OF 188RE-HEDP IN HEALTLY BEAGLE DOGS AND DOGS HAVING SPONTANEOUS OSTEOSARCOMA

G. Andocs, L. Balogh, K. Bodo, A. Polyak, D. Mathe, G. Janoki. National Research Institute for Radiobiology and Radiohygiene, Budapest, Hungary.

188Re labelled HEDP is a promising therapeutical radiopharmaceutical for pailiation of pain in patient with primery bone tumors and multiple bone metastases of breast and prostate carcinoma.
Aim of the study . We aimed at to examine the biodistribution and pharmacokinetics of the 188Re-labelled compound in healtly Beagle dogs. Pharmacokinetic evaluation in dogs having spontaneous osteosarcoma were also studied. Radiotoxicological side effects were followed throughout the study.
Materials and methods. 188Re-perrhenate received from a tungsten/rhenium generator (Oak Ridge National Laboratory). Radiochemical purity of 188Re-HEDP was determined by TLC before injection. For the pharmacokinetic study 20 MBq/body weight kg 188Re-HEDP was injected intravenously into 4 healthly Beagle dogs, and images were taken 1, 3, 6, 24 and 48 h after the injection by a digital gamma camera (Nucline X-Ring, Mediso LTD.) with HEGP collimator. To follow the radiotoxicological side effects blood parameters (blood cell counts) were investigated before and for 4 weeks following the injection. In dogs (2) having spontaneous osteosarcoma a whole body 99mTc-MDP scan was done before the rhenium injection, to localise correctly the primary bone lesion and the possible metastases. Fifty MBq/body weight kg 188Re-HEDP was injected intravenously into the dogs having spontaneous osteosarcoma, and images were taken 1, 3, 6, 24 and 48 h after the injection.
Results. The labelling efficiency of 188Re-HEDP injected into dogs was always more than 90 %. In healthly dogs late images were shown high 188Re-HEDP uptake in the skeleton. 188Re-HEDP was excreted mainly by the kidneys. Blood count analysis showed small decrease of the white blood cell count only, but it normalized without treatment within weeks. Dogs having osteosarcoma showed very high 188Re-HEDP uptake in the primary bone tumor. Investigation of therapeutical effects are in progress.
Conclusion. Our preliminary results are showed that 188Re-HEDP is a safe agent and localising in high extent in osteosarcoma lesion allowing possible therapeutical effects in future experiment.

PS_669

EFFICACY OF RADIOSYNOVECTOMY WITH YTTRIUM 90 IN THE TREATMENT OF INFLAMMATORY ARTHRITIS OF THE KNEE, RETROSPECTIVE ANALYSIS

S. Rodado (1), A.M. García (1), V.M. Poblete (1), A. Soriano (1), C. Rubio (2). (1) Department of Nuclear Medicine; (2) Deparment of Rheumatology,Alarcos Hospital ,Ciudad Real ,Spain.

Aim :To evaluate the efficacy of radiosynovectomy with yttrium 90 (Y90) in the treatment of arthritis of the knee , analysing retrospectively which factors influenced on the final success of our sample.
Methods :We retrospectively analysed a total of 36 joints (knees) in 30 patients (19 women and 11 men) with a mean age of 54 years (range:14-80 years) who were treated with intra-articular injection of Y90 between November 1995 and December 2000.The underlying disease process was rheumatoid arthritis in 21 patients and other arthropathies in the rest .The mean duration of the disease before the therapy was ten years (range :2-45 years).A „three-phases" bone scan for evaluating of degree of active synovitis of the treated joint was carried out some days prior to therapy .All treatments consisted of a intra-articular injection of 185 MBq of Y90.A scintigraphic imaging of activity distribution over the joint was performed immediately .Seven joints received a second therapy .We considered a good result when at least two of the next criteria improved :pain , swelling and limitation of motion ; medium if only one improved and no response if none improved .The factors which could be associated with response to the treatment were studied through logistic regression.
Results :Of the 36 joints evaluated we found a good result in 23 (64%) , medium in 5 (14%) and failure in 8.Therefore improvement was noted in 78% , the majority in the first month after therapy .Seven joints underwent a second treatment , four improved and three did not response definitely.In the joints in which the treatment was successful , the mean duration of the disease was 8.8 years .Imaging of activity distribution showed a homogeneous activity distribution in 42% of the cases , whereas 58% had an irregular or non intra-articular distribution.
Conclusions:-The radiation synovectomy with Y90 has proved to be an effective treatment of inflammatory arthritis of the knee.
-Patients who received the most benefit from the procedure were in the early stages of the disease.
-We did not find any relationship between scintigraphic distribution and the final result ; neither the age nor gender were predictors of results .This could be explained by the size of our sample and the reduced number of patients who did not respond to the treatment.

PS_671

PULMONARY DIFFUSING CAPACITY AND MULTIGATED RADIONUCLIDE VENTRICULOGRAPHY IN PATIENTS WITH HEART FAILURE – EFFECT OF MODERN MEDICAL TREATMENT.

C.L. Petersen, A. Kjær. Dept. Clinical Physiology & Nuclear Medicine, Frederiksberg Hospital H:S, University of Copenhagen, Denmark.

Aim: Substantial improvement in survival has been documented in patients with heart failure and reduced systolic cardiac function after the introduction of ACE-inhibitor treatment.
The purpose of this study was primarily to document a possible reduction in the lung diffusion capacity (TLCO) in patients with untreated heart failure (NYHA II-III). Secondly, to elucidate the effect of intensive medical treatment with diuretics and ACE-inhibitor/ angiotensin-II receptor antagonists on TLCO in patients with symptomatic heart failure and reduced systolic function.
Methods: Patients with a relevant history, symptoms of dyspnea and echocardiographically estimated LVEF< 0.40 were included. Patients were characterized according to the results of multigated radionuclide ventriculography as heart failure if left ventricular ejection fraction was reduced (LVEF < 0.50). A total of 20 patients fulfilled the criteria.
Patients were characterized by lung function test including diffusion capacity (TLCO) and by multigated radionuclide ventriculography (LVEF) before medical treatment (baseline) and after 1 year of treatment with diuretics and ACE-inhibitors/angiotensin-II receptor antagonists.
As control of baseline lung function test of an age - and sex matched group of healthy volunteers (n=17) was performed.
Results:
(Values are means)

Pulmonary diffusion capacity	Baseline, TLCO (mmol/sec x kPa)	1 year of treatment, TLCO (mmol/sec x kPa)
Healthy:	0,127 (94% of predicted mean)	
Heart failure:	0,099 * (76% of predicted mean)	0.094 (ns)
Left ventricular systolic function	Baseline, LVEF	1 year of treatment, LVEF
Heart failure	0.28	0.32*

*) P<0.05
Conclusion: Patients with symptomatic heart failure (NYHA II-III) and reduced systolic function have respiratory dysfunction in the form of reduced TLCO.
Intensive medical treatment did not have any effect on the reduced TLCO whereas a marginal increment in LVEF was observed within the first year.
The reduction in TLCO probably reflects permanent changes in the lung vasculature and may add to the dyspnea in these patients.

CARDIOVASCULAR 8

PS_670

CAUTION TO ESTIMATE CARDIAC FUNCTION IN PATIENTS WITH NONISCHEMIC HEART DISEASES USING ELECTRO-CARDIOGRAPHIC-GATED TECHNETIUM-99M TETROFOSMIN MYOCARDIAL SINGLE-PHOTON EMISSION TOMOGRAPHY

S. Isobe (1), A. Ando (1), M. Nanasato (1), M. Nonokawa (1), M. Hirai (1), M. Yokota (2). (1) First Department of Internal Medicine; (2) Department of Laboratory Medicine, Nagoya University School of Medicine, Nagoya, Japan.

Aim: It is now possible to obtain simultaneous assessment of perfusion and function using electrocardiographic-gated single-photon emission tomography (g-SPET) with Tc-99m_labeled tracers. It is important to estimate left ventricular (LV) function in patients with chronic heart failure noninvasively. However, recent studies have demonstrated some potential limitations to estimate LV function in patients with ischemic heart diseases using g-SPET. We intended to clarify factors which could influence LV function in patients with nonischemic chronic heart diseases using g-SPET.
Methods: Thirty patients with nonischemic chronic heart diseases (21 men, 9 women, mean age 54 ± 18 y, 22 with idiopathic dilated cardiomyopathy, 8 with primary valvular diseases) were subjected to eight frames per cardiac cycle g-SPET with Tc-99m-tetrofosmin, ultrasound echocardiography (UCG), and contrast left ventriculography (LVG). Quantitative g-SPET (QGS) software was processed to determine LV functional parameters from g-SPET. The LV myocardium on SPET was divided into 17 segments and defect score was defined a 4-point grading scale. Total defect score (TDS) was calculated.
Results: LV ejection fraction (LVEF) calculated by QGS was highly reproducible. There were significant correlations between LVEF from g-SPET and that from LVG as well as that from UCG ($n = 30$; $r = 0.71$, $P < 0.001$; $r = 0.75$, $P < 0.001$, respectively). When we excluded patients with a relatively large defect (TDS > 8), the correlations were slightly improved ($n = 25$; $r = 0.72$, $P < 0.001$; $r = 0.77$, $P < 0.0005$, respectively). If we excluded patients with LV enlargement (LV end-diastolic volume index > 120 ml/m^2), the correlations were moderately improved ($n = 25$; $r = 0.83$, $P < 0.0005$; $r = 0.82$, $P < 0.0005$, respectively). When we excluded patients with tachycardia (heart rate > 100 beats/min) or frequent premature beats (ventricular premature captures or supraventricular premature captures), the correlations were excellent ($n = 22$; $r = 0.97$, $P < 0.0001$; $r = 0.94$, $P < 0.0001$).
Conclusions: Because tachycardia or arrhythmia may be more influential to measure LV function of nonischemic chronic heart diseases, caution is necessary to estimate LV function of nonischemic chronic heart diseases using g-SPET at eight frames per cardiac cycle, albeit g-SPET is clinically useful. Heart rate should be appropriately controlled for this examination.

PS_672

AMBULATORY RADIONUCLIDE ASSESSMENT OF THE EFFECTS OF WALK TEST AT DIFFERENT LEVELS OF HEART RATE IN PATIENTS WITH HEART FAILURE

A. Ferro (1), C. Duilio (2), M. Santomauro (2), A. Cuocolo (1). (1) Department of Biomorphological and Functional Sciences; (2) Department of Cardiology, University Federico II, Napoli, Italy.

The effects of heart rate alone on left ventricular (LV) function during physical activity in patients with heart failure have not yet been investigated. The aim of this study was to assess the effects of changes in heart rate on LV function during walk test in patients with heart failure.
Methods: 13 patients (9 men and 4 women) with DDD pacemaker, implanted for complete heart block, were enrolled. Seven patients had depressed baseline LV ejection fraction (35±3%), history of congestive nonischemic heart failure (group A) and 6 patients had normal baseline LV ejection fraction (59±6%) without any relevant symptom at rest and during physical activity (control subjects, group B). In all patients, LV systolic and diastolic function was continuously monitored by ambulatory radionuclide system (Vest). All patients underwent three walk tests. Each walk test (6 min) was performed at 70, 90 and 110 beats/min achieved by a programmed stimulation at fixed rate.
Results: Under resting conditions, in group A, with increasing in heart rate, ejection fraction progressively decreased from 35±3% to 25±4% and to 22±6% at 70, 90 and 110 beats/min, respectively (all $p<.05$), as a consequence of slight reduction in end-diastolic volume and significant ($p<.05$) increase in end-systolic volume; whereas in group B, ejection fraction only decreased ($p<.05$) at 110 beats/min. At peak of the three walk tests, in both groups of patients, all parameters significantly ($p<.001$) increased, whereas end-systolic volume reduced (<.05) as compared to respective baseline value. In group A, comparison among rest-peak variations of all parameters during the three walk tests showed a significant ($p<.05$) reduction of LV ejection fraction and end-diastolic volume only during walk test performed at 110 beats/min. In contrast, in group B, no significant differences were observed.
Conclusions: In patients with heart failure, during walk test performed at 110 beats/min, there is a decline of LV performance as compared to walk tests performed at 70 and 90 beats/min. In contrast, in control group, the different levels of heart rate do not affect cardiac response to moderate physical activity. These data suggest the optimum heart rate ranging from 70 to 90 beats/min to perform a physiological and moderate stress-test, on the other hand there is a negative effect of faster heart rate on LV function in patients with heart failure.

PS_673

OBESITY AND ITS RELATION TO RESTING LEFT VENTRICULAR FUNCTION AND VOLUMES

O. De Winter (1), J. De Sutter (2), C. Van de Wiele (1), P. De Bondt (1), J. Versijpt (1), R.A. Dierckx (1). (1) Division of Nuclear Medicine; (2) Department of Cardiology, Ghent University Hospital, Belgium.

Aim: Obesity is a well-known risk factor for coronary artery disease. However, conflicting data exist on the relation between BMI and left ventricular (LV) volumes and function.
Methods: Data on BMI were collected in 297 consecutive patients (182 males, mean age 57±11 y, mean resting LVEF 58±11%) without a previous cardiac history who were referred for a diagnostic two-day Tc^{99m}-tetrofosmin gated SPET study. In all patients LV enddiastolic and endsystolic volumes (LVEDV and LVESV) were determined from the resting gated SPET studies using QGS". LV ejection fractions (LVEF) were calculated from the obtained volumes.
Results: Results for resting LV volumes and LVEF according to BMI are shown in the table.

	Resting study			
BMI (kg/m^2)	>35 (n=17)	30-34 (n=48)	25-29 (n=135)	< 25 (n=97)
LVEDV(ml)	106±59	94±33	102±35	104±48
LVESV (ml)	55±50	43±25	46±27	50±44
LVEF (%)	55±15	60±10	58±10	57±13

No differences for LV volumes and LVEF were noted between the different subgroups for the resting studies. No significant correlations were found between BMI and resting LV function and volumes.
Conclusions: When using gated SPET as a toll to measure LV function and volumes, obesity does not seem to be associated with a reduction of resting LVEF or an increase of resting LV volumes.

PS_674

EFFICACY OF WALL MOTION ANALYSIS IMMEDIATELY AFTER EXERCISE IN DETECTING CORONARY ARTERY DISEASE USING SEPARATE ACQUISITION, DUAL-ISOTOPE GATED SPECT

H. Ono, Y. Sato, M. Hashimoto, M. Mitsui, M. Muromoto, M. Kato, T. Horie, J. Kusama, T. Narumiya, T. Sakamaki, K. Kanmatsuse
The Department of Cardiology, Nihon University Surugadai Hospital, Tokyo, Japan.

Aim: The addition of regional wall motion analysis (WMA) using ECG-gated SPECT to myocardial perfusion SPECT alone has been reported to be of limited use in detecting coronary artery disease (CAD) because of reversal of ischemia after exercise cessation. We investigated whether nor not immediate data acquisition following exercise might improve the overall sensitivity of combined myocardial perfusion SPECT and WMA.
Methods: 62 patients with angiographically proven CAD and 46 patients judged to have low likelihood of CAD determined according to the AHA/ACC guideline entered the study. A high-resolusion collimator with 180-degree acquisition over 64 projections and 25-45 seconds / projection (Siemens E-cam) was utilized. Following rest ECG-gated Tl-201 imaging, the patients underwent symptom-limited, multi-stage bicycle ergometer exercise. 99mTc-tetrofosmin (740MBq) was injected at the end of exercise. Immediately after exercise cessation, the patients underwent gated 99mTc imaging for 13 min. This protocol allows post-stress imaging by 99mTc-tetrofosmin to be completed within 15 min following exercise cessation.
Results: The both rest and post-stress images were satisfactory for analysis of myocardial perfusion imaging and wall motion analysis in all patients with good separation of the heart from the liver. When only myocardial perfusion SPECT was applied, the sensitivity, specificity and diagnostic accuracy of the test were 89%, 87% and 88%, respectively. When perfusion SPECT and wall motion analysis were combined, the sensitivity was improved significantly to 92%. The specificity and the diagnostic accuracy were 85% and 89%, respectively. There were 3 patients who exhibited wall motion abnormality without significant perfusion defect.
Conclusion: The addition of WMA immediately after exercise to myocardial perfusion SPECT improves the sensitivity and diagnostic accuracy for detecting CAD.

PS_675

WHICH METHOD TO CALCULATE RIGHT VENTRICULAR EF CORRELATES BETTER WITH PEAK VO2 IN PATIENTS SUFFERING FROM CARDIOMYOPATHY: MUGA OR FIRST-PASS RNV?

M. Hacker (1), A. Tausig (1), S. St?rk (2), R. Angermann (2), D. Stratakis (3), R.M. Huber (3), M. Weiss (1), S. Dresel (1), K. Hahn (1).
(1) Department of Nuclear Medicine; (2) Department of Cardiology; (3) Department of Pulmonology, LMU, Munich, Germany.

Maximal exercise capacity (peak vO_2) predicts survival in candidates for heart transplantation. There have been reports that right ventricular ejection fraction (RVEF) calculated by multigated radionuclide ventriculography (MUGA) correlates well with peak vO_2. Due to partial overlap it is well known that first-pass radionuclide ventriculography (FP-RNV) is superior to planar MUGA in terms of calculating „true" RVEF. Aim of this study was to evaluate, whether MUGA or FP-RNV correlate closer with maximal exercise capacity.
Methods: In 87 patients (70 men, 17 women; age: 53 ± 11.8 yrs), suffering from dilated or ischemic cardiomyopathy, 121 cardiopulmonary exercise tests (upright symptom-limited bicycle ergometry) were performed within 2.5 years. During exercise ventilatory and gas exchange data were recorded and peak vO_2 was calculated. On the same day, patients underwent FP-RNV and MUGA (in vivo labeling of RBC's, 740 MBq ^{99m}Tc: FP-RNV; Picker SIM 400 multicrystal camera, projection: 30¡ RAO; MUGA: Picker Prism 2000, projection ~40¡ LAO) at rest.
Results: Mean peak vO_2 was 16 ± 4.8 ml/kg/min. Peak vO_2 has been ? 10 in 14 pts. and between 10 and 14 ml/kg/min in 43 pts. Mean FP-RVEF was 44% ± 10, mean MUGA-RVEF was 42% ± 12. Patients with a FP-RVEF of < 30% did have a significantly lower peak vO_2 (12 ± 3.8 ml/kg) than pts. with an FP-RVEF of ? 30% (16 ± 4.8 ml/kg; p=0,002). There was no statistically significant difference in peak vO_2 for MUGA-RVEF values < 30% and ? 30% (p=0.61). There was a moderate correlation between MUGA- and FP-RVEF (r=0.58).

Peak vO_2 (ml/kg/min)	RVEF < 30%		RVEF ? 30%		Total	
	FP	MUGA	FP	MUGA	FP	MUGA
Peak vO_2 ? 10	4	5	10	8	14	13
10 < peak vO_2 ? 14	6	3	38	32	43	35
Peak vO_2 > 14	1	12	63	61	64	73
Total	11	20	111	101	121	121

Conclusion: It is well known that RVEF calculated by planar MUGA does not represent true RVEF since the right ventricle and the right atrium cannot be distinguished appropriately. As expected we found only a moderate correlation for RVEF calculated by MUGA and FP-RNV in patients with cardiomyopathy. However, mean RVEF was similar for MUGA and FP-RNV. Nevertheless there has been a highly significant difference concerning peak vO2 if RVEF was measured below or above 30% for FP-RNV acquisitions but no significant difference was found for MUGA data.

PS_676

TOMOGRAPHY ADDS QUANTITATIVE AND QUALITATIVE VALUE TO RADIONUCLIDE VENTRICULOGRAPHY

I.P. Clements, B.P. Mullan, B.H. Brinkman, M.K. O'Connor. Mayo Clinic and Foundation, Rochester, Minnesota, USA.

Planar blood-pool radionuclide ventriculography (RNV) is currently the most accurate, reproducible and readily available non-invasive method for measurement of left ventricular (LV) function. However, the addition of tomography (SPECT) promises to expand the usefulness of RNV. The ability of SPECT RNV to measure LV and right ventricular (RV) ejection fraction (EF) and volumes and wall motion was evaluated in 26 patients (using a dual-headed gamma camera, 8-16 frames/cardiac cycle, 180? rotation, 30 images/rotation, 60 sec/stop). From this single acquisition, cardiac transaxial images were reconstructed to generate cardiac long (horizontal and vertical) and short axis image slices. Simultaneous display of all three sets of images with superimposition of bars identifying a specific slice location allowed identification of valve planes and facilitated quantitative analysis; horizontal long axis and short axis slices were optimal for analysis of the RV and LV respectively. Manually defined RV and LV regions of interest were used to determine RV and LV end-diastolic and end-systolic volumes and ejection fraction; background correction was found not to be necessary. Good correlations ($p<0.0001$) were evident between SPECT RNV and concurrently obtained planar RNV with regard to LVEF (0.86) and end-systolic (0.81) and end-diastolic (0.76) volumes. RVEF and volumes were readily determined with SPECT RNV but must be validated against another imaging method such as electron beam computerized tomography. The tomographic images also provided global evaluation of RV and LV wall motion. Thus a single tomographic acquisition maintained the ability of RNV to accurately assess the LV and greatly enhanced the qualitative and quantitative ability of RNV to evaluate the RV and cardiac wall motion.

PS_677

INDIRECT EVALUATION OF LV DIASTOLIC DYSFUNCTION WITH MYOCARDIAL PERFUSION SCINTIGRAPHY TC-99M MIBI IN PATIENTS WITH MYOCARDIAL INFARCTION - CORRELATIONS WITH ECHO-DOPPLER PATTERNS

C. Medrea, A. Bogdan, R. Petrovici, C. Suciu, S. Mot, R. Capalneanu, M. Barsan. Clinical Cardiology, Heart Institute, Cluij, Romania.

PURPOSE: To correlate the localization and the severity of the myocardial perfusion deffects in patients with MI with the degree of LV diastolic disfunction evaluated at cardiac echo-doppler.
METHODS: We studied 32 patients (age between 42-70 years, 22 male and 10 female) with MI older than one year. We excluded: moderate and severe LV hypertrophy, more severe than I-st degree mitral regurgitation, LVEF<40% and other disorders which could produce alterations in preload or afterload. All the patients underwent rest and stress myocardial perfusion scintigraphy with 99m-Tc MIBI SPECT in the two-days protocole. For regional analysis of perfusion, myocardium was divided in 16 segments. In each patient, corresponding resting and stress 99m-Tc MIBI tomographic images were evaluated for direct comparison and segmental tracer uptake was quantitatively analysed using a four-point scoring system (3=normal uptake, 2=slightly reduced, 1=severaly reduced, 0=absent). Also a Gated SPECT for LVEF quantification was performed. Each patient was further investigated by coronary angiography in order to establish the coronary anathomy. The following parameters were measured using PW doppler with the sample volume at the tip of the mitral leaflets and in the left upper pulmonary vein: E/A, deceleration time, isovolumetric relaxation time and velocities of pulmonary flow, obtaining different patterns of diastolic disfunction (abnormal relaxation, pseudonormal and restrictive patterns).
RESULTS: The terrytorial distribution of irreversible (i), accompanied or not by reversible (r) perfusion defects in the same or another region, was the following: 18p with necrosis in LAD teritory (10i and 8i+r),10p with necrosis in RC teritory (3i and 7i+r) and 4p with necrosis in Cx theritory (2i and 2i+r).12p of the LAD group, 4p of the RC group and 2p of the Cx group had scores 0 and 1. 6p-LAD, 6p-RC and 2p-Cx had scores 2 and 3.Echo-doppler evaluation of diastolic function revealed a normal pattern for 3p (2p–RC, 1p-Cx) with scintigraphic scores 2-3, abnormal relaxation for 20p(10p-LAD, 7p-RC and 3p-Cx), pseudonormalization for 2p of the LAD group and restrictive patterns for 7p (5p-LAD with score 0-1, 1p-LAD with score 2 and 1p-RC).
CONCLUSIONS: Myocardial necrosis situated in LAD theritory with a scintigraphic score 0-1 is more frequently associated with diastolic dysfunction of a restrictive type, compared to necrosis in RC or Cx theritory for the same scintigraphic score. Abnormal relaxation is more often found in patients with RC and Cx infarction without relation with the scintigraphic score and in LAD infarction with score 2-3.

PS_678

THE CLINICAL VALUE OF TC-99M-MIBI GATED SPECT FOR THE EVALUATION OF LEFT VENTRICULAR FUNCTION AND VOLUMES AS COMPARED WITH ECHOCARDIOGRAPHY

N. Alan (1), O. Özmen (1), M. Halaç (1), C. Nisli (1), L. Koldaş (2), I. Başar (2), L. Kabasakal (1), H. Karpuz (2), C. Önsel (1), I. Uslu (1).
(1) Department of Nuclear Medicine ; (2) Department of Cardiology, Istanbul, Turkey.

Technical improvement has recently permitted in the routine use of gated SPECT in myocardial perfusion imaging for evaluation of attenuation artefacts. Echocardiography is the standard method of evaluating left ventricular function in clinical practice.
Aim: The aim of this study was to determine if left ventricular function determined from gated-SPECT myocardial imaging adequately coincides with echocardiographic data
.Method: For this purpose we studied 75 patients, ages ranged from 38 to 83 years (mean 59.7±10.5), who referred for myocardial perfusion imaging (52f, 23m). All patients underwent same day stress-rest Tc-99m-MIBI gated-SPECT study and gated-SPECT was performed by 8 frames per cycle acquisition over a 180 degree rotation on 32 projections. Four gated-SPECT slices were obtained on midventricular vertical long axis, horizontal long axis, apical and basal short axis planes. Ejection fraction (EF), end diastolic volume (EDV) and end sistolic volume (ESV) were calculated from gated-SPECT data using an automatic edge detection algorithm from resting perfusion images. EF, EDV(n=28), ESV (n=28), end diastolic diameter (EDD) and end sistolic diameter (ESD) were obtained from echocardiography using a standard technique.
Results: EF values obtained from gated-SPECT ranged from 14 to 81 with a mean value of 57.2±11.4. EF values obtained from echocardiography were ranged from 27 to 72 with a mean value of 55.4±6.8 (p>0.5). The correlations between gated-SPECT and echocardiography with respect to left ventricular ejection fraction, end diastolic volume and end sistolic volume were ranged from good to excellent with correlation coefficients of 0.68, 0.61 and 0.93, respectively (p<0.001, Pearson's coefficient).
Conclusion gated-SPECT has a good correlation with echocardiography for the assessment of left ventricular function and these results support the clinical use of gated-SPECT technique.

PS_679

UTILITY OF SCINTIGRAPHY WITH 99MTC-PYROPHOSPHATE AND 99 MTC- TETROFOSMIN SPECT IN THE DIAGNOSIS OF ACUTE MYOCARDIAL INFARCTION

A.M. García (1), V. Poblete (1), S. Rodado (1), C. Rodriguez (2), L. Celemín (3), A. Soriano (1). (1) Department of Nuclear Medicine, Alarcos Hospital, Ciudad Real, Spain; (2) Department of Investigation, Alarcos Hospital, Ciudad Real, Spain; (3) Department of Cardiology, Alarcos Hospital, Ciudad Real, Spain

Aim: To determine the utility of pyrophosphate scintigraphy (PYP-S) in the diagnosis of acute myocardial infarction (AMI) and to assess the location. To study if the tetrofosmin SPECT (T-SPECT) is helpful in this group of patients.
Methods: 80 patients underwent PYP-S (59 males and 21 females) with an average age of 56 (16-82).
The suspicious diagnosis was AMI in 70 patients and myopericarditis in 10. All patients had at least two inclusion criteria (chest pain, high level of creatine kinase-MB and electrocardiogram alterations). Planar images (80 patients) and SPECT (23 patients) were carried out after administration of 740 MBq of PYP and 185 MBq of tetrofosmin within a medium time of four and eight days after the onset of the symptoms respectively.
Results: 44 patients were diagnosed of AMI, 10 of angor, 15 of myopericarditis and 11 with other no ischaemic diseases. The results of PYP-S were the following:

TP	TN	FP	FN
23	34	2	21

Of the 21 false negative, 15 corresponded to no Q infarction.
The values of sensitivity, specificity, PPV, NPV and accuracy for PYP-S were 52,3%, 94%, 92%, 61,8% and 71% respectively.
In 25 cases, PYP uptake was positive, 17 with focal uptake and 8 with diffused uptake.
There were 16 cases of AMI with positive PYP and focal standard, 10 of them had the same location with PYP-S uptake and AMI area.
The medium time of PYP-S was 3,9 days in true positives and 4,1 days in false negatives.
T-SPECT was realised in 23 patients. 14 of them showed an uptake defect compatible with infarction, 13 with final diagnosis of AMI and 1 with previous infarct (false positive for AMI) .5 cases resulted negative in both test. and only one of them was an AMI. 4 cases showed a diminished uptake within viability limits and the final diagnosis was ischaemia.
8 cases with negative PYP-S and final diagnosis for AMI (FN), showed positive T-SPECT in 7 cases, and only one resulted negative .
Conclusions: The PYP-S demonstrated to be effective in the diagnosis of AMI with Q wave and showed a high specificity and PPV. However, it was not very sensitive.
Final results of PYP-S were not influenced by the time of the scintigraphy.
T-SPECT can be helpful in AIM cases with negative PYP-S.

PS_680

THE RELATIONSHIP BETWEEN THE RIGHT SYSTOLIC VENTRICULAR FUNCTION AND LEFT DIASTOLIC VENTRICULAR FUNCTION DEPRESSED: USEFULNESS OF THE RADIONUCLIDE ANGIOGRAPHY(RNA)

M.J. Acosta-Gómez, A. Moral-Ruiz, M.D. Martínez, A. Rodríguez, M.A. Muros, G. Sabatell, S. Ortega, J.M. Llamas-Elvira. Department of Nuclear Medicine, Granada, Spain.

Aim: To prove if exists relationship in the incidence of systolic right dysfunction and the left diastolic function.
Patient and methods: Retrospective study of 650 patient sent to our laboratory by customary motives. All of them had measured through a RNA the ejection fraction of the left ventricle (LVEF), of the right ventricle (RVEF), and the following diastolic function parameters of the VI: peak filling rates(PFR) and average(AFR), time of the PFR (TPFR), filling fraction to the first third expressed in percentage of volume Tele-diastolic (FF_EDV) , and beat (FF_VL).
The population of study, the pathological groups and results are the following:

N=650	RVEF<42%	RVEF>=42%	T-test (2-Tail)
Male	228 (35.1%)	154 (23.7%)	N.S.
Female	152 (23.4%)	116 (17.8%)	
AURIC. FIBR.	73 (11.2%)	70 (10.8%)	N.S.
LV DISF./ISQ.	133 (20.5%)	72 (11.1%)	
VALVULAR	30 (4.6%)	26 (4.0%)	
CARDIOTOX.	61 (9.4%)	25 (3.8%)	
MISCELLAN.	83 (12.8%)	77 (11.8%)	
	Mean±Std.error	Mean±Std.error	
AGE	55.80 ± 0.83	57.18 ± 0.80	N.S.
HEART RATE	80.21 ± 1.05	74.24 ± 0.89	P<0.01
LVEF (%)	47.04 ± 0.82	55.13 ± 0.76	P<0.01
PFR (EDV/s.)	2.46 ± 0.05	2.66 ± 0.06	P<0.05 AFR
(EDV/s.)	1.32 ± 0.03	1.40 ± 0.03	P<0.05
TPR (ms.)	164 ± 3.67	173 ± 4.25	N.S.
FF_EDV (%)	44.88 ± 0.92	41.72 ± 0.88	P<0.05
FF_VL (%)	21.10 ± 0.57	23.16 ± 0.57	P<0.01

Conclusions: Our results express that exists a association between the alterations of the diastolic function of the LV and the systolic dysfunction of the RV. The diastolic parameter with greater power of association is FF_VL.

PS_681

RELATIONSHIPS OF LEFT VENTRICULAR MASS AND FUNCTIONAL PARAMETERS

B.C. Ahn, J. Lee, S.W. Lee, K.B. Lee. Department of Nuclear Medicine, Kyungpook National University Hospital, Taegu, South Korea.

The purpose of this study was to evaluate the relationship between left ventricular masses(LVM) and functional parameters measured by gated myocardial perfusion SPECT.
Methods: One hundred sixty-four subjects(M/F=94/70, ranged 32 to 84 yrs, mean age 58yrs) wenderwent ^{99m}Tc-MIBI gated myocardial perfusion SPECT with dual head SPECT camera. We measured LVM, end diastolic volume(EDV), end systolic volume(ESV) and ejection fraction(EF) of LV by AutoQuant program and evaluted the relationship of these parmeters using pearson's correlation test.
Results: Forty-seven subjects(27%)showed perfusion defect in myocardial SPECT. EDV and ESV were positively correlated with LVM, and EF was negatively correlated with LVM in Stress and rest gated myocardial perfusion SPECT.
Correlation of LVM and functional parameters(EDV, ESV, EF) measured by quantitative myocardial perfusion SPECT

Subjects with perfusion defect(n=117)			Subjects without perfusion defect(n=47)		
	Stress SPECT	Rest SPECT		Stress SPECT	Rest SPECT
EDV	r=0.882, p<0.01	r=0.852, p<0.01	EDV	r=0.875, p<0.01	r=0.892, p<0.01
ESV	r=0.859, p<0.01	r=0.827, p<0.01	ESV	r=0.830, p<0.01	r=0.861, p<0.01
EF	r=-0.558, p<0.01	r=-0.541, p<0.01	EF	r=-0.575, p<0.01	r=0.603, p<0.01

All data mean correlation coefficient(r) and p value(p) for LVM and functional parameters.
Conclusion: LVM was positively correlated with EDV and ESV and negatively correlated with EF.

PS_682

EFFECT OF L-CARNITINE SUPPLEMENTATION ON MYOCARDIAL ENERGY SUBSTRATE UTILIZATION IN PATIENTS WITH CHRONIC RENAL FAILURE AND RECEIVING HEMODIALYSIS

K. Fukushima (1), Y. Ishida (1), K. Fukuchi (1), M. Inubushi (2), K. Sugimura (3). (1) Department of Radiology, National Cardiovascular Center, Suita, Japan; (2) Department of Pharmacology, UCLA, LA, USA; (3) Department of Radiology, Kobe University, Kobe, Japan.

A decrease in intracellular L-carnitine (L-C) concentration, which is a key substrate for myocardial fatty acid metabolism, has been observed and recognized to possibly induce the life-threatening myocardial dysfunction in patients with chronic renal failure (CRF) after hemodialysis (HD). Based on this evidence, administration of L-C has been recommended for these patients. However, recent experimental studies in L-C deficient rats find that L-C increases glucose utilization rather than normalize fatty acid metabolism in myocardium associating with improvement of cardiac function. The aim of this study was to observe the effect on L-C treatment on myocardial energy substrate utilization in patients with CRF after HD and with L-C deficiency.
Methods: L-C was administrated orally at doses of 500 mg/day for 3 month in 5 CRF patients after HD. To evaluate myocardial fatty acid and glucose utilization before and after L-C treatment, 123I-labeled _-methyl-p-iodophenyl-pentadecanoic acid (BMIPP) SPECT imaging and 18F-labeled fluorodeoxyglucose (FDG) PET imaging were performed in the fasting state. In the 15-min early and 210-min delayed anterior planar imaging, myocardial BMIPP uptake estimated by the heart to mediastinum ratio (H/M) and myocardial BMIPP washout rate (WR) were determined. In the dynamic FDG PET imaging, myocardial glucose utilization (MGU) was determined by Patlak plot analysis.
Results: Free L-C concentration in blood increased from 37.5±9.1_mole/L to 75.5±13.5 _mole/L after the treatment. H/M and WR in BMIPP imaging did not change (2.78±0.43 to 2.60±0.20, 18.5±4.2 to 16.4±9.2, respectively), while MGU significantly increased from 1.52±0.96mg/g/min to 3.58±1.02 mg/g/min (p<0.05). In the 3-month follow-up, there was no significant improvement in cardiac function.
Conclusion: L-C administration augments glucose utilization rather than normalizes fatty acid utilization in myocardium under the L-C deficient state in humans. It may require further investigation whether this metabolic change improves cardiac function or not.

DIAGNOSTIC ONCOLOGY 14

PS_683

GALLIUM SCAN IN THE CLINICAL MANAGEMENT OF ADOLESCENTS AND CHILDREN WITH HODGKIN DISEASE

M. Castellani (1), G. Cefalo (1), C. de Graaf (2), M. Terenziani (1), S. Baio (1), G. Aliberti (1), M. Maccauro (1), E. Bombardieri (1). (1) Istituto Nazionale Tumori, Milano, Italy; (2) Leiden University Medical Centre, Leiden, The Netherlands.

Gallium scan is a well consolidated diagnostic approach in Hodgkin's diseases of adult age. Very few reports are available in pediatric age. Gallium scan results in 74 consecutive patients, observed in our Institute between Apr 1985 and Jul 1999 and subsequently followed until today, were retrospectively reviewed. The aim of this study is to assess the clinical impact of gallium scan in the management of patients with Hodgkin's disease, from the onset of disease, in correlation with response to therapy and, more in general, to the clinical course of disease.
Methods: Seventy-four patients (mean age:13) underwent gallium scans for initial staging, 71/74 (114 scans) repeated scintigraphy during the follow-up (usually two controls) to assess the achievement of complete response (CR), or in few cases (12) to confirm progression or relapse of the disease. A whole-body scan was performed after 48 or 72 hours of the injection of 37-111 MBq of ^{67}Ga citrate (related to body weight) using a large field gamma-camera with a medium energy collimator.
Results: Patients were classified 36 stage I-II, 21 stage III-IIIS stage, and 17 stage IV. At initial staging, gallium scans resulted positive in 72/74 patients (97%), detecting 264 of 309 lymph nodal sites of disease. Gallium scan was positive, concordant with the clinical findings, in 84% of the patients. The best sensitivity was observed in mediastinum 64/64 (100%) and neck 124./146 (84%) and was lower in the axilla 16/22(72%) and retroperitoneum (11/16: 69%). In case of visceral involvement gallium resulted effective for lung (11/15) and bone (4/5) detection. The aggressiveness of this lymphoma did not alter the sensitivity of the gallium scan for the detection of lymphnodes, as the sensitivity in stage I-II and IIIS-IV were similar. During the follow-up, gallium scan resulted concordant with clinical and radiological findings in 28/29 (97%) cases with confirmed or suspected relapse or progression. In 42 patients with a single scan, which achieved a CR during or at the end of the first line treatment, this CR was confirmed by gallium scans in 40 patients and by conventional techniques in 21 patients.
Conclusion: On the basis of this results we can confirm the clinical usefulness of gallium scan in the diagnosis and follow-up of patients with Hodgkin's disease. Gallium appears effective in confirming the absence of disease in patients with positive scan at staging.

PS_684

TECHNETIUM-99M-SESTAMIBI AS A PREDICTOR OF RESPONSE TO CHEMOTHERAPY IN INDIVIDUAL TUMORS OF PATIENTS WITH NON-HODGKIN'S LYMPHOMA

H.-.C. Song (1), H.S. Bom (1), J.J. Lee (2), H.J. Jeong (1), I.J. Chung (2), S.M. Kim (1), M.R. Park (2), H.J. Kim (2), J.Y. Kim (1). (1) Department of Nuclear Medicine; (2) Department of Hematology, Chonnam National University Hospital, Kwangju, South Korea.

Objective: We evaluated whether the tumoral retention of Tc-99m sestamibi was correlated with response to chemotherapy in individual tumors of patients with non-Hodgkin's lymphoma (NHL).
Methods: Seventeen patients (9 women and 8 men, mean age 57±12) with histologically proven NHL underwent MIBI scan before starting chemotherapy. Thirteen patients were treated with CHOP regimen, 2 CHOP followed by IFRT, and 2DHAP regimen. Both 10 min and 3 hr images were obtained after injection with 740 MBq of Tc-99m sestamibi using a dual-head rotating gamma camera. Tumor-to-normal soft tissue ratios (T/N) were measured. Percent retention (%R) was defined as T/N ratio at 3 hrs divided by T/N ratio at 10 min multiplied by 100.
Results: A total of 40 tumor lesions were detected in the patients by physical examination and CT scans. Twenty-two of them (55%) showed Tc-99m sestamibi uptake. %R of tumors which disappeared after chemotherapy was significantly higher than %R of tumors which remained after chemotherapy (91.1±14.9% vs. 66.9±1.86%, respectively, P = 0.04). Moreover, mean % R of tumors in patients showed negative correlations with serum LDH level (r=-0.742,P=0.04), the score of international prognostic index (r = -0.717, P = 0.009), and Ann arbor stage (r = - 0.620, P = 0.024).
Conclusion: These findings suggest that retention of Tc-99m sestamibi in individual tumors is related with response to chemotherapy as well as prognosis of patients with NHL.

PS_685

PROGNOSTIC VALUE OF GALLIUM-67 SCINTIGRAPHY AS A PREDICTOR OF RESIDUAL TUMOR VIABILITY AND CLINICAL OUTCOME IN LYMPHOMA'S PATIENT: A ELEVEN YEARS FOLLOW UP

M. Gasparini (1), M. Castellani (1), L. Maffioli (2), R. Benti (1), M. Rognoni (1), G. Biscontini (1), E. Bombardieri (3). (1) Department of Nuclear Medicine, Ospedale Maggiore-IRCCS, Milano, Italy; (2) Departmen of Nuclear Medicine, Ospedale A. Manzoni, Lecco, Italy; (3) Department of Nuclear Medine, Istituto Nazionale dei Tumori, Milano, Italy.

Aim. The aim of this study is to evaluate the ability of gallium scintigraphy after 4 cycles of chemotherapy (CT) to predict the clinical outcome of patients with Hodgkin's disease (HD) and non-Hodgkin's lymphoma (NHL).
Methods. The study included 77 patients (48 HD and 29 NHL) who were prospectively evaluated for 11 years (follow up 132 mths; range 7-132 mths). All pts underwent restaging 2-4 weeks after the end of 4 cycles of CT. In 65 pts the results were compared with Magnetic Resonance (MR) and in 12 with Computed Tomography (CT scan). Failure-Free Survival (FFS) in pts with positive or negative test were compared by means of Kaplan- Meier curves using the significance of the differences.
Results. Of 58 pts (41 HD and 17 NHL) with negative Ga-67 after 4 cycles of Ct, 53 (91%) remained in clinical remission (CR) after 132 mths (mean follow up 69.5 mths from presentation of the disease) and 5 pts died (mean follow up 16.5 mths) due to disease relapse. In this group the results of the scan was compared with MR in 51 pts; the results were discordant in 5 cases, 3 false positive for MR and 2 for Ga-67. The remaining 7 patient were compared with CT scan, wich showed one false positive result. Treatment failure occured in 13 of 19 pts with positive gallium scan after 4 cycles of CT (68.4%); the man follow up pf this group was 31 mths. Six pts were considered in CR (mean follow up 72 mths). There was a significant difference in FFS between pts with positive and negative Ga-67 scan after 4 cycles of CT ($p<0.0001$). Mr showed similar results, but with a large numenr of false positive results.
Conclusions. In conclusion Ga-67 scintigraphy after 4 cycles of Ct can be useful in predicting the outcome in HD or NHL patients. MR can be considered an imporatnt alternative. A change of treatment should be considered in patients with positive gallium scan. Early Ga-67 scintigraphy performed immediately after 1or 2 cycles of CT can better predict the outcome of lymphoma's patient.

PS_686

COMPARISON OF SESTAMIBI AND GALLIUM SCINTIGRAPHY IN THE ASSESSMENT OF LYMPHOMAS

L. Feggi (1), S. Moretti (2), S. Panareo (3), N. Prandini (1), G.L. Scapoli (2), G.L. Castoldi (2). (1) Nuclear Medicine , St. Anna Hospital of Ferrara; (2) Haematology, University of Ferrara ; (3) Nuclear Medicine , University of Ferrara, Italy.

The aim of this study is to evaluate the usefulness of MIBI versus Gallium scintigraphy in the assessment of the minimal residual disease in malignant lymphoma patients and to compare these results with the standard imaging techniques.
Material and methods: Between 1996 and 2000 we studied 51 patients (27 female, 24 male) affected by malignant lymphoma: 23 high grade NHL, 2 low grade NHL, 26 HD. At the time of the diagnosis all patients were studied with CT: total body scintigraphy with MIBI (MS) and Gallium (GS) always associated to SPECT were also performed for a total of 448 segments examinated. MS was performed 10 minutes after the administration of 740 MBq of the radiopharmaceutical while GS was performed on the third day after the injection of 370 MBq of Ga. The patients were treated with chemoterapy, radiotherapy and autologous peripheral stem cell transplantation. All the studies were repeated 6 months and 1 year after the time of the diagnosis. While we don't have a reference examination in the assessment of lymphoma we have compared our scintigraphical results with clinical and hematological remission status of the patients.
Results: At the diagnosis, CT showed 43 positive supra-diaphragmatic, 5 subdiaphragmatic and 19 both supra- and subdiaphragmatic localizations. Of 31 GS and 31 MS performed, respectively 90% and 87% resulted positive: on the basis of the intensity of the uptake the results were divided in high positive (respectively 60% and 50% of cases) and low positive (30% and 37%) showing a similar behaviour. At six months from the diagnosis 49 patients were studied: CT resulted completely negative in 31% of the patients and the lymphoma disease resulted decreased of more than 50% in 28.5% of patients. In the same patients GS and MS resulted negative in 57% and 64% showing a similar behaviour. At one year from the diagnosis 46% of CT resulted negative and 61% and 70% of GS and MS respectively resulted negative. At the Spearman and ROC curve analysis the results, considering all 448 segments, were not statistically significative ($p<0.05$).
Conclusions: Scintigraphy demostrated a high accuracy in the evaluation of minimal residual disease in lymphoma patients and we could not demostrate a significative difference between GS and MS, especially in supra-diaphragmatic localizations. Because the physical properties (energy and irradiation) of 99mTc-MIBI, its daily availability in a Dpt of General Nuclear Medicine, we suggest the replacement of GS with MS in the assessment of lymphoma patients.

PS_687

TECHNETIUM TC-99M-TETROFOSMIN SCINTIGRAPHY IN THE DIAGNOSTIC ASSESSMENT OF PATIENTS WITH LYMPHOMAS: COMPARISON WITH CLINICAL AND RADIOLOGICAL EVALUATION: PRELIMINARY REPORT

M. Kula (1), A. Tutuş (1), B. Eser (2), Hl. Sarı (3), O. Turhal (1), M. Çetin (2). (1) Department of Nuclear Medicine; (2) Department of Hematology; (3) Department of Internal Medicine, Erciyes University, Kayseri, Turkey.

Tc-99m tetrofosmin imaging has been used in nuclear oncology, but its role in detecting lymphomas has not been widely investigated.
Sixteen untreated patients (11 M, 5 F, aged 24- 70 years) with biopsy proven lymphomas (14 non-Hodgkin's and 2 Hodgkin's) underwent Tc-99m tetrofosmin whole-body imaging. Post-treatment investigations were also done in 6 of the 14 patients after first chemotherapy cycle. Focal pathological tetrofosmin uptake was seen in 37 sites in 11 patients, whereas computed tomography (CT) identified 42 pathologic regions 13 patients. Tc-99m tetrofosmin failed to visualize infradiaphragmatic 5 lesions in 3 patients. A total of six unknown tumor lesions in 3 of 16 patients were discovered on Tc-99m tetrofosmin scans. The tumor-to-background ratio ranged from 1.36- 2.12 (1.66+/- 0.24). A response to treatment was demonstrated by a reduction in localized Tc-99m tetrofosmin uptake in 4 of 6 patients, and by the disappearance of localized Tc-99m tetrofosmin uptake in 2 of 6 patients.
Tc-99m tetrofosmin scintigraphy may be useful in patients with lymphomas for localization tumor lesions, especially supradiaphragmatic ones, and, hence, may be considered an alternative to gallium scanning. Tc-99m tetrofosmin scintigraphy seems to be a suitable method for the prediction of therapy outcome.

PS_688

Abstract withdrawn

PS_689

TL-201 IMAGING IN PATIENTS WITH LOW-GRADE NON-HODGKIN'S LYMPHOMA RECEIVING LOCALISED LOW-DOSE IRRADIATION

R.A. Valdés Olmos (1), R.L.M. Haas (2), C.A. Hoefnagel (1), D. de Jong (3). (1) Department of Nuclear Medicine; (2) Department of Radiotherapy; (3) Department of Pathology, The Netherlands Cancer Institute, Amsterdam, The Netherlands.

Purpose: Localised low-dose irradiation has been introduced successfully in the treatment of low-grade non-Hodgkin lymphoma (NHL). We evaluated imaging with Tl-201 chloride in low-grade NHL patients receiving this treatment modality in order to establish parameters of metabolic tumour response for therapy outcome.
Methods: Total body images followed by SPECT were performed one hour after administration of 150 MBq of Tl-201 chloride in 43 patients (mean age 60.4y, range 39y-86y) with low-grade NHL scheduled for localised radiotherapy of the affected areas with a dose of twice 2 Gy. Images were performed before and 6-8 weeks after irradiation, and were compared with both clinical and radiological findings.
Results: Before radiotherapy Tl-201 imaging was positive in 39 patients (88%). Sensitivity to detect NHL at all affected sites was 65% (88/135), with 50% (23/46) for intra-abdominal lesions and 73% (65/89) for localisations outside the abdomen. The sensitivity for the neck was 81% (21/26). In 4 patients Tl-201 detected new lesions. Thirty-one patients with initially a positive Tl-201 study were investigated after radiotherapy. Tl-201 normalised in 20 of 22 patients who reached complete remission during follow-up (Fig. 1), and remained abnormal in 9 patients with partial remission or stable disease.
Conclusion: Tl-201 may be helpful in the management of low-grade NHL patients treated with low-dose irradiation. The method is especially sensitive in detecting extra-abdominal lymphoma sites. Tl-201 imaging appears to be very useful for the monitoring of response to radiotherapy, and both a negative and a positive test after treatment may be used to predict outcome.

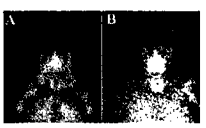

Fig. 1. Anterior planar Tl-201 images showing: A) Abnormal uptake in both sides of the neck as well as in both axillary and lung hilar regions before radiotherapy. B) A normal pattern after low-dose irradiation.

PS_690

COMPARISON OF TECHNETIUM-99M-TETROFOSMIN AND GA-67 CITRATE SCINTIGRAPHY IN THE ASSESSMENT OF LYMPHOMAS: PRELIMINARY REPORT

A. Tutuş (1), M. Kula (1), B. Eser (2), Hl. Sarı (3), A. Ünal (2), M. Caycı (1). (1) Department of Nuclear Medicine, Erciyes University, Kayseri, Turkey; (2) Department of Hematology, Erciyes University, Kayseri, Turkey; (3) Department of Internal Medicine, Erciyes University, Kayseri, Turkey.

The aim of this study was to compare Tc-99m tetrofosmin scintigraphy and Ga-67 scintigraphy in the diagnostic assessment of patients with lymphomas and to relate these results with those of radiological evaluation.
Method: Sixteen untreated patients (11 M, 5 F, aged 24- 70 years) with biopsy proven lymphomas (14 non-Hodgkin's and 2 Hodgkin's) were studied with 99mTc-tetrofosmin scintigraphy and then with Ga-67 scintigraphy before any therapeutic intervention. Post-treatment investigations were also done in 6 of the 14 patients after first chemotherapy cycle.
Results: The diagnostic accuracy of Tc-99m tetrofosmin and Ga-67 imaging for lesion detection was 88% and 90%, respectively. A total of seven unknown tumor lesions in 3 patients were discovered on Tc-99m tetrofosmin and Ga-67 scans. Tc-99m tetrofosmin failed to visualize infradiaphragmatic 5 lesions in 3 patients, but 3 of 5 lesions visible on Ga-67 images. The tumor-to-background ratio was 1.66+/- 0.24 (ranged from 1.36- 2.12) for Tc-99m tetrofosmin and 2.38+/- 0.48 (ranged from 1.68- 3.16) for Ga-67. A response to treatment was demonstrated by a reduction in localized pathological uptake (Tc-99m tetrofosmin and Ga-67) in 4 of 6 patients, and by the disappearance of uptake in 2 of 6 patients.
Conclusion: Tc-99m tetrofosmin scintigraphy may be considered an alternative to gallium scanning for the localization tumor lesions and the prediction of therapy outcome in patients with lymphomas. However, the intense Tc-99m tetrofosmin activity in the lower chest and abdomen may limit the diagnostic sensitivity of this radionuclide technique in patients with lymphomas.

PS_691

COMPARING STUDY OF GALLIUM-67 AND 99M TC—MDP SCINTIGRAPHY IN LYMPHOMA WITH BONE INVOLVEMENT

H. Wang (1), C. yu (2), T.I.A.N. Wei Jia (1), B.O. Min Fang (1), Z.H.U. Cheng Mo (1). (1) Department of Nuclear Medicine; (2) Department of Internal,Rui Jin Hospital,Shanghai,China.

Purpose: Evaluation of Ga-67 imaging in lymphoma with bone involvement was performed by the comprasion with Tc-99m-MDP bone scan.
Methods: In 63 patients with bone involvement of lymphoma proven by CT,X-rays or biopsy included 17 with Hodgkin's lymphoma(HL) and 46 with Non-Hodgkin's lymphoma(NHL),Ga-67 and ^{99m}Tc-MDP scintigraphy were performed after 48-72h of Ga-67 injection (10 mCi) and 3-4h of Tc-99m-MDP injection (20 mCi) in all patients.Of these,42 patients were imaged after 4cycles of chemotherapy.Result ananlysis:1.Diagnosis of bone lesions:Any spot abnormal uptake of radioactivity in bone will be considered as positive lesion.2.Comprasion of prior- and post-therapy Ga-67 imaging:1)If abnormal uptake of Ga-67 returned to normal after treatment,that suggested the complete remission of bone lesion.2)If Ga-67 bone uptake remained abnormal,the bone lesion was defined as no remission.3.Comprasion of Ga-67 and ^{99m}Tc-MDP uptake density in the same bone lesion.
Results: In 63 patients,total bone lesion is 128.The diagnostic sensitivity of Ga-67 and ^{99m}Tc-MDP scintigraphy is 89% and 98% respectively.The ^{99m}Tc -MDP uptake is higher than Ga-67 in 31 bone lesions,but there are 21 bone lesions with higher Ga-67 uptake than ^{99m}Tc -MDP.About monitoring therapy,accurate rate of Ga-67 imaging is 91%,the bone lesions with no remission were still have abnormal uptake of Ga-67.Average time of follow-up is 1.5 years.
Conclusion: Ga-67 scintigraphy correctly monitored the response to treatment in patients with bone involvement of lymphoma;Detection rate of ^{99m}Tc -MDP imaging was better than Ga-67 imaging in patients with bone involvement of lymphoma.

PS_692

TC-99M TETROFOSMIN SCINTIGRAPHY IN THE DIAGNOSTIC ASSESSMENT OF PATIENTS WITH LIMPHOMAS

F. Scopinaro, A. Filippis, AP. Anselmo, F. Monteleone, B. Campanella, R. Massa, F. Capoccetti, V. De Santis, R. Maurizi Enrici, O. Schillaci, A. Centi Colella Exp. Medicine, Section of Nuclear Medicine University of Rome , Rome, Italy.

Tc-99m tetrofosmin imaging has been used in nuclear oncology, but its role in detecting lymphomas has not been widely evaluated.
Methods: To assess the utility of Tc-99m tetrofosmin scintigraphy as a diagnostic modality in lymphoma, 17 patients (pts, 14 with Hodgkin's and 3 with non-Hodgkin's disease; 5 females and 12 males, age range: 10-59 years) were investigated. Planar and SPECT images of the supradiaphragmatic region (including neck and chest) were acquired starting 15 minutes postinjection. All pts had been untreated at the time of the first scintigraphy. Follow-up scans after therapy (ABVD chemotherapy, radiotherapy) were performed in 6 pts (in 5 twice), so a total of 28 scintigraphic studies were acquired. Mediastinal, pulmonary, cervical, supraclavicular and axillary activity was evaluated and results were compared in a blinded fashion with those of CT.
Results: Tc-99m tetrofosmin imaging demonstrated pathological focal uptake at 38 sites (16 in the mediastinum, 8 in the lungs, 4 in the axillas, 8 in the supraclavicular and 2 in the cervical region) in 16 out of 17 untreated pts; CT identified 24 lesions (16 in the mediastinum, 2 in the lungs, 2 in the axillas, 2 in the supraclavicular and 2 in the cervical region) in 17 pts. Scintigraphy detected 22 out of 24 lesions demonstrated by CT and revealed 16 unknown tumour sites in 10 pts. The only negative pre-therapy scintigraphy was in a case with axillary lymph-node involvement. In the first post-treatment scintigraphy, there was a reduction in the number of visualized pathological sites (7 vs 16) in 5 out of 6 investigated pts. The second follow-up study demonstrated only 2 lesions in 2 out of 5 evaluated pts. There was a good agreement between post-therapy scintigraphic results, response to treatment and clinical outcome of pts.
Conclusions: Our preliminary results indicate that Tc-99m tetrofosmin imaging is effective in depicting supradiaphragmatic lymphoma lesions in untreated pts and suggest that serial scintigraphic studies may be suitable for monitoring response to treatment. However, larger series are needed to better define the possible role of Tc-99m tetrofosmin scintigraphy in the follow-up of therapeutic response.

PS_693

USEFULNESS OF 67GALLIUM SCAN IN EVALUATING LONG-TERM EFFECTS OF CHEMOTHERAPY

I. Palumbo (1), B. Palumbo (2), A.M. Liberati (1), T.O. Moschini (2), M. Trottini (1), D. Siepi (2), S. Messina (2), R. Palumbo (2). (1) Dept. of Internal Medicine and Oncology, University of Perugia; (2) Dept. of Nuclear Medicine, University of Perugia.

Aim: ^{67}Ga scan was performed in patients with Hodgkin (HL) and non-Hodgkin (NHL) lymphoma to investigate the clinical outcome and long-term effect of different kinds of therapy: conventional and high dose chemotherapy followed by autologous bone marrow transplantation (ABMT) with or without radiotherapy (RT).
Methods: Fifty-two patients (24 M and 28 F, mean age ± S.D.: 35.5±15.8 yrs, range of age: 15-73 yrs) were studied with a mean follow up of 31±23.8 (S.D.) months. 33 subjects were affected by HL (24 nodular sclerosis, 7 mixed cellularity, 1lymphocyte rich), showing 13 bulky mass (12 mediastinal, 1 extramediastinal); 19 patients suffered from high grade NHL (6 mediastinal with sclerosis, 4 anaplastic large cell, 7 diffuse large cell, 2 lymphoblastic), showing 10 bulky mass (9 mediastinal, 1 extramediastinal). Mediastinal (M) involvement was present in 20 subjects, mediastinal and extramediastinal (M/ExM) in 26, extramediastinal (ExM) in 6. 24 patients were treated with high dose chemotherapy, while 26 with conventional chemotherapy; 31 subjects (10 NHL, 21 HL) underwent consolidation radiotherapy. ^{67}Ga scan and CT were performed at the same time, every 3-4 months and after last therapy cycle. 296 MBq of ^{67}Ga were injected to each patient. SPECT image acquisition (Starcam 3000, G.E.) was performed 72 hours after tracer administration.
Results: On the basis of Kaplan-Meier method a negative ^{67}Ga scan was predictive of a longer survival (mean ± S.E.: 87.29±8.89 months) as opposed to a positive ^{67}Ga scan (mean ± S.E.: 52.60±5.95 months), being the difference statistically significant ($p<0.001$). Considering the two different types of therapy (conventional and high dose chemotherapy) a negative ^{67}Ga scan in our patients undergoing high dose chemotherapy was predictive of a significantly higher survival (24 in disease free survival, 5 in continuous disease; mean survival ± S.E.: 91.67±4.21 months), while a positive ^{67}Ga scan in our subjects treated with conventional chemotherapy was predictive of a significantly decreased survival (mean survival ± S.E.: 52.57 ±5.95 months) ($p<0.05$). On the other hand a negative ^{67}Ga scan in our patients treated with conventional chemotherapy could be considered as a valid indicator of survival, although not statistically significant (mean survival ± S.E.: 66.50±12 months).
Conclusions: Finally our study discloses that ^{67}Ga scan is a useful predictor of survival and its ability to evaluate the long term effects of the two types of chemotherapy can suggest modification of therapy during treatment.

PS_694

MEDIASTINAL 'LAMBDA' SIGN IN THE SCINTIGRAPHY WITH 67 GA-CITRATE IN THE CHILDREN WITH MALIGNANT LYMPHOMAS AFTER CHEMOTHERAPY

I. Makaiova (1), S. Kovacova (1), V. Procka (1), S. Podana (1), J. Vesely (1), A. Cizmar (2), A. Foltinova (2), E. Kaizerova (2), I. Holincova (1), L. Plank (3), J. Kausitz (1)(1) Clinic of Nuclear Medicine Medical Faculty UK and St.Elisabeth Cancer Institute, Bratislava, Slovak Republic; (2) Pediatric Cancer Department of Medical Faculty, Bratislava, Slovak Republic; (3) Institute of Pathologic Anatomy Medical Faculty UK, Martin, Slovak Republic.

Aim: Residual anatomical masses of malignant lymphomas after therapy, especially in the area of the mediastinum cause in the CT or in MR imaging often difficulties, because can not give the information about the activity of them. On the other hand , the imaging with 67Ga-citrate (or with 18FDG) can give the information about the tumorous activity or viability of the lesions. This property is for the follow-up of the malignant lymphomas crucial and therefore radiogallium is a long time and 18FDG in the last years used in the managment of this disease also in the children. Despite of this, beacause of the functional basis of this imaging arrised also the disadvantage of äfalse positive„ uptake in other lesions as tumorous. Donahue et al. in 1981 the first time described the äfalse positive„ uptake of gallium in the area of upper anterior mediastinum, which corresponded with the hyperplastic thymus after chemotherapy. As we know, this disadvantage is visible also in the imaging with 18FDG because the similarity of them .
Methods: In this paper we refer about the retrospective study of the results gallium scintigraphy in the last 5 years (from 1995 till 1999) in the 100 children (in age from 2-18 years) suffering from malignant lymphomas after chemotherapy. The children were dividing in two groups: 91 children with hodgkin (HD) and 29 children with nonhodgkin (NHL) types of disease. The retrospective study was focussed on the the area of mediastinum and the finding of hypertrophic thymus which was notes as a älambda„ sign (a roof-shaped uptake on the anterior area of mediastinum). In 10 children was made also the PET scanning with 18F-fluorodeoxyglukose(FDG).
Results: From all 91 children with HD in 9 (9,9%) of them there was älambda„ sign, which from 20 patients with äpositive„ gallium uptake in mediastinum was 45% . In the group of all 29 NHL children was the älambda„ sign found in 8 of them (27%), and from äpositive„ gallium children it was 89% of them. Result of 18FDG was similar, but not the same as with 67Ga-citrate.
Conclusion: Mediastinal „lambda„ sign in the 67Ga-scintigraphy represents the hypertrophic thymus , which can be in correlation with the effectivity of the systemic treatment in malignant lymphomas and stronger delineated in the more agressive cytostatic treatment in the non-hodgkin typ of disease. The similar result can be visible in the PET with 18FDG.

PS_695

PREDICTIVE VALUE OF 99MTC-SESTAMIBI (99MTC-MIBI) IN PATIENTS WITH MULTIPLE MYELOMA (MM)

L. Pace (1), L. Catalano (2), S. Del Vecchio (1), A. De Renzo (2), N. Tedesco (1), C. Califano (2), G. Annunziata (1), F. Di Gennaro (A), B. Rotoli (2), M. Salvatore (1). (1) Medicina Nucleare e Centro CNR Medicina Nucleare, Dip. Sc. Biomorfologiche e Funzionali, Università Federico II, Napoli, Italy; (2) Ematologia, Dip. Med. Clin. e Sper., Univesità Federico II, Napoli, Italy.

Aim. 99mTc-MIBI scintigraphy proved to be useful in evaluating patients with MM. The aim of this study is to evaluate its predictive role in patients with MM Methods. 118 patients constituted the study group. All patients underwent a baseline whole body 99mTc-MIBI) scintigraphy (10 minutes after e.v. tracer injection and were clinically re-evaluated at a mean follow-up of 19+9 months. The scans were classified as N (physiological uptake), D (diffuse marrow uptake), F (focal uptake), and D+F. The intensity of diffuse bone marrow uptake was semiquantitatively scored. Results. At baseline 99mTc-MIBI, of the 51 patients with Pattern N only 8 (16%) were in stage II or III, of the 38 with pattern D 13 (34%) were in stage II or III, of 29 with pattern F or D+F 27 (93%) were in stage II or III (C2 63.6, $p<0.0001$). At clinical re-evaluation, 20 patients were in remission, 49 were in stable condition, 32 had disease progression, and 17 had died. Nine of the 51 (17%) patients with baseline pattern N had progression of disease, 23 (61%) of the 38 patients with pattern D had disease progression, and 17 (59%) the of 29 with pattern F or D+F had disease progression (C2 26.5, $p<0.001$). Baseline bone marrow uptake score was significantly ($p<0.05$) different among patients in remission (2.8+0.8), patients in stable conditions (3.1+1.3), and those with progression of disease (3.9+1.4) Multiple logistic analysis showed that monoclonal component (standardized coefficient=0.18), 99mTc-MIBI pattern (standardized coefficient=0.33), uptake score (standardized coefficient=0.39), and x-ray (standardized coefficient=0.33) were significantly related to the status at re-evaluation ($r=0.50$, $F=9.4$, $p<0.0001$). Conclusions. The results of this study indicate that 99mTc-MIBI scintigraphy may help in predicting the clinical status at follow-up in patients with MM. Both scintigraphic pattern and the uptake score have a potential prognostic role in these patients.

PS_696

WASH-OUT OF 99MTC-SESTAMIBI (99MTC-MIBI) IN EVALUATING RESPONSE TO CHEMOTHERAPY IN PATIENTS WITH MULTIPLE MYELOMA (MM)

L. Pace (1), L. Catalano (2), S. Del Vecchio (1), A. De Renzo (2), R. Fonti (1), G. Sica (1), G. Annunziata (1), C. Califano (1), B. Rotoli (2), M. Salvatore (1). (1) Medicina Nucleare e Centro C.N.R. Medicina Nucleare, Dip. Sc. Biomorfologiche e Funzionali; (2) Ematologia, Dip. Med. Clin. e Sper., Università Federico II, Napoli, Italy.

Aim. Wash-out of 99mTc-MIBI is reported to help in predicting response to chemotherapy in various tumours. The aim of this study is to evaluate the role of 99mTc-MIBI in predicting response to chemotherapy in patients with MM.
Methods. 40 patients with MM showing diffuse 99mTc-MIBI bone marrow uptake were included in the study. All patients underwent whole body scan at 10 and 60 minutes after tracer injection. Diffuse bone marrow uptake was semiquantitatively scored according to both extension and intensity on the 10 minutes scan. Wash-out was computed, after decay correction, as: (10 minutes counts/pixel minus 60 minutes counts/pixel) divided by 10 minutes counts/pixel. All patients were clinically re-evaluated (mean follow-up 26+9 months) after chemotherapy (14 MP, 9 VAD, and 17 VMCP).
Results. Of the 40 patients, 10 were considered to be in remission at re-evaluation and 30 showed disease progression. Neither the clinical status at presentation nor the therapeutic regimens were associated with the clinical status at re-evaluation (i.e. remission vs disease progression) (C2=1.8 and C2=1.0, respectively, p=n.s.). The bone marrow uptake score at the 10 minutes baseline 99mTc-MIBI scintigraphy was significantly ($P<0.05$) higher in patients showing disease progression (3.9+1.4) than in those in remission (2.7+1.4). 99mTc-MIBI wash-out was significantly ($p<0.01$) higher in patients with disease progression (18.3+9.8) than in those in remission (11.6+6.2). Of the 10 patients showing remission of disease after chemotherapy, the majority (7, 70%) had 99mTc-MIBI wash-out <15% (which was the median for the whole group), while of the 30 patients with disease progression after chemotherapy the majority (20, 67%) had 99mTc-MIBI wash-out > 15% (C2=4.1, $p<0.05$).
Conclusions. Our preliminary data suggest that in vivo evaluation 99mTc-MIBI wash-out may help in predicting response to chemotherapy in patients with MM.

PS_697

99M-TC MIBI SCINTIGRAPHY IN MULTIPLE MYELOMA: A POWERFUL IMAGING TOOL TO DETECT DISEASE ACTIVITY

A. Varraso (1), G. Martino (1), P. Musto (2), F. Dicembrino (1), F. Barbano (1), M. Guerra (1), M. Pirro (1), M. Greco (2), V. Frusciante (1).
(1) Department of Nuclear Medicine; (2) Department of Hematology, Casa Sollievo della Sofferenza, San Giovanni Rotondo, Italy.

Background: ^{99m}Tc-MIBI is a lipophilic cationic radiopharmaceutical which accumulates in tissues with high cell density and mitochondrial activation. Recently some papers have discussed the use of ^{99m}Tc-MIBI in patients with multiple myeloma (MM), where evaluation of bone involvement is of high relevance. The most widely accepted imaging technique to assess MM is plain skeletal x-rays; however positivity at plain radiography is often due to a non-active process; besides the results of biopsy are significantly conditioned by sampling errors; so an imaging tool, correlated to disease activity, is quite useful.
Patients and methods: We have enrolled 47 MM pts. Diagnosis was made according to standard criteria. Pts were classified as A-(33) active disease (untreated, refractory, relapsed), B-(5) stable disease (usually with reduction of monoclonal component >50%), C-(8) complete remission (absence of monoclonal component at immunofixation and no evidence of marrow plasma cells) after autologous stem cells transplantation, G-(1) incomplete remission after transplantation. 740 MBq of ^{99m}Tc-MIBI were injected; 15 mins after injection a whole body scan was acquired; scintigraphic pattern was classified on the basis of diffuse-D, focal-F, diffuse and focal -D+F uptake; D uptake was semiquantitatively scored according to the extension (E-three steps) and intensity of uptake (I – three steps). Four pts have been followed-up by sequential investigations (In).
Results: Considering clinical and hematological parameters:
In group A scintigraphy has correctly classified as diseased all the pts; in 18 In we have found D pattern, in 6 F pattern and in 9 D+F.
In all B group pts our results were concordant (negative)
In C group pts our results were discordant in 2/8 cases (6 cases negative, 1 F pattern and 1 D pattern).
In the one pt of G group scintigraphy was negative
Five follow-up In have been performed (4 A group, 1 G group); results were concordant in 4/5 cases; in 1 A group pt hematological and clinical parameters were negative but scintigraphy was clearly positive (D pattern).
Considering as true positive clearly evident focal scintigraphic lesions sensitivity of scintigraphy was 97.37 % and specificity 85.71 %.
Conclusions: Our data clearly demonstrate that ^{99m}Tc-MIBI scintigraphy has a very high sensitivity and specificity in MM pts. It demonstrates clearly focal lesions in pts without clinical or laboratoristic evidence of disease; it will be important to check the clinical course of the 3 pts with negative hematological findings of disease but with F or D pattern.

PS_698

USE OF THE 67-GALLIUM SCINTIGRAPHY IN THE PROGNOSIS IN HODGKIN'S DISEASE

I. Hervás (1), P. López-Tendero (2), P. Bello (1), A. Segura (2), A. Saura (1), P. González-Cabezas (1), A. Yuste (2), R. Pérez-Velasco (1), M. Pastor (2), R. Díez (1), A. Mateo (1)(1) Department of Nuclear Medicine; (2) Department of Oncology, University Hospital, Valencia, Spain.

Aim: Evaluation of the response to therapy is important in the clinical management of lymphoma. Gallium 67 scintigraphy has been considered a good technique for monitoring response after treatment of patients with Hodgkin's disease. The aim of this study is to assess the clinical impact of gallium 67 scintigraphy before and after treatment and to compare the overall survival between the patients whose gallium studies after treatment were negative and those whose studies did not become negative.
Methods: We have studied 71 patients (39 women, 32 men) with histologically confirmed Hodgkin's disease controlled by the Department of Oncology of our Hospital. All the patients underwent 67Ga scintigraphy at the moment of the diagnosis (basal study) and in the case that basal study was positive (abnormal hyper-uptake focus) we performed follow-up studies after the treatment. We have calculate the overall survival between the patients whose studies after treatment were negative (first group) and those whose studies did not become negative (second group) and between patients whose studies were negative at diagnosis (third group). Gallium scintigraphy were performed 48-120 hours after the injection of 185-296 MBq (6-8 mCi) of 67Ga citrate. The statistic analysis used to compare the overall survival of the three groups was chi-square test with Yate's correction.
Results: Gallium scintigraphy was positive at diagnosis in 42 patients (59,2%). In 34 of them we could perform the follow up study after the treatment. The follow up study was negative in 29 patients while in 5 patients the gallium scintigraphy remained positive after treatment. With a median follow-up of 8 years: In the first group (basal study positive and negative after treatment) the median overall survival was not reached (96.5% of patients remained alive). In the second group (basal study positive and positive after treatment) the median overall survival was 27 months (2 patients remained alive (40%)). In the third group (basal study negative) the median overall survival was 75 months (46% of patients remained alive).The overall survival was significant higher ($p<0.001$) in the first group comparing with the second group. The overall survival was higher in the first group comparing with the third one but statistic significance level was not reached.
Conclusion: In Hodgkin's disease, if the 67Ga scintigraphy is positive at diagnosis, the normalisation of the study after treatment can be considered as a good prognosis factor.

OTHER CLINICAL SCIENCE. NEPHRO-UROLOGY 3

PS_699

ESTIMATION OF RISK FACTORS FOR DIABETIC NEPHROPATHY BY RADIONUCLIDE METHODS

M. Rajic, M. Bogicevic, S. Antic, M. Avramovic, S. Ilic, M. Vlajkovic, V. Stefanovic. Department of Nuclear Medicine, Clinical Center, Nis, Yugoslavia.

Introduction: Glomerular hyperfiltration and nephromegaly are supposed to be predictive for progression from normo to microalbuminuria in patients with insulin-dependent diabetes mellitus (IDDM). **The aim** of this study was radionuclide assessment of nephromegaly incidence and its association with hyperfiltration, in order to select normoalbuminuric IDDM patients at risk of developing renal disease. **Methods:** IDDM patients (DM) with urinary albumin excretion < 20μg/min and duration of diabetes > 5 years were classified into groups with hyperfiltration (DM-h) and normofiltration (DM-n). Kidney size was expressed as a ratio of bipolar diameter on ^{99m}Tc-DMSA posterior images and patient's height (BPD/PH), while GFR was determined by measuring ^{99m}Tc-DTPA clearance. BPD/PH over 6.97×10^{-2} (control mean value + 2SD) and clearance values higher than 136 ml/min/1.73m^2 (control mean value + 2SD) were accepted as criteria of hyperfiltration and nephromegaly. **Results** are displayed in the following table:

Group	N°	Age (years)	^{99m}Tc-DTPA clearance	BPD/PH	Incidence of nephromegaly
1. Control	23	41.1±8.7	122±7	6.45±0.6	
2. DM	23	39.1±8.0	136±15[a]	7.19±0.55[a]	56.5% (N°=13)
3. DM-h	13	39.2 ± 7.9	147±7[a]	7.29±0.54[a]	69.2% (N°=9)
4. DM-n	10	39.0 ± 8.1	122±10[c]	7.09±0.55[b]	40.0% (N°=4)

Vs. control: [a]$p<0.001$, [b]$p<0.01$; vs. DM-h: [c]$p<0.001$

Conclusion: A markedly higher incidence of nephromegaly in diabetics with hyperfiltration than in patients with normal GFR was shown by the results presented. Considering that normoalbuminuric IDDM patients with association of elevated GFR and renal hypertrophy are at a greater risk for developing nephropathy, radionuclide methods should be used for follow up of their renal function.

PS_700

MEASURMENT OF KIDNEY TRANSPLANTS GLOMERULAR FILTRATION RATE USING RENAL SCINTIGRAPHY

F. Chehade, N. Droubi, H. Kazma, A. Zaatari, H. Abou Zainabe, M. Zaatari, F. Farhat. Hammoud Hospital,Sidon,Lebanon.

In order to assess the importance of expression of the cortical time of kidney transplants renogram in term of glomerular filtration rate (GFR) we have tested the correlations with the correspondent serum creatinine level (Cr).
Subjects : 71 scintigraphies with Technetium-99m-labelled diethylenetriamine pentaacetate (DTPA) were realized in 44 patients with renal allografts, transplanted between the years 1990 and 1999. Patients were 13 women and 31 men with mean age of 34±14 years (mean±SD) referred between the years 1997 and 2000 for scintigraphic exploration of function deterioration of kidney transplants mainly due to rejection.
Method : The GFR are calculated from renal scintigraphies using Gates method. The depth attenuation is corrected after measurement of transplants kidney depth, upon lateral view, between an anterior abdominal wall marker and the center of the transplanted kidney. Simple linear regression analysis over Cr and natural logarithm of Cr (Ln(Cr)) were calculated for GFR and natural logarithm of GFR (Ln(GFR)).
Results : The mean Cr and GFR are 2.5±2 mg/dl and 37±22 ml/min/1.73 m^2 respectively. A good correlation exists between the GFR and the Cr ($r=-0.65$, $P<0.001$). The correlation is closest between the GFR and the Ln(Cr) ($r=-0.67$, $P<0.001$), and even more between the Ln(GFR) and the Ln(Cr) ($r=-0.80$, $P<0.001$).
Discussion : Deducted linear correlation coefficients from this study, which is carried out on a large number of kidney transplants scintigraphies, are highly significatives ($P<0.001$). The weak mean GFR reflects the elevated mean Cr that indirectly reflects the renal cortical function. Moreover, this study shows that Cr is in good correlations with calculated GFR under different mathematical forms. Consequently, expression of the cortical time of DTPA renogram of kidney transplants in terms of GFR should adds an important quantitative data to the scintigraphic exploration. Since renal scintigraphy is a reproducible test, scintigraphic measurement of GFR may serves as objective data to follow close the function evolution of kidney transplant under anti-rejection treatment. The best correlation is found between the Ln(GFR) and the Ln(Cr). The following mathematical formula can be deducted: $Ln(GFR)=a.Ln(Cr)+b$, which also be written as $GFR=(Cr)^a.e^b$, where $a=-0.8$ and $b=4$.

PS_701

MEASURING TC-99M MAG3 CLEARANCE WITH CAMERA BASED METHOD IN PATIENTS WITH IMPAIRED RENAL FUNCTION: COMPARISON WITH MULTIPLE SAMPLE TC-99M MAG3 CLEARANCE: REPRODUCIBILITY, ACCURACY AND REPEATABILITY COEFFICIENT

T.Y. Erdil (1), F. Dede (1), S. Tuğlular (2), F. Şen (1), O. Noshari (1), C. Özener (2), E. Akaoğlu (2), T. Turoğlu (1). (1) Department of Nuclear Medicine, Marmara University Hospital, Istanbul, Turkey; (2) Nephrology Section, Department of Medicine, Marmara University Hospital, Istanbul, Turkey.

The aim of this study was to determine the reproducibility (REP), accuracy and repeatability coefficient (RC) of the Tc-99m mercaptoacetyltriglycine (MAG3) clearance measurements with camera based method in patients with impaired renal function.

Methods: Nineteen patients (10M, 9F, mean age:56.6±10.3yr, range:44-83yr) with chronic renal failure (Cr=3.4 mg/dl±0.68 mg/dl, range:2.1mg/dl-4.6 mg/dl) were included in the study. MAG3 scintigraphy and camera based clearance (CBCl) were performed according to QuanteEM method (2 sec/frame for 24 frames, 15 sec/frame for 16 frames, 30 sec/frame for 40 frames). In each patient, at the same time with MAG3 scintigraphy, MAG3 plasma clearance (PCl) was also determined using single injection, multisample (10 blood samples between 5 to 180 minutes), two compartment model of Sapirstein and corrected for body surface area. In 12 patients, scintigraphy and PCl studies were repetaed within a week under similar physiologic conditions. For the determination of accuracy, we calculated the differences between clearences obtained with CBCl and PCl methods. The mean and standard deviation (SD) of these differences represented the systemic bias and accuracy of the technique respectively. The mean difference between repeated CBCl studies in 12 patients were expressed as a percentage of the mean value of the two studies, and the SD of these percentages represented the reproducibility. CBCl were determined twice by the same physician in each patient and RC was measured according to Bland and Altman Method (2 SD of the differences between two measurements).

Results: The MAG3 clearance was found to be 56.7 ± 21.4 and 67.4 ± 32.1 for PCl and CBCl methods respectively (p = 0.06). The second measurement of the same camera study by the same observer was 67.4 ± 30.3 (p=0.86). The systemic bias and accuracy of CBCl, PCl method as a reference, were -8.8 and 29. REP of CBCl in 12 patients was found to be 40.31% and the mean difference was -5.31% (ranging from -40% to 74.3%. RC of of the same study was found to be 3.9.

Conclusion: We observed a poor accuracy and reproducibility of CBCl in patients with poor renal function. However, highly repeatable results of the same study was obtained. Therefore, CBCl is not sensitive to evaluate the alterations of the renal function in patients with impaired renal function.

PS_702

QUALITATIVE AND QUANTITATIVE ANALYSIS OF DELAYED TC99M DTPA IMAGES: DO THEY HAVE A STRONG IMPACT ON THE DIAGNOSIS OF OBSTRUCTION ASSOCIATED WITH UNILATERAL ADVANCED NEPHROUROPATHY?

S.H. Wagieh (1), O. Abdel Razzak (2), A. Khodier (3), H. Kiki (4).
(1) Department of Nuclear Medicine, Cairo University, Cairo, Egypt;
(2) Department of urosurgery, Cairo University, Cairo, Egypt;
(3) Department of Nuclear Medicine, Ain Shamas University;
(4) Department of Radiology, Cairo University, Cairo, Egypt

Diuretic renography is a valuable method for the diagnosis of equivocal UT obstruction, yet, with the presence of poor renal function and dilated collecting system, its results are unreliable, as they represent important etiological factors for poor drainage in response to diuretic stimulus without obstruction. The aim of this study is to assess the value of qualitative and quantitative analysis of 4 and 24 hours delayed Tc99m DTPA images in the diagnosis of obstruction.

Patients and Methods: Forty patients were included in this study after performing F+20 diuretic renography. They all have hydronephrotic changes of the affected kidney with split function < 20% and GFR < 16 ml /min associated with normal urine flow kinetics of the contralateral kidney. All were subjected to reviewing all clinical, laboratory and radiological data and abdomino-pelvic sonography. MRI was performed if all clinical and radiological data give equivocal results as regards obstruction. Delayed Tc99m DTPA images were acquired 4 and 24 hours postinjection for 5 and 15 minutes, respectively. Images were interpreted qualitatively for the assessment of obstruction and to detect its level and quantitatively by measuring the ratio between counts /pixel of the affected kidney to normal kidney in early and late images (O1 & O2, respectively) with calculation of obstructive index O.I. (O2/ O1).

Results: Clinical and radiological data confirmed the presence of obstruction in 19 patients and excluded the presence of obstruction in 21 cases. Obstruction was detected in 4 and 24 hours images in 19 patients with the detection of the level of obstruction in both sets of images. The 21 cases with non-obstructive dilatation showed complete clearance in 24 hours images, and only in 4 cases clearance occurred in 4 hours scintiscans. There was a statistically significant difference between O2 and O.I. values between both groups(p< 0.05).

Conclusion: Qualitative and quantitative assessment of 4 and 24 hours delayed Tc99m DTPA images are of great value in the diagnosis of obstruction associated with advanced unilateral nephrouropathy, avoiding the patient to proceed to more invasive and costy procedures with proper early therapeutic intervention.

PS_703

BACKGROUND SUBSTRACTION AND SPLIT RENAL FUNCTION IN TC-99M ETHYLENEDICYSTEINE RENOGRAPHY USING DIFFERENT TIME INTERVALS

O. Özmen, N. Alan, M. Halaç, L. Kabasakal, K. Özcan, C. Önsel, I. Uslu. Department of Nuclear Medicine, Cerrahpaşa Medical Faculty, Istanbul, Turkey.

Tc-99m EC is a new tubular tracer for renal studies. It is shown that type of region of interest (ROI) for background correction and the time interval that the parameters are generated has been a potential error for estimation of relative renal function. Aim: The aim of the present study was to determine the accuracy of relative renal function obtained from EC with different type of background ROIs generated from 1-2, 1.5-2.5 and 2-3 min. time intervals using DMSA as reference method. Method: For this purpose 41 patients ages ranged from 3 to 74 years with a mean of 31.6±21.0 years, were included to the study. Split renal function of each EC study was calculated from 1-2, 1.5-2.5 and 2-3 minutes of dynamic images using manually drawn perirenal, subrenal crescent, without background and lateral rectangular ROIs. Within the same week DMSA scintigraphies were performed 2 hours after injection and 6 planar images were obtained. DMSA split renal function was calculated for each patient either by using only posterior views without renal depth correction and also using the geometric mean of posterior and anterior views. The accuracy of EC split renal function was estimated by calculating the difference between the corresponding DMSA split renal function for the kidney with the lowest uptake. The mean of differences represented the systemic bias and the SD of the mean of the differences represented the accuracy of the technique. Results: No systematic bias was observed between first and second measurements giving a high reproducibility (SD<1.0%). When we compared DMSA split renal function calculated from only posterior views the highest accuracy was observed for perirenal ROIs generated from 1.5-2.5 min interval (2.3%). When we compared with the geometric mean the accuracy was lesser (4.2%). While the mean of the difference between EC and DMSA was giving a positive value for perirenal ROIs the other types were giving a minus value which meant that EC was overestimating the split renal function. These values were higher when they were compared with the geometric mean. The DMSA relative uptake calculated without renal depth correction was also overestimating the relative uptake calculated from geometric mean with a value of 0.6% and the accuracy between these two types was 3.8%. Conclusion: In conclusion, this study suggested that perirenal ROI obtained from 1.5-2.5 min is the most accurate method for determination of EC split renal function.

PS_704

NORMALIZED RESIDUAL ACTIVITY (NORA): USUAL VALUES AND ROBUSTNESS OF THE METHOD

A. Piepsz, J.D. Kuyvenhoven, M. Tondeur, H. Ham. Department Radioisotopes, CHU St Pierre, Free University Brussels, Brussels, Belgium.

Aim :the objectives of this study were twofolds. First, to investigate the robustness of the „normalized residual activity" (NORA), a parameter which has recently been proposed for the estimation of renal emptying during renography;secondly to define the usual values of NORA in two categories of kidneys : those with normal renogram and those with dilated but definitely non obstructed kidneys.

Methods : a large number of Tc-99m MAG3 renograms were extracted from a data base. NORA was defined as the renal activity at a given moment (end of renogram, end of furosemide acquisition, postmicturition image) divided by the renal activity between 1 and 2 minutes. Two variables which might influence the results of NORA were evaluated, the choice of background correction and an error in the estimation of the 1-2 min renal activity. In order to estimate the values of NORA in usual clinical conditions, two sets of data were analyzed :"normal" kidneys with normal renogram pattern; dilated but definitely non obstructed kidneys.

Results : Using a perirenal or a subrenal background correction, NORA was, on average, respectively 67% or 83% of the value obtained without background correction. The use of a 1min 20 sec to 2 min 20 sec renal activity instead of a 1 to 2 min activity resulted in a systematic 10-15 % underestimation of NORA. The percentile 90 values of NORA were, in the normal group, 0.70 at 20 minutes, 0.23 at the end of the furosemide test and 0.10 after micturition. In the operated kidneys, the percentile 90 values were 3.92 at 20 min, 2.91 at the end of the furosemide test and 1.99 after micturition. A good correlation was observed between NORA and output efficiency.

Conclusion : If adequately standardized, NORA is a robust and simple parameter, allowing the evaluation of renal emptying at any time of the acquisition. One should be aware of the fact that high NORA values, corresponding to poor renal emptying, can be observed in the operated non obstructed kidneys, even after micturition.

Poster presentation

PS_705

REPRODUCIBILITY OF SOFTWARE PACKAGES OF DICOM WORKSTATIONS OF DIFFERENT MANUFACTURES FOR SCHLEGEL ERPF AND GATES GFR MESAUREMENTS

G. Marotta, V. Longari, R. Matheoud, V. Salvatore, F. Voltini, P. Gerundini. Department of Nuclear Medicine, Ospedale Maggiore - IRCCS, Milano, Italy.

Aim: Because of ability to calculate the differential ERPF and GFR for each kidney and serial reproducibility in individual patients, the _camera methods to measure ERPF and GFR are widely used. Some recent _cameras transfer the data acquired with the DICOM protocol to their own workstations; so, all workstations with DICOM connectivity can process these data. Aim of this work was to investigate the reproducibility of Gates' GFR and Schlegel's ERPF measurements obtained by different software packages of four DICOM workstations and to evaluate the differences with the ERPF values from the single sample Tauxe method (Tx). Methods: Syringe static scans and dynamic renal scan, according to Schlegel's and Gates' methods, were performed in 10 patients (mean age 61 yrs, range 28-76) and 70 patients (mean age 54 yrs, range 21-82) respectively, with a GEMS Millennium VG5 _camera. Data were transferred to four workstations: GEMS eNTEGRA (eNT), Marconi Odyssey (Od), SMV Vision POWERstation (SMV) and GEMS XPertPro (XP). All kidney and background irregular regions of interest were manually drawn by one operator. Results: The tables show the coefficient of correlation (r) and standard error (SEE in ml/min) of ERPF values of 20 kidneys calculated by Od, SMV, XP and Tx and of GFR values of 140 kidneys calculated by eNT, Od, SMV and XP and the mean (_SD) of their differences (in ml/min). All differences were statistically significant ($p<0.0001$). There was a good correlation between ERPF and GFR values obtained by Od and XP, but the Bland-Altman plots showed considerable underestimation of GFR by eNT compared to XP and of ERPF by Od versus XP. There is also a poor correlation between the ERPF and GFR values obtained by SMV in comparison with all other workstations. Conclusion: This study showed statistical differences in the calculation of Schlegel's ERPF and Gates' GFR between different workstations. As a consequence, at any workstation upgrade it will be mandatory to revalidate the method on each system (_camera+new workstation) versus the blood sampling method.

ERPF	Od-XP	SMV-XP	SMV-Od	XP-Tx	Od-Tx	SMV-Tx
r(SEE)	.95 (19.3)	.80 (36.9)	.81 (33.7)	.89 (37.9)	.85 (44.3)	.56 (69.2)
diff_SD	-33.8_18.9	-22.7_42.1	11.1_41.8	-8.4_38.9	-42.2_45.2	-31.1_71.7
GFR	eNT-XP	Od-XP	SMV-XP	eNT-Od	SMV-Od	SMV-eNT
r(SEE)	.96 (6.0)	.98 (4.2)	.70 (14.7)	.98 (4.1)	.69 (13.9)	.66 (12.8)
diff_SD	-11.8_6.6	-7.2_4.3	-10.8_15.6	-4.6_4.4	-3.5_15.4	1.0_15.3

PS_706

COMPARISON OF PLANAR AND SPECT 99MTC-DMSA SCINTIGRAPHY FOR THE DETECTION OF RENAL CORTICAL DEFECTS IN PATIENTS WITH URINARY TRACT INFECTIONS

H. Demir, F. Berk, O. Erdinçler, S. Işgören, C. Aktolun. Department of Nuclear Medicine, Kocaeli University, Kocaeli, Turkey.

Renal cortical scintigraphy with ^{99m}Tc DMSA provides an excellent imaging modality for the assessment of cortical damage secondary to urinary tract infection (UTI). In this study we compared the detection rates of renal cortical defects with ^{99m}Tc dimercaptosuccinic acid (DMSA) using SPECT and planar cortical scintigraphy.
MATERIALS AND METHODS: We imaged 75 kidneys in 38 patients (10 males, 28 females) with recent or recurrent UTI. Patients' age ranged between 2 months and 23 years (mean 7.37 ± 4.44 years). Planar and SPECT studies of renal cortices were performed by Elscint SPX-6 gamma camera within 2 to 4 hours of injection 0,5-5 mCi ^{99m}Tc DMSA intravenously. All studies were evaluated by two experienced nuclear medicine specialist. Paranchymal uptakes were classified as; normal (grade 0), equivocal (grade I), single defect (grade II), more than 2 defects (grade III), contracted or small kidney (grade IV)and no visualization (grade V).
RESULTS: Fifty six of 75 kidneys were normal in both planar and SPECT studies. Thirteen kidneys were pathologic in planar scintigraphy however 19 kidneys were pathologic in SPECT studies. Six kidneys had normal paranchymal uptakes in planar studies. In SPECT studies; 3 out of 6 were classified as grade I and three of them as grade II. One kidney was grade I in planar study whereas it was grade II in SPECT study . All defects diagnosed by planar scintigraphy were also visualized by SPECT. Final grading were changed for, 7 out of 75, kidneys' according to SPECT results.
CONCLUSION: SPECT has no significant advantage over planar studies, although some cortical lesions are missed by planar imaging. It must be considered as a complementary technique to renal cortical imaging.

PS_707

OPTIMAL TIME WINDOW FOR CALCULATION OF TWO RENAL TRANSIT PARAMETERS: NORMALIZED RESIDUAL ACTIVITY AND OUTPUT EFFICIENCY

J.D. Kuyvenhoven, H. Ham, A. Piepsz. CHU St. Pierre, Brussels, Belgium.

Background: Normalized residual activity (NORA) and output efficiency (OE) have been proposed for the measurement of renal transit. The calculation of these transit parameters at fixed time is common usage. However, as these parameters are strongly time-dependent, the choice of moment for calculating these parameters may affect their discriminating power.
Aim: To evaluate whether there is an optimal time for calculation of transit parameters NORA and OE.
Materials and methods: A series of renograms were generated in a simulation model by convolution of a plasma disappearance curve with various created retention functions. Mean transit time (MTT) was set, increasing with 1-min. steps, between 3 and 60 min. For every MTT, 4 different shapes of retention functions were created. The ratio of the minimal transit time (MinTT) to MTT was fixed at 0.80 whilst the ratio of maximum transit time (MaxTT) to MTT varied between 1.10 and 2.00. A total of 232 retention functions and corresponding renograms were created. Mean and standard deviation of the MaxTT to MTT ratio were respectively 1.40 and 0.27. For each of the created renograms NORA-t and OE-t were calculated for t equal to 10, 20, 30, 40, 50 and 60 min.
Results: OE-20 is closely related to MTT for MTT shorter than 20 min. Therefore, for this range of MTT values, OE-20 is highly predictive of the value of MTT. If the MTT is higher than 20 min. OE-20 looses totally its discriminating power. The contrary is observed for OE-60, which varies only slightly when MTT is less than 20 min. This parameter reflects better the change in transit time in the range of 30 to 50 min. Similar patterns are observed with NORA. For MTT less than 20 min., NORA-20 has the highest discriminating power, whereas NORA-50 is best for MTT ranging from 30 to 50 min.
Conclusion: NORA and OE are strongly time-dependent and the choice of optimal time for calculating these parameters should be adapted to the clinical problem under investigation.

PS_708

INTEROBSERVER AND INTRAOBSERVER VARIABILITY AND REPEATABILITY COEFFICIENT OF RELATIVE RENAL TC-99M DMSA UPTAKE

T.Y. Erdil, F. Şen, F. Dede, O. Noshari, H.T. Turoğlu. Department of Nuclear Medicine, Marmara University Hospital, Istanbul, Turkey.

The aim of our study is to evaluate the intraobserver, interobserver variability and repeatability coefficient (RC) of relative renal function (RRF) obtained with Tc-99m DMSA (DMSA).
Methods: Two hundred and ninety three patients (pts) (mean age 6.9 ± 19.3, range 0.2-70 yr) underwent static DMSA studies in the supine position. Five hundred Kcounts were acquired in the posterior projection using high resolution collimator on a 256x256 matrix. All, but 7 pts had normal renal functions. In 26 pts, RRF of left kidney (LK) was above 60% and below 40% in 34 pts. Nine pts had hydronephrosis on right kidney and 30 on the LK. Atrophy or infection were present in the LK of 33 pts and in the right kidney of 18 pts. RRF was calculated with and without background (bcg) correction. The measurements for the intraobserver and interobserver variability and repatibility coefficients were performed by two independent observers for all pts (total), for LK having a RRF above 60% (Group1, n=26), between 40%-60% (Group 2, n=233) and below 40% (Group 3, n=34).
Results:

BCG (+)	Correlation (r)		Regression line (y=)		RC
	Intraobserver	Interobserver	Intraobserver	Interobserver	
Total	0.988	0.998	0.995x+0.23	0.995x+0.14	1.66
Group 1	0.996	0.997	0.982x+1.33	1.005x-0.85	1.11
Group 2	0.988	0.995	0.988x+0.59	0.989x+0.49	1.27
Group 3	0.997	0.998	1.006x+0.02	1.014x-0.41	3.4
BCG (-)	r =		y =		RC
Total	0.999	0.999	1.003x-0.2	1.003x-0.1	1.34
Group 1	0.998	0.996	1.005x-0.29	0.983x+1.64	1.28
Group 2	0.993	0.992	1.006x-0.3	0.985x+0.82	0.89
Group 3	0.997	0.999	0.999x-0.06	0.983x+0.38	3.01

A good correlation was found for both intraobserver and interobserver variability for all comparisons. RRF calculated without bcg correction showed slightly higher correlation and better repeatability results as compared to those (its counterparts) with bcg correction. However, this difference was not found to be significant. In Group 3, there was significant difference compared to other groups and the highest RC value was obtained from this group for both with and without bcg correction.

	BCG (-) vs BCG (+)	
	r =	y =
T	0.998	0.951x+213
G 1	0.985	0.946x+2.12
G 2	0.989	0.939x+2.83
G 3	0.998	0.986x+1.26

Conclusion: RRF obtained both with and without bcg correction gave highly repatable and correlated results. However, in kidneys with RRF lower than 40%, higher variable results were obtained as compared to kidneys with RRF higher than 60%.

PS_710

INTERFILE: OLD, SIMPLE BUT USEFUL

A. Dobbeleir (1), A. Vervaet (1), K. Melis (2), G. Dutoit (3), A.S. Hambye (1). (1) Middelheim General Hospital, Antwerp, Belgium; (2) Sint-Augustinuskliniek, Veurne, Belgium; (3) Dutoit Medical, Antwerp, Belgium.

In May 2000, several hospitals in Antwerp entered in partnership to purchase a GE Advance PET system. Each nuclear medicine department wanted to visualize interactively in 3D the PET whole body scans in his own location. Therefore the PET system provides besides the native attenuation corrected transverse slices also Dicom transverse slices. Transmission of data over network communication links to other sites is easy, but system compatibility remains a problem: no available nuclear medicine system was able to read native nor Dicom PET data. (GE, Elscint, SMV, Trionix, Hermes, Link). Freeware viewers developed for Dicom like Osiris or Acculite were able to read the data but ordered and/or normalized the GE PET images in a wrong way.

To solve the problem, we decided to transform the native GE PET whole body transverse slices to interfile.

Using Unix and C++, an interfile header was created from the data in the study header of the PET data. Position and individual image normalization factors were extracted from the image headers. Images were ordered according to their bed position before being stacked together and normalized to one factor. Absolute activity was preserved in order to allow calculation of standard uptake values (SUV) in normal tissue and tumors in the different referring nuclear medicine departments. The program output of the transformed whole body PET data consists of interfile data typically containing between 205 and 240 transverse slices of 128-128 pixels matrix size.

Thanks to the transformation into interfile, some nuclear medicine systems like SMV and Trionix succeeded to import this non-cubic volume and display the transverse, sagital and coronal slices in their 3D viewer. Furthermore ray tracing and volume rendering became available for tumor localization.

Despite the development of an elaborated transfer system like Dicom, the ability to easily convert images to interfile data readable by most nuclear medicine systems remains an important tool in daily practice. May be small developments in interfile deserves more attention by the nuclear medicine community.

PHYSICS / INSTRUMENTATION 3

PS_709

PACS IN NUCLEAR MEDICINE - ESSENTIAL PRECONDITION FOR PRACTICAL IMAGE FUSION

T. Kauppinen (1), P. Nikkinen (1), H. Pohjonen (2), I. Sippo-Tujunen (1), S. Savolainen (12). (1) Division of Nuclear Medicine; (2) Department of Radiology, Helsinki University Central Hospital, Helsinki, Finland.

Aim: Efficient routine use of image fusion requires a PACS (picture archiving and communication system) to provide storage of image data in a standard digital format, a high-speed image network as well as an accurate and reliable image fusion software. The Hospital District of Helsinki and Uusimaa (HUS) has a PAC system called HUSpacs with the total amount of 800.000 examinations (20 TB) per year by the end of year 2003. According to Finnish legislation images have to be stored for 20 years. The purpose of this study was to introduce a PACS for practical clinical use in the divisions of Nuclear Medicine, as a part of HUSpacs. The effect of PACS on customising image fusion in the division of nuclear medicine was also evaluated.

Methods: The architecture of HUSpacs is based on local on-line archives (RAID) and two regional image databases linked together. The capacity of online archives is approximately two years of image data. Each department a short-term archive of its own. Long-term archiving and back-up archiving are centralised. There are two separate campus areas with three nuclear medicine divisions and 7 gamma cameras. Both campus areas have a replicating hard-disk system of their own consisting of 3x60 GB disk space. All the data (approximately 10 GB per year) is transferred automatically to the global online database in a Dicom NM format. It is also possible to transfer images acquired by other modalities (e.g. MRI, CT) to this database for image fusion. The next step is to archive this data to the regional HUSpacs database.

Results: Combination of anatomical and functional image data from the same part of the body is important and can enhance the understanding of functional abnormalities. Hence image fusion is important in clinical work. The new fusion programs is based on several different registering algorithms and works fine in most cases. Registering with external landmarks is also an accurate technique if markers are available.

Conclusions: For routine use of image fusion it is essential to have a fast image network for transferring images from different modalities and a PACS for storing them. It is also essential to have a common commitment to Dicom standard. Open-architecture PACS seems to remove the remaining difficulties in customising image fusion. The introduced expanded HUSpacs will be one of the largest PACS in the world when completed in 2003.

PS_711

ON-LINE IMAGE PROCESSING OF A SMALL FIELD-OF-VIEW IMAGING PROBE

A. van Lingen (1), N.M. Bruin (1), E. Baumann (2), T. Ijbema (3), P.G.H.M. Raijmakers (1), G.J.J. Teule (1). (1) Department of Nuclear Medicine, Free University Medical Center, Amsterdam, The Netherlands; (2) Eurorad, CIT, Strassbourg, France; (3) PI-Medical Diagnostic Equipment Bv, Joure, the Netherlands.

Aim: To optimise by simulation the on-line processing of a 49x49 mm field-of-view (FOV) imaging probe for per-operative applications. The physical performance of the device (e.g. 6 mm spatial resolution) has been reported before. The imaging software displayed in a grey scale only a matrix of 16x16 pixels, in concordance with the array of the 256 CdTe elements of the collimated device.

Methods: Using Matlab 5.3 (SE) on a PC, the effect of different image smoothing and interpolation schemes was studied. All images were presented in colour (blue is background, yellow is medium and red is hot). The interpolation consisted of a 1-2-4 weighing scheme, with the higher weight applied to pixels closer to the central pixel. Subsequent application of the interpolation resulted in matrix sizes of 31x31, 61x61, and 121x121. With each interpolation a smoothing was performed either before or afterwards (pre- or post-smoothing).

The processing schemes were applied to the following test images (16x16 matrix): single pixel value, checkerboard, an acquired image of a high activity point source and a low activity point source (100:1 intensity ratio and 10 mm apart), an acquired image (60 sec) of a sentinel node near the injection site in a breast cancer patient. The criteria for the best scheme were reduction of coarseness, preservation of resolution and image uniformity.

Results: All test images showed too much coarseness if presented by a 16x16 matrix. More interpolation resulted in increased refinement, but also more noisy images. With pre-smoothing low activities tended to vanish, but were preserved with post-smoothing. The checkerboard images showed a better resolution with post-smoothing than with pre-smoothing. In the case of the 100:1 intensity ratio, the colder spot fused with the hot spot, when pre-smoothing was applied. This was not the case with post-smoothing. In the patient image, pre-smoothing caused an increase of activity between injection site and sentinel node, but not with post-smoothing.

Conclusions: For on-line imaging with a device consisting of 16x16 individual detector elements, the acquisition interface for the operator should be easy to interpret. A colour display is mandatory to resolve low contrasts. Furthermore, a 3-fold interpolation with post-smoothing is found to be optimal for on-line processing.

PS_712

MULTI-COMPARTMENT MODEL FOR INTRAOPERATIVE MEASUREMENT OF RENAL PLASMA FLOW DURING USE OF HEART-LUNG MACHINE IN CARDIAC SURGERY

D. Sandrock (1), S. Morgera (2), W. Heldwein (2), K. de Jonge (3), D.L. Munz (1). (1) Clinic for Nuclear Medicine; (2) Clinic for Nephrology; (3) Clinic for Cardiovascular Surgery, University Hospital Charité, Berlin, Germany.

Aim: The conventional measurement of the orthoiodohippurate (OIH) clearance for determination of renal plasma flow assumes a two-compartment model. During use of a heart-lung machine (HLM) in cardiac surgery these assumptions are not suitable. Aim of this study was to develop a multi-compartment model, which reflects the intraoperative situation in a more realistic manner.
Methods: The determination of the renal plasma flow was done by measuring intraoperatively obtained venous blood samples after i.v. injection of 10 MBq I-123-OIH in a gamma well counter. For creating the multi-compartment model, the following factors/spaces were taken into consideration (and measured by [volume corrected] fluid samples during 10 cardiosurgical interventions): blood volume (from nomogram), hematocrit (for calculation of plasma volume), infusion volumes, blood substitution, insensible water loss (IWL, open chest, 10 ml/kg body weight/h), urine/hemofiltration volume, filling volume of the heart-lung machine before use, volume changes according to the machine protocol, volume reflux of red blood cell concentrate at the end of use, blood loss.
Results: The model shown below represents the measured spaces/volumes of a single patient (example)
Conclusion: The multi-compartment model realistically describes the intraoperative volumes/spaces during the use of the heart-lung machine and allows the intraoperative measurement of the renal plasma flow.

PS_713

THE EFFECT OF AN INTRAMEDULLARY NAIL ON SEMI-QUANTITATIVE F18-BONE PET

B.G. Hoving, A. Van Lingen, T.J. Blokhuis, J.C. Roos, K. Boshuizen, A.A. Lammertsma. Clinical PET Center, Free University Medical Center, Amsterdam, The Netherlands.

Aim: To evaluate in a phantom whether an intramedullary vanadium nail in a long bone fracture affects the semi-quantitative results of PET F-18 bone scans.
Methods: A phantom was designed representing a human thigh: 28 cm long with three concentric cylindrical compartments: inner (marrow, 1 cm diameter, IC), mid (cortex, 4 cm, MC), outer (soft tissue, 17 cm, OC).
A static emission (Em) scan (15 min) was performed with the nail in the IC and 75 MBq F-18 only in the MC. After 12 hours of decay 10 min transmission scans (Tx) were obtained. All acquisitions were repeated with the nail removed and with F-18 activity in both MC and OC. The transmission μ-values were determined for all compartments in both situations. Each scan was reconstructed by filtered back projection with a Hanning filter (0.5 c/p), with and without attenuation correction. ROIs were drawn according to the cylinder diameters. The semi-quantitative parameters of interest were the ratios of activity concentrations (Bq/cc) of IC/MC and OC/MC.
Results: No streak artefacts were seen in the transmission scans. The OC density was not affected by the presence of the nail. However, the MC appeared more dense (0.102 vs 0.090) with the nail present:

μ-values (cm^{-1})	IC	MC	OC
With nail	0.137	0.102	0.095
Without nail	0.047	0.090	0.094

With attenuation correction and only activity in the MC, scatter into the OC was approximately 2%, with or without nail. Scatter from MC into the IC amounts to 22.4% without the nail and reduced to 14.7% with the nail. Adding activity to OC, the nail caused a decrease in total scatter (23.7% to 12.8%) from MC and OC into IC.

Without attenuation correction OC/MC scatter fraction seemed larger but was unaffected by the presence of the nail.

Act. conc. ratios	With nail		Without nail	
	IC/MC	OC/MC	IC/MC	OC/MC
Act. in MC only - with att. corr.	0.147	0.020	0.224	0.022
Act. in MC and OC - with att. corr	0.128	0.040	0.237	0.041
- without att. corr.	-0.070	0.043	0.414	0.045

Conclusions: An intramedullary nail reduces the cortical bone compartment density, as estimated from the Tx scan. However, the ratio of activity concentration (Bq/cc) in cortical bone and in soft tissue is not affected by the nail in the marrow compartment. Also, application of attenuation correction does not affect this ratio.

PS_714

COMPARISON OF TWO CT ORGAN VOLUME CALCULATION METHODS FOR MASS CORRECTION OF ORGAN BETA SELF-RADIATION ABSORBED DOSE ESTIMATES

W. D. Erwin, M. W. Groch. Department of Nuclear Medicine, Northwestern University Medical School, Chicago, USA.

Patient-specific organ beta self-radiation absorbed doses (_RAD) in radioimmunotherapy may be estimated by scaling absorbed dose according to organ mass. The purpose of this investigation was to compare calculated organ masses and corrected _RAD estimates using two different organ CT volume calculation methods.
Methods: Kidney, liver, lung and spleen _RAD estimates (rad/mCi) were calculated in seven (7) lymphoma patients undergoing Y-90 radioimmunotherapy, with mass correction based on reference phantom:patient mass ratios (Stabin, SNM '98). Two slice-by-slice (2D) CT volume definition methods were employed to calculate organ masses. Method 1 (GE Medical Systems) employed semi-automated edge tracking, while method 2 (Osiris, H™pitaux Universitaires de Gen?va) used pixel value histogram windowing and region growing. Volumes (cc) were converted to mass (g) by multiplication by organ densities specified by the MIRD schema (.2958 g/cc [lung] and .9869 g/cc [soft tissue]). Reference organ masses and uncorrected _RAD estimates were derived from the MIRDOSE version 3 program (Oak Ridge Associated Universities).
Results: Calculated organ masses (n = 28) were (mean [range] in g): 1083 [227-2288] (Method 1) and 1035 [192-2211] (Method 2). Linear regression of volumes demonstrated excellent correlation (Method 2 = 0.97×Method 1 – 15, r = 0.99). The mean absolute (g) and percent (%) differences (Method 2 - Method 1) were not statistically significant (-49 ± 60 g and -6.7 ± 7.5 %; p " 0.05, paired t-test). Bland-Altman analysis demonstrated slightly increasing absolute difference with increasing mass (Y = -0.03X – 18, r = -0.37), but slightly decreasing % difference with increasing mass (Y = 0.004X – 11, r = 0.40). Linear regression of resultant _RAD estimates was excellent (Method 2 = 1.08×Method 1 – 0.06, r = .99). Again, the mean absolute (rad/mCi) and percent (%) differences (Method 2 – Method 1) were not statistically significant (.76 ± 1.0 rad/mCi and 6.8 ± 7.5 %; p " 0.05, paired t-test). Bland-Altman analysis demonstrated slightly increasing absolute difference with increasing _RAD (Y = 0.09X – 0.2, r=0.50), and slightly increasing % difference with increasing _RAD (Y = 0.24X + 4.3, r=0.17).
Conclusions: In this study, the two CT organ volume calculation methods compared yielded no statistically significant difference in mass corrected _RAD estimates. Thus, the methods appear capable of producing essentially equivalent results.

PS_715

ESTIMATE OF PERSONNEL«S SKIN DOSE DUE TO CONTAMINATION BY RADIONUCLIDES USED IN NUCLEAR MEDICINE

V. Hušák, K. Kleinbauer, P. Koranda, M. Mysliveèek. Department of Nuclear Medicine, University Hospital, Olomouc, Czech Republic.

Aim: Personnel«s skin may become contaminated in incidents and accidents involving spills of unsealed sources of radioactivity. If contamination persists, an estimate of skin dose should be made. However, these estimates are very imprecise due to a series of factors a knowledge of which is often insufficient. Among them, two factors were investigated newly in our paper in an attempt to reduce partly an uncertainty in the determination of absorbed dose: an area of the contaminated skin and a residence time of radioactive substances on the skin.
Methods: Critically evaluating the literature, a table was compiled of beta and gamma dose rate to the basal layer of the skin at 0.07 mm depth from contamination by radionuclides used in nuclear medicine. In our calculation, the dose rate was considered as the arithmetic mean of dose rates corresponding to two extreme geometries: an extended contaminated area on the skin (≥ 100 cm^2) and droplet of radioactive substance on the skin (1 cm^2). A residual activity of any radionuclide which could not be removed by the repeated careful decontamination (performed immediately after incident), was supposed to be eliminated with the biological half-life T_b = 116 h as a consequence of the natural sloughing off of the skin. The residence time was calculated as $1.443T_fT_b/(T_f+T_b)$ where T_f is the physical half-life of the radionuclide. The skin dose was obtained as the product of the mean dose rate and the residence time.
Results: Values of dose rate in $mSv.h^{-1}/(kBq.cm^{-2})$ and dose in $mSv/(kBq.cm^{-2})$ (given in parentheses) for some radionuclides: ^{89}Sr 2 (306), ^{32}P 1.9 (238), ^{131}I 1.55 (161), ^{90}Y 2.1 (126), ^{186}Re 1.73 (127), ^{153}Sm 1.52 (73), ^{188}Re 2 (43), ^{111}In 0.37 (23), ^{67}Ga 0.36 (24), ^{201}Tl 0.25 (16), ^{123}I 0.35 (6), ^{18}F 1.9 (5), ^{99m}Tc 0.23 (1.9). Our approximative results are valid on the assumption that residual activity of radionuclides persists predominantly in the superficial layers of the epidermis.
Conclusions: It is possible to determine easily, without knowing the contaminated area and on the basis of one measurement of residual activity in $kBq.cm^{-2}$ by means of a monitor, rough values of doses to personnel«s skin and to interpret them in relation to the annual limit 500 mSv for the skin given in radiation protection regulations. The procedure suggested is assessed to diminish the usual large uncertainty by about 50 % (supported by State Office for Nuclear Safety, Prague).

PS_716

A GENERAL FORMULA FOR RADIATION DOSIMETRY ESTIMATES FOR SENTINEL LYMPH NODE BIOPSY IN BREAST CANCER SURGERY

C. Bagnara (1), G. Villa (1), F. Buffoni (1), P. Erba (1), F. Castagnola (1), M. Bagnasco (1), A. Pilot (2), G. Mariani (1). (1) Nuclear Medicine Service, DiMI - University of Genoa, Genoa, Italy; (2) Health Physic Unit, S. Martino Hospital - University of Genoa, Italy.

Growing interest is recently being devoted to radioguided surgery for sentinel lymph node biopsy, particularly in patients with breast cancer. In fact, after the pilot studies carried out under investigational protocols, this approach is quickly being translated into the clinical routine, although its long-term impact on the clinical outcome of patients has not yet been elucidated. In addition to the Nuclear Medicine staff administering the radiopharmaceutical and performing the in vivo evaluations (lymphoscintigraphy and intraoperative gamma-counting), the procedure intrinsically involves other personnel, such as the surgeon and the pathologist. Concern is therefore mounting on the possibility that the radiation burden to such personnel entails special protection procedures, especially when the number of such surgical procedures is relatively high.
Methods: In this work we reviewed the results of the following experimental studies on the radiation burden to non-nuclear medicine personnel involved in sentinel lymph node biopsy for breast cancer surgery, all based on the administration of ^{99m}Tc-labelled colloids:
1. Pijpers et al. *Tijdschr Nucl Geneesk 1997;* 19: 144-7.
2. Cremonesi et al. *Nucl Med Commun 1999;* 20: 919-924.
3. Glass et al. *Semin Nucl Med 1999;* 29: 57-68.
4. Stratmann et al. *Am J Surg 1999;* 178: 454-457.
5. Motta et al. *Tumori 2000;* 86: 372-374.
6. Waddington et al. *Eur J Nucl Med 2000;* 27: 377-391.
Results and conclusion: Our analysis showed that, despite some important differences in the methods employed for such determinations, there was a remarkable consistency in the results obtained, after normalizing for injected dose, time elapsed between tracer administration and surgical procedure, duration of the surgical procedure. A general formula was therefore derived thereby a certain radiation dosimetry estimate could be calculated after introducing any given combination of the variables involved in radioguided sentinel lymph node biopsy. The equivalent dose (D) to personnel can therefore be estimated emplying the following general formula:
D = f áA$_0$á_t /d^{2}áf$_{ret}$áf$_{decad}$(el_time)áf$_{atten}$(depht)
where:
f á = conversion constant (exposure-kerma-dose factor) for ^{99m}Tc
A_0 = injected activity
_t = duration of performance (surgery or pathology analysis)
d = mean distance from the source
f_{ret} = amount of injected tracer retained by in tissues
f_{decad}(el_time) = physical decay during time elapsed between tracer injection and surgery
f_{atten}(depht) = tissue attenuation of the source

PS_717

ASSESSMENT OF RADIATION SAFETY OF THE SENTINEL LYMPH NODE TECHNIQUE IN THE OPERATION ROOM

K. Nakamura (1), H. Kikuchi (2), H. Fujii (1), Y. Kitagawa (3), T. Ikeda (3), K. Nakazato (2), M. Kitajima (3), A. Kubo (1). (1) Department of Radiology, Keio University School of Medicine, Tokyo, Japan; (2) Radiation Safety Office, Keio University School of Medicine, Tokyo, Japan; (3) Department of Surgery, Keio University School of Medicine, Tokyo, Japan.

Aim: The purpose of this study is to assess radiation safety to the staff that performs the sentinel lymph node techniques by using radioactive materials in the operation room.
Methods: The radiation dose to two surgeons; Surgeon I conducting the excision at the primary tumor and Surgeon II performing probe-guided localization and excision of the sentinel nodes, was recorded using electronic personal dose meter in the chest and radiophotoluminescent glass dose meter at the fingers. The personal dose meter in her abdomen also determined the radiation dose to the nurse who assists surgeons.
Results: The surgery of breast or GI (gastric, esophagus, or rectal) cancer was operated for 2.24 hours or 5.30 hours on the average, respectively. The mean radiation doses to the surgeons (Chest: 0.42 (I) and 0.32 (II) (Sv/hr; Fingers: 12.2 (I) and 5.1 (II) (Sv/hr) and nurse (0.00 (Sv/hr) in the operation of breast cancer were smaller than those in the GI cancer operation (Chest: 0.54 (I) and 0.64 (II) (Sv/hr; Fingers: 12.6 (I) and 7.5 (Sv/hr; Nurse: 0.03 (Sv/hr), probably because Tc-99m was spread in the small area near injection tumour sites. When the operation of GI cancer was conducted under the endoscopes, radiation dose to the surgeon's chest was reduced to 0.16-0.34 (Sv/hr, and doses at fingers of Surgeon I and II were decreased into 1.03-1.44 and 1.71-1.12 (Sv/hr, respectively. The maximum radiation dose to surgical staff resulting from all surgeries (n= 20) performed on a sentinel node was 6 (Sv on the chest of Surgeon II and 129 _Sv at the finger of Surgeon I during the operation of gastric cancer.
Conclusions: the radiation doses to staff groups involved in any kinds of cancer operation were small enough for the personal radiation monitoring to be omitted.

PS_718

NEW CONCEPT OF POSITRON EMITTERS SHIELDING: DECLINE VIAL POSITION FOR QUANTITAVE WITHDRAWING OF RADIO-PHARMACEUTICALS

D. Janeba (1), P. Kralik (2), M. Penkava (2), J. Dudkova (1), O. Belohlavek (1), V. Vrana (3). (1) Na Homolce Hospital, Praha, Czech Republic; (2) Variotec Ltd., Rez u Prahy, Czech Republic; (3) Charles University General Hospital, Praha, Czech Republic.

Aim: Loading the dose of positron emitters into syringe causes radiation exposure, especially for the hands. The aim of this work was to develop an efficient shielding device for filling the syringes, which could be operated easily in the laminary flow box and would reduce radiation exposure.
Methods: Primary shielding of vial (20 mm lead) provides continuous protection even during short time manipulation with vial and it is housed in the secondary shielding (40 mm lead). The vial in primary shielding is taken out of the transport container and inserted in decline position into a system designed for loading radiopharmaceutical into syringe (see figure). Two needles are inserted to the vial, one for filling the syringe, the other to balance the air pressure. Then the whole device is closed with a cover (40 mm lead) and the syringe is housed into additional shielding (30 mm lead). No further movement with the vial is necessary and the technologist can immediately load the radiopharmaceutical into the syringe. After syringe is filled, it is placed into a syringe shield and mobile transportation container.
Results: The tests with the first prototype showed that the shielding considerably reduces radiation exposure (dose rate at 30cm from equipment is < 3μSv/hour for 5GBq 18FDG without any additional shielding). The conus of the needle is fixed which enables easy and exact connection and disconnection of syringes. The amount of radiopharmaceutical in the syringe can be continuously controlled by viewing the syringe scale in the mirror via a channel through the shielding. The mirror position may be optimised to lower the demands on accuracy of syringe positioning. The decline position of vial ensures almost total withdrawal of radiopharmaceutical inside.
Conclusion: The concept of the primary and secondary shielding with declined vial position showed its gain for reduction of radiation doses. The local shielding has proven to be very easy to handle and applicable in daily routine. The tests in routine practice showed that this system is compact for placement in laminary flow box and can be made compatible with different types and sizes of vials and containers.

Acknowledgements: The work was supported by projects LN00B122 and NC 5975-3 and the developed system is patented (PV2000-3151). Authors appreciate the effort of the Variotec Ltd. for manufacturing of the first prototype tested.

PS_719

EVALUATION OF RADIOISOTOPE EXPOSURES USING AUTOMATED QUALITY CONTROL SYSTEM AND AUTOMATED INJECTION SYSTEM AT PET INSTITUTE HANDLING LARGE AMOUNT OF SHORT HALF LIFE RADIOISOTOPES

K. Tomiyoshi (1), S. Nagata (1), S. Fujiwara (1), M. Shinoda (1), M. Kawano (1), T. Tomemori (1), K. Nakagawa (1), K. Abe (1), K. Uno (1), T. Kanoi (2), M. Sasaki (3)(1) Nishidai Clinic Diagnostic Imaging Center, Itabashi-Ku Tokyo, Japan; (2) Universal Giken, Odawara-City Kanagawa, Japan; (3) Sumitomo Heavy Industries.Ltd, Shinagawa-Ku Tokyo, Japan.

Because of a very short half life of radio-pharmaceuticals used for PET, a large quantity production of radio-pharmaceuticals is required for a clinical use. Attention has to be paid on the radioisotope (RI) protection. There are two chances for receiving large RI exposures. One is at production and quality control of radio-pharmaceuticals. The other is at injection of radio-pharmaceuticals to many patients. To attain a great reduction of RI exposure, we constructed an Automated Quality Control (Q.C.) System (M-200) and an Automated Injection System (US-2000) for routine production and for routine injection. We presented original scheme of these systems and we reported how much RI exposure was reduced before and after in their use.
Methods: Scheme of Automated Q.C. System (M-200) and Automated Injection System (US-2000)
M-200 has two main functions. One is to measure total volume and total activity of the radio-pharmaceuticals and distribute a designated activity into container made of tungsten. Other function is quality control of the radio-pharmaceuticals. Semiconductor RI detectors and liquid sensor was employed to measure activity and volume to get a concentration of radio pharmaceuticals. Tungsten shield container transferred from M-200 was directly placed in the US-2000 and a needle was connected to the sterile vial in the container. Radio-pharmaceutical was led by disposable sterile tubes controlled by several liquid sensors and RI sensors. A touch panel was used to obtain expected total activity and volume for injection. Patient is needle inserted to be ready to connected to a disposable tube from US-2000.
Results: By employing M-200 and US-2000, Exposure dose was decreased to in the range of one hundredth to one thousandth of that not employing the systems. A correlation factor in measurement of RI activity for M-200 and US-2000 was 0.99 in the range of 0.1GBq to 1.0GBq. Average injection dose was fluctuated less than 10 percents from an expected one. A residue activity in the system was about 10% to be improved.
Conclusion: These two systems are very valuable and indispensable for handling large amount of radio-pharmaceuticals and many patients at PET Institutes.

PS_720

DOSIMETRIC PROPERTIES OF LI2B4O7:CU,AG,P SOLID TL DETECTORS

M. Prokic. Institute of Nuclear Sciences, Vinca, YU.

Very fiew thermoluminescent materials are tissue equivalent with an effective atomic number which is very close to that of soft biological tissue (7.4). Lithium borate based TL dosemeters appeared to be the most attractive, with an effective atomic number Z_{eff}=7.3.
Methods: This paper presents the main dosimetric characteristics of newly prepared complete tissue-equivalent thermoluminescent detector $Li_2B_4O_7$:Cu,Ag,P in form of sintered pellets, developed at the Institute of Nuclear Sciences, Vin_a. As a result of an advancement in the preparation procedure by sensitizing of basical $Li_2B_4O_7$:Cu phosphor, significant improvement in the TL sensitivity of $Li_2B_4O_7$:Cu,Ag,P was gained.
The thermoluminescent properties of developed lithium borate TL detector examined in this study, include glow-curve shape, TL sensitivity, photon dose response, minimum detectable dose, relative photon energy response, fading, reproducibility, and recommended annealing procedure.
Results: From the experimental results it is evident its very wide linear dose response range up to 10^3 Gy. It is also evident that the glow curve consisted of well defined main dosimetric peak with a TL sensitivity which is about 4 times higher than that of commonly used TLD, LiF:Mg,Ti (TLD-100). $Li_2B_4O_7$:Cu,Ag,P is an efficient TL detector for dose measurements of X, photon, electron, proton and neutron radiation. Also, as a result of an advancement in the preparation procedure, $Li_2B_4O_7$:Cu,Ag,P sintered pellets have shown a resistance to adverse effects caused by handling procedure, with no change on the TL response.
Conclusions: Represented dosimetric characteristics make sintered solid lithium borate TL dosemeter promising for different dosimetry applications, particularly in medical and clinical dosimetry and radiation protection.

RADIOPHARMACY / RADIOCHEMISTRY 4

PS_721

EFFECT OF HIGHER 99MTC/99TC RATIO FROM A SECOND ELUTION IN LABELING COLLOID ALBUMIN

G.M.M. Gommans (1), R.O. Boer (1), A. Dongen van (1), E. Gommans (2), F. Zant van der (1). (1) Department of Nuclear Medicine, Westfries Hospital, Hoorn, The Netherlands; (2) Faculty of Chemical Engineering, University of Twente, Enschede, The Netherlands.

The Aim: Following our previous studies in which we proved a better labeling we tried in this study to Further improve labeling efficiency and radiochemical stability of ^{99m}Tc colloid albumin and to facilitate an optimal labeling protocol for ^{99m}Tc colloid albumin
Methods: To Further improve the labeling procedure of ^{99m}Tc colloid albumin, in-vitro stability of different concentrations prepared from a second elution of a ^{99}Mo / ^{99m}Tc generator at T= 2 hours were tested (ingrown T=0-2 h from a previous elution at T=0 hours. Concentrations of 2.5, 10, 20, 25, 30 and 37 MBq ^{99m}Tc /μg colloid albumin (Nanocoll) under nitrogen and in vacuum were prepared and the quality of the solutions, radiochemical stability and efficiency of labeling after 0.5, 2, 5 and 8 and 24 hours were tested.
Results: Using a second elution at T=2 (ingrown of 2 hours) hours for labeling ^{99m}Tc colloid albumin under nitrogen and under vacuum, a maximum acceptable concentration of 30 MBq/μg was found and a 3.0-fold greater efficiency over the entire period of 24 hours was achieved. Coincidental we found that eluting a 99Mo / ^{99m}Tc generator twice a day (T=0 h and T=2 h) will height the daily production of ^{99m}Tc with 20% without loose of strength of the ^{99}Mo / ^{99m}Tc generator.

Labeled under nitrogen T=0h (ingrown 24 h)					
MBq/mg	0.5 h	2 h	5 h ,	8h	24h
2.5	99.8	99.3	99.9	97.9	97.5
10	99.9	98.8	98.5	98.0	97.0
25	96.1	88.7	86.8	85.6	84.0
30	81.5	78.5	76.0	75.4	72.0
37	79.0	74.5	72.0	70.5	68.0
Labeled under nitrogen T=2h (ingrown 2h)					
MBq/mg	0.5 h	2 h	5 h	8h	24h
2.5	99.6	99.8	99.3	99.7	99,5
10	99.5	99.4	98.3	99.8	99,9
25	100.0	97.5	95.3	95.6	98.0
30	97.2	96.8	96.0	95.2	96.4
37	98.6	96.0	95.5	94.8	93.0

Labeled under vacuum T=0h (ingrown 24h)					
MBq/mg	0.5 h	2 h	5 h	8h	24h
2.5	98.5	98.0	98.0	99.0	98.2
10	99.6	98.0	97.5	96.7	96.0
25	98.1	97.8	97.9	97.1	96.6
30	96.5	95.1	93.9	93.7	92.0
37	94.5	88.3	85.5	83.9	82.6
Labeled under vacuum T=2h (ingrown 2h)					
MBq/mg	0.5 h	2 h	5 h	8h	24h
2.5	100.0	100.0	100.0	100.0	100,0
10	100.0	100.0	100,0	100,0	100,0
25	98.6	99.0	97.5	97.5	98.0
30	98.7	99.3	99.2	98.3	97.6
37	98.8	97.0	94.4	96.2	93.0

Conclusion: Labeled ^{99m}Tc colloid albumin from a second elution (T=2 h) with ingrown of two hours of a ^{99}Mo/^{99m}Tc generator shows a 3.0 fold greater efficiency of labeling and is more stable than labeled at time T=0 h with an ingrown ^{99m}Tc/^{99}Tc of twenty-four hours.

PS_723

EXTRACTION AND DEEP PURIFICATION OF ALPHA-EMITTING RADIONUCLIDES FOR MEDICAL APPLICATION

N. Nerozin, E. Smetanin, V. Pavlovich, D. Dubinkin, O. Vtorova. Department of Isotopes and Radiopharmaceuticals, Institute of Physics and Power Engineering, Obninsk, Russia.

Nowadays monoclonal antibodies labelled by radionuclides find more and more wide application in oncologic disease diagnostics and treatment. Alpha-emitting radionuclides have doubtless advantage over β- and γ-emitters due to a high value of their linear energy transfer and small free path.

Just few alpha-emitting radionuclides suitable for medical application can be picked out of a great number of them. Ac-225 is one of these radionuclides. It serves as the parent isotope for Bi-213 recovery.

Aim: This research has been carried out for studying chemical and engineering processes of recovery, purification and production of pure Ac-225 medications out of the seasoned Th-229.

Methods: Sorption methods of Ac-225 recovery and deep purification from Th-229 and daughter decay products have been used. Ac-225 produced has been analyzed for the chemical impurities and alpha-radionuclides concentration with the help of alpha-spectrometry. Chemical impurity concentration in Ac-225 is 10^{-4} – 10^{-5} mg/ml in 21 elements. Alpha- and gamma-radiometric control of process solutions has been carried out at every research phase.

Results: The research of Ac-225 generator basic design has shown that the most rational way is to develop Ac-225 generator consisting of the following operations:

Th-229(228) long-term storage in HNO_3 solution;

Th-229(228) sorption on anion-exchange resin;

Sorbent washing by the same solution;

Thorium desorption by HNO_3, correction by Th solution and long-term storage before the following processing;

Raffinate and washing solution correction in HNO_3 for Ac-225 sorption;

Ac-225 sorption on cationite from ~ HNO_3;

Sorbent washing by HCl solution of the same acidity prepared isothermally on the base of twice-distilled product made in a quartz device;

Ac-225 desorption by HCl distilled in the quartz device;

Analysis of the solution produced for Th-229(228) and Ra-224 contents, chemical and spectral analysis of chemical impurities.

Conclusions: The process of Ac and Th separation followed by Ac purification from Th-229 daughter decay products has been developed. The principle design of the generator system for Ac-225 production has been proposed.

PS_722

CLINICAL EXPERIENCE WITH PREPARATION OF IN-111 AND Y-90 LABELED ZEVALIN: RADIOCHEMICAL PURITY ASSESSMENT

A.M. Zimmer (1), P.C. Chinn (2nd), R.A. Morena (2nd), M.D. Wakefield (2nd), S.M. Spies (1st). (1) Nuclear Medicine Department, Northwestern University Medical Center, Chicago, IL, USA; (2) IDEC Pharmaceuticals Corporation, San Diego, CA, USA.

IDEC Pharmaceuticals has developed a cold kit for the preparation of In-111 and Y-90 labeled Zevalin (ibritumomab tiuxetan), an anti-CD20 murine IgG1 monoclonal antibody. The cold kit consists of four color-coded components including acetate buffer (50 nM sodium acetate), conjugated monoclonal antibody, formulation buffer (PBS, 7.5% human serum albumin, 1 mM DTPA) and a reaction vial. The purpose of the study was to evaluate the radiochemical purity of radiolabeled Zevalin utilizing thin layer and size exclusion high performance liquid chromatography.

Methods: At Northwestern University Medical Center, 38 In-111 Zevalin and 58 Y-90 Zevalin preparations were formulated using aseptic techniques with the cold kit components provided. Y-90 chloride (40 mCi) or In-111 chloride (5.5 mCi) was added to the reaction vial containing 50 nM sodium acetate in order to adjust the pH to approximately 4. Conjugated antibody was added and the reaction incubated for 5 or 30 minutes for Y-90 or In-111, respectively. Formulation buffer was then added (total volume 10 ml) to terminate the reaction and also to stabilize the radiolabeled antibody. Radiochemical purity (RCP) was assessed on each specific preparation in triplicate using instant thin layer chromatography-silica gel with normal saline. In addition, size exclusion high performance liquid chromatography (HPLC) was also used to assess radiochemical purity of selected radiolabeled antibody preparations. Chromatographic separation by HPLC was achieved using a TSKgel G3000SW molecular sizing column.

Results: The RCP of all preparations, except one, exceeded the release specifications of 95%. A mean radiochemical purity of 97.3% ± 1.8% (sd) and 97.7% ± 1.1% (sd) was obtained for In-111 Zevalin and Y-90 Zevalin, respectively. The RCP of the failed Y-90 Zevalin preparation was less than 10% and, upon further investigation, was attributed to a compounding error during the radiolabeling process. A close correlation in unbound radionuclide levels was observed between thin layer and size exclusion HPLC. Further analysis of HPLC elution profiles showed no radiolabeled antibody aggregates or other radiolabeled antibody breakdown products.

Conclusion: The formulation of radiolabeled Zevalin, using the cold kit components, is relatively simple and reliable and results in preparations with consistently high radiolabeling efficiencies, as shown by thin layer and size exclusion HPLC.

PS_724

STRUCTURAL COMPARISON OF THREE DOTATOC METAL COMPLEXES

A. Kühlewein (1), M. Deshmukh (1), G. Gemmecker (1), H. Mäcke (2), G. Scherer (2). (1) Institut für Organische Chemie und Biochemie II, Technische Universität München, Germany; (2) Institute of Nuclear Medicine Division of Radiological Chemistry University Hospital, Basel.

Introduction:DOTATOC (DOTA-D-Phe^1-Tyr^3-octreotide) has shown its suitability as a tumor targeting agent when labelled with diagnostic and therapeutic radionuclides. Patients with advanced somatostatin receptor positive tumors have successfully been treated with ^{90}Y-labeled DOTATOC. Other isotopes like ^{67,68}Ga and ^{111}In have been used for diagnostic applications. It was shown that sensitivity and biodistribution as well as receptor affinity depend on the metal ion which is complexed by DOTATOC. This result is quite surprising, given that it should be expected that the peptide part is solely responsible for receptor affinity, tumor uptake etc.This fact leads to the hypothesis that the nature of the metal ion has an influence on the three-dimensional structure of the peptide. Here we compare the structure of three M(III)-DOTATOC (M(III)=Ga, Y, Eu) complexes. As Eu(III)-DOTATOC is most likely isostructural to Y(III)-DOTATOC we included this metal because of potential additional distance information obtained due to the paramagnetic character of Eu(III).

Methods: Structural investigations were performed using 1D and 2D NMR experiments including TOCSY, DQF-COSY, E.COSY and ROESY. In addition, T1 relaxation measurements were performed to investigate the effect of the paramagnetic Eu(III) ion.

Results: Important differences were observed between Ga(III)-DOTATOC and Y(III)-DOTATOC with regard to the geometry of the metal complex. Whereas the NH proton of D-Phe coupled to the DOTA chelator is strongly shifted in Y(III)-DOTATOC to lower field, indicating an interaction of the corresponding carboxy oxygen with the metal, this proton shows no shift in the Ga complex compared to the uncomplexed DOTATOC. This is a strong indication that the Ga(DOTA-D-Phe) moiety is hexacoordinated whereas Y(DOTA-D-Phe) shows at least octacoordination in solution. Additionally, in Y(III)-DOTATOC two sets of signals appear, one set most likely belonging to the cis isomer (about 25%) at the amide bond to D-Phe. This is rather unusual as cis fractions in secondary amide peptide bonds are usually below 1 %. The solution structure of octreotide was shown to consist of two conformations, a sheet-like conformation and a 3-10 helical conformation. Our results indicate that the metal ions have an influence on the population of these conformations as well as on the cis/trans equilibrium.

Conclusion: High resolution ^{1}H NMR techniques allow the determination of structural and conformational differences of radiometal-peptide conjugates and help to understand differences in biological behaviour.

PS_725

IN-VITRO ADSORPTION OF TC-99M MIBI, TC-99M TETROFOSMIN, TC-99M FURIFOSMIN AND TC-99M O4- ONTO TUBES

M. Rodrigues, F. Chehne, H. Sinzinger. Department of Nuclear Medicine, University Hospital, Vienna, Austria.

Adsorption of radiopharmaceuticals onto disposable syringes has been reported to amount to levels of almost 50%. Data on adsorption of radiopharmaceuticals onto materials used for in-vitro studies are extremely limited. The aim of this study was to assess the extent of adsorption of Tc-99m hexakis(2-methoxyisobutylisonitrile) (Tc-99m MIBI), Tc-99m tetrofosmin, Tc-99m furifosmin and Tc-99m O_4^- onto tubes used for in-vitro measurement of cellular uptake of these radiopharmaceuticals.
Methods: In each experiment, for measuring the non-specific activity due to adsorption of radiopharmaceuticals, 1 ml of incubation medium for the cell lines was added to polystyrene round-bottom tubes and kept at 37°C for at least 1 hour for equilibration. The radiopharmaceutical ($7.4x10^5$ Bq) was added to each tube. The influence on adsorption of different incubation media [McCoy's 5a (for SK-BR-3 cells), RPMI-1640 (for MCF-7 cells) and Leibovitz's L-15 (for liposarcoma cells)], temperature of incubation (37°, 32° or 22°C) and time of incubation (10, 20, 30, 40, 60, 80, 100 and 120 minutes after the addition of the radiopharmaceutical) was evaluated. Six samples of each combination of the above mentioned experimental conditions (i.e. incubation medium, temperature and time) were studied. The human adenocarcinoma breast cells SK-BR-3 (poorly differentiated epithelial-like) and MCF-7 (differentiated epithelial-like), and the human liposarcoma cells SW 872 were chosen to demonstrate the need to correct cellular uptake after measuring the adsorption of the radiopharmaceuticals onto the tubes. The total (not corrected for adsorption) uptake was compared with the corrected, net cellular uptake in SK-BR-3, MCF-7 and liposarcoma cells.
Results: Levels of adsorption onto tubes ranging from 0.94±0.13% to 7.07±0.46% were found. The extent of adsorption of all the radiopharmaceuticals varied with the type of incubation medium (higher adsorption for Tc-99m MIBI, Tc-99m furifosmin and Tc-99m O_4^- with RPMI-1640, for Tc-99m tetrofosmin with Leibovitz's L-15) and the incubation temperature (22¡C>32¡C>37¡C). With Tc-99m furifosmin, adsorption was dependent on the incubation time as well on the incubation temperature and some of the incubation media investigated.
Conclusion: Systematic investigations to evaluate the residual, adsorbed activity of radiopharmaceuticals onto materials used during in-vitro studies should be regarded as a mandatory aspect of quality control.

PS_726

DEVELOPMENT OF TARGET SYSTEM FOR [18F]FLUORINE PRODUCTION VIA THE 18O(P,N)18F NUCLEAR REACTION WITH MC-50 CYCLOTRON

K.S. Chun, M.G. Hur, S.W. Kim, Y.S. Suh, S.D. Yang, S.H. Ahn, S.M. Lim, S.W. Hong. Cyclotron Application Lab., KCCH, Nowon-Ku, Seoul, Korea.

Aim: The number of PET scanner installed in Korea has been sharply increasing for a few years. [^{18}F]Fluorine has been gaining increasing importance in various F-18 radiopharmaceuticals production because its electrophilic reaction can afford many versatile pathways in [^{18}F]compounds synthesis. We have an experience of success in making the enriched O-18 water target for ourselves for the routine [^{18}F]FDG production with nucleophilic substitution reaction. In order to produce new [^{18}F]compounds, promising agents in oncology study, we decided to make the enriched $^{18}O_2$ gas target system to produce [^{18}F]fluorine. Method: Our target system for [^{18}F]fluorine production consisted of target chamber, enriched $^{18}O_2$ gas loading/cryogenic recovery system, collimator/energy degrader, gas and vacuum control system. Conically shaped target chambers were fabricated of aluminum and Ni-plated aluminum and the target chambers were mounted on the multi-target irradiation station made by ourselves. Also, 4 sectors carbon collimator(_ 1.0mm) was installed to control the proton beam on the target. All valves in the gas and vacuum control system were the VCO type of Swagelok product to maintain high pressure and vacuum. Conclusion: Now the target system is being tested for [^{18}F]fluorine production with two step irradiation protocol and it is expected to increase the beam current up to more than 60mA with improvement of target system. The results of testing of the target system will be discussed.

PS_727

A NEW METHOD FOR N.C.A. COPPER-64 PRODUCTION

M. Bonardi (1), C. Birattari (1), K. Abbas (2), F. Groppi (1), M. Severgnini (1), D. Shaw (2), E. Menapace (3), M.F. Stroosnijder (2). (1) Radiochemistry Laboratory, LASA, Università degli Studi and INFN-Milano, Segrate, Milano, Italy; (2) Institute for Health and Consumer Protection, Joint Research Centre, European Commission, Ispra (VA), Italy; (3) Enea, Applied Physics Division, Bologna, Italy.

^{64}Cu is a suitable radionuclide for labelling of a wide range of radiopharmaceutical compounds, for both PET imaging and therapy. In fact, Cu(II) forms a large class of stable complexes and chelates (acetate, TETA-octreotide, DOTA-biotin, DOTA-NR-LU-10, Shiff-base ligands, di-tio-carbamates (DTC) : ethyl-methyl-DTC and tio-semi-carbazonates: PTSM, ATSM, etc.). Several production methods have been investigated for ^{64}Cu production, such as those using neutron irradiation of Cu and Zn (natural or enriched targets) and also proton beam irradiation of an enriched ^{64}Ni target. The latter method yields a high specific activity product, however ^{64}Ni is obviously very expensive. Irradiation with neutrons is nowadays problematic since the nuclear reactors are shutting down one after the other. In addition, either the specific activity of the final product is low or the production yield of the radiotracer is low. In this study, we present preliminary results on another promising method for N.C.A ^{64}Cu production based on natural Zn irradiated with deuterons. A high purity (9N) Zn metal target was irradiated at the JRC Cyclotron (Ispra, Italy), which is a Scanditronix MC 40 variable energy machine, capable of accelerating deuteron beams up to 19 MeV, with a maximum extracted current of 30 _A. A few hours after the EOB, HPGe gamma spectrometry analysis, performed on the activated sample revealed the presence of the following radionuclides: ^{61}Cu, ^{64}Cu, ^{67}Cu, ^{66}Ga, ^{67}Ga, ^{65}Zn and ^{69m}Zn. ^{65}Ga and ^{68}Ga are cooled off. To proceed with the radiochemical separation, the activated Zn Target has been dissolved in 7 N HCl. The Ga nuclides have been liquid-liquid extracted from both Zn and Cu, with a yield greater than 99.99 %. In the residual solution of about 1 ml volume, radionuclides of Cu and Zn are well quantified with both gamma spectrometry and liquid scintillation counting. The Cu/Zn radionuclide separation has been carried out using an anion exchange column. The overall recovery of copper activity was greater than 95 % (^{64}Cu and ^{67}Cu). Impurities of Zn in the Cu fraction are determined by atomic absorption spectrometry, some days after separation to allow the radioactive decay. At present, traces of gallium radionuclides are present in the copper fraction, even if the gallium extraction yield is larger than 99.99 %.
Conclusion: This study presents a promising method for not only ^{64}Cu production, but also for ^{67}Cu and ^{67}Ga. The determination of both thick and thin target yields (cross sections) of the different radionuclides mentioned in this study is in progress.

PS_728

PREPARATION AND IN VIVO BIODISTRIBUTION OF 99M-TC LABELLED TRODAT-1 KIT

M. Csiszar (1), G. Toth (2), G. Jancso (3), B. Kanyo (1), L. Pavics (1). (1) Department of Nuclear Medicine, University of Szeged, Szeged, Hungary; (2) Isotope Institute Ltd., Budapest, Hungary; (3) Department of Physiology, University of Szeged, Szeged, Hungary.

^{99m}Tc is the most commonly used radionuclide in routine nuclear medicine imaging procedures. A novel ^{99m}Tc-labeled tropane derivative, ^{99m}Tc-TRODAT-1, is useful as potential dopamine transporter (DAT) imaging agent. According to the data of the literature we developed a TRODAT-1 kit. The aim of the present study was to optimize the kit formulation and to investigate the biodstribution of the complex in rats.
Methods: The composition of the lyophilized kit was varied. The amount of TRODAT-1 ligand, sodium-glucoheptonate and the other kit contents was changed. The optimal conditions for labeling were examined, the radiolabeling yield and the radiochemical purity was evaluated by HPLC method. The radioactivity for labeling was in the interval of 0,5-3,5 GBq. An ethanol solid phase extraction method on the Sep-Pak-Plus C-18 cartridge was developed to rid of the undesirable fractions. The reproducibility of our mensurmentes was also studied. The labeled and purified complex was i.v. injected into male Wistar rats (n = 9). After 60 minutes the rats was killed and biodistribution was measured. The regional brain biodistribution was analysed at the cerebellum, striatum, hippocampus and cortex.
Results: There is an optimal level for all kit components, the most drastical effect has the increased or decreased sodium-glucoheptonate content. The TRODAT-1 ligand amount has not influenced the complexing significantly. If higher radiactivity than 2 GBq was used at the optimal kit content the radiolabeling yield was about 50-70%. Much better yield can be obtained with 1-1,5 GBq ^{99m}Tc (80-95% over 6 hours). The labeling yield can be improved for 15-20% by the ethanol extraction and cleaning method. The highest uptake in the rats was in the liver (16,26 ± 5,26%). In the brain it was 0,12 ± 0,05%. Examining the brain regions the highest specific uptake was in the striatum, the lowest in the cerebellum (the striatal-cerebellar ratio was 2,21 ±0,47). Summarizing our results and comparing them with the literature data we conclude that our TRODAT-1 kit can be tested in human experiments.
Conclusion: ^{99m}Tc-TRODAT-1 binds selectively to DATs in the brain and that is potentially useful for in vivo assessment of the loss of dopamine neurons in Parkinson's and other neurodegenerative diseases.

PS_729

RUSSIAN TC-99M GENERATOR FOR NUCLEAR MEDICINE

A. Semenova (1), D. Stepchenkov (1), G. Davydov (2), A. Sokolov (1), V. Basmanov (1), D. Frolov (1). (1) State Scientific Center of RF - Institute of Physics and Power Engineering; (2) Medical Radiological Research Center, Obninsk, Russia.

Development of generator technology for Tc-99m radiopharmaceutical production shows that the aim is the impurity concentration reduction in eluate because the cold kits are very sensitive to stable chemical impurities.

Aim. The aim of the research is the development of Mo-99/Tc-99m generator of high activity with eluate of good quality for diagnostic radiopharmaceutical production in hospitals. During the eluate quality evaluation special attention was paid to its chemical purity, namely manganese concentration.

Manganese high concentration in eluate can result in its competitive participation in the following interactions between pertechnetate-ions and the cold kits during radiopharmaceutical synthesis at hospitals reducing their quality.

Methods. Multi-layer adsorbent has been used. One layer is silica gel modified by manganese dioxide in acid form and the other layers are chromatographic aluminum oxide in acid, alkaline and neutral forms.

Results. Optimization of molybdenum-99 dynamic adsorption has been carried out. It has been shown that the adsorption process from molybdenum-99 solution of pH 5.5 – 6.0 is efficiently carried out during technetium-99m generator production. It has been stated that the use of multi-layer adsorbent and molybdenum solution of the above mentioned pH results in the manganese concentration reduction at 1 – 2 orders in eluate and technetium-99m yield increasing at ~ 10% during the generator service life as compared with Russian adopted technology. The dependence of the manganese concentration in eluate on the generator service life has been studied.

Technetium-99m generator production technology of world level with 0.1 – 4.0 Ci activity has been developed with Tc-99m yield not less than 95%, Mn^{2+} and Al^{3+} ion concentrations – 0.1 – 5.0 μg/ml and 0.3 – 1.0 μg/ml, correspondingly, and molybdenum-99 concentration – 10^{-4} – 10^{-5}% of technetium-99m activity. The other quality characteristics correspond to the requirements of Russian, BP and USP Pharmacopoeia.

Conclusion. Tc-99m generator production technology possesses a patent #2153357 of 03.08.2000 „Generator for technetium-99m sterile radiopharmaceutical production".

Clinical application of the mentioned Tc-99m generators made in SSC RF IPPE (State Scientific Center of Russian Federation – Institute of Physics and Power Engineering) has persuasively presented the eluate high quality at the Department of Radioisotope Diagnostics of MRRC RAMS (Medical Research Radiological Center of Russian Academy of Medical Science). Wide range of cold kits made both in Russia (Diamed, Medradiopreparat) and in the foreign companies (CIS BIO, Nycomed Amersham, Mallinckrodt Medical) is used for radiopharmaceuticals production for scintigraphy of brain (Ceretec), cardiovascular system (Technetryl, MIBI, TCK-1, TCK-2, Cardiolite), lungs (Macrotech, Pulmocis), kidneys (TCK-6, MAG3, TCK-12, Pentatech, Technemec, Technemag), hepato-billiary system (Technetryl, Coren, Bromezida, Mezida, TCK-1, TCK-15), skeleton (Pyrphotech, Technefor, TCK-7) and tumors (Technetrul, Carbomec).

Clinical operation experience with Russian and foreign (CIS BIO, Nycomed Amersham, etc.) Tc-99m generators results in a conclusion that as for the eluate high quality, reliability and safety Tc-99m generators made in SSC RF IPPE (Obninsk, Russia) are as good as the similar products of the leading foreign companies.

* Variable collimator position: 0 = minimum collimation, 3 = maximum collimation.